National Academy of Sciences of Ukraine (NASU)
Russian Academy of Sciences (RAS)
National Academy of Sciences of Belarus (NASB)
Frantsevich Institute for Problems of Materials Science of NASU
Institute for High Temperatures of RAS
Lykov Institute for Heat & Mass Exchange of NASB
Bauman Moscow State Technical University (Russia)
Ukrainian Materials Science Association «Composites»
Financial & Industrial Group «Avangard» (Russia)
INTEM LTD (Ukraine)

SECOND INTERNATIONAL CONFERENCE

«Materials and Coatings for Extreme Performances: Investigations, Applications, Ecologically Safe Technologies for Their Production and Utilization»

20021231 151

PROCEEDINGS OF CONFERENCE

16-20 September 2002
Katsiveli-town, Crimea, Ukraine

OUR SPONSORS:

We wish to thank the following for their contribution to the success of this conference:

- *European Office of Aerospace Research and Development of USAF*

- *Science and Technological Center in Ukraine*

STCU

- *European Programme INTAS*

INTAS

- *Joint Stock Company "Ukranalit"*

- *Frantsevich Institute for Problems of Materials Science, National Academy of Sciences of Ukraine, Kyiv, Ukraine*

- *Bauman Moscow State Technical University, Moscow, Russia*

INFORMATION SUPPORT FROM:

Ukrainian Industrial Journal
«MM & Money «Technologies»

MM и ДЕНЬГИ и ТЕХНОЛОГИИ

Journal of Engineering Physics and Thermophysics

REPORT DOCUMENTATION PAGE

Form Approved OMB No. 0704-0188

1. REPORT DATE *(DD-MM-YYYY)* 30-09-2002	2. REPORT TYPE Conference Proceedings	3. DATES COVERED *(From – To)* 16 September 2002 - 20 September 2002

4. TITLE AND SUBTITLE

Materials and Coatings for Extreme Performances: Investigations, Applications, Ecologically Safe Technologies for Their Production and Utilization

5a. CONTRACT NUMBER
F61775-02-WF038

5b. GRANT NUMBER

5c. PROGRAM ELEMENT NUMBER

6. AUTHOR(S)

Conference Committee

5d. PROJECT NUMBER

5d. TASK NUMBER

5e. WORK UNIT NUMBER

7. PERFORMING ORGANIZATION NAME(S) AND ADDRESS(ES)
Institute for Problems of Materials Science
3 Krzhyzhanovsky Str.
Kyiv 03142
Ukraine

8. PERFORMING ORGANIZATION REPORT NUMBER

N/A

9. SPONSORING/MONITORING AGENCY NAME(S) AND ADDRESS(ES)

EOARD
PSC 802 BOX 14
FPO 09499-0014

10. SPONSOR/MONITOR'S ACRONYM(S)

11. SPONSOR/MONITOR'S REPORT NUMBER(S)
CSP 02-5038

12. DISTRIBUTION/AVAILABILITY STATEMENT

Approved for public release; distribution is unlimited.

13. SUPPLEMENTARY NOTES

14. ABSTRACT

The Final Proceedings for Materials and Coatings for Extreme Performances: Investigations, Applications, Ecologically Safe Technologies for Their Production and Utilization, 16 September 2002 - 20 September 2002

Principles of designing materials and coatings for operation in extreme conditions; scientific fundamentals and computer models for processing materials and coatings for operation in extreme conditions; advanced technologies for production and joining materials and products for operation in extreme conditions; structure and properties of materials and coatings for operation in extreme conditions; experimental data obtained from performance of materials and coatings in extreme conditions; and, potential technologies for recycling industrial waste aimed to production of structural, heat-insulation, facing and other materials.

15. SUBJECT TERMS
EOARD, Materials, Metals & alloys, Polymers, Ceramics

16. SECURITY CLASSIFICATION OF:			17. LIMITATION OF ABSTRACT UL	18, NUMBER OF PAGES	19a. NAME OF RESPONSIBLE PERSON Charles H. Ward, Lt Col, USAF
a. REPORT UNCLAS	b. ABSTRACT UNCLAS	c. THIS PAGE UNCLAS		658	19b. TELEPHONE NUMBER *(Include area code)* +44 (0)20 7514 3154

Standard Form 298 (Rev. 8/98)
Prescribed by ANSI Std. Z39-18

National Academy of Sciences of Ukraine (NASU)
Russian Academy of Sciences (RAS)
National Academy of Sciences of Belarus (NASB)
Frantsevich Institute for Problems of Materials Science of NASU
Institute for High Temperatures of RAS
Lykov Institute for Heat & Mass Exchange of NASB
Bauman Moscow State Technical University (Russia)
Ukrainian Materials Science Association «Composites»
Financial & Industrial Group «Avangard» (Russia)
INTEM LTD (Ukraine)

SECOND
INTERNATIONAL CONFERENCE

*«Materials and Coatings for Extreme Performances:
Investigations, Applications, Ecologically Safe
Technologies for Their Production and Utilization»*

PROCEEDINGS OF CONFERENCE

**16-20 September 2002
Katsiveli-town, Crimea, Ukraine**

AQ F03-03-0442

OUR SPONSORS:

We wish to thank the following for their contribution to the success of this conference:

- European Office of Aerospace Research and Development of USAF

- Science and Technological Center in Ukraine

- European Programme INTAS

- Joint Stock Company "Ukranalit"

- Frantsevich Institute for Problems of Materials Science, National Academy of Sciences of Ukraine, Kyiv, Ukraine

- Bauman Moscow State Technical University, Moscow, Russia

INFORMATION SUPPORT FROM:

Ukrainian Industrial Journal
«MM & Money «Technologies»

Journal of Engineering Physics and Thermophysics

INTERNATIONAL ORGANIZING COMMITTEE

Skorokhod V.   – chairman, Ukraine

Pavljukevich N.   – co-chairman, Belarus

Polezhaev Yu.   – co-chairman, Russia

Chernyshev L.   – scientific secretary, Ukraine

Ampleev N. – Russia

Antsiferov V. – Russia

Atamanenko B. – Ukraine

Byakova A. – Ukraine

Borisov Yu. – Ukraine

Drozdov Yu. – Russia

Froes F.H. – USA

Frolov G. – Ukraine

Gamulya G. – Ukraine

Haberko K. – Poland

Ivanchev S. – Russia

Ivasishin O. – Ukraine

Kamelin A. – Ukraine

Karpenko V. – Ukraine

Kostikov V. – Russia

Kostornov A. – Ukraine

Kuznetsov A. – Ukraine

Matsevityi Yu. – Ukraine

Molyar A. – Ukraine

Naidich Yu. – Ukraine

Nakamura T. – Japan

Neklyudov I. – Ukraine

Pokhmurski V. – Ukraine

Reznik S. – Russia

Ronen Y. – Israel

Rustichelli F. – Italy

Sitalo V. – Ukraine

Timofeev A. – Russia

Timoshenko V. – Ukraine

Vishnyakov L. – Ukraine

LIST OF ABBREVIATIONS

NASU   – National Academy of Sciences of Ukraine

RAS   – Russian Academy of Sciences

NASB   – National Academy of Sciences of Belarus

NSAU   – National Space Agency of Ukraine

SB   – Siberian Branch of RAS

MSAU   – Medical Sciences Academy of Ukraine

NTUU "Kiev Polytechnical Institute" – National Technical University of Ukraine "Kiev Polytechnical Institute"

Scientific Secretary of Conference
L. Chernyshev

CONTENT

III

SECTION B. SCIENTIFIC FUNDAMENTALS AND COMPUTER MODELS FOR THE PROCESSES OF MANUFACTURING MATERIALS AND COATINGS FOR OPERATION IN HAZARD CONDITIONS

VII

CONTENT

IX

CONTENT

X

CONTENT

XIV

CONTENT

SECTION E. EXPERIMENTAL DATA OBTAINED FROM PERFORMANCE OF MATERIALS AND COATINGS IN ON LOCATION HAZARD CONDITIONS

CONTENT

PLENARY SESSION

LAMINATED COMPOSITES: STRUCTURAL CLASSIFICATION, THERMAL, ACOUSTIC AND MECHANICAL PROPERTIES

Skorokhod V.V.

Frantsevich Institute for Problems of Materials Sciences National Academy of Sciences of Ukraine, Kyiv, Ukraine

In the report the major properties of multilayer composites as impact-resistant and high-temperature construction materials are esteemed in connection with the geometrical characteristics of their structure. The classification of laminated composites based on a commonality and discrepancy of structural parameters presented. Alongside with traditional periodic parallel-plane multilayer structures the ones having other elements of a symmetry (cylindrical or spheric multilayer objects) or not having them at all (irregular structures of all types) are reviewed also. The porous laminates are included also in a system of classification, in which the pores can be contained in both all, and only some of layers. Proprietary, but essential variety of porous laminated structures are composites which are composed of corrugated or grid layers which can alternate with continuous flat layers.

The special notice is given to a problem of an anisotropy of physical and mechanical properties of laminated composites. The methods of precise and approximated calculation effective values of thermal, thermoelastic, elastic and acoustic properties of unidimensional i.e. flat laminated composites lengthways and across layers are depicted the estimations of upper and lower values of properties for other types of composites, including for irregular structures are given. In most cases the effective values of physical and mechanical characteristics are confined from top and from bottom by known "fork" of Foight-Reiss. However, in spite of extreme simplicity of a geometrical arrangement of unidimensional laminated composites, in some cases the consecutive calculations of an anisotropy of averaged properties give nontrivial results. Most pronounced is for coefficients of the linear thermal extension and connected with them thermoelastic stresses.

The strength properties are reviewed for various groups of laminated composites - metallic, ceramic-metallic and ceramic - in connection with features of their fracture. Thus the considerable notice is given to influencing on hardness of "heritable" thermal stresses, and also conditions and processes at inner grain boundaries. It is pointed out, that in case of ceramic-metallic composites it is possible to achieve optimal combination of impact strength, modulus of elasticity and hardness of a material. Separately are considered ultra-light high-porous honeycomb structures having unusually a strong anisotropy of thermal, acoustic and mechanical characteristics.

The prospects of applying laminated composites in elements of constructions subjected to extreme thermal and mechanical loadings are shown. The tendency to transferring from discrete - laminated composites to gradient-laminated and gradient materials is noted with the purpose of decrease of their disposition to an inter-layer delamination under effect of thermoelastic stresses.

3

HEAT AND MASS TRANSFER IN POROUS MEDIA

Polezhaev Yu.V.

IVTAN (Institute of High Temperatures) Scientific Association, Russian Academy of Sciences, Moscow, 127412 Russia

The requirements for a porous material may be formulated depending on the efficiency with which the coolant blown through this material extracts heat supplied through the boundary layer from external high-temperature flow. The temperature of the external surface of the porous material will be defined in a first approximation by four parameters, namely, the level of external heat flux, the specific flow rate of the coolant, the thermal conductivity of the porous matrix, and the heat transfer inside the porous structure.

The first one of these parameters depends considerably on the completeness of mixing of the external and injected flows, and the last two parameters may vary in a wide range as a result of variation of the packing structure of particles. Apparently, this may explain the paradoxical fact that, in spite of the large number of publications in the Russian and foreign literature, not only does the disagreement between the experimental data with respect to the level of both external and internal heat transfer not decrease, but, on the contrary, this disagreement increases.

Naturally, numerous attempts were made at simplifying the formulation of the problem so as to derive its analytical solution. In particular, one can do this in the case when the intensity of internal heat transfer is sufficiently high to assume the temperatures T_s and T_c, to be equal.

Numerous experimenters extended, without ground, this relation to any case of percolation of coolant and tried to use the measured coolant temperature at the inlet, T_{c0}, and the external temperature of the porous wall, T_{sw}, to determine the hear flux q_w. It does not follow, however, that $T_{c0}=T_0$ and $T_{sw}=T_{cw}=T_w$ and, therefore, the actual value of q_w may vary considerably from the calculated one. This is but one of the possible explanation of the disagreement between the experimental data by different authors on the effect of injection into a turbulent boundary layer.

The situation with regard to generalization of the experimental data on the coefficient of internal heat transfer is likewise out of the ordinary. We will cite but a few published empirical dependences for the Nusselt number

$$Nu_v = \alpha_v d^2 / \lambda_c$$

$$Nu_v = 0.09 Re^{1.2},$$
$$Nu_v = 0.004 Re^{1.0},$$
$$Nu_v = 0.0175 Re^{1.65}.$$

It is obvious that the assumption of temperature equilibrium under conditions of percolation of coolant in a porous matrix is too rough, and the choice of the linear size d may help bring closer the empirical correlations for the coefficient of internal heat transfer.

The disagreement between the experimental data obtained by different researchers stimulates further the attempts to develop new physical models of the process.

The modified Darcy equation is often used to describe the percolation of liquids and gases inside a porous medium,

$$\frac{\Delta p}{H} = A\eta_c \frac{G_c}{\rho_c} + B\frac{G_c^2}{\rho_c},$$

where Δp is the pressure difference over the porous envelope thickness H; G_c is the mass rate of percolation, related to the total cross section of the porous material; η_c, and ρ_c denote the viscosity and density of the liquid being percolated, respectively; and A and B respectively denote the "viscosity" and "inertia' coefficients of hydraulic resistance of the porous material, which are assumed constant in the entire range of variation of the flow rate G_c.

This division of the total hydraulic resistance into two components is somewhat artificial, though rather convenient from the practical standpoint An analysis and companion of the published results of measurements of the viscosity A and inertia B coefficients are indicative of a considerable scatter of the values of the coefficients A and B even for porous structures of one and the same type. Apparently, it is both the porosity Π and the

characteristics of the starting material (such as the diameter of particles or fibers, as well as the density and structure of their packing) that may considerably affect the results of determining the values of A and B.

All this caused a considerable decrease in the interest of heat shielding specialists in the hydraulic characteristics of porous materials, however, serious problems associated with the estimation of the intensity of intrapore heat transfer made them once again turn to the modified Darcy law in search for the so-called "inherent" linear scale of the medium.

It is interesting to compare the linear scale $d_2 = 1/\sqrt{A}$ with the geometric characteristics of the tested mesh materials, as well as with other possible linear scales suggested by other authors.

Mesh materials offer a unique possibility of comparing these scales with the regular geometric characteristic, because the mesh number corresponds to the clear size of its pores in millimeters, and we will designate this sire as d_1.

The problem of the correct choice of the characteristic linear dimension of a permeable matrix, as well as the generalization of the experimental date on external and internal heat transfer using an adequate physical model, appears to be the most urgent problem in the field of investigations of heat and mass transfer in porous media. This will finally help solve the problem of optimization of the parameters of porous systems for various practical applications.

CAPILLARY TRANSPORT OF LOW-VISCOUS LIQUIDS IN POROUS METAL MATERIALS UNDER EFFECT OF GRAVITATION

Kostornov A.G.

Frantsevich Institute for Problems of Materials Science NAS of Ukraine, Kyiv, Ukraine

Porous metal materials are widely used as capillary structures in heat-exchange systems of evaporation-condensation and transpiration types.

In operation of above systems the capillary forces have key influence, which govern both transfer of working liquid over pore channels and foraing out of it by pressure or temperature gradient.

In the absence of pressure gradient the liquid in porous body moves under effect of a capillary pressure which in general case is balanced by losses in pressure due to friction in pores and difference of pressure in liquid due to gravity.

Neglecting the inertia effects at low flow rates one can obtain from the equation of pressure balance the following relationtship for average flow rate of liquid.

$$\overline{V} = \frac{Д_{эф}^2}{32\mu L B^2}\left(\frac{4\sigma\,|\cos\alpha\,|}{Д_{эф}} - \rho g L \sin\tau\right),\quad (1)$$

from which the maximum rate of capillary absorption under the conditions of full wetting of material is

$$V_{max} = \frac{Д_{эф}\sigma}{8\mu L B^2},\quad (2)$$

and the maximum heigh of capillary rising is

$$H_{max} = \frac{4\sigma}{Д_{эф}\rho g}.\quad (3)$$

In above expressions D_{eff} is average effective size of pores in material, which is equal to equilibrium value of average hydraulic diameter D_{h}^{eq} of pore channels in the case of regular porous structures, for which the coefficient of sinuosity is B; σ, g and μ are surface tension, density and absolute viscosity of working liquid at wetting angle α, respectively; q is gravitational acceleration; L is distance to which the liquid front displaced in material (its ultimate value equals to the specimen length Lo), which is located at the angle τ with respect to horizontal.

Based on traditional quantity which determines the structural characteristic of permeable material, namely general porosity θ, one can derive the following expression for average flow rate of liquid in pores

$$\overline{V} = \frac{2\sigma}{\mu}\frac{1}{S_o^2}\frac{1}{B^3 Lo}\frac{1}{Д_{гидр}^{равн}}\left(\frac{\theta^2\ln\theta}{1-\theta}\right)^2,\quad (4)$$

where So is specific surface of the unit volume of porous body.

High-porous specimens made from powders of copper PMS, bronze BrOF10-1, steels H18N10 and H18N15, titanium PTE, PTEM-2, PTM, PTOM and its alloy VT9 with varions dispersity and particle shape; discrette fibers of copper M1 and titanium alloy VT6 with different diameter, and also grid-like specimens made from steel H18H9T were used for experimental study of the kinetics of capillary transport of ethanol, distilled water and acetone.

All determining characteristics for the pore structure of materials under study were preliminary determined in the specimens-whitnesses.

Wide possibilities have been demoustrated concerning the forcast control of the capillar effects in powder structures by technological methods: pressing via elastic film; by adding pore-forming and agents; by vibroforming with both continuous and discrette variation in pore size; by precipitation of fine-grained particles in porous sceleton; by deformation of billets with wedge shape; by cyclic oxidation-reduction; by electric deposition.

The most promising capillar structures were shown to be materials from monodisperse fibers which capillar potential can be essentially varied through the control of adhesion work with the aid of high-temperature oxidation and vacuum treatment.

In such structures the most effect on the rate of capillar transport in horizontal location has the

variation in specific surface of pores and then in porosity and effective pore size.

Upon movement of liquid against gravitational force, porous materials having the most value of parameter of capillar pump K/O_h^{eq} showed the highest capillar rising.

For correct calculation of transport properties of capillar structures in various pore materials, we present the data about wetting them with different liquids (benzine, acetone, ethanol, methanol, water). The equilibrium wetting angles were determined by the methods of lying drop, photographine of shadow image of free meniscus upon wetting of vertically placed specimen with liquid and capillar rising.

Some examples of practical use of capillar mass transfer and its lows are shown for the resolving of methodical and technological tasks (determination of closed porosity in specimens, preparation of composite materials by impregnation, forecasting of service parameters of heating tubes and optimization of their mass and dimensions for different service conditions.

ADVANCED STRUCTURAL METALLIC ALLOYS AND TECHNOLOGIES FOR AIRSPACE USERS

Logunov A.V., **Timofeev A.N.**
Open Joint-Stock Company "KOMPOZIT", Institute of Metals, Korolev, Russia

The present review intends to demonstrate the results of the most important achievements of the Open Joint-Stock Company "KOMPOZIT" in a field of advanced structural metallic materials and technologies.

Metallic- and intermetallic structural alloys. Intermetallic alloys based on aluminides (Ni-Al, Ti-Al and some other systems) represent a new generation of advanced superalloys and are in a course of development in our Institute. A number of acceptable intermetallic compounds have a relatively high level of melting points, a good oxidation and scale resistance and a low density in compare with traditional metallic alloys (for example, Ni-base superalloys). However, the most acceptable intermetallics show room temperature brittleness that complicates their application as the structural materials. Fortunately, there exist the approaches that allow one to get over this difficulty and some of them have been developed in our Institute. One of approaches in an intermetallic alloy's design is based on a formation of a special microstructure that guarantees an acceptable level of the room temperature plasticity and a good structural stability at high temperatures.

Among traditional metallic structural alloys a group of the weld Al-base alloys with a service temperatures from - 235 up to 200 °C is at the center of attention. The alloys of this group have a number of preferences in compare with well-known Al-Li (01460) and Al-Sc (01545) alloys, for example, have a low tendency to formation of the micro cracks and show the highest level of the specific strength.

Advanced technologies. Our efforts that are made in a direction of the advanced materials design require an elaboration of the advanced technologies. The following decisions in a field of technologies can be especially marked:
- There exists an investment- and permanent-mold casting of Ti-base alloys that allows one to obtain the blown-free ingots having a very low level of impurities. A high quality of ingots is also achieved by means of using an electron-beam melting.

- An isothermal hot stamping is a progressive method of a hard-deformed materials production. It allows one to fabricate the complex-shape wares from intermetallic and titanium alloys having low room temperature plasticity. As a result of this process an improvement of a number of properties occurs. For example, the tensile ductility is increased; the low cycle fatigue is significantly improved.
- Hot Isostatic Pressing (HIP) of structural materials is a unique technology that allows one to strongly affect on the alloy's microstructure including the gas pore defects and shrinkages in the alloy. In this paper the effects of HIP on the microstructure of Ni-base superalloys is discussed in more detail. For example, a number of conventional cast alloys are known for their coarse γ' + γ eutectic areas and chunky carbides. The course structure and the unhomogeneity in the alloys result in not only reduced yield strength and low cycle fatigue property, but also hot workability. The data obtained demonstrate that after HIP and heat treatment the microstructure of Ni-base superalloys is greatly improved. The coarse γ' + γ eutectic areas can be effectively eliminated by transformation into fine γ' - γ regions. The composition segregation may be also remarkably eliminated by HIP treatment. As a result the several types of γ' - γ microstructures may by formed. It depends on the parameters of the HIP treatment: a uniform fine γ' – phase in the γ - matrix or duplex γ' - γ microstructure can be created.

An improvement of the microstructure and eliminated of the porosity provide marked quality and property improvements. For example, after HIP treatment of the cast blades made from the Ni-base superalloy type In 100 he following results have been obtained: the fatigue strength σ_{-1} = 22.6 kgf/mm^2 , yield strength σ_b = 92 kgf/mm^2 , tensile yield δ = 4.4 % (σ_{-1} = 16.6 kgf/mm^2 , yield strength σ_b = 85 kgf/mm^2 , tensile yield δ = 3 % for unHIPed blades). The long-term strength of the HIPed samples at temperatures 975°C, 900°C and 800°C increases in 1.5-3 times.

HIGH-TEMPERATURE CERAMOMATRIX COMPOSITES

Kostikov V.I., <u>Timofeev A.N.</u>[(1)], Bogatchev E.A.[(1)]

Federal State Unitary Enterprise NIIGrafit, Moscow, Russia

[(1)]Open Joint-Stock Company *Research, Development and Production Corporation "KOMPOZIT"*, Korolev, Moscow region, Russia

The works in the field of carbon-carbon composite materials [1-3] and high-temperature ceramics [4,5] had created a basis reliable enough for development of new generation of high-temperature materials, i.e. ceramomatrix composites (CMC). These composite materials must inherit all advantages of both carbon-carbon composite materials and high-temperature ceramics and get rid of disadvantages proper to them. The main reason causing researchers material scientists to start active exploration of composite materials with ceramic matrix and their manufacturing processes development was insufficiency of properties level of carbon-carbon composite materials (low resistance to oxidative media and insufficient resistance in erosive flows at high temperatures) and high-temperature ceramics (low resistance to thermal shocks and thermal cycling).

A review is presented in the report of domestic and foreign investigations in the field of development of high-temperature CMC. Results are considered of works in two directions.
➢ CMC efficient in neutral media;
➢ CMC efficient in oxidative medium conditions.

The first direction is presented by development of composites of the type C/MeC (TaC, HfC). Composites of this type have larger erosion resistance comparing to carbon-carbon composite materials. Thus the works we had carried out on introduction of tantalum carbide into a porous carbon preform had shown an opportunity of considerable increasing of ultimate compression strength and chiefly of decreasing erosion takeoff by 3-4 times comparing to a carbon-carbon composite material with the same reinforcement type. However in composites of that type at high-temperature exploitation eutectics are formed at the C-MeC, melting temperature of which is lower than the same of composite ingredients. Analysis of modern tendencies in creation of new thermal erosion resistant materials shows that further increasing of erosion resistance is connected with introduction of elements or compounds possessing ablation effect into a composite, or reinforcing of

carbide matrices by carbide fibers (TaC/TaC, HfC/HfC).

Concerning the second direction, the most investigated are composites C/SiC, SiC/SiC and their modifications with several types of additional protective coatings increasing the service temperature. Several integral and differential schemes are considered of surface protection of composites from oxidation. The authors had presented a classification of CMC developed on principles of material science, i.e. by material of filler and matrix. This classification is based on both developed composite materials and composites, which, in authors' opinion shall be developed in the nearest future.

Basic methods of obtaining of CMC are also presented in the report, advantages and disadvantages are analyzed of each of them as well as tendencies of their application in commercial industrial production.

Application fields are given of high-temperature CMC.

1. Костиков В.И. - Ж. Всес. хим. о-во им. Д.И. Менделеева, 1989, т.34, № 5, с. 492-501.
2. G. Savage. Carbon-Carbon Composites.- Chapman & Hall, 1993.
3. Ю. Г. Бушуев, М.И. Персин, В.А. Соколов. Углерод-углеродные композиционные материалы. - М.: Металлургия, 1994.
4. Р. Киффер, Ф. Бенезовский. Твердые материалы. Перев. с нем. - М.: Металлургия, 1968.
5. Косолапова Т.Я., Андреева Т.В., Бартницкая Т.Б. и др. Неметаллические тугоплавкие соединения. - М.: Металлургия, 1985.

THERMAL STABILITY OF NANOSTRUCTURED MATERIALS

Andrievski R.A.

Institute of Problems of Chemical Physics, Russ. Acad. of Sciences, Chernogolvka, Russia

Essentially all nanostructured materials (NM) in itself are far from equilibrium state. Many features such as large part of interfaces and triples, possible irregular distribution of alloying elements and admixtures, the availability of nonequilibrium phases, residual stresses and so on result in the excess value of free energy. So the thermal activation leads to enhancement of diffusion and recrystallization with partial or total annihilation of the nanocrystalline structure, nonequlibrium phases and residual stresses, that , in one's turn, changes the properties of NM. Thus, in many cases the thermal impulses could result in the critical conditions for NM. Besides, the understanding of the thermal stability regularities is also very important for the development of optimal technological regimes of the NM preparation which in many cases are connected with high temperatures.

In this paper, we attempt to review the progress in results of thermal stability of NM based on metals, alloys, intermetallics, oxides, borides, nitrides, etc. both in bulk and film forms. The attention is taken to the different aspects of grain growth such as the kinetics features, the availability of the growth stagnation and grain boundary segregation and so on. Interesting idea on the vacancy generation during grain boundary migration [1] is also analyzed in connection with experimental results which have showed that NM with small grain size are more stable than those with bigger crystallites.

The presence of triples and residual stresses exert important influence upon grain growth.

Analysis of thermodynamics of alloy nanocrystals has revealed the unmonotonous change of integral Gibbs-free energy as a function of grain size. This deduction has been done both from the Langmuir-McLean approximation and Fowler-Guggenheim that [2,3]. This result can be also used for explanation of stability of NM with small crystallites.

The behavior of supersaturated solid solution and nonequilibrium phases in nanostructured bulks and films are also discussed in detail.

The special interest is that now it is possible to obtain NM with crystallites of about 1-2 nm and lower [4]. This was realized by magnetron sputtering as applied to boride/nitride films. Such NM can be classified as cluster-consolidated solids. Their annealing at 1000°C does not effect on grain size but accompanied by some decrease of hardness. This situation is connected with residual stresses relaxation.

1. Y.Estrin, G.Gottstein, L.S.Shvindlerman. Acta Mater. **47**, 3541 (1999).
2. J.Weissmuller. Nanostructured Mater. **3**, 261 (1993).
3. D.L.Beke, Cs.Cserhati, I.A.Szabo. Nanostuctured Mater. **9**, 665 (1997).
4. R.A.Andrievski, G.V.Kalinnikov, A.E.Oblezov, D.V.Shtanskiy. Physics Doklady, 2002, submitted to publication.

THE METHODOLOGY OF SOLVING INVERSE HEAT TRANSFER PROBLEMS AS A TOOL FOR INTERPRETING THE RESULTS OF EXPERIMENTAL RESEARCH

Matsevity Yu.M.

A.N. Podgorny Institute for Mechanical Engineering Problems of the NAS of Ukraine, Kharkiv, Ukraine

In some cases, the complexity, labour intensiveness and high cost of thermophysical experiments make mathematical simulation an indispensable tool for investigating heat transfer processes. Its efficiency relies largely on the effectiveness of the methods of solving heat transfer problems and the computational tools used for implementing these methods. However, irrespective of the methods and tools used by the investigator, the results of solving the problems mentioned depend entirely on the correctness of selecting the mathematical model of the phenomenon and the validity of the available uniqueness conditions.

In view of their imperfection, special experiments in determining the thermophysical properties of materials and the boundary conditions cannot often serve as an exhaustive source of information about the uniqueness conditions. Moreover, each such experiment is unique in a definite sense, requires a special geometry of specimens and specific heating (cooling) regimes; special measurement methods, accessories and equipment. Accordingly, a great deal of attention has been paid recently to the solution of inverse heat transfer problems (IHTP), in which available (very limited) data about the temperature inside the body can be used to reconstruct its temperature field; determine its thermophysical properties and geometric characteristics; identify the initial and boundary conditions, as well as to specify the mathematical model of the phenomenon.

In other words, the methodology of solving inverse problems is a powerful tool for interpreting the results of a thermophysical experiment, making it possible to identify the parameters of heat engineering systems and processes by their indirect manifestations. This is particularly sensitive in diagnostics problems, which recently have been coming into the focus of researchers when estimating the residual life of power and industrial facilities. This is mandatory for identifying the strategy of upgrading and reconstructing these facilities.

Since, in essence, IHTPs are ill-posed problems because their causal links are violated, they were considered for a long time as non-solvable ones. After Academician Tikhonov A.N. introduced the notion of conditional correctness [1], and subsequent works were published by himself, Ivanov V.K, Lavrentiev M.M. and their progeny ([2-5] and others), there appeared the possibility of solving inverse problems. All this conditioned the development of the theory of ill-posed problems, the emergence of academic schools, progress in thermophysical research and obtaining of outstanding results when solving scientific and engineering problems [6-10].

The Institute for Mechanical Engineering Problems of the NAS of Ukraine has been conducting wide-scale research in heat processes. In so doing, methods of solving boundary, internal, geometric and combined IHTPs, as well as of optimisation and optimal control problems [8, 9 and 11-15] have been used.

As a result of these investigations, heat transfer conditions have been defined for the following cases: in cooling channels of turbomachines and on the surfaces of steam turbine casings; in ICE cylinders; on the surfaces of cooled caissoned components of metallurgical furnaces; during surface boiling of dispersed liquid; and in electronics components.

Thermophysical characteristics have been identified for polycrystalline superhard materials; for metal hydrides; for amorphous metals and for ceramic materials. The power of internal heat sources has been defined for induction heating of metals; for induction hard facing; and for activation annealing of semiconductor wafers.

The following geometric parameters have been defined: the substrate coating thickness; the depth of hardening of sheet products; the geometry of caissoned structures of fire engineering plants; and the depth of destruction of a flash smelting furnace bottom. Allocation of resistive components in the

plates of cermet heaters, and of cooling channels in cermet boards has been carried out.

The problem of concurrent identification of the thermophysical performance and boundary conditions of heat transfer has been solved for a rod cooled by a dispersed liquid and for induction hardening.

Optimisation has been carried out for the thermal regime of a steam turbine casing; for thermal processes during induction hardening; for activation annealing of semiconductor wafers and for the heat engineering process of slag granulation.

All the problems solved have demonstrated the high efficiency of parametric identification of heat processes by implementing the IHTP solution methods.

REFERENCES

1. Tikhonov A.N. On the stability of inverse problems // Dokl. AN SSSR. – 1943. – **39**, 5. – pp. 195-198.
2. Ivanov. V.K., Vasin V.V. and Tanapa V.P. The theory of linear ill-posed problems and its applications. – M.: Nauka, 1978. – 206 pp.
3. Lavrentiev N.M., Romanov V.G. and Shimateliy S.P. Ill-posed problems in mathematical physics and calculus. – M.: Nauka, 1980. – 288 pp.
4. Tikhonov A.N. and Arsenin V.Ya. Methods of solving ill-posed problems. – M.: Nauka, 1979. – 288 pp.
5. Glasko V.B. Inverse problems in mathematical physics. – M.: Moscow Univ. Publ., 1984. – 112 pp.
6. Alifanov O.M. Inverse heat transfer problems.– M.: Mashinostroenie, 1988. – 280 pp.
7. Kozdoba L.A. and Krukowsky P.G. Methods of solving inverse heat transfer problems. – Kyiv: Nauk. Dumka, 1982. – 360 pp.
8. Matsevity Yu.M. and Multanovsky A.V. Identification in heat transfer problems. – Kyiv: Nauk. Dumka, 1982. –240 pp.
9. Matsevity Yu.M. and Lushpenko S.F. Identifying the thermophysical properties of solids. – Kyiv: Nauk. Dumka, 1990. – 214 pp.
10. Simbirsky D.F. Temperature diagnostics of engines (film thermometry and optimal estimates). – Kyiv: Tekhnika, 1976. – 208 pp.
11. Matsevity Yu.M., Slesarenko A.P. and Tsakanian O.S. Spectral influence functions in multidimensional inverse heat transfer problems // Dokl. AN UkrSSR, Ser. A. – 1986. – № 5. – pp. 72–77.
12. Yerzhanov G.Zh., Matsevity Yu.M., Sultangazin U.M. and Sheryshev V.P. Lumped capacitance in thermophysical and microelectronics problems. – Kyiv: Nauk. Dumka, 1992. – 296 pp.
13. Matsevity Yu.M., Prokofiev V.Ye. and Shyrokov V.S. Solving inverse heat transfer problems on electrical models.– Kyiv, Nauk. Dumka, 1980. – 130 pp.
14. Matsevity Yu.M. Electrical modelling of nonlinear thermophysical engineering problems. – Kyiv, Nauk. Dumka, 1977. - 254 pp.
15. Matsevity Yu.M. Geometric inverse heat transfer problems. Statement and methods of solving // Elektron. Modelirovanie. – 1999. – **21**, 31. – pp. 3-10.

HOLLOW SUBMICRON-SIZED POLYMER PARTICLES AS WHITE PIGMENT FOR OBTAINING PIGMENTED POLYMERIC COATINGS AND COMPOSITIONS WITH INCREASED THERMAL STABILITY

Ivanchev S.S., Pavlyuchenko V.N., Sorochinskaya O.V., Skrifvars M.[1]
St-Petersburg Department of the Boreskov Institute of Catalysis of the Siberian Branch
of the Russian Academy of Sciences, St-Petersburg, Russia
[1]SICOMP AB, Pitea, Sweden

Hollow polymer particles with micron-sized air-filled hollows are effective light-scattering materials that determines the main area for their application in the production of pigmented coatings and compositions. The most convenient approach to obtaining hollow particles of this type is a synthetic technique (without using volatile pore forming agents) based on emulsion (co)polymerization of vinyl monomers in aqueous media. Technological and ecological advantages of the application of hollow pigments in the latex form in combination with waterborne polymeric binders (synthetic film forming latexes, aqueous solutions of condensation prepolymers) are obvious and connected with the simplicity of pigment-binder compatibilization and low energy required for this step, low density and high exploration performances of the pigmented compositions.

We have developed a method for the preparation of hollow particle latexes on the basis of styrene-acrylic copolymers [1,2]. However low glass transition temperature (T_g) of the polymer shell (about 100°C) does not allow the hollow pigment incorporation into the thermosetting binders cured and used at elevated temperatures. In addition, the anionic nature of the latexes makes impossible their application in thermosetting compositions cured in the presence of acidic catalysts. In order to resolve this problem we have developed a new method for obtaining hollow particle latexes with an additional thermally resistant outer shell comprising a thermosetting polymer.

The synthesis procedure involves the following stages:

- preparation of a carboxyl containing copolymer latex by emulsion copolymerization of methyl methacrylate, methacrylic acid and a small amount of a crosslinking comonomer (0.5%wt.);
- preparation of particles with the core-shell morphology by emulsion copolymerization of styrene, acrylonitrile and divinyl benzene in the presence of carboxyl containing seed particles;
- neutralization of carboxyl groups in the core with a base at temperatures above T_g of the shell polymer proceeding with a strong core swelling, shell expansion and formation of one central hollow (diameter 300-400 nm) in the latex particle;
- addition of a cationic colloid of melamine-formaldehyde resin (MFR) into the anionic hollow particle latex resulting in the cationic resin deposition onto the anionic hollow particles, their recharging and partial condensation of the cationic MFR.

The MFR cationic colloid was prepared by water mediated condensation of melamine (M) and formaldehyde (F) in the presence of hydrochloric acid at molar ratios of the reactants M:F:HCl from 1:2:0.4 to 1:8.4:1.3.

In order to avoid the latex system coagulation the procedure of anionic hollow particle recharging with a cationic MFR colloid was carried out with simultaneous feeding of the components into the reactor at vigorous stirring. The particle recharging was confirmed by the change in the particle ς-potential from – 50 mV (anionic latex) to +20 ÷ +50 mV (recharged latex). The ς-potential value of recharged particles depends on the ratio between the components in the used cationic MFR and cationic MFR colloid: anionic

hollow polymer weight ratio. We have found that this ratio should be no less than 0.3, otherwise a significant latex thickening or coagulation occurs.

Electron microscopy study of the prepared particles (Figures 1, 2) indicated remaining of the hollow size and some increase in the shell thickness after cationic MFR deposition onto the surface of anionic particles. DSC characterization revealed that a preliminary condensation of the outer MFR shell can be fulfilled at 70-90°C straight in the latex form. The final curing proceeds in a pigmented composition containing as a binder MFR etherified with methanol at 150-190°C within 5-35 min depending on the hollow pigment chemical composition.

Thermal stability of hollow particles modified with a cationic MFR was estimated by measuring optical properties of the coatings (based on etherified MFR) pigmented with hollow particles. The coatings comprising non-modified anionic styrene-acrylic hollow particles became almost transparent after exposure to the temperature 170°C thus indicating the destruction of hollow particles. The coatings based on the modified hollow pigment retained the initial opacity upon the similar treatment.

Recommendations for the application of the developed cationic hollow particles as components for thermally resistant pigmented polymeric compositions and multifunctional additives in pulp and paper industry are set forth.

Figure 1. Electron micrograph of anionic hollow particles. $D_n = 520$ nm, $D_v = 545$ nm
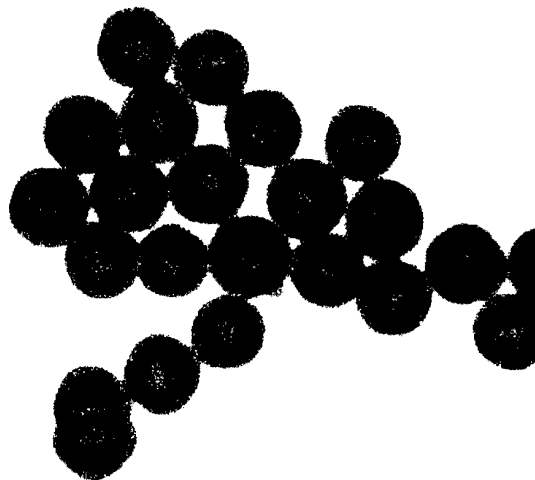
Figure 2. Electron micrograph of hollow particles after modification with cationic MFR (hollow polymer:MFR weight ratio 1:0.5). $D_n = 570$ nm, $D_v = 590$ nm

References:

1. V.N.Pavlyuchenko, N.A.Byrdina, S.S.Ivanchev et al. Russian Federation Patent No. 2128670 (1998).

2. V.N.Pavlyuchenko, O.V.Sorochinskaya, S.S.Ivanchev et al. J. Polymer Sci., Part A: Polymer Chem., Vol. 39, 1435-1449 (2001).

TECHNOLOGY OF MANUFAKTORING ALLOYS FROM INDUSTRIAL WASTER BY A METHOD OF THE LIQUID-PHASED REDUCTION OF OXIDES OF METALS IN IRON-CARBON MELT

Naydek V.L., Kostyakov V.N., Poletaev E.B., Chepel S.N.
Physic-Technological Institute of Metals and Alloys of National, Academy of Sciences of Ukraine,
Kiev, Ukraine

During the last years the Physic-Technological Institute of Metals and Alloys of National Academy of Sciences of Ukraine has intensively been working in the field of manufacturing metals and alloys from different industrial wastes by a method of reducing oxides of metals in iron-carbon melt.

Among numerous wastes of the economic activity a special place is occupied by high toxic wastes containing in particular such metals as Cd, V, Co, Pb, Hg, Mo and others. In this connection the problem of utilizing the referred to above wastes in particular electroplating sludge for industrialized countries, including, Ukraine, is one of the most important.

The fulfilled analysis of the compositions of electroplating sludge and worn-out catalysts from some Ukrainian enterprises has shown that all wastes by their chemical composition are close to polymetallic ores, and therefore, for their processing metallurgical technologies can be used.

The investigation of peculiarities of the technological process of remelting different wastes and melting alloys can be conducted in a plasma furnace. As a reductant in this case carbon in the form of electrode breakage is used.

It has been revealed that during melting at the arc current of 200-600 A up to 70 % of volatile matters is withdrawn from sludge and up to 30 % of a solid concentrate, consisting from metal and sludge, is formed.

The yield of metallic base and its chemical composition are presented in Table 1.

From Table 1 follows that at remelting electroplating sludge a high yield of metallic base with a high content of Cr and Ni is reached.

In future alloys melted of sludge have been used for melting alloy cast irons and steels.

Composition of sludge and chemical composition of manufactured melted cast irons and steels are presented in Table 2.

Chemical composition of these alloys is close to the composition of alloys, regulated by acting normative documents.

More effective process is the use of electroplating sludge in charge during melting, at which an intermediate metallurgical process stage is excluded. In this case the withdrawal of volatile matters and reduction of metal oxides carried out in iron-carbon melt during melting.

Chemical composition of melted alloys is presented in Table 3.

It should be hooted that the basis metal Cr and Ni are reduced in iron-carbon melt adequately and the degree of their reduction amounts to 80-90 %.

The implemented investigations gave an opportunity to develop scientific fundamentals for elaborating a technology of manufacturing alloys with the use of industrial wastes.

Thus, metallurgical technologies of processing industrial wastes enable to accomplish the following tasks:
- to withdraw volatile matters from different organic and inorganic compounds;
- to extract metallic base from sludge, containing deficit alloying elements;
- to eliminate the influence of toxic wastes on environment in places of their formation.

Tables to the abstract of the report by V.L. Naydek, V.N. Kostyakov, E.B. Poletaev, S.N. Chepel "Technology of Manufacturing Alloys from Industrial wastes by a Method of the Liquid-Phased Reduction of Oxides of Metals in Iron-Carbon Melt"

Table 1. Types of wastes, yield of metallic base and its chemical composition.

	Yield of wastes	Yield of metallic base, %	Chemical composition, % mas.									
			Si	Mn	Cr	Ni	Mo	Nb	W	Cu	S	P
1	Sludge from bath of electro-chemical treatment of chromi-um-nickel plating	22-26	0,53	0,05	14,9	61,2	1,42	0,87	0,55	-	-	-
2	Sludge from baths of copper, chromium, nickel plating	12-16	3,1	-	20,8	35,0	-	-	-	2,0	-	4,6
3	Sludge from baths of copper, chromium, plating	12-15	-	-	47,3	-	-	-	-	1,3	-	-
4	Positive electrodes of worn out iron-nickel accumulators	-	0,1	0,22	20,1	39,0	-	-	-	0,4	-	-
5	Worn-out nickel-bearing catalysts	-	2,55	0,35	0,16	11,1	-	-	-	-		0,3

Table 2. Composition of charge and chemical composition of melted alloys

	Alloy brand	Grade composition	Chemical composition, % mas.					
			C	Si	Mn	Cr	Ni	Cu
1	18Cr9Ni	Alloy of sludge from baths of electro-chemical treatment Steel3, FeCr90CO1; FeMn75, reductant	1,2	0,17	2,46	17,05	9,52	-
2	9Cr5Ni	Alloy of sludge from baths of electro-chemical treatment and copper-chromium plating Steel3, FeSi75; FeMn75, reductant	2,0	0,22	2,54	10,03	6,3	2,5
3	15NiO7Cu2Cr	Alloy of sludge from baths of copper-nickel-chromium plating and worn-out accumulator Steel3, FeSi75; FeMn75, reductant	2,6	0,33	2,44	2,23	14,3	0,73

Table 3. Types of wastes and chemical composition of melted alloys

	Alloy	Type of wastes	Chemical composition, % mas.									
			C	Si	Mn	Cr	Ni	Mo	Nb	W	Cu	S	P
1	13N2CrMoCu	Sludge from baths of electrochemical treatment, steel scrap	0,6	1,3	0,2	2,0	13,0	0,5	0,1	0,3	0,7	-	-
2	11Ni2Cu3P	Sludge from baths of electrochemical nickel plating	2,27	0,82	0,1	-	11,2	-	-	-	0,6	1,81	2,52
3	8NiCu2S2P	Sludge from baths of chemical nickel-chromium-zink plating	2,16	0,87	0,2	-	7,84	-	-	-	0,3	1,99	1,56

16

LIMIT POWER CONSUMPTION OF MAJOR FACTORS OF ABSORPTION OF HEAT AT THERMAL DESTRUCTION OF THE MATERIAL

Frolov G.A.
Institute for Problems of Materials Science of National Academy of Science of Ukraine

Undoubtedly, extreme conditions of a material operation involve material application at influence of big thermal streams. Here exist two opposite approaches: the first consists in use of concentrated streams of energy for cutting, weldings, and processings of a material surface with the purpose of increasing its employment characteristics, and the second implies application of a material, as sacrificial covering, for protection from influence of thermal streams of high density.

Both the first and the second cases are interesting in terms of finding out which conditions of thermal destruction enable a material to absorb a maximum amount of heat being brought.

The equation of heat balance on a surface of a collapsing material (1), which includes practically all major factors of absorption and dispersion of a brought thermal stream, shows that those factors are: heat absorption by heat conductivity (2), radiation from a surface $\left(\varepsilon\sigma T_w^4\right)$, thermal effect of physical and chemical transformations on a surface (ΔQ_w) and a blowing effect $(q_{вд})$.

$$q_0 + q_{л} = \varepsilon\sigma T_w^4 + \Gamma G_{\Sigma}\Delta Q_w + q_{вд} - \left(\lambda\frac{\partial T}{\partial y}\right)_w \quad (1)$$

at $\tau \to \infty$

$$-\left(\lambda\frac{\partial T}{\partial y}\right)_w = \rho\overline{V}_{\infty}c_p\left(T_w - T_0\right) = \rho\overline{V}_{\infty}H\left(T_w\right) \quad (2)$$

Here τ – time of heating; ρ, c, λ - density, a thermal capacity and heat conductivity of a material; $\overline{V}_{\infty}$ - quasistationary speed of weight ablation; q_0 - a convective thermal stream brought to a surface with temperature T_w; T_0 - temperature of a cold material; $q_{л}$ - a radiant thermal stream; ε - a degree of a surface blackness; σ - Stephan-Boltsman Constant; Γ - factor of gasification; $H\left(T_w\right)$ - enthalpy of a material at temperature T_w.

Absorption of heat by heat conductivity with use of a thermal capacity of the condensed systems (copper and graphite) can happen only under influence of small thermal streams during a short period of time. Limit value of this factor of heat absorb-tion is restricted to a material fusion temperature [1].

A maximal thermal stream, which can be removed from a surface due to radiation, can be estimated based on a graphite temperature in the triple point ($\sim$4200 K) $\varepsilon\sigma T_w^4$ =18000 kW/m^2

Thermal streams influencing lowered space vehicles, for example, to enter into an atmosphere of planets with 2-nd and higher space speeds, ten and hundred times exceed possibilities of such factors of heat absorption as accumulation and radiating cooling. This involves application only of either porous cooling or cooling of a surface with the help of sacrificial layer (ablation thermal protaction).

For simulation of such heating conditions, IPMS NASU developed installations which allow simulating not only convective heating of a heat-protective coating, but also joint influence of a radiation-convective heating. Considering a complex of installations of radiant heating with mirror concentrators in diameter from 1 up to 5m, the experimental base of IPMS of NAS of Ukraine enables researches of both external and internal thermal protection of space-rocket engineering products, including heat-shielding coverings of reusable space vehicles [2].

Analysis of the experimental results on research of heat protective materials on these stands and the installations which have been accumulated over 30 years, including processing of the literary data, allowed establishing of limit thermal opportunities of internal and surface processes of heat absorption at interaction of materials with a high-temperature environment.

It has been shown, that alteration of the total thickness of heated and removed layers Δ^* can be calculated with the formula:

$$\Delta^* = K\sqrt{a}\left(\sqrt{\tau} - \sqrt{\tau_{\xi}}\right),$$

and its speed with the expression

$$V_{\theta^*} = \frac{K\sqrt{a}}{2\sqrt{\tau}}.$$

Here K - temperature coefficient; a - effective thermal conductivity coefficient; $\sqrt{\tau_\xi}$ - a length cut with a straight line on the abscise axis. Thus, it was experimentally established that at

$$\theta^* = \frac{T^* - T_0}{T_w - T_0} > 0,2 \text{ for calculation } K \text{ it is necessary to apply the expression}$$

$$K = -\frac{1}{K_{T_p}}\theta^* + \frac{K_{T_p}}{1 - K_{T_p}},$$

which at $\theta^* = 1$ will be transformed to the equation of 3-rd degree and the determines value $K_{T_p} \approx 0,74$.

Further it was shown, that K_{T_p} determines laws of a surface temperature change, weight ablation speed, movement of a temperature field isotherms and characterizes the moment the end of non-stationary process of heat absorption in a surface layer of a collapsing material.

The temperature of a considered isotherm T^* determines the lower border of a heated layer. As the temperature T^* decreases, the speed of its movement grows. By the moment of the establishment of a quasistationary mode of heating τ_δ, the way covered by this isotherm, will be the more than less its temperature. At this moment the heated layer will reach the maximal thickness, and the amount of accumulated heat will achieve a limit value. Further all isotherms of a temperature field, which temperature are higher T^* will be moving with a speed equaling $\overline{V}_\infty$.

Calculations and experiments have shown, that at the moment of achievement of limit power consumption of internal processes of heat absorption, the thickness of an ablated layer will be equal to the disposition depth of isotherms θ^* practically all over the temperature field. This law functions up to dimensionless speed of ablation of weight $\overline{G}_\Sigma < 0,5$.

The received results do not contradict numerical calculations. For example, a model heat and ablation of weight from a crystal body surface, offered by J.V.Polezhaev [1], adequately confirms linearity of the experimentally established law. Numerical calculations on this model show, that ablation of weight and heated layer may vary under completely various regulations, but their total thickness during some time τ_δ, which establishes an equality of thickness of heated and ablated layers, with good accuracy (~5 %) may be described by a linear dependence. However, these calculations allow this conclusion only for isotherms with the dimensionless temperature $\theta^* \leq 0,1$. The experimental data confirming equality of thickness at the moment τ_δ even for an isotherm $\theta^* = 0,6$ are received at the same time. From here follows, that the process of heat accumulation in a surface layer of a material, determined by a constant K_{T_p} allows a precise identification of non-stationary and stationary modes of heating and ablation of weight.

Further it was established [3], that between a constant K_{T_p}, a material enthalpy at the boiling temperature and the evaporation heat there is an interrelation such as:

$$\Delta Q_u \approx \frac{\left(K_{T_p}^2 + 1\right)\sqrt{\pi}}{2K_{T_p}^3}H(T_\kappa) = 3,4H(T_\kappa) \quad ,$$

and for the dimensionless speed of evaporation, the equation is received

$$\overline{G}'_w \approx \sqrt{\frac{I_e - I_w}{H}} - 0,3, \text{ here } H = 2\Delta Q_w,$$

from which follows that a limit effective material enthalpy

$$I_{эфф} \rightarrow \sqrt{I_e H} \text{ при } I_e \gg I_w.$$

Thus, it is now possible to firmly established that the limit power consumption of a material thermal destruction process tends to a value equal to a square root from a product of a stream enthalpy and the total thermal effect of surface processes.

References

1. Polezhaev J.V., Jurevich F.B. Thermal protection.- Moscow: Energia, 1976.-392p. (Russia)
2. Frolov G. Application of the High Temperature Heating Installation for Gradient Material Obtaining // FGM News – 1995. - №28. P.16-20, Sindau, Japan.
3. Estimation of energy of destruction of a material on its enthalpy / G.A.Frolov, V.V.Pasichny, J.V.Polezhaev etc.// Inzhenerno-fizicheski zhurnal.-1986.-V.50, _ No 5.- p. 709-718. (Russia)

MATERIALS BEHAVIOR UNDER SPACE SIMULATION CONDITIONS

Gavrylov R.V., Eremenko V.V., <u>Pokhyl Yu.O.</u>
Special Research & Development Bureau for Cryogenic Technologies of Institute for Low
Temperature Physics & Engineering, NAS of Ukraine (SR&DB ILTPE NASU), Kharkov, Ukraine

The report contains review of researches carried out in SR&DB ILTPE NASU within last decade in the field of crygenic-vacuum and space material science, directed on an establishment of a nature of structural and functional materials physical properties changes under separated and combined laboratory simulating. Space factors influence. The aim of such researches is the definition of serviceability and durability of materials, used in space engineering, in extreme conditions influence of deep vacuum, electromagnetic radiation of the Sun, powerful flows of corpuscular radiation in radiation belts of the Earth, microgravitation, low temperatures, significant cyclic thermomechanical gradient stresses, magnetic fields, high dynamic loadings, vibrations and other factors. Each of the listed factors differently influences on changes of mechanical, optical, electrical, thermophysical, tribotechnical and other properties of materials, and their resulting joint influence is not additive.

Generally real Space negatively influences on materials and designs elements of space vehicles, resulting to essential degradation of their operational characteristics.

There are two approaches to decision of a problem of estimation and selection of materials, suitable to use in so specific conditions. The first consists in regular investigations of materials complex of physical&mechanical properties in conditions of separated and combined ground simulation of Space factors. The second assumes exhibiting of materials and designs elements in open Space conditions in real space flight with the subsequent investigation of their physical properties. These approaches are complementary, and in SR&DB ILTPE the works are carried out in these both directions.

The description of the created laboratory-test base with specialized cryogenic, vacuum and simulating equipment for various types of researches in conditions of ground simulation of major outer Space factors is given. The following set of equipment can be attributed to unique types:

- Complex system of the equipment for research of radiation stability of materials ensuring influence of vacuum (up to 3×10^{-4}Pa), extreme temperatures (80... 400K), ultra-violet (UV) radiation, vacuum ultra-violet (VUV) radiation, ultra soft X-ray (USX) radiation (range of wave lengths λ= 1.24-250 nm), flows of protons and electrons of energy up to 200 KeV.
- Setup for test of fatigue strength, cyclic crack growth and wear resistance of materials at low temperatures (4.2-300K) in cryogenic liquids (nitrogen, hydrogen, helium), vacuum, any gaseous medium.
- Series of test cryogenic machines for definition of quasi-static mechanical properties complex of materials in 4.2?300K temperature interval with an opportunity of parallel measurement of the magnetic and electrophysical object characteristics.
- Low temperature impactor for impact tests of materials in 4,2?300K temperature interval.
- Setup for thermocycling (4.2-500K) of samples at constant load and programmed low-frequency force cycling in the same interval of temperatures.
- Setup for research of shape and dimensional materials stability against gradient low temperature cyclic influence.
- Complex of setup for definition of thermophysical characteristics of materials within 5-300K temperature interval.
- The structural methods of investigation such as TEM and SEM, low temperature X-rays analysis are widely used.

he report is represent the results of numerous investigations and tests of space factors influence on:

- Fatigue characteristics of strength and crack growth resistance in vacuum and at low temperatures.
- Tribotechnical characteristics changes for solid lubricant coatings under influence of the radiating factors.
- Behaviour of mechanical properties of structural materials under influence of cyclic gradient thermal stresses.

•Processes of gassing out, surface state, structure and optical characteristics of functional coatings in vacuum under influence of temperature, radiation and atomic oxygen.

It is shown, that the improvement of the fatigue characteristics in vacuum is caused by more homogeneous distribution of microplastic deformation in a superficial layer of metal owing to change of adsorption conditions of oxygen atoms on juvenil surfaces of slip steps.

The best materials from the point of view of low temperature cyclic crack propagation resistance are the structural - stable alloys with FCC- lattice, which are characterized by increasing of crack growth resistance with temperature decreasing irrespective of a load level.

It has appeared, that for solid lubricant coatings with organic bond the frictional durability decrease under influence of VUV radiation but for coatings with inorganic bond is fixed significant (in 5 times) increasing of frictional durability.

It was established, that purposefully varying a combination of material structure and phase state and modes of cryogenic thermocycling treatment we can obtain the material with the optimum complex of mechanical properties.

It was shown, that the joint influence of space factors results also in changes of surface structure of functional coatings consisting in occurrence of a various nonhomogeneities such as cracks, holes, roughnesses, splitting and so on. Simultaneously the value of coatings integrated factor of radiation (factor of blackness) is increased also.

The found out effects of deterioration of surface conditions and corresponding reduction of reflecting ability and increasing of blackness factor of thermoregulating coatings are explained by Coulomb and recombination interaction of protons and electrons saved in undersurface layer.

The reasons of observed effects of the space factors influence from positions of a structural - phase state for the investigated materials are considered.

The physical criteria by justified of an estimation and selection of characteristic classes of structural and functional materials, suitable for use in severe operational conditions of cryogenic and space technique are formulated. These criteria are based on comprehensive analysis of the experimentally determinated interrelation of a wide spectrum of the factors (both external, and internal) comprising the cause-and effect sequence "history- structure phase state – mechanical properties -service conditions - application "

The data on SR&DB ILTPE NASU present-day developments on creation of onboard research and technological equipment and scientific programs of space technological experiments in conditions of real Space flight onboard of the International space station are given also.

CHEMICAL VAPOR DEPOSITED POLYCRYSTALLINE DIAMOND FILMS: PERFORMANCE AT ELEVATED TEMPERATURES

Ralchenko V., Khomich A.[1], Ivakin E.[2], Sukhodolov A.[2], Vlasov A., Salvatori S.[3]

General Physics Institute, Moscow, Russia; E-mail: ralchenko@nsc.gpi.ru

[1] Institute of RadioEng. & Electronics, Fryazino, Russia

[2] Institute of Physics, National Academy of Sciences, Minsk, Belarus

[3] Third University of Rome, Department of Electronics, Rome, Italy

Diamond is known to possess a combination of extreme physical properties, which make it the material of choice for many advanced applications. Those properties include, in particular, highest thermal conductivity at room temperature among other substances, record high hardness, transparency from ultraviolet to radio frequency range, ionizing radiation "hardness", chemical inertness, high mobility of charge carriers. Heat spreaders for electronic devices (laser diodes, microwave transistors), infrared optics, UV, X-ray and particle detectors, and of course, cutting tools are some well established applications for natural diamond crystals. However, small dimensions and high cost may limit the practical use of diamond single crystal, either natural or synthetic (produced at high pressures) ones in new fields.

In the last decade a big progress is achieved in synthesis of diamond at low pressure using a chemical vapor deposition (CVD) technique [1]. Thin coatings and macroscopic forms (wafers) of polycrystalline diamond can be produced using methane-hydrogen reaction gas decomposed thermally or in a discharge. As a result, new applications appear such as windows for CO_2 lasers and high power (~1 MW) gyrotrons, protective diamond coatings for exploitation of optics in harsh environment (e.g. against sand or high-speed water droplets), large area stable electrodes in electrochemistry, surface acoustic wave devices, and diamond-coated cutting tools.

Currently diamond wafers up to 75 mm diameter and up to 1.8 mm thickness are produced at joint facilities of General Physics Institute RAS and Diagascrown Co. using microwave CVD reactors (MPCVD) [2]. The deposition proceeds on a Si substrate at temperatures of 700-900°C with typical growth rate of 1-5 µm at pressures 70-100 Torr. The diamond films are chemically separated from the substrate to obtain free-standing films and plates. The material is essentially polycrystalline with arbitrary oriented grains (Fig.1).
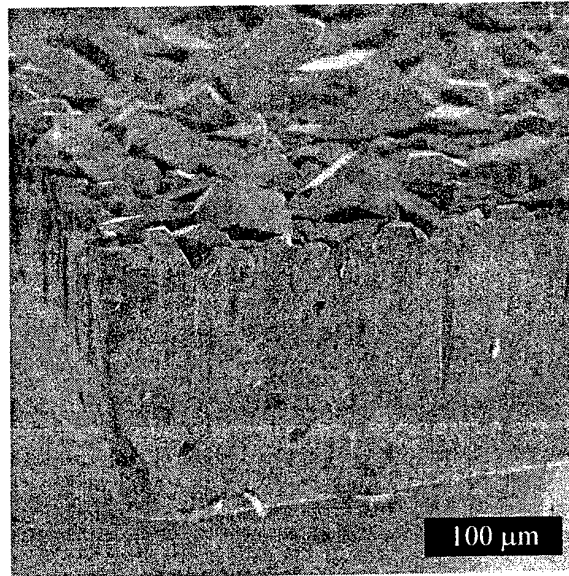
Fig. 1. A polycrystalline diamond plate 0.2 mm thick laser cut from a mother wafer produced by MWCVD. The upper, growth surface shows faceted crystallites of 20-40 micron size. The bottom, nucleation, side contains submicron grains.

In contrast to diamond ceramics the CVD films does not contain pores or a binder material. The main impurities are nitrogen and hydrogen with typical concentration of the order of a few ppm, (N), and tens or hundreds ppm (H), respectively. In many respects the quality of CVD diamond approaches to that of most pure natural diamonds. Here we touch only one aspect of this new material - the performance of polycrystalline diamond exposed to elevated temperatures.

The nominally undoped and semiconducting B-doped diamonds with resistivity of ~10^{13} and 10^3 Ohm_cm, respectively, show the thermal conductivity k=16-18 W/cmK at 20°C. In the temperature range T=20-200°C value of k decreases with T down to 10-12 W/cmK (Fig. 2), yet the diamond remains to be superior thermal conductor, that can be used as heat spreader for electronic devices operated well above R.T.
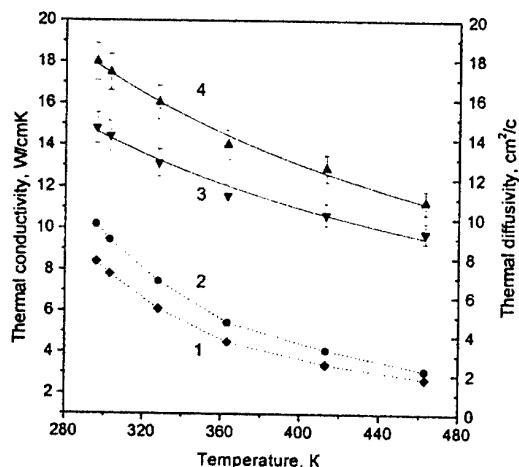
Fig. 2. Thermal diffusivity D (dotted lines) and thermal conductivity k (solid lines) of undoped (curves 1,3) and boron-doped (curves 2,4) diamond films [3]. The data are obtained using the laser-induced dynamic grating technique.

Fig. 3. Absolute quantum yield of 0.8 mm thick diamond film at different temperatures [4].

As the wide band-gap semiconductor (band gap 5.4 eV, fundamental absorption edge 225 nm) the diamond can be a solar-blind ultraviolet detector. The spectral discrimination (the ratio of the photoresponse at UV and visible range) exceeds 10^4 [4], and this selectivity is preserved upon heating at least up to 300°C, with temperature coefficient of quantum yield around 1%/°C (Fig.3). Diamond withstands much higher ionization radiation doses compared to silicon, that's why the diamond detectors are of interest for space research and high energy physics. Typical temporal resolution is in the range of 0.2-1 ns. Because of large area films are available, the position-sensitive detectors (pixelized) can be made.

CVD diamond preserves its optical properties after heating *in vacuo* up to 1300°C, however a darkening is observed after annealing to higher temperatures [5]. In contrast to single crystal diamond that shows a surface graphitization starting from about 1700°C, an *internal* graphitization takes place in CVD diamond at grain boundaries (GB). The de-bonding of hydrogen, which is located mostly at GB and extended defects, was studied at elevated temperatures using IR absorption spectra. The hydrogen loss is believed to trigger the internal diamond-to graphite conversion process.

It's interesting that the thermal conductivity measured perpendicular to the film plane is preserved (within 10% deviation) after annealing to at least 1500°C, in spite of the strong optical degradation of the diamond.
No decrease in Young modulus or fracture strength was found after such heat treatment [6].

In summary, the CVD diamond becomes is the emerging engineering material that can be produced in macroscopic forms for performance in extreme conditions, and today its unique properties are still far from being fully exploited.

References
1. *Handbook of Industrial Diamonds and Diamond Films*, M. Prelas et al (eds), Marcel Dekker, New York, 1997.
2. V.G. Ralchenko, A.A. Smolin, V.I. Konov, K.F. Sergeichev, I.A. Sychov, I.I. Vlasov, V.V. Migulin, S.V. Voronina, A.V. Khomich, *Diamond Relat. Mater.* 6 (1997) 417.
3. E.V. Ivakin, A.V. Suhkodolov, V.G. Ralchenko, A.V. Vlasov, A.V. Khomich, *Quantum Electronics* (Moscow), in press.
4. S. Salvatori, M.C. Rossi, F. Scotti, G. Conte, F. Galluzzi, V. Ralchenko, *Diamond Relat. Mater*, 9 (2000) 982.
5. L. Nistor, V. Ralchenko, I. Vlasov, A. Khomich, R. Khmelnitskii, P. Potapov, J. Van Landuyt, *Phys. Stat. Sol. (a)*, 186 (2000) 207.
6. V. Ralchenko, E. Pleurer, (to be published).

BODY ELECTRIZATION IN A HYPERSONIC TWO-PHASE FLOW

Vasilevskii E., Gorelov V., Kazansky R., Yakovleva L.
Central Aerohydrodynamic Institute, Zhukovsky Moscow region, Russia E-mail: vasilevs@netto.ru

Introduction

In the course of experimental investigations electro-optical effects caused by the presence of solid particles in gas flow were observed [1]. These factors can appreciably influence on particles flow, heat transfer and surface condition.

The electro-optical phenomena can be caused by different factors. In [2], the formation of a noticeable charge on aircraft traveling through clouds was considered and various accompanying electro-optical effects were discussed. Almost all studies refer to subsonic gas flows with liquid, essentially polydisperse drops. The polydispersion creates difficulties in interpreting experimental results. Perhaps, this is why the situation in this branch of science has not been considerably improved. However, as applied to space flights to the Mars, the problem of vehicle charging is very important [3].

In this report, we present the results experimental investigation of the charging of different segments of a sphere immersed in a supersonic gas flow with solid particles. The experiments were performed in a short-duration wind tunnel which makes it possible to obtain the results on a wide range of parameters with low cost. The particle concentration in a cross section of the flow was almost constant and the dispersion of particle size was only slight.

We note that for the supersonic flow, no disturbances penetrate into the region ahead of the bow shock. Accordingly, for the flow past a body the boundary conditions can be determined much more accurate than for subsonic and transonic flow.

For these investigations, we designed different models with different parameters of electric schemes. In the tests, the particle concentration and inertia parameter were varied.

Experimental technique.

The experiments were performed in the TsAGI UT-1 shock wind tunnel [1]. The tunnel operated in the Ludwieg scheme. The high-pressure channel was 12 m long. The Mach number of the undisturbed flow ahead of the model was $M_\infty = 6.04$ with the total pressure $P_0 = 23$ bar, stagnation temperature $T_0 = 600$ K, and the Reynolds number based on the free-stream parameters and the radius of curvature of the model $Re_{\infty,R} = 0.2*10^6$. The duration of the steady flow past the model was $\tau = 0.04$ s. The mean weight concentration of the particles in the air flow was below $n = 2$ %.

For introducing the particles into the gas flow, we used the "fluidized bed" method..

The models were spherical. Copper probes 5 mm in diameter and 12 mm long were flush-mounted on the external surface of the model. The radius of model № 1 was $r_w = 75$ mm and for models № 2 and № 3 $r_w = 40$ mm. Each probe was connected with direct-current amplifier through a load resistor R. The resistor of each amplifier channel was 2 MΩ. The amplifier coefficient of the signal was determined before the tests, it was varied on the range 100 - 15000.

Model № 1 was designed for measuring the potential on the external surface of the sphere for high electric resistance of the circuit. High-ohm resistors of the probes differed by more than an order of magnitude: $R_H1 = 680$ MΩ, $R_H2 = 51$ MΩ, $R_H3 = 6.2$ MΩ. The electric capacitance of the probes, including the adjoining electric circuits, was small: $C = 3, 7.5,$ and 2.6 pF, respectively. The effect of the electric-circuit high-voltage part capacitance on the generated current and potential can be neglected. To avoid electric break-down and leaking, the potential divider mounted on the model was covered by paraffin. The measuring under the normal conditions ($T=298$ K, $p=1$ bar) performed after the wind tunnel tests showed that the electric resistance between the probes of the model was greater than 3 TΩ. We note that in the two-phase dusted layer the electric resistance may be much lower than in the pure air under the normal conditions.

Model № 2 was designed for investigating the influence of the load resistor value on the current recorded ($R_1=100$ Ω for the probe mounted at the stagnation point of the model; $R_2=1000$ Ω and $R_3=10$ Ω for the probes mounted at a distance $\varphi=30°$).

23

Model № 3 was designed for investigation the distribution of the electric current along the sphere generatrix at a distance $\varphi=0$, 30°and 30°. The load resistance R of each probe on this model was R = 1000 Ω.

We used Fe_2O_3 and Fe particles with mean weight diameters 0.37 and 1.2 μm respectively.

For determining the temporal dependence of the particle concentration, we measured the voltage difference U on the load resistor likely [1].

The results.

A typical record of the potential U_m on the loading resistor during the test is presented in Fig. 1. The potential on the external surface increases with resistance and at 680 MΩ attains 5000 V
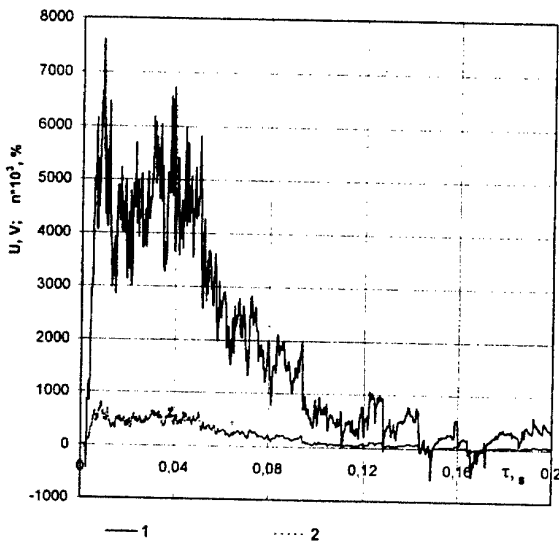
Fig. 1. Fe_2O_3, Model 1,
　　　　$1 - \varphi = 0$ at 680 MΩ
　　　　2 - n

Noticeable oscillations of the potential take place. This indicates that considerable temporal variations of the particle concentration may also take place. For the further analysis we performed averaging as a rule over 5 points: at each measuring we took the arithmetic mean for this instant, two preceding instants, and two subsequent instants.

The value of the potential on the load resistor makes it possible to determine the main required value, namely the current density i which is generated by the two-phase flow (i – the current in the circuit per the area of the exposed surface of the gage $S = \pi \cdot d^2/4 = 19 \cdot 10^{-6}$ m²).

The distribution of current density i in dependence of the sphere central angle ϕ is shown: at the angular distance from the stagnation point $\varphi = 30°$, the current density i is greater than at the stagnation point (Fig. 2).

The current density i increases about proportional to the particle concentration. For equal weight concentration, the ferric oxide generates greater charge than pure Fe. This may be caused by various reasons, e.g.: smaller particle number concentration of the Fe particles.
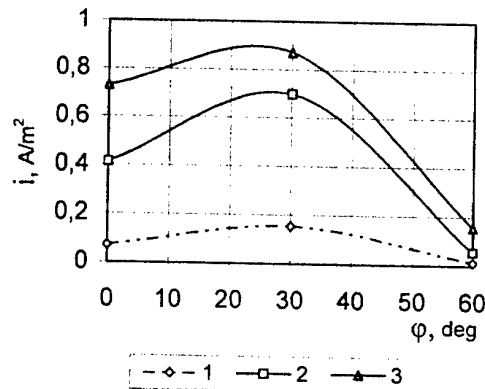
Fig. 2　　Fe_2O_3, Model 3
　　　　1 - n = 0.14 %,
　　　　2 - n = 0.8 %,
　　　　3 - n = 1.4%

In the pure gas flow (without particles), almost no charging is observed.

With increase in the electric resistance of the "probe-ground" circuit, the current density i is almost unchanged (Fig. 3).
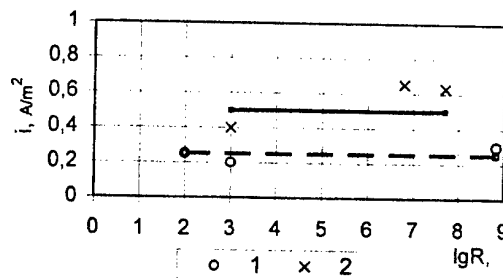
Fig. 2.　1 - $\varphi = 0$,　　2 - $\varphi = 30°$　(R - Ω)

References.
1. E.B. Vasilevskii, A.V. Chirikhin, A.N. Osiptsov, L.V. Yakovleva. JEP&T, 2001, No 6, pp. 31-42.
2. I.M. Imjanitov. "Electrization of aircraft in clouds and precipitations". Hydrometeorological publish house, Leningrad, Russia, 1980.
3. Joseph C. Kolecki, Barry Hillard, Mark Sielbert, Overview of Mars System-Environment Interactions// AIAA Paper 96-2333, 1996.

MECHANICAL PROCESSING AND HEAT TREATMENT OF SUPER-HIGH STRENGTH TITANIUM BETA-ALLOYS

Ivasishin O.M., Markovsky P.E., Semiatin S.L.[1], Fox S.[2]

Institute for Metal Physics, 36 Vernadsky Street, 03142 Kiev, Ukraine

[1]Air Force Research Laboratory, AFRL/MLLM, Wright-Patterson Air Force Base, OH 45433-7817 USA

[2]TIMET Henderson laboratory, Henderson, Nevada, USA

Titanium alloys are a unique material due high strength to density ratio, excellent fatigue properties and low elastic modulus, accompanied by good resistance against corrosion, that makes it irreplaceable for many critical applications. Due to higher than in alpha-beta alloys amounts of beta-stabilizing elements beta titanium alloys are capable of being heat treated to very high strength through solid solutioning followed by ageing [1, 2]. High strength levels are particularly attractive for an efficient application of beta alloys in the aerospace and automotive industries as materials for high-loaded parts and structures.

Important advantage of beta-titanium alloys consists of the possibility to employ cold deformation if the alloy comprises only metastable beta phase. In the present work the cold workability of four solution-treated beta-titanium alloys was determined and related to the initial substructure. Two alloys (TIMETAL®LCB and Ti-15-3), which retained a well-developed subgrain structure after solution treatment, exhibited excellent workability, while those alloys which did not (VT22 and TC6) exhibited inferior ductility. The difference in workability was explained in terms of the variation in strain-accommodation mechanism. Other factors that exacerbated the observed low ductility of the latter two alloys were also identified. These included the occurrence of deformation-induced martensite formation and the development of multi-component textures, both of which may lead to localization of deformation at grain boundaries and intergranular failure.

Cold worked material often requires intermediate and/or final annealing and ageing to eliminate cold work and restore ductility as well as to receive fine grained beta structure before final ageing. Most promising approach to receive such fine –grained condition is rapid annealing processes lasting seconds, which allow to unite heat treatment in line with the rolling operation. However, the development of such an approach requires detailed investigations because continuous heating of solid solutioned and subsequently cold rolled beta phase entails very complicated phase and microstructural transformations. In present study precipitation and recrystallization behaviour during the continuous heat treatment of above mentioned beta-titanium alloys with various molybdenum equivalents was established. Following solution treatment, the materials were cold deformed to various reductions and then heated at rates between 0.17 and 50 Ks^{-1} to peak temperatures below and above the beta-transus temperature. Precipitation below the transus was most rapid for the alloy with the least amount of beta stabilizing elements (VT22) and next fastest for the most-highly alloyed material (TIMETAL®LCB), an effect ascribed to its large iron content. Reduction level was found to have a very strong influence on the uniformity of recrystallization and the recrystallized grain size. Because of the competition between precipitation and the temperature-dependence of recrystallization nucleation and growth, the heating-rate dependence of the recrystallization temperature for the beta-titanium alloys was weak.

Influence of such thermomechanical + rapid heat treatment on the balance of titanium beta alloys mechanical properties was studied taking as an example TIMETAL®LCB. It was shown earlier, that strength level of 1300÷1350 MPa can be obtained with beta-grain size of about 50 μm easily attained by RHT of alloys thermomechanically processed in alpha+beta field [3]. Further increase in strength requires beta-grain size to be smaller than 50 μm, what can be achieved by RHT of alloys carefully processed in single-phase beta field. Material was solution treated either in a furnace at 820°C, 0.5 h (β-grain size 90 μm) or by rapid heating (β-grain size 20 μm), both followed by WQ. Following the solid solution treatment, the materials were cold drawn with a total reduction of either 50% or 70%. Cold drawn materials were then rapidly heated (20 Ks^{-1}) to produce recrystallization, water quenched from peak temperatures and finally aged at different temperatures. Results of tensile tests are listed in the Table. It is clear that aged material had an attractive combination of strength and ductility after the grain refinement to 30 μm achieved by cold deformation and RRA. The finest grain size achieved was 7 μm. The strength values of or in excess of 1600 MPa are the result of the high density of fine α precipitates produced by low-temperature ageing. The improvement in ductility may be attributed to the fine and very uniform β-grain microstructure. This represents a significant overall improvement in strength/ductility balance achieved in this alloy.

Table 1; Mechanical properties of TIMETAL®-LCB coil material in cold drawn/recrystallized conditions.

##	Solid solution	Reduc-tion	β-grain size, μm	Ageing	YS, MPa	UTS, MPa	A$_5$, %	RA,%
1	Furnace	50	30	538°C, 8h	1395	1425	6.8	24
2	RH	50	12	538°C, 8h	1420	1470	8.2	22.5
3	RH	70	7	538°C, 8h	1475	1490	10.3	25.5
4	RH	70	7	520°C, 8h	1600	1625	6.0	20.0
5	RH	70	7	500°C, 8h	1615	1690	4.2	13.5

References

[1] P.J. Bania in: D. Eylon, R.R. Boyer and D.A. Koss (Eds.), *Beta Titanium Alloys in the 90's*, TMS, Warrendale, PA, 1993, pp. 3-14.

[2] D. Eylon in: T. Kishi, N. Tanaka and Y. Kagawa (Eds.), *Proc. 3rd Japan International SAMPE Symposium*, SAMPE publishing, Tokyo, 1993, pp. 1588-1595.

[3] O.M.Ivasishin et. al. in: I.V. Gorynin and S.S. Ushkov (Eds.), *Titanium '99, Proc. of Ninth World Conf. On Titanium*, CRISM "Prometey" publishing, St.Petersburg, 2000, pp. 505- 512.

ТЕХНОЛОГИЯ ЖАРОПРОЧНЫХ УГЛЕРОД - УГЛЕКАРБИДКРЕМНИЕВЫХ КОМПОЗИЦИОННЫХ МАТЕРИАЛОВ

Костиков Валерий, **Черненко Николай**

ФГУП «НИИграфит», Москва, Россия

Разработана технология жаропрочных жаростойких композиционных материалов на основе углекарбидкремниевой матрицы, армированной углеродными волокнами. Процесс получения композита реализуется при последовательном термохимическом переделе полимерной коксообразующей матрицы исходного углепластика в углеродистую матрицу с открытой пористой структурой транспортного типа, которая, в свою очередь, превращается в углекарбидкремниевую матрицу путем капиллярной пропитки жидким кремнием и конверсии углерода в карбид кремния. Для предотвращения взаимодействия жидкого кремния с армирующим углеродным волокном на внутреннюю поверхность углерод-углеродной преформы наносится карбидкремниевая пленка - диффузионный барьер против диффузии углерода в жидкий кремний, который обеспечивает селективность взаимодействия жидкого кремния с компонентами углерод-углеродной преформы путем варьирования их химической активности.

Для объемного насыщения углеродистой матрицы углерод-углеродной преформы жидким кремнием, предложен новый принцип и разработан на его основе технологический процесс получения углеродистой матрицы, пористая структура которой характеризуется преобладанием открытой пористости транспортного типа. При этом пиролизу подвергается смесевая коксообразующая матрица, представляющая собой взаимопроникающие полимерные сетки ее компонентов, хотя бы один из которых при карбонизации газифицируется без возникновения углеродного остатка, образуя в формирующейся углеродной матрице сообщающиеся канальные поры открытого типа.

Получаемый по данной технологии конструкционный углерод-углекарбидкремниевый композиционный материал обладает высокими физико-механическими характеристиками в окислительной среде до температуры $1700^{0}C$, при которой его жаропрочность в 1,5 раза превышает соответствующие показатели при комнатной температуре.

SECTION A.
PRINCIPLES OF DESIGNING MATERIALS AND COATINGS FOR OPERATION IN HAZARD CONDITIONS

LARGE YBa$_2$Cu$_3$O$_{7-d}$ BULK MELT TEXTURED HIGH TEMPERATURE SUPERCONDUCTOR MATERIALS FOR POWER APPLICATIONS

Gawalek W., Habisreuther T., Zeisberger M., Litzkendorf D., Surzhenko O., Kracunovska S., Prikhna T.A.[1], Oswald B.[2], Kovalev L.K.[3]

Institut fuer Physikalische Hochtechnologie e.V., Winzerlaer Strasse 10, 07745 Jena, Germany

[1]Institute for Superhard Materials of NAS of Ukraine, 2, Avtozavodskaya Str., 254074 Kiev, Ukraine

[2]OSWALD Elektromotoren GmbH, Benzstr. 12, 63897 Miltenberg, Germany

[3]Moscow State Aviation Institute, Volokolamskoe shosse, 125871 Moscow, Russia

The dicovery of a new class of oxide-based superconductors by Paul Chu and his collaborators in early 1987 with T$_c$ above the boiling point of liquid nitrogen opened a new frontier for superconducting applications. Although the dissipationless current flow in superconductors is applied in many applications, the interaction of a superconductor with a magnet is also attractive for various practical applications, like magnetic levitation systems as frictionless and selfstabilising bearings for high speed or high load rotors and non contacting transport systems (MAGLEV).

Because of its unique magnetic properties melt textured especially single domain YBa$_2$Cu$_3$O$_{7-d}$ (YBCO) bulk HTS (High Temperature Superconductor) material has a large potential for MAGLEV and energy technique applications. Its material quality is nearing commercial demands in the superconductor industry. YBa$_2$Cu$_3$O$_{7-d}$ bulk HTS was tested successful in circular and linear superconducting magnetic bearings (fly wheels for the energy technique and MAGLEV transportation) as well as in electric motors and generators (hysteresis machines, reluctance machines and trapped field machines).

The magnetic material quality is given by the ability to store magnetic energy in supercurrent loops. It is measured by the current load as product of critical current density j$_c$ and smallest diameter of superconducting current loop d in a single domain. In a type II superconductor, the total magnetic moment is given by m=VAj$_c$d (V: superconducting volume fraction, A: geometrical factor) Because the perovskite lattice of the YBa$_2$Cu$_3$O$_{7-d}$ material is strong anisotropic, we have to look on the current flow in the ab-planes. The levitation force depends on the gradient of the magnetic field imposed by the lecitated magnet and the total magnetic moment m of the superconductor. However, it is important to note,

that between trapped field mapping results and levitation force results exists no simple relation in macroscopic disturbed material domains.

In small samples critical current densities up to 10^5 A/cm^2 @ 77 K are measured by vibration sample magnetometry. But there are indications of reduced critical current densities over full sample dimension also in single domain samples, caused by macroscopic inhomogeneities in thickness, as well as subgrain boundaries and cracks in lateral direction. Additionally, we have a typically growth induced sector structure

Because the critical current density seems to be limited to about 10^5 A/cm^2 for YBCO @ 77 K, the size of weak link and crack free regions (perfect domains) should be increased in order to increase the energy product. There are three ways to solve this problem:
1. better understanding and control of the melt textured growth process, in order to avoid small angle grain boundaries acting as weak links.
2. multi seeding in the top seeded process, and
3. superconducting joining of single domains in ab-direction.

In general the macroscopic growth sector structure of melt textured blocks has to be considered by using the material for magnetic applications. Growth structure related magnetic hard and soft regions influence the penetration of magnetic flux.

We produce YBCO material blocks in different shape in a batch process and compose cryomagnetic function elements for bearings and electric machines by cutting and bonding crystallographic oriented parts of sinlge domain blocks.

Safe passivation of function elements has to be solved.

31

High power density electric reluctance motors with output power up to 38 kW are constructed and successful tested in OSWALD Electromotors Company Miltenberg/Germany and MAI Moscow. Now, machines with output power of about 200 kW are under construction. A flywheel with 850 Wh kinetic energy storage capacity at 10 kW power was constructed in frame of an European project and a 2 MW power fly wheel for local energy tuning has been concepted in the DYNASTORE project in Germany.

For MAGLEV large scale application the economic permanent magnetic rail construction is an open problem. Also effective cryocoolers for MAGLEV and energy technique applications have to be developed.

Safe passivation of function elements has to be solved. At the time the step from material development to system development has to be made.

FORECAST OF CARRYING POWER OF CERAMIC SHELLS

Railyan V.S., Rusin M.Yu., Reznik S.V.[1], Gratsiansky Yu.A.
Federal State Unitary Enterprise "Obninsk Research and Production Enterprise
"TECHNOLOGIYA", Obninsk, Russia
[1]Bauman Moscow State Technical University

The passive methods of the study with workability selected check by destructive methods are used as a basis of the existing system of ground tests of flight vehicle ceramic components. Such approach conformed to the general level of technique development in 70-ties and 80-ties, particularly to the development level of measuring-information and computer technique. Over the past few decades the qualitative leap in these industries took place which made it possible to modify essentially the system of ground tests of missile head components from non-metallic materials.

In the present work the methods for improving the existing system of ground tests of fairing from non-metallic materials on the base of complex approach have been substantiated.

It is known that the every stage of ground tests consists of two parts:
- reproduction of necessary action on the fairing being tested;
- determination of the response of fairing being tested to the appropriate action.

At present time the normative documents, as a rule, determine only the complex of physical factors which is obligatory in the ground tests. The reproduction of this complex is necessary (but not sufficient) condition for guarantee of the workability of the flight vehicle component.

On the basis of generalization of experience gathered it was demonstrated that the transition of ceramic shell ground test system to a qualitatively new level would be possible with harmonious development of the methods and means of action and the methods and means of determining the response of the structure being tested.

The possibility of scanning the power load in the arbitrary direction and the methods for registering the deformation fields by limited number of sensors have been substantiated theoretically and by experiment. The method for forecasting the carrying power of ceramic fairing, the alternative methods for reproducing the mechanical interaction between the frame and the ceramic shell by means of heat action without structure disintegration, the possibility of estimating the dynamics of interaction between ceramic shell and metallic frame by use of displacement sensors have been substantiated.

The peculiarities of the improve system in comparison with the existing one:
- possession of the functions of forecasting the carrying power at low loads (not more than one-half the operating load);
- identify of evaluation of the stressed-strained state of the ceramic articles on all test stage;
- widened temperature range of evaluation of the stressed-strained state.

GRAPHITE AND CARBON-CARBON COMPOSITES AS MATRICES AND CLADDINGS OF STRUCTURES FOR CONFINEMENT AND STORING OF HIGH-LEVEL RADIOACTIVE WASTES

Gurin Vycheslav, Gurin Igor, <u>Zadvorny Arnold</u>, Kantsedal Valery, and Suchareva Tatyana
National Science Center "Kharkov Institute of Physics & Technology", Kharkov, Ukraine

Utilization of radioactive wastes (RAW) and their immobilization for further safe storing and/or disposal are the important stages of the nuclear fuel cycle. The RAW immobilization means RAW transformation into another form using the solidification, incorporating into the matrix or encapsulating into the cladding.

The main role of the matrix or the cladding of RAW consists in confinement and retention of the yield rate of RAW radionuclides at a level determined by the slow cladding destruction.

Requirements for matrix materials are as follows [1]. A matrix must have:
- unchangeable propeties under conditions of disposal
- high mechanical strength, proper elasticity and hardness
- low solubility in cold and hot water
- sufficiently high radiation resistance
- good heat conduction
- acceptable cost
- life time of the matrix or the cladding should be maximally long (hundreds - thousands of years).

Using the INIS Database (since 1972 up to the present day) and the site of papers on this problems [2] we have analyzed the composition of matrices and claddings for RAW (more than 600 papers).

As a RAW matrices one use different materials: glasses, bitumens, cements, concretes, synthetic organics, ceramics of a different compositions, clays, glass-like and mineral-like matrices (phosphate and borosilicate glasses, compositions based on perovskites, borobasalts and garnets). One uses crystalline materials of different types: based on zirconates, titanates, phosphates, silicates, including the analogues of natural materials.

One develops and studies different technological schemes of waste management using the advanced methods of solidification: induction melting in a cold crucible, vitrification by microwave heating, fusion-crystallization, solid-phase reactions, pressing.

A particular attention is given to the problem related with immobilization of excess amounts of weapon plutonium with the aim to prevent its propagation [3].

The study of available papers has convinced us that up to now one did not use a promizing material for matrices and claddings of RAW, namely, graphite and carbon-carbon composites.

Graphite is widely used in high-temperature gas-cooled reactors (HTGCR) with a helium coolant as a structural core mterial and as a neutron moderator as well as a component of a matrix composition for dispersive uranium-graphite fuel elements [4,5]. Spherical fuel particles having several protective covers of pyrocarbon with a different density, and of silicon carbide (micro-fuel elements) are homogeneously distributed in fuel elements of a tubular or spherical shape. A cladding of the tube or the sphere is made of graphite. This construction of the fuel element assures a confinement of solid and gaseous fission products (GFP) in the fuel element volume. The HTGCR fuel is efficient up to 1500°C and above, the radiation resistance is remained up to a fluence of $2.10^{22} n/cm^2$, a burn-up is permitted up to 30% without particle destruction [6]. Spherical fuel elements, according to specifications, possess an impact strength assuring that they be intact when falling multiply (up to 10^3 times) from a height of 4 m onto the spherical filling. They have a high wear resistance because under operating conditions they are moving constantly through the core. Fule elements have a high heat conduction. At a temperature of 1100-1350°C and a burn-up to 32% the fuel element GFP yield was 10^{-6} - 10^{-5}.

Spherical fuel elements were used in the 15 MW reactor AVR(Germany) operating at a coolant (helium) temperature of 950°C. The helium activity was several hundreds of curies that was

conditioned not only by the presence of defective fuel elements but also by the polution with uranium of the fuel element casing in the process of manufacturing.

At NSC KIPT the research works on spherical fuel elements become since 1963. They were conducted for the complete cycle of investigations in conformity with requirements of the technical task. Details are described in [6]. The recent paper on studying the radiation resistance of GSP graphite (NNC KIPT developments) is published (see Ref. [7]).

Furthermore, since 1980 at NSC KIPT developed is a gasostatic method of RAW compacting at pressures up to 6 thousands of atmospheres and temperatures up to 2000°C [8-9].

Proceeding from the foregoing it can be concluded that the matrix and the cladding of graphite and carbon-carbon materials meets all the requirements to materials used for RAW confinement.

REFERENCES

1. Gorsky V.V. Nuclear fuel with an inert matrix. Atomnaya Tekhnika za Rubezhom, 200, No10, p.4 (in Russian).
2. http:/www.iaea.org/programmes.irais.
3. Orlova A.I. , Dzhardin L..J. Immobilization of excess amounts of weapon plutonium in Russia. Radiokhimiya, 2000, v.42, N.3, p.284-286 (in Russian).
4. Beding D. High-temperature gas-cooled reactors Atomizdat, 1975 (in Russian).
5. Lebedev I.G. Radiation resistance of the reactor graphite with a higher performances. Atomnaya Ehnergiya, 2001, vol .91, No.2, p.114 (in Russian).
6. Kostikov L.E., Lozovetsky V.V. State and prospects of using the fuel and fuel elements for HTGCR, Atomnaya Tekhnika za Rubezhom, 1976, No 9, p.17-28 (in Russian).
7. Zelensky V.F., Gurin V.A., Konotop Yu.F. Spherical fuel elements and absorber elements of HTGCR. Voprosy Atomnoj Nauki i Tekhniki (VANT), ser.: Fizika radiatsionnykh povrezhdenij (FRP), 199, No 4(76), p.13-31.
8. Lebedev I.G. Radiation resistance of the reactor graphite with a higher performances. Atomnaya Ehnergiya, 2001, vol.91, No.2, p.114 (in Russian).
9. Neklyudov I.M. Kantsedal V.P., Lavruk A.G. Development of the technology and equipment for RAW and ENF conditioning by the method of gasostatic pressing under ecologically pure conditions. VANT, ser.: FRP, 2000, No4, p.185-187.
10. Kantsedal V.P., Kapustin V.A., Neklyudov I.M. Gas-fluoride reprocessing and mineralization of RAW - new environmentally safe technologies of NSC KIPT. Atomnaya Ehnergetika i promyshlennost' Ukrainy, 1999, No 2, p.20-23 (in Russian).

INDUSTRIAL GRAPHITE IMPROVEMENT BY THE METHOD OF A GASPHASE DENSIFICATION BY A PYROCARBON

Gurin I.V.

National Science Center "Kharkov Institute of Physics & Technology", Kharkov, Ukraine

As it was mentioned earlier [1,2] the volume of graphite usage is commensurable with the volume of all metals usage. Unfortunately Ukraine doesn't have a high quality industrial graphite production. For example there was stopped the production of graphite of MPG-6, MPG-7 marks due to the lack of the petroleum coke of KNPS mark. [3].

The works on improvement of the industrial graphite as well as the works on creation of a new graphite, carbon and carbon/carbon composite materials with a high consumer properties (mechanical strength, density, and etc.) are carried out in NSC KIPT. One of the ways of industrial graphite improvement is its densification by the pyrocarbon using thermal gradient gasphase methods and equipment of the NSC KIPT [5].

We have chosen the most used marks of the industrial graphite that are produced till the present day for the experiments.

Graphite EG-0. It is an electrode graphite with the grains up to several millimeters. EG-0 graphite is a well graphitized material with a low specific electro resistance (8-10 mOhmm). It is produced in Ukraine. Its density is ~1.6 g/ccm, open porosity – 20-25 %. The dimensions of the produced blocks allow producing items just without limitation to a size.

Graphite MG. It is a small grain material. It has a rather high density ~1.65 g/ccm and mechanical strength. Its specific electro resistance is about 15 mOhmm. The open porosity of graphite MG is ~18 %. It is produced in a form of blocks with the diameter 300 mm and height 300 mm. Performs are produced by the method of pressing out through the neck.

So we have chosen the most demonstrative cases: a small grain and small pores material and large grain material with large pores. The samples for densification were produced in a form of the tubes with the diameter 32x52 mm and length ~200 mm. The dimensions and form of the samples were chosen to allow producing the items with the minimum overdimensions.

Graphite densification was carried out using thermal gradient gas phase methods worked out in NSC KIPT [4-6].

Material density, open porosity and mechanical strength of the final products and samples were tested after densification.

The density was tested using the method of a hydrostatic weighting in water. The porosity was tested by boiling in water. Materials properties after densification are given in table 1.

The data on the density and open porosity of the samples from a high quality industrial graphite MPG-7 (MPG-6) are given for comparison.

The mechanical strength (σ_{comp}) definition was carried out on a tearing machine P05. The samples with the diameter 8 mm and height 16 mm were prepared. The samples were cut in two directions – along and perpendicular to the tube axis. Not less than 9 samples were tested. To test the method the strength of the samples from the industrial graphite without densification was determined.

The average data on the mechanical strength of the industrial graphite and graphite after densification by the pyrocarbon is given in table 2.

The results of compression strength for the samples from MPG-7 are given for comparison

As one can see from the offered tables densification by the pyrocarbon allows improving the consumer properties of the industrial graphite.

In addition to the density increasing and open porosity decreasing graphite after densification has the expanded oxidation resistance at high temperatures (1000 -2600 °C).

Unfortunately, we have not yet completed series of experiments on materials resistance to oxidation at high temperatures on an air definition, however, on our preliminary data, the

36

resistance of materials to oxidation after densification by the pyrocarbon is increased in 2-3 times. As one can see from the table 2 the mechanical strength of materials is increased more than in 2 times.

So according to our research densification of the industrial graphite be the pyrocarbon allows using them instead the graphite materials of a higher class. It is especially important for Ukraine taking into account that "Ukrainian Graphite" – the largest manufacturer of the industrial graphite in Ukraine – produces only electrode graphite [7].

Tabl. 1.

Materials properties after densification.

Material	Average density, g/ccm.	Average open porosity, %
MG	1,87	8,2
EG-0	1,78	11,3
MPG-7	1,65-1,8	24-15

Tabl. 2

Compression strength of materials before and after the densification.

Material	Compression strength	
	MPa	Kg/cm^2
Industrial graphite		
EG-0	19,8	201,6
MG	37,9	386,9
MPG-7*	118,6	1209,5
Graphite after densification		
EG-0	45,9	467,7
MG	87,2	889,2

♦ Note: due to a high mechanical strength of MPG-7 the samples dimensions were decreased up to diameter 5 mm, height – 10 mm.

References

1. Гурин В.А., Зеленский В.Ф. Газофазные методы получения углеродных и углерод-углеродных материалов. ВАНТ, 4/76/, 1999, стр. 13-32

2. УНТЦ, проект № 0293, Годовой отчет. 1999 г.

3. Виргильев Ю.С., Костиков В.И. Реакторные графиты на основе альтернативных видов сырья. XIV международная конференция по физике радиационных явлений и радиационному материаловедению.12-17 июня 2000 г., г. Алушта, Крым. Труды конференции. Стр. 105-106.

4. В.А. Гурин, И.В. Гурин, Ю.Е.Мурин, С.Г. Фурсов, В.В. Колосенко, А.А, Корнеев, Н.П. Одейчук, А.Н. Буколов. Некоторые особенности реализации метода движущейся зоны пиролиза при газофазном уплотнении пористых

наполнителей пироуглеродом., Вопросы атомной науки и техники 1/67/, 2/68/, Харьков 1998 г., стр.76-78.

5. В.А. Гурин, И.В. Гурин, В.В. Гуйда, В.В. Колосенко «Термоградиентные газофазные печи ННЦ ХФТИ». Труды научно-практического симпозиума «Оборудование и технологии термической обработки металлов и сплавов в машиностроении». ОТТОМ Харьков, Украина, 28-31 августа 2000 г., стр. 30-35

6. И.В. Гурин, В.А. Гурин, С.Г. Фурсов. Компьютерный расчет параметров уплотнения пористых сред методом движущейся зоны пиролиза /Тезисы/. Вопросы атомной науки и техники 1/67/, 2/68/, Харьков 1998 г., стр.79-82

7. http://www.ukrgrafit.com.ua

THERMAL AND RADIATING STABILITY OF MULTILAYER METAL SYSTEMS ON THE BASIS OF IRON

Kadyrzhanov K.K., Kislitsin S.B., Turkebaev T.E.
Institute of Nuclear Physics of National Nuclear Center, Almaty, Kazakhstan

The progress in present-day techniques demands the construction of novel materials operating under extreme conditions: high temperatures, intensive mechanical loads, aggressive and contacting environments. Development of radiation resistant construction materials, which will be maintained in conditions of high temperatures, aggressive environments and intensive irradiation, becomes urgent in connection with development of the fourth generation nuclear power reactors. Because of various requirement to surface and volume properties the employment of traditional technologies of production of the material with depth-homogeneous composition and structure are not perspective. For instance, a great amount of chromium atoms (5-10 at.%) are to be introduced into the high-temperature $(\gamma-\gamma')$ nickel superalloys to provide heat-resistance, however, their high-temperature strength and durability decreased in this case. The creation of protective coatings on industrial materials was the next stage in technology development. Nowadays the progress in the production of high-qualitative coatings is associated with ion-beam technologies (ion implantation, ion-plasma deposition and others). In the present report the common approach to development of stable multilayers metallic systems are given. The results on development stable at high temperatures of metal systems are illustrated on an example of systems on the basis of iron: iron with coatings from beryllium, from aluminum, from tin and steel with beryllium coatings.

Physical bases of ion-beam technologies of stable multilayer metallic material production

Previously we have proposed a thermodynamical approach to solve a problem of chemical compatibility of heat-resistant coatings with a high-temperature substrate [1]. The main idea of this approach consists in the determination of compositions and phase-structural states for a substrate and a coating that provide zero-gradients of chemical potentials for all components of an alloy at a given temperature. The following illustration will make this clear. A schematic phase diagram of an alloy A-B is represented in Fig. 1a.
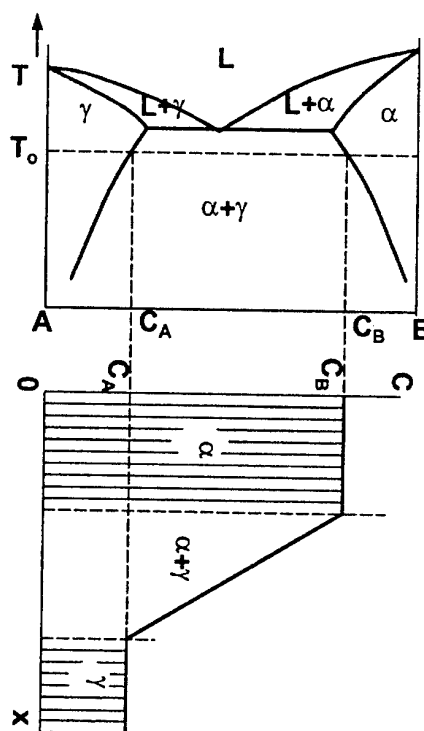
Fig. 1. Schematic phase diagram of alloy A-B (a) and thermodynamically equilibrium depth-distribution of phases and component composition at temperature T_0 (b).

Suppose that this alloy is exploited at temperature T_0, which corresponds to two equilibrium phases with various phase-structural states γ and α and chemical concentrations (C_A and C_B). Then creating the surface with the structure of the α-phase and chemical composition C_B on the matrix with γ-phase structure and chemical composition C_A we will obtain thermodynamically equilibrium two-layer system, where alloy component diffusion is absent (see Fig. 1b). Ion technology, as active method for formation of surface layers with high adhesion and the required chemical composition permit to realize this idea in principle. In contrast to the traditional methods of chemical heat treatment the presence of a two-phase intermediate region $(\alpha+\gamma)$ in ion-implanted layers can provide not only chemical

compatibility between coating and matrix but also physical compatibility. The proposed technology for the production of multilayer many-functional metallic materials consists of the following stages:
- determination of the working temperature T_0 for many-functional multilayer alloy;
- performing self-consistent thermodynamical calculations of a phase diagram for a system, including all chemical components of both the substrate and the coating;
- chemical potential calculation for all the components in various phase diagram regions at temperature T_0;
- selection of chemical compositions and phase-structural states for both the substrate and the coating on the base of calculated and experimentally obtained phase diagrammes;
- melting of alloys for substrate and coating materials and heat-treatment at temperature T_0;
- control of phase states and chemical compositions of heat-treated alloys to provide chemical compatibility of the prepared materials;
- selection of ion-beam (plasma) method for surface layer production with the given chemical composition;
- heat treatment of the produced multilayer material and depth-control of its phase state and chemical composition;
- testing of thermal and chemical stability of surface layers at temperature T_0 followed by the control of their composition.

Production of stable beryllium, aluminum and tin coatings on iron foils by means of magnetron sputtering technique

According to the thermodynamic approach, the stable at high temperatures layer enriched with coating element on iron can be created when volume of the material will represent a saturated solid solution of coating element in alpha iron. In this case diffusion of coating element deposited on the surface into volume of iron is negligible and stable structure with the high contents of coating element in near to surface area is formed. Therefore, if we preliminary create saturated solid solution in the sample of alpha - iron then deposited layer should be stable.

Another way for creation of stable coating is to deposit on thin alpha-iron film of coating element layers with both sides of sample and to heat it. Thickness of deposited element layers and duration of heating period should be such, that uring annealing period in a matrix saturated solid

solution was generated, and on a surface the excess of the deposited element has generated enriched by coating element phase.

We realized the second path on samples of alpha-iron and steel having the shape of thin foil by the thickness from 10 to 30 microns, the thickness for different deposited element layers was various for different elements. After deposition of coating element isothermal annealing in vacuum has been carried out. After annealing the structure of specimen was determined by the technique of Mossbauer spectroscopy and X-ray difractometry. Control of deposited Be layer depth as well as determination of the iron concentration profile over the depth have been implemented by the Rutherford back scattering method (RBS) at the electrostatic accelerator UKP-2-1 of Kazakhstan Institute of Nuclear Physics. In result of described procedure stable phase distribution along the depth of specimen was formed, see for example fig. 2 for beryllium coating.
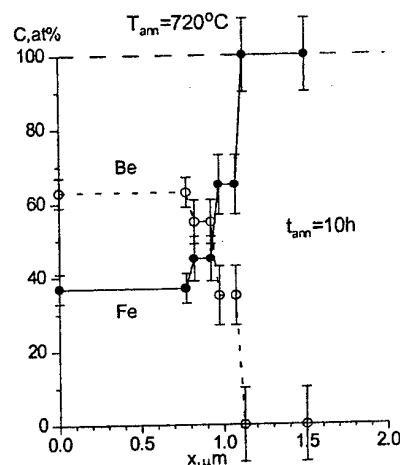
Fig. 2. The depth distribution of Fe and Be concentration along depth of specimen after 10 hours of annealing (RBS method).

Conclusion

1. The technology of many-functional multilayer material production consists of some stages is developed.
2. Stable at high temperature coatings on iron was produced with help of magnetron stuttering method and subsequent annealing.

References

[1] Kadyrzhanov K.K., Turkebaev T.E., Udovsky A.L., NIM **B 103**, 38 (1995).

39

WEAR AND FRICTION-RESISTANT POWDER MATERIALS FOR EXTREME CONDITIONS APPLICATIONS BY FRICTION LOADING

Slys I., Brakhnov N., and Berezanska V.
Frantsevich Institute for Problems of Materials Science,
National Academy of Sciences of Ukraine, Kyiv, Ukraine

The progress of modern technique requires advanced materials, which possess a variety of properties, sometimes contradictory but extremely useful. Friction and wear- resistant materials must have properties to be able to operate at elevated temperatures being in contact with aggressive media. The problem of friction and wear-resistant materials became the major one in machine engineering, space and aircraft construction, as well as in chemical, petrol, gas industries, etc.

Reliable operation of mechanisms and machines, either available or in stage of designing, shall require for the above industries friction and wear-resistant materials able for operation under gas or liquid aggressive media within a wide temperature range between minus 250 and plus 600 °C at high slip velocities (up to 60-80 m/s) and considerable loading values. Stability of physical and mechanical properties within a preset temperature range, resistance to aggressive media, either gas or liquid, at various temperatures and pressures, high wear resistance, good frictional characteristics (good running in, low and stable coefficient of friction, high bearing capacity, etc. of materials used for bearing application shall define a reliable operation of materials for bearing applications under such severe loading conditions.

The first two requirements shall be met due to the use of stainless steel nickel-chromium steels. However, they are prone to seize at friction, thus excluding their use as friction components.

The powder metallurgy being a technology of making materials with desired properties provides a number of routes permitting the tailoring of the required structure of composite materials based on stainless steels. We used the following methods to produce a series of corrosion resistant antifriction materials.

- Addition of chemically active agents to the material, which are able to interact with the metal of conjugated surfaces during the friction process to form protective wear resistant films upon them;
- Formation of a heterogeneous structure using alloying by strengthening elements (carbon or boron, for instance), that are able to resist seizing, chemical or abrasive effects;
- Combination of the alloying by strengthening elements and introducing of chemically active agents.

To achieve this aim, we have developed a method of introducing of sulfur in the stainless steel powder, which combined the sintering and sulfiding in a one step. This resulted not only in activation of the interaction process of the stainless steel components with sulfur, but also in activation of the sintering process, thus reduced the sintering temperature by 250-300 °C [1]. The process yielded a composite material based on stainless steels with uniformly distributed sulfide inclusions, based on iron, chrome and nickel. Such materials retain high corrosive resistance intrinsic for stainless steels and, at the same time, are able to form secondary separation antifrictional layers when friction loaded [2,3].

To prepare the heterogeneous structure, we developed a method of introduction of carbon and boron [4,5], and designed stainless steel-based friction and wear-resistant materials by combining the alloying through strengthening elements and the addition of chemically active agents [6-8].

Using the above materials, the IPMS, NAS of Ukraine, has developed methods of producing a number of corrosion, friction and wear-resistant materials based on powders of stainless steels and chromium [3,5-8] to be used under extreme conditions, and corrosion, friction and wear resistant coatings based on sulfided chromium [9-11].

The materials as designed have been tested by friction loading under extreme conditions, i.e. in contact with aggressive media at elevated temperatures. The friction and wear-resistant material base on X23H12 stainless steel, patented under the No. 449970 [6] has been successfully tested on the corrosion resistance in dissociating heat carrier, N_2O_4 at 500 °C and 5 atm.
References

1. L.Puguina, I.Slys. A method of producing metal ceramic materials. Certificate of Invention USSR No. 1943321, 1969.
2. I.Fedorchenko, L.Puguina, I.Slys, at al. Sulfided metal ceramic materials based on stainless steels for bearing application. In proc. Friction and wear at high temperatures. M. Nauka, 1973, p.115-117 (In Russian).
3. I.Fedorchenko, I.Slys, L.Puguina, at al. Antifrictional pair of friction. Certificate of Invention USSR No. 286413, 1970.
4. I.Fedorchenko, L.Puguina, I.Slys, at al. A method of producing friction and wear-resistant materials. Certificate of Invention USSR No. 224085, 1968.
5. I.Fedorchenko, I.Slys, L.Puguina, at al. Metal ceramic friction and wear- resistant material. Certificate of Invention USSR No. 276425, 1970.
6. L.Puguina, I.Slys, I.Fedorchenko, at al. Metal ceramic friction and wear- resistant material. Certificate of Invention USSR No. 311976, 1971.
7. L.Puguina, I.Slys, I.Fedorchenko, at al. Metal ceramic heat, friction and wear resistant material based on stainless steel for sealing application. Certificate of Invention USSR No. 339196, 1971.
8. L.Puguina, I.Slys, I.Fedorchenko, at al. Metal ceramic corrosion, friction and wear resistant material based on stainless steel for sealing application. Certificate of Invention USSR No. 449970, 1974.
9. I.Slys, V.Zozuya, I.Fedorchenko, at al. Sintered friction and wear-resistant material based on chromium. Certificate of Invention USSR No. 1494543, 1989.
10. I.Slys and V.Berezanska. A method of making sulfide-chromium coatings. Patent of Ukraine No. 10751A, 1996.
11. I.Slys, V.Berezanska, at al. Development of new corrosion-resistant and wear-resistant materials for the use in aggressive hydrogen medium. Inter. Journal of Hydrogen Energy 26 (2001) 531-536.

OPTIMIZATION OF DISING DATA OF BEARING BOXS SEM IN CONDITIONS OF DYNAMIC EFFECTS

Kurilov G.V. c.e.s.

The public corporation Special Design-technology Office of Submerged Electric Equipment "Potential", Kharkov, Ukraine

One of problems, directly bound with reliability and durability of submerged electric motors of a series SEM, is the problem of increase of up state of a bearing assembly. Terms of normal activity of bearing boxs are determined by a kind of a stuff of conjugate friction surfaces, features of cooling, lubrication and heat rejection, and also extreme operation conditions: by a slip velocity, load, temperature, medium (fluid, gas), where the direct and constant maintenance for SEM is impossible.

At designing of bearings of axes and shafts before the designer there is, first of all, problem that in the given concrete case the rolling-contact bearing or sliding bearing is more preferential. The essential role thus is played by economical reasons, condition of mounting and exploitation, and also requirement of trade off.

Conservatism concerning bearings of slip is conditioned by that popular belief, that the friction losses of slip at the identical operation conditions, always are higher than friction losses of rolling [1]. This error opinion cannot be diffused to sliding bearings working in a mode of fluid friction, when the layer of lubrication separating working surfaces of the bearing box and bush from each other, that eliminates a capability of their direct contact; the friction losses are in this case rather small and do not surpass friction losses in rolling-contact bearings.

However qualitative activity of sliding bearings is not provided of itself, and is possible only in that case, when a design of the bearing box, its sizes, stuffs rubbing of parts, kind of lubrication and other parameters are selected with allowance for of its operational conditions. Such selection is made with the help of the conforming calculations of bearing boxs and on the basis of usage of a stored case record in engineering. Only at exact, scientific and practically reasonable designing and calculation of bearings of slip, the success can be ensured at their technical application.

At the present stage of development of the introduced theory of friction and wearing it is possible to some extent to forecast the up state of a unit of friction and durability of the machine as a whole, outgoing from physico-chemical properties and mechanical characteristics rubbing of stuffs. The thermal processes developing at friction as a result of effect of load and a slip velocity, result in change of physical-mechanical properties rubbing of stuffs, and at simultaneous effect of fissile environment (fluid or gas) - to physico-chemical changes of surface layers, that, thus, results in change of the characteristics of friction [2], and, thereby, to decrease of up state of a unit of friction.

The uniqueness of a design SEM superimposes definite limitations on improvement of reliability of the bearing box.

Small external diameter SEM (103-123 mms at length of 6-8 meters) put in rigid frameworks critical dimensions of the bearing box.

The bearing case SEM works in a magnetic field of the electric motor, therefore, with the purpose of exception cranks and strong heating, the bearing box is necessary for producing from a non-magnetic material, which one is steady to induce of eddy currents. The stuff of the bearing box should be strong enough, not change geometry of the bearing box during activity and strong heating, have damping properties.

The replacement of oil on one more tenacious is not obviously possible, as the oil circulates and executes a heat rejection and other parts SEM, and also is the basic electric insulating material.

Therefore, the perfecting of the bearing box is possible only as at the expense of optimization of its design [3], and selection of a stuff he is made of which one.

The set forth above requirements to a stuff of a bearing case respond: a powder titanium ПТХ-4-2 and non-magnetic cast iron [4].

One of the main problems at mining a bearing assembly is the selection of a stuff of conjugate friction surfaces. Conducted before research The public corporation Special Design-technology Office of SE "Potential" on application metal-fluoraplastic of bushes in sliding bearings have shown their high enough maintainability [5].

In connection with the high requirements shown to characteristics SEM, actual there are problems, bound with definition of strength and compliance of sliding bearings used as bearings. The compliance of a bearing determines a series of the relevant dynamic properties of the machine, including resonant sites of a spectrum of vibration and dynamic forces which are operational on the part of a rotary table on a bearing assembly.

The reliability augmentation of activity of a bearing assembly is possible by maintenance of damping properties and exception crank of a bearing case. It is reached by that [3], that in a body of a bearing assembly, which one is set in a stator bore, three axial channels on external and internal cylindrical surfaces for transit of a cutting compound are made. The axial channels are arranged in such a manner that give to a bearing assembly damping properties.

As the monitoring mechanical characteristics of the bearing box two characteristics of its body are determined: hardness and destructive force.

The large concern by optimization of a design of the bearing box is introduced by researches of influencing of design data on value of internal stresses arising in a bearing case, for different stuffs and to a compliance of a design at different width of a groove and external loadings.

As a result of made activity the following problems were resolved:

- influencing design data, in particular width of a technological groove on an exterior of a bearing case, on value of internal stresses arising in a design under operating of external loadings of prescribed value for different stuffs (of a dust of a titanium and non-magnetic cast iron) is investigated;
- the compliance is investigated at miscellaneous external loadings of a design of the bearing box from different stuffs with varied width of a groove;

- the arc of a contact of the arbor and bush of the bearing box is determined, which one is characterized by angular coverage 2 φ_0;
- the distribution of contact pressures $p(\varphi)$ is determined;
- are determined maximum rating of contact pressure p_m and value of middle pressure at a contact;
- the experimental researches are conducted and the practical values of destructive force and compliance of bodies of bearing boxs with metalfluoroplastic by the bush and without it for different stuffs (dust of a titanium ПТХ-4-2 and non-magnetic cast iron) are obtained;
- the design of the bearing box with optimum design data which are conforming the requirements is determined which one are presented to bearings of slip used in SEM, the activity which one descends in rather the composite extreme operation conditions on conditions on fields at oil extracting.

1. Чернавский С.А. Подшипники скольжения. М: - Машгиз, 1963, 144 с.
2. Курилов Г.В. Некоторые аспекты сложной зависимости работоспособности твердых смазочных покрытий от глубины вакуума. ФХММ, 1979, №4, с. 80-86.
3. Курилов Г.В. и др. Патент РФ №1751489 от 25.03.93г. Подшипник скольжения для погружного электродвигателя.
4. Буланов В.В., Курилов Г.В., Суходольская Е.А. и др. Авторское свидетельство 1983г. №3659937/02. Чугун.
5. Курилов Г.В., Резников В.Д., Дроздов Ю.Н. Теоретические и экспериментальные исследования динамических нагрузок на подшипниковые узлы ПЭД. Трение и износ, 1981, т.2, №4, с. 678-686.

INSTALLATIONS AND BURNERS (GUNS) FOR HVOF AND HVAF SPRAYING

Kysil V., Kadyrov V., Yevdokimenko Y.
Institute for Problems of Materials Science of NAS of Ukraine, Kyiv, Ukraine

At present, high velocity gas flame spraying (**HVGFS – HVOF and HVAF systems**) is one of the most intensively developing directions of the thermal gas spraying. HVGFS technology allows to spray an functional coatings (wear and corrosion resistant, erosion resistant, heat protective and others) of practically any metal and many metal ceramic powder materials of high quality - low porosity (less than 1%) and high adhesion (up to 100MPa.). Technology of the HVGFS is based on spraying of the particles of applied material by high-temperature stream of the combustion products of hydrocarbon fuel in oxygen (HVOF process) or in air (HVAF process) having sub- or supersonic velocity.

The High Velocity Oxy-Fuel (HVOF) and Air-Fuel (HVAF) processes, an recent development in the field of thermal spray coatings, has attracted a lot of interest. Its high coating quality results from the use of a hot, combustion driven high velocity gas jet for thermal spraying. HVOF coatings cannot be considered generic because each is highly dependent on gun design, fuel type, operating pressure and energy input level. Particle velocity (i.e., the speed at which particles of coating material travel during their flight from the spray gun to he part being coated) is a critical factor in all thermal spray processes. Significantly, HVOF guns can produce particle velocities that are considerably higher than the other currently available commercial thermal spray processes. HVOF process can increase chamber pressure over Detonation Gun system and therefore can theoretically achieve higher particle velocity and coating quality. The particle velocities obtained are a function of chamber pressure. The only limits to a higher particle velocity in the HVOF process are the requirements to use higher oxidant and fuel pressure. Specific particle conditions that contribute to the HVOF advantages compared with other types of thermal spray processes in open air include:

- Favorable environment
- Much shorter exposure time in flight
- Reduced mixing with ambient air once the jet and particles leave the gun
- Lower ultimate particle temperatures compared to plasma or arc guns
- Higher particle kinetic energy upon impact against the substrate

The basic requirement of a HVOF system is to burn fuel and oxidant in an enclosed volume or chamber and build up pressure so that gases expand through an orifice as they exhaust and accelerate to the atmosphere. A number of burner designs can be used to accomplish this, each having advantages and disadvantages.

One of the main disadvantage of HVGFS technology is the difficulty and in most cases impossibility to apply refractory coatings. At the same time, the energy potency of the method allows to achieve for the particles of most materials the parameters (temperature and velocity), sufficient to produce high quality wear-corrosion resistant coatings of new composite materials based on refractory components and ceramic. However, the gas dynamic layouts of the burners in contemporary equipment for HVGFS don't able to realize energy potency of the method fully. At the best contemporary systems the processes of heating and acceleration of sprayed materials powder particles are taking place simultaneously at their move in high-temperature stream of burned products in sufficiently extended (up to 300mm) accelerating channel. The velocity of gas stream in such channel can be subsonic or supersonic, dependently on its configuration.

The possibility to increase particle energy, determined by their velocity and temperature, in burners of such design seems to be brought to the end. That is follow from the fact, that the conditions of further particles velocity and temperature increase are to be incompatible: to increase the temperature, it is necessary to increase the time of particles being in the stream, and at particle velocity growing the time of its presence in the channel decreases and, besides, the intensity of particle heat exchange with high-

temperature environments goes down as a result of their relative velocity decrease.

Further improvement of gas dynamic path of high-temperature two-phase stream generators and, in particular, HVGFS burners can be made by means of functional subdivision of the sections of particles heating and acceleration.

In present report is described new concept of gas dynamic burner channel with functional separation of dispersed powder heating and accelerating zones, which is aimed for:
• Disperse phase heating in transporting gas flow with high temperature and low velocity;
• Following accelerating of disperse phase in around sonic and supersonic flow;
• Accelerating of gas flow up to sonic velocity by means of consumption influence, which is reached by injection of certain portion of gas between heating and accelerating zones;
• Absence of convergent zones along the channel length.

Experimental air-fuel (HVAF) and oxy-fuel (HVOF) burners with the optimal gas flow channel are developed and described. Such materials as aluminum, nickel, nichrome, copper, tungsten carbide with cobalt matrix, alumina and composites were sprayed and investigated.

For experimental test spraying the experimental test stand was manufactured which is enable to perform the HVGFS.

For such purpose:
• The layout of the experimental installation for HVGFS was developed, which one ensures independent feeding of fuel components into consumption chambers of experimental burner. The modernization of the fuel and oxygen feeding system of the HVGFS installation "Struja" was done. Developed and manufactured the compressed air system of the experimental HVAF burner. Compressed air feeding system with extended maximum working pressure of 3.5 MPa, and air consumption of 5 m3/min. was modernized.
• Powder hopper was improved and modernizes. Remote control panel was developed to regulate and control feed rate with indications of the orifice size

• Developed and manufactured ignition system to ignite air-fuel burner, which was tested on the burners of the traditional layouts.
• Measuring method of working gases consumption determination, based on gas pressure in the combustion chamber and connection collectors was developed. PC software to calibrate the consumption of working gases by the results of cold blowing was developed.

As a result of experimental research of created burner installations were optimized their working parameters and determined main technological parameters (spray distance, working spray velocity pass, powder consumption and so on).

Technical parameters and coating properties obtained by traditional HVOF systems and new concept burners were compared.

Conclusions:

New gas dynamic concept and HVOF &HVAF burners (guns) based on consumptional regulation of gas flow parameters were developed which provides the following advantages:
• **Increase of coatings quality in terms of adhesion, cohesion, residiual porosity and hardness**
• **Increase of process thermal efficiency coefficient**

References:

1. M.L.Thorpe and H.J. Richter, A Pragmatic Analysis and Comparison of HVOF processes, J. Therm. Spray Technol., Vol. 1 (No. 2), 1992, p.161-170
2. V. Kadyrov, V. Kisel, Y. Evdokimenko, Interaction of Particles with Carrier Gas in HVOF Spraying Systems, J. Therm. Spray Technol., Vol. 3 (4), 1995, p.389-397
3.В.И.Тимошенко, И.С.Белоцерковец, В.П. Галинский., В.Х.Кадыров, В.М.Кисель , Ю.И. Евдокименко. Исследование процессов в горелочных устройствах для высокоскоростного газопламенного напыления порошковых материалов с использованием расходного способа воздействия на поток. Инженерно-физический журнал.-2001.-V.74, №6, с.156-161

DIAGNOSTICS OF THE PHYSICAL AND MECHANICAL CHARACTERISTICS OF MATERIALS OF MULTILAYER COATING DESIGNS

Nemirovsky Ju.V., Bogomolova O.A.
Institute of the theoretical and applied mechanics Russian Academy (Siberian Branch),
Novosibirsk, Russia

One of promising directions in designing of products to be used under extreme conditions is application of protective and strengthening coatings. Because there is an objective difference in operation conditions for bulk material and superficial layer this requires to provide different chemical, physical, mechanical and strength properties for the mentioned part areas. The experience of numerous research works shows, that in system «design - aggressive working environment» design surface is the weakest element that determines the allowable operational conditions and the resource of a system as a whole.

The design of products with applied coatings is based on optimization and strength analysis. Rather full information on physical and mechanical properties of both base material and coatings. While there is a comprehensive information on physical and mechanical properties of a base material, as a rule, but there is not enough information on the properties of coating materials, as the latter ones represent often new materials with unexplored properties. In the most cases it is impossible to study these properties using conventional equipment, as the material exists only as a thin layer on a certain base. Separation of sample from base material and then study of its properties represent a difficult engineering task and require development of a new equipment. Moreover, it shall be noted that a sample separated from the base has other properties, than the coating on the base, as in case of coating separation from the base a residual stress field inevitably arising in a coating material because of special technological features (different coefficients of linear expansion of base and coating materials, different shrinking properties etc.) disappears. At present the coating material properties are of particular interest. Only a few works on physical-mechanical properties of applied multi-layer coatings can be found. There are very few works, in which non-destructive tests of physical and mechanical characteristics of multi-layer coating materials are described.

The offered procedure generalizes the well-known methods of static and dynamic tests of isotropic samples taking into consideration the layered samples of different form. The procedure makes it possible to study mechanical properties of coating materials taking into account a field of residual stress with the aim to determine characteristics of macro-samples.

The essence of the technique is, that the required number of tests and minimum number of multi-layered samples which shall be analyzed as composite multi-layer designs and are described by the equations of the theory of elasticity are determined. The unknown values that shall be determined are physical and mechanical properties of multi-layer materials and their strength properties: modulus of elongation (Young's modulus), rigidity modulus (shear modulus), Poisson's ratio, specific weight densities, coefficient of linear thermal expansion, limit of elasticity and field of residual stress in these materials. Such samples as rods and bars are mostly used for mechanical tests therefore the offered technique is developed for multi-layer rod-type elements.

The tests shall enable to determine all physical and mechanical characteristics of materials and shall provide the information on a field of residual technological stress. Different stress diagrams can be used during the tests. However, because it is necessary to determine a wide range of characteristics, it is advisable to divide the tests into classes, this makes it possible to exclude some characteristics. For example, in static tests the influence of material density is excluded, in tests without heating or cooling of samples the influence of coefficients of linear thermal expansion is excluded.

46

Let's consider the most general class of tests: a dynamic bend with stretching or compression taking into account influence of temperature. In case of dynamic bend in plane with simultaneous stretching (compression) the stressed and strained state of a multi-layered rod, for which the Kirchhoff-Love hypothesis is assumed, is described by the following equations of plane motion:

$$\frac{\partial N}{\partial s} - \frac{Q}{R} + q_\tau = \rho_i F_i \frac{\partial^2 u_0}{\partial t^2} - \rho_i S_i \frac{\partial^2 \theta}{\partial t^2};$$

$$\frac{\partial Q}{\partial s} + \frac{N}{R} + q_n = \rho_i F_i \frac{\partial^2 w}{\partial t^2};$$

$$\frac{\partial M}{\partial s} - Q + m = \rho_i S_i \frac{\partial^2 u_0}{\partial t^2} - \rho_i J_i \frac{\partial^2 \theta}{\partial t^2};$$

$$N = \sum_i \int_{F_i} \sigma_i dF_i, \quad M = \sum_i \int_{F_i} \sigma_i z dF_i;$$

$$\sigma_i = E_i\left(\varepsilon_0 + z\ae - \alpha_i T\right) + \sigma_i''(s,z);$$

$$\varepsilon_0 = \frac{\partial u_0}{\partial s}; \quad \theta = \frac{\partial w}{\partial s}; \quad \ae = -\frac{\partial^2 w}{\partial s^2}. \quad (1)$$

Where N, Q, M - axial and shear forces and bending moment of section, respectively; u_0, w - axial movement and deflection of reference line of a layered rod; $q_\tau(s,t), q_n(s,t)$ - tangent and normal of distributed load; m (s,t) - distributed bending moment; $\rho_i(s), E_i(s), \alpha_i(s)$ - density, modulus of elasticity and coefficient of linear thermal expansion of "i" - layer material; $F_i(s), S_i(s), J_i(s)$ - known functions of distribution along the rod of area, static moment and moment of inertia of "i" –layer section; T (s, z) – rod temperature distribution; s, z, R (s) - coordinates longitudinally and perpendicularly to rod axes, radius of curvature of rod axis; $\sigma_i''(s,z)$ - distribution of initial stress in "i" layer (field of residual technological stress). For layers of small thickness the function of initial stress distribution can be approximated by the linear z-axis functions $\sigma_i''(s,z) = \sigma_{0i}''(s) + z\sigma_{1i}''(s)$. The field of initial stress is self-balanced: the functions $\sigma_i''(s,z)$ satisfy the equations (1), when external loadings and any movements are absent. In other words, the initial geometry of design is assumed

to be as the one after completion of technological process. Density, modulus of elasticity and coefficient of linear thermal expansion of materials are considered to be constant on Z-coordinate. If non-uniform properties of coating are observed on Z-coordinate, the mentioned layer can be considered as multi-layer design with piece-wise continuous distribution of material characteristics.

To obtain the set of equations that make it possible to determine the characteristics of materials, it is necessary to perform a series of tests. For each test a sample stress diagram, the forces and deformation parameters to be measured during tests are specified. After derivation of set of equations of motion, as a result of its numerical integration with use of additional experimental information stress, displacement and all necessary characteristics of materials are determined.

The procedure allows to specify for the given design with a multi-layer coating series of tests and sets of samples, which shall be cut out from the given design with the aim to determine all physical and mechanical characteristics of materials to be of interest for us.

The procedure has an advantage that makes it possible to determine coating characteristics not only of artificial samples but also of samples having properties very similar to the ones of a real design.

The next advantage of described procedure is possibility, using one sample, to determine a wide range of characteristics by means of different types of tests. For example, after determination of mechanical material characteristics with the help of static tests it is possible to determine material density by means of dynamic tests using the same sample. Then by sample exposure to the temperature field it is possible to determine coefficients of temperature expansion and thermal conductivity.

STRUCTURE AND PROPERTIES OF Al_2O_3 AND Al_2O_3+Cr_2O_3 COATINGS DEPOSITED TO USING PULSED DETONATION TECHNOLOGY

Pogrebnjak A.D.[(1)], **Tyurin Y.N., Kshnjakin V.S.**[(1)], **Kolisnichenko O.V.**

E.O.Paton Electric Welding Institute, NASU, Kyiv, Ukraine

[(1)]Sumy Institute for Surface Modification, Sumy, Ukraine

Coatings of aluminum oxide, which are produced by gas-thermal, plasma detonation deposition find their wide application due to their high wear resistant, corrosion resistant, heat protecting, electro-isolating, etc. properties [1-3]. When the powder Al_2O_3 is deposited by the plasma-detonation way, it undergoes phase transformations, which ratio depends both on the characteristics of initial material, and on the way and conditions of deposition, substrate temperature, the thickness of the deposited layer, the velocity of the incident plasma jet, its temperature, and, probably, other factors. In this connection, the servicing characteristics of the aluminum oxide coating seem to be determined by a quantitative content of various modifications of Al_2O_3 in it. As is known, in the process of exploitation under high temperatures, the phase composition may change. Therefore, one may assume that this change of phase ratio may influence the protecting properties of aluminum oxide and, naturally, affect the life of these coatings.

Modern techniques of deposition of high quality coatings have been developing now in such a way that to provide high rate deposition of materials. For these purposes, different devices for detonation deposition [2-4] as well as rocket nozzles or super-sonic deposition (of HVOF type), in which oxygen serves like a fuel are applied [6]. In spite of evident advantages of gas-detonation way of coating deposition, application of these coatings in industry is limited because the devices for proportioning and feeding of powders are complicated and there exist power limitations of a pulsed jet.

This paper proposes to apply non-stationary detonation burning processes of combustible gas mixtures in the device for deposition to increase the pulse power [5]. Realization of detonation of the combustible gas mixture in an electromagnetic field, which is formed between two coaxial electrodes in the reaction chamber seems to be an efficient way.

Therefore, the purpose of the presented paper was to investigate physical and chemical properties and phase composition of coatings of aluminum oxide and Al_2O_3 + Cr_2O_3 mixture, which were deposited using the plasma detonation technique (under high temperatures and high rates of the plasma jet) to the substrate of steel 3 (0.3wt.%C).

A plasmotron "Impulse-3" [5] purposed to deposit coatings has been applied. This plasmotron has a gas-dynamic combustion chamber, where the components of combustible gas mixture are mixed and their detonation with to 20 Hz frequency is initiated. Initiation of detonation is realized using a sparking plug. Total expenditures of the combustion mixture components are 2 m^2 per hour, the initiation frequency being 4 Hz. The energy of charging unit is 400 mF under 3.5 kV voltage. The length of the gas-powder jet limited by the cylindrical pipe was 350 nm, and a distance of deposition was 40mm. The velocity of plasma jet may be given in advance, it can reach 600 m/s to 8 km/s, plasma temperature in the jet being 2 x 10^3 to 3 x 10^4 K, and the power density of pulsed plasma can reach 5 x 10^7 W/cm^2. To investigate the element composition, we applied a beam of protons (1.744 MeV), using Elastic resonance on protons and Rutherford back scattering of He$^-$ ions of 2 MeV energy. To investigate the phase composition and structure, we applied X-ray phase analysis (XRD) with diffraction (the apparatus DRON-3, USSR) and transmission electron microscopy with diffraction (TEM) using the Electron microscope EM-125 (Electron, Selmi, Sumy, Ukraine) under accelerating voltage of about 125 kV. The surface morphology was studied using the raster electron microscope (REM 102 EM, Selmi, Sumy, Ukraine) and Atomic Force Microscope (AFM). Hardness was measured using PMT-3 apparatus with a pyramid KNUPA, adhesion was determined using sclerometry with indention of the diamond pyramid into a coating and its motion over it.

RBS analysis have been performed at three different points of the coating: near the surface, in the coating depth, and near the phase boundary of the film and the substrate. The energy RBS spectra and elastic resonance on protons show an evident surface peak of C (as a result of

resonance) in the vicinity of 1.755 MeV. Stoichiometry of the ceramic layer near the surface, which was averaged over the thickness of 1.6 mm, was as $Al_{35}O_{53}Fe_{0.5}$; carbon concentration was about 11at.%. Near the phase boundary, the stoichiometry of ceramic composition significantly changed and was $Al_{38}O_{58}Fe_3$. Iron concentration increased almost by a factor of 6, and the ratio of oxygen to aluminum was close to a classic one – $Al_{40}O_{60}$. Fe was present all over the whole thickness of coating, which evidenced some erosion (evaporation) of the electrode into the plasma jet. The coating, which was composed only by aluminum oxide, had an average density of $\rho = 3.9$ g/cm$_3$ (this was close to the value for α-Al_2O_3, i.e. $\rho = 3.98$ g/cm^3). Micro-hardness of some regions reached 1.95 x 10^4 H/mm^2, its minimum value being about 1.4 x 10^4 K. Measurements of heat conductivity of Al_2O_3 coating demonstrated a value of 38 W/m x K, which was close to that for the pure Al_2O_3 (40 W/m x K). One should note that the coating, which was produced from the mixture of Al_2O_3 + Cr_2O_3 powders, had higher value of hardness $\geq$ (2.1 to 2.2) x 10^{4}N/mm^2. However, the preliminary tests for adhesion demonstrated that under the same thickness of coating (about 0.8 mm), Al_2O_3 had better adhesion than that of the mixed one (composed of aluminum oxide and chromium oxide).

A phase composition of Al_2O_3 coating, which was determined by TEM with diffraction, demonstrated the presence of such phases as: α-Al_2O_3; β-Al_2O_3; γ-Al_2O_3; η-Al_2O_3; AlFe. α-Al_2O_3 was a poly-crystal with average crystal dimensions of about 250 nm. Crystallites were without defects, had a regular cut. β-Al_2O_3, α-Al_2O_3, and; η-Al_2O_3 were poly-crystals, dimensions of their crystals were from 100 to 300 nm. A defect structure was observed inside the crystallites. The region of a transition layer, which was contiguous with the substrate, consisted of FeAl poly-crystals, their average dimensions being about 20 nm. This transition layer consisting of FeAl had high dislocation density. One also should know that because of high deposition rate and high temperature of the plasma jet being incident on the substrate, some discrepancy of parameters of crystal lattices of the coating and table values was noticed (which was revealed in studies of electron diffraction). XRD analysis of the same coating demonstrated good correlation of these results with TEM analysis. In spite of the fact that XRD information was

obtained from a thicker layer, it was revealed that α-phase constituted about 60% of coating, γ-phase constituted about 30%, meta-stable phases as β- and η-, which could hardly be revealed in the XRD spectrum without special thermal annealing were the rest.

Phase analysis, which was performed using TEM with diffraction, demonstrated the following phases: α-Al_2O_3; β-Al_2O_3; γ-Al_2O_3; Cr_2O_3, and Cr_3O. α-Al_2O_3, and β-Al_2O_3 crystallites are of average dimensions (about 150 nm) and have no defects. γ-phase was the region of coating with crystallites, which dimensions were scores of nano-meters (20 $\pm$ 30 nm). Micro-electron patterns showed a ring-like structure. The regions of the coating containing Cr_2O_3 had crystallites of average dimensions of about 150 nm, dislocations-like defects were absent. Cr_2O_3 regions of coatings contained very large crystals of 0.5 mm dimensions. Dislocation-like defects were absent.

In such a way, the presented work has shown that the plasma-detonation way of deposition from Al_2O_3 and Al_2O_3 + Cr_2O_3 allows one to produce coatings of good quality, in which crystal dimensions are from 20 to 250 nm. They consist of α-, β-, γ-, η- phases and the transition layer of 15 µm thickness, which contains FeAl and has high dislocation density. Coatings of aluminum oxide are of high hardness to 1.95 x 10^4 N/mm^2, those of Al_2O_3 + Cr_2O_3 are of (2.1 to 2.2) x 10^4 N/mm^2. Heat conductivity of Al_2O_3 coatings was 38 W/m x K, which was close to that of α-Al_2O_3 (40 W/m x K). One should note that adhesion of the Steel 3 substrate with Al_2O_3 coating was higher than that of the coating deposited from the mixture of Al_2O_3 + Cr_2O_3 powders.

REFERENCES
1. A.L.Borisova, L.I.Adeeva. Automatic Welding (Ukraine, Kiev), 9 (1997) p.36
2. M.I.Thorpe and H.J.Richter. Symp.Thermal Spray: Inter. Advances in Coating Technology, Orlando, FL, USA (1992)
3. M.I.Thorpe. Adv. Material Processing 134 (1999) 69
4. P.Keng and E.Pfeinder. In: Combustion and Plasma Synthesis of High Temperature Materials. Ed.: Z.A.Munir and J.B.Hely. VCH Publishers Inc., New-York (1990) p.420
5. Yu.N.Tyurin and A.D.Pogrebnjak. Surf. and Coat. Tech. 111 (1999) p.269
6. S.Kuroda. Proc. 15th Inter.Thermal Spray Conference. 1998, Nice, France, p.539

49

ENGINEERING STRENGTH OF COATINGS: APPLICATION FOR DESIGN PURPOSES

Byakova A.V., Vlasov A.A.

National Technical University of Ukraine "Kiev Polytechnic Institute", Kiev, Ukraine

The study of the correlations of engineering strength of hard and brittle coatings with their composition, structural parameters, and stressed state has become of increasing interest to researches employed in both scientific and industrial applications. To evaluate engineering strength of coatings made of hard and brittle ceramic materials, the most effective criteria including the fracture toughness (K_{Ic}) combined with microhardness (HV) shared on the plasticity characteristic (δ_H), and the parameter of elastic deformation (ε_e) have been grounded in line with contemporary concept. Certain test methods procedures capable of determination the reproducible results for these criteria by the indentation technique were carried out and reported previously [1-5]. Effective application of the concept above for coating development and design purposes is considered in the present work.

Coatings in the TiN_{1-x}-Ti system of the specific composition, which was named by the 'window' structure, were developed to be alternative to those made of the TiN single layer or TiN-Ti multilayer composition of a gradient structure. The category of 'window' structure revealed in the TiN_{1-x} –Ti coatings was given on association with that of 'arched windows located in the wall' since numbers of discrete areas, which are made of ductile metallic material and put in order inside the parent TiN_{1-x} layer, were formed. Figure 1 demonstrates schematically the 'window' structure of the TiN_{1-x}-Ti coating.
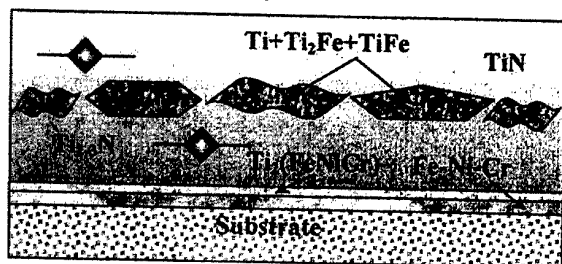
Fig.1. Schematic presentation of the TiN_{1-x}-Ti coating with 'window' structure (coating cross-section with indentations).

The particular method of several stages was employed for performance of the TiN_{1-x}-Ti coating. Deposition of the Ti- layer on thin metallic layer, which was made of Fe-Ni-Cr alloy and formed initially on the substrate surface, together with following ion-nitriding were used like the basic processes of this particular method.

It was found experimentally that ductile metallic areas consist of Ti-matrix with finely dispersed precipitates of intermetallic compounds (FeTi, Fe_2Ti), as shown in Figure 1. The structure observed for the metallic areas in the TiN_{1-x} –Ti coatings was found to be similar for nitriding zone of the □-Fe matrix with finely dispersed particles of the Fe_4N nitrides.

The metallic areas were very small (for each area ~$10^{-2} ... 10^3$ μm^3) in size and they were located in the central section of coating. It was shown also that additional thin layer made of the Ti_2Fe intermetallic compound alloyed by Ni and Cr is formed between initial layer made of Fe-Ni-Cr alloy and the parent body of the TiN_{1-x}-Ti coating.

The data for mechanical properties of coatings with 'window' structure of the TiN_{1-x}-Ti composition are shown in Figure 2. It could be seen that the fracture toughness criterion $K_{Ic}(0)$ of the $Ti_{2-3}N$ zone increases sharply as far as the specific volume (ψ) of the ductile metallic areas increases in the range of 15 to 25%, where the criterion $K_{Ic}(0)$ indicates the result determined in coating cross-section from the cracks occurred in the direction parallel to coating flat surface (Fig.1). Then, the $K_{Ic}(0)$ value of $Ti_{2-3}N$ zone increases slightly with increasing of the specific volume of the ductile metallic areas in the range $\psi > 25\%$. Under these conditions, the fracture toughness of the $Ti_{2-3}N$ zone was found to be comparable with that of the TiN zone placed above the metallic areas: $K_{Ic}(0) = 2.4$ MPa·m$^{1/2}$.

It is notable that the $K_{Ic}(0)$ value of the $Ti_{2-3}N$ zone indicated at $\psi > 25\%$ become almost doubled compared to that of continuous TiN_{1-x} layer.
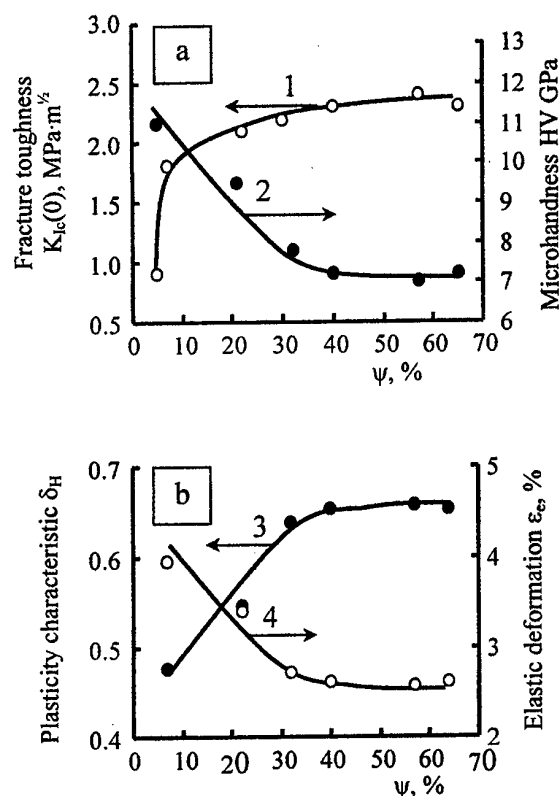
Fig.2. A summary of the data for (1) fracture toughness of the Ti_{2-3} N zone, together with the data, obtained in the ductile metallic areas for (2) microhardness HV, (3) plasticity characteristic δ_H, and (4) elastic deformation $\square_e$ (ψ is the structural parameter defined the specific volume of the ductile metallic areas).

In contrast with nitride zones the values of HV, δ_H, ε_e determined in ductile metallic areas were found to be dependent of structural parameter ψ. Figure2 illustrates that as structural parameter ψ decreases in the range of 35 to 5% the HV value increases in the range of 7 to 11 GPa. Because of this, the δ_H characteristic decreases in the range of 0.65 to 0.48 while the parameter ε_e increases in the range of 2.6 to 3.9%.

It was concluded that the increase of the K_{Ic} (0) value of the $Ti_{2-3}N$ zone with increasing parameter ψ could probably be · explained by the superimposition of local micro-scale field of structural stresses, which are formed in the vicinity of the metallic areas, on the macro-scale field of residual stresses.

Attention is drawn to the fact that engineering strength of the TiN_{1-x}-Ti coatings with optimised 'window' structure is great since their mechanical properties are found to be comparable with that for the best of conventional TiN coatings: HV=18...22 GPa, $K_{Ic}(0)$=1.8...2.2 MPa·m$^{1/2}$.

However, compared to conventional types of TiN and TiN-Ti coatings, the additional advantages in engineering strength of the TiN_{1-x}-Ti coatings are revealed due to the 'window' structure.

These advantages above fall in three categories, which are such as follow:
(i) First of all, the rigidity of the coating system is ensured by 'window' structure compared with the TiN-Ti multiplayer coating of a gradient structure;
(ii) The enlargement of coating fracture resistance due to crack braking by the ductile metallic areas;
(iii) Under conditions of mechanical loading the ductile metallic areas result in partial dissipation of energy by means of plastic deformation.

These advantages above allowed us to recommend the TiN_{1-x}-Ti coatings with optimised 'window' structure for high-performances in pneumatic and hydraulic systems used under extreme service conditions in aircraft industry.

References
1. Byakova A.V., Gorbach V.G., Fracture toughness and evaluation of coating strength with an initial residual stress field// Strength of materials. – 1994.-**26**, No1, pp. 40 -47.
2. Byakova A.V., Characteristic features of microhardness determination in assessing the structural strength of coatings// Strength of Materials. –1995. –**27**, No 9. - pp. 531 – 538.
3. Milman Yu. V., Galanov B. A., and Chugunova S.I. Plasticity characteristic obtained through hardness measurement// Acta Metall. Mater. – 1993.- **41**, No 9. - pp. 2523-2532.
4. Milman Yu. V., Galanov B. A., Chugunova S.I., Goncharova I.V. Investigation of mechanical properties of high-hardness materials by indentation method// Sverkhtverdye Materialy. – 1999. - No 3. – pp.25-38.
5. Byakova A.V. Structural aspects of strength and methods to increase the serviceability of carbide coating// Powder Metallurgy and Metal Ceramics.- 2000. - **39**, No 1. - pp. 85-90.

51

DESINING OF HETEROGENEUS COVERING WHICH HAVE DISPERSE FILLER FOR THE PROTECTION FROM IONIZING RADIATION

Ostrik A.V.
Institute of Problems of Chemical Physics RAS, Chernogolovka, Russia

Ionizing radiation (IR) cause in the irradiated structures a wide range of physical processes (thermal, ionizing, mechanical, chemical and so forth) [1]. The role of each of the phenomena varies depending on the IR quanta energies and properties of a material being irradiated.

To protect from IR one can use sets of screening covering external layers, having specific purposes (antistatic, dumping, radio absorbing and so on). Recently, however, universal heterogeneous materials (HM), which have integration the functions of several coverings are created. Particularly, unique protective properties are available to HM based on epoxies or rubbers with fillers of hollow metallized microspheres (MS) – spheroplastics. The most advanced use is the application in such materials of non-organic carbon or glass microspheres [2].

Integral part in protective coverings designing is solutions as follow [3]:
- determination of the IR energy deposited in the structure material;
- determination of the temperature and pressure fields, being formed in a structure as a result of pulsed energy excretion;
- determination of destructive factors caused by stress waves developing from initial pressure profile.

When calculating thermomechanical impact of IR on heterogeneous coverings there energy excretion profiles in the HM components will be needed with regard for energy redistribution by secondary electron radiation on the component boundaries. The effect of the redistribution is particularly noticeable when high-energy quanta are absorbed by disperse filler having dimensions comparable with the electron run length. In such conditions energy carrying out is executed not only from the inclusion boundary fields but practically from the whole volume of filler particles. The importance of considering the influence of the secondary electron radiation on energy excretion is determined by the small amount of time to transfer the energy by electrons (in the order of units of nanoseconds) and its commensurability with the radiation effect time of $\tau \sim 10^{-8}$ s discussed in the paper. Having been

formed for the time duration of τ (which are significantly less than typical time development of wave processes in a target) the IR energy distribution serve as primary data for calculation of initial pressure profile in the covering.
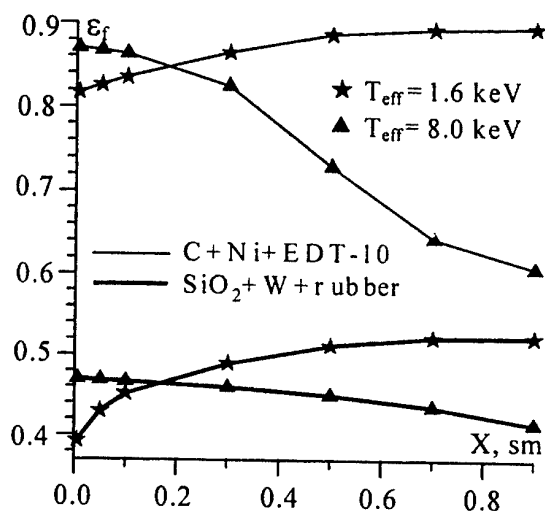
Fig.1. Portion of energy ε_f absorbed in the filler at the impact of the IR Plank spectrum.

Fulfilled numerical studies of IR impact on spheroplastics with the MS filler of glass (covered with tungsten) and carbon (covered with nickel) show that the portion of energy ε_f absorbed in the filling depends on the spectrum and changes depending on the covering thickness X (fig.1) which exert significant influence on initial pressure profile.

Pressure leveling at non-equalized energy excretion in the HM components occurs during the time significantly less then the development time of mechanical processes in the whole covering. In this case we can use the hydrodynamic model the pressures quasi-static leveling between the filler and the binder [4]. Figure 2 presents the calculation results according to the model (curve 1) and comparison they're of with the adiabatic (curve 3) and linear (curve 2) approximations.

In case of small specific absorbed energies Q disregarding for the shear deformations in the binder

may lead to errors in the initial pressure calculation. When warming-up the HM components near highly absorbing filler cores there plastic streams of the binder may be created. Disregarding for the material mechanical characteristic changes in this regions also leads to the errors in the calculation of radiation mechanical impact on HM. Figure 3 presents the results obtained from model [5] for change of energy excretion parameters (Q, ε_f) when various binder states are realized: elastic, mixed (the binder is near MS in the plastic state and the cells are in the elastic state on the periphery), purely plastic and hydrodynamic.
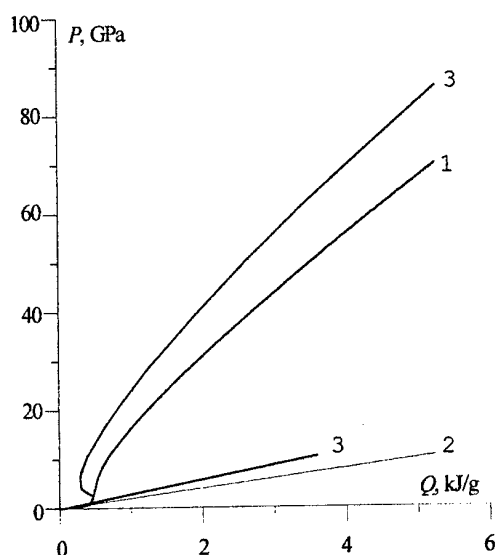
Fig.2. Dependence of the pressure in the material $SnO_2 + EDT - 10$ on specific absorbed energy Q.
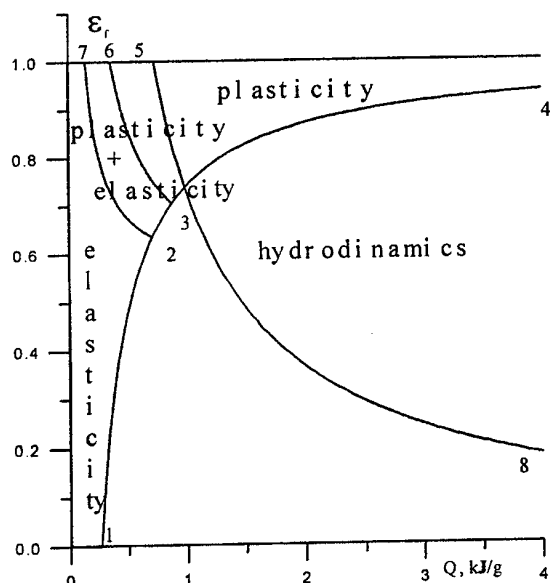
Fig.3. Regions of EDT-10 binder state (the filler is carbon MS covered with nickel).

As can be seen on fig.3 plasticity region is virtually present practically in the whole of the scope of specific energy Q, absorbed in HM change.

To optimize protective properties of spheroplastics one can use a model [6], regarding for not only peculiarities of the IR energy consumption by the HM components and porosity there of but also some technological peculiarities of coverings manufacturing (for example, MS destruction in process of a spheroplastic production).

Thus, a mathematical models complex has been developed that allows to conduct the studies of the IR mechanical impact on structures having high porous materials as well as design coverings of spheroplastics having required protective properties.

1. *Gribanov V.M., Ostrik A.V., Slobodchikov S. S.* Thermal and mechanical effects of x-ray radiation on materials and targets. Monograph. The nuclear explosion physics: In 2 Vols. Vol.2. An explosion effect. – M., RF Mod CIPT, 1997, 256pp.
2. *Ostrik A.V., Potapenko A.I.* Heterogeneous materials to protect structures from intensive energy streams // Composite Material Structures, 2001, P.1. P.48-53.
3. *Ostrik A.V.* Calculation-experimental prediction of the consequences of the x-ray mechanical effect on a aircraft structures. // Composite Material Structures, 2002, No. 1. P.10-28.
4. *Ostrik A.V., Ostrik E.A.* Quasistatic model to ascertain the pressure in multicomponent porous heterogeneous material under the impact of radiation. // Chemical physics, 2001, V.20, No. 8, P.90-93.
5. *Ostrik, A.V., Ostrik E.A.* Pressure calculation when RR impacting on heterogeneous material with plastic binder. // Composite Material Structures, 1999, No.2.
6. *Efremov V.P., Ostrik A.V., Potapenko A.I., Fortov V.E.* Pressure generation at pulsed volume energy output in heterogeneous material containing hollow microspheres. // Chemical physics, 2000.V.19, No. 2. P. 32-43.

CALCULATED-EXPERIMENTAL EVALUATION OF ULTIMATE POSSIBILITIES OF ADHESIVE-MECHANICAL JOINT OF GLASS-CERAMIC AND METAL TUBES

Kurakin V.I., Railyan V.S., Suzdal'tsev E.I., Hamitsaev A.S., Kolokolov L.I.
Federal State Unitary Enterprise "Obninsk Research and Production Enterprise
"TECHNOLOGIYA", Obninsk, Russia

Lap-joining of the tubes by means of elastic adhesive seam is considered. This seam was additionally strengthened mechanically by setting the sector keys into ring cuts made in both tubes. The key joint was also filled with the elastic compound. The quality of joint was monitored by X-ray pictures.

The joint is exposed to the complex force and heat action, and the level of loading varies up to the ultimate carrying power of the joint unit or one of the parts being joined.

The careful tensometering of the joint unit at various loading levels and with a variety of load application methods was carried out. Comparison of these pictures with the results of tensometering made it possible to determine the nature of total and local stressed state of the joint unit zone, which in turn allowed formulating the working hypothesis for the creation of the mathematical model describing the stressed-strained state of the tube joint zone satisfactorily.

It should be noted that at low temperatures the joint unit withstands such mechanical loads at which the failure on ceramic tube is observed due to the "normal" work of the adhesive joint. Key joint doesn't work under such conditions.

If the temperature goes up to 250-300°C, the adhesive loses its stiffness characteristics, admits of great (and practically unlimited) deformation. In this case the "sole mechanics" begins to act, i.e. only the key joint works, and adhesive may be neglected.

Under such conditions the joint carrying power decreases, the contact effects manifest themselves sharply, asymmetrical distribution of stressed along the circular coordinate is observed, which is confirmed by the experimental studies performed on a specially manufactured model without using the adhesive. The methods for up-grading the structure are proposed which increase the structure capability to transfer higher mechanical loads at high temperatures.

OPTIMAL DESIGN AND NUMERICAL COMPUTATION COMPOSITE COATINGS THAT FUNCTION IN EXTREMAL CONDITIONS OF EXTERNAL MEDIUM

Gusev E.L., Bakulin V.N.[(1)], Markov V.G.[(2)]

Unifed Institute Physical Technical Problems of the North Siberian Division, Russian Academy of Sciences, Yakutsk, Russia

[(1)] Institute of Applied Mechanics Russian Academy of Sciences, Moscow, Russia

[(2)] The Central Aerogidrodynamic Institute, Jukovsky, Moscow Region, Russia

In latter decades considerable attention is devoted to questions of development composite coatings with given complex of properties that function in extremal conditions of external medium. Variation perfomance of the problems of optimal design composite coatings with given complex of the properties is investigated. In variation perfomance the problems of optimal design composite coatings with given complex of the properties are formulated as a problems of optimal control complex systems. This complex systems are descrip-ted by interconnection totality of systems of differential equations. Set of materials for the decision problems of optimal design is discrete. This conduct to the problems of optimal control of combinatoric type. All totality of variables determinating the structure composite medium (physical properties of layers, thicknesses of layers, number of layers and also total thickness coating) is included in number of control parameters.

Necessary conditions of optimality and numerical procedures of optimization are developed, numerical experiments are realized. Different aspects of application of necessary condition of optimality in wave problems of optimal synthesis composite structures are investigated. Numerical procedures of optimization on the base necessary condition of optimality are developed. This procedures assume need-variation of admissible decison and allow to realize simultaneous variaton all parameters that determine the structure of layer coating: physical properties of layers, thicknesses of layers, number of layers and also total thickness layer system. Accordingly discretion change region of values of row control parameters corresponding to physical properties of finite set of materials is registered effectively. Constructive analysis of necessary conditions of optimality allow to establish row of qualitative regularities of structure of optimal composite coatings. The property of inner simmetry in strucrure of coatings that realize limit possibilities for the reaching given complex of the properties is established [1-5]. The established qualitative regularities of optimal composite construction allow apriori to realize effective narrowing admissible set variants that are analyzed for the optimality. And also admit to prognose optimal structure of composite coating.

The received results allow to realize effective design composite coatings with before given complex of the properties.

With the steadily rising requirements for the shell design it becomes increasingly important to choose its optimal construction. The more strong requirements for the weidht and security dived rise the concept of the undangerous damage construction. This concept allowes the undangerous fatigue crack growth before detecting by visual inspection. The optimisation of the undangerous damage construction is more complex task because of the next causes: it is necessary to determin the residual strength after cracking and the stress intensity factors at tips of standardized longitudinal and transverse cracks; it is necessary to develope the method of nonlinear mathematical analysis wich allowes to decide this task in appropriate time with the most accuracy.

This method assumes cylindrical sealed shells to be subjected to bending moments, shear forces and internal pressure and composed of three types of cylindrical panels. An optimum design is to be searched within a class of stringer-stiffened monocoque shells where none of skin portions buckles locally under ultimate loads [6-8]. The designed method synthesizes optimum pressure shell contours by varying a cross section shape and simultaneously searches for optimum structural concept by varying the number of load-carrying components and their sizes.

The optimization is made with due account of the following constraints: for static strength, for fracture mechanics, for stiffness characteristics of pressure shells under lateral bending and under torsion. The natural frequency constraints for skin portions of side panels can be considered. The limitations are considered also on overall dimensions of a cross section of a pressure shell as well as constraints for minimum and maximum allowable values of optimum design parameters.

Following the method of logarithmic internal penalty functions the problem of minimizing the pressurized shell mass with constrains reduces to the problem of unconstrained minimization for an auxiliary objective function. The designed method has made it possible to decrease the weight of three types of pressurized fuselage sections of aircrafts by 9-14% in comparison with models carefully designed with conventional methods at three different design bureaus.

LITERATURE

1. Gusev E.L. Optimal synthesis methodology of nonhomogeneous structures under the influence of electromagnetic waves //J. of Applied Electromagnetics and Mechanics, 1999, N 10, p. 405-416.

2. Gusev E.L. Narrowing of the region of search in problems of optimal synthesis of layered structures with a set of properties //J. of Applied Mechanics and Technical Physics, 1997, v.38, N 5, p. 768-773.

3. Gusev E.L. On optimization of synthesis of acoustical structures //Acoustical Physics, 1997, v.43, N 2, p.211-214.

4. Gusev E.L. Qualitative relationship in structures of optimal design with reference to optimal synthesis of acoustical systems //Acoustical Physics, 1997, v. 43, N 5, p.612-615.

5. Gusev E.L. Property of inner simmetry in optimal layer structures under the influence of elastic waves //Applied Mathematics and Mechanics, 2001, v. 65, N 6, p. 1025-1032.

6. Bakulin V.N., Gusev E.L., Markov V.G. (1999) Methods of optimal design of construction from composite and traditional materials. Collected abstracts of X anniversay international conference on Computational Mechanics And Modern Applied Software Sistem. Pereslavl-Zalessky. pp.234-235. (In Russian)

7. Bakulin V.N., Lagutin V.G., Markov V.G. (1994) The optimization of stiffened sealed shells with cracks. International aerospace congress (Theory, Applications, Technologies). Mosckow. Proceedings. v.2, pp.307-311.

8. Lagutin V.G., Markov V.G. (1990) Optimization of pressurized shell shape and dimensions and location of stiffeners. //Strength of materials. Kiev. N7, pp.102-107.

FORMING ENGINEERING PRODUCTS WORKING SURFACE FOR EXPLOITATION IN EXTREME CONDITIONS (INSTRUMENT)

Tyurin Yu.N., Zgadkeivich M.L., Kolisnichenko O.V.
E.O.Paton Electric Welding Institute, NASU, Kyiv, Ukraine

The E.O.Paton Electric Welding Institute developed the technology for pulse-plasma treatment of materials, which allows different methods of affecting the workpiece surface, such as elasto-plastic deformation, effect by sound and pulsed magnetic field, heat and electric-pulse treatment and deformation of metals and alloys during the process of reversible ($\alpha \leftrightarrow \gamma$) transformations, to be simultaneously implemented.

Non-stationary detonation conditions of combustion of fuel gas mixtures were used for formation of high-power plasma jets.

Energy parameters of the non-stationary detonation combustion products (pulse-plasma jet) can be determined by solving the known two-dimensional non-stationary problem of propagation of the detonation wave in the electric field between two co-axial electrodes. To derive a numerical solution, the problem was simplified, and the mean values of temperature, velocity, pressure and density of the combustion products along the axis of the electrodes were determined without allowance for their variations across the section [1].

The plasmatron consists of detonation chamber 1, where the fuel gas mixture is formed and its detonation combustion is initiated, central electrode - anode 2, conical electrode - cathode 3, consumable electrode 4 and power supply 5 (figure.1).

Energy characteristics of the plasma jets at the exit from the plasmatron, calculated from theoretical formulae, have a linear dependence upon the electric field intensity and inter-electrode length. Plasma jet can have temperature of 15000 K and velocity of 5 km/s.

Experimental evaluation of characteristics of the plasma jet was carried out using an industrial plasmatron with an inter-electrode gap 200 mm long. The time-averaged temperature of the plasma jet was determined by the results of spectral analysis of the jet. The temperature of the plasma was determined by a relative intensity of iron lines. Plasma radiation spectra integrated by time showed that temperature of the plasma at the plasmatron exit was 15000-20000 K.

Structure of the plasma jet is characteristic of a supersonic mode with the under-expanded flow of the jet and corresponds to the detonation character of operation of the plasmatron, at which pressure in the chamber can be much in excess of the atmospheric one. The pattern of interaction of the plasma jet with a barrier is characterized by the presence of jet and region of the shock-compressed layer (SCL).
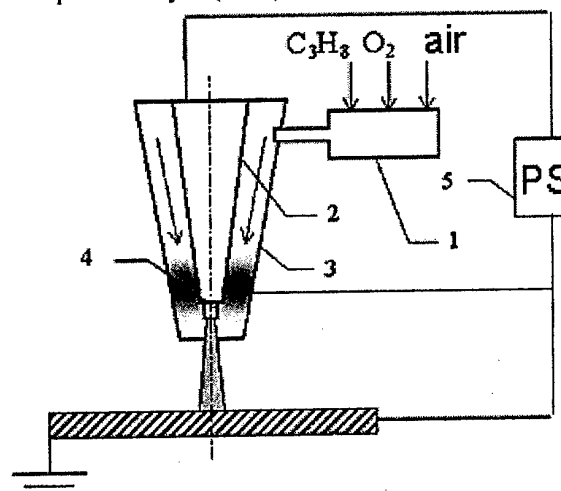
Fig. 1. Schematic of plasmatron for pulse-plasma treatment (designations of positions are given in the text)

After break-down of SCL the electric current will flow along the plasma jet from the central electrode in the plasmatron to the workpiece surface. Density of the electric current in the plasma jet, j, is $(1-7) \cdot 10^3$ A/cm^2 and temperature T is 15000-30000 K. The heat flow into a workpiece depends upon the current density and varies within a range of q= $(0.1-5.0) \cdot 10^6$ W/cm^2. Evaluation of heat flows was done on the basis of theoretical analysis of the non-stationary equation of thermal conductivity through thickness of the hardened layers of steels of the martensitic grade [2, 3].

The time of interaction of the plasma pulse and its energy parameters were controlled by varying capacitance C of the capacitors, voltage U_{charge} at plates of the capacitor bank, inductance L in the discharge circuit, distance B to the workpiece surface and variation in size of the active spot of

interaction of the plasma jet with the workpiece surface.

The experiments indicated that at the initial moment the workpiece surface is in elasto-plastic interaction with a shock wave and the pulsed plasma jet. Then, at break-down of SCL the surface is affected by the electric current (amplitude value of the current is 1-5 kA, time of interaction is 0.3-0.8 msec). This results in a formation of the pulsed magnetic field with an intensity of up to $1,6\cdot10^5$ A/м. Further on (within 3-5 ms) the surface will be affected by the flows of the combustion and electrode erosion products.

As indicated by the experiments and shown by the calculation data, treatment of the workpiece surface by the pulsed plasma containing alloying elements is accompanied by a complex (thermal, electromagnetic and deformation) pulsed effect. This provides alloying of the workpiece surface with components of the plasma and hardening of this surface. Alloying elements are added into the plasma in the form of metal electrode (rod) erosion products and gas (propane, nitrogen).

Pulse-plasma treatment of a workpiece of iron-based alloy results in the formation of a microcrystalline alloyed layer. Structure of the layer depends upon the plasma composition and quantity of the treatment pulses. Composition of the plasma is determined by a oxidizer to fuel ratio [4].

The highest value of microhardness of the hardened layer on samples of steel U-8, which were preliminarily subjected to quenching and high tempering, was chieved in the case of using tungsten and molybdenum electrodes (Figure 2). Treatment was performed without surface melting, specific power of the jet was $1\cdot10^6$ W/cm^2. Microhardness was measured on transverse sections using the PMT-3 hardness meter. The Knoop diamond pyramid was used for the measurements. The load on the pyramid was 1 N.

X-ray phase analysis of the pulse-plasma hardened layers on samples of carbon steels detects widening of the ⸬-Fe lines and emergence of the Fe residual austenite lines. An increase in the number of pulses favours further widening of the ☐-Fe lines with a decrease in their intensity, as well as an increase in the relative intensity of the ⸬-Fe lines. Comparison of the intensities of the residual austenite and ferrite lines shows that the amount of austenite under the same treatment conditions.
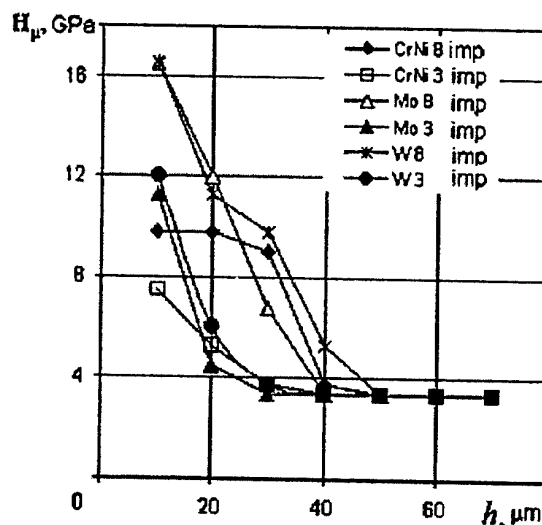
Fig. 2. Distribution of microhardness in the hardened layer of a sample of iron alloy (0.8 %C) after pulse-plasma treatment using different electrodes; h - layer thickness

Pulse-plasma hardening of the tools at the Open Stock-Holding Company "Cherepovets Steel-Rolling Plant" is done using an upgraded milling machine tool [5]. Metal cutting tools, dies and punches for hot and cold deformation of metal were subjected to hardening. Prior to hardening, the parts were subjected to standard heat treatment and machining. Pulse-plasma treatment was used as a final operation. Hardening was done only to surfaces of cutting edges of the tools. The experience of commercial application showed that performance of the tools increased 2-6 times.

REFERENCES

1. Tyurin. Yu. N., Pogrebnjak A.D. Advances in the development of detonation technologies and equipment for coating deposition. Surface and Coatings Technology. -111. 1999. 269-275.

2. Tyurin. Yu. N., Kolisnichenko O.V. Impulse - plasma modifying. Interplay of radiations with a solid. Materials of the third international conference, Minsk, October 1999. 214-216.

3. Losko D.V., Milman Yu. V., Yefimov N.A., Korzhova N.P., Tyurin Yu. N. Physical Nature of Hardening of Sleel U8 by Plasma-Detonation Working // VOX - 1999. №6. 764-771.

4. Tyurin, Yu.N., Pogrebnjak A.D., Kolesnichenko O.V. Formation of plasma pulses in the process of detonation of combustion gas mixtures in electromagnetic field. 7-th International Conference on Plasma Surface Engineering. Garmisch-Partenkirchen. 2000. P. 145-149.

5. Tyurin. Yu. N., Kolisnichenko O.V., Sigankov N.G. Impulse-plasma hardening the tool. Autowelding, Kiev, № 1, 2001. P. 13-18.

THE STRUCTURE AND PROPERTIES OF A HARD ALLOY COATING DEPOSITED BY HIGH-VELOCITY PULSED PLASMA JET ONTO A COPPER SUBSTRATE

Pogrebnjak A.D.[1], Tyurin Y.N., Iljashenko M.I.[1], Kolisnichenko O.V.

E.O.Paton Electric Welding Institute, NASU, Kyiv, Ukraine

[1]Sumy Institute for Surface Modification, Sumy, Ukraine

Using a plasmatron operating in specially calculated regimes, tungsten carbide (WC) based coatings were deposited onto a copper crystallizer plate. It was found that a local hardness of the WC-Co coating may reach up to 1.3×10^4 N/mm^2 and the coating adhesion to substrate may be as high as 270 MPa. The elemental and phase compositions of coatings were studied by Rutherford backscattering spectroscopy, X-ray diffraction, and transmission electron microscopy with electron diffraction. The surface morphology and depth-composition profiles of the coatings were studied by optical and scanning electron microscopy. The coating is composed of WC crystal grains with hexagonal close packed (hcp) lattice, α- and β-Co grains, and cubic WC grains. The average size of the hcp WC grains is 0.15 μm and that of the cobalt particles is about 25 nm. In addition, the grain boundaries contain W$_3$CO$_3$C particles with an average size of 15 nm.

Pulsed beams of charged particles and plasmas have been extensively used for the surface modification of various materials since the beginning of 1980 year [1-2]. The action of such concentrated energy fluxes upon a solid sample leads to a high-rate ($10^{-3} - 10^{-8}$ s) heating of the surface layer followed by its rapid quenching with a fast heat removal in depth of the processed target. As a result, the target material exhibits significant structural and phase transformations, including the formation of metastable phases, dispersed nanoinclusions, amorphous layers, and high densities of dislocations and nonequilibrium point defects frequently accompanied by the ion-beam-induced mixing [2-4]. Pulsed energy fluxes are also employed for depositing thin films, applying coatings, and obtaining dispersed nano-particle powders [4]. In particular, by introducing a WC-Co powder (VK-12 grade) into a pulsed high-velocity plasma jet, one may obtain a coating of this composition with good adhesion to a copper crystallizer plate (solving this task is important for the molding technology).

The sample coatings were prepared using a pulsed plasmatron supplied with a VK-12 powder with an average particle size of 35-56 μm. Using preliminary mathematical modeling and variation of the plasmatron parameters, nozzle geometry, the distance from the nozzle to substrate surface, and the reaction chamber dimensions, we determined optimum values of the pulsed plasma jet velocity, plasma temperature, and optimum nozzle to substrate spacing. These parameters were as follows: jet plasma temperature, 2.4×10^4 K; jet velocity, ~7 km/s; jet power density, up to 10^7 W/cm^2; nozzle to substrate spacing, 30 mm. The gas mixture components and powdered material were supplied to the plasmatron in a continuous regime. The jet pulse duration was 0.3 ms.
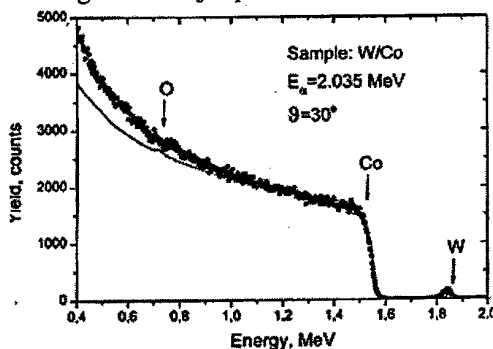
Fig. 1. RBS He^{4+} spectrum of a WC-Co coating on a copper crystallizer surface.
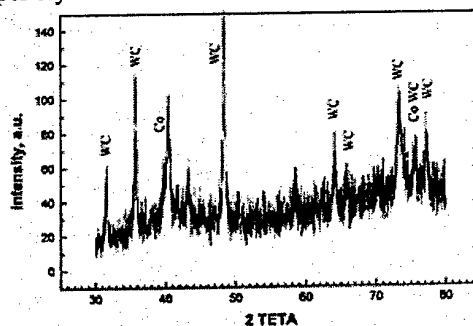
Fig.2. X-ray diffractogram (CuK_α radiation; Sunya, Japan) of a WC-Co coating deposited by a pulsed plasma jet onto a copper crystallizer surface.

Figure 1 shows the Rutherford backscattering (RBS) spectrum of He$^+$ ions for a tungsten carbide-cobalt coating. As is seen, the spectrum displays the peaks of tungsten and oxygen and a kinematic threshold of Co. The relative content of Co, W, C, and O in the surface layer with a

thickness of 2.8 μm corresponded to the following composition: WC_{89}; Co_8; C_2; O_2. Note that the concentration of tungsten on the film surface was very small (~1 at. %), while the carbon concentration reached 30 at. %. As is known [5-8], the tungsten carbide films deposited by the HVOE and HEP techniques are characterized by the tungsten content increased up to 84.38 and 87.98%, respectively. This may even be accompanied by the partial amorphization of complex phases at the carbide and cobalt grains. The cobalt content also changed to reach 12.98% (HVOE) and 9.22% (HEP), while the carbon concentration decreased from 4.09% in the initial powder to 2.5% (HVOE) and 2.52% (HEP). In our case, the coating contained phases which were mostly present in the initial powder, although some other phases formed in the course of rapid quenching appeared as well.

Fig. 3. Micrograph of the transverse cross section of a WC-Co coating on a copper substrate with indenter pyramid marks: (1) in the middle of the coating; (2) near the film-substrate interface; (3) at the film-substrate interface.

The X-ray diffraction analysis performed on a DRON-3 diffractometer using K_α-Cu radiation showed that the main phase in the coating was WC with an hcp lattice. The presence of other phases was evidenced by reflections in the 37°-47° angular interval (Fig. 2). Unfortunately, the diffraction peaks observed in this interval exhibited overlap, hindering the identification of phases.

The interplanar spacings calculated for the reflections that could be resolved suggested the presence of the following phases: W_2C, Co_7W_6, Co_3W, W, and Co. Complex phases occurring in the intergranular regions may be amorphous, in agreement with. This state is explained by a high-temperature cycle involved in the coating formation.

Additional analysis of the sample structure and

phase composition was performed with the aid of the transmission electron microscopy with electron diffraction. According to these data, the coating has a poly-crystalline structure including grains of the hcp WC phase and the cubic α-Co, β-Co, and WC phases. The average size of the hcp WC grains is 0.15 μm and that of the cobalt particles is about 25 nm. In addition, the grain boundaries contain W_3Co_3C particles with an average size of 15 nm. A dislocation substructure was observed inside the cubic WC grains.

Figure 3 shows a micrograph of the transverse cross section of a WC-Co coating with prints of a diamond indenter pyramid used for the microhardness measurements (scale: 1 cm ~ 200 μm). As is seen from this image, the coating contains local regions possessing significantly different microhardnesses (ranging from 8 x 10^3 to 1.3 x 10^4 N/mm²). The adhesion of coating to substrate was determined for the films deposited onto M-00 grade copper plates. This characteristic, determined after about ten measurements of the groove made by a diamond pyramid scribing the sample surface, was calculated by the formula $H_u = 4P/b^2$ (here P is the load and b is the groove width). The results of these measurements showed that the adhesion is on the average 250 MPa (ranging from 210 to 280 N/mm²).

REFERENCES

1. A. N. Valyaev, Kishimoto Naoki, and A. D. Pogrebnyak, Modification of Materials Properties and Synthesis of Thin Films under Irradiation by Intense Electron and Ion Beams (Vostochno-Kazakhstanskil Tekhnicheskil Univ., Ust'-Kamenogorsk, 2000).

2. V. L. Yakushev, B. A. Kalin, and V. I. PoFskikh, Metally, No. 4, 74 (1994).

3. Yu. N. Tuyrin and A. D. Pogrebnjak, Surf. Coat. Technol. III, 269 (1999).

4. A. D. Pogrebnyak, Yu. N. Tyurin, Yu. F. Ivanov, et al., Pis'ma Zh. Tekh. Fiz. 26 (21), 53 (2000) [Tech. Phys. Lett. 26, 960 (2000)].

5. Surface Modification and Alloying by Laser, Ion and Electron Beams, Ed. by J. M. Poate, G. Foti, and D. C. Jacobson (Plenum, New York, 1983; Mashinostro-enie, Moscow, 1987).

6. J. Nerz, B. Kushner, and A. Rotoliko, J. Therm. Spray Technol. 1 (2), 147 (1992).

7. C. J. Li, A. Ohmori, and J. Harada, J. Therm. Spray Technol. 5 (1), 69 (1996).

8. R. B. Bhagat, M. F. Amatean, A. Papyrin, et aL, ASM Thermal Spray Society, 1997, pp. 361-37

EVALUATION OF THE STRESSED – STRAINED STATE OF THIN – WALLED SHELLS USING READINGS OF THE SENSOR OF DISPLACEMENT AT THERMAL LOADING

Railyan V.S., Gratsiansky Yu.A.
Federal State Unitary Enterprise "Obninsk Research and Production Enterprise "TECHNOLOGIYA", Obninsk, Russia

The most effective method for estimation of the stressed – strained state (SSS) of the constructions is to use tenso - resistors. Their work is based on the tenso – effect, consisting in sensor resistance change when deformed. When the sensor heat up, the estimation of SSS becomes difficult, because it is not easy to separate changes in resistance, caused by heating, from changes, caused by deformation of the surface. Conventional methods of accounting for thermal characteristics cannot properties of the material of the sensitive element in the sensor and whose of the the surface and substantial heating.

Use of displacement sensor, measuring the movements in meridional, circumferential and radial directions, where sensitive elements are at the distance from the heated surface and which design allows for providing of sufficient cooling, which in is turn , provides constant temperature of sensitive element, make it possible to obtain objective information about the field of displacement on the inner surface of the shell to the field of deformations of the whole shell.

The allgorithm is offered for the transition from the measured transition from the masured displacement to the fields of deformations for the whole shell. Check on the testing samples showed good precision of the offered algorithm and errors stability in estimation of displacements.

COATINGS FOR THE SIMULATION OF TEMPERATURE FIELDS DURING THE GROUND-BASED TESTS OF THE CERAMIC COMPONENTS FOR FLYING VEHICLES

Railyan V.S., Rusin M.Yu., Reznik S.V.[1]

Federal State Unitary Enterprise "Obninsk Research and Production Enterprise "TECHNOLOGIYA", Obninsk, Russia
[1]Bauman Moscow State Technical University, Moscow, Russia

The analysis of the validity of temperature field specification during the ground-based tests of the flying vehicle components in the radiation heating plant shows that the magnitude of ΔT error mainly depends on the geometrical dimensions of the infrared heaters and on the variation of the optical parameters of the surface being heated, temperature detectors and reflecting screen. This component of the temperature field error can be reduced in two ways:
- through the reduction in the geometrical dimensions of the heaters and thus the increase in the number of the heating zones;
- through the use of coatings with a varying extent of blackness.

The method and the composition of the coating for the simulation of temperature fields during the heat-resistance tests of nonmetallic fairings have been theoretically substantiated. The coating makes it possible to decrease the error of specification of the radiation heating field in the range 20 to 2000°C by a factor of three.

The coating in question is based on the high-temperature oxides of chromium, silicon and aluminium. After heating the coating is easily removed from the surface being tested which allows one to investigate the dielectric properties of the shell material.

The formula for the temperature field correction at any point on the surface being heated has been deduced. The results of the experimental studies with the use of coatings with the controlled extent of blackness are given in the paper.

ETHYLENE-HEXAFLUOROPROPENE COPOLYMER AS BASIS OF PROTECTIVE COATINGS STABLE IN AGGRESSIVE MEDIA

Voznyakovsky A.P., Sokolov Yu.P., Lovchikov K.V., Krivoruchko E.M.
Lebedev Rubber Research Institute, St.-Petersburg, Russia

Many industry branches lately increase their need in protective coatings stable in aggressive media at high temperatures. This need is generally due to strict requirements of ecological safety as well as industrial technologies power consumption decreasing.

User generally makes a complex of strong demands to the same polymer coating including stability in aggressive media, electrochemical corrosion stability and heat resistance. Such a demand complex makes fluorine-containing polymers the most suitable material as a basis of protective coatings. Higher price of fluorine-containing polymers as compared to the hydrocarbon polymers should not prevent from its application in the areas where high reliability is the main guideline.

Fluorine-containing polymers can be divided into fluoroplasts and fluoroelastomers according to their elastic properties. Rheological characteristics show that fluoroplasts are thermoplasts. They have a minimal diffusion permeability that causes many attempts of their using as the protective coatings. Best fluoroplast coatings usually can be applied from the polymer melt. This method requires the heating of the protected surface up to $300 - 350 \,^\circ C$ that constricts the area of its practical application.

Fluoroelastomers unlike fluoroplasts contain in polymer chains the units provided the high elastic properties. Fluoroelastomer based films are practically not inferior to fluoroplasts in their chemical resistance. In respect to protective coating application method fluoroelastomers are preferable due to their ability to form the films from polymer solutions in volatile solvents. Moreover, mechanical properties of such fluoroelastomer coatings are much higher as compared to fluoroplast films. Most prevalent fluoroelastomer material for protective coatings are the copolymers of vinylidene fluoride with some perfluorinated unsaturated compounds. The main disadvantage of these polymers is in their low resistance in polar and nucleophilic media. Copolymers of ethylene with perfluorinated alkyl vinyl ethers (PFAVE) synthesized by the authors do not have this weakness. Nevertheless, the

shortage of PFAVE and their high price hinder the PFAVE based copolymers from their wide application.

High-molecular copolymer of ethylene with hexafluoropropene (EHP) synthesized by the authors has much lower price as compared to PFAVE based polymers.

^1H and ^{19}F NMR study shows that EHP backbone structure is near to alternant and can be controlled by the polymerization conditions.

Experiment shows that EHP has practically the same high stability in aggressive media like ethylene-PFAVE copolymers and much more stable than vinylidene fluoride based analogs.

Table 1

Swelling of EHP and vinylidene fluoride based copolymers in some liquid media

Media	Swelling, %			
	EHP	filled EHP	Viton A	Viton B
Tetrahydrofurane	35	11	200	190
Acetone	15	7	200	175
Ethyl acetate	17	10	230	250
Heptane	3	2.7		
Dimethylformamide	6	3.5		
Acetonitryle	15	12		
Decane	6	3		
H_2SO_4 (98%)	2	3.1		
HNO_3 (57%)	2.3	3.3		
HCl (31%)	1.5	3.2		
H_2O	1.5	2		
$H_2O + K_2Cr_2O_7$ (5%)	1.5	2		
$H_2O + K_2S_2O_8$ (5%) + $AgNO_3$ (0.01%)		3		
$H_2O + NaOH$ (20%)	2.5	2.9	*	*

* complete destruction

Special attention should be paid to the solvent selection at films preparation since the solvent

thermodynamic quality is one of the most important factors determining the formed films properties.

EHP chemical structure features substantially constrain the range of potential solvents. It is known that vinylidene fluoride based copolymers have the limitless swelling in polar solvents (e.g., in acetone) whereas EHP swelling level does not exceed 15 – 20% (see Table 1). Two most appropriate solvents for EHP films forming are hexafluorobenzene and 1,1,2-trifluoro-1,2,2-trichloroethane (Freon-113). We used the last one in our study due to its low cost.

The most important characteristic of protective coatings is their diffusion permeability in respect to various environment components. Such data for EHP under study were obtained by means of inversed gas chromatography method. Table 2 displays the EHP calculated values of diffusion and permeability coefficients for hexafluorobenzene (thermodynamically 'good' solvent) and cyclohexane (thermodynamically 'bad' solvent). Also Table 2 displays for the comparison purposes the diffusion and permeability coefficient values of polydimethylsilicone (PDMS) in respect to the same sorbates. Permeability coefficients were calculated according to the well-known expression $P = D*S$, where S is the solubility coefficient calculated from the inversed gas chromatography data.

Obvious approach to films diffusion permeability reduction consists in using of filled systems. We have chosen as a filling agent the ultradisperse carbon nano-particles obtained with detonation synthesis. Filled materials have been prepared by means of solution technology where dry powder of filling agent was dispersed into EHP solution in 1,1,2-trifluoro-1,2,2-trichloroethane. It was found that using of nanodisperse carbon particles without preliminary treatment causes an appreciable deterioration of protective properties of the coatings as well as of their mechanical properties. We suppose that this deterioration is due to the aggregation of nanodisperse carbon particles as a result of their high surface energy. Aggregation processes do not allow achieving the uniform particles distribution in the whole volume of polymer matrix that causes cracking of the coating surface.

Authors have found the method of chemical modification of the nanodisperse carbon particles that substantially increases the affinity of particles surface to the solvent and decreases the aggregation processes. Application of the suggested method allows forming the EHP based coatings with high protective properties as well as with appropriate mechanical properties.

Table 2
Diffusion coefficient D (cm^3*s) and permeability coefficient P (cm^3*m*cm^{-2}*s*atm) for EHP and PDMS at 20 °C

Sorbate	EHP		PDMS	
	D*10^8	P*10^8	D*10^8	P*10^8
Hexafluoro-benzene	0.082	3.6	0.473	9.3
Cyclohex-ane	0.127	1.2	0.278	10.6

Table 2 data analysis shows that EHP has a typical for the ethylene based copolymers feature – relatively high diffusion permeability regarding the hydrocarbons. High diffusion permeability of EHP is a drawback within the framework of this study, though the above-mentioned EHP feature gives a good chance to apply EHP as a material for permselective membranes.

MANUFACTURE OF CONTAINERS RESISTANT TO MOISTURE, BIOLOGICAL THREAT AND RADIATION, FOR THE PACKING AND BURIAL OF SOLID NUCLEAR WASTE

Demichev V.I., **Meleshko A.I.**
Scientific-manufacturing association "Kompozit", Korolev, Russia

One of the most serious global problems connected with environmental issues is that of pollution caused by nuclear waste.

In Russia the current practice is to pack solid nuclear waste in stainless steel barrels before burying it in chambers which are faced with cement and covered in bitumen. This method has the following disadvantages:

- bitumen presents a fire risk and is subject to biological degradation;
- cement cracks, allowing both water from the atmosphere and the soil to seep in;
- exposure to moisture, microorganisms in the soil and the corrosion process caused by the effects of radiation mean that the barrels have an expected life of 20 – 25 years.

At "Kompozit", the joint-stock company and scientific-manufacturing association, research has been carried out regarding how moisture, radiation, and biological factors affect polymer composite material (PCM). Research using the Fik equation for total saturation time has confirmed the potential application of PCM. The total saturation time for PCM with a diffusion ratio of 10^{-9} and a plate thickness of 20mm is 116 years, while for PCM with a diffusion ratio of 2.10^{-10} and a plate thickness of 100mm is 144 years. The results of environmental testing show that in corrosive conditions PCM will be serviceable for over 100 years.

It is suggested that fibre-glass reinforced plastic and basalt reinforced plastic should be used to develop containers for the packaging of nuclear waste: fibre-glass reinforced plastic is the most thoroughly researched, cheapest, and most widely produced material, while basalt reinforced plastic has a higher density and is more resistant to corrosion.

In choosing fibre-glass reinforced plastic the matrix material is of great importance. The binding material should satisfy the following conditions:

- radiation resistance of not less than 10^7 rad;
- a moisture diffusion ratio of not more than $10^{-9} - 10^{-10}$ cm^2/sec;
- resistance to fungi and bacteria.

In accordance with these requirements an epoxyphenol (ЭНФБ) binder was chosen. It is strong and has high technical specifications.

The structural framework of the container has been developed using T10-80 glass cloth and an (ЭНФБ) binder. The containers are produced in sections using vacuum autoclave moulding. Experimental models have been produced and tested by burying.

The vessel is a cylindrical shell 20mm thick, with a diameter of 500mm. The specifications of plates made from glass cloth are as follows:

$E = 2700$ kg(f)/mm^2
$\sigma = 56$ kg(f)/mm^2

Critical load leading to loss of stability:
$T'_{кр} = 2\pi KE\delta^2$;

where $K = 0.3$ – ratio of stability;
$T'_{кр} = 6.28 \cdot 0.3 \cdot 2700 \cdot 20^2 = 19963.35$ kN

Critical load leading to compression of the container;
$T''_{кр} = \sigma F$

where $F = \pi d\delta$ – sectional area
$T''_{кр} = 56 \cdot 3.14 \cdot 500 \cdot 20 = 17246$ kN

It is intended that the fibre-glass reinforced plastic containers will be supplied with hermetic lids rather than the type normally used with metal containers. The hermetic joint between the lid and the container means that it will be possible to manufacture the containers as a single unit by

using excess compound to fill up the container of solid nuclear waste. At the same time this ensures that the clearance between the lid and the container is as small as possible. Such containers provide a reliable method of packing nuclear waste of low or medium specific activity for burial. Using containers made of PCM is substantially cheaper than using those made of stainless steel, both in terms of man hours spent and the price of the containers.

Calculations show that the strength of cylindrical containers made of basalt is somewhat lower than that of containers made of fibre-glass reinforced plastic, but they still meet requirements. Basalt has higher heat, chemical and water resistance indices, higher dielectric properties and does not contribute to air pollution.

In order to improve radiation resistance the production of a hybrid structural PCM has been developed. The material, which is reinforced with glass cloth, consists of a thermoactive polymer base which contains a densely dispersed (высокодисперсный) filling agent. The filling

agent is finely dispersed (тонкодисперсный) (4 – 10 microns) tungsten. Production engineering means that the filling agent can be between 30% to 80% by volume. This increases radation resistance, ensuring a long life together with high strength and structural specifications. The limit of stability of the above material under compression is 200 – 400 mega Pascals. As radiation testing of experimental models at NPO "Radon" have shown, the attenuation ratio of the material under research is 3-7. If the material is 70% filling agent and 10mm thick then the attenuation ratio is 3.8.

It is suggested the radiation permeability of the container shells can be controlled by varying the quantity of material with low radiation permeability. In such a case the container is produced in two parts; an outer and an inner wall made of fibre-glass reinforced plastic 3 – 5 mm thick, with a 4 – 10 mm clearance between the two. The gap is filled by a filling agent such as lead shot, microspheres, powder or suchlike, which is distributed throughout the compound or binding material.

References:
1. Patent No. 2174467, Russia

TRIBOLOGICALS ASPECTS OF POLYFAUNCSHIONAL CRADIENT COATING CREATION BY CEC METHOD

LUCHKA M.V.
Fransevich Institute for Problem of Materials Science,
National Academy of Science of Ukraine, Kyiv, Ukraine

The theoretical conditions for reception gradient and composite of a matrix and skeletal type coatings have been developed. The intense state which arises within the friction in such structures, have been investigated and their gabitus is a matrix layer with in regular distributed and normally orientated formation by pillar formations. The tenacity distribution into a layer depth on a metal matrix model containing continuous fibers have been investigated to determine the evaluation of stress concentration in the matrixes with their mechanical properties including the interaction of components in the composition if a transitive zone is present.

The character of stress state in the composition loaded by a friction and sliding forces have been investigated on a model with such circular zone between a matrix and a filling according to known law of mechanical properties changing only in the normal direction from the matrix boundary-line with a filling.

It have been shown, that the kind of dependence and distribution of local stress fields in composition from a loading kind of chosen elementary volume with typical gabitus, may have 3 structural types of a transitive zone, which is formed as a result diffusion interaction of a matrix material and filling according to the equilibrium diagram, of such systems. The knowledge of stress distribution in stratification gives by an opportunity of creation of coverings, in which the rule of a positive gradient on opportunity of coating creation in which the rule of positive properties is realized.

These it is a new and most expedient for formation in tribocontact zone a friction pair of gradient composite matrix filled layer with following mechanical hart treatment in vacuum, protective medium, diffusion infiltration and eutectic melting, including different concentrated energy sources (solar, laser, НВЧ). Such coverings were formed on detail surface from constructional material as a were resistance layer with non-uniform structure by means composite electrolytic codeposition method (CEC) based on nickel with definite particles distribution.

The necessary gradient of properties provided during chemical-heat treatment (CEC) in vacuum for CEC, which contain actively interaction inclusions (B, C, Cr, Mo), or in powder sating mixes of boron, chrom and aluminium saturation for CEC containing inert inclusions (Ti, TiB_2, TiC, CrB_2).

According to the phase x-ray, metallographic and microduromentric analyses CEC based on nickel with refractory powders inclusions steel 45, 20X13 after chemical-heat treatment is Ni-B, Ni-Cr, Ni-AL matrix, which contains about 30 volume % of wear resistance particles (carbides, borides, nitrides) with the granularity from 3 to 300 mkm and their quantity and size changes both on a composition depth and on a tribocontact surface.

The existence of the optimum size, quantity and distribution in coatings promote redistribution in a friction zone without oil for wear resistance secondary structures. Thus the plasticity of matrix metal in CEC promote the leading redistribution, which perceive by the stronger inclusions effectively holding in matrix, which are reliably kept in matrixes. It's typically that with temperature increase in friction zone to 700 °C the coupling processes are braked, that is caused by stable oxide film formation and optimum filler contents in coating depth is moved in the direction of its volume part increasing and at that time the level of diffusion infiltration of matrix is smoothly decreases.

NEW LAMINAR COMPOSITE MATERIALS FOR THE OPERATION UNDER EXTREME CONDITIONS

Neklyudov I., Borts B., Lopata A.T., Chevtchenko S.
National Science Center "Kharkov Institute of Physics and Technology", Kharkov, Ukraine

Composite material articles reveal the unique performances; it is impossible to obtain the combination of these performances in articles produced of material of one kind. Laminar composite materials (LCM) represent the specific kind of composite and are of great importance for the material use under extreme conditions. The use of LCM permits to solve some of complicated technical problems, to economize the deficient and expensive materials, to increase the structure operation reliability. The unique method to produce the composite materials that contain easy oxidizable materials or alloys on its base, namely: titanium, tantalum, niobium, zirconium, vanadium, aluminium, copper, iron, steels is the method of simultaneous deformation (SD). The method is based on the simultaneous deformation of preliminary arranged billets (layers) of heterogeneous materials in specially selected artificial medium. At optimal choice of relationship between billets of carrier, damping and barrier layers also as at high-speed deformation optimal conditions (pressure pulse, temperature, oxidizing-reducing atmosphere, residual pressure) this method provides the strength and ductility of heterogeneous metal joint zones close to the designed. Due to the vacuum purity and the pulsed pressure at the metal joining the metal permits to obtain LCM of any material combinations. Developed now LCM operate in quasi-stationary temperature pattern, field of forces. At article operation under the variable temperature-force fields the decrease of strength and ductility characteristics is typical due to the crystalline structure change and due to the stressed state near the boundaries of heterogeneous materials junctions [1-3].The fuel elements of some thermal reactors also as the transducers and probes of reactor measuring and control devices contain the compounds of zirconium and steels. In nuclear thermal power there is no alternative to the disengaging adapters that guarantee the joints reliability; so, the problem of reliable safe adapters production is very actual.Now one can produce the joints between zirconium and steel by different methods: by explosion welding, simultaneous extrusion, diffusion welding, brazing etc. These methods of adhesion joints production between zirconium and steel provide the high strength (30-45 kg/mm^2) and may be successfully used in articles operating at low temperatures. The high temperature effect on such joints causes the formation of brittle phases on the conjugated part boundaries and to the loss of composite materials service properties.Laminar composite materials on the base of titanium-steel with barrier and damping interlayers of copper and niobium, zirconium-steel with interlayers of copper, chromium, niobium, vanadium and others materials ,developed in NSC KIPT, are used now in some members of contemporary space facilities, in nuclear reactor core; these members operate in the extreme conditions of quasi-stationary force and temperature regimes.The increase of thermal cycling endurance of LCM titanium-steel, zirconium-steel in wide temperature range is one of priority problems. Samples after some thermal cycling demonstrate the geometric parameters deviation of their initial value. The damping interlayer is subjected to the more forming: inside and outside diameter of copper ring near copper-niobium boundary is increased and near copper-steel boundary is decreased in comparison with the initial values. The main component (titanium and steel) forming is small. Independently of copper damping interlayer thickness the forming increases with the thermal cycles number increase.; after the equal number of thermal cycles the forming is the more the smaller is the copper layer thickness.Microstructure studies demonstrate the relationship between the composite structure change and its loss of strength under the variable thermal fields effect; these studies allow to examine the experimental data on the base of internal stresses gradient effect in composite on the monatomic processes defining the thermal fatigue progress kinetics. With the damping layer thickness decrease the stress gradient increases that causes the intensification of structure damage processes and the intensification of irreversible plastic deformation also as the redistribution of the "injurious" impurities and the accumulation of the excess vacancies.

The considered dependencies of LCM thermal fatigue evolution on different factors give the possibility to control the thermal cycling strength by the damping interlayer structure stability increase

and by the decrease of "injurious" .impurities content and by the decrease of excess vacancies concentration. Introduction of damping interlayer of microalloyed copper with one or some elements such as: scandium, yttrium, rear earth metals, zircinium, aluminium, boron, chromium, tin or phosphorus and of interlayer of microalloyed niobium with the addition of one or some elements such as: scandium, holmium, dysprosium, neodimum, praseodium, gadolinium, zirconium, boron and the interlayer thickness holding in the range of 0,2-1,2 mm results in the thermal cycling endurance rise in 1,7-3,5 times. In NSC KIPT the production of LCM of type titanium-steel, zirconium-steel is developed on the vacuum rolling mill DUO-170 [4]. Experimental-industrial batches of composite materials were produced with the use of microalloyed copper, niobium, chromium, vanadium as barrier and damping interlayers; physical-mechanical properties and the operating performances of obtained composites are investigated in extreme conditions.

REFERENCES.

1. Ivanov V.E., Amonenko V.M., Trony A.S. High-temperature vacuum rolling of metals, alloys and multilayer materials// UPhJ. -1978.-V.23. №11- P.1782-1789.

2. Amonenko V.M., Trony A.S., Lopata A.T. Production and properties of three-layers bands tantalum-niobium-tantalum. Electronics technique. Issue 2, -series 6. Materials. 1975. p. 22-28.

3. Lopata A.T., Neklyudov I.M., Chevtchenko S.V. Termal cycling of bimetal zirconium-steel for the adapting elements// Proceedings of the Conference: Problems of zirconium and hafnium in nuclear power. VANT, Kharkov, 1999.

4. Lopata A.T., Neklyudov I.M., Borts B.V., Chevtchenko S.V. Proceedings of 6-[th] International Vacuum Conference. Lyon, France,1999, p.35

PRINCIPLES OF CHOICE OF MATERIAL COATINGS FOR WORK IN MICROSHOCK OF A CAVITATION

Cherenega S.M., Loskutova T.V., Loskutov V.F., Iantsevitch C.V.

National Technical University of Ukraine "KPI", Kiev, Ukraine

The generalization of the researches, carried out by us, has allowed presenting dependence of size of deterioration of a material at cavitation (dV/dt) from microhardness and crack of stability by the following dependence:

$$\frac{dV}{dt} = \frac{dE/dt}{K_{1c}^{m} H_{\mu}^{n}} \quad (1)$$

Where E - energy of hydraulic impact. Under constant conditions at cavitation of influence size of capacity of hydraulic impact dE/dt = const. In view of it (1) it is possible to present as

$$\frac{dV}{dt} K_{1c}^{m} H_{\mu}^{n} = const = A_1 \quad , (2)$$

That is for identical conditions of experiment the size A_1 is constant. Factor of proportionality And reflects size of capacity cavitation, causing destruction of a material and there is a dimension [n · m/s] = [Dg/s]. We receive empirical dependence of deterioration at cavitation with microhardness (H_{μ}) and crack by stability (K_{1c}) of researched materials. Definition of parameters of a degree m, n and factor of proportionality A_1, connecting the specified characteristic with meaning of deterioration at cavitation (loss of weight on unit of the area for a time unit, or change of volume from time, if weight to normalize on density) carried out by the experimentally received results for coatings:

$Cr_{23}C_6$, Cr_7C_3, VC, ZrC, NbC, TiC, (Zr + Cr) C, [1] which rendered from a gas phase at the lowered pressure with use of powders of transitive metals, wood coal and four chloride carbons:

$$\frac{d\left(\dfrac{m}{\rho}\right)}{dt} K_{1c}^{m} H_{\mu}^{n} = const = A_1 . \quad (3)$$

For a presence of parameters of a degree m and n, at construction of dependence (2), used minimization functional

$$f(m,n) = \sum_{i=1}^{k} [[\Delta G_i - (K_{1c})_i^{m} (H_{\mu})_i^{n}]^2 , (4)$$

Here ΔG - loss of weight at cavitation i-ro of a sample. The parameters m and n, determining a minimum f (m, n), calculated with the help of a combination of methods of general and casual search and have established, that n = -0,313, and m = -0,724. After of a linearization of the equation (4) have received dependence of a kind:
$$\Delta G = A(K_{1c})^{m} (H_{\mu})^{n} , (5).$$
Also we used a method of the least squares for definition of size m, n and A, and have received the following meanings of factors:

A =1,953; m = -0,733; n = -0,384.

The equation connecting at cavitation of deterioration of coverings to their characteristics of cracks stability and microhardness, received on the basis of experimental results has the following kind:
$$\Delta G = 1,953 K_{1c}^{-0,733} H_{\mu}^{-0,384} . (6)$$

Carbide coatings in process of reduction of deterioration at cavitation settle down in the following line: (V-Nb)C → NbC→ ZrC → (V-Cr)C → TiC→ (Zr-Cr)C → VC→ $Cr_X C_Y$.

A similar line can be constructed for product of parameters $(K_{1c}^{0.733} H_{\mu}^{0.384})$, designed for carbide coatings

(V-Nb)C→ NbC→ ZrC → (V-Cr)C→ TiC →(ZrC-Cr)C →VC→ $Cr_X C_Y$.
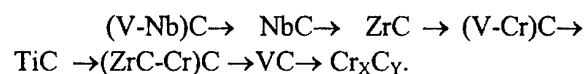
The submitted lines completely correlate, as against a line constructed in process of growth of microhardness carbide coatings and having the following kind:

(V-Nb)C → NbC→ ZrC → (V-Cr)C → TiC→ (Zr-Cr)C → VC→ Cr_XC_Y.
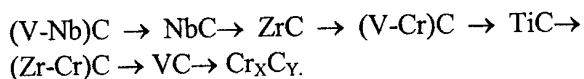
Also there is no correlation's between lines a crack of stability and deterioration of stability. Estimation of the characteristic of deterioration at cavitation on the offered dependence $K_{Ic}^{-0,738} \cdot H_\mu^{-0,384}$ A, will well be coordinated to experimental data cavitation deterioration of coatings, thus to the large meanings $K_{Ic}^{-0,738} \cdot H_\mu^{-0,384}$ there correspond higher stability of a material of blanket. [2-6]

The deduced mathematical dependence (5) on experimental data at cavitation of deterioration carbide coatings has proved to be true for bored and alloyed bored of phases, and also for gas thermal coatings. The comparison of settlement meanings at cavitation of deterioration, for a phase FeB 0,053 with experimental 0,075 has made an error 29 %, and for a phase (Fe, Cr) $_2$B (0,04 -0,033) - 17 %. Thus results at cavitation of deterioration bored of phases both the meanings of the characteristics of hardness and crack of stability will be coordinated on of a linearization of dependence of the equation (3), though the accounts of factors m, n and A in the equation (3) on the data for bored coatings did not carry out. By us are in addition investigated silicon - chromium coatings, as there was it borrows an intermediate rule both on stability at cavitation and on size of product of the characteristics a crack of stability on microhardness $K_{Ic}^{0,733} \cdot H_\mu^{0,384}$ from the investigated line of coatings. The experimental results at cavitation of deterioration (0,04) of a coatings of system Si-Cr and designed meanings (0,0029) of deterioration received according to the equation (2) under the characteristics of hardness (21) and crack of stability (0,02933) are close (divergence of results has made 0,75 %).

For multicomponent carbide coatings of system (V-Cr) the difference between experimental (0,032) and settlement meaning (0,03) of deterioration at cavitation has made 2,8.

Conclusions:

1. The criterion at cavitation of stability is offered which allows to carry out an estimation and to predict at cavitation of deterioration high and rigid metal diffusion and gas and thermal coverings on steels on parameters of their microhardness (H_μ) and crack of stability (K_{Ic}.) The mathematical parity of these sizes and display is received, but, that than more meaning $K_{Ic}^m \cdot H_\mu^n$, the less size of deterioration at cavitation. The parameters of a degree m and n, and n < m < 1 are determined.

2. Is established that the offered mathematical dependence allows estimating at cavitation of deterioration of various classes coatings on parameters of microhardness and crack of stability.

High cavitational stability can have the materials have or very high significance's of microhardness (H_μ) or very much plastics materials with large significance of a drag coefficient of intensity of distribution of a crack (K_1c).

.The literature.

1 .Лоскутов В. Ф., Хижняк В. Г., Куницкий Ю. А. Диффузионные карбидные покрытия. – Киев.: Техника, 1991. – 168 с.

2 .А. Г. Ворошнин, М. М. Абачараев, В. М. Хусид. Кавитационностойкие покрытия на железоуглеродистых сплавах. - Минск.: Наука и техника, 1986. – 248 с.

3. Чернега С. М., Лоскутов В. Ф., Хижняк В. Г. В сб.: Защитные покрытия на металлах. Киев.: Наук. Думка. 1986. – Вып. 20. – с. 44 – 83

4.Чернега С. М. О механизме разрушения композиционных эвтектических покрытий при кавитации.// Порошковая металлургия. 1998. № 7/8 с. 36 – 43.

5.Э Evans A. G., Charles E. A. Fractur toughness determination by indentation// V.Amer. Geram. Sos. – 1976. – vol. 59 № 7 – 8 – p.371 –372.

6 .Evans A. G., Wilshaw T. R. Quasi-static solid particle damage in brittle solids - I. Observations, analysis and implications // Acte Metallurgica. – 1976 y. Vol. 24 № 10 – p.936 – 956.

THE RESEARCH OF THE INFLUENCE OF ALLOYING ELEMENTS OF THE TRIBOTECHNICHAL PROPERTIES OF COMPOSITIONAL ANTIFRICTIONAL SELF-LUBRICATING MATERIALS

A.G. Kostornov, <u>O.I. Fuschich</u>, T.M. Chevychelova, A.D. Kostenko
Frantsevich Institute of material science problems, National Academy of Science, Kiev, Ukraine

Researches of tribological properties of powder materials on the basis of copper at the pressures till 10 Mpa and speeds of sliding till 1,0 m/s, i.e. at the conditions that are identical to the conditions of the work of the joints of friction of machines and devices have been conducted.

Powdered compositions on copper basis, containing alloying elements, some of them strengthen the load–carrying part of the composition, increase its mechanical properties, the others perform the role of a solid lubrication, responsible for the formation of a shielding pellicle have been researched.

Powder compositions were got form the powder mixtures by pressure with the followed agglomeration in the hydrogen. The mass content of alloying elements was changed in the range of 8-15 mass %.

The research of the friction was conducted in the air on the friction machine allowing at the same time to define the coefficient of the friction and the intensity of weariness. The friction was conducted on the steel XBG at the variable speeds of sliding and graded pressure.

The research was conducted in the air without the supplying of lubrication to the friction zone and at the presence of lubrication incoming to the working zone out of the sample interstices presenting in them in the result of their impregnation.

On the basis of the structure research and frictional properties of powder compositions the optimum content of the strengthening materials and their structural distribution necessary for the getting of non-wearable ground with good frictional characteristics was defined.

It was determined that with the toughening of the regimes of the tests the optimum content of strengthening elements is increasing in quantity.
While working without the lubrication anti-friction ability of the powder composition is developed in the course of the formation on the working surface of a shielding pellicle, the appearance and action of which is determined by the presence of a solid lubricating element in the material.

In the result of researches conducted the quantity of solid lubricating component that from one side is no leading to the weakening of the powder composition as a whole and from the other side is contributing to the formation of effectively acting shielding pellicle was optimized.

STATISTICAL MODELLING IN APPLICABLE SCIENTIFIC INVESTIGATION. PROBLEMS AND PERSPECTIVES

Murzin Lev, Murzin Aleksandr
Sevastopol National Technical University, Sevastopol, Ukraine

In mathematical modelling, it is possible to allocate two methods of modelling: analytical and statistical. The greatest distribution at the decision of technical problems was received with methods of analytical modelling.

For example, in materials of the international symposium" Advanced thermal technologies and materials" [1], in a significant part of reports directly or are indirectly used methods of mathematical modelling of an analytical direction on the basis of phenomenological theories. Use of such approach in the decision of complex technical and technological problems provides application of some assumptions which frequently have the important character and may serve as sources of essential sinfulnesses. Most typical such assumptions: the assumption of uniformity of structure of a material, an assumption of monotony of time dependences of change of internal sources of heat, etc., are used. The Account of such effects in model in the form of strict mathematical dependences while is impossible at a modern level of development of scientific representations about a nature of materials and the mechanisms determining course of technological processes.

For example, in work [2] authors mark complexity of use of the experimental data received in one conditions and their carry to other conditions on the basis of construction of the common mathematical model of complex process what, erosion of thermal protection for example is.
At construction of analytical models in complicated problems where are taken into account: the structure of a material, external influences, thermal and mass streams, - usually makes the common number of factors 20-30, at complex interrelations between them.

In analytical model, owing to mathematical difficulties of the strict description of interrelations it is necessary to be limited to consideration individual sections of multivariate space, it is artificial fixing all other connections between factors.

At use of statistical models such difficulties do not arise, as the formal description regressive model does not demand a formulation of a specific kind of connections between factors.

It is typical, that statistical estimations of errors do not result in publications, or the generalized estimations without revealing structure of making errors are given. Other example mathematical model of work ablating heat-shieldings, allowing to take into account in the obvious form interrelation of physical and chemical transformations and accompanying them swelling with structure and properties of a material [2]. The model is under construction on the basis of fundamental laws, such as: laws of preservation, the equation of a condition in system, the equations of the mechanics of polymers, reological equation of a condition etc., however, use of such powerful mathematical device for the description of the complex phenomenon nevertheless demands significant number of assumptions concerning structure of materials frame, matrix and other types that should cause essential errors in the received decisions on the basis of model.

Thus, large number of analyzed factors, and plurality of the physicomechanical and physical and chemical phenomena in investigated processes, compel authors of researches to accept significant assumptions and the simplifications lowering accuracy of received models.

On the other hand, for the description of the complex phenomena are used, as a rule, original under the form and on structure of model that complicates their use at change of conditions and research of the new phenomenon or new technological process.

All this complicates use of analytical models for wide application in various branches of engineering, technology of mechanical engineering.

Statistical models are deprived many of the listed lacks by virtue of their universal character

determining a kind of model and its structure. Due to universality of the mathematical form of record of model as a polynom of the certain degree it is possible to receive the unified decisions for various problems both practical, and theoretical character. On faculty of mechanical engineering and transport SNTU experience of application of statistical models is saved up at the decision of practical problems in various areas of a science and engineering.

So, program CORREAPPRO developed on the basis of methodology multifactorial modelling - oriented the correlation analysis and modified for use on IBM PC [3], allows to carry out the correlation analysis of a file of the experimental or literary data.

The analysis may be carried out on a file, volume of 200 data representing 40 parameters - properties of investigated objects. As parameters may be used physicomechanical properties of materials, heat-phisiical and thermodynamic characteristics, data about which it is possible to find in the literature or to receive in experiment.

Feature of statistical modelling is use at construction of model of statistical estimations as the quantitative measure determining influence of chosen parameter on an investigated parameter of process. Thus, within the framework of the correlation analysis it is enough to determine the appropriate factors of correlation between factors - parameters and parameters of investigated process and, in view of size of these factors to construct formal regressive model as a polynom of the certain degree for each of the factors included in model.

Factors of correlation characterize the interactions caused by a nature. Thus the mechanism of these interactions has no value for construction of statistical model.

In this connection, at construction of statistical model disappears necessity of revealing of functional interrelations between parameters of process and a spelling of mathematical expressions for the account of influence of the chosen parameter on an investigated parameter.

Hence, the errors connected to discrepancy of used models or with their wrong application, at such approach practically do not arise, that is essential advantage of statistical modelling in comparison with analytical.

The bibliographic list

1. Polezhaev J.V., Mihatulin D.S. Erosion: problems of modelling and improvement constructions /J.V. Polezhaev, D.S.Mihatulin//Col. Advanced thermal technologies and materials. Transactions of the international symposium (October 1997, s. Kaziveli, Crimea, Ukraine) part.2.-P.107-112., M.:Pub..-in MGTU named Bauman, 1999.

2. Timoshenko V.I. Problems of mathematical modelling of processes destruction heat-shielding materials and coverings in highenthalpic a stream gas./ V.I. Timoshenko //Col. Advanced thermal technologies and materials. Transactions of the international symposium, part 2. P. 116 - 118., M.: Pub. - in MGTU named Bauman,1999.

3. Murzin L.M. Program CORREAPPRO as means of the decision of problems of modelling in technology of machinebuilding/L.M.Murzin, A.V.Glushkov, F.A.Korneev//Tr. "Technology of machinebuilding. Problems and perspectives. Materials of scientific and technical conference. P. 115-118. SNTU, Sevastopol, 2000

ТЕПЛОВАЯ ЗАЩИТА СТЕНОК ВЫСОКОЭНЕРГЕТИЧЕСКИХ УСТАНОВОК

Аринкин С.М.

Институт тепло- и массообмена НАН Беларуси, Минск, Беларусь

Рассмотрена эффективность тепловой защиты стенок установок с температурой активного объема, исчисляемой тысячами и десятками тысяч градусов [1,2]. Это – плазменные реакторы [3], газофазные ядерные двигатели [4], камеры сгорания авиационных и ракетных двигателей, выполненные из пористых тугоплавких материалов с транспирационным охлаждением [5]. В работе [6] предложено в энергоустановках с водородным рабочим телом использовать легкокипящие соединения тугоплавких металлов, которые при температуре 15 – 350 °C переходят из твердого в газообразное состояние. Проходя через горячую пористую стенку они ее охлаждают, а на выходе при температуре 1200 – 1700 °C восстанавливаются. В пристеночном слое создается газопылевая завеса частиц металла. Она поглощает и рассеивает тепловое излучение в широком диапазоне длин волн. В работе [7] установлено, что такая среда при движении по каналу интенсивно укрупняется. Происходит непрерывное изменение поглощающих и рассеивающих свойств. В работе [8] получено, что в диапазоне длин волн теплового излучения $0{,}005 < \lambda < 1$ мкм наибольшую величину массового коэффициента ослабления излучения обеспечивают частицы с радиусами $0{,}03 \le r \le 0{,}1$ мкм.

С уменьшением размера частиц максимум ослабления излучения сдвигается в область ультрафиолета, для которого наибольшее экранирование обеспечивает газопылевая среда с размерами частиц $0{,}005 \le r \le 0{,}03$ мкм [9].

При температуре в активном объеме установки $10\ 000 \le T \le 100\ 000°C$ основное излучение приходится на диапазон длин волн $0{,}005 < \lambda < 0{,}04$ мкм. Это диапазон рентгеновского излучения и вакуумного ультрафиолета. Для поглощения и рассеяния излучения в этой области температур необходимо создать газопылевую завесу с размерами частиц порядка нескольких десятков ангстрем. Частицы с такими и меньшими размерами появляются только при непосредственном восстановлении соединений WCl_6, WF_6 на выходе из пористой стенки.

Источники информации.

1. Аринкин С.М. Способ защиты и диагностики стенки камеры сгорания. ИФЖ, том 74, №6, 2001.

2. Хеберлайн В., Пфендер Е. Пористое охлаждение стенок камеры сгорания. Теплопередача, №2, 1971.

3. Дресвин С.В. и др. Физика и техника низкотемпературной плазмы. М., Атомиздат, 1972.

4. Том Г.К., Швенк Ф.К. Системы на основе газофазного ядерного топлива. РТК, том 16, №1, 1978.

5. Газоохлаждаемые высокотемпературные реакторы. М. Атомиздат, 1975.

6. Аринкин С.М., Третьяк М.С. Способ защиты стенки высокоэнергетической установки, а.с. №130724, 1992.

7. Ослабление лучистой энергии газопылевыми потоками. Сб. "Теплообмен-78", Минск, ИТМО, 1978.

8. Хьюст Г. Рассеяние света малыми частицами. М., 1961.

9. Исследование коэффициентов ослабления излучения и индикатрис рассеяния газопылевыми средами. Отчет №1298, ИТМО – Нью-Йоркский университет,1976.

SECTION B.
SCIENTIFIC FUNDAMENTALS AND COMPUTER MODELS FOR THE PROCESSES OF MANUFACTURING MATERIALS AND COATINGS FOR OPERATION IN HAZARD CONDITIONS

"TWO_PHASE" SOFTWARE PRODUCT FOR SIMULATION OF ACCELERATION, HEATING AND MELTING PARTICLES IN GAS-DYNAMIC DEVICE PASSAGES

<u>Timoshenko</u> V.I., Belotserkovets I.S., Galinsky V.P., Zagny V.V., Kadyrov V.Kh.[1],
Kysil V.M.[1], Evdokimenko Yu.I.[1]
Institute of Technical Mechanics of NASU and NSAU, Dniepropetrovsk, Ukraine
[1]Institute for Problems of Material Science of NASU, Kiev, Ukraine

The following physical picture of processes is characteristic for technological devices of a high-speed gas flame spraying of coatings, thermo-abrasive processing and jet grinding. The particles together with combustion materials move to the gas-dynamic passage, in which there is their acceleration, heating and, in a case necessities, melting. The additional acceleration of particles takes place in a free supersonic jet. The acceleration of carrier gas in a gas-dynamic passage is made at shape of passage or by using of additional gas feeders. Terminating processes happen in an shock layer generated at impact of a two-phase jet about handled surface or at collision of jets. "Two_phase" [1] software product designed, in which the following computational model is implemented for a simulation modeling of above-stated processes.

The two-phase flow is described by a mathematical model of two-speed and two-temperature continuum. The gas phase is a mixture of combustion products of hydrocarbon fuels in a flow of an oxidant (oxygen, air). The solid phase consists of particles of a powder material. The two-phase flow in a gas-dynamic passage of the gas-dynamic device is described by quasi one-dimensional equations of gas dynamics which are taking into account friction and convective heat exchange of for a two-phase flow with the passage walls as well as friction and heat exchange between phases. The calculation of flow field in the gas-dynamic passage with a geometric way of flow control is carried out continuously from the inlet to outlet section of the passage. The calculation of a flow field in a passage of the gas-dynamic device using additional gas feeders for flow control is carried out with a series of calculations of sections between feeders and recalculation of flow parameters past the feeder. The parameters of a two-phase flow at the feeders outlet are calculated using balance rations on known parameters at feeder inlet and ones supplied through its walls.

The flow in a free two-phase jet is described by two-dimensional equations of turbulent boundary layer for a gas phase and two-dimensional equations of hyperbolic type for a disperse phase. Power and heat interaction between phases is taken into account through the additional source terms included in termed named combined equations. The influence of particles on a turbulence is not taken into account. The numerical integration of equations implements a stepping procedure along an axis of a jet.

The calculation of two-phase flow parameters in an impact layer is realized in two stages. Parameters of a gas phase calculates of installation method at first. Then monitoring particles place in a field of gas flow and their parameters are calculated along their motion trajectories. Thus the influence of particles on parameters of a gas flow is not taken into account.

"Two_Phase" software product allows calculating the parameters of two-phase flow in gas-dynamic passages in view of power and heat interaction between phases, passage walls friction and heat transfer through its lateral surface. The software product can be used for researches of thermogas-dynamic processes in the passages of gas-dynamic devices to most fully use chemical energy of a fuel for heating and acceleration of particles, as well as to select rational geometric parameters of passages. The software product provides a user with the information on its purpose, structure and capabilities. A brief description of physical and mathematical formulations of the problems solved is given. The software product provides means for formation and remembering of the problem input data to carry out current calculations. It ensures processing and storage of the calculation results.

The software product works in the interactive dialogue mode with using the terms and determinations from the data domain of software product purpose. The practical work with the software product does not require from the user a special training in the area of programming and learning special operating instructions.

The user's work with the software product is reduced to the following sequence of operations: choice of a problem; specifications of the input data of the problem according to the submitted prototype of

their defaults; the problem start-up for calculation; solution results representation of the selected problem on the monitor screen in the form of numerical or graphic information depending on selected kinds of solution processing; comparison of the obtained results with the earlier obtained results of the selected problem under different input data of the problem.

The use of the software product allows:
– to estimate discharge characteristics of the installation, gas-dynamic and thermo-physical characteristics of combustion products;
– to estimate the range of change in dynamic and power parameters of particles in the gas-dynamic device passage, in a free jet and in an impact layer;
– to calculate the field parameters of gas and particles in the gas-dynamic device passage and two-phase jet flowing out of the passage;
– to choose the geometric and regime parameters values of the gas-dynamic device for obtaining the maximum values of the particles power parameters;
– to calculate the composition of combustion products, their thermodynamic and thermophysical properties;
– to determine the disperse phase thermal condition (temperature field, degree of melting) at its motion in the of gas-dynamic device passage, in a free jet and in an impact layer.

User has an opportunity to present results of calculations as: tables of parameters at the gas-dynamic device passage outlet at various values of input parameters of the problem; diagrams of gas-dynamic parameters distributions along the gas-dynamic device passage axis; diagrams of parametric dependencies of flow parameters at the gas-dynamic device passage outlet on input parameters of the problem; isoline fields of flow parameters in the gas-dynamic device passage and free jet.

The designed "Two_Phase" software product utilized for research process of acceleration, heating and melting of particles from refractory materials in a gas-dynamic passage of a burning installation with using of additional combustion products feeders [2]. Feature of this process is the commensurability of melting temperature of particles with equilibrium stagnation temperature of combustion products of fuel. Therefore melting of such particles in a gas flow is possible only under condition of effective organization interchange of energy between combustion products of fuel and particles. For definition of a rational way of power transmission of combustion materials of fuel to particles the flow in gas-dynamic passages and jets was explored.

The optimization of regime and geometrical parameters of a gas-dynamic passage was made by measure of a maximum total energy of particles on outlet of gas-dynamic passage, thus the capability of their full melt was admitted. Optimum distance up to a substrate, on which the coating was put, was determined from the analysis of results calculations of the particles characteristics before it. The characteristics last were determined by series calculation of flow in a gas-dynamic passage, free jet and in an impact layer.

The carried out calculations for refractory materials (chromium, alumina, zirconium oxide and tungsten carbide) have shown [3], that for heating, melting and acceleration of particles from these materials are advisable use the gas-dynamic passage with two additional combustion products feeders. The dependencies of two-phase flow parameters on outlet of gas-dynamic passage with using of additional combustion products feeders from length of a site of heating (site between additional combustion products feeders) and ratio of consumption factors in additional Is shown, that the full degree of particles melt has an extreme at defined values of length of heating site and ratio of consumption factors in additional combustion products feeders. With increase of a dispersion of particles the efficiency of optimization of selection of these parameters grows.

1. Timoshenko V.I., Belotserkovets I.S., Galinsky V.P. Software and methodic support for numerical simulation of particles acceleration and heating processes under flame spraying / International conference "Materials and coats in extreme conditions: investigation, application, environmentally appropriate technology fabrication and utilization production", 17-22 September 2000, Katsiveli, Crimea, Ukraine. Thesis reports. - M.: Pb.h. MGTU nm. N.E.Baumana, 2000.
2. Timoshenko V.I., Belotserkovets I.S., Galinsky V.P., Kisel V.M., Evdokimenko Yu.I., Kadyrov V.Kh. Investigation operations in burner devices for a high-speed gas-flame powder material spraying with using flow effect // Engineering physical journal. - 2001.- V.74, N 6.
3. Timoshenko V.I., Belotserkovets I.S., Galinsky V.P., Kisel V.M., Evdokimenko Yu.I., Kadyrov V.Kh. Investigation operations of acceleration, heating and melting the particles from refractory materials in burner devices for a gas-flame spraying // Engineering physical journal. - 2002. - V.75, N 2.

COMPUTER MODELLING OF TEMPERATURE AND STRESSED-DEFORMED CONDITIONS OF COLD ROLLED STRIP AT ANNEALING

Timoshenko M., Timoshenko V.[(1)], Prykhod'ko I.[(2)]

[(1)]Institute of Technical Mechanics of the National Academy of Sciences of Ukraine and National Space Agency of Ukraine, Dnipropetrovsk, Ukraine

[(2)]Iron and Steel Institute of the National Academy of Sciences of Ukraine, Dnipropetrovsk, Ukraine

The production technology of cold rolled steel provides after rolling the re-crystallization annealing in units of continuous action or in bell-type furnaces. In bell furnaces heat treatment of strips conduct in densely winded rolls in a protective atmosphere of a nitrogen-hydrogen mix circulating on a closed contour or in the environment of pure hydrogen. Annealing process of strips coils pile from low carbon steel, for example, consists of stages of heating (1-3 steps) up to temperature 680-700 C°, endurances at this temperature during 15-20 hours, adjustable cooling with speed 5-25°C/hour up to temperature 550-650 °C under bell, noncontrollable cooling under muffle up to temperature 100 °C and the subsequent natural cooling up to an ambient temperature.

The bell-type annealing, besides known advantages, has the lack connected with adhesion (welding) of strips in coils at annealing process. At the subsequent unwinding a strip from a coil, owing to adhesion of coils at a separation of an external coil from a roll lines the plastic bend of a strip are formed. There is a defect of a surface "fracture". On conditions of adhesion (welding) at annealing process influence inter-coil pressure (which dependent in many respects from a roughness of a surface, deviation of thickness and non-flatness of strips), the maximal temperature of coils and duration of its action.

Distribution of inter-coil pressure on radius of a coils is formed depending on a roughness of a surface of a strip, a mode reeling (distributions of a tension and temperatures of a strip at reeling). Specificity of a problem consists that at cooling and heating of a roll in it there is a variable temperature field which causes additional thermal pressure which render essential influence on the condition of a roll is elastic - intense. In turn, at presence of thermal resistance on adjacent surfaces of coils which sizes are appreciably determined by inter-coil pressure, change of temperature in a roll depends on it is elastic-intense conditions. Mutual influence temperature and intense-deformed conditions of rolls essentially. Additional features in

statement of a problem are caused by a condition of surfaces of contacting coils (the roughness, the form of micro profiles). It may result in rapprochement of contacting surfaces in result micro profiles crumpling, and also to occurrence of breaks in distribution of temperature.

In connection with complexity of process of coils processing, the choice of technological parameters demands the all-round analysis of elements of technological process. Effective methods of this analysis are methods of mathematical, computer modeling of processes.

On the basis of the techniques submitted in [1,2,3], the algorithm is developed and the program is created for numerical modeling non-stationary thermal and intense - deformed conditions of strips rolls during the reeling on a drum, removals from a drum, heating and cooling of rolls. For calculation of temperatures with using set heat transfer coefficients and the protective gas temperatures cyclorama, simulating conditions heat exchange of a roll with high-temperature protective gas circulating on a closed contour in the bell-type furnace. The algorithm allows to take into account non-ideal thermal and mechanical contact on adjacent coils surfaces.

Components of algorithm.

1. Calculation of formation of the intense condition of a roll at strips reeling on a drum with the given law of change of a tension of a strip and distribution of temperature of a strip.

2. Calculation of change of the intense condition of a roll at its removal from a drum .

As a result of it initial distributions of temperature and parameters of intense - deformed condition of a roll are determined.

3. Step-by-step on time the decision of a problem with use of a method of splitting on physical processes:

- On the first half step on time parameters of thermal resistance are defined under given at the previous moment of time values of temperature and pressure (calculation on final ratio or interpo-

lation of the tabulated data) and the problem of calculation of a roll temperature is solved. The common algorithm of the numerical decision of this problem is described in [2].

- On the second half step it is settled an invoice the intense condition at the given temperature field in view of change of character of mechanical contact between the next coils. This problem is considered under quasi-steady approximation. The system of the equations is solved by a sweep method.

Opportunities of the developed algorithm are illustrated by results of numerical modeling of a temperature and a inter-coil pressure in the rolls received coiling of 2600 coils of 0,5 mm thickness strip steel. Reeling it was carried out with a constant tension of a strip $\sigma_0 = 25$ N/mm^2. The condition of a roll is analyzed at winding on a drum, after removal from a drum with the account contacting surfaces micro profiles crumpling and a thermal resistance.

Calculations strips reeling on a drum were carried out in view of change of a thinness coils adjacency. It is shown, that as result of strip surfaces micro profiles partly renewing a pressure upon a drum in process of a strip winding grows and asymptotically tend to a constant value. Since 600 coil pressure upon a drum, reaching value $0,095\,\sigma_0$, does not depend on amount of the reeled - up coils. It is shown also, that as result of the partial restoration surfaces adjacency at unloading a roll after removal from a drum, inter coil pressure in the most part of a roll remains same as in a roll on a drum.

Taking into account the thermal resistance caused leaky coils adjacency results in essential increase of gradients of temperature in external coils of a roll.

Calculations of a roll intense condition in view of thermal resistance and at ideal thermal (but not ideal mechanical) contact between surfaces of layers show, that the account of thermal resistance results in the big temperature pressure . Therefore at computer modeling it is important to have the most exact, it is better – experimental, data about dependence of thermal resistance from inter-coil pressure.

As follows from the analysis of the received results, because of surfaces rough strips thermal resistance, the thermal pressure is located on the sites adjoining to external and internal coils, where their level initially (after removal from a drum) lower.

Therefore in the basic internal part on radius of a roll thermal pressure and consequently also probability adhesion (welding) in conditions of high temperatures are less.

1. Mazur V.L., Timoshenko V.I. Calculation of the intense condition coil-type cylinders// Mechanics of composite materials. Riga: Zinatne, 1982.-N 5.-P.880-886.
2. Timoshenko M.V. Numerical modeling of heat exchange in multilayered designs with the generalized nonideal contact//ÈÓÆ. - 1996. - Ó.69, N 5.-P. 773-778.
3. Timoshenko M.V. Temperature and is stressed-deformed conditions coil-type cylinders.// Technical mechanics.- N 2, 1999. - P. 53-61.

COMPUTER SIMULATION STUDY OF THE ATOMISTIC PROPERTIES OF ARTIFICIAL METALLIC SUPERLATTICES AND SEMICONDUCTOR HETEROSTRUCTURES

Masuda-Jindo K., Kikuchi R.[1]
Department of Materials Science and Engineering, Tokyo Institute of Technology, Nagatsuta 4259, Midori-ku, Yokohama 226-8503, Japan
[1]Materials Science and Mineral Engineering, University of California, Berkeley, CA 94720-1760, U.S.A.

The atomic and electronic structures of both metallic and semiconductor heterostructures are studied by using the path probability method (PPM) coupled to the tight-binding electronic theory. We focus our attention on the following features: (i) For metallic multilayers, like Cu/Pd, Cu/(Ni,Fe), Ag/Pd and Au/Ni systems, we investigate the effects of interface mixing and modulation period on their elastic and mechanical properties, (ii) For semiconductor heterostructures like $Ge_xSi_{1-x}/Si(001)$, GaAs/AlAs and GaN/sapphire, we investigate the stability and properties of the heteroepitaxial layers in conjunction with the interface defects and interface mixing. The atomic diffusion through the heterostructures is studied via vacancy mechanism of diffusion using the pair approximation of PPM. The effective pair interaction energies between the constituent atoms are derived using the zeros-poles method taking into account the misfit strains at the interface. It has been found that the interface defect structures and interface mixing influence quite significantly the mechanical, electronic and optical properties of the above mentioned heterostructures.

Keywords: Path Probability Method, Semiconductor Heterostructure, Tight-Binding Method, Metallic Superlattice, Supermodulus Effect

PROBLEMS OF THEORY AND PRACTICE OF CREATION OF CARBON - CARBON COMPOSITE MATERIALS

Karpenko Vladimir, Skachkov Victor[1]
State works of carbon carbon composite materials «Uglecompozit», Zaporozhye, Ukraine
[1]Zaporozhye State engineering academy, Zaporozhye, Ukraine

CCCM is a three-component composite based on carbon. One of its components are fibrous forms i.e. carbon fibres, the second component is a carbonized polymeric matrix based on phenol-phormaldehyde resins, the third component is pyrolytic carbon deposited in the porous structure of the composite.

The dependence of basic structural components of viscose-based carbon fibres on their formation temperature has been shown (interplanar spacing is d002, crystallite sizes La, Lc). The parameters of the structure uniquely determine macroscopic mechanical properties of fibres. The dependence of the modulus of elasticity, the strength on the treatment temperature of carbon fibres, sizes of crystal formations and basic parameters for obtaining carbon fibres are given.

Integrated study of matrix-forming material, i.e. a binder based on phenol-phormaldehyde resins has been carried out. Kinetic equations for the binder curing have been stated, the dependence of modulus of elasticity as well as shear on temperature and duration of curing have been presented.

The problems of modification of the binder with carbon and carbide-forming components have been considered. The mechanism of influence of modifying components on the basic properties of CCCM has been studied. Special consideration has been given to the determination of quality indices of modified binders (sedimentation of components, density, viscosity, period of viability).

Carbonization processes which specify the structure and properties of CCCM are of utmost importance. The methods of thermal gravimetric analysis were used for the determination of carbonization rate, chemical composition of CCCM dependent on the process temperature has been studied. The basic parameters of carbonized CCCM under various process conditions have been evaluated, the dependence of porosity on thickness of the carbonized materials, distribution of thermochemical shrinkage and strength properties has been defined.

Using the methods of statistical micromechanics of non-uniform media a mathematical model of CCCM carbonization process has been defined, which takes into account thermochemical shrinkage as well as thermochemical expansion of components and makes it possible to determine elastic and strength characteristics of the material for a predetermined temperature. The obtained calculation results with sufficient reliability coincide with the test results of carbonized CCCM. The constructed model makes it possible to optimize carbonization processes and minimize thermochemical shrinkage, to decrease porosity and improve mechanical characteristics of carbonized CCCM.

The most crucial stage of the manufacturing technique for CCCM is the densification of the porous structure (filling of pores with pyrolytic carbon). The densification is carried out in an isothermal-type flow reactor. In such a reactor both homogeneous and heterogeneous reactions are observed. The reactor gas, methane, is decomposed within a reactor with formation of radicals, heavy saturated and unsaturated hydrocarbons as well as commercial carbon. Initial gas and products of its homogeneous transformation spread to heated CCCM surfaces, spread to porous structure and decompose on the surface as well as in the pores with formation of a solid deposit, i.e. pyrolytic carbon.

A homogenous and heterogeneous-type mathematical model containing equations for the transfer of products and substances with due regard of their chemical transformation within a reactor as well as a porous structure of CCCM in the process of densification, has been developed for the description of the densification processes. The methods for determination of constants for the rates of homogeneous and heterogeneous reactions accompanying the process of pyrolytic densification have been developed.

The suggested mathematical model has been successfully tested for the calculation of densification processes for long profiles (angles, channels), shell structures and plates from CCCM. Design parameters of density and porosity distribution over the wall thickness of the material to be densified with an error not exceeding 8 %, corresponded to the data received in actual processes.

The technology for CCCM manufacturing, used at production sites, makes it possible to obtain products with various geometrical shapes and sizes: cylinders and cones with any cross section, long profiles, thin and thick plates, pipes and disks.

The manufactured CCCM are used as constructional materials, high-temperature insulation, heating elements, crucibles and thermal units in electrical vacuum furnaces.

MATHEMATICAL MODELING OF NITRIDE MATERIALS COMBUSTION SYNTHESIS UNDER THE HIGH PRESSURE

Grachev V.V., Borovinskaya I.P.

Institute of Structural Macrokinetics and Materials Science, RAS, Chernogolovka, Russia

Nitride ceramic materials (e.g. BN, AlN, Si_3N_4) possess a great potential for wide application in different areas of industry. This is due to good combination of their properties for use at high temperatures in corrosion environment. One of the promising methods of the nitride materials production is a combustion synthesis (self-propagating high-temperature synthesis - SHS) from compacted powders of corresponding components (e.g. B, Al, Si) under high pressure of gaseous nitrogen (an order of several hundreds of MPa). Already in the first experiments [1] studying combustion mechanism of such systems, the important role of the process of gaseous reagent filtration through a porous substance towards the reaction front was revealed. Practically, the combustion modes at natural filtration of an oxidizer, when a pressure difference controlling filtration appears spontaneously due to the oxidizer consumption in the combustion front, are widely applied. These combustion regimes are the subject of theoretical modeling in this work.

The compacted sample composed of a solid reagent and diluent powders in the atmosphere of gaseous reagent is considered. The left edge of the sample is ignited by a short-term thermal pulse, which initiates the combustion wave propagation due to the heat released during the exothermic gas - solid reaction yielding a solid product (nitride material). Lateral surface and edges of sample are assumed to be gas-impermeable. Physically, it is possible either when the sample is jacketed or it occupies entire inner volume of reactor. In this case the combustion is possible only due to the gaseous reagent located in the sample pores, and the initial gas pressure is assumed sufficiently high so that the combustion wave propagation could have place.

For describing the processes of heat-mass transfer, proceeding in the sample during the filtration combustion, the time-dependent system of equations [2] is used, which reflects the laws of the conservation of masses for solid and gaseous reagents, energy, the equation of state of perfect gas and Darcy's law. In the absence of heat and gas flows through the sample surface, the distributions of temperature, pressure and conversion degree are the functions only of longitudinal x coordinate. Previously, one-dimensional steady state combustion modes were analyzed in [3], where the criterion of the realization of combustion modes with the monotonic and non-monotonic pressure profiles of gaseous reagent was obtained. The same result is obtained in this work by another method, which made it possible to derive distribution and maximum value of pressure in the sample in the explicit analytical form. Furthermore, in contrast to [3] it became possible to obtain a physically correct dependence of the maximum pressure value and the coordinates of maximum in the entire range of a change in the important parameter L, which is the ratio of the scales of the filtration zone and the heat effected zone.

Actually, a steady state combustion mode can be observed only if the characteristic scales of the heat effected zone and the filtration zone are substantially lower than the length of the sample. The first condition usually is satisfied, and the latter can be broken. Evaluations of the filtration zone scale d for the characteristic values of combustion velocity $\sim 10^{-3}$ -10^{-2} m/s, filtration coefficient $\sim 10^{-11}$ - 10^{-9} $m^4/(N\ s)$ and the stoichiometric pressure $\sim 10^8$ Pa give the values of $d \sim 10^{-1}$ -10^2 m, i.e., in the best case, the filtration zone scale is compared with (if the sample length is several tens of centimeters), or considerably exceeds the length of real samples. Under these conditions, quasi-stationary combustion modes are realized, which have not been described earlier in the literature for the situation in question.

In connection with the open systems (presence of the gas exchange through one of the ends of the sample), quasi-stationary regimes were analyzed in works [4, 5]. In this work quasi-stationary combustion modes in the closed volume at high initial pressures of gas are examined, when initially in the pores a significant quantity of an oxidizer is contained (in [4, 5] the initial content of

gas in the pores was disregarded, it corresponds to low pressures).

The pressure difference, which controls the delivery of the oxidizer to the reaction front, appears after the stage of ignition. Since in the analyzed case the size of the filtration zone is compared with or exceeds the length of the reactor, the gas, which is initially located in the pores, manages to reach the front in the quantities, which are sufficient for the complete conversion of the solid reagent, the quasi-stationary regime with the maximum velocity of combustion is realized. In proportion to the propagation of the combustion wave and gas consumption there comes a moment, when the pressure difference varying in the magnitude does not ensure the required filtration flow any longer, and the combustion transforms to the regime of incomplete conversion with the progressively reduced conversion degree. In contrast to [4, 5], in the case of the closed volume, the quasi-steady-state of the process is developed not only in the constantly varying length of the filtration zone, but also in the varying value of the pressure in the end (in [4, 5], pressure in the open end is preset). The specific character of the problem is developed also in the fact that although the propagation of the combustion front is controlled by the filtration counter flow, the observed process picture is a reverse one that is described in [4]. At first, the combustion regime with complete conversion is realized, then it transforms to the regime with incomplete conversion.

It is well known, that with the specific values of the parameters, the steady state combustion mode can become unstable due to the unbalance of the processes of heat-mass transfer inside the combustion wave. In this case the realization of self-oscillating combustion mode is possible. In [6] on the basis of the numerical calculations of the one-dimensional time-dependent system of equations, the conclusion was made that at high pressures, the self-oscillating regimes were realized only at the degeneration of the filtration system into the gasless one. The calculations carried out in this work show that the self-oscillating regimes are possible in the wider parametric area. The profiles of temperature θ and conversion degree η at the self-oscillating combustion are shown in figure with the equal time intervals. It is possible to see that the

pulsations appear only at the stage of the combustion regime with complete conversion and disappear at the subsequent quasi-stationary stage with the incomplete conversion.
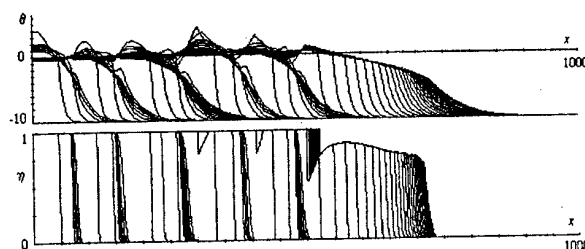
A difference in the combustion modes during the nitrides synthesis can affect the structure of the obtained material, since in the self-oscillating regime during the flash, the maximum temperature in the reaction zone considerably exceeds the temperature reached in the mode with the constant combustion velocity.

LITERATURE

1. Merzhanov A.G., Borovinskaya I.P., Volodin Yu.E. "On the Mechanism of the Combustion of Porous Metallic Samples in Nitrogen", Dokl. Akad. Nauk SSSR, 1972, vol. 206, № 4, pp.905-908.
2. Grachev V.V., Ivleva T.P., " Surface and Layer-by Layer Combustion Modes in Gas-Solid Systems", Inter. Journal of SHS, vol.7, no1, 1998, pp.1-19.
3. Aldushin A.P., Merzhanov A.G., Seplyarskiy B.S., "For the Theory of the Filtration Combustion of Metals ", Fiz. Gor. Vzryva, 1976, no.3, pp. 323-332.
4. Aldushin A.P., Ivleva T.P., Merzhanov A.G., Khaykin B.I., Shkadinskiy K.G., "Combustion Front Propagation in the Porous Metallic Samples during the Filtration of Oxidizer ", The Combustion Processes in Chemical Technology and Metallurgy, Chernogolovka, 1975, pp.245-252.
5. Aldushin A.P., Seplyarskiy B.S., Shkadinskiy K.G., "For the Theory of Filtration Combustion", Fiz. Gor. Vzryva, 1980, no.1, pp. 36-41.
6. Seplyarskiy B.S., Aldushin A.P., Shkadinskiy K.G., " Non-steady-state Phenomena during the Filtration Combustion", Chemical Physics of the Processes of Combustion and Explosion. Condensed Systems Combustion., Chernogolovka, 1977, pp.29-32.

87

INFLUENCE OF A RANDOM STRUCTURE OF RAW MATERIAL ON SHS-PROCESSES IN THIN FILMS

Grinchuk P.S., Rabinovich O.S., Pavlyukevich N.V.

Luikov Heat and Mass Transfer Institute, National Academy of Sciences of Belarus, 220072, 15 P.Brovka Str, Minsk, Belarus. E-mail: gps@hmti.ac.by

In the present work a case of combustion in a two-dimensional heterogeneous *random* medium is considered when the characteristic scales of combustion wave are less than the sizes of structural elements of a reacting system. Mechanically activated powder mixtures of intermetallic compounds (e.g., Ni-Al, Fe-Al, Ni-Ti, etc.) diluted by an inert component with the purpose to improve some physical properties (solidity, heat resistance, etc.), are the prototypes of such systems. It is shown that in these systems a *percolation combustion regime* is possible. In this regime the combustion process has a form of successive ignition of connected combustible (mechanically activated) particles constituting a percolation cluster. This cluster extends over the whole system, contrary to finite clusters, which locate in the small regions of the system. In this work we investigate the conditions, under which the propagation of the SHS process can occur in the percolation regime.

Numerical simulation of gasless combustion of 2D heterogeneous random systems have been performed. The following model of such system is adopted in the present study. The basic element of the model is an elementary cell. It includes a solid phase (the effective particle) and chemically inert gaseous inter-layers. The elementary cells are placed in the nodes of a square lattice of the size $L \times L$. All cells have similar physical properties (density, thermal conductivity, etc.) and geometrical characteristics (shape and size). They are different only in chemical composition of the solid phase: a cell contains either the mixture of components in a fixed proportion (a reactive cell) or an inert substance (an inert cell). It is supposed that, in the initial state, the components in a reactive cell are mixed uniformly. The kind of each cell is determined on the random basis: a cell is either reactive (with a given probability p) or it is inert (with the probability $1-p$). The local chemical composition of a reactive cell (conversion degree $\_(x,y)$) varies in the course of reaction propagation. Unlike the existing models of random-media combustion [1,2], the developed approach treats each particle as a macroscopic object with its own nonstationary temperature and concentration fields.

Proposed model is described by the following system of equations for dimensionless variables:

$$\frac{\partial}{\partial \tau}\left[\Theta_{ij}(x,y,\tau)\right] = S\left(\frac{\partial^2 \Theta_{ij}}{\partial x^2} + \frac{\partial^2 \Theta_{ij}}{\partial y^2}\right) + c_{i,j}^{(0)} W\left(\Theta_{ij}, \eta_{ij}\right) - \chi\left(\Theta_{ij} - \Theta_0\right),$$

$$\frac{d}{d\tau}\left[\eta_{ij}(x,y,\tau)\right] = \gamma W\left(\Theta_{ij}, \eta_{ij}\right),$$

$$W\left(\Theta_{ij}, \eta_{ij}\right) = \exp\left(\frac{\Theta_{ij}}{1 + \beta \Theta_{ij}}\right) \cdot \exp\left(-m\eta_{ij}\right),$$

where $i=1..L$ and $j=1..L$ are sequence numbers of a cell in x- and y-direction, L is the size of the system, $c^{(0)}$ is the initial concentration of the fuel in a cell ($c^{(0)}$ is equal to 1 or 0), Θ is dimensionless temperature and χ is dimensionless heat-loss parameter. The heat fluxes at the boundaries of a cell are determined by the temperature difference and Biot number Bi.
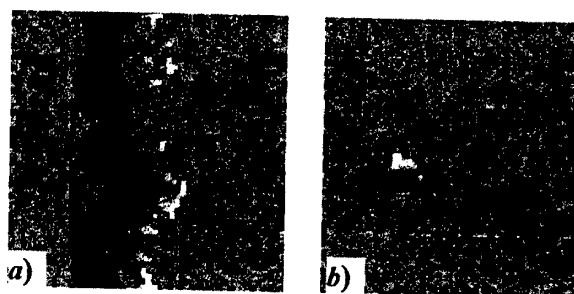
*Fig.*1. *Frontal (a) and percolation (b) regimes of combustion wave propagation in a random heterogeneous medium (temperature field). The increase in the temperature is represented by the change of color from dark to light. Part of combustible particles p is 60 %.(□- inert cells,▦- reactive cells belonging to finite clusters, ▩ - reactive cell belonging to a percolation cluster).*

Some of our modeling results presented in Figs. 1-3. Figure 1 demonstrates the examples of two different combustion regimes in 2D random heterogeneous system. Estimations and numerical modeling have shown that percolation regimes are possible if three conditions are satisfied. The first of them is that each particle can burn independently, i.e. the ratio of the combustion zone scale to the particle size should be less than

unity and the heat exchange between particles should be hampered. The second condition says that the heat losses should be not far from the extinction limit. The third condition relates to the initial organization of a medium: the percolation regime of combustion is possible if the concentration of combustible particles is in a vicinity of a percolation threshold [3].
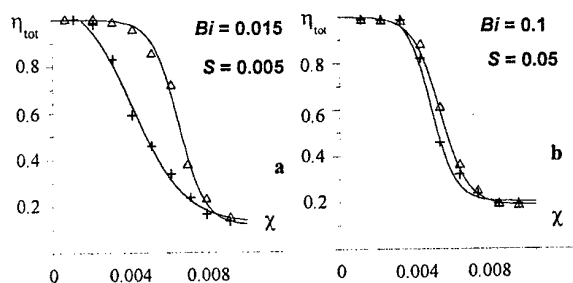
Fig. 2. *Mean conversion,* η, *in the random heterogeneous systems of the size* 25×25 *versus dimensionless heat-loss parameter,* χ *(see comments in text).* $\triangle$ - *percolation cluster is present;* + - *percolation cluster is absent.*

The influence of a combustion regime on a final product structure can be obviously shown by the example of mean degree of conversion of combustible cells (Fig.2). In this figure case *a)* corresponds to percolation regime and case *b)* to frontal regime of combustion. The critical values of the heat-loss parameter χ have been also found for regions of system parameters, when existence of a percolation cluster of reactive particles possesses key advantages for combustion wave propagation in comparison with the case when such a cluster is absent.
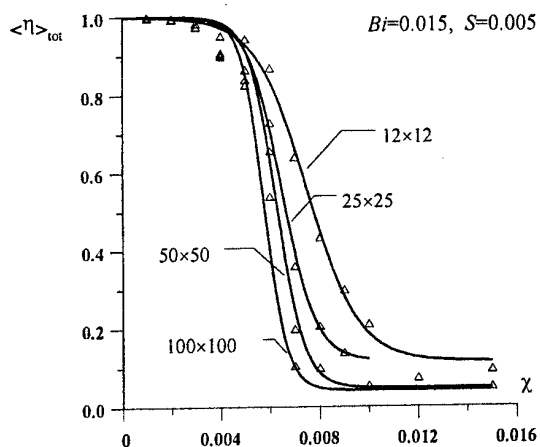
Fig. 3. *Dependencies of the mean conversion on the heat-loss parameter for different system sizes (all other parameters are the same). Only cases, when percolation cluster is present.*

The influence of the system size on the mean degree of conversion has been studied for systems with the number of particles 12x12, 25x25, 50x50 and 100x100 (Fig.3). We have to point out once again that predicted regime of combustion could essentially influence the structure of SHS-products. So, in a number of experimental works on burning of SHS-systems, samples were observed which did not burn out or burned very for a certain ratio of mixtures [4-6]. In the proposed approach, the given phenomenon finds natural explanation.

We suppose that the first candidates for percolation regimes of combustion are SHS-processes in thin films and coatings. The following list presents SHS-systems where percolation combustion could be also reveal:

1. SHS-systems near the concentration limits of combustion;
2. Mechanically activated systems with relatively low degree of activation (Ni-Al, Fe-Al, *etc.*);
3. Diluted metal-oxide systems (Al-Fe$_2$O$_3$, Al-NiO, *etc.*);
4. Multi-component systems with substantial difference in adhesion properties of components.

ACKNOWLEDGEMENTS

REFERENCES

1. A. Varma, A. S. Mukasyan, and S. Hwang, *Chem. Eng. Sci.,* **56**, 1459 - 1466 (2001).
2. N. Provatas *et al.,* *Phys. Rev. E*, **51**, 4232 (1995).
3. D. Stauffer and A. Aharony, *Introduction to Percolation Theory*, 2nd ed., Taylor & Francis, London (1995).
4. Frolov Yu.V, Pivkina A.N. *Comb. Explos. Shock Waves*, **33** (5), 3-19 (1997).
5. S. W. Jo et al., *Acta Mater.*, **44**, N 11, 4317 (1996).
6. A. E. Grigoryan et al., Refractories and Technical Ceramics, N 11, 7 – 11 (1999).

ESPECIALLY STRONG AND DURABLE POROUS BLANKETS HAVING HONEYCOMB STRUCTURE

Shapovalov V.I., Loutfy R.L.
Materials and Electrochemical Research Corporation, Tucson, USA

Introduction. Porous surface on article is necessary when one would like to give the surface special property, which is different from the bulk material. For example, porous surfaces can results in components with surfaces with a low friction coefficient, increased light absorption coefficient, controlled heat and acoustical wave absorption, or increased intensity of heat exchange between a surrounding medium and the articles. Porous surfaces can also results in the increase surface area of an article to change decorative properties, or to reduce the level of mechanical resistance of surface layer to an attrition or cutting. It is also extremely important to have a strong interface between the porous surface and the bulk materials even at high level of porosity. A unique method is proposed to produce novel materials with special porous surface that is strongly bonded to desired structure bulk materials as space structure of high-performance heat exchangers and cooling panel for hypersonic and space vehicle.

Unfortunately, the currently available ways of obtaining of porous coverings on metal or ceramic do not allow having sufficient durability at porosity more than 40 %. It is almost impossible to supply strong enough adhesion of the porous layers to solid body. Besides the organization of required pore space structure represent very serious technical problem and obtaining of honeycomb structure is almost impracticable in real technological process.

Technical Approach. We offer to create rather simple and inexpensive technological process, which will allow solving two most serious problems with creating porous structure on a surface of monolithic metals and ceramics articles:

*   Considerably to increase toughness of a layer and its junction with a monolithic matrix,
*   To realize honeycomb type porosity forming, either closed spherical or ellipsoidal pores.

Scientific basis of the proposed project is based on the recently discovered gas eutectic transformation [1-3]. This concept is based on the decomposition of hydrogen saturated fluid into solid and gaseous phases simultaneously, at temperatures lower than gas eutectic equilibrium. This phenomenon creates porosity and the degree of porosity; shape and the pore size are determined by: hydrogen concentration, direction and rate of solidification, and gas phase pressure at the solidification. The porous materials obtained in such a way (named *gasars*) differ from the conventional porous materials by having much higher toughness and structure variety as contrasted to traditional [1-3]. No melt foaming occurs because the gas is evolved as the melt freezes. The main process variables that govern the amount of porosity and the size, shape, and orientation of the pores are the hydrogen level in the melt, gas pressure over the melt in solidification, direction and rate of heat removal, and alloy chemical composition. By changing these variables, one can control the gasar pore structure over a wide range.

The technological scheme to produce the porous coatings includes two subsequent stages:

*   melting of solid article surface layer with simultaneous saturation of melt with hydrogen to required concentration,
*   solidification of the melted layer at specific external parameters.

Melting of a surface metal layer while keeping up the larger part of the article in solid state is today an easy realizable technical problem. For this purpose may be used electrical arc, laser, plasma flux, induction heating, flow of elementary particles or ions, intensive friction, concentrated solar radiation, energy of explosion. The first four methods are the most suitable to for our proposed technology. To ensure the required level of hydrogen concentration in the melted layer, three methods we used:

*   Preliminary product surface saturation with hydrogen from the gaseous phase or by the way of electrolysis in other unit.
*   Coating of the surface before melting with the layer of substance which actively releases

hydrogen on heating (hydrides, liquid, solid or viscous hydrocarbons, paper type porous materials impregnated with water).

- Placement of articles in hermetically sealed chambers, filled with hydrogen or a mixture of hydrogen with nitrogen or argon.

The general model of the saturation of the technology is shown in the Figure 3. Commonly we obtain thing solid skin on the top of article (see top figure). The skin can be removed by machining or chemical etching. Using soft energy blasting we can make open pores directly after scanning (se bottom figure).
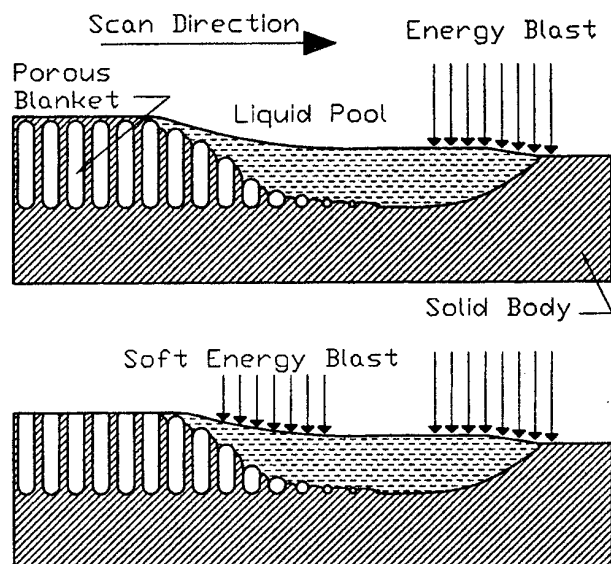
Model of the process taking place at the liquid pool saturation from the gaseous phase (displacement of the sample from the right to the left in present figure): vertical arrows denote the flux of energy (arc, plasma, laser ray)

1. Shapovalov V., Method for manufacturing porous articles U.S. Patent No. 5,181549, January 26, 1993.
2. Shapovalov V. Porous Metals. MRS Bulletin, April, #4,1994,p.24-29
3. Shapovalov V. Formation of Ordered Gas-Solid Structures via Solidification in Metal-Hydrogen Systems. Porous and cellular materials for structural applications. Symposium held April 13-15, 1998, San Francisco, California, USA. MRS Symposium Proceedings Volume 521, p. 281-290
4. Shapovalov V., Apprill J., Baldwin M., Maguire M., Miszkiel M., Production of Gas-Solid Structures in Aluminum and Nickel Alloys by Gasar Processing. Proceedings of the 1999 International symposium on Liquid Metal Processing and Casting, Santa Fe, New Mexico, February 21-24, 1999, p. 322-329
5. Shapovalov V.I. Porous Metals. Invited paper from Massachusetts Institute of Technology, for book "Materials in the next Millenium", 2000.

MATHEMATICAL MODELING OF CHEMICAL CONVERSION OF THIN-LAYER EXOTHERMIC MIXTURES UNDER REPEATED ACTION WITH AN ELECTRICAL SPARK DISCHARGE

Seplyarskii B.S.[(1)], **Ivleva T.P.**[(1)], **Levashov E.A.**[(2)]

[(1)]Institute of Structural Macrokinetic and Materials Science RAS, Chernogolovka, 142 432 Russia
[(2)]Research Center of SHS at the Institute of Steel and Alloys, Moscow, 117 936 Russia

The thermic regimes of a novel version of the process of thermoreactive electrospark strengthening (TRES) of the surface [1] has been for the first time studied with the use of the methods of mathematical modeling. The experimental procedure has been performed according to the following scheme. A 40-100 μm thick layer of a reactionable mixture of a certain composition is placed onto the surface. An electrical discharge induced by the repeated contact of the electrode to the sample to be strengthened provides the green mixture heating at the contact point. An as-initiated chemical exothermic reaction of the components results in the formation of a protecting layer on the sample surface. The present version of the method saves the electrode material and the required performance characteristics of the coating are achieved by variation of the green mixture composition, the thickness of the working layer, and the power and duration of the spark discharge.

The following model process is considered. At $t = 0$, an electrode-cathode is brought to the contact with the green mixture layer placed onto the alloyed surface and closes the electrical circuits. The components of the reactionable layer are heated with the electrical current applied. A sharp increase in the rate of the chemical reaction in the surface layers brought about by the substance heating may lead to the green mixture ignition and its burning out. It is believed that the main resistance is located on the electrode-green mixture interface and the greater portion of heat is evolved therein. It is also supposed that the energy of the heat release is constant and proportional to that of the electrical discharge. Therefore, a permanent thermal flow on the surface of the electrode-green mixture interface (the boundary conditions of the 2nd kind) can be used in the mathematical description of the TRES process. At $t = t_h$, the electrode is removed from the alloyed surface, the electrical circuit is broken and the adiabatic boundary condition is achieved on the surface layer of the green mixture. In $\Delta t = t_{ad}$, the electrode is again brought to a contact with the alloyed surface and the process of heating is resumed. Thus, mathematics modeling of the process of the alloying coating deposition with the use of the TRES modified method is reduced to the study of the thermic regime of the process of chemical conversion of the reactionable substance layer. The main goal of the study is to find such values of the governing parameters that could allow one to perform TRES under controllable conditions, i.e. to perform the green mixture conversion to a coating without considerable overpassing of the pre-given level of heating. In our calculations, the heating level has been fixed at the temperature of the green mixture layer of a large thickness (an infinite one in the limiting case) ignition T_{ig} with a constant energy flow - q_0. As known from the thermic theory of ignition [2], if the temperature on the green mixture surface is 2-3 characteristic intervals RT_{ig}^2/E higher than T_{ig}, the further temperature growth is of a progressive character (the higher is the temperature, the high is the heating rate) and is well described by analytical formulas used in the theory of adiabatic thermic explosion [3]. It is particularly important that the control over the temperature growth at the stage of thermic explosion is practically impossible. Therefore, one must not let the green mixture heating over T_{ig}, since it can lead to the coating overburning and non-uniformity of its physicochemical properties. In the present study, the T_{ig} value has been determined with the use of the methods of the thermic theory of ignition [2, 3].

The $L_l = L_{cr}$ values for various θ_N, P, c_λ, that could provide overheating of the green mixture at $L_l < L_{cr}$ and the condensed products at $0 < \tau \le \tau_{cov}$ not higher than 1-1.5 characteristic

intervals RT_{ig}^2/E, have been derived by numerical computation of the initial problem. It has been found that such conditions can be practically always achieved at $L_1 < 1$. Therefore $L_1 = 1$ has been taken for L_{cr}.

θ_N, P, c_λ - are non-dimensional initial temperature gradient, the period duration, and the ratio of the thermal conductivity of the substrate to the green mixture, respectively; $L_1, L_2 - L_1$ - are respective thickness of the green mixture layer and the metallic substrate; τ_{cov} - is nondimensional time of the coating deposition. The latter has been determined in the following way: the process of alloying is believed to be accomplished if the degree of the green mixture conversion η on the green mixture-substrate interface has achieved 98%.

At $L_1 > L_{cr}$, intense conversion of the green mixture can start only after the temperature on the external boundary ($\xi = 0$) has become equal to or exceeded the ignition temperature, i.e. $\theta_1(\tau, \xi = 0)$ is higher than zero. Then the temperature on the green mixture surface is sharply increased and the greater portion of the starting reagents is converted to the products in the combustion wave propagating from the heated surface to the green mixture-substrate interface. It should be noted that at the stage of combustion, the reagent heating in the reaction zone exceeds the adiabatic temperature of the reagent mixture combustion at the given initial temperature $\theta_{1ad} = -\theta_N + 1/\gamma$. A more detailed analysis shows that the upper estimate for the maximum heating can be the $\theta_{1max} = -1 + 1/\gamma$.

The process of TRES is quite different at $L_1 < L_{cr}$. In this case, intense conversion of the initial reagents also begins at $\theta_1(\tau, \xi = 0) \leq 0$. However, chemical heat release does not evoke the exponential growth of the temperature inside the green mixture, since additional heat has time to be removed to the inert substrate. Complete conversion of the reactionable substance is accomplished when heating at the green mixture-substrate interface is approximately equal to the ignition temperature $\theta_1(\xi = L_1) \cong 0$. At that moment the surface temperature does not exceed

the 1-1.5 values, i.e. at $L_1 < L_{cr}$, the process of chemical conversion is of a quasi voluminal character.

The following practice-important conclusions have been made.

1. The value of the characteristic temperature of chemical conversion can be regulated by varying the discharge power and , consequently, the value of the heat flow at the active stage of the process.

2. To let the coating be formed at the characteristic temperature the active layer thickness should be less than some critical one.

3. The actual values of the discharge power and the thickness of the green mixture layer depend on the properties of the green mixture used and can be evaluated in the independent experiment on ignition and combustion of the samples pressed of the same mixture.

References

1. Levashov E.A, Kudryashov A.E., Nikolaev A.G. et al. Book of Abstr. of the 4th Intl. Symp. on SHS (Toledo Spain, 1997), p. 150.
2. Vilyunov V.N. The Theory of Ignition Of Condensed Substances, Nauka, Novosibirsk, 1984.
3. Voronin K.Yu. and Seplyarskii B.S. Ignition of a condensed matter with a constant heat flow at two competing exothermic reactions running, Khim. Fizika, 1991, v. 10 (9), p. 1251.

COMPUTER MODEL OF FRACTAL STRUCTURE OF A BRITTLE CRACK IN HAZARD CONDITIONS

Usov V.V., Shkatulak N.M.
South Ukrainian State Pedagogical University, Odessa, Ukraine

The brittle failure of a plate can be caused by set of alternate processes. All mechanisms for such processes are determined by operation of breaking stress. In theoretical homogeneous compact solids the crack will have the form of a straight, but in practice the heterogeneity of a material determines zones mainly approaching for destruction, and, therefore, it inevitably determines a stochastic nature of a crack.

The tree structures of cracks were considered as fractal objects, for which it was fair $S \sim (L^d)$, where S - the mass of structure, length - L. Generally, the tree-like cracks can accept one of two main forms [1]:
1) "Branched" (fractal dimension in limits $(d_f = 1,2 - 1,8)$;
2) "Sectional" $(d_f = 2,5)$.

It is known that branched tree-like structures are propagated faster, than sectional (which can even stop body height) and thus they are more dangerous at operating loads. It is important to understand mechanisms, which cause destruction of compact solids, and also factors defining a fractal size of the tree-like structures.

Firstly we shall consider the elementary process of the brittle failure. We shall assume that one of the extremities of a thin friable rod is clipped fixedly, and another is free. If the moving d of the free extremity is less than some critical d_c, the modulus of rigidity is constant. When d exceeds d_c, the rod can break, and the modulus of rigidity G suddenly lowers to the very small value. Further we shall consider a plane square lattice composed from such friable rods. This lattice will simulate a plate. If we assume, that moving in sites of such lattice is perpendicular to the plane (problem about anti plane shear), equilibrium equation of forces is written as:

$$\sum {}^k G^k(i,j)\{U^k(i,j) - U(i,j)\} = 0, \quad (1)$$

Where U (i, j) - vectors of moving, and the index k indicates the direction. In a limit of the continuous environment (plate) the relation (1) passes in the fundamental conservation law:

$$\nabla(G\nabla U) = 0 \quad (2)$$

In the specific case from the equation (2) it is possible to receive the Laplace law at G = const.

It is possible to set temporary evolution of a friable lattice with the help of the following algorithm:

1). Give a set of a rigidity modulus {G} for each rod, thus it is necessary to take into account heterogeneous character of structure of a lattice;

2). Set boundary conditions on $\{U^k\}$ (they should correspond to such physical situation, when the tensile strain is affixed on the upper edge, and the lower edge is fixed);

3). Test each rod (which is undestroyed); if the condition of destruction is satisfied $|U^k(i, j) - U(i,j)| > V_c$, you should produce replacement $G = \lambda G$, where $\lambda \ll 1$;

4). Change boundary conditions, if at execution of prior stages of the procedure any new rod was not destroyed, otherwise return to item 2 and prolong execution of the procedure. Stop the process, if the percolation structure was formed across the lattice.

The density of the function of probability determines the registration of heterogeneities of a friable lattice:

$$P(x) = p\, d(x - G) + (1 - p)\, d(x - 1\,G), (2)$$

Where p is probability of appearance of a rigid rod. A the probability of the appearance of the through structure from friable rods is:

$$R(p) = N/F, \quad (3)$$

Where N - number of the appeared through clusters, F - complete number of the

94

configurations from rods of two types. The graph of the given function is shown in the fig. 1.
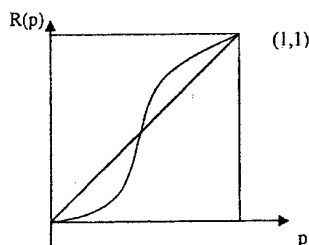
Fig. 1. The graph of the function R (p)

If to suggest that the destruction occur by a multilevel image, it is possible to define, how the breaking stress varies at transition from one level to another.
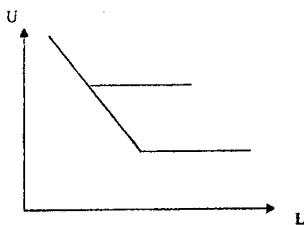
Fig. 2. A stress variation of destruction with a scale of a non-uniform flat plate

If the concentration of heterogeneities is defined by the law

$$R (p) = p, \qquad (4)$$

then the stress of destruction will depend on numbers of a level under the law $U \sim L^f$ (see fig. 2).
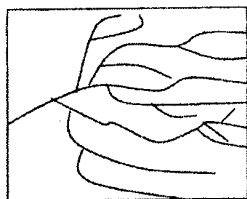
Fig. 3 (a) One of the typical configurations a crack for the branched fractal
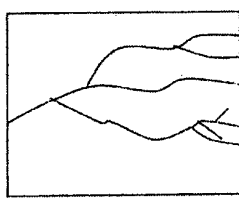
Fig. 3 (б). One of the typical configurations of a crack for the sectional fractal

In the fig. 3 (a) and 3 (b) the characteristic configurations of cracks generated at uniform expansion are shown. The configurations are self-similar with fractal dimension 1,62 ± 0,05 at extension for the branched fractal and 1,9 ± 0,05 for the sectional fractal.

We investigated propagation of a fragile crack in an ideal square lattice, in which rigid rods connect the nearest nodes among themselves. His appeared that the configuration of the cracks in such system has a fractal nature. We pay attention to the following:

1). Lattice relaxes in the field of the destroyed links.

2). There is the large deformations are watched on active extremities of the configuration.

3). The symmetry imposed by boundary conditions is clearly appreciable on the configurations of cracks.

The by us conducted operation, could give a start for the series of researches of gradually becoming complicated models of destruction. Using fractal geometry, such researches could promote the best understanding of appearances of destruction in materials. One of the above described attractive outcomes, is, that the fractal dimension weakly depends on boundary conditions. At the comparison of above mentioned fractal dimensions of cracks and clusters obtained in a two-dimensional case at a restricted diffusion of cauterization and a breakdown of dielectrics, all three fractal dimensions coincide [2].

1. Sinergetika i fraktaly v materialovedenii / V.S. Ivanova, A.S. Balankin, I.J. Bunin, A.A. Oksagoev. - M.: Nauka, 1994. - 383s.

2. Olemsky A.I., Flat A.Y. Ispolsovaniye konzepzii fractala v fizike kondensirovannoj sredy // Uspechi Fisicheskich Nauk - 1993. - Vol.163, N12. S. 1 - 50

MODELING OF A POROUS BODY CLOSED DIE DENCIFICATION WITH USE OF PERMEABLE ELEMENTS METHOD

Baglyuk G.A. Yurchuck V.L.
Institute for Problems of Materials Science NAS of Ukraine, Kiev, Ukraine

The way of reception of powder parts and preforms by dencification in the closed die with rigid walls under action of applied axial strength is one of widely distributed methods in th technology of hot and cold forging of sintered porous preforms. In turn, development o technological processes of powder forging promoted the development of various methods of accounting and analysis of the stressed and deformed condition of the preform material during its processing, which are reduced, mainly, to analytical [1-2] and numerical methods [3-5], the widest application among which has received a method of final elements [4-5].

In a present work the attempt of description of densification process of a porous body, which material submits to a condition of plasticity of a kind [1]:

$$\frac{p^2}{f_1(\Theta)} + \frac{T^2}{f_2(\Theta)} = \sigma_s \qquad (1)$$

is undertaken with use of advanced in a work [6] method of petrmeable elements method. The technique of account is based on a principle of a minimum of complete power of deformation, according to which from all the kinematically possible speeds of particles movings fields of the deformed body the valid one renders minimum to a functional of complete power of deformation, and kinematically possible field of speeds thus is considered as the approximation of the valid one and gets out from the classes of rather simple functions (for example - polynomal).

Thus, the function of a speeds field should satisfy boundery conditions, which, for our case, look like:

$V_z = 0$ at $z=0$;
$V_z = V_0$ at $z=h$; $\qquad$ (2)

where V_0 is a speed of the upper punch movement , h - is a current height of the preform deformed.

Accepting assumptions about equality to zero of radial deformations in volume of a porous body, for the description of a speeds field that satisfy to boundary conditions (2) we shall
sostojiania uplotniaemogo osesimmetrichnogo poristogo tela s ispolzovaniem variatsionnich

accept dependences:

$$V_z = -V_0 \frac{z}{h}\left[1 - a_1(1 + a_2 \frac{r^2}{R^2})(1 - \frac{z}{h})\right] \qquad (3)$$

$$V_r = 0;$$

where R is radius of preform forged, a_1 and a_2 are the varied parameters, which value at every step of deformation can be found of a condition of minimization of the variational function for rigid - plastic porous body of a kind [7]:

$$J = \sum_{k=1}^{K} \iiint_V (pe + TH)dV + \\ + \sum_{m=1}^{M} \mu\sigma_s\sqrt{3} \iint_F \sqrt{f_2(\Theta)V_{fr.}}\, dF \qquad (4)$$

For numerical simulation of a process the deformed axisymmetrical porous body has been conventionally broken into the ring elements with rectangular cross sections having equal initial porosity, in which units parameters included in the equation (4) were defined.

Account had been made by consecutive small deformations mode. On each step of deformation parameters value that minimize the quantity of functional (4) were found and the value of porosity reduction and current meaning of each elementary cell porosity defined. The last ones served as the initial data for the subsequent settlement step of deformation.

The analysis of the modeling results has shown, that on the first stage of deformation density difference in volume of preform is increased, whereas at the final stage of deformation is observed the tendency to decrease of density difference up to its complete elimination with achievement of practically pore free stage of a material deformed.

References

1.Shtern M.B., Serdiuk G.G., Maksimenko L.A. et al. Fenomenologicheskie teorii pressovaniya poroshkov. - Kiev, Nauk. Dumka, 1982. -140 p. (In Russian).

2.Laptev A.M. Deformirovanie poristogo metalla v zakritoi matritse // Izv. Vuzov. Mashinostroenie. 1979. - №7. -P.89-94. (In Russian).

3.Baglyuk G.A., Radomiselskiy I.D., Yurchuck V.L. Analiz napriajonno-deformirovannogo metodov // Poroshko-vaia metallurgia. - 1986. - №10. -P.26-30. (In Russian).

4.Petrosian G.L., Nersisian G.G., Malchasian S.A., Petrosian A.S. Uplotnenie poristich materialov v jostckih konicheskich i tsilindricheskic matritsach
//Poroshkovaia metallurgia. - 1982. -№5. -P.22-27. (In Russian).

5.Petrosian G.L. Plasticheskoe deformirovanie poroshkovich materialov. -M.: Metallurgia, 1988. - 152 p. (In Russian).

6.Olevsky E.A., Shtern M.B., Michailov O.V. Raspredelenie plotnosty pri pressovanii izdelii s perechodom po visote // Poroshkovaia metallurgia. - 1989. -№3. -P.15-21. (In Russian).

7.Baglyuk G.A., Shtern M.B., Yurchuck V.L. Sravitelniy analiz schem nagrujenia pri goriachem douplotneniy poristoi zagotovki v zakritom shtampe // Poroshkovaia metallurgia. - 1989. - №11. -P.19-22. (In Russian).

HIGH STRAIN RATE SUPERPLASTICITY OF ALUMINIUM - LITHIUM ALLOYS

Myshlyaev M.M.[1], Kamalov M.M.[2], Myshlyaeva M.M.[2], Medvedev A.S.[2]

[1]Baikov Institute of Metallurgy and Material Science RAS, Moscow, Russia

[2]Institute of Solid State Physics RAS, Chernogolovka, Russia

INTRODUCTION: Scientists and technologists have been displaying recently an active interest in aluminium-lithium alloys due to unique combination of their properties, namely, an increased elastic modulus, sufficiently high strength and low density. Nowadays much work is in progress aimed at improvement of properties of these alloys, also by forming in them nano- and microcrystalline structure via intensive plastic deformation. It is generally acknowledged herewith that equal-channel angular pressing (ECA-pressing) is one of the most promising methods to achieve the goal. In this work precisely this method was employed for the formation of a microcrystalline structure. The object to study was the prospective lightest (density 2.47 $g \times cm^{-3}$) corrosion resistant weldable alloy 1420 (Al-5.5%Mg-2.2%Li-0.12%Zr). It is superplastic and is widely used to fabricate workpieces of a complicated profile. Typical characteristics of its superplasticity (SP) are as follows: strain to failure is 350% and the coefficient of strain rate sensitivity of stress is 0.45 at a strain rate of $5 \times 10^{-3} s^{-1}$ at T=480°C [1].

PROCEDURES, RESTULTS AND DISCUSSION: The rods (20 mm in dia, 70 mm in length) were produced by sequentially ECA-pressing the material for 10 passes at 370°C. Structure and phase state were studied by an electron microscopy (JEM-100CX). Three sample sections, i.e. normal to the rod axis and two mutually perpendicular and parallel to the rod axis were examined. Flat samples (0.85 mm in thick, 5 mm in gauge length) to be tested under tension in Instron machine were prepared.

The investigations showed. Rods demonstrated grained structure. About 50% of grains measured from 0.5 to 3 μm, grains measuring from 3 to 5 μm made up 30-40%, from 5 to 8 μm – 10-20%. Normally, the grains exhibited subgrains containing both individual dislocations and dislocation cells and tangles. The subgrain misorientations were 2-8°. The subgrain boundaries consisted of dislocations. Often they were quite regular dislocation networks and single-row walls. They measured from 0.3 to 2 μm, depending on the grain size. Fractured and broken subgrain boundaries were frequent. Dislocation motion and migration of subgrain boundaries were observable when examining the structure. In individual cases bent extinction contours were observed that is suggestive of the occurrence of internal stresses. The rods demonstrated numerous particles of the Al_2LiMg phase of various sizes and configurations and small particles of the δ' (Al_3Li) phase. The formers were found in the grain and subgrain interiors and at their boundaries as well as on dislocations. In the latter case particles were small.

The diagrams describing the connection of true stress σ with true strain e were experimentally obtained. They showed three stages of plastic deformation. The first one was rather continuous stage of deformation hardening. The second stage was characterized by constancy σ. The third one was a stage of monotonous fall of σ with increase in e value. This stage was the most continuos in true strain and, consequently, in elongation. To determine the true strain rates in these stages we obtained a dependence of $\dot{e}$ on e using the same testing conditions. This dependence showed that strain rates $10^{-2} s^{-1}$ and $10^{-3} s^{-1}$ corresponded to the first and the third stages, correspondingly. The former indicated strain rate is characteristic for SP deformation (SPD) at the expense of sliding inside grains [2]. The last indicated strain rate is typical for SPD of fine-grained materials, when SP is conditioned by grain boundary sliding [3,4].

Studies of the dependence of deformation up to failure on the initial strain rate and testing temperature (T) showed that the range of 365-400°C and $\dot{e}_{in}=1.7 \times 10^{-2} s^{-1}$ were the most optimum to attain the largest strain. The greatest value of the attained elongation was 1878%. Note (see Introduction) that this alloy, not subjected to ECA-pressing, exhibited the SP elongation (350%) and its SP manifested itself at a much higher Temperature (480°C) and a noticeably smaller strain rate ($5 \times 10^{-3} s^{-1}$).

The analysis of the collected experimental data with take into account the ones presented in literature showed that the connection among $\dot{e}$, σ and T can be well described by the known relationship:

$$\dot{e} = \dot{e}_0 \times exp(-U/kT) = A\sigma^n T^{-1} \times Exp(-U/kT), \quad (1)$$

where $n = 2$, and U – activation energy of SPD, k – Boltzmann constant, A – constant. Estimation of value n and U were evaluated using standard techniques. According to our experiments $n = 2.235$ and $U = 1.4$ eV in the first stage and $n = 2.3$ and $U = 0.98$ eV in the third stage. The experimental values n coincide with rather a high accuracy in the value $n = 2$ in Eqn. (1). Using these values of n and U values of parameters $\dot{e}_0 = 5 \times 10^{10}$ s^{-1} and $A = 1.6 \times 10^6$ K·mm^2·MPa^{-1}·s^{-1} were calculated. The aforementioned of SPD activation energy value of $U = 1.4$ eV corresponds to self-diffusion energy (1.4 – 1.5 eV) inside of grain [5]. The value of $U = 0.98$ eV corresponds to grain boundary self-diffusion energy $Q_{zp} = W + R_{gb} = 0.99$ eV, where $W = 0.8$ eV [5] – vacancy formation energy and $R_{gb} = 0.19$ eV [6] – vacancy migration energy along grain boundaries or dislocations (pipe diffusion). The obtained different values of activation energy which correspond to the first and third stages point to the presence of plastic deformation under different mechanisms during these stages. Thus, the second stage is a transitory one and transforms from one mechanism to another.

TEM studies were carried out to investigate structure of the samples subjected to tensile straining. The first stage shows overall continuous rearrangement of structure with domination of hardening processes over dynamic recovery ones, and active sliding inside grains. As a result, the grains became elongated in the strain direction. Elongation of grains decreased during the deformation in the third stage. As a result, the grains became elongated in the strain direction. Elongation of grains decreased during the deformation in the third stage. By the end of the stage grains became nearly equiaxed. Important circumstances attract attention in the whole stage: Absence of dislocations in many grains and the presence of fine Al$_2$LiMg particles in them and in grain boundaries. The important fact is also that Al$_2$LiMg particles make chains in grains and situated as grain boundary profiles. All these points to continuous and overall dynamic recrystallization with grain boundary sliding and

migration. One should note that the described herewith in agreement with aforesaid activation energies.

CONCLUSION: The structure and mechanical behaviour of the ECA pressed 1420 alloy have been studied in SP conditions. Three stages of SPD have been shown. The data showing intra-grain sliding during the hardening stage and dynamic recrystallization with participation of grain boundary sliding and migration during the stage of the decrease of true stress have been obtained. It has been shown the elongation up to 1878% corresponds to alloy, and n ≈ 2 and m ≈ 0.45 for both stages.

REFERENCES:
1. Novikov I.Y., Portnoi V.K., Konstantinov I.L., Kolobnev N.I. Physical metallurgy of aluminium alloys, Nauka, Moscow, 1985.
2. Likhachev V.A., Myshlyaev M.M., Sen'kov O.N. Laws of the Superplastic Behavior of Aluminum in Torsion, Lawrence Livermore National Laboratory, Livermore, 1987.
3. Grabskii M.V. Structural superplasticity of metals, Metallurgia, Moscow, 1975.
4. Kaibyshev O.A. Plasticity and superplasticity of metals, Metallurgia, Moscow, 1975.
5. Friedel J. Dislocations, Pergamon press, Oxford, 1964.
6. Stark J.P. Diffusion in solids, Energiya, Moscow, 1980.

EXPERIMENTAL AND THEORETICAL STUDY OF INTERACTION OF AN ARC AND SPARK DISCHARGES WITH ELECTRODE MATERIAL

Kurochkin V.D., Kravchenko L.P.
Institute for Problems of Material Science, NAS of Ukraine, Kyiv, Ukraine

Erosion resistance, life cycle of electrode materials and quality of coatings to a large extent depend on processes in discharge plasma and foots of a discharge. Previous investigations reveal complex nature of processes of interaction discharge plasma with surface of electrodes or coatings at power flux density up to 10^{10} W/m^2 [1].

This report presents results of mathematical simulation of spark and arc discharge parameters as function of electrode material. The model includes flow continuity conditions for each component of electrode, quasi-neutrality condition for plasma, the equation of state, the equation of energy conservation for electrons, equations of equilibrium for reactions of dissociation- molization for main gas components and Saga equations for all plasma components, equation stated the constant relationship between nucleus of O and N in air plasma. Parameters of a plasma (temperature, electron density, concentrations of all particles, etc.) depend on evaporation rate of materials and later depends in its turn on power flux into electrodes. Such system is described by self-consistent sets of equations that have been calculated in loops until they reach self-consistent values. As an example, dependence of electron density in discharge axis on power and pressure is shown in Fig.1.

Calculations show that changing of ambient conditions - pressure, discharge power produce such change of T and effective ionization potential that minimize changes of N_e. In the practice this means that increase in discharge power results in appearance of new higher available for the system levels and in increasing of dissipation of energy. This effect slows down increase in T and N_e.

Stationary arc discharge in argon atmosphere also was a subject of investigations. Experimental setting was designed to measure temperature in the anode spot of a direct current arc on materials having wide range of melting points (Fig.1). Radiation of material was compared with standard tungsten lamp with high resolution spectrometer used as monochromator.
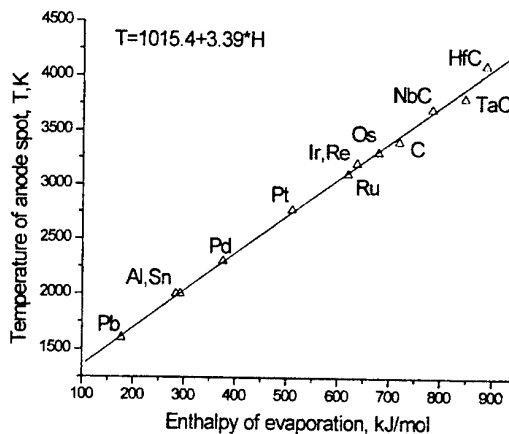
Fig 2. Dependence of temperature in anode spot of enthalpy of evaporation anode materials in argon direct current arc at 20 A.

As indicates Fig.2, temperature with good precision linearly depends on enthalpy of evaporation of anode materials. This dependence was described by mathematical model that takes into account power balance in anode.

Experimental data on evaporation rates of metals from anode spot area allows to conclude that this process is described by the same lows as in vacuum despite it occurs at atmospheric pressure. This effect is due to the high velocity of transfer by field of ions of evaporated atoms from the electrode

Fig.1. Normalized values of N_e for W-Cu electrode with 5% of La against pressure and power. $N_{e\,max} = 1.3E18$ cm^{-3}, $P_{max}=1.2E6$ Pa.

surface. Equation for evaporation rate ($1/s \ m^2$) was found in the approach of theory of excited complex:

$$dN/dt = N \ kT/h(Q^*/Q)\exp(-E^*/kT), \qquad (1)$$

where N -atom density in the surface of metals, k - Boltzmann constant, T - temperature, h - Planck constant, E^* - activation energy, Q^* - statistical sum of atoms in intermediate state. It depends on symmetry of orbitals and it was found expressions for Q^* that gave best fit to the experimental results. Q is statistical sum of atoms in solid metals. E^* is energy of activation. This value depends on temperature and was calculated for metals investigated [2].

Measurements of evaporation rates indicate that dependence observed can not be attributed to the energy losses due to evaporation only since they do not exceed several percents in sum losses. The curve in Fig.2 is result of summed effect of losses on evaporation, radiation, thermal conduction and first of all inelastic collisions of electrons in thin boundary layer.

Results of measurements and calculations with use of formula (1) are presented in a table.

Table Evaporation rates from the anode foot at current 20 A.

Materials	Measured evaporation rate, $1/s \ m^2$	Calculated evaporation rate, $1/s \ m^2$
Ag	1.0E25	1.0E25
Pd	1.5E24	1.6E24
Sn	2.2E24	2.2E24
Pt	2.0E23	2.3E23
Ru	4.0E22	4.4E22
Os	1.0E22	1.1E22
TaC	4.1E21	4.5E21
HfC	8.0E21	6.0E21

Model proposed takes into account the main features of processes in the area of anode foot and gave ability to calculate evaporation rates of materials with good precision.

REFERENCES

1. Kurochkin V., Kravchenko L. Interaction of a Spark Discharge with W-Cu electrodes Alloyed by REE. // High Temperature Materials and Processes. - 2000.- v.19. - No 6.- P. 427 - 433.

2. Курочкін В.Д., Кравченко Л.П. Кінетика випаровування речовини у плазму дуги постійного струму.// Доповіді АН УРСР. - 1979. - сер. А. - №12. - С.1051 - 1053.

COMPUTER MODELLING of THREE-DIMENSIONAL PHYSICAL FIELDS in ALUMINIUM ELECTROLYSERS

Panov E.N., Karvatskiy A.Ya., Leleka S.V.
National Technical University of Ukraine "KPI", Kiev, Ukraine

Generally thermal and electric fields in aluminium electrolysers can be described Poisson equation

$$\Delta\varphi + b = 0, \tag{1}$$

where Δ – Laplacian; φ - potential; b – volumetric loading.

At the decision of a task by definition of a temperature field under variables (1) understand

$$\varphi = t, \quad b = q_v/\lambda,$$

where t – temperature; q_v – volumetric density of an internal source of heat; λ - thermal conductivity.

Boundary conditions for a thermal problem can be put as:

$$\text{I sort} - t\big|_{\Gamma_1} = t(x,y,z), \tag{2}$$

$$\text{II sort} - \lambda\frac{\partial t}{\partial n}\bigg|_{\Gamma_2} = q(x,y,z), \tag{3}$$

where n – normal to a surface of a body; q – normal density of a thermal stream,

$$\text{III sort} - \lambda\frac{\partial t}{\partial n}\bigg|_{\Gamma_3} = \alpha\big(t\big|_{\Gamma} - t_c\big), \tag{4}$$

where α - heat transfer coefficient; t_c – ambient temperature, IV sort (conjunction)

$$\begin{cases} t\big|_{\Gamma_{4-}} = t\big|_{\Gamma_{4+}}, \\ -\lambda_-\frac{\partial t}{\partial n}\bigg|_{\Gamma_{4-}} = \lambda_+\frac{\partial t}{\partial n}\bigg|_{\Gamma_{4+}}. \end{cases} \tag{5}$$

where $\pm$ - concerns to the connected environments.

At the decision of a problem of electric potential as variables (1) sizes are used

$$\varphi = u, \quad b = 0,$$

where u – electric potential.

Thus boundary conditions of type are considered (2), (3), (5):

$$u\big|_{\Gamma_2} = u(x,y,z), \tag{6}$$

$$-\chi\frac{\partial u}{\partial n}\bigg|_{\Gamma_3} = i(x,y,z), \tag{7}$$

where χ - specific electroconductivity; i – normal density of an electric current;

conditions of interface of various environments

$$\begin{cases} u\big|_{\Gamma_{4-}} = u\big|_{\Gamma_{4+}}, \\ -\chi_-\frac{\partial u}{\partial n}\bigg|_{\Gamma_{4-}} = \chi_+\frac{\partial u}{\partial n}\bigg|_{\Gamma_{4+}}. \end{cases} \tag{8}$$

The technique of the numerical decision of the formulated task is constructed on a direct of boundary elements method (DBEM) [1], that allows to lower dimension of a task and to avoid a problem of a triangulation of an internal part of area.

To the basic stages of realization DBEM concern:

- triangulation of boundary surfaces Γ_i $(i = 1,...4)$;
- calculation of influence matrix (coefficients);
- formation of a matrix of system of the linear algebraic equations (SLAE) under the given boundary conditions on Γ_i $(i = 1,...4)$;
- elimination singularity SLAE and her solution;
- definition a component of density of a stream on borders Γ_i $(i = 1,...4)$.

The original technique of a triangulation is developed Γ_i. The offered technique based on display of an any flat quadrangle in an individual square that considerably allows to facilitate and automate procedure of breakdown of any piecewise flat border. Unit of a triangulation is the any flat quadrangle (side) into which the surface of an any body is broken. And units on a contour of the next sides Γ_i $(i = 1,...3)$ are double, that is untied and may not correspond at all each other on the next sides. Performance of conformity between units is imposed only on units on all area of a side Γ_4. As boundary elements linear triangular elements are chosen. It allows to execute analytical integration singularity at calculation of coefficients of influence.

Nonsingularity coefficients of influence are calculated numerically with the help Hammer's quadrature formulas of the fifth order of accuracy [1].

The technology of compression of sides is applied to exception singularity matrixes SLAE on a contour on 0,05-0,1 % from the maximal linear size. This procedure is carried out at a stage of a triangulation.

It is offered also an original design procedure a component of a vector of density of a stream on borders Γ_i.

On the basis of original techniques and classical BEM [1] the universal software for calculation of fields of temperatures and electric potential in three-dimensional bodies of the complex form is developed. In a basis of development of the given software principles of object-oriented programming are fixed. The given software is developed in the programming language C++. Universality of software is reached by application of special files - tasks which creates and writes down the module of input of the initial data for specific tasks. In these files the geometrical data and physical properties of object are set. With the help of the module of calculations these files are analyzed by the linguistic analyzer. Thus is analysed errors of the file - task and at their absence it is settled an calculation.

The structure of the submitted software includes 3 modules:
- preprocessor - the module of input of the initial data and preliminary viewing of designs on the entered data;
- processor - the module of the solution of Laplacian's and Poisson's equations;
- the postprocessor - for visualization of results of calculations. It is used standard software.

Calculations of fields of temperatures (Fig. 1) and electric potentials (Fig. 2) in elements of a design aluminium electrolyser are executed.

Level	1	2	3	4	5	6	7	8	9	10
t, °C	161	176	190	204	219	233	247	262	276	290
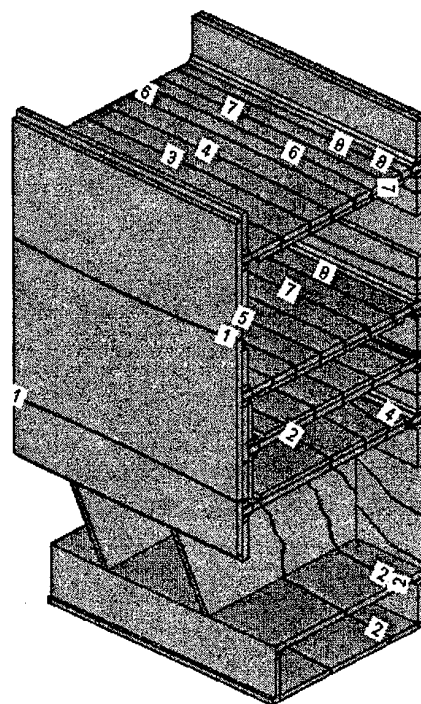
Figure 1. Field of temperatures of a part of a cathode casing aluminium electrolyser.

Level	1	2	3	4	5	6	7	8	9	10
U, mV	134	342	550	758	966	1175	1383	1591	1799	2007
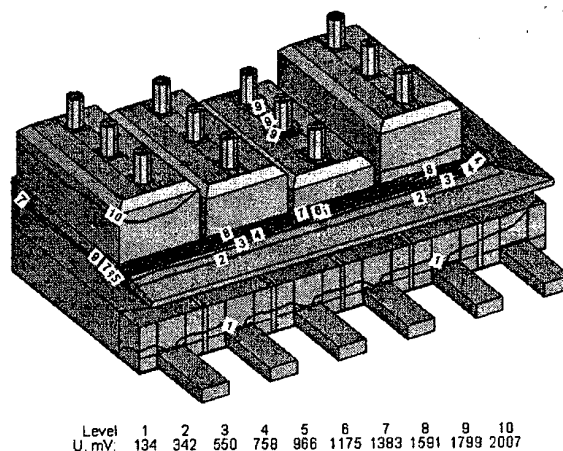
Figure 2. Field of electric potential of a aluminium electrolyser.

Literature.
1. C.A.Brebbia, J.C.F.Telles, L.C.Wrobel - Boundary element techniquus. – Springer-Verlag, Berlin, New York, Tokyo. – 1984.

MODELING OF THE INFLUENCE OF RHEOLOGICAL PARAMETERS OF WORKPIECE SURFACE LAYER ON LOADS AND ITS DAMAGE UNDER DRY FRICTION CONDITIONS DURING HIGH TEMPERATURE PLASTIC DEFORMATION

Barykin N.P., Valeeva A.Kh.
Institute for Metals Superplasticity Problems RAS, Ufa, RUSSIA

The paper considers the influence of a strain rate sensitivity factor of a near-surface layer material on homogeneity of deformation and power-consuming of the process under dry friction conditions. Mathematical modeling performed shows that in spite of high values of friction constants it is possible in principle to decrease a scalar parameter of damage and strain loads due to high strain rate sensitivity of a near-surface layer material.

As a first approximation a finite element model of the axially symmetric isothermal compression of the workpiece with different rheological properties of separate layers has been applied. The problem formulation was reflected in work [1]. The rheological ratio for the near-surface layer and the material of the body being deformed is in the form:

$$\sigma_s = A\xi_i^m(1+\varepsilon_i)^n,$$

where: σ_s - flow stress; ε_i and ξ_i – deformation and deformation rate intensities respectively; A, m, n – rheological parameters of the near-surface layer and the body being deformed. The scalar parameter of damage (ω) accumulated in the process of plastic metal working may be estimated from the known ratio [2].

The technological parameters, influencing contact surfaces upon interaction, are the following: geometric sizes of the deformed workpiece (D_0 and H_0- initial diameter and height) and rheological parameters of the deformed body and near-surface layer. Calculations were performed within the range of the strain rate sensitivity of stress m_1 varying from 0,1 to 0,9. The following workpieces were considered: a low workpiece (D_0/H_0=10), a high workpiece (D_0/H_0 =0,5) and a workpiece with the ratio D_0/H_0=2 (all workpieces are similar in height). Thickness of the near-surface layer is equal to 0,1 of the initial height (h_0=0,1H_0). The boundary conditions on the surface of contact with the tool: $v_w=v_T$; $\tau_k=\sigma_s F_z$, where v_w, v_T - normal constituents of moving speeds of the tool and the

object being deformed on the contact surface; F_z - Ziebel friction factor. Its range is from 0,1 to 0,9 that corresponds to conditions of dry friction. While solving the problem of numerical modeling it is taken that values of the other parameters do not change during the whole technological process $A_1=A_2$=120; m_2=0,1; $n_1=n_2$=0. Moreover, characteristics of plasticity (relative reduction) of materials of the near surface layer (ψ_1) and the base (ψ_2), $\psi_1=\psi_2$=0,5 are set. (While solving the task of mathematical modeling values of rheological parameters of a deforming body corresponding to the aluminum alloy Al4.4Cu1.5Mg at the temperature 450°C and the strain rate ξ=2·10⁻¹c⁻¹ [3] were taken.). The following constant technological parameters were established: velocity of deformation v_t=0,1 mm/sec; strain value ε = 0,5.

The following parameters of the stress-strain state obtained by mathematical modeling were analyzed: maximum normal stresses (σ_{max}) on the contact surface and the scalar parameter of damage of the deforming material and the near-surface layer (ω_2^{max}; ω_1^{max}).

As seen from Fig.1 the increase in the strain rate sensitivity of stress m_1 of the near surface layer leads to the decrease in strain loads. This tendency is apt to all the size ratios under consideration. However, in case of the high workpiece the decrease in the strain load is not so significant: when m_1=0,1 the maximum normal stress is 165 MPa, then, when m_1=0,5 σ_{max} – 102 MPa and further increase in m_1 does not exert a significant effect on strain load. In case of the workpiece with D_0/H_0=2 varying m_1 from 0,1 to 0,9 decreases the maximum normal stress by twice. The most significant decrease (approximately by a factor of 3) occurs in case of the low workpiece: when m_1 is equal to 0,1 σ_{max} is 1360 MPa and when m_1=0,9 σ_{max} – 505 MPa.
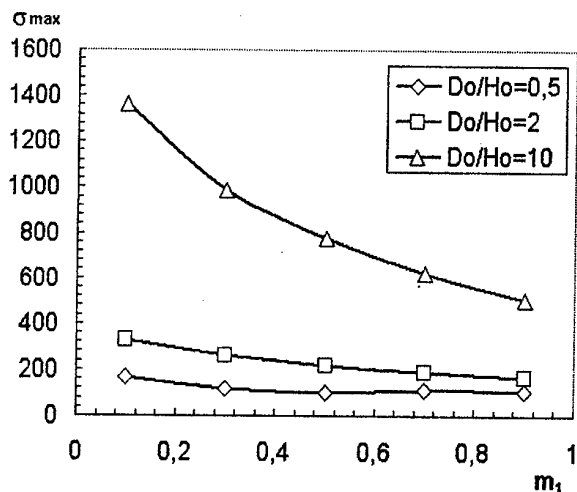
Fig. 1. Dependence of maximum normal stress on strain rate sensitivity of stress m_1 of the near surface layer.

Fig.2. shows the influence of strain rate sensitivity of stress of the near surface layer on values of the scalar parameter of damage of the base material.

Fig. 2. Dependence of the scalar parameter of damage on the strain rate sensitivity of stress m_1.

The most noticeable decrease in the scalar
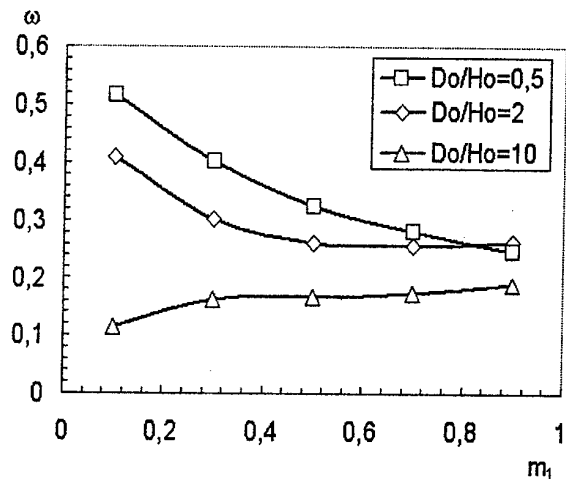
parameter of damage is observed in case of the high workpiece: as m_1 increases from 0,1 up to 0,9 ω decreases by twice.

In case of the workpiece with the ratio $D_0/H_0=2$ the increase in m_1 from 0,1 up to 0,5 causes a drop of ω by approximately 80 %; further increase in m_1 does not influence the scalar parameter of damage of the base material.

In case of the low workpiece the lowest values of the scalar parameter of damage have been obtained. These values, of coarse, increase with

increasing the strain rate sensitivity of stress, though in all cases their values do not exceed 0.3.

On the basis of results of mathematical modeling of the process of axially symmetric compression of the workpiece with the ratio D_0/H_0 ranging from 10 to 1 under conditions of dry friction $F_z=0,9$ the considerable influence of the strain rate sensitivity of stress (m_1) of the near-surface layer material on maximum normal stresses on the contact surface (σ_{max}): as m_1 achieves values 0,4 – 0,6 the maximum values of σ_{max} decrease by 1,5-2 times as compared to the values when $m_1=0,1$. In terms of increasing the quality of articles (the decrease in the scalar parameter of damage) the near-surface layer having the strain rate sensitivity of stress m_1 of about 0,4-0,6 is most efficient under conditions of dry friction.

References.

1. Barykin N.P., Vasin R.A., Ermachenko A.G., Mathematical modeling of technological ensuring of service life of articles processed by deformation under conditions of superplasticity. // KShP. 1994. N 4. P.18-21.
2. Bogatov A.A., Mizhiritztkyi O.I., Smirnov S.V., Resource of plasticity during plastic working M.: Mashinostroenie, 1977.- 88 p.
3. Polukhin P.I., Gun G.Ya., Galkin A.M. Plastic deformation resistance of metals and alloys. Ref.book. M.: Metallurgia, 1983. 352 p.

COMPUTER SIMULATION AND EXPERIMENTAL RESEARCH OF COMPACTING OF CUMULATIVE CHARGES FACINGS

Yepifantseva T., Mikhailov O., Martyukhin I.
Institute for Problems of Materials Sciences, Kiev, Ukraine

The high performance at a perforation oil and gas wells is ensured with applying cumulative charges facings. The shape of a facing is a thin-wall cone. The facings make from composition heterogeneous powdered materials by a method of a pressing. The density of parts should be uniform.

Computer simulation and the experimental studies were carried out. The study of distribution of the density fields - was in the focuss of interest.

The powder of electrolytic copper was used for experiments. The shape of powders was dendritic. This powder is a ground of a material for facings.

The experimental study method was proposed.

The xeroradiography method was used [1].

The special mold tool was designed and manufactured (Fig.1).

Fig.1. Experimental plant

The copper powder was covered together with interlayers from lead shots. The pressing was carried out step by step. At each stage the position of lead shots was determined by a radiographic method.

Constructions of an integral lower punch, and also demountable lower punch were studied.

The simulation was carried out by use of the finite element method [2]. The system GID (http://gid.cimne.upc.es) was applied (pre- and post- processor). The familiarization (one month password) version of a system was used.

In case of an one-sided pressing with an integral lower punch has appeared, that the maximal vertical displacement of lead shots is observed near to the upper punch. These displacements are minimum near to the lower punch.

The horizontal displacement of lead shots is observed in the field of broad angles of an part.

The horizontal displacement of a powder above and below has an opposite direction.

The experimental data and the results of computer simulation [3] are closed each other.

In case of an one-sided pressing the field of a density is very nonuniform (Fig.2) [4].
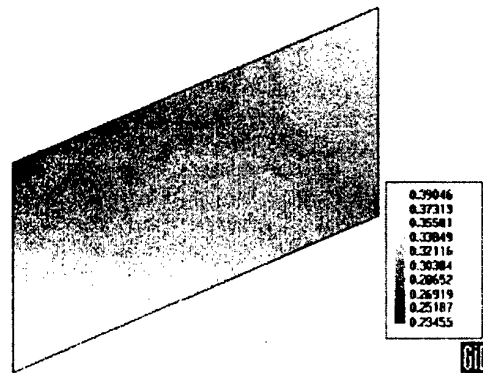
Fig.2. Contours for equal porosity

In case of use of demountable punches the bulk of an part is divided on a series of areas. The compacting of each area is carried out separately. The density distribution is uniform.

The influencing of a direction of friction forces was studied also. The direction of friction forces influences a field of a density.

If the friction forces are directional to broad angles, the variance of a density increases. The density in the field of broad angles increases, and the density in the field of acute angles is diminished.

If the friction forces are directional to acute angles, the variance of a density is diminished. The density in the field of acute angles is diminished, and the density in the field of broad angles increases.

The carried out studies have enabled to define the optimum scheme of a pressing of powdered facings.

The demountable lower punch is applied. The compacting of each area is carried out separately. The active friction forces are applied. The friction forces are directional to acute angles. The density of facings is uniform.

REFERENCES

1. *T.A. Yepifantseva, Ph.D. thesis, Kiev,1992*
2. G.G. Serdyuk and O.V. Mikhailov, The mathematical modelling of plastic deformation of PM materials in the presence of a free surface, *Powd. Metall. Metal Ceram., (translated from Russian), N4, 18-22 (1986)*
3. T.A. Yepifantseva, I.D. Martyukhin, O.V. Mikhailov, G.G. Serdyuk, Features in density distribution during axial pressing of porous parts bounded by surfaces sloped to pressing axias. The numerical analysis, *Powd. Metall. Metal Ceram., (translated from Russian), N 5/6, 43-52 (1997)*
4. T.A. Yepifantseva, I.D. Martyukhin, O.V. Mikhailov, G.G. Serdyuk, The effect of sealing scheme on the properties distribution of material for cumulative charges facing during their forming from heterogenous powder composition, *Powd. Metall. Metal Ceram., (translated from Russian), N 11/12, 21-27 (2000)*

MODELLING OF COMPACTING OF PM PARTS OF COMPLEX SHAPE

Mikhailov O., Shtern M.
Institute for Problems of Materials Sciences, Kiev, Ukraine

The computer simulation is used here to improve existing metods of manufacturing the PM - parts. The study of distribution of the density fields - is in the focuss of interest. The effect of the pressing diagrams on finite properties of parts is studied.

The experimental information concerning the final distribution of a density and all geometrical parameters of part are taken from work [1]. The first of all the simplest diagram is considered: two lower punches are immobile. Then the diagram for which rates of punches are proportional to current heights will be analyzed. Finally, the pressing diagram suggested in [1, 2] will be considered. In the last case the process of pressing consists of three stages.

1. Methods of simulation

The simulation is carried out by use of the finite element method. The modified relationships of plasticity theory for porous body are used. It has been considered rigid - plastic behaviour of material.

The similar ideas were used in [3,4]. The boundary value problem reformulated in a finite element form has been solved using the step by step computation. For each step of loading (or straining) the system of non-linear algebraic equation has been solved by use of Newton – Rafson procedure. Iterations were finished if the convergence criterion was satisfied. On the base of obtained rate field the density field as well as the stress components has been defined. Than the same procedure has been carried out for the next step of loading. The rate of convergence was controlled by the choice of initial estimate. For this purpose the extrapolation on the base of previous rate field (obtained for previous moments) has been used. Besides we have used solution obtained on the base of linearization as a first estimate.

All punches, core – pine and sleeve are supposed to be rigid. At the surface of these elements the external friction is taking place.

To prevent the complications due to the strong deviation of the mesh of elements (because of deflection) special procedure has been used. The given mesh of finite elements is mapped at the final configuration of part. Then it was mapped onto initial configuration.

The creation of initial geometric model, generation of finite elements mesh, formulation of material properties, formulation of boundary condition and visualization of final results are carried out on the base of package GiD: pre- and post- processing system for F.E.M. calculations (International Center For Numerical Methods In Engineering CIMNE).
Academic and professional (one month password) versions of system have been used.

2. Obtained results

One-side pressing. The given diagram is the simplest one, but can be practically used only when the ratio of height /diameter is very small. In our case the density variation is very significant. The shear strain rate achieves the largest value in the neighborhood of internal angle. It should be emphasized that the contours of equal shear strain rates remind to the paths of the overconsolidated cracks propagation are known from practice [2].

Diagram for which rates of punches are proportional to current heights. One should note that in condition of the absence of external friction the given diagram unlike to one – side pressing provides the uniform density distribution [5]. The presence of external friction results in irregular distribution of a density. Controlling a direction of external friction, it is possible to reduce the noted effect, however nonuniformity of a density remains.

Modified pressing diagram. Unlike to both previous diagrams in the case considered in paper [1] rates of punches is variable for period of compaction.

Pressing diagram now consists of three parts. At the first stage the rate of the second punch - V_2 is less then V_1. At the second stage the second punch passes ahead the first one and at the third

stage $V_2 = 0$. The initial properties is not uniformly distributed. The densities of the upper and lower parts are correspondetly 3.5 g/sm^3 and 3.4 g/sm^3.

This stipulates the same level of shear strain rates that in previous case and provides the most uniform density field.

The results of computer simulation and experimental data [1,2] are closed each other.

REFERENCES

1. Doremus, P.,Pavier, E., Kergadalan, J., Puente, G., Axisymmetric Part Compaction: Data Base For Numerical Simulation, *The International Journal of Powder Metallurgy*, Vol.35, N3, 1999, pp. 63 –68

2. Kergadalan, J., Puente, G., Pavier, E. and Doremus, P., Compression of an Axisymmetric Part with an Instrumented Press, In *Proc. Int. Workshop on "Modelling of metal powder forming processes,* Grenoble, France, 1997, 227 -285.

3. Zang, Z.L.and Niemi, E., A class of generalized mid-point algorithms for the Gurson-Tvergaard material model, *Int. j. numer. methods eng.,* **38**, (1995), 2033-2053.

4. Mikhailov, O., Integrated scheme of computer simulating for PM articles pressure treatment, *Powd. Metall. Metal Ceram., (translated from Russian)*, N **9/10**, (1995), 99-104

5. Yurchenko, E. and Shtern, M.Control of Complex Forms by the Density Distribution During Axial Compaction of Objects, *Powder Metall. Metal Ceramics* **4** (1993), 286 - 291

THERMODYNAMIC SIMULATION OF THERMAL TREATMENT OF ALUMINUM NITRIDE POWDER IN HYDROGEN ATMOSPHERE

Morozov I.A.,* **Gordiyenko S.P.,** **Panashenko V.M.,** **Morozova R.A.,** **Dubovik T.V.**
Institute for Problems of Material Science of NAS Ukraine

INTRODUCTION

High chemical activity of hydrogen and its capability to form volatile compounds are the basis of purification of substances and materials from contaminants during the thermal treatment in hydrogen atmosphere [1]. The aluminum nitride powder, which is under study of this work, contains in wt%: Al - 63.50; N - 31.90; O - 1.87; Fe - 0.70; C - 0.30; S - 0.26; Ti - 0.12; and Si - 0.08. As a potential method of aluminum nitride purification from contaminants can be its thermal treatment in hydrogen atmosphere at elevated temperatures and pressures.

The first stage in the development of technology of aluminum nitride purification from contaminants is its thermodynamic simulation. The gas-thermal treatment simulation of aluminum nitride in hydrogen atmosphere was accomplished with the use of Astra Program [2] within the temperature range of 1000 to 1500 K with the 100 K gain, and pressure of 0.2 MPa. The computation results only included components with a concentration over 10^{-7} mol/kg.

RESULTS OF THERMODYNAMIC SIMULATION

Equilibrium concentrations of vapor-gas components and condensed components for each temperature within said temperature range are shown in Tables 1 and 2. The computation at 1200 K revealed the presence of Si_3N_4 in condensed products while silicon nitride was not observed both at 1100 K and 1300 K. Therefore, computations were made at 1150 K and 1250 K, which allowed to establish the temperature range of silicon nitride existence.

Table 1 gives the temperature relation of the main gas-vapor component concentrations. As can be concluded from the data of Table 1, the outflow of carbon into the gas phase is preferentially caused by the formation of methane and molecules of CO and HCN; of sulfur due to formation of hydrogen sulfide and molecules of SiS; of oxygen due to molecules of water and CO; of silicon due to molecules of SiS and SiO. Besides, an insignificant transition of atoms of nitrogen (N_2, NH_3), aluminum and iron to the gas phase can be observed.

Table 2 gives the temperature relation of condensed component concentrations expressed in mol/kg. As can be seen from the data of Table 2, at 1000 K, AlN, Al_2O_3, TiC, TiN, SiS, and Fe coexist in equilibrium. With the temperature rise, the TiN concentration drops while the TiC concentration growths. At 1200 K, TiN disappears and the TiC concentration reaches 0.019 mol/kg and then does not change with temperature. Iron in free state is present up to 1400 K, and at an above temperature, products contain Fe_3C. Silicon at low temperatures is bound in SiS compound, the concentration of which reduces with temperature, on the other hand, within the 1150-1250 K range, it is accompanied by Si_3N_4, concentration of which is lower than of SiS. Above 1250 K, no compounds of silicon in the condensed phase can be observed. The main condensed components of the system under study are AlN, concentrations of which negligibly rise at 1500 K, and Al_2O_3, concentrations of which decrease at 1500 K. All the above condensed substances are minor contaminants.

As can be concluded from the results of thermodynamic simulation of hydrogen-thermal treatment of aluminum nitride under study, such contaminants as sulfur, silicon, and to some extent, carbon and oxygen can be removed from an initial substance in the form of gases or vapors. Removal of these contaminants is of great

* imorozov@materials.kiev.ua

significance as they considerably deteriorate properties of finite products when being present during further treatment of aluminum nitride (sintering). Concentration variations of condensed phases containing iron and titanium during the gas-thermal treatment (formation of TiC and Fe_3C; disappearance of TiN) result in no removal of iron or titanium contaminants. However, compounds of these contaminants as being refractory ones produce negligible effect on the product properties made of aluminum nitride.

Table 1
Concentrations of vapor components, mol/kg

Component	1500 К	1400 К	1300 К	1250 К	1200 К	1150 К	1100 К	1000 К
I_2I	$1.3*10^{-4}$	$8.9*10^{-5}$	$4.9*10^{-5}$	$3.3*10^{-5}$	$1.8*10^{-5}$	$9.2*10^{-6}$	$3.2*10^{-6}$	$2.6*10^{-7}$
I_2S	0,041	0,041	0,041	0,041	0,041	0,041	0,041	0,041
N_2	$4.5*10^{-3}$	$6.7*10^{-3}$	$7.3*10^{-3}$	$0.6*10^{-2}$	$2.5*10^{-4}$	$1.5*10^{-3}$	$2.5*10^{-4}$	$3.1*10^{-6}$
NH_3	$0.9*10^{-4}$	$1.5*10^{-4}$	$2.3*10^{-4}$	$2.6*10^{-4}$	$2.3*10^{-4}$	$0.2*10^{-4}$	$1.1*10^{-4}$	$2.2*10^{-5}$
CO	$8.5*10^{-3}$	$2*10^{-3}$	$2.6*10^{-4}$	$7.3*10^{-5}$	$1.6*10^{-5}$	$3.2*10^{-6}$	$4.1*10^{-7}$	–
NI_4	0,133	0,169	0,174	0,175	0,175	0,176	0,189	0,190
HCN	$2.2*10^{-4}$	$9.5*10^{-5}$	$2.4*10^{-5}$	$9.6*10^{-6}$	$2.9*10^{-6}$	$7.6*10^{-7}$	$1.2*10^{-8}$	–
SiO	$4.2*10^{-5}$	$2.6*10^{-5}$	$1.3*10^{-5}$	$4.3*10^{-6}$	$7.1*10^{-7}$	$1.0*10^{-7}$	$1.2*10^{-8}$	–
SiS	$2.2*10^{-2}$	$2.2*10^{-2}$	$2.1*10^{-2}$	$1.3*10^{-2}$	$4.4*10^{-3}$	$1.4*10^{-3}$	$4*10^{-4}$	$2.2*10^{-5}$
Al	$3.6*10^{-7}$	$7.2*10^{-8}$	–	–	–	–	–	–
Fe	$8.0*10^{-6}$	$9.2*10^{-7}$	$6.6*10^{-8}$	$1.5*10^{-8}$	–	–	–	–

Table 2
Concentrations of condensed components, mol/kg

Component	1500 К	1400 К	1300 К	1250 К	1200 К	1150 К	1100 К	1000 К
AlN	17.683	17.678	17.677	17.677	17.677	17.677	17.677	17.677
Al_2O_3	0.3	0.302	0.3025	0.3026	0.3026	0.3026	0.3026	0.3026
TiC	0.019	0.019	0.019	0.019	0.019	0.018	0.005	0.0044
Fe_3C	0.032	0.0033	–	–	–	–	–	–
Fe	–	0.087	0.097	0.097	0.097	0.097	0.097	0.097
SiS	–	–	–	0.0075	0.011	0.013	0.022	0.022
Si_3N_4	–	–	–	$6.8*10^{-4}$	$2.1*10^{-3}$	$2.5*10^{-3}$	–	–
TiN	–	–	–	–	–	0.0018	0.014	0.015

CONCLUSIONS

The hydrogen-thermal treatment of AlN containing O, C, S, Si, Fe and Ti at the hydrogen pressure of 0.2 MPa within the temperature range of 1000 to 1500 K should result in the purification of nitride from S, Si, and partially, from C and O. The aluminum nitride purification from above contaminants shall contribute an amelioration of sinterability of treated aluminum nitride powders and improvement of properties of sintered specimens.

REFERENCES

1. Trefilov VI, Morozov IA, Morozova RA et al. Effect of Hydrogen on improving purity of WC and AlN Powders. Int J Hydrogen Energy 1996;21(11-12):1097-1099.

2. Sinyarev GB, Vatolin NA, Trusov BG, and Moiseev GK. The use of computer in thermodynamic computations of metallurgical processes. Moscow: Nauka, 1982, 263 p. (In Russian)

BRAZING OF JOINTS OPERATING UNDER EXTREME CONDITIONS

Khorunov V.F., Maksymova S.V.
Paton Electric Welding Institute of the NAS of Ukraine, Kyiv, Ukraine

It is a known fact that brazed joints successfully operate in many heavy-loaded structures, e.g. elements of space vehicles and rockets (shells, rocket rudders), gas turbine engines, cathodes of high-power plasmatrons, etc. Also, the brazed joints play an important role in fusion reactor plants.

In development of a fusion reactor (FR) the special consideration is given to power-intensive elements of discharge chambers of FR, such as divertors, limiters and internal walls. These structural elements are located in an immediate proximity to plasma and subjected to the simultaneous effect by thermal and corpuscular flows, as well as by neutron radiation. Alloys on the base of graphite, tungsten, copper, molybdenum and niobium were selected as candidate materials for fabrication of the above structures [1]. The issue of a paramount importance for fabrication of a serviceable structure is to ensure a reliable joint between the above dissimilar materials.

Physically, the receiving divertor device for a period of the technology phase is a joint of the tungsten-copper type. Difficulties with joining the above materials are caused by a large difference in their thermal expansion coefficients and low oxidation resistance of the refractory metal. Therefore, a proper selection of brazing filler metal, temperature range and shielding atmosphere is very important for brazing. The brazing filler metal should wet well the materials brazed, be sufficiently strong and, at the same time, ductile to be able to deform to relax stresses during brazing and cooling to room temperature. The brazing temperature should not be too high, as in this case it may cause growth of residual stresses.

The authors elaborated the technology for producing dissimilar brazed joints in tungsten-copper, using a brazing filler meal based on the cooper-manganese system, developed by the E.O.Paton Electric Welding Institute.

Brazing of the joints was performed in a vacuum furnace with radiation heating by evacuating the work space to 10^{-3} Pa. The brazing filler metal used was in the form of wire 1 mm in diameter.

Imbedded elements in the form of semi-rings and strip 0.3 mm thick were made from the wire. The butt brazed joints passed the strength tests at room temperature in the as-brazed state, after heat treatment conducted to restore strength properties of the copper alloy and after neutron irradiation at different temperatures. Performance of the units under conditions of thermal-cycling loading was determined [2].

As proved by the tests conducted, strength of the brazed joints greatly depends upon the neutron irradiation conditions, and first of all upon the temperature. So, irradiation at a temperature of 100-200 °C and dose of 5×10^{21} neutron/cm^2 leads to a substantial increase in strength, which is associated with low-temperature radiation strengthening of the copper alloy. Further increase in the exposure temperature does not lead to strengthening of the copper alloy (Fig.). Fracture of the brazed samples occurred in base metal.
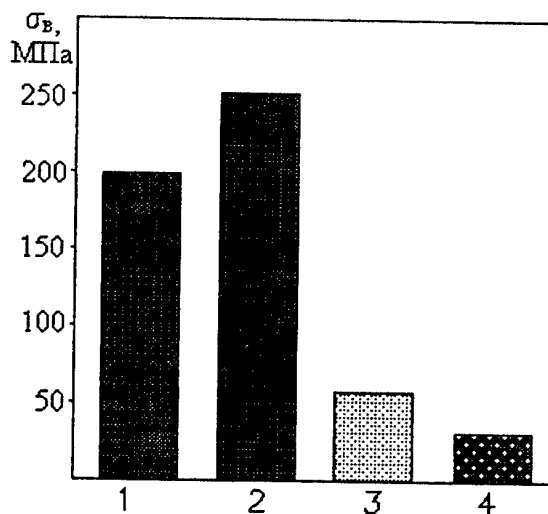
Fig. Strength of tungsten-copper brazed joints after neutron irradiation:
1 – as-brazed;
2 – 100 °C, dose 5×10^{21} neutron/cm^2, reactor SM-2;
3 – 310 °C, dose 5×10^{21} neutron/cm^2;
4 – 400 °C, dose 5×10^{21} neutron/cm^2, reactor BOR-60

The brazed joint has a homogeneous structure of copper-based solid solution with a small amount of silicides detected along its boundaries.

X-ray microanalysis of the brazed joints shows an intensive diffusion of manganese into the base metal (width of the brazed joint is about 30 μm and depth of diffusion of manganese is more than 45 μm).

Performance of brazed models of the copper-tungsten diverter plates was evaluated by thermal cycling tests. Powerful pulsating heat flows result in a temperature and stress-strain state of structural members, which is close to that observed under actual conditions. Power of the heat flow and duration of its effect were selected so that maximum temperatures on the surface and in the zone of joining to the substrate corresponded to temperatures of the structure in constant heating by the heat flow with a power of $\theta = 10$ MW/m^2. It was established that the brazed joints retained their thermal cycling strength on a base of 2×10^3 cycles. No losses of thermal contact or separations were detected.

Analysis of the results obtained allows a conclusion that for brazing of joints of the tungsten-copper (copper alloys) type a decisive characteristic in selection of a brazing filler metal is its ductility (impact toughness, elongation), rather than tensile strength.

Therefore, the developed brazing filler metal possesses the required combination of the above properties, which makes it possible to produce joints which retain performance under the effect of powerful cyclic heat flows and neutron radiation at increased temperatures.

References

1. Roth J., Bondarsku J., Ottenberger W., Materials for fusion reactor plasma fusing components / Rep. IPP. – 1979. – 9/26. – 12 p.
2. Maksymova S.V., Khorunov V.F., Barabash V.R. Problems of producing fusion reactor diverter units / Svarochnoye Proizvodstvo. – 1994, No. 5. – P. 6-8.

COMPETITION OF THE HYDROGENATION AND HYDROGENOLYSIS UNDER INTERACTION OF THE INTERMETALLIC COMPOUNDS WITH HYDROGEN

T.I.Bratanich, T.V.Permyakova, V.V.Skorokhod

Frantsevich Institute for Problems of Material Science of NASU, Kiev, Ukraine

The interaction of the intermetallic compounds with hydrogen may go not according to direct but destructive hydrogenation (hydrogenolysis) accompanied by the decomposition of the initial intermetallid. That is why the destructive hydrogenation may be one of the method for the obtaining of the high dispersive composite metallic powders.

The objective of the present work is the thermodynamical analysis of the direct and destructive hydrogenation of the intermetallic compounds and the delimitation of the hydrogenation and hydrogenolysis fields. The objects of the investigation were the intermetallic compounds of AB_5 - type ($LaNi_5$, $LaNi_{5-x}Al_x$) and AB - type (TiNi,TiFe, $TiFe_{1-x}Me_x$).

The calculation of the free Gibbs energies for the reactions of the successive hydrogenation of $LaNi_5$, $LaNi_4Al$, TiNi, TiFe up to the different absorption levels and for their hydrogenolysis reactions at 298, 473 and 773 K have been fulfild. The border hydride is shown to exist for each temperature and its formation is equiprobably to the hydrogenolysis reaction. The formation of the border hydride takes place at the border temperature and hydrogen pressure. The hydrogenation field is higher and the hydrogenolysis fild is lower than the border hydrogen capasity.

The dependences of the relative border hydrogen capasity of $LaNi_5$, $LaNi_4Al$, TiFe, TiNi upon the temperature are presented on fig.1. $LaNi_5$ is shown to be the most stable and TiFe is the least stable against the hydrogenolysis. TiNi is some stabler than $LaNi_4Al$. Thus the investigated intermetallic compounds according to the increasing stability against the hydrogenolysis may be placed as $LaNi_5$, TiNi, $LaNi_4Al$, TiFe.
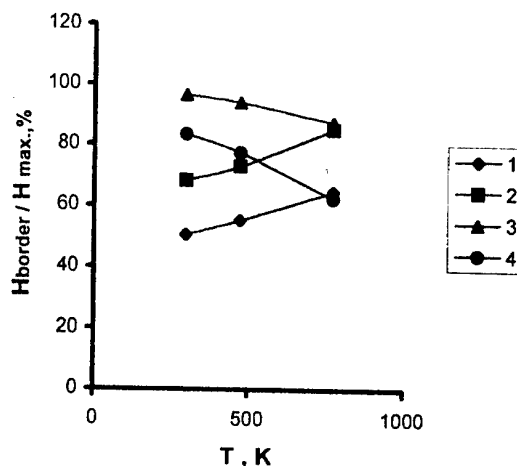
Fig. 1. Relative border hydrogen capasity of the hydrides on the base of $LaNi_5$(1), $LaNi_4Al$ (2), TiFe (3), TiNi (4) vs temperature.

The dependences of the border equilibrium pressure upon the temperature for the border hydride composition determine the work conditions of the material in the hydrogenation or hydrogenolysis fields. The presented on fig.2 curvers deliminate the hydrogenation and hydrogenolysis fields of $LaNi_5$ and $LaNi_4Al$ according to the equilibrium pressure in the specifie temperature conditions of their exploitation. Thus when $LaNi_5$ works as the hydrogen accumulator the increase of the temperature up to 393K leads to the neccessity of the preassure increase higer than 4,5 MPa to avoid the problems with the hydrogenolysis. This problem is still more critical for TiFe - hydrogen accumulator as even at 293 K it must be hydrogenated at the pressure not lower than 5 MPa and the long thermal processing are extremely undesirable. And under the destructive hydrogenation intermetallic compound must work at the pressure lower than the border equilibrium one that is in the fields occupied lower than the presented curvers.
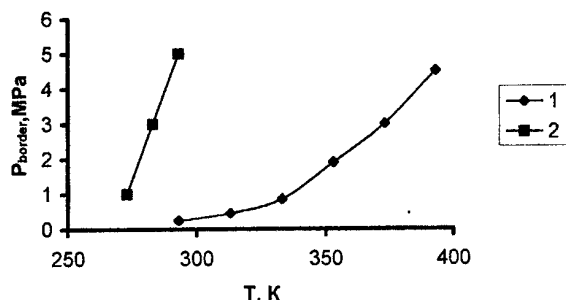
Fig. 2. Equilibrium pressure vs temperature for the border hydrides on the base of $LaNi_5$ (1), $LaNi_4Al$ (2).

From the practical point of view it is important to control the border between the hydrogenation and hydrogenolysis fields. Obviously the dose doping of the intermetallic compounds may be one of the version of the such control. The dependences of the relative border hydrogen capasity upon the aluminium content in the alloys $LaNi_{5-x}Al_x$ for 298, 473 and 773K are showed on fig.3. With the increase of the aluminium content in the intermetallic compound the hydrogenation - hydrogenolysis border moves to the hydrogenation that is the $LaNi_{5-x}Al_x$ stability against the hydrogenolysis decreases.

Thus the thermodynamical analysis of the direct and destructive hydrogenation (hydrogenolysis) of the intermetallic compounds $LaNi_5$, $LaNi_{5-x}Al_x$, TiFe, $TiFe_{1-x}Me_x$ (Me – Al, Mn, Co, Ni) and TiNi has been fulfilled. The fields of these processes realization are established to be divided by the hydrogenation – hydrogenolysis border which are determined by the border hydrogen capacity depending upon the temperature and thermodynamical characteristics of the intermetalid (metal) – hydrogen system. The control of the border between the hydrogenation and hydrogenolysis fields is possible by means of the intermetallid doping with the elements influencing on the thermodynamical characteristics of the hydriding system. During the exploitation of the intermetallic compounds as the hydrogen sorbents and to avoid the destructive hydrogenation it is necessary to work at the pressure higher than the border equilibrium one for given temperature.

Fig. 3. Relative border hydrogen capasity vs aluminium content in $LaNi_{5-x}Al_x$ and temperature. 1 - 773 K, 2 - 473 K, 3 - 298 K.

Investigation of the doping additions influence on the $TiFe_{1-x}$ (Me - Al, Mn, Co, Ni) stability against the hydrogenolysis showed that aluminium additions to TiFe decreas its stability against the hydrogenolysis and manganese, cobalt, nikel increase it.

115

MULTILEVEL MECHANISM OF PHYSICAL PROPERTIES FORMATION IN CERAMIC AND COMPOSITE REFRACTORY COMPOUNDS

Goryachev Yu., **Dekhteruk V.**, **Siman N.**, **Fiyalka L.**
Institute of Materials of Science NAU, Kyiv, Ukraine

Ceramic and composite materials are now known to have a number of unique worthy pecularities (from technological to electronic ones) [1, 2]. In the former our papers [3, 4] it was shown that composites of the types: semiconductor – dielectric and semiconductor – metal in thick films preserve many worthy properties of the compact semiconductor (for example, high thermoelectric and resistive sensibilities). In addition, they gain some advantages (simple technology, small size, cheapness).

At the same time such systems yield to common semiconductors in the thermoelectric figure of merit and stability. There are many external factors and internal papameters leading, on the one hand, to new possibilities of controling functional characteristics and,on the other hand, to the apearance of worse reproductivity and reliability. To optimize the characteristics investigations of the mechanisms of composite properties formation were carried out [4, 5, 6]. In particular, the contribution of separate component properties to the composite properties was shown.

It was also shown that cjmposite and ceramic materials are usually composed of components which, in their turn, are composites as well (at least of two levels- micro- and macroscales) [6, 7]. The analysis of the properties of such components showed that they often have a higher thermoelectric figure of merit and efficiency than those of the whole composite. The task is to find a method for fixing the properties of the most effective composite level and controlling them in a vide temperature region up to the temperatures of using refractory ceramic materials.

The experimental investigation of concentration and temperature dependences of the thermoelectric properties of ceramics and semiconductor – metal composites (for example, $Si_{0,7} Ge_{0,3}$ - Mn_4B) has been carried out. The method for analysis and calculation of internal electron-transfer parameters in the systems investigated has been worked out on the base of taking into account of different levels of parameter

formation (macro-, micro-, nano- and electron scales).

The results obtained are shown in Table.

T a b l e – Resistivity and thermoelectric coefficient for the composite $Si_{0,7}Ge_{0,3}$ – Mn_4B and its components (ρ_{ik},α_{ik}) in two-levels

	T, K/ X	500/ 0.1	800/ 0.1	500/ 0.4	800/ 0.4
Compo-site	ρ, Om·cm	0.47	0.35	0.10	0.04
	α, $\mu V/ K$	72	42	40	12
Phase "A" Si-Ge	ρ_{1a}, Om·cm	0.90	0.68	0.48	0.29
	ρ_{0a1}, Om·cm	1.25	0.96	1.25	0.96
	ρ_{0a2}, Om·cm	0.09	0.04	0.09	0.04
	α_{1a}, $\mu V/ K$	210	235	130	150
	α_{0a1}, $\mu V/ K$	240	250	240	250
	α_{0a2}, $\mu V/ K$	40	70	40	70
Phase "B" Mn_4B	ρ_{1b}, Om·cm	0.06	0.10	0.003	0.006
	ρ_{0b1}, Om·cm	0.32	0.56	0.32	0.56
	ρ_{0b2}, Om·cm	$3.2 \cdot 10^{-5}$	10^{-4}	$3.2 \cdot 10^{-5}$	10^{-4}
	α_{1b}, $\mu V/ K$	30	15	10	6.0
	α_{0b1}, $\mu V/ K$	81	52	81	52
	α_{0b2}, $\mu V/ K$	2.0	0.0	2.0	0.0

For these data a model for the interrelation of the composite compositions at different levels was worked out. In the simplest case an exponential dependence of compositions is supposed:

$$X_i = A + B*X_{i+1} + C*(X_{i+1})^2 + \ldots \qquad (1)$$

Here X_{i+1} and X_i – the content of the second phase of higher and lower levels correspondingly.

Besides, the ideal interdependence of properties for the lowest level of composites was supposed [7]:

$$(V_{i=1})^{n(i=0)} = \Sigma\, X_{i=0}(k)*[\, V_{i=0}(k)]^{n(i=0)};$$

$$1 < n(i=0) < +1; \qquad (2)$$

Here k – the component index; i – the index of the corresponding composite level.

Such an interaction leads to the following s ---stem of transcendental equation:

$$V_{i,k}(k)*[1 + (V_{02}/V_{01})^{n(1)}]^{1/n(1)} =$$

$$= V_{i1}(1)*[1 + (V_{02}/V_{01})^{n(k)}]^{1/n(k)}; \qquad (3)$$

Here k and 1 – the index of the corresponding composition at the its level.

The minimum quantity of composition s (N) meeted for the solution of the equation system (3) is equal to:

$$N = (M - L)*L + 1; \qquad (4)$$

Here M – the quantity of the levels analused, L – the quantity of theadjusted coefficients in the model for the interrelation of the composite composition. When the model is described by the equation (1), $L = 3$.

The system of transcendental equation (3) was solved using the itteration method for $(N - 1)$ equation.

Conclusions

-The multilevel analysis of physical properties formation in ceramic and composite materials permits technology of the systems investigated to be optimized in order to get the maximum efficiency and thermoelectric figure of merit.

- The $Si_{0.7}Ge_{0.3} - Mn_4B$ system is perspective as a working body for thermoelectric converters of energy and thermoelectric sensors.

Literature
1. Скороход В.В., Петровский В.Я., Бойцов О.Ф. Structure matrixity and the dimentions of conducting cluster in "dielectric – metal" composite. Труды 1-го Международного семинара по керамичуским композитам с организованной структурой "IOM-98", 19-22 мая 1998г., Киев, Украина, 1998. С.15.
2. Фиялка Л.И., Горячев Ю.М., Симан Н.И., Шварцман Е.И. Thermistor – like properties of thick films of the composite system Ni – B – O. Труды 1-го Международного семинара по керамичуским композитам с организованной структурой "IOM-98", 19-22 мая 1998г., Киев, Украина, 1998. С.16.
3. Горячев Ю.М., Дехтярук В.И., Фиялка Л.И., Шварцман Е.И. Electronic structure and properties of composites of oxide – carbide type. Сб. Теория и моделирование электронного строения и свойств тугоплавких соединений, сплавов и металлов.Киев, ИПМ НАНУ, 1997, С.44-49.
4. Горячев Ю.М., Дехтярук В.И., Симан Н.И., Фиялка Л.И. Thermoelectric properties of composite thick films of semiconductor – dielectric type. Сб. Электронное строение и свойства тугоплавких соединений и сплавов и их использование в материаловедении. Киев, ИПМ НАНУ, 2000. С. 112-118.
5. Горячев Ю.М., Дехтярук В.И., Симан Н.И., Фиялка Л.И. Шварцман Е.И. Thermoelectric properties of semiconductor ceramics. Сб. Передовая керамика третьему тысячилетию. Киев, ИПМ НАНУ, 2001, С.161.
6. Скороход В.В. Technology ptinciples, stucture and physico-chemical properties of ctramic composites. Сб. Передовая керамика третьему тысячилетию. Киев, ИПМ НАНУ, 2001, С..3.
7. Горячев Ю.М., Симан Н.И., Фиялка Л.И. Шварцман Е.И. Electron transfer in unhomogeneous semiconductors with regard for two levels of its formation. Труды 19-го Научного семинара "Элекутронное строение и свойства тугоплавких соединений, сплавов и металлов в физическом материаловедении." 23-23 января 2002 Киев, ИПМ НАНУ, 2002. С. 2

117

INTERACTION IN THE ZrO_2-HfO_2-CeO_2 SYSTEM.

Gerasimjuk G.I., LopatoL.M., Red'ko V.P.

Frantsevich Institute for Problems of Materials Science NAS of Ukrajina, Kyiv, Ukrajina.

The system ZrO_2-HfO_2-CeO_2 is interesting for the creation of materials with enhanced physico-mechanical properties for high-temperature application. However, the phase diagram for the ZrO_2-HfO_2-CeO_2 system has not been reported.

The phase equilibria at the boundary binary systems are known. The ZrO_2-HfO_2 system is one with unlimited mutual solubility of the components in the solid state It is characterized by the formation of the solid solutions fields based on monoclinic (M), tetragonal (T) and fluorite- type (F) forms of the ZrO_2 and HfO_2. The ZrO_2-CeO_2 and HfO_2-CeO_2 systems are of the same type. They are characterized by a limited mutual component solubility in the solid state. The last investigation [1] of the ZrO_2-CeO_2 system defined of the tetragonal and cubic ZrO_2 solid solutions regions as well as the solid solution on the base of fluorite type CeO_2 (1500 °C). In this investigation the solubility regions on the base of M- and F- HfO_2 and F-CeO_2 were determined in the HfO_2-CeO_2 system. No compounds were found in the systems.

In this communication we present the results of interaction for the ZrO_2-HfO_2-CeO_2 system and isothermal section at 1500 °C.

The samples were obtained from nitrate solutions with their subsequent evaporation and decomposition at 1200 °C for 2 h. Thermal treatments were conducted in air in the furnaces with heating elements based on SiC (1200 °C) and ZrO_2 (1500 °C for 40 h). The phase composition of the samples was investigated by X-ray, petrographic and microstructural analyses. X-ray diffraction analysis of the samples was performed by a powder method at room temperature (Cu kα radiation). The scanning speed of 1-4 ° 2Θ/min was used in the 15-90° 2Θ range. The unit cell parameters were calculated by the least-squares fit method. The refractive indexes were measured in highly refractive immersion media (sulfur-selenium alloys or solutions of arsenic tribromide in methylene iodide).

As a result of investigation undertaken it was found that features of phase equilibria in the bounding binary systems are also observed in this ternary diagram: formation of solid solutions based on the different polymorphic modifications of the initial oxides. No ternary compounds were found in the system.

Reference.
1. Andrievskaya E.R., Red'ko V.P., Lopato L.M. Interaction of the CeO_2 with the oxides of hafnium, zirconium and yttrium at 1500 °C.// Powder metallurgy and ceramics.- N7/8.- 2001.- p.109-118.

ATOMIC ISOMORPHISM AND THEORETICAL ESTIMATES OF ENERGY COMPATIBILITY FOR ADMIXTURE *1H – 94Pu* ELEMENTS IN COMMON ELEMENTARY CELL OF *d*-METAL SOLID SOLUTIONS

Lidiya N. Grishchishyna, A.A. Lisenko, D.A. Grishchishyn, G.A. Baglyuk
Institute for Problems of Materials Science, NAS of Ukraine

It is thought that the atomic isomorphism is foundation property of elements for the crystalline isomorphism and of the solubility of components in solid-state. This report dealt with problem of the theoretical option of an energy profitable admixture/alloying of components (from *1H-94Pu*) with atoms of *3d-, 4d-, 5d*-metal-solvents [1-4].

In report the advantages and deficiencies of traditional approach (estimates by atomic radius R, electronegativity En) are considered. The microscopical approach of the energy aspect for the atomic isomorphism theory, we are accounting now, bears on combined approach [1]. Efficiency of it has been provided by using of an experimental atomic and electronic parameters for calculations of special auxiliary microscopical parameters of mutual energetic influence /AMPEI/ $PEICh = [\pm f(En,R)(\pm)]$, $PEV = [\pm f(K_E,\Omega)(\pm)]$ $VMP = [\pm f(\Sigma_m,\Omega)(\pm)]$, other, – here Ω – is volume per atom for solid solution matter, K_E – is energydynamical potential of atom, as function of the isolate atome own energy formation ε and Σ_m – Voltchenkova's S_{3F} atomic energy capacity).

To simplify the discussion it must be mention of that the isomorphic and isoenergetic compatibilities of a component atoms are the conditions necessary and sufficient to secure of their mutual solubilities and for phase stability of thermodynamical macrosystem as a whole.

To begin with the local thermodynamic potentials of microvolum for any macrosystem form by own characteristics of a component atoms.

It is widely recognised that the local decrease of atomic parameters in any micro-volume of macrosystem gives rise to diminution of a local thermodynamic potentials, in particular, for a local Gibb's energy Δg.

The mathematical expressions of Gibb's equations in general and local task are: $\Delta g = (\Delta h - T\Delta s)$, $\Delta g<<0$, $T\Delta s>\Delta h>0$, if pressure p – const.,
$$h=(u – pdv), \quad u=(u_0 + j_0), \text{ then,}$$
$$dg = \{dh - Td(s_0 + s_k^{A,C})\} =$$
$$\{(du_0 + dj_0) - Td(s_0 + s_k^{A,C})\} = \{(\varepsilon_i - \varepsilon_j/\varepsilon_j + h_0) -$$
$$Td(s_0 + s_k^{A,C}) - \Sigma\mu_k dm_k\} \text{ and for macrovolume}$$

$$\Delta G = \sum_{i=1}^{\infty} \Delta g_i,$$ here Δg – is change of local Gibb's energy, Δh – a local enthalpy, Δs – entropy one, T – temperature, $s_k^{A,C}$ – configuration enthropy deposit, u_0 – a local crystalline grating energy, local anharmonism $j_0 \rightarrow 0$, μ – chemical potential, m – atomic mass. This local characteristics are functions of atomic and electronic parameters.

Application of AMPEI for quick-forecast of donor / acceptor activities of the admixture atoms, of energy equivalent components for same atomic structure and isomorphic mixtures, for estimates competitive of elements in formation process for the multicomponen subgratings in macrosystem will be discussed.

AMPEI forecust results are correlating with the first-principle one for the same effects in solid state of materials (see table) [2-4].

In report the special attention has been paid to the rules of the pre-diagrams option of the energy equivalent components and elements for a part exchange of components into hydrogen-acumulating-subgrate "Met-Hydrogen" system.

Such an combined approach proves to be extremaly helpful and gives some rules for identification of the energy equivalent atoms for acumulate-subgrate (or for an energy compatibilities with atoms) of solid solution.

Table Auxiliary microscopical parameters *AMPEI* and first-principle data for isomorphic mixtures

Admix-ture→(sol-vent)	$\Delta R/R$, %	$PEICh=$ $[\pm f(En, R)(\pm)]$	$PEV=$ $[\pm f(K_B, \Omega)(\pm)]$	$VMP=$ $[\pm f(\Sigma m, \Omega)(\pm)]$	ΔH, eV/at. [4]	$-E_{coh}$, at. ed. [2]	Isomorphic mixtures
1	2	3	4	5	6	7	8
Al→(Ni)	+14,89	+ 1,075(+)	+ 0,333(+)	+ 1,112(+)	–	**1,3803**	Ni₃Al
Ni→(Al)	–12,96	– 1,470(–)	– 0,431(–)	– 1,071(–)	–		
Co→(Al)	12,58	– 1,244(–)	+ 0,339(–)	– 1,097(–)	–0,006	**1,3780**	(Ni, **Co**)₃Al
Co→(Ni)	**+ 0,44**	**+ 6,553(+)**	+ 3,256(+)	**0,000**			
Cr→(Al)	–10,24	– 0,531(–)	– 0,759(–)	+ 0,285(–)	+ 0,047	**1,3976**	(Ni, **Cr**)₃Al
Cr→(Ni)	**+ 3,12**	**+ 3,659(+)**	– 0,767(+)	**+ 7,213(+)**			
Hf→(Al)	**+10,43**	**+ 1,565(+)**	– 2,220(+)	**– 2,225(+)**	–	**1,4013**	Ni₃(Al, **Hf**)
Hf→(Ni)	+26,87	+ 1,031(+)	– 0,696(+)	– 0,607(+)	– 0,475		
Ti→(Al)	**+ 2,09**	**+ 1,258(+)**	– 3,725(+)	**– 2,759(+)**	–	**1,4140**	Ni₃(Al, **Ti**)
Ti→(Ni)	+17,28	+ 1,422(+)	– 0,170(+)	+ 0,426(+)	– 0,319		
Nb→(Al)	**+ 2,72**	**+ 6,005(+)**	– 4,386(+)	**– 6,462(+)**	–	**1,4293**	Ni₃(Al, **Nb**)
Nb→(Ni)	+18,01	+ 1,650(+)	– 0,395(+)	– 0,418(+)	– 0,329	–	
Ta→(Al)	**+ 2,78**	**+ 3,425(+)**	– 7,649(+)	**– 8,519(+)**	–	**1,4300**	Ni₃(Al, **Ta**)
Ta→(Ni)	+18,08	+ 1,327(+)	– 0,916(+)	– 0,880(+)	– 0,386	–	

Notes: *1. PEICh – auxiliary microscopical parameter of electron-chemical mutual influence of atoms;*

PEV – parameter for estimates of atom ability to homogeneous alloying;

VMP – high temperature parameter for estimate of the relation change of atomic cohesion force.

2. About a parameter signes: first sign /before parameter/ points out energy deposit and second one /after parameter/ – is dimentional difference between admixture and a basic component atoms.

Conclusions

1. The pre-diagrams option of principal element composition for any materials can be done by *AMPEI*-parameters of four types.

2. Quick-forecast of the atomic competitive for substitution in common atomic structure for many components, estimates of the donor/acceptor activities may be done by agency of microscopic parameters *PEICh*.

3. The auxiliary microscopical parameters $PEV=[\pm f(K_v, \Omega)(\pm)]$ gives estimate of effect cohesive strength in atomic structure.

4. Results of theoretical investigations by *AMPEI* are agreed with the first-principle calculation results and with the experimental measurements of mutual solubility for metals and of the hydrogen solubility in ones.

3. ΔR/R, % value determines preferablest for substitution of admixture element into common ele-mentary cell of solid solution.

4. Competitive between admixture atoms with equally ΔR/R, % to substitution in common elemen-tary cell of solid solution dependents from PEICh-value and signes (see table col. 3).

5. Rule [+VMP(+)] determines substitution into common elementary cell of component without change type interaction but [–VMP(+)] – with one; VMP-value /for same signe rule/ points out relative increase /decrease/ of strength for cohesion force in atomic structure.

References

1. Grishchishyna L.N. Microscopicheskaja teorija dodiagrammnogo vybora elementnogo sostava novogo materiala na osnove 3d-, 4d-, 5d-metallov. // Sb. Trudov IPM:Sovrem probl. fizich materi-alovedenija Kiev:1999, T.1, S.76

2. Bogdanov V.I., Ruban A.V., Fuks D.S. Ener-giya svjazi i termodinamicheskaya stabilnost fazy Ni₃Al // Fiz. met. metalloved. 1982, 53, S.521

3. Grishchishyna L.N., Lisenko A.A., Trefilov V.I. Metod izutchenija effecta perenosa zarjada i ego vlijanija na svoistva. // Ibid S.16

4. Watson R.E., Bennet L.H. Optimized prediction for heats of formation of transition metal alloys // CALPHAD, 1981, 5, 1, P.25

MODELLING OF HIGH-TEMPERATURE DEPENDENCES FOR THE CHARACTERISTICS OF THE GRAIN BOUNDARY SEGREGATION IN THE Al-Ti AND Al-Ni ALLOYS

Yagodkin V.V., **Danylenko V.M.**

J.N. Frantsevich Institute for Problem of Material Science NAS of Ukraine, Kyiv, Ukraine

Very valuable construction materials on the basis of Al-Ti and Al-Ni alloys are intercrystallite fragile mainly due to the grain boundary impurity segregation. In our the grain boundary equilibrium segregation substitution atoms model [1] polycrystal assumed to be two-phase system of solid solution (s) and grain boundary (b) phase which have small volume fraction $a \ll 1$. Introducing internal deviation parameter X from mean impurity concentration Z, we may determine the middle-phase concentrations as follows $Z^s = Z + X$ for solid solution and $Z^b = Z - (1-a)X/a$ on the grain boundaries. Assume that molar Gibbs potential of policrystal is: $G = (1-a)G^s + aG^b$, where G^s and G^b are molar potentials of solid solution and boundary phases, respectively. Substracting the non-segregation G^s_0 and G^b_0 potentials we obtaine the energy dependences of the segregation relaxation potential $-G_R$ and the grain forming one $-G_F$, respectively: $G = (1-a)G^s_0 + aG^b_0 + G_R = G^s_0 + G_F$. If the volume of grain boundary phase is constant (a = const), this two-phase system is in equilibrium state when the condition $dG/dX = 0$ is fulfilled. Using for potentials of both phases the model of subregular solutions where all G_q are thermodynamic potentials components phases, constants of interaction in solid phase and in grain boundary phases depending on the temperature by four-term formula $G_q = A_q + B_qT + C_q \ln T + D_qT^2$ [2] we obtaine the transcendental equation for segregation, which we must resolve by numerical methods.

We investigated at high-temperatures the grain boundary segregation in the liquid-like grain boundary model [1] with a = 0.01 for systems with the broad homogeneity regions: α(HCP-Al,Ti), β(BCC-Al,Ti), α_2(AlTi$_3$), γ(AlTi) and γ(AlNi). The consistent description for all condensed phases in the Al - Ti and Al - Ni alloys firstly developed with help of phase diagrams calculation. We took the thermodynamic properties of the phases of elements from SGTE [3].

We have obtained by computer modelling the temperature dependences of the grain boundary concentration Z^b and the temperature dependences of the energy characteristics G_R, G_F. We have obtained also the regions of phase existence (consistent with corresponding phase diagram) and zero- segregation lines L_0. There are general tendency of increasing the isoconcentration sections Z^b for Al - Ti and decreasing Z^b for Al - Ni with temperature growth.

In the α_2 - Al,Ti phase we obtained zero-segregation line L_0 is external for the region of phase diagram existence. Impoverishment of aluminium atoms on the boundary under cooling was found for whole region of α_2 phase: $Z^b = 27.5$ at.%Al at the top of this region (1472 K, 33 at.% Al) and at 1000 K we have Z^b from 37 at.%Al (Z = 45 at.%Al) to $Z^b = 0.85$ at.%Al (Z = 20 at.%Al). In the α - Al ,Ti phase we obtained L_0 line from (Z = 31 at.%Al , T =1530K) to (Z =33 at.%Al, T=1470K), and the segregation maximum $Z^b = 86$ at.%Al for Z =50.1 at.%Al , T = 1793K. In the β - Ti,Al phase we obtained L_0 line from (Z = 6 at.%Al, T =1970K) to (Z =31 at.%Al ,T =1620K), and segregation maximum at $Z^b = 55$ at.%Al for Z = 42.7 at.%Al, T = 1793K . In the γ - Al,Ti phase we obtained L_0 line from (Z = 47.5 at.%Al, T =1650K) to (Z =61at.%Al, T =1350K), and the segregation maximum at Z^b =77 at.%Al for Z =65 at.%Al, T = 1483K, with tendency of increasing Z^b changes to saturation at Z = 65.5 at.% Al with instability at T ≤ 1200K. Regions of phase domaines intersections reveale decreasing of grain boundary equilibrium segregation with cooling: Z^b/Z changes from 1.2 (Z=52 at%Al, T=1793K) and later to 0.42 at 1000 K.

For the γ phase in the Al – Ni system the zero-segregation line L_0 goes from the melting point (1911K, 50 at.% Al) to (1370K, 36 at.% Al). For the γ - Al,Ni phase we have tendency of Al atoms segregation with its atomic fraction increasing and cooling: $Z^b = Z$ (1911 K, 50 at.% Al) at 1000 K through $Z^b = 63.9$ at.%Al (Z = 45 at.%Al) up to $Z^b = 84$ at.%Al (Z = 65 at.%Al). When Z < 50 at.%Al Z^b/Z=0.67 (1668K,30 at.% Al). For Z ≥ 50 at.%Al the atoms of

aluminium go to boundaries: at 1000K Z^b/Z changes from 1.42 ($Z = 45$ at.%Al) to 1.29 ($Z = 65$ ar.%Al).

We have obtained also general tendency of correlation between the temperature dependences of the energy characteristics G_R, G_F and the temperature dependences of the concentration Z^b on grain boundaries under the equilibrium segregation substitution atoms.

Conclusions

The Al-Ti and Al-Ni alloys with aluminium content of about and higher then 50 at.% revealed the segregation of aluminium atoms on the grain boundaries. Analysis of the grain boundary segregation tendencies for the γ phases in the Al –Ti and Al – Ni systems also permit other intermediate micro-phases nucleation prognozis on boundary regions. These effects may explain the high-temperature intercrystalline fragility of these alloys.

References

[1]. Danylenko V.M., Yagodkin V.V. Modelling of the temperature dependence of the equilibrium substitution atoms segregation on grain boundaries of binary alloys , Kyiv, Preprint of Institute for problems of material science NASU; 1993, N2 , P.22 . (in Russian).

[2]. Danylenko V.M. Real crystals models , Kyiv: Naukova dumka, 1983, P.224.(in Russian).

[3]. Dinsdale A.T. SGTE data for pure elements, CALPHAD, 1991, 15(4) , P.317 .

PHASE INTERACTION IN THE TERNARY SYSTEM ZrO_2-Y_2O_3-Eu_2O_3 AT HIGH TEMPERATURES

<u>Andrievskaya Elena R.</u>, Lopato Lidiya M.

Institute of Materials Science Problems, Kiev 03142, Ukraine

ABSTRACT

Phase equilibria in the binary ZrO_2-Eu_2O_3, Eu_2O_3-Y_2O_3 systems and ternary ZrO_2-Y_2O_3-Eu_2O_3 system were studied in the wide range of temperatures (2500-1250 °C) and concentrations (0-100 mol % Eu_2O_3) by thermal analysis in air, X-ray diffraction, microstructural and petrographic analyses, electron microscopy using melted and annealed samples. Phase diagrams of the Eu_2O_3-Y_2O_3, ZrO_2-Eu_2O_3 and ZrO_2-Y_2O_3-Eu_2O_3 systems are developed.

INTRODUCTION

Europia as well as yttria is useful dopant to refractory oxide such as zirconia. Because of its high capture cross section in fast neutron fluxes and because this absorption worth is sustained by chains of high cross-section daughter isotopes, europia is attractive as a control and shutoff rod material in fast reactors. Europia is a suitable for these purposes since it is relatively stable chemically, has a high melting point (2320°C), can be fabricated easily into dense bodies with a high europia density, and is readily available. However, disadvantage associated with the use of pure europia is that when it is fabricated at temperatures above 1100°C the higher-temperature monoclinic B form is produced which exhibits undesirable swelling under fast neutron irradiation. The cubic structures can be stabilized at sintering temperatures by using suitable additives. Additions of zirconia and yttria to europia suppress grain growth and improve its elastic properties [1].

The main purpose of this work is to investigate the physics and chemistry of phase interactions in the ternary ZrO_2-Y_2O_3-Eu_2O_3 system at high temperatures and wide concentration range. This system is perspective from the standpoint of creation high-refractory materials and ones with increased strength characteristics in which the composition of both matrix and strengthening phase is the same.

Phase relations in the boundary binary systems Eu_2O_3-Y_2O_3, ZrO_2-Eu_2O_3 were studied in the wide range of temperatures (1250-2800°C) and concentrations (0-100 mol % Eu_2O_3). Phase diagrams of these systems were developed [2, 3].

Phase equilibria of the system Eu_2O_3-Y_2O_3 are characterized by the formation of the fields of solid solutions of various extent based on the hexagonal (A- and H-type), monoclinic (B), cubic (C- and X-type) modifications of the rare-earth oxides, that is known for the majority of cerium subgroup oxides. There is the peritectic-type transformation on the liquidus at 2370 °C, 58 mol % Y_2O_3 and point of minimal temperature at 2310 °C, 10 mol % Y_2O_3.

In the subsolidus region of the phase diagram ZrO_2-Eu_2O_3 system the fields of solid solutions based on tetragonal (T) and cubic (fluorite-type, F) modifications of zirconia, pyrochlore-type compound $Eu_2Zr_2O_7$ as well as solid solutions on the basis B, A, H and X forms of Eu_2O_3 were found. The dopants of zirconia to europia have stabilized the C-phase at the higher temperatures, increasing the range of its existence. The liquidus of the system ZrO_2-Eu_2O_3 is characterized by eutectic transformation at 2310°C, 26 mol % ZrO_2. The compound $Eu_2Zr_2O_7$ is not observed on the liquidus surface but is created in the solid phase at temperature ~ 2000 °C.

Solid solutions based on T, M and F modifications of zirconia as well as C and H modifications of yttria are known to form in the system ZrO_2-Y_2O_3 at high temperatures. The higher yttria content the higher is the liquidus temperature in the ZrO_2-Y_2O_3 system which reaches its maximum at 20 mol % Y_2O_3 [4]. There is an eutectic transformation at 2360 ±25 °C and 87 ±2 mol % Y_2O_3. The liquidus of this system is also characterized by a peritectic transformation at 2440 °C and 76±2 mol Y_2O_3 [5].

EXPERIMENTAL PROCEDURE

The samples for investigations of the phase equilibria in the ternary ZrO_2-Y_2O_3-Eu_2O_3 system were prepared from 5 to 10 mol % by both mechanical mixing of oxides and coprecipitation of hydroxides. Part of these samples was used for the investigation in the as prepared form (melted specimens). Other samples were annealed at

1550 °C for 70 h in air. The boundaries of the phase fields were determined by thermal analysis in air up to 3000 °C using a solar furnace. The phase compositions were investigated by petrography, X-ray phase analysis, electron microprobe X-ray analysis, chemical and X-ray fluorescence spectrum analysis.

RESULTS AND DISCUSSION

An investigation of interaction in the system ZrO_2-Y_2O_3-Eu_2O_3 and over the whole range of concentrations at temperatures above 2000 °C revealed no new phases. The results of this investigation showed that the liquidus surface of this system is consisted of four fields of phase-primary crystallization: namely, solid solutions based on ZrO_2 phase with a fluorite-type structure F, H and C forms of Y_2O_3 as well as X- Eu_2O_3. There are two invariant points four-phase equilibria of peritectic-type on the liquidus with the coordinates 20 mol % ZrO_2, 50 mol % Y_2O_3 at 2340 °C (U_1) and 20 mol % ZrO_2, 40 mol % Y_2O_3 at 2310 °C (U_2).
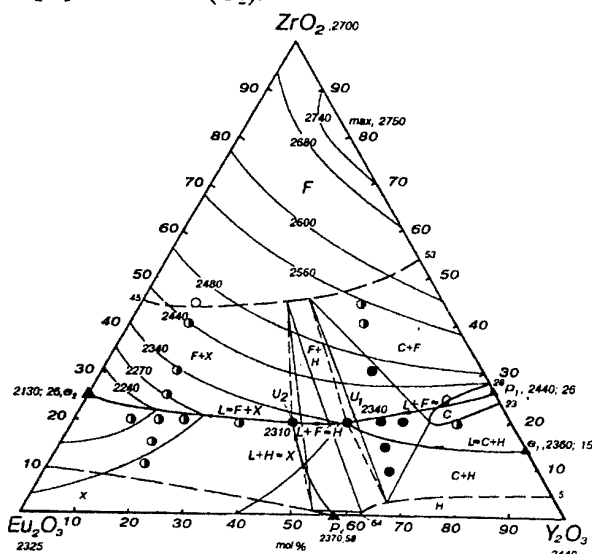
Fig. 1. Crystallization paths for the ZrO_2-Y_2O_3-Eu_2O_3 system (O -single phase, ◑ - binary phase, ● - ternary phase samples).

The minimal melting temperature for the ZrO_2-Y_2O_3-Eu_2O_3 system is 2130 °C(e_2), maximum temperature of the liquidus surface is equal to 2750 °C, which corresponds to the melting point of 80 mol % ZrO_2-20 mol % Y_2O_3. The liquidus surface of this system contains the same fields as do the solidus surface, and the most extended field is that of the fluorite based solid solutions. Solidus surface in the investigated system consists of 2 ternary-phase fields corresponding to the

transformations L+H→X+F and L+C→H+F. The crystallization of the alloys was investigated using the data on structure of the liquidus and solidus surfaces. The crystallization paths for the alloys and the schematics of the reactions were constructed (Figs. 1, 2).
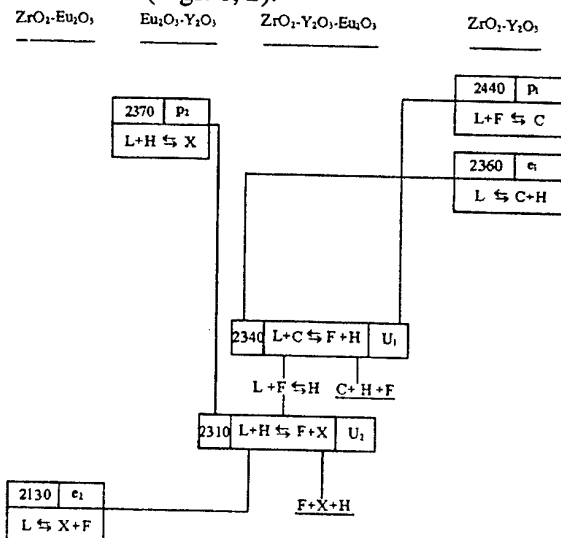
Fig. 2. Schematic of the reactions proceeding during equilibrium crystallization of melted samples in the ZrO_2-Y_2O_3-Eu_2O_3 system.

The isothermal sections were developed at 1550 °C and 1250 °C. Some similarities and differences are observed. At 1150-1250°C we identified single fase regions of solid solutions based on T- and F-ZrO_2, B- and C-Eu_2O_3, C-Y_2O_3 and $Zr_3Y_4O_{12}$ (δ).

REFERENCES

[1] D.A. Moore and J.F Fergusson: J. Am. Ceram. Soc. Vol. 65 (1982), 414.

[2] E.R. Andrievskaya, Z.A. Zaitseva, A.V. Shevchenko, and L.M. Lopato: Inorganic Materials. Vol. 33, No. 4 (1997), 390.

[3] L.M. Lopato, E.R. Andrievskaya, A.V. Shevchenko, and V.P. Red'ko: J. Inorganic Chemistry. Vol. 42, No. 10 (1997), 1736.

[4] A.V. Shevchenko, V.D. Tkachenko, L.M. Lopato et al.: Powder Met. and Metal Ceram. No. 1 (1986), 91.

[5] M.F. Trubelja and V.S. Stubican: J. Am. Ceram. Soc. Vol. 71 (1988), 662.

ACKNOWLEDGEMENTS

COMPLEX HIGH-TEMPERATURE OXIDE MATERIALS IN THE SYSTEMS Al$_2$O$_3$ – ZrO$_2$ – RARE EARTH OXIDES

Lakiza S.M., Lopato L.M., Red'ko V.P.

Frantsevich Institute for Problems of Materials Science NAS of Ukrajina, Kyiv, Ukrajina

Systems Al$_2$O$_3$ – ZrO$_2$ – RE-oxides attract much attention as a source for design of refractory oxide materials with complex composition. The initial oxides are very hard, stiff, have low thermoconductivity and high chemical stability. RE-oxides are the best ZrO$_2$ stabilizers, alumina improves thermomechanical properties as well as inhances the stability of ceramics at hydrothermal conditions.

Phase diagrams are the best technologist assistant for constructing advanced materials. So the aim of the present investigation was to study Al$_2$O$_3$ – ZrO$_2$ – RE-oxides phase diagrams, where Ln – La and Y. These RE-oxides are the representatives from Ce and Y subgroups.

Samples for the investigation were prepared of pure "ч" qualification oxides, melted in high-temperature DTA set and analysed by DTA, X-ray, petrodraphic and microstructural methods. The results of investigation are presented in Fig. 1 and 2 as isothermal Al$_2$O$_3$ – ZrO$_2$ – RE-oxides phase diagram sections at 1250 °C.

phase fields. It is the result of interaction differences in binary bounding systems Al$_2$O$_3$ – RE-oxides and ZrO$_2$ – RE-oxides. In the Al$_2$O$_3$ – La$_2$O$_3$ system only two compounds LaAlO$_{18}$ and LaAlO$_3$ are known. Three compounds Y$_3$Al$_5$O$_{12}$, YAlO$_3$ and Y$_4$Al$_2$O$_9$ are known in the system Al$_2$O$_3$ – Y$_2$O$_3$. There is only in ones compound in bounding systems ZrO$_2$ – RE-oxides and both are superstructures: La$_2$Zr$_2$O$_7$ with pyrochlore-type structure melts congruently at 2340 °C, and Zr$_3$Y$_4$O$_{12}$ with rombohedral structure decomposes in solid state above 1382 °C.
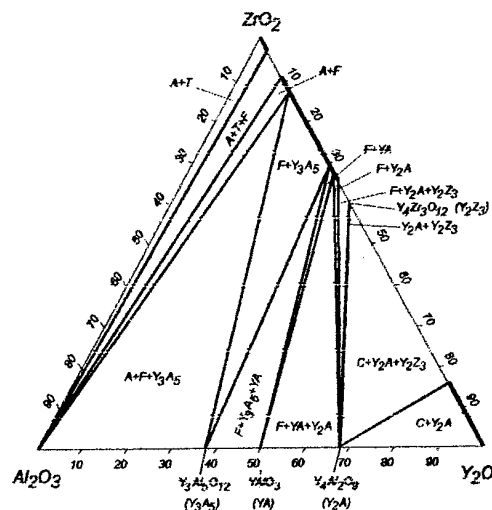
Fig. 2. Isothermal section of the Al$_2$O$_3$-ZrO$_2$-Y$_2$O$_3$ phase diagram at 1250 °C.

One should draw attention to the wide area (up to 40 % mol. Y$_2$O$_3$) of solid solutions on the base of ZrO$_2$ in the binary bounding system ZrO$_2$ – Y$_2$O$_3$. The La$_2$O$_3$ solubility in ZrO$_2$ does not exceed 1,5 % mol. in the bounding system ZrO$_2$ – La$_2$O$_3$. All these differences leads to the different interactions in the system studied.

But these two systems have also some common features.

First, no ternary compounds and solid solution areas were found in both systems. Second, the interaction in the systems is defined by the phases on the base of ZrO$_2$; they are in equilibria with majority of other phases. This fact is the scientifical base for constructing composite materials, in wich reinforcement phases do not react with a matrix.

Fig. 1. Isothermal section of the Al$_2$O$_3$-ZrO$_2$-La$_2$O$_3$ phase diagram at 1250 °C.

At first site the interaction in these systems are quite different. Really, the isothermal section of the Al$_2$O$_3$-ZrO$_2$-La$_2$O$_3$ system contains four three-phase fields and four two-phase fields. The same section in the Al$_2$O$_3$-ZrO$_2$-Y$_2$O$_3$ system contains six three-phase fields and seven two-

PERSPECTIVE EXTREMELY HIGH-FREQUENCY ELECTRO-ACOUSTICAL TRANSDUCER OF HYPERSOUND ON BASE OF BN-NANOTUBE/SiC-NANOWHISKER

Pokropivny V.V., Bezymjany Yu.G., Pokropivny A.V., Prilutskii E.V., Partch R. [1]
Frantsevich Institute for Problems of Materials Science, of Ukrainian NAS, Kiev, Ukraine
[1] Clarkson University CAMP, Potrdam NY, USA

Generators and receivers of irradiation are known to determine the progress in many branches of science and technology. To present time electroacoustical transducers for generation and reception of hypersound waves in a range up to hundreds of giga-hertz on base of surface acoustical waves were developed that were excited on resonant frequencies in the thin piezoelectric films of quarts, LiNbO3, AlN, ZnS, CdS, ZnO, etc. However for high frequencies the wafer becomes to be brittle and difficult to fabricate, because of it ultra-thin width is comparable with half of wave length $d=l/2$. Up to now, there are no effective hyper-sound generators in tera-gertz range, thought the need of which is requested when activating a sintering of ultradisperse superhard particles, when generating of coherent phonons (phaser), and many other applications.

Discovery of nanotubes presents us an unique possibility to solve this problem. The nanotubes posses a number of advantages over the thin films. Firstly, the diameter of nano-tubes lie in the range of 1 - 1000 nm, therefore the extreme frequency of natural transverse hypersound vibration can be raised to ~ 1 - 10 TGz. Secondly, the vibrate spectrum of cylindrical nanotubes is characterized by the number of peculiar circular modes called as whispering gallery modes, such as breathing A_{1g}, whispering/squash E_{2g}, silent E_{1u}, and other modes. Thirdly, by a singularity of this modes is a low attenuation. Fourthly, in some nanotubes the inversion symmetry centers are absent, and in hexagonal layers of hetero-geneous nanotubes an electron charge transfer is presented, so the nanotubes and BN nano-tubes in particular become to be piezoelectric. Fifthly, the quantum chemical calculation of BN nanotube polarization under axial stretching gives non-zero values of piezoelectric constants.

Propagation of hypersound vibrations is known to be possible only in crystals, because in gases the hypersound can not propagates due to it wave length is less then a mean free path, and in liquids it strongly attenuates. Therefore to transfer the hypersound vibration an crystalline rod, for example SiC, must be placed inside the core of nanotube. The scheme of such an electo-acoustic transducer is shown in the figure. The calculations are presented to confirm the BN-nanotube/SiC-nanowhisker as an extremely high-frequency hypersound transducer in giga-tera gertz range.
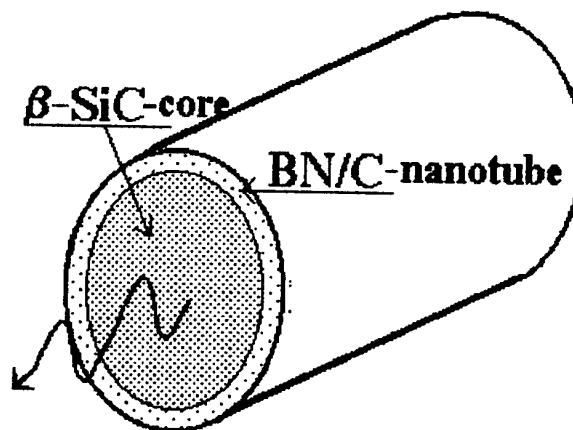
THEORETICAL PREDICTION OF THE ELEMENT COMPOSITION AND INVESTIGATIONS OF THE WEARPROOF FACTORS FOR EUTECTIC COATINGS ON THE d-METALS BASE

N.A. Uskova, A.G. Moljar[1] L.N. Grishchishyna
Institute for Problems of Materials Science, NAS of Ukr., Kyiv, Ukraine
[1]ASTC «Antonov», Kyiv, Ukraine

The Tribotechnical and phisical-chemical properties of the eutectic coatings by our technology [1] compared favourable with analog ones after a sliding friction force tests.

This report is devoted to governing of the properties by the agency of the defect structure forming and by initiation in the multi-component coatings of the eutectic effects.

Investigation was made in the complex approach [1-5].

Theoretical part:

The primary task of investigate is to provide estimations of the energy and dimentiona contributions to the d-metal solvents atomic structure from alloying elements and admixture atoms. It is now that the properties of an materials are function of a structure stability but the local decrease of thermodynanic potentials for microvolume of the grain atomic structure can gives rise to diminution of Gibb's energy G (G is criterion of the material phase stability).

It is widely recognised, that the thermodynamic potentials of the material grains are formed from a local atomic (electronic) characteristics o components in an elementary cells of soli solution.

The energy profitable defect structure must not give rise to break of the material phas stability, but it will be strengthening for one. This question will be considered in detail in report.

The second step towards the solution of this problem consists in calculation of auxiliary microscopic parameters (it uses of the individual atomic /electronic/ characteristics of components).

The author [2] has elaborated the combined approach for estimates of ability to mutua solubility of chemical elements in a solid state materials and has calculated a system of the special auxiliary microscopical parameters of a mutual energetic influence (AMPEI) of four types: normal temperature parameters are

$PElCh = [\pm f(En, R)(\pm)]$, $PEV = [\pm f(Ke, \overset{\circ}{U})(\pm)]$;

high temperature $-$ $VMP = [\pm f(\Sigma m, \overset{\circ}{U})(\pm)]$,

$PIEMR = [\pm f(\Sigma m, S)(\pm)]$ (here En /eV/– electronegativity, R /nm/ – atomic radius, KE /106 J mol/ kg m3/ – energodynamical potential of chemical elements and Σm / J/K, a.u.m. / – atomic energy-contents by Voltchenkova, $\overset{\circ}{U}$ /nm/ – volume per atom).

Application of two types of AMPEI, – PElCh – PEV for quick-forecast of donor/ acceptor activity (the first), of the energy compotibility elements (second) and the solid-solution strength will have been discussed in report.

To anticipate, if the atoms of admixtures and metals have parameters with combination signs [–PElCh(+)]⇔[–PEV(+)] (see table) they are giving rise to formation of an energy profitable of the chemical nature defect structures after the type of the admixture-saturated d-metal complexes /CTC –eng. KPZ-rus., [4]/. CTC d-metal complexes typical formula is:

$$\{ [(H_3N)_6 M_z G L_y ((OH)_2 H)_5]^{4+} + + L_{(x-y)} M_{\{1-[(x-y)+z]\}} \}$$

here L, M – basic components, G – halogen atoms, other – are admixture elements. If the atoms of admixtures and metals have parameters with combination signs [–PElCh(–)]⇔[–PEV(–)] (see table) they are giving rise to isomorphical substitution (solid-solution with intermetallic effect).

Experimental part: The crystal structure, the phase composition and properties of the plaz-ma deposyted eutectic coatings on a Fe-base were investigated in complex approach [1-3].

The research samples were made in ammonia atmosphere.

The complex researches of samples had been carried out by Oge spectroscopy, electro-chemical methods and by X–ray difraction method and microanalyser «Camebax» (operators – M.V. Karpez, V.M. Vereshchaka) .

It was found out that, the investigate plazma deposyted eutectic coatings are characterized by the good systems «dendrites–intermetallics–the topology bond nets of defects after the type of CTC».

127

Table Auxiliary microscopical parameters of electrochemical actyvity [± PElCh(±)] and mutual energy influences [± PEV(±)] for the some mixture components of coatings

A base components (sol) Alloying elements	Sc	Ti	Cr	Mn	Fe	Ni
1	2	3	4	5	6	7
H→(sol.) PEV	− 1,789(+)	− 0,925(+)	− 0,443(+)	− 0,447(+)	− 0,433(+)	− 0,389(+)
H→(sol.) PelCh	− 5,037(+)	− 2,039(+)	− 0,760(+)	− 0,684(+)	− 0,589(+)	− 0,390(+)
N→(sol.) PEV	−10,422(−)	− 3,462(−)	− 1,106(+)	− 1,145(+)	− 1,065(+)	− 0,918(+)
N→(sol.) PelCh	−48,713(−)	−15,293(+)	− 4,157(+)	− 4,043(+)	− 3,577(+)	− 2,748(+)
O→(sol.) PEV	− 3,160(−)	− 58,985(−)	− 2,195(+)	− 2,325(+)	− 2,075(+)	− 1,673(+)
O→(sol.) PelCh	−16,786(−)	−296,5(−)	− 9,604(+)	− 9,648(+)	− 8,207(+)	− 6,013(+)
B→(sol.) PEV	+31,109(−)	+22,986(−)	+35,309(−)	+49,959(−)	+31,490(−)	+39,552(−)
B→(sol.) PelCh	− 2,255(−)	− 2,383(−)	− 2,507(−)	− 2,100(−)	− 2,044(−)	− 1,713(−)
C→(sol.) PEV	+39,957(−)	+30,393(−)	+50,423(−)	+70,464(−)	+45,437(−)	+59,326(−)
C→(sol.) PelCh	− 3,692(−)	− 4,322(−)	− 6,261(−)	− 5,398(−)	− 5,692(−)	− 6,147(−)
Al→(sol.) PEV	+ 3,333(−)	+ 5,182(−)	+ 0,695(+)	+ 2,284(+)	+ 0,250(+)	+ 0,333(+)
Al→(sol.)PelCh	− 1,766(−)	− 5,562(−)	+ 0,452(+)	+ 0,765(+)	+ 0,855(+)	+ 1,075(+)
Si→(sol.) PEV	+ 6,813(−)	+ 3,379(+)	+ 0,609(+)	+ 1,596(+)	+ 0,321(+)	+ 0,364(+)
Si→(sol.)PelCh	− 6,320(−)	− 7,448(+)	− 0,659(+)	− 0,493(+)	− 0,315(+)	+ 0,026(+)
Zr→(sol.) PEV	− 8,480(−)	− 2,315(+)	− 0,794(+)	− 0,706(+)	− 0,798(+)	− 0,678(+)
Zr→(sol.)PelCh	− 0,719(−)	+ 0,784(+)	+ 0,862(+)	+ 0,996(+)	+ 1,004(+)	+ 1,058(+)

Notes: *PelCh −auxiliary microscopical parameter of electron-chemical mutual influence of atoms; PEV − one for estimations of relation ability of components to homogeneous alloying. First sign /before parameter/ points out an energy deposit but second one /after/ − is a dimentional difference between admixture atom and basic one.*

Investigation of phase state for coatings had been carried out by X–ray diffractometer DRON–UM1 and by the transmission electronic microscopy.

It is a matter of common experience clusters of defects after the type of CTC were disposed on (110), (112), (111) crystallographical planes of the d-metal solid solution; embryos of carbides, intermetallic compounds, eutectic phases had been formated on a cluster nonvalency bonds of CTC; scandium and hydrogen are general the CTC initiate elements in composition of this coatings. It was found out that the plazma deposyted eutectic coatings have the adhesion strendth to Fe-base very high.

Conclusions: **1.** As thermodynamical potentials are function of atomic characteristics, the relation energy contributions of components from powder mixture can be determined by agency PelCh – PEV.

2. It was found out that the **simbios** of some factors for system «dendrites–intermetallics–the hydrogen-saturated topologybonding cluster-nets of CTC defects» **forms the strength framework**, and the general load from an external factors is carry out by it.

References:
1. Uskova N.A. Osobennosti formirovanija structury pokrytij i eje vlijanie na phiz-mech. svoistva. //Sbornik trudov IPM NAN Ukr. Adgezija rasplavov i paijka materialov. –Kiev, 1997, v.33, S.113
2. Grishchishyna L.N. Microskopicheskaja teorija dodiagramnogo vybora elementnogo sostava na osnove 3d-, 4d-, 5d-metallov // Sb. trudov IPM NAN Ukr.Sovrem. probl. phizich. mat. –Kiev, 1999, t.1; t.2
3. Uskova N.A., Trefilov V.I., Grishchishyna L.N. O roli electronnoij structury scandija v usilenii effectov, «porjadok-besporjadok» v sisteme s 3d-metallami. //Sb. trud. IPM NAN Ukr Electronnoe stroenie i svoijstva tugoplavkih soedineniy –Kiev, 2000, S. 79.
4. Grishchishyna L.N. O roli phiziko-himicheskoij prirody promegjutochnyh soedin. tipa CTC v formirovanii svoijstv 3d-binarnyh splavov. // Sb. trudov IPM NAN Ukr., Aktualnye probl. v materialoved. – Kiev, 1996, S.28
5. Uskova N.A., Moljar A.G., Trefilov V.I. About role of hydrogen-saturated defects after the type of CTC /KPZ-rus./ in formation of wearpoof for eutectic coatings //Col. Report ICHMS`01, Alushta, Ukr., 2001, 16-22 sept., P.422

SIMULATION OF THE PROCESS OF GLASS PRODUCT HOT PRESSING

<u>Sereda G.N.</u>, Samsonov V.I.
Federal State Unitary Enterprise "Obninsk Research and Production Enterprise
"TECHNOLOGIYA", Obninsk, Russia

The process of hot pressing the complex-shaped profile glass products on the Walter type automatic line with the natural cooling of the mold and product open surfaces is discussed in the paper.

The line consists of:
- rotary table with a set of mold matrices fixed circumferentially at regular intervals;
- furnace-matrix glass feeder, press with a punch, lift for transferring molded items from the matrix onto the line of annealing which are fixed at definite positions over the table;
- driving systems for the line elements;
- systems of programmed parameters for pressing mode control.

The molding process is of cyclic character. It consists of several stages: successive uniform movement of the table with the matrices along the positions in the turn-stop mode, glass feeding, glass product molding, transfer of the glass product from the matrix onto the line of annealing.

Hot pressing is accompanied by the continuous cooling of the glass mass at the expense of heat transfer from this glass mass through the forming surfaces onto the heat removal surfaces of the tooling, line equipment and into the environment and also by the transformation of the product material from the viscous state into the aggregative solid state. In this case thermal stresses may occur in the product the amount of which depends on the rate of material cooling at the temperature close to the temperature of softening and on the viscous properties of the material. Thus, hot pressing is a complicated heat exchange process which requires a consideration of press line technical characteristics, geometrical dimensions of the molds, physical properties of the press mold and product materials in order to obtain appropriate products.

A model of glass product hot pressing based on solving the problem of nonstationary thermal conductivity for the system of bodies with the variable boundary conditions is proposed. A heat exchange model makes it possible to examine the processes of heat exchange between a glass product (drop), matrix, punch, table and the environment during separate stages or during the whole cycle of pressing. The problem of nonstationary thermal conductivity was solved in the cylindrical system of coordinates using Krank-Nickolson implicit scheme and the method of elemental heat balance for each separate stage. This method is characterized by the constant boundary conditions of heat exchange for the process elements and by the initial conditions determined by the temperature fields in the elements according to the last time interval of the previous stage. The initial conditions in the elements for the first cycle were determined from the temperature and thermophysical properties of the glass mass fed onto the line, from the quantity of heat released to the glass mass during one cycle, from the duration of the cycle and from the temperature of press mold forming surfaces calculated for the conditions when a glass product does not adhere to the press mold and there are no cracks in the glass product.

Heat removal from the open surfaces of the elements at all stages was considered to be a process caused by natural convection and (or) radiation.

The peculiarities of heat transfer in the "product-tooling-environment" system during one cycle for the glass type product were studied with the help of a heat exchange model. The quantity of heat released to the tooling elements and into the environment through the forming surfaces of the product was determined. An important role of matrix geometry and material in the process of heat removal was found.

The problems of a steady process of heat exchange for the case with a water-cooled punch and two matrices from the 40x13 steel are considered in the paper. One matrix is manufactured by the conventional method and the other – with the use of the

evaporation/condensation system (ECS) of the heat exchange.

The measurements made during the real process of pressing revealed the agreement between the calculated and experimental temperature values of the forming surfaces with an accuracy of 10 %. The results obtained point to an essential decrease in the scatter of temperatures of the forming surfaces of the matrix with ECS as compared to the conventional matrix.

The effect of each parameter controlling the process on the magnitude of steady temperature field in the press mold was evaluated on the basis of a multifunctional analysis.

The algorithm for bringing the line with the tooling to the required initial conditions has been developed. Simpler ways of adaptation of the heat exchange system to the changed initial conditions (glass mass temperature) was found in the case of using the matrix with ECS. The validity of the pressing mode chosen was evaluated based on the maximum thermal stresses occurred in the glass product.

A heat exchange model constitutes software with a set of subprogrammes intended for solving the heat problem at each stage. Combining the subprogrammes in varying sequence, one can significantly increase the number of the problems which can be solved.

COMPUTER-AIDED MODELING OF THERMAL ELASTOPLASTIC STRESSED-STRAINED AND LIMITING STATES OF MULTILAYER COMPOSITES COATED WITH STRUCTURE-INHOMOGENEOUS MATERIALS

Shestakov S.I.

Bakul Institute for Superhard Materials of the National Academy of Sciences of Ukraine, Kiev, Ukraine

A new approach to the assessment of adhesion and cohesion strengths of multilayer composites has been developed. The approach is based on the computer-aided modeling of the thermal elastoplastic stressed-strained and limiting states of the composites after coating and when operated.

Studied were multilayer composites produced by the CVD and PVD coating of substrates with structure-inhomogeneous materials and other traditional methods (welding, hard-facing, diffusion).

A data bank has been formed that includes the key physico-mechanical properties both of the individual layers and the composite as a whole as well as the most typical schematic diagrams of their loading. The bank can be supplemented with the results of analysis of the basic regularities of the local straining and fracture of the composites under the loading conditions similar to those in operation.

The stressed state, static and fatigue strengths of multilayer composites have been FEM-studied using the specially developed "KOMPOZIT" set of software. The program takes into account the sputtering technology, structure inhomogeneity of materials of individual layers and dependence of their properties on the scale factor. The "KOMPOZIT" includes a number of service programs that assist essentially in the preparation of the initial and in the processing of the FEM-calculated information.

The potentialities of the suggested approach are illustrated by modeling the stressed-strained and limiting states of a composite. The composite has been produced by sputtering of an a-C:H structure-inhomogeneous diamond-like carbon film onto a polymeric substrate of polyethylene terephthalate by butane decomposition in a glow discharge plasma [1]. As a rule, the two-layer composite is used as an external protective layer for multilayer optical elements operating in corrosive media and can be subjected to extreme heat and power loads. The hardness, Young modulus and fracture toughness coefficient used in calculations have been measured on a Nano Indenter II mechanical microanalyzer (Nano Instrument Inc., USA) [1].
The thickness of the polymeric substrate was 100 µm and the thickness of the coating sputtered at a temperature of about 70-150 °C was varied from 5 to 10 µm.

Our calculations have shown that residual compressive heat stresses act in the coating. They increase with sputtering temperature and diamond-like film thickness. In terms of the limiting state criterion [2] it follows that at a sputtering temperature of about 150 °C the adhesion strength of a composite on cooling is close to zero. This can result in a spontaneous peeling of the coating.

We have modeled the lengthwise elastoplastic deformation of the two-layer composite by tensile stresses, which are close in value to the respective strength of the substrate material. We have found and experimentally verified that the diamond-like coating with residual stresses starts to fail in the region of the peak tangential and equivalent stresses. The failure is accompanied by the initiation of cross cracks spaced 15-20 µm apart.

References

1. M.A. Voronkin, S.N. Dub, V.G. Malogolovets, G.A. Podzyarei, T.A. Nachalnaya, and B.A. Maslyuk, Structure and mechanical properties of a-C:H films deposited onto polymeric substrates, Diamond and Related Materials, 1994, no. 4, pp. 5-9.
2. S.I. Shestakov, The working out of the extreme state criteria for the structurally inhomogeneous materials and their application at the static and cyclic loading, Int. Conf. on Assessment and Substantiation of the Extension of the Service Life of the Structural Elements, Abstr. in 2 volumes, vol. 2, pp. 488-489, Kiev, 2000.

A KINETIC STUDY OF CLUSTERS EVOLUTION UNDER VVER-TYPE REACTOR CONDITION

Gokhman A., Britavskaya E., Boehmert J.[(1)]
South Ukrainian Pedagogical University, Department of Physics, 65020 Odessa, Ukraine
[(1)]Forschungszentrum Rossendorf e.V., Institut für Sicherheitsforschung, PF 510119, 01314 Dresden, Germany

It is well-known a lot of successful applying of the nucleation theory [1] to the different actual problems: glass transition, alloys decomposition, phenomena in biological systems, melting of clusters and bulks, gas-liquid- crystal transition near the triple point and some others. One of the perspective developments of [1] is the so-called multistate kinetics theory (MSKT) when the evolution of thermodynamics system is considered step-by-step from the nucleation (fluctuation) stage to the growth (deterministic) stage and then to the coarsening (ripining) stage.

The goal of the present paper is applying the MSKT approach to the problem of the neutron stimulated damage structure of the reactor pressure vessel (RPV) steel. Most damage caused by fast neutrons results from the creation in elastic collisions of energetic primary cnock-on atoms (PKAs), for they in turn produce cascades of atomic displacements.

A cascade produced by a PKA occupies a region only 10 nm across, yet within in the concentration of displaced atoms may be as high an as a few percent. A cascade of displacements at the end of collision phase consists principally of a core of vacancies surrounded by a mantle of the associated self-interstitial atoms. The kinetic energy density in the cascade can be much higher than equilibrium melting point of the solid, though this declines quickly as heat is dissipated by the surrounding lattice. Nevertheless, the lifetime of the thermal spike phase is of the order of several ps, and it is expected that this should permit extensive atomic rearrangements to occur in the highly disorded structure.

The configuration of the foreign atoms in the irradiated material is a result of competition between disorder due to atomic jumps induced by nuclear collisions (ballistic jumps) and thermally activated reording due to the usual atomic jumps. Cascade stage has been investigated by molecular dynamics, molecular statistics and kinetic lattice Monte Carlo simulations [for example, 2] and probably can be considered in frame of the spinodal decomposition theory under adiabatic condition [3].

Only after this stage when temperature and pressure became the constant ones the MSKT with it correlations of the equilibrium thermodynamics can be used. Foreign atoms diffusivity increase in many times due high value of the free vacancies concentration. Resulting high mobility of the point defects and foreign atoms is a good background of the nanoclusters formation. Their distribution on chemical content and size effects on the mechanical integrity of the RPV steels.

Sophisticated micro-structural analysis methods like small angle neutron scattering (SANS), atom probe field ion microscopy (APFIM), high resolution field emission scanning transmission microscopy (FEGSTEM), or, less direct, positron annihilation spectroscopy (PAS) have been proven the existence of nanoscale micro-structural features in reactor pressure vessel (RPV) steels after irradiation under typical reactor condition. Their size amounts to approximately 1 to 2 nm in the radius.

In RPV steels with high content of copper Cu-rich precipitates (CRP) has been detected experimentally and in computer simulation. Cluster dynamics (CD) approach is used to

obtain the size distribution functions (SDF), mean size R_m, number density (N_p) and volume content (C_v) of the pure copper clusters time dependence in the electron irradiated dilute FeCu binary alloys. Fluence dependence of the R_m, N_d and C_v values of the CRP in the neutron irradiated RPV steels is investigated on the nuclear, deterministic and coarsening stage in.

The best way to describe the experimental results of low Cu steels is to assume the presence of the multi-component clusters (MCC) consisting of Fe, Cu, Ni, Mn, Mo and other foreign atoms but also, probably, of vacancies. Furthermore the evolution of stable vacancy clusters (VC) is often discussed. Unlike to CRPs and MCCs pure VC-defects can hardly directly be identified. Nevertheless, simulation studies have been shown their significance.

First in [4] it was proved that VC can be considered as an ensemble of vacancies in 2 n-n or 4 n-n nearest locations. This approach corresponds to the maximum position of the pair distribution function in iron. Stoller [4] investigated the nucleation stage of the VC evolution. Future progress of this approach is expected concerning the calculation of the time dependence of the VC radius and SDF.

Our models the CRP and VC evolution beginning at the nucleation stage and finishing in the coarsening stage. For this typical VVER-type reactor conditions are considered. The results are compared with the results of SANS experiments which were carried out at specimens irradiated

Additonal to approach [4] the accounting of the elastic interaction between VC and matrix provide the stopping of the VC growth in the neutron irradiated materials that correspond to the experimental data. Analytical it was found the possibilty of the small decreasing of the VC radius under increasing of the G_{dpa} value. On the other hand calculated VC radius at the end of the deterministic stage smaller then the experimental finding one. It points out on the necessarity of the more precise determination of the elastic potential $\Phi^{(\varepsilon)}$ first, and second to consider the visco-elastic effect too.

The following progress in the investigation of the VC on the coarsening stage is connected with working out of the more adequate approach to find SDF. Method [5] is valid in full measure for great size of the VC when the linearity approximation of the Thomas-Freundlich term. It is easy to find analytical that using of this approximation doesn't produce the mistakes in the SDF values near the peak of it only. Other restriction of the [5] approach to the RPV steels is the life- time of the nuclear power plants less then time is recommended for application of it. Calculated SDFs of CRP are found closely to ones for irradaited alloy B but not alloy A that proves the validness of our approach.

VC evolution in the nucleation stage is analysed on the base of the computer simulation according to [4]. The final data of this stage are taken for the initial data of the deterministic stage. In this stage elastic interaction between iron matrix and VC is considered. For VC evolution in the coarsening stage the Lifshitz-Slezov approach with an additional accounting of the elastic effect is used. CD approach is used to investigate the CRP evolution.

Reference

1. Selected Papers of Research Workshops Nucleation Theory and Applications, ed.J.W.P.Schmelzer, G.Roepke, V.B.Priezzhev, JINR, Dubna, (1999), p.510
2. R.E.Stoller, Nucl.Eng.Des. 195 (2000) p.129
3. A.Mishev, I.Gerrof, J.Schmelzer, J.Z.Phys. B94, (1994) p.101
4. R.E.Stoller, J. of Nucl. Mater. 276 (2000) p.22
5. I.Lifshitz, V.Slezov, J.Chem.Phys., 19 (1961) p.35

EVOLUTION OF APPROACHES TO CREATION OF MATERIALS FOR HIGH-LEVEL WASTE IMMOBILIZATORS

Azhazha Zh.S., Vakulenko S.V., Gabelkov S.V., Danilov P.A., Kantsedal V.P.,
Lavruk A.G., Mironova A.G., Neklyudov I.M., Pilipenko A.V., Poltavtsev N.I., Tarasov P.V.,
Sayenko S.Yu., Surkov A.E., Kholomeev G.A., Shevyakova Eh.P.
Institute for Solid-State Physics, Materials Science and Technology at National Science Center
"Kharkov Institute of Physics and Technology" (ISSPMST NSC KIPT), Kharkov, Ukraine

A problem concerned with isolation of high-level wastes (HLW) from nuclear power plants and spent nuclear fuel (SNF) not subjected to radiochemical reprocessing engendered a variety of approaches to solving this problem. One of approaches is SNF and HLW disposal into deep geological formations. This approach can be realized by different ways such as HLW vitrification, encapsulating the spent fuel assemblies (SFA) on whole or their fragments with applying diverse shielding barriers: metallic, ceramic, glass-ceramic etc. [1-5].

Since the end of the eighties of XX century the researchers of our Institute developed a concept for encapsulating RBMK spent fuel assemblies with the use of different natural rocks (mainly of magma origin) as a source materials for creation of shielding barriers [6].

At a level of laboratory technologies different rocks were tested to create ceramic and glass-ceramic materials of protective immobilizing forms for HLW and shielding barriers for SFA encapsulation.

Preconditions for these experiments were R&D works, being carried out successfully during foregoing years, on gasostatic treatment of different materials, gasostatic pressing, development of high gas pressure cryogenic sources - cryogenic thermocompressors, and later on designing and manufacturing half-scale commercial gasostats for pressures (400-600 MPa) much higher than commonly applied in the industry (100-150 MPa) [7-8]. High gas pressures were used for needs of the aircraft industry, military-industrial establishment, radio-electronics and automotive industry. In most cases the use of high gas pressures for the high-temperature gasostatic treatment (HTGT) and hot isostatic pressing (HIP) provided a significant improvement of technical characteristics of

materials treated. Particularly, remarkable results were gained during treatment of the non-ferrous castings (values of mechanical properties were increased by a factor of 2-2.5).

The majority of rocks (granite, basalt, gabbro etc.) were formed under conditions of high temperatures and pressures during thousand years. On the other hand, formation of clay materials frequently is a final process of fracture of the rocks such as granite. Therefore, application of HIP with the use of high pressures, at first sight, was reasonable and necessary.

The first experiments on the hot isostatic pressing of magma rocks (granite, basalt) were carried out at a temperature not higher than 1000°C and pressure of working gas argon not higher than 80 MPa. Because of the incongruent character of melting these rocks and the processes of dissolving more refractory components in the melt, it was not succeeded to compact granites, basalts and gabbro in the solid phase. Plagioclases (for example, albite) being melted at a low temperature dissolved a part of other rock-forming mineral phases (α-quartz, potassium feldspars, mica and accessory materials). As a result, the mass of a material being pressed was redistributed with volume decreasing. A metallic capsule, in which the rocks were subjected to the HIP process in the vertical gasostate furnace along the vertical axis, took a droplet-like form.

A try to create, using the HIP method, matrix materials based on rocks in the form of clay (kaolin and bentonite) evidenced on the necessity of applying more higher pressures (up to 300 MPa) in order to obtain a high-density ceramic material. It was conditioned by the presence in the clay structure of 13 wt.% water (interlayer, interplane and in crystal) liberated by heating up to 800°C. In cavities of the closed capsule with the clay "green" blank a water vapor pressure

~200 MPa was created. The carrying out of HIP at a pressure less than 200 MPa resulted in metallic capsule breaking. It was found that the ceramic material with a theoretical density can be obtained at a pressure not less than 300 MPa. However, the water released from clay did not enter back into the ceramic material. The water took place under the capsule envelope. The use of the powder composition (clay + granite) makes it possible to eliminate this effect. However, a moisture-saturated glass-ceramic material does not possess a sufficient radiation resistance.

Therefore we have offered a two-stage method of manufacturing the glass-ceramic material enabling one to avoid these disadvantages. Parameters of the processes of manufacturing this material completely coincide with available industrial values: temperature not higher than 1050°C and pressure not higher than 100-150 MPa.

Using the mathematical simulation of the processes occuring in glass-ceramics when forming the structure by HIP and subsequent cooling we substantiated the conditions for obtaining sufficiently firm glass-ceramics and the criteria for selection of source rocks taking into account the mineral composition, radiation and corrosion resistance [9,10, 11].

On a basis of experimental results and mathematical simulation we have determined more precisely the parameters of designing and manufacturing a commercial gasostatic installation for encapsulating the spent fuel assembly.

REFERENCES

1. Concepts for conditioning of spent nuclear fuel for final waste disposal, Technical Report IAEA, ser. No 345, Vienna, 1992.
2. Report "ABB atom and the Swedish methods for management of the fuel cycle back end", 1991-01-03.
3. Kedrovsky O.L., Shishits I.Yu., Gupalo T.A. et al. Substantiation of conditions for localization of high-level waste and spent nuclear fuel in geological formations. Atom. Energ., 1991, v.70, No 5, p.294-297 (in Russian).
4. Gustafson, Radioactive waste management in Sweden experience and plans, Int. Conf. Radio-active Waste. Storage, Transportation, Recycling. Environment and Human Impact, RF, S.-Peterburg, 14-18 Oct., 1996, P12.
5. D.A. Knerht, Glass-ceramic waste forms developed at the Idahochemical processing plant for immobilizing HLW and actinides, Int. Conf. Radioactive Waste. Storage, Transportation, Recycling. Environment and Human Impact, RF, S.-Peterburg, 14-18 oct., 1996, A 25.
6. Patent of Ukraine No 25986, Method of fixing radioactive materials. Kantsedal V.P., Tarasov R.V., Saenko S.Yu.
7. Lavruk A.G., Linnik Yu.A., Azhazha Zh.S. et al. Concept for a gasostat - installation of hot isostatic pressing for encapsulating RBMK fuel assembly wastes, Proc. 14th Internat. Conf. on Radiation Phenomena Physics and Reactor Materials Science, 12-17 June 2000, Alushta, KIPT, Ukraine, p.304-305.
8. Lavruk A.G., Linnik Yu.A., Ledovskaya L.N. et al. Upgrated cryogenic thermocompressor KRIT-6M for the closed cycle of the gasostatic installation. Proc. 14th Internat. Conf. on Radiation Phenomena Physics and Reactor Materials Science, 12-17 June 2000, Alushta, KIPT, Ukraine, p. 360-361.
9. Azhazha Zh.S., Gabelkov S.V., Tarasov R.V., et al., Mathematical model of development of mechanical stresses in glass-ceramics under irradiation, Abstracts of Internat. Conf. "Ad-vanced ceramics for the third millenium", Kiev, IPM, 5-9 November, 2001.
10. Sayenko S.Yu., Neklyudov I.M., Kholomeev G.A. et al., "Mathematical simulation of heat- and mass-transfer in the geologic shielding barrier after disposal of the spent nuclear fuel", Zhurn. "Yadernaya i radiatsionnaya bezopasnost'", No 4, 2000, p.66-72 (in Russian).
11. Sayenko S.Yu., Tarasov R.V., Gabelkov S.V. et al. Corrosion resistance of glass-ceramic matrix manufactured by the HIP method in aqueous medium. Proc. 14th Internat. Conf. on Radiation Phenomena Physics and Reactor Materials Science, 12-17 June 2000, Alushta, KIPT, Ukraine, p. 298-299.

FEATURES OF A COMPACTION KINETICS OF POWDER MATERIALS IN NONISOTHERMAL CONDITIONS

Stelmakh L.S., Stolin A.M.[1]
Institute of Problems of Chemical Physics Russian Academy of Sciences
[1]Institute of Structural Macrokinetics and Materials Science, Russian Academy of Sciences,
Chernogolovka, Moscow region, 142432, Russia
E-mail:stelm@ism.ac.ru

Numerically analized the compaction kinetics of powder materials in nonisothermal conditions. For studying the processes of deformation of powder compressible materials the rheodynamic model, including the equations of continuity, heat diffisitivity, motion, rheological rations is used. It takes into account the initial density and temperature distributions in the material. The features of the model is taking into account the transition from liquid state of the material to solid one and the melting of the material in front of the reaction zone.

The new features of a nonisothermal kinetics of compaction are established, which one are characterized by the following main characters - presence of an induction period, during which one the compacting does not take place practically, and capability of "explosive" nature of compaction. The carried out numerical calculations have allowed to update a picture of compacting in a wave mode and to dedicate two autonomous processes: propagation of a compression area in space from a layer to a layer and compacting of a material in compression area.

Is rotined, that at increase of an altitude of a compressed sample there is a continuous transition from a regular mode to a wave mode of compaction. In intermediate area on sizes the so-called transitional modes will be realized, which are characterized by a wide, blurred wave front of compaction.

On the basis of a numerical solution of a problem about nonisothermal compaction and cooling of a viscous compressible media in the cylindrical chamber the analysis of influencing of the thermal factors and geometrical sizes of a sample on characteristic times of two autonomous processes is conducted: spatial propagation of a compression area along a sample from a layer to layer and temporary extracompacting of a material in the compression area. It is revealed, that the effect of slowing the induction period down is increase on remoteness of cross-section of a sample from the migrating cylinder piston and conditions impairment of a thermal insulation of a sample ends. The known earlier experimental result about the presence of two critical sizes of a sample determining condition for obtaining poreless materials is affirmed and justified.

ECOLOGY OF THINKING, A GARANTEE OF PURE TECHNOLOGIES AND THE HEALTHY PLANET

Lavriv L.V.

Institute for Problems of Materials Science, National Academy of Sciences of Ukraine,
Kyiv, Ukraine

Nowadays the ecology of an environment demands for itself new steadfast attention and understanding of the deep reasons of sharp deterioration of a condition of the planet: destruction of an ozone cloud, earthquake, war, flooding, sharp climatic differences etc. It is held back deliberately by originators of the situations, managing representatives of the leading states. Here are infringed interests of the big groups of people which pursue the narrow own purposes which in the obvious image miss a problem of improvement of an environment.

What does it mean "new steadfast attention"? It means that, it is necessary to look at a status of ecological conditions not only from positions of without waste high technologies of manufacture, problems of recycling of harmful waste products, nevertheless proceeding from the purposes which are formed in a brain of the person, i.e., his thinking. It is necessary to observe pure ecology of thinking which, in turn, results in pure harmless technologies and recovery, thus, the planet as a whole. The rough material world is dependent and closely connected to the thin world of thinking, interaction of electromagnetic fields of both biological objects and a lifeless matter.

The unique LITOVIT's properties were emphasized in Ref. [1]. Now we would add new information in particular about LITOVIT "K".

Wave LITOVIT's characteristics can influence the structure of a biological field of the person and thus to change his own wave characteristics which, in turn, influence a condition of an organism as a whole [2]. In particular, taking into account creative specificity of the scientist's work namely to improve a brain's condition, to concentrate attention more quickly and to improve memory, it is necessary to use LITOVIT "K". This preparation contains laminaria in addition to a mineral basis. The optimum ratio of these components is capable to improve wave characteristics of a biological field around of a head of the person. At significant improvement of power parameters of a brain, it is possibly for the person to achieve significant

creative successes because in this condition the human body is capable to perceive much more information from an environment as compared with that in a usual condition.

Influence of a human body of one person, in turn, changes a condition of biological characteristics of people which surround the given person. If characteristics of a field are big enough, that, being rather long time in a field of such person, it is possible to change own parameters of power. On a physical level, it is expressed by quieter condition of nervous system and by reduction harmony of work of some bodies. At this condition, activity of internal bodies of the person is normalized, in addition, disappearance of painful symptoms is observed.

The group of people with similar characteristics is capable to influence any process in both alive and lifeless matters. The main thing is to coordinate the actions of these group. Furthermore, it is necessary to emphasize that, the brain of the person in positive extreme conditions is adjusted on positive creative force, creation of the pure advanced technologies, instead of on destruction and on improvement and manufacture of the weapon in particular.

As a whole for safety of the Earth and improvement of its field characteristics, in the ideal case it is necessary of 50-70 % of such category of people. They are capable to change wave characteristics of the Earth. And the content of ionosphere and nanosphere in particular will be changed as well.

Such condition of the Earth will result in creation and utilization of modern technologies, which being different from modern one, carry in itself pure creation, instead of destructive actions or collateral, negative elements.

Nowadays, advanced distributing technologies demand improvement with the purpose of liquidation of negative factors which are integral components at creation of modern ways of manufacture.

At present the newest technologies which do not demand the further elimination of

collateral negative factors are created. Nevertheless, these technologies demand new thinking and absolutely new scientific approach with respect to all phenomena in a nature and in particular to creation of the world. They are based on such interactions which are caused by torsion fields. Knowing laws of existence of torsion fields, it is possible to create highly effective technologies. They do not require recycling waste products or systems of clearing of air, ground and water. They are absolutely non-polluting. To use these technologies, it is necessary to own absolutely in another way thinking. This is due to the fact, the virtue of such mechanisms cleanliness depends on thinking. These technologies should work on creation of harmony, instead of on destruction which results in chaos.

The persons should possess their own thinking. And if such persons are capable to supervise over the thinking they are capable to consult with emotions and own physical bodies. High parameters of own biological fields are inherent in such people. These are people of new epoch. Increase of their number will result in a sharp qualitative level of the new relations, the new technologies, new life on the Earth.

It will be the change similar to a chain nuclear reaction. At enough amount of such people (critical weight) on the Earth there will be sharp changes which will capture all spheres of life on the Earth, switching both biological objects and inorganic life on the planet. There will be people with pure both heart and ecological thinking. It will be a guarantee of creation of the updated harmless technologies and the improved planet as a whole.

[1] Lavriv L.V., Proc. Int. Conf. "Materials and Coatings for Extreme Environments Performance: Investigations, Applications, Ecologically Safe Technologies for their Production and Utilization", Catsively, Crimea, Ukraine, 2000, p. 429 (in Russian).

[2] S.M. Zakirov and I.V. Orzhelsky, Patent of Ukraine, No. UA-34389-A (pub. on 15.02.2001) (in Ukrainian).

THE MATHEMATICAL SIMULATION OF THERMAL PROCESSES IN THE CONDITIONS OF RADIANT ENERGY STREAM INFLUENCE ON POWDER SYSTEMS WITH PERITECTIC TYPE EXOTHERMAL REACTIONS

Scorohod V.V., Solntsev V.P., Baranov V.L.[1], Frolova E.G.[1]
Francevich Institute for Problems of Materials Sciences NSA of Ukraine, Kiev
[1]Puhov Institute of power engineering simulation problems NSA of Ukraine, Kiev

The study of thermal processes at distribution of exothermal reactions in powder systems represents the special practical interest in connection with problems of creative effective, energy inexpensive technology of inorganic compound synthesis and functionally gradient materials. Also no minor importance is attach to the fundamental aspect of a physicochemical interaction in reaction powder mediums, bounds with collective character of processes, which appropriate to high level of complexity of heterogeneous systems.

Dominating till now formal-phenomenological approach [1] can not explain a line of observable phenomena, to which one concern occurrence of concentration waves and macroscopic splashes of temperature [2], indicative about rather composite differentiating of material and energy. Taking into account a high level of complexity of existent processes at distribution of exothermal reactions, the most prime systems with peritectic character of interaction are selected first of all, where the physicochemical model can be represent in the form of two-dimensional, which taking into account concentration modifications of one of components and temperature. The concentration of other component is hardly constrained with concentration of first. Therefore in case of melting a low-melting component the kinetic model of process can be represent by a following system of two differential equations

$$\dot{c} = k_1(c_R - c) - k_2 c - \eta l(T - T_Q),$$

(1)

$$C\dot{T} = -k_1(c_R - c)h + k_2 cH + g - l(T - T_Q),$$

(2)

where c - concentration of one of components, c_R - its equilibrium concentration in a melt, k_1 and k_2 - constants of dissolution and fusion reaction velocities, h - an enthalpy of solid component dissolution, H - an enthalpy of compound formation, C - thermal capacity, T - temperature,

T_Q - environment temperature, l - heat transfer coefficient, g - magnitude of a heat stream.

The constants of dissolution and fusion reaction velocities generally are functions of temperature

$k_i = k_{0i} \cdot e^{-\frac{E_i}{RT}}$, however by virtue of a small variation value δk_i, at high temperatures they can be constants. If the parameters of the equations (1) and (2) satisfy to an inequality

$$\left(\frac{l}{C} - k_2 - k_1\right)^2 < \frac{4l\eta}{C}(k_2 H + k_1 h),$$

(3)

the solutions of a system (1), (2) are described by damping harmonic functions of a kind

$$T(t) = P_T + N_T e^{-\alpha t} \sin(\omega t + \varphi_T),$$

(4)

$$c(t) = P_c + N_c e^{-\alpha t} \sin(\omega t + \varphi_c),$$

(5)

where the constants P_T, P_c, N_T, N_c are determined in parameters of the equations and initial conditions.

The system of equations (1), (2) has exponential solutions in case of substitute sign of an inequality (3) for opposite

$$T(t) = \overline{P}_T + N_{1T} e^{\lambda_1 t} + N_{2T} e^{\lambda_2 t},$$

(6)

$$c(t) = \overline{P}_c + N_{1c} e^{\lambda_1 t} + N_{2c} e^{\lambda_2 t}.$$

(7)

All constants in dependence (3) - (7) are concrete physicochemical values, defining velocity of dissolution processes of a solid component in a melt, reaction rate, power of a radiant energy stream, velocity of heat rejection at prescribed value of environment temperature. Varying the given values, it is possible effectively to influence modification of trajectory and concentration of components and temperature, thereby driving

macroscopic sintering processes and shaping of structure FGM.

The harmonic fluctuations occurrence (solutions (3) and (4)) of temperature and concentrations reduces in a gradient medium to initiation of temperature and concentration waves, which one are found experimentally in work [2]. The obtained result practically dissects the true physicochemical nature of exothermic synthesis process in a condensed medium, where temperature and components concentrations are determined by collective interaction of four processes. The represented model (1), (2) can be put in a basis of the microscopic theory of a condensed medium off-gas combustion. It is obtained with a particular degree of reductions and considers local representation, which one can be spread on macroscopic only in case of systems

heat with peritectic reactions to solid-liquid state. At the same time considering a powder medium as the collection of local combustion sources, which are described by model (1), (2), is possible directly to approach to a problem of creative of the macroscopic physicochemical theory of condensed matter off-gas combustion.

Reference.
1. A.G. Merzhonov and E.N. Rumanov. Physics of reaction waves. Reviews Physics, Vol. 71, № 4, July 1999, p. 1173 - 1211.
2. V.V. Scorohod, V.P. Solntsev. About dynamic stability in reaction powder systems. Dop. of Ukraine National Academy of Science 2001, № 11, p. 74 - 80. (Russia).

CERAMIC ARMOR – DEVELOPMENTS OF MATERIALS AND PENETRATION PROCESSES

Galanov B.A., Grigoriev O.N., Ivanov S.M.
Frantsevich Institute for Problems in Materials Science, National Academy of Sciences of Ukraine

The results of researches and developments of new ceramic materials, perspective for use as the armor and also for other adjacent applications are described. There are the main materials under investigation: Ceramic and ceramic matrix composites (CMC) on the boron carbide as well as borides base (B_4C, B_4C - MeB_2 system, Me - Ti, Zr; TiB_2-W_2B_5, W_2B_5, W_2B_5- B_4C- TiB_2); Ceramic and CMC on the silicon carbide base (SiC, SiC- MeB_2); Ceramic materials on the nitrides base (TiN, TiN-AlN); Laminated ceramic composites: Composites on the Ti base, produced by SHTS-process.

The investigations were fulfilled in the the following directions:
- -Development of physical and chemical principles of selection of the components of heterogeneous materials based on refractory compounds;
- - Calculations and experimental determinations of the internal stresses fields in ceramics and CMC;
- - Optimazation of the structural and streses-strain state of the CMC by using a proper termo-mechanical model of CMC.
- - Researches of fracture and deformation under contact loading, the contact strength determination.
- - Researches of ballistic properties

Developments are concentrated in the following directions:
- light armor ceramic plates
- materials for armor and radiation protection simultaneously
- materials for adjacent applications (wear-resistant, ceramics for high temperature)

In all practical actual development programs, ceramics are not a single-phased, but represent some form of ceramic matrix composites. Elastic interaction of phases at temperature and pressure changes during production and under external thermo-mechanical effects results in a complex stress-strain state of a material, which determines the features of its mechanical behavior. The thermo-mechanical approach to the problem of optimization of composition and structure of composites, as well as distribution of internal stresses is described.

An analysis of penetration resistance of these materials was performed using the modified Alekseevskii-Tate model for nonstationary penetration of long rods into targets. This model describes both initial and primary penetration into target. In accordance with the components of the main model's equation, total resistance to penetration is decomposed into three components, which can be conditionally called static R_t, kinematic p_k and dynamic p_d. Here R_t has the usual sense, p_k depends on penetration velocity, and p_d is associated with acceleration and cavity expansion. Relative contributions of those are different and varying during the penetrator — target interaction. Kinematic and dynamic components are short-lived and affect only nonstationary phase, while long-term resistance is defined by static component. In accordance with the accepted model, the value R_t is defined by the system of elastic and strength characteristics of target material: ρ, E, ν, Y, σ_f, etc., while values of p_k and p_d depend not only on target properties, but also on projectile parameters. Resistance to penetration was characterized by the penetration work per the unit volume of penetrated material: "penetration hardness" HP= $1/P \int p_c dP$ (P — depth of penetration, p_c – contact pressure), where p_c and P are taken from the model of nonstationary penetration. In the case of brittle material, the comminuted (pulverized) zone is formed in the contact area as a result of multiple fragmentation and value Y is defined by the strength characteristics of material and is obviously close to strength limit under compression. If under impact radial cracks are formed outside the comminuted zone then their formation must be defined not by material's tensile strength but by «tensile contact strength» of material. The technique of contact strength measurement is presented.

The mechanical and service properties of new materials are given and a prognosis of their ballistic properties is provided.

ИССЛЕДОВАНИЕ УСЛОВИЙ ФОРМИРОВАНИЯ ФАЗОВОГО СОСТАВА ПЛАЗМЕННОГО ПОТОКА ПРИ ВАКУУМНО-ДУГОВОМ НАНЕСЕНИИ ПОКРЫТИЙ

Лойко В.А., Кулеш Ю.А., Казакевич Д.А.
Институт порошковой металлургии Беларуси, Минск, Беларусь

В настоящее время плазменно-вакуумные покрытия, полученные конденсацией с ионной бомбардировкой, позволяет незначительно увеличить стойкость деталей и инструмента. Процессу плазменно-вакуумного нанесения упрочняющих покрытий характерен преимущественный разогрев в процессе ионной очистки выступающих элементов, а также отпуск кромок при интегральной температуре материала, значительно более низкой, чем температура отпуска. Неконтролируемый разогрев детали в процессе нанесения плазменно-вакуумных покрытий объясняется в основном высоким (до 50 %) и не поддающимся контролю в обычном процессе содержанием расплавленных частиц (капель металла катода), снижающих износостойкость. Осаждение расплавленных частиц на упрочняемую поверхность детали не только приводит к ее перегреву и разупрочнению, но и формированию в слое и на поверхности включений металла, существенно ухудшающих условия трения и усиливающих адгезионный износ.

Решение указанных выше проблем возможно, если свести к минимуму или исключить разупрочняющее воздействие потоков металлической плазмы на поверхностные слои материала. Поэтому, актуальным является изучение закономерностей формирования бескапельных вакуумных электродуговых покрытий.

В данной работе исследовалось влияние физических и поверхностных характеристик расходуемого катода, а также параметров электродугового испарения в вакууме на формирование фазового состава плазменного потока с низким содержанием нейтральных частиц (расплавленных капель и паров металла катода).

На основании оценочных измерений состава потока плазмы и энергии ионов и тока дугового разряда получены зависимости осевой плотности, зарядового состава и средней энергии ионной компоненты плазменного потока.

Было установлено влияние на фазовый состав плазменного потока теплофизических характеристик материла расходуемого катода, температуры плавления и теплопроводности, интегральной температуры расходуемого катода, давления и состава газовой среды в вакуумной камере, состояния и микрогеометрии поверхности расходуемого катода, наличия и напряженности внешнего аксиального к поверхности расходуемого катода магнитного поля.

Проведенные исследования также показали, что формирование на поверхности расходуемого катода физически адсорбированных примесей существенно снижает содержание микрокапельной и макрокапельной компоненты плазменного потока вследствие более высокой температуры плавления указанных примесей. Выявлена зависимость фазового состава поверхностного слоя электродугового покрытия от продолжительности ионной очистки и взаимосвязанной с ней температурой подложки.

Результаты выполненной научной работы будут применены при разработке новых плазменно-вакуумных процессов нанесения бескапельных функциональных покрытий и устройств для реализации этих процессов.

SECTION C.
ADVANCED TECHNOLOGIES FOR PRODUCTION AND JOINING MATERIALS AND PRODUCTS FOR OPERATION IN HAZARD CONDITIONS

THE USAGE OF THE COMBINED INFLUENCE OF THE BIG PLASTIC DEFORMATIONS FOR THE OBTAINING OF THE ULTRADENSE AND ULTRAFIRM BLANKS FROM THE POWDER MATERIALS

Perelman Vladimir, Zubro Svetlana
Moscow Institute of Fine Chemical Technology named after M. Lomonosov, Moscow, Russia

The report considers some aspects of the influence of big deformation combinations on the heterogeneous materials' structure and characteristics.

The most of mediums subjecting to pressure treatment posses evident or non-evident characteristics' heterogeneity. As a rule, inside these kinds of mediums the shears go along uneven sliding surfaces. The value of medium deflection of sharing micro-grounds from main direction of sliding surfaces determines the level of deformations' influence upon the structure and characteristics of material. Under the big enough shrinking tensions (and only under such tensions big deformations are possible) the shears lead not to defects' rise and accumulation (micro-cracks, micro-pores, etc.) but to breaks' smoothing on the sliding surfaces. After finishing of this process the possibility of deformations' effect upon the materials' structure and correspondingly upon the characteristics disappears.

The effect of "deformation's localization" is the second factor limiting the big influence of deformations upon the materials' structure and characteristics. In this case the deformation goes only along some narrow sliding zones and does not spread upon the whole materials' volume. The Dr Pice's gives detail enough basis of this process. It depicts the critical conditions under which forming correlation of plastic flow assume bifurcation of homogeneous or smoothly changing deformation with very much localized sliding zone. The main hypothesis runs that the localization of deformations may occur in mediums, which equations of keeping balance of material's element are hyperbolic. It means that they have characteristics along which the fields of velocities and tension bear breaks. Materials' plastic shares are known being described with equations in particular derivatives of the second order (plane task) of hyperbolic type. There is enough quantity of data confirming the existence of the localized sliding zones not only on the stage of the material's destruction (Chernov – Luder's line) but on the stage of its consolidation, too.

These two above mentioned factors restricts the possibilities of technologies which set their aim as an object of gaining the high degree of transformation of materials under processing by big deformations as considerable volumes of the material inside the grating formed by the system of the sliding zones do not get the required levels of deformation for the structures' changing. These restrictions can be overcome by the combined influence of the different type of deformations upon the mediums under processing.

The correct choice of the deformation types' combinations, their succession, etc. allow to destroy "frame" of the smooth sliding surfaces, get the new system of non-smooth sliding surfaces and with the help of these factors provide the more fool processing of the whole material's volume.

The following data have been received on the pressings from powders of the plastic and firm materials. These are the mediums with strongly marked heterogeneous characteristics (fractions, inter-fractions borders and pores). It allows watching the processes inside the structurally heterogeneous mediums exposing the combined influence of the big deformations of the different types.

The schemes of the immersion were used for the fulfillment of the investigations. It allows not only providing of the combination of different types' deformations, but also regulating of the degree of the materials' deformation, repeatedly changing of the direction of one or two deformations in the combination with the effect of the applied body. It also allows creating of the required temperature rate in the processing material by the controlling the deformation velocity.

The method of Staged Changing of Pressing (SCP) provides the permanent pressure of the material along the axle direction, cyclical share in two directions along the horizontal plane and pressure following this share. The pressure is the

expansion of the material along the orthogonal to the axle of pressing direction.

The comparable pressures of pressing the SCP method gives 15% density increase. The effect of the additional density increase is more considerable and reaches 20 – 25% while pressing super-dispersion nickel powder (60nm).

Pressing method (International Application PCT/IL97/00196) combining the sharing and twisting, represents a rather flexible scheme. It allows the wide spectrum of the influence upon the material by choosing the inline angles of the matrix' channels, their longitudinal profiling, choosing of the material's volume of feeding for one revolution and also by changing the sign of the deformation transmitted to the material.

The following results, gained on long rods of 30mm in diameter, defines the potentialities of the method:

- Iron powder is packed to 99 – 100% and the pressing gains 24 – 27HRS destiny;
- Chromium Electrolytic powder (of scales of 5 – 7mm in diameter) with 0,5% content of oxygen and 24 27 HRC density of scales is packed to 99 – 100%, the same as iron powder does (fig.1);
- It is possible to make the integral rod from the materials different in composition and also the combination of the powder material with the casting metal (fig.2).

Conclusion: the results of the investigations showed that combined, of different signs and directions influence of big deformations upon the pressing material allows gaining the practically compact material with the high level mechanical characteristics from the hardly pressing powder compositions and even from the powders of the hard and brittle materials by the repeated distractions creating in structures' processing.
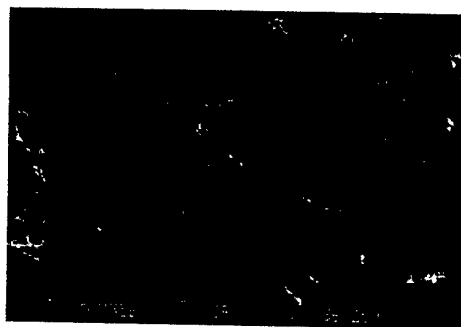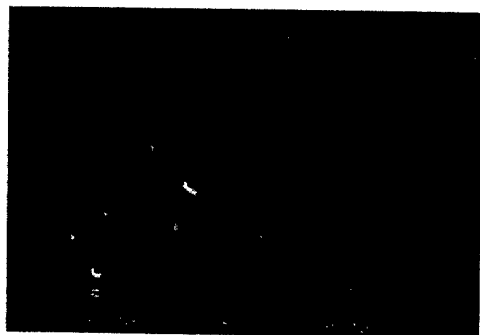
Fig.1
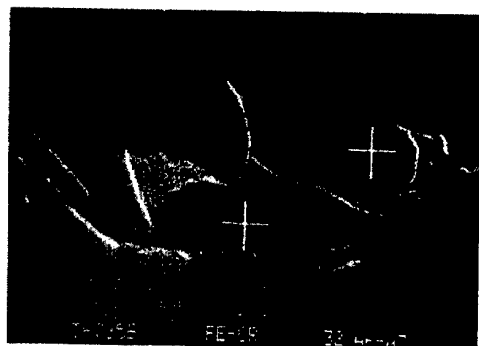
Fig.2

SINTERING OF NON-EQUILIBRIUM COMPOSITIONS BASED ON REACTIONARY- DIFFUSION SYSTEMS TITANIUM TRANSITION METAL CARBIDE OF IV - VI GROUPS OF PERIODIC SYSTEM

Scorokhod V., Solntsev V., Solntseva T., Tkachenko L., Maslyuk V., Koval A.
Institute for Problems of Materials Science of NASU, Kyiv, Ukraine

In most cases technological processes of powder metallurgy occur under conditions, that are far from equilibrium. Non- equilibrium of processes occurring in powder systems, admits the existence of excess free energy, which is necessary for accumulating to a greater extent and directing toward processes of obtaining materials. The powder metal mixes with compounds of various physico-chemical nature have the greatest free energy excess. These compounds or the products of their interaction with a metal matrix determine functional properties of materials. In such systems the gradient of concentration causes excess of free energy and significant thermodynamic non-equilibrium of the system respectively. Under diffusion homogenization with the inter-diffusing atoms of different elements some flows of matter of various intensity arise. It causes the appearance of excess vacancies in diffusion zone, compressing stresses, dislocations and related processes, resulting in collective effects. In addition to cooperative interaction in multy-flow diffusion system the chemical reactions make the whole physico- chemical process more complex. The whole system and the interactions in it has a mark of synergetic effects peculiar to reactionary sintering. The interest in reactionary sintering with development of high-energy methods of obtaining composite materials (Dynamic Hot Pressing, Hot Pressing, Hot Stamping, Pressing by explosion, etc.) has slightly decreased. However, recently in the context of development of non-equilibrum thermodynamics, synergetics and also in view of necessity of search for low power- consuming technologies, the reactionary sintering, probably, will become one of the basic methods of obtaining the new class of materials. It is necessary to pay attention to its specific, technological and functional potentialities.

During the sintering of diffusion- reactionary coarse-dispersed systems based on vanadium the facts of active condensation, autodispersion of structure and initiation of dynamic character of stability are fixed[1,2]. The detailed research of mechanisms of active sintering in such systems allowed to establish that in the given area of concentration and controlled parameters (constants of speed, diffusion coefficients, volume share of constituents in a metal matrix) there appeared processes of the non-linear interaction causing given character macrobehaviour (increase or shrinkage).

The non-linear character of interaction may occur in greater part in diffusion - reactionary systems based on titanium with carbides of transition metals of IV- VII groups because of its high affinity to carbon. Besides, titanium forms a continuous series of solid solutions with the majority of metals of these groups. Electrolitic titanium powders with the 100-200 microns particle size may exhibit low activity, so macroscopic effects at sintering may be present to a greater extent owing to processes of diffusion-reactionary interaction. Addition of carbides of transition metals up to 20 vol. % increases essentially the shrinkage and lowers the sintering temperature. Carbides of transition metals of VIA group activate processes of sintering most effectively. Thus the increase of the volume content of carbide results in increase of shrinkage of samples. In most cases volume changes (shrinkage)-sintering temperature relationships have a maximum. With increase in the sintering temperature the volume shrinkage decreases. Electron-microscopic researches allowed to find out the area of carbide interaction with a titanium matrix. Thus the transition metal forming the initial carbide, is partially dissolved in a titanium matrix, forming a 5-15 microns zone of interaction. The stable coarse-dispersed structure with carbide patches , strongly bonded with a titanium matrix through a transition layer of complex compounds is fixed. In this way the application of any metal carbide of IV-VIA groups as ingredient of powder compositions makes it possible to activate

effectively the sintering processes of materials, based on titanium and the choice of compound of one kind or other is dependent only on functional and service characteristics of the developing composition.
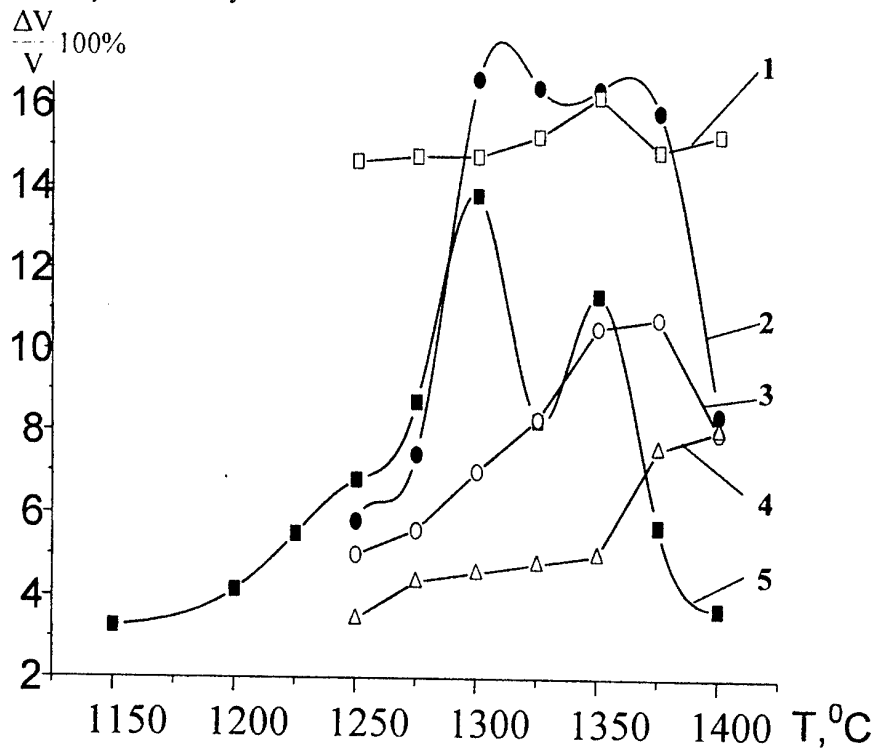
Fig. Dependence of volume shrinkage during sintering of compositions Ti-WC (1), Ti-Cr$_3$C$_2$ (2), T i-TiC (3), Ti-VC (5) and Ti (4) on temperaturez

1.Радомысельский И.Д.,СолнцевВ.П., Евтушенко О.В. и др. Объемные изменения при спекании брикетов ванадия с диселенидами ниобия и молибдена// Порошковая металлургия.- 1983.- № 9.- С.13-17.

2.Солнцев В.П. Неравновесные процессы в реакционных системах и их роль в технологии получения слоисто-градиентных материалов //Nowe Kierunki technologii badan materialowych .- Warsava: ATOS, 1999 . - P. 321-324.

HIGH QUALITY CARBON MATERIALS ON THE BASIS OF GRAPHITE FILLERS

Gurin V.A., Gurin I.V., Gujda V.V., Kolyanda S.I., Rizhgov V.P., Kaplenko O.G., Fursov S.G.

National Science Center "Kharkov Institute of Physics & Technology", Kharkov, Ukraine

Carbon and graphite materials have unique physical, chemical and mechanical properties and are used when we need characteristics such as high-temperature resistance, electro conductivity, resistance for aggressive media, low density at a high mechanical strength and elasticity. That is why they are widely used in the modern engineering. All producers of carbon and graphite are working on the improvement, of their materials. Such research is also carried out in NSC KIPT. For example there was worked out graphite bond by the pyrocarbon (GBP) that has a wide range of unique properties: high density, mechanical strength, low open porosity and extremely high radiation stability [1,6]. But the most of the high quality industrial graphites as well as graphite GBP have a high cost and the cost of the final products is increased due to the material losses at machining.

To increase the competitiveness of our materials by the method of decreasing their cost we have formulated and realized the principle of production «to a size». The essence of this method is in the fact that blanks are produced with the minimal machining allowance or even without machining. Besides that the greatest part of our products for example crucibles has a modular construction that allows decreasing material losses [2].

To realize the production principle «to a size» in case of graphite GBP items we have developed a unique method of blanks forming. Graphite powder is used as a raw material at GBP production. This powder is appeared while machining and is collected in the special traps in exhaust ventilation. The traps have such construction that graphite powder is automatically sorted by fraction. Above that we collect the powder from machine pallets while producing carbon and graphite items. This powder has the largest particles grain that can achieve several millimeters. For experiment conduction we have produced special lots of powder of industrial graphite EG-0 and ARV. According to the requirements of the products we chose the appropriate fraction of graphite powder.

We have selected a usual sugar as a binder. It more than on 99,7 % consists from sucrose. Sucrose belongs to a large class of natural organic substances called as carbohydrates (compound of carbon atoms and molecules of water) with the general formula: $Cm (H_2O)n$. This class includes sugars more or less sweet on taste such as monosaccharides (for example, glucose and fructose), and oligosaccharides (for example, sucrose), and also polysaccharides, (for example, cellulose and starch).

Sucrose (a reed, beet sugar) is a disaccharide with the general empirical formula $C_{12}H_{22}O_{11}$ and consists of two equal parts of monosaccharide: d-glucose and d-fructose. These monosaccharides connect each other by glucose groups: glucose in an a-configuration and fructose in a b-configuration. In a sucrose molecule glucose is in the form of pyranose (pyrane ring), and fructose is in the furanose form (furane ring фурана). A sucrose molecular mass is 342,296. It contains 42,11 % of carbon, 6,43 % of hydrogen and 51,46 % of oxygen.

Sucrose is a crystalline substance, which molecular structure has a natural for it special lattice. A density of a sucrose crystal without inclusions at 20°C is 1,5915 g/ccm, specific volume is 0,628 ccm. It melts at the temperature of 186-188°C, a so-called "caramelization" of sucrose or formation of a complicated, painted in a brown color substances of a bitter taste takes place [3].

Sugar powder was milled in a porcelain mill by the steel balls up to the fraction commensurable with the fraction of the graphite powder-filler. While milling a graphite powder was added in a proportion of 1:1 to avoid sugar balling and decrease milling time. Milling degree was controlled by taking the probes and calibrated sieving. After milling the rest part of a graphite powder was added and the compound was mixed

in the same mill. The final mixture contains 20 % of a sugar. This ratio was selected experimentally and allows on the one hand to make performs with the necessary mechanical strength and on the other hand after heat treatment the coal residual of sugar is minimum and does not render essential influence to a perform properties.

For performs shaping we used paper forms that burn out at carbonization. Carbonization was carried out at the atmosphere of the natural gas at the temperature of 900 °C. The achieved performs have all the necessary properties for the further gasphase densification: they have a sufficient electrical conductivity, appropriate dimensions, mechanical strength and open porosity.

Thermal gradient gasphase methods of a porous media densification by pyrocarbon with a resistive heating that were worked out in NSC KIPT were used for performs densification [4-5]. Density, open porosity and mechanical strength of the produced materials were tested.

Using this method we have produced the items with the maximum dimensions: length 900-1000 mm, diameter- ~150 mm. The maximum density of these items was 1.9-1.95 g/ccm at an open porosity 2-3 %.

As it was earlier mentioned the mechanical strength of the produced materials was tested. For this aim samples with a diameter of 5 mm and length of 10 mm were cut. Tests were carried out on a tearing machine P05 with the maximum load of 500 kg. To compare the results we have also prepared large samples with the diameter of 10 mm and length of 20 mm. These samples were given for tests to an independent expert. The results of the tests are given in a table 1.

As one can see from the given data the produced materials have high consumer properties. Mechanical strength of these materials exceeds in several times the strength of the high quality industrial graphite.

Tabl. 1.

Mechanical strength of the samples on the basis of ARV graphite powder.

Samples	Breaking point at compression , MPa			Breaking point at compression , kg/cm^2.		
	av	max	min	av	max	min
∅5 mm. H=10 mm	236,13	266,21	202,573	2408,487	2715,325	2066,2
∅10 mm. H=20 mm.	260,53	293,34	229,682	2657,433	2992,113	2342,8

References

1. Зеленский В.Ф., Гурин В.А., Конотоп Ю.Ф., Одейчук Н.П. Графит ГСП. Вопросы атомной науки и техники 4/76/, Харьков 1999 г., стр.67-79.
2. www.carbon.com.ua
3. http://www.sugarindustry.ru/what/encyclo paedia/1/1.shtml
4. В.А. Гурин, И.В. Гурин, Ю.Е.Мурин, С.Г. Фурсов, В.В. Колосенко, А.А, Корнеев, Н.П. Одейчук, А.Н. Буколов. Некоторые особенности реализации метода движущейся зоны пиролиза при газофазном уплотнении пористых наполнителей пироуглеродом.,

Вопросы атомной науки и техники 1/67/, 2/68/, Харьков 1998 г., стр.76-78.
5. В.А. Гурин, И.В. Гурин, В.В. Гуйда, В.В. Колосенко «Термоградиентные газофазные печи ННЦ ХФТИ». Труды научно-практического симпозиума «Оборудование и технологии термической обработки металлов и сплавов в машиностроении». ОТТОМ Харьков, Украина, 28-31 августа 2000 г., стр. 30-35.
6. Лебедев И.Г., Кочкарев О.Г. Радиационная стойкость графитов сповышенными эксплуатационными свойствами. Атомная энергия т.91, вып.2. 2001 г. стр. 114-120.

OUTLOOK FOR INDUSTRIAL PRODUCTION OF CARBON THREADS AND FABRICS OF VISCOUS PRECURSOR

Vishnyakov L.R., Vdovenko V.A.[1], Tonkovid A.N.[1]
Frantsevich Institute for Problems of Materials Science, National Academy of Sciences, Kyiv, Ukraine
[1]Government Plant of Powder Metallurgy, Brovaru, Ukraine

A great demand is now observed on the worldwide market in carbon threads and materials produced of viscous threads. This is associated, firstly, with the reduction of their production for engineering composite materials of military application, because of failed attempts to achieve high values of strength and Young modulus. In these areas, carbon fibers prevail in manufacturing and consumption, as produced of polyacrylic (PAN) and pitch-based fibers, secondly, because of closing of some plants producing viscous, which use primarily wood of conifers and foliates. Here, some ecological factors play a role, such as cutting out forests, chemical treatment of wood, etc.

A great significance was recently attached to the following applications of carbon fibers and materials, for which primarily importance acquires non-engineering, heat insulation properties, chemical and radiation resistance, sorptive capacity, etc.
The hydrated cellulose precursor carbon fiber costs between USD 80 and 110$/kg in the market. For comparison, the costs of carbon fibers of PAN precursor have been lowered for last years and now reach $40-70/kg depending on physical/mechanical characteristics and delivery volume.

A rather great demand is observed in market in carbon fabrics of functional application (resistive, filtering, screening, sorbents, electrodes, etc.). They are produced of hydrated cellulose (HC) fibers, while tailoring of their structures and consumer's properties is determined primarily by the properties of initial HC fibers, degree of carbonization, pattern of interlacing, areal density of the initial HC and fabric, and finite product.

Due to the reduction of the volume of output of carbon fabrics of HC precursor because of the reduction of their use as reinforcements for composites for missile application, demands and proposals have been reduced in market. Besides,

the ecological factor has played a certain role in this concern.

Having such unique properties as high corrosion resistance in aggressive media (gases, vapors, fluids), filtering, resistive, electromagnetic wave protective and other useful properties, these fabrics become the major functional element in the filters, heaters, screens, etc. to be used in industry, building, medicine and other areas.
Producers of the following materials and products are among the potential customers of carbon fibers made of hydrated cellulose:
   carbon-carbon composite materials (aircraft brakes, etc.);
   electrical thermal equipment (vacuum, and in protective medium);
   filters for hot gases, vapors or aggressive media in chemical and petroleum industries;
   reinforced composite materials based on polymers for the use in processing units of chemical and other productions, sliding bearings, stuffing boxes;
   clothing for protection against electromagnetic radiation;
   electrically heated systems for medicine, building erection, agriculture, tourism and recreation industries;
   products of medical application - napkins for therapy of burns and wounds, sorbents, implantants to restore ligaments and tendons;
   miscellaneous.

Currently, there is no production of continuous carbon thread in Ukraine in industrial scale. Nevertheless, due to existence of production facilities, experience of engineers and workers, technical documentation in respect to the basic technology according to the following scheme: viscose thread → viscose fabric → carbon fabric → carbon thread shall provide restoration of the production within a short term. It is assumed that the physical and mechanical properties of the product as obtained shall be similar to those of УН-2 carbon threads (Ukraine) and УВИС-Н

carbon threads (Russia) and will have the following characteristics: areal density: 140 tex; breaking load: 20 g/tex, elongation: 1-1.5 %, diameter of elemental fiber: 7-8 microns, strength of single threads: 1.2-1.3 GPa.

The carbon threads are expected to cost at least 10-20 % lower the worldwide price provided the production growth is stable. The basic carbon thread is believed to be subjected to modification (by thermal, electro-chemical or other treatment) in order to tailor specific final properties for the thread or products (as per Customer's specification).

Science and production staff having a great experience shall be involved into processing of the thread into a product, and in its modification.
For applications, where a desired temperature range is required with a narrow temperature scattering, or programmable conditions of the resistive element use are needed, the carbon fabric is subjected to thermally stabilizing chemical-thermal treatment. In this case, the cost of fabric shall include the cost of thermal stabilizing treatment. For many other uses, where an additional thermal stabilizing annealing is not required, other treatments have to be done like activation to increase the specific surface of carbon fibers (sorbents, filters, etc.), or special modification for fibers, for instance to enhance the adhesion to polymers, increase the electrical conductivity or screening ability.

Areas which shall use carbon fibers are of high technologies, therefore, their production increase shall be of commercial gain and profitable.

ELECTRICAL AND HEAT-INSULATING MATERIAL BASED ON BORON NITRIDE WITH ELEVATED STRENGTH

Vishnyakov L.R., Pereselentseva L.N., Okhrimenko V.V., Vishnyakova E.L., Barschevska A.K.

Frantsevich Institute for Problems of Materials Science, National Academy of Sciences of Ukraine, Kyiv, Ukraine

The well known physical and chemical properties of boron nitride make it irreplaceable in the techniques of high temperatures, where high electric and heat-insulating properties, corrosive media resistance and differential temperatures are required. However, application of graphite-like boron nitride is restricted because of its low hardness, low elastic and strength properties due to its crystalline structure and difficulty to prepare high-density products, therefore, the above shortages should be avoided.

The last two decades the materials science in its area of refractory or hardly-sintered materials has been developing through creation of multicomponent and multiphase composites. To produce the above composites, agents are used able to activate the sintering processes, and physical and chemical processes able to form new phases. These phases can improve the functional properties and provide new features to materials.

Hence, our objective is in this work to design a composite materials on the base of boron nitride and new refractory phase, which shall have adjustable structure formation during the process of activation sintering (hot pressing). Using the idea of creation of composite materials, new phases of which are formed in situ, materials have been prepared of boron nitride-sialon family, the latter being known due to its high hardness and corrosion resistance in various media, through selection of the mixture and method of its preparing (blending and grinding). The main phase (BN) in composites is at least 75 vol %.

Sintering (hot pressing) of these materials at rather low temperatures causes eutectic transformations of the Al_2O_3 — SiO_2 system, which enhance the densication process at earlier stages to a great extent. Further rise of the sintering (hot pressing) temperature contributes conditions for the processes of recrystallization via the melt of aluminum nitride and silicon nitride alumosilicates as components of the mixture, and the synthesis of new refractory hard phase, i.e. sialon as was confirmed by X-ray and spectra analysis. As electron microscope examinations have shown, the process of recrystallization involved also boron nitride via the alumosilicate melt. This process is accompanied with coarsening of boron nitride particles, preferentially in the normal direction to the applied pressure at hot pressing, thus producing a distinct layered gradient structure of the composite.

Fig. 1 shows typical electron microscop photos of the boron nitride-sialon composite structure.

Parallel to pressing direction

Normal to pressing direction

Fig. 1. Typical micostructure of boron nitride-sialon composite

The liquid phase formation process at earlier phases of sintering (hot pressing) and the presence of liquid phase at all the subsequent stages strongly enhance the densification of composite allowing production of essentially poroless material at pressures of hot pressing two times lower of those needed for preparing high-density boron nitride. The materials acquire an elevated strength (1.5-2 times versus boron nitride) and high hardness (HV=1.1-1.3 GPa) while retaining all important properties of boron nitride needed for application in techniques (electric and heat-insulating properties, and corrosion resistance). This opens opportunities for their use under conditions of increased mechanical loads and erosion attacks by corrosive media.

The researches resulted in developing of a technology of hot pressing for large-sized items of boron nitride — sialon composite material. The material can be made using the cold pressing technique with subsequent sintering.

Fig. 2 gives the photo of hot-pressed cube with edge of 180 mm made of composite developed.
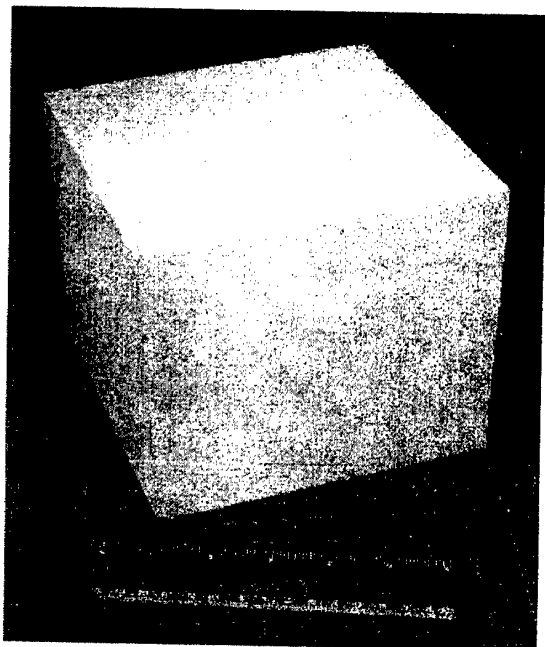
Fig. 2. Hot-pressed cube made of boron nitride-sialon material

JOINING OF POROUS AND COMPACT TITANIUM WITH LASER WELDING AND PLASTIC DEFORMATION

Savich V.V., Pilinevich L.P., Tumilovich M.V., Tolochko N.K.[1]
Powder Metallurgy Research Institute of the NAS of Belarus, Minsk, Belarus
[1]Technical Acoustics Research Institute of the NAS of Belarus, Vitebsk, Belarus

Titanium filters have gained wide application for cleaning food liquids, chemical solutions, medical preparations [1]. Porous titanium elements are used as parts of surgical implants [2]. These parts often look like built-in constructions, consisting of porous elements and different main and auxiliary parts (flanges, connecting pipes, etc.). As a rule, they use welding for their assembling. But conventional methods of argon and electron-beam welding of titanium, which are widely used in aircraft and space industries [3, 4] for welding of porous parts do not provide necessary quality of welded joints.

The present paper modes of laser welding and conditions of preliminary preparation of joint surfaces, influencing quality of a weld during their welding porous parts produced from technically pure titanium ПТХ2-1 with parts from compact technically pure titanium ВТ1-0 are studied.

In a sheet of compact titanium there was cut out a hole with diameter $\varnothing185$ mm in which there was tightly inserted a porous disc of the same diameter. These parts were welded by laser along the joint perimeter.

Impulse Nd:YAG laser ($\lambda=1.06$ µm) was used as a source of laser radiation. The best quality of welded joints characterized by absence of pores and cavities, smooth and flat surface of solidified metal in a weldpool, the same dimensions along the whole weld perimeter were obtained at the following conditions: impulse radiation energy - 2-4 J, impulses time - 4 milliseconds, frequency of impulses repetition - 5 Hz, diameter of laser spot - 0.7-1.1 mm, speed of laser spot motion - 30-50 mm/min.

Treatment of titanium in technological processes, characterized by thermal effect is carried out in vacuum or inert protective gas environment [5]. But our experiments have showed that you can achieve appropriate quality of a titanium weld in the air when using impulse laser radiation.

In Figure 1 you can see a photo of such a welding joint of porous and compact titanium after etching.

Figure 1. Cross-section metallographic specimen of a welded joint of compact and porous titanium after etching. ×50

In Fig. 1 you can determine that at optimal treatment modes the weld is dense and smooth. Its width is 1.5-1.7 mm and depth 1.1-1.3 mm. The weld is recessed below the welded parts surface at the depth of about 200 µm, which is connected with titanium melting and the melt infiltration into pores. Preliminary mechanical treatment of porous titanium, due to its high viscosity and plasticity, leads to compaction of the materials in the zone of cutting and «smoothing out» of pores. As an effect of that reduction of the material shrinkage degree during welding and limitation of the melt infiltration into pores takes place, which reduces possibility of formation of the mentioned defect.

The weld metal heats to the temperature higher than the melting point and after cooling has plate structure of fast-cooled casted metal of martensite type [6]. As for near-weld zone, it is typical to observe partial melting of grains boundaries. Average width of this zone is 90-105 µm. Zone of thermal influence includes a zone of phase refining, where the metal got a meta-stable α'-transformed structure, and a transformation zone from α'-transformed structure to the basic metal structure.

155

Multi-zone type of the weld structure was proved by results of hardness measuring.

During tensile testing of all the samples under investigation we have observed breaking not in the place of a weld but along the body of porous elements. Equivalent tensile strength was 50-70 MPa, and strength of the weld was, accordingly, higher than this number.

We have also carried out investigations of the process of a permanent joint from compact and porous titanium production by expansion [7]. This method enables to join easily parts having different plastic properties. Due to the fact that compact titanium has higher hardness and stiffness, a porous part should be deformed. According to this hypothesis the porous part is the one under straddling, so the other one should have a cut pit, with a closed groove inside along its perimeter. This groove should be «filled in» with the material of the porous part due to local plastic deformation.

There was carried out a number of experiments on models, which scheme is presented in Figure 2.
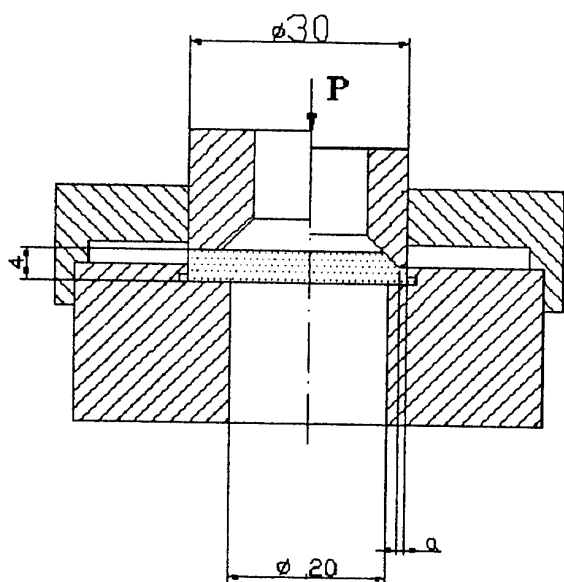
Figure 2. Scheme of expansion of a model porous sample into a compact mandrel.

For our experiments we were using porous discs from titanium powder with height 4 mm and diameter $30_{-0.1}$ mm calibrated along their diameter. We were cutting standard cartridges with central hole 20 mm in diameter, pits $30^{+0.05}$ mm in diameter of different depth with square grooves along their sides. The outer diameter of the groove was the same for all the cartridges (34 mm). Only 2 parameters were under variation - depth of the pit and height of the groove. With the help of special ring punches, mounted directly along the axes of the cartridges and porous discs, we have carried out local inserting of the discs to the level of the cartridge surfaces. As for the punches we were varying width of deformed ring surface and degree of deformation. Height of the groove was 12, 24 and 36% of the disc height.

After shrinkage and compacting the porous discs into the cartridge we were measuring force of ejecting a disc out of the cartridge.

The results of the investigations carried out have showed that optimal ejecting force (higher than 700-750 N) is achieved at the following parameters: relative deformation degree - 2-3 mm; relative groove height - 35-38%.

The achieved results can be used for optimizing processes of joining porous and compact materials.

References

1. Vityaz P.A., Kaptsevich V.M., Sheleg V.K. Porous Powder Materials and Parts Made from Them // Minsk, «Vysheishaya Shkola» Publishers, 1987, 164 p. (in Russian).

2. V. Savich, A. Ilyuschenko Porous and Nonporous Titanium for Surgical Implants of Various Application // Proceedings of the 1998 Powder Metallurgy World Congress & Exhibition. Granada, Spain, 1998, vol.5, p.352-356.

3. Technology for Production of Titanium Aircraft Parts // A.G. Bratukhin, B.A. Kolachev, V.V. Sadkov and others / M., «Mashinostroyeniye» Publishers, 1995, 448p. (in Russian).

4. G.Yu. Pinchuk. Laser Welding of Porous Materials // «New Materials and Technologies». Theses of reports at Republican Scientific-Technical Conf., Minsk, 1994, p.186 (in Russian).

5. Technology of Non-ferrous Metals and Alloys Thermal Treatment // B.A. Kolachev, R.M. Gabidulin, Yu.V. Piguzov / M., «Metallurgy» Publishers, 1992, 272 p. (in Russian).

6. Laser Welding of Porous and Compact Titanium Elements // N.K. Tolochko, V.V. Savich, L.P. Pilinevich and others / Physics and Chemistry of Materials Treatment, 2000, #4, p.75-78 (in Russian).

7. Permanent Joint of Implant Parts from Compact and Porous Titanium Produced by Their Cold Plastic Deformation // V.V. Savich, S.A. Bedenko / Powder Metallurgy, 2001, issue 24, p.79-82 (in Russian).

ALTERNATIVE CAST IRONS PRODUCTION TECHNOLOGIES FOR METALLURGY

Lubyanoi D.A., Shulgin Yu.F.[1], Elansky G.N.[2], Karachentsev N.V.[3], Yazykov A.V.[3]
West Siberian Steel Corporation, Novokuznetsk, Russia
[1]Kuzmashzavod, Novokuznetsk, Russia
[2]Moscow Evening Metallurgical Institute, Moscow, Russia
[3]Novokuznetsk Department of KemSU, Novokuznetsk, Russia

Nowadays, the requirements on quality of castings in metallurgy and engineering increased considerably with the simultaneous rise in cost of charge materials and utilities used in cast iron production [1].

One of major production phases of high-strength nodular cast irons is mold inoculation of cast iron with silicon-magnesium inoculants of specially chosen definite chemical composition.

However, domestic production of such inoculants has been practically curtailed.

In this connection, the development of new resource-saving technologies of high-strength cast irons production, including the stage of complex silicon-magnesium inoculant production, becomes urgent. To choose the optimum composition of the inoculant, the latter should be produced either at metallurgical works located geographically close to the works which produce high-strength cast iron and have special equipment or directly at the works which produce high-strength cast iron.

On basis of this, the creative group of specialists from West Siberian Steel Corporation, Kuzmashzavod and Kuznetsk Ferroalloys has developed a complex of techniques including the following:

-iron smelting from steel scrap with thermotime treatment and superheating temperature up to 1510°C by recarburization with a carburizing agent as well as remelting of ingot mold scrap and mold plate scrap;

-production of silicon-magnesium inoculants which correspond to the best world analogs of such alloys of different chemical and grain composition using cheap off-size high-grade ferrosilicon fractions in induction furnaces;

-mold inoculation of cast iron with the use of inoculants of variable composition and selection of the optimum structure of the latter for production of castings from high-strength cast iron;

The results of introduction of such technologies have shown that the burden cost decreased 3 – 4 times and ferroalloys consumption decreased 10 – 14 times.

It became possible to obtain stably the initial cast iron with specified properties, inoculants with magnesium content from 7% to 30% and a high degree of assimilation of expensive and scarce metallic magnesium and the high-strength cast iron in accordance with the State Standard requirements.

Thermotime treatment (TTT) of metallurgical melts is in progress at metallurgical works, wide implementation of which is favored by growing use of induction melting in ironmaking and continuous casting in electric steelmaking. When iron is produced in induction furnaces, the metal temperature in the furnace is 200 to 300°C higher than the liquidus temperature. In both cases the temperature reaches the phase transformation range in liquid iron and steel under TTT [2].

Critical phase transformation temperatures in liquid iron and steel were determined by the high-temperature microscope "Leitz" from the surface tension by the lying drop method in the range from 1300 to 1600°C (Figure 1). The analysis of the experimental data obtained in laboratory conditions has shown that main transformations in the liquid phase take place in the range from 1485 to 1550°C both in the natural titanium and vanadium alloy iron and chrome-nickel alloy iron for mill rolls. The thermotime treatment opens possibilities for production of iron with specified properties for machine-building plants. The iron desulfurization technology in acid induction furnaces with the use of TTT has been developed. This technology provides the stable sulfur content in iron (below 0.01%) after treatment. For example, West Siberian Steel Corporation produced for Kuzmashzavod some amount of cast iron with sulfur content of 0.009% and optimum TTT parameters in the induction furnaces ИЧТ-10M of its Foundry shop. This low sulfur content in iron with inoculant allows production of high-

strength nodular and vermicular cast iron.
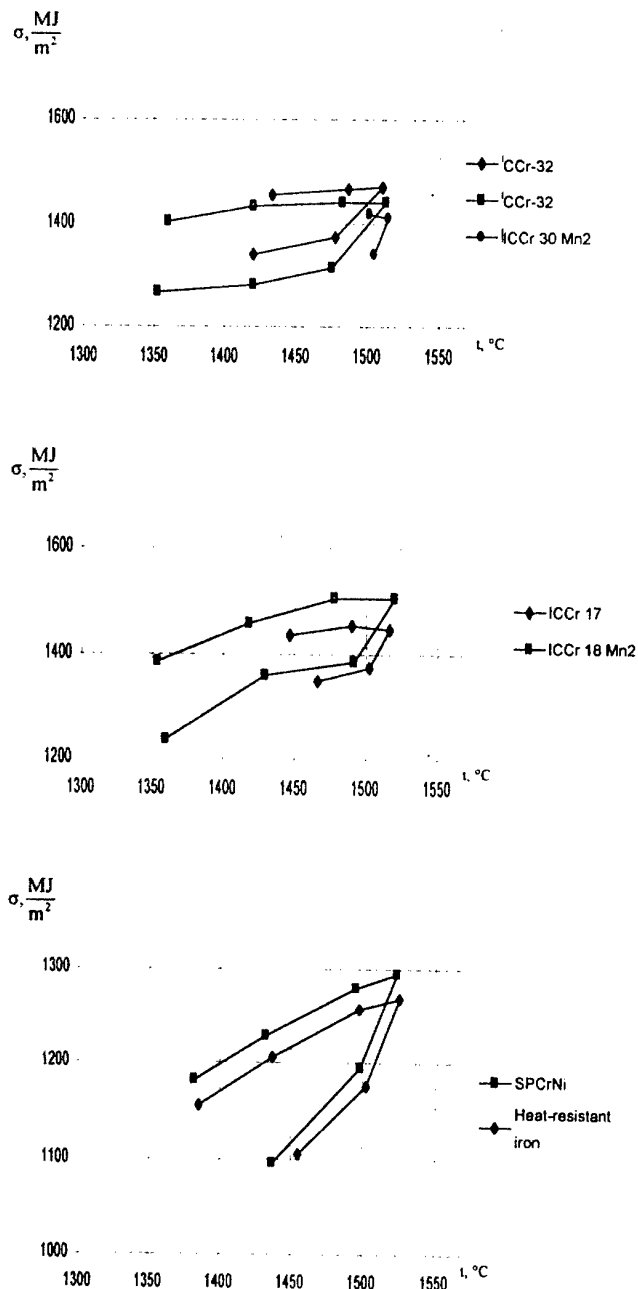
Figure 1. Effect of σ on t

Iron pigs produced after desulfurization but without microstructure inoculation have good graphite form.

It is known that presence of titanium and vanadium in cast iron influences favorably its microstructure. Alloying of such iron with silicon- and manganese-bearing ferroalloys at West Siberian Steel Corporation is done on basis of initial titanium and vanadium content in cast iron.

When making the optimum alloying, the important role is given to the express determination of the initial admixtures. With production of cast iron in induction furnaces of the Foundry shop, admixtures determination is done by the optical quantometer "Spectrovac 2000".

In production of molds from cast iron, the express determination of admixtures is done by optical quantometers "JY32" and "GVM-1014" before alloying, and certification of chemical composition of pig iron is done by the optical quantometer "GVP1-1014" if shipped to the customer.

Information on the initial content of admixtures in cast iron allowed prompt introduction of corrections during the alloying process; this gave a saving of up to 2 kg of silicon-bearing alloys and 0.67 kg of manganese-bearing alloys per ton of steel.

Application of these approaches makes possible a considerable reduction of ferroalloys consumption. Decrease in ferroalloys production, in its turn, allows improvement of the ecological situation.

The development is introduced at West Siberian Steel Corporation and Kuzmashzavod. The products made in accordance with the given technology are used at West Siberian Steel Corporation, Kuzmashzavod, Kuznetsk Ferroalloys as well as mining enterprises of the branch.*

REFERENCES
[1]A.A. Bondaryev, D.A.Lubyanoi, Yu.F.Shulgin, V.I.Brylyakov, Ye.I.Molchanov, A.Ye.Bazegsky, N.N.Tyuleneva, A.A.Peremitin. Alternative technologies of inoculants production and high-quality cast irons for needs of metallurgy and engineering // VI International Scientific and Practical Conference of Students, Post-graduates and Young Scientists: "Modern Techniques and Technology MTT'2000" – Tomsk: Russia, 2000. – P.122.

[2]D.A.Lubyanoi, I.V.Kokolevsky, Ye.V.Mantrova, Ye.A.Belyugov. Improving properties of iron-carbon alloys by thermotime treatment// Russian-Chinese International Symposium: "Fundamental Problems and Development of Advanced Materials and Processes in XXI Century". – Baikalsk: Russia, 1999. – P.233.

MINING AND APPLICATION OF NEW STRUCTURAL MATERIALS FOR BEARING UNITS SEM

Kurilov G.V. c.e.s., **Bednaya K.L.**, **Kurilov A.G.**
Research-and-production corporation "Technology - 2000"Ltd, Kharkov, Ukraine

Now creation of a universal stuff capable to work in units of friction of different assigning practically it is impossible, therefore there is a necessity of mining of stuffs for the concrete working conditions. Rational guard ropes of a stuff and production process enables to receive parts of heightened reliability, minimum weight and low-level cost, that is characteristic for parts and units SEM.

As has shown experience on fields [1], in a general flow of failures of the electric pump installations of one of the most widespread causes of rise of the submerged equipment from well is the failure of the electric motor, that is conditioned by a design SEM (upright arranged electric machine with external diameter 103, 117, 123 mms; in length of a body of 6-18 meters and multi-supported rotor). The observations by electric pump fund during several years have revealed the following main causes of failure of engines: an rupture of a core coil; an rupture in a frontal part; an rupture in a current lead; jamming and demolitions of arbors; a decrease of insulation; wearing of couples of friction.

The operation conditions and the mechanical tension of separate units, in particular of sliding bearings, and parts of the SEM results in necessity to apply to their manufacturing new progressive stuffs, more modern technology of processing; permanently to perfect their design; to pinpoint geometrical parameters and mechanical characteristics at the expense of the improved computational methods and bench tests.

Usage of powder metallurgical techniques allows to decide a series of the relevant technological problems.

The powder composite materials distinguish valuable of advantage, namely capability of obtaining and regulation of the different characteristics: strength, high-temperature strength, corrosion resistance, porosity, hardness damping and antifriction properties at the expense of the introducing of different dopes, doping of a fundamentals, change of production process.

One of the basic unit of the SEM are the sliding bearings: persistent and reference.

The body of block bearing works in a variable magnetic field and should have a high specific resistance as much as possible ease eddy currents, induced in the bearing box, and heating. The stuff of the bearing box should be strong enough, tear-proof, have damping capacity, to provide vibration resistance of the bearing box and to content to the following requirements: magnetic permeability of 1,1-1,3 mcHn/m; specific resistance not less than 1,0 Ohmmm^2/m, hardness 135-150 HB, ultimate tensile strength 500 MPa.

Such properties has nickel-chromium-manganous cast iron of a following elemental composition: 3,2-3,6 % C; 2,2-2,8 % Si; 9,0-10,3 % Ni; 6,0-8,0 % Mn; 1,5-2,0 % Cr; up to 0,12 % S; up to 0,3 % P. The long-lived operational check confirms necessity of application of the given stuff.

In connection with a deficit included in a structure nickel-chromium-manganous of cast iron of the most relevant component - nickel (9,0-10,3 %), is put a problem of definition of a capability of a decrease of the contents of a nickel at the expense of increase of doping of non-magnetic cast iron by manganese and nitrogen.

However manufacturing of bodies of bearing boxs from hire or casting method gives low operating ratio of a stuff. With the purpose of its increase, the decrease of laboriousness of manufacturing, increase of a wear resistance, improvement of up state, decrease of a friction coefficient of bearing assemblies are offered are to produced their powder metallurgical technique.

The successful combination of transferred properties of a stuff of a bearing case is obtained on the basis of powder titanium ПTX-4-2, which one and was selected for the basis for manufacturing of a body of block bearing [2].

Conducted idealized and experimental researches on analysis of up state persistent and block bearings [3] have shown, that 80 % of failures of

thrust bearings descend because of melting or intensive wearing it layer of a babbit in the extreme working conditions.

Way of obtaining of an antifriction stuff [5] a powder metallurgical technique on the basis of cuprum for a thrust bearing including mixing of dusts of cuprum, graphite, zinc and disulphide of molybdenum, pressing and sintering, has allowed to receive an antifriction stuff, due to cladding of a disulphide of molybdenum by monoxide of a boron. The obtained stuff has found broad application for manufacturing of thrust bearings in SEM [4].

The researches have shown, that parts made a powder metallurgical technique for SEM (turbine and a bore protector of a stuff ЖГр1, bearing case from a stuff ПТХ-4-2 [2] and support from a stuff ДО4Ц4Гр2Мс3Б [4,5]) respond the shown requirements and are advised to exploitation. The footstep from a powdered material ЖГр1 demands padding heat treatment. After improvement of this process also can be advised to exploitation.

The perspective application of items made of the set forth above stuffs, has allowed to economize raw, intermediate products and specially, that is very important, to lower costs of manufacturing of parts SEM at simultaneous preservation of the basic figure of merits and reliability of electric motors.

1.Основные характеристики работы УЭЦН в нефтяных скважинах Миннефтепрома. Технические материалы. М.: 1983.

2.Курилов Г.В. А. с. 1751489 (СССР) от 20.10.89. Подшипник скольжения для погружных электродвигателей серии ПЭД.

3.Филлипов В.Н. Надежность установок погружных центробежных насосов для добычи нефти. Обзорная информация. М.: ХМ —4 Насосостроение., Цинтихнефтемаш, 1983, 50с.

4.Курилов Г.В. и др. А. с. 1521948 (СССР) от 15.07.89 . Подпятник для машин с вертикально вращающимся валом.

5. Гребень А.М., Курилов Г.В. и др. А.с. 1455743 (СССР) от 01.10.87. Спеченный антифрикционный материал на основе меди и способ его получения.

NON – GALVANIZATION METHOD OF BONDING OF FRICTION MATERIAL TO THE STEEL BODY

Siroeshco G.S., Pascuk S.E., Gricel P.V., Leshok A.V., Zvonariov E.V.[1]
Molodechno Powder Metallurgy Plant, Molodechno, Belarus
[1]Institute of Powder Metallurgy, Minsk, Belarus

Frictional materials (FM) have a great role for automobile and tractor industries. FM is the material wich has got frictional coefficient (f) above 0,05 in conditions of wet rubbing and 0,2 in conditions of dry rubbing.

Working speeds increase permanently and conditions of operation become extremely high/ For example the speed is up to 100 m/s, the contact temperature is achieved up to 1000^0 C and working pressure is used up to 20 MPa.

The metal ceramic FM have got a wide range of appliance in industry. These materials include both metal components and non-metallic compounds.

Therefore there are many different problems in the manufacture technology of frictional products.

One of then is the creation reliable bonding of FM with steel body.

Traditional technology of producing frictional articles embodies protective coating on the steel body having thickness 2,5...150 mm. The coating protects the steel surface and prevents the formation compounds or films by oxidation process by of oxygen from air or gases entrained in the FM mixture.

There were made some experiments substituting an copper electrolytic coating which provide appliance harmless processes for people and nature.

Taking into account capillary effect and its property to constrict particles there is developed the flux giving an opportunity for activity steel surface and construction particles simultaneously.
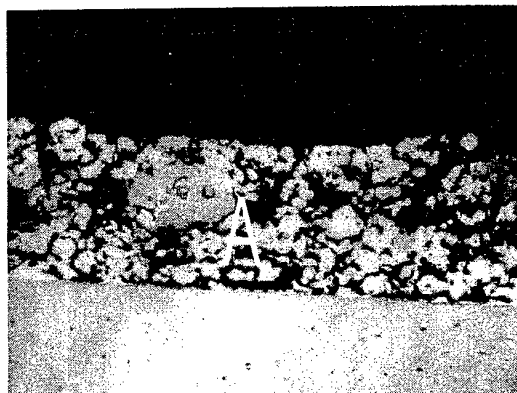
Fig. 1.
The border FM (A) – steel body(B).

The flux isn't found on the border frictional material – steel body and it provides efficient bonding of the sintered FM to the steel. The high quality of the bonding is provides by the diffusion process of powder material to the steel body.

Experimental tests of frictional disks have been carried out in hard conditions and the results were satisfactory.

The flux using allows to simplify the technology of producing frictional disks and to avoid quite harmful process and to use technology without purification constructions. Thereto it gets an opportunity in reduction in the price of final products.

161

DISPERSION STRENGTHENED MATERIAL BASED ON COPPER POWDER C 0/97 OF DISCOM® TRADE MARK FOR CURRENT REMOVING STRIPES USED IN CURRENT-COLLECTING DEVICES OF ELECTRIC TRAINS

Shalunov E.P., Matrosov A.L., Wendland St.[1]
Scientific and Technological Company TECHMA Ltd, Cheboksary, Russia
[1] RÖTECH G.m.b.H., Mühlheim –an-der-Ruhr, Germany

As in any electric circuit, a device commuting current form the contact net to the electric drive of the locomotive is one of its most important elements. Stable operation of the whole electric circuit and electric engine of the locomotive, as a power consumer including, depends on the safety and working ability of this device. If under quiescent conditions electric energy removal and its transfer to the locomotive electric drive is carried out relatively easy, fulfillment of the same function when electric train is moving, i.e. under conditions of the sliding electric contact, becomes a complicated technical task. Due to the availability of movement this contact is notable for instability causing possibility of sparking or electric arc. Sparking increases wear of the contact pair, i.e. "contact wire - current-removing stripe", and arc results in material evaporation, which in its turn increases roughness of the contacts. Ice on the wire causes interrupted movement and increases sparking. Rain also increases the wear of the contact pair. Sparking and arc, the power of which increases as collected current rises, and mechanical friction in the contact pair as well stipulate for sufficient temperature rise of the current-collecting element as compared with the temperature of the environment. The higher is the strength of the collected current and speed of the train, the higher is the temperature. Taking it into account it's necessary for material used for current-collecting elements to provide high arc-resistance, wear-resistance, high hardness cha-racteristics at high temperatures, and antifriction characteristics as well.

As the speed exceeds 160 km/h, the temperature in the contact zone reaches 500...600°C. That is why, many materials used earlier (bronze CuCr1Zr, sintered powder compositions on the base of copper and iron saturated with lead and tin alloys etc.) having lower recrystallization temperature have become improper for such operational conditions. Materials possessing higher heat- and wear-resistance are required. To prevent current

loss and consequent temperature rising due to the self-heating these material should be of high conductivity as well. Due to the high temperature appearing in the contact zone of current-collecting devices, materials used for the current-removing stripes shouldn't contain easy fusible chemical elements, especially those which are able to go into the atmosphere and cause along the railways unfavorable ecological background for human beings and animals. Good processing ability requirements for materials used to produce current-removing stripes (milling, grinding, drilling etc.) should also be taken into account.

Current-removing stripes made of various carbon materials widely used in railways in different countries of the world at alternating voltage from 15000 V to 25000 V (at the average current of 700...800 A) endure high temperature and contact wire wear is minimal. Such current removing stripes are often used in electric trains inside and outside the city at constant voltage (1500 and 3000V) in the contact net, where current reaches from 700 to 2800 A.

Calculations show that the consumption of power increases by 8...12% at such current and electric conductivity of carbon current removing stripes of 0,03...0,06% from copper electric conductivity as compared with the power consumption level, when it is commuted by current removing stripes, their electric conductivity making up 88 % from copper electric conductivity.

Due to the low electric conductivity current removing stripes made of carbon materials cause overheating resulting in extra heating of the contact wire. Besides current removing stripes are worn quickly and the products of their wear go into the atmosphere and fall down to the neighboring grounds. Production of such stripes also faces certain ecological and technological difficulties.

Oxide and Carbon Dispersion Strengthe-ned Material based on copper powder (OCDS-Copper) C 0/97 of DISCOM® Trade Mark developed by TECHMA Ltd (Cheboksary, Russia) meets the above requirements in the highest degree. It is a copper matrix strengthened by ultra-dispersion particles (0,02...0,03 µm) of Al_2O_3 and contains carbon in addition.

Technological process of this material production, mechanical alloying of powder composition Cu-Al-C in attritors being the major operation, is based on the technology developed and patented by TECHMA Ltd.

OCDS-Copper C 0/97 of DISCOM® Trade Mark possesses the following physical and mechanical characteristics at room temperature:
Electrical conductivity, % IACS...........90±2
Rockwell Hardness (HRB)...............70...74
Ultimate tensile strength, N/mm².....410...460
Conditional tensile yield limit,
N/mm².................................350...390
Relative elongation, %....................20...23
Compressive yield point,
N/mm².................................1800...2000
Compressive relative settling, %........63...67

After annealing at 800°C during 1 hour strength characteristics of the material are reducing only by 10...15 %.

Apart from high electrical conductivity, strength characteristics and wear resistance the material also possesses high recrystallization temperature, which makes up not less than 800°C, whereas traditional and sintered Bronze looses its strength characteristics already at the temperature of 350...550°C. It means that DISCOM® C 0/97 material can be successfully applied without loosing its characteristics not only at the speed of 160 km/h but also at considerably higher speeds.

Tests of the developed material having been conducted in German Metal Studying Scientific and Research Institutes (Max-Planck-Institute, IFAM and others) and current-removing stripes produced from this material having been tested on the testing grounds and in operational conditions of high speed main lines of Italian Railway, the material in question was recommended to be used in electric trains moving at a speed over 160 km/h apart from the American oxide dispersion strengthened material (ODS-Copper) Cu+Al_2O_3 GlidCop® AL-15.

OCDS-Copper C 0/97 of DISCOM® Trade Mark is manufactured as hot pressed (by means of extrusion) rods of rectangular section according to Technical Requirements TU 1479-002-13092819-2001 registered by State Standard of Russia and after mechanical processing is delivered as ready-made current-removing stripes of various sizes and weight from 2 up to 3 kg to the Italian Railway via the German firm RÖTECH G.m.b.H. Every lot to be delivered undergoes independent testing beforehand in one of the branches of Fraunhofer Institute and obtains Quality Certificate of this Institute. The volume of delivery at the moment makes up more than 20 tons of ready-made current-removing stripes annually and this volume will steadily grow since Glidcop® AL-15 is being replaced by it. A possibility to substitute material C 0/97 DISCOM® for Bronze CuCr1Zr, used in electric trains moving at a speed under 160 km/h, is also being considered.

To prevent the contact wire from wear between current-removing stripes made of DISCOM® C 0/97 material there should be fixed a graphite plate used as a source of dry lubricant for the contact pair "current-removing stripe – contact wire" (Fig.).
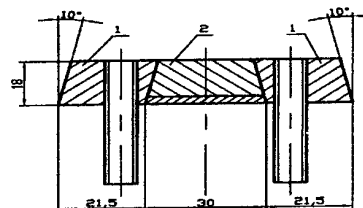
Fig. Current-removing device of a high speed electric train moving at 160km/h and over: 1- current-removing stripes; 2 – a graphite plate.

163

SUPERCONDUCTIVITY NIOBIUM CARBIDES, NITRIDES, CARBONITRIDES AND GLASS COMPOSITES AND NEW POSSIBILITIES OF THEIR APPLICATIONS IN CRYOGENIC TECHNICS

O.I.Shulishova, N.V.Shevchuk, I.A.Shcherbak

Institute for Problems of Materials Science of NANU, Kiev, Ukraine

The high temperature superconductivity discovery that evoked incredible expectations concerning the possibility of room temperature superconductivity achievement caused a significant decrease in public interest to conventional "low-temperature superconductors" that hardly reached hydrogen temperatures over the past decades.

However, even if these expectations come true the demands for facilities and materials that are necessary for the operation at helium level of cooling will not disappear or diminish. Electronics, e.g., remains such a field where the need for helium level of cooling will always exist. Any electronic circuit consists of passive elements – resistors and conductors – 60-80 %. These elements determine the whole circuit operation in many respects. The thermal noise electromotive force of resistor that is determined by the production of its resistance and temperature limits the threshold power of the useful signal. It is impossible to increase the sensitivity of receiver decreasing its input resistance, and the only radical measure of noise reduction is the decreasing of devices operating temperature. Circuit cryostatting in the liquid helium allows to decrease resistors thermal noise level by two orders of magnitude that will allow to decrease the threshold power of the signal received in the same times. It is especially important for the long distant Earth's and space communications.

The thick film production process initial materials are paste-like compounds. The thick film production process is widely used in nowadays electronics to fabricate passive elements. This techniques offers some advantages over the thin film one among which there are the simplicity and lower cost of equipment, less sensitivity to contamination, the lower surface finishing class of substrates applied, higher reliability and reproduction of operating characteristics.

The thick film production process initial materials are compounds that comprise a conductive phase powder suspension mixed with configuration and thickness films are deposited mechanically through the mask on the ceramic substrate, an organic is removed by drying, and afterwards films are subjected to heat treatment. The films obtained in such a manner comprise not uniform disordered structure of three-dimensional chains of randomly oriented contacts that are formed by the conductive phase particles in the glass matrix.

The quantity of conductors in large-scale integrated circuits may be so big that their total input in the resistance becomes comparable with the good resistor input. As thick films comprise disorder media in which a substantial resistance growth is observed with the temperature drop, it is clear that at the circuit cryostatting aimed to improve resistors operation conductors become a source of substantial additional power losses and circuit operation parameters degradation. Thus, the problem of such thick conductor films creation that would not degrade circuit operation at the cryostatting but would fulfil their role as ideal as possible reducing the electrical loss to zero at all, arises. We have solved this problem by means of pastes based on superconductive niobium carbides, nitrides and carbonitrides having T_c 11.1 K, 16,3 K and 17,9 K respectively.

Carbides, nitrides and carbonitrides have a simple crystal structure B1 (of NaCl-type) and form a wide class of superconductive compounds having unlimited mutual solvability and wide areas of homogeneity. It allow to obtain superconductive materials and, correspondingly, superconductive thick films with virtually and desirable superconductive temperature T_c from the lowest one to 18 K. Superconductive thick films properties do not depend only on chemical composition, but on the superconductive component grading composition as well as the superconductive and dielectric paste components quantitative relation (Fig. 1,2).

Thus, changing the chemical and grading Composition of the superconductive component

glass powder in organic solvent. The necessary to obtain superconductive thick films varying slightly their properties combination in superconductive and normal state:
- T_c from the lowest one to 18 K,
- superconductive width ΔT_c from the part of one degree to 18 K,
- film resistance in the normal state , ρ_n , from the tenth parts to tens Ohm/ □ ,
- temperature coefficient of resistance TCR in the normal state positive, negative, or practically equals zero.

Superconductive thick films critical fields H_c are several orders greater than those of the initial components in solid state, their critical currents I_c depend on phase ratio and comprise 10^2- 10^4 A/cm^2 at 4,2 K.

It is known that superconductive metals and compounds possess much lower conductivity in the normal state that normal metals such as copper and silver. Introducing normal metal with high conductivity, e.g., silver, in the paste compound one can obtain unique films having such a high conductivity at temperature higher than T_c that cannot be achieved for any superconductors and having zero resistance at temperatures lower than T_c .

Thick films based on niobium carbides, nitrides and carbonitrides properties allow to apply them as:

and its quantitative part in a paste, it is possible conductive elements with zero electric losses in integrated circuits of helium level of cooling;
- conductivity elements having superconductivity at $T<T_c$ and extremely high conductivity at $T>T_c$ (compounds with silver);
- thermal switches, switches that are converted in the normal state by the current passed;
- resistance cryogenic thermometers with the linear dependence (transition to the super-conductive state with wide ΔT_c);
- sensors for liquid helium level gauges having reliable potting automatization (high , small TCR, T_c = 4,2 K);
- materials for superconductive screens having any dimension and form deposited by the paste spraying technique.

Apart from practical application in cryogenic electronics, instrument engineering, and cryogenic engineering superconductive thick films may be used in scientific researches as model systems for phase transition investigations, for superconductivity and localization competition, for laws of percolation theory study as well as for the investigation of charge effects role in systems having Josefson's junctions.
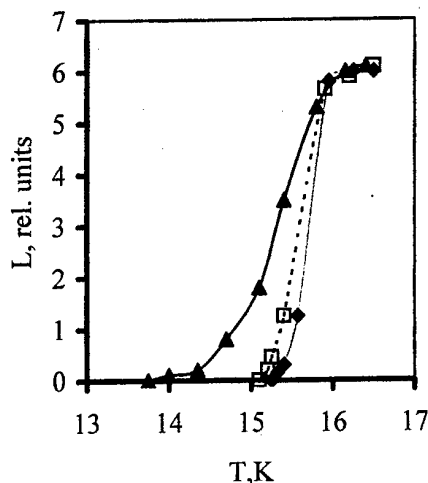
Fig.1. Superconducting transition for $NbC_{0,3}N_{0,7}$:
◆ - sintered sample,
□ - fraction for particles size ≥ 40 μkm,
▲ - fraction for particles size < 40 μkm.
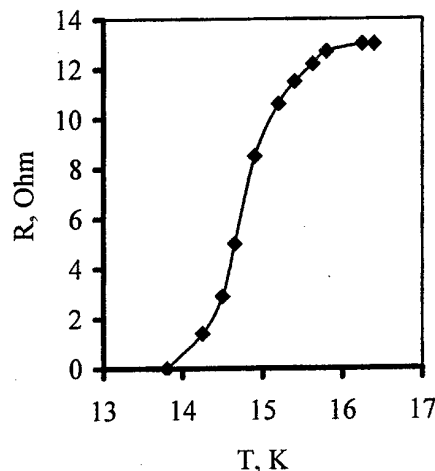
Fig.2. Superconducting transition (4) for thick film with powder from fraction < 40 μkm. (superconducting transition ▲ from Fig.1).

165

NEW COMPOSITE COATINGS FOR REINFORCING HEAVILY LOADED PARTS

Rudenskaya N.A., Shveikin G.P.
Institute of Solid State Chemistry, Ural Branch of the Russian Academy of Sciences, Ekaterinburg, Russia

Gaseous thermal deposition technology for reinforcing parts operating under extreme conditions should be developed employing composite materials, whose composition, micro- and macrostructure can be formed in a controlled manner during deposition, thermal treatment and operation of coatings.

A new class of composite powders and universal gaseous thermal coating based on refractory compounds with a special structure has been elaborated.

We were the first to study experimentally and theoretically the processes of shperoidization, pulverization and conglomeration of polydispersion powders TiC, Cr_3C_2, NiN, TiCN, CrB_2, TiB_2, ZrB_2, $TiCrB_2$, AlB_{12} under low-temperature plasma conditions; migration of reinforcing phase particles in melted coatings; as well as wear of composite coatings during abrasive treatment. These processes were simulated to put forward criteria for evaluating and predicting the composition, structure and properties of composite materials (universal incommensurate criterion of spheroidization, analytical equations for determining the thickness of a cladding layer on refractory granules and residual porosity of melted coatings with the reinforcing phase, semi-empirical equation for calculating relative wear resistance of composite coatings in abrasive treatment).

Some unfamiliar self-organizing processes of modification of the composition and structure of gaseous thermal coatings occurring during their formation were found and investigated. They proved to considerably improve physical and mechanical characteristics of (i) deposited layers (phases with enhanced microhardness 3200-4929 kg/mm^2) formed during the interaction between composite particle components; (ii) multilayer oxynitride shells (2800-3500 kg/mm^2) on titanium nitride inclusions resulted from interaction of deposited particles with a plasma-forming gas (self-cladding effect); (iii) gradient-layer coatings and multilayer interfaces coating – base metal; (iv) refractory phases and phases with enhanced microhardness arising when composite coatings interact with the environment.

A unified complex approach to the creation of reinforcing coatings used under extreme conditions has been proposed, substantiated and approbated. It involves the choice of the composition of the reinforcing ingredient and the matrix alloy with the optimum physico-mechanical properties; individualizing the composition based on the structure and method of obtaining the reinforcing phase particles; the choice of the system for modifying the coatings' micro- and macrostructures. The structure and properties of gaseous thermal coatings made of 93 different composite powders have been examined. The proposed approach was employed to develop 20 novel compositions and composite materials types. The problem of high-temperature working capacity of parts exposed to simultaneous wear and shocks was solved for the first time in this country by using protective coatings. Comparative analysis between coatings made of the developed complex powders and those produced by domestic and foreign firms showed that cladding and conglomeration of reinforcing phase powders result in (i) properties comparable to those of <u>Castolin</u> coatings when they operate in a flow of abrasive-containing liquid (the proposed materials are tungsten-free); (ii) 3 to 5 times better wear-resistance in an abrasive air flow as compared to Ni-Cr-B-Si alloys; (iii) 2 to 22 times increased stability to abrasive wear (reference – steel 50 quenched to HRC = 52-54 units). Owing to the synthesized compositions, the thermal stability of deposited layers is raised by a factor of 2 to 20 in comparison with stellite and melting from powder wire ПП25Х55ФСМ.

The elaborated composite powders and technological innovations were tested and adopted at a number of enterprises of the Ural region and Western Siberia thus improving the operation stability of heavily loaded parts.

OBTAINING OF WEAR-RESISTANT CHROME COATINGS WITH NANODIAMONDS OF DIFFERENT ORIGINS

Burkat G.K.[(1)], **Fujimura T.**[(2)], **Dolmatov V.Yu.**[(1)], **Orlova E.A.**[(1)], **Veretennikova M.V.**[(1)]

[(1)]Special design bureau "Tekhnolog" at the St.Petersburg State Technological Institute
(Technical University), St. Petersburg, Russia
[(2)]"VISION DEVELOPMENT CO., LTD", Tokyo, Japan

At the beginning of the eighties of XX century it was found that detonation synthesis ultradispersed diamonds (or UDD, or nanodiamonds) (of 4-6-nm size) are able to co-deposit with metals by their electrochemical or chemical reduction from aqueous solutions of salts. It allows one to form the two-phase composite electrochemical coating (CEC) consisting of metallic matrix and introduced dispersed nanodiamond particles [1-3].

The method of chrome-UDD-plating for edge tool and parts are widely used. This method was realized on an industrial scale at the enterprise "Elektrokhimpribor" (t. Lesnoy) et al. Many scientific-research works were devoted to that process, and they described very contradictory results – from enthusiastic up to negative ones [1, 2].

The present work has for an object to investigate a process of electroplating of chrome-diamond CEC and its quality with nanodiamonds of different origins: UDD industrial-manufactured by SDB "Tekhnolog" according to Specs TU 05121441-275-95 and static synthesis nanodiamonds ASM 0,1/0 (crystal size up to 100 nm). The results of the work can be widely used in practice.

Chrome plating process (standard and diluted electrolytes of chrome plating) allowing to obtain the hard chrome at temperature of 45-48°C over the current density range of 50-130 A/dm² and the wear-resistant chrome at temperature of 52-56°C (current density 50 A/dm²) was studied.

Introduction of UDD- and ASM-additives to the electrolyte of chrome plating does not exert a great influence on the microhardness of chrome coatings. An increase in the microhardness is observed in a high current density region, it is equal to 30-35% of the microhardness of chrome without additives.

An influence of concentration of UDD on the microhardness of chromic coatings is presented (Fig.1) for the standard chrome electrolyte

(concentration of chromic anhydride of 250 g per l). On Fig.1 there is the maximum of microhardness for UDD-concentration of 15 g per l, and the microhardness of chromic coatings is higher, the higher the current density. At the high current density region (100-130 A/dm²) the maximum of microhardness is shifted to the region of 30 g per l of UDD. But, concentration of UDD in an electrolyte should not be increased more than 15 g per l as Russian enterprises do not practically work at high current densities. Optimum current densities are usually 50-75 A/dm² for the chrome plating process. An increase in microhardness at the presence of UDD occurs equally in both standard and diluted electrolytes. Thermal treatment of samples at 200°C during 2 hours naturally decreases the microhardness over the all current density range by about 15-20%.
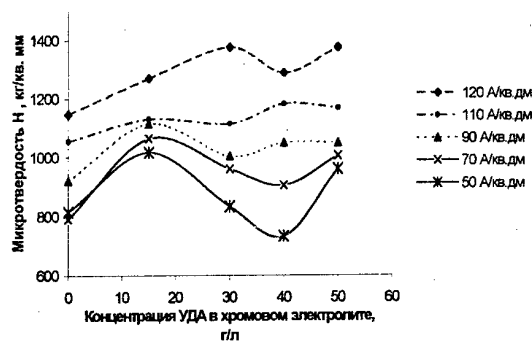
Fig. 1. An influence of UDD-concentration in the electrolyte (CrO₃ – 250 g per l) on the microhardness of chrome coating at different current densities.

It is found that the coatings with ASM have smaller microhardness than these with UDD because ASM do not have a high surface activity in contrast to UDD. ASM are included into the coating only due to mechanical capture of particles by growing the chrome-deposit. As an increase in concentration of ASM-additive the microhardness smoothly increases up to the concentration of 5 g per l. Therefore, the concentration of ASM in electrolyte can be limited to 3-6 g per l. UDD being included into the chrome deposit promote

the grinding of coating-grains due to surface-active properties of UDD.

The results of studying of wear-resistance of the chrome coatings in the presence of both UDD ASM are presented in Fig.2. As a rule, the attrition time is limited to 20 hours.

As it follows from Fig. 2, the chrome coating obtained under conditions of wear-resistant chrome plating but from the standard electrolyte with no any additives for 20 hours' attrition loses 15% of its mass. The coatings obtained from the electrolyte containing ASM-additive have the maximum wear-resistance. The samples of chrome coatings which have lost little more than 1% of theirs mass for 20 hours of attrition time were obtained from solutions containing 3-6 g per l of ASM. An increase in the concentration of ASM up to 10 g per l in the electrolyte does not change the microhardness of chrome coatings. That fact once more confirms the conclusions about the optimum content of ASM of 3-6 g per l. However, during testing the chrome coating with ASM-additive (at different concentration in an electrolyte) abrades a counter-body 1,5 –3,0 times as intensive as that without additives.

The wear-resistance of the chrome coatings in the presence of UDD was studied over a wide range – up to 50 g per l. The wear-resistance of the chrome-coatings with UDD is a little worse than for the ones with ASM. Nevertheless, wear of the chrome coatings obtained from the electrolyte containing 15 g per l of UDD amounts to about 3%, that is greatly better than for the coatings obtained from the electrolyte without additives (wear amounts to 15%). In addition, during testing the obtained chrome-UDD-coatings the attrition of a counter-body was not practically observed.

Moreover, the wear-resistance of the chrome coatings obtained from electrolytes containing mixed additives of UDD and ASM was investigated. The coatings obtained from the electrolytes containing 2,5 g per l of UDD and 5 g per l of ASM have the same wear-resistance as the coatings obtained from the electrolyte containing 15-20 g per l of UDD. However, attrition of a counter-body is increased.

Addition of ASM despite the fact that it has a positive impact on wear-resistance of chrome coatings is not very effective, in particular as that does not practically influence the uniformity of a

coating (in contrast to addition of UDD). An increase in the uniformity of a coating for the chromic electrolyte is one of the most important problems. Thus, addition of UDD into the electrolyte of chrome plating does not have an alternative.

The conclusions:

The carried out investigations shown that in the presence of UDD (UDD-content of 15-30 g per l) the microhardness of the chrome coatings is increased by 30-35% (up to 1400 kg/mm^2), the wear of that coatings is decreased from 15% (without additives) to 3% (in the presence of 15 g per l of UDD in the electrolyte) and to 1% (in the presence of 3-6 g per l of ASM 0,1/0).
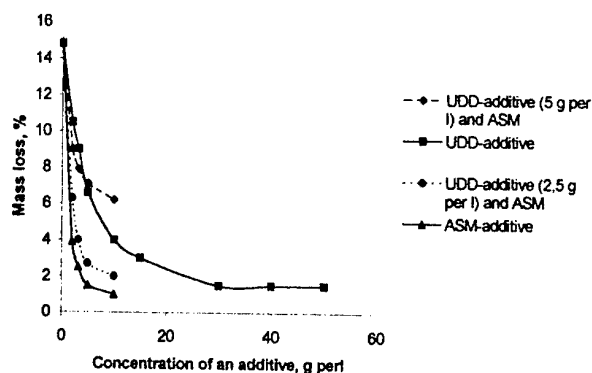
Fig. 2. An influence of UDD- and ASM-additives on the wear-resistance of chrome coatings

References:

1. A.s. № 1694710, C25D15/00, The method of obtaining of composite coatings on the basis of chrome/ A.I.Shebalin, V.D. Gubarevich, P.M. Brilyakov. – Publ. 30.11.91 .Bul. № 44 (A.c. № 1694710, C25D15/00, Способ получения композиционных покрытий на основе хрома/ А.И.Шебалин, В.Д. Губаревич, П.М. Брыляков. – Опубл. 30.11.91. Бюл. № 44)

2. Dolmatov V.Yu. Detonation synthesis ultradispersed diamonds: properties and applications// Russian Chemical Reviews. – 2001. – 70, №7. – P. 607-626

3. V.Yu. Dolmatov, G.K. Burkat. Detonation synthesis ultradispersed diamonds as the base of a new class of composite metal-diamond galvanic coatings//Sverkhtv. Mater. – 2000. - №1. – P. 84-95.

OZONESAFE COOLANTS AND SOLVENTS: SYNTHESIS AND OPTIONS FOR PRODUCTION, PROPERTIES AND POTENTIAL APPLICATIONS

Shatalov V.V., Orekhov V.T., Ryabakov A.G., Skachedub A.A.[1], Lunin A.I.[2]
[1]State Unitary Enterprise All-Russian Research Institute of Chemical Technology, Moscow, Russian Federation
[2]Moscow Technical University, Russian Federation

Since 2001 international legal documents on the Earth ozone layer protection have banned Russian Federation to produce ozone depleting substances (ODS), i.e. khladon-11, -12 and −13 − coolants and propellents, khladon-113 and tetrachloro-methane − solvents, bromine containing khladons (halons) − fire suppressing agents [1].

Under the circumstances during the transitional period Russian Federation is planning to stop the consumption of ozone depleting substances and to make the various fields of national economy produce and use ozonesafe substances and technologies.

MinAtom of Russia has executed such works since 1988 owing to their own finance and made possible for State Unitary Enterprise All-Russian Research Institute of Chemical Technology together with Kirovo-Chepetsk Chemical Plant to carry out researches in the ozonesafe khladons and solvents syntheses.

Methods of khladons, solvents, foaming agents, fire supressing agents syntheses on base of depleted hexafluorinated uranium (UF6) have been developed and ozonesafe fluorine-organic substances have been produced [2, 3].

The syntheses of the following substances were studied at the pilot plants and experimental industrial installations:

HCFC:

$$122a: CHCl{=}CCl_2 + UF_6 \xrightarrow{t} CHClF\text{-}CCl_2F + UF_4$$
$$_{122a}$$

$$132c: CH_2{=}CCl_2 + UF_6 \xrightarrow{t} CHF_2\text{-}CCl_2F + UF_4$$
$$_{132c}$$

$$142a: CH_2{=}CHCl + UF_6 \xrightarrow{t} CH_2F\text{-}CHClF + UF_4$$
$$_{142a}$$

HFC:

$$152: CH_2{=}CH_2 + UF_6 \xrightarrow{t} CH_2F\text{-}CH_2F + UF_4$$
$$_{152}$$

$$134a: CH_2{=}CF_2 + UF_6 \xrightarrow{t} CH_2F\text{-}CF_3 + UF_4$$
$$_{134a}$$

$$CH_3\text{-}CF_3 + UF_6 \xrightarrow{t} CH_2F\text{-}CF_3 + HF + UF_4$$
$$_{143a} \qquad\qquad _{134a}$$

$$125: CH_3\text{-}CF_3 + 2UF_6 \xrightarrow{t} CF_3\text{-}CHF_2 + 2HF + 2UF_4$$
$$_{125}$$

FC:

$$116: CH_3\text{-}CF_3 + 3UF_6 \xrightarrow{t} CF_3\text{ - }CF_3 + 3HF + 3UF_4$$
$$_{116}$$

$$218: CF_3\text{-}CF{=}CF_2 + 3UF_6 \xrightarrow{t} CF_3\text{-}CF_2\text{-}CF_3 + UF_4$$
$$_{218}$$
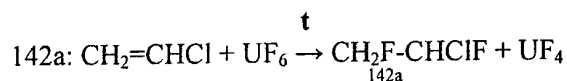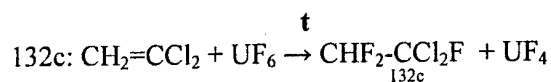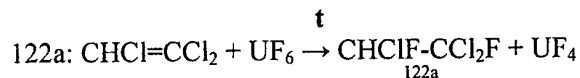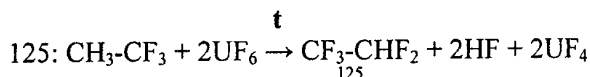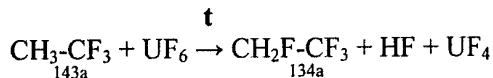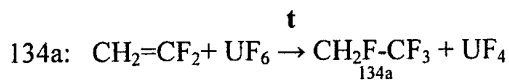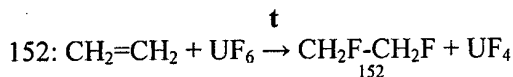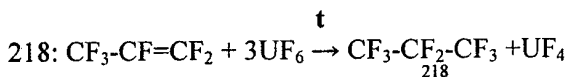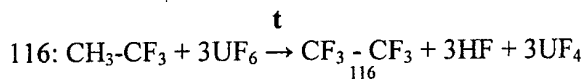
Proposed technology of the ozonesafe compounds suntheses with the help of UF6 has the following advantages over the technologies based on catalitic fluorization:
- the construction of the reactor is the same;
- the ratio of the reagents is close to stoichiometric instead of large excess of fluorizating agent;
- the low temperature of the synthesis;
- weak vacuum instead of pressure of 3-10 atm.
- depleted uranium hexafluoride utilization.

As a result of the research works of State Unitary Enterprise All-Russian Research Institute of Chemical Technology ,Kirovo-Chepetsk Chemical Plant, a number of Moscow enterprises and high educational establishments a nomenclature of ozonesafe khladons for domestic needs, trade and industrial refrigerators was defined. The substances isolated and approved in Russia were given the preference, as there are home raw materials base, ready-made technology and minimal financial

outlays would be necessary for their introduction in the shortest possible time.

Transitional (up to 2020) ozonesafe mixture of khladons X-22 + X-142b with low ozone depleting potential ODP= 0,02-0,04 was investigated in details and proposed for uses instead of ozone depleting coolant X-12. This mixture makes it possible to utilize equipment both new and old, which had run on khladon-12, and cheap home mineral oil. Kirovo-Chepetsk Chemical Plant produces up to 1000t of this mixture annually, this quantity is enough both for needs of Minatom and 10 Russian plants of domestic refrigerators.

The most promising ozonesafe coolant is CM-1 (mixture of khladon-134, -218 and butane). CM-1 has unlimited period of work.

Moscow Technical Univercity calculated the equation of state, determined heat properties, held exploitation tests for both mixtures in different types of refrigerators.

Both of the appointed coolants coexist with mineral oils, electric insulators and constructional materials that have been utilized before, that is why these coolants may be applied in new equipment as well as in already functioning equipment. In some cases, in particular in two-compartments refrigerators ozonesafe mixture coolants make it possible to reduce electric energy consumption up to 10% as compared with khladon-12. Special ozonesafe noncombustible mixture on base of home industrial coolants was chosen for climatic chambers. At the moment the optimization of the mixture composition to replace X-13 is executed and stand tests were held to confirm the calculated parameters.

All-Russian Research Institute of Chemical Technology together with Kirovo-Chepetsk Chemical Plant elaborated technology and produced experimental industrial batch (~50t) of ozonesafe solvent – khladon-122a, held enlarged industrial tests in Russia, South Korea and apointed the most promising potential applications [4].

Azeotropic mixtures on base of khladon-122a were developed to clean the metal details. They have high solvent power and can dissolve a number of contaminations and technical products. Before the industrial manufacturing of khladon-122a it is recommended to make use of stable ozonesafe chlorine-organic solvents and their mixtures with other organic solvents to remove contaminations and fat from various technological equipment.

1. Report of the 13-th Conference of the Parties of the Montreal Statement on the Substances Depleting the Ozone Layer (Sri Lanka, Colombo, October, 13-19, 2001).
2. A.N.Golubev, V.U.Zakharov, V.T.Orekhov et al. The method of production of the fluorine containing substances of ethane series. Russian Patent № 2030380.
3. A.N.Golubev, V.U.Zakharov, V.T.Orekhov, V.V.Shatalov et al. The method of khladon-134a production. Russian Patent № 2116287.
4. V.V.Shatalov, V.T.Orekhov, A.A.Skachedub. Khladon-122a – synthesis, properties, applications. The theses of the reports. The 3-d International Conference "Chemistry, Technology and Applications of Fluorine-substances" CTAF, 2001, St.-Petersburg.

FUSION WELDING OF PARTICULATE REINFORCED METAL MATRIX COMPOSITES

Chernyshov G., Shiganov I., Panichenko S.
Bauman Moscow State Technical University, Moscow, Russia

Metal Matrix Composites (MMCs) can be reinforced by particulates, continuous fibers, chopped fibers or whiskers. Most attention is currently to particulate reinforced aluminium alloys, magnesium, titanium and copper alloys. SiC is the preferred particulate reinforcement, although other material such as ceramic phases Al_2O_3, TiC, B_4C, TiB_2, graphite particles and intermetallic phases Al_3Ti, Ni_3Al, NiAl have also been used in matrix alloys. MMCs are now widely used for structural applications due to low cost and more high properties compared to most monolithic metals such as specific strength, specific stiffness, hardness, damping capacity and wear resistance. Selecting the kind and quantity of particulate reinforcement and matrix chemical composition can tailor a level of particle/matrix intefactal bouding and coefficients of thermal expansion and thermal conductivity. Existing and potential applications for MMCs are including: automative drive shaft tubes, cylinder liners, aircraft stabilizer, heat exchanger material for hypersonic aircrafts electrodes for power semiconductor devices. In many of these applications it is also desirable to fabricate of MMCs into complex shapes via joining processes. Joining technologies are essential for practical application of MMCs.

There are a few reports about the fusion joining of the MMCs, from wich it can be seen that main goal into these processes is limitation of chemical reactions at the particle/matrix interface. The most of the MMC systems are not thermodynamic stable, therefore any joining process that involves high heat input will inevitably upset the existing metastable micro-environment. In particular, prolong exposure of Al-based/SiC particulate composites at reasonably high temperatures may promote reactions between the matrix and reinforcement, in that the formation of brittle Al-carbide phases Al_4C_3 would cause the corrosion resistance and the fracture toughness of the weld to be reduced to an unacceptably low level. The fusion joining of these MMC, however, is possible if the duration of particle/melt contact can be decreased or the weld pool temperature can be kept below the temperature at which the formation of aluminium carbide is inhibited by silicon content in the aluminium matrix alloy [1,2].

An additional complication of fusion welding is the increased viscosity of the molten pool due to presence of the particles and the products of interfacial reactions. The high viscosity and lesser wetting of this molten region prevents manipulation of the pool. During laser-beam welding the viscous drag effect of the reinforcement results in lack of fusion. The addition of filler alloys has been used successfully to improve the fluidity of the weld pool, especially during gas metal arc welding.

MMCs produced by powder metallurgy techniques are often subject to the formation of porosity in the fusion zone and heat-affected zone. The porosity is caused by the presence of large amounts of hydrogen associated with the oxides on the surface of the metal powder. Upon melting, the hydrogen coalesces and forms large pores in the weld. Another concern of fusion welding is the rejection of the particles by the solidification front and damage of the uniform particle distribution in matrix. It appears from published works [3,4], that during argon tungsten-arc welding of SiC_p-Al alloy (АЛ2) composites the ceramic particles generally do not melt or do not dissolve in weld pool, however near to a line of fusion and in central fusion zone by weld surface is possible the formation of zone free from particles. The size of these zone a depend on welding conditions. At minimum power density of welding it is possible to receive more uniform macrostructure of a weld, best particle distribution in matrix, major dispersity of matrix structure compounds.

Reference
1.Ellis M.B.D. Materials and Manufacturing Processes. 1996, vol.11, N1, pp.45-60.
2.Iseki T., Kameda T. And Maruyama T. J.Mater. Sci., 1984, v.19, pp.1692-1698.
3.Чернышов Г.Г., Чернышова Т.А., Кобелева Л.И., Болотова Л.К. ФизХОМ, 1999, № 4, с.57-62
4.Чернышов Г.Г., Рыбачук А.М., Чернышова Т.А., Кобелева Л.И., Болотова Л.К. Сварочное производство, 2001, №11, с.7-13.

Oxidation Behavior of Al-Cr-N Films Prepared by a DC Reactive Sputtering

Yukio Ide[1], Takashi Nakamura [2] and Katsuhiko Kishitake[3]

[1]Yamaguchi Prefectural Industrial Technology Institute, Ube, Japan

[2] Tohoku University, Sendai, Japan

[3] Kyushu Institute of Technology, Kitakyushu, Japan

Introduction

It is well known that oxides formed by Al and Cr under high temperature make strong adhesion to substrates. AlN and CrN are believed to be high temperature protective coating materials due to the high excellent oxidative resistance. The high temperature oxidation characteristics of Al-Cr-N films composed of AlN and CrN may be superior to that of Ti-Al-N films that have been widely used under severe oxidation environment. We have proposed and discussed Al-Cr-N films composed of AlN and CrN. This study deals with the high-temperature oxidation properties of Al-Cr-N films that were deposited using a DC reactive sputtering apparatus.

Experimental

Commercial Stainless steel sheets and SKH51 steel sheets were used as substrate materials. Since Al/Cr ratios of the targets are considered to be important for the performance of the films in the reactive sputtering method, three different Al/Cr ratio targets, Type A (75at%Al25at%Cr), Type B (50at%Al50at% Cr) and Type C (25at%Al75at%Cr) were selected. Targets of pure Al, Cr, Ti and Al-Ti (50at%Ti 50at%Al) were used to make AlN, CrN, TiN and Ti-Al-N films.□Details of a dc magnetron sputtering apparatus used in this study were already described previously[1].

The samples were heated at 800□, 900□ and 1000□ in air for 10 min and 60 min followed by air cooling. The oxidized films were characterized by a low angle X-ray diffraction (XRD). The compositional depth profiles of the oxidized films were measured by auger electron spectroscopy (AES). The oxidation properties of Al-Cr-N films were compared with a Ti-Al-N film by the thermogravimetric-differential thermal analysis (TG- DTA) method.

Results and Discussion

Figure1 shows the XRD patterns of Al-Cr-N films after oxidation at 800 □ and 1000 □ for 60 min. The crystal structure of Al-Cr-N films was B1 (NaCl) type in the range up to 50 at% of aluminum and B4 (Wurtzite) type over 75 at% of aluminum. Any oxide crystals were not detected on the films(Type A, B and C) heated at 800□for 60 min in air. The crystal structure of Al-Cr-N films heated at 800□ is almost the same as that of at room temperature.
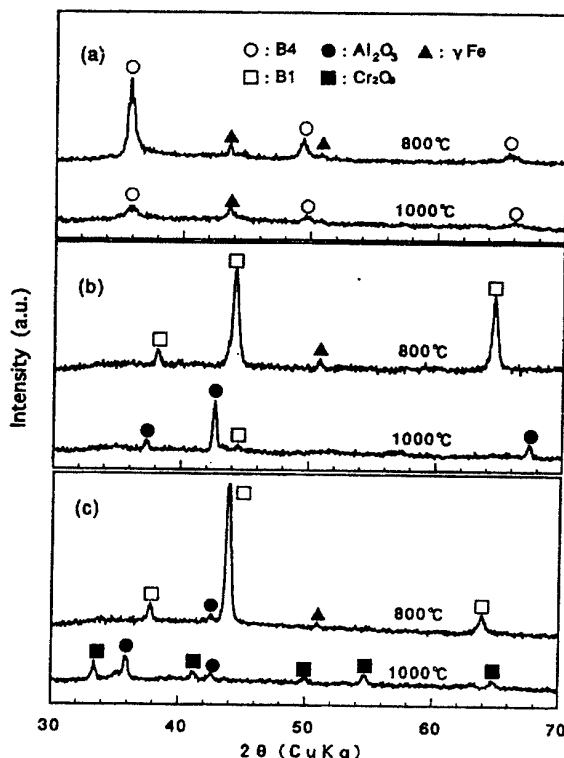
Figure 1   X-ray diffraction patterns of Al-Cr-N films heated at 800□ and 1000□ for 60 min followed by air cooling. (a); Type A, (b); Type B, (c); Type C.

172

The Al-Cr-N films (Type A) quenched from 1000□ (Fig. 1(a)) didn't form the crystal structure of oxides. The diffraction pattern (Fig. 1(b)) observed in Al-Cr-N films (Type B) at 1000□ showed strong crystallized peaks of Al_2O_3. And the Al-Cr-N films (Type C) at 1000 □formed the weak crystallized Al_2O_3 and Cr_2O_3.

Figure 2 shows the depth profiles of AES analysis for Al-Cr-N films quenched from 1000□ The distribution of aluminum, chromium and nitrogen is very uniform in the films. The composition ratio of Al and Cr of the film approximately agrees with the composition ratio of the target. Thickness of the films before oxidation was approximately 1.5□m. The protective layers of Al oxides and Cr oxides were observed on top of the Al-Cr-N films (Type A, Type B and Type C). It is found that the oxide layer thickness of Al-Cr-N film made from Type B is the thinnest of the three Al-Cr-N films.

In order to investigate the high temperature oxidation characteristics of the Al-Cr-N films, the samples were heated in air for 60 min and quenched. Exfoliation was not recognized in any film quenched from 900□ however, those quenched from 1000□ exfoliated except for the sample using Type B target. Then the films made from Type B target shows a strongest resistance against oxidation.

The TG-DTA measurements showed oxidative resistance up to 1200 °C, 1210 °C and 1260 °C for the Al-Cr-N films prepared using targets of type A, C and B respectively. These values are higher with about 200□compared to that of the Ti-Al-N films prepared also by dc reactive sputterings.

Conclusions

(1) Any oxide crystals were not detected on the Al-Cr-N films (Type A) heated at 1000□for 60min in air. The Al-Cr-N films (Type B) formed the crystallized Al_2O_3. The Al-Cr-N films (Type C) formed two-phase mixtures of crystallized Al_2O_3 and Cr_2O_3.

(2) The protective layers of Al oxides and Cr oxides were formed on top of the Al-Cr-N films (Type A, Type B and Type C) heated at 1000□for 10 min in air.
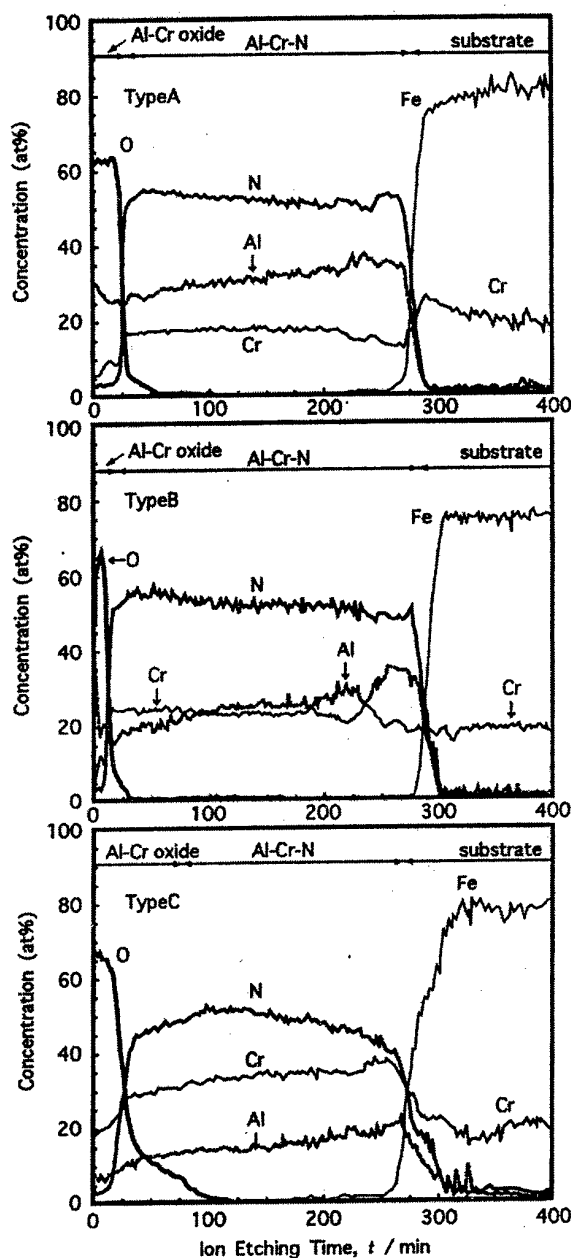
Figure 2 Auger depth profiles of the Al-Cr-N films quenched from 1000□ The samples were annealed for 10 min in air.

(3) The oxidative resistance of the Al-Cr-N films were improved by more than 200 □compared to that of the Ti-Al-N films.

References

1) Y.Ide, K.Kishitake and T.Nakamura□J. Japan Inst. Metals 63 (1999)1576-1583.

INVERSE OPTIMIZATION OF ALUMINUM INGOT COOLING PROCESS

Moultanovsky Alex, Rekada Mohammed[1]
Bergstrom Climate Systems, Inc., Rockford, Illinois, USA
[1]Quebec University of Montreal, Montréal (Québec), Canada

The thermal investigation of the studied aluminum alloy is carried out during its cooling process. Our research has shown that heat transfer between hot aluminum surface and cooling system depends upon several parameters. The most important and decisive parameters are the sprayers geometrical dimensions and the fluid-dispersing coefficient. The last one represents the ratio between the amount of pulverised cooling fluid and the temperature of the cooled surface. The experiments were conducted in the specially built test rig. Temperatures are measured for a series of tests involving several sprayers of different geometry and various dispersing coefficients. The obtained results are comparable to those of two-phase high volume boiling regime. The change from nucleating boiling regime to film boiling is observed at a mean critical temperature.

The suitable numerical algorithm of Adaptive Iterative Filter (AIF) is used for solving number of non-linear unsteady external and combined inverse Heat Transfer Problem (IHTP) that appeared during investigation. Specifically, AIF has been proposed to identify the influences of the sprayer properties on the convection heat transfer coefficient of two-phase regime during the process of intensive cooling of aluminum ingot.

The well-known method of Adaptive Iterative Filter [1] has been proposed and previously used as a mathematical and numerical instrument for identification of thermophysical and technological parameters including simultaneous identification of different thermal parameters [2 – 4], for solving IHTP [3, 5 - 7] and optimum control problems [1, 8], for thermal system simulation [1, 5, 8], etc.

As known, the inverse problems are ill-posed ones in sense of existence, uniqueness and stability and, as such, in general case they do not have a universal solution. Therefore, on the stage preceding the actual solving real inverse problem, the simulating inverse analysis should be done. This analysis, which include the solution of methodical inverse problem, are required to investigate the range of stability of the obtained results. The above simulation allows:

- To design the test plan that includes but is not limited to determination of the influence on the identification results of position and number of temperature measured devices.
- To figure out the optimal numerical algorithm of AIF that allows refinement or updating the measurement and covariance matrices to indicate reliability of the estimates.
- To optimize a weight matrix of AIF associated with each problem under study.

The proposed approach can be utilised at the aluminum manufacture facilities to optimize the properties of fluid's spray during the cooling of aluminum ingots. The method of adaptive iterative filter could be used as a powerful method for solving the similar inverse problems as well as problems for porous materials and cooling electronic systems.

1. Matsevity, Yury M. and Moultanovsky, Alexander V. (1988). Solution of Parameters' Optimization and Control Problems in Thermal Systems by Means of Local Adaptive Filter. In: *Mathematical Research, Systems, Analysis and Simulation*, Vol. 2, Academie-Verlag, Berlin, Germany, pp. 175-178.

2. Moultanovsky, Alexander. V. (1994). A comprehensive method of adaptive filter for solution multiparameter inverse problems, Proceeding of *the Sixth Annual on Inverse Problems in Engineering Seminar*, University of Cincinnati, Cincinnati.

3. Moultanovsky Alexander V. (1996). Identification of boundary conditions & thermophysical characteristics during the rolled stock thermal hardening process for the purposes of determination of rolled sheets thermal hardening zones, Proceeding of the *2nd International Conference on Inverse Problems in Engineering: Theory and Practice*, Le Croisic, France, Published in behalf of Engineering Foundation, The

American Society of Mechanical Engineering, New York, 1996, 481-489.

4. Moultanovsky, Alexander V., Rekada, Mohammed. (2002). Inverse Heat conduction Problem Approach to Identify The Thermal Characteristics of Super-Hard Synthetic Materials, *Inverse Problems in Engineering,* Vol. 10, No. 1, Taylor & Francis Group Ltd., pp. 19-41.

5. Matsevity, Yury. M., Moultanovsky, Alexander V., Timchenko, Victoria. (1992). Modelling of Thermal Processes and Identification of Local Heat-Transfer Parameters with the Help of an Adaptive Iterative Filter. *High Temperature*, Vol. 30, No1, Consultants Bureau, New York, USA, pp. 71-78.

6. Moultanovsky, Alexander. V., Khawaja, Aamir. (1997). Inverse Heat Transfer Calculation for Automotive Evaporator Design, Proceeding of the *32nd National Heat Transfer Conference*, HTD-340, 2, The American Society of Mechanical Engineering, New York, USA, pp. 33-39.

7. Moultanovsky, Alexander V., (2002). Mobile HVAC System Evaporator Optimization and Cooling Capacity Estimation by Means of Inverse Problem Solution, *Inverse Problems in Engineering,* Vol. 10, No. 1, Taylor & Francis Group Ltd., pp. 1-18.

8. Moultanovsky, Alexander V. (1999). Optimum Control problems Solution by Means of Inverse Method of Adaptive Iterative Filter, Proceeding of the *3rd International Conference on Inverse Problems in Engineering*, The American Society of Mechanical Engineering, Port Ludlow, WA, USA.

EFFECTIVE LONG-LIFE EMITTER SHELLS FOR THE THERMIONIC ENERGY CONVERTERS

Dekhtyar O.I., Kobyakov V.P.[1]
Kurdyumov Institute for Metal Physics, NAS of Ukraine, Kiev, Ukraine
[1]Institute of Structural Macrokinetics and Materials Science, Russian AS, Chernogolovka, Moscow, Russia

Great promise of the employment of termionic nuclear energy units (TNEU) for power service of space stations makes the problems of guarantee of their effectiveness and long-life to be extremely actual. These problems equally concern with other wide field of potential application of termionic energy converters (TEC) such as utilization of irreversibly lost heat by heat electrical power stations and by metallurgical industry .Decision of such problems is to a considerable extent determined by achievement of suitable values of characteristics of TEC basic units namely of the tube electrodes and in the first of the emitters. Emitter shells serve in extreme conditions (temperature up to 2100 K and internal stresses about 10 MPA). Apart, they are in the conditions of reactor irradiation with nuclear fuel in and cesium plasma out the tube. Since interelectrode gap (IEG) in TEC is a small part of millimeter the questions of high shape-stability (extremely low high temperature creep rate) of emitter shell are of the fundamental importance. Besides, the shell material should be the effective diffusion enclosure relatively to neutron fuel and its decay resultants in IEG. Mentioned requirements are related to emitter material as construction material. On the other hand not less strong requirements have been made to this material as to functional one. The main of them is the extremely high emission-adsorption behavior at temperatures higher than 2000 K to ensure the required level of output electric power.

Carried out during the last half of left century of study uniquely have determined tungsten, as the basic emitter material of TEC. In former USSR was made selection for the benefit of tungsten in a single-crystal state, the methods of deriving of crystallographic oriented tungsten tubes were elaborated. From the point of view of usage of such materials in modern TEC with the easily ionizable component of cesium in an IEG, the maximal interest was introduced with the most highly-packed plane of tungsten (110). This plane ensures a maximum high scale of coating of a tungsten surface at a high temperature adsorption of cesium, i.e. plays a defining role in formation in working TEC of the effective metal-film cathode W-Cs, generated current, supplying high output power.

Today developers of termionic TEC use single-crystal tungsten tubes with a cylindrical lateral surface and with axial orientation <111>. At such orientation 6 poles with most favorable orientation <110> go out on a cylinder surface. The plane of single-crystal tungsten with indexes (110) has maximal for tungsten a work function 5.3 eV and maximal adsorption capacity. However polyside tubes at its best have a work function 5.0 эB. Such tubes are made on capacity vapor deposition (CVD) "chloride" technology by epitaxial precipitation of tungsten on molybdenum undercoat with the applicable orientation. By the published data obtained on the experimental prototypes, the output power such TEC does not reach 8 W/cm^2. The creep rate of a material of such tubes is not lower 10^{-9} s^{-1}, i.e. the period of their reliable exploitation does not exceed 2 years.

In the given paper the technologies are esteemed permitting it is essential to augment both work function, and high temperature strain resistance of single-crystal tungsten tubes. First of all, there is a creation of tubular electrodes with monoside (110) cylinder surface. It means, that in any point of a lateral surface of a tube the orientation practically does not differ or differs from (110) plane orientation very little.

In this point of view two concepts of monoside tubes are esteemed. One of them is the logical progressing of CVD technologies of polyside tubes. In this case tungsten is epitaxially deposited on a cylindrical molybdenum undercoat with axial orientation <111> up to self facing a settling by crystal planes. Adsorption-kinetic conditions of epitaxy are selected by such, that facing originated by plains (110). In the total the single-crystal tube receives with a cylindrical internal surface, faced outside by six planes (110). It is reached in that case, when in a gas phase of process enter the

oxygen component shifting adsorption dynamics on a surface of rising planes in such a manner that the plane (110) becomes slowly rising and, in the end, habit forming. Thus has appeared, that the part of oxygen remains in a crystal, forming solid quasi-solution in tungsten with concentration up to 10^{-2} wt %. This circumstance by a cardinal image influences emission characteristics of such "oxygenated" tungsten. The completely unexpected temperature dependence of a work function was obtained and the high values of this performance for hexagon-side tubes (up to 5.8 эВ) are reached anomalously. Usage of such tubes (turn on the cylinder) as emitters of experimental TEC has allowed even in this case to increase a level of output electric power up to 25 W/cм^2. In the long term, the high level of output characteristics can be elaborated much less "porous" and more effective from the point of view of power and mass-dimensional parameters.

However this new concept has not given anything new in the field of a heightening shape-stability of emitter shells, since the high temperature creep of a material of shells has remained practically at a former level.

Other concept of monoside tungsten tubes differs by the principally new approach to know-how of their forming. This approach was proposed by Kononenko and his colleagues and was carried to a state of pilot production. The essence here is encompassing by usage of technological reception, known in multi-tonnage tube production, helical twisting of steel pipe blanks with their consequent welding on a helical junction. In this case single-crystal (110) tungsten bars were twisted and welded. Twisting was effected at high temperature on a special tube mandrel of necessary diameter. The welding of a helical joint was carried out by an electron beam.

The internal essence of happening is that at particular technological conditions of hot twisting and annealing in a material the strengthening dislocation substructure representing a homogeneous net of close located subboundaries of one sign, composed predominantly from edge dislocations also of one sign will be formed. Such dislocation distribution with total density up to 10^{-2} cm^{-2} ensures a considerable angle of integral misorientation of substructure (δ), with which one

the creep rate ($\dot{\varepsilon}$) correlates: $\dot{\varepsilon} \propto \delta^{-2}$. Enough homogeneous on a bulk the distribution of subboundaries prevents the appearance of long-range fields of elastic stresses and consequently allows to avoid recrystallization of a material during its heating up to working temperature. In result the steady state creep rate of emitter shells from such material at temperature 2073 K and internal stress 10 MPa reaches record low values 10^{-12}-10^{-11} s^{-1}. Thus, the substructure-strengthened tungsten single-crystal obtained on "deformation" know-how, in conditions of high temperature creep becomes a unsurpassed constructional material. The indicated level of creep ensures rather long-life shape-stability of emitter shells in service conditions, that eliminates this performance from a list of probable reasons confining durability of TNEU.

However if to judge under the preliminary items of information, this new concept and this new material do not give anything new in a functional sense with reference to its usage in an emitter unit of TEC. The work function of an emitter shell of this material is 5.0 eV, that is instituted by high density of defects of the latter. The truth, is necessary to be stipulated, that in this case high and correctly organized defects' density of tungsten will be doubtless to be tracked by a heightening of its high temperature adsorptive capacity. On these reasons, the final deductions can be made only after trials of experimental TEC with emitters from monoside tungsten obtained on "deformation" technology.

In any case, from the reported results the deduction about perspective of the alternative combining both reviewed concepts arises. There is two-layer a monoside emitter shell, in which one the substructure strengthened tube obtained on "deformation" know-how, serves a undercoat for epitaxial precipitation on CVD technology of a layer of oxygenated tungsten. Thus it will be possible to aggregate in one article record levels both functional and constructional materials. Such unite are harboring miscellaneous capabilities. For example, as a strengthening undercoat it is possible to take monoside molybdenum tube, the substructure by which one will be inherited by an epitaxial tungsten undercoat, and then this undercoat to eliminate. The alternative versions are possible also.

INVESTIGATION OF MULTILAYER THERMAL PROTECTION STRUSTURES FOR REDUCING THEIR EFFECTIVE HEAT CONDUCTIVITY

Kuryachii A.P., Paderin L.Ya.
Central Aero-Hydrodynamic Institute, named N. E. Zhukovsky, Zhukovsky, Russia

The problems of thermal protection and thermal control of constructions exist in various branches of engineering and industry (aerospace, power engineering, metallurgy, ceramic industry). At present time there are many methods thermal protection and corresponding structures. In the most degree this direction of investigations is developed in aerospace engineering [1, 2, 3]. Selection of method and creating of thermal protection structure depend on operating conditions of protecting object, first of all, values and difference of environment and object temperatures, gas media composition and pressure, geometric, weight, firmness of thermal protection structure, physical-chemical compatibility of using materials in surmising temperatures and gaseous media.

In present work the thermal protection structures intended for numerous missions and long time exploitation constructions are considered. In this case the passive methods of thermal protection are preferable. Realization of these methods do not demand heat exchangers, ablative and sublimation materials, physical-chemical, in that number phase transformations, mass - change and other processes with heat absorption. By present time the known passive thermal protection systems are monostructures of two types. The structures of the first type are manufactured of thermal insulation materials of specific thickness, which depends on heat load and is selected on the basic of calculations or experiments. In particular, such approach was used in high temperature thermal protection systems of "Space Shuttle", "Buran" and other aerospace vehicles as well as various high temperature furnaces. The similar approach isused for thermal protection of constructions operating at low temperatures down to cryogenic temperatures. Further progress of this thermal protection systems type is provided, in the main, by means of creating the new rigid and flexible materials with improved thermophysical properties. Other type of effective passive thermal protection structures is a set of parallel high reflective screens, which are used in vacuum

conditions. These structures (multiscreen vacuum insulation) widely applied in thermal control systems of space vehicles as well as in cryogenic engineering at relatively low temperatures (T<500K). At that the screens are manufactured of polymeric films with metallic coatings. Furthermore similar structures are used at high temperature in electric thermic vacuum furnace. In this cases the screens are manufactured of high temperature metal (molybdenum, tungsten, tantalum) and applied at temperature T>2000K.

In proposed report the following investigations will be presented:

1) The numerical-experimental method for studying heat transfer in multiscreen thermal protection structures. Experimental part contains the test of a model, consisting of three screens, irradiated by the known radiant flux. The test results include the determination radiant characteristics and temperatures screens. Mathematical model and numerical alghoritm permit on the basic of above experimental data to evaluate the heat transfer and thermal resistance of multiscreen structures, consisting of arbitrary number screens. The investigation of series of multiscreen structures were performed.

2) The method and facility for experimental studying effective thermal conductivity of insulation materials, mono- and multilayer structures, consisting of various materials as well as the transient thermal regimes of above objectswere developed. The facility permits to carried out the investigation in temperature range T=500-2000K and gas pressure $P=10^0$-10^5 Pa. By present time the experimental data were obtained for many porous insulation materials.

3) The method for comparative analysis of heat resistance of above types thermal protection structures is developed. The numerical comparison for the known insulation materials and multiscreen systems were carried out. Calculation results obtained for known modern and advanced screen materials and thermal insulation materials and reflective coatings as well as porous insulation materials permit to determined the temperature ranges preferable in

dependence on operating conditions for using either multiscreen systems (T<1000K) or porous insulation materials (T>1500K).

4) On the basic result obtained it is proposed combined thermal protection structures consisting of two substructures, set successively relatively temperature gradient in structure. The first and second substructures are manufactured of high temperature porous material and high reflective screens accordingly. Calculation results demonstrate using multiscreen substructure in low temperature zone of structure provides the significant increasing a thermal resistance of one These approach permit to optimize the thermal protection structures destined for application at high maximum temperatures (T > 1500K) and large-scale difference (ΔT > 1000K) due to reducing thickness and weight of ones in comparison with porous insulation monostructure.

References

1) Yu.V. Polezhaev. Teplovaya Zashita
2) L.J.Korb, et al, The Shuttle Orbiter Thermal Protection System. Ceramic Bulletin, 1981, v. 60, N11, pp1181-1193.
3) D.L. Rasky, Thermal Protection System for Future Reusable Launch Vehicle. SAE Technical Paper N 951618, 1995.

ABOUT THE MECHANISM OF METALS'HARDENING AT EXPLOSIVE ALLOYING

Sitalo V.G., Usherenko S.M.[1], Gubenko S.I.[2], Bunchuk J.P.
Yuzhnoye state design office, Dnepropetrovsk, Ukraine
[1]Institute of pulse processes, Minks, Byelorussia
[2]National metallurgical academy of Ukraine, Dnepropetrovsk, Ukraine

The method of volumetric alloying of metal materials is carried out at deep penetration of disperse particles (inclusions) as a result of explosive influence. Disperse particles dispersed by energy of explosion punch a target as a result of overcoming forces of intermolecular links, raising before themselves shock-plastic waves and moving area of a high pressure that results in formation of a zone of strongly disordered condition of a matrix. For a way of movement of a particle the channel is formed separating it from a matrix and creating an own field of stresses. Channels are partially collapsed. The particle may be in the channel, but its mechanical coupling with a matrix is also possible then the new phase boundary on type welding by explosion is formed and a stress field from a particle is created which character is determined by discrepancy of radiuses of a particle and the channel, constrained by strain of a matrix and an inclusion.

Structural changes of character near to channels (channel zones) and near to braked particles at materials with different type of a lattice (Armco-iron, steel E3 and 08X18N10T, Mo, Ti) are revealed which allowed establishing the mechanism of hardening at explosive alloying. The thin layer of a matrix, adjoining to walls of channels, undergoes amorphization and superficial saturation by elements of particles. Character of relaxation processes testifies that the local high-speed deformation takes place which has resulted in formation of complex dissipative structures – fragmented, cellular, crossed dispositions along trajectories of movement of particles on which background zones of the located deformation were allocated, the curved doubles, large-scale heterogeneity crystallographic orientations of ε-martensite, packages of defects of the packing, the split borders and dispositions.

Martensitic transformation caused by explosive influence, has strongly pronounced crystallographic selectivity. Explosive kinetic of transformations results in formation of the certain ensembles flat martensitic crystals. According to the wave theory of martensitic transformations, origin and growth of ε-martensite crystals is accompanied by energy liberation and its part at origin of ε-martensite goes on excitation of displacement waves which at a stage of crystals' growth are stabilized due to energy of transformation and providing the deformation necessary for overcoming of a barrier, dividing γ- and ε-conditions. The lamellar form of ε-martensite crystals is connected to the two-wave concept of managerial process by their growth according to which loss of stability γ-conditions is connected to area of imposing of two managing waves of displacement as pulses with the flat fronts, made of quasi-longitudinal flat waves. The heterogeneous nature of origin of ε-martensite on dispositions and defects of packing is compatible to a wave picture of growth of martensite crystals, and process of their formation elastic field of the dislocation origin centre is influenced.

Near to channels, channel zones and particles non-equilibrium structures with high charging density of dispositions and extensive far-ranging stresses are formed. Distinction in character of relaxation processes is caused by type of lattice of a matrix and equal energy of stacking fault.

To features of the titan structure after processing it is necessary to relate folded and circular configurations which are found out in all structural zones. At explosive influence concentration of point defects, in particular, vacancies sharply grows that cause a lot of structural effects: gradients of concentration of vacancies change effective factors of diffusion and self-diffusion which essentially grow; when concentration of vacancies becomes non-equilibrium, their redistribution occurs, a leaving to dispositions and other drains, in result crawling and growth of regional occurs in a diffusion field, dispositions become unstable and may change the form. At buckling of dispositions aside their movements the gradient of a field of vacancies grows that results

in increase of a stream of vacancies at a dislocation center and its further buckling; the vacancy structure becomes unstable and breaks up, that results in formation point defects' clusters, collapsing of vacancy disks occurs, and dislocation loops in the size 100-300 Å are formed. It is necessary to note, that in the titan it is not revealed coordination of concentration of these dislocation loops with the general density of dispositions on structural zones.

Moving particles, affecting resistance on the part of a matrix, reduce the speed, broken and stopped. In places of their braking arise the far-ranging fields of stress inducing relaxation processes which have obviously wave nature. Shock waves raise pulses of impact. Stress waves generated by these processes, being imposed, and form superposition of pulses. Relaxation processes near to particles are carried out by consecutive dumps of stresses as a result of emission from borders a particle – matrix of defects (dispositions and disclination). Relaxation shifts owing to non-isotopic of transmitting streams inevitably derivate a field of the rotary moments working on a particle and an adjoining zone of a matrix. High-frequency fluctuations of particles and grains of a matrix serve in shock waves the reason of occurrence of turbulent plastic current. Streams of the defects proceeding from particles, form new sources of power fields.

Presence stress fields close to broken particles testifies to occurrence spidery extinction contours of wave type which character testifies about them elastoplastic origin. In all cases these fields are shielded by a field of the dispositions arising around of particles. Extinction contours have arisen as a result of localization of whirl deformation in a place of braking of particles. This fixed condition of the plastic deformation proceeding at impact with very high speed and resulting in occurrence of strong stress fields of elastoplastic character around of particles.

Process of hardening of metal materials at explosive alloying is multiple-factor and agrees an additive principle includes making explosive hardenings, reinforcing by channels or channel zones, amorphization, micro-alloying at particles dissociation, dispersive hardening by particles, deformation hardening and far-ranging fields:

$$\sigma = \sigma_{exp} + \sigma_{rein} + \sigma_{amor} + \sigma_{alloy} + \sigma_{disp} + \sigma_{def} + \sigma_{far\text{-}r}$$

On the basis of the carried out researches the way of hardening of surfaces of the products is offered, including cyclic influence on a surface by high-speed jets of working substance. The group of technologies is developed and tested and experimental batches of various products with the increased operational stability are manufactured.

OBTAINING OF α-Si$_3$N$_4$ – BASED COMPOSITE UNDER COMBUSTION MODE

Borovinskaya I.P., Zakorzhevsky V.V.
Institute of Structural Macrokinetics and Materials Sciences Problems, Chernogolovka, Russia

Introduction

Silicon nitride is widely used as a material for producing structural ceramics characterized by high strength, hardness, and crack resistance. The items produced from the material can successfully work under a wide range of temperatures (up to 1400°C), they are stable to acids, alkalis, melted salts and metals.

Creation of composite materials based on α-Si$_3$N$_4$ allowed us to improve the properties of silicon nitride ceramics. The best results were obtained in the case of Si$_3$N$_4$-SiC composite, in which silicon carbide can exist as fibers or nanoparticles. Conventionally, such materials are obtained by thorough mixing of preliminarily synthesized initial components in a liquid medium with the following drying and dispersing of the mixtures obtained. The paper describes some synthesis peculiarities and properties of composite materials based on Si$_3$N$_4$ and obtained under the combustion mode.

Experiment

The synthesis was carried out in an SHS reactor of 30 l capacity. The combustion temperature was determined by thermocouples WRe5/WRe20. The specific surface area was established by the BET method according to nitrogen adsorption. Particle morphology was studied by means of SEM JEOL-733.

Results and Discussion

It was possible to obtain silicon nitride with α-phase content being 95 mass % by the SHS method only by introducing some gasifying agents [1] into the green mixture composition and organizing a special heat regime of the synthesis process [2]. Synthesis of α-Si$_3$N$_4$ with salts allows regulating a temperature mode of the synthesis and phase composition of silicon nitride (Fig. 1).
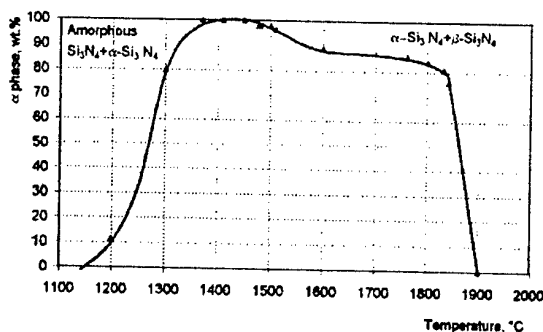
Fig. 1. Silicon nitride phase composition as a function of synthesis temperature.

Carbon introduction into the green mixture of α-Si$_3$N$_4$ allows synthesizing α-Si$_3$N$_4$ -β-SiC. Silicon carbide content can be varied from 0 up to 85 mass %. Two parallel reactions are carried out during the synthesis:

$$3Si + 2N_2 = Si_3N_4;$$
$$Si + C = SiC.$$
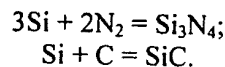
Predominance of this or that direction of the synthesis is regulated by the combustion temperature and possible nitrogen filtration to the combustion front. Also, duration of the process is of great importance.

Fig. 2 shows the morphology of α-Si$_3$N$_4$ -β-SiC powders obtained under various modes of synthesis. The silicon carbide content is from 25 up to 70 mass %. The specific surface area depends on the synthesis temperature and grows from 3.6 up to 20.6 m^2/g at the temperature decreasing from 1900°C to 1300°C. α-Si$_3$N$_4$ -β-SiC particles are fibrous, equiaxial or needle-shaped. It depends on the synthesis temperature and α-Si$_3$N$_4$/β-SiC phase ratio.

Analysis of chemical composition of α-Si$_3$N$_4$ -β-SiC (Table 1) synthesized at T= 1300 and 1800°C, SiC content being about 70 mass %, proved that free carbon content was 11.5 mass %. The product was gray in color. At T=1300°C the composite was light green. We observed a low content of nitrogen and free carbon. The X-ray
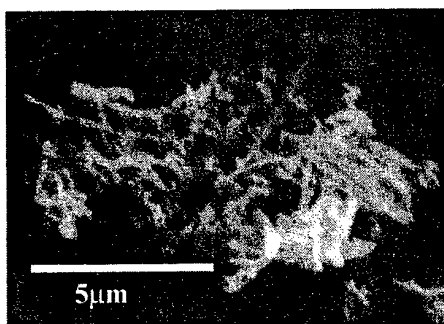
Fig. 2a. α-Si$_3$N$_4$ -β-SiC, T$_{syn.}$=1300°C, S$_{sp.}$=14.1 m^2/g, SiC - 65 mass%.
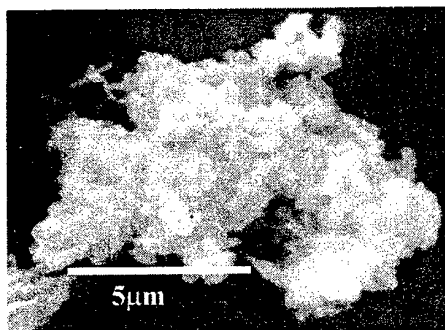
Fig. 2b. α-Si$_3$N$_4$ -β-SiC, T$_{syn.}$=1700°C, S$_{sp.}$=6.6 m^2/g, SiC - 50 mass%.
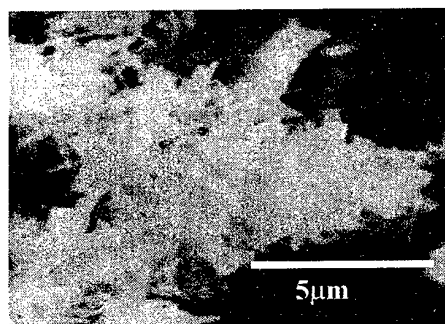
Fig. 2c. α-Si$_3$N$_4$ -β-SiC, T$_{syn.}$=1800°C, S$_{sp.}$=3.6 m^2/g, SiC - 25 mass%.

phase analysis showed only two phases: α-Si$_3$N$_4$ and β-SiC. Therefore, we can suppose that α-Si$_3$N$_4$ -β-SiC is not stoichiometric, in such case there would be an excess of carbon, about 6 %. The lattice parameter of such silicon carbide is c=4.344A, it differs greatly from the literature datum of c=4.359A. The decrease in lattice parameters favors our supposition. The product was gray in color. At T=1300°C the composite was light green. We observed a low

Superstoichiometric carbon in silicon carbide was reported in [3]. The authors pointed out two characteristic features of the phenomenon: low synthesis temperature (1200-1400°C) and existance of gas-transport reactions. We also observed these conditions in our process. Besides, a dependence of lattice parameters on a synthesis temperature was discovered (Fig. 3).
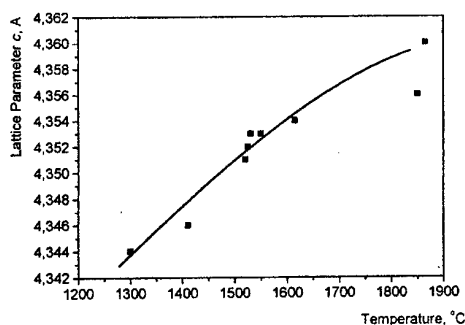
Fig. 3. Lattice parameter c of β-SiC as a function of synthesis temperature.

Conclusion

A possibility of one stage production of a composite material based on α-modification of silicon nitride and β-SiC under the combustion mode was shown. The synthesis main parameters affecting the material properties were determined.

Si-N-C material of nonstoichiometric composition was obtained by low-temperature SHS.

References

1. A.G. Merzhanov, I.P. Borovinskaya, V.M. Shkiro, L.S. Popov, N.S. Makhonin, L.V. Kustova. A production method of silicon nitride. Patent RF No. 1696385.
2. V.V. Zakorzhevsky, I.P. Borovinskaya. Some regularities of α-Si$_3$N$_4$ synthesis in a commercial SHS reactor. Int. J. SHS. vol.9, No.2, p.171-191 (2000).
3. N.F. Gadzyra, G.G. Gnesin, A.V. Andreev, and others. On superstoichiometric carbon in silicon carbide crystals. Neorg. materialy, vol.32, No.7, 1996, p.816-820.

Table 1.

Composition, mass%	N$_2$	O$_2$	C$_{total}$	C$_{free}$	Si$_{free}$
T=1300°C	20.3	2.5	16.9	0.7	1.1
T=1800°C	32.1	0.7	13.5	11.5	0.08

PECULIARITIES OF ACTIVATED SINTERING OF BORON NITRIDE BASED MATERIALS

Dubovik T.V., **Rogozinskaya A.A.**, **Itsenko A.I.**, **Panashenko V.M.**, **Morozov I.A.**,[*]
Morozova R.A.
Institute for Problems of Material Science of NAS Ukraine

INTRODUCTION

Boron nitride (BN) is nonmetal refractory compound which crystallizes in ordinary conditions like a graphite and has the hexagonal lattice with periods of a=2.504 A, c=6.661 A, c/a=2.66. Such structure is characterized by heterodesmic of "boron-nitrogen" chemical bonds due to strong covalent interaction within one monolayer and weak van-der-vaaltz one between layers [1].

The features of boron nitride structure determine on the one hand is critical properties: stability upon thermal shock, high electrical resistance, dielectric stability in wide frequency range, chemical inert relative to metallic and alloy melts, and on another hand hinder the possibility of sintering compact isotropic material.

THE RESULTS AND DISCUSSION

In powder materials the great part of the particles surface is passivated by the atoms of adsorbed impurities which hamper the sintering. The effective means to remove the adsorbed impurities from powder surface and to effect their structure is hydrogen-thermal treatment of powder over catalysts at temperatures in the range of 900-1200 °C. Such treatment allows to get the purified powders with improved structure which in turn makes it possible to design the materials with definite physics-chemical properties [2].

The goal of this work is to study the influence of hydrogen-thermal treatment of BN powder on the properties of compact BN based materials.

The hydrogen-thermal treatment of this powder was carried out in the hydrogen ambient at temperatures of 900 °C and 1100 °C during 1, 2 and 3 h at each temperature. Chemical composition of BN powders before and after treatment is listed in table 1.

It is evident from table 1 that the quantity of B_2O_3 and C impurities decreases and of nitrogen increases in treated BN powders. At the same time the increase in the temperature and duration of treatment results in

more efficiency of treatment . The powder BN treated at temperature 1100 °C for 2 h was used later on. Crystal lattice parameters of treated BN are identical to literature data [1].

Table 1. Variation of BN powder chemical composition with treatment conditions in hydrogen environment

Treatment		Content, mas%			
°C	hour	B	N	B_2O_3	C
Initial	-	42,1	54,4	2.0	1,4
900	1	42,9	55,2	0,2	-
900	2	43,0	55,7	0,1	-
900	3	43,0	55,5	0,1	-
1100	1	43,3	56,0	-	-
1100	2	43,5	56,3	-	-
1100	3	43,5	56,2	-	-

The samples for laboratory examination of precursor powder and of hydrogen treated one were manufactured by hot pressing at temperatures 1600-2000 °C (in each 100 °C), pressure 30 MPa for 1-10 min (in each 1 min) exposure at maximum temperature.

Experimental data show that the character of density variation of initial and treated BN powders in hot pressing is mostly the same: the samples density quickly increases for 1-5 min then asymptotically approaches its maximum value at given temperature. The lower temperature of hot pressing, the more difference between initial and final density of sample and the more time is necessary to reach the maximum density. The treatment time interval, above which the density does not increase, corresponds to each pressing temperature. This behaviour could be explained from the point of view of the theory of bulky-tough yielding of porous material created by M.Kovaltchenko [3].

---

[*] *imorozov@materials.kiev.ua* (for Dubovik)

The findings show that only samples of hydrogen treated BN powders can have density close to theoretical one. This is because of considerable increase in reactive surface of BN due to refining of powder from surface impurities. Being the very active reagent the hydrogen removes oxides and other impurities from the powder surface and forms the volatile compounds with these impurities.

The strength characteristics of boron nitride before and after refining have been studied (table 2). The obtained data show that the preliminary hydrogen-thermal treatment results in an increase in the mechanical strength of material by 2-2.2 times.

Table 2. Comparative strength characteristics of hot pressed BN samples at different temperatures (pressure resistance time 10 min).

Hot pressing temperature, °C	Compression strength, MPa	
	Initial BN	Treated BN
1600	12	27
1800	15	41
2000	23	47

The pressing of samples of initial and treated BN powders followed by sintering has been studied. The samples were pressed at pressure 2 tone/cm and sintered in nitrogen ambient at temperature of 1900 °C (1 h). The results are listed in table 3.

Table 3. Properties of sintered samples of boron nitride

BN	Properties		
	Relative density	Compression strength, MPa	Resistance, Ohm·cm
Initial	0.6	4.8	10^{11}
Treated at 1100°C, 2h	0.8	10.3	10^{18}

Data of table 3 show the hydrogen-thermal treatment to increase the density, strength and electroinsulating properties of boron nitride.

The effect of hydrogen treated BN powder on the properties of base on it the composite material - boron carbonitride (BNC) - has been investigated. The samples were manufactured by the above mentioned pressing and sintering regimes for BN. The data are listed in table 4.

Crystal structure of this BNC consists of two phases - BN and B_4C - with lattice periods: a_{BN}=2.504 A, c_{BN}=6.675 A; a_{B4C}=5.610 A, c_{B4C}=12.120 A.

Table 4. Properties of the sintered boron carbonitride (BNC).

Property	Temp., °C	BNC based on:	
		initial BN	treated BN
Resistance, Ohm cm	20	$>10^{13}$	$>10^{13}$
	1000	$1,5·10^7$	$1,6·10^9$
	1800	$2·10^4$	$1·10^6$
Coefficient, of thermal expansion, degree^{-1}	200-1800	$4,6\ 10^{-6}$	$3,0·10^{-6}$
Compression strength, MPa	207	15,9	29,8

It is evident from table 4 that hydrogen-thermal processing of initial BN increases physical and mechanical properties of boron carbonitride. On the base of such boron carbonitride it was developed the device for temperature measuring of metal melts [4]. Refractory entrance bushing made of boron carbonitride permits to execute continuous temperature measuring during entire melting process of steel #45 in crucible furnace (2 h).

CONCLUSION

The investigations revealed the perspective of using the method of hydrogen-thermal treatment of initial powders for activation of densification processes of BN and materials on its base. Further investigations in this field have to be carried out.

REFERENCES

1. Kosolapova TJa, Andreyeva TV, Bartnitskaya TS et al. Non-metal refractory compounds. - Moscow: Publishing House «Metallurgiya». - 1985. - 224 p.
2. Trefilov VI, Morozov IA, Morozova RA et al. Effect of Hydrogen on improving purity of WC and AIN Powders. Int J Hydrogen Energy 1996;21(11-12):1097-1099.
3. Kovaltchenko MS. Theoretical bases of hot treatment of the porous materials with pressure. - Kiev: Publishing House «Naukova dumka». - 1980. - 240 p.
4. Pat. 33418 A Ukraine, MPI⁶ G 01 K 7/02. Device for melts temperature measuring / Itsenko AI, Dubovik TV, Morozov IA, Morozova RA. N 99020989 15.02.2001, Bull. N 1.

REFRACTORY CARBIDES GALVANIC COATINGS DEPOSITION ON DIAMOND SURFACE FROM IONIC MELTS

Novoselova I.A., Gab A.I.
V.I. Vernadskii Institute of General and Inorganic Chemistry, NAS of Ukraine, Kiev, UKRAINE

Abrasive tool efficiency can be significantly improved by its production technology development. One way to increase efficiency of such tools usage consists in diamond grains metallization by refractory metals carbides. New method of direct electrochemical diamond metallization suggested by us has a number of advantages over common methods including the following possibilities:

1) to coat superhard materials grinding powders fine grains;

2) to deposit coatings of fixed composition;

3) to simplify metallization procedure (no need in special protecting atmosphere and in conducting precoat deposition).

The possibility of diamond using as conducting cathode material and of refractory metals carbides synthesis at diamond grains surface during simultaneous reactions of refractory metal and carbon electrodeposition was shown in [1, 2]. Appearance of surface conductivity of diamond being in contact with complex melts based on alkali metals molybdates, tungstates and carbonates was determined. This phenomenon is caused by redox reactions appearance at diamond surface. Sodium molybdate, dimolybdate, tungstate, ditungstate, and carbonate being a part of Mo and W deposition electrolytes can simultaneously be a source of refractory metals and of carbon during respective carbides coatings deposition on diamond surface.

Diamond powders AS15 (315/250) and ASS (630/500) widely used for diamond abrasive tools production were used for coatings deposition. Nickel net container filled by diamond powder and immersed into the melt with the help of nickel wire was used as cathode. W or Mo rod was used as anode. Molten electrolyte was contained in glassy carbon or graphite crucible.

Oxide system $Na_2WO_4 - WO_3$ was chosen for tungsten containing coatings deposition on diamond surface. It was established that optimal conditions for continuous coatings deposition are the following: WO_3 content 0.02-0.2 % (mass); T = 1123-1173K; i_k = 0.03-0.1 A/cm²; τ = 60-

90 min. In these conditions coatings of W_2C-WC (1:1) composition were deposited.

For molybdenum carbide coatings deposition on diamond surface the system $Na_2WO_4 - MoO_3$ (4 mol. %) was used. Metallization degree dependence on cathode current density and electrolysis duration for AS15 diamonds of different fineness was shown on Fig. 1. It should be noted that under the same electrolysis conditions diamond metallization degree and coating deposition rate are increasing with diamond grains dimensions decrease. Thus, metallization degree Δm was 10% for diamonds AS15 (315/250) and 25% for AS15 (160/125) (T = 1123K; τ = 50 min; i_k = 0.05 A/cm²). Coating deposition rates were 0.58 and 0.97 μm/h, respectively. Optimal conditions for coatings deposition from this system are the following: τ = 90 min; i_k = 0.05-0.1 A/cm².
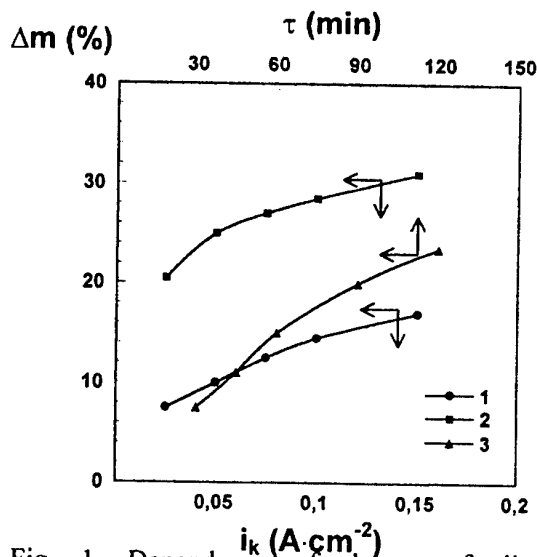
Fig. 1. Dependence of degree of diamond metallization by Mo_2C on cathode current density for AS15 (315/250) (1) and AS15 (160/125) (2), and on electrolysis duration for AS15 (315/250) (3) in the following system: Na_2WO_4-4mol%MoO_3 T = 1173.

In order to diminish electrolyte consumption we decrease MoO_3 content to 2.5 mol. %. Using this system for AS15 (315/250) and ASS (630/500) diamonds metallization there is also lower

metallization degrees for larger and less defective diamonds. Metallization degree was 8 and 5%, and deposited coatings thickness was 0.5 and 0.4 µm for AS15 (315/250) and ASS (630/500) diamonds, respectively. Also, using this system at optimal conditions (T = 1173K; τ = 90 min; i_k = 0.08-0.12 A/cm^2) we succeeded in coating type I natural diamond with molybdenum carbide (coating thickness was 1 µm).

With the purpose of electrolyte price reduction we turn to the following dilute chloride-tungstate(molybdate)-metaphosphate systems: NaCl-KCl – Na$_2$WO$_4$ (6 mol. %) – NaPO$_3$ (0.4 mol. %), and NaCl-KCl – Na$_2$MoO$_4$ (5 mol. %) – NaPO$_3$ (0.75 mol. %). Optimal electrolysis conditions (T = 1023-1073K; τ = 60 min; i_k = 7-10·10^{-3} A/cm^2) were established for these systems, as it follows from Fig. 2. Thickness of coatings deposited on AS15 (315/250) diamonds in systems (1) and (2) was 0.40 and 0.46 µm, respectively. Also, use of these systems allows us to lower electrolysis temperature and current density, and therefore, power consumption.
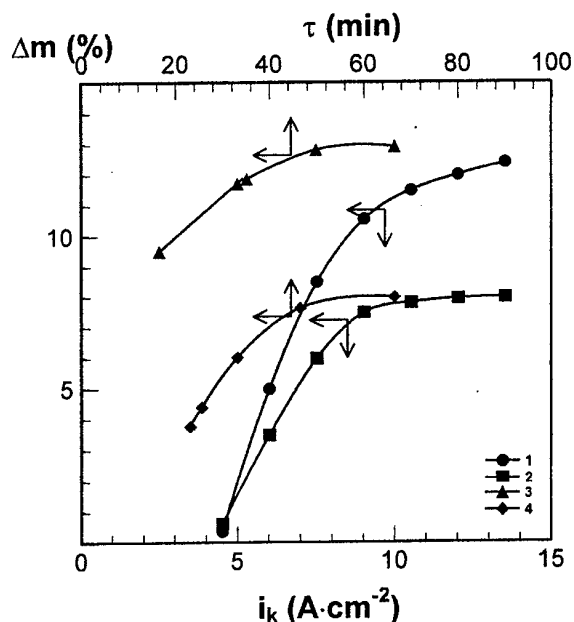
Fig. 2 Dependence of diamond AS 15 (315/250) metallization degree by Mo$_2$C (1,3) and W$_2$C (2,4) from systems NaCl-KCl – Na$_2$MoO$_4$ (5 mol. %) – NaPO$_3$ (0.75 mol. %) and NaCl-KCl – Na$_2$WO$_4$ (6 mol. %) – NaPO$_3$ (0.4 mol. %), respectively on cathode current density (3,4) and electrolysis duration (1,2). T=1123 K

Molybdenum and tungsten carbides coatings form some kind of shell on diamond grains. It brings

about loading redistribution between different sides with differing characteristics, and makes them more durable for different loading types. Thus, after molybdenum and tungsten carbides coatings deposition on the surface of AS15 (160/125) diamonds its rupture loading coefficient measured by «Tornado» apparatus at Lviv Polygraphic Institute was 1.4-2.3 times depending on electrolysis conditions. Besides, coatings deposition leads to increase of diamonds wettability by binder material, and therefore, to increase of their stability in tools structure. Capillarity, characterizing abrasive materials wettability, and being determined from water level raising height in glass tubes filled with unmodified or metallized diamonds, increases by a factor of 2.1-2.4 when diamonds are coated.

Pilot tools lots with AS15 diamonds (160/125) coated with ditungsten carbide in NaCl-Na$_2$WO$_4$-Na$_2$CO$_3$ were tested in optical glass coarse grinding operation at Poltava Factory of Artificial Diamonds and Diamond Tools. Testing reveals that polishing disks productivity increases by a factor of 1.4-1.8 after metallization.

LITERATURE

[1] Shapoval V.I., Kushov H.B., Malyshev V.V. Molybdenum carbide deposition on diamonds surface by ionic melts electrolysis // Poroshkovaya Metallurgiya. – 1986. – No. 7. – P. 43-45.

[2] Malyshev V.V., Novoselova I.A., Gab A.I., Pisanenko A.D., Shapoval V.I. High-temperature electrochemical synthesis of molybdenum carbide on dielectrics and semiconductors surface in ionic melts // Zhurn. Prikl. Khim. – 1996. – V. 69, No. 8. – P. 1314-1320.

[3] Malyshev V.V., Novoselova I.A., Shapoval V.I. Molybdenum and molybdenum coatings electrochemical deposition from ionic melts // Zhurn. Prikl. Khim. – 1996. – V. 69, No. 8. – P. 1233-1247.

[4] Baraboshkin A.N. Metals electrocrystallization from molten salts. – M.: «Nauka», 1976. – 260 p.

THE CREATION OF STABLE NANODIAMOND SUSPENSIONS IN LIQUID MEDIUMS IS THE WAY TO OBTAIN NANOCOMPOSITE MATERIALS FOR EXTREME PERFORMANCES

Voznyakovskij A.P.[(1)], **Fudjimura T.**[(2)], **Dolmatov V.Yu.**[(1)], **Veretennikova M.V.**[(1)]

[(1)]Special design bureau "Tekhnolog" at the St.Petersburg State Technological Institute (Technical University), St. Petersburg, Russia

[(2)]"VISION DEVELOPMENT CO., LTD", Tokyo, Japan

One of the perspective directions of up-to-date material-science is the creation of nanocomposites able to work in extreme performances. Particularly, the investigations on the use of detonation synthesis ultradispersed diamonds (UDD, nanodiamonds) are strongly developed [1-3].

As suspensions the UDD are used in many fields of application. UDD-suspensions in aqueous salt solutions of electrolytes are applied for electrochemical technologies (high-strong metal-diamond coatings [2]); UDD-suspensions in liquid non-aqueous mediums are useful for preparation of polymeric protective coatings and membranes with the improved complex of service properties [3]. Stabilisation of degree of dispersion of UDD and suspension structure are achieved by modification of their surface.

The present work has for an object to choose the ways of stabilisation of UDD-suspensions to use them for the creation of the nanocomposites with improved service properties.

In order to purify a surface from absorbed substances the UDD were previously warmed up to $T=420^{0}C$ at a high vacuum ($1.33*10^{-4}$ Pa).

Curve of line ion current for UDD has two extremums of desorption at $110^{0}C$ and $280°C$. As a practical matter the satisfactory purification efficiency of UDD-surface can be attained by pre-warm-up ($T=350^{0}C$) at a high vacuum for 4 hours. Such the UDD were used for the next experiments.

Features of dispersion of UDD in an aqueous medium. Polydispersivity curves of UDD-particles in water are presented on the figure. The figure data show that UDD relate to nanodispersed substances by a degree of dispersion (~ 90% of particles are over the range of 18...32 nm – curve 1). Initial type of polydispersivity curve is constant for 15 minutes subsequent to that the bigger particles begin to precipitate, and the whole curve shifts to bigger sizes direction. In order to stabilise

an initial dispersivity of UDD the suspension is withstood under ultrasonic field (US) action. It is established that the dispersivity of a system depends on insonification time (exposure to US). The polydispersivity curve shifts to bigger sizes direction (an increase in average numerical diameter from staring 23,0 up to 95,6 nm) for the first 5 minutes of US-treatment. For the next 5 minutes US-field action results in recovery of the polydispersivity curve similar to that in the initial state (the average numerical diameter of 31,2 nm – curve 3). The reached degree of dispersion remains constant under US-field action for 20 minutes. Over a long period of time of US-field action the aggregation processes resulting in the intensive precipitation of UDD are registered again.

After stopping the US-field action the dispersivity of the solution remains constant for 2 hours, subsequent to that agrregation processes begin. So, to hold the optimum dispersivity of UDD over a long period of time the recurrent (not continuous) US-treatment is necessary. At the same time it should be taken into account that for every cycle of the process (alternation of insonofication and non-insonofication) some part of UDD-particles (in our experiment it amounts to about 11 wt. %) keeps as indestructible aggregates and precipitates.
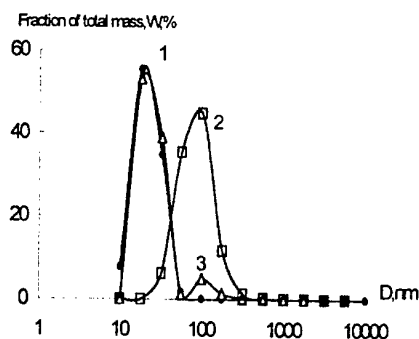
Figure. Relative distribusion of the initial UDD-particles in water without US-treatment (1-•), under US-treatment during 5 minutes (2 - □) and 10 minutes (3 - Δ).

Features of dispersion of UDD in non- aqueous mediums. Dispersion of UDD in non-polar mediums demands the corresponding modification of a surface (we modified it by means of sililization).

The surface texture are characterised by implanted trimethylsililic groups, i.e. water-repellency treatment of the surface was carried out. A degree of water-repellency treatment can be regulated by a quantity of the sililizing mixture to a certain degree, and also by a choice of chemical nature of chlorosilane in the sililizing mixture.

In the present work three variants of water-repellency treatment of UDD-surface were studied.

1. Modification was carried out by an excess quantity of sililizing mixture (sililizing agent) – equimolecular quantity of $(CH_3)_3SiCl + ((CH_3)_3Si)_2NH$ (double excess with respect to calculated quantity).

2. Modification was carried out by 50%- quantity (with respect to modification I) of sililizing mixture. Like the modification I the isolation of ammonium chloride (in a smaller quantity) was observed.

3. In some cases in order to stabilise the UDD-particles in organic non-polar mediums (for example, toluene) the insertion of double bond groups may well be useful. The insertion of such groups onto the UDD-surface was realized by means of substitution of trimethylchlorosilane in sililizing mixture by dimethylvinylchlorosilane (sililization with vinyl-group). The modification was carried out using sililizing mixture (50% from UDD-mass). The isolation of ammonium chloride confirmed the reaction passage.

UDD-samples of these three modifications were dispersed in non-polar liquid. Toluene was chosen as a medium.

Modification of the surface by trimethylsililic and dimethylvinylsililic groups allowed one to reach the dispersivity of UDD-particles over the range of 14,5 – 18 nm in non-polar organic liquid.

The conclusions:

Desorption of gases and volatile matters from UDD-surface was investigated. For the practical use the following conditions: desorption temperature - 350^0C, pressure - $\sim 10^{-4}$ Pa and treatment time - 4 hours were recommended.

The dispersivity of UDD-suspensions in aqueous medium under US-field action was investigated. The complex dependence of polydispersivity of UDD in water on time and US-treatment cyclicity is shown. The preparation of a stable UDD-suspension in water with the particle size of 18-32 nm at cyclic US-treatment is possible.

It is shown that the modification of UDD by sililizing agents appreciably changes properties of nanodiamonds. At the same time the preparation of a stable UDD-suspensions in non-aqueous mediums becomes possible. The modification of UDD by trimethyl- and dimethylvinylsililic groups allows one to reach the dispersivity of nanodiamond particles of 14,5 – 18 nm in toluene (better than that in water).

References:

1. Dolmatov V.Yu. Detonation synthesis ultradispersed diamonds: properties and applications//Russian Chemical Reviews. – 2001. – 70, №7. – P. 607-626

2. Dolmatov V.Yu., Burkat G.K. Detonation synthesis ultradispersed diamonds as the base of a new class of composite metal-diamond galvanic coatings// Sverkhtv. Mater. – 2000. - №1. – P. 84-95.

3. Voznyakovskij A.P., Dolmatov V.Yu. Antifriction coatings on the basis of nanocomposite of fluoropolymers and detonation nanodiamonds//Materials and coatings for Extreme Performances, Katsiveli, Crimea, the Ukraine, 18-22, September, 2000. – Proceedings of Conf. 2000. – p. 85

PHYSICAL BACKGROUNDS OF MANUFACTURING OF COMPOSITE MATERIALS BY CRYSTALLISATION IN ULTRASONIC FIELD

Prokopenko G.I., Mordyuk B.N.
Kurdyumov Institute for Metal Physics, Kiev, Ukraine

The conventional approach to control of properties of materials is based on using of alloying by some impurities. However in a number of cases this approach comes across principled limitations conditioned by absence in the nature of impurities indispensable for obtaining of materials with given properties.

Materials consisting from a component that do not dissolve in each other in a liquid-phase is of interest both with fundamental and technological points of view.

If the components will not form a liquid solution, the customary metallurgical melting methods do not allow to obtain qualitative ingots with an even distribution of components in ingot volume, as the unsolvable components will form layers or zones in ingot or settle out on a floor. Such ingot becomes unsuitable for the technological or scientific purposes. At the same time the modern industry requires materials with the improved service characteristics in extreme conditions (wear resistance, high-temperature strength etc.).

The acoustic mixing of the system ZnPb in microgravity conditions was used in [1]. Coalescenting drops in molten alloy, were dispersed by ultrasound, and well-dispersed structures were obtained; however these experiments were carried out only at small concentration of Pb and low ultrasound intensity.

In the present work the possibility of producing of composite materials of systems Al-Pb, Zn-Pb with application of ultrasonic and centrifugal fields was investigated. Such composites can be used for self-lubricating bearing boxs.

Ultrasonic action on a melt initializes a cavitation phenomena and acoustic flows within a melt. There are a number of consequent processes in indurating melt, having different structural components under ultrasonic treatment [2]:
1) Equalization of a solidified front;
2) Dispersion and metalization of solid phase particles and distribution in volume of centers of crystalline phase;

3) Initialization of acoustic flows in a melt that lead to intensive stirring;
4) Removal of capillary limitations at a stage of growth of crystallization centers and improvement of a wettability by stayed liquid.

To selection of optimum regimes of ultrasonic treatment of melts the following features of formation of cavitation area were taken into account:

The cavitation area size are directly connected with dimensions of ultrasonic horn (diameter of area $d = (0,9...1,1)$ d_h and its altitude $h = (2,6...4,3) \cdot d_h$).

The threshold power of a beginning of cavitation is connected to a wettability of the waveguide (horn) and may be defined with allowance of Blake's threshold [1]:

$$P_c = P_o + \frac{2}{3\sqrt{3}} \sqrt{\frac{(2\sigma_L / R_0)^3}{P_0 + (2\sigma_L / R_0)}},$$

here $P_0 = 5 \cdot 10^{-4}$ MPa is a static pressure in melt, R_0 is a radius of cavitation bubble.

For zinc a surface tension of melt $\sigma_L = 0.787$ J/m^2, threshold Blake's $P_C = 0,22$ MPa, threshold power $W = 37...43$ Wt; for lead - $\sigma_L = 0.442$ J/m^2, $P_C = 0,16$ MПа, $W = 18...23$ Wt.

Obviously, the ultrasonics preferentially affects on that frame of a structure, which one crystallizes first of all (Al, Zn). Ultrasound increases wettability of disperse particles because of local raise of temperature and pressure on the boundary between disperse particle and melt due to cavitational bubbles shocks. Besides, action of powerful ultrasound on a melt with disperse particles (crystallization centers) or liquid drops, causes intensive dispergation of this particles and drops. So this effect consist in dispersing of crystallization centers and after its metalization by a Pb melt in arranging them uniformly (or pursuant to acoustic flows) in melt volume.

A series of experiments were carried out on a special centrifuge. It allows to clearing up the influence of acceleration on crystallization processes of composites in ultrasonic field.

It is necessary to mark, that due to difference of composite component densities the installation for ultrasonic producing of composite materials developed on the vertical scheme for compensation of gravitational forces by acoustic pressure. Besides the influence of centrifugation on structure of obtained composites was investigated.
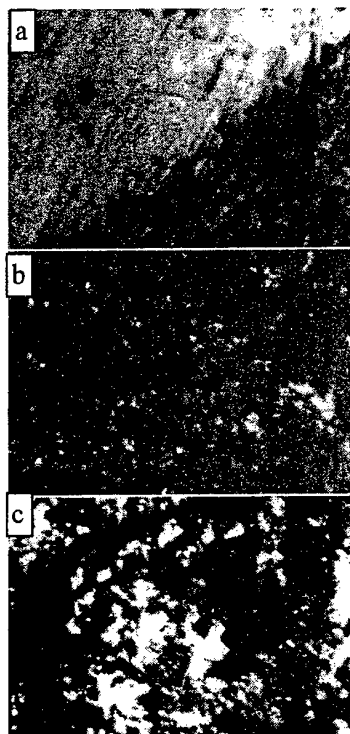
Fig.1. Microstructures of Zn – 15% Pb composite
        produced in different conditions:
a – conventional crystallization of melt;
b - crystallization with ultrasonic treatment of melt;
c - crystallization with ultrasonic treatment of melt in centrifuge (accelaration g=10).

Several microstructure images of Zn-15%Pb composite produced in different conditions are shown on fig.1. As one can see ultrasonic treatment of melt leads to uniform distribution of Pb disperse globules in Zn matrix (fig.1 b). Crystallization of ZnPb composite in ultrasonic and gravitation fields brings to coagulation of disperse Pb globules (fig.1 b). The degree of this coagulation depends on acceleration of centrifuge rotation.

The results obtained by experiments on crystallization under ultrasound and different accelerations of centrifuge after theoretical analysis may be used to extrapolation on the case $g = 0$ and thus suppositions about possible properties of these composites and crystallization processes with ultrasound in zero gravity may be made.

References

1. Schonholz R., Dian R., Nitsche R. Proc. 5th european Symposium on Material Science in Microgravity, Schoss Elman, Nov 1984, ESA SP-22, 1984, p.163-167.
2. G.I. Eskin, V.I.Skopin // New processing techniques of metals by ultrasonic. M., 1986 - P. 47-50. in Russian.
3. Physical Acoustics, Edited by W.P.Mason. - V. 1. Part B. - 363 p. - in Russian.
4. Abramov O.V. Crystallization of metals in a ultrasonic field. M.:Metallurgy, 1972, 256 p. – in Russian.

COMBUSTION SYNTHESIS AND PROPERTIES OF SiAlON-BASED COMPOSITE CERAMICS

Smirnov K.L.

Institute of Structural Macrokinetics and Materials Science Russian Academy of Sciences, Chernogolovka, Moscow oblast, Russia

The main features of self-propagating high-temperature synthesis of β-sialon ceramics and their properties were studied. The process was carried out according to the following reaction scheme:

$$(6 - 1{,}5z)Si + zAl + 0{,}5zSiO_2 + (4 - 0{,}5z)N_2 \rightarrow Si_{6-z}Al_zO_zN_{8-z}.$$
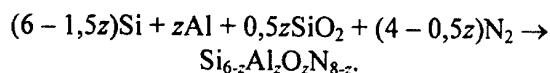
Two more components, diluent and sintering regulator, were added into the reaction mixture. The former one is necessary for suppressing the dissociation of product and coalescence of melted combustible components (Si, Al) into inactive aggregates. The latter one favors a homogeneous structure of synthesized ceramics. End product, sialon that corresponds to element composition of synthesized one, as well as other refractory compounds (SiC, TiB$_2$) were used as diluents. BN that formed during combustion was used as a sintering regulator. Approximately 10 % wt of BN was enough to inhibit capillary processes in the combustion wave.

Two factors determine the density of SHS ceramics: volume change during nitriding and sample shrinkage. These were characterized by the ratios of product volume to volume of starting reactants (V_p/V_r) and initial sample volume to the final one (V_0/V_f), respectively. In the system under consideration, the V_p/V_r values were below 1.2. Therefore, their expected relative density of synthesized materials never will exceed 0.75. For this reason, a key problem for us was to find out combustion conditions that favor sample shrinkage.

The value of V_0/V_f increases within the range 30–100 MPa and then levels off. The burning velocity and combustion temperature attain their maximum values (u_c = 1–1.6 mm/s and T_b = 2300–2600 K). This is accompanied by changes in a combustion mode from the surface to the layer-by-layer one. This is supported by the distribution of product composition and density over the sample cross section. Low conversion degree and low density in the internal area of the samples synthe-

sized at 30 and 60 MPa are associated with poor infiltration in surface combustion. In the central area of the sample synthesized at 30 MPa there is no reaction between silicon and nitrogen. For the sample synthesized at 90 MPa, nitriding is incomplete due to self-densification of product in the central area of the sample. Upon going from surface into layer-by-layer combustion the shrinkage increases. The ratio of relative linear shrinkage along the combustion axis and the perpendicular axis also increases by a factor of 5–10. Thus, the sample shrinkage should be caused by pressure gradient around the reaction zone. According to the theory of infiltration combustion during layer-by-layer combustion the pressure gradient should attain it's maximum value and be oriented largely along the direction of combustion wave propagation.

The sample shrinkage was found to increase nearly proportional to the content of combustible components in the green mixture. The measured V_p/V_r turned out lower than the calculated one due to increase in the content of unreacted silicon. The relative density of synthesized ceramics is determined by variation in sample shrinkage. The sample shrinkage increases with increasing content of oxides in the green mixture. This tendency is observed for oxides both soluble and insoluble in β-sialon.

The shrinkage also depends on the sample diameter of initial: it begins to diminish at two critical diameters (~30 mm and ~70 mm). In both the cases, the heat loss suppresses sample shrinkage. The maximal critical diameter exists due to impossibility to provide good heat insulation from cold walls of the reactor for large samples. The minimal one exists due to an increase in specific heat loss determined by the ratio of surface area of the sample to its volume. Heat losses effect directly on the inequality of shrinkage resulting in unequal density distribution in the sample cross-section. The density in outlying zones is a little less than in the center.

Addition of nonsialon refractory compounds into the green mixture allows us to produce composite materials. Formation of high-density structure upon combustion was found to provide stability of refractory compounds. When the relative density of β-$Si_{4.3}Al_{1.7}O_{1.7}N_{6.3}$-SiC-BN is less than 0.85, SiC reacts with N_2. For more dense materials, the SiC content is in exact agreement with the calculated value.

When TiB_2 is used as a diluent, changes both in the structure and composition of synthesized ceramics are more sophisticated. There is a discontinuity in the dependence of the ratio V_0/V_f on the content of diluent in green mixture. In case of sample shrinkage ($V_0/V_f>1$), the most of TiB_2 remains in the initial state, while in case of sample swelling ($V_0/V_f<1$), it readily reacts with N_2. Formation of BN explains sharp change in conditions of structure formation and reaction of TiB_2. Large amount of BN inhibits the shrinkage, which facilitates supply of N_2 into the reaction zone and further reaction between TiB_2 and N_2. Due to such a positive feedback, some compositions exhibit both the types of changes in volume.

The electrical resistivity of sialon composites was found to vary within wide limits: from 10–10^4 $\Omega \cdot \mu m$ for compositions containing transition metals compounds (β-SiAlON-TiB_2), to about 10^{11} $\Omega \cdot m$ for compositions containing only dielectric phases (β-SiAlON-BN). For materials containing SiC, the resistivity ranges between 10^3 and 10^4 $\Omega \cdot m$. For the latter two systems, even small amount of unreacted silicon markedly reduces value of electrical resistivity by several orders of magnitude.

The flexural strength as a function of ceramic porosity obeys the expression $\sigma = \sigma_0 \exp(-4P)$, where $\sigma_0 = 240$–300 MPa. The greatest value of σ_f is exhibited by composites containing SiC. For the compression strength, this function complicates. For β-$Si_{4.3}Al_{1.7}O_{1.7}N_{6.3}$-SiC-BN, the maximum value of σ_c is about 700 MPa (for porosity $P\sim10\%$). For ceramics of lower porosity but with higher content of free silicon, σ_c comes down 400 MPa. Above 1300°C, the values of σ_f for all of the compositions studied range between 80 and 120 MPa.

The initial temperature of decomposition of composite materials in vacuum (10^4 Pa) is within the range 1650–1700°C, which corresponds to the dissociation temperature for pure silicon nitride

under our conditions. The rate of high-temperature decomposition depends on the porosity as well as on sialon content.

Synthesized materials exhibit extremely high corrosion resistance to molten metals and slag. In this respect, they are much better than commercially available refractories and their analogs fabricated by conventional methods (table 1). These materials have also high thermal-shock resistance (more than 30 cycles without destruction at "furnace - water" temperature overfall of about 1300°C). At quenching in running water, SHS sialons withstand temperature overfall of 550–600°C without deterioration of their flexural strength.

Table 1

Ceramics	Weight losses % wt	
	in slag	in steel
ZrO_2 – graphite	60	20
Al_2O_3	–	30
ZrO_2	–	50
RBSN	–	100
HP Si_3N_4	–	17
SiAlON (sintered)	–	5
SiAlON–SiC–BN (SHS)	**0**	**0**
Si_3N_4–SiC–TiN (SHS)	–	40
BN (SHS)	30	20
BN–SiO_2 (SHS)	20	20

193

SOLDERING OF MELT-TEXTURED YBCO USING Tm123 POWDER

Prikhna T.A.[(1)], **Gawalek W.**[(2)], **Moshchil V.E.**[(1)], **Sergienko N.V.**[(1)], **Surzhenko A.B.**[(2)], **Sverdun V.B.**[(1)], **Litzkendorf D.**[(2)], **Kordyuk A.A.**[(3)], **Melnikov V.S.**[(4)], **Dub S.N.**[(1)], **Habisreuther T.**[(2)], **Alexandrova L.I.**[(1)]

[(1)]Institute for Superhard Materials, Kiev Ukraine
[(2)]Institut fur Physikalische Hochtechnologie, Jena, Germany
[(3)]Institute of Metal Physics, Kiev, Ukraine
[(4)]Institute of Geochemistry, Mineralogy and Ore-Formation, Kiev, Ukraine

Of known high-temperature superconductors (HTSC) the melt-textured $YBa_2Cu_3O_{7-\delta}$- based (MT-YBCO) is considered as a material to be successfully used for bulk applications like flying wheels, frictionless bearings, electromotors, levitation transport etc. The widespread use of HTSC bulk materials is restricted by the absence of technologies that allow the manufacturing of high-quality large (larger than 40- 60 mm) and complex-shaped parts. The attempts to grow up large blocks of MT-YBCO using multi-seed growth up to now haven't given very encouraging results due to the crystallization of a great deal of impurity phases at the boundary where two fronts of crystallization (from different seeds) meet each other [1, 2]. A relatively good boundary, using multi-seed growth, can be obtained if the distance between the seeds is of about few millimeters. So, in this case it is not quite clear whether the multi-seed growth has advantages over the single seed one.

Soldering of MT-YBCO to obtain the SC junctions is a very promising way of producing large superconductive items of complex shapes. A lot of papers on the problem describe the processes of joining MT-YBCO bulk using spacer layers [3, 4] in the form of thin plates (of about 1 mm thick) cut from various materials with lower melting temperatures than that of the joined one, e.g., from MT-TmBCO or MT-YBCO with Ag aded. Thus, the problem arises of manufacturing of large high quality auxiliary layers. Besides, such soldering process is complicated and rather time-consuming.

We have developed a method to solder MT-YBCO using a $TmBaCu_3O_{7-\delta}$ (Tm123) powder under a pressure of about 3-4 kg/cm^2 that allows us to produce high-quality superconductive junctions between MT-YBCO parts excluding the stages of slow cooling during soldering and preparation of auxiliary layers. This method imposes no restrictions on the size of the joint surfaces, quantity of parts to be joined and their arrangements relative to each other.

The structure of MT-YBCO is usually constituted of one or a few (well oriented relative to each other) large textured SC grains of Y123 with finely dispersed small inclusions of the non-superconductive Y_2BaCuO_5 (Y211) phase. The melt-texturing process of Y123 supposes a slow cooling (about 0.3 K/h) in the 1000-1030 °C range. To form the soldered seam, the MT-YBCO samples should be repeatedly heated (above 1030 °C) that may induce changes of their structure: variation in oxygen content of Y123, decomposition of Y123, recrystallization and coarsening as well as redistribution of Y211, etc. So, it is important to find compromised soldering conditions in order to provide a high-quality joint and not to impair properties of MT-YBCO.

The determined-from-DTA study temperature of incongruent melting of MT-YBCO was 1016 °C and that of Tm123 was in the range of 984 – 986 °C.

To estimate the critical current density (j_c) through the junction, we have drilled rings from single-domain MT-YBCO blocks and estimated the j_c in these initial rings from the loops of magnetization using a vibrating sample magnetometer. Then these rings have been cut into two pieces along the diameters (the width of cut was about 0.7 mm) and soldered using a Tm123 powder under the 3-4 kg/cm^2 pressures. The soldered rings have been again placed into the magnetometer to estimate the j_c. The results are given in Fig.1. An increase in jc in 1.5-1.6 times through the ring from MT-YBCO soldered by a Tm123 powder as compared with that in the singledomained ring was observed up to the 2.5 T field. For the joined sample, at 0 T field j_c=34.4 kA/cm^2. The obtained seam was practically

invisible under a polarizing microscope and was about 40 μm in width (as the SEM study have been shown). In fields higher than 2-3 T some decrease of j_c took place.

The bending strength of the seam was even higher than that of the material being joined. During investigation of bending strength of the seam the breaking occurred mainly through the joined material. Thus the estimated value of the bending strength was of about 32 MPa.

REFERENCES

1. Schatzle, P., Krabbes, G., Stoever, G., Fuchs, G. and Schlafer, D. Supercond. Sci. Technol. **12**, 69 (1999)

2. Veal, B.W., Zheng, H., Claus, H., Chen, L., Paulikas, A.P., Koshelev, A., Hull, J., Crabtree G.W., in "The extended abstracts of 2000 International Workshop on Superconductivity", June19-22, 2000, Shimane, Japan, 2000, pp.211-214.

3. Zheng, H., Jiang, M., Nikolova, R., Welp, U., Palikas, A.P., Huang, Yi., Crabtree, G.W., Veal ,B.W., Claus, H., Physica C **322**, 1 (1999).

4. Mendoza, E., Puig, T., Varesi, E., Carrillo, A.E., Plain, J., Physika C, **334**, 7 (2000).
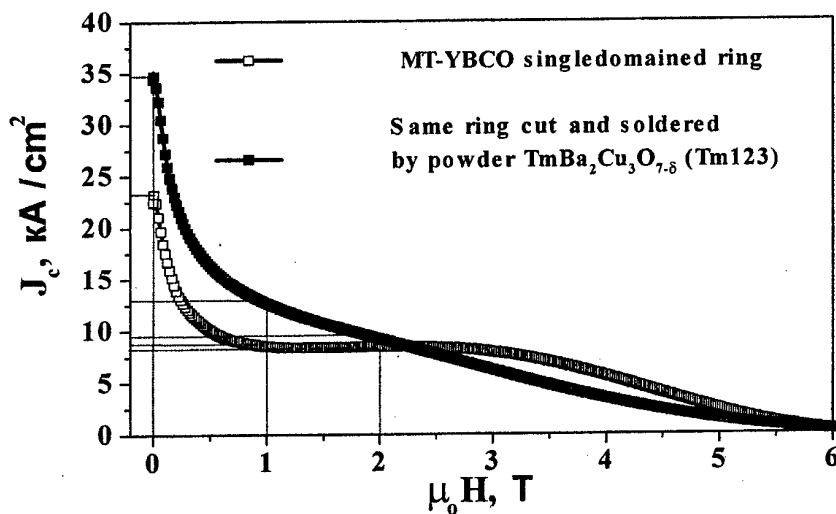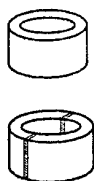
Fig.1 Critical current density, j_c, vs magnetic field, μ_0H, of the singledomained ring and of the same ring cut and soldered by a Tm123 powder at 1010 °C (the temperature raised and decreased with a rate of 500 K/h, after the soldering, the sample was oxidized in a separate process).

MANUFACTURING OF PERMEABLE CELLULAR MATERIALS OF HIGH POROSITY (PCMHP) BASED ON KXH-15

Antsiferov V.N., <u>Khramtsov V.D.</u>
Scientific Centre of Powder Material Study, Perm, Russia

The development of technologies for Ni-Cr alloy PCMHP [1] production and its implementation have shown that heat resistant PCMHP are always needed. The main area of their implementation – catalyst carriers, filters operating in oxidizing atmosphere at high temperatures. Because Ni-Cr alloy PCMHP can operate for a long period up to temperature 700-750^0 C only, the development of more heat resistant PCMHP is of great interest. Powder compositions of carbide-metal - cermets [2] - proved themselves as strong, chemically and heat resistant materials. Carbide Cr cermets of KXH and 608 mark containing from 10 to 40% of Ni resist to abrasive wear, corrosion in alkali and acid, mineral salt solutions, sea water, melted glass.

Various methods for cermets manufacturing: impregnation of sintered ceramic frame with melt metal; parts molding of plastic mixture and sintering at high temperature; molding in steel moulds; extrusion molding, slip casting.

KXH manufacturing and implementation are based on some properties of chromium carbides [2]. The most stable and often used Cr_3C_2 in the interval of 800-1100^0 C does not change the weight in the air. Its wetting angle Si, Mn, Fe, Ni, Co is about 0 ^{0}. Eutectic temperature with Ni, Fe Co – 1255, 1280, 1285^0 C, respectively [4, 5].

Methods, Results and their Discussion

To produce PCMHP the mixture of KCXH-15 was used, it contains 85 % of Cr_3C_2 and 15 % of Ni powder (mass). 99.5 % of powder is < 40 µm.

Cr_3C_2 particles are of shiver form. KCXH-15 apparent density, (γ_H), and density after shaking, (γ_y) amount to 1.85 and 2.87 g/cm^3, respectively. Mixture specific density after shaking amounts to 37.1 % only, it results in large shrinkage at sintering.

So that to increase the particles placement density the influence of mixing in mixer and moulding in closed mold were studied (Table 1, 2).

Mould items can be crushed very easily by hands up to moulding pressure of 120 MPa. At moulding the consolidation is worse. Repeated mouldings do not serve to placement density as well. Evidently, it is connected with morphology and polydispersity of powder mixture and is explained by high hardness and strength of Cr carbide particles. Plastically deformed particles of Ni prevent from crushing.

Table 1 – Relationship of particles placement density (apparent density and density after shaking) of KCXH-15 mixture to the moulding pressure

P, MPa	N*	γ_H, g/cm^3	γ_y, g/cm^3	c_H, vol %	c_y, vol. %
0	0	1,89	2,94	24,4	37,5
50	1	2,14	3.09	27,6	39,9
100	1	2,17	3,13	28,0	40,4
100	2	2,.13	3,18	27,5	41.1
100	3	2,19	3,20	28,3	41,3

N* - number of moulding cycles.

The other way to increase particles placement density – processing in the mixer. The mixing was fulfilled in the mixer with rotation axis displaced, ½ charge, relation of grinding balls and powder is1:1 by volume. On mixing (Table 2), after 15-20 hrs of processing they can reach the saturation, rather small consolidation effect (placement density growth up to 0.42-0.43).

Table 2. Relationship of KXH-15 mixture characteristics to the mixing time

Time, hr	γ_H, g/cm^3	γ_y, g/cm^3	c_H, vol %	c_y, vol. %
0	1,89	2,94	24,4	37,5
8	1,89	3,16	24,4	40,9
21	2,22	3,33	28,7	43,0
32	2,41	3,40	31,1	44,0

The samples of polyurethane foam (PUF) (cell average diameters - 4.5, 2.4 and 1.15 mm) were used to produce PCMHP.

One of the problems in PCMHP production is the elimination from the blanks of PUF and water suspension organic stabilizer. The organic matters should be preliminary eliminated to prevent pollution of sintering oven. As the experiments have shown, it is to no purpose to apply the thermal destruction in the air because near destruction temperatures (450-550 ^{0}C) Ni powder oxidizes intensively. For example, KXH-15 mixture weight increase equals to 2.0 % at 470 ^{0}C in 0.5 hr. It is accepted optimal to eliminate organic matter in reducing atmosphere.

The experiments showed that the optimal sintering will be one hour in vacuum at 1255-1240 ^{0}C. The samples provide the expected shrinkage; no fractures, deformations, warping. At 21-25 % linear shrinkage (horizontal plane), the height shrinkage is 2-7 % more, i.e. despite liquid sintering and low particles placement density, the height creeping is not so considerable.

Mass loss is slightly more than organic matter mass, it is explained by partial Cr evaporation. Fe-magnetic phase absence caused, obviously, by Cr dissolution in Ni and partial dissolution of Ni in carbide.

Microstructure analysis revealed inhomogeneous hardness of matrix, hilly surface of metallographic specimen. Under the microscope two phases and micro-pores are seen on metallographic specimen without pickling.

Micro hardness of KXH-15 PCMHP matrix was measured under load of 100 g.

Clearly distinguished PCMHP matrix components have micro-hardness 1450 and 900, respectively, there are local parts of HV $_{100}$ 1800.

Derivatogram of heating in air and at velocity of 7.5 degree/min showed that KXH-15 PCMHP with d_{cell} = 3.69 mm and specific density (θ) of 7.17 % increases evidently in mass from 995^{0}C, the mass increases by1.0% at 1145^{0}C. Ni-Cr PCMHP possessing similar characteristics has mass increase from 830 ^{0}C, the mass increases by % at 1000^{0}C.

The samples of KXH-15 and X24H75 PCMHP, similar cell average diameter of 3.4 mm and density of 0.39 and 0.55 g/cm^{3}, respectively,

undergone the comparative oxidation in air up to 5 hours at 900^{0}C. KXH-15 showed slight mass loss, X24H75 – mass increase: -0.12 and +0.90 %, respectively. Therefore, we can conclude: KXH-15 PCMHP is more (165-140) ^{0}C heat resistant than Ni-Cr.

Strength properties of KXH-15 PCMHP were estimated during compression test of samples processes by diamond grinding wheel, speed 0.2 mm/min (Table 3). KXH-15 PCMHP crushes in fragments, it is untypical.

KXH-15 PCMHP showed compression strength like Ni-Cr PCMHP, its strength essentially more than that of PCMHP based on oxide ceramics which compression strength does not exceed 1 MPa at θ=10 %.

Table 3. KXH-15 PCMHP strength properties

d_{cell}, mm	γ, g/cm^{3}	θ, %	σ_{compr}, MPa
3,66	0,55	7,1	1,9
1,92	0,50	6,4	1,7
0,92	0,72	9,3	4,9

Conclusions

The method for KXH-15 PCMHP suspension molding is developed. Determined that its compression strength is similar to SiC and Ni-Cr alloy PCMHP and much exceeds PCMHP based on oxide ceramics. Heat resistance of KXH-15 PCMHP exceeds Ni-Cr PCMHP.

References

1. V.N. Antsiferov, V.D. Khramtsov, O.P. Koshcheev. High-Porous Ni-Cr: Production, Structure and Properties.// High School Transactions. Non-Ferrous Metallurgy. #5, 1998, p.56-60.
2. Encyclopedia of Inorganic Materials. Two Volumes. V.I – Kiev: Main Editorial Office Ukr. Sov. Encyclopedia, 1977. 840 p.
3. G.V. Samsonov, I.M. Vinnitsky. Refractory Compounds (Reference-Book).M., Metallurgy, 1976.560 p.
4. Heat and Corrosion Resistant Cermets. Translation from German. M., 1959.
5. U.D. Kingery. Introduction into Ceramics. Translation from German. M., 1967.

DEVELOPMENT AND REASEARCH OF TECHNOLOGY OF RECEIVING OF SEMI-FINISHED PRODUCT MADE OF METAL POWDERS FOR CONTACT SPOT WELDING

Kuimov Sergey, Filonov A.
Join-stock company « Revda Non Ferrous Metals Processing Works », Revda, Sverdlovsk reg, Russia

Traditionally in Russia and abroad contact spot welding electrodes of sheet and other products are produced from cast bronze (БрХ, БрХЦр, БрБНТ) etc. However these materials with their operational characteristics do not completely meet to the requirements of welders and are expensive because of irrational use of material resources: low operating ratio of metal, complex technology, ecological problems, and the trouble-free technology is not found up to now.

The researches of the various authors in the field of contact welding have resulted to development and introduction into an industry a perspective class of dispersible - harden composite materials (DHCM) on the basis of powdered copper. The technology is simple, the resistance of electrodes made of DHCM in welding is higher in compare with electrodes made of cast bronze. Nevertheless cost of electrodes made of DHCM is also high because of large price on copper electrolytic powder.

In join-stock company « Revda Non Ferrous Metals Processing Works » the perspective technology of receiving of bars made from DHCM having diameter 12-80 mm (patents of Russia № 2159297, 2161084) for electrodes of contact spot welding in mechanical engineering, ferro-concrete products etc. with use of electrolytic and sprayed copper powders is mastered.

A basis of the technology of semi-finished items from DHCM is:

• Manufacture of the sprayed copper powders and copper alloys from waste (Scrap of wire, bars, pipes, rejected semi-finished items);
• Chemical-mechanical doping of initial powders;
• Cold pressing received granules into briquettes on hydraulic (vertical or horizontal) press – machines, or into the bars, which can be subjected, if necessity, heat treatment (hardening, ageing), smelting, calibration, raising accuracy of the sizes and improving their properties and quality of a surface.

With the purpose of increase of electric conductivity, heat conductivity, and operational characteristics of electrodes in welding process the technology of reception be-metallic bars is developed: as an environment serve cold-drawn thick-walled tubes made from cast electrolytic copper, core – bars made of DHCM with various structures. Cost of be-metallic bars is lower than cost of mono-bars made of DHCM and the more so, then cost of the best electrotechnical bars made from cast bronze.

Developed construction of compound electrodes made: a tip – from be-metallic bars, base - from drawn cast copper bars (the patent of Russia for model № 20270), allows considerably to reduce the charge of materials, to make welding works cheaper.

In the table the comparative characteristics of semi-finished items made from DHCM (mono and be-metal) and traditionally used in welding of Russia and abroad are submitted.

№	Material, grade, country - manufacturer	Brinell hardness, HB	Electric conductivity, (%) from electric conductivity of copper	Temperature of crystallization, "C
1	DHCM, KM-4, Russia	190-200	55-65	>800
2	DHCM, KM-25, Russia	200-250	50-55	>850
3	Be-metal: envelope, M-1 with rod DHCM KM-4 - with rod DHCM KM-25	70-90 190-200 200-250	80-85	>800
4	Copper M-1, Russia	70-90	98	150-300
5	Bronze БрХ, Russia	110-130	70-80	350-450
6	Bronze БрХЦр, Russia	120-130	80-85	480-500
7	Б Bronze БрБНТ, Russia	170-240	45-55	500-550
8	Element HA, Germany	220-240	35-52	500-600
9	Mallori-3, USA	130-135	80-84	450-500
10	Mallori-100, USA	190-240	45-50	500-550

Taking into account, that the resource of electrodes made from DHCM exceeds a resource of similar electrodes made from traditional bronze, the need of product made from DHCM (including be-metal) in a result receives significant benefit.

Joint-sock company "Revda Non-Ferrous Metal Processing Works" is ready to cooperate with the interested consumers of our production on mutually advantageous conditions.

SYNTHESIS OF FULLERENKS AND THEIR DERIVATIVES DURING SIMTERING OF POWDER STEELS

Antsiferov V.N., Grevnov L.M.
Research Center of Powder Material Science, Perm, Russia

Recent achievements in the field of carbon compounds allow to presuppose that in iron-carbon alloys the formation of free carbon such as fullerenes, bakitubes and globuls is possible [1,2]. It has been investigated the Influence of kind and quantity of alloying elements on synthesis of fullerenes and their derivatives in the process of low temperature sintering of powder steels in the field of α-γ transformation. For this purpose steels on the basis of ПЖРЗ.200.28 iron powder alloyed with nickel, copper and silicon were prepared.

Concentrations of alloying elements were changed within 5 to 20 % at 1% carbon. Part of the samples having 15 % nickel content was prepared based on P10 carbonyl iron and ОСЧ.6-2 iron. Samples were pressed at 400 MPa and sintered in vacuum at 700 - 900 °C for 1 - 5 hours.

It has been established by radiographic analysts that after sintering at 850 °C for 5 hours, metal fullerite based on C60 fullerene with 4.23 Å lattice period was formed in P10 iron steel with 15 % nickel content. The synthesis goes more actively in surface layers of the sample (4.27, 4.14, 3.34 and 2.54 Å lines). In a sample core it was observed only one intensive enough 3,34 Å line of metal fullerite.

In steel with the same nickel content (15 %), but on the basis of ОСЧ 6-2 iron, after the same sintering mode, it was generated much less fullerene and only in a surface layer, and this is testified by single 3,34 Å line of average intensity.

Changing the nickel content from 5 to 20 % in steel based on ПЖРЗ-200.28 iron powder results in the most active formation of metal fullerene at 15 % nickel content. Crystaliograms of this steel sample show the most intensive lines of a metal fullerene. On a surface it is 3.36 Å and 3.65 Å lines, and in a core- 3,56 Å and 3,35 Å.

So, the synthesis of a fullerene most actively occurs in P10 and ПЖРЗ.200.28 iron steel alloyed with 15 % of a nickel, and in this process the metal fullerite with the 14,23 Å lattice period is formed.

The study of sintering duration effect at 850 °C and 1 to 5 hours has shown that formation of metal fullerite on a surface of samples practically does not depend on duration of sintering. In a core of samples the synthesis of fullerenes most intensively occurs when sintering for 3 hours.

It has been determined that change of sintering temperature from 700 to 900 °C renders insignificant influence on formation of fullerenes.

It has been established that the synthesis of fullerenes occurs also in steels alloyed with silicon.

The sintering is most actively in 5 % silicon steel. In a copper steel a metal fullerene with 14,23 Å lattice period is also formed. The synthesis of fullerene occurs most actively in steel containing 15 % of copper. So, nickel, copper and silicon promote the synthesis of fullerenes In powder steel.

References
1.V.S.lvanova, D.V.Kozitsky, P.Kuzov, M.M.Zakirlchnaya About self-similarity of fulierenes formed in product structures of thermal graphite evaporation // Advanced Materials 1998. N 1. P.5-15.
2.A.A.Zhukov. R.L.Snezhnoy, S.V.Davydov. About formation of compact graphite in cast iron // МиТОМ, 1981.No.9. P.21.

DETONATION SYNTHESIS NANODIAMONDS AS A COMPOSITE FILLER OF POLYSILOXANE BLOCK-COPOLYMERS

Voznyakovskij A.P.[(1)], Fujimura T.[(2)], Neverovskaya A.Yu.[(1)], Dolmatov V.Yu.[(3)]
[(1)]The S.V.Lebedev Scientific-research institute of synthetic rubber, Saint-Petersburg, Russia
[(2)]"VISION DEVELOPMENT CO., LTD", Tokyo, Japan
[(3)]Special design bureau "Tekhnolog" at Saint-Petersburg State Technological Institute (Technical university), Saint-Petersburg, Russia

Polyblock polysiloxane copolymers of the (AB)$_n$ type consisting of rigit polysiloxane with a high vitrification temperature (A) and flexible polysiloxane (B) blocks have a complex of important applied properties. So, a frost resistance of articles of their basis amounts to about -100°C; a heat resistance – up to 400°C [1]. The combination of a wide temperature range of serviceability and high adhesion and dielectric properties allows one to use these block-copolymers as the basis of creation of the film-forming materials for the wide potential application fields – from protective coatings to selective-permeable membranes. Disadvantage of the obtained films is a unsatisfactory complex of elasticity and strength parameters. Because of the last circumstance the formation of a chemical net in addition to a spatial physical one being characteristic for block-copolymers is recognised as necessary. The formation of the chemical spatial net is the more effective to increase the strength parameters at maximum deformations. But, as a practical matter attainment of the strength parameters as much as possible at deformation up to 300% is often required. In order to solve this problem filled compositions might be used. Reinforcement effect is closely bound up with so called "size effect", i.e. physical and chemical properties of substances change as the particle size decreases [2]. At the same time a maximum "size effect" is observed as the dispersivity of particles increases up to 10 nm, when a part of surface atoms is commensurable with a part of atoms being in the substance volume.

The present work has for an object to obtain the high-strong polymer film materials on the basis of nanocomposites of polyblock polysiloxane block-copolymers designed for use in corrosion medium.

As a polymer matrix the polyblock block-copolymer of "ladder" phenylsilsesquoxane and polydimethylsiloxane (LPhS-PDMS) produced at the S.V.Lebedev Scientific-research institute of synthetic rubber (Saint-Petersburg) on an pilot-industrial scale was used. When choosing the nanofillers their availability on an industrial scale was taken into consideration. This criterion limited the choice by a high-dispersed silicon dioxide (Aerosil A-300) and detonation synthesis ultradispersed diamonds (UDD). Because of renewal of high-dispersed glass spheres (GSph) production the study of prospects of their use as a filler is also expedient.

In order to obtain the filled materials the solution technology was used. According to this technology a dry powder of filler particles were dispersed into a toluene solution of block-copolymer. To reach the uniformity of surface characteristics of fillers they were previously warmed up at 400°C in the vacuum cabinet. The strength parameters of non-filled films of LPhS-PDMS were used as initial strength parameters for comparison with the filled ones obtained at the same conditions. It turned out that the use of selected fillers by themselves even after preliminary treatment is ineffective. That fact is likely to be bound up with intensive processes of aggregation of filler particles in non-polar medium. Aggregation processes did not allow one to reach the uniform distribution of the filler particles in the volume of a polymer matrix, that in combination with a high surface activity of particles resulted in the formation of structurization units and, as a result, the cracking of films. The aggregation processes of particles with hydrophilic surface groups in non-polar mediums may be decreased by means of chemical modification of a surface with the result that active functional surface groups will be blocked by non-polar ones. With that object some variants of hard-phase sililization were used. A number of water-repellency treated fillers (A-300m and UDDm) was obtained.

Some characteristics of polydispersivity curves at the more effective way of modification of a surface are presented in the Table 1.

The data of the table 1 show that the average numerical diameter values (D) reached during the

modification of a surface allow to refer the used fillers to nanodispersed substances. The suspensions of modified fillers in toluene remain stable for a long time that allowed one to use them for obtaining of nanocomposite films. But, it was found that the use of fillers in individual state results in structurization of the films and the loss of strength properties.

Table 1
Some characteristics of polydispersivity curves of filler particles

Parameters of polydispersivity curve	Aerosil A-300m	Glass spheres GSph	UDDm
Average numerical diameter of particles, D, nm	22,0	39	14,5
Content of particles with the size ≤ 10 nm, %	20,6	--	54,0

At the same time a maximum degree of filling foregoing structurization depends on a filler type (minimum one for UDD and maximum one for GSph). To explain this effect the parts of particles with the size ≤ 10 nm, i.e. the parts of particles with the well-marked "size effect" (table 1) were calculated from polydispersivity curves. As shown in the table data, both UDDm and A-300m have a great part of particles with the size ≤ 10 nm. One can suppose that the surface activity of these particles is not compensated for by surface modification and, accordingly, the structurization processes are not blocked. The possible way to reach the uniform distribution and reduction of the high surface activity of particles is the use of compositions of nanometric and low-dispersed substances. At the same time the character of distribution of a filler in a volume will be characterised by the presence of ensembles formed by big particles of one filler surrounded with small particles of other filler. Fields of forces and the surface activity of fillers of different sizes due to superposition and interference determine a larger isotropy of properties than when using of an individual nanometric filler. In the given work the glass spheres were used as a low-dispersed component. The work on optimisation of a composition of the composite fillers GSph -A-300m and GSph-UDDm was carried out. That work showed that the composite fillers on the basis of UDDm is more effective to use. So, the filling with the 5% composite filler (2,5% GSph+2,5% UDDm) allowed one to obtain practically a double increase in strength parameters at satisfactory elasticity (table 2).

Table 2
An influence of filling on strength parameters of LPhS-PDMS (T=20°C)

Block-copolymer film	M_{100}, MPa	M_{300}, MPa	P, MPa	L, %
Initial	2,0	3,7	5,2	550
Filled*	4,3	6,4	7,0	300

where M_{100} – modulus at 100% deformation
M_{300} – modulus at 300% deformation,
P – rupture stress,
L – elongation at rupture,
* - filler composition (2,5% GSph + 2,5 UDDm)

The conclusions:

Based on the work results one can conclude that an effect of the UDD-use as a nanofiller allows one to reach a great reinforcement at a degree of filling less than 3%.

References:

1. Dolgoplosk S., Savchenko V., Martyakova N., Aleskovskaya E. // Proceedings of the 5th International Conference on Silicone in Coatings, Brussel, 1996, p.17
2. Uvarov N.F., Boldirev V.V.//Uspekhi khimii, 2001, v.70, № 4, P.307

CRYSTALLIZATION OF CUBIC BORON NITRIDE SINGLE CRYSTAL POWDERS IN THE Li - B - N (H, P) SYSTEM

Vityaz P.A., Gameza L.M., Antonovich Ya.V.
The Institute of Machine Reliability of NASB, Minsk, BELARUS

Phosphorus is very active doping element that allows one the synthesize single crystals of cubic boron nitride (cBN). In this connection we report here a research focused on the influence of phosphorus additions (0.10 – 1.00 mass %) on the degree of the graphite-like boron nitride (gBN) → cubic boron nitride (cBN) conversion and the growth peculiarities of cBN single crystals during spontaneous crystallization of the latter in the Li - B - N system with the use of LiH (10 mass%) as a catalyst in the mixture with easily decomposable nitrogen-containing additions and phosphorus additions at a pressure of 4.3 GPa over the temperature range 1940 to 2080 K for the time interval of up to 300 s. It is found that the phosphorus concentration over 1.0 mass % in the mixture suppresses the nucleation and growth of cBN single crystals. Therefore the doping addition concentration in our experimental study on the kinetic parameters of synthesis did not exceed 0.5 mass %. The graphite-like boron nitride had the following lattice parameters: a = 0.2504 and c = 0.6658 nm, degree of three-dimensional ordering p = 0.85, graphitization index G = 1.45. The dimension of the starting graphite-like boron nitride varied from 1 to 20 μm.

The kinetic dependences of the degree (@(t) of the gBN → cBN conversion and the largest crystal sizes (L(t) were explored at a pressure of 4.3 GPa and the temperatures of 1940, 2010 and 2080 K for the time interval of 300 s. Thereafter the reaction products were treated with the potassium oxide melt to result in the complete decomposition of the graphite-like boron nitride and the as-obtained crystallites were investigated.

Fig. 1 gives the kinetic dependences of the degree @ (@ = m $_{cBN}$ x ρ $_{hBN}$ / m $_{hBN}$ x ρ $_{cBN}$, where m $_{cBN}$ and ρ $_{cBN}$, m $_{cBN}$ and ρ $_{hBN}$ are the mass and density of cBN and hBN, respectively) of the hBN →cBN conversion at temperatures of 1940, 2010 and 2080 K and a pressure of 4.3 GPa on the addition of phosphorus: 0.10 mass.% (curves 1, 4 and 7); 0.25 mass.% (curves 2, 5 and 8); and 0.50 mass.% (curves 3, 6 and 9).

For 0.10, 0.25 and 0.50 mass % phosphorus additions the character of temperature dependences

(α(t) is, practically, identical, i.e. the degree of conversion rises with increasing temperature and it also enhances as the phosphorus concentration increases from 0.10 to 0.50 mass %. It is significant that the induction period decreases with rising temperature from 60 s at 1940 K to 30 s at 2010 K and 20 s at 2080 K for all the concentrations. It is obvious from the figure that all the curves have either a sigmoidal-like shape or are the lower branch of a sigmoidal curve, thus testifying to fairly equilibrium conditions of crystallization [1]. The maximum value @ is noted at the synthesis temperature equal to 2080 K, and the phosphorus concentration with the addition of 3.0 mass. % measures 0.26.
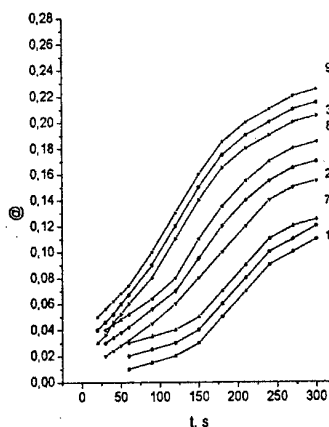
Fig. 1. Time dependencies of the degree, @, of BN conversion in the BN – LiH(N, P) system for phosphorus concentration of 0.10, 0.25 and 0.50 mass.% at temperatures of 1940, 2010 and 2080 K. The pressure is 4.3 GPa.

The analogous character of the temperature and concentration dependence is observed for the largest linear size of the single crystals L, indicating the similiarity of the processes occurring during the nucleation and crystal growth (Fig. 2).

The degree of phase transformation is described by the Kolmogorov - type expression:

$$\alpha(t) = 1 - \exp(-K t^m),$$

where the temperature dependence of the reaction rate constant K is expressed in terms of the Arhenius equation

$$K = K_o \exp(-U/kT)$$

while

$$m = (|\ln|\ln(1-\alpha)-\ln K)/\ln t.$$
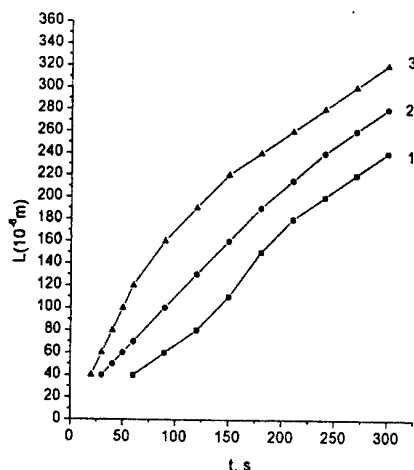
Fig. 2. Time dependences of the largest size L of cBN crystals for phosphorus concentrations of 0.10, 0.25 and 0.50 mass.% at temperatures of 1940, 2010 and 2080 K. The pressure is 4.3 GPa.

The kinetic parameter m, as shown from the calculations based on the experimental values of α at the given temperatures, is independent of temperature and is very close to 4, which testifies to fairly equilibrium conditions under which the crystal growth has taken place. The value of m in the initial stage of conversion for which the activation energy of the cBN formation processes was determined from the slope of the straight dependences $\ln|\ln(1-\alpha)|$ - $\ln t$. The activation energy of the gBN $\rightarrow$ cBN conversion was evaluated from the slope of the straight linear for $\ln K$ as a function of $1/T$. These values appeared to be 53.0 kJ/mol when introducing 0.10 mass % phosphorus into the mixture, 48.0 kJ/mol when introducing 0.25 mass %, and 43.0 kJ/mol on the addition of 0.50 mass % phosphorus. In our earlier work we used Li_3N (10 mass%) as a catalyst. The energy of the process of cBN formation is found to be 60 kJ/mol [2]. The as-obtained syngle crystals were yellow, light yellow or amber in colour. The length of the largest crystals made up 200 - 450 μm.

It is recognized that the kinetics of crystal nucleation and growth can be affected by either soluble or insoluble impurities in the melt [3]. In a heterogeneous solution, the crystal nucleation is made easier as the value of free energy change needed for a new phase to appear is lower than that in the case of nucleation in homogeneous solutions. This is due to the reduction in the surface energy at the interface between the insoluble impurity and the melt. At a pressure of 4.3 GPa, the fine-grained phosphorus particles in the temperature range 1940 – 2080 K are molten. Because the degree of conversion, @, increases with the addition of 1.0 mass. % phosphorus into the mixture and decreases with the addition of 1.0 – 3.0 mass.%, it may be suggested that phosphorus is either dissolved or is present in the form of insoluble aggregates whose density is higher than that of the melt. In this case, the nucleation takes place at the interface of phases with various densities. For small phosphorus concentrations up to 0.1 – 0.5 mass. %, its soluble fraction influences the melt viscosity insignificantly and, as a result, an increase in @ is observed since the thermodynamic factor dominates and nucleation occurs at the surface of insoluble particles. Adding phosphorus above 1.0 mass. % brings about an increase in its concentration in the solution and that of its viscosity. In this event, the kinetic factor prevails and the nucleation rate decreases, leading to the reduction of the degree of the hBN $\rightarrow$ cBN conversion and crystal growth rate. At the same time, a lowering of the eutectic temperature is observed. All these observations show clear evidence of the effect of the phosphorus additions to the mixture in the kinetic processes of cBN crystallization. The mechanism of the effect of phosphorus on the crystallization process is so complicated that further investigation is needed.

The as-obtained crystals demonstrated n-type conductivity, their resistivity ranged from 10^5 to 10^7 $\Omega \cdot$ cm, the dislocation density in the best crystals varied from 10^3 to 10^5 cm^{-2}.

[1] V.B.Shipilo, L.M.Gameza, A.I.Lukomskii, Superhard Mater. 5 (1995) 16 (In Russian).
[2] V.B.Shipilo, L.M.Gameza, N.V.Semashko, and T.S.Bartnitskaya, J. Phys. Chem. 63, 6 (1989) 1599 (In Russian).
[3] N.I.Galperin, G.A.Nosov, Fundamentals of the melt Crystallization Techniques, Chemie, Moscow, 1975, p. 351 (In Russian).

PROBLEM OF DEPOSITION OF HEAT PROTECTION AND CAVITATION COATINGS ON SLEEVE-PISTON GROUP OF INTERNAL COMBUSTION ENGINES

Tretiyak M., Petukhov A.[(1)], Chuprasov V.[(2)]
[(1)]Minsk Motor Factory, Minsk, Belarus
[(2)]Luikov Heat and Mass Transfer Institute, NAS of Belarus, Minsk, Belarus

Improvement of internal combustion engines requires creation of new materials ensuring decrease in heat losses from a working medium into a cooling system, diminution of influence of high temperatures on efficiency of details, increase in their resistance to wear, etc.

An effective method of solving some problems is deposition of coatings on a working surface of details of an engine. The application of ceramics and cermets for creation of heat protection coatings leads to essential improvement of performance of engine work [1].

The more effective and full combustion of fuel takes place as a result of which consumption decreases by approximately 3-9 g/(kW·h) and the amount of unsaturated hydrocarbons and hydrogen in exhaust gases decreases.

The character of fuel combustion changes, which causes decrease of maximum pressure in combustion chamber and, as a consequence, decrease of vibration and noise; "softer" operational mode reduces wear of bushes of the cylinder and conrod inserts.

The rate of accumulation of polymerization products and condensation of hydrocarbon in oil decreases, causing decrease in carbon varnish deposition.

The thermal stresses in the piston diminish, which leads to increase of its service not less than by a factor of 1.5.

In connection with an essential modification of combustion process, the application of heat protection coatings requires development of new constructions, but even their use in existing engines can considerably improve characteristics of these latter.

It is usual to employ plasma units for deposition of coatings of various composition with thickness of 0.1-1.0 mm on details of engines. However, this complicates the process and rises its price, so, for example, the specific costs in electric arc metallization are almost two orders of magnitude less [2].

In electric arc metallization, sputtering of metal wires is carried out, and thermal conductivity of coatings is rather high. However, it is possible to select operational modes of the unit, for which deposited coating can contain up to 60 % of oxides [3], i.e. the layer deposited is practically composed of cermet. Besides, a metal coating, for example, aluminum one, can be hereinafter subjected to electrochemical processing with formation of the Al_2O_3 layer . As a result, the multilayer coating with a metal sublayer and ceramic surface is generated.

In this connection, we investigated a possibility of manufacture of coatings from metal wires by a method of electric arc metallization for the purpose of their further use for protection of details of the combustion chamber of internal combustion engines. As an adding material, the wires of aluminum and nichrome with a diameter of 1.8–2.2 mm were used.

Thermal conductivity, hardness, heat resistance, and structure of coatings are determined. To determine thermal conductivity, samples of 2.5–5 mm thick were sprayed. The thermal conductivity of "aluminum" coatings for density $(2.1–2.15) \cdot 10^3$ kg / m^3 in the temperatures range of 25–125° C was equal to 49 W·m^{-1}·K^{-1}, which is less than the value for pure aluminum (210 W·m^{-1}·K^{-1}) [4] by a factor approximately equal to four [4]. The thermal conductivity of "nichrome" coatings in the range of 25–150° C is equal to 4 W·m^{-1}·K^{-1}, which in 3–5 times is lower than for monolithic material (12–22 W·m^{-1}·K^{-1}) [4]. For comparison, the thermal conductivity of partially stabilized zirconium dioxide, recognized as one of the most perspective materials for protection of a working surface of the combustion chamber, is equal to 1

$W \cdot m^{-1} \cdot K^{-1}$ [5].

The microhardness of an "aluminum" layer depending on a procedure of metallizator ranges up to $(80-150) \cdot 10^7 \, N \cdot m^{-2}$, which is to two times more than [1] reports and considerably more than the hardness of annealed aluminum ($18.4 \cdot 10^7 \, N \cdot m^{-2}$).

An investigation on thermal shock was carried out with the specially manufactured samples. The coating of size of 160x30x5 mm was deposited on a plate of steel 20 kp at both sides (A and B). The thickness of coatings is presented in the Table.

Table

No. of a sample	Thickness of coating, mm	
	A	B
1	0.50-0.60	0.20-0.30
2	0.30-0.35	0.15-0.25
3	0.40-0.45	0.20-0.30
4	0.70-0.80	0.25-0.35

The essence of the technique of tests was that the samples were subjected to heating in the furnace from a cold state, to endurance within 20 minutes at temperature of 600° C, and further to cooling in water at temperature of 18° C for all the samples.

It is found that after 348 tests cracks appeared on the A sides of all four samples (thickness of the coating on the side A was more than on the side B by a factor approximately equal to 2–3). Thereafter the number of tests was enlarged up to 446, however for all the samples cracks in the coatings did not form on the sides B and any mechanical damages (exfoliation, increase in number of cracks, etc.) were not revealed on the sides A.

The analysis of metallographic investigation shows that pores, cracks, and exfoliations of coatings from substrates are not revealed in the transitional zone "substrate material–coating". The observable cracks in coating after tests on thermal shock do not result in "peeling" of coating and do not reduce an adhesion of coating with a substrate.

Except for the listed investigations, the Institute together with the engine-repair enterprises carry out works on deposition of anticavitation coatings on the outside of sleeves of cylinders of internal combustion engines by a method of electric arc metallization.

At present the tests of erosion of coatings of powder wire PP-MM-63 and PP-TP1 on cavitation stability under operating conditions of engines are conducted.

References

1. M.D. Nikitin, A.Ya. Kulik, I.I. Zakharov. Heat Protection and Wear-resistant Coatings of Details of Diesels, Leningrad (1974).
2. Scientific and Technical Report, State Registration No. NIOKR 1994499, Minsk (1995).
3. A. Khasui, Sputtering Engineering, Moscow (1975).
4. I.K. Kikoin (Ed.), Tables of Physical Magnitudes, Handbook, Moscow (1976).
5. A.F. Ilyushchenko et al., Heat Protection Coatings Based on ZrO_2, Scientific Research Institute of Powder Metallurgy, Minsk (1998).

EXPERIMENTAL INVESTIGATION OF TEMPERATURES INFLUENCE ON PROCESSES IN THE RAMMING PASTES AT THE ALUMINIUM ELECTROLYSER BAKING MODE

Shilovitch Tanyana

National Technical University of Ukraine "Kiev Polytechnical Institute", Resources-Economy Technique Research Center, Kiev, Ukraine

Modern aluminium cell cathode lining designs are based on prebaked carbon bottom blocks with joints between individual bottom blocks. Joints seald with a carbonaceous ramming paste. Cold ramming paste (CRP) is a composite carbon material. It is used at the aluminium electrolyzer cathode manufacturing. In fact, burning is the most important step of electrolyzer cathode preparing before it will be put into operation at high temperatures (about 1000°C) as well as upon corrosive medium (such as the electrolyte, melted aluminium).

During burning a CRP carbonization is occurred, at that a cathode becomes a solid structure. Burning temperature impact on the carbonization process was investigated in [1, 2]. Typical temperatures of the basic carbonization steps are ranged:

1 stage: 20 - (200...220)° C - a binder softening of the cold ramming paste, evaporation of the dissolved gases and a water as well as binder volatile fractions, a binder migration in the seal.

2 stage: (200...220) – 350° C – a process of the semi-coke structure forming which is completed with a CRP solidification;

3 stage: 350 - (450...500)° C – a semi-coke structure transformation into coke.

The most important in technology is the burning process second step which is completed with a semi-coke creation. To make a binder coke residuum greater could be possible by burning rate decreasing [3]. Therefore at burning drawing up development it is necessary to determine temperature boundaries of the second step.

In this research a gassing processes from ramming pastes samples produced by different manufacturers (conditional names A and B) research results (fig. 1) are represented. The gassing process mass rates plots

analysis shows the second step is determined by the following temperature intervals:
- paste A – 250...330° C (fig. 1, a).
- paste B 230...300° C (fig. 1, b).
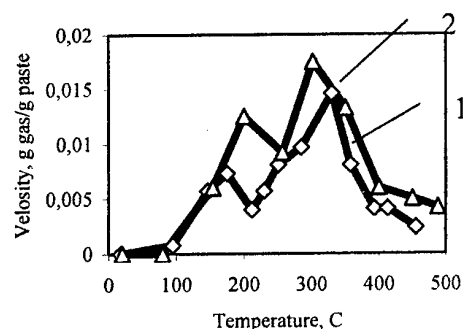
a) 1 – *1* °/min; 2 – *1,5* °/min;
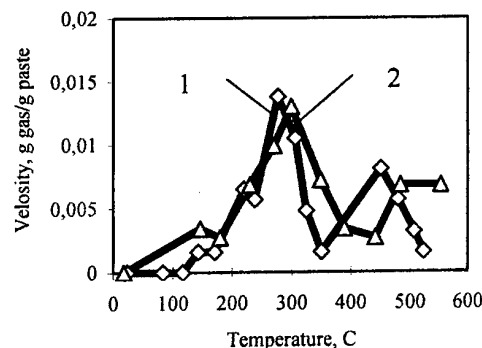
b) 1 – *1,3* °/min; 2 – *1,6* °/min

Fig. 1.

At the aluminium electrolyzer burning time-table development it is recommended to take into account results of ramming pastes coking investigation; namely to make heat flux rate rather lower during semi-coke

formation. It will allow to raise a coke yield output from binding on 5 %.

Литература

1. Шилович Т.Б. Експериментальне дослідження впливу температури на процеси коксування набивної маси при обпаленні алюмінієвого електролізера. //Наукові вісті НТУУ «КПІ». № 6, 2000, - с.41-45.

2. Громов Б.С., Панов Е.Н., Боженко М.Ф. и др. Обжиг и пуск алюминиевых электролизеров// -М.: Руда и металлы. – 2000. – 336 с.

3. Чалых Е.Ф. Обжиг электродов. – М.: Металлургия, 1981. - 116 с.

SYNTHESIS AND PHYSICAL PROPERTIES OF LaYO3 ·YScO3 AT HIGH TEMPERATURES

V. Dubok, V. Lashneva

Frantsevitch Institute for Problems of Materials Science Ukraine, National Academy of Sciences, Kiev, Ukraine

Study of physical properties of complex refractory oxides attracts attention due to search of new oxygen ion conducting materials. The most essential of them are the oxides with perovskite like crystal structure, which have manifold electrical, magnetic, optical and other properties stipulated by their crystalline structure. Special kind of the compounds consists of inter rear earth or interlanthanoid oxides which are formed by two rare earth oxides (ORE). Owing to features of 4f electron shells of rare earth cations, availability of several degrees of oxidation and difference of their ionic radiuses exists a lot of capabilities to regulate physical characteristics of the interlanthanoid oxides.

The method to regulate gradually properties of the interlanthanoid perovskites consists in synthesis of their mutual solid solutions, i.e. synthesis of phases with three or more different rare earth cations. The synthesis and properties of solid solutions between $LaYO_3$ and $YScO_3$ are presented in this report.

Synthesis and properties of individual perovskites $LaYO_3$ and $YScO_3$ were studied earlier. It was described that their electrical conductivity σ is determined by the oxides' non-stoichiometric disordering and substantially depends on impurities concentrations. The impurities can both increase and decrease the value of electrical conductivity σ as well as activation energy E_σ.

In temperature range 900-1350 °C σ of the $LaYO_3$ and $YScO_3$ changes under the exponential law, at the partial pressure of oxygen $P_{O2} > 10^2$ Pa the electrical conductivity is predominantly nonionic of p-type. At $P_{O2} < 10^{-2}$ Pa the electroconductivities of the compounds are predominantly ionic.

To study properties of solid solutions on the basis of $LaYO_3$ и $YScO_3$ the samples were synthesized with composition $LaYO_3$ ·$YScO_3$ (1:1) and their electrical conductivity was studied vs. temperature (in the interval 700 -1550 °C) and vs. partial pressure of oxygen (from atmospheric pressure up to 10^{-15} Pa) in conditions, whenever possible close to a thermodynamic equilibrium with gas environment.

The technology of the samples manufacturing included continuous chemical coprecipitation of hydroxides La, Y and Sc from aqueous solutions of nitrates by ammonia solution, grinding of the precipitate and its calcination at temperature 1200 °C during 2-3 h to decompose the mix into oxides, repeated grinding of the obtained oxides, molding of the samples' green compacts by isostatic method in elastic rubber envelopes at pressure 400-500 MPa with preliminary vacuumization. The green compacts were calcined in air at temperature 1200 -1300 °C 2 h, then sintered in vacuum furnace at temperature 1750 - 1800 °C during 1 h, then annealing in air at 1300 °C not less than for 2 hours.

Open porosity of the samples were less than 0,5 %; a mean grain size - 6 - 7 microns. Petrographic analysis reveals that the samples have optical inhomogenities and consist of the mixture (1:1) of optically isotropic and anisotropic phases.

Electrical conductivity were measured by 2 probe method at alternating current with frequency of 1500 Hz. Electrodes for measurements were burn-in on the samples with platinum paste at temperature 1200 °C. Partial pressure of oxygen P_{O2} in the camera for measurements were regulated by solid electrolyte ceramic pump made of zirconia stabilized by yttria ZrO_2 (8 mol.% Y_2O_3).

Results of measurement electrical conductivity of $LaYO_3$·$YScO_3$ vs. temperature in air are presented in tab. 1, and in the environments with controlled P_{O2} - in tab. 2.

Electrical conductivity of $LaYO_3$ ·$YScO_3$ vs. temperatures measured in air can be described by Arrhenius equation. In temperature range 1000 - 1550°C in Arrhenius coordinates it represents by straight line, and activation energy of electrical conductivity calculated from this plot is $E_\sigma = 1,5$ eV. Comparison of the electrical conductivity of the studied samples $LaYO_3$·$YScO_3$ with measured earlier σ $LaYO_3$ and $YScO_3$ reveals that σ $LaYO_3$ ·$YScO_3$ has intermediate value: it is above σ $YScO_3$, but is lower than σ $LaYO_3$ in the same conditions of measurement.

At temperature range 700 - 850 °C the conductivity $LaYO_3$ ·$YScO_3$ practically does not

depend on the oxygen partial pressure P_{O2}, thus testifies to predominantly ionic nature of electrical conductivity in such conditions.

The obtained results can be utilized for synthesis of new kinds of thermistors, sensors of oxygen and other high temperature ceramic sensors, as well as functional materials.

Table 1 – Results of measurement of electrical conductivity of $LaYO_3 \cdot YScO_3$, $LaYO_3$ and $YScO_3$ vs. temperature in air.

T °C	$LaYO_3 \cdot YScO_3$ σ, Ohm^{-1}×m^{-1}	$LaYO_3$ σ,Ohm^{-1}×m^{-1}	$YScO_3$ σ,Ohm^{-1}×m^{-1}
1000	$1,0 \times 10^{-2}$	$2,2 \times 10^{-2}$	$2,7 \times 10^{-3}$
1100	$2,8 \times 10^{-2}$	$6,3 \times 10^{-2}$	$8,7 \times 10^{-3}$
1200	$6,6 \times 10^{-2}$	$1,6 \times 10^{-1}$	$2,5 \times 10^{-2}$
1300	$1,4 \times 10^{-1}$	$3,3 \times 10^{-1}$	$6,0 \times 10^{-2}$
1400	$2,6 \times 10^{-1}$	$6,3 \times 10^{-1}$	$1,3 \times 10^{-1}$
1500	$4,0 \times 10^{-1}$	$1,2$	$2,8 \times 10^{-1}$
1550	$6,3 \times 10^{-1}$		

Tab.2. - Isotherms of electroconductivity σ of $LaYO_3 \cdot YScO_3$ vs. oxygen partial pressure P_{O2}

T °C	P_{O2}, Па	σ, Ом$^{-1}$×м$^{-1}$
700	$1,66 \times 10^4$	$4,0 \times 10^{-4}$
	$1,0 \times 10^2$	$4,0 \times 10^{-4}$
	$1,0 \times 10^{-5}$	$4,0 \times 10^{-4}$
	$1,0 \times 10^{-10}$	$4,0 \times 10^{-4}$
	$1,0 \times 10^{-15}$	$4,0 \times 10^{-4}$
750	$1,66 \times 10^4$	$5,8 \times 10^{-4}$
	$1,0 \times 10^2$	$5,8 \times 10^{-4}$
	$1,0 \times 10^{-5}$	$5,8 \times 10^{-4}$
	$1,0 \times 10^{-10}$	$5,8 \times 10^{-4}$
	$1,0 \times 10^{-15}$	$5,8 \times 10^{-4}$
800	$1,66 \times 10^4$	$9,6 \times 10^{-4}$
	$1,0 \times 10^2$	$8,7 \times 10^{-4}$
	$1,0 \times 10^{-5}$	$8,7 \times 10^{-4}$
	$1,0 \times 10^{-10}$	$8,3 \times 10^{-4}$
	$1,0 \times 10^{-15}$	$8,3 \times 10^{-4}$
850	$1,66 \times 10^4$	$1,6 \times 10^{-3}$
	$1,0 \times 10^2$	$1,3 \times 10^{-4}$
	$1,0 \times 10^{-5}$	$1,3 \times 10^{-4}$
	$1,0 \times 10^{-10}$	$1,2 \times 10^{-4}$
	$1,0 \times 10^{-15}$	$1,2 \times 10^{-4}$

KINETIC OF PYROCARBON DEPOSITION ON CONTINUOUS SIC FIBERS

Silenko P.M., Shlapak A.M.
Frantsevich Institute for Problems of Materials Science of Ukrainian National Academy of Science,
Kyiv, Ukraine

Continuous silicon carbide fibers are obtained by chemical vapor deposition (CVD) method and are used mainly as reinforcement for composites with metal and ceramic matrices. Such composites can service at temperatures up to 1273K and higher. Reliability of work of such composite products depends on fiber-matrix interface interaction essentially.

Rresearches carried out before are showed that for prevention of interaction (or for it essential decreasing) reinforcing SiC fibers with carbides, borides and nitrides of refractory metals and pyrocarban coatings are successfully used [1- 3].

With the purpose of choice of the most suitable composition (from a point of view of least temperature of pyrocarbon synthesis) in this work performance we carried out the following:

(a) thermodynamic analysis of pyrocarbon deposition reactions from some hydrocarbons (acetone, toluene, methane, n-geptan and tetrachloride of carbon);

(b) experimental determination of pyrocarbon deposition rate from indicated above composition on SiC fibers;

(c) determination of activation energy of pyrolysis of specified above combinations.

Thermodynamical analysis allows to determinate a conditions of probable progress of reactions in gaseous phase. As base of thermodynamic analysis is values of Gibbs free energy of reactions (1) in temperature range 500-2000K :

$$C_xH_y \rightarrow xC+yH \qquad (1)$$

Since the reactions of pyrolysis of hygrocarbous take place at high temperafures that dotation of changes of heat capacities of reactions components for temperafure dependence of Gibbs potential is insignificant and therefore we use admission ΔCp=const. in our calculations. Then

the equation for determination of ΔG_T value becomes the forms:

$$\Delta G_T = \Delta H^\circ_{298} - T\Delta S^\circ_{298} - (\Delta C_p)_{298}TM_o \qquad (2)$$

$$\text{where} \quad M_o = \ln\frac{T}{298,2} - 1 + \frac{298,2}{T} \qquad (3)$$

ΔG_T values for investigated hydrocarbons was calculated wit the formula (2). Obtained results for temperature range 500-2000K are showed in figure.

ΔG_T, kJ/mol
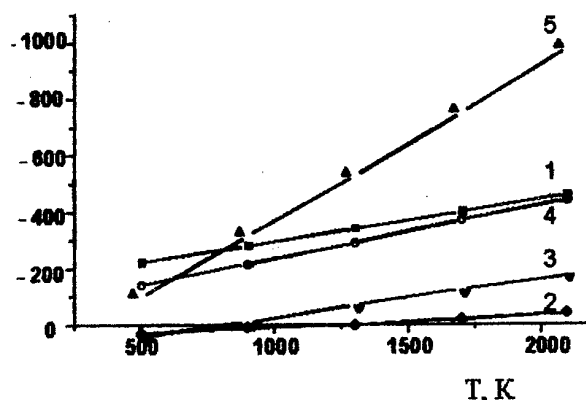
Figure. Dependence of a Gibbs free energy of temperature for pyrolysis reactions of hydrocarbons: 1-C_7H_8, 2-CH_4, 3-CC_4, 4-(CH_3) 2CO and 5-C_7H_{16}.

As will be seen from the obtained data most favorable substances, from a point of view of lower pyrolysis temperature, is n-geptan and toluene, least favorable - methane and tetrachloride carbon.

Experimental definition of rate of a pyrocarbon deposition was conducted on such procedure. The carrier gas argon was sated with pairs of hydrocarbons in glass a bubbler, which was placed in a calorstat at temperature 293K and then inputed in the chamber of pyrolysis. In the pyrolysis chamber a silicon carbide fiber was heated by an electric current, which was connected

shutters. Measuring of temperature of a silicon carbide fiber was conducted by an optical micropyrometer OMP-054. The time of a presence of a fiber in a reactor was 5, 10, 15, 20 and 25 seconds. A pyrocarbon was deposited on a fixed silicon carbide fiber. Thickness and surface quality of pyrocarbon, obtained at different temperature-time parameters, measured by an optical microscope MIM-8. It is determinated that optimum temperature range of a pyrocarbon deposition from various hydrocarbons is 1673-1773K. The coatings obtained at lower temperatures had small thickness (less than 0, 1 micron) and at higher temperatures of a deposition occured degradation of silicon carbide fiber that is intolerable from a point of view of further use of a fiber as reinforcing phase of composites. Obtained dependences of thickness of a pyrocarbon layer on time at temperatures 1673K and 1773 K have shown, that the greatest rate of a pyrocarbon deposition takes place at pyrolysis of a toluene and n-geptan, and least - at pyrolysis of methane and carbon tetrachloride. The pyrocarbon deposited from a toluene and n-geptan were dense, with an equal smooth surface and fine grained structure.

It was interesting also to determinate values of an activation energy for pyrolysis reactions of investigated substances.

According to paper[4] for determination of an activation energy it is enough to measure a time of deposition of pyrocarbon layer that have the same thickness at two different temperatures:

$$E_a = \frac{4{,}575 T_2 T_1}{T_2 - T_1} \lg \frac{1/\tau_{T2}}{1/\tau_{T1}} \qquad (4)$$

where τ_{T_2} - time of obtaining of a coating at temperature T_2;

τ_{T_1} - time of obtaining of a coat at temperature T_1;

Date of temperatures T_1 and T_2 was found experimentally.

The results of calculation of date of activation energies for all investigated substances are shown in the table.

Table. Date of activation energies for investigated types of reactions

#	Type of reaction	E_a, kJ/mol
1	$C_7H_{16} \rightarrow 7C + 8H_2$	36
2	$C_7H_8 \rightarrow 7C + 4H_2$	72
3	$(CH_3)_2CO \rightarrow 3C + 2H_2 + H_2O$	78
4	$CCl_4 \rightarrow C + 2Cl_2$	171
5	$CH_4 \rightarrow C + 2H_2$	398

As we can see from the obtained data, the greatest values of an activation energy are obtained at pyrolysis of methane and tetrachloride of carbon, least - at pyrolysis of n-gektan and toluene, that is coordinated well with the kinetic data of pyrolysis of these substances.

Conclusion
1. The thermodynamical analysis of obtaining of pyrocarbon from carbon substances in wide temperature range is carried out.
2. The greatest velocity of obtaining of pyrocarbon takes place at pyrolysis of a toluene and n-geptan, and least at pyrolysis of methane and carbon tetrachloride.
3. The activation energies of reactions of pyrolysis C_7H_8, C_7H_{16}, $(CH_3)_2CO$, CCl_4, and CH_4 are determinated.

References
1. Ning X.J., Pirouz P., Lagerlof K and DiCarlo J. The structure of carbon in chemically vapor deposited SiC monofilaments//J. Mater. Res., Vol. 5, No. 12 .-1990.-P.2865-2876.
2.Choy K.L. Effect of surface modification on the interfacial chemical stability and strength of continuous SiC fibers after exposure to molten aluminum//Scripta Metallurgica et Materialia, Vol.32, No.2.-1995.-P.219-224.
3.Silenko P., Shlapak A., Upadhyaya D. and Froes F. Hf and Zr carbide barrier layers for Sic/Ti-MMCs/ in International conference "Novel processes and materials in powder metallurgy".-Kiev.-1997.-P.254.
4. Emanuel N.M. and Knore D.H. Chemical kinetic, High school, 1969, 432 p. (in Russian).

THE RECEPTION OF WEAR-RESISTANT STEEL COMPOSITES AT THE EXPENSE OF CARBIDE PHASES FORMATION FROM MATRIX PCEUDO-ALLOY

Baglyuk G.A., Pozniak L.A., Gumeniuk S.V.

Institute for Problems of Materials Science NAS of Ukraine, Kiev, Ukraine

The application of a new class of too materials - carbide steels allows both to increase wear resistance of cutting, forming and other tool and constructional parts that are working in conditions of friction, and to save expensive alloying elements.

At the same time, traditional technology of carbide steels reception by liqid phase sintering of a mix of titanium carbide and steel powders is characterized by presence of such problems, as unsatisfactory wetting of titanium carbide particles by alloys of iron owing to presence of oxygen films on a surface of TiC grains and th phenomenon of active growth of a carbide phase grains during liqid phase sintering .

Developed in IPM technology largel eliminates the specified problems at the expense of use as initial materials powders of titanium and graphite instead of titanium carbide. Sintering of the samples, pressed from such mixes at 1180-1200^0 C is accompanied by occurrence in Fe-Ti system low temperature eutectic with subsequent its interaction with particles of graphite and formation titanium carbide grains.

The research of sintered material structure has shown, that the optimum contents of carbon in initial mix may be estimated according t reception of titanium carbide, appropriate to meaning $TiC_{0.8}$, that provides the reception of free carbon minimal contents in a sintered pceudo-alloy.

The further application of hot deformation of sintered porous preforms (extrusion, forging) allows to achieve high relative density of carbide steel with fine structure of a material owing to use lower sintering temperature in comparison with common liqid phase sintering. At the same time, the formation of TiC from a matrix alloy provides durable adhesive connection of a steel matrix with TiC particles .

The annealing of forged preforms with TiC contents up to 20 % (weight) gives an opportunity of realization of material machining by a hard alloy tools, and optimum modes of heat treatment (hardening and tempering) chosen according to chemical structure of steel and TiC contents , allows to achieve hardness of material up to 85-88 HRA.

References

1.Komac M., Novak S. Mechanical and wear behaviour of TiC cemented carbides // Int. J. Refract. and Hard Metals. -1985. -Vol.4, №1. -P.21-26.
2.Weber J. Cutting-drawing-forming and bending with steel-bonded titanium carbide // Sheet Met. Ind. - 1981. -Vol.58, №4. - P.270-276.
3.Gurievitch Ju.G., Narva V.K., Frage N.R. Karbidostali. M.: Metallurgia, 1988. -144 p. (in Russian).
4.Kiubarsepp J. Tviordie splavi so stalnoi sviazkoi. Tallin: Valgus, 1991. - 164 p. (in Russian).

213

STUDY OF DENSITY AND STRUCTURE OF Mo-(30-70)%TiC COMPOSITES PRODUCED BY SINTERING AND HIGH-ENERGY PRESSING

Laptev A.V.

Institute for Materials Science Problems of UNAS, Kiev, Ukraine

Refractory metals of VA and VIA groups of the Periodical System of the Elements as well as composites based thereon are the most potential materials to be used under extreme conditions. Among the above refractory metals of said groups, molybdenum is of interest because its melting temperature is among the highest ones, i.e. 2890 K [1] and it is not among the very scarce materials. The capability of refractory metals to withstand extreme impacts is a positive feature in operation, however, this feature makes the production process of semi-products of tungsten or molybdenum more complicated and energy consuming. Besides, conventional methods of making items are unable to tailor an ultrafine-grained structure, furthermore, restrict possibilities of preparing dispersion-strengthened materials containing a high volume of ultrafine strengthening particles. Said shortages can be avoided through the use of advanced powder metallurgy techniques. One of these is high-energy hot pressing under vacuum, which provides pressing for heated powder bodies under high pressures of up to 1500 MPa with a relatively high strain degree and strain rate. Some success in this method application was yet attained when compacting of submicron-size powder of molybdenum [2]. In particular, it was shown that specimens with insignificant porosity can be prepared at a low temperature, however, a high tendency of wrought molybdenum to recrystallization allows no possibility for retention of the fine-grained structure. One of efficient method of inhibiting of the recrystallization up to 0.5-0.9 Tmelt, and also increasing of the material heat resistance is the reinforcing it with refractory fine-grained particles [3]. Titanium carbide was chosen as reinforcing phase for this study as in the Mo-TiC system, an enhanced mutual solubility of elements can be observed. This must contribute an improved shrinkage of composite during sintering, and formation of a more strong interphase boundary. Three compositions were taken to study the compacting process, each having volume content of titanium carbide of 30, 50 and 70 %,

respectively. The composite with lower TiC content had composition nearing that of Mo-Ti-C (28.7 vol.% TiC) eutectic alloy and belonged to the class of dispersion-strengthened materials, while the composite with higher content of carbide particles corresponded to the class of hard alloys. Powder mixtures of said composites were prepared by grinding of Mo and TiC commercial powders in a ball drum. The grinding was in acetone for 72 hours with 9:1 ratio of ball to powder mass. The grinding yielded fine-grained powder mixtures. The average particle size as measured by the mercury porometry method was 0.3-0.5 μm. The prepared mixtures were used to produce green briquettes at room temperature and the 100 MPa pressure without use of any plasticizer. The green briquettes had initial density of 55 %, 40 %, and 45 %, respectively for composites with 30, 50, and 70 vol.% of TiC. The briquettes were compacted at 1300, 1500 and 1700 °C by two methods of sintering and high-energy pressing. Isothermal holding duration of the sintering and before pressing was 20 min. The sintered and pressed compacts were cut to produce rectangular bars useful for measuring of the structure density and properties. The measured densities of composites under study are shown in Fig. 1. The composite
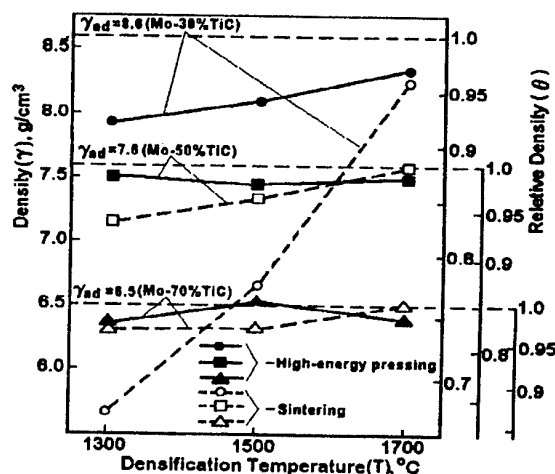
Fig.1. The density of Mo-(30-70)% TiC composites versus densification temperature in sintering and high-energy pressing

compacting behavior is dependent both on the content of titanium carbide and compacting method. At low temperature, the greater tendency for shrinkage at sintering was exhibited by the Mo-70%TiC composite, the density of which reaches the value of 96 % at 1300 °C. The Mo-50%TiC composite is also prone to prompt compacting as, at T=1300 °C, its density is ≈95 %. The most hardly compactable are specimens of the Mo-30%TiC composite. The latter have the 66 % density at the above temperature, however, their initial density was 55 %. The temperature rise up to 1700 °C yields practically poroless composites with 50 or 70 % of titanium carbide, whereas the composite with 30 % of TiC has porosity of about 5 % . In contrast with the above art, another situation is with the high-energy pressing. High pressure applied to sintered specimens provides a noticeable increase of the density only on a low carbide composite. High content of carbide phase (≥50 %) in the Mo-TiC system reduces the efficiency of press treatment. Further more, the Mo-70% TiC composite produced by pressing at 1700 °C exhibited reduction of the density in comparison with that of sintered specimens. This indicates that composites containing very high volume of carbide phase are rather brittle even at 1700 °C and the applied pressure causes macro- and microfractures.

The strength characteristics of resultant specimens were tested at room temperature by three-point bending. It should be noted that specimens fracture without a noticeable plastic deformation in all cases. An increase of green compact consolidation temperature caused increased bending strength. Maximum values of transverse rupture strength, σ_b=1000-1200 MPa, achieved on the Mo-30% TiC composite produced by high-energy pressing at T=1700 °C. The sintered specimens of this composites have the 300 MPa bending strength due to residual porosity (ref. above). Increased volume content of the carbon phase deteriorates the specimen strength characteristics. The strength of Mo-50% TiC and Mo-70% TiC composites is at the 600-500 MPa level, further more, in high TiC composites, the strength is reached rather through sintering than pressing.

The fracture surface of Mo-(30-70) TiC composites was examined by scanning electron microscopy in dependence on the temperature of pressing and shown in Fig. 2. As can be concluded from the photos of structures: i) the structure is

a   b
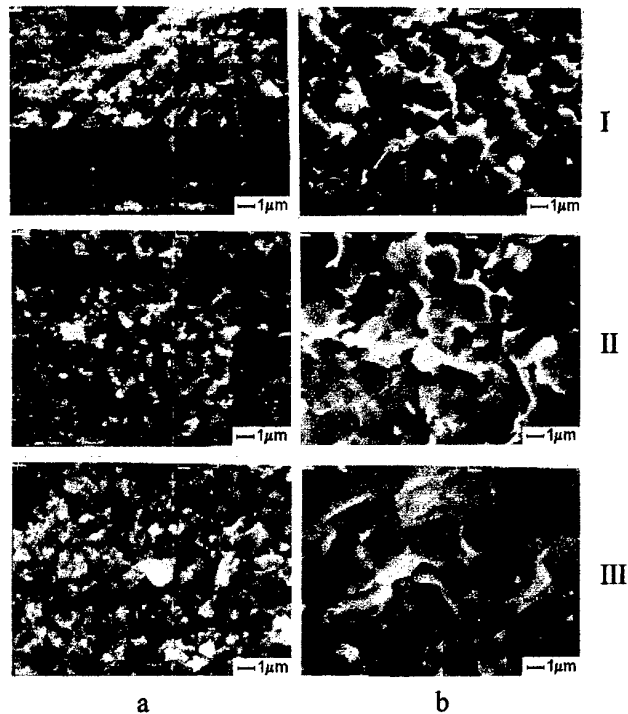
Fig.2. The fracture surfaces of Mo-30TiC (I), Mo-50TiC (II) and Mo-70TiC (III) specimens obtained by pressing at 1300 °C (a) and 1700 °C (b).

coarsening with consolidation temperature, and ii) particles in high TiC composites are growing more intensively. Thus, as a preliminary estimation of particle sizes shows, a rise of temperature of sintering for the Mo-70% TiC composite from 1300 °C to 1700 °C causes particle to grow by 4 to 6 times, i.e. from 0.3-0.5 μm to 2.0-3.0 μm. In the Mo-30% TiC composite, there is no visible particle growth up to the sintering temperature of 1500 °C, while at 1700 °C, the particles have sizes of around 1.0 micron. A distinguishing feature of the composite under study comparing with other two-phase materials such as WC-Co hard alloys implies that the dissolution of metallic phase in carbide phase prevails the reverse dissolution. This phenomenon is discussed in the report to highlight the mechanism of particle growth of composite of the Mo-TiC system and to compare this mechanism with that of WC particle growth in cobalt.

References

1.The Properties of Elements. Part 1. Physical Properties. Edit. G.V. Samsonov, M.: Metallurgy, 1976.-600p. (Rus)
2.Laptev A.V. Potential of the method of high-energy hot pressing under vacuum to produce materials with ultrafine structure and high strength. Powder metallurgy, 2001.-N3-4.-p.8-19 (Rus)
3.Trefilov V.I., Moiseev V.F. The Dispersed Particles in Refractory Metals.-Kiev: Naukova dumka, 1978.-240p.

BRAZING JOINTS OF CONSTRUCTION CERAMICS TO METALS

<u>Moskalenko S.A.</u>, Durov O.V., Kostyuk B.D., Naidich Y.V.

Institute for the Materials Science Problems of National Academy of Sciences of Ukraine, Kiev, Ukraine

Ceramic to metal joining is important technical problem, the brazing by metal filler is one of the most extensively used method of its solving.

In this work the processes of formation of such joints and its properties are considered.

The ceramic based on ZrO_2 partially stabilized by 3% Y_2O_3, bend strength near 400 MPa and thermal expansion coefficient (TEC) $\sim 9 \times 10^{-6}$ K^{-1}, and Si_3N_4 hot pressed ceramic with bend strength $\sim 700 - 800$ MPa and thermal expansion coefficient $\sim 2.5 \times 10^{-6}$ K^{-1} were studied.

To elaborate the brazing technology two problems have to be solved:

1) high wetting of the ceramic by melt filler;
2) decreasing or removing of stresses arising due to difference of the thermal expansion between ceramic and metal in the joint.

To provide the necessary wettability high chemical active additions of titanium or zirconium in based on copper or silver brazing fillers were used. The number of brazing fillers compositions based on the copper and its alloys ensured low enough values of contact angles were elaborated [1, 2].

The data for some composition are represented in table 1.

Table 1. Contact angles (degrees) for wetting of ceramic by brazing fillers at 1150 °C in vacuum

Filler \ Ceramic	Cu-Ga	Cu-Ga-Ti	Cu-Ga-Zr	Cu-Sn-Ti	Cu-Sn-Pb-Ti
ZrO_2	130	60	40	–	–
Si_3N_4	135	15	–	15	<10

Cu-Ga-Ti, Cu-Ga-Zr and Cu-Sn-Pb-Ti melts were used for brazing of ceramics.

For ZrO_2 ceramic after the addition of titanium or zirconium to the Cu-Ga melt contact angles still were not low enough (60° and 40° respectively). So the additional covering of the ceramic by the layer of titanium powder was used, the full spreading of brazing melt was realized on it. Si_3N_4-ceramic was brazed by Cu-Sn-Pb-Ti filler.

The problem of thermal stresses lowering was solved by different ways for every sort of ceramics.

For joining to ZrO_2-ceramic the forgeable cost iron was selected because its TEC is close to that for ceramic (10×10^{-6} K^{-1}).

Taking into consideration possibilities of wetting by the Cu-Ga-Ti and Cu-Ga-Zr filler of the ZrO_2, for it brazing the method of impregnation of titanium powder layer by melting filler was applied.

The brazing procedure was carried out in high vacuum at 1150 °C.

The Si_3N_4-ceramic has especially low value of TEC, and it is difficult to choose the metal with such low TEC in wide temperature range.

The lowering of thermal stresses may be achieved by a few ways: using of the ductile laying between joined materials, application of the metal laying with low TEC values (Mo, W), use of interlayer with high deformation, fabricated for example in spiral shape. The volume changes due to phase transformations of one of the joined material also may be used.

Japanese researchers [3] have used steel with composition (Fe, Cr3, Ni3, Mo0.5, Mn0.4, C0.3) for brazing of Si_3N_4-ceramic and have obtained the joint strength ~ 250 MPa when the Ag-Cu-Ti filler was used. The strength characteristics was measured on single samples by shear method.

In this work Si_3N_4-ceramic to metal joints were obtained:

a) with elastic copper layering
b) with application of steel analogous to [3] as the metal part of joint. The aim was to study in detail the bend strength characteristics of joints use statistic analyze.

The Cu-Sn-Pb-Ti without any noble metals filler was used in both variants ("a" and "b"). The Invar was used as the metal part of joint for "a" variant (TEC $\sim 13 \times 10^{-6}$ K^{-1}).

The brazing procedure was carried out in high vacuum at 950 °C.

The shear strength of obtained ZrO_2-ceramic to cost iron joints was tested on special device. The average strength of joint was about 250 MPa,

maximal — 330 MPa, minimal — 200 MPa. The statistic processing of obtained results use the Weibull theory was carried out. The Weibull plot for this joints is represented on Fig. 1, Weibull coefficient m = 6.5.

The samples of joints by the capillary impregnation of the copper-gallium melt through the zirconium powder layer were also fabricated. The average strength of joint was about 260 MPa, maximal — 292 MPa, minimal — 220 MPa. The Weibull plot for this joints is represented on Fig. 2, Weibull coefficient m = 11.3.

The bend strength of Si_3N_4-ceramic / copper / Invar joints was about 110 MPa (the copper layering width was 1 mm), failure occurred through the ceramic. The results are represented in Table 2.

Table 2. The band strength of Si_3N_4-ceramic / copper / invar joints

№ of sample	1	2	3	4	5	average strength
strength, MPa	100	110	108	105	104	105

The bend strength of Si_3N_4-ceramic / special steel joints was studied in detail use the Weibull statistic. Results are represented as the plots on Fig. 3. The failure occurred through the ceramic near the interface. The average strength of the joint is about 220 MPa, maximal — 242 MPa.

The investigation of the special steel thermal expansion shows such peculiarity: in 300 – 400 °C range the sample size increase is observed. It take place due to martensitic transformation, so the common TEC of steel from 900 °C to room temperature is ~8 – 10×10^{-6} K^{-1}.

When analyzing of obtained results conclusion was done that thermal expansion coefficients difference of joined materials significantly influence ceramics / steel joint strength. Also one can marc, that the martensitic transformation in the steel leads to volume change and lower TEC in low temperature region (martensitic transformation region (start at 350-400°C)) is especially favorable, because the ductility of materials (metal base, filler) is low, and high TEC in this temperature region will lead to large stresses in the joint.
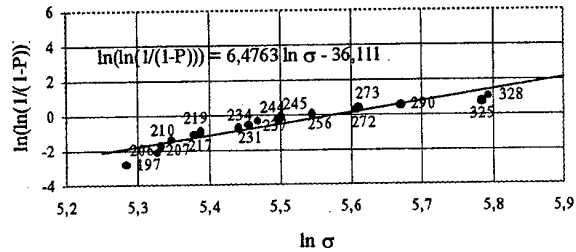
Figure 1. The Weibull plot for shear strength of ZrO_2-ceramic to forgeable cost iron joints, brazed by capillary infiltration of Cu-Ga through the Ti powder.
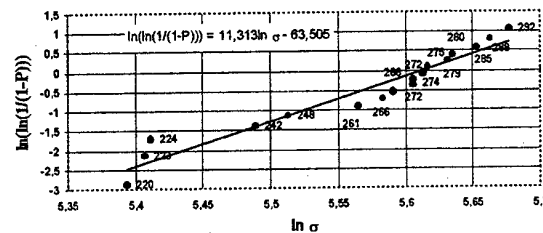
Figure 2. The Weibull plot for shear strength of ZrO_2-ceramic to forgeable cost iron joints, brazed by capillary infiltration of Cu-Ga through the Zr powder.
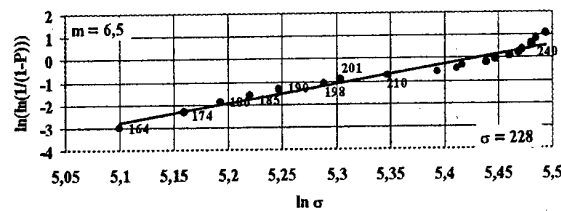
Figure 3. The Weibull plot for bend strength of Si_3N_4-ceramic to special steel joints.

1. Ю.В.Найдич, И.А.Лавриненко, Г.А.Колесниченко, В.С.Журавлев. Поверхностные свойства расплавов и твердых тел и их использование в материаловедении.— Киев: Наук. думка.— 1991.—280 с.
2. А.В.Дуров, Б.Д.Костюк, В.А.Мельникова, Ю.В.Найдич. Исследование смачивания и контактного взаимодействия диоксида циркония с припоем состава Cu-Ga-Ti // Адгезия расплавов и пайка материалов.— 1999.
3. Y.Matsuo, M.Ito, M.Taniguchi. R&D Center, NGK Spark Plug Co. Ltd. Ceramic-metal Joining for automobiles // Industrial Ceramics № 3 volume 19.—1999.

Si$_3$N$_4$-SiC-AlN and SiC-AlN BASED COMPOSITE MATERIALS at EXTREMAL SOLAR ENERGY AFFECT

Lyudvinskaya T.A., Panasijuk A.D., Neshpor I.P., Subbotin V.I.
Institute for Problems of Material Science, National Academy of Science, Ukraine, Kiev.

Composite ceramic materials based on Si$_3$N$_4$-SiC-AlN and SiC-AlN systems have high level of physic-mechanical properties and rather high oxidation resistance.

The investigation of influence of solar radiation at Si$_3$N$_4$-SiC-AlN and SiC-AlN system composite materials is the aim of this work. Using of solar heating is unique possibility for investigating of such influence on material due to the possibility of achievement of high temperatures (3000°C) in the air, one side and easy regulated non inertial heating. Surface heating of ceramic composites at solar energy affect in the air allows to determine high temperature corrosion resistance of the material and possibility of making up the new surface structural formations. It makes possible to obtain gradient materials with new complex of properties. Experiments were carried out by using solar furnaces of Institute for Problems of Material Science, Ukraine with concentrators of 4-8 mm. Different regimes of heating were used with both different angle of opening of curtain and time of acting at full opened curtain. The heating temperature and heating stream were measured at heating zone.

The investigated specimens were obtained by hot pressure method at temperature range 1750-1800°C and pressure 35 MPa from SiC-AlN and Si$_3$N$_4$-SiC-AlN composite powders. The composite powders were obtained by original technology of simultaneous formation of Si$_3$N$_4$, AlN and SiC phase at carbothermal reduction of corresponding oxides in nitrogen flow. This method allows to obtain powders of high purity, given composition and ratio.

The rayed specimens were investigated by TG, DTA, XRD, EPMA and matellographic analyses methods.

It has been established by TG and DTA methods for AlN-SiC ceramics that both 80%AlN-20%SiC and 50%AlN-50%SiC composition have extremely high corrosion resistance in air (fig. 1). At short times of exposure in air and at comparatively low temperatures, β-cristobalite and aluminum oxynitride proved to be the main oxidation products while at longer oxidation and higher temperatures (1350-1550°C), 3Al$_2$O$_3$·2SiO$_2$ (mullite) is the main interaction product.

The dense scale formed on 80%AlN-20%SiC ceramic is characterized by heterogeneous structure according to XRD and EPMA analyses data identification of Al, Si and O corresponds to 3Al$_2$O$_3$·2SiO$_2$ and β-SiO$_2$ phases (fig. 2).

The comparative analyze of experimental date showed that practically all materials Si$_3$N$_4$-SiC-AlN and SiC-AlN systems at affect of solar radiation stream of 1500-1700°C Vt/sm^2 (2500°C) have high oxidation resistance. Formed thin oxygen film has high adhesion to the surface of Si$_3$N$_4$-SiC-AlN and SiC-AlN composites.

It is known that at oxidation in the air up to 1500°C of SiC-AlN system materials form mullite of 3Al$_2$O$_3$.2SiO$_2$ composition on their surface and plentiful oxygen, very often, in amorphous state, arranges on the outward surface. At the oxidation up to 1800°C at solar radiation stream affect the surface layer is removed and partial melting of oxygen film is observed.

Composite ceramics based on Si$_3$N$_4$-SiC-AlN system form more dense oxygen films which serve as distinctive barrier for oxygen diffusion inside specimen.
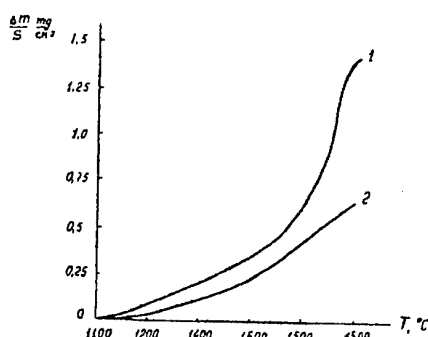
Fig. 1. Non-isothermal oxidation of AlN-SiC ceramics samples: 1 - 80%AlN-20%SiC; 2 - 50%AlN-50%SiC.
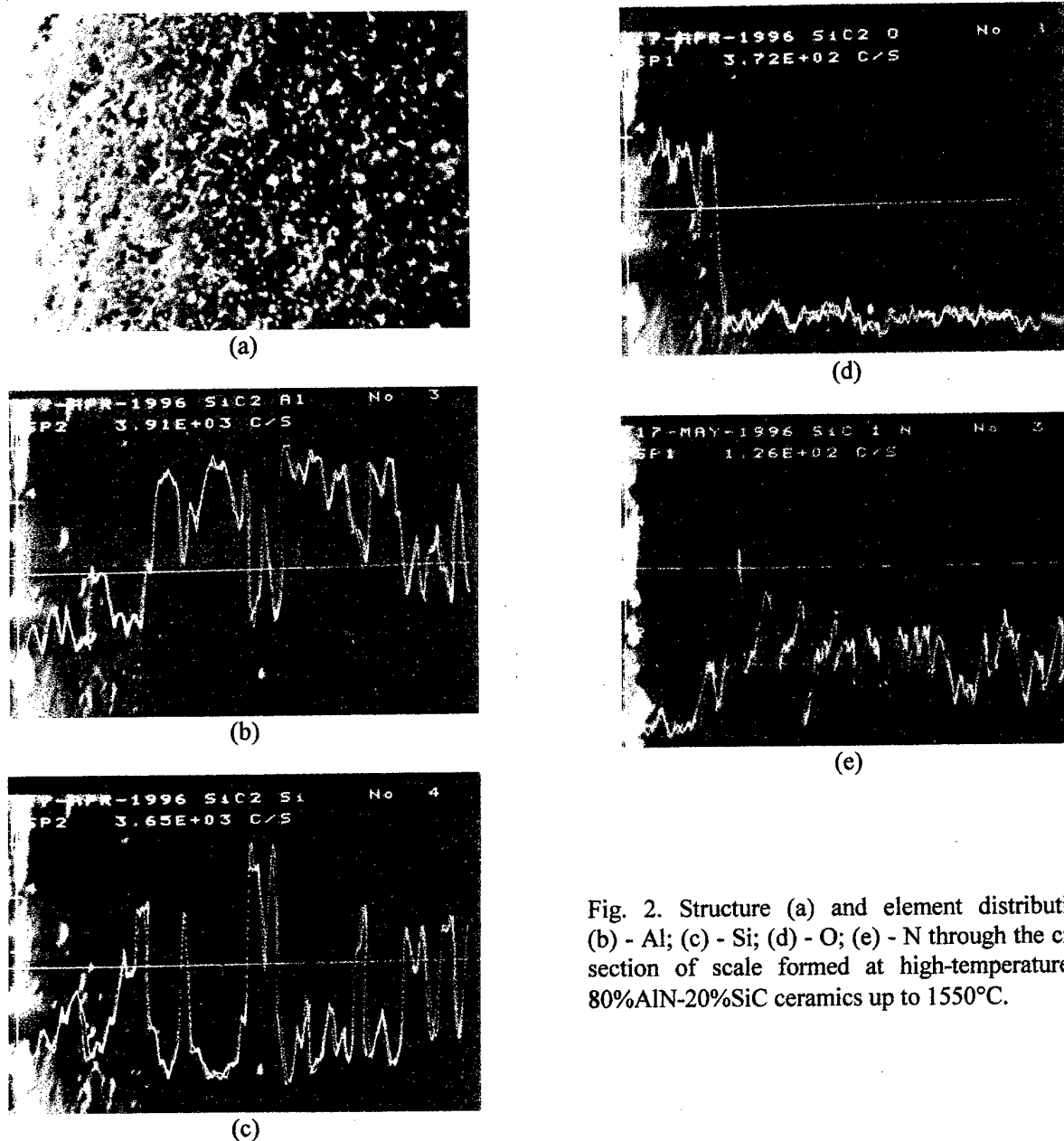
Fig. 2. Structure (a) and element distributions: (b) - Al; (c) - Si; (d) - O; (e) - N through the cross-section of scale formed at high-temperature on 80%AlN-20%SiC ceramics up to 1550°C.

Perspective technologies of reception of a powder of system Y-Ba-Cu-O, used for superconducting products.

Flis A.A.
Frantzevich Institute for Materials Science Problems NAS of Ukraine, Kiev, Ukraine

The intensive examinations, directional on reception of volumetric superconducting ceramic products and superconducting films, require considerable quantity single-phase HTS - high-temperature superconducting powder [1]. The greatest attention from all class HTS of materials is yttrium ceramics (compound $YBa_2Cu_3O_{7-\delta}$) [2,3].

The properties of any products fabricated by powder metallurgical techniques always depend on a method of reception of powders. To products from a HTS material many requirements are showed. The products should be made of a single-phase material. This most important requirement. After synthesis the mix should consist of 100 % HTS phases $YBa_2Cu_3O_{7-\delta}$, and the ratio of components should be Y:Ba:Cи = 1:2:3.

The purpose of the present research was the examination of an opportunity of reception single-phase HTS of yttrium powder at use of different methods of opening-up of mix material and operations.

The yttrium powders of HTS ceramics synthesized with use of three basic methods: ceramic, chemical, explosive squeezing. The superconducting targets for a pulse-laser deposition HTS epitaxial $YBa_2Cu_3O_{7-\delta}$ films were fabricated of the received powders.

Element charge makeup explored in chemical-analytical and spectral laboratories IPM NAS of Ukraine. A phase composition of yields of synthesis of compound $YBa_2Cu_3O_{7-\delta}$ determined by an X - ray method.

Powder of HTS yttrium ceramics received by a ceramic method.

After careful intermixing of initial components taken in required quantity (a) - oxides Y_2O_3, BaO. CuO; 6) - oxides Y_2O_3, CuO and salt $BaCO_3$; в) - oxides Y_2O_3, BaO and powder Cu) and repeated sifting, carried out preliminary synthesis of a charge in an interval of temperatures 150 - 200 °C or 400 °C during 4 - 16 h. Further annealing of mix material carried out at temperatures 400 - ≥ 800 °C during 4 - 24 h depending on temperature of annealing. Through everyone 4 h of annealing synthesized mix material repeatedly intermixed and sifted through a bolter. Thus, series of intermediate annealings and immixtures have allowed to receive a homogeneous powder with a

high yield ratio 85-100 % basic HTS phase $YBa_2Cu_3O_{7-\delta}$. The analysis of results of examination has shown, that for synthesis of a powder of a single-phase composition it is necessary to carry out treatment of initial mix material as a minimum in two stages. The first stage is necessary low-temperature - 400 °C and second - high-temperature >800 °C. Such mode of heat treatment can be given at use as initial components of yttrium, barium and cuprum oxides. The introduction barium in a mix material as salt $BaCO_3$ results in necessity of realization of an intermediate annealing at T - 600 °C. However even at realization of an intermediate annealing at temperature 600 °C collateral phases remain. The increase of temperature > 830 °C results in sintering a powder in a conglomerate. Is shown, that the process of a solid-phase sintering is labour-consuming. The infringement of operations gives in deterioration of reproducibility of experiment.

The yttrium powders of HTS ceramics received by a chemical method.

Taking into account chemical features of yttrium, the cuprum and barium, as initial builders used nitrates of yttrium $Y(NO_3)_3$, cuprum $Cu(NO_3)_2$ and hydroxyd of barium $Ba(OH)_2$, as cleaner and accessible compounds [4]. At reception of HTS powder $YBa_2Cu_3O_{7-\delta}$ by coprecipitation from a solution the important role is played by the used precipitating agent, as it should ensure dropout of nonsoluble precipitates, i.e. the deposition should be complete. Picking the precipitating agent, regarded its nature, pH of a solution, relative miscibility of a precipitate in medium, temperature, concentration reagents. The coproducts, generated as a result of response, of interaction should well be washed, and the stayed microimpurities should not worsen properties HTS of materials. Therefore as the precipitating agent the solutions hydroxyds of barium $Ba(OH)_2$ and kalium KOH were used. They provided a joint deposition of yttrium and cuprum as hydroxyds $Y(OH)_3$ and $Cu(OH)_2$. The optimum value pH for a complete deposition of cuprum as $Cu(OH)_2$, is equal 10, for a deposition of yttrium as $Y(OH)_3$ it is equal 7. After a deposition of yttrium and cuprum in received washed from intermediate yields of response a precipitate, inlet stoichiometric ratio of miscible

linking of barium as a water solution $Ba(OH)_2$ [4]. The received intermixture have steamed up to a thickening, dried up to a stationary value of mass, carried out the relevant heat treatment.

At use of the precipitating agent $Ba(OH)_2$ and at all temperature отжигах the secondary phases and microimpurities are always observed. The measurings of relative electroresistance R (T) have shown, that the microimpurities partially change a type of conductance with metal on semiconductor. Therefore use as the precipitating agent $Ba(OH)_2$ requires the relevant completion. The received intermixture have steamed up to a thickening, torrefied up to a stationary value of mass, carried out the relevant heat treatment.

At use of the precipitating agent $Ba(OH)_2$ and at all temperature отжигах the secondary phases and microimpurities are always observed. The measurings of relative electroresistance R (T) have shown, that the microimpurities partially change a type of conductance with metal on semiconductor.Therefore use as the precipitating agent $Ba(OH)_2$ requires the relevant completion. The precipitating agent KOH provides reception single-phase of HTS powder at heat treatment in an interval of temperatures $T = 700 - 920\ ^0C$ during t = 6 h.

The yttrium powders of HTS ceramics received by a method of explosive squeezing.

The initial burden constituents immixed in the ratio, ensuring ambassador of heat treatment formation of a superconducting phase $YBa_2Cu_3O_7$. $_\delta$, added condensed explosive substance (relation explosive substance and mix material – 6 : 1 or 3 : 2), molded charges by a diameter of 60 mm of blanket mass of 1,2 kg and blew up them in the strong metal chamber in medium of a coolant (water). After explosion the powders have separated in dewatering tanks and on a centrifugal machine, dried up in air medium at temperature $350\ ^0C$ during 0,45 - 1 h.

Optimum and restrictive concentration of a charge in explosive substance determined experimentally: bottom – 15 %, top – 40 %. The best conditions at explosive squeezing were pressures 11 - 12,5 GPa and temperature in an interval 3000 - 3300 ^{0}C.Is established, that during explosive compression of an initial powder mix the superconductive phase "«123" is not formed.

Therefore received powder have annealing on a many-stage mode: I a stage - T- 920 - 950 ^{0}C, t- 6 h, II a stage - T - 350 ^{0}C, t- 10 h.

At a shock compression of a powder the degree of bucking of particles raises, there is a

unsoundness of structure, the new not superconducting phases are formed. After heat treatment and saturation by oxygen these phases transfer in compound $YBa_2Cu_3O_{7-\delta}$.

The targets for a deposition of films were made of HTS yttrium powders, which were received by all by three methods. Temperature of superconductive transition - T_c and width of superconductive transition - ΔT_c were measured. In the present research is shown, that the selection relevant of initial components and realization of necessary operations allows to use all methods for reception single-phase of HTS yttrium powder, and, hence, of products from them with the following superconducting parameters: $T_c = 92 - 98\ K$, $\Delta T_c = 3 - 7\ K$. The researches of a kinetics of formation of phases have allowed to determine optimum conditions of heat treatment necessary for reception single-phase HTS of a powder with a phase $YBa_2Cu_3O_{7-\delta}$ (a phase "«123").

References

1. Попков А.Ф. Физические свойства и возможные области применения высокотемпературных сверхпроводников // Высокотемпературная сверхпроводимость. -1989. – N 1. – с. 5- 16.

2. Eab C.H., Tang I.M. The orthorhombic – tetragonal structural phase transition and effect on the T_c of the high temperature superconductors // Physica C. - 1991- 174,N1-3, - P.149 – 154.

3. Procceding of the workshop on chemical designing and processing of high - T_c superconductor / H.Komatsu, Y. Kato, S. Miyashita et al. // Ranazawa Japan, July 27 – 29, 1991 , 20с.

4. Оськина Т.Е., Третьяков Ю.Д., Кулаков А.Б. Твердофазные превращения и кислородный обмен в купрате иттрия – бария // Неорганические материалы . – 1989. – 25, N1.- С. 98 – 102

VACUUM-TIGHT LOW STRESSED WELDED
GLASS CERAMICS / METAL UNITS

Naidich Yu.V., Gab I.I., Kurkova D.I., Stetsyuk T.V., Abramov Ye.V.[(1)]
Frantsevich Institute of Materials Science Problems, NAS of Ukraine, Kiev, Ukraine
[(1)] State firm "Central design office "Arsenal", Kiev, Ukraine

In modern radio engineering, electronics and other areas of engineering brazed [1] and welded [2] metal/glass and ceramics/metal units are used for a long time and successfully. Glass ceramics materials find still greater application in laser devices and apparatus. Optical glass ceramics SO-115 M has the high optical and physic-mechanical characteristics, in particular, very low thermal expansion coefficient which remain stable in extreme conditions (repeated thermal cycling, sharp thermal shock, microwaves radiation etc.). It allows to widely use this material in the laser industry, frequently as single-piece brazed [3, 4] or welded joints with metals, in particular, with aluminium details. Severe requirements are imposed on glass ceramics/aluminium units prospective to application in new more perfect designs laser apparatus, in particular, high vacuum tightness of units (leakage not more $6,5 \times 10^{-12}$ Pa· m^3/s) and very low level of mechanical residual stresses in glass ceramics detail which require difference of rays path in polariscope no more than 25 nm. Besides this units heating during joining process up to temperatures higher then 400 ^{0}C is not permitted deterioration of the characteristics of an aluminium detail usually being the cathode. Thus, the application well-known technology of active nonmetals soldering with metals which requires heating of details being joined up to 600 ^{0}C and higher [5] is not usable in this case. Procedure of cold joining of nonmetallic materials with metals by pressure through indium gasket [6] is known but it gives very unstable results and does not provide sufficient vacuum tightness of unit.

This paper concerned with development of manufacture procedure of welded vacuum-tight glass ceramics/aluminium unit of the ring-type laser with a low residual stress level in glass ceramics detail at room temperature. This unit is the polished monoblock from glass ceramics SO-115 M 60x40x40 mm with internal cavity and output channel closed hermetically from the above by the aluminium cathode in 20 mm diameter and 20 mm height. As a solder we used high-plastic adhesion-active indium alloy. The developed process of the

joining of aluminium detail with glass ceramics one consist of two following stages:
1 - separate preliminary metallization of glass ceramics and aluminium details by indium solder;
2 - pressure welding of metallized details at room temperature.
Metallization of glass ceramics details was made by indium solder in vacuo at 600 ^{0}C [4] and aluminium details metallization was also by indium with the use of ultrasonic soldering iron at temperature not exceeding 200 ^{0}C.

Metallized indium layers on both details were subjected to mechanical clearing and processing to give them the appropriate form and then details were collected in appropriate technological equipment which keep their centring and mutual fixation and pressure welding process was carried out in vacuo on the special installation UTS-1 [7] at temperature 20 ^{0}C. Finished samples of units were tested on vacuum tightness, mechanical strength and presence of residual stresses in glass ceramics detail. The joints strength testing at a separation and shear have shown values of their strength close to indium strength especially, as the destruction happened just on indium interlayer.

Vacuum tightness of units was determined with the help of helium leakage-finder STI-11 by helium ventilation of joint place inleakage speed not exceeding $6,5 \times 10^{-12}$ Pa·m^3/s was obtained.

Residual stresses presence in unit was determined by polariscope-polarimeter PKS–250 and the maximum stresses initiated difference of rays path not exceeding 25 nm were measured.

Thus the tests results give the basis to recommend the developed manufacturing technology of vacuum-tight low-stressed glass ceramics/metal units for using them in production of high-quality assemblies of new laser instrumentation.

The literature
1. Heat-resistant dielectrics and their junctions with metals in new engineering / M.A.Rubashev, G.I.Berdov, V.N.Gavrilov etc. – M.: Atomizdat, 1980. – 246 p. (in Russian).

2. Kazakov N.F. Diffusion bonding of materials. - M.: Engineering, 1976. – 312 p. (in Russian).

3. Thermovacuum characteristics of glass ceramics/metal junctions, obtained with the use of plastic adhesion-active solders / Zhuravlev V.S., Severyanina Ye.N., Protsenko D.P., Naidich Yu.V. // Adhesiya rasplavov i paika materialov. – 1977. – No. 2. – P. 87-89 (in Russian).

4. Grain size and continuity influence of a titanium powder in coating on glass ceramics wettability by lead and stresses in soldered joints / Zhuravlev V.S., Krasnobaeva I.N., Severyanina Ye.N., Abramov Ye.V. // Adhesiya rasplavov i paika materialov. – 1981. – No. 7. – P. 96-98 (in Russian).

5. Development of obtaining methods and properties study of brazed metal/quartz portholes for cryogenic engineering / Naidich Yu.V., Kondratskii V.A., Zhuravlev V.S. etc. // Adhesiya rasplavov i paika materialov. – 1976. – No. 1. – P. 74-78 (in Russian).

6. About a possibility of pressurized joining of metal and glass or crystalline details by cold welding with indium / Bresler P.I. // Optic-mechanical industry. – 1969. – No. 2. – P. 28-30 (in Russian).

7. Obtaining vacuum - tight quartz/aluminium joints by method of solid-phase joining with pressure application / Gab I.I., Zhuravlev V.S., Pilipenko S.A., Naidich Yu.V. // Adhesiya rasplavov i paika materialov. – 1982. – No. 10. – P. 76-79 (in Russian).

PROPERTIES AND MICROSTRUCTURE OF SI$_3$N$_4$-BASED CERAMICS SINTERED UNDER MICROWAVE HEATING

Getman O.I.,[1], Panichkina V.V.,[1], Plotnikov I.V.,[2], Holoptsev[2] V.V.[2],

[1] Institute for Problems of Material Science, Kiev, Ukraine
[2] Institute of Applied Physics, Nizny Novgorod, Russia

Producing silicon nitride ceramics with high maximum strength and fracture toughness values are impossible without achievement of the maximum density and creation of a certain microstructure. As known, best strength and plasticity characteristics were demonstrated by Si$_3$N$_4$ ceramics whose microstructure consisted of a skeleton of elongated grains and a matrix of polyhedral β-Si$_3$N$_4$ phase grains. Such a "self-reinforcement" bimodal structure promotes an increase of the fracture toughness through the bridging crack mechanism [1]. It is also known that a bimodal structure is formed when two competing processes – densification and growth of β-Si$_3$N$_4$ phase grains – proceed at different rates [2].

During sintering of Si$_3$N$_4$ ceramics with ytterbia and alumina additions under microwave heating (MWH) both the densification temperature and the temperature of the beginning of the α-β-phase transformation decrease [3]. Also, the end of densification and phase transformation processes under MWH occurs earlier than in samples produced with a traditional heating (TH).

The mechanical properties and microstructure formation processes in Si$_3$N$_4$+3% Al$_2$O$_3$+5% Yb$_2$O$_3$ ceramic compacts sintered under MWH and under TH were investigated.

The initial ceramic materials were powder blends of silicon nitride with oxides. The mean powder particle sizes were 0.5-1.0 μm. The α-phase content in the Si$_3$N$_4$ powder was more than 95%. Samples sizing 3x5x35 mm were prepared in the same manner as in [1]. MWH sintering was carried out in the 30 GHz gyrotron system for microwave processing of materials [4]. TH sintering was carried our in a muffle furnace. The specimens were sintered at 1800^{0}C in a nitrogen atmosphere at normal pressure, the heating rate in all experiments was 60^{0}C/min. There were determined the Vickers hardness (*HV*) by standard procedure and fracture toughness (*K$_{Ic}$*) by the microindentation technique. The fracture surface microstructures of samples were studied by SEM. The quantitative microstructure analysis was carried out by SIAMS computer analyzer [5].

As shown by tests, at close values of the relative density, the hardness of ceramic samples sintered under MWH were higher as compared with those of samples sintered TH (see Table). The change in mechanical properties is undoubtedly associated with a change in the evolution of the microstructure at MWH as compared with that at TH.

Table - Properties of Si$_3$N$_4$+3% Al$_2$O$_3$+5% Yb$_2$O$_3$ samples sintered at 1800^{0}C

Heating method	Time, min	Porosity %	β–phase content, %	*HV*, GPa	*K$_{Ic}$*, MPa* (m)$^{1/2}$
MWH	1	6.3	100	13.4	8.7
TH	60	6.3	76	9.8	7.2
MWH	60	2,4	100	18.2	9,5

The microstructure of samples had the form of elongated grains in a matrix of polyhedral grains of the β-Si$_3$N$_4$ phase. Size distributions of the following microstructure parameters were determined: the mean size of grains regardless of their form; length of elongated grains and their elongation factor (the minimum-to-maximum size ratio) (see Figure). Measurements showed the mean size of grains in samples produced under MWH to be greater than in samples produced under TH, 2.3 and 0.8 μm respectively. This was due to formation in the former case of a larger number of elongated grains, which also were longer. The mean length of elongated grains was of 3.7 and 1.3 μm respectively. Values of the average elongated factor of grains for the two series of samples were close to each other (0.480 and 0.465 for MWH and TH respectively), but the distribution curve for MWH sintered samples is shifted towards lower values, which evidences a greater elongation of β-phase grains. It is to be taken into account that the phase transformation at 1,800 °C in the former case occurs completely and the content of the β-phase equals 100%. In TH sintered samples the content of the β-phase was of 76%, and the residual porosity, of 6.3%.

MWH

TH

MWH

TH
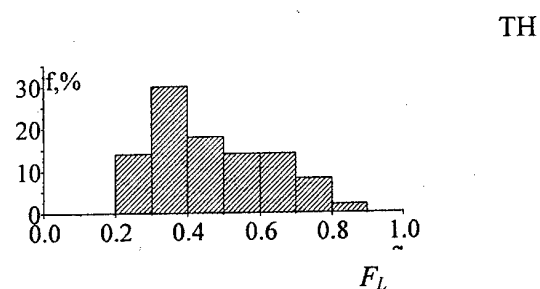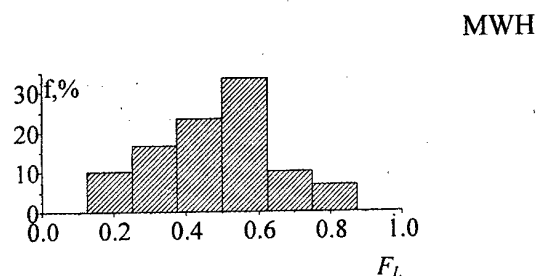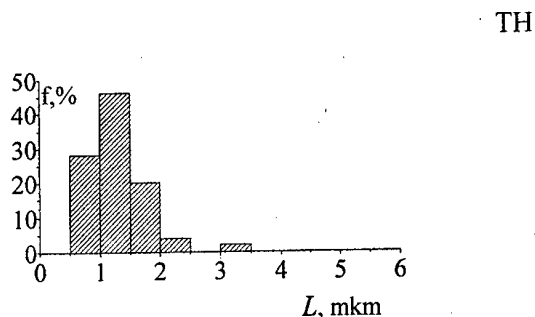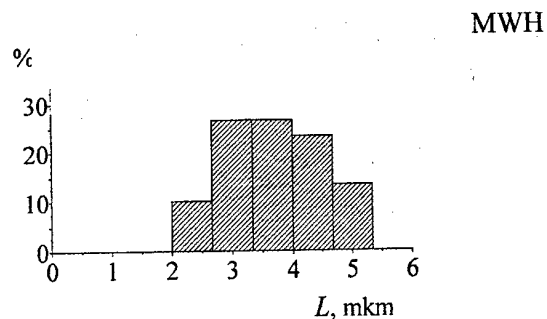
Figure. Length size distributions of elongated grains (L) and distributions of their elongated factor (F_L) for the samples sintered under MWH and TH at 1800^0C during 60 min.

In the latter case a growth of elongated grains at continuation of the phase transformation after the isothermal hold of 60 min is hardly possible.

Thus, it can be concluded that at the sintering under MWH of $Si_3N_4+3\%Al_2O_3+5\%Yb_2O_3$ ceramics the decrease of the initial phase transformation temperature not only speeds up the phase transformation, but also promotes growth of elongated Si_3N_4 grains and formation of the

"reinforcement" microstructure. Thereby the hardness and fracture toughness of such ceramics increases.

References
1. Becher P.F., Sun E.Y., K.P.Plucknett et al. Microstructure Design of Silicon Nitride with Improved Fracture Toughness: I, Effects of Grain Shape and Size, J.Am.Cer.Soc., 1998, v. 81, p.2821-2830.
2. Kim H.-D,, Han B.D., Park D.S., Lee B.T., Becher P.L. Novel Two-Step Sintering Process to Obtain a Bimodal Microstructure in Silicon Nitride. J.Am.Cer.Soc., 2002, 85, (1), p.245-252.
3. Быков Ю.В., Гетьман О. И., Паничкина В. В., Плотников И. В., Скороход В.В., Холопцев В.В.. Спекание Si_3N_4-керамики с добавками, содержащими оксид иттрия и оксид иттербия, при микроволновом и традиционном нагревах. Порошковая металлургия, 2001, № 3/4, С.20-30.
4. Yu. Bykov, A. Eremeev, V. Flyagin, V. Kaurov, A. Kuftin, A. Luchinin, O.Malygin, I. Plotnikov, and V. Zapevalov, "The Gyrotron System for Ceramics Sintering", in Microwaves: Theory and Application in Materials Processing III, Ed. by D. E. Clark, D. F. Folz, S. J. Oda, R. Silberglitt (Ceramic Transactions, v.59, The American Ceramic Society, Westerville, OH, 1995, pp. 133-140
4. Промышленная система анализа изображений "SIAMS 600". Екатеринбург, а/я 96, 1998.

SYNTHESIS OF FULLERENES USING ECONOMIC ARC DISCHARGE POWER SOURCE

Chujko A.A., Dymenko V.V.*, Kasumov M.M.,
Malashenkov S.P., Ogenko V.M., Paton B.E. *
Institute for Surface Chemistry of the NAS of Ukraine, Kyiv, Ukraine
* E.O.Paton Electric Welding Institute of the NAS of Ukraine, Kyiv, Ukraine

The method of synthesis of fullerenes, well-known since 1990 [1], i.e. the arc discharge using graphite electrodes in an inert gas atmosphere, is still the most productive and widely applied in the art. This method is employed to produce fullerene-containing carbon black in the discharge. Fullerenes are separated from carbon black by means solvents and filters. Liquid chromatography is used for separation of fullerenes. Out of the above operations, the arc discharge one is considered to be the most power-consuming process, making up the major part of the cost of a synthesized material and, therefore, the main limiting factor [2].

1.Calculations. Parameter S, defined as a ratio of mass of synthesized fullerenes, M, to power Q consumed for the synthesis process, may serve as an objective parameter for estimation of power efficiency of the discharge, i.e

$$S = M/Q, \qquad (1)$$

where values M and Q are determined as follows:

$$M = \alpha_{es} \cdot \alpha \cdot q \cdot t, \qquad (2)$$
$$Q = W \cdot t, \qquad (3)$$

where: α_{es} is the coefficient of transformation of the electrode material into the fullerene-containing carbon black [relative units, < 1];

α is the content of fullerenes in carbon black [relative units, < 1]; (4)

q is the electrode erosion [g/s];

t is the fullerene synthesis process duration [s];

W is the arc discharge power [kW].

The calculations were made using equalities (1-4), experimental results [3] and data on different fullerene synthesis methods taken from review [2]. Our calculations show that the highest value of parameter S is achieved in the *He* arc discharge: $S \approx 0{,}8$ g/kW·h (5)

With such a value of parameter S fullerenes synthesized in the arc would have been advantageous as compared with conventional materials in a number of important area [2], such as pharmaceutics and diamonds synthesis. ...However, an objective calculation of costs of synthesis considerably diminishes optimism. Power losses for ballast resistance used to provide

stability of the discharge decrease the value of parameter S in 1.5-4.0 times. These losses are minimum if the arc is powered from a source with a steeply drooping characteristic. A welding transformer has the most economic operation among other power sources with a steeply drooping characteristic.

2. Description of an experimental installation. 2.1. For the investigations we developed a source for synthesis of fullerenes, based on the arc discharge. Graphite electrodes for the discharge were made with a geometry similar to electrodes for the HF-discharge described in [4]: rod with a diameter of 6 mm and conical aperture in a disc with a minimum diameter of 5 mm. The possibility is provided for feeding the rod type electrode as it burns down .

The next unit is a space for drift and collection of the synthesis product, attached to the discharge chamber. In our source it is a quartz cylinder 50 mm in diameter and 500 mm long. The cylinder is covered by a lid with an orifice. In initial measurements the quartz cylinder was replaced by a copper one 100 mm long.

The discharge chamber, components to which the discharge electrodes were secured, and walls of the drift space were cooled with water. For this the quartz cylinder was fitted with a system of copper tubes. Locations of attachment of the components were sealed with fluoroplastic. Seals protect cavities from ingress of the atmospheric air in the case of an excessive pressure in the cavity, as compared with the atmospheric one. Auxiliary gas *Ar* and working gas *He* were fed to the cavity of the source through a buffer volume at the location of the rod electrode attachment. The gas supply lines were equipped with pressure regulators and rotameters.

An experimentally selected orifice was made in the drift tube lid to ensure a controlled gas flow from the point of introduction and over the entire volume of the fullerene source.

2.2. To power the arc, our source uses a commercial frequency transformer with a regulated dispersion flow, i.e. the TDM-317 U2

stabilizer. The stabilizer comprises the a.c. capacitor and thyristorized switch with an electronic control unit [5, 6], connected in series. Connection of the USGM arc stabilizer to the transformer makes the power source versatile and equivalent to the rectifier.

With such a connection of the transformer and USGM, the arc is initially ignited by a contact method. Upon ignition, at the moments of transition of the mains voltage through zero the arc is maintained by a voltage pulse with an amplitude of 200-500 V and duration of 10^{-5} s, formed by USGD. With the discharge ignited, the electrodes are drawn apart and installed at a distance optimal for the working conditions.

3. *Experiment.* 3.1. Prior to ignition of the discharge, the atmospheric air in the fullerene source cavity was replaced by purging with *Ar* and then, immediately before the discharge,with *He*. The arc was reliably ignited by bringing the electrodes in contact, and was burning until the electrodes were drawn apart to a distance of 3-7 mm. The tests were conducted for 0.5-5.0 min at a current of 60-200 A, the *He* gas flow rate amounting to 20 l/min. Bright glow of the discharge electrodes prevented observation of a clearly defined plasma jet, such as that observed in the HF-discharge [4].

With the discharge ignited, the working gas carries the products of plasma-chemical reactions out of the electrode materials. The product is deposited on the water-cooled drift space walls. The amount of the material produced was monitored visually by formation of a deposit on the quartz cylinder walls. Density and length of the deposit along the length of the quartz cylinder increased with an increase in the discharge current and the working gas flow rate. It was noted that a deposit of a small thickness might have a different color, i.e. from purely black to black and brown.

3.2. Oscillograms of current and voltage of the arc with the graphite electrodes are similar to those of the welding arcs using conventional materials: a clearly defined ignition peak at a change of polarity at the arc, rising to a half sine ave length, and then a constant voltage (plateau) for half a period.

the oscillograms some time after ignition of the graphite electrode arc, as opposed to the conventional arc. They are characterized by a steep leading front and a quiet tailing front. The spikes in the oscillograms correspond to wandering of the cathode spot [7] along a contour of the graphite electrode. This results in elongation of the arc and, therefore, decrease and increase in the arc voltage by a value of the spike. *The high power density at the cathode spot (about 10^7 W/cm^2) and, accordingly, the high concentration of plasma in the plasma column adjoining the spot, as well as their chaotic wandering over the cone surface, are the effective sources of particles C, C* and C+. Formation and the probability complete formation of fullerenes of them are determined by temperature, concentration of carbon vapor and working gas flow rate.*

After turning off of the discharge the discharge space and the quartz tube are cooled down by continuous flows of gas (Ar) and water through the cooling system.

4. *Investigation of the synthesized material.* Carbon black deposited on the walls of the quartz cylinder and copper tubes was removed mechanically and immersed into benzene. The presence of fullerenes in this solvent showed up as a marked coloring of the solution. It is in this way that the discharge conditions necessary for synthesis of fullerenes were established. These conditions correspond to formation of a brown tint of a deposit on the quartz cylinder walls.

The fullerene-containing carbon black was also treated in xilol. A solution produced in this case had a less marked coloring. And only the concentrated solution acquired first a slightly yellow-brown tint. Evaporation of the solvent resulted in crystals characteristic of fullerene associates, that formed on the surface [1].

To obtain the IR-spectrum, several successively evaporated layers of the concentrated benzene solution of fullerene were deposited on the KBr-glass. The IR-spectrum differing from the known ones [1, 8] was obtained on our sample. It is likely that this is associated with the presence of a mixture of fullerenes in the sample.

[1].W.Krätschmer,Lowell D.Lamb,K.Fostiropoulos & Donald R.Huffman. Nature.- 1990.- 347 .- № 6291.- P.- 354. [2]. A.A.Bogdanov, D.Draiger, G.A.Dyuzhev // Zhurnal Tekhnicheskoj Fiziki. – 2000.- 70.- №5.- P. 1. [3].D.Afanasiev,I.Blinov,A.Bogdanov,G.Dyuzhev,V.Karagaev, A.Kruglikov // Zhurnal Tekhnicheskoj Fiziki.-1994.- 64. - №10.- P. 76. [4]. G.N.Churilov. Pribory i Tekhnika Eksperimenta - 2000.-№1.- P.5. [5].B.E.Paton, V.A.Zavadsky // Avtomaticheskaya Svarka. –1956. - №3. – P.26-35. [6]. I.I.Zaruba, V.V.Dymenko, V.V.Bolotko // Avtomaticheskaya Svarka . –1989. - №10. – P.46-52.[7]. I.G.Kesaev. Cathode processes of the electric arc.- Nauka Publ. House.- 1968. [8]. A.P.Shpak, Yu.A.Kunitsky, V.L.Karbovsky. Cluster and nano-structural materials.- V.1.- Kyiv: Akademperiodika, 2001.- P.206.

THE STRUCTURE OF ELECTRIC CONTACT COMPOSITE MATERIALS OF TRADITIONAL COMPOSITION IN THE EXTREMAL CONDITION OF CONVERSION

Minakova R.V., Homenko E.V., Yenevich V.G., Pomarin Y.M.[1], Orlovsky V.Y.[1], Grechanyuk N.I.[2]

I.N. Frantsevich Institute for Problems of Materials Science, NASU, Kyiv, Ukraine
[1] E.O. Paton Electric Welding Institute, NASU, Kyiv, Ukraine
[2] Scientific Production Enterprise «Gecont», Vinnitsa, Ukraine

The functional properties of different-purpose articles predominantly are structure responsivity. This is concerned with properties of the electric contacts. It is ascertain [1] that dispersing of original structure in the contact work layer for instance Cu-Cr composite material (CM) under arc discharge effect establishes an elevated serviceability of these contacts [2]. It is known too, that increase of dispersivity of CM on the Ag-base is the effective method for attainment of required physical and chemical properties these CM and functional properties of middle loaded electrical contacts. Different processes of dispersing CM structure have been used in the production articles by powder metallurgy methods. In the present work is studied opportunity of using alternative (for powder metallurgy) methods CM structure dispersing: plasma-arc smelting; electron-beam high-velocity evaporation-condensation, working by pressure under elevated temperature. Electric-contact CM in the systems Cu-Mo, Cu-Cr, Ni-Fe-W were chose as objects for present investigation. Optical and electron microscopic examination, determination of high temperature oxidation resistance and others were used for confirm of CM structure dispersing.

This research allowed to studying morphological modifications of the powder CM Cu-Cr (1:1) under plasma-arc smelting. It is concerned with consolidation of initial Cr-particles, dispersing new conglomerates with forming of coarse columnar or small crystals of the Cr-component dendrite and other forms, fig. 1. It is concluded from the microscopic examination, that the structure forming features is concerned with possibility existence in the system Cu-Cr for the super-cooling of the liquid phase. That is why in the system Cu-Cr (as in Cu-Fe and Cu-Co [3]) the limit of immiscibility (T_o) is at the temperature below T_L (liquidus temperature). It is probable, that structure of CM Cu-Cr exhibits an anomalous behavior if liquid alloy breaks up into two phases.

The value of (T_l -T_o) interval and velocity of cooling influences the form of Cr-component crystallization in the liquid Cu. Necessary condition for crystallization may be realize, for instance, in the commercial production of Cu-Cr CM vacuum contacts with lower impurities content.
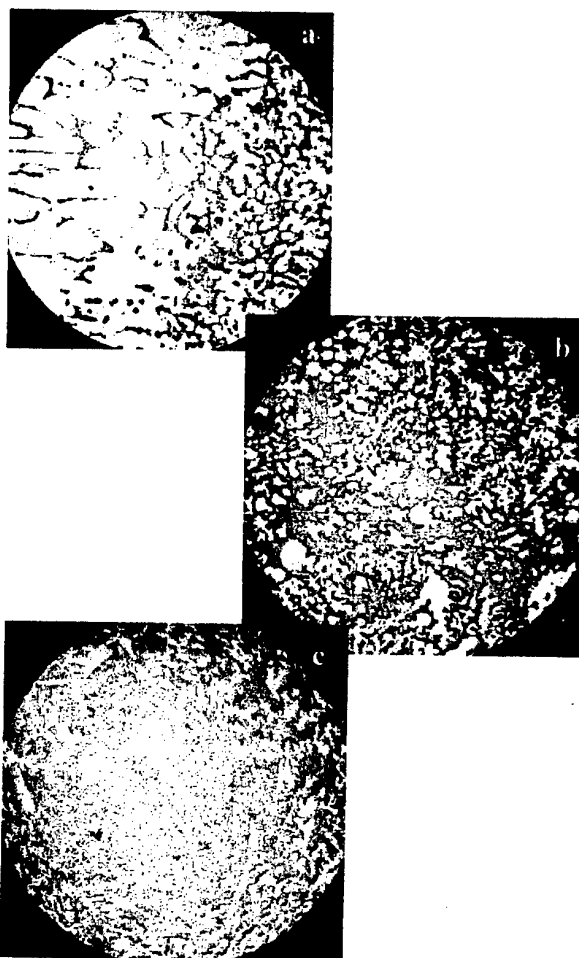
Fig. 1 - Consolidation of initial Cr-particles with forming of coarse columnar crystals (a); Cr-component dispersing and forming of small crystals with different forms (b, c).   x 400

228

CM on the base of Cu and Mo (in form of articles) were received by method of electron - beam high velocity evaporation - condensation in Ukraine for the first time [4]. Earlier these CM have produced by powder metallurgy method partially for substitution of powder W-content contacts. New CM has a specific micro-dispersed and micro-layered structure. In contrast to powder CM on the same base condensed CM have the higher resistance to oxidation in the air. This resistance to high temperature corrosion was achieved by alloying but with lower content of additions then in powder matrix CM. Slightly alloying condensed CM has high level of electric conductivity, what allows to use new CM for change Ag-content CM in middle loading switches.

In this work the changes of alloy Ni-Fe-W structure were considered in connect with influence on it of high temperature (1085-1645 °C) and pressure (6-8 GPa). After short-time influence of these parameters CM followings structure changes were established in the Ni-Fe-W: W-grains dividing and originating splinter W-particles, fig. 2, a, b; redistribute of component on the base Ni and W; forming the dendrite W-crystals locally between initial grains or in the whole volume of specimen, fig. 3, a, b. Complex influence of temperature and pressure allows increasing CM hardness from 3000 to 6400 MPa.

Fig. 3 - Dendrite W-crystals forming: locally between initial grains (a); in the whole volume of specimen (b)
x300

Received results have used for choice of properties increase condition of these CM.

REFERENCES

1. Лафферти Дж. Вакуумные дуги. Теория и приложения. - М: "Мир", 1982. - 463 с.
2. Правоверов Н. Л. Скорость эрозии катодно-поляризованных контактов в различных системах сплавов серебра / Электротехника. - 1979. - N 9. - C. 42-44.
3. Nakagava Y. Liquid immiscibility in copper-iron and copper-cobalt systems in the supercooled state / Acta metallurgica. - V. 6. - November 1958. - P. 704-711.
4. Гречанюк Н.И., Осокин В.А., Афанасьев Г. Б., Гречанюк И.Н. Электронно-лучевая технология получения материалов для электрических контактов / Сб. трудов «Электрические контакты и электроды». Киев: ИПМ. - 1998. - C. 51-66.

Fig. 2 - W-grains dividing (a); originating splinter W-particles (b)   x 200

IMPRUVEMENT OF EXPLOATATION CHARACTERISTICS OF MOLIBDENUM USING LAYER-BY-LAYER ELECTRIC-SPARK ALLOYING AND LASER TREATMENT

Podchernyaeva I.A., Frolov G.A., Panasyuk A.D., Kravchenko V.S., Teplenko M.A., Bloschanevich A.M., Kostenko A.D.

Institute for Problems of Materials Science of National Academy of Science of Ukraine

Nowadays there is an important problem to increase the resistance to high-temperature corrosion and the level of mechanical characteristics of molybdenum as material of jet and space industry. The conventional way to decide this task is surface modification using laser alloying or vapour deposition (PVD or CVD methods) [1]. The electric-spark alloying (ESA) being characterized by expedient application and ecological safety may be one of the ways to decide such task. The goal of this study is to investigate the composition, structure and corrosion properties of Mo after its ESA with AlN-TiB$_2$/ZrB$_2$-based composite ceramics. As Mo samples the ЦM-10alloy (Al – 0.02%, B – 0.002%, C – 0.003%, O$_2$ – 0.002%) was used. The choice of coating materials was conditioned by high corrosion resistance of these ceramics till 1400°C [2].

ESA was implemented under high-frequent alloying in air at the following regime: short circuit – 0.9 A, impulse energy – 0.08 J, impulses frequency – 1200 Hrz. The «Квант-15» solid laser was used for the surface treatment. The electrodes (3 x 4 x 35 mm) with the porosity ~ 2.0 –2.5% were fabricated by powder metallurgy methods. ESA was carried out using layer-by-layer procedure. The outer layer was formed with the use of MoSi$_2$ electrode, the latter being applied to silicide the surface. Another way to silicide was the laser treatment of ESA-coating or initial Mo, using SiC powder. The composition and structure of surface were studied using XRD, EPMA, SEM, and metallographic methods. The kinetics of interaction with oxygen under isothermal conditions (up to 1400°C) was studied by TG method. The mechanical tests were carried out at the temperature of 1150°C in vacuum not worse 0.1 Pa. The sample heat rate till the test temperature was 30 °/min.

It was found that the ESA-coatings obtained had an island-like nature and consisted of three parts. The surface of sample with coating (a thickness ~ 5-20 μm) proved to be reinforced by granules of fine-dispersion composite material on the base of electric erosion solid-phase products. They occupied approximately 20-30% of working area whereas the greater part of coating was Mo, mainly, alloyed with aluminium, and also contained the uncoated molybdenum, the latter being explained by peculiarities of ESA method. According to XRD data as well as EPMA spectra of a cross section of globule for both the AlN-TiB$_2$ (ТБHA) and AlN-ZrB$_2$-ZrSi$_2$ (ЦБCAH) electrode materials, one can conclude that the gradient structure of globule sintering layer is formed on the Mo surface. In the case of AlN-TiB$_2$ alloying electrode, the outer globule later proved to be the titanium diboride while the layer near Mo substrate is double titanium-molybdenum diboride, and the middle one is alumina. In the case of AlN-ZrB$_2$-ZrSi$_2$ alloying electrode, the surface sintered layer consists of the alumina whereas the lower layer is zirconium borone silicide with the additive of Al$_2$SiO$_5$ mullite. Hereby on the "globule-Mo" boundary there is a transition zone of about 1 ⎕m, enriched, mainly, with aluminium. It was shown that the deposition of ESA coating promoted to a rise of corrosion resistance of technical Mo samples (up to 1200°C) by ~ 8 times. Hereby the vaporization of MoO$_3$ oxide was the process limiting high-temperature corrosion, on the whole. On the base of both data concerning the temperature dependence of linear vaporization rate and thermodynamic calculation of diminution of oxidation/ vaporization active centers amount one can evaluate the magnitude of working area of uncoated sample surface that proved to be equal to ~ 16%. The influence of layer-by-layer ESA on the molibdenum resistance to high-temperature oxidation is presented in the table for the different annealing temperatures (Tan) of samples. The total affect of an increase of corrosion resistance of molibdenum conditioned by formation of complex compounds of the Ti-Zr-Al-Si system in the material of sintered layer as well as a presence of molibdenum regions alloying with aluminium. The layer-by-layer ESA process improved the molibdenum mechanical characteristics as well (Table). The most magnitude of relative uniform lengthening ($\delta_{un.}$) was 6.7% for the case of layer-by-layer ESA using ТБHA+MoSi$_2$ scheme. This value is higher by 5.6 times compared with the initial uncoated Mo specimen.

230

Table

Effect of ESA on the molibdenum properties

Electrode material (treatment scheme)	Mass loss $\square m/s$, mg/cm^2		Relative uniform lengthening $\delta_{un.}$, %
	Tan. = 1200 °C, t = 30 min	Tan. = 1400 °C, t = 30 min	
ЦБСАН-5 (ESA)	-47.30	-	-
ЦБСАН-5 + Mo-Si$_2$ (layer-by-layer ESA)	-7.32	-30.5	4.3
ЦБСАН-5 (ESA) + SiC (laser treatment)	-9.70	-	-
ТБНА (ESA)	0	-37.5	6.7
ТБНА + MoSi$_2$ (layer-by-layer ESA)	-88	-	-
MoSi$_2$ (ESA)	-115.80	catastrophic mass loss	1.2
Initial uncoated Mo	-15.95	-	-
Laser treatment of uncoated Mo	-	-	3.7

References

1. M.Nagae, T.Yoshio, J.Takada and Y.Hiraoka. Surface modification of molibdenum alloys by carburazation / 2000 Powder Metallurgy World Congress. Abstract. November 12-16, 2000. Kyoto. Japen. P. 95.

2. A.D.Panasyuk, I.A.Podchernyaeva, R.A. Andrievsky, M.A.Teplenko, V.P.Katashinsky, I.I.Timofeeva. Structure and properties of electric-spark, laser and magnetron coatings using AlN-TiB$_2$/ZrB$_2$ composite materials. Function materials, v.8, # 1, 2001, P. 129-134.

DEVELOPMENT OF A TECHNOLOGY FOR PRODUCTION OF THE MULTI-LAYER AXIALLY SYMMETRIC SEMIFINISHED ITEMS

Kulmov S. D.[1], **Bychkov T.A.**[2], Rostovchikov V.A[3], Loginov Ju.V[3]

[1]JSC "Revdinsky Zavod po obrabotke cvetnykh metallov" (JSG "RZ OGM"), Revda, Sverdlovskoj obl., Russia

[2]JSC "ELKAM-Neftemash", Perm, Russia

[3]JSC "Perm Research Technological Institute" (JSC "PNITP'), Perm, Russia

The upgrading of quality of parts, especially determining the service life of art ides, remains as an urgent problem in machine building. Here, we have to do with the widely used axially symmetric parts: shafts, axles, tubes et al.

Traditional techniques for increase of service life of such parts consist in an application of protective wear resistant coatings on working surfaces in various ways, Even these coatings are not necessarily efficient for rust protection. For parts to be exposed simultaneously to high temperatures, intensive mechanical, corrosion and erosion wear, high impact loads, another technical decisions are required.

Along these lines, interesting perspectives open through the use of advantages of granule metallurgy and radial forging in a complex.

Abroad, the following firms attained some successes in this field: ASEA (Sweden), Krupp Forschungsinstitut (Germany), AVCO Ryconing DJY (USA).In the former Soviet Union the analogous works were conducted at: the All-Union Institute For Light Alloys (VILS),Moscow; the Ukrainian Research Scientl4-fical Institute For Special Steels and Alloys (UkrNIISpec-Stal), g.Zaporozhie; VNIIStal, Moscow; NPO "Tulachermet" et al

These works go on at present too. However, rates of progress are reduced and there is no coordination between leading institutes of this direction.

The accepted technology for manufacturing large-sized blanks from granules consists of the following operations: capsules are filled with granules, degased and sealed. Hot pressing is carried out on gas static presses. If required, the produced blanks are exposed to the hot deformation, heat treated and machined.

For production of axially symmetric semi finished items, radial forging machines of the Austrian firm GFM (radial forging machines of the type SXP 16.SX 25, SX 40. SX 55 et al.) are heavily used all over the world. On these machines, a high degree of precision and dimensional stability of parts are achieved; a metal consumption decreases by a factor of 1,5 ... 2; the labour productivity increases 5 to 6 times. The specialists of the Perm Research Technological Institute have used the complex of possibilities of radial forging process and granule metallurgy when elaboration of a fundamentally new technology for manufacturing shafts and tubes and for perfection of design of these parts. In so doing, the operation of pressing of granules in a capsule on the gas static press was replaced by operation of hot packing and then by the hot deformation on the radial forging machine of the type SXP 16 with the use of special hammers. The present method makes it possible to simplify and reduce the price of the technological process. And at the same time this method allows the use of heterogeneous alloys which provide the increase of wear and erosion resistance, high-temperature strength and other characteristics. This technology makes it possible to vary the chemical composition, both through the length and the cross-section of a semi-finished item. Field of application of this new technology does not restrict only to production of special articles. In such a way it is possible to manufacture multi-layer axially symmetric blanks, such as blanks from tool steels for production of cutting tools and machining attachments, tubes, incl, multilayer tubes with use of powders (granules) of satellites, nimonics et al. for general machine building use (oil and gas industry et al.)

For production of oil well sucker-rod pumps and other pumps of various modifications, the specialists of the JSC "ELKAM-Weftemash" have developed a perspective technology for making of a radial forged bimetallic cylinder with an inner cladding layer from materials with higher wear and corrosion resistance -stainless steels, brass, bronze et al. (Patent of the Russian Federation

No.2095179).

The JSC "Perm Research Technological Institute" and the JSG "ELKAM-Neftemash" are ready for the joint cooperation for making of new materials and technologies for production of axially symmetric semi finished items with interested firms on the basis of the agreed understanding.

THE OBTAINING OF AMORPHOUS-MICROCRYSTALLINE COATINGS WITH HEIGHTENED AUXILIARY CHARACTERISTICS BY LASER EFFECT

Skrypka N.N.
Physico-technological institute of metals and alloys of National Academy of Science of Ukraine, Kiev, Ukraine

Now one of actual problems is obtaining high-quality coatings and surfaces of details. For solution of this problem the local methods of effect with application of high energy sources such as laser radiation, plasma arc, electron beam, currents of a high frequency etc. will be even more often used.

The laser surfacing consists in obtaining topcoats from powdered materials on details by laser bundle. High efficiency of this process, possibility of regulation of thermal modes of a surfacing, obtaining of coatings by width from tens micrometers up to several millimeters, including on restricted sites of workpieces, causes high versatility of a laser surfacing, which allows to plot coatings with a wide spectrum of the auxiliary properties. The soul interest represents one of sorts of such processing, when as a result of a smelting-down and subsequent superfast cooling in a thin surface layer the metal gains amorphous or microcrystalline structure. Obtained two-phase (amorphous phase + crystalline) or microcrystalline (one or several phases with a very mesh size of a grain) the coatings can have a high corrosion stability, endurance, magnetic properties, heightened hardness etc.

The work is devoted to research of the process of a surfacing of metal alloys on a base of transition metals by laser radiation with the purpose of development of the technology of a plotting of coatings, which have amorphous-microcrystalline structure. The purpose of the given operation was detection of legitimacies of influence of technological modes of a surfacing of alloys FeNiB and FeMoCrB on physical-mechanical properties of received coatings.

The surfacing was conducted by continuous laser radiation. The focus of radiation was carried out by a lens with focus distance F = 300 mm. The hard facing powder was moved under a corner of 45 degrees following to driving of a sample. The thermal source was displaced with speed of 2...5 mm/s, providing obtaining hard facing platens of width 0,5-1,5 mm and height up to 1 mm.

Structural-phase researches of coatings were conducted by diffractometer. The corrosion tests of the obtained laser coatings in the different environments were carried out. With the help potentiometer the anode and cathode curves of each sample were removed and are defined by EMF and speed of staining. We conducted wearing tests in the mode of a rubbing friction with loads 5,1-15,3 MPa at speed of abrasion of 20 mm/s.

The analysis of X-ray photographs of coatings, that in structure of hard facing layer are present both amorphous, and crystalline structural components. Hard facing coatings from FeNiB obtained at speeds of refrigeration 10^4 K/s, have in main crystalline structure and consist of a hard solute of iron (Fe,Ni)$_3$-B on the basis of a tetragonal lattice of boride of a nickel Ni$_3$-B (a = 0,863 nm; c = 0,437 nm). The coatings obtained at speeds of refrigeration of the order 10^5 K/s, in top layers have microareas of amorphous structure. Its amount depends on technological parameters of processing. On a base of a structure analysis it is possible to assume, that at plotting one track hard facing of a stratum on a metal substrate on a surface there is an amorphous layer, which at the subsequent heat (originating at plotting adjacent surfacing of a stratum) passes in a crystalline state. It is reconfirmed by that on a surface hard facing of a stratum is gained tetragonal, instead of the trimetric boride, i.e. crystallization goes not from a melt, and from an amorphous state.

The similar outcomes are obtained for FeMoCrB.

The analysis of polarization curves has shown, that the researched coatings in a wide interval of potentials behave practically identically. At anode polarization in active area the current intensity linearly depends on a potential, and at further increase of a potential the saturation current is

achieved and the current intensity varies unsignificantly with rise of a potential.

The researched coatings have high corrosion stability. However, if on a potential of staining of a coating practically are identical, on speed of staining the essential discrepancy is watched. So, for example, in the neutral environment for FeNiB coating with amorphous structure the speed of staining constitutes 0,56 mkA/sм^2, with amorphous - crystalline 0,79 mkA/sм^2, microcrystalline 1,77 A/sм^2, in slightly alkali she is diminished in 5 times order, in sour – by 1 order.

The high corrosion stability of microcrystalline coatings is explained to the following. It is known that the boundaries of grains in crystalline alloys are sites of the facilitated origin of staining. The crystalline coatings obtained as a result of fast refrigeration consist of very shallow crystallites and consequently the specific surface area of boundaries in them is great. However, during fast refrigeration there is no fluctuation of chemical composition. Therefore, alloys obtained by fast refrigeration of a fluid, though are crystalline, but have not local oscillations of chemical composition on such defects, as the boundaries of crystallites, i.e. are characterized by a high chemical homogeneity. Thus, the boundaries of crystallites in high cooling alloys do not render essential influence on their corrosion behavior.

In overwhelming majority of cases the real details are subjected combined influence - corrosion, friction, cyclic powers, heat etc. Therefore we spent test on friction. It is visible, that the sample with microcrystalline structure has the greater endurance, than sample with amorphous structure of a surface. It's established the sample with amorphous structure of a surface has losses of a mass in 1,5-2 times above, than sample with microcrystalline structure. I.e., at decrease of a running speed of a laser beam and increase of an amount of a given dust in a workpiece range, and, therefore, at decrease of speed of refrigeration the value of a wear is reduced, as microcrystalline

structure in this case is shaped. I.e., at decrease of a running speed of a laser beam and decrease of an amount of a given dust in a workpiece range, and, therefore, at increase of speed of refrigeration the value of a wear is reduced, as microcrystalline structure in this case is shaped.

High wear resistance the characteristics has the amorphous-crystalline structure. The outcomes are obtained for coatings marked at speeds of refrigeration 10^5 K/s, which provide creation of a high-strength and rather plastic amorphous matrix with the uniformly distributed dispersible particles of hardening phases. Presence of microcrystalline inclusions in an amorphous matrix boost hardness and improve триботехнические sharply characteristics is model. I.e., the coatings having amorphous - crystalline structure have to a rather high resistance of outwearing, which is higher than subjects, than more degree of dispersion of particles of borides and is more uniform their allocation in bulk coatings.

Experimentally is established, that at a laser surfacing it is possible to gain both amorphous, and microcrystalline structures.

Is exhibited that speed of staining is model with a coating having amorphous structure higher, than having microcrystalline. Thus of speed of staining of a coating with amorphous - crystalline structure unsignificantly differs from coatings with amorphous structure.

The researches on influence of technological modes of obtaining of coatings on their endurance are carried out. Is established, that the microcrystalline coatings have losses of a mass in 1,5-2 times smaller, than amorphous coatings.

I.e. the amorphous-microcrystalline coatings can be classed as intermediate structure, which has rather high both corrosion and tear-proff properties. Therefore it is expedient to apply coatings with such structure on details operating in conditions of a wear in hostile environments.

SUPERHARD MATERIALS ON THE BASIS OF DIAMOND AND CUBIC BORON NITRIDE FOR USE IN EXTREME CONDITIONS

Starchenko I.M. Tolkachev A.N.
Institute of Solid State and Semiconductors Physics of NASB, Belarus, Minsk

Synthetic diamonds are manufactured by the following basic methods:
1. The methods of high pressure and high temperature treatment of graphite in the region of thermodynamic stability of diamond. Under such conditions the synthesis of powders of poly- and monocrystals of diamond is carried out;
2. By methods of explosive synthesis the powders of ultradisperse diamond with the very small sizes of particles and large specific surface are manufactured;
3. The methods of chemical vapor deposition (CVD) allows one to manufacture diamond films.

The synthesis of cubic boron nitride are carry out by the first method.

It is known, that the basic reasons for failure to achieve the theoretically designed parameters of synthesis of diamond near the line of thermodynamic balance at high pressure, are the processes connected with nucleation of diamond particles and formation of a critical nucleus of growth.

Ultradisperse diamonds, manufactured by the methods of explosive synthesis, have a number of unique properties connected to the features of their structure [1]. The basic properties determining their special behavior while interacting with other substances are the extremely small size of particles (2-40 nm) and large specific surface (up to 300 m^2/g).

In this sense the research of the influence of the ultradisperse diamonds additives on direct and catalytic synthesis of diamond under high pressure conditions is of practical interest.

In the manufacture of diamond materials the challenge is to create highly dispersive diamond containing compacts with the nanophase structure useful as abrasive tools in optics and microelectronics for obtaining high purity of the machined surfaces [2,3].

As the polymorphic modifications of carbon (graphite, diamond) and boron nitride (hexagonal boron nitride, cubic boron nitride) have a number of similar physical-chemical properties and are analogous in the crystal structure with the close parameters of the crystal lattice, the study on interaction of ultradisperse diamond with boron nitride holds considerable practical interest too.

The special interest is the investigation of the interaction of ultradisperse diamonds with hexagonal boron nitride in P, T area of phase transformation hexagonal boron nitride - cubic boron nitride.

In the work the X-ray diffraction analysis data on the influence of the additives on conditions of synthesis and output of diamond and cubic boron nitride in wide area of pressure (P=4.0-7.0 GPa) and temperatures (T=500-1700^{0}C) at a time of high pressure and temperature treatment from 10 up to 300 s are presented.

The phase structure of the samples was investigated by the methods of X-ray diffraction analysis on X-ray diffractometer DRON-4. The study of the dependences of density and microhardness of the samples on the conditions of high pressure and high temperature treatment was carried out.

It is established, that when graphite or hexagonal boron nitride interact with the ultradisperse diamond over the wide temperature and pressure range there occurs the transformation graphite and hexagonal boron nitride into cubic modifications (Fig.1).

The X-ray patterns of the sample of an starting composition with 50 wt. % of ultradisperse diamond and 50 wt. % of hexagonal boron nitride are given on a Fig. 1. Samples were subject of high temperature high pressure processing under pressure 7.0 GPa during 10 minutes at a various temperatures (T=1000^{0}C, T=1600^{0}C).

In the sample, with the temperature T=1000^{0}C of high temperature high pressure treatment only the lines of hexagonal boron nitride and ultradisperse diamond are observed (Fig.1,b).

In the sample, which the high temperature high pressure treatment was carried out in the field of stability of cubic boron nitride (T=1600°C) the phase transformation is clearly seen (Fig.1,a).

Characteristically that the line for ultra- disperse diamond have disappeared.

It is established, that the transformation goes through amorphous of hexagonal boron nitride and the crystallization of cubic modification of boron nitride from the amorphous phase of boron nitride.(Fig.2)

The X-ray patterns of the sample of an starting composition with 80 wt. % of ultradisperse diamond and 20 wt. % of hexagonal boron nitride are given on a Fig. 2.

The high temperature high pressure treatment was carried out with the following conditions: pressure P=7.0 GPa, temperature T=1300 C with various time of proceedings: a) 10 c, b) 30 c.

It is shown, that the hexagonal boron nitride transform in the amorphous state, then it begin crystallization as cubic boron nitride from an amorphous phase.

The similar processes occur when a graphite transform to diamond.

In work the received data are discussed
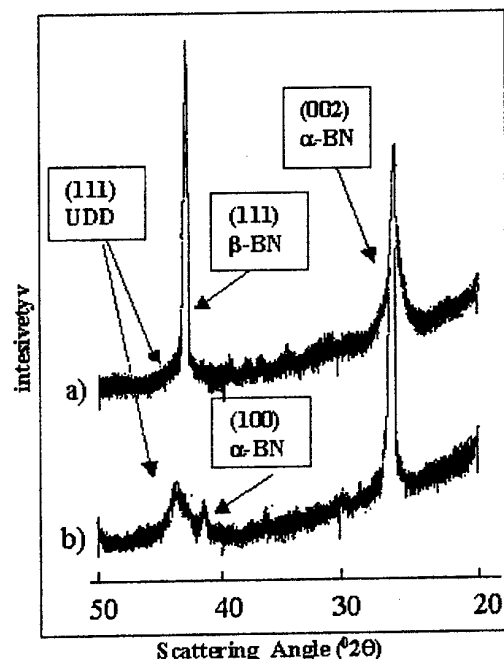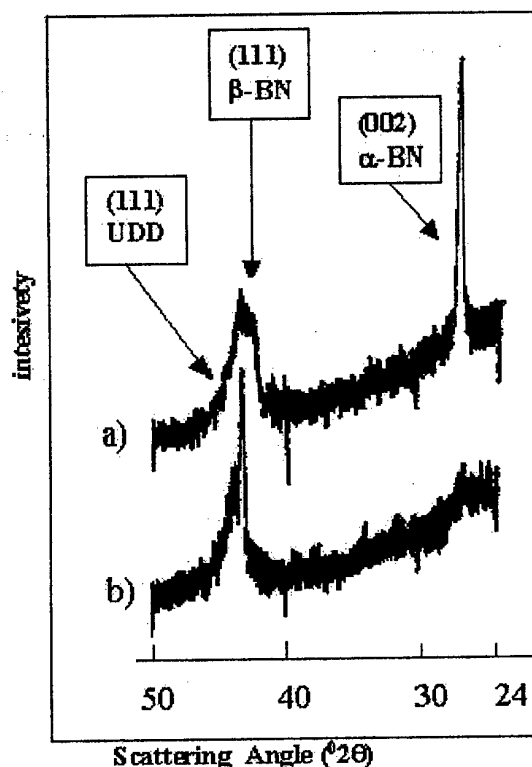
Fig. 2. X-ray diffactograms of the patterns measured with $CuK_{\alpha1}$ – raiation (λ=1.5405 A).

REFERENCES

1. Lyamkin, A.M., Petrov, E.N., Eremin, A.P. et al. (1988) Fabrication of Diamonds from explosive material, Dokl. the USSR Acad. Sci. 302 / 3, 611-613.
2. Shipilo, V.B., Starchenko, I.M., Gubarevich, T.M. et al. (1995) On sintering of UD powders under high pressures and temperatures, Powder Metallurgy 18, 126-130.
3. Shipilo, V.B., Starchenko, I.M., Zvonarev, E.V. et al (1995) Sintering of ceramics from UD diamonds under high pressures and temperatures, Prospects for Diamonds application in Engineering And Electronics Industry 5, 64-65.

Fig. 1. X-ray diffactograms of the patterns measured with $CuK_{\alpha1}$ – raiation (λ=1.5405 A).

237

PECULIARITIES OF INFLUENCE OF A DISPERGATION MEDIUM (WATER AND ETHANOL) ON STATE AND PROPERTIES OF TITANIUM DISPERGATED

**Kharlamov A.I., Khomko T.V., Ushkalov L.N., Gubareni N.I., Fomenko V.V.[1],
Bondarenko M.E.**

Frantsevich Institute for Problems of Materials Science, National Academy of Sciences of Ukraine,
Kyiv, Ukraine

[1]National University of Food Technologies, Kyiv, Ukraine

High-capacity metals in respect to hydrogen require the certain treatment before the first sorption of hydrogen. Especially when we deal with such high-active metals, as Be, Al, Mg and Ti. After direct contact with hydrogen, they do not tend to form hydrides without being previously activated. However, these very elements and their alloys form hydrides characterized the highest content of hydrogen.

In our work the method of mechanochemical treatment of metals and alloys for activation materials before sorption of hydrogen was used. Titanium was chosen as an model object because of its high capacity and modest cost of metal itself.

Mechanochemical treatment was carried out in a high-rate planetary mill with metallic drums and metallic balls. Water and alcohol were used as dispergation media. Weights of titanium loaded were 6, 10, and 20 g. X-ray patterns were taken using DRON-3M (CuK$_\alpha$) X-ray diffractometer. Hydrogenation of Ti powders was performed directly after the treatment in a mill on Siverst's type device. Absorption of hydrogen was measured regarding the change of pressure in a closed system with volume about 65 cm^3. Initial pressure 0.1 M Pa was fixed to the normal in constant intervals (5 min.) with following noticing

of hydrogen absorbed. Dehydriding was carried out in vacuum 13 Pa. Temperature at which hydrogen started to evolve and its amount were noticed as well.

Analysis of X-ray spectra showed that under the mechanical activation during 20 min. the peak corresponding to TiH$_x$ hydride phase ($2\Theta \approx 86^0$) is present in X-ray patterns (fig.1). On the other hand, peaks corresponding to titanium oxide formation are absent. Further increase of the treatment duration results in lowering of this peak and after 40 min. of activation in a mill one can observe transformation of Ti powder in the X-ray amorphous state occurred due to significant

dispergation, which could be attributed to formation of "fragile" TiH$_x$ phase.
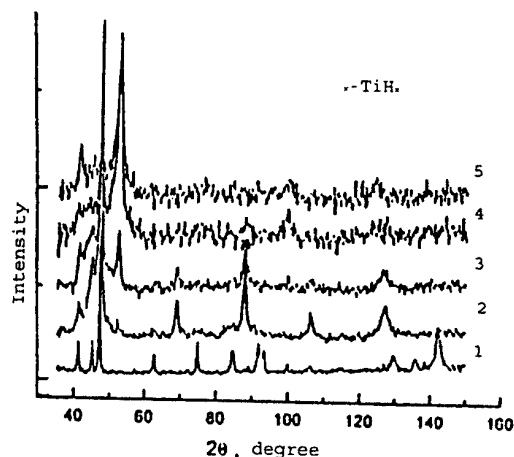
Fig.1 X-ray patterns of titanium powder. 1-initial Ti, 2, 3, 4 and 5-treated in water during 20, 30, 40 and 80 min., respectively.
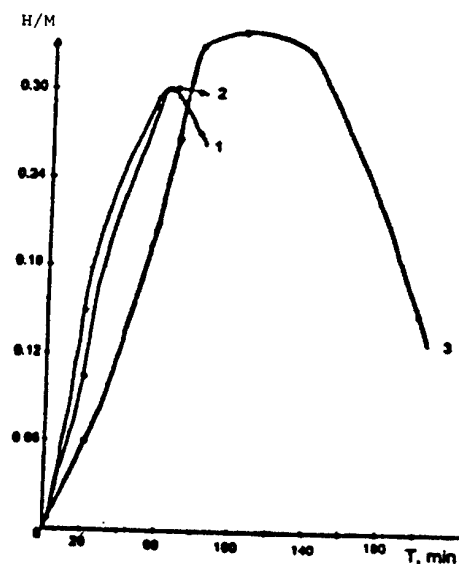
Fig. 2 Dependence of hydrogen content in the hydride phase on duration of Ti milling in water. Weight of titanium loaded in a drum: 1-6 g., 2-10 g., and 3-20 g.
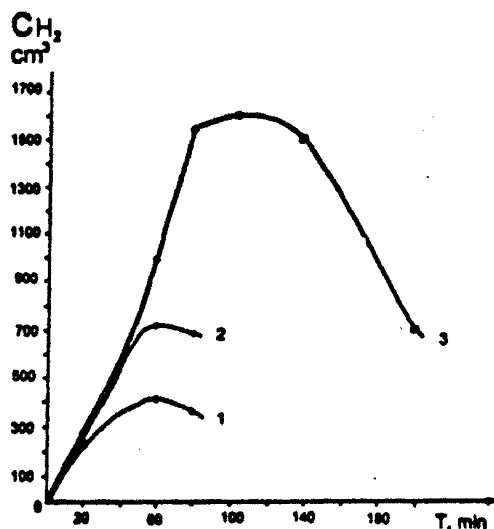
Fig. 3 Dependence of total content of hydrogen in a hydride material on duration of milling. Weight of titanium loaded in a drum: 1-6 g., 2-10 g., and 3-20 g.
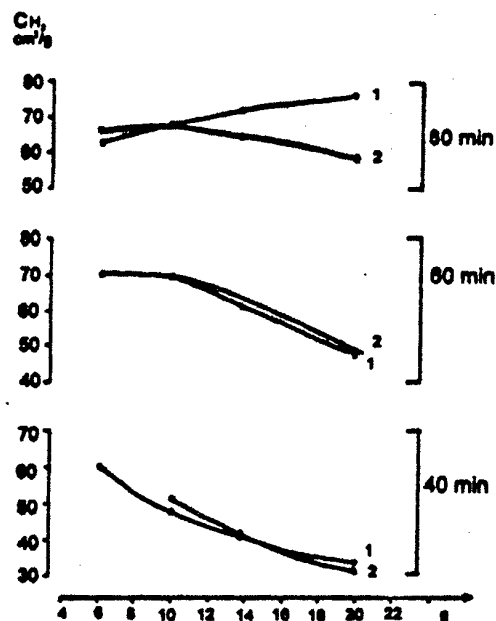
Fig. 4 Influence of the mechanical treatment medium on concentration of hydrogen in a hydride material. 1- water, 2-alcohol.

It was found out that hydrogen concentration in the hydride phase is higher when weight of loaded in a drum titanium powder is lower (fig.2). Total content of hydrogen in the whole weight loaded in a drum is higher when mass of powder is higher (fig.3). It is worth noticing that formation of the hydride phase occurs when, as dispergation medium was also used alcohol. It was shown that amount of hydrogen evolved insignificantly depends on medium of the treatment up to 80 min. of activation. After the treatment exceeds that time, it was noticed that for 10 and 20 g. loaded titanium powder we have more hydrogen evolved in water than alcohol (fig.4). The process of mechanical activation of titanium powder was also accompanied by grinding of iron from metallic drums and balls (fig.5). It was shown that the highest amount of iron has been ground when 20g. of titanium powder was treated in a mill.
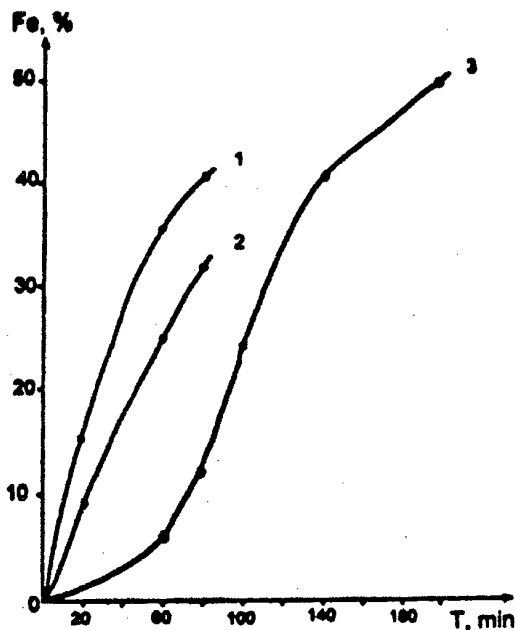
Fig. 5 Dependence of Fe content in titanium powder on milling duration and amount of Ti powder. Weight of titanium loaded in a drum: 1-6 g., 2-10 g., and 3-20 g.

Thus, mechanochemical treatment of titanium powder results in both the activation of titanium powder itself and, what is more interesting, formation of titanium hydride phase TiH_x. Moreover, the formation of titanium hydride occurs under treatment of the powder in water as well as alcohol. Therefore, mechanochemical activation is a promising method for development of new and improvement of existing as hydride materials as methods of their obtaining.

239

CREATION OF EQUIPMENT AND TECHNOLOGIES FOR A HIGH-TEMPERATURE GASOSTATIC TREATMENT OF VARIOUS NEW-ENGINEERING OBJECTS

Neklyudov I.M., Kantsedal V.P., Ashikhmin V.P., Linnik Yu.A., Ledovskaya L.N., Azhazha Zh.S., <u>Kholomeyev G.A.</u>

Institute for Solid-State Physics, Materials Science and Technology at National Science Center "Kharkov Institute of Physics and Technology" (ISSPMST NSC KIPT), Kharkov, Ukraine

The gasostatic equipment and technologies are the new advanced developments which are gaining wide application, extending to the leading branches of national economy such as air-space and nuclear industries, metallurgy, mechanical engineering, chemical industry, etc.

The most important advantage of the gasostatic treatment method lies in the possibility of providing a uniform force action at high temperatures on the products, workpieces and other objects of any shape and composition. In this case, optimum conditions are provided for healing various structural defects, sintering of powdery blanks, synthesis of mineral-like and other-type materials. Abroad, this method received the name hot isostatic pressing (HIP) which is sometimes preceded by cold isostatic pressing (CIP) [1].

The groundwork of the gasostatic facility involves a high-pressure gas compressor (gas drive) and a container with a device for heating the items to be treated.

To compress gases to high pressures, various boosters, piston- and diaphragm-type compressors have gained wide acceptance in the world practice. Depending on the operating parameters of gas and the kind of production tasks, the containers of gasostatic facilities can vary in design, they may be single-layered, multilayered, reinforced by winding special strips, with axially loaded or unloaded frames, etc.

The efforts at ISSPMST NSC KIPT have been aimed for many years at developing gasostatic equipment and methods to immobilize radioactive high-level wastes (HLW) and spent nuclear fuel (SNF). Studies are made to elucidate the possibility of using various natural minerals and their synthetic analogs, ceramic, glassceramic and other materials for immobilization of HLW and SNF.

To perform these studies, high-temperature gasostatic installations appear an efficient kind of equipment. A series of these installations (GAUS type) was designed and manufactured at ISSPMST NSC KIPT [2].

Their distinctive property and advantage consist in the use of the cryogenic gas thermocompressor of KRIT type as a high-pressure gas source[3]. The KRIT-type cryogenic gas thermocompressor was developed at ISSPMST NSC KIPT and has an original design, free of a variety of drawbacks inherent in piston- and diaphragm-type compressors, and also in boosters of various kinds. Its operation is based on a sequential liquefaction and evaporation of working gas - argon. The pressure increases as a result of change in the aggregative state of working gas.

The thermocompressor design comprises no mechanisms, and hence, no moving parts, owing to which there are no sources to contaminate the gas compressed with the grit of moving parts and lubricants. By varying the quantity, connections and the operation order of thermocompressor elements, one can readily provide the required performance characteristics of the KRIT-type thermocompressor. The highest possible pressures of gas, attained with these

compressors, make about 800 MPa. As a working container in the GAUS-type gasostatic installation, a one- or two-layer cylinder choked with threaded plugs is used, depending on the operating conditions.

The special features and the simplicity in the design of the GAUS-type gasostatic facility, and hence, its ease of manufacture, high performance characteristics, and also, its moderate size make the GAUS-type facility more favorable as compared to the other-type facilities.

The ISSPMST NSC KIPT has manufactured over 10 cryogenic thermocompressors and GAUS-type high-temperature gasostatic installations of various modifications, which are now in service at ISSPMST NSC KIPT and at several industrial enterprises and institutions of Chelyabinsk, Zlatoust and St. Petersburg (RF).
Activities at ISSPMST NSC KIPT are continued to create GAUS-type gasostatic

installations intended for use in different industries.

References
1. Status and prospects for the development of gasostatic technologies in Ukraine and abroad. Kantsedal V.P., Lavruk A.G., Basic Centre of Critical Technologies "ORTER" at NSC KIPT, Kharkov, ORTER preprint, 1994.
2. Creation of gasostatic installation for conditioning HLW and SNF. Azhazha Zh.S., Ashikhmin V.P., Zelensky V.F., Kantsedal V.P. et al. (In Russian). "Voprosy atomnoj nauki i tekhniki. VANT". Proc. of the 14th International Conference on Physics of Radiation Phenomena and Radiation Materials Science, 2000, pp. 287-289.
3. A modified cryogenic thermo-compressor KRIT-6M for the closed circuit of gasostatic facility (in Russian). Lavruk A.G., Linnik Yu.A. et al. Ibid, pp. 360-361.

THE CHEMICAL METHODS OF PREPARATION OF ULTRA FINE POWDERS OF ZIRCONIUM, TITANIUM, ALUMINUM BORIDES AND NITRIDES

Petukhov A., Ragulya A.

Institute for Problems in Materials Science, Ukrainian National Academy of Sciences, Kiev, Ukraine

The materials prepared from nano-size powders from borides and nitrides of transition metals and aluminum have sufficiently high properties for successful work in extreme conditions.

In this report studies of the chemical methods for synthesis of ultra fine powders of Ti, Zr, Al borides and nitrides and processes, occurring during these reactions, are reviewed.

The main problems of preparing of nano-size powders by chemical methods are synthesis of "precursors"[1], concentration of impurities, stochiometric composition and formation of conglomerates of prepared powders [2].

The dominant chemical methods are described:liquid-phase reduction [3-7]; gas-phase reduction (CVD-method) [8-12]; gas-phase flaming reduction [13-14], pyrolysis of chemical "precursors" [15-17]; topochemical methods [18].

The liquid-phase reduction includes the preparation of solid "precursor" from a solution and vacuum annealing it in high (about 1000^0C) temperature. CVD- and gas-phase flaming reduction include converting of initial components to gas phase, where the chemical reaction passes with formation of a solid nano-size product. The particular feature of gas-phase flaming reduction is the exclusively high exothermic effect.

The chemical "precursors" can be synthetized, for instance, by sol-gel method, initial metalamides preparation from halogen containing binary compositions of metals and alkyds of alkaline metals.

The data on specific surface, sizes of particles, phase compound, crystallographic properties, impurity content of powders, prepared by the chemical methods, are adduced.

Such methods are suggested as perspective: the pyrolysis in nonisothermic conditions the hybride organic-inorganic gel, prepared by chemical modification of titanium n-tetrapropylate and ethylenediamine for synthesis of nano-size powder of TiN; compositions, derivative of ammoniem, for AlN preparation; titanium boron-hydride $Ti(BH_4)_3$ and fine mixture H_2TiO_3-H_2BO_3-$C_{12}H_{22}O_{11}$ for TiB_2 ultra fine powder synthesis.

1. Kuznetsov N.T.// Materials Science of Carbides, Nitrides and Borides. – Dordrecht, 1999. – P.223-245.
2. Скороход В.В., Уварова I.В., Рагуля А.В. – Київ, Академперіодика, 2001.- 179 с.
3. Способ получения сверхтонких порошков/ Като Акио// "Хемэн".- 1983.- 21, №2.- С.65-76 (яп.).
4. Axelbaum R.L., Bates S.I., Buhro W.E. a.o.// Nanostruct. Mater.- 1993. – 2, №2.- P.139-147.
5. Axelbaum R.L., Bates S.I., Buhro W.E. a.o.// Particul. Sci. Technology: Proc. Fine Part. Soc.- 1992.- 10, №3-4.-P.11.
6. Andrievski R.A., Kravchenko S.E., Mozgina N.G. a.o.// Nano 94: 2nd Int. Conf. Nanostr. Mater., Stuttgart, October 3-7, 1994: Programe and Abstr.- Stuttgart.- 1994.- P.146.
7. Андриевский Р.А.., Кравченко С.Е., Шилкин С.П.// Неорг. матер.- 1995.- 31, №8, С.1048-1052.
8. Elger G.W., Traut D.E., Slavens G.J. a.o. // Metall. Trans. B.- 1989.- 20 B, №4.- P.493-497.
9. Заявка Японии №64-37407, пр.30.07.87 №62-191308, публ.08.02.89. МКИ C01B 21.06., B01 J4/02/ Доноуэ К., Танака Х., Канэсаку Я.
10. Junishi Hojo, Akio Kato.// J. Ceramic. Soc. Jap.- 1981.- 89, №1029.- P.277-279.
11. Заявка ФРГ №3415611, публ. 31.10.84 №44, пр.США 26.04.83 №488870, МКИ C01B 35/04 C04B 35/58, 35/66.
12. Зуоквиан Каи, Кенонг Занг// Хуасюэ Тунбао , Chemistry.- 1987.- №5. – С.35-38. (кит.).
13. Axelbaum R.L., Lottes C.R., Huertas J.I. a.o.// Materials of 26th International Symposium on

242

Combustion.1996/ The Combustion Institute
.- P.1891-1897.

14. Axelbaum R.L., Dufaux D.P., Frey E.A. a.o.//
Metallurgical and materials transactions B.-
1997.- V.28B.- P.1199-1211.

15. Maya Leon.// Transform. Organomet. into
Common and Exotic. Mater.: Des.and Activ.:
Proc. NATO Adv. Res. Workshop, Car
D'Adge, Sept. 1-5, 1986.- Dordrecht etc.,
1988.- P.49-55.

16. Moalla S., Amara Ch.B., Zarrouk H.// Journal
of Mat. Synth. and Procc.- V.4, №4.- 1996.-
P.265-273.

17. Власова М.В., Серебрякова Т.И., Килимник
А.А. и др.// Пор. мет.- 1994.- №5/6.- С.70-
75.

18. Горовой М.А., Голтвяница С.К.. Миннева
Л.К.// Пор. мет.- 1986.- №9- С.76-78.

INTENSIFICATION OF ALLOYING PROCESSES IN HETEROGENEOUS COMPOSITE UNDER ELECTRIC CURRENT ACTION

Raychenko O.I., Derev'yanko O.V., Popov V.P.
Frantsevych Institute for Problems of Materials Science, Ukrainian National Academy of Sciences,
3, Krzhyzhanivs'ky St., Kyiv, 03142, Ukraine,
tel.: (044) 444 22 55, e-mail: raitch@ipms.kiev.ua

Introduction

The mixtures which are intended for production of the composition materials (CM) contain often some components that have relatively low-melting points. Arising of liquid during the thermal processing may sometimes hinder the complete technological process. Using an electric current passing through a proper mixture mainly makes more active the diffusion and alloying due to electroconvection [1-3].

Experimental researches

The spherical solid copper particles (of diameter ~ 50 μ) were taken as an addition (20 mass. %) to tin. The electric current density passing through the original mixture was equal to 100-150 A/cm^2. The duration of processing was equal to 120 s. In order to compare, the experiment at annealing of the same composition in the muffle furnace (at temperature ~ 350 ^{0}C and 1200 s) also.

The X-ray analysis has shown that the copper particles under the electric current action were dissolved in the liquid tin. As the result the following structure was obtained: the intermetallides Cu_6Sn_5, Cu_3Ssn and tin (Fig. 1a). The intermetallides mentioned were arisen in the plates shape (with length up to 20 μ and thickness of 0.5-1.0 μ). The material obtained after processing in the muffle furnace contains the pure copper particles surrounded by the "shaping strips" of the Cu_6Sn_5 – C_3Sn and tin phases (Fig. 1b).
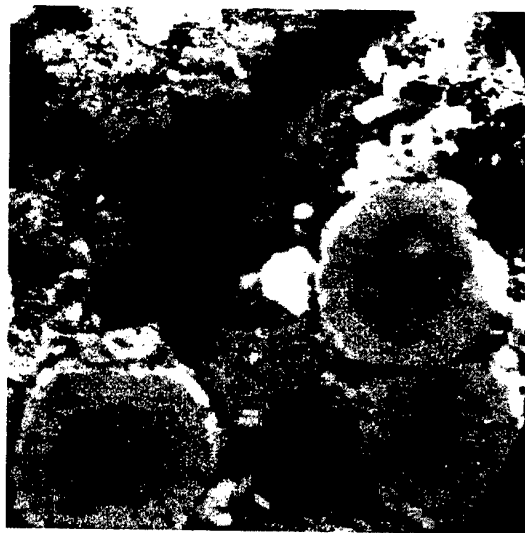
Figure 1- Microstructure of Cu-Sn samples: a- sintered by electric current (intermetallides Cu_6Sn_5 and C_3Sn), ×60; b- sintered in muffle furnace by conventional method (intermetallides as "shaping strips" of the Cu_6Sn_5, – C_3Sn and copper in center), ×500.

244

This allows to conclude that the more intensive mass transfer, than it is at convectional sintering, occurs under the electric current action. We think that the mechanism of the phenomenon observed is the electroconvection.

The second experimental series consists of processing the mixtures containing 80 % copper particles with dimensions 0.7 mm and 20 % tin. The sintering of such objects by the electric current (at temperature 600-670 ^{0}C and 120 s) results in the alloy structure: intermetallides Cu_6Sn_5 and C_3Sn in the plate shape (with length up to 100 μ and thickness 0.7-5.0 μ), pure tin.

In order to compare the same mixture was processed in the muffle furnace, the temperature at this processing was the same. It was shown that the complete alloying has occurred after the sintering named above at temperatures 650-700 ^{0}C after time 2400-2600 s. The composition of the samples obtained was similar to the composition of the samples sintered by electric current described above: the intermetallides named with length 1.6-1.7 mm and thickness 5-25 μ.

Figure 2- Microstructure of Cu-Sn samples, sintered under by electric current action (copper particle is surrounded by the thin layer of the Cu_6Sn_5 phase and intermetallide Cu_6Sn_5 as "rays from Sun"), ×200.

The additional metallographic investigation of the samples obtained after the short sintering by electric current (15-20 s) allows to fix some intermediate state during alloying.

So, the copper particle is surrounded by the thin layer of the Cu_6Sn_5 phase, besides that the plates of such an compound are located with directions as "rays from Sun". This picture maybe is caused by the peculiarities of the electromagnetic exertion at electric sintering of solid-melt compositions. During this processing some small pieces are separated from the intermetallide plates and more off these plates.

Conclusions

The intensification of mass transfer and alloying in heterogeneous materials under the electric current action was observed. This occurs often due to the electroconvection and the electroconvection diffusion. Such phenomena can be used for shortening sintering process. This will allow in some cases to prevent, or to minimize for example, graphitization of diamond grains in tool CM due to increase of temperature during sintering and to short this technological process. The other objects, which may be retained by this method, are CMs containing reinforcing fibres and thin rods.

References

1. Chow C.-Y. Flow around a nonconducting sphere in a current-carrying fluid // Phys. Fluids. – 1966. – Vol.9. – №5. – P. 933-936.
2. Raychenko O.I.,. Raychenko O.O., Chernikova E.S., and Miroshnichenko A.A.Analysis of the electroconvection dissolving of a conductive solid sphere in a current-carrying liquid // Magnitnaya gidrodinamika. – 1994. - N 1. - Pp. 71-76. (In Russian).
3. Raychenko O.I., Popov V. P., and Derev'yanko O. V. Alloy concentration fields resulting at dissolving of solid particle in the surrounding current-carrying liquid metal // Metal Physics and Advanced Technologies.- 1999. - Vol.21. - N 10. –Pp. 80-86.

PHYSICAL PROPERTIES OF HTSC CERAMICS $Bi_{1.8}Pb_{0.2}Sr_2Ca_1Cu_2O_8$ OBTAINED UNDER HIGH PRESSURE CONDITIONS

Nemoshkalenko V.V., Shevchenko A.D.
Kurdyumov Institute for Metal Physics, N.A.S. of the Ukraine, Kyiv, Ukraine

Abstract

On the HTSC ceramics $Bi_{1.8}Pb_{0.2}Sr_2Ca_1Cu_2O_8$ obtained by sintering under high pressure conditions the gravimetric investigations in the range of temperatures 300–1100 K and under magnetization M at 4,2 and 79 K in magnetic fields H till 7 T were performed. The gravimetric data of the experiment carried out in static air atmosphere with heating and cooling rate of 10 gr/min showed an insignificant loss (0,1 %) of the sample mass. The critical transport current density of $Bi_{1.8}Pb_{0.2}Sr_2Ca_1Cu_2O_8$ samples j_c and their granules, j_c^g, low H_{c1}=420 e and upper H_{c2}=180000 e critical magnetic fields were calculated from the dependencies M(H). It was determined that at 4,2 K and H=0 j_c=2,5•10^4A/cm^2, j_c^g =7•10^6A/cm^2; at 79 K j_c=70A/cm^2 and j_c^g =2•10^4 A/cm^2. At 4,2 K and H=7T j_c=4,1•10^3 A/cm^2, j_c^g =1,17•10^6 A/cm^2.

Introduction

The investigation of the metallo-oxide HTSC ceramics physical properties is of great interest. However, as it well known, common porous HTSC ceramics obtained by the standard solid phase synthesis technology is characterized by the degradation of critical parameters under external effects, such as follows: thermocycling, agressive medium, etc. Absence of the HTSC ceramics operating reliability is a serious obstacle for its wide application. In connection with this/the development of other technologies to obtain the metallo-oxide HTSC ceramics, for example, using high pressure technology, is of interest. Presented paper is dedicated to the investigation of the HTSC ceramics Bi-Sr-Ca-Cu-0:Pb samples obtained under high-pressure conditions (up to 5 GPa), thermogravimetry in the temperature range 300–1100 K and magnetization M at 4,2 and 79 K.

Experimental Results and Discussion

The investigations were carried out on the $Bi_{1.8}Pb_{0.2}Sr_2Ca_1Cu_2O_8$ samples prepared by sintering of the 2-2-1-2 compound powders powders under high' pressure conditions (up to 5 GPa) using high pressure solid phase chambers of "Toroid" and "Lens" types and hydraulic press of 2000 tonnes stress. While thermobaric processing the oxygen loss was eliminated by using special technological methods allowing to provide air-tightness of the high pressure chamber in which protective medium with 2-2-1-2

compound powder was. X-ray phase analysis was performed with the help of X-ray diffractometer "DRON-2.0" using CuK radiation. The X-ray structural analysis of the samples showed that they have mainly the structure of 2-2-1-2 type. The parameters 2-2-1-2 pseudo-tetragonal phase are as follows: a= =5,39 Å, c=30,78 Å; for 2-2-2-3 phase a=5,39 Å, c=37,04 Å. The temperature control of superconducting transition T_n was carried out by measurement of magnetization temperature dependences M and electrical resistance R. It was determined that the investigated samples had the value T_c=86 K at R=0 and the metallic dependence R(T) at the temperature which is higher than T_c. Critical transport current density $j_{c}j_g$ for the samples and critical current density of the sample granules (size of granules ?3 μm) were determined from the dependences M(H) at 4,2 and 79 K. The value j was calculated through the loop width of the curve M(H) in the Bin-London model. The samples for the magnetic measurements were prepared in the form of balls with 0.84 mm diameter. Dependences M(H) in the range H= 500e were performed for 79 K and in the range H=7T for T= 4,2 K. Magnetic measurements were carried out according to the standard technique with the help of "SKVID"-magnetometer, and at 4,2 K – with the help of the "ballistic magnetometer; electrical measurements were performed by the four probe methods Thermogravimetric investigations were performed on the Hungarian "G-1500" derivatograph of MOM firm in the static air atmosphere, rate of cooling and heating was 10 dg/min. The thermograms were taken in the temperature range 300–1100 K on the samples of 2g weight. It was turned out, that sintering of HTSC ceramics under high pressure conditions, using it as a solid medium transmitting pressure, leads to the structure deformation both 2-2-1-2 and 2-2-2-3 phases that was expressed in widening of the diffraction lines and in decreasing of peak intensity. It is explained by the presence of the internal microstrains in the sample which, however may be removed, by the following thermocycling. Offered thermocycling up to 1100 K with heating rate 10 dg/min of the mass HTSC ceramics Bi-Pb-Sr-Ca-Cu-O obtained by sintering under high pressure conditions brings to essential regeneration of the 2-2-1-2 and 2-2-2-3 phases crystal structure without changing the unit cell parameters.

As the content of oxygen in metallo-oxide HTSC ceramics determines superconducting properties then for determination of the ceramic thermal stability its thermogravimetric investigations are very important. In Fig.1 the temperature changing of
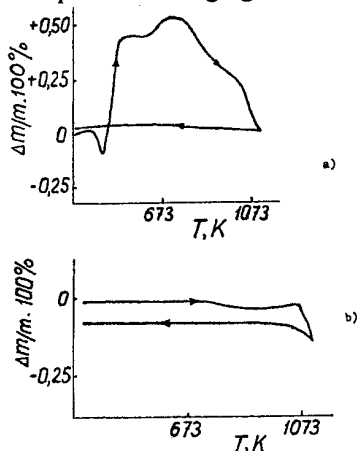
Fig. 1. Temperature changing of mass of HTSC ceramics samples obtained under high pressure conditions (5GPa): a) first cycle heating-cooling; b) second cycle heating-cooling.

mass of $Bi_{1.8}Pb_{0.2}Sr_2Ca_1Cu_2O_8$ samples obtained under high pressure conditions (2GPa) are presented. After the first cycle of heating-cooling the mass changing of the sample is insignificant (0.1%). After the second heating-cooling cycle mass of the samples doesn't practically change. Comparison of obtained by us experimental results on thermogravitometry of the HTSC ceramics $Bi_{1.8}Pb_{0.2}Sr_2Ca_1Cu_2O_8$ samples sintered under high pressure conditions (5GPa) with The literary data for common porous ceramics, for example, yttrium HTSC ceramics obtained by standard solid phase synthesis technology, gives the possibility to make following conclusions:

a) the general changing of mass is lower on one order of value for the HTSC ceramics $Bi_{1.8}Pb_{0.2}Sr_2Ca_1Cu_2O_8$ samples obtained by sintering under high pressure conditions;

b) the cycling stabilizes the change of mass for the samples obtained by sintering under high pressure conditions in heating-cooling regime;

c) the single-step change of mass takes place at heating for the HTSC ceramics samples obtained under high pressure conditions. Thus, the experimental thermogravimetric results for HTSC ceramics $Bi_{1.8}Pb_{0.2}Sr_2Ca_1Cu_2O_8$ samples obtained under high pressure conditions point at thermal stability of such samples till 1050 K and more stable connection of oxygen atoms in volume in comparison with common porous HTSC ceramics obtained by sintering under the standard solid phase synthesis technology. The low H_{c1} and upper H_{c2} critical magnetic fields, j_c and j^g_c were

determined from the dependences M(H). The value H_{c1}, was determing at 4,2 K upon the beginning of the deflection of the dependence M(H) from linear dependence considering the magnetization factor. The value H_{c2} was determing the dependence M (H) at 4,2 K by extrapolation of the dependence M (In H) till intersection with the axis "X". It is turned out that H_{c1}= 420 e and H_{c2}= 180000 e. The critical current density data are presented in the Table.

Table Meanings of critical transport current density of the samples j_c and critical current density of granules j^g_c at 4.2 K for HTSC ceramics $Bi_{1.8}Pb_{0.2}Sr_2Ca_1Cu_2O_8$ obtained by sintering under high pressure conditions in the different magnetic fields H

H,T	0	1	2	3	4	5	6	7
$j_c 10^3 A/cm^2$	25	14,3	10,8	7,9	6,5	5,7	4,8	4,1
$j^g_c 10^6 A/cm^2$	7	4	3,03	2,2	1,8	1,6	1,35	1,17

It is seen that in the HTSC ceramics obtained under high pressure conditions the critical transport current density j_c depends weakly from the value of the magnetic field intensity H. As it is known, in mass porous HTSC ceramics obtained by the standard solid phase synthesis technology, the value j_c decreases catastrophically under the influence of outer magnetic field, that is an obstacle for wide practical application of porous HTSC ceramics. From the analysis of the dependences M(H) in the range of H= 500 e it is turned out that at 79 K in H=0 j_c =70A/cm^2 and j^g_c = 2$\cdot$10^{4}A/cm^2. It is the fact that critical transport current density at 79 K in $Bi_{1.8}Pb_{0.2}Sr_2Ca_1Cu_2O_8$ samples obtained under high pressure conditions, is approximately equal to 10^2A/cm^2, makes such material to be ineffective for applying in special assignement devices at the temperatures of liquid nitrogen.

Conclusion

On the basis of performed investigation (thermogravimetry and magnetization) of mass HTSC ceramics $Bi_{1.8}Pb_{0.2}Sr_2Ca_1Cu_2O_8$ samples it is-possible to make following conclusion: the thermally stable mass ceramics with critical transport current density j_c 10^2 A/cm^2 at 79 K was obtained by sintering under high pressure conditions (up to 5GPa); it makes possible to apply such ceramics in special assignement devices.

247

WETTING OF THE HT$_c$SC -CERAMICS SURFACE BY COPPER UNDER HIGH PRESSURE

Shevchenko A.D.

Kurdyumov Institute for Metal Physics, N.A.S. of the Ukraine, Kyiv, Ukraine

Abstract

Technology of wetting the metallo-oxide HT$_c$SC-ceramics surface by copper under high pressure (up to 5 GPa) has been developed with the held of high pressure techniques. The high pressure is produced by the hydraulic press of 2000 tons stress and high pressure solid-phase chambers of "toroid" type. The copper layer on the surface of metallo-oxide HT$_c$SC -ceramics is formed as a result of copper reducing reaction from copper oxide in the presence of carbon.

Introduction

The problem of metallo-oxide HT$_c$SC-ceramics surface metallization is an actual task of HT$_c$SC physics and techniques and, in particular, physics of surface of HT$_c$SC materials, Solution of this task gives possibility to obtain, for example, ohmic electric contacts on the boundary metal-HT$_c$SC ceramics and, therefore, to perform successfully fundamental experimental investigations of kinetic and galvanometric properties of the HT$_c$SC samples for determination critical parameters of investigated metal-oxide HT$_c$SC ceramics. In so doing it is necessary that metallization of HT$_c$SC ceramics surface won't lead to destruction of internal structural bonds and as a results of this – to the loss of high-temperature superconductivity. In the previous scientific works the author has shown that use of high-pressure techniques (hydraulic press of 2000 tons stress, high pressure solid phase chambers of "toroid" and "lens" types and special instrumentation for sintering of HT$_c$SC-ceramics under pressure) gives possibility to obtain thermo-stable HT$_c$SC ceramics by sintering under high pressure (up to 10 GPa) conditions suitable for practical application at the liquid nitrogen temperatures. The present paper contains the results of technology invented by author for wetting of the HT$_c$SC-ceramics surface by copper under high pressure with an aim to obtain ohmic electric contacts on the boundary metal – HT$_c$SC-ceramics and, therefore, to determine the boundaries of practical applying HT$_c$SC as a constructive elements, which in real conditions of exploitation are under thermomechanical loads. Up to the present time there are no, however, the works dealing with studying the wetting of the HTSC-ceramics surface by copper under high pressure. Therefore the investigation of this problem is clean with point of view of scientific importance.

Results and Discussion

To wet by copper the surface of metal-oxide HT$_c$SC-ceramics under high pressure conditions, the copper oxide is deposited on the surface of ceramics and heat under pressure 0,1–10 GPa in the presence of oxygen to 900–1300°C, Heating under pressure is performed in a protective shell of high-melting metals one can use, for example, tungsten or molybdenum which do not interact with elements of ceramics, and as a source of carbon-graphite. In a given case pressure was created by hydraulic press of 2000 tons stress and high pressure solid phase chambers of "toroid" type. An electric contact in the form of a thin layer of copper on the surface of metal-oxide HT$_c$SC-ceramics is formed due to reducing reaction of copper from the copper oxide in the presence of carbon. Because of high temperature reduced copper in the form of melt is distributed along the HT$_c$SC-ceramics surface. As far as HT$_c$SC-ceramics contains copper oxide, it part, being in the surface layer, also reduces that assists good wetting the surface of metal-oxide HT$_c$SC-ceramics by copper and, therefore, – strong coupling of them at wetting. Presence of the shell made of high-melting metal in combination with high pressure excludes the loss of oxygen and prevents disarrangement of inner structural bonds in HT$_c$SC ceramics at heating under pressure. The shell also protects HT$_c$SC-ceramics from penetration of carbon into ceramic bulk and prevents partial reduction of metals from oxides. Moreover, oxygen loss in the volume of HT$_c$SC-ceramics also takes place under pressure below 0,1 GPa as a result of bad airtightness of the high pressure chambers. Both pxygen loss in the volume of HT$_c$SC-ceramics due to penetration of carbon into ceramics mass and breakdown of airtightness of high pressure chambers lead to loss of high-temperature superconductivity. Application of pressure higher than 10 GPa, as is known, is limited by technical capabilities of used high pressure devices. High pressure solid phase devices provide uniform pressing of the shell and protect its content from undesirable contact with environment during heating under pressure. Heating below 900°C doesn't provide melting of reduced copper, heating higher than 1300°C – isn't technically advisable,

In Figure 1 the scheme of the high pressure chamber equipment for wetting the surface of metal-oxide HT$_c$SC-ceramics by copper under high pressure conditions is presented. The high pressure chamber

contains two anvils 1 with container 2 made of pyrchophilite or catlinite in their pockets. HT_cSC-ceramics 5 is placed in protective shell of high-melting metal consisting of cylindrical part 4 and two discs 5 with apertures 6. The pellets 7, made of copper oxide, are placed outside of discs 5 and through the apertures 6 in the discs contact with the faces of HT_cSC-ceramics samples 3. Outside of the pellets 7 the graphite discs 8 are installed.

Wetting the surface of metal-oxide HT_cSC-ceramics by copper under high pressure conditions is realized by the following way, The anvils are brought together with the help of the hydraulic press of 2000 tons stress (it isn't shown in Fig. 1).
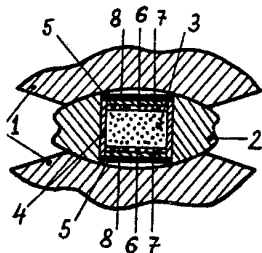
Fig. 1. Scheme of equipment of high pressure chamber for wetting the surface of HT_CSC ceramics by copper under high pressure conditions: 1 – anvils; 2 – container made of pyrchophilite or catlinite; 3 – HT_CSC ceramics sample; 4 – rotective shell made of high-melting metal in the form of cylinders-protective shell made of high-melting metal in the form of disc; 6-aperture in the disc; 7 –copper oxide pellet; 8 – graphite disk.

In this case deformation of material of the container 2, which transfers pressure through high-melting shell 4 and 5 on the HT_cSC-ceramics sample 3, takes place. On attainment required pressure heating is turned on. Heating is realized by gating of electric current along the curcuit: anvil 1 – graphite disc 8 – shell of high-melting metal 4, 5 – graphite disc 8 – anvil 1. On attainment required temperature due to contact of copper oxide pellet 7 and graphite disk 8 the reducing reaction of copper takes place. Through the aperture 6 in the disc 5melt copper falls on the face surface of HT_cSC sample 3 and is distributed upon it in a thin layer. After finish of reducing reaction, electric heating is stopped and pressure is taken off. After cooling the HT_cSC-ceramics sample with face surfaces metallized by copper is derived, For wetting the face surface of HT_cSC-ceramics by copper under high pressure c conditions either ready preliminary sintered HT. SC ceramics c sample should be placed into the shell 4, 5 or HT_cSC-ceramics o in the form of powders, which are sintered under action of high pressure and temperature into the sample of required form, whose face surfaces are simultaneously metallized by copper, As a source of carbon one can use not only graphite disc 8 out thin layer of graphite deposited, for

example, by detonation deposition on copper oxide pellet 7. Below some concrete examples of realization of wetting method the surface of HT_cSC-ceramics by copper under high pressure conditions are. Pressure was achieved with the help of hydraulic press of 2000 tons stress. The high pressure chamber of "toroid" type was used, Into tungsten shell 4,5 the preliminary obtained HT_cSC-ceramics $YBa_2Cu_3O_{7-\delta}$ sample was placed. Outside of the shell of copper oxide the pellets 11 mm in diameter, 1 mm thickness and graphite discs 11 mm in diameter, 1 mm thickness were placed. The diameter of aperture in disc 5 was 3 mm, Container was produced of catlinite. Pressure of 5 GPa was created in the chamber and then heating to 1300°C was promoted, Under these conditions exposure 60 sec was made, then heating was stopped and pressure was removed. After cooling the HT_cSC-ceramics $YBa_2Cu_3O_{7-\delta}$ sample with layer of copper 0,4 mm in thickness on it faces was derived, Copper layer was used as electric contacts to bind them with copper wire with the help of light-melting solder, Measurements have shown that obtained contacts are ohmic ones and HT_cSC-ceramics sample with wetted by copper faces preserved superconducting properties at a liquid nitrogen temperature. An another series of experiments HT_cSC-ceramics $YBa_2Cu_3O_{7-\delta}$ in the form of powder has been used, The scheme of equipment was the same as in the first series of experiments, Molybdenum was used as a material for the shell. Under pressure 5 GPa and temperature 1300°C the sintered HT_cSC-ceramics sample with metallized by copper faces has been obtained. The sample possessed superconductivity at a liquid nitrogen temperature and had ohmic contacts. Checking by thermocycling has shown that the contacts were not "aged" under thermocycling.

Conclusions
The method of wetting the surface of metal-oxide HT_cSC c ceramics by copper under high pressure conditions up to 10 GPa has described, Its realization has a great scientific and practical significance as it gives possibility to obtaine long-dimensional conductors from HT_cSC-ceramics samples with c metallized by copper faces useful for practical application at a liquid nitrogen temperatures in the special assignement devices.

249

MANUFACTURE OF NEW MATERIAL WITH HIGHER DAMPING ABILITY FOR SUPERHARD CUTTING TOOLS

Shevchenko A. D.
Kurdyumov Institute for Metal Physics, N.A.S. of the Ukraine, Kyiv, Ukraine

Introduction

The purpose of given work is to obtain under high pressure conditions using specialized technology' the material with thermoelastic martensite, material that would provide high level of deformation accumulation E_h, in the martensite transformation process and, therefore, the increase of Q^{-1}. It may be realized, for example, if to create necessary quantity of closed pores in the material bulk with thermoelastic martensite. Necessary quantity of closed pores, which would realieze displacement of phase boundaries increasing mobility of boundaries of martensite microdomains that would lead to effective relaxation of external strains, growth of E_h and amplification of Q^{-1} in this case it is necessary for "closed" porosity in the material with thermoelastic martensite to be such in magnitude that Q^{-1} amplification mechanism would work and simultaneously structural material would possess necessary mechanical strength. One may expect that mechanism giving rise to the growth of En and Q^{-1} in the material with thermoelastic martensite will also lead to strengthening of the material itself in the thermoelastic martensite state as a result of manifistation of the plasticity effect at martensite transformation in the field of external strains.

Experimental

To create high pressure, solid-phase high pressure chambers ("toroid" and "lens"-types) and a hydraulic press of 2000 tons stress were used. Physical-mechanical characteristics of "avibrite" in comparison with those, studied by the author, of cast alloy with composition analogous to that of new material are listed in this work. Complex of "avibrite" physical and mechanical characteristics, and efficiency of cutting and drill tool, equiped by vibration-damping elements made of new material, at permanent, impact and impact-rotation load on the tool has been investigated. The microhardness magnitude H_b was measured by the Vickers method at load on indentor 50 g. Compressive strength limit value σ_c was determined by-compression of cylindric samples with plane-parallel polished ends between hard-alloyed bearing on the static test machine "P-5". Investigation of damping ability Q^{-1} was performed over ultrasound damping in the frequency range of $40 \div 1500$ kHz on the samples of "avibrite" and ones of analogous composition cast alloy using the resonance method based on measuring of the resonance curve with on the level $A_{max}/\sqrt{2}$ (A_{max} is a resonance maximal amplitude). Structure investigations of obtained composite material "avibrite" were performed with X-ray diffractometer "DRON-2" Composition of obtained material was determined with the help of X-ray fluorescent spectrometer VRA20 and VRA30 of the "Karl Zeiss Ienna", Germany and English electron scanning microscope with electron probe of the "Camscan" firm. The value E_h m the alloy was determined by the formula $E_h = c/2r = c/l + a^2/4l$ (c is thickness of the sample, r is a bending radius, a is the distance between quarts bearings, l is a sag) from investigations of the shape memory effect (SME) by the three-point bending method of rectangular samples with concentrated load. Investigation of SME according to this method was realized by measurement of the temperature dependences of the sag l(T) formed by bending deformation of rectangular "avibrite" plates and ones of analogous composition alloy. The composite material microstructure was investigated with "Camscan" and optic microscope "Neophot-2", Germany.

Results and discussion

It is determined that at T<323 K obtained composite material "avibrite" is characterized by availability of pores placed along the boundaries of microdo – mains having martensite structure. It is known that SME is related to inelastic properties of materials, it is an effect of phase thermoelastic equilibria and occurs at martensite transfor-mation. It is also known that the martensite transformation is accompanied by big shift deformations (effect of transformation plasticity – decrease of resistance to shift deformation) leading, in its turn, to accumulation of deformation in the martensite transformation process in the field of external strains, realizing by the way of displacement of interphase boundaries of microdomains with followed directed orientation of domains under effect of external load; in this case, such displacement realizes relaxation of external strains and thereby motivates damping ability Q^{-1} characteristic for a given material with thermoelastic martensite. As a rule, good damping materials have $Q^{-1} = 10^{-3} - 10^{-4}$. It has been turned out that in "avibrite" $E_h = 4,5\%$ and it exceeds E_h for the analogous composition alloy approximately in 17 times, in this case reversible deformation $E_r = 3,0\%$ for "avibrite", and SME is characterized by incomplete return of accumulated deformation – remanent deformati on $E_{rem} = 1,5\%$. Investigation of Q^{-1} in "avibrite" and in alloy showed that in the alloy $Q^{-1} = 0,005$, and it is impossible to measure ultrasound damping in "avibrite" because offtill absorption of ultrasonic oscillations in it, i. e.

250

"avibrite" is characterized by raised Q^{-1}. Investigation of mechanical properties of a given composite material and analogous composition alloy showed that in "avibrite" σ_c =2300 MPa and exceed <7c of the alloy in 1,7 times under compression of the samples made of a new material in response to the external, raising in time load the displacement of martensite phase of the latter (at the room temperature "avibrite" is already in the state with thermoelastic martensite) and following direct disposition of domains in the field of external strains, at which the process of accumulation of deformation proceeds, take place. The result as to σ_c correlates with the data on microhardness H_b, also resulting in that H_b, in "avibrite" exceeds H_b of analogous composition alloy in 1,8 times. It is determined that for H_b=4,8 GPa. Influence of "avibrite" vibration-damping elements on capacity of work of cutting tool made from polycrystalline super-hard material on the base of the boron cubic nitride from and other superhard materials, developed at the Institute of Superhard Materials, Academy of Sciences of Ukraine, under dynamical loads on tool, arising while processing heatproof steels, has been studied. The tests has proved that "avibrite" dampts effectively vibrations arising under dynamical load on cutting instrument and increases wear resistance of the tool in 1,8-3,0 times. It has been determined that application of a new material while core drilling of the boreholes also increases wear resistance of the diamond drill bits and reduces the consumption of diamonds by 59%. The properties of "avibrite" to reduce dynamical loads on tool in the process of cutting were investigated and were compared with analogous characteristics of hard alloy BK8. "Avibrite" and alloy BK8 were used as backing plates at attaching in a jack of a holder of cutting element made of superhard materials. Comparative tests were performed under following conditions, equal to "avibrite" and BK8. Cylindric blank 70 mm in diameter of steel 9XC with hardness 60HRC was machined on screw-cutting lathe with numerical-program control (NPC), model 16K2003CI. To imitate impact loads, six grooves were done on a blank along the generating line. Cutting rate was 1, 8 m/sec. Thus, the impact cycles repeated every 0,02 sec. Turning was performed with longitudinal feed 0,1 mm/rot., depth of cut 0,2 mm without lubricating-cooled liquids. Kiborite was used as instrumental material; round cutting plate made of it was mechanically fixed in the groove of a holder, forming front and back angles γ =-10° and α =10° without face on cutting edge. Cutting instrument was isolated above and below from the clamp and bearing surface of a holder by intermediate plates of "avibrite and alloy BK8. In the process of cutting the force components P_x, P_y and P_z were measured with the help of universal dynamometer, model YDM-100. The dynamometer was connected with the computer ECM CM-4 that asked the data unit with the frequency 10^4 imp./sec. Obtained information was entered into computer operating memory and then was reproduced on the graphic plotter. In Figure I diagrams of change of the main cutting force component P_z on cutting time after 3 second of contact of cutting instrument with the blank are presented. In the first case (see Fig. 1, a) hard alloy of BK8 was used as bearing bearing blanks, in the second one – "avibrite" (see Fig. 1, b).
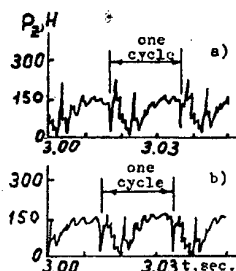
Fig. 1. Dependence of cutting force on time using the alloy BK8 (a) and "avibrite" (b) as a pad for the instrument.

The cycles of duration 0,02 sec. are well seen. At the moment of unloading, when the instrument falls in a groove on the blank, the curve is sharply descended, however, at the expense of elastic elements of the dynamometer vibration of instrument takes place, having pyramidal form both for BK8 and "avibrite" that points at equal test conditions. While contact of kiborite instrument with following part of blank, the cutting force is reply grown it is stabilized with the time and goes out a nominal regime, characterizing for every test by mean load 150 H (H is Newton). New cycle begins with unloading. Comparative analysis of dependences in Figure 1 shows that cutting process is characterized by smaller intensity when using "avibrite" as a bearing plate. One can judge about this by the height of splashes at the moment of impact and also after unloading. For the new material the height of splashes doesn't exceed mean level of 150 H, while for BK8 the splashes achieve 200 H and more that exceeds by 40% splashes when "avibrite" is used. Analogous character of dependences was observed for axial P_x and longitudinal P_y cutting force components, up to 12 sec. Thus, "avibrite" at compared to BK8, possesses better ability to damp vibrations in the process of cutting under impact load on instrument and may be recommended for use as backings in collecting instrument and for armoring of clamp pressure surface, too.

Conclusions

A new composite material with higher damping ability has been created with the use of specialized technology. Application of vibration-damping elements made of new composite material in the cutting and drilling tools proved the effective damping of the vibrations arising under permanent loads, impact and impact-rotations ones. resulting in considerable increase of wear resistance of cutting tools and diamond drill bits.

DIFFUSION-VACUUM TECHNIQUE FOR POROUS MESH MATERIALS

Pelevin F.V.

Bauman Moscow State Technical University, Moscow, Russia

Development of materials with predetermined properties makes it necessary to establish relationships between the strength, hydraulic resistance and geometrics of the structure and factors determining its formation.

Mechanical properties of porous metals are dependent on mechanical properties of the particles, fibers, wire material, their dimensions; material porosity; number and dimensions of post-sintering interparticle contacts, sintering process. An increase of mechanical properties is contributed by an increase of strength of the particles, fibers, wire material, decrease of porosity, increase of a number, dimensions and quality of interparticle contacts. For the evaluation of mechanical properties of porous materials conventional characteristics are used, i.e. ultimate strength, compression and shear strength, elongation, impact elasticity, etc.

Porous mesh materials (PMM) have the best mechanical and hydraulic properties among other porous materials [1,2]. PMMs are used to manufacture filters, thermal protection systems, and various-purpose heat exchangers. They have a well-defined anisotropy of the structural, hydraulic, thermal and mechanical properties ($\sigma_{Bx} \neq \sigma_{By} \neq \sigma_{Bz}$), as an initial material for PMM is a mesh, that itself is an anisotropic material [3].

In PMM production wire gauze meshes are most widely used, namely filter meshes GOST 3187-76 and meshes with a square cell GOST 6613-73. Filter meshes have a regular and controlled structure. Anisotropy of PMM is made more evident in PMM made of filter meshes [2,4].

Presently PMM are manufactured by using two processes, i.e. 1) by a hot rolling of a pack of meshes in vacuum; 2) by a diffusion welding of metallic meshes in vacuum (Fig. 1). Strength characteristics of PMM produced by these processes are different.

Diffusion-Vacuum Welding of Mesh (PMM)

Rolling of Mesh Pack
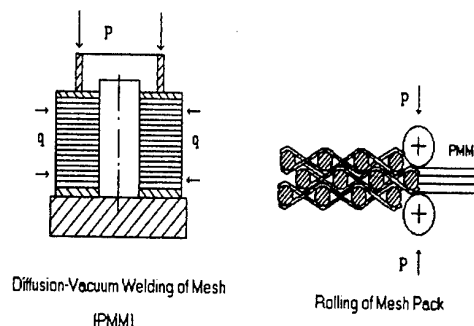
Fig. 1. PMM Production Techniques

The technique of producing porous sheets by hot rolling developed at N. Bauman MSTU is well known [1]. However, when producing cylindrical, conical shells of a thick sheet we do not succeed in keeping repeatability of structural, and consequently hydraulic properties, that significantly limits the area of their application [5]. Concurrently the results of activities on manufacturing complicated axisymmetric porous welded joints showed that these problems can be resolved by using diffusion-vacuum welding of filter meshes.

A diffusion-vacuum technique for manufacturing porous axisymmetric elements of metallic meshes has been developed at M. Keldysh research center with the participation of N. Bauman MSTU personnel. In manufacture of complicated axisymmetric porous elements of the Laval nozzle type based on this technique the mesh structure and PMM are not impaired during all production phases.

The strength of the intermesh joint is determined by a relative strength of the welding joint ϕ ($0 \leq \phi \leq 1$). The quality of the intermesh welding is improved through an increase of the contact time of the mesh wires in diffusion welding. A relative strength of the welded joint is $\phi \approx 1$.

The joint strength is dependent on the diffusion processes passing in time. If the exposure time and pressure are low and insufficient for complete relaxation of stresses in a contact, a break of established joints is not excluded, that is caused

by a known effect of elastic aftereffect [6]. In this context low values of σ_B and ϕ for PMM produced by rolling a mesh pack can be explained [7]. In fact, at a rolling rate of (0.15...0.5) m/s the time of a single contact exposed to the deformation factor is (0.6...2) · 10^{-3} s (the contact length is taken 0.5 of a wire diameter of a weft of mesh П60). This time is not sufficient for diffusion processes to go. Therefore, for PMM produced by mesh rolling, ϕ = 0.25...0.35. PMM produced by a diffusion welding of meshes in vacuum have $\phi \approx 1$ due to a lengthy contact of wires in welding (5...10 minutes).

In diffusion-vacuum welding of metallic gauze wire filter meshes of a twill weave C200 and at a degree of reduction of mesh pack of $\varepsilon \geq 0.45$ a very high strength of PMM is achieved. Such meshes with a large number of bases and wefts are commended for specifically significant porous articles. If $\varepsilon < 0.45$, the required mechanical strength of PMM can be provided in the course of the diffusion welding in a sintering mode. In the first mode the pack is being formed up to the specified linear dimensions in a temperature range sufficient for complete relaxation of elastic stresses. In the second mode the sintering in vacuum or hydrogen is taking place at a temperature of about 0.9 of the temperature of melting for 4...6 hours. The heating source is a RF tube generator ЛЗ - 107B.

By using a diffusion-vacuum technique one can make porous mesh axisymmetric billets of a large thickness (height), which are needed for manufacture of porous heat exchangers. The external diameter of PMM is about 200 mm,

height of PMM is 300 mm. PMM dimensions have no technological limitations. They depend only on dimensions of the vacuum chamber and RF tube generator magneto.

REFERENCES

1. Sinelnikov Yu.I., Tretyakov A.F., Maturin N.I., et al., 1983, Porous Mesh Materials, Moscow, *Metallurgy*, 64 pages.
2. Pelevin F.V., 1998, Heat Transfer and Hydraulic Resistance in Porous Mesh Materials, Moscow, *Proceedings of the 2nd National Conference on Heat Transfer*, Vol. 5, pp. 254-257.
3. Polyaev V.M., Pelevin F.V., Reprintsev D.M., 1999, Analysis and Summary of Investigation Results on Hydraulic Resistance of Packs of Meshes with One-Dimensional Coolant Filtration, Voronezh, *Heat Power Engineering*, pp. 39–43.
4. Polyaev V.M., Gorbatovsky A.A. Thermal Conductivity of Porous Latticed Materials., 1992, *Experimental Thermal and Fluid Science*, №5, p.p. 417-424.
5. Polyaev V.M., Kremensky I.G., Avraamov N.I., 1978, Penetration Factor of Conic Shells Stamped from a Porous Sheet, *Powder Metallurgy*, №7, p.p. 48-51.
6. Kostornov A.G., 1983, Penetrable Metallic Fiber Materials, Kiev, *Technology*, p. 128.
7. Polushkin G.P., Tretyakov A.F., 1984, Pull Strength of Porous Mesh Materials, *Strength Problems*, №2, p.p. 37-46.

SECTION D.
STRUCTURE AND PROPERTIES OF MATERIALS AND COATINGS FOR OPERATION IN HAZARD CONDITIONS

BORON NITRIDE – MATERIAL FOR HIGH-TEMPERATURE ENGINEERING

Rusanova L.N., <u>Gorchakova L.I.</u>, Kulikova G.I., Alexeev M.K.
Federal State Unitary Enterprise - Obninsk Research and Production Enterprise
"Technologiya", Obninsk, Russia

A number of boron nitride sintered materials have been developed which have certain advantages over hot-pressed and pyrolytic materials in respect to manufacturability and achieved level of properties. A high-pure isotropic material with satisfactory strength has been produced by reaction sintering of turbostratic boron nitride powders with an addition of amorphous boron. The material has stable physical-mechanical properties over the temperature range of up to 2000°C. The boron nitride content in the material is up to 99 wt.%.

Over the investigated temperature range of up to 2000°C, a temperature coefficient of dielectric permittivity does not exceed 3%. Absolute value of dielectric permittivity is within the range of 2.8-3.3 depending on ceramic density. Dielectric loss at 2000°C is less than 10^{-2}. Electrical resistance of reaction-sintered ceramics is $10^{12} - 10^{14}$ Ohm·m at 20°C and 10^5-10^7 Ohm·m at 1000°C.

Using reaction-sintered boron nitride as a porous inert matrix to provide impregnation with organosilicon compounds followed by pyrolysis, several materials of the $BN\text{-}SiO_2$, $BN\text{-}SiC$, $BN\text{-}Si_3N_4\text{-}SiC$ systems have been produced which have the strength level approaching that of pyrolytic materials over the testing temperature range of up to 1400°C.

The $BN\text{-}SiO_2$ and $BN\text{-}SiC$ materials are high-temperature dielectrics.

Boron nitride falls within destructible thermal protection materials. When heated up to a destruction temperature, boron nitride transfers the heat easily from the heated surface due to its high thermal conductivity. High value of dissociation temperature and relatively high value of thermal capacity assure high efficiency of boron nitride as a thermal protection material.

At a temperature of around 3000°C boron nitride sublimates with a considerable endothermic effect. Under sublimation conditions its thermal protection ability is the most efficient. At the same time boron nitride oxidation is accompanied by exothermal effect which somewhat impairs the thermal balance on the surface of an article operating in the oxidizing flow.

All over the investigated temperature range (above 3000°C) at high powers of a plasma flow as well as when tested using a powerful laser plant, reaction-sintered boron nitride shows high resistance. It has superior thermal-erosion characteristics to those of all known kinds of thermal protection materials.

ELECTROSPARK ALLOYING BY SHS-ELECTRODES

Stolin A.M., Stelmakh L.S.[1]

Institute of Structural Macrokinetics and Materials Science, Russian Academy of Sciences,
Chernogolovka, Moscow region, 142432, Russia

[1]Institute of Problems of Chemical Physics Russian Academy of Sciences

e-mail: amstolin@ism.ac.ru

The various aspects of development of SHS-extrusion for producing long-measuring products from powders of refractory materials are considered, in which the processes of combustion and shift deformation are combined. As against known methods of powder metallurgy this method requires less power expenses, the number of technological operations is considerably reduced (up to 5), and the time of products producing is reduced up to ten seconds (instead of hours). The basic stages of SHS-extrusion and processes, proceeding at these stages are considered.

The application of SHS-extrusion, most developed on all directions, is the producing of electrodes for electrospark alloying from wide scale of hardalloyed materials on a basis of carbides and borides. These electrodes are multifunctional, with diameter of 1-2 mm, length 30-40 mm and they used in installations for drawing wearproof coverings (thickness 10-100 microns) on a metal surface of details and the tool for various purpose. The electrospark alloying method most frequently is applied to local treating of a working surface in places of the greatest wear. Thus the high bond strength of the marked material with a ground is achieved, it is absent heating details in process alloying.

The data on electrodes producing from synthetic hard-alloy tool materials (STIM) are given, the properties and microstructure of these materials, including density, hardness, average size of a grain are investigated. For all these materials the optimum modes electrospark alloying are chosen. The characteristics of the put coverings are investigated: thickness, continuousness, microhardness, corrosion resistance and wear resistant. The results of industrial tests strengthened of the tool at the various enterprises, and also comparison with wear resistant of the tool, alloyed by industrial firm alloys are submitted.

FORMATION OF SIC MATRIX OF AL$_2$O$_3$-SIC AND C-SIC COMPOSITES FROM POLYCARBOSILANE

Bogatchev E.A., Chtchetanov B.V.[1], Timofeev A.N.

Open Joint-Stock Company Research, Development and Production Corporation "KOMPOZIT", Korolev, Moscow region, Russia

[1]State Enterprise "VIAM", Moscow, Russia

Tendencies of engine building in aerospace technology in recent years confirm evidence of necessity of development of relatively cheap and reliable material for high-temperature applications in an oxidative medium. Composite materials with silicon carbide matrix including C-SiC and Al$_2$O$_3$-SiC composites in principle fit a lot of designers' requirements. Service life values typical for aviation allow relying on especially prospective using of a composite material consisting of Al$_2$O$_3$ fibers and SiC matrix, both components of which are resistant to oxidative medium at least to 1300-1400°C.

In this work principles were investigated of silicon carbide matrix formation from polycarbosilane by means of a liquid phase method developed in the Open Joint-Stock Company *Research, Development and Production Corporation "KOMPOZIT"* [1]. Porous aluminum oxide plates from chopped fibers (80%Al$_2$O$_3$ - 20%SiC by mass) manufactured by the State Enterprise "VIAM" and carbon-carbon composite material of the type *Grauris* were used as porous preforms.

As a result of thermodynamic calculation of changes in content of components in Al$_2$O$_3$-SiC composite material vs. temperature it was revealed that aluminum oxide and silicon carbide are stable up to 1600°C. At higher temperatures, interaction of oxide and carbide occurs with formation of volatile oxides of aluminum (Al$_2$O), carbon (CO) and silicon (SiO).

It was ascertained that as a result of 6 cycles including densification of porous preforms with 50% solution of polycarbosilane and subsequent carbonization in carbon backfilling, density of Al$_2$O$_3$-SiC composite material obligate grows, porosity decreases approximately by five times,

and strength increases by an order of magnitude. At this, not decrement but increment of mass of samples is observed after each carbonization. This phenomenon is connected with thermal destruction peculiarities of polycarbosilane. During carbonization in the temperature interval from the room temperature to four hundred degrees, partial oxidation of the polymer occurs due to the air remaining in pores, and this entails mass increment by 7-12% .

Microstructural and diffractometer analysis reflect changes of composition and structure of a composite during its formation. In a densified and carbonized sample, amorphous polymer coats fibers with continuous film and fills pores. Together with absence of SiC peaks, α-Al$_2$O$_3$ peaks disappear in a difractogram, and this seems to be caused by a contact interaction of the polymer and alumina fibers with formation of mullite. After thermal treatment at 1600°C crystalline silicon carbide is formed.

Performing densification of a porous preform of carbon-carbon composite material (density 1.1 g/cm^3) with polycarbosilane results in gasification of a portion of the volume during the high-temperature treatment due to interaction between carbon and silicon dioxide present in matrix.

To avoid gasification of components of Al$_2$O$_3$-SiC and C-SiC composites, it is necessary to perform carbonization of organo-silicon polymer and thermal treatment of a composite material in inert medium.

1. Bogatchev E.A. Method of Obtaining of A Composite Material. Patent of the Russian Federation No2130509 dated 20.05.1999.

PLASTIC DEFORMATION AND FRACTURE OF POROUS TITANIUM-SILICEOUS CARBIDE Ti$_3$SiC$_2$

Firstov S.A., Ivanova I.I., Pechkovsky E.P.

Institute for Problems of Materials Science, N.A.S.U., Kiev, Ukraine

By testing methods on 4 dot bending, axial compression, the measuring of hardness and fractography examinations are investigated regularities, features and mechanisms of strain, strengthening and fracture in an interval of temperatures 20-1300 °C of one of representatives nanolaminates - titanium-siliceous carbide Ti$_3$SiC$_2$, porous, obtained by a solid-phase reactionary sintering [1]. The temperature-deformation boundaries of its existence in a plastic state set. The model of course of strain and fracture processes in it is offered. The obtained results are compared with known for a dense material of same stochiometric composition.

Fractography examination of a surface destroyed samples with a porosity q=0,28 had shown, that the particles - grains of ternary compound Ti$_3$SiC$_2$ have the shape of plates by thickness 1-2 microns and cross size 5-10 microns. These plates are curved, ramified, polythickness, with salients and dimples. During formation and growth such flat particles, adjoining among themselves in different places, realize contacts of a different degree of strength - from negligible touch up to mutual intergrowth with formation of bridges-necks. The presence of this structure element in a porous titanium-siliceous carbide is its essential structural feature, which defines features of a plastic deformation and fracture.

Test for a microplasticity by a bending of samples with a porosity q=0,42 at T=20 °C has shown presence of a plastic deformation at a level e =3,5*10^{-4}, that corresponds to value for a dense material [2]. A deforming by compression executed in vacuum with a strain rate $\dot{\varepsilon}$ =10^{-3} c^{-1}.

By results of examinations the model of a plastic deformation and fracture of porous titanium-siliceous carbide Ti$_3$SiC$_2$ in an interval of temperatures 20-1300 °C is offered. The model are put in its bottom the representations, developed by M.W. Barsoum [3, 4].

The model takes into account features of a structure of a crystal lattice (lamination in an arrangement of atoms of a titanium and silicon, and also small constraint forces between them), behaviour of dislocation structure (presence at a loading at room temperature only of edge dislocations and opportunity of their glide only in basis slip planes, and also its ability for crawl in adjacent

planes at temperature above 700 °C with the subsequent annihilation in boundaries of the cells, that had formed), features of generated microcracks, and also morphology of grains - particles of a porous material and their interaction at a loading.

In connection with the plates of a porous material are connected among themselves by bridges-necks, stresses concentrate, primarily, in these necks, and first of all in that of its, which have the least cross-sectional area.

The plastic deformation in this material is realized by slide of edge dislocations in basis planes with formation of flat bundles [3, 4]. The overcoming of resistance of a crystal lattice and other hindrances on trajectories of a motion of edge dislocations under influence of the thermal factor (so-called crawl in adjacent slip planes) can happen at temperatures, which ensure a diffusion of atoms of a crystal lattice. As a result diffusion mechanisms of a plastic deformation come into action.

If temperature of a loading is those, that the diffusion processes in this material can not intensively evolve, the bridges-necks after some small quantity of deformation strengthening fail. It can result to formation of a microcrack of the critical size and subsequent fracture of a sample.

Plastic deformation at T=20 °C at a level e=3,5*10^{-4} could provided by incurvated bridges-necks due to an opportunity of an exit of edge dislocations on a free surface of pores. In a dense material, as follows from [3, 4], a necessary condition of embodying of a plastic deformation is the formation on boundaries of grains of cavities, pores. In a material, investigated in at present work, already there are pores, where the moving dislocations can go out and thus to not create concentration of a stresses, i. e. the necessity for a relaxation of a stresses by power-intensive process of a delamination of grains, reference for a dense state, disappears.

At test for an uniaxial compression of a material with a porosity q=0,28 the absence of macroplastic strain is noticed in an interval of temperatures T=20-600 °C (Fig.). Above this temperature there are indications of macroplastic strain, which reaches quantity of e=6 % at T=1000 °C. It means, that the edge dislocations have gained
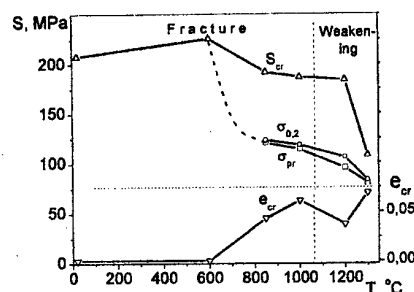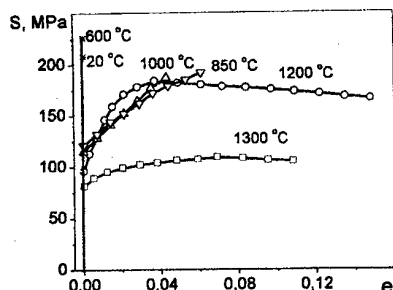
°C. It means, that the edge dislocations have gained an opportunity to transfer in adjacent planes by crawl, i. e. the atoms of a crystal lattice (and vacancy) became to diffuse actively.

At an uniaxial compression of a porous sample at higher temperature - 1200-1300 °C it is possible to present such scheme of sequentially performing processes. The plastic deformation starts in bridges-necks of plates with a microstrain by shear, which is ensured with edge dislocations due to their exit on a free surface of pores. As a result bridges-necks are bended, that gives in coming together of plates among themselves, and then and touch in separate places (points, lines, surfaces). Under activity of force of compression in these places due to intensive course of diffusion processes there is a welding of plates, the conglomerates of plates form - peculiar mechanism of integration of crystalline structure will be derivated. It gives that in adjoining to conglomerates areas are diminished extent and cross size of pores , the part from them collapses, the communication trenchs between remained pores is diminished. There is a transition of a material to a new qualitative state, it easily gives in to a plastic deformation, which reaches tens percents, the values of strength properties are reduced.

It is possible to explain the observed character of process of deformation strengthening at T> 1200 °C as follows.

The parabolic course of a deformation curve strengthening of a porous titanium-siliceous carbide at a loading at T=1200 °C, as well as in metals, is bound that despite of raising of an integrated dislocation density in a material there is a slowing down of its rate of rise, that is result of magnification of interaction force between dislocations. After reaching critical strain, at which as a result crawl of edge dislocations in adjacent planes will be derivated highdisorienting cellular structure, the activity is entered by(with) one more factor of interaction of dislocations - there is an annihilation of some part of dislocations of an opposite

mark in boundaries of cells. The annihilation of dislocations gives in slowing down of rate rise of a dislocation density. At this high temperature of strain, when are ensured fissile diffusion mobility of atoms of a crystal lattice and, accordingly, intensive crawl of edge dislocations, the velocity of an annihilation of dislocations can become such considerable, that it will exceed a generation rate of new dislocations, - there will be lowering an integrated dislocation density, i. e. the dynamic weakening takes place. Accordingly, on a strain curve at value of critical strain at a level 5-7 %, is observed decline of a flow stress, the plasticity increases up to e=30-40 %.

At elevation of temperature of strain of a porous titanium-siliceous carbide up to T=1300 °C the character of both parts of a stress-strain curve (strengthening and weakening) is maintained same, however, there is a considerable decline of a level of a flow stress during all interval of strain (in 1,5-2 times). It is possible to explain it to that at maintenance of process of an annihilation of dislocations and its intensification there is one more factor rendering essential influence to course of process of a plastic deformation. In a hexagonal crystal lattice the activity is entered by new systems of slide, which are capable to provide work of 5-th independent systems of slide, that gives in a decline of a weakening and elevation of a plasticity.

1. Brodnikovskyy N.P., Burka M.. P, Demidik A. N, Ivanova I.I., Pechkovsky E.P., Polushko G.P., Firstov S.A. / International Conf. « Advanced Ceramics for Third Millennium », Kiev, 2001. - P. 115, 116.
2. Li J.F., Pan W., Sato F., Watanabe R. / Acta Mater. - 2001. - Vol. 49. - P. 937-945.
3. Barsoum M.W. / Prog. Solid St. Chem. - 2000. - Vol. 28. - P. 201-281.
4. Barsoum M.W., El-Raghy T., Radovic M. Ti3SiC2: / Interceram. - 2000. - Vol. 49, No. 4. - P. 226-233.

261

INHERITABLE FRAMES of ALUMINIUM OBTAINED FROM OVERHEATED, PREVIOUSLY CONVECT MELT I

Maiboroda V.P., **Golovkova M.E.**, **Molchanovskaya G.M.**
I.Franzevich Institute of Materials Sciense Problems of National Academy of Scienses of Ukraine, Kiev, Ukraine

Not detracting advantage of the macroscopic thermodynamic concepts, theory of nucleation and spreading of a solidified front, which one satisfactorily describe process of an induration, it is necessary to recognize, that the processes of gelation in ingots, either particulate, or completely, simply are not regulated by these theories. It is bound as to influencing not up to the end studied of the constitution of structural motives of a liquid, dynamics of its condition, and also way of submission of a melt in a crystallizer or on a crystallizing surface and conditions of cooling.

The variation only in these parameters allows to change on the orders, for example, disperse of different hierarchically bound among themselves the structural pieces of ingots, of ribbons and hardened models of other forms.

The given activity is dedicated to mining of effective ways of control of processes of fragmentation of frame and analysis of a constitution of structural motives of a melt of aluminium, using effects of inheriting.
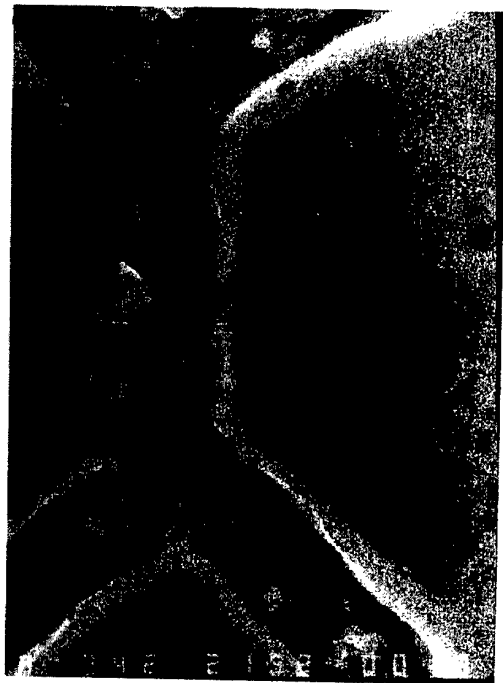
In activities [1-3] intercommunicated about specific influencing of preliminary stream stirring of a melt on the subsequent frame of rod samples. Using a technique of activities [1,3], the cylindrical sample Al (purity 99,995 mas %) was obtained, the frame of which was investigated on a bevel cut. For exception of artefacts, bound with etching, in a fig.1 the frame is resulted, we shall call of an initial sample, the melt which one before a solidification did not subject to convective effect. The melt temperature in both cases made 1100^0C.

Fig.2

In a fig.2 the frame of an investigated rod is resulted. Etching of samples implemented etching acid in identical conditions, but with a difference of duration of etching twice for a rod sample. Over-etching of frame, the fig.1, however does not reveal a flap-type fragmentation, reference sample, fig.2.

The electron-microscopic research confirms these structural differences. The electron diffraction pattern of an initial sample, fig.3, has a standard view. The substructure of a cylindrical

Fig.1

sample, fig.4, a, has microflap-type, blended with type of certain micrograins constitution.
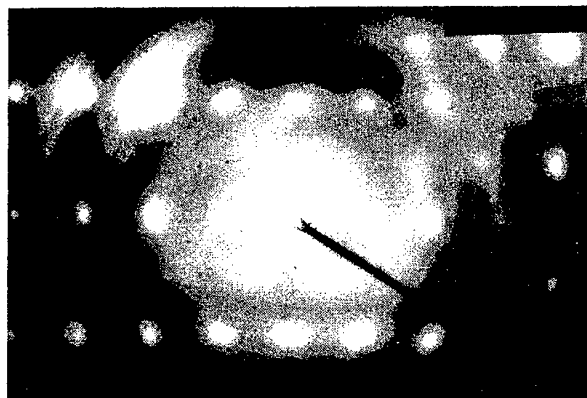
Fig.3

The padding jerks and pulls of an electron diffraction pattern, fig.4,b, convincingly testify to availability of a fine-plate fragmentation in case of obtaining a sample at preliminary covectation of a melt.

a
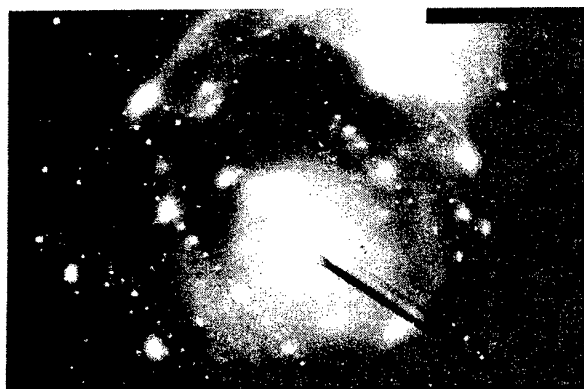
b
Fig.4

Conditions of experiment [1,3] eliminate a solidification of metal during retraction of a melt in alund tube with a diameter of 6 mm, that is why the microbanding is not a consequent of freezing during flow.

Is enabled, that melt of a liquid, except a cluster microgrouping has more extended polystructural motives, hereditable orientationaly the crystal-grains.

Therefore the method of flow of metal through narrow foramens is applied with the purpose of attempt of splitting of colloid on its composite motives, if those are available. Thus there is no necessity to approve, that the cluster has a crystalline state.

The essence of the alone given experiment is encompass byed finding - out of nature of distant ordering of a melt, which, is adopt to consider, one can resemble a system of the frozen polyhedrons of Voronoy-Bernal, or the Delone simplexes. However, the outcomes of the given activity can testify to availability only of plate-like polystructural composite motives in a melt of aluminium overheated up to $1100-1200^0C$.

The literature
1. Maiboroda V.P. // Rasplavy - 1991, - №3.-p.115-117.
2. Maiboroda V.P. // Metallu.-1993, - №3.-p.43-45.
3.V.P.Maiboroda,V.A.Makara, G.M.Molchanovskaya, M.E.Golovkova, S.L.Revo, R.O.Ivanenko // Dopovidi natzionalnoi academii nauk Ukrainu, №11, -2001.-p.64-67.

The NANOSTRUCTURAL CONDITION of an ALUMINIUM INGOT OBTAINED by SPLASH of a MELT III

Maiboroda V.P., Maksimova G.M., Revo S.L.[1], Ivanenko E.A.[1], Molchanovskaya G.M.
I.Franzevich Institute of Materials Sciense Problems of National Academy of Scienses of Ukraine, Kiev, Ukraine
[1] T.Shevchenko Kiev National university of Ukraine, Kiev, Ukraine

In the maiden two reports of this book the specific structures and substructures of aluminium obtained from an overheated melt are adduced. The wobble of their interpretation can be connected to absence of studing of influencing of a cooling rate of a sample. In the first report the cylindrical sample was cooled in alund tube of a diameter of 6 mm during 40-50 sec, and in the second report – ~ 10^{-3} sec. However both in maiden, and in the second cases, the approximately identical tendency to formation of a microflap-type fragmentation, but of a miscellaneous degree, is watched. To reduce influencing of a cooling rate and to approach conditions of a solidification to cooling conditions of an ingot with a crucible on air, the metal was obtained on technology of filling of a warm steel mold by a quasicontinuous thin spray with exhaust velocity ~ 0,5 m/s.

The indicated way is close to technology of obtaining of welds by a method of splash. Therefore in a title of the report is used a word "splash".

At obtaining an ingot the molten metal moved in alund crucible heated up to 500^0C, the diameter of 20 mm and during experiment was spacefilled on an altitude of 12-15 mm. After ending submission of metal, the melt was in a steel mold in a liquid state some seconds. For matching the identical ingot was obtained also at a customary melting of a blend in board of resistance, overflow of metal through a broad foramen and cooling on air.

In a fig.1, a, b, are adduced the lightfield map of substructure and electron diffraction pattern of a comparative sample with jerks conforming to a FCC-lattice of Ai. We suppose, that these data do not require the special ininterpretation.

a

b
Fig.1

In a fig.2, a, b, c, are adduced the structural data of an ingot obtained by "splash". Also, as well as in case of a fast crystallization (the previos report II) the substructure of metal differs by a fine-plate fragmentation (~ 20 nm), generatrix a superstructural system. It confirms by nature of electron diffraction patterns, fig.2, b and c, which are obtained from two adjacent areas (screw racks) figured in a fig.2 a.

The outcomes of experience testify to prevailing influencing of processes of preliminary melt flow on gelation in aluminium as contrasted to by factor of speed of a crystallization. To the same conclusions has come Chadwick at research of originating of banding in ingots of aluminium.
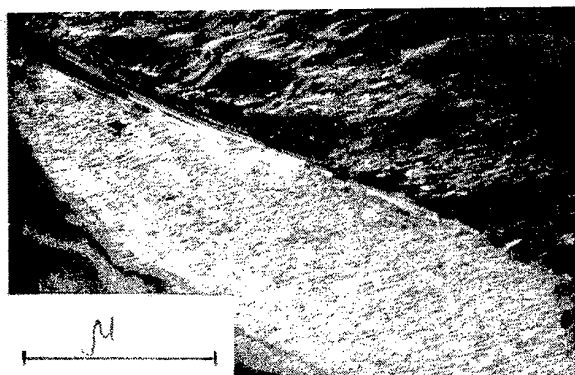
a
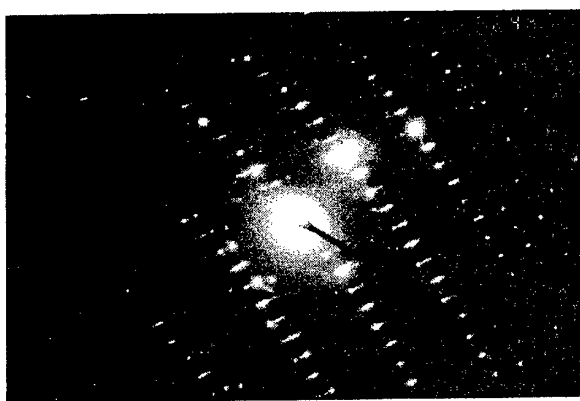
b

c

Fig.2

It is necessary to mark, that the indicated methods of effect on a melt do not allow while to receive metal with isotropic nanodispersiv frame.

The literature
1. Poluhin V.A., Vatolin N.A. // Rasplavu.-1987.-V.1, №5. p. 29-65.
2. Chadwick G.A. Decanted interfaces and ground forms //Acta met.-1962-10,N1,-P.1-12.

We suppose, that observed naostrip pieces and the screw racks of micron width mirror the composite motive of short-range and distant ordering of a melt of aluminium at the temperature of up to 1100⁰C. These data can be utilised at application of a statistic-geometrical method of computer simulation of a constitution of a melt. At simulation of a crystallization on a Voronoy method, apparently preference should be returned to a set of sequence of digits identifying tetragons [1].

THE STUDING of INHERITABLE FRAMES of ALUMINIUM, OBTAINED by SPINING of a MELT II

Maiboroda V.P., **Maksimova G.M.**, **Revo S.L.**[(1)], **Molchanovskaya G.M.**
I.Franzevich Institute of Materials Sciense Problems of National Academy of Scienses of Ukraine, Kiev, Ukraine
[(1)] T.Shevchenko Kiev National university of Ukraine, Kiev, Ukraine

In activities [1-3] show, that if in overheated up to ~ 1100^0C melt of Al before a solidification to call somehow convection, the frame of last has a flap-type constitution. At a direct researches of a building of microdrips of indium and tin [4,5] the availability of nanosize rectangular zones of width 30-40 nm, and also flap-type formations of two scales - size ~ 200 nm and 1-2 microns was watched except for a cluster microgrouping. Last fragment a drip or colloid.

Unconditionally, listed the structural-hierarchical system exists in a mobile condition such as Brownian motion and, apparently, introduces structural motives of a constitution of melts. The life time of such motives makes, on supervision, tens seconds.

Not excepting influencings of conditions of a crystallization (these factors will be studied in following, III report), we suppose, that the increase of speed of a convection of a melt or its expiration from a nozzle and speed of a rotated crystallizer will allow before a solidification to disperse colloid on the conforming more dispercive structural fragments of compositional motive of melt structure.

In the given activity the researches of substructure of films of aluminium by depth of 0,3-0,5 mm and width 8 mm obtained on rotated copper disk. The speed of the rotated disk was 3600 turns/min. Vacuum in system was 10^{-2}Pa. Mean radius of a place of deposition of an aluminium drip makes 25 mm. The melt had temperature 1100-1200^{0}C. The speed of velocity of metal from a nozzle made 0,5-0,8 m/s.

As shown in activity [3], the surface of a film has microstriate morphology. In the given experiment at obtaining of foil the similar outcome was watched. Realization of electron microscopic research of the foil therefore was meaningful. The substructure of a film resembles a lath-similar constitution. The electron diffraction pattern from inter-lath space, fig.1,a, testifies to availability of a fine-plate nanosize fragmentation, the basis of which can be made the defects of packaging or doubles derivated in the conditions of a crystallization. At deformation, as is known,

originating of defects of packaging is improbable. The lightfield, fig.1,b, and the darkfield map in matrix reflex, fig.1,c, confirms availability of fine-plate contrast with parameter ~ 50 mm.
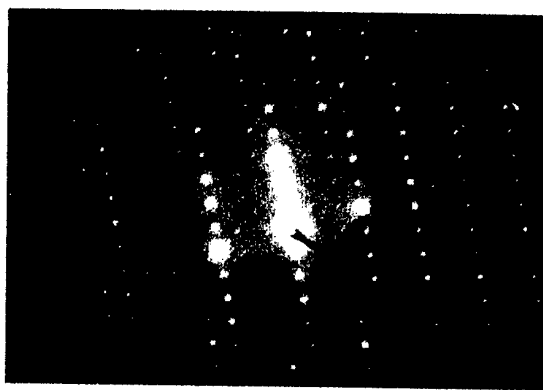
a

b

c

Fig.1

Electron diffraction pattern from area of "screw rack", fig.2,a, and darkfield map, fig.2,b, also testify to availability of two systems of fine-plate superstructure, but more finely divided on depth (25 nm). It is necessary to attribute the given phylum of frame, apparently, to a plate nanostuctural condition.

a

b
Fig.2

The literature
1. Maiboroda V.P. Rasplavu - 1991, - №3.-p.115-117.
2. Maiboroda V.P. Metallu.-1993, - №3.-p.43-45.
3. V.P.Maiboroda, V.A.Makara, G.M.Molchanovskaya, M.E.Golovkova, S.L.Revo, C.O.Ivanenko. Dopovidi nazionalnoi academii nauk Ukrainu, №11, -2001.-p.64-67.
4. Maiboroda V.P. // Thin Solid Films. 195, N1-2 (1991), p.357.
5. Maiboroda V.P., Maksimova G.A., Sinelnichenko A.K. Ukrainian physical journal - 1991, - №11, p. 1752-1758

The obtained nanostrip frame on parameter coincides the size of an intermediate zone observed in activity [5] (30-40 nm), or with the size of the prolated cluster on a large axis(axes) [4].

Following element of frame, it is the lath-similar pieces of the micron depth. These forms, apparently, can not be referred to polyhedrons of Voronoy-Bernal. Most likely composite motive of a melt consists of "pieces" of the rectangular-like or flap-type-like extended forms. As follows from the reduced data for implementation of nanostructural, also while anisotropic condition of metal the considerable efforts of effect on a melt are indispensable.

267

HARDMETALS FOR MINING TOOLS WORKING UNDER HARSH OPERATING CONDITIONS

Konyashin I.Yu.

Boart Longyear GmbH & Co. KG, Technical Development Centre, Burghaun, Germany

The need for improved hardmetals intended for production of mining tools for drilling and cutting hard and soft rock is rapidly growing. This need is created by the demand for utilisation of ores of lower and lower grade, for drilling tough and abrasive rock, and for general improvement in the efficiency of rock-removal methods. Wear of hardmetal buttons or inserts in the drilling bits and road-planing and coal coal-cutting picks is a major factor in determining the energy requirements and the penetration rate in drilling or cutting and usually dictates the choice of rock-removal methods for a given type of rock [1, 2]

Hardmetals for mining tools work usually under extremely harsh operating conditions including temperatures of nearly 1000°C, high impact loads, thermal shocks, intensive abrasive wear and severe fatigue. Such unfavourable operating conditions dictate special features of the hardmetal grades employed for fabrication of mining tools. The mining grades of hardmetal have to possess a combination of high hardness and wear-resistance on the one hand and enhanced strength and fracture toughness on the other hand. Although these properties are known to be contradictory in the manufacture of WC-Co hardmetals, they have to be optimised by choosing the best combination of WC mean grain size, Co content and other microstructure characteristics of hardmetal.

Some new results on wear mechanisms of hardmetal buttons and inserts in drilling and cutting of hard rock and soft rock will be reported. The understanding of the wear mechanism and defining the weakest consistent part of the WC-Co materials have allowed the hardmetal microstructure to be designed and optimised from the viewpoint of improving tool lifetime in rock drilling and cutting under unfavourable operating conditions.

One of the major characteristics of the hardmetal microstructure is thought to be the uniformity of WC grain size distribution [3, 4]. The microstructure of the hardmetals intended for production of mining tools is usually middle-, coarse- or ultra-coarse grained, and the presence of either very fine fraction or excessively coarse WC grains is undesirable from the viewpoint of both mechanical properties and performance. One can improve the WC homogeneity in the hardmetal microstructure only by producing more uniform W and WC powders. The influence of WC grain size uniformity on the performance and mechanical

properties of different hardmetal grades will be presented.

Other decisive properties of WC-Co hardmetal are the Co mean free path and WC average grain size, which have a strong influence on the physical and mechanical properties of WC-Co materials. Results on optimisation of Co mean free path and WC grain size in the hardmetal grades intended for different applications in percussive drilling of hard rock as well as in road planing and coal cutting will be reported. A wide variety of up-to-date hardmetal grades with improved physical and mechanical properties and enhanced performance for mining applications will be briefly described. A number of examples of their employing in different operations of rock drilling and cutting in comparison with conventional hardmetals will be given.

References
1. J.Larsen-Basse, Powder Met., 16(1973)1.
2. K.G.Stjernberg, U.Fischer et at., Powder Met., 18(1975)89.
3. I.Konyashin, V.Senchihin et al., Int. J. Refractory Met. Hard Mater., 14(1996)41.
4. I.Konyashin, T.Eschner, et al. Z. Metallkd., 90(1999)403.

THE CONCEPT OF THE STRUCTURE FORMATION IN CEMENTED CARBIDES DESIGNED TO OPERATE UNDER EXTREME CONDITIONS AT DYNAMIC LOADING

Lisovsky A.F.
Institute for Superhard Materials, Kiev, Ukraine

Advantageous development of mining, metalworking industries and some subbranches of mechanical engineering is, to a great extent, due to a wide application of carbide articles that operate under extreme conditions. Among such articles are included drilling and rock-cutting tools, dies, broaching tools, milling cutters, carbide elements of high-pressure apparatus, punches of compressors, etc. To ensure a high performance of these articles, a new concept of the formation of them should be developed. The concept should be based on particular conditions of the operation of carbide articles and take into account the interaction between an operational member and an article, and between the latter and a workpiece material.

According to this concept, at the first stage, the computer-aided simulation of the carbide article is performed. The computer-aided simulation includes the calculation of the stressed-strained and limiting states of the article under cyclic loading, the calculation of the adequate limiting values of such characteristics of the cemented carbide as bending strength (R_{bm}), compression strength (R_{cm}) and yield stress ($R^c_{0.1}$). The limiting values of these characteristics define the range of stresses within which the article can operate. If, as the situation requires, this region must be extended the values of R_{bm}, R_{cm} and $R^c_{0.1}$ of this cemented carbide should be increased. If the values of these characteristics meet the conditions of the article operation, they should be remained unchanged (at the existing level). Based on the obtained values of the fields of stresses, which generate in the bulk of the article during its operation, the computer-aided simulation of gradient structures in this article is performed. The development of gradient structures makes it possible to maximize the adaptation of an article to the extreme conditions of its operation.

At the second stage the problem of the formation of the cemented carbide structure at all the levels of its hierarchy (submicro-, micro- and mesolevels) is solved. To accomplish this, the working article should be considered as an open system which absorbs energy from without. In this case, the system stores entropy, and dynamic structures develop in this system. In cemented carbide articles defects are one of these dynamic structures. TEM observations have shown [1-5] that in cemented carbides under the action of external loads there initiate defects that accumulate and form three-dimensional structures at submicro-, micro- and mesolevels. The initiation of defects and the organization of them into three-dimensional structures cause the degradation of the cemented carbide initial structure and, ultimately, to its failure. The processes of the initiation, development of defects and organization of them into three-dimensional structures are directly related to the energy absorption by a cemented carbide article. The ability of cemented carbides to absorb energy is given in terms of the energy absorption coefficient λ [6] and the work of deformation A_{def}. These characteristics correlate well with the fatigue strength of the cemented carbide, e.g., with the values of the threshold stress intensity factor K_{th} and the critical stress intensity factor K_{fc}. It follows from the foregoing that the structures must be formed which would ensure a high energy absorption of a cemented carbide thus inhibiting the initiation and organization of defects.

At the third stage one should choose the adequate technologies to develop the required structures in the bulk carbide article. We think that the treatment of a sintered article with a metal melt (MMT technology) offers promise for the formation of gradient structures. The MMT-process allows the formation of new structures in a cemented carbide article after its final sintering. Additionally, this process enables one to control the polymorphic transformation of the cobalt phase and thus to develop or to suppress the formation of nanostructures in the cemented carbide at the submicrolevel [7].

The above-considered concept was implemented when designing high-pressure apparatus to synthesize diamonds [8] as well as when making rock-cutting tools. The computer-aided simulation

was performed with a cone rotary cutter operating in the system which included an operational member (a П220 entry-driving machine, in our case), a cone cutter and a rock (strength = 100 MPa, abrasive ability = 15...18 mg). According to our calculated results, the following limiting values of the main characteristics of cemented carbides are adequate for these working conditions: R_{bm}=2300 MPa, R_{cm}=3300 MPa and $R^c{}_{0.1}$=2800 MPa. Within the range of allowable stresses the performance of the rock-cutting tool will be specified by the processes of initiation and development of defects in the bulk of a cemented carbide insert. The foregoing and analysis of the results reported in [1- 5] show that to inhibit the development of defects at submicro-, micro- and mesolevels, a high energy - absorption ability of a cemented carbide should be ensured, the cubic modification of cobalt should be stabilized and steps should be taken to strengthen WC/WC and WC/Co interfaces. To implement the above statesmens, we chose standard grades of cemented carbides used in rock-cutting tools (WC-8CoT, WC-10CoT and WC-12CoT) and have developed new grades on the base of then by alloying the former by nickel and silicon following the MMT-process. This has allowed the cemented carbides to be produced having high values of A_{def} and λ (see Table).

Field tests of rock-cutting tools inserted with WC-12CoT (Ni,Si) cemented carbide have shown that they outperform tools inserted with standard WC-12CoT carbide by a factor of 2.8.

Referens

1. Manlang L., Xiaoying H., et. al. Int. J. of Refractory Metals and Hard Materials, 1983, vol.2, No 3, pp. 129-132.
2. Vasel C. H., Krawitz A. D., et. al. Metall. Trans. A, 1985, v.16A, pp. 2309-2327.
3. Jonsson H. Pranseeberichte fur Pulvermetal., 1976, No 2, pp.108-134.
4. Rowcliffe D. J., Jayaram V., et. al. Materials Science and Engineering A, 1988, vol. 105/106, pp. 299-303.
5. S. Lay, J.L. Chermant, J. Vicens. Proc. Int. Symp. Plast. University Park, July 20-22, 1989. New York, 1984, pp. 87-96.
6. Лебедев А. А., Чечин Э. Проблемы прочности, 1980, №4, с. 32-34.
7. Lisovsky A. F. Proc. European Conference on Advances in Hard Material Production, Turin, EPMA(ed.), 1999, pp. 301 – 306.
8. Lisovsky A. F. and Shestakov S. I. Сверхтвердые материалы, 2001, №4, с.3-6.

Table. Physico-mechanical properties of specimens

Specimens	Co, mass %	HRA	K_{IC}, MPa·м^{0,5}	R_{bm}, MPa	R_{cm}, MPa	A_{def}, MJ/м^3	λ
WC-8CoT	8	88,0	15,9	2200	3900	126	3,2
WC-10CoT	10	87,1	17,6	2320	3600	145	4,0
WC-10CoT(Ni)	10	87,2	18,4	2450	3520	182	5,5
WC-10CoT(Ni,Si)	10	87,2	19,0	2560	3500	193	5,9
WC-12CoT	12	86,6	18,7	2460	3400	165	4,9
WC-12CoT(Ni)	12	86,7	19,8	2640	3310	214	6,8
WC-12CoT(Ni,Si)	12	86,6	20,5	2810	3300	219	7,1

HIGH-PRESSURE SYNTHESIS AND SINTERING OF MgB₂ –BASED SUPERCONDUCTIVE MATERIALS

Prikhna T.A.[(1)], Gawalek W.[(2)], Savchuk Ya.M.[(1)], Sergienko N.V.[(1)], Moshchil V.E.[(1)],
Melnikov V.S.[(3)], Dub S.N.[(1)], Surzhenko A.B.[(2)], Nagorny P.A.[(1)], Abell S.[(4)],
Habisreuther T.[(2)], Wendt M.[(2)], Herdt R.[(2)], Schmidt Ch.[(2)], Dellith J.[(2)]

[(1)]Institute for Superhard Materials, Kiev, Ukraine
[(2)]Institut fur Physikalische Hochtechnologie, Jena, Germany
[(3)]Institute of Geochemistry, Mineralogy and Ore-Formation, Kiev, Ukraine
[(4)]University of Birmingham, Birmingham, United Kingdom

MgB_2, superconductive properties of which have been recently discovered, can be easily synthesized both under ambient and high pressures. A lot of different methods of MgB_2 preparation are known [1-6]. Manufacturing of bulk MgB_2 under high pressure is one of the promising methods of producing highly dense superconductive material with mechanical properties of a high level. In our experiments on synthesis and sintering we used pressures of about 2 GPa Our high-pressure apparatuses allows to produce samples of about 60 mm in diameter and 20-30 mm in height that can be practically used in electromotors or generators.

We have studied the peculiarities of high-pressure synthesis of MgB_2 from Mg and B and sintering of commercial MgB_2. The high-pressure-synthesized samples have exhibited a density of 2,4-2,5 g/cm², microhardness of 12.1-15.6 GPa at the 4,96-N load, fracture toughness of 4.1 MN m$^{-3/2}$ at 147.2-N load, Young Modulus of 220 GPa, critical current density of 170-200 kA/cm² at 10 K and 58- 62 kA/cm² at 20 K in 1T field. The irreversible field was 9 T at 10 K and 6 T at 20 K. We have found evidence indicating that the presence of Ta during synthesis positively influences the critical current density of the material in magnetic field as well as the field of irreversibility. In our experiments on synthesis of MgB_2 we have used boron containing a H_3BO_3 impurity phase and have come to the conclusion that Ta reacts with hydrogen to form Ta_2H and TaH, indirectly causing the formation of finer (of a submicron size) inclusions of MgO in MgB_2 that may be the reason for an increase in critical current density. We have found some evidence that intergrowth of MgO and MgB_2 may occur by (111) planes of MgO and (0001) planes of MgB_2.

Addition of Ta (10 %) to the sintered MgB_2 samples allowed us to increase fracture toughness from 4.4 to 7.6 MH m$^{-3/2}$ (under the 147.2 N load). The Young modulus of high-pressure sintered MgB_2 was in the range of 223 to 382 GPa and under the 0.5-N load the nanohardness was 17.3 GPa, while some grains exhibited 43.4 GPa.

The structure of both synthesized and sintered samples contained uniformly distributed single crystals of MgB_2 with the sizes from 10 to 0.1 μm. The MgB_2 sample obtained under high pressure was a nanostructured material with the separate inclusions of larger grains.

References

1. Y.Takano, H.Takeya, H. Fujii, H. Kumakura, T.Hatano and K.Togano, Superconducting properties of MgB2 bulk materials prepared by high pressure sintering, cond-mat/0102167 (2001)
2. Y.Bogoslavsky, G.K. Perkins, X.Qi, L.F. Cohen and A.D. Caplin, critical currents and vortex dynamics in superconducting MgB₂, cond-mat/0102353 (2001)
3. Y.Bogoslavsky, L.F. Cohen, G.K. Perkins, M. Polichetti, T.J. Tate, R. Gwillian and A.D. Caplin, Enhancement of the high-field critical current density of superconducting MgB₂ by proton irradiation, Nature C04852 (2001)

4. Amish G. Joshi, C.G.S. Pillai, P. Raj and S.K. Malik, Magnetization studies on superconducting MgB_2-lower and upper critical fields and critical current density, cond-mat/0103302 (2001)

5. S.X. Dou, X.L. Wang, J. Horvat, D.Milliken, E.W. Collins and M.D. Sumption, Flux jumping and bulk-to- granular transition in the magnetization of a compacted and sintered MgB_2 superconductor. cond-mat/0102320 (2001)

6. K. Togano, The current status of the research on critical current related issues in Japan, in Abstracts of Joint workshop on : High-current Superconductors for Practical Applications, 8-10 June 2001, Alpbach, Austria, p.10
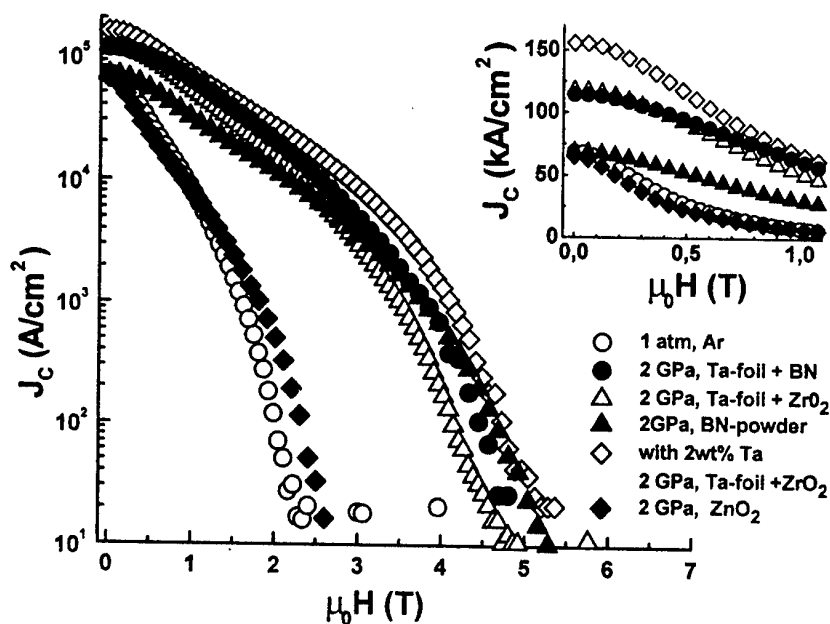
Fig. 1. Critical current density j_c vs. magnetic field at 20 K of the samples synthesized at 2 GPa, 800°C, 1 h from Mg and B of commercial purity in contact with a BN powder, Ta foil and from Mg and B of commercial purity with additions of a Ta powder (2wt%) in contact with a Ta foil. The same dependence for the sample synthesized from the same raw materials at an Ar pressure of 1 atm and 800 °C for 4 h is given for comparison.

MACRO STRUCTURE AND MODULUS OF ELASTICITY (MOE) OF HIGH ALUMINA HCCBS*-BASED MATRIX AND CASTABLE

Rozhkov Y.V., **Kashcheyev I.D.**[(1)], **Belooussova V.I.**[(2)], **Pivinsky I.Y.**[(3)]

"NVF Ognjeuporniye Materyaly & Teploviye Agregaty" Ltd, Pervouralsk, Russia

[(1), (2)] Urals State Technical University (USTU- UPI), Yekaterinburg, Russia

[(3)] "NVF Kerambet" Ltd, Obninsk, Russia

Introduction

Recently, large interest has focused on studying of structure of various refractory materials because the development of effective composite materials promotes the formation of the most important service properties of refractory linings, such as high corrosion- and steel melt resistant and thermal shock resistant [1].

One of the most advanced directions in technologies of refractories is improving of conventional materials by optimization of their macrostructure.

The forward-looking refractories are HCCBS-based refractories (in Russian *keramobetony*). Their matrixes are formed of the high concentrated suspensions or slurries at ambient temperatures. The HCCBS-based materials are applied successfully at Russian ferrous metallurgical enterprises, especially as shaped and unshaped refractories for steel ladles and blast furnaces at the temperatures up to 1600 °C.

An important feature of the unshaped HCCBS-based refractories (plastic mixes, rammables, castables) is a formation of their structure under service conditions. In the works [2, 3] technology of HCCBs-based castables of sintered brown alumina (sintered Chinese bauxite) is described. The purpose of the present work is to investigate the character of macrostructure (porosity) of the matrix of such castables and the module of elasticity (MOE).

As started material for the specimens the high concentrated ceramic binder suspension made of sintered Chinese bauxite has been applied. It's characteristics were: suspension density $\rho_s = 2.65$ g/cm^3; bulk concentration of solid phase $Cv = 0.62$; pH = 7.6; water content W = 13.6 mass %; the rest on 63 mkm sieve (230 mesh after Taylor) R = 1.4 %. The experimental specimens were cast in plaster and metal molds and cured at the air at ambient 22 °C for 24 h before measurement.

Using the method of mercury pressure there have been received the experimental curves of integrated and differential distribution of pores of the matrixes after their thermal treatment at temperatures between 100 and 1450°C.

The dynamic MOE of the HCCBS-based matrix and castable under heating and cooling conditions was measured on the specimens with sizes 160x40x40 mm in a range of temperatures of 100 - 1450°C.

Figure 1 demonstrates the results of dynamic MOE measurement at the heating and cooling temperatures *and* dominant pore radius of the matrixes as a function of pre-heating temperature. Despite the thermal differences in the experiment conditions both of the mercury presses and MOE the same character of the curves on thermal lengths "350 - 900 °C" and "900 - 1200 °C" is observed. Thus the first thermal length shows a constancy of pore structure of the matrix, that also the MOE data confirm.
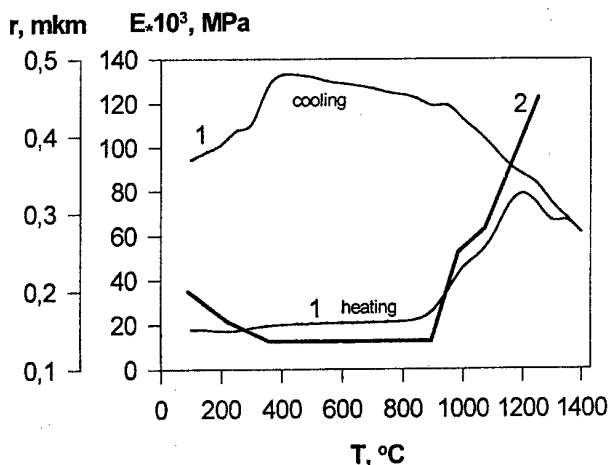
Figure 1. Dynamic MOE under heating and cooling conditions (1) *and* pore distribution curve as a function of pre-heating temperature (2) of sintered brown alumina-based (HCCBS-based) matrix

---

* HCCBS – High Concentrated Ceramic Binder System (aqueous suspension of pre-heated ceramic materials with bulk concentration $C_v = 0,5 – 0,7$ (fused silica, fired clay, sintered brown alumina, fused alumina and alumina-spinel material)

This length of the curves shows that pore size doesn't depend on the pre-heating temperature. At 900 °C process of silica fine particles sintering begins. This process connects with pore radius increasing because of silica phase transition and bulk expansion.

At this stage the process of sintering is accompanied by growing of particles and coalescence. In the range 100 - 1400 °C the apparent porosity changes from 24 up to 5 %. The "heating" curve of MOE between 900 and 1200 °C shows the similar behaviour or gentle increasing caused by sintering process (MOE is increased with strength increasing [3]) and also formation of a liquid phase and porosity reduction.

At the temperature of 1200 °C the whole process of particle sintering and process of mullite formation with the bulk expansion are observed. These processes are accompanied by disappearing of the small pores and increasing of the large ones. The matrix pre-heated at 1400 °C shows abrupt decreasing of pore volume (from 0.120 after firing at 100 °C up to 0.014 sm^3/g).

Coefficient K as a function of the temperature is shown at figure 2. At heating to the temperature of 500 oC the behaviour of the matrix and the castable do not differ from each other. MOE increase sharply for the castable and does not change for the matrix between 500 and 1000 °C (K < 1) Sintered brown alumina aggregate compensates the low elasticity of the matrix. After 1000 °C the sintering and hardening of the matrix begins, and the parameters of its MOE exceed those for the castable. During the cooling process the materials have a remarkably growth of their MOE and the character of MOE's changing is the same for both materials. Thus MOE is more for the matrix because it has the best elastic properties.

Conclusions

(1) The pore structure of the HCCBS-based matrix of the high alumina castable is investigated.

(2) The direct influence of the character of pore structure of the matrix on dynamic MOE between 400 and 900 °C and 900 - 1200°C is observed.

(2) The coefficient K that shows the differences of "matrix" MOE and "castable" MOE is offered.

References

1. Кащеев И.Д., Семянников В.П. Роль структурного фактора в повышении коррозионной устойчивости огнеупоров // Огнеупоры, 1993. № 9. С.2 – 4.

2. Гришпун Е.М., Пивинский Ю.Е., Рожков и др. Производство и служба высокоглиноземистых керамобетонов. 1. Набивные массы на основе модифицированных ВКВС боксита // Огнеупоры и техническая керамика. 2000.- № 6.- С.21 - 27.

3. Пивинский Ю.Е., Добродон Д.А., Рожков Е.В. и др. Материалы на основе высококонцентрированных керамических вяжущих суспензий (ВКВС). Оценка способов формования бокситовых керамобетонов // Огнеупоры и техническая керамика. 1997. №5. С. 11-14.

4. Buyukozturk O. and Tseng, T., "Thermomechanical Behavior of Refractory Concrete Linings", Jour. Am. Cer. Soc., 65, 301 (1982).

Figure 2. Ratio coefficient K = Ematrix / Ecastable as function of temperature

To find out the role of the matrix in the castable dynamic MOE for the castable has been determined. Analyzing MOE data the differences for both materials were observed. For their explanation the authors of this paper has offered a coefficient as a ratio of MOE both matrix and castables:

$$K = E_{matr}/E_{cast}$$

SHAPE MEMORY EFFECT AND SUPERELASTICITY IN TITANIUM-NICKEL SINGLE CRYSTALS

Chumlyakov Yu.I., Kireeva I.V., Panchenko E.Yu., Zakharova E.G., Aksenov V.B.
Siberian Physical-Technical Institute, Tomsk, Russia

At titanium-nickel single crystals $Ti_{50}Ni_{50}$ (I), $Ti_{50}Ni_{48}Fe_2$ (II), $Ti_{49.5}Ni_{50.5}$ (III), $Ti_{49}Ni_{51}$ (IV), $Ti_{48.5}Ni_{51.5}$ (V), $Ti_{50}Ni_{30}Cu_{20}$ (VI), $Ti_{50}Ni_{40}Cu_{10}$ (VII) the systematical investigations of functional properties – shape memory effect (SME) and superelasticity (SE) – has been carried out at tension/compression in wide temperature interval $T = 77-673K$ depending on orientation of crystal axis, size, volume fracture and quantity of variants of Ti_3Ni_4 particles.

In single-phase single crystals I-V at B2-B19' martensitic transformation (MT) the value of SME depends on crystal axis orientation and deformation way – tension/compression. And experimental values of SME coincide with theoretically calculated values taking into account the lattice deformation only. Therefore, at $T < M_s$ (M_s - temperature of start of direct martensitic transformation) at deformation a single crystal of B19' martensite arises, which transforms to single crystal of B2-phase at heating higher then $T>A_f$ (A_f - temperature of finish of reverse martensitic transformation). Superelasticity in single-phase crystals I-III has not been observed at tension/compression. In single-phase single crystals IV-V superelasticity is observed at compression of <001> crystals, where $a<100>\{110\}$ slip in B2-phase is suppressed due to zero Schmid's factors, and the main deformation mechanism of B2-phase in this crystals is mechanical twinning.

Thermomechanical treatment of single crystals I-III (the deformation at $T < Ms$ +heating) leads to changing of MT type from B2-B19' to B2-R-B19', increasing of stress level of B2-phase and occurrence of SE. SE was found out in <001>, <111>, <123>, <157> investigated orientations at tension in temperature interval $\Delta T = 30$ K. The value of SE depends on orientation of crystal tension axis and the maximum SE equal 6 % is observed in crystals <111> orientations. At tension of <001> crystals the SE value = 2.7 % is equal to value of SME for quenched crystals. The value of SME and SE in <001> crystals means, that after the thermomechanical treatment the final product after deformation at $T<M_s$ at measurement

of SME and at $T> A_f$ in experiments at studying the SE is the same and represents a single crystal of B19' martensite.

In single crystals of <111> orientation after thermomechanical treatment the size of SME is less those in quenched state. As researches of dislocation structure show it can be connected with residual twining in the given crystals after thermomechanical treatment. Residual twinning in <111> crystals, apparently, reduces crystallographical resource of SME value.

The physical reason of SE occurrence in crystals I-III after thermomechanical treatment is established and it is connected with origin of martensite crystals on dislocations and increasing of stress level of B2-phase with respect to quenched crystals.

In crystals VI the B2-B19' martensitic transformation is observed. The value of SME and SE, their dependence on orientation and sign of applied stresses coincide with theoretically calculated values taking into account the lattice deformation only. Hence, at $T<M_s$ at deformation a single crystal of B19 martensite arises and it transforms to B2-phase single crystals at heating at $T>A_f$.

In crystals VII the B2-B19-B19' martensitic transformations are observed and B19-B19' transformation is unfinished. So, at cooling at $T<M_s$ and at $M_d>T>M_s$ deformation the finish product of transformation is mixture of two martensitic phases. For the first time the experimental data of dependence of SME and SE on crystal orientation have been carried out. It has been found that volume fracture of B19' phase arising at loading is dependent on crystal orientation and way of deformation.

The aging without external stress of single crystals IV-V results in precipitation of four crystallographically equivalent variants of particles Ti_3Ni_4 and changes mechanical behavior of the given crystals in comparison with a single-phase state. Experimentally it has been revealed, that the precipitation of dispersed particles Ti_3Ni_4

30-440 nm in size leads to reduction of SME value with respect to quenched crystals and occurrence of SE in all orientations at tension/compression. The value of SME, SE and temperature interval of thermoelastic MT is defined by volume fracture of dispersed particles and their size. It has been revealed, that particles 440 nm in size are the primary places of R and B19' martensite nucleation and R-B19' MT proceeds in two stages: at first - close to particles, then at the further cooling - in volume of material. The reduction of distance between particles and size of particles till 30-40 nm results in absence of double-stage R-B19' MT and shift of temperatures of MT in area of low values up to 120K, that testifies to accumulation of elastic energy in material at origin of B19' martensite crystals, containing fine dispersed particle. The distinction in character of interaction of dispersed particles with crystals of B19' martensite leads to changing of temperature interval of SE occurrence from 30 K up to 150 K depending on the size of particles.

It is supposed, that in crystals with dispersed particles Ti_3Ni_4 in comparison with single-phase crystals the values of SME and SE are defined by additional deformation of martensite crystals by twinning, that is necessary for achievement of compatibility of martensite deformation of matrix and elastic deformation of particles. Morphology of martensite crystals and type of twinning alter in crystals with particles in comparison with single-phase one. It is revealed experimentally, that in aging single crystals IV-V of titanium-nickel plate martensite is formed, instead of usually observable triangular self-accommodated microstructure [1]. The basic type of twinning of martensite in crystals with particles represents compound twinning (001) [100] [2], whereas in single-phase crystals twinning is realized as type I (-111), (011) and type II [011]. It is possible to consider compound twinning as "geometrically necessary twinning" for preservation of compatibility on "particle - matrix" boundary at MT [2]. In single-phase crystals untwinning of martensite B19' crystals occurs completely as in experiments on change of SME at deformation at $T < M_s$ as at deformation at $T > M_s$. In aged crystals particles interfere with complete untwinning of B19 ' martensite crystals and it results in reduction of SME value and, hence, it fails to receive a single crystal of B19'.

Loops of SE in aged single crystals of titanium-nickel have asymmetrical view showing that the processes of origin and disappearance martensite under external loading proceed not in strict return sequence. With growth of test temperature the reduction of value of mechanical hysteresis has been revealed. The speed of collapse of SE loop in crystals with fine particles 30 nm in size is larger than in crystals with large particles 100-440 nm in size.

The aging under stress of single crystals IV-V <111>, <011> orientations allows to receive structures containing one and two variants of particles Ti_3Ni_4, accordingly. The reduction of number of variants of dispersed particles results in reduction of shape memory effect and superelasticity values. Aging under loading at 823K for 1.5 hours, the size of particles 440 nm lead to shift of martensite transformation points into the area of higher temperatures, reduction of critical stresses in M_s point and inducing of a temperature interval of SE occurrence. The precipitation of one variant of particles 40 nm in size at aging 673K for 1.5 hours leads, on the contrary, to shift of MT points in area of lower temperatures, more significant hardening of B2-phase and increase of a temperature interval of SE from 120 K up to 135 K.

The micromechanical model of martensite transformation development in heterophase crystals of titanium-nickel has been developed. It has been shown, that the important moment in management of functional properties – shape memory effects and superelasticity - in aged single crystals of titanium-nickel is the mechanism of interaction of martensite crystals with dispersed particles and performance of compatibility conditions on boundary "martensite-particle".

References

1. C. M. Wayman, M. Nishida, A. Chiba. Microscopy studies of martensitic transformation in aged Ti-51at%Ni shape memory alloy // Metallography, 1988, vol. 21, pp 275-291
2. M.F. Ashby. The deformation of plastically nonhomogeneous materials// Philos. Magazine, 1970, vol. 21, pp 399-424

WAY OF MANUFACTURING OF PRECISION COMPOSITE CARBON PRODUCTS FOR HIGH-TEMPERATURE ENGINEERING

Kolotylo D.M., Kolotylo O.D.[1]

Kyiv National University of Economic, Kyiv, Ukraine

[1]Institute for problems of materials science NAS, Kyiv, Ukraine

The modern carbon materials such as graphite of high density, synthetic carbon fibers and fabrics, pyrographite which were developed during last 50 years, have unique technical properties especially valuable for high-temperature technologies.

So, in a range of temperatures 1500-1700 °C when short-term tensile strength for the majority of known refractory materials falls up to zero, durability of graphite rises and at diapason 2400-2600 °C nearly into two time above than durability of it at temperature of room.

Due to high durability, of thermal conductivity and low module of elasticity and small value of temperature factor of linear expansion of graphite, its thermostability, appreciated as the relation of product of durability and heat conductivity to factor of linear expansion and the module of elasticity, on two - four order is higher, than of carbides and the most fire-resistant oxides.

At the temperature higher 1000 °C thermal conductivity of dense graphite of one order with thermal conductivity of metals, but at pyrocarbon and graphite fabrics's is lower, than at fire-resistant oxides. The true density of carbon materials of various structure of interatomic bonds changes from 1400 up to 2200 kg/m^3, and specific volumes of these graphite differs in 2-3 times.

The characteristic of various graphite to accumulate heat have wider range in the field of high temperatures, than all group of fire-resistant materials. Evaporation of graphite in vacuum at temperature up to 2000 °C does not exceed million shares of gram from square centimeter.

Surprises a unique variety of structure and properties of such materials as "graphites" containing only one chemical element - carbon of the condensed condition and the fact of their theoretical unpredictability. Our surprise amplifies the opening of new kinds of crystal carbon, as, for example, icosahedral C_{60}, so-called «buckminsterfullerene» [1].

In author opinion the reason of it is inadequate reflection by out-of-date but still prevailing theoretical structural models of parameters of interatomic connections in carbon of various electronic configurations [2].

Backlog of the theory from experimental researches and practice constrains development of new carbon materials and their wide application in high-temperature technologies.

First of all it is connected to oxidation and by destruction of carbon materials when they heat in air. It creates technological problems of manufacturing of carbon products of high accuracy.

The most simple way of manufacturing of such products might be process of compressing on model of compositions of carbon filler (grains, powder, fiber, fabrics) and of thermosetting resin in the inert environment. However in consequence of elasticity of a composition at pressing and changes of volume of resin at heating not controllable deviation of the final size of a product (V_f) from nominal (V_n) will take place always.

Allocation of gases at plastic condition of resin results in increase of volume of a composition at an initial stage of heating. At a stage of roasting and cooling a product not controllable reduction of volume (shrinkage) follows. On the figure 1 the combined modeling diagram of volumetric changes of product at various technological stages is given:
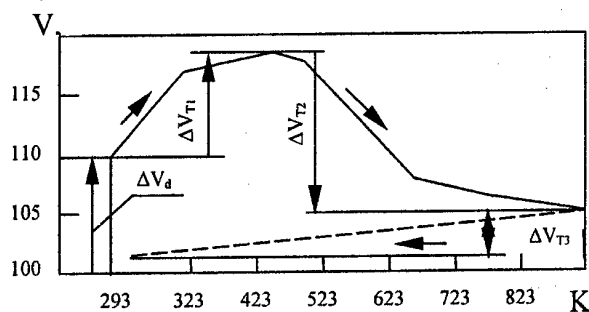
Fig.1

ΔV_d - dynamic (elastic) increase of volume;

ΔV_{T1} - increase of volume in consequence of decomposition of resin at heating;

ΔV_{T2} - thermal reduction of volume (shrinkage) at stage of carbonization of resin;

ΔV_{T3} - thermal reduction of volume at cooling a product;

From the given diagram follows, that the final volume of a product (V_f) will be equal to the algebraic sum of components:

$$V_f = V_n + \Delta V_d + \Delta V_{T1} - \Delta V_{T2} - \Delta V_{T3}$$

Thus a maximum of a gain of volume (20%) corresponds to temperature 250-300 °C.

The preventing of a gain of volume was put into practice by way of heating of product directly in rigidly fixed volume of equipment at temperature which corresponds to maximum of a gain of volume V_{T1} [3]. Fig.2
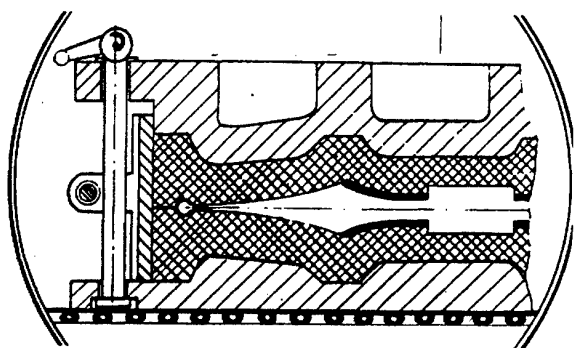
Fig.2

The received products precisely reproduced the sizes and a spatial configuration of form-building equipment and kept stability of properties at operation in a range of temperatures of heat treatment. However at higher temperatures at carbonization of resin there is not controllable reduction of volume (shrinkage).

Thus the volume of resin of a composition decreases on 40-50% that breaks its safety margin and, as consequence, under action of elastic forces of graphite materials causes deformation and destruction of a product.

For thermosetting resins of furan both an aromatic series, the volume and weight and consequently also durability of coke depend on content of oxygen in their chemical structure, which oxidizes carbon of resin. According to theoretical calculation and experiment the content of oxygen in hard furan resins up to 24% that reduce formation output of coke on 30-40% in comparison with theoretical calculation for conditions of absence of internal-molecular oxidation of carbon.

The temperature of disclosing of double bonds of furan and oxidation of carbon is revealed by the thermic analysis in a range 420 - 440 °C.

Synchronism of peaks of loss of weight (DTGA) and heat (DTA) is the convincing proof of legitimacy early the executed theoretical calculations of energy of transformation of two double carbon bond of furan cycle in four ordinary [4].

In this connection, the important practical problem is prevention of oxidation of resins by own oxygen and, as consequence, increase of density and durability of a product.

The decision of this problem would be found by selection of the additive to resins which actively connected oxygen of resin and was simultaneously chemically built in periphery of valents bonds of the condensed carbon.

It is of interest to consider the possibility of application of the theory of structural models of an electronic configuration of atoms of substance of the additive to resin to choose the most suitable. As the closest analogue for an electronic configuration of carbon $(2s^1 2p^3)$ is boron $(2s^1 2p^2)$. The thermal analysis has confirmed the assumption, that boron actively connected oxygen of resin in heat-resistant and to oxidation of structures (- C - B - O - B - C -) given on figure3.
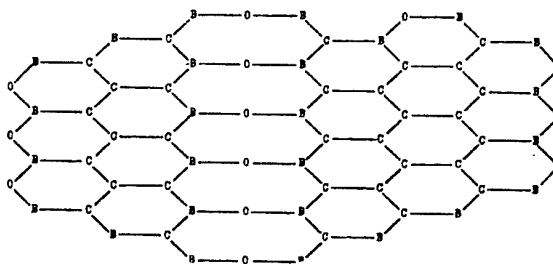
Fig.3

Behind the stated technology various precision products such as frictional disks of coupling, of protective signalling screens of melting furnaces, of foundry forms for refractory d-metals IV-V of groups were made.

References.

1.   P.A. Heaney, Duckyballs: Icosahedrel C_{60}, *Condensend Metter News* 1, 4 (1992).
2.   Д.М. Колотило, К теории электронной структуры непредельной углерод - углеродной связи и ее изменения при высокотемпературной обработке органических соединений. *Химия твердого топлива* 3, 45- 54, 1968.
3.   Д.М. Колотило, В.В.Казарцев, О.Д. Колотило. Авт. свид. № 1546202, БИ № 8, 1990.
4.   D.M. Kolotilo, II. Vědecká konference s mezinárodní účastí. Brno- květen (1978).

ANTIFRICTION Fe-Cu-S-P ALLOYS AS BRONZE SUBSTITUTES FOR SLIDER BEARINGS

Gavrylyuk V.P., Markovsky E.A., Ilchenko V.D.

Physics and Technology Institute for Metals and Alloys, National Academy of Sciences of Ukraine, Kiev, Ukraine

It is argued that one of the most urgent tasks of materials science is the improving of wear-resistant properties of various mechanisms and units, and enhancing their performance. Composites made up of metallic (base) and non-metallic (solid lubricants) parts obtained with cost-effective casting technology seem to be the most promising materials for that matter.

The rationale for the current research is the idea that one can obtain solid lubricants (MoS_2, WS_2, graphite) in Fe-C alloys structure. The study of the properties of simple and complex sulfide compounds as well as pertinent thermodynamic calculations made it possible to choose a certain system of alloying elements. Due to the changes in thermodynamic potential, the most likely compounds housing simple and complex sulfides to be formed when obtaining Fe-C-Cu-S-P alloys have been identified. MnS, Cu_5FeS_4, $CuFeS_2$, FeS, Cu_2S, compounds forming in Fe-C-Cu-S-P alloy structure at cooling and crystallizing were found to have the lowest free energy and thus improved stability when being cooled within the $1000-25^0$C temperature range.

The influence of alloying elements, C, and also thermal processing on the specific characteristics of heterogeneous structure of Fe-Cu-S-P alloys was studied. Steel-based alloys containing ~0,2% of C have ferrite-perlite matrix. Their structure houses compact, evenly distributed inclusions of Cu phase, as well as complex non-metallic sulfide inclusions. The increase of C content in the alloys up to ~1% causes certain changes in alloy base (the latter is turns from ferrite-perlite to perlite structure). As a result, the alloys hardness increases. Employing thermal processing (quenching with tempering) in the experimental samples has revealed some changes in alloys base structure, and leads to the considerable increase in hardness (3000 to 5800 MPa). The phase structure analysis with X-ray microspectroscopy and X-ray microstructure techniques has shown that Cu inclusions are in fact Cu-based solid solutions. The composition of non-metallic sulfide inclusions is made up of Cu_5FeS_6, Cu_2S, Cu_5FeS_4,

FeS, MnS compounds. The highest concentration of Cu_5FeS_6, Cu_2S is obtained in Fe-Cu alloys by means of $\geq 1\%$ S and $\geq 0,4\%$ P alloying. The mentioned compounds have in most cases hexagonal lattice with a high $c/a>2,7$ correlation and 600-1400 MPa hardness. Thus, the compounds may well be used as solid lubricants. The main structure parameters of sulfides were obtained with X-ray structure analysis (see Table 1.)

Table 1
Parameters of sulfide inclusions in alloys

Compund	Lattice parameters Å	Type of lattice
Cu_5FeS_6	a=3,894 c=17,403 c/a=4,469	Hexagonal
Cu_2S	a=4,012 c=11,213 c/a=2,795	Hexagonal
FeS	a=6,012 c=11,803 c/a=1,963	Hexagonal
Cu_5FeS_4	a=11,08 c=22,129 c/a=1,997	Tetragonal

The wear-resistant properties of the alloys were studied on the basis of Fe-Cu-S-P alloys structural characteristics. Cu and non-metallic sulfide inclusions parameters were also taken into consideration. The dominant influence of mean area and the mentioned phases (Fig. 1, 2) in the alloyed structure of sulfide inclusions structure on wear-resistant properties of the alloys have been identified. The study of the working surface of friction pair has revealed the processes of Cu and sulfides mass transfer on the surface of mated sample.

The study of load influence (5 to 25 Mpa) has also been performed. Thus we could identify the range alloying elements content that make for high wear-resistant properties of the alloys (1,5 times higher than those of bronze).

Fe-Cu-S-P alloys under study have shown high wear-resistant (antifriction) properties not only due to Cu content, but also to the effect of solid lubricant on the basis of non-metallic sulfide inclusions in the alloy.
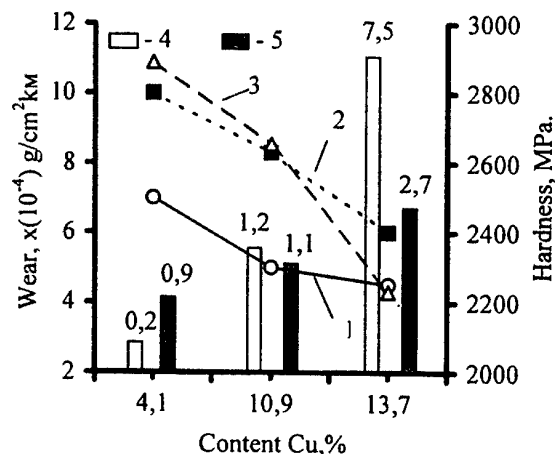
Fig.1. The influence of Cu amount on the wear-resistant properties of the alloys under conditions of oiled friction (U-20 oil) and 10Mpa load: 1-sample wear; 2- friction pair wear; 3- alloys hardness; 4-content of Cu-phase, %; 5- content of non-metallic sulfide inclusions, %;
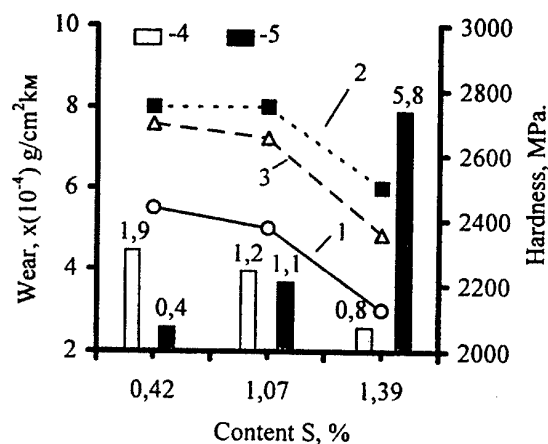
Fig. 2. The influence of S amount on the wear-resistant properties of the alloys under conditions of oiled friction (U-20 oil) and 10Mpa load: 1-sample wear; 2- friction pair wear; 3- alloys hardness; 4-content of Cu-phase, %; 5- content of non-metallic sulfide inclusions, %;;

The technological properties of the alloys were also studied. The temperature regime of casting Fe-Cu-S-P alloys was also identified. The influence of alloying elements on liquidus, solidus temperatures and crystallization interval was addressed. The dominant influence of sulfide

inclusions in Fe-Cu-S-P alloys on alloys castability (fluidity) and linear shrinkage was also considered. Taking into account physical and chemical processes of Fe-Cu-S-P alloys casting, the impact of frequent remelting of the alloys on their chemical content changes and structural characteristics (amount, mean area, content) of Cu and sulfide inclusions has been studied. Such inclusions are crucial for technological properties of Fe-Cu-S-P alloys and their performance. Prospects for the possibility of Fe-Cu-S-P alloys' reprocessing and recovery have also been outlined.

280

REFRACTORY CONCRETES OF INCREASED HARDNESS AND HEAT RESISTANCE

Tropinov A., Tropinova I.
Scientific private company «ALINEKA», Kiev, Ukraine

The introduction of new types of burners, fur – naces (f.ex.: a primary furnace), fuel (f.ex.: biofuel) leades to the change of the field conditi – ons of the thermo sets: temperature elevation and air – blast gas mixtures speed with the simultaneous increase of abrasive impact of incombustible particles, slags, etc. Besides, in this case, great demands are made of heat resistance. The use of traditional lining materials such as, fireclays or refractory chamotte concrete on alumina cement doesn't meet the changed used conditions in view of low thermomechanical properties, that lead to the frequent shut - downs for lining repair [1].

In the connection with the above – said, the compositions of the dry – shake: **BRAB50T15*** for the refractory concrete, the properties of which are indicated lower, have been worked out.

R_{com}, MPa
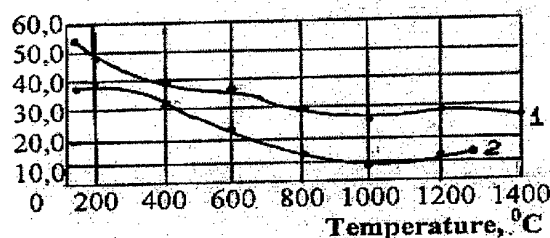
Fig. 1. The dependance of compressive strength of refractory concrete on temperature heating: 1 - BRAB50T15*; 2 – refractory concrete № 19 [2]

The dry shake BRAB50T15* is the composition of gray – white colour, consisted of aluminate cement and aggregates, fractions from 0,2 mkm to 7 mm of aluminosilicate mix. Dry shakes samples have been produced and tested on standard technique [3]. In the aim of the received data comparisson, the traditionally used concrete samples (composition №19) on Pashiysk EME alumina cement and class «SHA» chamotte aggregate, 0 – 20 mm fraction have been produced and tested.

The concrete average density after hardening constitutes p=2480 kg/m³,after drying (t=105⁰C) – p=2160 kg/m³. BRAB50T15* mark density is in 1,44 times higher in comparisson with concrete

based on alumina cement and is being explained by formation of resistance hidroaluminate CAH_{10} aggregates (peaks of high intensity A=14,3;3,56 and 2,55 mkm) in contact hardening zone. The samples heating t=105⁰C (drying up fixed mass leads to 11% strength decrease, that's explained by physically connected water removal and hidroaluminate CAH_{10} modification into C_2AH_8 and C_3AH_{10}, that's proved by high peaks, correspondently: A=10,7;2,87;2,55;1,67 and A=5,14;2,30;2,23;2,04, less strengthable on data [4].The temperature heating increase to t=1000⁰C leads to53,8% strength decrease in comparison with mark strength and explained by formation in the cement stone on the contact zone with aggregates:the main phaze, possibly a-Al_2O_3 A=2,54;2,08;1,59;1,37 mkm and CA_2 (peaks A=4,44;2,88;2,71 and 2,61 mkm), as well as the small portion of C_2AS (peaks A=2,85;2,43;2,41;2,40 mkm) and three-wedged anorthite CAS_2 (peaks A=3,20;2,95;2,51;1,83 mkm). It's necessary to stress that the worked out composition posseses much less strength loss in comparison with the concrete based on alumina cement, that testifies to dehydration of hydrosilicate without structure breakdown, proving results [3]. BRAB50T15*concrete strength, after heating up to t=1400⁰C, is increased in 28% in comparison with the strength under t=1000⁰C, that's explained, possibly, by a small structure seal (shrinkage 0,37%) and stable properties a-Al_2O_3 and CA_2 in this temperature range that proves data [4], as well as in 126% higher of concrete strength based on alumina cement. Deformation temperature strain 0,2Mpa makes up :HP-1290⁰C, 4%- 1480⁰C that corresponds to the 15class maximum tolerance temperature of use (t=1500⁰C) and 200⁰C higher in comparison with the concrete based alumina cement. The thermal linear expansion coefficient in the temperature range of t=105 – 1100⁰C makes in the limit a=4,8-7,1x10⁻⁶x⁰C⁻¹. The coefficient of heat conduction depends on temperature: under t=20⁰C makes 1,78Wt/mK, and under heating t=100-1100⁰C changes in the limit of: 0,54-1,82 Wt/mK. The distinctive feature of the refractory concrete BRAB50T15* is increased heat resistance and hardness. The heat resistance,

defined according to the standard technique [3], has made 46 water heat changes, that corresponds to the class $T_1 45$ and higher of the concrete based on the alumina cement on 25 water heat changes and explained by "fragmental" structure, that presuppose higher prolongivity of the concrete use in the conditions of often shut – downs on the cause of technological necessity (a boiler furnace cleaning from slag, based on biofuel, as well as the fall of the output, electric power, etc. The concrete hardness has been defined on cube samples 7,07 mm on edge, by heating procedure $(t=105 - 1400^0 C)$ and the following definition on Moos scale. It has been determined, that concrete hardness in this temperature interval is being changed in the range of 9,0 – 8,5, that is 2,5 units higher of analogical concrete indicator based on alumina cement and testifies the raised BRAB50T15*concrete hardness, explained by high hardness of aggregates and contact zone, the aggregate – cement stone, probably: hardness CA_2 – 6,5;a-Al_2O_3 – 9,0; that presuppose the high longlivity as well.

Thus, laboratory tests have proved higher thermomechanical properties in the comparison with chamotte concrete based on alumina cement. The technological properties check in the condition of working production has been done during primary furnace production (the furnace of the "complex" geometry) E1/9 of Dvurechye elevator (Dvurechye, Ukraine) and private firm "VAG"(Alchevsk, Ukraine). The dry shake BRAB50T15* has been produced at the company plant, packed into polipropylene bags of 75 kg/bag and dispatched to the above mentioned installation. The refractory concrete has been produced from the dry shake, the hardness of which equalls 20 sec and placed into the formwork (table 2). The concrete strength after 3 days of hardening $(t=7 - 11^0 C)$ made R=48,9 MPa (with 9% errow and explained by the use of the gravity type concrete mixer, that lead to the 17% water overexpenditure. The concrete longlivity has made 2,5 years that is in 2,2 times higher than the chamotte refractory primary furnace. Primary furnaces are intended for buck – wheat husks burning and in the process of operation are

undergone by high temperature $(t=1380 - 1500^0 C)$, frequent shut – downs (putting in operation service), electricity switchingoffs, non – burn husks abrasive wear. High thermomechanical properties are proved in production conditiones, that have given way to dry shakes introduction at 37 Ukraine and foreign (Belorussia) installations: boiler sets components, oil – processing and shaft furnaces.

Conclusion:

1. The lining material has been produced and characterized by ductility properties at the production stage, that allows to produce "complex geometry" lining.
2. The correspondence of high thermomechanical properties of refractory concrete to the operation conditions determines high lining longlivity and the repair as a whole.
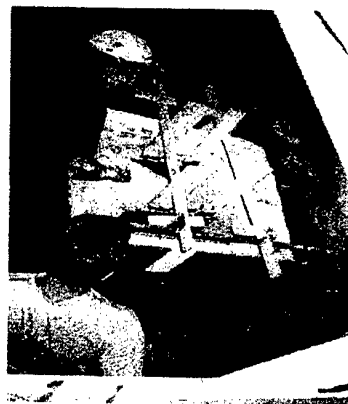
Fig. 2. Refractory concrete placement into the E1/9 boiler primary furnace, Dvurechye, Ukraine

Literature
1. V.P.Yegorov, V.G.Vifatnyuk, A.M.Tropinov / The dry shake experience use for embrasures: J: "Concrete and iron – concrete in Ukraine", 2000: №2 -p.13 – 15.
2. SNiP 2.03 – 04 – 84. – M: 1998. – 52 p.
3. K.D.Nekrasov "Refractory concrete": M: Promstroyizdat, 1957. – 283 p.
4. T.V.Kuznetsova, others "Special cements", S.P.: 1997. – 314 p.

BHATIA – THORNTON STRUCTURE FACTORS FOR LIQUID ALKALI-ALKALI ALLOYS

Dubinin N.E., Malkhanova O.G., Vatolin N.A.
Institute of metallurgy Ural's Division of the Russian Academy of Science, Ekaterinburg, Russia

From the practical point of view, investigation of alkali metals melts used as coolants in different areas of industry is interested.

For binary alloys the study of the Bhatia-Thornton [1] structure factor "concentration - concentration" in the long-wavelength limit, $Scc(0)$, is important, since its dependency on alloy composition is connected with a tendencies for phase separation or strong association in system.

We investigate $Scc(0)$ for Na-K, Na-Cs, Na-Rb, K-Rb, K-Cs and Rb-Cs systems at T=373K theoretically. For this aim the local Animalu-Heine [2] model pseudopotential and variation method [3] of the thermodynamic perturbation theory are used. Exchange – correlation function is considered in the Vashishta – Singwi [4] approximation. Earlier, this method was successfully used on thermodynamics study for the systems under consideration [5,6].

Obtained results are represented in Fig.1-6.

Fig.2. $Scc(0)$ for Na-Cs system at T=373K.
——— Our calculation ....Experiment [10]
——— Experiment [11] ● Experiment [12]
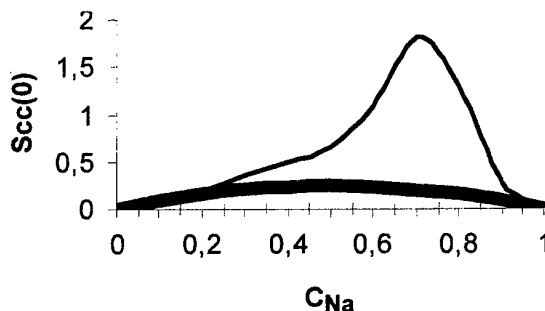
Fig.3. $Scc(0)$ for Na-Rb system at T=373K.
——— Our calculation
——— Calculation from [13]

Fig.1. $Scc(0)$ for Na-K system at T=373K.

——— Our calculation ———Experiment [7]
.... Experiment [8]   ● Experiment [9]

In the most cases a good agreement of our results with experimental data and other theoretical results is achieved.
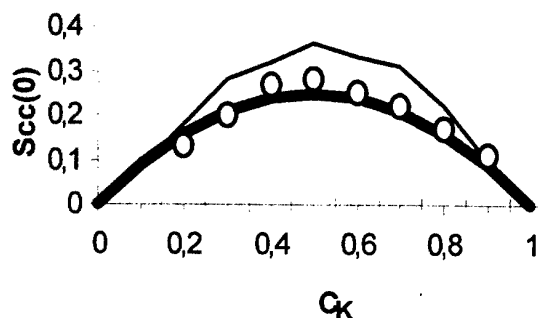
Fig.4. $Scc(0)$ for K-Cs system at T=373K.
━━━ Our calculation
──── Calculation from [13]
O   Experiment [14]
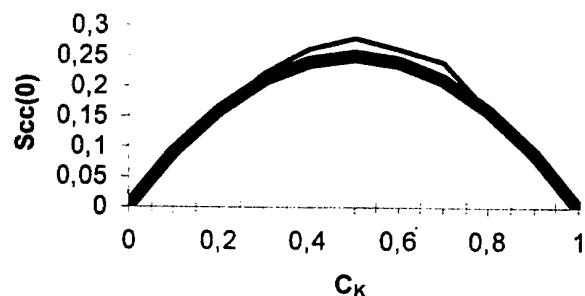
Fig.5. $Scc(0)$ for K-Rb system at T=373K.
━━━ Our calculation
──── Calculation from [13]
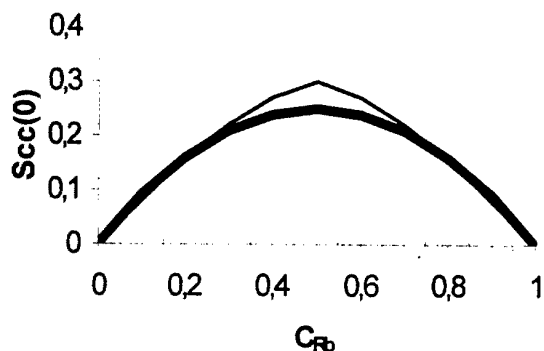
Fig.6. $Scc(0)$ for Rb-Cs system at T=373K.
━━━ Our calculation
──── Calculation from [13]

References

[1] Bhatia A.B., Thornton D.E. Phys. Rev.B, 1970, v.2, p. 3004- 3012.

[2] Animalu A.O.E., Heine V. Phil.Mag., 1965, v.12, № 120 , p.1249-1270.

[3] Mansoori G.A., Canfield F.B. J. Chem. Phys., 1969, v.51, №11, p.4958-4967.

[4] Vashishta P., Singwi K.S. Phys.Rev.B, 1972, v.6, №3, p.875-877.

[5] Дубинин Н.Э., Ватолин Н.А., Юрьев А.А. Расплавы, 1994, №.2, с..9 – 14.

[6] Dubinin N.E., Yuryev A.A., Vatolin N.A. Thermochimica Acta. 1998, v.316, p.123-129.

[7] Hultgren R.R., Orr R.L., Anderson P. D. and Kelly K.K. Selected values of thermodynamic properties of the elements, 1963, New York: Wiley.

[8] Caffasso F.A., Khanna V.M., Feder H.M. Adv. Phys., 1967, v.16, p.535.

[9] Alblas B. P., W van der Lugt. J.Phys.F:Metal Phys., 1980, v.10, p.531-539.

[10] Ichikawa K., Granstaff S.M., ThompsonJ.C. J.Chem.Phys., 1974, v.61, p.4059-4062.

[11] Neale F.E., Cusack N.E. J.Phys.F:Met.Phys., 1982, v.12, p.2839-2850.

[12] Huijben M.J. et.al. Physica B., 1979, v.97, p.338.

[13] Y.Tanaka, N.Ohtomo, K.Arakawa. Physical society of Japan , 1983, v.52, №6, p.2093-2101.

[14] Alblas B.P. , W van der Lugt., Mensies O., C. van Dijk. Physica B., 1981, v.106, p.22.

284

SYNTESIS AND SOME CHARACTERISTICS OF THE BNC – BASED SHS COMPOSITE

Bunin V.A., Borovinskaya I.P., Senkovenko M.Yu.

Institute of Structural Macrokinetics and Materials Science Problems RAS, Chernogolovka, Russia

Investigation of a ceramic boron carbonitride composite obtained by the method of furnace sintering has proved [1, 2] that it is characterized by high electroinsulating properties, excellent resistance to melted metals, alloys, slags, and salts.

So, this system is of great interest due to possible production of a promising ceramic material which is inert to an aggressive medium and resistant to high temperatures. Boron carbonitride composite can be obtained by the method of self-propagating high-temperature synthesis [3] which allows forming material structures in the combustion wave; the structures differ from those of the conventional ceramics [4,5].

Within our work we investigated synthesis of boron carbonitride ceramics under the mode of layer-by-layer infiltration combustion of boron and carbon mixtures in nitrogen, phase composition, elctroconducting and mechanical properties of the product.

Amorphous boron, lamp black, gaseous nitrogen (extra pure), and boron carbide were used as initial materials. The powders were mixed in ball mills. Cylindrical samples were made of the green mixture by a gasostatic method. The samples were 30 mm in diameter, 50 mm in height. The synthesis was carried out at nitrogen pressure ranging from 40 to 200 MPa.

The synthesis was realized by two reactions:

$$B + C + 1/2N_2 \longrightarrow BNC \quad (1)$$
$$B + B_4C + N_2 \longrightarrow BNC + B_4C \quad (2)$$
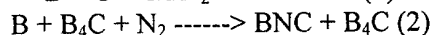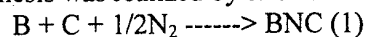
Within our investigations we determined a dependence of the combustion rate on the initial composition. Also, we studied the influence of nitrogen pressure on the combustion rate. It is shown to be dependent on the gaseous reagent pressure. Minimum nitrogen pressure necessary for realization of stationary self-sustaining combustion is 40 MPa. If the pressure is increased, the combustion rate grows.

The final product composition was studied by the methods of X-ray and chemical analyses. The product composition was obviously dependent on the initial mixture composition and synthesis terms. The product composition and electroconducting properties are shown in the Table below.

Product characteristics

Synthe-sis method	Product composition, mass %					Specific resistance (T=20°C) Ohm·cm
	C_{total}	C_{free}	B_{total}	B_{free}	N	
SHS	8.8	0.2	45.3	0.42	38.6	$4 \cdot 10^3$
SHS	12.2	0.4	46.6	0.24	36.7	$4 \cdot 10^2$
SHS	25.9	0.6	30.3	0.17	39.1	$(0.5\text{-}3.2) \times 10^{-1}$
SHS	27.6	0.7	29.9	0.15	37.9	$(1.7\text{-}7.4) \times 10^{-1}$
Furnace method	32.9	-	30.9	-	36.6	$>10^{13}$

We can see that the samples have insignificant content of free carbon, it is proved by DTA. IR analysis shows the existence of C-C fragments (a line at 1390 cm^{-1}) and B-N fragments (a line at 825 cm^{-1}). When we were studying the specific resistance of the products, we observed some unusual data in comparison with the conventional ones known from the literature. So, taking into account the data of chemical, thermogravimetric analyses and specific resistance of the samples, we can conclude that the composite is not a mechanical mixture of hexagonal boron nitride with carbon. The results of the composite investigation by the X-ray structure method prove that there is no interplanar expansion between the layers. It contradicts the supposition of carbon penetration into the interplanar area. That is why, we can suppose that the monolayers of the synthesized composite are either hexagonal rings of B-N structure and these rings form block fragments with C-C, or cluster distribution of carbon which in the case of a definite carbon concentration leads to formation of percolation cluster.

Therefore, a significant percentage of bound carbon, this carbon stability at burning out, abnormal specific resistance of the sample with 28 mass % of carbon prove that under the SHS conditions unordinary boron carbonitride is formed. The peculiarities of the SHS method (nonequilibrium, short times of the process, high temperatures, and high pressure in this case) allow us to assume that variation of these conditions can result in formation of unusual structures in the case of the trisystem of BNC.

The results obtained in specific resistance prove this idea and substantiate the research in this direction. Besides, an additional treatment of the nonequilibrium structures formed should lead to obtaining of novel materials with unusual properties.

REFERENCES
1. T.Ya. Kosolapova, G.N. Makarenko, Serebryakova, E.V. Prilutskij, O.T. Khorpyakov and O.I. Chernysheva, Poroshk. Metall. (Kiev) 1, 97 (1971),p.27-33.
2. G.V. Samsonov, A.I. Eroshenko, V.I. Ostroverkhov, V.A. Krat, T.V. Dubovik, Poroshk. Metall. (Kiev) 12 ,120 (1972),p 46-48.
3. A.G. Merzhanov and I.P. borovinskaya, "Self-propagating high-temperature synthesis of inorganic compounds", Dokl. Akad. Nauk USSR, 1972,vol..204,N 2, p.366-369.
4. Borovinskaya I.P., Bunin V.A., Vishnyakova G.A., and Karpov A.V. Some Specific Features of Synthesis and Characteristics of (TiB$_2$-AlN-BN)- Based Ceramic Materials // Int.J.SHS. 1999. vol.8.№4. p451-457.
5. Filonov M.R., Levashov E.A., Shylzenko A.N., Borovinskaya I.P., Loryan V.E., Bunin V.A. Indastrial Application of SHS Heat-Resistant Materials // Int. J. SHS. SHS.2000. Vol.9. №1. p. 115-121.

286

EFFECT OF ALUMINIUM ON SLIP AND TWINNING IN HADFIELD STEEL SINGLE CRYSTALS

Zakharova E.G., Kireeva I.V., Chumlyakov Yu.I.
Siberian Physical -Technical Institute, Tomsk, Russia

At single crystals of Hadfield steel Fe-13Mn-1.3C, wt.% with low stacking fault (SF) energy (γ_{SF} = 0.023 J/m^2) and Fe-13Mn-2.7Al-1.3C, wt.% the investigations of stages of plastic flow, strain-hardening coefficients (SHC) and mechanism of deformation depending on orientation of tension axis and way of deformation (tension/compression) have been carried out at room temperature of test using the methods of optical and electron microscopy, X-ray diffraction.

Experimentally it has been shown that the combination of low stacking fault energy and high level of friction forces (due to high concentration of carbon atoms) in Hadfield steel results in development of mechanical twinning from the beginning of plastic flow at tension at room temperature. In $[\bar{1}11]$ single crystals of Hadfield steel from the beginning of plastic flow the deformation develops by twinning in several systems simultaneously with high value of SHC. In $[011]$ orientation of Hadfield steel without aluminium the plastic deformation develops in two stages: the first, with low strain-hardening coefficient, is connected with development of deformation by twinning in primary system, the second - with interaction of twins in several systems simultaneously. The axis of single crystal during all plastic deformation goes to direction of $[\bar{2}11]$ pole - twinning in primary system. SHC at the second stage of hardening is as well as in $[\bar{1}11]$ crystals, hence, the high speed of hardening is defined by hardening on boundaries and in body of twins at their intersection [1, 2].

It has been shown that the increase of γ_{SF} up to 0.048$\pm$0.005 J/m^2 at alloying with aluminium [3] results in change of the deformation mechanism of Hadfield steel from twinning to slip. In $[\bar{1}11]$ single crystals of Hadfield steel with aluminium from the beginning of plastic flow the deformation develops by slip in several systems simultaneously with high value of the SHC, exceeding the SHC in Hadfield steel without aluminium, where the deformation is realized in several systems of twinning from the yield stress.

The thin twins in several systems after 10 % of deformation experimentally have been found out, at preservation of slip as a basic mechanism of deformation. Alloying with aluminium results in suppression of twinning in single crystals of $[011]$ orientation. The deformation develops with the high SHC from the beginning of plastic deformation, stage with low strain-hardening coefficient is not observed. The axis of single crystal at deformation moves in $[\bar{1}01]$ direction - slip in primary system. Thus, the increase of SF energy results in suppression of deformation by twinning in $[\bar{1}11]$, $[011]$ orientations, where twinning acts as the basic mechanism of deformation in Hadfield steel without aluminium.

In Hadfield steel without aluminium in $[\bar{1}23]$ crystals the change of the deformation mechanism from slip in one system to twinning mainly in one system is observed and it is proved by electron microscopy and X-ray researches. From the beginning of plastic deformation the axis of single crystal goes to $[\bar{1}01]$ direction - slip in primary system, twinning is not revealed. In Hadfield steel the pile-ups of dislocations and slip traces on specimen surface are not observed due to the high mobility of carbon atoms in matrix [4, 5]. The possible reason is fast restoration of the local order of carbon during movement of dislocation on slip plane. The important feature of deformation of $[\bar{1}23]$ single crystals is that at action only one systems of slip the SHC at the first stage exceeds the SHC at deformation of pure FCC materials and FCC substitutional alloys. At ϵ = 20 % the axis moves in $[\bar{2}11]$ pole - twinning in primary system. The increase of the SHC at this stage, in comparison with the first one, is caused by interaction of slip and twinning dislocations in different systems of shear simultaneously.

The slip mainly in one system defines deformation of $[\bar{1}23]$ single crystals down to fracture in Hadfield steel with aluminium, twinning experimentally has not been revealed. From the early degrees of deformation the traces of slip are observed as against in Hadfield steel

without aluminium. Hence, the aluminium decreases the diffusion mobility of carbon and first dislocation on slip plane destroys the local order and subsequent dislocations test smaller resistance to the movement on slip plane on the part of the local order forming the pile-ups of dislocation.

As electron microscopy and metallographic researches have shown in [001] single crystals at tension in Hadfield steel without aluminium the high SHC is connected with interaction of slip and twinning dislocations in several systems. Twinning is realized here with formation of extrinsic SF. Such type of twinning in FCC crystals is observed for the first time and these data allow to consider a role of new type of twinning in hardening of polycrystals of Hadfield steel. In Hadfield steel with aluminium the high speed of hardening is connected with intersection of powerful pile-ups of perfect dislocations and it causes hardening similar to hardening at intersection of slip and twinning in several systems simultaneously.

At compression of single crystals of Hadfield steel without aluminium of $[\bar{1}11]$ orientation the deformation passes in two stages: first with low SHC is caused by formation and propagation of macro shear bands (MSB). MSBs are rejected on corner 7-10^0 from {111} plane - plane of slip in FCC crystals. Thus low value of strain hardening is connected with effect of geometrical softening of lattice during plastic flow inside of MSB [6]. MSB arising does not extend in volume of specimen. Electron microscopic researches, repolishing and etching have shown that in MSB the high density of twins of deformation is formed. The deformation in MSB is stopped due to twinning inside of MSB and further deformation at the first stage is realized by origin and stopping of new MSBs. When all volume of specimen is filled with macro shear bands there is a transition to the second stage of hardening with higher SHC in comparison with the first stage. Here hardening is defined by interaction of slip and twinning in several systems simultaneously.

At compression of Hadfield steel with aluminium the $[\bar{1}11]$ single crystals have two stages on the curve of plastic flow. MSBs are not observed. The first stage of deformation is connected with slip mainly in one system. The second - with activation of slip in conjugative systems. Thus,

alloying with aluminium moderately raises SF energy of Hadfield steel that results in suppression of deformation by twinning as a basic mechanism determining all plastic deformation of crystal. The aluminium reduces diffusion mobility of carbon in austenitic matrix so that the processes of dynamic strain aging appear to be suppressed at room temperature [3] as against Hadfield steel without aluminium, and from the early stages of deformation the powerful pile-ups of dislocation are formed. The intersection of pile-ups causes the high speed of strain hardening of Hadfield steel single crystals with aluminium similarly to intersection of slip and twinning dislocation in several systems in Hadfield steel without aluminium.

References:
1. K. S. Raghavan, A. S. Sastri, M. J. Marcinkowski. Nature of the work-hardening behavior in Hadfield's manganese steel/ Transactions of the metallurgical society of AIME, vol. 245, 1969, pp.1569-1575
2. P. H. Adler, G. B. Olson, W. S. Owen Strain hardening of Hadfield manganese steel/ Metallurgical transactions A, vol. 17A, 1986, pp. 1725-1737
3. B. K. Zuidema, D. K. Subramanyam, W. C. Leslie. Effect of aluminum on the work hardening wear resistance of Hadield manganese steel/ Metallurgical transactions A, vol. 18A, 1987, pp. 1629-1639.
4. Y. N. Dastur, W. C. Leslie. Mechanism of work hardening in Hadfield manganese steel/ Metallurgical transactions A, vol. 12A, 1981, pp. 749-759
5. W. S. Owen, M. Grujicic. Strain aging of austenitic Hadfield manganese steel/ Acta mater., vol. 47, No. 1, pp.111-126, 1999
6. M. A. Schtremel. Durability of alloys. P.2. Deformation. Moscow "MISIS", 1997, 525 p.

SLIP AND TWINNING IN AUSTENITIC STAINLESS STEEL SINGLE CRYSTALS WITH DIFFERENT STACKING FAULT ENERGY, HARDENED BY NITROGEN

Kireeva I.V., Luzginova N.V., Chumlyakov Yu.I.
Siberian Physical -Technical Institute, Tomsk, Russia

On single crystals of austenitic stainless steels Fe-17%Cr-8%Ni-2%Mn with γ_{sf}=0.01 J/m^2 (I), Fe-18%Cr-12%Ni-2%Mo with γ_{sf}=0.025 J/m^2 (II), Fe-26%Cr-32%Ni-3%Mn with γ_{sf}=0.08 J/m^2 (III) the systematical investigations of the influence of crystal axis orientation, the value of stacking fault energy, test temperature and nitrogen concentration on the level of resolved shear stresses τ_{cr}, deformation mechanism – slip/twinning, the type of dislocation structure – planar and cellular, work-hardening rate θ, plasticity and fraction by means of optical, transmission electron and scanning electron microcopies, X-ray diffraction at tension have been carried out.

It has been shown that austenitic stainless steels without nitrogen are characterized by low values of resolved shear stresses ~ 50 MPa at T=300K. As the temperature decreases the increase of resolved shear stress in 2.5 times: from 50 MPa at T=300K up to 125MPa at 77K is observed in steels (I-III). It has been established that in these steel (I-III) crystals without nitrogen resolved shear stresses are not dependent on crystal orientation, i.e. in these crystals Schmid's law about independence of RSS on crystal axis orientation takes place. The exception is single crystals of steel (I) without nitrogen in which the orientation dependence of RSS is observed. In <001> crystals RSS is higher than RSS in <111> crystals and <001> crystals is "hard", <111> - "soft" in temperature interval T=77-573K.

Alloying with nitrogen of steels I-III up to C_N=0.2-0.7 wt.% leads, firstly, to strong solid solution hardening. The level of RSS is increased in 3-3.5 times compared to crystals without nitrogen. Secondly, the value of stacking fault energy is decreased in 2-2.5 times compared with nitrogen-free steels. Thirdly, the change of type of dislocation structure from cellular in nitrogen-free steels to planar in steels with nitrogen is found out. Fourthly, in II-III steels there is an orientation dependence of RSS, which becomes stronger with the increase of nitrogen concentration and the

decrease of test temperature, the maximal its effect are reached at C_N=0.5-0.7 wt.% and T=77K. The investigation of dislocation structure in <001> and <111> crystals shows that orientation dependence of RSS correlates with orientation dependence of type of dislocation structure. Two types of orientation dependences of dislocation structure are established: the first is at C_N=0.2-0.4 wt.%, when RSS is determined by the value of dislocation splitting, i.e. in "hard" <001> crystals the perfect dislocations interact with nitrogen atoms whereas in "soft" <111> crystals – partial dislocations. The second type of orientation dependence of dislocation structure at C_N=0.5-0.7 wt.% is connected with the change of deformation mechanism from slipping in "hard" orientations to twinning in "soft" orientations.

It has been established that the high level of stresses reached by solid solution hardening with nitrogen C_N=0.5-0.7 wt.% in steels I-III results in the appearance of twinning in <001> crystals at tension, these crystals are earlier considered to be untwinned. It has been established by transmission electron microscopy that in <001> crystals twinning is realized by extrinsic stacking faults whereas in <111> - by intrinsic stacking faults. Hence, in high-strength crystals of austenitic steels with nitrogen twinning becomes polar deformation mechanism as compared with established conformities for twinning in low-strength FCC materials.

It has been experimentally shown that the stages of strain-stress curves, plasticity, the values of work hardening rate are dependent on crystal axis orientation, nitrogen content, test temperature and the type of dislocation structure.

It has been shown that stress-strain curves for single crystals <111>, <001>, <011>, <012>, <123> of nitrogen-free steels have two stages: stage 2 of linear hardening with work-hardening rate θ_2/G ~ 4×10^{-3}, which is not dependent on test temperature and crystal orientation, and stage 3 of dynamical recovery connected with the development of cross slip processes. The

investigations of crystal axis precession in crystals <012>, <123>, <011> show that deformation occurs by slipping. In <111>, <001> crystals the axis precession is absent, it means that multiple shear takes place.

Alloying with nitrogen of <111> single crystals of II-III steels up to $C_N=0.3-0.4$ wt.% leads to the drop of work-hardening rate (WHR) and to the development of deformation in one slip plane compared to these crystals without nitrogen. This changing of WHR, as shown by the investigations of dislocation structure, is connected with the change of the type of dislocation structure form cellular in crystals without nitrogen to planar structure with pile-ups in crystals with nitrogen. The increase of nitrogen content up to $C_N=0.5-0.7$ wt.% results in the sharp increase of work hardening rate, the decrease of plasticity. It is connected with the change of deformation mechanism from slip to twinning and with the interaction of twinning in several systems.

In <001> crystals of II-III steels the alloying with nitrogen up to $C_N=0.3-0.5$ wt.% doesn't lead to the principal change of stress-strain curves and work-hardening rate compared with nitrogen-free crystals. The absence of WHR dependence on nitrogen concentration is connected with likeness of dislocation structure.

In <011>, <123>, <012>, <122> crystals the alloying with nitrogen leads to the increase of strength properties, the suppression of the cross slip processes, the increase of stage 2 and stage 3 of dynamical recovery is not reached compared with nitrogen-free crystals. In these orientation WHR on the stage 2 of linear hardening as well as in nitrogen-free crystals is not dependent on orientation and test temperature. X-ray investigations show that the change of deformation mechanism from slip to twinning in <123>, <122> orientations after significant slip deformation in the moment when the crystal axis reaches "symmetral" takes place. Two stages on stress-strain curves are observed: the first is connected with slipping in one plane, the second – with the appearance of twinning in one system. As the test temperature decreases the transition to twinning shifts into the region of lower deformation.

It is experimentally established that alloying with nitrogen of crystals of II-III steels leads to the change of fracture mechanism from ductile in nitrogen-free crystals to mixed and brittle in crystals with high content of nitrogen $C_N=0.5-0.7$

wt.%. It has been shoun that in <001>, <111> crystals of I, II steels without nitrogen the fracture is ductile with the neck formation in the temperature interval 77-573K. At alloying with nitrogen up to $C_N=0.2-0.4$ wt.% the fracture is ductile as well but without the neck formation over planes close to slip planes (111).

In high-strength state at $C_N=0.5-0.7$ wt.% and T=77K in <111> crystals the fracture occurs by the mechanism of quasi-cleavage with good-represented volume character. The crack of quasi-cleavage spreads through several equivalent planes close to (111) and serrated structure is formed, traces of localized deformation are observed.

In <001> crystals at $C_N=0.5-0.7$ wt.% and T=77K the mixed fracture takes place, brittle component being 50% from total fracture surface of crystal.

Thus, in crystals with high nitrogen content the orientation dependence of fracture mechanism is found out: in <111> crystals – brittle, in <001> - mixed fracture. The orientation dependence of fracture mechanism is connected with difference in work hardening and dislocation structure formation processes. So, brittle fracture in <111> crystals at $C_N=0.5-0.7$ wt.% and T=77K is realized after plastic flow with high work hardening rate connected with interaction of twinning in several systems. In <001> crystals the main mechanism of plastic deformation is slip, which leads to the ductile fracture. Twinning, found in these crystals, is additional deformation mechanism and the interaction of twinning and slip results in the appearance of brittle component on fracture surface of these crystals.

The comparison of fracture stresses of differently orientated crystals shows that not only the level of fracture stresses determines fracture mechanism, but also the important is the character of dislocation structure – the transition to twinning.

The correlation between the type of dislocation structure and fracture is experimentally established: plastic deformation by slip determines ductile fracture at all states $C_N=0.2-0.7$ wt.% and T=77-573K in <001> crystals whereas twinning deformation at $C_N=0.5-0.7$ wt.% and T=77K leads to brittle fracture.

Obtained results may be used at the analysis of deformation hardening mechanisms of high-nitrogen steel polycrystals and at the determination of the role of texture in the formation of strength properties of steel articles.

INTERACTION OF ATOMIC OXYGEN WITH COPPER AND SILVER

Zheludkevich M.L., **Gusakov A.G., Voropaev A.G., Vecher A.A., Sobeski A.S.**
Belarussian State University, Minsk, Belarus

This work is devoted to the interaction of flows of atomic oxygen with copper within the temperature range of 473 to 1073 K and with silver within the temperature range of 423 to 673 K. Experiments were performed by using a high-vacuum system that was earlier described in more detail [1]. Atomic oxygen was generated by dissociation in microwave discharge.

The degree of dissociation was varied between 5 to 50 % depending on the gas mixture composition and the discharge power. The density of the atomic oxygen flow was measured by the method of chemiluminescent titration by nitrogen dioxide [1]. To investigate the kinetics of copper and silver oxidation, the time dependence of electric resistance of a sample was measured. The composition of the scale formed during oxidation was analyzed by X-ray diffraction method.

Oxidation of silver by flows of atomic oxygen with the density of $2.7 \cdot 10^{16}$ atoms·cm^{-2}·s^{-1} was studied within the temperature range between 423 and 673 K. X-ray diffraction analysis of oxidized samples proved that during oxidation oxide Ag_2O is formed on the silver surface within the above temperature range.

The silver oxidation rate within the temperature range of 423 to 623 K and at the atomic oxygen flow density of $2.7 \cdot 10^{16}$ atoms·cm^{-2}·s^{-1} obeys the parabolic kinetic dependence, which is the evidence of diffuse limitation of oxidation. The parabolic kinetic dependence of silver oxidation by atomic oxygen was previously observed in the work [3] at temperatures between 293 and 373 K. Increasing the temperature to 648 K changes the parabolic kinetic law to linear, which is the evidence of a change in the oxidation mechanism. The linear kinetic law is probably preconditioned by that the limiting stage of the oxidation process is the reaction at the solid-gas interface.

The kinetic dependence also changes with a decrease in density of the atomic oxygen flow falling on the sample. Increasing the temperature within the range of 423 to 573 K increases the silver oxidation rate. Further increase in

temperature decelerates the oxidation rate. Due to this, a fracture is observed for the silver oxidation rate in the region of 573 K on the Arrhenius dependence.

The activation energy at temperatures between 423 and 523 K makes 33 kJ·mol^{-1} (Fig. 1). With further increase in temperature up to 673 K silver oxidation ceases and the previously oxidized sample reduces to metal silver. The non-linear Arrhenius dependence for silver oxidation by atomic oxygen flows within the temperature range of 423 to 673 K is probably connected with that not only oxidation reaction (1), but also opposite reactions of silver oxide dissociation (2) and "recombination reduction" (3) can proceed in a silver-oxygen system.

$$2Ag + O \rightarrow Ag_2O \qquad (1)$$
$$Ag_2O \rightarrow 2Ag + \tfrac{1}{2}O_2 \qquad (2)$$
$$Ag_2O + O \rightarrow 2Ag + O_2 \qquad (3)$$
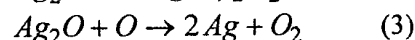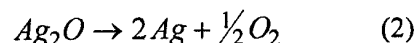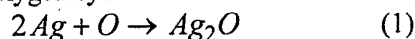
To back up the thermodynamic probability of these processes, the Gibbs energies for the respective reactions were calculated. The obtained results prove that all the three reactions are thermodynamically probable within the entire temperature range being investigated.

According to the calculations, with the atomic oxygen flow density of $2.7 \cdot 10^{16}$ atoms·cm^{-2}·s^{-1}, the formation of silver oxide Ag_2O is thermodynamically probable up to the temperature of the order of 1100 K, but, as the experimental data prove, already at 673 K silver is not oxidized by atomic oxygen and, moreover, the reduction of oxide formed at lower temperatures starts. This occurs because at temperatures above 673 K processes of thermal dissociation and "recombination reduction" of silver oxide start.

When copper is oxidized by atomic oxygen, Cu_2O is formed on the surface as distinct from oxidation by molecular oxygen, when Cu_2O-CuO scale is formed. And the probability of interaction of atomic oxygen with copper is by six orders of magnitude higher than that of molecular. Between 473 and 773 K, like in case with molecular oxygen,

the oxidation kinetics of copper by atomic oxygen obeys the parabolic law. A more complex kinetic dependence is observed between 873 and 1073 K.

At the initial stage, which lasts 20 to 80 minutes, oxidation obeys the linear kinetic law. With further oxidation the linear kinetic dependence changes to parabolic. Based on the temperature dependence of the parabolic constant of the copper oxidation rate by atomic oxygen, the activation energies of this process were calculated within the entire temperature range (Fig.2). In the high-temperature area, the effective energy of activation made $E_a=16\pm5$ kJ·mol^{-1}, which is much lower than the activation energy of copper oxidation by molecular oxygen - 165 ± 9 kJ·mol^{-1}.

Within the temperature range of 473 to 823 K, the found activation energy made $E_a=62\pm4$ kJ·mol^{-1}, in molecular oxygen, at T=723-873 K, $E_a=107\pm15$ kJ· mol^{-1}. Such difference at low temperatures may be due to that oxidation by atomic oxygen decreases one of the components of the summary activation energy – the energy necessary for dissociation of oxygen molecules.

At high temperatures, the difference by an order of magnitude between the activation energies of copper oxidation by atomic and molecular oxygen is probably caused by that the oxidation process is accompanied by the processes of dissociation and "recombination reduction" of the formed copper oxide.

Thermodynamic analysis proved the probability of the reaction of "recombination reduction" of copper oxide by atomic oxygen within this temperature range

$$Cu_2O + O \rightarrow Cu + O_2, \qquad (4)$$
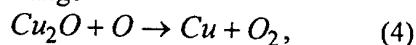
whereas the thermodynamic probability of oxidation reaction decreases considerably with increasing temperature. As a result, at temperatures above 1123 K the oxidation rate starts decreasing.
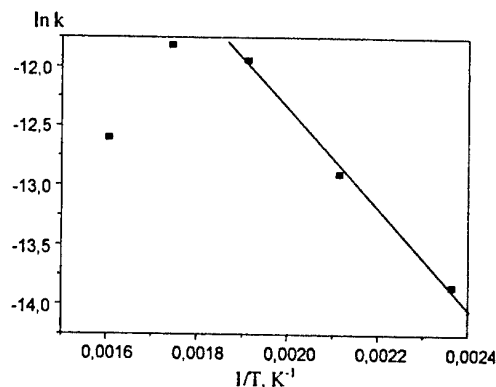
Fig. 1. Temperature dependence of the rate constant of silver oxidation by atomic oxygen.

$\square$ T=823-1073 K, $E_a=16\pm5$ kJ·mol^{-1}

$\blacksquare$ T=473-823 K, $E_a=62\pm4$ kJ·mol^{-1}

$\blacktriangle$ Ref. [3]
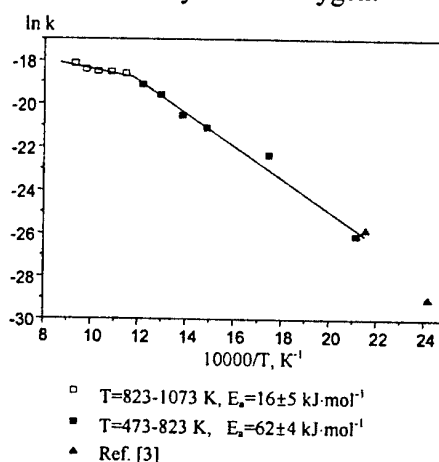
Fig. 2. Temperature dependence of the rate constant of copper oxidation by atomic oxygen.

References

1. A.G. Gusakov, S.A. Raspopov, A.A. Vecher, A.G. Voropaev. Interaction of tantalum with diatomic and atomic oxygen at low pressures//J. Alloys Comp. 1993. V. 202. P. 67.
2. De Roij A, European Space Aqency Journal, 1989, 13, 363.
3. B.G. Gibson, J.R. Williams, J.A.T. Fromhold, M.J. Bozack, W.C. Neely and A.F. Whitaker. The interaction of atomic oxygen with thin copper films//J. Chem. Phys. 1992. V 96. P. 2318.

INTERACTION OF NIOBIUM AND PCW-10 ALLOY (NIOBIUM-ZIRCONIUM-CARBON) WITH FLOWS OF ATOMIC AND MOLECULAR HYDROGEN

Zheludkevich M.L., Gusakov A.G., Voropaev A.G., Vecher A.A., Kozyrski E.N.
Belarussian State University, Minsk, Belarus

This work investigates the interaction of flows of atomic and molecular hydrogen with niobium within the temperature range between 573 and 773 K and with the PCW-10 alloy within the temperature range between 573 and 873 K.

Experiments were performed by using the high-vacuum system that was previously described in more detail [1]. Atomic hydrogen was generated by dissociation in microwave discharge. To examine the kinetics of dissolution of hydrogen in niobium, the dependence of electric resistance of tape metal samples on the exposure time was investigated.

The dependence of the niobium resistance on the concentration of hydrogen dissolved in it is known [2]. The values of dissolved hydrogen concentration obtained from the data of sample resistance measurements coordinated well enough with the concentrations calculated on the basis of a change in the crystal lattice constant. The study of the dissolution kinetics was carried out in flows of molecular hydrogen 10^{18} molecules·cm^{-2}·s^{-1} and atomic hydrogen 10^{17} atoms·cm^{-2}·s^{1}.

Molecular hydrogen is dissolved in niobium in the flow of 10^{18} molecules·cm^{-2}·s^{-1} only at temperatures above 673 K. At lower temperatures the process is kinetically decelerated and no dissolution of hydrogen in niobium was recorded by the method of measuring the sample resistance.

Increasing the temperature increases the molecular hydrogen dissolution rate. The energy of activation of this process within the temperature range of 673 to 773 K made 5 kJ·mol^{-1}.

Investigated was also the kinetics of reaction of niobium with atomic hydrogen within the temperature range of 573 to 723 K. When treating the niobium samples with flows of partially dissociated hydrogen 10^{17} atoms·cm^{-2}·s^{-1},

dissolution occurs with a higher rate that in case of molecular hydrogen.

At the temperature of 673 K the hydrogen absorption rate increases by the factor of 4. The process of dissolution of atomic hydrogen obeys the parabolic kinetic dependence, which is the evidence of diffuse limitation of the process. Increasing the temperature increases the rate of dissolution of atomic hydrogen in niobium.

The activation energy of this process is close in value to the activation energy of molecular hydrogen dissolution and is equal to 5.3 kJ·mol^{-1}. Studied was also the saturation of niobium with hydrogen up to high concentrations. The initial stage of dissolution of atomic hydrogen at the temperature of 673 K is described by parabolic dependence. At the hydrogen concentration of the order of 11 at. %, the process kinetics changes to linear and the dissolution rate increases considerably (see Fig.1).

In this case practically all atoms of hydrogen, which fall on the sample surface, dissolve in niobium. The change of the kinetic law and the rate of hydrogen dissolution in niobium may be connected with the formation of a new phase. The X-ray diffraction analysis of the samples proves that hydrogen dissolution causes formation of a solid solution (α-phase) in niobium; when the concentration of dissolved hydrogen reaches 11 at. %, β-phase is formed.

Dissolution of atomic hydrogen in PCW-10 with a notable rate begins only at a temperature above 573 K. The dissolution rate obeys a complex kinetic dependence. At the initial stage, rapid dissolution of hydrogen in PCW-10 occurs. It obeys the linear kinetic law. Increasing the exposure time decelerates the process and a parabolic dependence is observed. Increasing the temperature within temperature range between 573 and 773 K increases the hydrogen dissolution rate. The energy of activation of atomic hydrogen dissolution within this temperature range is equal to 85 kJ·mol^{-1}.
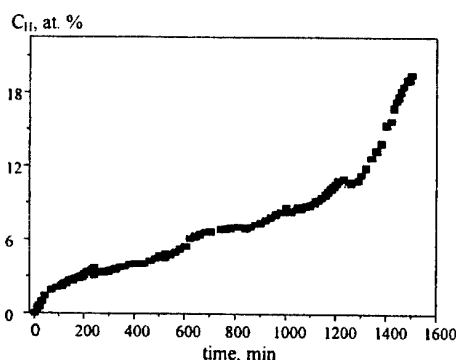
Fig.1. Kinetic curve of dissolution of atomic hydrogen in niobium at 673 K.

Further increase in temperature decreases the rate of atomic hydrogen dissolution in PCW-10 which is probably conditioned by the increase of the recombination coefficient of hydrogen atoms on the alloy surface.

When a flow of molecular hydrogen reacts with PCW-10 at 773 K, a considerable decrease in the dissolution rate is observed as compared with the atomic hydrogen (approximately by 25 times), see Fig. 2.
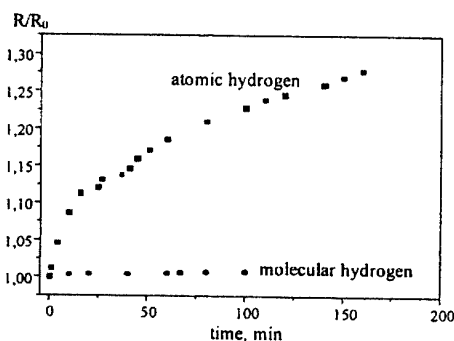
Fig. 2. Kinetic curves of dissolution of atomic and molecular hydrogen in PCW-10 at 773 K.

The comparative analysis of the kinetics of hydrogen dissolution in niobium and PCW-10 proved that the dissolution rate of atomic hydrogen in PCW-10 exceeds the dissolution rate in niobium under similar conditions. In case of molecular hydrogen, the dissolution rate in niobium is, in its turn, higher than in PCW-10.

The obtained results make it possible to state that preliminary dissociation increases to a considerable extent the rate of hydrogen dissolution in niobium and PCW-10, the

dissociation having a much greater effect on the kinetics of hydrogen dissociation in PCW-10 than in niobium. This fact should be taken into account when selecting structural materials for work in media containing atomic hydrogen.

References

1. A.G. Gusakov, S.A. Raspopov, A.A. Vecher, A.G. Voropaev. Interaction of tantalum with diatomic and atomic oxygen at low pressures//J. Alloys Comp. 1993. V. 202. P. 67.
2. De Roij A, European Space Aqency Journal, 1989, 13, 363.

INFLUENCE OF THE STRUCTURE AND TEXTURE ON THE FAILURE ANISOTROPY OF THE LOW ALLOYED STEELS

Shkatulak N.M., Usov V.V.
South Ukrainian State Pedagogical University, Odessa, Ukraine

Texture and anisotropy of the failure after controlled rolling (final rolling temperatures $t_{r.f.}$ were as high as 650, 700, 750 and 850^0C) of the low-alloyed steels were investigated. The relatively small grain (20-30 μm), slight quantity (0,007%) of the non-metal inclusions characterized the structure of the steels. The chemical composition of the steels was practically homogeneous through the cross-section of the sheets. Crystallographic texture was considerably heterogeneous through the cross-section of the sheets. The shear texture component {110}<100> was formed in surface layers. Nearing to the middle of the sheets the intensity of the mentioned texture component decreased and the intensity of the {001}<110>-texture component increased. The latter of the mentioned orientation was major in the middle of the sheets. Above-mentioned heterogeneity of the texture increased if $t_{r.f.}$ decreased. The rapid cooling after rolling at $t_{r.f.}=850^0$C led to the practically non grain-oriented state of the sheets.

The researched steels have the brightly expressed anisotropy of impact elasticity. Thus the resistance to the failure decreases at temperature fall. The fractographical analysis of the fracture after testing in the field of temperatures that is lower than temperature of a cold brittleness t_x, showed the presence of macroscopic separations. The centers of origin of similar separations are, apparently, the non-metallic inclusions (oxides, nitrides, sulfides), detected in secondary cracks. The further development of a brittle crack is determined by crystallographic texture of a material.

The layered brittle failure in researched specimens of low-alloyed steels mainly is carried out on the mechanism of the trans-crystallite friable chipping on planes {001}. It is confirmed also by data of the micro-fractographical analysis. The oblong concavities by the size (20 × 100) micron (fig. 1) are detected, which sizes are comparable to the dimensions of the pearlite components, deformed at the rolling.
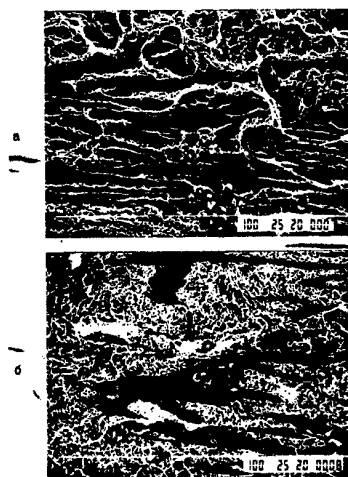
Fig. 1. Electronic micro still picture of the steel fracture ($t_{r.f.} = 750^0$ C) after testing on impact elasticity at – 40^0 C: a – layered viscid failure; b – layered brittle failure

There are numerous separations, which have particular crystallographic trend. Alongside with it on adjacent sites of a fracture there are facings of a chipping, commensurable with a size of ferrite grains (20 – 50 microns). In texture of ferrite of steels after rolling the component of texture {001} <110> predominates. Main planes of a chipping in BCC - metals are the crystal planes {001}. In case of favorable orientation of such planes in relation to a direction of the affixed normal stresses the development of a friable crack is facilitated, as the transition from one grain to another is bound to smaller deviation of a crack from a tentative direction of its development. For the trans-crystallite crack this, in turn, is promoted by the fact, that the sub boundaries of dislocation structure of the texture component {001} <110> are parallel to rolling plane. As a result a plasticity of a material is lowering at appropriate above described crystallographic texture there. It appears in origin of a three dimensional anisotropy of mechanical characteristics of researched steels and lowering of resistance to failure at temperature fall.

Thus, at increase of the intensity texture components {001} <110> in different sections of sheets of low-alloyed steels the brittle failure

should be expected. In case of increase in texture of sheets of the component {110} <UVW> it is necessary to expect a viscid character of the failure.

We suggest the texture parameters, which allow estimation the tendency of mentioned steels to the layered brittle destruction. We define such parameters as volume parts of «brittle» {001} and «viscid» {110} texture components.

It is possible to characterize the above-mentioned distribution of the texture trough cross-section of the low-alloyed steel sheets by relation of pole density P_{110}/P_{100} in each layer of sheets.

By comparison of this ratio in different sections of sheets with the appropriate value of impact elasticity, the correlation is found out: the higher is the value of the ratio P_{110}/P_{100}, the more value of impact elasticity.

The correlation is watched also by comparison of an impact elasticity for different directions in a plane of rolling (fig. 2, a) with the appropriate value of the above-stated ratio (fig. 2, b), obtained by results of research of polar density on a direction in a rolling plane.

In the field of temperatures of layered viscid failure the enough tight nonlinear correlation is detected. Thus the coefficient of correlation made up 0,895 with reliability 95 %. The equation of regression for a nonlinear correlation between the value of an impact elasticity a and P_{110}/P_{100} is:

$$a = 265,2 - 100,7 \, (P_{110}/P_{100}) + 19,6 \, (P_{110}/P_{100})^2.$$

This equation in a graphic form is represented in a fig. 2, c, curve 8.

In the field of temperatures of layered brittle failure (fig. 2, a, the curve 4) linear correlation is detected. Thus the coefficient of correlation made up 0,977 with reliability 99 % between value of impact elasticity and value P_{110}/P_{100} (fig. 2, c, curve 7).

It is interesting to remark, that in the field of temperatures of viscid destructions the maxim of impact elasticity coincides with a minimum of the above-stated ratio in, declined from rolling direction on an angle 45^0 the direction (fig. 2). It confirms the crystallographic mechanism of development of a crack.
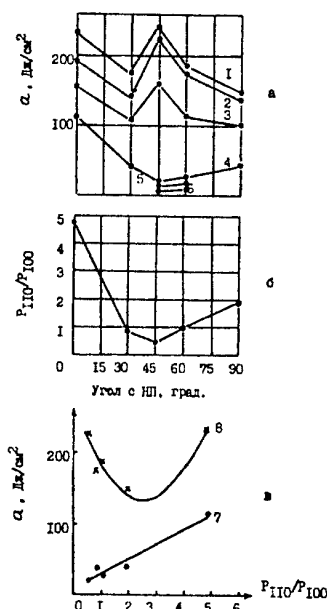
Fig. 2. Dependences of an impact elasticity (a) and ratio (b) from a angle of a cutting of the specimens in a plane of a steel sheet at viscid (1-3) and friable (4-6) failure, c - correlation dependences of an impact elasticity on the ratio P_{110}/P_{100} at friable (7) and viscid (8) character of failure

And vice versa for a temperature of the cold brittleness t_X: the higher is the ratio P_{110}/P_{100}, the below t_X (fig. 3)
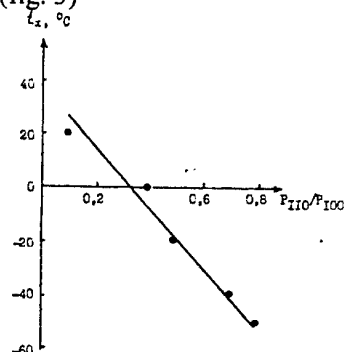
Fig. 3. Dependence t_x, obtained from the data of testing on impact elasticity of the specimens, oriented in normal direction to a plane of rolling from the appropriate ratio P_{110}/P_{100}.

Thus, increase of the {001}<110> texture component is one of the main causes firstly of the rise of the fracture anisotropy and secondly of the tendency of the above-mentioned steels to the laminar brittle failure.

STRUCTURE STATE OF TEMPERED MARAGING ALLOYS

Danilchenko V.E.
G.V. Kurdyumov Institute for Metal Physics NAS of Ukraine, Kyiv, Ukraine

Heat treatment of maraging steels and metastable phase-hardened iron-nickel alloys includes heating to within the $(\gamma+\alpha)$– phase limits. The heating is necessary either for producing the intermetallic phases on aging or for initiating the reverse $\alpha-\gamma-$ transition. These processes in iron-nickel-based alloys are accompanied by the redistribution of the alloying element between the $\gamma-$ and α–phases. This work deals with X-ray study of structural and composition changes in single crystals caused by heating the maraging alloys to within the $(\gamma+\alpha)$– limits.

The test material was Ni29Ti2 and Ni28Ti2Al2 alloys, which is used for the fabrication of stamps and press molds. The specimens contained (70-85)% martensite at room temperature. The reverse transition occurred on heating in salt bath at $(400-500)^0$C. The transition kinetics and the amount of martensite were controlled by magnetometry. Selected area X-ray diffraction patterns were taken on a KAMEBAX spectrometer. Nickel content of the $\gamma-$solid solution was estimated from the previously built concentration dependences of fcc-lattice parameter of binary iron-nickel alloys. With this purpose, a set of single crystal specimens containing from 25 to 100% Ni were prepared. The alloys containing 25 and 28% Ni were two-phase $(\gamma+\alpha)$ at room temperature. Thus, their lattice parameters a_γ corresponded to the retained austenite. The lattice parameters of the fcc-crystals were close to those of iron-nickel polycrystals.

The tempering of freshly quenched alloys reduced the parameter c_α and the tetragonality c/a_α of the martensite lattice even at room temperature. At temperatures between 100 and 300° C, the parameter c_α reduced further, and the reverse $\alpha-\gamma-$ transition occurred during tempering at 400° C. The reduced in c_α is associated with the loss of matching of the martensite and retained austenite lattices, as well as with the formation of a Ni_3Ti-type phase and the subsequent depletion of the α-solid solution in the alloying elements due to the formation of intermetallic compounds and the nickel redistribution between the between the $\gamma-$ and α–phases.

Annealing of the two-phase specimens at 520°C for several minutes shifted the martensite reflections having high third indices toward higher Bragg angles. The retained austenite reflections were blurred at the side of low angles, and weak first-order satellite reflections appeared at the blurring at 520°C (for 10 h) or higher annealing temperature (600°C) attenuated and eliminated the latter reflections, and the retained austenite reflections started blurrings. Holding at 600°C increased the Bragg angles and intensities of the satellite reflections. The Bragg angles of the retained austenite reflections also increased.

The appearance of the satellite first- nd second-order reflections indicated the recovery of the initial austenite phases having an fcc-lattice and larger and smaller lattice parameters, respectively. The disappearance of first-order satellite and the appearance of the second-order ones with increasing tempering time and temperature were accounted for by the permanent shifting of the first-order reflections, which were temporally superposed with the strong reflections of the retained austenite. These satellites are produced by the reverted austenite that forms during the reverse $\alpha-\gamma-$transition.

The lattice parameter of the reverted austenite, which was initially higher than of the retained austenite, decreased which increasing time of tempering at 600°C. After 1 h of tempering, the parameter was already considerably smaller than for the retained austenite. Each austenite reflection split in two reflections having different intensities. The amount of the reverted austenite increased with decreasing lattice parameter.

The splitting of the austenite reflections, which indicates a decomposition of the γ–solid solution was observed during heating of the $(\gamma+\alpha)$–specimens. This rule was true for heating in air, in pyrophyllite environment, in salt bath, and in ealed quartz ampoules at 10^{-3} torr. The splitting was strongest in air, i.e., in an oxidizing environment. Splitting pattern and intensity ratios

297

in ampoules were similar to these parameters for air only after 5-8 times longer tempering.

The shift and change in intensity of the satellites is probably due to the permanent increase of nickel concentration in the reverted austenite. The decrease and subsequent increase of the Bragg angles were due to the nonmonotonic variation of the fcc-lattice parameter of the iron-nickel alloys with increasing nickel concentration: the parameter a_γ increased until a nickel concentration of 41% was reached, and then it considerably decreased. The calculation of nickel concentration in the reverted austenite from the parameter a_γ showed that tempering enriched the fcc-lattice in nickel to above 90%. The concentrations of titanium and aluminum were not taken into account.

The enrichment of the reverted austenite in nickel during the reverse $\alpha-\gamma$-transition and isothermal holding of metastable austenite alloys and maraging steels was reported earlier. However, the large enrichment obtained in this work can hardly be accounted for by only the nickel redistribution between the $\gamma-\alpha$-phases.

The major cause of the enrichment of the γ-solid solution in nickel was deduced by analyzing the microstructural and layer-by-layer phase composition data of the tempered specimens.

The superficial layer was removed by abrasion, chemical etching, and electropolishing. The intensities of the nickel-rich austenite reflections decreased beginning from a depth of 20 μm, and only retained austenite reflections were observed at a depth of 40 μm. The metallographic data taken from a tilt section showed the presence of an oxide layer with well-developed cracks on the surface. Fe_2O_3 and Fe_3O_4-type oxides were revealed by X-ray diffraction.

Oxides of other alloying additions were not revealed by X-ray diffraction because of the low concentrations. X-ray probe concentration depth profiling showed that, at depth of > 50 μm, the nickel-to-iron ratio were close to those for the mean composition, whereas at a depth of 5-8 μm from the oxide/matrix boundary, this ratio was more than 5:1. Even higher nickel concentrations were observed immediately at the surface.

The data proves that the γ-solid solution is laminated at the surface. The appearance of continuous reflection zones of polycrystalline oxides simultaneously with the splitting of the single crystal reflections allowed the austenite lamination to be attributed to the surface oxidation.

The surface oxidation was selective because the specific heats of the formation of iron and nickel oxides differ by 4-6 times. The scale was formed by the growth of two layers. The upper layer grew by the diffusion of iron cations to the surface, and the inner layer grew by the inward oxygen diffusion along the lattice defects. The diffusions of iron into the oxide layer and nickel into the suboxide layer enriched the latter layer in nickel and depleted it of iron.

The lamination of the γ-solid solution was observed only on heating of two-phase alloys containing large amounts of the martensite (>20%). Thus, the diffusion was enhanced by the phase hardening, and the mechanism and kinetics of the reverse $\alpha-\gamma-$ transition at the surface differed from these in the bulk.

The data proves that diffusion may be enhanced even on the martensite/coarse-grained reverted lath austenite boundary. This is the only reasonable explanation of the γ-solid solution lamination because the lattice of the nickel-rich regions had the orientation of the retained austenite.

Thus, heating of two-phase iron-nickel-based alloys during the reverse $\alpha-\gamma-$ transition causes the surface lamination of the γ-solid solution. The surface of the quenched alloy is nickel because of the nickel redistribution between the $\gamma-$ and $\alpha-$phases during the $\alpha-\gamma-$transition, selective iron oxidation, and increase in the concentration of the unoxidized component in the suboxide layer.

PROPERTIES OF Fe-B (10wt%) OBTAINED FROM MECHANICALLY ALLOYED Fe-B (50wt%) POWDERS

Abenojar J., Velasco F., Mota J.M., Martínez M.A.
e-mail: abenojar@ing.uc3m.es
Dpto. de Ciencia de Materiales e Ingeniería Metalúrgica. Universidad Carlos III de Madrid.
Av. de la Universidad, 30 – E-28911 – Spain.

Boron, with a effective section of 755 barns, is the perfect candidate to absorb neutrons. It is one of the few elements that does not emit ☐radiation after being irradiated [1] [2]. In some reactors, steels with 3-4 %B have been used, as they give many metallurgical problems.

So high content boron steels (10–20%B) can be of great interest as radiation barrier for waste containers or controlling elements in reactors. Boron is added as liquid phase forming element in powder metallurgy [3], where boron additions are around 1%.

Boron additions substantially modify the mechanical properties of carbon steels, increasing their tensile strength (it doubles when passing from 1% to 3%B) and reducing their deformation capability [2]. Higher boron amounts (10%-wt) and manual mixing of elemental powders produce, after sintering, very brittle materials that can not be used in this kind of applications [4].

In this work, the objective is to carry out the mechanical alloying of iron powders with 50%-wt boron, for their ulterior application. However, there are other procedures to obtain Fe-B solid solution [5, 6, 7], depending on the way of boron mixing. Mechanical alloying allows maximum boron contents $Fe_{60}B_{40}$ [5] and $Fe_{50}B_{50}$ [7].

Raw material powders used are as follows: ASC300 atomised iron powder with 99,9% purity, from Höganäs (Sweden), with particle size less than 45 ☐m, for mechanical alloying process; amorphous boron from Strem Chemicals, with 92-95% purity (magnesium impurities); natural graphite, with particle size less than 50 ☐m; atomised iron powder ASC100.29 used to dilute

Fe-B(50%), 99,9% purity, from Höganäs (Sweden), with particle size less than 150 µm.

Using mechanical alloying, this work tries to form a Fe-B amorphous phase, that can be diluted in iron to manufacture a steel with 10%-wt boron, possibly with an iron matrix and a Fe/B solid solution, so mechanical properties are improved.

So that, the powder mix Fe/B+1% C is introduced in a high energy mill, with a charge/balls ratio of 15:1 at 700 rpm, for 36 h using an inert atmosphere. Samples were taken each 6 h, characterizing the powder through differential thermal analysis (DTA) up to 1400 °C in inert atmosphere, X-ray diffraction and scanning electron microscopy (SEM).

As can be appreciated in the X-ray diffraction patterns (figure 1), after 36 h milling, peaks do not correspond to iron, and the peaks corresponding to borides are found. So that, this powder milled for 36h was chosen for the next step of the research, being labelled as Fe/B (50%).

This powder was diluted with more iron (ASC100.29), to get a steel with 10% boron. This material was named A. This mix is uniaxially compacted at 500 MPa. In order to compare results, a mix of Fe/B (50%) without milling (0 h) was also diluted with iron to get the same composition and compacted in the same conditions. This material was named B. Green density was evaluated. Then, materials were sintered in argon at 1150°C and physical (sintering density) and mechanical properties (hardness and bending strength) were measured. Finally, a microstructural study and fracture analysis were carried out.
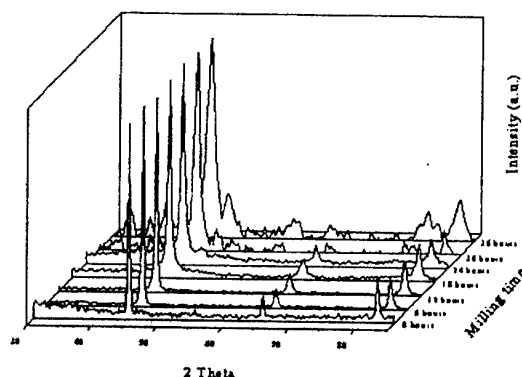
Figure 1. Normalised X-ray diffraction of Fe/B (50wt%) + 1%C powders obtained each 6 h of milling.

Table 1. Physical and mechanical properties of studied materials. A and B materials are explained in the text.

Material	Relative density (%) green	Relative density (%) sintering	Hardness (HRA)	Bending strength (MPa)
A	61	65	XX	82
B	68	76	64	128

Materials obtained with this Fe/B(50wt%) powder (milled for 36h) present higher green density. For example, B material (from not mechanically alloyed powders) has a relative density of 60%, while the same material (A) using 36 h milling powder has a 67% density. Once sintered, this material also improve their properties (table 1).

In conclusion, more research has to be developed in this field in order to obtain more adequate results, although this line seems to be very promising.

REFERENCES

[1] H.C. Cowen. Boron and boron-containing materials. Nuclear engineering. 1 (1959) 11-17

[2] M.Lopez Rodríguez, F.Pascual Martinez. Materiales Nucleares Tomo 1. Publicaciones científicas de la junta de Energía Nuclear, (1971).

[3] D.S. Madan, R.M. German, W.B. James. Iron-boron enhanced sintering. Progress in powder metallurgy. Vol.42 (1986) 19.

[4] J. Abenojar; F. Velasco; M.A. Martínez. Microstructural analysis and X-ray diffraction of Fe-10%B (wt.) system and carbon addition influence. AMPT'01 International Conference on Advances in Materials and Processing Technologies. (2001) 1313-1319.

[5] Ratnesh Gupta, Ajay Gupta. Mechanical alloying of Fe-B powders. Materials Science and Engineering A. 304-306 (2001) 442-445.

[6] Pekka Ruuskanen, Oleg Heczko. Formation of amorphous $Fe_{1-x}B_x$ alloys during solid state alloying with hexane. Journal of Non-Crystalline Solids. 224 (1998) 36-42.

[7] Toshio Nasu, Masaki Sakurai, Kenji Suzuki, Carl C.Koch, Ann M.Edwards, Dale E.Sayers. Structural changes in Fe-B powder mixture during amorphization process by mechanical alloying. Materials Transactions, JIM. 36-8 (1995) 1088-1090.

KINETIC LAWS OF METALLIC COMPOSITES DESTRUCTION

Bobonazarov Kh.
Khujand scientific center of Tajik Academy of sciences, Khujand, Tajikistan

It is settled that destruction of soled bodies is a kinetic thermofluctuatioanal process. Such an understanding was, first of all, formulated on the basis of study and analysis of their durability dependence (τ) from the tension (σ) and temperature (T) [1]. Such dependence is described by the equation

$$\tau = \tau_0 \exp \left[(U_0 - \gamma \sigma) / \kappa T \right], \quad (1)$$

in which τ_0 is identical for all bodies and $\approx 10^{-13}$c, and U_o is a structurally insensitive constant of a material which characterizes the energy of stirring up an elementary act of its destruction process; parameter γ depends on the structural condition of the material and it represents an indicator of a local tension level; k is a Bolzman constant.

Thus, a study of temperature – force dependence of durability and analysis of parameters of this dependence (especially U_o and γ) allows to obtain information about the mechanism of destruction and intensively of its development.

This paper deals with the results of analysis of durability of fibrous, flaky and dispersal strengthened metallic composites.

These materials now acquire the important value by way of their application in details and constructions working in extreme conditions in particular at high and low temperatures, effects of the different exterior factors and so on.

Undirected fibrous composites Cu-W and Al (Am$_r$ 61) – B were respectively obtained by a diffusion welding and a plastic sprinkling. The value of W was changing from 4 to 26 %, but the value of B constituted 20 %. The orientation angle of fibers y for Cu-12%W was from 0^0 to 26^0, but for Al-B was from 0^0 to 90^0. Flaky composites Al-Ni and Al-Cu were prepared by electro besieging Ni and Cu. The value f Ni constituted 11 and 35 %, but the value of Cu changed from 15 to 60 %.

Industrial flaky and dispersal strengthened composites Al-Ni-Al, and САП-1, САП-2 (baked aluminum powders) were prepared by a cool rolling and contained respectively 82 % Ni, ≈ 8 % and ≈ 11 % of Al$_2$O$_3$ particles.

On the basis of a systematic research of temperature – temporal laws of destruction of the above mentioned composites the following results were received.

1.   There is temporal dependence of society for all materials studied by us. This dependence in definite interval σ, T depends on the equation (1)

2.   By the change of volumetrically content of tungsten the value of U_0 energy discretely (by leaps) from the value ≈ 335 kJ | mol, which is typical of the copper, till the value ≈ 900 kJ | mol which is typical of tungsten. The achieved values U_o coincide well with the values of sublimation warmth accordingly Cu and W. As the analysis shows the energy leap is connected with the equality condition of leads in the matrix and filler. The conducted value showed that with regard for the equation (1) the energy leap takes place with the value of volumetrically quota of tungsten (v*) which is defined by the formula

$$V^* = [\gamma_w (U_o^{Cu} - C)] / [\gamma_{cu}(U_o^w - C) + \gamma_w(U_o^{Cu} - C)] \quad (2)$$

in which U_o^{Cu} and U_o^w is an activation energy of copper destruction and tungsten, γ_w and γ_{Cu} is a value of structural sensitive coefficient of tungsten and copper; $C = kT \ln(\tau|\tau_0)$.

Calculation with the formula (2) gave the value V*=5±1% which agrees well with the experimental data. By the change of y about the wasp of tension the value U_o also changes by leap from its value for fibre till its value for a matrix. Perhaps , it is connected with the fact that the extension of the angle y causes the diminution of volumetrically quota of fibres bearing loads. For de composite Cu – 12 % w this leap (from ≈ 900 LM ≈ 335 to kJ / mol) takes place in the interval of angles 8 – 14 % , but for the composite Al - 20% B this leap (from ≈ 550 till ≈ 220 to kJ / mol) takes place in the interval of angles 0 –5% dependents from the angle of φ showed a that for de composite Al + 20% B the value y grows linearly with the growth φ, but for the composite Cu – 12 % w with the transitional critical angle it diminishes by leap and then in grows again. The

achieved data permit us to conclude that filler the durability is limited by a dislocational mechanism of destruction increase in the filler. A study of temperature – power dependence of durability and an analysis of activation energy U_o of flaky composites showed that the value U_o by the change of volumetrical quota of components also changes by leap from the value which is typical of matrixes material (Al) till the value which is typical of the filler (Ni, Cu), in this case the value of critical quota of filler (V*) calculated with the formula (2) agrees well with its experimental value. By $V<V^*$ the value U_o is typical of a sublimationonal mechanism of destruction and by $V>V^*$ agrees with the energy of self diffusion of electro besieged Ni and Cu respectively.

Consequently, galvanic besieged metals are destructed by a diffusional mechanism that represents natural with due regard for the specificity of their structural state (initial porosity and concentration of vacancies formed in the case of creepiness [2]) Research off dispersal consolidated composites (fusion) САП-1 and САП-2 after a cool rolling and annealing with $T \geq 350°$ showed that the value of activation energy U_o takes two discrete values. Under a cold rolled state the value $U_o \approx 150$ to kJ|mol and after a four hour annealing at the $T \geq 350°C$ $U_o \approx 220$ kJ|mol which respectively coincide well with the energy of self diffusion and sublimation of aluminum.

Thus, it can be stated that the durability of dispersedly strengthened composites is limited by the development of destruction by a vacancy or dislocational mechanism in the material of matrix. High porously and concentration of unbalanced vacancies in reveled powder composites, probably, cause a vacancies mechanism of their destruction; after the annealing of the vacant volume, which, probably, leads to the formation of a stable substructure [2], the development of the cracks is realized by a dislocational mechanism.

Literature:

1. Regel V.P., Slutsker A.I., Tomashevsky A.E. Kinetic nature fern of body's solidity – L, "Nauka", 1974, - 486p. (in Russian).
2. Leksovsky A.M. Kinetics of composite materials destruction. Doc. dess L, Ph t,1, 1983- 396p. (in Russian).

INFLUENCE OF THE STRUCTURAL STATE ON MECHANICAL BEHAVIOR OF TIN BABBIT

Sadykov F.A., Barykin N.P., Valeev I.Sh.

Institute for Metals Superplasticity Problems, Russian Academy of Sciences, Ufa, Russia

The tin babbit (Sb – 10 - 12 wt. %, Cu – 5 - 6 wt. %, Sn – rest) is widely used for producing bushes of steam turbine sliding bearings. Service properties of babbit considerably depend on its chemical composition and structural state [1-2]. Small ductility (~ 6 % elongation) is one of drawbacks of the tin babbit that negatively influences service properties of the alloy. Treatment of a material causes its structural changes and affects physical and mechanical properties.

The present paper deals with investigations of the structure and the influence of a structural state on mechanical properties of the tin babbit.

Babbit of the chemical composition (Sb – 10 - 12 wt. %, Cu – 5 - 6 wt. %, Sn – rest) was selected as an object of investigations. For forming different structural states the cast babbit was cooled at different velocities. The obtained β - phase crystallite size was 50, 100 and 250 μm. Moreover, for obtaining the structure of babbit with a β - phase grain size of 30 μm some specimens were subjected to rolling at room temperature.
The results of mechanical tests of specimens in various structural states are shown in Fig. 1.
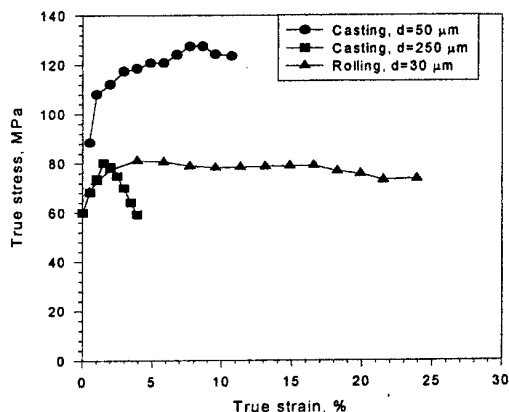
Fig. 1. Curves "true stress - true strain" of babbit at different structural states at strain rate of 10^{-3} c^{-1}.

There is a noticeable dependence of the flow stress on the grain size of β - phase. The decrease in the β - phase grain size from 250 to 50 μm for the cast alloy increases ductility and flow stress. For example, relative elongation increases from 5 to 12 %, respectively. Moreover, rolling results in a significant increase in ductility of the alloy as compared to the cast state. In particular, elongation of the rolled specimens was increased up to 26 % and flow stress was decreased by 50 - 60 % as compared to the cast specimens with a β-phase grain size of 50 μm.

The data on the strain rate sensitivity coefficient m shows that for the cast alloy it depends on a strain rate and is 0.01 - 0.03 and 0.14 - 0.17 for a β - phase grain size of 50, 250 and 100 μm, respectively. However, the alloy subjected to rolling displays rather high strain rate sensitivity, namely m values vary from 0.07 to 0.31 with decreasing the strain rate from 10^{-2} to 10^{-4} s^{-1}.

For explaining the influence of the structural state of babbit on its rheological behavior let us consider structural changes occurring during deformation of the alloy.

For more precise definition of the alloy's composition and phase constituents the X - ray structure analysis of the alloy has been carried out.

On the basis of full-scale investigations it has been ascertained that cast high-tin Sn – Sb - Cu babbit consists of three phases: α – phase being solid antimony and copper solution in tin with a submicrocrystalline grain size of 0.5 - 1 μm; β – phase consisting of SnSb crystals and a small phase being η – phase (Cu_6Sn_5).

It is known that β – phase belongs to a cubic syngony [3, 4]. The obtained experimental data shows that β - phase of such babbit, obviously, has a hexagonal lattice.

Investigations of the deformation relief of the alloy were carried out after tension of specimens. There are many cracks on the surface of the cast alloy with a β - phase grain size of 250 μm. The cracks mainly initiate on matrix- β - phase crystal. The inspection of the deformation relief of the cast babbit with a β - phase grain size of 50 μm shows that the number of cracks is less than in the previous case. As for the rolled alloy the inspection of its deformation surface shows that cracks are observed only in rare areas of specimen's surface.

The fracture study of broken surfaces was made by means of an electron microscopy. The analysis indicates that there occur fragile fracture of β - and η - phases and viscous fracture of main α - phase. The low ductility of babbit is apparently conditioned by brittleness of β - phase which due to hexagonal lattice has a limited number of slip planes at plastic deformation.

The X - ray diffraction investigation shows a decrease in a width of peaks of X - ray lines of the rolled babbit as compared to the cast babbit. This explains softening and, perhaps, recrystallization of the α - phase of the alloy after rolling.

In general, ductility and other mechanical properties depend on α - and β - phases, since the amount of η - phase is small. When the size of α - phase is similar in different alloys (cast alloys with grain size of 50, 100 and 250 μm) the β - phase effect ductile and other mechanical properties of the alloy as a whole. The increase in β - phase grain size leads to the decrease in elongation of the alloy. After rolling, the recrystallization of α - phase occurs and ductility controls by both of α - and β - phases.

A significant distinction in deformation behavior of the cast alloy from the rolled alloy can evidently be explained by processes of breaking of cast structure basis, recovery and recrystallization of alloy phases after rolling that decreases significantly flow stresses and increase ductility.

[1]. M.M. Khrushchev, *Fatigue of babbit* (in Russian), USSR Academy of Sciences, Moscow, 1943, p 143.

[2]. M.V. Zernin and A.V. Yakovlev, On the investigation of fatigue durability of highly loaded sliding bearings babbit layer (in Russian), *Plant laboratory,* 1997, No.

[3]. Y.M. Lakhtin. Metals Science and heat treating of metals (in Russian). Metallurgia, Moscow, 1976, p. 407

[4]. A.P. Smirygin, N.A.Smirygina, A.V. Belova. Commercial metals and alloys (in Russian). Metallurgiya, Moscow, 1974, p. 483.

THE PROPERTIES OF PIEZOCERAMIC MATERIALS AND PLASMA COVERAGES ON TITAN AND CHROME CARBIDES BASE, ALLOYED BY ZIRCONIUM INTERMETALLIC HYDRIDES UNDER THE CONDITIONS OF EXPLOITATION

Dubrovskaya G.N., **Gubar E.Y.**, **Butenko T.I.**, **Okatova T.P.** [(1)], **Sharapov V.M.**

Cherkassy state technological university, Ukraine

[(1)]Concern of powder metallurgy, Minsk, Byelorus

The aim of this work is the processing of experimental results on change of the properties of the coverages ПГ-CP4 and TiC-Cr$_3$C$_2$-NiCr, alloyed by hafnium and zirconium, and also piezoceramic ZTL-19 and ZTL-83 under the conditions of exploitation.

The titan and chrome carbides powders were produced by method of self-propagating high-temperature synthesis in Byelorussian Concern of powder metallurgy. Powder ПГ-CP4 - (ТУ 14-1-3785-84) was made at the Torez plant, fraction particles' dimension being equal 40-60 mkm. Piezoceramic was made in the laboratories of CSTU and Chernigov technological institute by method of diffusive welding in smouldering digit [1, 2, 3].

The study of microstructure of initial individual powders and obtained coverages allowed to characterize the dimension, form and distribution of phases in elementary stage of process of plasma spraying and after experiments under the conditions of working cauldron БКЗ 220 (Cherkassy ТЭЦ).

For the research of microstructure, elementary and phase composition of materials the methods with such devices as X-ray diffractometer ДРОН-2, microhardmeter ПМТ-3, power-mass-analyzer laser ЭМАЛ-2 were used.

The study of peculiarities of the process and the speed of the diffusion of coverage elements Cr-B-Si-Fe-Zr(Hf) and TiC-Cr$_3$C$_2$-NiCr-Zr(Hf) on the base of 12Х1МФ steel, the determination of phase composition of transitional contact zones allow to make conclusion about their chemical and mechanical compatibility under the conditions of exploitation.

Change of the adgesive strengths indicates weak eonnection matrix-coverage. For the increasing of strength on grains boundaries of refractory Me-oxidery coverage on the base Cr-B-Si-Fe and the regulation of grain and coverage density the addition of Hf and Zr in amounts from 3 to 20% were brought

During exploitation under high temperatures in the air the "self-healing" of pores and microcracks in coverage takes place for account of liquid phase in case ПГ-CP and HfO$_2$-ZrO$_2$-TiO$_2$-Cr$_2$O$_3$ is formed in case carbid-Ni-In this case the dimension, form and distribution of the basic carbide constituent is preserved in the microstructure. A complicated glass crystalline matrix B-Si-Fe with isolated chrome carbides is made in ПГ-CP the carbides are isolated in the continuous hard solution Ni-Cr of matrix in the system TiC-Cr$_3$C$_2$-NiCr.

The distribution volume of all phases is researched and concentration gradients Ni, Cr in separate grains and phases are defined.

The changes in the material structure take place during exploitation (under the oxidation). Firstly the formation of unstoichiometric composition of phases of oxycarbides takes place. The restoration process products in complicated system depend on temperature and are the result of diverse combinations. The stable and instable phases are exposed under the temperature of oxidation 200-1000^{0}C. The metastable oxycarbides are formed under 200^0 C, and the oxides of complicated composition are formed under 1000^0 C is.

The second part of the work deals with the research of piezoceramics.

The results of the mass-spectrometric analysis of piezoceramic are given in the table.

305

Table

Elementary composition of piezoceramics ZTL-83 and ZTL-19

Piezoceramics	Maintenance of elements, mass%							
	O	Si	Ti	Fe	Sr	Zr	Nb	Pb
ZTL-19	4,17	1,07	16,75	0,45	10,9	37,5	4,37	17,47
ZTL-83	0,02	-	18,12	-	12,25	34,8	0,79	33,86
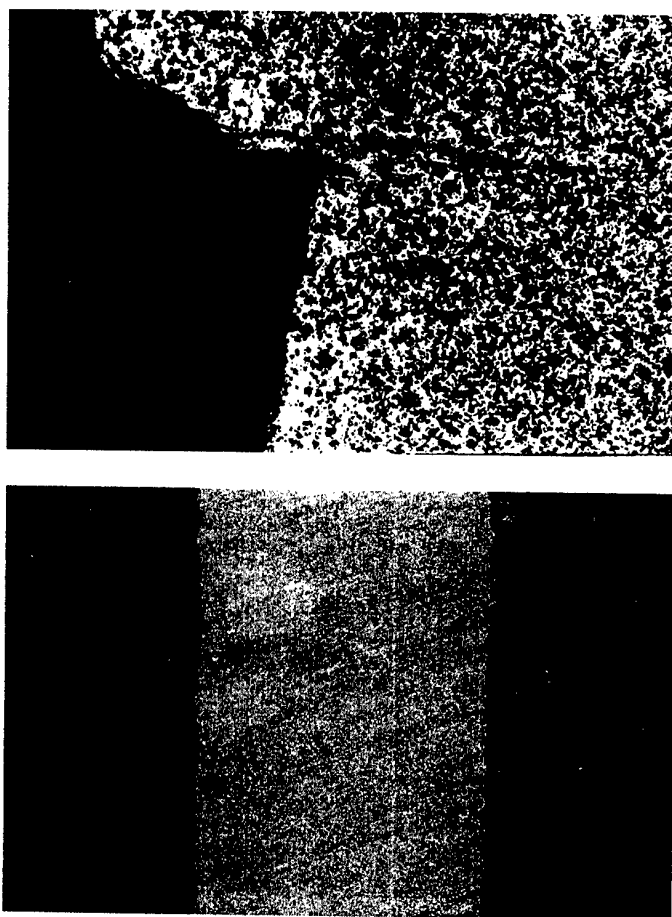
Pic. Electronically-microscopic photos of the surface of piezoceramics .

Literature

1. Патент Украины 30706 А "Материал для плазменного напыления покрытий", авторы –Дубровская Г.Н., Быков В.И., Губарь Е.Я., Частоколенко И.П.. Шматков В.Ю.

2. Патент Украины 43964 А "Пьезокерамический преобразователь механических величин", авторы –Шарапов В.М., Лега Ю.Г., Мусиенко М.П. и др.

3. З.Дубровская Г.Н., Божко Н.И., Котельников Д.И. Локальный анализ на РЭМ-100У формирования переходных слоев в композиционном материале пьезокерамика-медь // XII российский симпозиум по растровой электронной микроскопии и аналитическим методам исследования твердых тел, Черноголовка, 2001, с.45.

INVESTIGATION INTO THERMAL DEFORMATION AND STRENGTH OF CARBON-CARBON COMPOSITE MATERIALS AT HIGH TEMPERATURES

Gracheva L.I.

Institute for Problems of Strength, National Academy of Sciences of Ukraine, Kiev, Ukraine

The reliability and serviceability of structures operating under conditions of ultimate force and heat loads are mainly determined by the strength of materials for which successfully employed are polymeric matrix and carbon matrix composites.

In order to determine most reliably the strength of real heat-resistant coatings whose time of heating to temperatures above 1000°C is estimated in minutes, the consideration of the material heating rate and change in the chemical composition and pressure of the structure gaseous environment is of the great importance in the experimental investigation of the physicomechanical properties.

The goal of the present investigation is to determine the deformation and strength of thick-walled composite shells from carbon composites depending on the type of their binder and orientation of the carbon filler during heating under conditions simulating the actual ones.

Specific character of the changes in the physicomechanical properties of composites at high temperatures imposes essential restrictions on the use of the standard test facilities. In this connection, the unique procedures were developed and a setup was created. Which enable one to determine the regularities of deformation and change in the strength of composites including those which destroy on heating at temperatures to 3000°C.

The investigation of temperature strains of composites including the distracting ones was performed along three mutually orthogonal axes simultaneously using a three-coordinate optoelectronic dilatometer.

A dilatometer-type DKM-3 created at the Institute for Problems of Strength enables one to measure volume thermal strains of specimens and structural elements of an arbitrary shape along three axes of anisotropy simultaneously in the temperature range from 0 to 1700°C in air or neutral atmosphere and in vacuum without breaking the continuity of the material and structure.

A running record of thermal strains for the specimens from composites was made by an electronic recorder in the coordinates $\Delta l - T$ for each of the three directions or in the form of the tape digital printing; the difference in time of the Δl records along three axes did not exceed 0.01 s.

The strength characteristics of the composites were determined using a high-temperature setup-type KM-10 built around a standard general-purpose testing machine and equipped with a heating system, a system for creating vacuum and inert atmosphere, and a load/strain recording system.

A characteristic feature of the sealed water-cooled thermal chamber developed is its possible application for all the types of static tests involving displacement of the moving crossbar in the direction ease manipulations on the replacement of the internal tooling (block heads, grippers, etc.). heating was conducted by the radiation method which excluded the action of electromagnetic fields on the specimen; the gaseous atmosphere of the tests was varied depending on the experiment requirements.

The materials investigated were carbon-carbon composites. Heating was carried out to the preset temperature at the rate of 100°C/min in a neutral gaseous atmosphere (argon).

The relative strain was computed from the $\varepsilon = \dfrac{\Delta l}{l_0}$ where Δl is the variation in the specimen length and l_0 is the initial length.

The temperature dependences of the thermal strain for carbon composite with a simultaneous change in linear strains along three mutually orthogonal coordinates are shown in Figure 1.

In this case, the specimens were cut from the sheath fragments rather than specially manufactured plates, and the direction of the specimen faces did not correspond to the anisotropy axes of the carbon composite. The angle between the specimen face and the direction of the measuring axes, (φ, varied from 3° to 9°.

Investigated were, in fact, the fragments of heat-protective structures with a sufficiently arbitrary spatial orientation rather than the specimens.
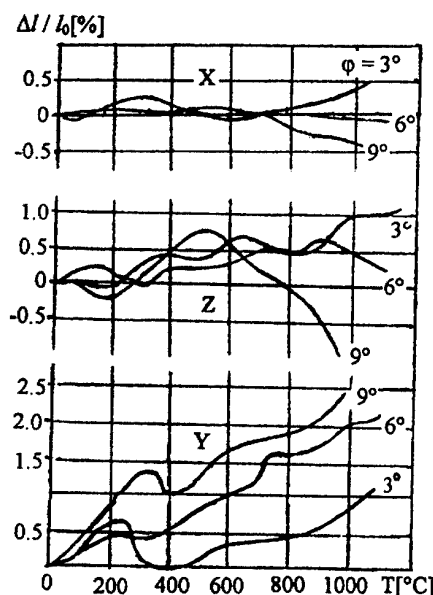
Fig. 1. Carbon composite thermal strain as a function of temperature for different angles of winding the carbon filler fabric in the X, Y, Z - directions.

Measurements of the specimen thermal strains during heating were made simultaneously for each of the axes of anisotropy of the material in the coordinates Δl (displacement) vs T (temperature) by an optoelectronic automatic system.

To determine the mechanical characteristics using the KM-10 setup, specimens were heated to the required temperature, held for one minute and loaded at the strain rate of 2 mm/min.

The main mechanical characteristics were obtained from stress-strain diagrams $P - \Delta l$, which took into account the compliance of all the elements of the testing machine power circuit, including strikers, over the entire temperature range.

The modulus of elasticity, E, was determined as the slope of the linear portion of the σ - vs - ε diagram.

All the diagrams were obtained in the two mutually-orthogonal directions in the plane of reinforcing at a heating rate of $100\,°C$ /min.

Figure 2 shows the variation in the strength characteristics of the carbon matrix composite with heating. In the temperature range from 20 to 3000°C, the curves of the modulus of elasticity, E,

has a clearly defined peak near T = 1000°C, a region of stability in the temperature range from 1500 to 2000°C and a sharp drop in its magnitude down to 10% from the initial value at T = 3000°C.

The ultimate strength, σ_u, also decreases in the temperature range T = 0 to $500\,°C$, its variation curve has a portion which is nearly stable in the temperature range T = 500 to $1500\,°C$, the sharp spike at T = $2000\,°C$ and the value drop (a dotted line on curve 2) when fracture does not occur with increasing strain, and the material transits completely to the plastic zone.
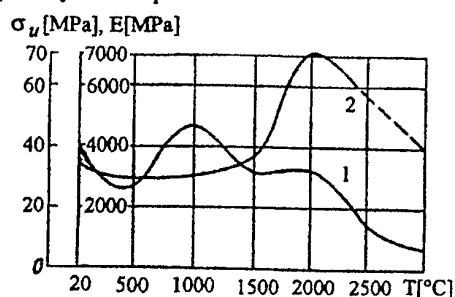
Fig. 2. Temperature dependence of the modulus of elasticity, E, (1) and ultimate strength, σ_u, (2) for the carbon fiber composite in compression.

A comprehensive experimental and theoretical investigation has been carried out on the influence of the thermal deformation character on the stress state of the shell-type structural elements made from high-temperature composites. As a result of the experimental study on the carbon/carbon composites with their heating at a rate of 100°C/min in a neutral atmosphere, it has been found that:

- thermal deformation of a carbon carbon composite in the temperature range from 20 to 1200°C in three orthogonal directions is characterized by a strong dependence on the angle of winding of the carbon filler,
- moduli of elasticity and ultimate strengths of the carbon matrix composites in the temperature range from 20 to 3000°C have a more pronounced nonlinear character; here, the highest value of the modulus of elasticity, E, were obtained at temperatures T = 1000°C, whereas those of the ultimate strength, σ_u, at 2000°C.

THERMAL STRESSES IN HEAT-PROOF SHELLS FROM CARBON-CARBON COMPOSITES IN CHANGING THE FILLER WINDING ANGLE

Gracheva L.I., Borisenko V.A.
Institute for Problems of Strength, National Academy of Sciences of Ukraine, Kiev, Ukraine

This paper presents the investigation of the strength of the shell-type structure for heat protective coatings. The problem of the stress-strain state of structural elements from anisotropic composites has been solved taking into account the distribution of the physicomechanical characteristics obtained with the use of the unique equipment which enables one to simulate the actual operating conditions of the object under study. The data obtained have made it possible to determine the stress state of the constructive shell elements depending on the matrix and orientation of the carbon heat protective coatings in the temperature range from 20 to 1500° C. The calculations performed show that the normal stresses in the cylindrical thermal-protective shell from carbon-carbon materials grow with an increase in the value of the winding angle φ.

Solution to the given problem is built through rational combination of analytical transformations in the initial equations of elasticity theory and the numerical analysis method.

As initial equations of the three-dimensional equations of the elasticity theory in the curvilinear system of coordinates α,β,γ are taken. There is one plane of elastic symmetry tangent to each point of body surface γ = const or perpendicular to the axis of rotation α = const. The generalized Hook law for the i-th layer ? $\gamma_i \leq \gamma \leq \gamma_{i+1}$, i $=1,...,N)$ has the form

$$\bar{e}^i = B^i \bar{\sigma}^i + \bar{f}^i, \bar{e}^i = \{e^i_\alpha, e^i_\beta, e^i_\gamma, e^i_{\alpha\beta}, e^i_{\alpha\gamma}, e^i_{\beta\gamma}\}$$

$$\bar{\sigma}^i = \{\sigma^i_\alpha, \sigma^i_\beta, \sigma^i_\gamma, \tau^i_{\alpha\beta}, \tau^i_{\alpha\gamma}, \tau^i_{\beta\gamma}\} \quad (1)$$

$$B^i = \|b^i_{lp}(i)\|, \quad l, p = 1,2,...,6$$

Here, $e^i_\alpha, e^i_\beta, e^i_\gamma, e^i_{\alpha\beta}, e^i_{\alpha\gamma}, e^i_{\beta\gamma}$ are the strain tensor components, $\sigma^i_\alpha, \sigma^i_\beta, \sigma^i_\gamma, \tau^i_{\alpha\beta}, \tau^i_{\alpha\gamma}, \tau^i_{\beta\gamma}$ are the stress tensor components. The coefficients of linear thermal expansion and the coefficients of shear may be set in the form

$$\hat{\alpha}^i = \alpha^i_\alpha \cos^2\varphi + \alpha^i_\beta \sin^2\varphi \quad (2)$$

$$\hat{\alpha}^i_\beta = \alpha^i_\alpha \sin^2\varphi + \alpha^i_\beta \cos^2\varphi$$

$$\hat{\alpha}^i_\alpha \quad \beta = 2(\alpha^i_\alpha - \alpha^i_\beta)\sin\varphi\cos\varphi$$

$$\hat{\alpha}^i_\gamma = \alpha^i_\gamma, \hat{\alpha}^i_{\alpha\gamma} = \hat{\alpha}^i_{\beta\gamma} = 0$$

where φ the angle of inclination to the axis β.

Equations (1) are also valid for orthotropic bodies with principal directions of elasticity are turned about the normal to the surface γ = const or α = const through the angle φ.

The temperature field for the i-th layer of the multilayer hollow body is defined by the equation of heat conductivity.

$$K^i_\alpha \frac{\partial}{\partial\alpha}\left(\frac{H_2 H_3}{H_1}\frac{\partial T}{\partial\alpha}\right) + K^i_\beta \frac{\partial}{\partial\beta}\left(\frac{H_1 H_3}{H_2}\frac{\partial T}{\partial\beta}\right) + K^i_\gamma \frac{\partial}{\partial\gamma}\left(\frac{H_1 H_2}{H_3}\frac{\partial T}{\partial\gamma}\right) = 0 \quad (3)$$

where $K^i_\alpha = K^i_\alpha(\gamma), K^i_\beta = K^i_\beta(\gamma), K^i_\gamma = K^i_\gamma(\gamma)$ are the coefficients of heat conductivity acting in the directions α,β,γ. It is assumed that thermal continuity conditions of layers over the entire surface of contact are fulfilled

$$T^i = T^{i+1}, K^i_\gamma \frac{\partial T^i}{\partial\gamma} = K^{i+1}_\gamma \frac{\partial T^{i+1}}{\partial\gamma} \quad (4)$$

Then conditions on the limiting surfaces $\gamma = \gamma_0, \gamma = \gamma_N$ may be set as follows: temperature of surface T^i, flow of heat $K_\gamma \frac{\partial T}{\partial\gamma}$; conditions of the ideal thermal of surface $\frac{\partial T}{\partial\gamma} = 0$; conditions of conventional heat exchange $K_\gamma \frac{\partial T}{\partial\gamma} = p[T_0 - T(\alpha\beta)]$, where p is the coefficient of heat exchange, T_0 is the temperature of the surrounding environment.

Taking into account the equilibrium equations, the strain-displacement relations, the Hook law for a non-homogeneous anisotropic body Eq.(1) and the equation of heat conductivity Eq.(5), the system of partial differential equations describing the thermo-stressed state of laminated hollow elastic bodies is received.

$$\frac{\partial\bar{\sigma}^i}{\partial\gamma} = B^i_0 \bar{\sigma}^i + B^i_1 \frac{\partial\bar{\sigma}^i}{\partial\alpha} + B^i_2 \frac{\partial\bar{\sigma}^i}{\partial\beta} + B^i_3 \frac{\partial^2\bar{\sigma}^i}{\partial\alpha^2} + B^i_4 \frac{\partial^2\bar{\sigma}^i}{\partial\alpha\partial\beta} + B^i_5 \frac{\partial^2\bar{\sigma}^i}{\partial\beta^2}$$

$$\bar{\sigma}^i = \{\sigma^i_\gamma, \tau^i_{\alpha\gamma}, \tau^i_{\beta\gamma}, u^i_\gamma, u^i_\alpha, u^i_\beta, T^i, T^i\} \quad (5)$$

$$B^i_p = \|b^i_{mq,p}(\gamma)\| \quad (m,q =,2,.........,8, \quad p = 0,1,.....5)$$

$$\alpha_0 \leq \alpha \leq \alpha_n; 0 \leq \beta \leq 2\pi; \quad \gamma_{i-1} \leq \gamma \leq \gamma_i; \quad i = 1,2,...,N)$$

309

where $T^{bi} = K^i_\gamma \dfrac{\partial T^i}{\partial \gamma}$.

Here, the resolving functions are taken as the basic ones with the help of which we can formulate the conditions for the limiting surfaces $\gamma = \gamma_0$, $\gamma = \gamma_N$ and for the surfaces of layers conjugation $\gamma = \gamma_i$. Presentation of all factors of the thermo-stressed state in double rows with orthogonal trigonometric and special functions for some types of boundary conditions on the surfaces $\alpha = \text{const}$, $\beta = \text{const}$ allows strict separation of the variables in Eq. (5) and for each i layer to receive a system of 8 ordinary differential equations with variable coefficients. This system is solved with the stable numerical method that makes it possible to solve one-dimensional problems with the required accuracy level.
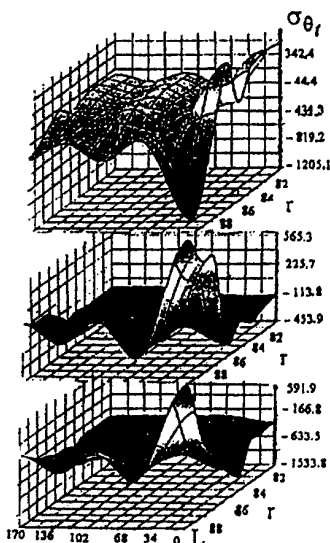
Fig. 1. Distribution of normal stresses σ_θ over the length and thickness of the cylinder depending on the change of the winding angle.

Calculation of the thermal stress states of heat-protective coatings from carbon composites (Fig. 1) was made for a cylinder of length L = 340 mm, midsurface radius R = 90 mm, thickness δ = 10 mm. The mechanical and thermal characteristics α, E and G of the materials were determined experimentally for the conditions which simulate the actual ones, namely, variation of the heating rates, the composition and the pressure of the gaseous atmosphere, the anisotropy of materials taking into account the direction of the filler fiber orientation.

Some of the computational results are presented in

the form of plots of fields of normal stresses σ_θ along the length and thickness of the cylinder made from carbon composite.

Thermal stresses are generated in the bulk of the cylindrical shell as a result of the thermal loading during heating without any external forces applied. As an example, Fig. 2 presents the variation of the minimum and maximum values of normal thermal stresses $\sigma_{\theta(r)}$ depending on the changes in the filler winding angle φ in heating from 20 to 1200°C. It can be seen that with an increase in the angle φ in the extreme on the stress curves also increase their magnitudes both under tension and compression.
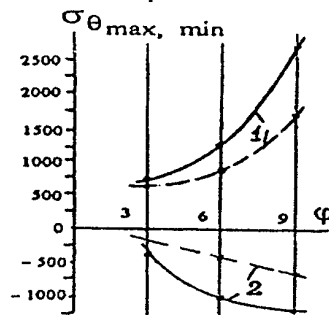
Fig. 2. Dependence of the maximum and minimum values $\sigma_{\theta(r)}$ on the angle of the filler winding φ (– in the zone of tension, – in the zone of compression), 1 – max, 2 – min.

Analysis of normal thermal stresses acting through the thickness and along the length of a cylindrical shell with the angle φ varying from 3° to 9° in the temperature range from 20 to 1200°C revealed that:

- the maximum values of σ_z and σ_θ increase: σ_z in the tension zone 2.5 times, σ_θ 4 times; σ_z in the compression zone 4 times, σ_θ 3 times.
- the maximum values of $\sigma_z(r)$ are 6 times higher than those of $\sigma_z(r)$ in the tension zone and 5 times in the compression zone;
- the zone of action of the maximum stresses of $\sigma_{\theta(r)}$ is shifted by 38 – 40% towards the outer surface of the cylinder in the zones of both tension and compression.

310

PECULIARITIES OF FORMATION OF THE STRUCTURE OF SOLID ELECTROLYTES WORKING UNDER THERMAL SHOCK

Yakushkina V.S., **Korablyova E.A.**, **D'yachenko O.P.**, **Vikulin V.V.**
Federal State Unitary Enterprise "Obninsk Research and Production Enterprise "TECHNOLOGIYA", Obninsk, Russia

Zirconia solid solutions-based cersmics, having such valuable properties as high temperature of melting, chemical stability in the melts of metals and anion conductivity, is widely used as solid electrolytes for the oxygen concentration sensors for various applications:
- in the systems of electronical adjustment of fuel injection in the automobile engine;
- monitoring of the physical/chemical processes in liquid- metal media;
- measuring of the oxygen content in liquid steel in express-analysis in metallurgy.

The materials (for solid electrolytes) working under thermal loads in liquid-metal media (steel, special alloys, lead, cuprum) must possess high indices of density, anion conductivity, heat resistance which in turn results from the structure and phase composition.

The interconnection between the structure of solid electrolytes made of ceramics (produced from high-activity-, homogeneous, fine-dispersed powders) on the base of zirconia partially stabilized by yttria and magnesia, and heat resistance has been studied. The mechanisms for improving the thermo-mechanical properties by the use of polyphormic transitions and thanks to distinction between the phase linear expansion coefficients are determined. The tests of solid electrolytes as a part of oxygen concentration sensors in the various liquid-metal media have been carried out in production conditions. The graphs of the dependence of the sensor electromotive force on the test time, phase composition and the structure of the ceramics produced are presented.
It is shown that the results of the studies carried out are applied in manufacturing the pilot batch of solid elecrtolytes for the work in production conditions.

INVESTIGATION OF BRITTLENESS OF ANNEALED METALLIC GLASS BY BOTH MICROINDENTATION AND U – METHOD

<u>Ushakov I.V.</u>, Feodorov V.A., Permyakova I.J.
Derzhavin Tambov State University, Tambov, Russia

INTRODUCTION

Fabrication and application of metallic glasses (MG) is of particular scientific and practical interest. The considerable attention focused on MG is motivated by the complex unique properties of these materials [1-3].

One of the negative moments in application of MG exhibits tendency to brittleness accompanying thermal treatment [4, 5]. Thus reception of an information about this question is of great significance.

MATERIALS AND EXPERIMENTAL TECHNIQUE

We studied an 82K3KhSR metallic glass of the composition (wt %) 83.7Co+3.7Fe+3.2Cr+9.4Si in the form of a ribbon 30 μm thick. Prior to experiments, samples (3×10 mm) were annealed in a furnace, in the temperature range of T_{an}=538-1183K and held at a specified temperature for 10 min.

The character of deformation and fracture of the MG were investigated by U – method and by method of microindentation of the MG deposited on a substrate. We tested 15 samples at each temperature for statistics.

In the traditional U – method we estimated the deformation of bend ε at which take place brittle fracture of the MG [2]:

$$\varepsilon=h/(d-h) \qquad (1)$$

where h is the thickness of the sample, d is the distance between two parallel plate of the specific designed measuring instrument at the moment of fracture.

The microindentation of the MG deposited on substrate (composite with microhardness of: 1 ≈ 151 kG/mm^2; 2 ≈ 16 kG/mm^2; 3 < 10 kG/mm^2, thickness of ≈ 1 mm) was carried out on a PMT-3 microhardness gauge.

EXPERIMENTAL RESULTS AND DISCUSSION

a) It is found by U-method:

Dependence of the deformation of bend (Fig. 1)

At the T_{an}<628K the deformation MG proceed on the flatness of sliding. The fracture is not observed, if we bring bend to contact of ends of sample.

It is happened thanks to the plastic deformation, which display in rise of slip bands.
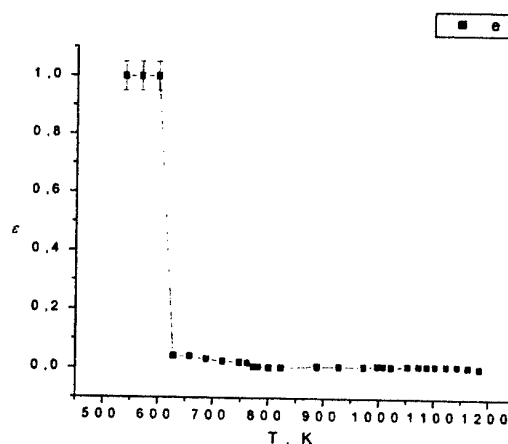
Fig. 1 Influence of thermal treatment on the deformation of fracture ε in the temperature range of T_{an}=538-1183K

The visible loss plasticity starts at a T_{an}≈628K accompanying formation main crack and leading to fracture of sample. The further reduction occurs with beginning crystallization MG. The loss plasticity lead to growth brittleness correspondingly.

At a T_{an}≈823K conform to maximum brittleness connect with transition in a submicrocrystallic state. This temperature coincides with data of differential scanning calorimetry at which runs crystallization MG.

312

b) It is found by method of microindentation:

The critical temperature of annealing at which emerges of cracking formation during indentation. T_c depends for material of substrate. T_c is revealed on elastic substrate better than on the hard ones.

It is estimate that macropictures of destruction and deformation of the metallic glass after indentation depends from properties of used substrate. At the same time, the experimentally established critical temperatures, which correspond to ductile - brittle transition, are near-by for all substrates. At all substrates similar statistical regularities are obtained.

The endurance to cracking is lowered exponentially after exceeding T_c and reaches the minimal value near temperature of crystallisation (Fig. 2)
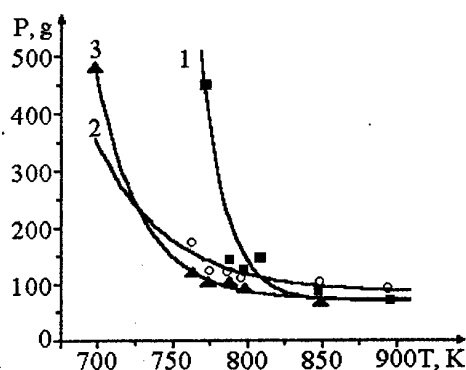
Fig. 2. Dependences of load P upon indentation on the annealing temperature T, for probability of the crack formation $W=0,5$: ■ – substrate № 1, ○ – substrate № 2, ▲ – substrate № 3.
Substrate № 1. $P_0=106,8g \pm 14,8g$; $A=345,2g \pm 29,5g$; $T_0=475$ K; $C=7,2 \pm 2,4$ K.
Substrate № 2. $P_0=84,8g \pm 18,9g$; $A=271,6g \pm 23,7g$; $T_0=673$ K; $C=49 \pm 35,7$ K.
Substrate № 3. $P_0=72,1g \pm 3,9g$; $A=408,8g \pm 6,6g$; $T_0=673$ K; $C=31,3 \pm 1,7$ K [6].

Thus, the brittleness is raised exponentially after exceeding T_c and reaches the maximal value near temperature of crystallisation correspondingly. These results tally with analogous results of U – method.

CONCLUSIONS

A change the brittleness of annealed metallic glass is investigated by traditional U – method and by method of microindentation on polymer substrates. The satisfactory concurrence of data is found. As a result, the data of U - method and data of microindentation may be united and may be used for analysis of structure and mechanical properties of metallic glass. In some case the method of microindentation is alternative method for research mechanical characterristic.

ACKNOWLEDGMENTS

REFERENCES

1   *A. M. Glezer and B. V. Molotilov*, Structure and Mechanical Properties of Amorphous Alloys (Moscow, 1992).

2   *A. V. Likhachev and V. E. Shudegov*, Organization Principles of Amorphouse Structures (St. Petersburg Gos. Univ., St. Petersburg, 1999).

3   *K. Sudzuki, H. Fudzimori, K. Hasimoto* Amorphouse alloys (Metallurgiy, Moscow, 1987)

4   *Sestak J.* // Thermochimica Acta. 1987, Vol. 110, P. 427-436

5   *C. A. Pampillo, D. E. Polk* // Mater. Sci. and Eng. 1978, Vol. 33, No 2, P. 275-280

6   V. A. Feodorov, I. V. Ushakov, Technical Physics. 2001 Vol. 46, No. 6, P. 673-676

INVESTIGATIONS OF RADIATION CHARACTERISTICS OF SPACE VEHICLES EXTERNAL SURFACES

Aksyutenko A., Bass V., Smelaya T.
Institute of Technical Mechanics of National Academy of Science (NAS) and
National Space Agency (NSA), Dniepropetrovsk, Ukraine

The luminescence processes observed in the vicinity of space vehicle (SV) surfaces are one of symptoms of surrounding self-atmosphere action. Physicochemical processes in the surrounding SV self-atmosphere are complicated and multiform. Recently more works appear where metastable NO, NO_2, N_2 and OH radiant particles arising as a result of SV interaction with the multicomponent free stream in upper atmosphere, and first of all with atomic oxygen, are considered as the main factor luminescence. A number of regularities were discovered as a result of great amount of the orbital data processing [1]:

in the vicinity the low-orbital SV surfaces:

- luminescence intensity depends on their temperature, kind of finish material and is proportional to the $\cos\theta_s$, where θ_s is the local angle of attack (the angle between the normal to the surface of the SV and the motion direction of the vehicle);

- continuous luminescence takes place mainly at the visible spectrum diapason with the wave length of $\lambda \sim 6800$ Å and covers the surface area of ~ 20 sm, which corresponds to the life time of NO_2 radiant molecules equal to $\sim 0.6 \div 0.7$ ms;

in the vicinity the high-orbital SV surfaces:

- luminescence intensity, mainly of OH particles, is proportional to the $\cos\theta_s$, but to $\cos^3\theta_s$;

- the thickness of luminous layer in the vicinity of the object riches $\sim 1 \div 10$ m and its brightness increases in the direction of red diapason spectrum.

In the work [2] the results were summarized and presented as the mathematical model of the SV external surface luminescence at altitudes of 100–600 km during the motion along the shady orbit part. By the use of these models the analytical expressions for calculations of spatial distribution radiation power density (indicatrix of dispersion) have been obtained for various configuration of SV. The dependence of spectral density $M_{e,\lambda}$ of SV surface element energetical luminance as a function of angle of incidence was taken as

$$M_{e,\lambda} = M^o_{e,\lambda}(\cos\theta_s)^n,$$

where $M^o_{e,\lambda}$ is the spectral density of SV surface element energetic luminescence when this element is normal to the free stream velocity. The coefficient n is equal to 1 for the low-orbit SV and to 3 for SV moving along the comparatively high-orbits (~ 600 km).

As a result of natural data processing the expressions for $M^o_{e,\lambda}$ as a function of the orbit height h, finish design material, its temperature and wave length λ are obtained in the work [2].

Radiation power $I_{e,\lambda}$ (luminescence) of the flat element is characterized by the expression

$$I_{e,\lambda}(\theta_s, \theta_a) = \frac{M_{e,\lambda} \cdot F}{\pi}\cos\theta_a,$$

where F is a surface element, θ_a is the angle between the normal to the surface of the SV and the direction to observer in the assumption that one is at the infinitely large distance from the SV along the sight ray $\vec{r}_a(\theta_a, \varphi_a)$. Under such assumptions analytical expression for the radiation power of the simple shape SV (spherical, conical and cylindrical) are obtained [3].

Using corresponding quantities of $M^o_{e,\lambda}$ for the given orbit height h, surface material type, its temperature and wave length λ we can determine the dependence of SV radiant force $I_{e,\lambda}$ on the direction of its sight vector $\vec{r}_a$ by the numerical integration of local luminescence characteristics along the SV surface.

The main attention was paid to the development of effective numerical algorithms and realization with their aid of multiparametric investigation of integral characteristics of SV luminescence having complicated geometrical shape taking into account structure elements mutual shading.

The results of radiation normalized power indicatrixes calculations $I_{e,\lambda}(\varphi_{\acute{a}})/I_{e,\lambda}\max(\varphi_{\acute{a}})$ for SV, which configuration is similar to the main block of "Mir" orbital complex and also to one of versions of the main satellite and subsatellite of the experimental space complex "Poperedjennja" planning for realization of complex researches in the upper atmosphere and Earth magnetosphere at altitudes of ~ 600 km [3], are given. It is shown that screening effects introduce the essential contribution to the total indicatrix of dispersion.

These results were used to formulate the requirements concerning the radiation conditions in the neighborhood of spectrophotometric equipment established on these satellites.

Created software has appeared rather effective for solution of the broad circle of satellite photometry problems. As an example a comparison of calculation results for theoretical luster curves R (in stellar quantities) for "Raduga" type SV (curve 1 is for the case without shading, and curve 2 is for the case with shading) with the data of ground observations (wavy curve) made in October 12,1990 for a time period from 19.30 up to 20.05 [4] is shown.

correspond to calculation results without taking shading into account and taking into account SV structure elements mutual shading. The calculated results (curve 2) coincide well with ground observations. During SV motion SP were turned periodically for the corresponding orientation to the sun. It caused SP "oscillation". Panels oscillate with 1^0 amplitude explains well the wavy behavior of the observed luminescence curve.

Capabilities of laboratory modeling by vacuum and aerodynamic unit VAU-2M ITM NAS and NSA of chemiluminescence and ion-molecular responses causing SV luminescence were considered. The unit allows to simulate SV flight conditions at high altitudes ($H > 150$ km). The unit description and its basic characteristics are given in [4,5]. The main responses causing luminescence are chosen to be:

- gas-phase reaction or the reaction of gas with a solid body causing formation of exited particles, f.e. OH;
- molecular dissociation as a result of collisions with object materials and the subsequent recombination of atoms causing formation of electronic-exited and oscillatory-forced states;
- interactions in plasma;
- O and O_2 adsorption on SV surfaces;
- recombination with NO_2 molecules formation radiating in an continuous spectrum;
- reactions causing material ablation from SV surface or change of their structure.

The problems related to practical realization of laboratory experiment are discussed.

Vehicle orientation had following features during this period. The normal to solar panels (SP) was directed to the sun, and the angle between the normal and the direction to the observer varied from 6^0 up to 20^0. In calculations the specular-diffuse scheme of solar stream reflection from SV finish materials, which coefficients were determined as a result of specially carried out experiments, was used. Curves 1, 2 in the Figure

References

1. Garret H. B., e.a. Journal of Spacecraft and Rockets. –1988. –Vol.25. –№ 5. –P. 321–340.
2. Vasilyev V.N., Mishin G.S. Astronautics and Rocket Manufacturing. –1994. –№ 2. –P. 72–78.
3. Bass V.P., Smelaya T., Zabluda S.M. Technical Mechanics. –1998. –№ 8. –P. 19–25.
4. Bass V.P. Technical Mechanics. –2001. – № 2. –P. 52–63.
5. Bass V.P. Space Science and Technology. – 2000. –Vol.6. –№ 4.– P. 57–60.

OPTICAL AND OTHER PROPERTIES OF NEW SUPERHARD CUBIC MATERIAL

Dmitruk N.L.[(1)], Kondratenko O.S.[(1)], Litovchenko V.G.[(1)], Piryatinskii Yu.P.[(2)], Solozhenko V.L.[(3)]

[(1)]Institute for Physics of Semiconductors, National Academy of Sciences of Ukraine, 45 Prospekt Nauki, Kyiv, 03028, Ukraine
[(2)]Institute of Physics, NAS of Ukraine, 46 Prospekt Nauki, Kyiv, Ukraine
[(3)]Institute of Superhard Materials, NAS of Ukraine, 2, Avtozavodskaya st., Kiev, 04074, Ukraine

In additional to diamond and cubic c-BN existent in the B-C-N composition triangle, dense phases of carbonitrides and boron carbonitrides are considered as potential superhard material [1]. Recently cubic BC_2N was synthesized from graphite-like BC_2N at pressures above 18 GPa and temperatures higher than 2200 K [2]. The hardness of c- BC_2N is higher than that of c-BN single crystals, and only slightly less than of diamond [3].

In this paper some optical properties of this material were investigated by ellipsometric and luminescent methods.

The optical parameters of synthesized samples of c-BC_2N the refraction index (n) and extinction coefficient (k), have been determined by the multi-angle-of-incident ellipsometry (MAI), using laser ellipsometer with the He-Ne laser as source of monochromatic light (λ=632,8 nm).

The measurement of the polarization angles ψ and Δ were carried out with the LEF-3M laser ellipsometer in the range of the angles of incidence φ = 50-70°. The angles ψ and Δ were measured using a double-zone method [4,5].

The optical parameters n, k have been determined with solution of inverse ellipsometric problem in the semiinfinite model for multiangles of incidence. For calculation of these parameters the developed program solution has been used [4]. It is based on a modified method of general search and a specific choice of the fitting function. Since the fitting function had many minima, the search of a global minimum was performed using the ψ, Δ for 10-15 angles of light beam incidence.

Figure 1 shows the polarization angles ψ and Δ in dependence of the incidence angle φ. The characteristic point of the $\psi(\varphi)$ curve is minimum caused by the Brewster's angles φ_B where the $\Delta(\varphi)$ curve is arrived at the value of Δ=90°. Using the values of φ_B, $tg\varphi_B$ we can obtain the first approximation for the optical constants:

$$n \cong tg\varphi_B$$

$$k \cong tg\Psi(\varphi_B)\frac{(\sin^2\varphi_B + n\ cos\varphi_B)^2}{\sin\varphi_B \cdot \sin2\varphi_B}$$
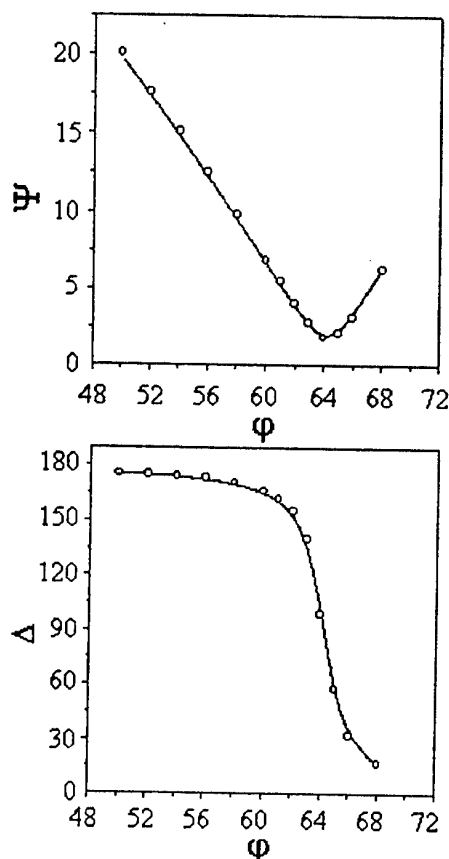
Fig.1 Polarization angles ψ and Δ vs angle of incidence φ for multicrystalline c-BC_2N.

As the final result of following solution of inverse ellipsometric problem it was obtain: n = 2.06 ± 0.01, k = 0.16 ± 0.06. The dependence of n on ρ for the related cubic materials is shown in fig.2.Besides, the value of n can be connected with the density of material ρ by the so-called molecular refraction [6]:

$$M = w/\rho \cdot (n^2 - 1)/(n^2 + 2),$$

where w is the atomic weight.

316
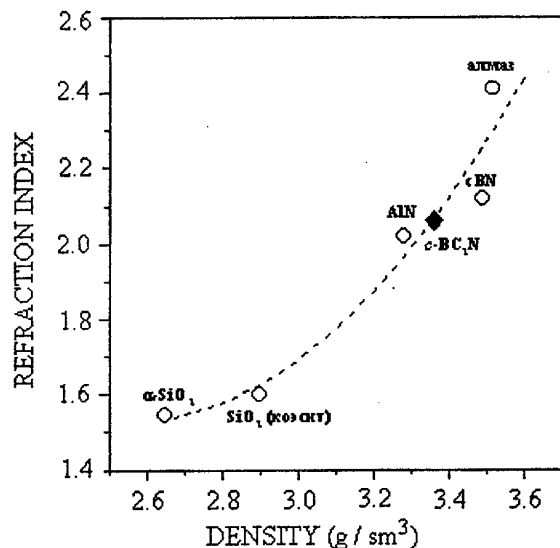
Fig.2.Dependence of refraction index on density for various cubic phases.

The value of molecular refraction M in dependence of density ρ is shown in Fig.3 for several related materials.
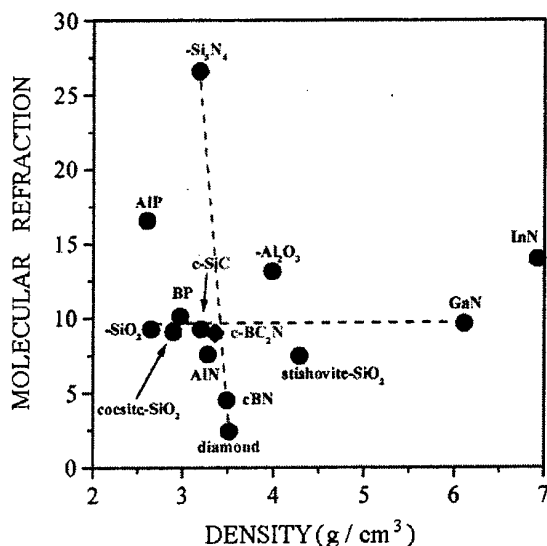
Fig.3 Dependence of molecular refraction on density.

Some support of nonhomogeneous surface we obtain from time-resolved photoluminescence spectrum (PLS), see Fig.4. That were measured in two regimes in case of all surface illumination and when only "defected region" was illuminated through small diaphragm. The experiment shows mainly all intensity of PL take place from the mentioned "defect spots". As to the spectra shape: 1) that have very broad band (about 2 eV), with long tail, beginning in fact, directly from excitation quanta energy, and, hence it is probably begin from near to edge of energy gap, penetrating deeply inside of sample. The spectra, begging in generally monotonous, have some

slight structure at energy of ~ 3eV, demonstrate existing relatively shallow levels. Probably, that is nitrogen N-origin donor levels, which is known for diamond, doped by N_2 with approximately the same energy (about $1\div1,5$ eV below conductive band edge). As to kinetic of PL, relaxation process of PL have short – time component, (mainly for high energy spectral range), $t \sim 10$ nsec. and more long time nonexponential decay.
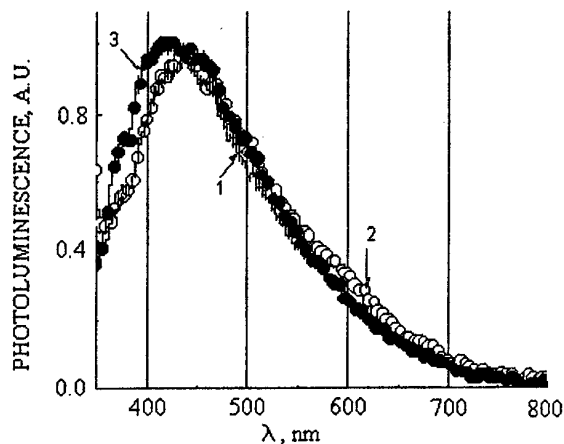
Fig.4. Photoluminescence spectra of BC_2N measured with different time delay: 1-0 ns, 2-4 ns, 3-6 ns.

[1] V.G. Litovchenko, Ukr.J. of Phys.,V.44, #9, 1064-1068, 1999; Physics of Low-Dim. Structures, 7/8, p.129-134,1999.
[2] SolozhenkoV.L., et.al. Synthesis of superhard cubic BC_2N // Appl. Phys. Lett. – 2001. – 78, No.10. – P. 1385-1387.
[3] SolozhenkoV.L., et.al. Mechanical properties of cubic BC_2N, a new superhard phase // Diamond & Related Mater. – 2001. – 10. – P. 2228-2231.
[4] Ellipsometry. General editor A.V. Rzhanov,– Novosibirsk: Nauka.1978 (in Russian).
[5] V.N. Antonyuk, N.L. Dmitruk et.al. In book: Ellipsometry in Science and Technique.– Novosibirsk.1987, p. 66-71 (in Russian).
[6] M. Born, E. Volf. Optics.– M: Nauka, 1470, p.846.

317

STRUCTURAL STABILITY OF SUPERALLOYS: A CONTROL OF THE KEY PARAMETERS OF MICROSTRUCTURE

Logunov A.V., Razumovskii I.M., Timofeev A.N.
Open Joint-Stock Company "KOMPOZIT", Institute of Metals, Korolev, Russia

One of some moments in a superalloy's design is a formation of the stable microstructure that guarantees an acceptable level of service parameters. There is a diffusion coarsening of the given microstructure under high temperatures and stresses, which leads to a lowering of the service characteristics. That is why a prediction of the superalloy's structural stability is the important problem of physical metallurgy.

The different types of microstructures in structural alloys can be divided into three main groups:

i) the isolated particles of the second phase in a matrix phase. Such a structure is formed, for example, in the Ni-base superalloys and consists the small inclusions of γ' – phase in γ - matrix.

ii) Lamellar structure that is formed, for example, in the Ni-base superalloy single crystals under uniaxial loading along <100> direction of fcc lattice at high temperatures (so-called raft-structure); the same type of structures is found in the intermetallic Ti-Al alloys (lamellas of γ (TiAl) and α_2 (Ti$_3$Al) phases).

iii) Fibrous (rod) structure that is formed, for example, in the eutectic superalloys like CoTaC, obtained by unidirectional solidification.

Analysis of the models of diffusion coarsening of the microstructures under consideration (Lifshiz-Slezov-Wagner [1], Lozovoi-Razumovskii [2], Cline [3]) shows that the kinetics of the processes in all cases is described by the following expression:

$$V \sim s\, c_i\, \sigma D_{eff},$$

where s is the structural factor, c_i are the concentrations (solubility's) of the diffusing components in the matrix and\or in the second phase, σ is the surface tension between the phases, D_{eff} is the effective diffusion coefficient of the microstructure. Therefore, the stability of the microstructures is controlled by a number of structural (s), thermodynamical (c_i and σ) and kinetical (D_{eff}) parameters.

The alloy's microstructures having a high level of stability against the process of diffusion coarsening have to have an acceptable combination of the given parameters. In this paper the most effective approaches to affect on the parameters under consideration is discussed.

1. **The structural parameter** s. The considered models of diffusion coarsening of different microstructures are based on assumption that the initial microstructure is imperfect. For example, in the 1 type microstructure the isolated particles of the second phase in the matrix have the different sizes. Such a microstructure is unstable against the process of diffusion coarsening: the small particles begin to dissolve in the matrix, and the large particles grow. As a result of this process the mean size of the particles in the matrix increases with time at high temperatures. Therefore the efficient approach to increasing the stability of microstructure in superalloys is a production of more perfect microstructure. The rule is "the structure has to be as perfect as possible".

2. **Thermodynamical parameters** c_i **and** σ.

- c_i - the solubility's (concentrations) of the diffusing components in the matrix and\or in the second phase. The model analysis shows that the lower c_i - values, the higher the stability of microstructure. Therefore to improve the stability of a given microstructure the addition of elements with a low solubility in the matrix can be used. For example, in the Ni-base superalloys Re can be classified like a such element.

- σ - the surface tension between the phases. The rule is: the lower σ - values, the higher the stability of microstructure. For example, the coherent interphase boundaries $\gamma'\gamma$ in the Ni-base superalloys are characterized a very low σ-value. If the interfaces in a given alloy are incoherent ones, a possibility of producing so-called "special boundaries" have to be considered. For example, the special interphase boundaries are found in the eutectic superalloys type $\gamma\backslash$MC [4].

Further, microalloying additions can be considered as a power tool to improvement of the

structural stability. Actually, some microalloying elements (for instance, boron) tend to segregate to the internal interfaces (grain- and interphase boundaries). This result was obtained in [4] by means of the radiotracer technique. A segregation of the microalloying additions decreases the σ - value in the alloy. As a result of this fact the stability of microstructure increases.

2. Diffusion parameter D_{eff}.

The effective diffusivity of the microstructure D_{eff} is given by the relation

$$D_{eff} \approx D_v + (\delta \backslash l) \, D'.$$

Here D_v and D' are the diffusion coefficients of the components in the lattice and interphases, δ is the diffusion depth of the interphases, l is the characteristic size of the phases in the microstructure. In [4] one can find information about the parameters D_v, D', δ and l in the superalloys.

From the point of view of the D_{eff}- parameter, to increase the stability of microstructure one has to find an approach to decreasing the D_{eff}- values in the alloy. For example, in the Ni-base superalloys such an approach consists in the addition to the alloys number refractory metals (W, Mo, Ta, Re etc.).

The microalloying additions are also useful ones in this context because these elements usually tend to low the diffusivity of interfaces in the alloys [4].

Let us specially consider important results that were obtained in [5,6,7]. It was established that in the Ni-base superalloys the diffusivity of the interphases $\gamma'\backslash\gamma$ strongly depends on the value f = $(a_\gamma - a_{\gamma'})\backslash a_\gamma$ (so-called misfit); here a_γ and $a_{\gamma'}$ are the lattice parameters of the γ and γ' – phases, respectively. It was also found that the minimum diffusivity was observed for the interphases with a small positive f –value. That is why the Ni-base superalloys with a small positive value of misfit have a number of preferences. The "positive misfit" factor especially important for the Ni-base

superalloys intend to a long-time service under high temperatures and loading. In such conditions the raft-structure can be fast created in the alloy and the time-to-rupture will be depend on the diffusivity of interphase boundaries $\gamma\backslash\gamma'$ in the lamella-like microstructure.

In conclusion, the approaches under consideration are applied to prediction of the structural stability of the Ni-Al-base intermetallic alloys at high temperatures. A temperature dependence of the diffusion coefficients of the bulk and grain boundaries in the Ni-Al-base intermetallic alloys is analyzed in compare with behavior of the same characteristics in the Ni-base superalloys [4,8]. It is established that the Ni-Al-base intermetallic alloys at high temperatures T > 1300° C have a preference in compare with the traditional Ni-base superalloys.

References

1. Lifshiz I.M., Slezov V.V. Sov. Phys. JETP, 1958, **35**, 479.
2. Lozovoi A., Razumovskii I. Materials Science Forum, 1996, **207-209**, 513.
3. Cline H.E., Acta metall., 1971, **19**, 481.
4. Bokshtein S.Z., Ginzburg S.S., Kishkin S.T., Razumovskii I.M., Stroganov G.B. Autoradiography of interfaces and structural stability of alloys (in Russian). Moscow, Metallurgiya, 1987.
5. Bokshtein S.Z., Bolberova E.V., Kishkin S.T., Kuleshova E.A., Logunov A.V., Mishin Y.M., Razumovskii I.M. DAN SSSR, 1980, **253**, 1377.
6. Bokshtein S.Z., Bolberova E.V., Ignatova I.A., Kishkin S.T., Razumovskii I.M. Physical Metallurgy, 1985, **5**, 936.
7. Petrushin N.V., Ignatova I.A., Logunov A.V., Samoilov A.I., Razumovskii I.M. Izv. AN SSSR, Metals, 1981, **6**, 154.
8. Zulina N.P., Bolberova E.V., Razumovskii I.M. Acta metall., 1996, **44**, 3625.

AB INITIO INVESTIGATION OF 3C-SiC:Zn

Yuryeva E.I.
Institute of Solid State Chemistry, Ural Branch of RAS, Ekaterinburg, Russia

It is known that Zn atoms in III-V nitrides used as doping defects bring about hole conductivity of the compounds. Theoretical LMTO-FG studies of SiC:Zn were carried out earlier only within Zn->Si substitution model. An overview of literature on SiC revealed a total absence of experimental evidences concerning the influence of Zn-doping atoms on the properties of this compound. At the same time it was found that the introduction of Me3d-atoms into the crystal structure of SiC can affect its properties. For example mechanical properties of SiC matrix may be improved by introducing TiC as the second phase. On the other hand, Ti-, Ni coatings are reported to be strengthened in the presence of SiC, TiC_4, TiB_2. At the same time Ni/SiC, Ni/C(diamond) coatings also show much promise. In the series of Me3d elements, titanium and nickel atoms are located respectively at the beginning and the end of the row and have either two electrons (Ti) or two holes (Ni) on the Me3d-valence orbitals. Probably the latter circumstance determines the similarity of Me-C chemical bonding.

In this report we present the results of our calculations of SiC:Zn electronic structure and compare them with the pecularities of interatomic interactions in SiC: (Ti, Ni). The investigations were carried out within the density functional theory (DFT) in the local spin-density approximation by X_a-method of discreet variations; the calculation details were used as published earlier. The electronic structure of perfect and doped silicon carbide was modeled by $[Si_{1-x}Zn_xC_{10}]^{24-}$ clusters. Substitutional (Zn->Si) and interstitial (Zn->i) defects have been examined. The following investigations parameters have been considered: atomic charges, ionicity parameter of interatomic Si-C, Zn-(Si,C) bonds, the distribution of electronic states on the electronic scale, total and partial interatomic atom-atom and orbital-orbital bond orders, total energies of clusters and bonding energies of constituent atoms.

The following findings have been obtained. In the Zn->Si substitution model with the nearest tetrahedral C-environments, the degree of ionicity of Si-C chemical bonding is 0.33, whereas when an impurity atom is located in Si-tetrahedral interstice this value decreases to 0.25. Here Zn atom exhibits a similar tendency: 0.25 in the substitution position and 0.23 in the interstitial site. This tendency is indicative of a weakening of interatomic interactions when going from the substitutional model to the interstitial model. This tendency is also supported by the variations in the overall covalence (reduced to atom) and valence of the clusters: these parameters are maximum in the substitutional model. Detailed analysis shows that in the substitutional model Zn atoms interact both with C atoms (average bond population is 0.314e) and Si atoms of the second coordination sphere (0.005e). Zn3d AO interact almost not at all with Si atoms of the second coordination sphere, whereas their interaction with C(2s,2p)-AO is nonzero. In the substitutional model, the basic interactions in the Zn-C chemical bonding are the Zn(4s,4p)-C(2s,2p)-AO interactions, the diffuse C2p-AO exhibiting a much greater activity. The introduction of a Zn atom into the interstitial position with Si_4 nearest tetrahedral surrounding results in an active interaction of all Zn3d,4s-,4p-AO. The interaction of Zn-AO with Si atoms nearest to Zn atoms is of a weakly covalent type (mean bond population 0.072e), with carbon atoms from the second coordinate sphere it has an antibonding character (mean bond population - 0.022e), and with carbon atoms from the third coordinate sphere – a bonding character (mean bond population 0.015e).

The matrix (Si,C) and doping atoms (Zn) in our calculations are in the non-magnetic state.

Ti and Ni doping atoms in 3C-SiC have the largest values of partional covalence parameters in these clusters as compared with Zn.

SLIDING WEAR BEHAVIOUR OF PARTICULATE REINFORCED ALUMINIUM BASED COMPOSITES

Chernyshova T., Kobeleva L., Bolotova L.
Baikov Institute of Metallurgy and Material Science RAS, Moscow, Russia

Particulate reinforced aluminium matrix composites are considered as an ideal substation for antifriction materials to be used on engine parts in aerospace and particularly in automotive industries, wich require good wear resistance and friction properties.

In our previous work, sliding wear behavior of aluminium alloy composites reinforced with SiC particles have been studied [1,2]. It was showed that the wear rate of the composites was lesser than that of the bronze (Table) and it further decreased with particle volume fraction and particle size in the matrix alloys. The value of the coefficient of friction of Al-12%Si alloy containing up to 5 vol. % SiC was ≤0,01 in sliding against a hard steel counterface (>45 HRC) with lubricant limited.

To analyze wear mechanisms, wear surface were examined by optical and electron (TEM and SEM) microscopy. It was found that the hard ceramic particles act as load-supporting elements carryed the normal load and prevent the softer matrix from becoming directly involved in the wear process.

The friction surface is contained traces of plastic deformation in the form of the light and grey bands. In the grey bands micrographs are showed the initial features of structural self-organization in the surface layers similar to matrix cells surrounding by the particles. A major wear mechanism was the abrasion wear with partial particle cracking. Increase in the applied load increased the wear severity by changing the wear mechanism from abrasion to intensive particle chipping induced delamination wear.

The purpose of this work is to study the effect of the interfacial bond strength between particles and matrix on the wear resistance of composites. Samples of composites are prepared by the method of mechanical mixing of SiC particles (7 vol.%) with average diameter of 28 μm in a molten matrix alloy Al-12% Si. To arise the particle/matrix interfacial bonding the additions of magnesium (5 wt.%) and/or scandium (up to 1,5 wt.%) to matrix alloy are selected. The quality of adhesion bonds between SiC particles and matrices is estimated by compression testing in

three stages with an upset of 50, 75 and 87,5%. Uniform distribution of SiC particles in the matrix is analyzed by the microstructural method of the equal-cell division. Wear tests (dry friction) are carried out by using a pin(composite)-on-disk (steel 45, HRC ≥45) set-up by a constant load of 5 kg and speed of 0,02 ms^{-1}.

The results indicate that a noticeable effect of surface-active Sc and Mg addition to Al-Si-matrix alloy is the grain refinement and a more homogeneous distribution of SiC particles in the matrix (Fig.1). The solidification of the composite melt begins with the formation of the crystals of intermetallic phase Al_3Sc that act as α-dendrites nucleation sites due to close face centered cubic crystal structure matching of Al and Al_3Sc. The interdendritic regions contain SiC particles pushed by the growing α-dendrites, Al-Si- or Al-Si-Mg-eutectics and a fine dispersion of $AlSi_2Sc_2$ and Mg_2Si precipitates. Several SiC particles capturing within the grains of Al-Si-Sc-Mg matrix are suggested a good particle/matrix wetting during solidification.

The hardness of Al-12%Si alloy is about 500 HB. Samples of the composites have higher hardnes: 1 (Al-12%Si)/SiC_p – 735 HB; 2 (Al-12%Si-5%Mg-1,5%Sc)/SiC_p – 751 HB; 3 (Al-12%Si-1,26%Sc)/SiC_p – 768 HB. Certain distinction between hardness of the composites may be due to the presence of hard phases Al_3Sc, $AlSc_2Si_2$, Mg_2Si, Si-needles in the matrices. The analysis of failure nature of the samples after the compression test showed that the clusters of particles and the weak interface bonds cause cracks at the periphery of the samples already after 50% upset. According to the increasing strength of adhesion bonds the composites form the following series: 1, 3, 2.

In Fig.2 the results of wear test of composites are presented. The wear results were computed from weight loss measurements. The wear volume, ΔV, was calculated from the ratio of weight loss to density and wear rate was calculated using sliding distance S and wear volume. One can see that samples alloyed with Sc and Mg have a higher wear resistance than the samples with a Al-Si matrix. It is probable that the

coarse rigid phases from the matrices (Si-needles, Al_3Sc) can improve the wear resistance of composites as well as reinforcing particles SiC designing a role of padding supporting elements. Data on the steady state wear rates of the composite pins was equal 0,029 (1), 0,056 (3) and 0,035 (2) mm^3m^{-1}.

According to the Archard wear equation, the wear rate is related to the material hardness and applied load as:

$$\Delta V/S = KN/H,$$

where N is the applied load, H is the material hardness and K is the wear coefficient. Values of the wear coefficient, K, for the composite pins were: $1,4\cdot10^{-4}$ (1), $1,01\cdot10^{-4}$ (3) and $0,72\cdot10^{-4}$ (2).

The similarity of the wear coefficients for the three composites indicate that no change in wear behaviour has occurred. A wear mechanism was abrasion.

Conclusion. The high wear resistance of the Al-12%Si/SiC_p composites alloyed with Sc and Mg additions correlates with the increase a hardness, strength and matrix/particle bounding strength.

Reference.

1. T.A.Chernyshova, L.I.Kobeleva, A.V.Panfilov and P.Šebo, Interaction of Metallic Melts with Reinforcing Fillers, Nauka, Moscow, 272 p. (1993)
2. T.A.Chernyshova, L.I.Kobeleva, A.V.Panfilov and T.V.Korzh, J.Adv.Mater., 3 (1), pp.20-27 (1996)

Table
Comparative characteristics of bronze (1) and composite alloys (2,3)

Parameters	(1):Бр06Ц6С3	(2): AK9 + 5%SiC_{28}*	(3): AK9+ 2,5% SiC_3
Specific pressure at stable friction mode, MPa	7,0	64,0	120
Friction coefficient at specified pressure	0,038	<0,01	<0,01
Temperature developing in the friction zone, °C	110	<55	<70
Rates of wear at pressure 7,0 MPa, c.u. Block material Counterbody material	$4,5\cdot10^{-10}$ $1,8\cdot10^{-10}$	$3,7\cdot10^{-12}$ $1,3\cdot10^{-12}$	$0,5\cdot10^{-12}$ $0,7\cdot10^{-12}$
Weight of the billet of 0,084 dm^3, kg	0,740	0,235	0,235
*) Average diameter of particles, μm: SiC_{28} - 28, SiC_3 - 3			
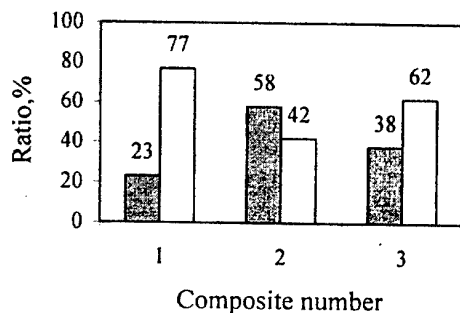
Figure 1. Evaluation of uniformity of distribution of the SiCp in the matrix of composites. Columns give the percent of cells occupied (dark) and not occupied (light) by the particles.
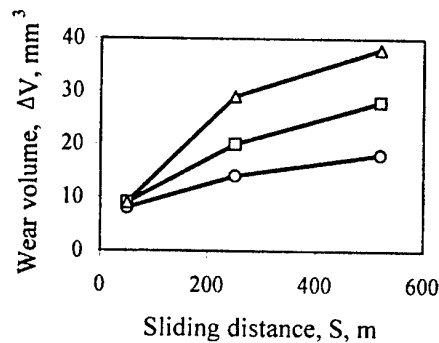
Figure 2. Wear test results of composite samples
1 -△, 2 – O, 3 -□

MECHANICAL CHARACTERISTICS OF COMPOSITE MATERIALS THERMOEXFOLIATED GRAPHITE-ORGANIC COMPONENT

Matzui L., Vovchenko L., Zhuravkov A., Stelmakh O., Fedorov V.

Kyiv National Taras Shevchenko University, Kyiv, Ukraine

The aim of our work was to investigate the influence of organic modifiers on mechanical properties of composite materials based on thermoexfoliated graphite (TEG) such as the compression strength and the creepage.

The modification of TEG powder (the bulk density was $0.005 g/cm^3$, specific surface was 50-60m^2/g [1]) with organic components such as phenol-formaldehyde resin (PFR) and silicon-organic binder (SO) was performed via several stages as described in [2]. The bulk samples of CM were produced from powders by cold pressing. The investigations of compression strength and creepage were carried out by using ИМАШ-20-78 device. The values of compression strength σ_c and deformation of destruction ε_D for CM based on TEG are presented in Table 1. As it was shown in paper [2] the destruction of compacted TEG samples occurs due to the increase of intrinsic pressure in closed pores

Table 1

CM	ρ, g/cm^3	ε_D *	σ_c, MPa,
TEG	1.80	0.22	53
TEG(2,38%H$_2$O)	1.81	0.21	44
TEG(5,93%H$_2$O)	1.73	0.25	32
TEG+50%Ni	2.81	0.21	79
TEG+73%PFR	0.82	0.44	26
TEG+96%SO	1.06		~5**

* - $\varepsilon=\Delta l/l_0$; ** - viscous destruction.

under the application of external load and at increased temperature. The modification of TEG by nickel yields better strength characteristics of composite materials at the concentration of Ni >30%mas [2]. The cracks produced under external pressure are stopped from spreading by nickel particles metal that are uniformly distributed on the TEG particles in the form of spherical particles, which are (0.01-0.05) μm in size [3]. The investigations of the strength σ_c of the compacted samples of TEG in dependence of their

moisture have shown that the strength properties of compacted TEG become worse with increase of sample's moisture due to the increase of intrinsic pressure in closed pores filled by vapour of H$_2$O (Tabl.1). The introduction of organic component in TEG leads to decrease in strength σ_c and to viscous destruction of these materials. In the samples of TEG-SO the process of mechanical destruction when the sample cracks up into separate pieces does not occur at all. Under increase of loads $\sigma(\varepsilon)$ dependence reaches the maximum but sample's crumbling does not occur. Instead the intensive viscous squeeze out is observed when the material escapes through the gap between the press punches.

The more detailed information about plastic characteristics of materials under study and in particular about fluidity process we obtained by using the method of static loading. The investigations by using static loading allows us to calculate $\varepsilon_{pl}(\sigma)$ dependence and $\varepsilon_{pl}(t)$ dependence at $\sigma = const$.

The analysis of the obtained results for compacted pure TEG had shown that the rate of creepage $\dfrac{d\varepsilon_{pl}}{dt}$ decreases essentially as the time of exposure t is increased (for the sample with density $\rho=1.14 g/cm^3$ the rate of creepage decreased 500 times after two hours exposure). The characteristic time τ_0 for creepage slowening decreases as the density of material grows: in the sample with large value of density ($\rho=1.9 g/cm^3$) the duration of creepage process was several minutes. Further exposure of the sample under load almost does not change its dimensions. The measurements under static loading (in condition $t > \tau_0$) give direct and almost precise information about the dependence of residual plastic deformation ε_{pl} on mechanical stress σ.

Fig.1 presents the typical curves for time dependence of relative change of length $\varepsilon(t)$

obtained for the samples of CM based on TEG-SO under permanent loading σ.

Figure 1. Creepage curves for CM based on TEG-SO: 1- $C_{TEG}=25\%$mas, $\rho=1.07g/cm^3$; 2 - $C_{TEG}=14\%$mas, $\rho=1.26g/cm^3$; $C_{TEG}=25\%$mas, $\rho=1.32g/cm^3$; $\sigma_1=0.3$MPa, $\sigma_2=0.8$MPa, $\sigma_3=2.7$MPa.

The characteristic feature of these curves is that after the load is taken off the so-called reversible creepage is observed, i.e. complete (or partial) return of the sample to its initial length. It should be remembered that for CM based on pure TEG and TEG modified with metals the phenomenon of reversible creepage does not occur. The phenomenon of reversible creepage is inherited in the materials belonging to the class of visco-plastic composite materials. A small instantaneous modulus of elasticity and intensive process of creepage at steady loading is characteristic of such composite materials as TEG-SO. Direct creepage prevails over the reverse one and the sample does not recover in its sizes even after many hours' exposure with the load taken off. As it is seen from Fig. 1 the creepage process is more intensive in the samples TEG-SO with low density and low concentration of TEG. Table 2 presents the values of effective rate of creepage $\dfrac{\Delta\varepsilon_{eff}}{\Delta t}$ calculated on the part of $\varepsilon(t)$ dependence at $\sigma_3=2.7$MPa and residual deformation ε_{pl} for TEG-SO samples. It

was found that these values decrease with increase of TEG concentration.

Table 2

CM	ρ, g/cm^3	$\dfrac{\Delta\varepsilon_{eff}}{\Delta t}$, s^{-1}	ε_{pl}
TEG	1.14	$1.8 \cdot 10^{-7}$	
TEG+86%SO	1.26	$1.25 \cdot 10^{-4}$	0.075
TEG+75%SO	1.07	$2.0 \cdot 10^{-4}$	0.15
TEG+75%SO	1.32	$5.9 \cdot 10^{-5}$	0.046
TEG+48%SO	1.49	$4.0 \cdot 10^{-5}$	0.036
TEG+38%SO	1.59	$3.3 \cdot 10^{-5}$	0.031

Thus, modification of TEG with organic component leads to decrease in strength σ_c and viscous destruction of these materials. The mechanism of deformation is visco-elastic with considerable plastic component. The residual deformation is observed in all "loading-unloading" cycles.

REFERENCES
[1.] E.I.Kharkov, V.I.Lysov, L.Yu.Matsui, L.L.Vovchenko, M.F.Tsurule, N.A.Morozovskaya. Patent N 33777A, 15.02.2001, bul.1.
[2.] L.L.Vovchenko, E.I.Kharkov, A.G.Rudenko, T.L.Tzaregradska. Abstracts, EuroCarbon – 2000, 1st World Conference on Carbon Germany, Berlin, July, 2000, 305.
[3.] I.Ovsienko, M. Thurule, A. Brusilovetz, E. Kharkov. Abstracts, EuroCarbon – 2000, 1st World Conference on Carbon Germany, Berlin, July, 2000, 849.

ELECTRICAL CONDUCTIVITY OF COMPOSITE MATERIALS GRAPHITE-ORGANIC COMPOUND

Vovchenko L., Matzui V., Stelmakh O.
Kyiv National Taras Shevchenko University, Kyiv, Ukraine

Electrical resistivity of composite materials (CM) based on graphite (natural disperse graphite, thermoexfoliated graphite (TEG)) and organic compounds (silicon-organic binder based on polyorganosiloxane (SO) and polyvinylpyrrolidone (PP)) have been investigated. The concentration of graphite in CM varied from 4 to 73%mas. The modification of TEG powder [1] with silicon-organic binder was performed by using method described in [2]. The powders of TEG modified with PP were obtained by mixing the TEG and PP in presence of water. The samples of compacted CM were prepared in press moulds by using hydraulic press and had the density of $(0.8-1.6)$g/cm^3. The measurements of electrical resistivity along compression axis (ρ_c) were carried out by using four-probe method.

As we used high-porous TEG-particles and modified these particles by polymer impregnation the bulk density of modified TEG-powders can be increased significantly because open pores had been filled by polymers (see Table 1).

Type of material	Bulk density of powder, g/cm^3	Density of CM, g/cm^3
TEG	0.005	
TEG-SO:		
51%TEG	0.165	1.47
25%TEG	0.220	1.27
14%TEG	0.270	1.22
TEG-PP:		
10%TEG		1.12
40%TEG		1.28
Gr (50μm)	0.328	
Gr-PP		
10%Gr		1.21
40%Gr		1.42

Modified TEG-particles with filled open pores became more rigid and save their initial configuration during the pressing process. It is obvious that the bulk density of conducting component (TEG, modified TEG) which is the analog of packing density determines the percolation threshold in electric conductivity: the

low values of packing density give low values of percolation threshold.

The investigations of electrical resistivity of CM have shown that all TEG samples modified with organic substances (at $C_{TEG}\geq4$%mas) are electric conductors, and their electric resistivity does not exceed ~ 1Ohm·m. For graphite-organic modifier systems there exists a threshold value of graphite content in CM below which the electrical resistance grows abruptly and above it the system's electrical resistance decreases inconsiderably (Figs.1).
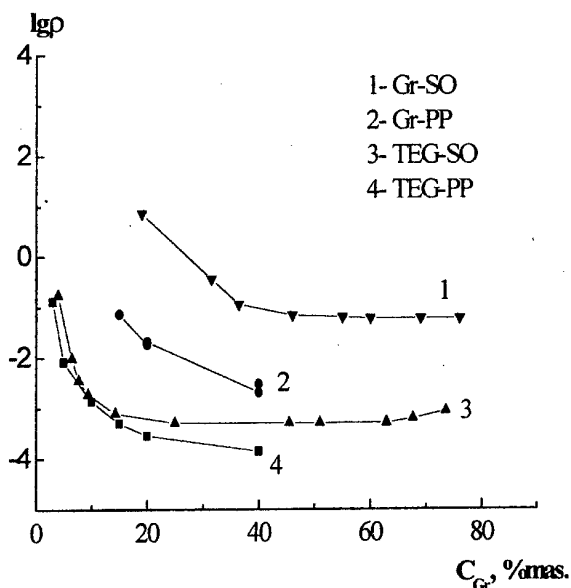
Fig.1 The dependence of electrical resistivity on the concentration of graphite in CM based on graphite and organic binder: 1 - ρ_V of graphite-SO; 2 - ρ_c of CM Gr-PP, 3 - ρ_c of CM TEG-SO, 4 - ρ_c of CM TEG-PP.

Electrical resistivity in this case can be described as [4]:

$$\rho_{CM}(C) \sim \rho_0(C - C_k)^{-t}, \qquad (1)$$

where ρ_0 - is the electrical resistivity of TEG, C is arbitrary concentration of TEG and C_k - critical concentration, i.e. at which an abrupt decrease of

electric resistivity has been observed, t is critical index which consist 1.7 for the model of three-dimensional electroconducting net with fixed nodes [3].

In the case of direct contacts between TEG-particles in compacted samples contact resistance of particles R_k plays important part, while the resistance of material the particles are made up r is sometimes less significant. For the general case the electrical resistance of compacted sample R may be presented as follows:

$$R = R_k + r ,$$

$$R_k \sim k, S, F^{-1/2}, r \sim \frac{1}{n}, \frac{1}{L_{ef}} \quad (2)$$

where total contact resistance R_k depends on the number of contacting particles k, contact area S, pressure on contact F and degree of thermochemical treatment of contacting surfaces [4]; r is determined by concentration of charge carriers n and effective free path of charge carriers L_{ef} at various scattering processes.

For the systems under study the threshold values of graphite content are $\sim$ (20-30)%mas for graphite-SO, graphite-PP and (4-10)%mas for TEG-SO, TEG-PP accordingly. As it is seen from figure the percolation transition in the system based on TEG and SO or PP occurs in very narrow interval of concentration (C=(5-15)%mas.) in comparison with composite TEG-polyethylene [5], (C=(15-50)%mas.). This fact testifies about small number of isolating films on TEG particles and gaps between particles of TEG in the case of using SO or PP as binders. Using the relation (1) experimental dependence $lg\rho(C)$ for the systems TEG-SO can be approximated by following expression:

$$\lg \rho(C) = \lg(A \cdot \rho_0) - t \lg(C - C_k) \quad (3)$$

where A is constant. The increase of the value of electrical resistivity ρ with increase of TEG content is caused by increase of structure anisotropy of compacted samples at increase of TEG anisotropic particles concentration. The obtained samples of TEG-SO have anisotropy of electrical properties: $\rho_c/\rho_a \sim 2$ for the samples with low content of TEG ($\sim$8%mas) and $\rho_c/\rho_a \sim$ (7-9) for the samples with maximal content of TEG ($\sim$60-70%mas). The temperature dependence of electrical resistivity $\rho(T)$ in CM based on TEG-

SO is analogous to temperature dependence in TEG $\rho(T)$: the greater is the concentration of TEG the more similar are the temperature dependence of electrical resistivities in TEG-SO and pure TEG.

TEG-organic modifier CM have slight anisotropy of electrical properties: ρ_c/ρ_a ratio is $\sim$ 10, which is 2-3 times less than in pure TEG of similar density.

Thus, it was shown that for the systems of TEG-organic modifier a threshold value of TEG concentration below which the electrical resistivity grows abruptly and above which it slightly decreases is $\sim$ 5% mass. The low percolation threshold in CM TEG-organic component is associated with special configuration of TEG particles and low bulk density of TEG powders.

REFERENCES

[1] E.Kharkov, V.Lysov, L.Matsui, L.Vovchenko, M.Tsurule, N.Morozovskaya. Patent of Ukraine N 33777A, 15.02.2001, bul.1.

[2] L. Matzui, A. Zhuravkov, E. Kharkov. Abstract of ISIC11, Moscow, Russia, (2001) 114.

[3] B.I. Shklovsky. A.L.Efros. Electron properties of alloyed semiconductors. Moscow, Nauka (Eds.), 1979.

[4] A.I. Lutkov. Thermal and electrical properties of carbon materials [in Russian], Moscow, Metalurjiya (Eds.), 1990.

[5] L. Semko, I. Chernysh, L. Vovchenko at al. Plastmassy [in Russian], №8 (1991) 20.

MICROSTRUCTURE OF POLYMER CHAINS AND RELAXATIONAL PROPERTIES OF POLYISOPRENES

Egamov M.CH., Karimov S.N.
Khujand centre of science AS of Republic of Tadjikistan
E-mail: muchtor@khj.tajik.net

The purpose of work is the influence of microstructure synthetic stereoregularity polyisoprene (PI) on relaxational processes and findings - out of a nature of this phenomenon under operating conditions. As microstructures PI have accepted the contents 1,4-cis-, 1,4-trans-, 1,2- and 3,4-units in percentage ratio. In elastomers such as PI main relaxational transition by arrival is glass transition (α-transition) with the basic characteristic it is in glass transition temperature T_α [1]. It is important to note, that, T_α as well as temperature others relaxational transitions, T_i depends on temporary pegimes of tests: time of supervision τ (stress relaxation), frequency of deformation V and speed of heating ω.

For cis - and trans - PI, not containing of 1,2-units, glass transiton temperature low $(T_g = -71^0 C)$. Presence 1,2 - or 3,4 - units strongly raises up T_g to $30^0 C$ on glass transition temperature the intramolecular influences in itself elastomers chains circuits determining inretnal rotation, i.e. flexibility of a polymeric chains, and molecular interactions, density of energy cohesion can influence as inside. In this aspect the reason of change T_g with change of microstructure of polymeric chains for same PI becomes urgent.

The given works, [2] in which the dependence T_g PI have contents 1,2-units in the polymers chain was studied, testify that the microstructure does not influence density of energy cohesion and, hence, on intermolecular interactions. From here it is possible to make a conclusion, that the dependence T_g, observable by us, on structure is connected not to intermolecular interactions, i.e. power factor, and with change of character of internal rotation in chains brought in presence 1,2 - units, i.e. flexibility of a chain, namely, entropy by the factor. Other factors, such, as cristallization and stereoregularity, in researched polyisoprenes are absent. Hence, nature of influence of microstructure PI on wholly entropy.

For finding - out influence of microstructure on others relaxation transitions the researches PI by methods relaxational spectrometres [1] and IR-spectroscopy are carried out. On the data IR-spectroscopy of a chain PI 92 % - 1,4-cis-units, 6 % 1,4-trans units and 2% 1,2 units contained. For more precise revealing relaxational transitions the basic researches carried out on poorly network elastomers (vulcanization from 2 % of sulfur on standard technology) for giving elastic properties to samples, and on occassion carried out measurements on not network initial PI.

From izoterm relaxational pressure at different temperatures the continuous and discrete spectra of times relaxational τ_i were received, and the temperature dependences them in arrenius coordinates have allowed for everyone relaxational transition to find predexponential factor B_i and activation energy. From all relaxational transitions only basic process glass transition α_i and additional α_1 are characterized by dependence by activation energy U_α and $U_{\alpha 1}$ of from temperature and frequency.

Above α - and α_1 - transitions in the field of high elasticity a line known for elastomers relaxational transitions is observed. Their identification can be made, having calculated temperatures relaxational transitions T_i on the equation

$$T_i = U_i / [2,3 k \lg(C_i / 2\pi v B_i)]$$

where relaxational constants B_i and U_i also are taken from given on relaxational pressure. At account it is necessary to have in view of, that for

small-scale transitions, $C_i = 1$ and for large-scale transitions $C_i = 10$.

On with earlier found out relaxational transitions in elastomers [1,2], we reveal splitting chemical processes relaxational on $\delta_{s1} = \delta_{s2}$ and δ_c high-temperature transitions. First two are observed for rubbers, vulcanizational by sulfur. The received results allow to assume, that the δ_{s1}-transition is connected to disintegration polysulphide, and $-\delta_{s2}-$ by disintegration monosulphides of cross communications connections. These transitions do not depend neither on a type of rubber, nor from microstructure of chains. The strongly expressed δ_c-transition on a spectrum is explained by disintegration of weak communications connections C-C at high temperatures.

The superslow physical process δ_1 is absent in spectra not vulcanizational elastomers. It results in a conclusion that it is connected with vulcanized by a grid, but is not connected to disintegration observable at δ_{s1}-and δ_{s2}-processes. Than activation energy of δ_1- process relaxation is much lower activation energy of chemical processes, and consequently the δ_1- process concerns to one of physical relaxational processes. The large sizes of factor B_i testify that cinetics units participating in δ_1- processes larges. Under our assumptions them are in vulcanizational to a grid more densely network microsites. It is explained by more regular structure of polymeric chains PI, which owing to not of branching ways to be packed into larger ordered micro of area and under certain conditions to form crystals.

Literature

1. Bartenew G.M. Structure and relaxational property elastomers. -M.; Science, 1979 - 280c.
2. He T., Li B., Ren Sh. // g. appl Polymer. Sci. 1986. V31. №3. P.837

EFFECT OF HIGH POWER ULTRASOUND ON STRUCTURE IN POLYCRYSTAL ZINC

Ryumsnyna T.A., Pylypenko N.P.[1]

Donetsk National Technical University, Donetsk, Ukraine
[1]Physicist-Technical Institute NAS of Ukraine, Donetsk, Ukraine

Making of materials that operate in extreme conditions is one of actual directions of materials science. High power ultrasound influence creates a complex of these conditions in the material. Alternated big frequency and amplitude loads stimulate an appearance of mechanical stresses and heating in specimens. Investigation of ways to relaxation of the energy droved in materials under high-power ultrasound, study of influence of mechanical and temperature stresses induced by ultrasound on the structure take in interest for understanding evolution processes and for reliability prediction of functioning the products in complex conditions alternating loads.

Experiment Description. Polycrystalline Zn specimens, purity 99.95% were as an object of studies. Specimens was cut out by 7×7×90 mm (length of specimen equals to half-wave), then surface was chemical polished. A sample was connected to the magnetostriction converter which was agitated from the ultrasonic generator on the frequency 22 kHz by tread joint. Fluctuation amplitude was checked by electrodynamic's sensor, which was bolted on the concentrator and was adjusted within 3-10 mcm. Processing the samples by the ultrasound was realized at room temperature without cooling. Temperature of heating was checked by thermocouples, bolted in the sample center.

Defect structure was checked by measurement of microhardness and by methods optical metallography (selective etching of boundary grains in 5% alcohol solution of hydrochloric acid).

Simples with different defect structure were used: poured, recrystallized and hydroextruded zinc. Poured zinc had big grain (average size of grain 3-5mm) and microhardness was H_μ = 300 MPa. Recrystallized samples were prepared from beforehand deformed, but then annealed zinc (recrystallized annealing within 2 hours under 360^0C) had microhardness 420 MPa and average size of grain 100 mcm. Hydroextruded samples (degree of deformation was 98%), had very small grain d = 5 ± 2 mcm, but large H_μ = 750 MPa.

Experimental results. In the sample of half-wave length was formed standing longitudinal wave, and antinode of wave was located in the sample center. Experiments have shown that poured sample was destroyed already after 25 seconds of ultrasound action (amplitude of oscillations was 5 mcm). It was observed the brittle fracture in the antinode's region. Main crack was appeared and destroyed the sample.

In recrystallized specimen the intensive growing of grain from 0.1 mm before 10 mms was observed in the oscillation's antinode already at 15 sec ultrasonic irradiation. Active development of bands of slide and grain crushing were observed in central grain after 1 minute irradiation. A sample is destroyed in central part after 2 minutes of the ultrasonic effect.

The fine-grain structure of hydroextruded sample was changed from initial moments. Already as from 5 sec of irradiation a strong grain was growing took place in the specimen center. Grain sizes were increased in dozens of times. Grains grow along the direction of spreading a wave from the center to sample ends. Big part of boundaries was situated parallel to axis. Temperature measurements in the antinode's region has shown that sample powerfully became heat. Maximum of temperature about 400^0C was reached under 2 minutes of irradiation, but then temperature was decreased. After 2 minutes of ultrasound's action the intensive intragrained sliding was developed in sample center. Twinning and started cracking were observed inwardly grains alongside with sliding lines. These processes caused grain crushing. Further ultrasound treatment led to increasing the sizes and numbers of cracks, forming a main crack and destroying a sample. Time life's of sample before destroying was 9 minutes.

Discussing the results. High-power ultrasonic irradiation introduce into material an energy

$$W = \frac{\rho\omega^2}{2}\int_0^{\lambda/2}\left(A_0^2\cos^2 kx\right)S dx$$

where ρ is density of material, ω is frequency, $k = \frac{2\pi}{\lambda}$ and λ is the wavelength, S is a cross-section of sample, dx is a elementary length of sample, A_0 is a oscillation's amplitude in antinode's place.

The energy relax in the material by mechanical deforming and by heating. The gradient accumulated mechanical energy is force, acting toward spreading a wave along specimen axis and having maximum value in the center. The force oscillates with the frequency ω: $F = kA_0 \sin kx \cos \omega t$.

There is an essential nonhomogeneity of stress and strain field along sample under high-power ultrasonic irradiation. Maximum values of alternating straining and compressive forces exist at center of specimen. At ends this forces are absent. A moving of defects occurs from the center to ends under the action gradient forces

Strong heating of material is other particularity of high-power ultrasonic action. It reveals in that event, when structure can render a greater counteraction to mechanical deforming. So, if poured zinc is destroyed after 25 sec of

included deforming channel to relaxations an energy. Then is observed strong heating sample (a temperature increases to 400 ^{0}C), grain begin intensive to grow, but temperature begins decreases. The further evolution is realized by intensive intragrained deformation, which lead to crushing of grain, secondary hardening of material in the region of stress antinode, and then cracking development in the sample.

Conclusion. Effect high-power ultrasound creates a complex nonhomogeneous alternating stress field as well as a heating of material. Deforming or heating channels of energy relaxation depend on the defect structure. Than smaller grain, that more loss of energy on the heating and that above stability of material to the ultrasonic influence.

Study to evolutions a structure has shown that different mechanisms to deformation are realized under high-power ultrasound. It is possible to regulate a structure in the material by selecting the parameters of influence, as a value of amplitude, oscillation's frequency, time of the ultrasonic influence, that create the ability to control of material's properties.

Fig. 1. Microhardness distribution along hydroextruded specimen after 3 minutes of ultrasonic irradiation
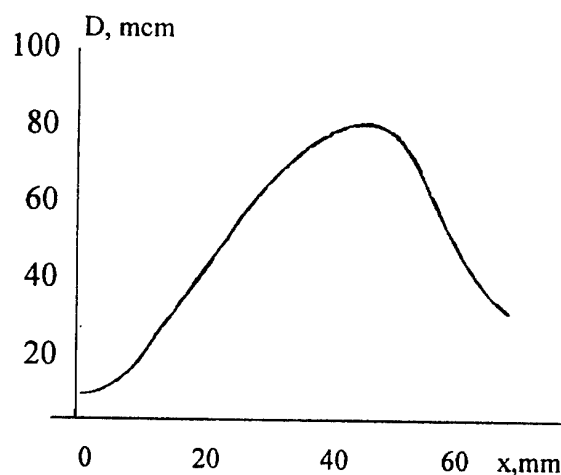
Fig. 2. Size grain distribution along hydroextruded specimen after 3 minutes of ultrasonic irradiation (x is distance from sample end)

ultrasonic irradiation without heating, in the event of the fine-grained material, presence of large number high-angle incoherent grain does not enable will be

330

STRUCTURAL FEATURES OF THE FAST HARDENED METAL PAPERS OF ALLOYS Bi-15 at. % Sb

Gretchannikov E.E., Savenko V.S., Chepelevich V.G.
Mozyr state pedagogical institute, Mozyr, Byelorus

Alloys of bismuth and antimony containing 6-22 at. Than % Sb at temperatures is lower 180 To contain a forbidden region and are the most successful materials for manufacturing cold thermoelectric converters of energy. The application of single crystals of the indicated alloys is hindered by some lacks, intrinsic by them: by predilection to a dendritic segregation considerably aggravating electrical properties of materials, low dissolubility of addition agents in bismuth and antimony, low mechanical strength. The frame largely influential in physical properties and as a consequent in technical parameters of systems in many respects depends on conditions of obtaining of alloys and subsequent heat treatment. In this connection, in the given activity the findings of investigation of frame of alloys Bi-15 at is resulted. % Sb-obtained by a method of a superfast hardening from a fluid phase, permitting to eliminate the indicated lacks.

For cooking alloys 99,9999 % were used bismuth and antimony by purity. Doping of binary alloy Bi-15 at. % Sb implemented aluminium, gallium, germanium, indium, tin, sulfur and Zincum. The purity of addition agents was not worse than 99,999 %. The superfast hardening implemented belching of a drip (~0,2) melt on an internal polished surface of a rotated copper barrel. In such conditions the cooling rate made v » 106 K/c.

The research granular of frame of the fast hardened metal papers was conducted with the help of a metallographic microscope " Neophot-21 X-ray crystallographic analysis was conducted on a diffractometer ДРОН-3 in cobaltic radiation. The polar density of diffraction lines $10\bar{1}2$, $10\bar{1}4$, $11\bar{2}0$, $10\bar{1}5$, $10\bar{1}7$, $20\bar{2}0$, $20\bar{2}2$, $21\bar{3}0$, $21\bar{3}2$, $20\bar{2}5$ settled up on a method Harison . Interplanar spacing interval $d_{10\bar{1}2}$ was determined from a Bragg equation. The X-ray spectral microanalysis was executed on installation IComeca I with usage of a microprobe MC-46, dia 2 microns.

The fast hardened metal papers of investigated(studied) alloys were received by the way of belts(ribbons), length 5-10 cm, width about 1 cm and depth 10-50 microns. The metallurgical surveys have shown, that the fast hardened metal papers have microcrystalline frame, that is connected to a considerable frigorism of a melt at a superfast hardening and bound with it by high speed of nucleation. In the fast hardened metal papers of non-alloy alloy Bi-15 at. % Sb of a grain have predominantly paxillate form much of them are limited simultaneously to two surfaces of a metal paper that is the certificate that the germing of crystallization centres is heterogenous. Doping of alloy 0,2 at. % Ge and 0,25 at. % Sn does not change form of grains. For the fast hardened metal papers of alloy Bi-15 at. % Sb, doped 0,4 and 0,8 at. % Ge, Ga, In, Al and S the equiaxial grains are characteristic predominantly. Most coarse grains were watched in the fast hardened metal papers of non-alloy alloy Bi-15 at. % Sb . The introduction of addition elements reduces aggregate size, that is connected to increase of quantity of centres of a germing of a solid phase at a crystallization of alloy. So, doping of alloy Bi-15 at. % Sb by sulfur and aluminium

The table 1
Values it is medium-sized of grains promt solidication of metal papers

Alloy	An angle diameter of grains, micron
	Reset state
Bi–15 ат.% Sb	5.0
Bi–15 ат.% Sb–0,2 ат.% Ge	4.6
Bi–15 ат.% Sb–0,4 ат.% Ge	3.6
Bi–15 ат.% Sb–0,8 ат.% Ge	3.7
Bi–15 ат.% Sb–0,4 ат.% Ga	2.9
Bi–15 ат.% Sb–0,8 ат.% Ga	2.5
Bi–15 ат.% Sb–0.4 ат.% S	2.5
Bi–15 ат.% Sb–0,8 ат.% S	2.6
Bi–15 ат.% Sb–0,25 ат.% Sn	3.6
Bi–15 ат.% Sb–0,8 ат.% Al	1.9
Bi–15 ат.% Sb–0,8 ат.% In	3.1
Bi–15 ат.% Sb–0,8 ат.% Zn	3.9

Reduces an angle diameter of grains in 2 and more time, while the doping by Zincum, small quantity of tin and germanium a little bit reduces aggregate size.

The outcomes of X-ray crystallographic analysis demonstrate, that the fast hardened metal papers of alloy Bi-15 at. % Sb is characterized by the legiblly expressed texture $(10\bar{1}2)$. On a share of the given orientation it is necessary up to 100 % of volume of a metal paper. The formation of the indicated texture is stipulated by the gear of growth of chips at a superfast hardening. Each atom of crystal lattice is connected to three other covalent bonds Two from them are in planes $(01\bar{1}2)$, $(\bar{1}012)$ and $(1\bar{1}02)$, and third binds two atoms of adjacent planes. On interphase border the chip - liquid conterminous with the indicated planes will be derivated high density of fissile centres by the way of non-saturated covalent bonds. The atoms from a melt are easily affixed to them, that causes a tachyauxesis of crystallites of the given orientation. Doping of alloy Bi-15 at. % Sb does not render noticeable influencing on texture.

The outcomes of a X-ray spectral microanalysis demonstrate, that bismuth and antimony of the in bulk fast hardened metal paper are distributed uniformly, that is a consequent diffuse-free of a crystallization, the weep by which one becomes possible (probable) at a superfast hardening from a melt and during which one the solidification of a fluid phase descends without redistribution of components of alloy..

Dependence of change of interplanar spacing interval $d_{10\bar{1}2}$ in the fast hardened metal papers of alloy Bi-15 at. % Sb from the contents in them of alloying components (fig. 1) testifies to a solid-solution formation of replacement. As the equilibrium dissolubility Ga, Ge, S, In, Zn in bismuth and antimony is lower 0,8 at. %, the data the solid solutions are supersaturated. Their formation becomes possible (probable) thanking diffuse-free of a crystallization, at weep by which one the melt indurates without redistribution of components and allocation of the second phase.
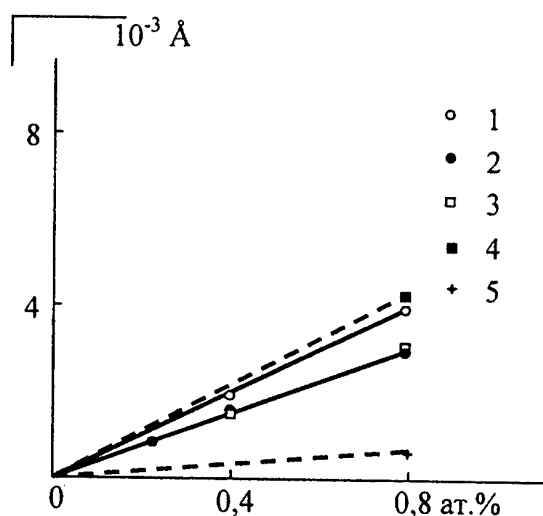
Fig. 1 Dependence of change of interplanar spacing interval $d_{10\bar{1}2}$ from the contents (1) - sulfur, (2) - germanium, (3) - gallium, (4) - indium, (5) - Zincum.

CORROSION AND HIGH-TEMPERATURE OXIDATION RESISTANCE OF SI$_3$N$_4$-BN COMPOSITE MATERIAL

Ershova N.I., Kelina I.Yu.
Federal State Unitary Enterprise "Obninsk Research and Production Enterprise
"TECHNOLOGIYA", Obninsk, Russia

The results of an investigation into hot-pressed Si$_3$N$_4$-BN material behavior under the thermocycle and high-temperature conditions and under the action of corrosive medium are presented.

The material under investigation has a variable composition, boron nitride content may vary from 0 to 60 %; in so doing there are regular changes in mechanical and thermo-physical characteristics which approach the pure boron nitride properties. On the basis of the material being developed a manufacture of a functional-gradient multilayer material is possible.

The resistance of the material to high-temperature oxidation was studied in different temperature conditions: at 1300°C for 10 and 50 hours and on longer standing for 250 hours at 700-950°C. The dependences of relative mass changes on material composition, holding time and testing temperature have been investigated. The samples of multilayer ceramics were tested in high-rate gas flow with ten-fold heating up to 1530°C and cooling. In all cases resistance to oxidation and erosion carry-over was found.

The process of the composite material corrosion in aggressive medium is rather complicated by virtue of the fact that this material presents a multiphase system. The determination of acid resistance was carried out at standard conditions throughout the entire composition range. HF, HCl, HNO$_3$, H$_2$SO$_4$, KOH were used as aggressive media. The material was demonstrated to have resistance to attack by acids HCl, HNO$_3$, H$_2$SO$_4$ and alkali KOH without regard to its BN content. Hydrofluoric acid has a pronounced effect on the composite material containing more than 30 % BN even after 10 days of interaction. The corrosion process is most pronounced after 60 days of interaction (fig.1). Under these conditions boron nitride is the most chemically resistant. The material containing 10 % BN possesses high acid resistance without regard to interaction duration which results from low porosity obtainable during the hot-pressing of ceramics of a given composition.

The non-uniformity of the corrosion process in the Si$_3$N$_4$-BN composite material stemming from the inherent in hot-pressed materials texturing was observed.

Fig.1. The samples of Si$_3$N$_4$-BN composite material containing (from left to right) 10, 20, 30, 40, 50, 60 % BN after 60 days of interaction with HF

NOVEL ORGANOSILICON PRECURSORS TO SILICON CARBIDE/CARBON BASED CERAMICS

Belyaeva E.I., Baklanova N.I., Suchkova G.A., Lyakhov N.Z.
Institute of Solid State Chemistry and Mechanochemistry of SB of RAS, Novosibirsk, Russia[*]

Ceramic matrix composites (CMC) especially SiC/SiC composites, as structural materials for hot-section components in advanced aerospace and land-based gas turbine engines, offer a variety of performance advantages over current metallic materials. Organo-silicon preceramic polymers can provide a unique approach to the process of ceramic shape forming. At relatively low temperatures, these polymers can be converted into the components of SiC/SiC composites, namely, coating, fibers, matrix, and monolithic ceramics [1].

Organosilicon polymers containing germanium atoms in main chain can be interested as precursors to SiC-based ceramics with approved high-temperature oxidation resistance.

The goal of this work is to study the features of transformation of organosilicon polymers with germanium atoms in main chain poly(germasilethyne) (PGSE) into silicon carbide/carbon/germanium-based ceramics under mechanical treatment.

PGSE $\{-(SiMe_2C\equiv C)_4-GeMe_2-\}_n$ was treated in planetary high-energy mill AGO-2 (the ball acceleration 600 ms^{-2}) under argon atmosphere for different intervals of time. The initial polymer and products obtained at different stages of mechanical treatment were investigated using X-ray diffraction analysis, IR and Raman spectroscopy, as well as SEM analysis and Energy dispersive X-ray spectrometry.

The results show that mechanical treatment for a short time (10 min) leads to substantial changes in the polymer. For example, the IR bands at 3280 and 2040 cm^{-1} attributed to the stretching vibrations of C-H and C≡C in monosubstituted group C≡CH, respectively, disappear. Additional bands appear, namely, a band at 2120 cm^{-1} which can be attributed to the vibrations of C≡C bond of disubstituted acetylenes, ~1700 cm^{-1} connected with the presence of the carbonyl group, ~1580 cm^{-1} assigned to aromatic bonds, and a band

at 1350 cm^{-1} which is responsible for bridging vibrations of the -CH$_2$- group. Also the intensities of bands attributed to methyl group vibrations decrease. The Raman spectrum exhibits the disappearance of all the characteristic bands of the polymer, and a very broad halo appears in the region 950-1650 cm^{-1}. The product obtained after milling for 10 min is X-ray amorphous, similarly to the initial polymer. Longer mechanical treatment (20 min) leads to even more profound organic-to-inorganic transformation. This is confirmed by a substantial decrease in the intensities of all the characteristic IR bands. According to SEM analysis, the particle size of the product obtained after milling for 20 min is from 0.5 to several micrometers. So, mechanical treatment for 10 min and 20 min leads to the cross-linking of polymer, accompanied by the opening of triple carbon bonds of carbon and by binding the molecules through the -CH$_2$-, -C=C-, and conjugated carbon bonds. At the same time processes of thermal decomposition of polymer and the release of inorganic phases occur.

According to the IR, Raman, and XRD data, a 30 min mechanical treatment of polymer is sufficient for its practically complete mineralization to occur. Characteristic bands of PGSE disappear in the IR spectrum of the product, which is the evidence of practically complete transformation of the polymer into inorganic product. The data of Raman spectroscopy are another evidence in favor of this observation. Fig. 1 shows a Raman spectrum of carbon phase released during the decomposition of polymer.

The most intensive bands are those attributed to so-called disordered carbon (D-band) and graphite (G-band) [2]. X-ray diffraction patterns of the product exhibit the appearance of the β-SiC phase. So, one can assume that practically complete decomposition of the polymer occurs at this stage, along with the release of β-SiC, carbon and possibly germanium phases. The ordering of these phases also occurs.
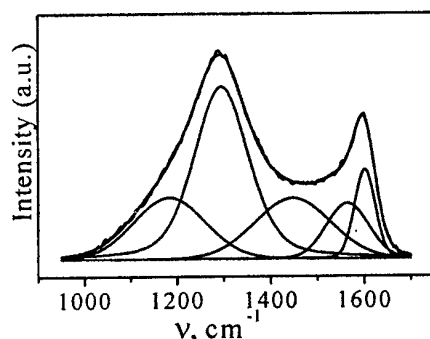
Figure 1. Raman spectrum of polymer treated for a 30 min.

A further 40 min. mechanical treatment leads to the broadening of the patterns attributed to β-SiC-phase in X-ray patterns and to the decrease of their intensity, as well as to the decrease of the intensities of the Raman bands of the carbon phase.
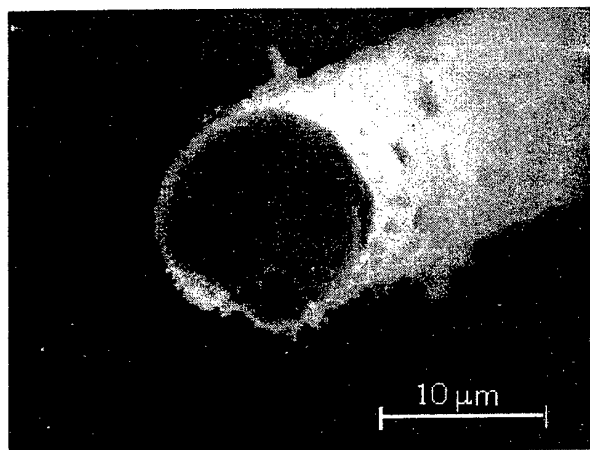
Figure2. PGSE-derived coating on Nicalon fiber.

According to SEM analysis data, the grinding of particles is observed at this stage together with their aggregation. Particle size is about 1μm. They are rounded. One can assume that a 40 min milling causes partial amorphization of the products of polymer decomposition.

PGSE under investigation was used to obtain thin barrier coatings on silicon carbide fibers of the "Nicalon" grade. The diameter of fiber was 12-15 μm. The coating was obtained by dipping the fibers into PGSE solution in chloroform, followed by centrifuging and thermal treatment within temperature range 20-1000°C. As one can see in Fig. 2, the coating is rather uniform in thickness

and fiber length, and strong adhesive to monofilament. Its thickness is less than 1μm. The coating is X-ray amorphous.

On the basis of the presented results, the use of poly(germasilethyne) for the formation of thin barrier coatings on reinforcing fibers for structural materials may be estimated to be favorable.

References

[1] Fiber Reinforced Ceramic Composites. Editor K.S. Mazdiyansi, 1990.
[2] N.I. Baklanova, V.N. Kulyukin, V.G. Kostrovsky, N.Z. Lyakhov, V.V. Terskikh, G. Yu Turkina, L.V. Zhilitskaya, O.G. Yarosh, M.G. Voronkov, J. of Materials Synthesis and Processing v.7, №5, 1999, p.289-296.
[3] N.I. Baklanova, S.S. Shatskaya, T.M. Zima, E.I. Belyaeva, N.Z. Lyakhov, N.O. Yarosh, O.G.Yarosh, M.G. Voronkov, Polymer Science, Ser.A, 2002, accepted.

POLYCRYSTALLINE MATERIALS BASED ON MODIFIED ULTRADISPERSED DIAMOND

Senyut V.
The Institute of Machine Reliability National Academy of Sciences of Belarus, Minsk, Belarus

Shown is the dependence of compact's physical properties on the ways of ultradispersed diamond's (UD) treatment and sintering modes.

Changing the ultradispersed diamond's surface it is possible to control the processes of graphitization and recrystallization of a diamond grain and produce the materials with the given structure which influence the properties of the compacts. Reverse transformation of diamond into graphite is highly essential even when compacting UD powders is being conducted within the diamond's stability range.

The graphitization process can be significantly reduced when substances such as B_2O_3, SiO_2 and B enhancing formation of glass with the oxides of UD surface during the sintering are added into the mixture.

The glass phase which is formed facilitates sintering process and reduce the porosity of the material in comparison to the samples where the additions are not used.

x200

Fig 1 a) Structure of the compact obtained without additions.

x200

Fig 1 b) Structure of the compact obtained with 1% mass. of B_2O_3.

Another way to improve quality and physical properties of the compact is to modify the surface of the initial diamonds particles. In the work different modificators were used. Such substances as CH_4, C_2H_5OH, H_2 intensify the transition of the carbon during the treatment under high pressure and temperature. As the result the porosity is lowered and the density and the hardness of the samples are increased (Fig 2)

X15000

Fig 2 TEM of the compact based on UD-powders modified with H_2.

Further compactivity of the UD with B and Ti on the diamond's surface was investigated. From one point boron and titanium can accept oxygen which impedes the sintering process, from another point these elements provide the filling of the pores during the thermal treatment.
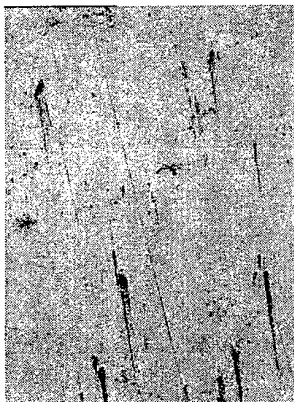
x200

Fig 3 Shows the image of the compact based on UD-powders with Ti.

Hardness and density of the samples were higher than that of the compacts which had been obtained before and made up 30 GPa (Vickers method, load 200g) and 2,7-2,8 g/cm₃ respectively.
Sintering of the UD-powders modified with metal-catalist's also was carried out. Hardness of compacts obtained on the base of such powders were 30-40 GPa (Vickers method, load 200g), density 2,8-2,85 g/cmqq.

In spite of this the porosity of the material also in creased (Fig 4)
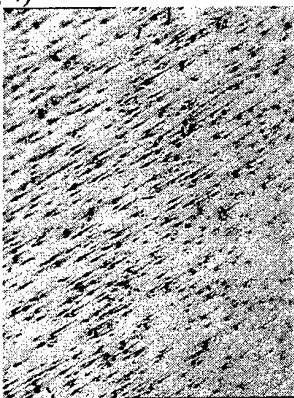
x200

Fig 4 Structure of the compact based on UD-powders with Co.

There was determined ability of UD to influence catalitically on the transformation of the non-diamond carbon into diamond. During the sintering of the UD-powders modified with the graphite and the soot formation of dense carbon phases took place. It was shown that physical-mechanical properties of produced compacts are defined by a kind and dispersivity of the non-diamond carbon. The samples obtained on the base of the UD modified with carbon have a hardness up to 70 GPa (Vickers method, load

200g) and a density raging from 2,5 to 2,7 g/cm₃ (Fig 5).
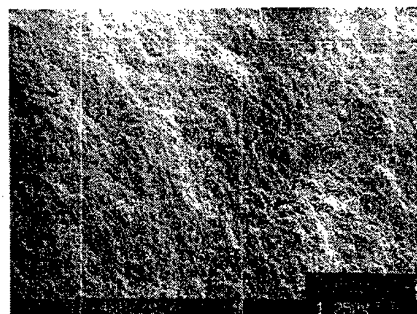
X250

Fig 5 SEM of compact based on UD-powders modified with carbon.

The results of the work shows that combining UD-powders modified in the different ways it is possible to get the compacts that have the fine structure (Fig 6) which determine high hardness of the samples (up to 100GPa, Vickers method, load 200g).
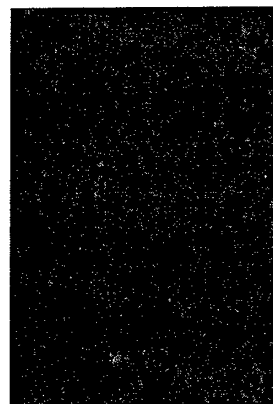
x200

Fig 6 Structure of the compact based on UD obtained in optimum conditions

X-ray analysis shows that the samples obtained in optimum conditions possess an ultradispersed structure with small amount of the graphite in the compacts.

Grain Boundaries and Properties of Alumina Ceramic.

L.L. Sartinska
Institute for Materials Science Problems, NAS of Ukraine, Kyiv, Ukraine.

Abstract.
A microstructure - properties study of the hot-pressed pure alumina materials and finegrained alumina matrix composites containing 5 wgt. % of nano-dimension nonoxide and oxide particles with different thermal expansion coefficients: SiC, Si_3N_4, SiO_2, ZrO_2 has been undertaken. The structure, hardness, fracture toughness, wet erosive wear and worn surface have been investigated. Dominant influence of hot pressing conditions on the properties of the produced materials has been demonstrated. It has been confirmed that composition and condition of the grain boundaries play an increasingly important role in nanomaterials, in correlation with their large volume fraction.

Introduction

Previous studies have demonstrated that wear behavior of pure polycrystalline alumina is strongly dependent on grain size and for a wide range of wear modes the rate increases significantly with increasing grain size [1,2]. However, because alumina is usually in the polycrystalline form, its properties are also influenced by grain boundaries that occur in the microstructure [3]. Thus, the present work presents the preliminary findings to investigate the pressing conditions, microstructures and physico-mechanical properties of ceramic nanocomposites.

Experimental procedure

Dense alumina materials of a range of grain sizes were produced from α-Al_2O_3 powder (Sumitomo AKP-50, Japan). 5 wgt% nanoparticles: SiC, Si_3N_4, SiO_2, ZrO_2 were incorporated into alumina. Discs were produced by hot pressing under pressure 20 MPa, temperature 1300-1700°C and time 8-211 min. Thermal etching of polished surfaces was carried out in air at 1470°C for 1 hour. Microstructures of thermally etched surfaces, worn disc surfaces and fracture surfaces were examined by scanning electron microscopy (SEM). Mean grain size was determined by the standard linear intercept method. Wet erosion was carried out in a modified high-torque attritor mill by special technique [1].

Results and Discussion

SEM examination of polished and thermally etched surfaces of aluminas hot-pressed at high and low temperatures, showed fairly equiaxed grains. Materials that have been hot-pressed at high temperature are developing grains of nonuniform size. Aluminas hot-pressed at low temperature have more uniform size and their porosity is distributed as intergranular micropores at grain boundaries, especially at triple points. Nevertheless, there is correlation between grain size, hardness, fracture toughness, wear rates of aluminas and temperature of hot-pressing. At low temperatures such correlation is not so obvious and materials with the same grain sizes can demonstrate different properties because of the influence of the large difference in dwell times of hot-pressing. It can be explained by long dwell time of hot-pressing or any annealing of hot-pressed materials which not only can increase grain sizes but also can help to get some changing (or ordering) grain boundaries [4], effecting of the resulting properties.

It has been demonstrated that aluminas hot-pressed at high temperature can contain pores inside grains due to grain boundary evolution and their fracture mode partially changes from inter- to transgranular. The worn surface had a very rough appearance with localized chipped area; the intergranular nature of the grain failure process in the rough regions can be seen. Presence chipped areas in rougher areas shows that transgranular failure takes place too.

Relatively smooth and finegrained structure of fracture surface of the alumina composite with 5 wgt% SiC demonstrates changes in morphology in contrast to the Al_2O_3 – 5 wgt.% Si_3N_4 composite that has rougher nonuniform structure of fracture surface with elongated grains and only partial transformation of the fracture mode from trans- to intergranular.

The worn surfaces of composites with different additives are strongly different. The best nanocomposite Al_2O_3 – 5 wgt.% SiC has an overall smooth appearance, that is a microscopically uniform surface, but with some localized very fine roughness covering up to 30% of the all surface (Fig. 1a). Addition of Si_3N_4 in alumina leads to a

338

very rough worn surface with some regions of grain pulled out by intergranular fracture, areas of plastically deformed material and particulate wear debris which have collected in recesses on the surface (Fig. 1b). The little difference of the thermal expansion coefficients for SiC and Si_3N_4 is not responsible for the better wear resistance of the first composite and for the worn surfaces in that case. Moreover, Si_3N_4 must produce additional strengthening due to the presence of elongated columnar grains in the matrix. However, the microstructure can not enhance wear resistance of the Al_2O_3 - 5 wgt.% Si_3N_4 nanocomposites. Very smooth, with fine structure response of composite material to wear by alumina grits on adding 5 wgt.% SiO_2 have been demonstrated. The occurrence of fracture due to strengthening all the grain boundaries and preventing of crack initiation became suppressed and the surface was plastically deformed instead. Perhaps, the reason is the strength of the grain boundaries of composition Si-C-O-Al which form in the material. The worn surface of alumina with 5 wgt% ZrO_2 is similar to the worn surface of coarse-grained pure alumina, but with significant increase in the proportion of the chipped areas.

All composite materials produced at the temperature 1700°C have the lowest wear rate when the dwell time of hot-pressing is short, leading to amorphous grain boundaries. By contrast, pure aluminas exhibit a decrease in the wear rate for low temperatures of hot pressing and long dwell times, resulting in ordered grain boundaries.

Conclusions

Hot-pressed alumina materials from high purity α-Al_2O_3 exhibit dominant influence of hot pressing conditions on the properties of the produced materials.

It has been demonstrated that aluminas hot-pressed at high temperature (1600-1720°C) can contain pores inside grains due to grain boundary evolution and their fracture mode partially changes from intergranular to transgranular.

The fracture mode changed from predominantly intergranular for the pure alumina to predominantly transgranular in some of the nanocomposites. The difference in the thermal expansion coefficients is not the main reason for this phenomenon.

The best composite material containing 5wt.% SiC particles exhibits transgranular fracture and

excellent wear resistance because the grain boundary composition is Si-Al-O-C. Other composite materials containing 5 wt.% Si_3N_4 or SiO_2 also exhibit predominantly transgranular fracture, but with a large proportion of intergranular cracking or with the plastically deformed surface, so their wear resistance is lower. Perhaps this is because the composition of grain boundaries does not include carbon. The composite materials produced at 1700°C have the lowest wear rate when the dwell time of hot-pressing is short, leading to amorphous grain boundaries. By contrast, pure aluminas exhibit a decrease in the wear rate for low temperatures of hot pressing and long dwell times, resulting in ordered grain boundaries.

References

[1] M. Miranda-Martinez, R.W. Davidge and F.L. Riley: Wear Vol. 172 (1994), pp. 41-48.

[2] R.W.Davidge, F.L. Riley: Wear Vol.186-187 (1995), pp.45-49.

[3] S. Blonski and S.H. Garofalini: J.Am.Ceram.Soc. Vol. 80 [8] (1997), pp.1997-2004.

[4] Lena.K.L. Falk: The 6th Conf. and Exh. of the Eur. Ceram.Soc. Vol.2 [60] (1999), pp.15-16.
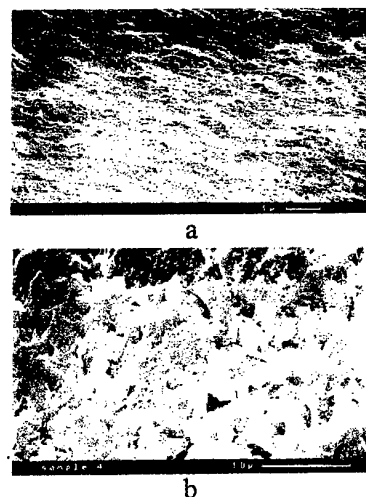
Fig. 1. SEM of worn disc surface of alumina composites: Al_2O_3 – 5 wgt.% SiC, Al_2O_3 - 5 wgt.% Si_3N_4 .

RESEACH OF THE INFLUENCE OF TECHNOLOGICAL FACTORS ON STRENGTH OF MATERIALS ON THE BASIS OF SILICON OXIDE

<u>G. Okhrimenko</u> [(2)], L. Dubikowsky

Institute for Problems of Materials named of Frantsevich of National Academy of Science, Kiev, Ukraine

[(2)] Institute for Problems of Strength Science NAS of Ukraine, Kiev, Ukraine

Problem definition. According to researches [1, 2]the Silicate materials on the basis of SiO_2 can be used for responsible constructions in the field of squeezing, as at small unit weight ρ, comparative small flexural strength σ_I, are characterized by a high compressive strength σ_c и and rather acceptable Young's modulus E and Puasson's coeficient μ for structural materials. The above mentioned datas are submitted at table 1 for six grades of materials. . The improving of operational properties of these materials has the important practical value. The present research is devoted to the given problem in connection with lack of similar information in the technical and scientific literature.

Brief information about technology of manufacture. The stock materials from a glass and glassceramic were gained from a melting of charge of a given elemental composition in electric furnaces by molding or by pressing on pneumatic presses in the metal shapes. Work material was annealed after congelation. After baking glassceramical workpieces were exposed to a heating in electric furnaces on particular mode due to what 70-80 % of crystals appeared in their structure. Stock material of chemically resistant solid porcelain (CRSP) were gained by casting of ceramic slurry (CCS) with moisture of 32...36 % in gypsum molds or shaping of crude mass (SGM) with moisture of 16...18 %.

Table 1. Physical - chemical properties of some technical glasses					
M*	ρ**,	σ_C, MPa	σ и, MPa	$Ex10^5$, MPa	μ
1	2,23	1580	57	0,91	0,20
2	2,52	1330	45	0,82	0,21
3	2,24	1300	64	0,71	0,16
4	2,53	2200	71	0,91	0,22
5	2,55	1200	56	0,69	0,26
6	2,45	1600	70	0,83	0,19

*) <u>Materials</u> : 1. Alumoborosilicate glass. **2.** Optical glass K-8. **3.** Glass MKR-1. **4.** Glass 13v. **5.** Glass S93-2. **6.** Sheet glass.

**) In kg/dm^3

Testing technique was described in researches [1, 2]. Samples Ø10x30 mm fabricated by diamond tool were tasted. The high of microasperity formulated $R_a \leq 0,63$ mkm on lateral area. Samples of TSM506 glass were exposed to a fluid temper after tooling [3].

The test data , their argument and deductions. The test data of four grades of material are submitted in tab. 2. Amount of sampling is designated as n_O, influence on strength on a concret technology factor - parameter γ_T, is equal to the attitude of samples strength, that are characterized by this factor and initial samples.For glass S93-2 and ceramicglass STL-10 initial samples fabricated from molten slabs were taken. As an estimation of influence on strenth on a structural state of glassceramic STL-10 boundary stress for glass S-57, from whish it is obtained was taken. As to CRSP it was initial strenth for samples cut out from workpieces obtained in casting of ceramic slurry in gypsum molds .

It follows from tab. 2 , that for a composition S93-2 the replacement of casting by molding is capable to increase strength on 35 %, while for STL-10 this increase has not exeeded 5 %. However transision to a crystalline structural state hase raised strenth almost on 50 %. The special attention is deserved to CRSP because manufacture of workpieces from crude mass promotes a strength improvement on squeezing almost on 60 %. The greatest relative increase of strenth (up to 80 %) was reached for a glass TSM506 after a temper in fluid PES-5. That circumstance deserves attention that a molding of workpieces from glassceramic STL-10, chaping from a crude mass CRSP, tempering in fluid promoted a decrease of selective coeficient of variation. In this connection we can mark that attitude of selective coeficients of a variation of glassceramic STL-10 strength bound, fabricated from moulded and molded stock materials has reached almost 3,5. Due to this the inferior boundary of a confidence interval of 340 ultimate strength essentially increases in samples

Table 2. The test data according to influence og technology factors on strength at an axial compression σ_C of silicatematerials

M*	T**	σ_C, MPa	v,%	n_O, piece	γ_T
Method of obtaining of stock material					
1	P	1200	8,5	10	1,00
	P	1625	13,2	20	1,35
2	P	2670	9,5	50	1,00
	P	2777	2,6	20	1,04
3	CCS	560	4,3	24	1,00
	SCM	880	3,7	30	1,57
Structural state of stock material					
2	A	1801	6,8	8	1,00
	CR	2700	6,0	267	1,49
Fluid temper					
4	IG	1225	8,5	20	1,00
	HT	2149	5,1	30	1,76

*) Materials : **1.** Glass S93-2. **2.** Glassceramic STL-10. **3.** CRSP **4.** Glass TSM506.
**) Tyechnology: C – casting. P – pressing. CCS-casting of ceramic slurry . SCM – shaping of crude mass. A and CR - amorphous и cristalline state. IG и HT – initial and heat-treated glass

The feature of studing material is presence in their composition K = 15 - 60 % SiO_2, and also A = 20 - 70 % of aluminium oxide Al_2O_3. In research [4] set that the strenth on axial compression depends on the content of above mentioned oxides and can be estimated on the following stating:

$$\sigma_C \approx e^{3,32}A^{0,98}; \qquad \sigma_C \approx \frac{e^{9,69}}{K^{0,79}}, \text{ where}$$

$e = 2{,}7128$ is basis of natural logarithm. The studyed materials are pespective for making responsible highly stresses workpieces such ascylindrical or spherical shells working at extremal pressure. Value of limiting forecast pressure of strenth σ_{CPR} according [5] it is possible to estimate from expression

$$\sigma_{CPR} = \sigma_{C}/\gamma_1/\gamma_2/\gamma_3\cdots\gamma_n,$$

here $\gamma_1...\gamma_n$ are relative coefficients of influence on strenth bound of used material similar to ours γ_T, stipulated by influence not only technological but also both constructural and operational factors.

Thus for increasing of bearing capacity at an axial compression of highly stresses workpieces on a basis of SiO_2, the materials with crystalline structure , for example, glassceramics are rational. Whenever possible it is nessesary casting to exchange by a molding , to make articles from CRSP and similar technical constructional ceramics preferably on the basis of crude mass at an oppotunity for glasses, to utillize a fluid temper. For surveyed materials the relative magnification σ_C due to surveyed technological reseptions thus makes from 5 up to 80 % and essentially depends on the content of silicon oxides and aluminium oxides. The boundary pressure loads in article from datas of materials are proportional to product of of its ultimate strength on coefficient of influence of technnlogical, design and operational factors.

Literature

1. Конструкционная прочность стекол и ситаллов/ Г.С.Писаренко, К.К.Амельянович, Ю.И.Козуб и др.- Киев: Наук. думка, 1979. - 284с.

2. Прочные оболочки из силикатных материалов/ Г.С.Писаренко, К.Амельянович, Ю.И.Козуб и др. - Киев: Наук. думка, 1989.- 224с.

3. Оценка влияния термической обработки на прочность стекла при осевом сжатии / Р.П.Келина, А.А.Андреев, Е.М.Ковалёва, Г.М.Охрименко // Пробл. прочности. – 1990. - № 8. – С. 112 – 115.

4. Влияние технологических факторов на прочность керамических материалов /К.П.Белоус, М.И Кушель, Ю.Н.Евплов, Г.М.Охрименко// Там же. – 1989. - № 2. – С. 42 - 49.

5. Дубиківський Л.Ф., Охріменко Г.М. Вироби із конструкційної кераміки в умовах стиску. – В кн.: Ceram-2001. Международная конференция "Передовая керамика – третьему тысячелетию. Тезисы докладов." - Киев, Украина. 5 – 9 ноября 2001 года. С. 166.

341

THE STRUCTURAL CHANGES in IRON at COOLING

Maiboroda V.P., **Adeev V.M.**, **Maksimova G.M.**, **Molchanovskaya G.M.**
I.Franzevich Institute of Materials Sciense Problems of National Academy of Scienses of Ukraine, Kiev, Ukraine

The exploitation of outer shells of space flight vehicles descends in conditions of leaps of temperatures. On the solar party the surface temperature of a stuff reaches 450K, and in shaded - 4K. The indicated temperature cycling can cause structural changes in metal and introduce the definite contribution in degradation processes of a surface of external parts of flight vehicles.

Earlier intercommunicated [1], that cooling of iron up to temperatures of fluid azote and helium originates dislocation processes. Accumulation of crystalline defects for a surface of a sample, specially around of actuations can be one of the causes of a level-by-level degradation of a metallical skin of a space engineering.

Research of similar processes [1] is conducted on refined to iron РЖ05 and on steel 05. The steel 05 is selected in connection by that contains in the volume enough impurities, which one can be utilised as the natural set dresser structural gradient. With the purpose decreasing of artefacts, bound with opening-up of a metal paper for a translucent microscope, the samples were mechanically thining in identical conditions. Then one part of samples were electrolytic thining, and its frame executed a role "of reset state". The second crew, before a final procedure electrolytic thining, was chilled in fluid azote with the subsequent heating on air up to room temperature.

In a fig.1, a, the substructure of initial iron РЖ05 is adduced, in which one are watched in the main single dislocations. After cooling, fig.1,b, quantity of dislocations increases sharply. The dislocation congestions will derivate type of cellular frames [2].

Change of morphology of a surface of a sample of steel 05 conducted in a Auger-microscope in vacuum 10^{-6}Pa. Diameter of a surface of a microsection made 3 mm and, after a polishing the sample was annealed in vacuum 10^{-3}Pa at the temperature of 1100^0C.

a
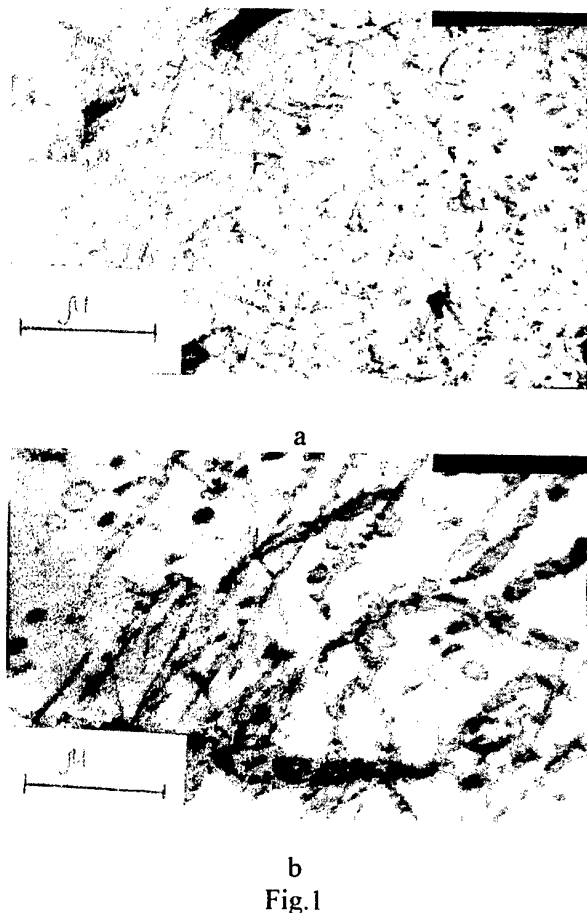
b
Fig.1

In a fig. 2,a, the reference surface structure of a microsection of an initial sample is adduced, which one practically did not vary both after maiden, and after the second -minute cleanings by ions Ag.

In a fig. 2,b, the map of the same place, but at the temperature of, close to -150^0C is adduced. Cooling and exposure (~30 minutes) are carried out in column of an Auger spectrometer. Before obtaining of a snapshot, fig. 2,b, the surface subjected to minute cleaning. The essential increase of density of pits, fig. 2,b, is a consequent of increase of density of dislocation congestions in iron at cooling and exposure. At the greater sanction of a snapshot, the fig.3, is visible, that the pits contain microactuations of impurity of metal.

342

a

b
Fig.2
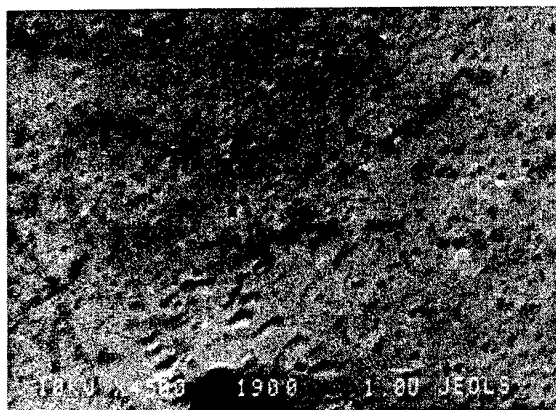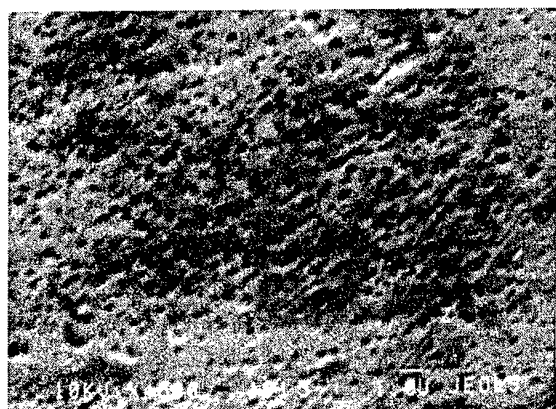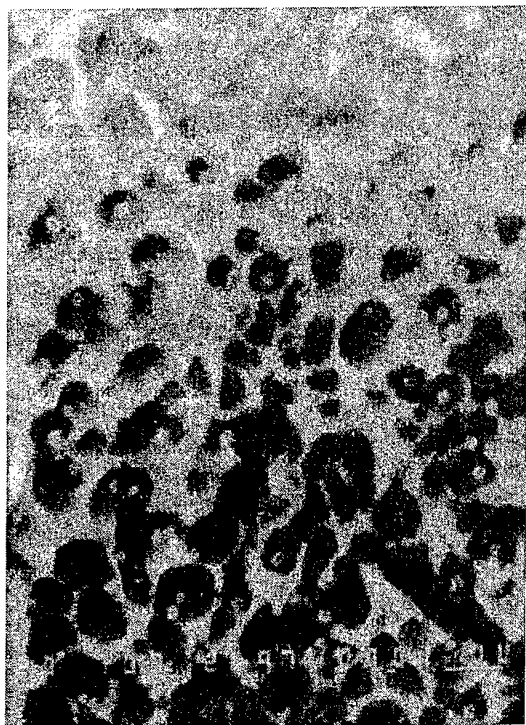
Comparing these data with outcomes, reduced in activity [1], it is necessary to mark their coincidence up to temperature of metal ~ (130-150⁰C). Therefore it is necessary to expect, that fall of metal temperature in conditions of actual space (4-10)K, will cause the formation including relief, reference twinning, which one arises at more steep cooling [1].

The obtained data testify, that steep temperature fall of metal of a surface of a skin of a space vehicle, availability of intrinsic contaminants and ionized radiation of space can essentially influence strengthening of degradation processes in conditions of outside space.

The literature
1. Maiboroda V.P., Maksimova G.A. Metals, №1, 1933, p. 117-121.
2. Trefilov V.I.//Moscow, Metallurgizdat. 1963.

Fig.3

PHASE FORMATION IN THE Si_3N_4-Al_2O_3-ZrN SYSTEM.

Khorujaya V.G., Martsenyuk P.S., Meleshevich K.A., Lysenko S.I., Fomichev A.S., Velikanova T.Ya.

Institute for Problems of Materials Science, NAS of Ukraine, Kiev, Ukraine.

Unique characteristics of SiAlON – based ceramics attract researchers' attention to it as a basis for development of new high – performance metal – ceramic materials of the Si-Al-O-N-Me class which are capable of operating under extreme conditions.

The aim of the present work is to investigate the interaction in SiAlON – based composites with an addition of the ZrN reinforcing phase during hot pressing and to determine the factors promoting an increase in some mechanical properties.

Using the methods of differential thermal analysis (DTA) and X-ray diffractometry (XRD), the character of interaction in the composites of five–component Si-Al-O-N-Zr system, in particular in its element Si_3N_4-Al_2O_3-ZrN and the forming pseudobinary Si_3N_4-ZrN, Si_3N_4-Al_2O_3 and Al_2O_3-ZrN subsystems, is established.

Literature data concerned the Si_3N_4-Al_2O_3-ZrN system are unavailable. As to the forming pseudobinary systems, it is known that as a result of the interaction of Si_3N_4 with Al_2O_3, the following exchange reaction occurs: $Si_3N_4 + 2Al_2O_3 \leftrightarrows 4AlN + 3SiO_2$ [1]. The intermediate products of the reaction are mullite $3Al_2O_3 \cdot 2SiO_2(M)$, X-phase $Si_4Al_4O_{11}N_2$, oxynitride Si_2N_2O and five AlN polytypes. DTA of green compacts of the concerned subsystem which were subjected to heating up to 1870°C and cooling to room temperature shows the effects corresponding to the formation of SiO_2 and the X-phase. XRD analysis of the sintered samples detected the presence of β-SiAlON, SiO_2 X-phase and mullite. Therefore, our data are in full agreement with the data of the investigation [1].

During studying of the interaction in the Si_3N_4-ZrN system it has been shown by us for the first time that heating of the samples in the DTA unit up to 1850°C with the subsequent cooling to room temperature leads to free silicon (which is a product of the Si_3N_4 dissociation) reacting with ZrN. The latter results in the formation of $ZrSi_2$ which is determined via XRD analysis. During cooling $ZrSi_2$ forms a eutectic with the unreacted silicon, $ZrSi_2 + Si$ (1340°C).

DTA of the Al_2O_3-ZrN subsystem composites carried out by us for the first time has shown that in heating them up to 1900°C with subsequent cooling to room temperature on heating curves an exothermic effect is observed corresponding to the allotropic transformation in Al_2O_3 as well as the effects at 1705, 1840 and 1860°C. XRD analysis of the samples which were sintered in the DTA unit indicates that ZrN, α-Al_2O_3 and ZrO_2 (impurity in the starting ZrN component) are present in them. It follows from that that the effect at 1860°C corresponds to the ($Al_2O_3 + ZrO_2$) eutectic. The effects at 1705 and 1840°C similarly to a known system Al_2O_3-TiN are interpreted by us as corresponding to the formation of spinel (AlON) and melting of its eutectic with Al_2O_3.

DTA and XRD analyses of the Si_3N_4-Al_2O_3-ZrN system composites indicate that the same processes take place in this system as in its limiting pseudobinary systems. However, depending on the content of the component in the composites particular processes prevail. For instance, in the $40Si_3N_4$-$10Al_2O_3$-50ZrN (mol. %) composite heated up to 1862°C, the formation of zirconium disilicide and the ($ZrSi_2 + Si$) eutectic is determined, whereas in the $25Si_3N_4$-$50Al_2O_3$-25ZrN (mol. %) composite heated up to 1900°C apart from the described processes the effects corresponding to the formation of spinel and the ($AlON + Al_2O_3$) eutectic are registered on the heating curve.

Thus, it has been established for the first time, that in the Si_3N_4-Al_2O_3-ZrN system during hot pressing of the composites the following phases form: SiO_2, AlN, X-phase, mullite, $ZrSi_2$ and spinel. The amounts of these phases depend on the starting composition of the composites. The effects corresponding to the eutectics $L_1 \leftrightarrows Si + ZrSi_2$ (1340°C) and $L_2 \leftrightarrows Al_2O_3 +$ spinel (1840°C) are also registered on the heating curves.

1. Gauckler L.J., Lukas H.L., Petzow G.J. Contribution to the phase diagram Si_3N_4-AlN-Al_2O_3-SiO_2 / J. Amer. Cer. Soc., V. 58, No 7,8, 1975. – P. 345-347.

MICROSTRUCTURE OF CrSi₂ AMORPHOUS-CRYSTALLINE THIN FILMS

Dvorina L.A., Dranenko A.S.
Institute for Problems of Materials. Ukrainian Academy of Sciences Kiev, Ukraine

Thin films of chromium disilicide have attracted attention because of their unique combination of electrophysical properties, increased stability under temperature gradient, mechanical stresses, aggressive media. Thin films of chromium disilicide solid solutions have been intensively studied from both fundamental and applied points of view, due to their important application in very large integrated-circuit technology as metallic materials for gate electrodes, interconnection and surface resistors in hybrid integrated circuit, sensor and other. In this work we present the results of evolution parameters of microstructure in amorphous-crystalline films in thickness range 20-80 nm.

The films were prepared by the ion-plasma method sputtering chromium disilicide targets, produced by hot forming powder CrSi₂. The residual gas pressure was about 1×10^{-4} Pa, and the pressure of argon during deposition was 4×10^{-2} Pa. At a target voltage of 1 kV and a target current of 50 mA, the film thickness was 10-100 nm.

To investigate the structure by transmission electron microscopy, the films were condensed on (100) surface NaCl, from which they were separated by distilled water and supported by grids of copper or molybdenum. Resistivities were calculated from the sheet resistance, measured with a foir-point probe method. The sample composition was controlled by a standard Auge-sputter depth-profiling technique, which combined argon-ion milling technique with Auger electron spectroscopy (AES) and SIMS. Ellipsometric measurements were made with ellipsometor LEF-2. The light source was He-Ne laser (λ =632,8 nm).

Films deposited at T_s = 333 K are amorphous. The transmission electron micrograph shows a fine – grained contrast which is typical of amorphous structures. It is shown, that films deposited on the substate at T_s = 573 K have amorphous and crystalline phase. For annealing temperatures >973 K the amorphous films crystallized into polycrystalline hexagonal phase CrSi₂ type (C40) [1]. Transition from amorphous to crystalline phase take place on the narrow temperature range as shown in fig 1. AES and SIMS depth profiles
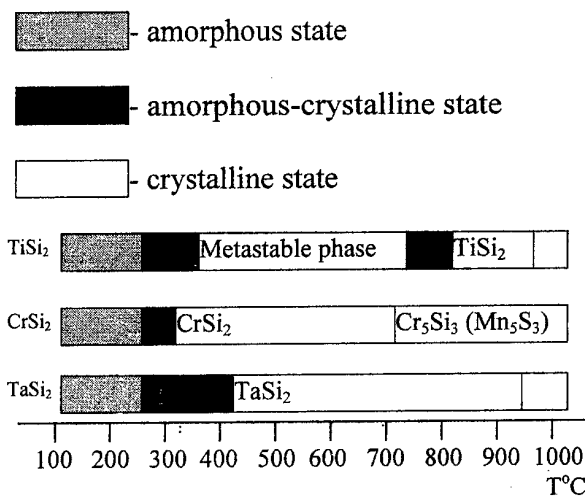
Fig.1. Diagram of phase transitions on crystallization of disilicides in thin films.

showed uniform distribution metal and silicon throughout the film thickness, and its ratio corresponded to target compositions. In all samples, carbon with some oxides (<1,5 nm) was detected on the surface, presumably in form of native silicon oxide. The oxygen concentration in the layer is normally not uniform in depth. No other contamination was found.

The studies of microstructure are an important stage of material research. The knowledge about the relationship between the parameters of structure and properties is necessary for the development of advanced ceramic thin films. For this purpose the quantitative analysis of structure is used as a significant research tool. This work aimed at the application of computer aided quantitative analysis for the description of microstructure of amorphous-crystalline thin films.

In the quantitative analysis of amorphous-crystalline thin films the following microstructural parameters were determined:

D_f - Feret"s diameter,

Θ - volume fraction of phase, $\Theta = S_p / S_o$ (S_p - surface crystalline phase, S_o -surface window of measurement),

N_Θ - specific number of grains,: $N_\Theta = N / S_o$;

L – mean chord of grains, $L = 4\Theta/S_v$; (S_v - spesivic surface of grains),

345

t – mean intergrain distance, $t = 4(1-\Theta)/S_v$;

F_c - factor configuration of grains, $F_c =2(\pi S)^{1/2} /P$ (S – surface of grain, P – perimeter of grain).
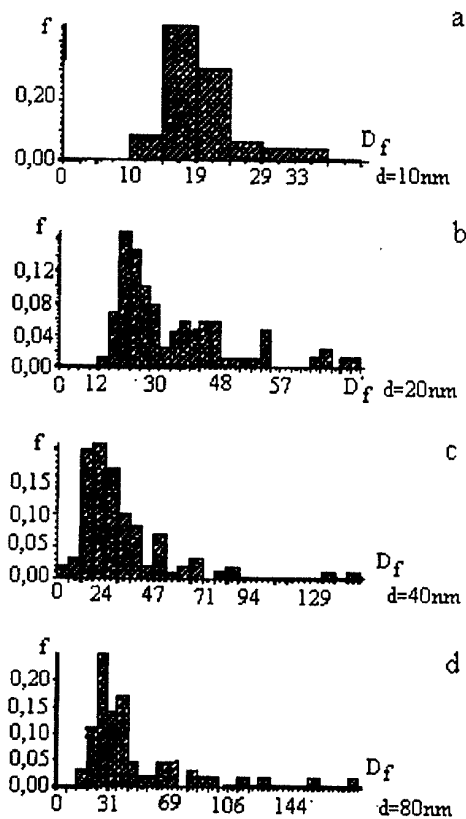
Fig.2. Histograms of Feret"s diameters for $CrSi_2$ amorphous-crystalline films for variety thinks: a - d=10 nm; b - d=20 nm; c - d=40 nm; d=80 nm.

Fig.3. Thickness dependence of microstructure parameters of $CrSi_2$ amorphous-crystalline films:a- Feret"s diameter, b- mean intergrain distance (1) and mean chord of grains {2}, c- volume fraction of phase (3) and specific number of grains (4).

In Fig.2 the examples of distribution of Feret"s diameter of crystalline phase are shown. It should be noticed that the histograms are stretched in right-hand. Thickness dependence of lines, volumes and configuration parameters of crystalline and amorphous phase of microstructure of $CrSi_2$ thin films thus calculated are shown in Fig.3. Mean intergrain distance of crystalline phase and its specific number are decrease with the growth of films thickness. Experimental results were calculated in terms of Skorochod"s theory [2]. Using relations from this theory of volume characteristic of crystalline phase [3], we have obtain the evolution of microstructure from matrix to matrix-statistic type which happen stipulate crystallization effect in the process of film setting, coalescence isolated standing by crystalline and "caking" of contacting particles.

1. L.A.Dvorina, I.V.Kud, G.Beddis Regularities crystallization of thin films of transition metals disilicides // Powder metallurgy.-1987.-1.-P.81-84.
2. V.V. Scorochod Theory of physical properties of pocket and composition materials and regulation principles of microstructure in technological operation //Powder metallurgy-1995.-1/2.-P.53-71.
3. A.S.Dranenko, L.A.Dvorina, O.I.Gatman Thickness dependency of microstructure characteristiks of $CrSi_2$ thin films, Powder metallurgy //-2001.-5/6.-P.112-116.

346

RESEARCH OF STRUCTURE AND PROPERTIES OF THE CAST MODIFIED ALLOYS OF SYSTEM Cr-Re-La.

Pisarenko V., Kusnetsova T., Rogul T., Sameluk A.
Institute of problems of Materialsciens NAS of Ukraine, Kiev, Ukraine.

The necessity of significant increase effectiveness of the power blocks in the Ukraine, and also revival of an air space-rocket industry requires creation the new generation of high-temperature alloys and heat-resistant alloys, and also their manufacturing technologies. The perspective decision of this problem is use of high-temperature alloys and heat-resistant alloys on basis of chromium. For example it can be used to produce locks of the vanes which could work at temperatures up to 1573 K. The Cr-Re-Ti-La system can be discussed as a suitable alloy.

The temperature of cold brittleness of such alloy is below room temperature, the temperature of recrystallization of the deformed metal is about 1573 K, tensile strength in the deformed state reach almost 250 MPa at1573 K, but the "viscous" intergranular breaking tendency in a cast state at test temperatures higher than 1373 K is a serious difficulty to its use. First of all, it is connected with increased alloys impurity by the implantation impurity and low cast quality of alloys. Besides, the electric arc melt of this system is incomplete, because the melting temperature of the rhenium is almost 3570 K, and the chromium melting temperature - 2090 K, therefore there is always probability of detection some slice of the unfused metal in the alloy. This problem also adds the question of the decreasing contamination by the powder rhenium implantation impurity, because there is 0.2-0,25 % wt in a condition of delivery content of carbon in rhenium Re-2 and as the alloys Cr-Re consist up to 40% weight of rhenium the consequence is that content of impurity introduction (carbon) is more than limiting value, because it cause significant increase of cold brittleness temperature (almost up to 473 K).

The carried out physic-chemical researches and thermodynamic calculations have shown, that the reduction of carbon in rhenium powder is possible in high vacuum (10^{-2}-10^{-3} Pa) processing at temperatures above 1773 K at the expense of the carbon evaporation. It is established that the annealing at temperatures 1673-1773 K allows to reduce the carbon weight from 0.25 % up to 0.02-0.01 %. There is no problems with oxygen because the oxide Re_2O_7 already evaporates at temperature 560 K. At the same time the accounts have shown,

that there is an opportunity to decrease contents of the carbon at much lowest temperatures (1073-1473 K) by the simultaneous expense dioxidation and carbon removal at reaction

$$Re_2O_7 + C = 2ReO_3 + CO$$
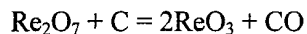
At these temperatures the products of reaction can evaporate easily. This assist increasing kinetics of process at the expense of optimum stock porosity. There for was explored the possibility of pressing rhenium powder together with the chromium mark ERC in order to further annealing pressed material in vacuum and exploring their use in melt abilities. It was investigated and established the optimum pressure at pressing compacted stocks and temperature of its annealing. Experimental melt Cr-Re alloys was carried out in vacuum-arc furnace in copper crater of 50mm diameter. The researches have shown that melting of common pressed compact stocks of system Cr-Re was more technological, melting stocks occurred smoothly, without additional superheating and with small losses of metal.

At melt of ingots by an electric arc method their crystallization occurs in very adverse conditions. The results are both the rather large size of grains and their non-uniform growth in various directions. Taking into account, the fact that in fine crystalline deformed state is absent the propensity to high-temperature "viscous" intergranular destruction a temperature of test up to 1573 K was put a task to receive a uniform fine grain in a cast state. It can be reached only by casting the metal in the copper chill. But attempts to pour out the metal in the chill were unsuccessful because the metal quickly transformed into a mix of liquid and crystal particles even at essential superheating. The study has shown the temperature interval of the Cr-Re system crystallization is very large ((t_{sol} = 2178 K, t_{liq} = 2253 K) that has a negative effect for cast properties of an alloy.

For reduction the temperature interval of crystallization and increasing the cast technological properties of these alloys the titanium has been choose as alloying component. The insertion of titanium into alloys enables to narrow an interval of crystallization till 10-15 K, and considerably to increase the fluidity of alloys. The titanium is very active carbide forming element which clear an

alloy from the carbon as well. We hope that the particles of the titanium carbide will crystallize first of all, which can be as additional centers of crystallization (modified alloys), creating the preconditions for the fine crystalline structure. Besides this in according to the phase diagram Ti-Re the titanium solubility into the rhenium is very insignificant, so there is a possibility of formation the intermetalic compound Ti_5Re_{24} at high temperatures which can create additional centers of crystallization also (melting temperature of the Ti_5Re_{24}-3023K).

The implantation of the titanium into the alloy in insignificant quantity (0.2-0.3% weight) leads to the melted metal cast into the chill very

easily. In addition the crystallization is extremely uniform with fine crystalline structure. In this case the size of grains is within the limit of 25-40 microns arise unlike the usual electric arc melt which produce grains size of 0.5-2 mm.

The structural researches have shown that it was impossible to clear completely the borders of crystalline grains from harmful impurity. The electron-microscopic researches have found out both slag impurities and other cast inclusion. It can testify about the insufficient size of the cast feeder head. There for at melting and casting the very pure alloys should be paid attention to the cast technological process features.

The mechanism of structure formation of titanium – carbide chromium with high wear - resistance

A.M. Petrova

Institute for Problems of Materials Science of NAS of Ukraine, Kiev, Ukraine

The material Ti - Cr - TiC, having increased wear- resistant on air is known at friction without greasing in pair with chilled steel , and steels after of borating , siliconizing, chromizing (hardness up to 60 HRC).

In the given work the mechanism of structure formation of a material of composition Ti - Cr - TiC, received as a result of reactionary interaction of components of charge Ti – Cr_3C_2. The research was carried out on extrusion samples made of from powders of electrolytic titanium and carbide chromium of fractions accordingly - 0,25 and -0,056 mm, annealing in vacuum 0,13 Па during 15, 30, 60, 90,120 mines.

The process of dissolution of carbide chromium particles in titanium is investigated on the basis of research of redistribution of making components in dissolved carbide to a particle and basis annealing titanium of a material. With this purpose was carried metallography research on raster electronic microscope JSM – U3 and x-ray microanalyzer "«Самеса". The use of raster microscope has allowed to lead three-dimensional research of separate phases or site of sample, and the application of the adaptation to microscope - x-ray spectrometer - has enabled to receive the electronic image dissolved of a particle carbide chromium with a x-ray picture of distribution in it Ti, Cr, C .

The contents titanium and carbon in a basis of new phase formed around of initial carbide as the shell, is shown, than in dissolved carbide chromium particle are much above. The curve of distribution of chromium shows his high contents in an initial particle, sharp decrease in the formed shell of a new phase and presence it in a basis. I.e. on a place of an initial arrangement of a particle carbide chromium is present chromium, around of which the phase carbide titanium was formed. Chromium and the carbon contains also in titanium to a basis. The application of the x-ray microanalyzer "«Самеса" has allowed to define

the contents Ti, Cr, C in separate structural components and to establish comhjsition of formed phases that depending on the size of inclusions initial carbide chromium (0,01- 0,05 mm).

Is established, that the dissolution of particles carbide chromium is accompanied at first diffusion of carbon, and after that chromium in titanium. In result diffusion goes leaning carbide Cr_3C_2 on carbon with transition it in the lowest forms Cr_7C_3, $Cr_{23}C_6$, and then chromium. Carbon diffuse in titanium with formation carbide titanium stechiometric of composition TiC, chromium - with formation of a solid solution in titanium.

The research of structure and microhardness of phases annealing of samples has shown, that diffusion of carbon in titanium accompains of formation of solid solution in titanium the carbon in the beginning around of initial carbide of inclusions , then there is a redistribution it on borders of particles titanium, as to the most defective and close located places to dissolved carbide chromium, and, at last, as a result of aspiration of system to an equilibrium status, on borders of grains titanium and in their volume.

At cooling from supersaturaton of a solid solution titanium - the carbon is allocated carbide titanium stechiometric of composition TiC, the form and place which arrangement depends on annealing time and redislocation of carbon in a basis: as the shell around of initial carbide inclusions, continuous strips superpose of crystals on borders of particles titanium, separate fine rounding of inclusions on borders of grains of titanium basis. Chromium diffuse in titanium after carbon and also forms a solid solution titanium – chromium.

The structure containing plastic titanium – chromium basis, in which the fine even inclusions carbide titanium are in regular intervals distributed, responds a principle of creation wear - resistant materials which have received the name « a rule Charpi« (a plastic matrix - firm inclusions).

THERMODYNAMIC PROPERTIES OF LaNi$_{5-x}$Co$_x$ ALLOUS IN THE WIDE TEMPERATURE RANGE

N.P. Gorbachuk, A.S. Bolgar, V.B. Muratov, A.A. Skrypai, M.V. Karpets
I.N. Francevich Institute for Problems of Materials Science, National Academy of Science of
Ukraine,Krzhyzhanovsky Str., 3, 03680 Kiev, Ukraine

Intermetallics LaNi$_5$ is widely known due to extreme opportunities is convertible to absorb hydrogen in significant quantities (6-7 atoms per formula unit) at temperatures close to room. However equilibrum pressure in system LaNi$_5$-H$_2$ makes about 3 atmospheres, that essentially reduces opportunities its practical application. Doping LaNi$_5$ by other transitive metals allows to operate process of hydride formation without deterioration its absorbtion of properties. For example, for an alloy LaNi$_{4.5}$Mn$_{0.3}$Al$_{0.2}$ the equilibrum pressure at room temperature managed to be lowered to 0.2 atmospheres [1]. The thermodynamics is one of the fundamental approaches by development of the theory of management hydrogenation. At the same time of items of information on thermodynamic properties of alloys on a basis LaNi$_5$ in the literature are absent.

The purpose of the present work was the research heat capacity and enthalpy of LaNi$_{5-x}$Co$_x$ (X=0; 0.5; 1.0; 1.5; 2.0; 2.5) alloys in the temperature range 55 – 1500 K. The intermetallides under study were produced from lanthanum, nickel and cobalt (99,8 %) by arc melting with tungsten nonconsumable electrode in purifild argon.

Heat capacity at 55 – 300 K were measured by adiabatic calorimetry method with periodic input of heat on low temperature standard thermophysical unit [2], and enthalpy - by drop calorimetry method on high-temperature differencial calorimetry [3]. The error of the heat capacity measurement not to exceed 0,4 %, and of enthalpy - 1,5 %. The experimental data (fig.1) of heat capacity smoothed out by a method of sliding approximation by the cubic multimembers with weight factors [2].

To obtain main thermodynamic functions under standard conditions the experimental data on the low temperature heat capacity for the alloys studied were extrapolated to 0 K using equation of follows [2]:

$$C_P^0(T) = \gamma \cdot T + D\left(\frac{\theta_D}{T}\right) + \sum_{i=1}^{n-1} E_i\left(\frac{\theta_{Ei}}{T}\right), (1)$$

were γ is coefficient of electron heat capacity, $D\left(\frac{\theta_D}{T}\right)$ and $E_i\left(\frac{\theta_{Ei}}{T}\right)$ is Debye and Einshtein heat capacity, respectively, n is numbers of atoms in the substance formula.

Fig.1. Low temperature heat capacity for LaNi$_{5-x}$Co$_x$ compounds

○ X=0   ● X=0.5   × X=1.0   ■ X=1.5   □ X=2.0   ▲ X=2.5
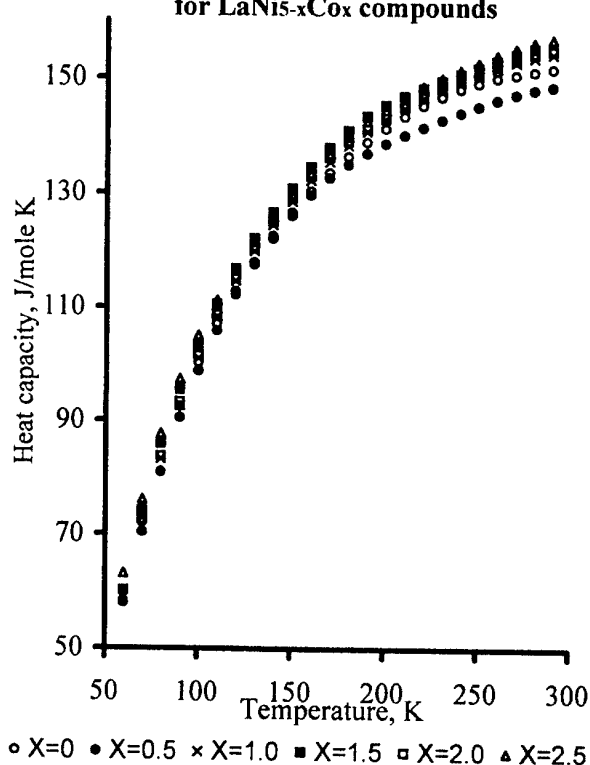
The enthalpy (J·mole^{-1}), heat capacity, entropy and Gybbs's energy (J·mole^{-1}·K^{-1}) of LaNi$_{5-x}$Co$_x$ alloys at 298,15 K were obtained: 31383; 152,26; 211,4; 106,1 (LaNi$_5$); 30970; 149,04; 211,6; 107,8 (LaNi$_{4.5}$Co$_{0.5}$); 31942; 154,70; 219,0; 111,9 (LaNi$_4$Co); 32408; 156,76; 222,5; 113,8 (LaNi$_{3.5}$Co$_{1.5}$); 32195; 155,27; 224,1; 116,1 (LaNi$_3$Co$_2$); 32461; 157,2 220,9; 112,0 (LaNi$_{2.5}$Co$_{2.5}$).

Experimental data (fig.2) of the alloys studied enthalpy (J·mole^{-1}) in the temperature range of 298,15 – 1500 K were approximation using Mayer – Kelly equation:

$$H^0(T) - H^0(298,15K) = A\cdot T^2 + B\cdot T + C\cdot T^{-1} + D (2)$$

At confidential probably 0,95 values of enthalpy, designed on (2), are characterized by an average relative confidential interval not to exceed 1,5 %.

Proceeding from (2) the temperature dependencies of heat capacity, entropy and Gybbs's energy ($J \cdot mole^{-1} \cdot K^{-1}$) function are as follows:

Fig.2. Experimental data for enthalpy of LaNi₅₋ₓCoₓ alloys

$\triangle$ X=0 $\square$ X=0.5 $\blacktriangle$ X=1.0 $\circ$ X=1.5
$\times$ X=2.0 $\bullet$ X=2.5
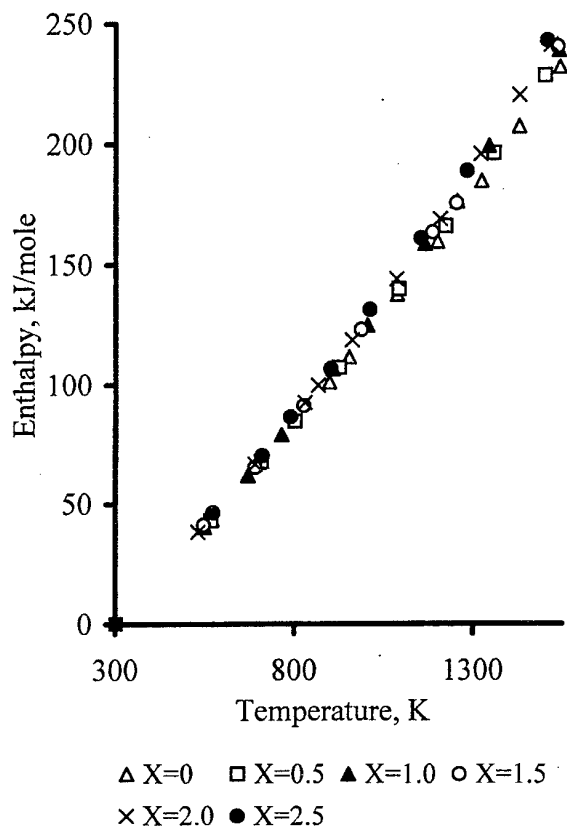
$$C^0{}_p(T)=2 \cdot A \cdot T + B - C \cdot T^{-2} \qquad (3)$$
$$S^0(T)=2 \cdot A \cdot T + B \cdot \ln T + 0,5 \cdot C \cdot T^{-2} + E \qquad (4)$$
$$\Phi'(T)=A \cdot T + B \cdot \ln T - D \cdot T^{-1} - 0,5 \cdot C \cdot T^{-2} + (E-B) \quad (5)$$

Coefficients of temperature dependences (2 – 5) were calculated by the least square method using two boundary conditions, i.e. zero value of enthalpy at 298,15 K and standard value of allow heat capacity to provide agreement between high and low temperature heat capacity values. The parameters A,B,C,D,E are equal, respectively: $23,60 \cdot 10^{-3}$; 142,94; 422020; -46130; -619,5 (LaNi₅); $28,23 \cdot 10^{-3}$; 139,09; 611006; -42029;- 601,2 (LaNi₄.₅Co₀.₅); $30,05 \cdot 10^{-3}$; 138,00; 101068; -44155; -585,9 (LaNi₄Co); $27,69 \cdot 10^{-3}$; 142,97; 302063; -46100; -610,3 (LaNi₃.₅Co₁.₅); $31,73 \cdot 10^{-3}$; 140,10; 332457; -45706; -594,9 (LaNi₃Co₂);

$34,40 \cdot 10^{-3}$; 138,12; 126669; -44664; -587,3 (LaNi₂.₅Co₂.₅).

Heat capacity at low temperatures is determined on the one hand by insignificant shift phonon mode on frequency in result doping, with another - presence of magnetic transition peculiar of cobalt compounds. As shown in [4], the Curie temperature grows in process of increase of the contents cobalt from 20K for LaNi₄.₅Co₀.₅ up to 400K for LaNi₂.₅Co₂.₅. Heat capacity of this alloy has the greatest meanings owing to superfluous absorption of heat on destruction of the magnetic order.

At higher temperatures, when phonon spectrum is completely exited also magnetic transitions are completed, the important role is played by(with) changes in elastic - dynamic characteristics at doping LaNi₅ by cobalt, and also electronic specific heat. In [5] is shown, that the high meaning of factor electronic specific heat LaNi₅ is completely determined in densities of states N(e) $5d^1$ of a zone La close Fermi level and the power structure of this zone is given. Increase heat capacity of alloys LaNi₅₋ₓCoₓ in proportion to parameter x can be quite connected to shift of a Fermi level in the party of more dense condition in a zone of conductivity.

REFERENCES

1. Filatova E.A., Yacovleva N.A., Semenenko K.N / The calorimetry investigation intermetallic compound of LaNi₄.₅Mn₀.₃Al₀.₂ with hydrogen (in Russian) // Westnic MGU. Hymiya.- 2000.- **41**, №5.- p. 331-334;
2. Bolgar A.S., Krykla A.I., Suodis A.P. / Low Temperature Heat Capacity of Praseodymium, Neodymium and Samarium Sesquicarbides (in Russian) // Zh. Fiz. Chim.- 1998.- **72**.- p. 439-443;
3. Bolgar A.S, Gorbachuk N.P, Blinder A.V / Enthalpy of Gd₅Si₃, Gd₅Si₄, GdSi, GdSi₁.₈₈ in Temperature Range 298.15 – 2200 K. Enthalpy of the Melting (in Russian) // Teplophiz. Visok. Temperatur.- 1996.- **34**.- p. 541-545;
4. Van Mal H.H., Buschow K.H.J. and Kuijpers F.A. / Hydrogen Absorbtion and Magneic Properties of LaCo₅ₓNi₅₋₅ₓ compounds // J. Less.-Comm. Metals.- 1973.- **32**.- p. 289-296;
5. Wallase W.E. / Bonding of Metal Hydrides in Relation to the Characteristics of Hydrigen Storage Materials // J. Less.-Comm. Metals.- 1982.- **88**.- p. 141-157.

POWDER POROUS TiNi MATERIAL WORKING IN EXTREMAL CONDITIONS OF VOLUME SELFDEFORMING

Solonin Sergey M., Kolomiets Lyudmila L.
Institute for Problem of Material Sciense NAS of Ukraine, Kiev, Ukraine

Powder intermetallic compounds titanium nickelide possessing save memory and super-elasticity properties must work in particular conditions of the considerable volume self-deforming under influence of the martensitic transformation. It is difficult problem creating strong undestroyed powder carcasses.

Synthesis TiNi results from combining the pure elemental metal powders by powder metallurgy method has produced by many authors, but they have obtained mixture of the intermetallic phases TiNi, Ti_2Ni, and Ti_3Ni. The goal of homogeneous TiNi would seem to be difficult to achieve because titanium and nickel-rich phases existed in addition to the TiNi phase although they showed a tendency to shift further toward the TiNi single phase when heat treatment as applied to effect homogenization.

The second method used for the production of porous nitinol is self-propagating, high temperature synthesis. The technology of this method is based on utilization of the exothermic heat of formation upon interaction of various elements. But this porous material contained both TiNi and Ti_2Ni phases.

Another method of powder metallurgy is proposed to produce homogeneous one phase powder porous TiNi in this work. Produced TiNi by this method allowed also to increase the reversible deformation up to 20-30%, to extend the temperature range of phase transformation up to 300^0C, to assure the manufacturing of parts of complicated shape without mechanical processing.

It was studied the characteristic temperature of martensite transformation in porous TiNi.(fig.1). It is seen the range of martensite

transformation in powdered TiNi is about 300^0C. This means the our TiNi to be two-phase at room temperature and lower one: both austenite and martensite are present. This, in turn, stands for after deformation at those temperature the material will reveal both super-elasticity and shape memory phenomena, thus making the powdered TiNi more universal in application.

It was established the character of dependencies of reversible deformation and height recovery degree for sintered porous material.
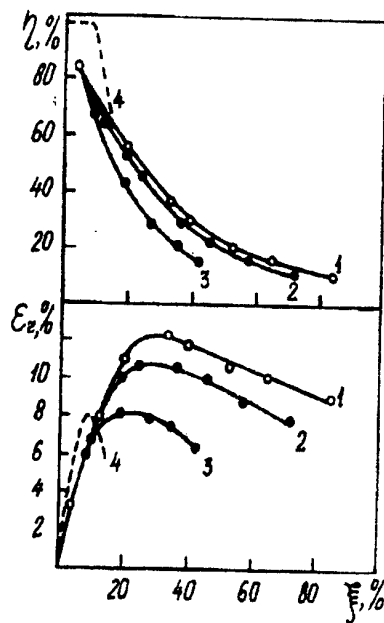
Fig.2. Height recovery degree (η) and reversible deformation (ε_r) for sintered specimens with different porosity: 50%(1); 43%(2); 30%(3) vs. direct deformation (ξ) under uniaxial compression. The dotted curve is the same for nonporous TiNi under tension.

The curves are obtained from the data of height change of the sintered specimens under loading and unloading. The maximum value and its position are changing with the sample porosity, increasing in both coordinates for higher porosity. These curves are formed as a result of common contribution of two deformation channels. One of them is martesitic deformation, which provides an increase of the reversible deformation, and the second is the deformation in accordance with traditional mechanisms of plastic flow, which
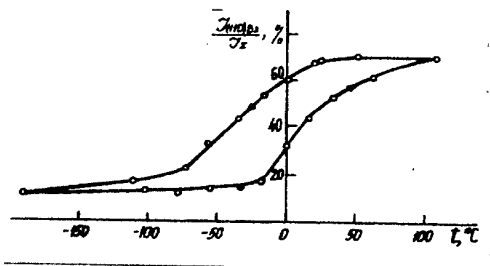
Fig.1. The hystheresis curve of martensite transformation for TiNi powder. The ordinate shows an amount (%) of high-temperature ("austenite") phase B2.

decreases the reversible deformation. This is also a reason of decreasing of the recovery degree. So We have established the following characteristic features of shape memory and super-elasticity effect during one-time loading of the porous TiNi associated with heterogeneous deformation of porous bodies: shape recovery degree not achieving 100%: back deformation of the porous TiNi materials significantly exceeding that of nonporous materials; the maximum on the back deformation curve as a function of that of the direct one shifting to the region of the higher values of direct deformation.

In case of a repeated loading of the porous TiNi materials, the following peculiarities of the super-elasticity effect realization were distinguish: occurrence of significant delay in shape recovery during the first cycle as compared with other cycles; repeated loading with the same load value causing further material densification which ceases with the increase of the number of cycles; practically complete deformation reversibility achieved after 10 loading cycles.

It was shown the powder porous TiNi produced by special method has the developed coral-like particle shape. The usage of such
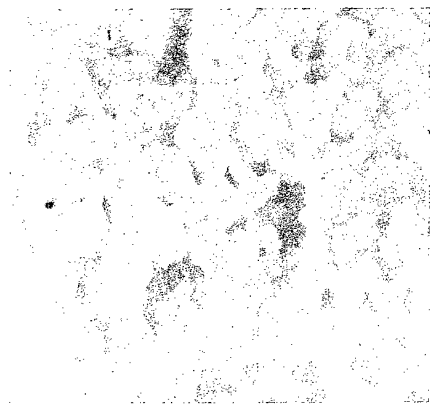
Fig.3. Porous structure of samples from coral-like powders with developed surface. (x200)

powders permitted to produce the porous structure of compacts with two sizes pores: fine pores inside the powder particles and coarse interparticle ones. Such a structure assures the effective dissipation of vibrations and high damping properties.

The practical meaning of proposed work consists in that new sort of functional material TiNi manufactured in the porous version is universal material as it has wider interval of permissible strengths and deformations than cast TiNi. It is also established porous TiNi possess the

volume memory effect and higher damping properties.

TiNi is known as the material with high damper properties due to effective dissipation of vibrations on the interphase "austenite – heat temperature elastic martensite" boundary. In proposed porous TiNi materials (porosity is 30-50%) besides microstructure level of damping more powerful macrostructure level works dissipation of vibrations on the pore free surface and inter-particle contacts. That allowed not only increasing the coefficient of damping by 100 times but also to wider significantly amplitude-frequency interval of effective damping. Such material is prospective for the development of the effective vibroinsulating systems for cryocoolers and optical platforms in airspace and for using as damping layers for cutting instruments from superhard ceramics.

Some constructions of the tank dizel engines need the effective thermal compensators for assembles of jet joining. Porous TiNi material permits to replace large and less reliable buffer cast springs due to super-elasticity effect.

Due to its high hardness TiNi material possesses also high wear resistance. Such materials for tribotechnical using in the conditions of friction without lubricant may be created on the porous TiNi basis both as details and as plasma coatings. Specifics of wear-resistant friction in the extreme conditions is caused by deformative properties of porous surface which is reversibly restored after removal loading without wear due to shape memory and super-elasticity effects. Besides, its contribution in the process of wear-resistant friction process is to bring in also the damping ability of the porous TiNi surface.

SOME FEATURES OF PREPARATION OF MAGNESIUM DIBORIDE

Marek E.V., Ljashenko V.I., Klochkov L.A., and Makarenko G.N.
Institute for Problems of Materials Science, NAS of Ukraine, Kiev, Ukraine

In the Mg – B system, the existence of four boride phases, namely, MgB_2, MgB_4, MgB_6 and MgB_{12}, has been established. However, only magnesium diboride has found practical application. It is used as a catalyst in the reaction of synthesis of cubic boron nitride [1] and in preparation of superconductors [2].

In this connection, in the present work, methods of synthesis of magnesium diboride which can be the base of the full-scale production of MgB_2 with a composition close to the stoichiometric composition were sought.

For the preparation of MgB_2, the method of synthesis from elements was used, and the processes of interaction of magnesium salts with boron were investigated.

The synthesis from elements was carried out in an argon atmosphere at temperatures below the dissociation temperature of magnesium diboride, i.e., at 780-800° C. The composition of mixtures, the influence of the exposure time, and the purity of initial magnesium on the quality of the end product were studied.

It was established that, to compensate magnesium losses caused by its evaporation, a 5% magnesium excess should be present in the mixture. The preparation of the product of optimum composition requires an exposure time of 2–3 h.

The compositions of the reaction products were studied by X-ray phase analysis. The contents of magnesium, boron, and oxygen were determined by methods of chemical analysis.

The oxygen content in all samples was found to be somewhat below that in initial magnesium. That is why, to prepare MgB_2 with a composition close to the stoichiometric composition, magnesium with a minimum oxygen content (which is usually present in the form of stable MgO) should be used.

In investigation of interactions between magnesium salts and boron, the process was carried out in a neutral atmosphere and vacuum.

It was established that the use of magnesium carbonate as an initial component did not lead to the preparation of single-phase boride. The boride formation process proceeds slowly, and, in the end product, along with magnesium diboride, magnesium oxide and free boron were present.

The magnesium halogenides can become more promising materials for the preparation of oxygen-free magnesium boride [3].

The literature.

1. Samsonov G.V., Serebrjakova T.I., Neronov V.A. Borides. – M.: Atomizdat, – 1975. – p. 142.
2. Karapetrov G., Ivarone M., Kwok W.K., Crabtree G.W., and Hinks D.G. Scanning Tunneling Spectroscopy in MgB_2 // Internet, February 20, 2001.
3. Kartvelishvili J.M., Mchedlishvili D.I., Kochalava Z.D. To a question of preparation chromium borides // High-temperature borides and silicides. - K.: - 1978. - p. 36.

ENTHALPY OF LANTHANUM SELENIDE HAVING THE La$_3$Se$_4$ COMPOSITION AT HIGH TEMPERATURES

Bolgar A. S., Kopan A. R.

I. N. Frantsevich Institute for Problems of Materials Science, National Academy of Sciences of Ukraine, Kiev, Ukraine

Halcogenides of rare earth metals (REM) having the Ln$_3$H$_4$ (here Ln-REM, H – halcogen) composition are characterized by the thermal stability, the high melting temperatures (~ 2000 K) and the electrical conductivity (for La$_3$Se$_4$ the concentration of conduction electrons is equal 5,4·10^{21} cm^{-3}). They have the superconductivity properties, high values of electronic works function and resistance to the metals melt and halcogen salts [1,2]. The estimation of Ln$_3$Se$_4$ compounds thermoelectric efficiency (Z) [3] showed that the halcogenides of mentioned composition will be available as a promising high temperature (1300 – 1700 K) thermoelectric materials for the n - branch of thermogenerator. The application of these compounds allows to increase the temperature and , thus, the efficiency of hot junction to 1700 – 1800 K. Therefore they are considerably promising for application as structural materials for some parts of magnetohydrodynamical transducers and in a different branches of techniques.

A knowledge of the thermodynamic properties of substances is necessary for optimization of synthesis process and manufacturing of new materials with the previously predetermined properties.

The estimations of standard entropy magnitude and the enthalpy of formation for La$_3$Se$_4$ were presented in [4]. Values of these characteristics are equal to $S^0(298,15 \text{ K}) = 282,42 \pm 8,37$ J·mol^{-1}·K^{-1} and $H_f^0(298,15 \text{ K}) = 131796 \pm 83680$ J·mol^{-1}, respectively. Heat capacity measurements by adiabatic calorimetry are reported for indicated compound between 60 and 300 K in [5]. The heat capacity, entropy, reduced Gibbs energy and enthalpy of La$_3$Se$_4$ at 298, 15 K were also determined therein. Up to the present time the thermodynamic properties of La$_3$Se$_4$ have not been investigated experimentally at high temperatures.

The goal of our presentation is to study of La$_3$Se$_4$ enthalpy in the range from 450 to 2260 K as well as to calculate the temperature dependencies of principle thermodynamic

functions for these compounds in both solid and liquid states.

The sample of the selenide was prepared[1] by ampoule method from the elements. From the results of XRD analysis the synthesized selenide proved to be single-phase compound of Th$_3$P$_4$ structure. The lattice parameter was determined for the compound investigated and is equal to: a = 0,9045 nm. This result correlates well with the literature data [6]. From the results of chemical analysis, the La$_3$Se$_4$ sample contain La – 56,91, Se$_{general}$ – 43,02 mass., %. The free selen was not founded in the sample. Consequently, the composition of sample is stoichiometric LaSe$_{1,33\pm0,01}$ and formula of the compound pointed out is La$_3$Se$_4$.

The enthalpy of lanthanum selenide was measured by the mixing method between 450 – 2260 K. After experiments have been carried out before the compound melting the mass change of calorimetric sample was no from the initial one more than 0,1 % and 1 % after the melting temperature.

The results of measurement for La$_3$Se$_4$ enthalpy are given in Fig. 1. The enthalpy of compound investigated changed monotonically up to some temperature interval (for La$_3$Se$_4$ – 2070 –2102 K) followed by an increase of enthalpy stipulated with the appearance of a liquid phase.

In the solid state the experimental data concerning the enthalpy were approximated by Maier – Kelly equation:

$$H^0(T) - H^0(298,15) = AT^2 + BT + CT^{-1} + D \qquad (1).$$

The A, B, C and D parameters in this equation were determined by the method of least squares [7] using two boundary conditions $H^0(T) - H^0(298,15) = 0$ at 298,15 K, $C_p^0(298,15 \text{ K}) = 182,4$ J·mol^{-1}·K^{-1}. Such expedient makes possible to reconcile low and high temperature heat capacity data for our selenide. The temperature dependencies of thermodynamic functions (heat

---

[1]Synthesis and attestation of samples were carried out with the participation of M. Y. Pribilskiy

capacity, entropy and reduced Gibbs energy of compound were determined as:

$$C_p^0 = 2AT + B - CT^{-2}; \qquad (2)$$

$$S^0(T) = 2AT + B\ln T + 0,5CT^{-2} + E; \qquad (3)$$

$$G^0(T) = AT + B\ln T - DT^{-1} - 0,5CT + (E-B). \qquad (4)$$

Here E is numerical parameter. The parameters of (1)-(4) equations are equal to: $A = 3,464 \cdot 10^{-3}$, $B = 147,383$, $C = -42738$, $D = -1276890$, $E = -489,38$.
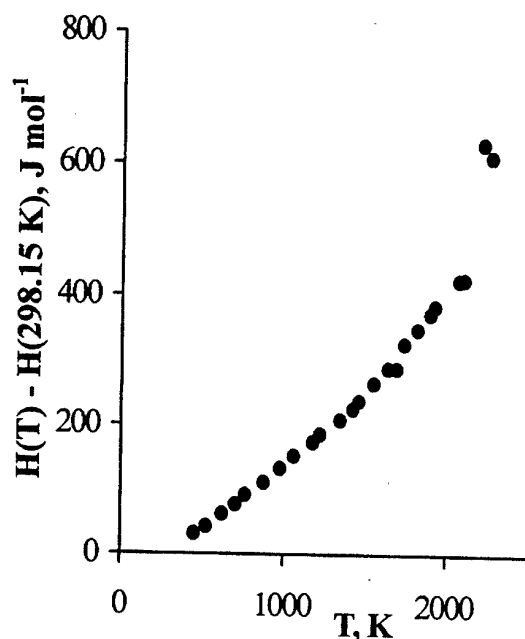
Fig. 1. Experimental data of La$_3$Se$_4$ enthalpy at high temperatures

In the liquid state two values of La$_3$Se$_4$ enthalpy were obtained and then they were approximated by following linear dependence (5):

$$H^0(T) - H^0(298, 15\ K) = f + gT. \qquad (5)$$

The f and g parameters were evaluated only taking into account the first boundary condition $H^0(T) - H^0(298, 15\ K) = 0$ at 298,15 K and they are equal to −95308 and 319,67, respectively. The deviation of values of La$_3$Se$_4$ enthalpy as they were calculated from (1) and (5) equations were characterized by 0,9 and 2,12 % magnitudes of averange confidence interval, respectively.

The calculated melting point of indicated lanthanum selenide (2108 ±55 K) is 15 K below than values given in [8]. The melting enthalpy and

entropy for La$_3$Se$_4$ were at first found by extrapolation of (1) and (5) dependencies to the melting point: $\Delta_{tr}H(La_3Se_4) = 157,3 \pm 8,474$ kJ·mol^{-1}, $\Delta_{tr}S(La_3Se_4) = 74,62 \pm 4,02$ J·mol^{-1}·K^{-1}.

Such information about La$_3$Se$_4$ thermodynamic properties should be interesting to work with material containing this substance in extreme conditions.

References

1. Golubkov,A.V., Goncharova, E. V., Juze, B. R. and other,Physical Properties of the Rare Earth Elements Halcogenides [in Russian], Nauka, Leningrad (1973).
2. Yarembash, E. I., Eliseev A. A., Rare Earth Elements Halcogenides (Synthesis and Crystal Chemistry) [in Russian], Nauka, Moskow (1975).
3. Rudnik, I. M., " Thermoelectric Properties of Rare Earth Elements of the Cerium Subgroup,"PhD Thesis [in Russian],(01.04.10), Leningrad (1978).
4. Mills, K. C., Thermodynamic Data for Inorganic Sulphides, Selenides and Tellurides, Butteworth, London (1974).
5. Kriklya, A. I., Bolgar, A.S., Blinder, A.V., Gorbachuk N. P., Kopan A.R ., "Thermodynamic characteristics of La$_3$Se$_4$", in:Electronic buildingand properties of refractory compounds and alloys the using of their in materials sciencees [in Russian], I.N. Frantsevich Institute for Problems of Materials Science NASU, Kyiv (2000).
6. Kosolapova T. Ya. (ed.), Handbook of the Properties, Production and Application of Refractory Compounds [in Russian], Metallurgiya, Moscow (1986).
7. Litvinenko, V. F., Bolgar A.S., Muratov V.B. and other "The Experimental Data Processing on enthalpy with Conciderations", Institute for Problems of materials science AS USSR, Kyiv (1984), dep v VINITI 19.09.84; № 6300 V.
8. Gordienko, S. P., Fenochka, B. V., Viksman, G. Sh. Handbook of the Thermodynamics of Lanthanides Compounds [in Russian], Nauk. Dumka, Kyiv (1979).

STRUCTURE AND PROPERTIES OF HOT PRESSING MATERIALS FROM MECHANICAL SYNTHESED POWDERS OF TITANIUM ALUMINIDES.

Oliker V. E., Sirovatka V. L.
Institute for Problems of Materials science NAN of Ukraine, Kiev, Ukraine.

INTRODUCTION

Due to low density (4,2 g/sm^2 for Ti$_3$Al and 3,9 g/sm^2 for TiAl in comparison from 8,9 g/sm^2 for superalloys on Ni -base) and high temperature of melting (1600^{0}C for TiAl and 1460^{0}C for Ti$_3$Al in comparison with 1650 – 1800^0 C at superalloys), intermetallics on a basis titanium aluminides the find wide application in quality of materials of details of modern aircraft engines and designs [1-5].

It is established, what microalloying γ - aluminides the titanium scandium can to provide increase of their heat resistance, refinement and modifying structures, formation of the dispersion strengthened structure with coherent connection between strengthening and matrix phases. Proceeding from this it is possible to expect increase of mechanical characteristics in a wide range of temperatures. The given material it is possible to use in chambers of combustion as it has sufficient durability at working temperatures up to 1000^0 C.

It is established, what such properties the materials on a basis has γ - aluminides the titanium with additives of scandium.

On the basis of carried out researches it is established :

1. During mechanical synthesis formation no governing structures with simultaneous formation metastable phases (hadness solution, intermetallics, oxides) takes place.

2. Application hot isostatic pressing allows to realize effect of a structural heredity and durable characteristics at hot pressing from this alloy of a material, due to formation at high values of temperature and loading of pressing of a refined substructure with nanostructural grains.

3. It is established, that covering on a basis γ - aluminides have good heat resistance and high mechanical characteristics.

4. The accent of the further researches in this area should be done on reception no porous the dispersion strengthened materials on nanometrical a level with the raised mechanical characteristics.

REFERENCES

1. S.J. Balcone, J.M. Larsen, D.C. Maxwell, J.W. Jones, Mater. Sci. Eng. A192/193, 457- 464 (1995)

2. J. Kumpfert , Y-W. Kim and D.M. Dimiduk, Mater. Sci. Eng. A192/193, 465-473 (1995).

3. K. S. Chan and Y-W. Kim, Metall. Trans. 23A, 1663-1677 (1992).

4. K.S. Chan and D.S. Shin, Metall.Trans. 29A, 73-87 (1998).

5. J. P. Campbell, K.T. Venkateswara Rao and R. O. Ritchie, Mater. Sci. Eng. A 229-240, 722-728 (1997).

COMPOSITE MATERIAL ON THE BASE OF DOUBLE TITANIUM – CHROMIUM CARBIDE WITH THE HIGH RESISTENCE AS FOR WEAR AND HIGH – TEMPERATURE OXIDATION

Umansky A.P., Panasyuk A.D.

Institute for Problem of Materials Science, Kiev, Ukraine

The double titanium – chromium carbide is the solid solution of Cr_3C_2 in TiC. It is the material having the high hardness and resistence to high – temperature oxidation. This enables to consider TiCrC as a perspective components of wear– and heat – resistant composite materials.

In order to develop the composite materials on the base of double titanium – chromium carbide we carried out the study of wetting of TiCrC by Ni – Cr nickel alloys, the chromium content in alloys being in the concentration range of 1 – 25 mass.%. Hereby the nature of interface interaction zone was studied for the "TiCrC – (Ni – Cr)" system. For the composite materials on the base of TiCrC double carbide, the Ni – Cr metallic binder was chosen because it was characterised by a high enough heat – resistance. This allows to use the TiCrC – (Ni – Cr) material for the manufacturing of parts working at high temperatures. It has been established, resulting from investigations carried out, that the chromium additives into nickel in the concentration range of 10 – 15% under the wetting of TiCrC by Ni – Cr alloys promote to formation of zerro contact angles.

In the interaction zone, the heterogeneous fine – grain structure consisting of complicated carbide grains was found. The metallic phase proved to be uniformly distributed between these carbide grains. For the fabrication of composite material, the Ni – 15 mass.%Cr metallic binder was chosen, the content of metallic binder being 20 and 30%.

The TiCrC, Ni and Cr powders, in the coorelation pointed out, were subjected to hot pressing in the graphite moulds at the temperature 1550^0C. It has been established that the microstructure of TiCrC – 20%(Ni – 15%Cr) material, investigated using the SX – 50 microanalyser, consists of carbide grains of sphere shape with the size of 1 – 5 µm. The metallic melt is uniformly distributed between these grains.

The tribologic characteristics of TiCrC – 20%(Ni – Cr) composite material were studied using the MT – 68 friction device. Hereby the values of friction coefficient and relative wear resistance of material were determined at different velocities (in the region of 5 – 15 m/s) and loads (2.5 – 10 MPa).

It has been shown that the friction coefficient is diminished with the increase of test velocities, and at V = 15m/s it is equal to 0.25. Hereby the relative wear resistance is decreased. If at the small values of velocity the sample wear did not exceed 3.5µm/km, under the maximum test velocities it increased up to 11 µm/km (fig. 1).
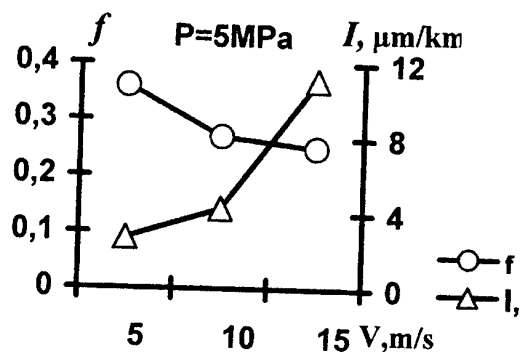
Fig.1. Influence of speed of the test on the material TiCrC–20%(Ni – Cr) value of wear and friction coefficient meaning by constant load of P = 5 MPa.

Tribological tests by constant speed and different loads (fig.2) showed the same tendentions: the increasing of the load was followed by diminishing of the friction coefficient and increasing relative wear resistance. The process of the wear, as it was detected, with increasing of load becoming more intensity againist increasing speed.
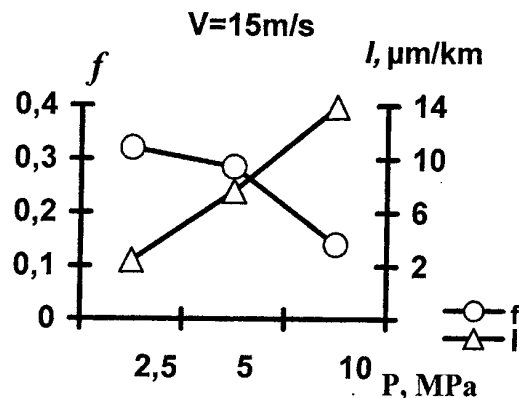
V=15m/s

Fig. 2. Influence of load of the test on the material TiCrC–20%(Ni – Cr) value of wear and friction coefficient meaning by constant speed of V = 15 m/s.

The resistance of material as for high – temperature oxidation is one of the most important parameters characterizing the material. In study the oxidation behavior of TiCrC – 20%(Ni – Cr) composite powders has been investigated under the heating in air up to 1000^0C using the OD – 103 derivatograph.

It has been established that the interaction of composite on the base of TiCrC with oxygen (in air) proceeds during four stages, the first stage beginning at $\sim 550^0$C. The formation on powder surface of protective films consisting of both titanium and chromium oxides significantly decreases the oxidation rate. Havever, the oxidation rate is essentially increased at the temperatures exeeding 800^0C.

The investigations carried out have shown that the material developed may be recommended for the work under condition of intensive loads at high temperature.

STRUCTURAL STABILITY OF HIGH-ALLOY CHROME-IRON ALLOYS AT HIGH TEMPERATURES

Dan`ko S.V., Minakov V.M.

Institute for Problems of Materials Science by I.M.Frantsevich NAS of Ukraine, Kiev, Ukraine

High-alloy chrome-iron alloys have a row of unique and specific properties, that allows to recommend them as perspective heat-resistant and construction materials for needs of chemical and power-generating machine-building, active zone of fast reactors. Investigation of structure change and alloys properties during exploitation at high temperatures is an actual task.

Objects for research were alloys, containing 54-60% Cr, 0,8-2,8% Al, 0,18-0,64% Ti, 0-1,35% V, 0,01-0,1% rare-earth metals, the rest - Fe. They were obtained by vacuum-induction melting of pure charge materials with next vacuum-arc remelting or refining by electron-beam method in vacuum with use of intermediate reservoir. Primary treatment by pressure of cast metal was concluded in extrusion. Than metal was forged by sledge hammer to sheet-bars, which afterwards were rolled to the sheets in a few passes.

Essential obstacle for wide application of Cr-Fe alloys at high temperatures is their embrittlement owing to dissolution (foliation) of solid solution in the temperature range 670-820 K and owing to sigma-phase forming at 820-1020 K.

Investigation of peculiarities of these processes at duration up to 1000 hours allows to estimate an exploitation possibility of explored materials in stated temperature range, to define influence of admixtures, alloying elements, structural state on the embrittlement. Analysis of strengthening which takes place at long-term annealing at T = 770 K shows that dissolution process approaches to equilibrium state at duration more than 100 hours. Zones (phases) α и α` enriched by iron and chrome have a dimension ~ 10-20 nm. They are effective barriers for dislocation movement, that is why strengthening and lowering of plasticity occur. During long-term annealing precipitation of carbide particles takes place in cast and recrystallized metal. These particles can precipitate along grains boundaries and embrittle metal additionally.

It was observed that amount of nitrogen influences on the embrittlement speed essentially (fig. 1). Increasing of total amount of nitrogen determines raise part of this element in free

(dissolved) state, which first of all tends to fill octapores of crystalline lattice, that circled by big amount (four-six) of chrome atoms owing to considerable electron affinity of nitrogen to chrome. Atom complexes Cr-N serve as the centers for creation of zones depleted by iron, apparently. Presence of interstitial atoms accelerates dissolution and accordingly embrittlement as a result of higher extent of solid solution overcooling at 770 K. At certain level of total amount of nitrogen (more than 0,03%) amount of it in free state runs up to maximum presumably. This part of nitrogen participates in complexes forming and accelerating this process. Further increasing of concentration of this admixture does not accelerate embrittlement already. As a whole this argumentation is confirmed by plasticity degradation of alloys with different structural state. Amount of nitrogen in free state which is situated in the interstices of crystalline lattice in metal with grain structure is higher than in material with cellular dislocation substructure. This is takes place owing to bigger segregation "capacity" of cell boundaries. They accumulate a greater amount of admixtures than grain boundaries. Recrystallized material (pure by nitrogen) reaches maximal temperature of cold brittleness after lesser time (fig. 2). For alloy with high nitrogen amount structural state does not determine embrittlement speed already: amount of impurity atoms participating in the forming of Cr-N complexes reaches maximum for cellular as for recrystallysed structure presumably. Concentration of carbon does not have an influence on embrittlement speed.

Thus in order to decrease the embrittlement extent at dissolution of solid solution for investigated group of alloys it is necessary to decrease amount of nitrogen in free state during melting and by fixing it in stable chemical compounds. Creation of cellular structure which accumulate considerable part of impurities on cell boundaries allows to slow plasticity degradation essentially.

Also long-term annealing (duration up to 1000 hours) of alloys at T = 970 was carried out. Initial material state is cellular dislocation structure

(cell size - 0,5 -2,0 mkm). The alloys with different aluminium amount were investigated. Sigma-phase precipitates on grain and cell boundaries at duration less 500 hours already in alloy with amount of Al equal 0,8% and results in catastrophic embrittlement. Amount of sigma-phase increases from internal layers of specimen towards its surface. That is explained by depletion of surface layers by aluminium which is consumed for oxide film forming. Sigma-phase does not precipitate in alloys with high aluminium amount (1,9-3,1%) at explored annealing duration up to 1000 hours. Alloying of vanadium (~1%) results to forming fine-dispersed carbonitrides of this chemical

element after few hours of annealing. These particles prevent migrations of cells boundaries and recrystallization.

Thereby in order to prevent forming of sigma-phase at exploitation of materials in temperature range 900-1100 K it is necessary to alloy them with aluminium not less 1,5-2,0%. Increasing of chrome concentration in accordance with equilibrium diagram of alloys Fe-Cr-Al diminishes tendency to creation of this phase also. But raised chrome amount causes plasticity degradation and problems with industrial melting of alloys.
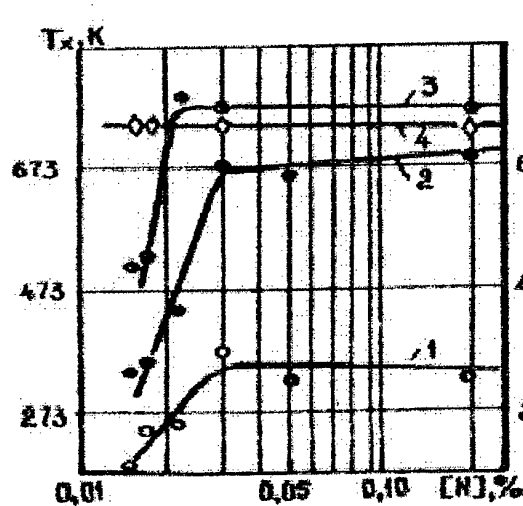
Fig. 1. Change of cold brittleness temperature of alloys in dependence on amount of nitrogen at dissolution of solid solution (T=770 K) at duration:
1 - 0 hours, 2 - 10 hours,
3 - 100 hours, 4 - 1000 hours.
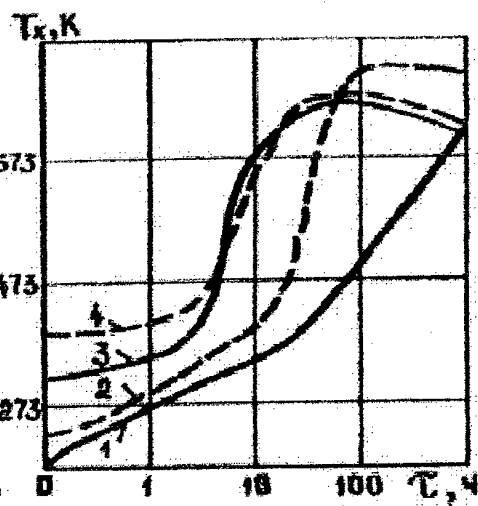
Fig. 2. Temperature dependence of tough-brittle transition of alloy which contains 0,014% N (curves 1, 2) and of alloy which contains 0,120 % N (curves 3,4) on annealing duration at T = 770 K and structural state:
1,3 - cellular state,
2,4 – recrystallized state (grain size = 10 mkm).

361

DESTRUCTION SURFACE ANALYSIS OF TITANIUM IN WIDE TEMPERATURE RANGE

Adeev V.M., Minakov N.V., Minakova A.V., Puchkova V.U., Rudyk N.D.
Institute for Problems of Materials Science by I.M.Frantsevich NAS of Ukraine, Kiev, Ukraine

Technically pure titanium obtained by technology of Joint-stock company "FIKO" was investigated. The melting method through intermediate reservoir with use electron gun of high-voltage glowing discharge cold cathode was used in this work.

Admixtures such as Na, K, Ca, S, Cl in condensates taken from chamber surface in zones over melting electrode and over bath as well as over crystallizable metal were detected with use of Auger-electron spectroscopy. These admixtures were revealed in the samples which were remelted after vacuum arc melting.

These admixtures were not detected on destruction surfaces of technically pure titanium and alloy VT-6 (Ti-6%Al-4%V). These data testify to metal refining from harmful admixtures at electron-beam melting method.

Destruction of titanium obtained by technology of Joint-stock company "FIKO" at low temperatures takes place at high strength level. Grain boundaries, particles and other defects highly influence on the passing of the tests. Destruction of technically pure titanium occurs by mechanism of dimple forming and merger in the examined temperature range.

Researching of destruction surfaces of technically pure titanium displays that the intensive displacement bands are formed on side-cut surface of specimens. Interaction of these bands with grain boundaries generates the cracks. Crack initiation takes place on grain boundaries. Dimple forming takes place on grains boundaries which are ortogonal to specimen axis. That's why tough destruction passes here.

High ingots quality permits to deform theirs with high reduction. High-quality foil was obtained from ingots of technically pure titanium without intermediate annealing and structure preparation by thermomechanical treatment.

Fulfillment of this treatment allows to obtain fine-grained (~1 mm) and coarse-grained (~5 mm) structure.

Fine-grained structure is formed during dynamic recrystallization. Grain size of coarse-grained structure correlates with extraction coefficient.

Results of tension tests in co-ordinates true deformation e - true strength S testify to rise of plasticity modulus at temperature lowering from $+200^0C$ to -253^0C. At temperatures -253^0C and -196^0C true breaking stresses coincide practically and are equal $S_f = 2200$ MPa E/50, where E is modulus of elasticity of titanium.

Data of mechanical tests at 20^0C are presented in the table.

Table. Properties of technically pure titanium obtained by melting method of Joint-stock company "FIKO" after different thermomechanical treatment.

	Structure type	σ_{02}, MPa	σ_B, MPa	δ, %	ψ, %	Sf, MPa	HV, MPa
1.	fine-grained	378.3	467.7	21.05	85.2	2366	1920
2.	fine-grained	404.9	474.7	24.04	85.2	2271	
3.	coarse-grained	358.2	454.7	10.53	73.0	1175	1840
4.	coarse-grained	327.6	336.2	5.44	50.5	765.9	
5.	Grade 2 *	275	345	20	30		
6.	Grade 3 *	380	450	18	30		

*ASTM B348

RELATION OF ACOUSTIC CHARACTERISTICS AND SRUCTURE PARAMETERS OF FOAM NICKEL

Bezimyanniy Y.G., Burlachenko Y. V.
I.N.Frantsevich Institute for Problems of Material Science of NAS of Ukraine, Kiev, Ukraine

The possibility of controlling of foam metals structures using acoustic methods is examined in this work. Specifically the evaluation of structure elements sizes and degree of material destruction is investigated.

Specimens of foam nickel with porosity level 95% consist of elementary cells has been investigated. The elementary cell is a penetrable sphere composed by bridges combined with nodes. Bridges are represented by hollow prisms with cross-sections in the form of triangle with concave sides.
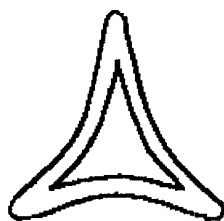
Fig.1. The cross-section of a bridge

The spectrum of a signal passed through a specimen of a material been investigated normalized by spectrum of an emitted signal can be interpreted as a material's transitional characteristic. Maximums of the transitional characteristic can be associated with resonance of a certain material's structure elements. Therefore the possibility of a material's structure units sizes evaluation by analysis of the spectrum of an acoustic signal passed through the pattern exists.

Specimens of foam nickel were investigated by acoustic signals with ultrasonic wavelength of such order as a material's structure elements sizes. This allows us to examine our patterns as a submesostructure. In this case with acoustic point of view the material is a system of bridges making vibration. So the bridge is an expected resonant element.

To calculate fundamental frequencies of bridges the series of measurements with a microscope has been provided. As a result following situations of node's and bridge's sizes distribution were obtained.
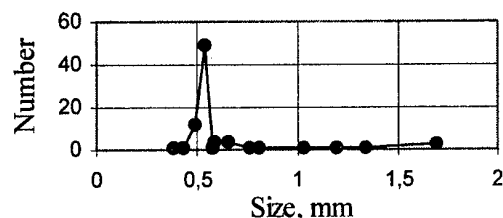
Fig.2. Node's sizes distribution.
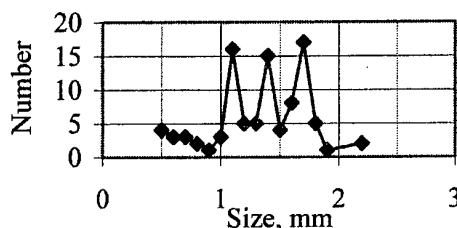
Fig.3. Bridge's sizes distribution

Fundamental frequencies for three types of bridge's sizes were calculated: 1) the size of bridge; 2) the size of bridge measured from the centers of nodes; 3) the size of bridge and two nodes together.

The character of bridge's mutual orientation allow to suppose two types of vibration: longitudinal and transverse vibration. For the theoretical computation a bridge has been approximated by the bar and the tube of triangle cross-section respectively for both types of vibration.

For the case of longitudinal vibration the wave equation has the following form [1]:

$$\frac{\partial^2 u}{\partial x^2} = \frac{1}{c^2}\frac{\partial^2 u}{\partial t^2}, \quad c = \sqrt{\frac{E}{\rho}}. \quad (1)$$

Here E - the Yung module, ρ - density.

The frequency equation for the case of a bar with nonfixed ends is

$$\sin \frac{\omega l}{c} = 0. \qquad (2)$$

Here l - the length of a bridge.
The solution of the frequency equation (2) is

$$\omega_i = \frac{i \pi c}{l}, \quad f_i = \frac{\omega_i}{2\pi}. \quad (3)$$

Here f_i - fundamental frequencies of longitudinal vibration of a bar.

Expressions for the case of transverse vibration are reduced below [1].

The wave equation:

$$\frac{\partial^4 y}{\partial x^4} = -\frac{1}{c^2}\frac{\partial^2 y}{\partial t^2}, \quad c = \sqrt{\frac{EI}{\rho S}} \quad (4)$$

Here I - moment of inertia of the cross-section [2]; S - the area of the cross-section of a bridge.

The frequency equation and fundamental frequencies calculation:

$$\cos k l ch k l = 1;$$

$$\omega_i = k_i^2 c; \quad f_i = \frac{\omega_i}{2\pi} = \frac{k_i^2 c}{2\pi}. \qquad (5)$$

In the experimental part of the research specimens of the foam nickel were disturbed by the shock excitation and excitation by radiopulse train. The analyses of the experimental results shows that a series of typical frequencies close to theoretically calculated fundamental frequencies of bridge's longitudinal and transverse vibration forms signal's passed through the specimen spectrum.

Comparing of the theoretical and experimental data shows that in the case of longitudinal vibration the third variant of the bridge's length measurement (including node's sizes) must be used and in the case of transverse vibration - the second one (the length of a bridge is measured between the centers of nodes).

Comparing the values of foam nickel's bridge's fundamental frequencies calculated theoretically with frequency maximums in the spectrum of ultrasonic signal passed through a specimen verified the adequacy of the acoustic model has been proposed. The results obtained in the present research allow us to develop a methods of foam metal's structure controlling on the submezolevel.

References

[1] Тимошенко С.П., Янг Д.Х., Уивер У.: Колебания в инженерном деле/Пер. с англ. Л.Г. Корнейчука; Под ред. Э.И. Григолюка. - М.: Машиностроение, 1985.
[2] Ицкович Г.М.: Сопротивление материалов: Учебник для учащихся машиностроит. техникумов. - М.: Высшая школа, 1982.

364

VIBRATION DAMPING OF AIRPLANE ENGINE MOUNT AND METAL FIBROUS MATERIAL

Zorin V., Rutkovskiy A., Kriushin V., and Ivanchuk A.

Frantsevich Institute for Problems of Materials Science, National Academy of Sciences of Ukraine, Kyiv, Ukraine

The engine mount vibration damping (attachment system) of engine mount is provided by specially built-in shock absorbers. A shock absorber is made in the form of a hollow cylinder or housing having a coaxial cylindrical rod and a number of washers of flexible material within it. With the axial displacement of the housing and the rod in relative to each other direction, they interact through the compressible washers, then a portion of the washers shall act in one direction while the other portion shall act in the reverse direction during the rod travel. Thus, the washers in the shock absorber shall play the role of damping members and the rubber shall be usual material for them.

The temperature of under cowling space of nacelle of an up-to-day airplane, where the engine is mounted, can reach so high values that rubber damping members are needed to be replaced by those made of material which shall provide the desired level of damping at high temperatures too.

The IPMS, NAS of Ukraine had designed and produced experimental damping members of metallic fibers forming a flexible anisotropic structure, hardly removable. The use of metallic fibers has to provide operation capability for damping members at high temperature, power, vibration or other differentials.

Tests of a shock absorber with rubber damping members and that with metallic fibers were conducted independently for comparison of characteristics of experimental metal fiber members and those made of rubber being in practice. Shock absorbers together with corresponding rig were located on a electrodynamic vibration table and loaded with charges simulating those caused by the airplane engine weight and its torque. Vibration pickups were attached to the cylinder and rod along the shock absorber axis. Vibrodamping amplitude-frequency characteristics (AFC) of both shock absorbers were tested and recorded by both pickups within the frequency range of 5 to 2000 Hz at the 1 to 15 g vibration overcharge amplitudes and the 0.5 to 2.5 mm vibration displacements. The frequency scanning was by the logarithmic relationship with the 1 oct/min velocity up to 50 Hz and 0.5 oct/min above 50 Hz.

After the AFC were recorded, the same conditions were used to test both shock absorbers on a vibration strength by frequency pumping technique. The frequency was varied by logarithmic relationship with the 1 oct/min velocity. The test time was 27 hours in total, the total number of vibration cycles was at least 10^7. The shock absorbers were fully dismantled each 9 hours of vibration strength testing in order to check the surface conditions of their members.

The comparative table tests and analysis of their results provided conclusion that the vibration damping and vibration strength characteristics of experimental metallic fiber damping members as developed by the IPMS, NAS of Ukraine and used in engine mount shock absorbers, are not inferior to those of rubber damping members, and in contrast to the latter, high temperature of the space under the cowling of engine nacelle can not be a restricting factor for the metal fibrous damping members.

PROPERTIES OF THE HIGH-STRENGTH NI-CR-AL BASE ALLOYS OBTAINED BY METHODS OF POWDER METALLURGY

Alfintseva R.F., Laptev A.V., Brodnikovskyy N.P., Chevychelova T.M., Rogozinskaya A.A.

Institute for Problem of Materials Science, Kiev, Ukraine

Use of an impact molding allows to receive practically dense material and at that the time of sintering is considerably abbreviated. At high energy impact on a material the series of competitive processes of dissipation of the delivered energy take place. It's the volume strain and cracking of powder particles, slipping particles relatively each other with an intensive local strain and even by melting of a material at the field of contact of powder particles, actuation of new diffusion mechanisms, phases changes and others. Setting structure and the phase composition of a material, temperature and magnitude of impact impulse it is possible to control the contribution from different mechanisms for dissipation of energy with the purpose to optimize mechanical characteristics and process of powdered materials shrinkage.

The present work is devoted to analysis of possibility of using of the high energy hot pressing method for obtaining of the Ni - Cr - Al system cermet alloys. The Ni - Cr - Al system is a conventional system for creation high hot strength and wear-resistant alloys. The Ni - Cr - Al system is interesting to use for analysis of capabilities of the high energy hot pressing method for obtaining materials due to preliminary different degree sintering of clean component of the system allows to vary over a wide range structure and phase composition of alloy before high energy affecting. It permits to track out influence of phases properties both on process of shrinkage, and on strength of contacts which arise between cramped surfaces of pores.

For preparation powder compositions the powder of the electrolytic nickel GOST 97-22-74 with dispersion ability no more than 40 microns, powder of chrome ПХМ with dispersion ability less than 40 microns, and also powder of aluminum ПАП 41 with dispersion ability less than 20 microns were taken.

From the prepared mixtures at room temperature and stress 300 MPa the preforms of diameter 25 mm and height of 10-13 mm were pressed. The preforms are located in an evacuated chamber with stress 0,13 Pa , heated to 900 –

1200 °C and were held out 20 minutes then exposed to an impact molding in an enclosed matrix with maximal stress 1000 - 1200 MPa. The elemental composition of obtained alloys was instituted through x-ray fluorescent spectral analysis on a spectrometer VRA - 90 (Table 1).

The table 1
Physic-mechanical characteristics of Ni-Cr-Al cermet alloys.

№ alloy	Compo-sition, mas.%	HEHP Tempe-rature,° C	grav-ity, $Г/см^3$	Poro-sity, %	Specific resis-tance mkOm* sm
1A	Ni-50,5 Cr-49.5	900	7,66	3,04	28,0
		1000	7,69	2,65	99,7
		1100	7,83	0,88	86,4
		1200	7,90	0,00	101,5
		1200*	5,68	28,1	216,9
2A	Ni-51.3 Cr-41.7 Al-2.0	900	7,61	2,5	98,8
		1100	7,75	0,7	72,1
		1100	7,55	3,7	82,7
		1200	7,76	0,6	102,6
3A	Ni-52,0 Cr-41,7 Al-6,3	900	7,33	2,1	37,4
		1000	7,23	2,9	59,9
		1100	7,43	0,0	91,2
		1100*	5,34	28,2	763,0
4A	Ni-50,3 Cr-40,2 Al-9,5	900	6,82	5,7	48,4
		1000	7,01	3,1	67,2
		1100	7,08	2,1	71,4
		1150	7,07	2,2	88,6
		1200*	5,28	27,0	520,0
5A	Ni-42,2 Cr-38,5 Al-19,5	900	6,09	2,6	87,9
		1000	6,15	1,3	73,0
		1150	6,32	0,0	43,1

In the table 1 temperature of high energy hot pressing (HEHP) of preforms, and also data of measuring of their gravity and specific electric resistance is introduced. For matching are cited data obtained on samples gone off the same heat treatment and not subjected to high energy ardent pressing (sintering).

The magnitude of alloys porosity after sintering at 1150 - 1200 °C without high energy hot pressing depends on composition of alloy (table 1). In alloy 1A sintering is solid-phase and the shrinkage practically misses. The introducing about 2 mas. % of aluminum (the alloy 2A) results in appearance of a liquid phase at sintering and abatement of porosity from 28 % up to 3.5 %. At further magnification of the contents of aluminum in alloy the liquid shrinkage again practically misses. As a result of sintering samples of alloys 3A and 4A (containing 6.3 and 9.5 mas. % Al accordingly) even augmented in bulk. Not looking on distinction of processes happening in alloys with different composition during sintering, the applying consequent of high energy hot pressing allows to solve the problem of dense materials obtaining. The magnitude of temperature which is needed for obtaining of 100 % gravity samples varies in a spacing 1100 – 1200 °C depending on composition of alloys.
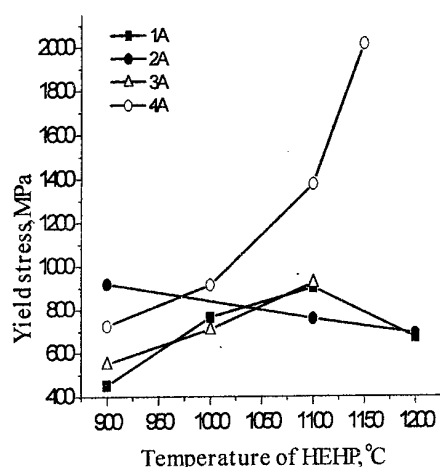
Fig. Fig. 1. Dependence of yield stress on temperature of high energetic hot pressing of Ni-Cr-Al alloys

The data of definition of specific electric resistance, X-ray and metallographic analyses has allowed to define the phases composition of the obtaining alloys. At the conditions of HEHP, which supply with obtaining of practically dense materials, solutions on the basis of chrome and nickel. In 3A and 4A alloys intermetallic compound NiAl are formed as well. 5A alloy contents the solid solutions on the basis of chrome and intermetallic compound.

The data of definition of specific electric resistance, X-ray and metallographic analyses has allowed to define the phases composition of the obtaining alloys. At the conditions of HEHP, which supply with obtaining of practically dense materials, phase content of 1A and 2A alloys is two solid solutions on the basis of chrome and nickel. In 3A and 4A alloys intermetallic compound NiAl are formed as well. 5A alloy contents the solid solutions on the basis of chrome and intermetallic compound NiAl.

Table 2. Hardness, endurance and friction coefficient of Ni-Cr-Al alloys getting by high energetic hot pressing

Alloy, #	tempe-rature, °C	Hard-ness, HRC	Endu-rance, Мкм/км	friction coef-ficient
1A	1200	16	120	0,28
2A	1200	20,3	104	0,30
3A	1100	36,4	20	0,26
4A	1150	46	12	0,20
5A	1150	48	4	0,18

Strength properties and the endurance of obtained alloys is determined by a proportion of phases components and condition of materials getting. With magnification of HEHP temperature compression yield strength (fig.1) and stress of bending failure (fig.2) grow. The HEHP at 1200 °C gives growth of grains and so some decrease of strength. The introducing of aluminum slashes plasticity of a material. By growth of the contents of aluminum strength properties at compression test are increased, but bending properties are slashed. The endurance is decreased with magnification of the contents of an intermetallic phase (table 2).

References
1. Nesterenko V. F. Capability of shock-wave methods of deriving and sealing quick quenched materials//Physics of combustion and detonation,1985,v.21,#6,p.85-98.
2. PovarovaK.B.,Bannyh O.A., Kazanskaya N.K., Antonova A.V. Heat resisting composites with matellical and intermetallic matrix// Metalls, 2001,#5, p. 68-78.

RHENIUM CONTENT EUTECTIC ALLOYS BASED ON ALUMINIDE NICKEL FOR AIROSPACE CONSTRUCTIONAL DETAILS

M.YU. Barabash, V.E.Oliker

Institute for Problems of Materials Science of NAS of Ukraine, Kiev, Ukraine

INTRODUCTION

High physico-mechanical properties intrinsic to nickel-aluminium materials make them rather promising for manufacture of the heat loaded parts of gas turbine and a number of other components used in modern engineering. Intermetallic NiAl compound has a number of advantages important for aerospace engineering due to its high melting point (1640°C), high thermal conductivity, low density of 5,95gm/cc which is approximately 2/3 those of state-of-the art nickel base superalloys and high resistance to oxidation [1]. Improvement of its mechanical properties may be achieved through its microalloying, which affects the level of structure perfection and morphology of eutectic compositions and allows to develop a number of composite eutectic alloyed materials with high mechanical characteristics. However, increase of ductility and high-temperature strength of nickel aluminides still remains a topical problem. Some projects of the National Aerospace Plane (NASP) and The High Speed Civil Transport (HSCT) [2-8] were dedicated to investigation of nickel aluminides. Ternary Ni-Al-Re alloys, which produce eutectic two-phase β-NiAl+γ-Re systems, are of interest, because the provide a possibility to achieve a successful combination of strength properties characteristic to intermetallic NiAl compound and to rhenium [1]. The Ni-Al-Re system was partially studied previously in [9]. There were studied the phase equilibrium states in the area of rhenium content from 0.1 to 33 at.% and the liquidus surface of state diagram of the Ni-Al-Re system was built in the plane of the triangle of concentrations. In was shown that introduction of rhenium dopes into nickel super-alloys allows to reach an increase of ductility and high-temperature creep resistance.

The area under consideration is peculiar for its rather wide range of β-NiAl homogeneity, which allows to vary the ratio of Ni and Al concentrations without any change in phase composition of the alloys. In this concern, the objective of this work, aimed at determination of the area, where two-phase (β-NiAl+γ-Re) alloys do exist at crystallization, and at finding location of the quasi-binary sectional view within the said area, seems to be quite topical. Besides, the precise location of the said area at the state diagram was not found by far.

THE RESULTS AND DISCUSSION

The Ni-Al-Re alloys were studied by the methods of differential thermal analysis and metallographic examination. Aluminium 99.999% pure, nickel, at least, 99.9% pure and powdered rhenium 99.85% pure were used as starting materials. The alloys were prepared in the arc furnace with a tungsten nonconsumable electrode placed at a brass water-cooled bottom, in the atmosphere of purified argon. The compositions of the made alloys are shown in Table 1. The differential thermal analysis was carried out in corundum Al_2O_3 crucibles using the thermal analyser VDTA-3 with symmetrical placement of thermocouples. The rate of heating and cooling was 60 degrees/minute. The X-ray phase analysis was done in Cu K_α rays using the diffractometer DRON 2.0. The structures of alloys were studied by methods of optical and electronic spectroscopy using microscopes Neophot-32 and JSXA-733.

The chemical composition of phases was determined using the electron probe X-ray analysis. The metallographic examination of the alloys falling on the equiatomic NiAl-Re section of the ternary fusibility curve of Ni-Al-Re system has shown that the alloy structure successively changes with Re content increase from a typical solid solution to a pre-eutectic-eutectic and eutectic structure.

Table 1. Composition of alloys

Content of elements, at. %				
Ni:Al	Ni	Al	Re	Structure
1:1	50.00	50.00	—	Nominal
1:1	49.90	49.90	0.2	Solid. sol.
1:1	49.00	49.00	2.0	Before eutectic
1:1	48.75	48.75	2.5	Binary. eutectic.
1:1	48.00	48.00	4.0	After eutectic
1:1	47.00	47.00	6.0	After eutectic
1:1	43.00	43.00	14	After eutectic
4 Ni	50.50	46.50	3.0	After eutectic
4 Al	46.50	50.50	3.0	After eutectic
8 Al	44.50	52.50	3.0	Ternery eutectic
12 Al	42.50	54.50	3.0	Ternery eutectic

The metallographic examination has shown that metal matrix in the eutectic state is a solid NiAl solution, which contains 0.2 at. % of rhenium, where rhenium leads eutectic crystallization and creates a frame with about 0.2 at.% of NiAl dissolved inside. The area of eutectic inside an alloy increases with Re concentration increase. At Re content of 2 at.% first crystals of refractory rhenium γ-phase appear.

According to DTA data, eutectics in all the alloys of NiAl-Re section melt at the constant temperature equal to 1665°C. Results of metallographic examination allow to discern the range of alloy compositions (2-2.5 at.% of Re), where eutectic should exist. The eutectic structure of (NiAl+Re) alloys may be classified as an anomalous. The detailed morphology study of the eutectic colony using the scanning electron microscope allowed to find out that it has a fibred structure.

The study of the microstructure of alloys at different values of Re/Al ratio allowed to determine the width (from 46 at. to 53 at.% of NiAl) of the area of the two-phase equilibrium between the solid solution formed by Inter-metallic NiAl compound (β-phase) and Re (γ-phase).

CONCLUSIONS

It was found that polythermal NiAl-Re section of the ternary system is quasi-binary. Any deviation of compositions of the monovariant eutectic alloys from this section results in decrease of the eutectic equilibrium temperature. The area of existence of the two-phase alloys (β-NiAl+γ-Re) was found for crystallization of the ternary Ni-Al-Re system.

REFERENCES

1. *Darolia R.,Lahrman D. F. Field R.D.* Overview of NiAl for high temperature structural application, Ordered Intermetallics-Physical Metallurgy and Mechanical Behaviour, 1992. P. 679-698
2. *Darolia R.* NiAL for High-Temperature Structural Applications // JOM 1991. **43,** 44.
3. *Sauthhoff G.* // Metallkde 1989. **80**, P. 337.
4. *Sauthhoff G.* in High Temperature Aluminides and Intermetallics, ed. al. (Warrendale, PA: TMS), 1989. P. 329.
5. *Law C. C., Blackburn M. J.* Rapidly Solidified Lightweight Durable Disk Material (Final Report AFWAL - 1987. TR - 87-4102)
6. *Noebe R. D., Bowman C.L.* in HIGHTEMP Review 1990 (NASA CP 10051 20-1), 1990.
7. *Noebe R. D., Bowman C.L.* Gibala R. in High Temperature Aluminides and Intermetallics, ed. S.H. Whang et.al. (Warrendale, Pa: TMS), 1989. P. 271.
8. *Vedula K., Pathare V.,* in High Odered Intermetallics Alloy IV, ed. Koch C. C. et.al. (MRS Symposium Proceeding **39**), 1985. P. 411.
9. *Cornish L. A., Witcomb M. J.* A metallographic study of the Ni-Al-Re phase diagram, // Material Science and engineering. — 1997.— A **239-240**, P. 75-87.

ALN-BASED HIGH-STRENGTH CERAMIC COMPOSITE

O.V.Pshenichna, G.K.Kozina[t)

Frantzevich Institute for Problems of Materials Science NAS of Ukraine, Kyiv, Ukraine
[t)Bakull Institute for Superhard Materials Science NAS of Ukraine, Kyiv, Ukraine

Aluminum nitride is challenging for using in technology as a basis for constructive materials due to its high specific modulus of elasticity, good strength properties and high heat resistance. The major problem faced by the formers of ceramic constructive materials – increasing of fracture failure resistance – is usually solved by creation of heterogeneous structure with considerable grain and phase boundary extension, effectively dissipating energy of the extending crack.

We worked out the heterophase material AlN-TiN, in which the matrix phase – aluminum nitride–is reinforced by dispersed particles of titanium nitride [1-3]. It was produced by hot pressing (HP) of charge comprising a mixture of industrial powders of nitrides of furnace (fs) and plasma chemical synthesis (pcs), sintering of preforms in the nitride medium without pressure impressing (SN), sintering of composite powder AlN-TiN received by titanium aluminide nitriding (NS), reaction sintering of AlN and titanium hydride mixtures in nitrogen (RS). In the limits of 60-80 % (mass.) of TiN, the material possesses high compression and flexural strength, significant hardness to 800 °C (figure), fracture toughness and thermal resistance (Table 1 and 2). The obtained properties are conditioned by formation of

strong bonds on phase boundary, high density, structural homogeneity and self-reinforcement effect.

To improve the material's properties and increase their repeatability, specialties of formation of the structure and bonding on phase boundary under various conditions of the material preparation and there influence over the properties were studied in the present work by application of a complex of up-to-date methods.
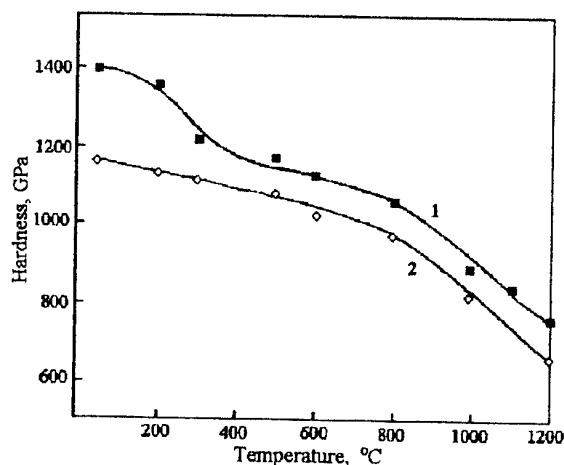
Figure. Dependence of hot pressing (1) and sintering (2) AlN-TiN materials hardness on temperature.

Significant influence of impurities, in particular of oxygen, on formation of strong bonding between the phase components of the material and on structural transformations in it in the process of sintering and prolonged high-temperature exposure time was revealed. Formation of the bonding at the phase boundary of AlN-TiN in the process of sintering or hot pressing is determined mostly by diffusion of titanium into the near-surface layers of AlN particles forming finite solid solution of replacement of aluminum by titanium in the

Table 1. Hardness, friction coefficient and wear of AlN-TiN-heterophase materials

material	γ, %	Hv, GPa	f*	W*, μm/km
NS	= 93	12	-	-
HP	= 98	14	0,12	6,0
SN	93- 97	12	0,17	7,2
RS	87	8	-	-

*P=2 MPa,   v =16 м/s

narrow edge area. It is determined by considerable concentration of point defects in them in particular vacancies in the aluminum sublattice and impurity oxygen atoms. Relaxation of the point defects results in thickening of spinel phase layer with soluble titanium at the phase boundary under influence of electrostatic forces and lattice elastic resistance forces.

Eutectic interaction at 1830°C of spinel with oxide film, covering AlN particles due to partial hydrolysis of nitride in the air, results in appearing of a liquid phase at the boundaries in the process of sintering and hot pressing. The liquid phase activates mass transfer in the process of phase diffusion interaction as well as the process of densification of AlN-TiN under sintering including diffusion enrollment of AlN and TiN grains with formation of coherent boundaries.

The latter mechanism is believed to be responsible for binding oat phase boundaries when receiving heterophase material AlN-TiN by nitriding of titanium aluminide and by reaction sintering.

Table 2.Compression and flexural strengths and fracture toughness of AlN-TiN heterophase materials

material	σ_c, MPa	σ_f, MPa	σ_f**, MPa	K_{1C}, MPa.м-$^{1/2}$
NS	1650	580	525	3,4
HP	1930	670	-	4,6
SN	1600	610	560	4,2
RS	720	240	200	-

**after 10 temperature quick changes from 1200 to 20 °C

Heterophase material strength is determined - besides the bond strength - by dispersity and homogeneity of phase aggregate distribution and grains morphology. High strength of the materials (HP and SN) remaining after 2.5-hour heating at 1950°C is connected with dispersed homogeneous structure in which grains of one phase resist growing of the other phase grains. The

material (NS) possesses high purity and superfine homogeneous structure at the "chemical mixing" level. To receive similar structure aluminide nitriding should be conducted at the possible low temperature. It allows preserving distribution of nitride-forming elements close to that of the phase-precursor.

Evolution of the microstructure of AlN-TiN materials received by sintering and hot pressing of the charge from industrial powders in the process of high-temperature annealing is substantially determined by influence of oxygen dissolved in matrix phase lattice. It is connected with poly-type transformations caused by segregation of solid solution of substitution of nitrogen by oxygen in AlN with formation of lamellar and needle-shaped crystals, the quantity of which increases with the rising of the temperature and exposure time. Separation of anisometric crystals in the material favors growing of its strength and crack resistance due to self-reinforcement effect.

Analysis of the received characteristics of strength and other properties of the worked out materials and evaluative costs allow suggesting (HP) and (SN) as constructive materials for using in conditions of wear, considerable temperature and loading, more low (RS) material - as refractory brick and (AS) - as functional material with special electric and thermal properties.

1. Кузенкова М.А., Кислый П.С., Пшеничная О.В. Структура и свойства композиционных материалов на основе нитридов Ti, Zr и Al. // Изв.АН СССР, Неорганические материалы. - 1976. - т.12, №3. -С.430-434.

2. Пшеничная О.В. Гетерофазные материалы на основе нитридов титана, циркония и алюминия. - Дисс....канд. техн.наук. - Киев: ИПМ АН УССР - 1981.-207 с.

3. ТУ 88 УССР, ИСМ 736-80. Футеровочная плита для плавильных ванн.

TO MODELING OF INFLUENCE OF THE CHARACTERISTICS OF POROUS COVERINGS AND STRUCTURES ON LIMITING HEAT FLUX DENSITY AT STEAM PHASE GENERATION

Kostornov A.G., Shapoval A.A., Shapoval Art.A.[1]

Frantsevich Institute for problems of materials science NAS of Ukraine, Kiev, Ukraine

(1) National technical university of Ukraine "KPI", Kiev, Ukraine

The researches of influence of the characteristics of porous coverings and structures on heat transfer at phase transformations of heat-carriers liquids are necessary for the decision following urgent of thermophysical tasks and problems: 1) creation the universally recognized theory of boiling on heat intensive technical surfaces; 2) finding-out of mechanisms of heat transfer at boiling on porous surfaces; 3) reception of the formulas and dependence allowing to expect parameters of heat transfer at phase transformations of liquids on porous surfaces in view of the determining characteristics last. A number of researches of heat transfer at boiling on surfaces with porous coverings and structures [1,2] has shown that except for essential increase of intensity of heat transfer (10-12 multiple increases in comparison with smooth technical surfaces). (2-4) multiple increases limiting (so-called critical) values of a heat flux density are also possible.

Some results of researches of heat transfer are submitted at boiling water on surfaces with metal fibrous porous coverings and structures created in IPMS of Ukraine presented in [3]. Approached semi-empirical model of heat transfer at vaporization in such conditions is offered in [4]. Within the framework of proposed model was possible to logically interpret complex influence of a number of the structural, geometrical and thermophysical characteristics of porous coverings on intensity of heat transfer at boiling. Also may be used the modeling of vaporization at the large values of density and at the conditions of critical parameters of heat transfer. As is known, there is so-called "a hydrodynamic theory of crises of boiling ", stated in works S.S.Kytateladze [5]. However within the framework of this theory it is impossible to explain essential increase limiting density of a heat flux typical of porous

surfaces. G.F.Smirnov in [6] and S.A.Kovalev in [7] are offered other mechanisms of heat process for these conditions. These mechanisms however still require verify by experimental measurement. By us, in the present work it is offered to consider influence on limiting density of heat flux at steam generation (in particular, at boiling) such factor, not taken into account in similar researches, as presence of the additional centers of steam generation on fractions (particles of porous coverings), arising on some removal from the basic surface of heating. It is obvious, that at the large sizes of density of a heat flux the potential centers of steam generation are capable to be made active and to ensure additional (except for the basic centers which are taking place in places of contact of a litting surface with particles of a porous covering) of a steam phase generation. By development of physical model of the mechanism of generation pair at the expense of the additional (removed) centers of a steam phase generation the following assumptions simplifying the valid real process of boiling are made. An assumption 1: the separate fraction (in our case - piece of a fibre) represents the vertically located cylindrical core having ideal contact to a litting surface. The following assumption 2: the metal core is covered with a microfilm of a liquid, which thickness is constant on his height. Further - 3: the roughness of a surface of the cylinder corrsponds to a roughness of a litting surface. In view of the made assumptions by us the temperatures on a surface of a core paid off. Thus were set: 1) superfluous temperatures at the basis of a core; 2) physical characteristics of a core and liquid; 3) thickness of a microfilm of a liquid covering a surface of a core - edge and other necessary parameters. As a first approximation, proceeding from a number of known

works, the thickness of a microfilm was equated to thickness of a microlayer of a liquid under bubbles of liquids at boiling. Further, in dependence, basically, from high heat conductivity of a core, the falls of temperature pressures on height of a core (dependence paid off are given in the report). The data of accounts were compared to known sizes overheating of a liquid [5], necessary for activation of the potential center a steam phase generation. The results of accounts are compared to experimental data received earlier in [2,3]. They are satisfactorily coordinated with experiment, confirming that fact, that porous coverings and the structures executed from heat conductivity metal fibres, provide essential (up to 4 times) increase of limiting density of a heat flux in comparison with smooth technical surfaces. For real processes the complication of a picture of heat transfer takes place in comparison with our assumptions. First, a number of fibres not ideally contact to a litting surface. Secondly, the significant part of fractions is in a flux of a liquid. Thus boundary conditions for accounts of a task of heat transfer change. Thirdly, it is necessary to take into account contacts of monoparticles of a porous covering to others at particles that essentially complicate model. However our results confirm the following conclusions: 1) at steam phase generation the occurrence of the additional centers vaporization on particles removed from a litting surface, is real; 2) generation pair by such additional centers in many respects explains the reasons of increase of limiting density of a heat flux at vaporization on porous surfaces.

REFERENCES

1. Николаев Г.П, Токалов Ю.К. Кризис кипения на поверхностях с пористым покрытием. – Инж.-физ. журн., 1974, 26, №1, с. 5-9.
2. Шаповал А.А., Зарипов В.К., Семена М.Г. Влияние характеристик пористых покрытий на первую критическую плотность теплового потока при кипении. - Атомная энергия, 1988, 64, № 4, с. 62-63.
3. Шаповал А.А., Зарипов В.К., Семена М.Г. К расчётам интенсивности теплообмена при кипении на поверхности с пористыми покрытиями. - Известия АН СССР. Энергетика и транспорт, 1989, № 3, с. 63-68.
4. Шаповал А.А. К моделированию процессов теплообмена при кипении на поверхностях с неупорядоченными пористыми структурами. – Тепломассобмен ММФ-2000. IY Минский международный форум (22-26 мая 2000 г.). Т.5. Тепломассоообмен в двухфазных системах, с. 198-204.
5. С.С.Кутателадзе. Основы теории теплообмена. М.: Атомиздат, 1979. – 416 с.
6. Смирнов Г.Ф. Основы теории замкнутых теплопередающих испарительных систем: Автореф. дис. ... докт. техн. наук. – Л., 1979. – 45 с.
7. Ковалев С.А., Соловьёв С.Л. Испарение и конденсация в тепловых трубах. М.: Наука, 1989. - 112 с.

ELECTRONIC STRUCTURE AND ELECTRICAL PROPERTIES OF LANTHANUM NICKELITES BASED CONDUCTING MATERIALS

Bondarenko T., Zyrin A. [(1)], Uvarov V. [(2)]
(1) Institute for Problems of Materials Science NAS of Ukraine, Kiev, Ukraine
(2) Institute of Metal Physics NAS of Ukraine, Kiev, Ukraine

INTRODUCTION

The modern power, electrothermie, analytical chemistry etc. need of electroconducting materials, which can durable work at high temperatures in gas environments with high oxygen partial pressure. The unique thermodynamic stable in these conditions materials are oxide compounds. The high already at room temperature conductivity can be created at such compounds, which contain oxides of metals with variable valency. The beforehand given electron or hole current carriers concentration in such materials is possible to be created applying so the named regulation of valency method [1]. These electroconducting oxide materials are used wide as fuel cells and other current sources electrodes, gas sensors, electric heating elements etc. Mainly such materials are doped rare earth manganites, cobaltites, chromites. Nickelites are less investigated. But they cause interests due to their metal type conductivity at increase temperature. The present message is devoted to research of their electronic structure and electrical properties.

RESULTS AND DISCUSSION

The homologous lanthanum nickelites row is known, which composition can be expressed by the formula:

$La_{(n+1)} Ni_n O_{(5n+3+x)/2}$ [2]. The index x reflects a possibility of nickel valence increase with 2^+ up to 3^+, to what is connected significant hole conductivity of these substances. The number of nickel atoms with increased valency depends on conditions of synthesis and operation of a material.

Measured by us the conductivity temperature dependence of ceramic samples $La_2NiO_{(4+x/2)}$, $La_3Ni_2O_{(6,5+x/2)}$ and $La_4Ni_3O_{(9+x/2)}$ had a semiconducting character in arrange of temperatures from 20°C up to (200... 300) °C and metallic for want of higher temperatures. The measurements were realized in air atmosphere by the 4-th contact method. Synthesis of nickelites from oxides NiO and La_2O_3 made in air at the temperature of 1100 °C. Ceramic samples was sintered in an air at temperature 1300 °C. On datas of XRD-analysis all samples were single-phase and had K_2NiF_4 structure.

For want of diminution of magnitude La/Ni conductivity decreased (for example, for want of 800°C - from 330 up to 67 $Ohm^{-1} \cdot cm^{-1}$). For stabilization of current carriers concentration in a material by us are synthesized hetherovalentic solid solutions of composition $La_{(2-y)}Ca_y Ni O_4$. At the expense of substitution La^{3+} on Ca^{2+} in a material should be fixed an equivalent number of current carriers connected to emerging in the lattice Ni^{3+}. Calcium doped lanthanum nickelite ceramic samples (for want of y = 0,4) conductivity was really more than in 3 times above, than at undoped nickelite. Temperature of transition from semiconducting conductivity to metallic for want of it has remained former (Fig.1).

For clarification of the researched nickelites electronic structure the X-ray spectroscopy methods were used. The emission fluorescent $NiL\alpha$-, $OK\alpha$- spectra were obtained on a spectrometer САРФ-1 with the copper anode and crystal-analyzer RbAP. These spectra resolution has made ~0,2 eV.

Researched nickelites have a K_2NiF_4-type structure. For a comparison the NiO (structure of type NaCl) spectra are obtained. The availability of Ni-containing oxygen octahedrons is characteristic of both structures types.

$OK\alpha$- spectra characterize the oxygen p (genetically 2p)- energy distribution. $NiL\alpha$-spectra show of valence ds(genetically 3d4s) - electrons distribution.

That the Ni4s- electrons density in compounds is small, $NiL\alpha$-spectra characterize practically in the pure state Ni3d-electrons distribution.

The charge state of atoms is determined on a of spectral lines shift.

The $NiL\alpha$-spectra shape and width in La_2NiO_4 show, that this element d-states are distributed in a zone width about 23 eV. This the most intensive density of states maximum is near the zone ceiling. The less maximum is located approximately on 4,5 eV below the main maximum. There is a weak inflow in the smallenergy part of the spectra. It means Nid-states presence in a bottom part of the valence zone. La_2NiO_4 $OK\alpha$-spectra testify that the oxygen p-

states are distributed in a band about 8 eV width. The main maximum of these states distribution is in a band's upper part. The less intensive maximum adjoins to it on the part of smaller energies.

The spectrum shape shows two types of bonding Me-O (π- and σ-) presence.

In spectra of nickel and oxygen in La_2NiO_4 there are common features with spectra of the same elements in $LaNiO_3$,wich has perovscite structure [3]. It is connected to availability in structures of both types Ni-containing oxygen octahedrons, i.e. with preservation for Ni atoms of coordination number and of the first coordination polyhedron structure. For atoms of oxygen the structure of the first coordination polyhedron (the nickel atoms) also is the same.

The doping of nickelites by calcium changes slightly nickel and oxygen density of states (the parity of maxima intensity is changed both for NiLα- and OKα-spectra). It is accompanied by the atoms charge density redistribution. For want of transition from La_2NiO_4 to $La_3Ni_2O_{6,5}$ and $La_4Ni_3O_9$ an electronic structure and charge state of Ni- and O-atoms also is changed. It fairly and for want of transition from nickelites to NiO.

The X-ray spectra reveal most typical features of these compounds valence zone structure. In its upper subzone (width about 11-12 eV) are concentrated hybrid Ni3d- and O2p-states. The upper subzone's XRE-spectra shape shows the decomposition of Ni3d-states by a crystalline field (states of eg- and t2g-type). The lower subzone is generated mainly subvalent La5p- and O2s-electrons with small impurity of Ni3d-electrons.

The SW Xα - method calculation of full and partials dencity of states was executed for $La_{(2-y)}Ca_yNiO_4$ (y=0; 0.1; 0.2; 0.3 and 0.4). There is good agreement with the experimental data.

CONCLUSIONS

1.Valence zone in lanthanum nickelites consists of several subzones.
2.Doping La_2NiO_4 by calcium (that increased concentration of current carriers and diminution of the La-contents in isostructure nickelites) result in some changes of the electronic structure and charge on atoms .
3.The nickelites composition change (variations of the ratio La / Ni) gives any changes in their electronic structure and in nickel and oxygen atoms charge states.

4.There is a large rebuilding in nickelites valent Nid-electrons distribution relatively Ni metallic. The nickelites electron structure changes visible the same of NiO. But nickelites and oxide's electron structure has also a row of common character lines.
5.Of a nickel and oxigen atoms charge in nickelites differs from those in NiO.
6.La_2NiO_4 electron structure may be calculated by SW Xα-method.
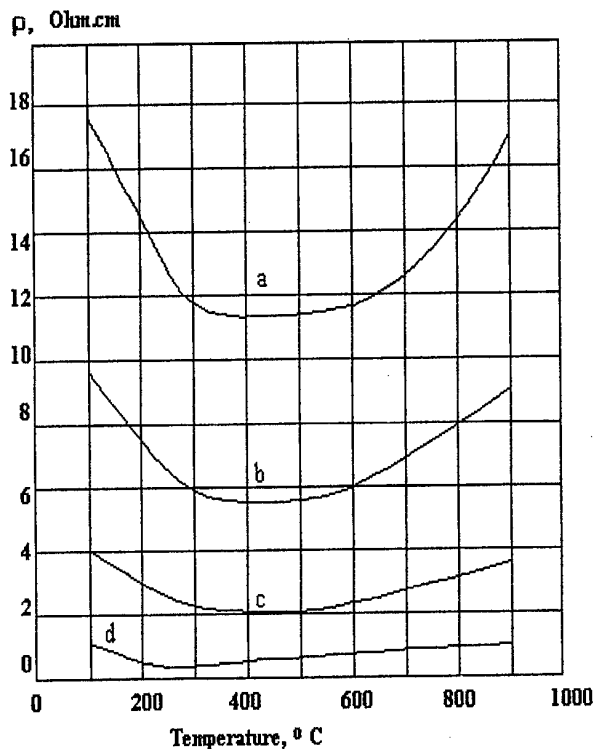
Fig.1.Resistivity of $La_{(2-y)}Ca_yNiO_4$ as a function temperature:y=0(a); y=0.1(b); y=0.2(c); y=0.3(d).

REFERENCES

1.Зырин А.В., Тресвятский С.Г. Оксидные электропроводные полупроводниковые материалы. В кн."Новые материалы из оксидов и синтетических фторсиликатов".-К.:Наукова думка.1982.

2. Mohan Ram R.A., Ganapathi L., Ganguly P., Rao C.N.R., J. Solid State Chem.1986; 63:139.

3.УваровВ.Н.,НемошкаленкоВ.В.,НедилкоС.А. и др. Особенности электронного строения окисла $LaNiO_3$, обладающего металлическим типом проводимости.-Металлофизика и новейшие технологии,2001,т.23,N4,с.419-429.

POROUS COMPOSITES OF METALLIC FIBERS AND POWDERS. PRODUCTION AND PROPERTIES

Kostornov A.G., Moroz A.L. and Verbylo D.G.

Institute for Problems of Materials Science, National Academy of Sciences of Ukraine, Kyiv, Ukraine

Methods [1,2,3] are known for the improvement of properties of powder and fiber materials. Improvement of structural and hydrodynamic characteristics is achieved through a non-uniform porous structure created, for instance, by the methods of dry or wet powder and fiber blending, settling of fine particles in sintered large-porous compacts, alternating of the charge of fibers and that of powders in a die with subsequent pressing and vibration damping. However, the above methods have disadvantage because of difficulty of making porous materials of metallic fibers and powders having a homogenous porous structure and large-sized.

This paper describes peculiarities of the manufacture of porous sheet materials made of metallic fibers and powders, and of their properties. Formation technique for porous sheet materials was studied by vibration dispersion and settlement of fibers and powders in layers. It was found that powders are able to be introduced into a high-porosity fibrous preform through a desired depth.

A simple and efficient method of formation was developed, which allowed preparation of various potential structures:

- in the form of separated high-porosity fiber/powder layers settled in a proper consequence;
- in the form of high-porosity fibrous frame filled with powder to the desired depth.

Structural and hydrodynamic characteristics of single-layer and two-layer materials made of fiber/powders of stainless steel are given below.

Specimens of 30 mm in diameter and porosity of 20 to 75 % were used for study. Specimens of fiber/powder layers having initial heights of 8 and 2 mm, respectively, produced by joint and separate sintering and pressing at 1.25 to 40 MPa, were cutting shaped.

As investigations revealed, layered specimens were superior to porous «pure» fibrous fiber or powder materials .in terms of complexity of properties «permeability-pore size». Thus, material containing a layer of 50 micron fibers, and a layer of powder with 60 to 80 micron grain sizes and 60 % porosity, has two times smaller pores in comparison with a single-layer material of similar fibers, and 5 times higher permeability in comparison with a single-layer materials made of similar powder.

The porous fiber/powder composites as designed can include either one or several coarse-pore layers; or one or several fine-pore layers. The pore sizes in the bulk of these materials can vary by 1 to 2 orders in dependence on the ratio of fibers and powder particles. This was supported by the integral and differential curves for the material containing a layer of fibers averaging from 100 to 45 microns, and a layer of powder of 40 microns having the 9 and 2 microns maximum and mean pore sizes. The pore size gradient in the bulk of biporous material is 10, proceeding from the maximum sizes, and 22 as proceeding from the mean pore sizes.

An interest should also be paid to the investigation results of physical/mechanical properties of «pure» fiber, layered or frame-like materials made of stainless steel.

Rectangular specimens measuring 1 to 5 x 6 mm and of porosity from 30 to 90 % produced using the above route, were used for experiments. Microdeformation of the materials under study was examined by the results of four-point bend testing on the testing unit of CERAM-type [5].

As revealed the test results, conductivity and elasticity of materials reduced with porosity increased. «Pure» fiber materials then are superior to layered ones by electrical conductivity and elasticity through all the pore variation range, whereas frame-like materials are only superior in the high-porosity region (over 60 %). Different values of electric conductivity and elasticity of the materials under study are due to peculiarities of densification process of materials, fibers and powders, and to a totally contact nature of densification, and flexible-rigid mechanism of densification of fibers with formation of multiple interfiber contacts of high performance.

Layered materials include a strong and plastic fiber layer and rigid powder layer, that causes the decrease of electrical conductivity and elasticity. Under loading, these materials always exhibit the fracture of their more rigid and less plastic powder layer.

In frame-like materials, the main load is taken up by the strong and plastic fiber frame. Therefore, materials in the form of high-porous fiber frame retaining thin working fiber/powder layers feature high permeability and plasticity. These materials are good to produce efficient tubular filter elements of any size through bending and welding. of them. Materials in the form of fully filled fiber frame having porosity less than 60 % have higher rigidity than «pure» fibrous materials.

The studies resulted in the design of sheet composite materials having an efficient porous structure and improved strength characteristics. These materials have potential for the use in filters, heat exchangers of evaporation-condense type, phase separators, noise- and sound absorbers.

References

1. Tumilovich M.V., Kostornov A.G., Leonov A.N. at al. Porous fiber/powder materials based on copper. Poroshkova metallugia. 1992, No.3, c. 56-60.
2. Certificate of Invention No. 1014657 USSR. Vityaz P.A., Sheleg V.K., Kantsevich V.M., at al. Bul. Izobr., 1983, No.16.
3. Leonov A.N., Tumilovich M.V., Kostornov A.G., Sheleg V.K. Porous fiber/powder materials based on copper. Poroshkova metallugia. 1997, No.9/10, c. 23-28.
4. Kostornov A.G. Permeable metallic fibrous materials. Kyiv: Technica, 1983, 128 p.
5. Firstov S.A., Shlesar M. Structure and strength of powder materials. Kyiv: Naukova dumka, 1993, 170 p.

THE STRUCTURE AND SOME PROPERTIES OF COMPOSITES ON THE BASE OF TITANIUM NITRIDE.

T.M. Evtushok, A.D. Kostenko, O.N. Grigorev, G.L. Zhunkovskii, and V.A. Kotenko
Institute for Problems of Materials Science, National Academy of Sciences of Ukraine, Kiev, Ukraine

An analysis of the literature [1] and our investigation on the development of antifriction materials [2-4] show that significant improvements of tribologic properties can be obtained by using, as a hard component, refractory compounds with a low adhesion activity. In this respect, titanium nitride is the most attractive compound. Works on the improvement of the wear resistance of parts and tools by application of titanium nitride coatings, that, in essence, serve for decreasing the adhesion interaction in the pair with a counterbody, have long and widely been known.

We developed frame and matrix-filled type composites on the base of titanium nitride.

The physicomechanical conditions of the formation of the dense and strong structure of new powder composites with a high wear resistance under conditions of dry friction were studied.

The influence of the ratio of components in the composites on their physicomechanical properties was investigated. The ranges of the strength properties of these materials (bending strength σ_{bend} from 700 to 1150 MPa, hardness HRA from 78 to 87 units) and their optimum levels that are 890-900 MPa and 83-85 units, respectively, for using in the pair with hardened steels were determined.

The tribologic characteristics of the composites, namely, the friction coefficient and wear at sliding rates from 5 to 25 m/s under a load of 1 MPa in the pair with hardened 65G steel in dry friction in air were studied (Fig. 1).

It was established that the frame type materials prepared by the impregnation method have the level of tribologic properties which is twice or trice that of materials prepared by sintering.

The test results show that the new composites exhibit a high level of the tribologic properties which is an order of magnitude higher than that of familiar composites on the base of such refractory compounds as TiC and Cr_3C_2.

The prepared materials can be recommended for dry friction assemblies at sliding speeds from 20 m/s under a load of up to 1 MPa inclusive.
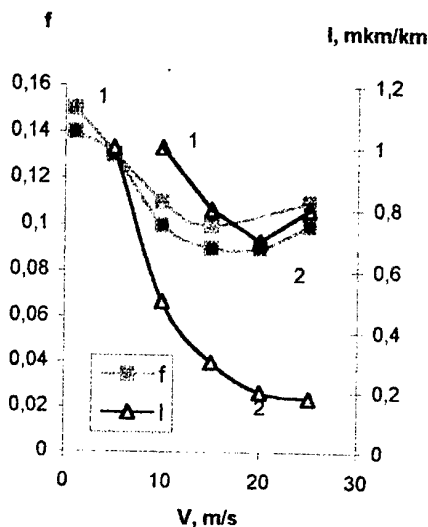
Fig. 1. Dependences of the friction coefficient and wear on the sliding speed of friction pairs under a load of 1 MPa:
1 – [TiN-(60BrO10C10-40(Cu-Ni))] – 65G;
2 – [TiN-Ni₃Al] – 65Г.

REFERENCES

1. Fedorchenkp I.M. and Pugina L.I.//Sintered Composite Materials. -Kiev: Naukova Dumka. 1980 -404 p.
2. Zhunkovskii G.L., Evtushok T.M, Mazur P.V, et al.// Borides and Materials on its Base: Collection of Works. Kiev: IPM AN USSR, 1994. P. 147-150.
3. Zhunkovskii G.L., Evtushok T.M, Strashinskaya L.V., et al.// Refractory nitrides and materials on their base: Collection of Works. Kiev: IPM AN USSR, 1992. P. 184-190.
4. Evtushok T.M., Zhunkovskii G.L., Koval'chenko A.M., et al. Structure and tribologic properties of cermets prepared by the impregnation method, Adgez. Raspl. Paika Mater., No. 29, 1993, P. 73-77.

THERMOELECTRIC MATERIALS ON BASES BOTH OF LEAD AND OF LANTAN'S GROUP ELEMENTS TELLURIDES

Freik D., Mykhajlyonka R., Mezhylovsjka L.

Physics-Chemical Institute at Vasyl Stefanyk Precarpathian University, Ivano-Frankivsk, Ukraine;
Email: freik@pu.if.ua

The lead telluride is a perspective semiconductor material for making of thermoelectric devices, which function in an interval of temperatures from room up to 900 K [1]. The efficiency of use of a material is determined by opportunities of achievement of high values of thermoelectric parameters: α, σ and $\alpha^2\sigma$ [2], and also its stability both to thermal fields, and to atmospheric gases. One of probable ways of enriching of the specified performances is introduction geterovalence of substitutional atoms.

To attention there were selected solid solutions $(PbTe)_{1-x}$ $(Gd_2Te_3)_x$ of a composition $0,0 < x < 0,06$, $(PbTe)_{1-y}(Tb_2Te_3)_y$ of a composition $0,0 < y < 0,10$, and also $(PbTe)_{1-z}(Eu_2Te_3)_z$ of a composition $0,0 < z < 0,08$. Synthesis carried out at temperatures 1200-1500 K, which was determined by the content of an alloy and got out on the basis of the analysis T-x (y, z) phase charts [3,4,5]. Then samples gave in homonization annealing at temperatures 750-850K on an extent 550-600 h. Is confirmed, that in system PbTe-Gd_2Te_3 sideways lead telluride there are restricted series of solid solutions, which depend on temperature and have 3,5-5,5 mol. % Gd_2Te_3 at 300-1000K accordingly. Thus small contents Gd_2Te_3 (up to 2 mol. %) causes sharp decrease of a direct-current conductivity (σ) both thermal conductivity (χ) and ascending of coefficient thermal electromotive force (α). It also gives in ascending thermoelectric power ($\alpha^2\sigma$) and thermoelectric quality factor (Z) (fig. a). In a solid solution PbTe-Tb_2Te_3 the addition Tb_2Te_3 to PbTe essentially variates an electrical conductivity (σ), coefficient thermal electromotive force (α) and thermal conductivity (χ): the thermal conductivity monotonously decreases, and electrical conductivity and coefficient thermal electromotive

force are unmonotonously variate. Such doping Tb_2Te_3 gives in ascending thermoelectric power ($\alpha^2\sigma$) and thermoelectric quality factor (Z) (fig. b). Lead telluride with europium telluride Eu_2Te_3, according to results of operations [8], forms restricted series of solid solutions. At 1123 K at solid solutions the concentration of Eu_2Te_3 is 6 mol. % and at decrease of temperature to room smoothly decreases up to 5 mol. %. With augmentation of contents of europium telluride in a solid solution $(PbTe)_{1-x}(Eu_2Te_3)_x$, in boundaries of homogenity field, have decrease of a thermal conductivity (χ). A direct-current conductivity (σ), and coefficient thermal electromotive force (α) are unmonotonously variates with a composition. Note, that the inappreciable doping lead telluride by Eu_2Te_3 gives in ascending thermoelectric power ($\alpha^2\sigma$) and thermoelectric quality factor (Z) (fig. c).

By methods of crystallochemistry is analysed defect status of the basic matrix PbTe in solid solutions PbTe-Gd_2Te_3, PbTe-Tb_2Te_3, PbTe-Eu_2Te_3. Taking into account, that nuclear radiuses [6] of рідкісноземельних elements, which close to lead nuclear radius, it is possible to assume, that the atoms of рідкісноземельних elements substitute octahedron hollow of lead in lead telluride p-type. That is the mechanism of replacement is implemented which is implemented by the equation:

$$(1-x)[(Pb^x_{1-\beta}V''_\beta)_{Pb} Te^x_{Te} + 2\beta h^{\cdot}] + x[(R_{2/3}V''_{1/3})_{Pb} Te^x_{Te}] -$$

$$\rightarrow [Pb^x_{(1-\beta)(1-x)} R^x_{\frac{2}{3}x} V''_{\frac{1}{3}x+\beta(1-x)}]_{Pb} Te^x_{Te} + [2\beta(1-x) + \frac{2}{3}x]$$

,

Where b – diversion from stechiometry, and R – atoms of Gd, Tb, or Eu.
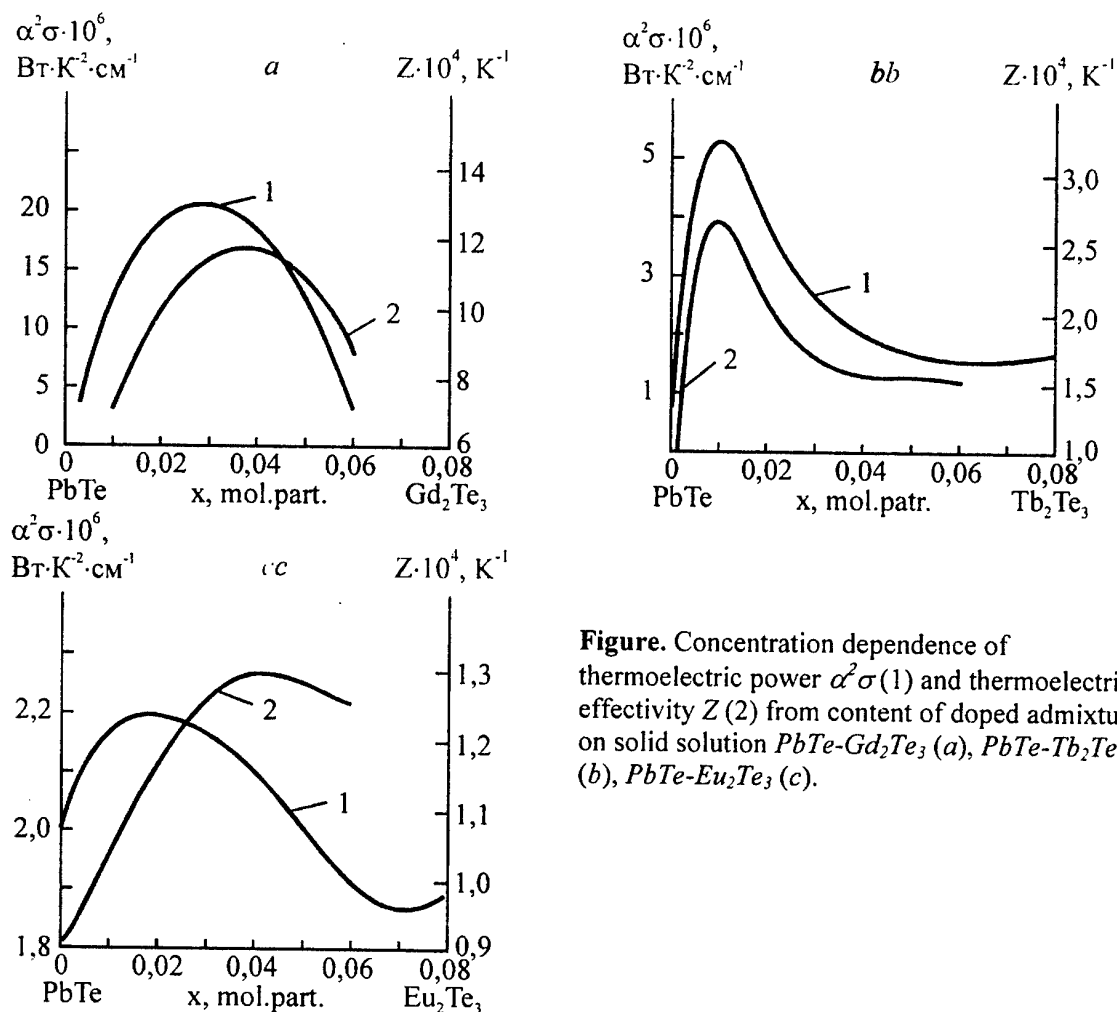
Figure. Concentration dependence of thermoelectric power $\alpha^2\sigma$ (1) and thermoelectric effectivity Z (2) from content of doped admixture on solid solution $PbTe\text{-}Gd_2Te_3$ (a), $PbTe\text{-}Tb_2Te_3$ (b), $PbTe\text{-}Eu_2Te_3$ (c).

Optimum values of a thermoelectric quality factor ($Z=11{,}64\cdot10^{-4}$ K^{-1}, $Z=2{,}65\cdot10^{-4}$ K^{-1}, $Z=1{,}296\cdot10^{-4}$ K^{-1}) have solid solutions of the relevant compositions $(PbTe)_{0,96}(Gd_2Te_3)_{0,04}$, $(PbTe)_{0,99}(Tb_2Te_3)_{0,01}$, $(PbTe)_{0,96}(Eu_2Te_3)_{0,04}$.

1. V.M. Shperun, D.M. Freik, R.I. Zapukhlyak. A thermoelectricity of lead telluride and its analogs. Play. Ivano-Frankivsk. (2000).

2. L.I. Anatychuk. Thermoelements and thermoelectric devices: the manual. A scientific idea. K. (1979).

3. I.O. Nasibov, T.I. Sultanov, M.I. Murguzov, V.K. Valiev, S.M. Alidjanova. Alloys of system PbTe - Gd$_2$Te$_3$, Inorganic materials, **21**(12), 2090-2091 (1985).

4. I.O. Nasibov, T.I. Sultanov, M.I. Murguzov, V.K. Valiev, S.M. Alidjanova. Field of solid solutions on PbTe basis in system PbTe - Tb$_2$Te$_3$, Inorganic materials, **21**(12), 2019-2020 (1985).

5. I.O. Nasibov, T.I. Sultanov, V.K. Valiev, S.M. Alidjanova. Properties of solid solutions (PbTe)$_{1-x}$(Eu2Te3)$_x$ (x < 0,14), Inorganic materials, **22**(5), 515-517 (1986).

S.A. Semiletov. Tetrahedronical and octahedronical covalent radiuses. Crystallography, **21**(4), 752-758 (1976).

PHASE EQUILIBRIA AND THERMODYNAMIC CHARACTERISTICS OF THE Cu-Zr SYSTEM

Semenova E.L., Sidorko V.R.

Institute for Problems of Materials Science, National Academy of Sciences of Ukraine, Kyiv, Ukraine

Introduction

The Cu-Zr liquid alloys over a range of 25-75 at. % Zr can be transformed into a glassy state. This ability make them one of the basic systems for obtaining a new class of advanced materials, which possess a high electrical conductivity, ferromagnetism, superconductivity.

The Cu-Zr alloys can be considered as the oxide dispersion alloys (fine dispersion of ZrO_2 in copper matrix). Such material exhibits a combination of high electrical and thermal conductivity, good mechanical properties, stability of microstructure at high temperature.

Due to Shape Memory Effect discovered in an equiatomic alloy a class of smart materials, displayed the unusual physical-mechanical properties at various temperatures can be developed.

The Cu-Zr alloys are used in electrical and electronic applications where conductivity, strength and formability are requied.

Literature Data

The literature data up to 1988 are given in the review by [1] and up to 1991 by [2]. Subsequently the Cu-Zr system phase equilibria were studied by several techniques and for different composition ranges and temperature. The following intermetallic compounds of the system are fairly well established: $Zr_{14}Cu_{51}$, Zr_3Cu_8, Zr_7Cu_{10}, ZrCu and Zr_2Cu. No one of them has a homogeneity range. Data as to stoichiometry of some intermetallic compounds were not agreed.

The copper rich phase is formed in the diffusion zone after annealing at 704°C for 20 h is $ZrCu_4$, that was estimated by EPMA and X-ray studies [3].

For the compound richest in copper a $ZrCu_5$ formula was proposed by [4] and [5] based both on their own data that were obtained by SAD and energy dispersive spectrometry and STEM, EDX methods, respectively, and on [6] data. The stoichiometry $ZrCu_5$ was accepted by [2] in their thermodynamic assessment.

The vast DTA data in [7] match certain elements of phase equilibria determined in [8] and certain elements of the Cu-Zr phase diagram version presented in [1].

[7] data supported those of [8] as to existence of two modifications of Zr_2Cu compound and of a phase formed by a peritectic reaction in the 63-70 at. % Cu composition range.

[9] determined the critical temperatures of martensitic transformation of the ZrCu equiatomic phase and crystal structure of its high and low temperature modifications.

[10] found that ZrCu being annealed at 550°C decomposed into two phases, Zr_7Cu_{10} and Zr_2Cu.

[11] reviewed the values for enthalpies of formation of the Cu-Zr intermetallic compounds obtained early by high-temperature direct synthesis calorimetry.

Basing on the old versions of the Cu-Zr system the thermodynamic data were obtained for the compositions which were attributed to the stoichiometry of the Cu-Zr intermetallic compounds known that time. However there was much confusion regarding their compositions. In case of calorimetry, data obtained in experiment can characterize the alloy, that is why they are valid and will be shown here.

The last thermodynamic description of the Cu-Zr system [2] considered the following formulas: Cu_5Zr, $Cu_{51}Zr_{14}$, Cu_8Zr_3, $Cu_{10}Zr_7$, CuZr and Cu_2Zr.

Solid Phases

The assessment of the Cu-Zr system made by us covers the data appeared in literature after 1989.

[7] inferred from the analysis of DTA experiments that another phase is stable between Zr_3Cu_8 and Zr_7Cu_{10} and in the 960-915°C temperature range. It can be $Zr_{13}Cu_{24}$ or $ZrCu_2$ phases suggested by [8]. $Zr_{13}Cu_{24}$ is accepted as this phase is in a structural conformity with other phases of the Cu-Zr system.

[7] confirmed [1] as to congruent melting of the ZrCu equiatomic phase.

[10] determined that the equiatomic alloy being annealed at 550°C for 24 h and quenched into liquid nitrogen exhibited two phase structure: Zr_7Cu_{10} and Zr_2Cu. The ration of Zr_7Cu_{10} to Zr_2Cu estimated by TEM is about 2.

According to [8] and [9] ZrCu undergoes martensitic transformation at ~140°C. The high temperature phase with cubic of CsCl type crystal

structure exists above this temperature and according to [9] is preserved at room temperature in cast alloy. The crystal structure of the products of martensitic transformation is monoclinic. So on a rapid cooling of the equiatomic alloy the eutectoid decomposition is suppressed.

[7] confirmed the data obtained by [8] on the transformation of the Zr_2Cu phase and determined its temperature close to 960°C.

Phase Equilibria

[8] made more occurate liquidus in the ZrCu system in the 6-80 at. % Zr range and therefore the compositions of liquid phase in invariant reaction were made more accurate too. The decomposition of ZrCu was found in [7] to occur at temperature somewhat higher than that assessed in [1], 725°C.

Thermodynamics

Enthalpies of formation of the intermetallic compounds and some alloys of the Cu-Zr system determined by solution calorimetry were considered.

The partial molar enthalpies of mixing of the overcooled liquid zirconium at infinite dilution and enthalpies of mixing of liquid alloys are listed.

It may be drawn the following from the analysis of these data:

! the values of and $_mH$, obtained by the same researches in different studies are in conformity with each other;

! discrepancies in these values, obtained by different researches exceed the errors, pointed out;

! the value of enthalpy of mixing depends on temperature;

! the minimum of $_mH$ is displaced to copper and is observed at $x_{Zr} = 0.45$. 0.50, as it follows from the majovity of works.

Activities of the components in the Cu-Zr liquid alloys were measured by the Knudsen effussion method.

Miscellaneous

The liquid Cu-Zr alloys over a wide concentration range can be amorphizided by rapid quenching. The enthalpies of formation of the Cu-Zr amorphous alloys, obtained by a solution calorimetry method in liquid aluminium are considered.

References

1. Arias D., Abriata J.P., "Cu-Zr (Copper-Zirconium)" *Phase Diagrams of Binary Copper Alloys; edited by Subramanian, P.R., Chakrabarti, D.J., Laughlin, D.E.,* ASM Materials Park, OH, 497-502 (1994).

2. Zeng, K.J., Haemaelaeinen, M., "A New Thermodynamic Description of the Cu-Zr System", *J. Phase Equilibria,* **15** (6), 577-586 (1994).

3. Bhanumurthy K., Kale G.B., Khera S.K., "Authors Reply", *Metallur. Trans.,* **23A**, 3393-3394 (1992).

4. Singh R., Lawley A., Friedman S., Murty Y., "Microstructure and Properties of Spray Cast Cu-Zr Alloys", *Mater., Sci. Eng.,* **145A**, 243-255 (1991).

5. Anzel I., Kneissi A.C., Kosec L., Krizman A., "Internal Oxidation of Rapidly Solidified Cu-Zr Alloys", Z. Metallkd., **88** (1), 38-44 (1997).

6. Lou M.Y.-W. Grant N.J., "Identification of Cu_5Zr Phase in Cu-Zr Alloys", *Metal. Trans.,* **15A** (7) 1491-1493 (1984).

7. Braga M.H., Malheiros F.M., Castro F., Soares D., "Experimental points and invariant reactions in the Cu-Zr system", Z. Metallkd., **89** (8) 541-545 (1998).

8. Kneller E., Khan Y., Corres U., "The Alloy System Copper-Zirconium", Part I. Phase Diagram and Structural Relations", *Z. Metallkde,* **77**, 43-48 (1986).

9. Koval Yu.N., Firstov G.S., Kotko A.V., "Martensitic Transformation and Shape Memory Effect in ZrCu Intermetallic Compound", *Scri. Metallur.,* **27**, 1611-1616 (1992).

10. Liu Z.Y., Aindow M., Hrijiac J.A., Jones I.P., Harris I.R., "Microstructural Characteristic of the Eutectoid Mixture Zr_2Cu and Zr_7Cu_{10}, *J. Mater. Sci. Lett.,* **20**, 543-545 (2001).

11. Guo Q., Kleppa O.J., "The Standard Enthalpies of Formation of the Compounds of Early Transition Metals with Late Transition Metals and with Noble Metals as Determined by Kleppa and Co-workers at the University of Chicago. - A review, *J. Alloys Compd.,* **321** (2), 169-182 (2001).

THE ESTIMATION OF THE DEPENDENCE OF TWO PHASE CERAMICS FRACTURE TOUGHNESS ON PHYSICAL AND MECHANICAL PROPERTIES OF ITS COMPONENTS

Popov Alexey, Kepich Tiberiy, Makara Vladimir, Kazo Jgor
Taras Shevchenko University, Kyiv, Ukraine

The results of the theoretical investigations of the dependence of two-phase composite fracture toughness (K_{1C}) on the volume fractions and mechanical properties of both components (fracture toughness of each phase sintered alone, theoretical strength. Plasticity) as well as grain sizes of matrix and inclusion are represented in this work.

The foundation of the reviewed model consists of followed basic hypotheses and assumptions:
1. The length of the investigated crack front is far more then the average grain size.
2. The process of the crack propagation is discussed in terms of quasi-brittle destruction (1).
3. It is considered that the crack front may bend only on the plane which is perpendicular to the crack moving direction.
4. The presence of strong chemical connections between grains of different phases is also considered.
5. All the grains are equal exist polyhedrons.
6. All the crack tip sectors begin their motion simultaneously.

The value of the stress intensity coefficient needed for the crack tip advancement is estimated as an average value of all the local coefficients needed for the motion of different sectors passing through grains of different phases. It is taken into consideration that the evaluation of each local coefficient depends not only on properties of the grain being passed by the specific crack tip sector, but also on those of its closer neighborhood. The volume fractions of the grains of each phase restricted with different contact surfaces are calculated using formulas obtaining in (2). It is also appreciated that under some circumstances (shown in the report) the crack tip sector moving to the stronger grain (the reference is to so called theoretical strength which may be estimated as $0,1E$) may scert this grain. The estimation of local values of critical stress intensity coefficients is carried out using generalized energy G-riffits' criterium.

So the crack tip is considered to be a line consisting of recliner sectors passing through the weaker phase and bent sectors in places of skirting of stronger phase grains.

The result of the investigations is the analytical formula of the dependence of critical stress intensity coefficient K_{1C} of a composite material obtained with powder metallurgy methods on physical and mechanical properties and volume fractions of its components.

It is pointed that this formula may be used to estimate the fracture toughness of cermets, being obtained in presence of liquid phase but in this case the model should be developed.

In conclusion the model is used to evaluate the fracture toughness dependence in such private cases:
- The improvement of the material with the involving chemical interaction leading to ideal gluing of grains of different phases. In this case mechanical properties of the phases are considered to be identical.
- The improvement of the composite is connected not only with the chemical interaction (as in the previous case) but also with the difference in mechanical properties of its components:$K_{1C1}= K_{1C2}; \sigma_{C2} > \sigma_{C1}$.

The analysis of the obtained regularities allows to make the next conclusions:
1. Fracture toughness – composition dependence (when the chemical interaction between different phases takes place) has an external character.
2. Suitable choosing of mechanical properties makes the introduction of the second phase considerably more efficient.
3. The optimal second phase fraction as the maximum fracture toughness value

depends on the inclusion-matrix grain size ratio.

LITERATURE.

1.Черепанов Г.П. «Механика хрупкого разрушения».М.74.

2.Скороход В.В. «Теория физических свойств пористых и композиционных материалов и принципы управления их микроструктурой в технологических процессах»//Порошковая металлургия – 1995. - №1/2. – С.53-70.

HIGH - STRENGTH HEAT-RESISTANT GLASSY MATERIALS FOR OPERATION IN EXTREMAL CONDITIONS

ROMASHIN A.G., KELINA R.P., SAMSONOV V.I.

Federal State Unitary Enterprise "Obninsk Research and Production Enterprise "TECHNOLOGIYA", Obninsk, Russia

Space and supersonic velocities, gigantic overloads, aerodynamic heating, pressure of kilometers of water thickness, influence of aggressive media and nuclear radiation - such are the conditions under which have to operate optical and radiotechnical systems, devices and machinery. The elements of construction optics are to provide for their normal functioning as well as for the work of people under these severe extremal conditions.

One of the basic materials, widely used in elements of construction optics is the high-strength, heat-resistant glassy material.

Arising from conditions of operation glass as a construction material should provide for:
- high resistance to mechanical and thermal loads;
- stability to the influence of aggressive media, physical fields and other extremal conditions;
- functioning of products at high temperatures;
- preset spectral and optical characteristics;
- stability of properties within the whole range of working temperatures.

These characteristics are necessary for safe work of people and equipment under severe operation conditions.

Thus, the glass should have a complex of features, namely, high heat-resistance and strength together with the given spectral and optical characteristics and their stability under operating conditions.

This work presents the results of complex research in synthesis of heat-resistent colourless and coloured glasses and technology of their production.

The created materials are intended for load-bearing glazing of pilot cabins for flying apparatus with working temperature up to 700 K, strength up to 300 MPa, heat-resistance 450 K. They practically do not change their transparence at gamma-irradiation with doses up to 10 x 6 Roentgen.

High-strength glasses found their application in observation or sight glasses and level indicators of liquid in boilers, vessels and apparatus, operating at high pressure up to 30 MPa.

Heat-resistant glasses of special strength are used in sea craft, in particular, in under-water lamps as protective covers. Such glasses have improved chemical stability and high thermal resistance. The manufactured products are functioning in sea water at working pressure up to 60 MPa.

One of the perspective construction and fundamental materials is the glassceramic or piroceramic material (sitall) with ultra-low temperature coefficient of linear elongation with the order of $0.3-0.5 \times 10^{-7} K^{-1}$, with working temperature up to 1000 K. This material is used in laser gyroscopes of navigation systems and can be also used for high-temperature glazing of flying apparatus.

The heat-resistant colour glasses are widely used in aviation and aero-space equipment as products for light signals, in particular, as air-borne aeronavigation lights and inside-cabin indicators. In the field of production of coloured heat-resistant glasses main attention is paid to receive light-technical characteristics that provide for the increase in distance of signal observation. This presumes the development of glass materials with high brightness, good contrast and coordinates of colouring, cor- responding to the international system IKAO.

The materials, developed by us, do not yield in their features to materials produced by the leading world glass firms, such as: Corning Glass, USA; Schott, Germany; Nippon Electric Glass, Japan; Kovaler, Czechia; etc.

The developed materials, technologies and received on their basis glass products found wide application in many fields of contemporary engineering. Glass products are used at space station MIR, spacecraft SALUT, spacecraft of multiple use BURAN, aircraft AN-72, IL-96, TU-204, TU-334, etc., in apparatus used in the regions of the world ocean, that allow to dive to the depth of 8 000 m, in power equipment, in automobile and railway transport, as well as in the equipment for rated airports.

CORROSION RESISTANCE AND PASSIVATION OF ALLOYS UNDER EXTREME CONDITIONS

Vyazovikina N.V., Mandich N.V.[1], Ponomarev S.S., Vyazovikin I.V.[2], Donchenko M.I.[3]

Institute for Problems of Materials Science of UASU, Kiev, Ukraine
[1]HBM Electrochemical and Engineering Co., Lansing, Illinois, USA
[2]Voronezh Technological Institute, Voronezh, Russia
[3]Kiev Polytechnic Institute, Kiev, Ukraine

Presented is method for the improvement of corrosion resistance and passivation ability of the selected alloys by alloying them with anodic additions. The mechanisms for improving passivability and corrosion resistance of alloys by anodic additions were previously proposed [1]. The main purpose of the present work is to study the wear and corrosion resistance of high-chromium and high-strength aluminum alloys that are additionally alloyed with small additions of selective electronegative metals, under different extreme corrosion conditions.

The voltammetric, chronopotentiometric, gravimetric methods, scanning microscopy, Auger-electron spectroscopy and X-ray microprobe analysis were used. It was shown that the passivation potential, E_p, critical passivation current, i_{cr}, and the current of passive dissolution of alloys, i_p, in sulphuric acid solutions, aerated and deaerated by argon, decrease pronouncedly when alloying the high purity and commercial Cr-Fe alloys containing from 16 to 60 of wt. % Cr with small additions of aluminum and some d-transition metals. The additions of Al, La, and Sc also increase the passivability and corrosion resistance of the Cr-Fe alloys in dilute NaCl solutions under aerated conditions. High resistance to pitting and intergranular corrosion was exhibited by rolled and annealed Cr-Fe-Al commercial alloys in aerated 3 % NaCl as well in 2 M $HClO_4$ + 1 M NaCl solutions [2]. Similarly, cast and hardened commercial alloys, containing more than 27 % Cr, exhibited a high corrosion resistance and ability to passivate in aerated 0.5 M H_2SO_4 solution during a wear test under conditions of extrusion processing of polymers [3]. In both cases alloying by aluminum with a small addition of La or Sc increased the passivability of the high-chromium alloys. Also, annealed commercial Cr-Fe-Al alloys containing less than 60% Cr exhibited high hardness and wear resistance in contact with SFD SV composite polymer at temperatures of 60 to 100°C.

According to our published data [3], the annealed alloys containing more than 40% of Cr are highly competitive in wear resistance with well-known hard facing wear resistant materials of type XN80C4P4 and PC-12NVK-0.1 used as reference samples under these extreme conditions. Actually, the wear resistance of the alloys, (g h^{-1}), in tribological couples with the SFD SV composite polymer is: 0.0109 for XN80C4P4; 0.0083 for PC-12NVK-0.1; 0.0110 for Cr27Al5; 0.0094 for Cr40Al2; 0.0079 for Cr45Al4; and 0.0037 for Cr60Al2. Consequently, annealed commercial Cr-Fe-Al alloys containing more 40% of Cr that are alloyed by anodic additions can be used successfully in practice under these extreme conditions. Their wear resistance exceeds that of XN80C4P4 and PC-12NVK-0.1 type materials used as reference samples under these extreme conditions. The ability to passivate and the corrosion resistance of alloyed commercial Cr-Fe-Al alloys to total, pitting and intergranular corrosion in aerated 0.5 M H_2SO_4, 3% NaCl and 2N $HClO_4$ + 1N NaCl solutions increased correspondingly after testing them for wear resistance in contact with polymer. Hence, annealed commercial Cr-Fe-Al alloys containing more than 40% of Cr can be used as long-term materials due to the high hardness, wear, and corrosion resistance under different extreme conditions.

The total effect of aluminum on the corrosion resistance of commercial chromium-iron alloys was recognized when testing them in high-temperature power-generating plants when they come in contact with liquid metal heat-transport medium (sodium). The corrosion resistance of investigated alloys substantially exceeds that of the austenitic stainless steels usually used under these conditions as previously shown in [4]. Thin

oxide films enriched in aluminum that have good surface adhesion, provide under this extreme medium high corrosion resistance of commercial chromium-iron-aluminum alloys.

Anodic additions also increased the passivability and resistance to overall as well pitting corrosion of high-strength aluminum alloys in aerated solution of 3% NaCl. It is shown [5] that the corrosion and pitting potentials of aluminium and its alloys alloyed by small additions of Sc are increased. Also, anodic dissolution, overall and pitting corrosion rates are decreased in comparison with aluminum and Al alloys that do not contain Sc. Small additions of other d-metals facilitate the effect of Sc on corrosion resistance of Al and its alloys in seawater. As a result, aluminum and its alloys alloyed with small additions of Sc and other d-metals can be used under extreme seawater conditions.

----

1. N.V. Vyazovikina, *Zashchita Metallov*, **33**, 372 (1997).
2. N.V. Vyazovikina and N.V. Mandich, *Voprosi chimii I chimicheskoi technologii*, **29**, 72 (1999).
3. N.V.Vyazovikina, S.V.Dan'ko, N.P. Korzhova and E.Yu.Shestakova, *Zashchita Metallov*, **31**, 31 (1995).
4. E.Yu. Shestakova, N.V.Vyazovikina and V.N. Minakov, in "Extended Abstracts of Congress "Zashchita-92", **1**, 201,Moscow (1992).
5. N.V. Vyazovikina, *Zashchita Metallov*, **35**, 493(1999).

THERMALLY STABILIZED CARBON FABRICS FOR ELECTRICALLY HEATED SYSTEMS APPLICATIONS UNDER EXTREME CONDITIONS

Vishnyakov L.R., Holenevich V.A., Kokhana I.M., Kokhaniy V.O., Kovalchuk N.M., Dyadechko O.G.

Frantsevich Institute for Problems of Materials Science, National Academy of Sciences of Ukraine, Kyiv, Ukraine

We have been developing for a number of years different types of flexible electric heaters made of thermally-stabilized electrically-conductive carbon fabric for surface warming.

The flexible heater preferentially uses an electrically-conductive element or multiple elements made of carbon fabric and embedded in two layers of an electrically insulation material.

As initial carbon materials for heaters, UUT-2 and G3 fabrics produced by Brovary Government Plant, and Etan-type fabric produced by Vuhlecomposite Plant, Zaporizhya are used. As major disadvantage of these commercial fabrics is a non-sufficient stability of their resistance associated with peculiarities of their production under plant conditions. Therefore, thermal stabilization requires an additional step, i.e. chemical processing of fabrics. A selective thermal stabilization of fabric pieces designed for making real heaters shall be the most efficient route.

Our flexible heaters have a number of features allowing their use in different industries, medicine, household, and under extreme conditions. Flexible heaters can be designed and manufactured of desired sizes in dependence on applications or requirements. The heaters are powered from an AC or DC current source. The rating of its heat production may vary within a broad range depending on the heat take-off. Selection of a proper insulation coating influences the admissible operating temperature on the heater surface.

Various constructions of heater with desired performance have been developed. We studied possibility of the UUT-2 fabric application for different thermal conditions. In order to simplify the use of this fabric to specific items, a quantity of experimental data was obtained useful for constructing nomographs showing the heater surface power dependence of its length, specific surface resistance and voltage applied.

Electrically-heated systems may be used to the following extreme conditions:
- Blankets for victim or patient warming;
- Electrically-heated ambulances or tents;
- Clothing for drivers of vehicles subjected to extreme environments.

For the above applications and for hypothermia prevention, in particular, stationary hospitals shall require devices for precision (programmable) warming. Stringent requirements shall be provided to meet an uniform heat distribution all over the surface of the carbon fabric. The paper describes the ways how to achieve these goals.

STUDY OF MECHANICAL PROPERTIES AND STRUCTURE OF THERMALLY EXPANDED GRAPHITE REINFORCED WITH PYROLYTIC CARBON AT HIGH TEMPERATURE EXPOSURE

Vishnyakov L.R., Hurin I.V.[(1)], **Kossiguin E.P., Moroz V.P., Sinaiskiy B.M., Vereschaka V.M.**

Frantsevich Institute for Problems of Materials Science, National Academy of Sciences, Kyiv, Ukraine

[(1)]National Scientific Center, Kharkiv Physical & Technology Institute, Kharkiv, Ukraine

Thermally expanded graphite (TEG) products have a potential due to their high temperature, radiation and corrosion resistance, compressibility and recovering ability, and formability at room temperature without binder use, at low pressures [1]. One among the methods of designing composite materials (CM) based on TEG having improved functional properties including high temperature resistance can be the reinforcing of TEG with pyrolytic carbon through gas-phase impregnation of TEG porous frame with pyrolytic carbon.

This paper describes the study of strength and deformation properties, structure of CM made of TEG frames differing in their density (0.07 - 0.5 g/cm^3) in their initial states and after the thermal heating.

To produce TEG particles, a technology was used involving a chemical treatment of graphite powder with sulfuric acid, and thermal expansion of oxidized graphite. As porous medium for pyrolytic carbon impregnation, products were taken in the form of ring (of 35/24 mm in diameter and 15-17 mm in height) produced by unilateral pressing technique [2].

The TEG ring impregnation was made using the radially-driven pyrolizing zone [3] as developed by the NSC PTI technology. A rod with impaled rings or frames made of TEG has been resistively heated up to the T_c temperature. This was accompanied with formation of a relatively narrow area of gas-phase precipitation reactions of pyrolytic carbon around the rod. We reached the desired compactibility of the composite material due to high affinity of the graphite and pyrolytic carbon as precipitated. Thus, at the initial density of ring-frames of 0.07 g/cm^3 achieved after the impregnation, the CM density was 0.3 - 0.5 g/cm^3.

The strength and deformation properties of ring-type samples were tested at the end-direction compression while recorded the strain diagrams. The high-temperature effect was experienced within the range of peak temperatures, i.e. 500-1000^{0}C whereas the holding at the above temperatures. Moreover, taking into account the fact that the CM components are subjected to heating/cooling cycles during the operation, the rings were undergone to thermal cycles at 200 ^{0}C - T_{max}-200 ^{0}C. The peak temperatures during the thermal cycling, T_{max} were similar to those of the steady heating stage. Said high temperature exposure was made in air using the SGU-2 unit Heliostation, Katsively, and, for comparison, under vacuum (10 $^{-5}$ mm of mercury column) using the 1246 P-2 unit.

To evaluate the damages caused by preliminary temperature effects, relative changes of strength σ_{10} and elastic E_{comp} characteristics were used.

A comparative analysis of the compression diagrams for TEG and CM samples containing different pyrocarbon fractions showed that the reinforcing with pyrolytic carbon may produce considerable changes in the behavior of the material at compression depending on its composition. Thus, for TEG samples within the 0.3 to 0.9 g/cm^3, the compression diagram of porous isotropic materials is of typical nature. The transition from the elastic deformation to the elastic-plastic deformation of samples occurs at a lower density. The TEG samples have been deformed without fracture even at high stresses and levels of accumulated plastic deformation.

Evaluation of the CM compression diagrams concludes that a relatively small amount of pyrolytic carbon (up to 27 %) increases the strength, σ_{10} and modulus of elasticity, E_{comp}, but the diagram patterns are similar to those for TEG of equal densities, while the sections having similar curvatures shift to the area of great stresses. With the pyrolytic carbon concentration increase up to 80-85 %, the strain diagrams

change their behavior. The elastic deformation contribution increases while the samples fracture showing multiple cracks initiated.

The CM samples studied in their initial states and after the thermal exposure showed that the damage occurrence of the sample tested is dependent on the upper temperature level, nature of temperature exposure under air (oxidizing) or vacuum) neutral medium.

Using the «COMEBAX SX-50» scanning electronic microscope, the TEG and CM structures having different densities and pyrocarbon concentrations were investigated and also TEG and CM samples subjected to preliminary temperature exposure under the above conditions were studied.

The results of fracture studies showed an uniform impregnation of the TEG frames with pyrocarbon. The non-reinforced TEG has particles with the 300 to 400 micron sizes, the particle surface is non-uniform exhibiting visible porosity between them. The pyrocarbon impregnation up to 80-85 % produces a significant fragmentation of the graphite grains having spherical accumulations of pyrocarbon among them, which completely penetrate the sample. A lower concentration causes the CM structure to lay between the above states.

As the studies of non-reinforced TEG and CM revealed after the high temperature exposure, the structure change is dependent on the peak temperature, oxidizing or neutral medium presence.

The method of designing composite materials using the impregnation of a TEG porous frame with pyrocarbon has been developed. Investigations of microstructures and mechanical properties showed a superiority of the obtained CM in terms of strength and elastic characteristics in comparison with TEG having similar densities. A different behavior was shown when the compression of initial TEG sample and CM of TEG-pyrocarbon samples differing in pyrocarbon contents. The damage occurence was evaluated as caused by the preliminary temperature exposure.

The composite material products of the TEG-pyrocarbon system feature a combination of low porosity and elevated load-carrying capability including at high temperatures, and can be used for various modern devices applications.

REFERENCES

1. Vishnyakov L.R. Reinforced composites based on thermally expanded graphite for sealing applications.// Voprosi atomnoi nauki i techniki, Issued by NSC KPTI, 4/76/, 1999, P.93-100 (In Russian).
2. Vishnyakov L.R., Gurin I.V., Kossiguin E.P. et all. Influence of gas-phase impregnation with pyrocarbon on structure and mechanical properties of thermally expanded graphite // Functional materials, 8, 1, 2001. P.125-128.
3. Zelenskiy V.F., Gurin V.A., Gurin I.V.. Gas-phase impregnation by a pyrocarbon of the porous media by a methods of a radially-driven pyrolysis zone, in : Twenty Fourth Biennial Conference on Carbon, Lightsey Conference Center, Charleston USA (1999), P.50.

INTERCOUPLING OF STRUCTURE AND PHASE COMPOSITION WITH CHEMICAL AND RADIATION STABILITY OF STONE-CAST MATERIALS

Kosinscaia A.V., Bogatiriova J.D.
Physico-technological institute of metals and alloys NAS of Ukraine, Kiev, Ukraine

The cast oxide materials (the stone casting), made from melt of mountain rocks and slag are characterised by sufficient toughness, low porosity and thermal conductivity, high stability against corrosion and attrition. On this reason using of the products to equipment protection at extreme conditions of influence aggressive and abrasive ambiences influence, has conditioned. At studies was installed that radiation stability of stone casting and intercoupling of the enumerated characteristics of material with its construction and phase composition.

The castings has crystalline structure, formed from different minerals. In structure of castings the glassy phase is present as separate formations in interaxes spaces of dendrites or interdendrite zones of crystals. At influence of aggressive solutions, corrosion is connected with dissolution of the intercrystal free glass. Glass bounded phase does not interact with acids. Depending on phase composition of material, increasing of mass loss occurs on initial stage of destruction of crystalline forming. It is stated, for instance, that magnetite and olivine have more high stability, than pyroxene. In solutions of acids and alkalis akermanite, monticellite, manganosite - main minerals which form materials on the base of silicomanganese slag have low steadfast. So slag-cast products more chemical unstable, than from melts of mountain rocks.

Size of crystalline formation have the greater influence upon chemical stability of stone casting. When crystals size of the main crystalline phase increas in 4 - 4,5 times, stability of material falls in 2 times, under close contents of free glass in them.

Stability of stone-cast material studied at influence of solid, fluid, gaseous, radioactive environment and γ-rays. After γ-rays influence (under average energy 0,662 MV and powers of absorbed dose 0,1116 Gy/s) change of their forms, linear sizes, colour did not exist in samples. Forming of the defects in free glassy structures component in the case of its partial crystallisation is stated. This, obviously, cause appearance of strain in material and a certain reduction of strength.

Central part of casting is composed from large dendrite formation. Surface and intermediate zones has the fine-grained structure. At surface thick layer with fine-grained structure characterised by low open porosity which provides to products an absence permeability to water, high stability at influence of aggressive fluid, solid, radioactive environment. At submersion of samples in solutions of different radionuclides mixtures with total three-demential radioactivity $3,03 \cdot 10^6 \ldots 4,07 \cdot 10^6$ Bq/m^3 and endurance in them during 3 day, with the following deactivation by water, radioactive contamination of surface of material does not exist. It is established also that diffusion processes do not cause essential penetration of radionuclides. The mass-transfer coefficient of radioactive cesium from hard forming in 350 once lower, beside concrete. Liquid permeability exists in a surface layer only at microdefect presence in him and on distance of order 500 μm. Herewith minimum possible velocity of cesium penetration from fluid inviroment in stone-cast material in 27 once, but strontium - in 630 once lower, than concrete.

The data were a reason for recommendation of stone-cast products using on objects of keeping of radioactive materials, as a facing of premiseses and devices, subjected to influence aggressive and radioactive solutions.

ELASTIC BEHAVIOR OF HIGHPOROUS MATERIALS

Podrezov Yu.N., Verbylo D.G., Chernyshov L.I., Slyunyaev V.N., Firstov S.A.
Frantsevich Institute for Problems of Material Science NAS of Ukraine, Kiev, Ukraine

Creation of high porous materials is one of the most perspective directions of materials science. There are numerous examples of successful usage of such materials in the most responsible designs of space, air and automobile engineering. The structure of cellular solids ranges from near perfect order honeycomb cells to the disordered three-dimensional network of powders and forms.

Literature analysis shows the displacement of priorities from complex technologies for preparing of high porous constructions with the regular geometrical form (for example, honeycombs structure) to more simple technologies for preparation of such materials by melting, powder metallurgy or other structural engineering methods. According to this tendency, there is some displacement of accents in the development of the models which describes the mechanical behaviour of such systems with the purpose of optimization of their structure.

A regular geometrical construction may be described by some array of identical cells nested together to fill a plane. The cells for honeycombs are usually hexagonal in section, but they can also be triangular, or square, or rhombic. Ashby and his co-workers [1, 2] developed the mechanical approach to the analysis of deformation of high porous materials. Large–scale deformation models were obtained from stress – strain analysis for structural elements of unit cell under loading.

Such approach gives good correspondence with experiment for regular structures (such as honeycombs), but is not suitable for high porous materials with stochastic structure. In materials with stochastic distribution of porous it is necessary to take into account that such structure consists of diverse structural elements chaotically located in designed object (Fig. 1).

In this case representations about an elementary cell can be accepted only as the first very rough approximation. For deeper analysis it is necessary to involve representations about effective properties advanced in the theory of porous powder bodies, and statistical theory of effective medium. The key moment of these theories is the opportunity of the independent account of influence of structure of solid phase and powder space in formation of properties of a material as a whole.

To account for stochastic nature of structure of high porous materials it is offered in works [3, 4] to use statistical models based on the percolation theories and the fractal approaches. For the analysis of durability of porous materials from our point of view it is the most correctly to use the physical approaches advanced in works of S.A. Firstov with co-workers [5].

gasar process   foamed metals

metallic foam-rubbers   bi-porous materials

powder materials   sintered fibers
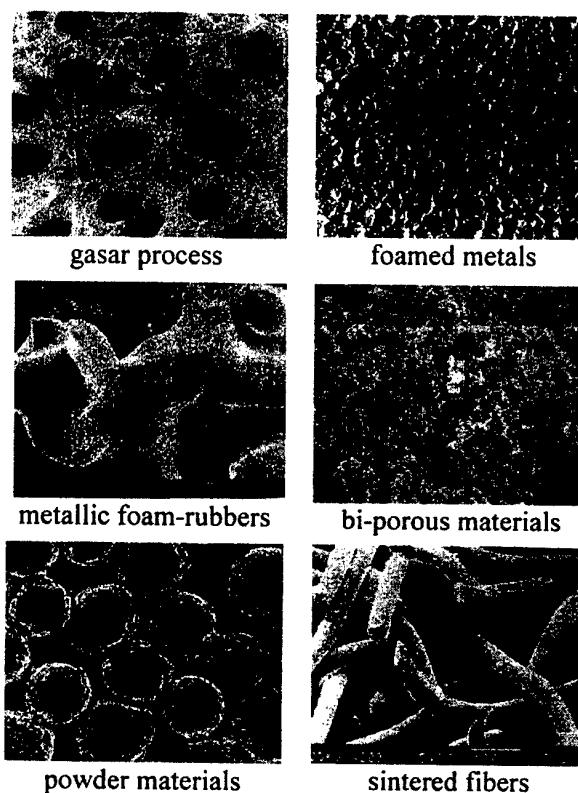
Fig. 1. Types of structures of porous space

As objects of research the distributions, having stochastic porous structure (Fig. 1) were chosen high porous materials obtained by using of various technologies of materials science.

Four-point bends with registration of microplasticity curve was test procedure used in this work. The influence of porosity on the modulus of elasticity of the investigated materials was analyzed. The results of these researches are shown in Fig. 2 as the schematic curve.

One can see from these data, that the morphology of porous space essentially influences on dependence of the modulus of elasticity on porosity. None of the known mechanical schemes does not allow

to describe the obtained results correctly. In particular, it concerns the usage of simple geometrical models, for example, Ashby sell. The analysis
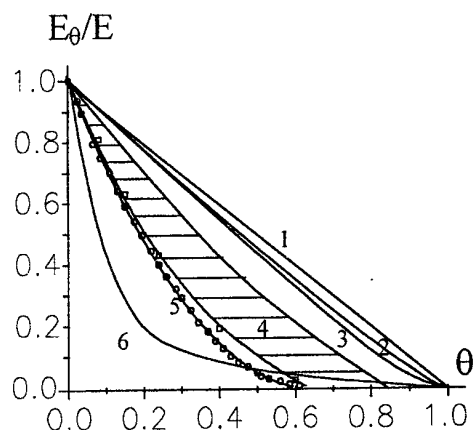
Fig. 2. Dependence of the relative modulus of elasticity on porosity for various types of materials

of dependence of the modulus on porosity is especially complicated in area of near limiting high porous states. At the same time equation of the percolation theory allows to describe experimental data satisfactorily. For case of the modulus of elasticity it is possible to write this equation in the following form:

$$E_\theta = E_0 \left(1 - \frac{\theta}{\theta_c}\right)^\beta \qquad (1)$$

where E_θ - modulus of a porous sample;
E_0 - modulus of a compact sample;
θ - porosity of a material;
θ_c - limiting porosity;
β - parameter of porous structure.

The calculated values of θ_c and β for various types of porous structures are listed in the table:

Material	Θ_c, %	β
Gasars	100	1
Foamed metals	100	1,65
Metallic foam-rubbers	100	1,85
Bi-porous materials	65-85	1,2 – 1,6
Powder materials	65	1,65
Sintered fibers	100	3 – 4

One can see, that for a case of isotropic structures, parameter b changes from 1,6 up to 1,8, corresponding to predictions of the percolation theory. Limiting porosity in case of powder systems does not equal to 100 % and depends on structure of porous space.

The influence of porous structure on the elastic modulus of this class of materials is shown in Fig. 3. One can see from the diagram, that at given porosity the following tendency is observed: the more is relation of the powder former size to the size of a powder λ, the more is value of the elastic modulus of high porous materials.

⊙ - Ni, $\lambda = 60$
● - Mo, $\lambda = 30$
x - Fe, $\lambda = 8$
△ - Ni, $\lambda = 6$
▲ - Mo, $\lambda = 4$
□ - Fe, $\lambda = 1$
O - Fe without powder-former
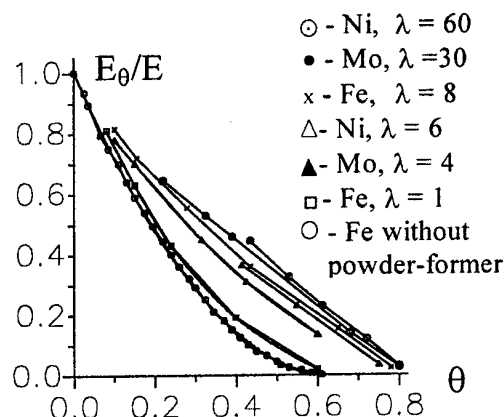
Fig. 3. Dependence of the relative modulus of elasticity on a volumetric share of pores.

Limiting porosity of a bi-porous material also depends on a ratio of the sizes of a powder and powder former. Geometrical model offered in work [4] allows to describe this dependence as follows:

$$\theta_c = \frac{0,85(1 - \theta_{micro})}{\left[1 + \frac{1}{\lambda}\left(\sqrt[3]{0,85\frac{1 - \theta_{micro}}{0,65 - \theta_{micro}}} - 1\right)\right]^3} + \theta_{micro} \qquad (2)$$

where θ_{micro} - porosity of a powder subsystem;
θ_{macro} - porosity, determined in volume of macropores.

The proposed expressions (1, 2) describes experimental data satisfactorily, from what follows, that the principles of the percolation theory are applicable for the description of behaviour of high porous materials working in extreme conditions.

References:

[1] Gibson L.J., Ashby M.F. Cellular Solids - Structure and Properties, Pergamon Press, Oxford, 1988.
[2] A.G. Evans, J.W. Hutchinson, M.F.Ashby. Progress in materials science **43** (1999) 171-221.
[3] Yu.N. Podrezov, N.I. Lugovoy, L.N. Chernyshev and L.G. Shtyka. *Powder metallurgy and metal ceramics.* 33, 628-633 (1994).
[4] R. Graninger, F.Simancik, H. Degischer: Fracture Mechanics and Quality Manegement, Vol.2, Vienna University of technology, 1997, 701.
[5] S.A. Firstov and M. Shlessar (Eds.), *Structure and Strength of Powder Materials* (Naukova Dumka: Kiev, 1993, in Russian).

393

NEW RIGID MATERIALS WITH HIGH ELEVATED-TEMPERATURE STRENGTH BASED ON INTERMETALLIC ALUMINUM PHASES

Podrezov Y.N., Barabash O.M.[(1)], Milman Y.V., <u>Korzhova N.P.</u>, Legkaya T.N.[(1)], Mordovets N.M., Voskoboinik I.V.

Institute for Problems of Materials Science of NAS of Ukraine, Kiev, Ukraine
[(1)]Institute of Metal Physics of NAS of Ukraine, Kiev, Ukraine

Unique properties of Al_3Ti intermetallic compound are determined by its crystalline and electronic structure. This material has Young's modulus of 170-220 GPa that is very high for aluminum-based alloys and high elevated-temperature strength. According to literature data, the compression yield point of Al_3Ti in the wide temperature interval of 20-900 °C is not less the 300 MPa. Because of low density of the alloys based on Al_3Ti (3-4 g/cm^3) their specific properties per unit weight are even more attractive. However, the features of crystalline structure of the intermetallic cause very high brittleness of this class of materials.

Low strength and brittleness of intermetallic Al_3Ti prevents the utilization of these attractive compounds. New methods to solve the problem of brittleness were proposed in recent years. The methods are based on the principles of rational alloying. It was shown that alloying of Al_3Ti with Cr, Mn, Ni, Fe, Cu and other elements converts the crystalline cell of the intermetallic from the tetragonal DO_{22} to the cubic $L1_2$ [1-7]. Such transformation of the cell provides the possibility to improve the plasticity of Al_3Ti-based intermetallics [8].

In the present work it is shown that further increasing the strength and plasticity in bending and tensile tests may be achieved by using multiphase alloys. The structure of such materials must be prepared by a special way. It is necessary to remove the porosity, to decrease the size of structural elements and to create optimal conditions for energy dissipation at the crack tip. All these requirements may be fulfilled in the Al-Ti-Cr alloys, which crystallize as eutectic with $L1_2$ intermetallic phase. The task of this investigation is the selection of Al-Ti-Cr alloys with the optimal structure and investigation of their mechanical properties.

The alloys of Al-Ti-Cr system were prepared by arc melting in gettered argon atmosphere with a nonconsumable tungsten electrode on a water-cooled copper hearth. The line of the monovariant eutectic transformation (LMET) with the

participation of $L1_2$ phase was determined by the methods of metallographic, thermal and X-ray analysis, and the region of two-phase aco-existence was established as well. The structure of alloys in the investigated region changes from hypoeutectic with primary $L1_2$ dendrites and eutectic formed by cubic $L1_2$ and β-phases (Fig.1) to eutectic $L1_2+\beta$.
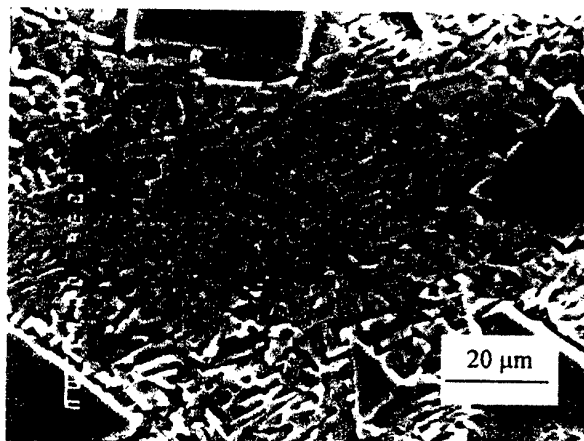
Fig. 1. Microstructure of hypoeutectic $L1_2 + (L1_2+\beta)$ alloy.

Mechanical properties of alloys with different volume parts of the eutectic were investigated by testing in compression, bending and high temperature hardness. It was established that hardness and compression strength increase with the rise of the volume fraction of the eutectic; the concentration dependence of plasticity is non-monotonous, having a maximum in the hypoeutectic range. In the phase diagram of the Al-Ti-Cr system the lines of isohardness are parallel to the LMET. Alloys with the eutectic structure have the maximum compression strength (σ_m^c=2000 MPa). Hypoeutectic alloys with a large fraction of the eutectic phase have the maximum value of plasticity (ε^c=20.5 %). Compressive stress - strain curves of the eutectic alloys of Al-Ti-Cr system are shown in Fig. 2.

The value of Young's modulus was obtained from four-point bending test. All investigated eutectic alloys have similar values of elastic modulus of 175-190 GPa. Four-point bending was used for analysis of microplasticity deformation curves. It

was found that the eutectic alloys, which have maximum strength under compression test, in the case of bending test have no signs of plastic deformation. From this point of view, the hypoeutectic alloys are more suitable. These alloys have high bending strength (σ_m=550-600 MPa) and appreciable microplastic deformation (ε=0.04 %). The microplastic deformation curve of the hypoeutectic alloy #4 is shown in Fig.3.
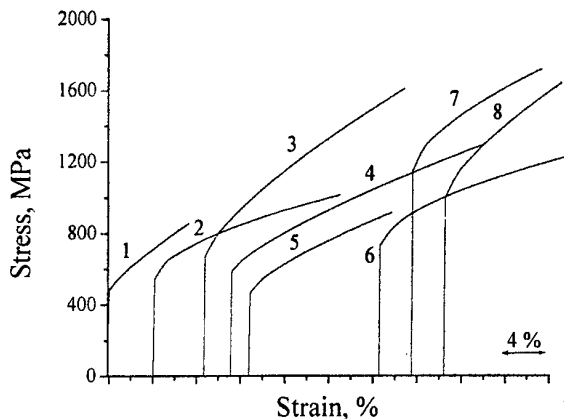
Fig. 2. Compressive curves of the eutectic alloys of the ternary Al-Ti-Cr system: 1 – single phase $L1_2$; 2-8 – alloys with different volume fraction of eutectic.
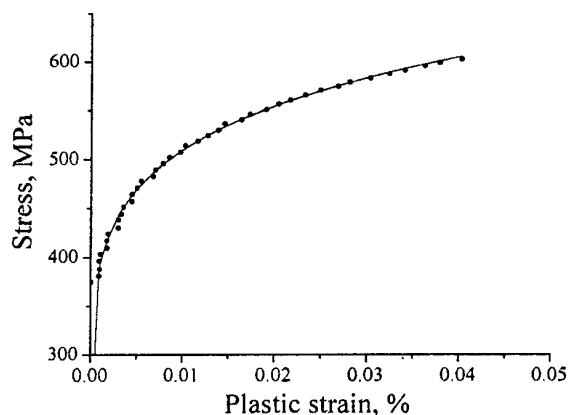
Fig. 3. Bending curve of the hypoeutectic alloy.

Alloys based on the $L1_2$+β eutectic have high melting temperature (1275 °C). That is one of the main reasons of high elevated-temperature strength of this class of materials. Hardness in the temperature interval of 20-800 °C is not less than 3.1 GPa. This value is significantly higher then hardness of the single phase intermetallic compound (Fig.4).
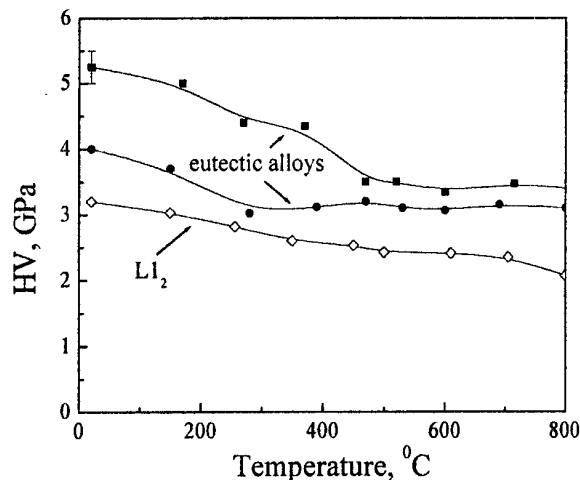
Fig. 4. Temperature dependence of hardness.

Conclusions

It is shown that eutectic alloys, formed by cubic $L1_2$ and β-phases, have an unique balance of mechanical properties: Young's modulus up to 190 GPa; hardness up to 3000 MPa in the temperature interval of 20-800 °C; compressive and bending strength up to 2000 MPa and 600 MPa, respectively.

It is established that the occurrence of the eutectic component in alloys structure results in the increase of their plasticity. Thus, binary hypoeutectic $L1_2$+β alloys have the value of the parameter ε^c in compression in the limits of (11-20) % in contrast to 7 % for the single-phase intermetallic $L1_2$. These alloys have also a low density of 3.5 g/cm^3. The eutectic character of alloys ensures their high cast properties.

The unique balance of properties allocates this class of advance materials for application in extreme conditions.

[1] Lee J.K., Park J.Y., Oh M.H., Wee D.M. Intermetallics 2000; 8: 407-416.
[2] Jewett T.J., Ahrens B., Dahms M. Intermetallics 1996; 4: 543-556.
[3] Mabuchi H., Kito A., Nakamoto M., Tsuda H., Nakayama Y. Intermetallics 1996; 4: 193-199.
[4] T.Y.Yang, E. Goo, Met. and Mater. Trans.A. 1995; 26A: 1029-1033.
[5] Fu Y., Shi R., Zhang J., Sun J., Hu G. Intermetallics 2000; 8: 1251-1256.
[6] Mabuchi H., Tsuda H. et al., J. Japan of Powder Metallurgy 1997; V.45, 3: 225-230.
[7] Klansky J.L., Nic J.P., Miccola D.E. J. Mater. Res. 1994; V.9, 2: 255-258.
[8] Milman Yu.V., Miracle D.B., Chugunova S.I. et al. Intermetallics 2001; 9: 839-845.

SIMILARITY CRITERIA OF POWDER SPRAYING OF PLASTIC MATERIALS

Uryukov B., Yevdokimenko Yu., Kysil V., Tkachenko G.
Institute for Problems of Materials Science of National Academy of Science of Ukraine

Materials erosion under the impact of hard particles against a target (powder spraying) is observed in many technical processes and is a negative phenomenon on the whole. By normal particles impact a crater is formed with a bead along its edges as a manifestation of residual deformation due to the material plastic flow under impact stress. The bead is removed from the surface by other particles impacts or under the influence of the flow carrying the particles.

The compression of a hard material is accompanied by the shift of its layer [1]. If the shear stress is exceeds the corresponding critical value the material turns into plastic state. Equating critical load to pressure difference on a shock wave we can determine the critical shock velocity:

$$V_{cr} = \frac{2}{\omega\gamma}\frac{1-v}{1-2v}\sigma_{\tau cr} \qquad (1)$$

where v is the Poisson's ratio; $\sigma_{\tau\,cr}$ – critical shear stress; $\omega = \rho_0\,a_0$, $\omega' = \rho'_0\,a'_0$ – acoustic impedances of materials, the dash concerns a particle; $\gamma = \omega'/(\omega + \omega')$.

The calculations have shown that critical velocity is within the limits of 35 – 60 m/s for such materials as aluminium, duralumin, copper and steel.

Thus, plastic deformation erosion can take place only when $V > V_{cr}$. If $V < V_{cr}$, the erosion is stipulated by the material disstrengthening by the accumulation of fatigue cracks. The duration of particle contact with a target under shock interaction is of an order of double time of shock wave passing the particle (in one direction as a shock wave, in another one as an unloading wave).

The erosion process under particles interaction with a target is very complicated. It depends upon many factors being random sometimes, which cannot be taken into account practically. It proves the availability of a great number of published theoretical approaches and theories [2] and at the same time there is no such theory which answers all the known experimental data. In such cases good results can be obtained by the generalization of the experimental data with the help of the system of similarity criteria.

The purposeful works on the generalization of the experimental data on the basis of similarity criteria have not been carried out for the investigation of powder spraying of plastic materials.

When similarity criteria are being selected it is necessary to determine the parameters of the physical process being considered, which influence upon it most strongly. In this case one should be oriented on general conceptions of the process being grown up already, by those parameters and their combinations which have already been used for the experimental data treatment.

The analysis has shown that the following parameters can be assumed to be the basic ones: for a particle: V, ρ', a', d, for a target: ρ, a, T, τ_T, T_m, where d is particle diameter; τ_T – yield stress of target material; T – target temperature; T_m – melting point.

The following functional dependence was considered by the orientation on the thorough work of Polezayev and Mihatulin [3] on powder spraying analysis:

$$W_m = \frac{V^2}{2H_{er}}f\left(\frac{V}{a};\frac{T}{T_m};\frac{\rho'}{\rho};\frac{a'}{a}\right) \qquad (2)$$

where H_{er} is the energy consumed for the erosion of the unit of erosion mass (erosion enthalpy).

By the authors' of work [3] opinion it is a characteristic of backing material depending upon temperature only.

As a result of the generalization of the known experimental data the following criterion formula has been obtained:

$$W_m = \frac{V^2}{2H_0}\frac{M^{0.6}}{\cos^{1.8}\theta_T}\left(\frac{\rho}{\rho'}\right)^{0.76} \qquad (3)$$

$$\theta_T = \frac{\pi}{2}\frac{T-T_0}{T_m-T_0}; \quad M = \frac{V}{a}$$

The value H_0, which has the dimension of specific energy turned out to be constant and equal to $H_0 = 1.5 \cdot 10^6$ J/kg. The squared mean error of the formula was 36%. The generalization of all the data based in the usual for many works form: $W_m = b\,V^n$ gave minimum error being equal to 85% by the $n = 1,9$. The comparison of the dependence calculated

by the formula (3) with the experiments is shown in the Fig.1.
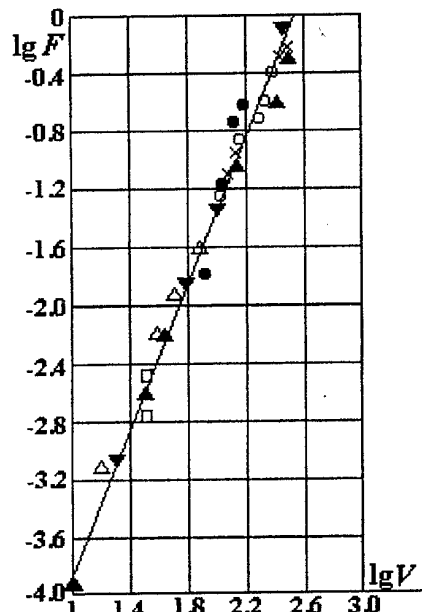
Fig.1. Experimental data treatment by the formula (3).

The following criterion formula was considered also

$$W_m = f\left(\frac{\gamma \rho a V}{\tau_T}; \frac{\rho' V^2}{2\tau_T}; \frac{T}{T_m}; \frac{\rho'}{\rho}\right) \qquad (4)$$

Where the first and second criteria characterize the contribution of the erosion of shock and pressure stages to particle interaction with a target.

As a result of the generalization the following formula has been obtained

$$W_m = C\left(\frac{\rho' V^2}{2\tau_{T0}\cos\theta_T}\right)^n \left(\frac{\gamma \rho a V}{\tau_{T0}\cos\theta_T}\right)^m \left(\frac{\rho}{\rho'}\right)^l \qquad (5)$$

where $C = 4,82 \cdot 10^{-4}$; $n = 1,0$; $m = 0,50$; $l = 2,0$; the index 0 concerns normal temperature. The squared mean error of the formula (5) is equal to 37.4%.

It is interesting to note that the difference between the experiments with single particles and the particles flow did not influenced on the criterion formulae. It is important also that the independence of the erosion upon particles dimensions has been confirmed.

The experimental data set is not representative enough obviously. There are only 30 points and the criterion formulae will be corrected when the new results are obtained. Nevertheless, it can be expected the criteria set will remain in its basis because the range of the parameters change was large enough during the experiments.

So, the particles velocity changed from 10 up 300m/s, target temperature − from room one up to 0,8 T_m, the densities relation − from 0,3 up to 3, the particles diameter − from 40 up to 3000 μm.

Powder spraying rate depends upon the angle of attack at which the particles get on target surface. The optimum angle of attack is between 20 and 50° from the point of view of metals maximum damage. The influence of the angle of attack can be represented in the form of:

$$W_m(\alpha) = W_m(90°) \, g(w_m, \alpha) \qquad (6)$$

where $W_m(90°)$ is calculated by the formulae obtained above and the function $g(w_m, \alpha)$ depends upon the relation of erosion maximum rate to erosion rate by normal particles impact and the angle of attack.

For the determination of the function $g(w_m, \alpha)$ the data published in the [2] on aluminium erosion under different angles of incidence and target temperatures have been approximated:

$$g(w_m, \alpha) = \frac{w_m \alpha}{\alpha_n\left(\dfrac{\alpha - \alpha_m}{\alpha_n - \alpha_m}\right)^2 (w_m - 1) + \alpha} \qquad (7)$$

where α_m is the angle of attack when erosion is maximum; $\alpha_n = 90°$.

As the analysis has shown the value w_m depends linearly upon the relation of backing temperature to its melting point:

$$w_m = 3,25 - 2,25\frac{T - T_0}{T_m - T_0} \qquad (8)$$

The squared mean error of the calculations by the formula (7) does not exceed the error of the formulae (3, 5).

The criterion dependencies for erosion rate enable to estimate for example the crater depth h, because

$$\mathbf{W_m} \approx \frac{3\rho}{K_M \rho'}\left(\frac{\mathbf{h}}{\mathbf{d}}\right)^2$$

where K_M is the number of the particles taking part in a single erosion act.

1. Зельдович Я.Б., Райзер Ю.П. Физика ударных волн и высокотемпературных гидродинамических явлений. – М., Наука, 1966, 686с.
2. Эрозия. Под ред. К. Прис, М., Мир, 1982, 464с.
3. Михатулин Д.С., Полежаев Ю.В., Репин И.В. Препринт ИВТАН, № 2-402, – М.,1997, 87 с.

STUDY OF CORROSION PROPERTIES OF POROUS COLD-PRESSED ITEMS MADE OF CUPRUM – TUNGSTEN POWDEROUS CONSTRUCTION MATERIAL

Scherbakova L.N., Epifanceva T.A., Kayuk V.G.

Institute for Problems of Materials Science NASU, Kiev, Ukraine

The usage of powderous materials in order to increase efficiency of the detonation effect directly related to conditions of medium of their application as well as to the preservation of their storage. Development of a composite material for these purposes must suppose the finding out of a particular feature of structure and physical-chemical characteristics changes of an item in dependence on the corrosion influence when an item is exposed to sea atmosphere, sea water and NaCl solution. The usage of a composite material predicts experimental investi-gations on efficiency of its application to be carried out.

In the present work investigations on influence of the corrosion affect on changes of physical-chemical properties of a porous nonsintered cold-pressed item made of a construction material with the determined structure characteristics are reported.

By means of metal-graphical investigations of pressings the presence of phases and impurities characterizing composition of the materials was shown. Fracture-graphical inve-stigations revealed the presence of hollow pores and conglomerates of tungsten alloy particles on the surface of the cuprum frame particles.

It was found out that the difference in the surface parameters of items is predetermined by different percentile-weight content of the tungsten alloy.

Experimentally it was established that the corrosive behavior of powderous construction materials based on the cuprum-tungsten alloy is determined through the content of the tungsten phase in a material. Kinetics of a relative change of the samples weight (Δ g/g, g/g) and the rate of their oxidation (K, g/cm^2 24 hours) under exposure in a sea atmosphere are presented in Fig.1. Materials with the high content of tungsten are oxidized and this process is accompanied with the weight of samples increases in time. The rate of oxidation has the extreme dependence. The oxidation of a powderous material with the lower content of tungsten when exposed less then 2400 hours proceeds with the weight of samples decreases. It occurs due to the formation of friable not continuous films on the surface of samples. When exposed during 2800-8600 hours, a dense thin film is formed on the surface of samples and the oxidation process proceeds at rates 2-3 times lower than those when materials with higher content of tungsten are used.

Tests on corrosion in sea water showed that samples with 20 mass % of W-phase corrode with the weight of samples increase (K=1,1 · 10^{-4} g/cm^2 24 hours), on the other hand, when the content of tungsten is raised the material dissolves with the total balance of a weigh lost (K=2,0 · 10^{-4} g/cm^2 24 hours). Character of the surface dissolved is unequal, the main dissolving component is iron contained in W-phase and products of its oxidation are distributed between the surface and electrolyte. Character of the corrosion potentials changes ($E_{corr.}$) of Cu and W containing materials (fig.2, a) in sea water testifies about stability of the corrosion process proceeding in time in case with samples in which content of W-phase is up to 50 mass % and about oxidation of the surface of samples with lower content of W-phase that is similar to samples of pure cuprum.

The anode dissolving of the both materials in 3% NaCl solution proceeds analogically. However, the rate of dissolving of the material with 20 % mass of W-phase is almost one order higher (fig. 3). During the anode polarization one can observe the change in control from kinetic (in region of linear function lgi-E) to diffusion (in the area of the limit currents). At the process of dissolving soluble cuprum and iron chloride particles are formed and on the surface dissolved cuprum particles and con-glomerates of tungsten particles are deposed with the rate almost 2 orders lower than that of cuprum. The latter is proved by the significant difference of $E_{corr} - \tau$ function of the materials with different content of W-phase after the anode dissolving.
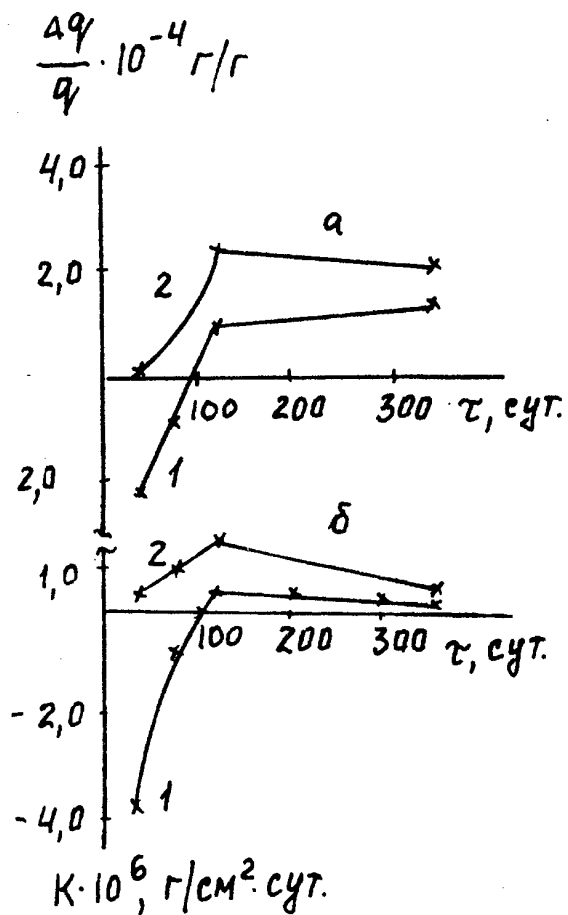
Fig. 1, a, б
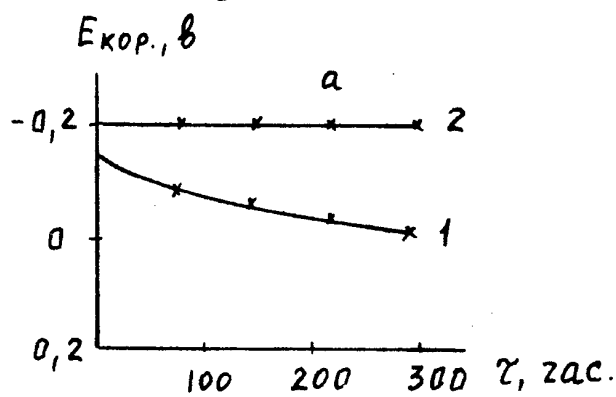
Fig. 3

Fig. 2, a
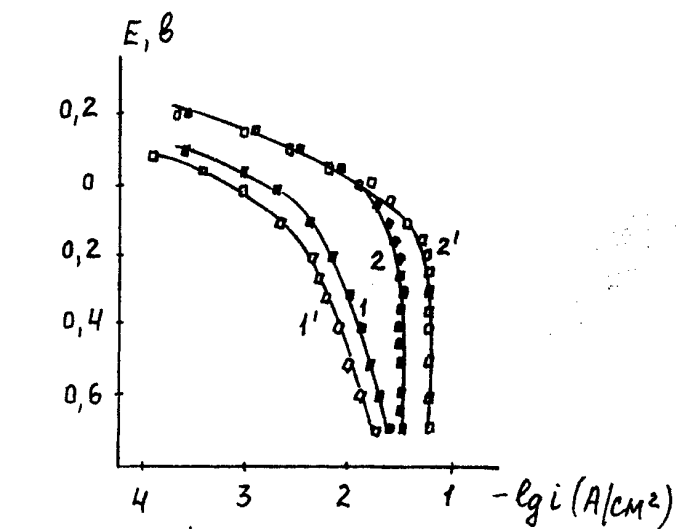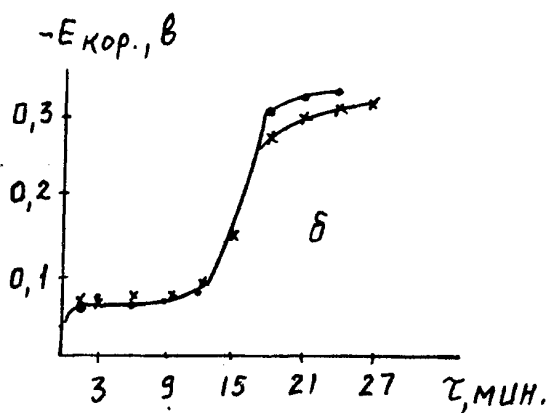
Fig. 2, б

THERMODYNAMIC PROPERTIES of Ni-Al, Ni-W, Al-W, Ni-Al-W MELTS

Sudavtsova V.S., Vovkotrub N.E.

Kiev National Taras Shevtchenko university, 64 Volodymyrska Str., 01033, Ukraine

The alloys on a Ni-base are widely used in engineering as heatproof and corrosion resistant materials, which frequently are reinforced by refractory metals. In this case it is expedient to study thermodynamics of ternary alloys of system Ni-Al-W(3d), which unknown till nowadays. By mixing isoperibolic calorimetry were studied thermochemical properties of 4 sections of binary boundary systems for ternary Ni-Al-W system. Thermochemical properties of Ni-W liquid alloys were studied by mixing isoperibolic caloremetry earlier at 1910 K [1] and in the given work at 2000 K. In novel technique at 1910 K solid W (T=298 K) entered in calorimetric bath with liquid nickel. As Ni-W alloys are characterized by weak interpartial interaction, we have improved the experimental technique. In new technique instead of the thermocouple is applied thermobattery and samples of refractory metals entered in pipe with mobile bottom Nb-foil made screwed on rotated molybdenum core. After sample throwing down on a plate it maintained to const temperature, that fixed using special thermocouple. After that, by shifting of niobium plate, the pipe opened and heated sample add into liquid alloy. This technique has been allowed to increase accuracy of obtained results that is very important at researching in such sort of systems characterized by weak interpartial interaction. It is deals with that the contribution of heat necessary for samples heating from 298 K up to temperatures of endurance considerably decreases. Heat, which is necessary for heating of component entered in calorimetric bath, from 298 K up to experimental temperatures calculated from Hultrgen handbook data. The defined values of partial and integral enthalpy of formation in studied alloys with accuracy up to 2-10 %, accordingly, are given in the table. In calculation used tungsten enthalpy of melting for defined alloys enthalpy of mixing formed by liquid Ni and overcooled liquid W. In the table are given enthalpy of mixing of liquid alloys of Ni-W system up to x_W =0,3. It have been established, that the data [1] slightly more exothermal, in system Ni-W in a solid state such compounds are formed: Ni_4W, NiW, NiW_2 and its correlates with the obtained thermal effects of binary alloys. Evidence of data reliability for Ni-W alloys are same parameters for Fe-W, determined by other authors. As well as it was necessary to expect thermal effects of liquid Ni-W alloys are a little more exothermal, than for Fe-W.

Table
Enthalpy of mixing of liquid alloys of binary Al-Ni (W), Ni-W and sections of Ni-Al-W systems (kJ/mol)

$x_{2(3)}$	0	0,1	0,2	0,3	0,4	0,5	0,6	0,7	0,8	0,9
Ni-Al, T= 1870 K										
-ΔH	0	18	32	42	50	54	54	44	30	16
Al-W, T= 1870 K										
-ΔH	0	2,4	3,9	7,1	8,1	8,6	7,4	6,2	4,3	2,4
Ni-W, T= 2000 K										
-ΔH	0	2,4	3,5	5,8	5,6	4,9	3,9	2,9	1,9	1,0
$-\Delta H'_W$	28	22	16	100						

Ni-Al-W								
$x_{2(3)}$	0,1	0,2	0,3	$x_{2(3)}$	0,1	0,2	0,3	0,4
ΔH(1)	20	32	39	-ΔH(3)	33	34,8	29,6	26
ΔH(2)	22	34	42	-ΔH(4)	50	44	38	32,2

1,2 – section x_W/x_{Ni}= 0,16/0,84; 0,24/0,76.
3,4 -section x_{Al}/x_{Ni}= 0,8/0,2; 0,6/0,4.

Thermochemical (TCh) property of Al-W system were investigated by us earlier at 1870 K [2]. The meanings of integral enthalpy of mixing defined in this work on an advanced technique are given in the table. It is visible, that they will be coordinated to the data [2] and characterize moderate interpartial interactions between different atoms. The comparison has shown first partial enthalpy of mixing of 5d-metals in liquid aluminium, that the minimal interpartial interaction is characteristic for liquid Al-W alloys. TCh of property of liquid alloys of system Ni-Al are determined by caloremetry at 1928 K in Ni interval of concentration $0,6 < x_{Ni} < 1$ by Yu. Esin ($\Delta_m H_{Al}^{\alpha}$ in Al-Ni is -147,5 kJ/mol by A. Stomakhin). These data well coordinated with us-defined at 1870 K in an interval $0,5<x_{Al}<1$ [3] and correlate with estimated from standard enthalpy of formation for Ni_3Al, $NiAl$. In the table are given $\Delta_{mix}H$ of Ni-Al alloys. In the table are given experimental $\Delta_{mix}H$ of 4 sections Ni-Al-W system. It is visible, that $\Delta_{mix}H$ for sections beginning from

alloys of system Ni-Al, decrease. It is clear, that the W adding into Ni-Al alloys results in reduction exothermal effects, which are observed in binary Ni-Al alloys. From partial $\Delta_{mix}H_W$ values of a_W activity in binary Ni-W system in approximation of regular melts are designed. Has appeared that they find out small negative deviations from Raoults law. For Ni-Mo melts is earlier studied by us in [1], that of Mo activity show small positive deviations from ideal solutions. This implies, that melts of Ni–W system, as well as it was necessary to expect, are not regular, and their components should show moderate positive deviations from the Raoults law. The components of Al–W melts, are more probable than everything, will show similar behaviour. As Ni-Al find out the very large negative deviations from ideal solutions, in the ternary Ni–Al–W system, activity of components will show sign changing of a deviation from ideality. It is necessary to expect negative deviations from ideality for alloy components, which structures are close to binary boundary Ni–Al system, namely they have the important practical application. We extrapolated defined enthalpy of mixing of binary Ni (Al)–W systems, defined in an interval $0<x_W<0,3$, on all concentration interval, were based on experimentally defined TCh data on aluminium and nickel-based alloys, and also standard enthalpy of intermetallics formation. Using them have simulated enthalpy of mixing of ternary Ni-Al-W system by Bonier-Caboz and Tuppa eqn. components of the appropriate ternary systems. In figure are given isoenthalphy of mixing for ternary Ni–Al–W melts. The comparison of the experimental and settlement data has shown that they correlate better with the data defined on the Tuppa equation.
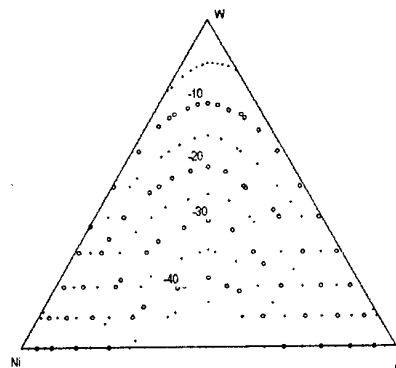
Figure. Points of isoenthalphy of mixing for Ni-Al-W liquid alloys at 2000 K, and Tuppa eqn. calculated.

It has been allowed to make conclusions about an opportunity of correct contribution of TCh properties of Ni-Al-M systems from given for double boundary systems. Enthalpy of mixing of the investigated ternary system smoothly decrease from alloys of system Ni-Al to W and the minimum on this surface corresponds to area of concentration close to equi-atomic to an Ni-Al alloy. And in all interval of concentration enthalpy of mixing is negative ($\Delta H<0$), that it is possible to explain by determining influence of properties of system Ni-Al on properties of ternary Ni-Al-W system. It is no wonder, as interaction between components in liquid Ni (Al)-W alloys is small. From known isothermal section of Ni-Al-W state diagram 1523 K is clear, that ternary intermetallics don't formed. It correlates with defined TCh properties of the investigated ternary system. Thus, from the limited quantity of experimental thermodynamic given for binary boundary systems and sections of ternary melts it is possible to define the authentic information in all a concentration interval. It is especially important for practically important systems, which contain aggressive, refractory or scarce components. Besides the defined in such a way data can form the basis specification of the state diagrams.

Reference:

1. Sudavtsova V. S. *Metally* 1999 №5 97
2. Sudavtsova V. S., Batalin G.I. *Ukr Khim Zh.* 1989. **55** 2 144
3. Sudavtsova V. S., *et al*, *Rasplavy.* 1990 1 97

COMPOSITE COVERINGS CONTAINING REFRACTORY COMPOUNDS

Kudin V.G., Makara V.A.
Kyiv National Taras Shevchenko University, 64 Volodymyrska Str., 01033 Kyiv, Ukraine

Materials based on carbides and borides of transition metals, are refractory, firm, posses high thermal and corrosion stability, but often are fragile. Therefore they are best for rendering on a surface for working in aggressive environments.

The coverings usually are obtained from a gas phase and plasma, by ionic and detonation sputtering on a surface using boron, carbon, nitrogen, that is very expensive, though in the many cases highly effective. For this case it is necessary to develop cheap, but in the same time not less qualitative methods for obtaining of such coverings. Last years composite coverings are used more widely, especially based on polymers. We obtained a number of composite coverings on a basis of polymeric compounds containing powders of refractory substance additives. The composite coverings were prepared from various polymers: polyurethane (P), Teflon (TF), silicon polyurethane (SiP), polyvinylic spirit etc.) with addition of powders of refractory compounds (WC, W_2B_5, VC, B_4C, TaC etc.).

Obtained pastes rendered on steel plates, the plates previously cleared of wastes and oils by a chemical and mechanical way, and then washed out by distilling water. The pastes were fixed by paint on plates and dried at room temperature within day. The coverings on basis fluorine plastics (Teflon) were heated up to 733 K during 0,5 h.

After that measurement of layer thickness, microhardness determination was proceeded. The covered samples after study were placed in the solutions of a sulfuric acid, sodium hydroxide, in the boric acid solution and distilled water. The results on resistance measurement *vs* time for best coverings in various environments are given below.

Table

Coverings	Stability			
	H_2O	20 mass % H_2SO_4	20 mass % NaOH	H_3BO_3
TF+WC	+	-	-	-
P	+	-	-	-
P+W_2B_5	+	+/-	+/-	+
P+Mo_3B	+	-	+	+
P+B_4C	+	+	+	+
P+VC		-	-	+/-
P+WC		-	+	+/-
P+CrB_2		-	+	+
P+C	+	-	-	+
SiP+WC	+	+	+	+
SiP+B	+	-	+/-	+
SiP+B_4C	+	+	+	+
SiP+W_2B_5	*	-	+	*

+ stabile, - unstable; +/- stabile more than 1 day, *collodized

It is observable from the given table, that among the investigated coverings there are such, which are steady in acidic or alkaline-based solution. The most perspective in this respect are such polymers as Teflon, polyurethane and silicon polyurethane because they uncollodized in the water solutions. Therefore it is necessary to develop new compositions on the basis of polymers, which can be longtime-used in aggressive environments, as well as at high temperatures. As many coverings should work up to 700 K, we studied the thermal stability of the all powdered composites in isothermal conditions, also by DTA-DTG analysis in air environment using quasi «Q-1500» derivatograph. It is established that all refractory materials - composites were thermal-proof up to 750 K.

PHYSICAL-CHEMICAL PROPERTIES OF BINARY AND TERNARY SYSTEM CONTAINING SILICON, CARBON, BORON AND ALUMINIUM

Kudin V.G., Makara V.A.
Kyiv National Taras Shevchenko University, 64 Volodymyrska Str., 01033 Kyiv, Ukraine

The properties of materials (alloys) in a wide interval of temperatures and pressure can be predicted from state diagrams of appropriate systems. As the construction of DS is a complex experimental problem, they are expedient for simulating from thermodynamic properties of various solid phases. For this purpose it is necessary for modelling to defined these properties by various experimental methods (EMF, caloremetry, Knudsen effusion and etc.), even by narrow concentration interval.

Carboborides, siliconborides, carbooxides of aluminium and other metals widely use as abrasive, heatproof or corrosion resistive materials. For synthetic methods improving and best best conditions search is necessary to know physical-chemical properties of binary, ternary alloys, one of most important among them is knowledge on liquid state thermodynamics. For researchers in these branch especially in this kind on difficult-in-study systems the liquid state is the uneasy task, thus several prospect techniques for calculation from appropriate binary boundary systems are developed now. For alculation used Toop and Bonnier-Caboz equations because they are most suitable for systems forming compounds in the solid-state. For this purpose were defined using isoperibolic calorimetry the enthalpy of mixing in alloys of binary systems Al (Si)-B at 1873 K and $0 < x_B < 0,4$ and system Si-C at 2000 K up to $x_c < 0.1$ in a liquid by technique described elsewhere in [1]. Initial materials used are silicon (KPS, 99.999%), crystalline boron purified by r.f. heating, spectral-pure graphite, and aluminium AB-000. As boron and carbon at temperature of experiment are in a solid state, from thermal curves were defined partial and integral enthalpy of dissolution, which have recalculated on enthalpies f mixing for process of alloys formation from liquid Al(Si) and overcooled liquid B(C). For this purpose used enthalpy of heating and melting of aluminium, silicon, carbon and boron, given in Hultrgen handbook. The relative errors integrated and partial enthalpy of mixing is equal to be 1-2 and 10%. Processing of common experimentally established enthalpy of mixing for these systems and calculated from standard $\Delta_f H^0_{298}$ of selected compounds, we have defined thermochemical property in all concentration range. These parameters in kJ/mol at the given concentration of the second component are given in the table.

Table
Enthalpy of mixing in melts of binary Al (Si)-B, Al (Si)-C, B-C. System Al-B

x_2	0.1	0.2	0.3	0.4	0.5	0.6	0.7	0.8	0.9
System $-\Delta H$									
Al-B	5	9	14	17	19	20	21	15	6,6
Si-B	2	6	10	15	20	19	16	12	7
Al-C	10	18	23	28	29	27	23	18	10
Si-C	13	21	28	33	36	36	34	19	9
B-C	10	14	15	13	11	9	8	7	3,5

For melts of systems Al-C and B-C the modeling is executed in view of dH values appreciated from $d_f H_{298}$ (AlB$_2$, B$_4$C). Though in this system other compounds - AlB$_{10}$ are formed also, AlB$_{12}$ [8], but for them are not established $d_f H_{298}$. Therefore we have tried to predict them. Has appeared, that they are equal to be -66 and -78 kJ/mol, accordingly.

It is visible, that for all systems in a liquid condition are characteristic moderate exothermal effects of alloy formation. It is no wonder, as all components have close radiuses and properties, and in periodic system are located beside.

It is a little more exothermal dH for melts of system Si-C, in which the most refractory and stable compounds SiC is formed.

Very perspective there is a prediction of physical-chemical properties of melts of ternary systems, especially because their of refractory properties, fugitively it is difficult to investigate now. We have executed accounts of enthalpy of mixing in melts of ternary systems Al-Si-B (C), Al (Si)-C-B using Toupee and Bonier-Caboz eqn. in all interval of concentration, using most reliable thermochemical properties for binary boundary systems (for results see figure) It is observed that small thermal effects characterize all of them. The minim on surfaces of enthalpy of mixing of these systems have on binary alloys Al (Si)-C. It is not

surprising, as enthalpy of mixing in the Al (Si)-B-C system reach the extreme to be equal to -30 and -36 kJ/mol. It is caused by strongest interpartial interaction between different by sort atoms, which is characteristic for these binary boundary systems, and fact that these systems formed any stable ternary compounds. As if to melts of ternary systems Al-Si-B (C), the minimum on enthalpy of mixing is necessary on average concentration area with x_B equal to 0,4-0,7. Those alloys of binary boundary systems Al (Si) cause it -B is characterized approximately by identical interpartial interactions. Therefore on a surface enthalpy of mixing there is a dim plateau of a local maximum. It is possible to make from this a conclusion, that in these systems the unstable ternary compounds can be formed.
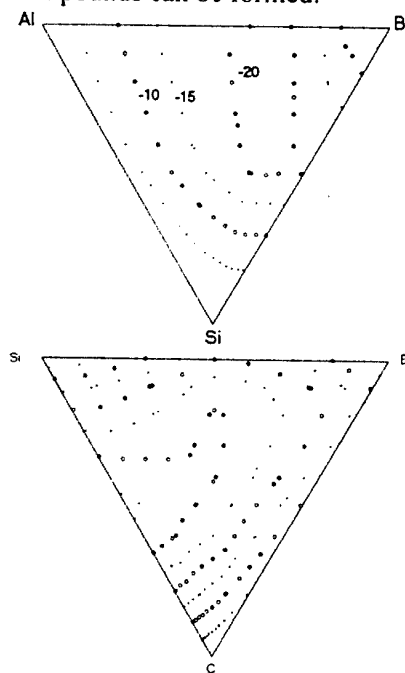
Figure. Plot of isoline (points) for calculated and studied Al-Si-B systems.

For alloys using in a wide concentration and temperatures range it is necessary to know the state diagrams of appropriate systems. Now phase balance in binary systems are well studied and critically analyzed, that cannot be told about situation in the ternary or more complex alloys. Phase equilibrium has been calculated on the base of thermodynamic properties of stable and metastable phases in studied systems. A combination of phases with a global minimum of free Gibbs energy equilibrium and their characteristics used for state diagram graphical-fitting. The values of free Gibbs energy of transformations for pure components were borrowed from literature data. It has been established, that designed and experimentally constructed diagrams for studied systems are in good agreement among themselves.

In isoperibolic calorimeter were determined partial and integrated enthalpy of mixing of binary Aluminium(Silicon)-Boron systems liquid alloys at 1873 K and at 2000 K for Silicon-Carbon one. All enthalpies of mixing are exothermal and relatively small by eigenvalues, which is in a good agreement with literary data. Enthalpy of mixing for Metal-Boron (Carbon) alloys was calculated from $\Delta_f H^0_{298}$ for metals borides and carbides. The mixing enthalpy concentration dependence for liquid ternary alloys of Al, Si, B, C-based systems is defined.

[1] V.S. Sudatsova, V.G. Kudin, *Inorg. Mat* **2001** *37* 396.

COMPOSITE HEAT-RESISTANT MATERIALS: METALLIZED OXIDE GLASSES

Lisnyak V.V., Stus N.V., Sudavtzova V.S., Slobodyanik N.S., Popovitch P.[(1)]
Chemical Department of Kyiv National Taras Shevchenko University, 64 Volodymyrska Str.,
01033 Kyiv, Ukraine
[(1)]Facultät für Physik, Tubingen universität, Universitätstraße 10, D-10452 Tubingen, Deutschland

INTRODUCTION

The metal glasses obtained by rapid quenching of multi component liquid alloys always contain metal nanoscaled crystallites dispersed into amorphous matrix. In such a way materials with high mechanical stability, thermal proof, and also unusual electrical properties are received [1-3].

The interaction of metal particles with ionic liquids (high-temperature molten salts) is accompanied by their partial oxidation with formation of various cluster groups containing metals in low oxidation states. The fast cooling led to incorporation of metal clusters groups, which can be united in a circuit or grids in glassy oxide matrix. That is one of possible ways for a new class of refractory composite materials creation.

RESULTS AND DISCUSSION

Our research in this area is concentrated on synthesis of metallized nano composites in glassy oxide matrix using systems M_xO_y-Mo-MoO$_3$ and M_xO_y-W-WO$_3$ (where M - s- or d- metal), containing small amount of p-elements oxides (it is usual B, Si, P, Ge) as admixture.

Processing of initial components in conditions of high pressure and high temperature (4-7 GPa, 1073 K) with future fast cooling of the system was used for composite synthesis.

The size of tungsten and molybdenum metal inclusions in the glassy matrix changes from atomic units, clusters up to nm-scale particles (see. a fig. 1) depending on stoicheometry of initial composition, dispersion of substances, temperature, pressure, and interaction technique.

Obtained metallized composites were characterised by X-ray diffraction, also ESR, and XPS. The study by scanning and transmission electronic microscopy (SEM, TEM) also was carried out. The properties of the obtained samples i.e. mechanical: micro hardness, crack resistance; thermal stability, electrical conductivity were studied.
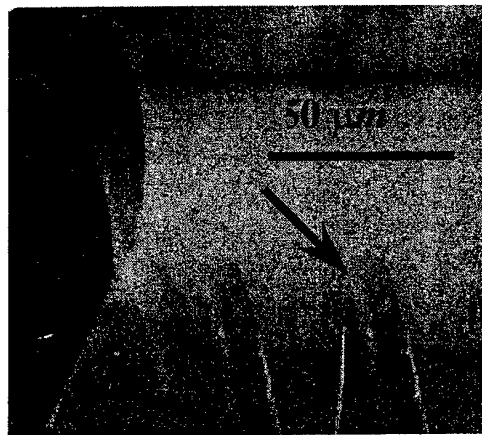
Fig. 1. Morphology of inclusion in glass of system BaO-W-SiO$_2$-WO$_3$, TEM microphoto.

The comprehensive information on initial systems melts properties is necessary for the directed synthesis of metal-oxide composites: viscosity, melting temperature, overcooling liquid temperature, enthalpy of mixing, glass forming ability and tendency [4, 5]. For the subsequent modelling of processes in the melt we defined state diagrams and thermodynamic properties of pseudo binary boundary systems M_xO_y-MoO$_3$ and M_xO_y-WO$_3$ and also number of sections of M_xO_y-GeO$_2$-WO$_3$, M_xO_y-GeO$_2$-MoO$_3$, M_xO_y-SiO$_2$-WO$_3$, M_xO_y-SiO$_2$-MoO$_3$, M_xO_y-B$_2$O$_3$-MoO$_3$, M_xO_y-B$_2$O$_3$-WO$_3$ systems has been investigated.

The tendency to amorphization in mentioned systems was estimated according to criterion GFT, by Zielinski and Matyja [6]. The formula for the analysis of the tendency to amorphization when melt enclosed pseudo-binary M_nO_m associates in multi component systems is proposed:

$$GFT = -0,434 \left[\ln\left(1 - 2\frac{\Delta_{mix}H(z)}{RT_{ov}} \right) + \frac{\Delta_{mix}H(z)}{RT_{ov}} + \frac{1}{3}(1-z)^{m+n} \cdot \ln\left(\frac{N_a}{m+n} \right) \right]$$

where z - is a third component mole fraction, T a temperature of overcooled liquid, $\Delta_{mix}H(z)$ is a concentration dependence of mixing enthalpy; N_a is Avogadro`s number, $m+n$ are the stochiometrical coefficient of cluster composition.

CONCLUSIONS

The new class of refractory composite materials containing metal cluster groups in glassy oxide matrix is synthesised. The thermodynamic properties of initial systems melts were estimated.

REFERENCES:

1. Young Kwan Kim, Jeong Ryong Soh, Hyoung Seop Kim, Hyuck Mo Lee. *CALPHAD* **1998** *22*, 2. 221.Zhang Z.J., Jin O., Liu B.X. *Physical Review B.* **1995** *51*, 13 8076.

2. Liu B.X., Zhang Z.J., *Physical Review B.* **1994** *49*, 18 12519.

3. Bohmer, R. Nanoscale heterogeneity of glass-forming liquids: experimental advances, *Current opinion in solid state & material science* **1998**, *3* 378.

4. Greer, A.L. Metallic glasses, *Current opinion in solid state & material science* **1997** *2* 412.

5. Zielinski, P.G. Matyja H. Int. conf. Cambridge: Mit Press, **1975** 237.

INFLUENCE OF A TEXTURE OF TUBES FROM AN ALLOY TITANIUM ON THEIR STABILITY IN REQUIREMENTS OF BOOSTED DANGER

Tarasov A.F., Koncha A.A., Timoshenko E.S.
South Ukrainian State Pedagogical University, Odessa, Ukraine

The texture essentially influences corrosion properties of tubes from titanium and alloys on its basis. Most proof appear pipes with the texture of a central basic type, i.e. with an arrangement of a basic plane parallelly surfaces of a wall of a tube. We explore influence of a texture on stability of tubes from alloys OT4 and OT4 - 1 (system Ti-Al-V) depending on its basic parameters (blanket dispersion, amount of deflection of maximums of pole density and their arrangement - in an axial or tangential direction), and also the technological plan of reception of tubes with a sharp texture is designed.

The development of the plan of reception of a sharp texture in explored alloys was carried spent previously on leaf materials. The Initial alloys leaves and trumpet purveyances got by ingots processing after double arc vacuum fusion. Then the ingots exposed to homogenizing annealing in atmosphere high clean of argon and by consequent cooling with stove, whereupon them exposed to division, a surface cleaned out.

A Cold leaves rolling took on laboratory rolling figure with smooth cylindrical felling, trumpet purveyances on experimental figure of cold tubes rolling. Texture of initial purveyances is the separate domains of raised pole closeness asymmetric pole figures distributed on all area. On elementary stages of warm deformation (15 – 20%) takes place some regulating texture and her reinforcement attached to augmentation of deformation to 40– 50%.

Has appeared, that the most suitable initial texture is the rather feeble texture of a central basic type with a strong blanket dispersion both in a direction rolling (DR), and in a transverse direction (TD) to DR, however dispersion in TD should surpass a dispersion in DR not less than in 2 times. Subsequent rolling should thus be carried spent in new DR, conterminous with old TD. Already at 20-40 % of strain under such plan the texture begins will become aggravated, and the dispersion decreases, and at strains ~ 60 % in new DR, it practically comes nearer to circular. The intensity of centre of a pole figure is sharply incremented and exceeds initial ~ 2,5 times, and at the deformation degree ~ 80 % in 3 times.

At rolling of tubes, because of difference of the plan of the intense state (taking into account also features tube-rolling mill) the quantities of deformation degree are displaced on 5-15%. Besides it is necessary to take into account and degree of strain not only on thickness of a wall, but also on a diameter. It is important as well to maintain acceptable parameters of structure which can be levelled by realization extra annealing (however annealing can give in decrease of stability).

The changes of a texture in tubes (as well as similar changes in leafs at realization of prestress examinations) were analysed with the help the texture of parameters, that enables in a self-acting mode conduct the check of changes of a texture at rolling. At the same time texture parameters have a high correlation with changes of an anisotropy of properties in tubes, that enables to estimate their anisotropy during manufacture and to work up the recommendations on improvement of tubes production technology from explored alloys with made better operational descriptions.

REFLECTANCE AT 10.6 μm OF CARBON-CARBON COMPOSITES HEATED IN THE AIR BY CW CO₂-LASER RADIATION

Dlugunovich V.A., Zhdanovskii V.A., Snopko V.N.
B.I. Stepanov Institute of Physics of the National academy of sciences of Belarus,
68 F. Skaryna Ave., Minsk 220072, Belarus, e-mail: tsaruk@dragon.bas-net.by

Carbon-carbon (c/c) composites consist of a carbonaceous matrix, reinforced with carbon fibers. The matrix is formed using successive cycles of carbonization of high carbon yield resins. The enhanced mechanical properties combined with thermal endurance of c/c composites find their applications in cases where extreme environments of heat and stress exist like in aerospace and rocket engines. Difficulties of mechanical processing of high-strength c/c composites have caused laser cutting application. Efficiency of laser-material interaction depends on the reflectivity of the ablating material surface at the laser wavelength and any meaningful modeling of this materials laser-ablation process requires accurate reflectivity data. There for the directional-hemispherical reflectance at 10.6 μm of c/c composites during its heating on air by CW CO₂-laser radiation was measured. Three modification of this material were investigated without an oxidation protection, and with two types of protections. The investigated materials density was $1,2 \cdot 10^3$, $1,7 \cdot 10^3$ and $1,8 \cdot 10^3$ kg/m³ accordingly.

The samples 20×20 mm with a standard thickness 4 mm where placed in the center of integrating sphere and exposed under a ~ 150-watt CW CO₂-laser beam focused to three different spot sizes ~ 12; 8 and 1 mm. The incident radiation intensity q was 90; 200 and 16 000 W/cm² accordingly. During the treatment and reflectance measurement, the target temperature was simultaneously recorded by thermocouple on the rear side of the sample.

It is summarized, that reflectance R_0 of the investigated composites before laser treatment have essential disorder of values for different samples of the same material. The greatest disorder of reference is characteristic for less dense material. Therefore change of the investigated materials reflectance $R_{10.6}$ during laser influence is convenient to characterize by relation of the current values of reflectance to initial one R_0 for each sample ($R_{10.6}/R_0$).

Increase of $R_{10.6}/R_0$ for all investigated c/c composites, heated by CO₂-laser radiation with a power density 90 W/sm², is uniquely connected with materials temperature rise and apparently is caused by thermal activation of electrons from the valency zone to the conductive zone. However, the reflectance of the c/c composites depends on the perfection of the structure so as, from the material porosity, the admixtures and surface relief also. Reduction of the surface porosity with a pore size more than 10 μm during material shrinkage at the laser heating may increase $R_{10.6}/R_0$ too. The investigated c/c composites reflectance change at the incident power density over 200 W/sm² depends not only on material temperature, but also from its modification and incident power density.

SURFACE X-RAY PHOTOELECTRON SPECTROSCOPY AND REACTION ABILITY OF ALLOYS BASED ON RARE-EARTH METALS AND ZIRCONIUM

Dobrovolsky V.D., Khyzhun O.Yu., Solonin Yu.M.

Institute for Problems of Materials Science, National Academy of Sciences of Ukraine,
Kyiv, Ukraine

Multicomponent hydride-forming alloys of the AB_5 and AB_2 types based on rare-earth metals and zirconium are widely used as perspective electrode materials of nickel/metal-hydride storage cells. These alloys show different behavior during electrochemical hydriding-dehydriding. The alloys with similar bulk characteristics (e.g., equilibrium hydrogen pressure and hydrogen capacity) may exhibit different real electrochemical activity because of different surface states. The main process that influences alloy activity is the formation of thin surface oxide layer and related element redistribution during exposure of the alloys to air. However, the above process has not been sufficiently investigated for the mentioned multicomponent hydride-forming alloys.

Difference between surface energies of the components and their affinity with oxygen may cause different content and charge states of atoms, which are catalysts in the reaction $H_2 \Leftrightarrow H + H$, in surface layers of Zr- and rare-earth-based alloys exposured to air [1,2]. As a result, these alloys will possess different electrochemical activity. Polarization measurements allowed to evaluate activity of different alloys at initial stages of hydriding-dehydriding [2]. The X-ray photoelectron spectroscopy (XPS) method reveals information about chemical states of atoms that are catalytically active centers and atom centers in the surface layer [3-7].

The purpose of the present investigation was to study correlation between surface chemical states and electrochemical activities of alloys of the AB_5 and AB_2 types and to determine the influence of the composition and structure of the surface oxide layer and different elements in this layer on the activity of alloys during electrochemical hydriding and dehydriding.

The studying alloys were the following: $LaNi_{4.5}Al_{0.5}$, $Zr_{0.59}Ti_{0.41}Ni_{0.78}V_{0.53}Cr_{0.22}Fe_{0.2}Co_{0.27}$ and $Zr_{0.9}VCo_{0.55}Ni_{0.55}$. The alloys have been prepared by arc melting [2]. For the XPS measurements, powders of these alloys were pressed to obtain pellets with d = 10 mm, h = 2 mm. The XPS spectra were derived with an ES-2401 spectrometer at 2×10^{-7} Pa using Mg Kα radiation. The polarization measurements were carried out using an impulse potentiometer PI-50-1 over the range -0.2 V to -0.95 V in the alkaline electrolyte (30% KOH solution). The three-electrode cell, Hg/HgO comparative and nickel counter electrodes were used. Negative electrodes were the hydrogen-sorption alloys studied. The electrodes were prepared by cutting plates from the alloys ingot or by pressing pellets (d = 10 mm, h = 1.5 mm). The pellets were pressed from powders of the arc melting alloys (p $\approx 1.5 \times 10^7$ Pa).

The XPS Zr 3d, Ti 2p, Ni 2p, Ni 3p, Mn 2p, V 2p, Co 2p, C 1s and O 1s core-levels spectra for the Zr-based alloys were recorded, and La 3d, Ni 2p, Ni 3p, Al 2p, O 1s and C 1s spectra for the $LaNi_{4.5}Al_{0.5}$ alloy. The XPS analysis of specimens in initial states (i.e., exposed to air for a long time) showed that the spectra of Ni, Co and V are almost not detected [2,7]. As shown in our previous works [1,7], on the surface of the zirconium-based alloys Ni is covered by the compact layer of Zr (or Ti) oxides and only its destruction may lead to alloy activation. In surface layers of the alloys investigated, the Ni atoms are observed after Ar^+ cleaning. When the Zr-based specimens were exposed to air (1 h or 24 h) after Ar^+ cleaning of their surfaces the quantity of the nickel atoms in oxidized states increased in comparison with those in metallic state [1,2,7]. The part of the atoms in Me^0 states in surface layers of the alloys exposed to air decreases in the sequence Ni, Co, V. In the zirconium-based alloys investigated after their cleaning and exposing to air, Zr and Ni atoms are mainly in oxidized states.

Results of the XPS studies have been compared with data of polarization measurements as well as the electrochemical behaviors of the alloys over the potential range $-0.95 \text{ V} \leq E \leq -0.2$ V [2]. These measurements allowed to evaluate the alloys activity. A course of cathodic curves,

especially in initial area of small currents, should reflect initial states of surfaces, and first of all presence of active centers [2,7]. The more such centers on the surface, the higher activity and less overpotential at certain cathodic currents. Thus the activity of the initial surface can be characterized by an inclination of cathodic curves especially in their initial area. The higher activity, the more flat course of these curves.

A course of curves in the region of small currents indicates that activities of the zirconium-based alloys, $Zr_{0.59}Ti_{0.41}Ni_{0.78}V_{0.53}Cr_{0.22}Fe_{0.2}Co_{0.27}$ and $Zr_{0.9}VCo_{0.55}Ni_{0.55}$, are smaller than that of the alloy $LaNi_{4.5}Al_{0.5}$ [2]. The XPS analysis of the specimens in initial states (i.e., exposed to air for a long time) showed that the spectra of Ni, which is the most active catalyst of the processes of H_2 $\Leftrightarrow$ 2H dissociation, could be measured in the case of the alloy $LaNi_{4.5}Al_{0.5}$, nevertheless, these spectra could not be practically detected in the case of the zirconium-based alloys (for more detailed information see Refs. 2 and 7). This fact can be explained if we suppose that on the surface of the zirconium-based alloys Ni is covered by the compact layer of Zr oxides and only destruction of this layer may lead to alloy activation. Creation of this compact layer that covers Ni^0 plays the important role in decreasing activity of the Zr-based alloys investigated.

Comparison of the XPS spectra of the rare-earth- and zirconium-based alloys exposed to air for a long time [1,7] allowed to choose the most important factor which couse fast activation of the alloy $LaNi_{4.5}Al_{0.5}$ as compared with the zirconium-based alloys. This factor is that, the oxidized layer La_2O_3 is broken on the surface of the $LaNi_{4.5}Al_{0.5}$ alloy, therefore, this layer is permeable for molecular hydrogen. The XPS Ni 2p core-level spectra, which could not be detected for the zirconium-based alloys [2,7], could be measured for the $LaNi_{4.5}Al_{0.5}$ alloy due to brokeness of the La_2O_3 oxidized layer (i.e., due to its islet-type form). It should be noted that a significant part of the Ni atoms on the initial surface of the $LaNi_{4.5}Al_{0.5}$ alloy are in the Ni^0 state. Ni atoms in the Ni^0 state are the most active centres on which hydrogen dissociative chemisorption is realized. These centers are weakly blocked by carbon- and oxygen-containing structures absorbed on the alloy surfaces. Amount of these structures on the surface of the $LaNi_{4.5}Al_{0.5}$ alloy is larger as compared with those on the Zr-based alloys.

The two types of selected area electron diffraction of the Zr-based alloys exposed to air in the form of diffraction rings were observed. The first one was obtained from thin films attached to the edge of bulk alloy and attributed to TiO_x with cubic structure. The second one was derived from the edge of bulk alloy in the form of very diffuse rings attributed to rutile-like structure [2,7].

In conclusion, it should be mentioned that, the present study revealed some correlation between data of the polarization measurements and the XPS investigations. These data indicate that, a course of cathodic curves, especially in initial area of small currents, reflects an initial state of the surface, and first of all the presence of active centers. The present study and some of our previous investigations indicated that, the alloy that contained on its surface the greatest amount of catalytically active centers observed by the XPS technique (e.g., segregation of the nickel atoms in the metallic state, Ni^0) possesses the more flat polarization curve in the range of small currents as well as the smaller potential at the same cathodic currents. These alloys are the studied rare-earth-based alloy that displays higher electrochemical activity as compared with those of the zirconium-based alloys. It is general for the studied zirconium-based alloys that on their surfaces Ni^0 is covered by the compact layer of Zr (or Ti) oxides and only destruction of this layer may lead to alloy activation.

[1] V.D. Dobrovolsky, Yu.M. Solonin, V.V. Skorokhod, O.Yu. Khyzhun, J. Alloys Comp., **253-254** (1997) 488.

[2] Yu.M. Solonin, V.D. Dobrovolsky, V.V. Skorokhod, O.Z. Galiy, O.Yu. Khyzhun, Proc. Summer School on Advanced Materials for Industrial Application, June 20-27, Kavala, Greece, p. 331.

[3] L. Schlapbach, T. Riester, J. Appl. Phys., **A32** (1983) 169.

[4] L. Schlapbach, N. Riester, J. Less-Common Metals, **101** (1984) 453.

[5] Yu. Xin-Nan, L. Schlapbach, Int. J. Hydrogen Energy, **13** (1988) 429.

[6] V.D. Dobrovolsky, S.N. Yendrzheevskaya, A.K. Sinelnichenko, V.V. Skorokhod, O.Yu. Khyzhun, Int. J. Hydrogen Energy, **21** (1996) 1061.

[7] V.D. Dobrovolsky, Yu.M. Solonin, V.V. Skorokhod, O.Yu. Khyzhun, Int. J. Hydrogen Energy, **24** (1999) 195.

IMPROVEMENT OF PHYSICO – MECHANICAL PROPERTIES OF COMPOSITION MATERIAIS BY POLYORGANOSILOXANE HYDROPHOBISATION

Kostornov A.G., Beloborodov I.I., Sukhostavets S.V.
Frantsevich Institute for Problems of Material Science of National Academy of Science of Ukraine, Kiev, Ukraine

Polymer based composition materials are widely exploited in moisture medium. Due to their value properties (anticorrosion stability, small weight, simplicity of making etc) they are often non-alternative in practice.

Epoxy and polyether resins based composition materials play important roll in various industry branches.

However, machine details from such materials change essentially their geometric dimensions and physico – mechanical properties under action of moisture. As it was shown after 10 days exploitation in moisture medium the polymer samples increased their dimensions because of smelling. Simultaneously a bending strength was lowered in 1,5 – 1,7 times.

An influence of the fillers hydrophobisation by the polyorganosiloxanes on compositiom materials properties was investigated with using marshalit and tripoly.

As hydrophobic substance the polyethilenhydrosiloxane liquid GKG – 94 was used.

The treatment in a ball mill showed considerable influence of the polyorganosiloxane addition: spesific surface of the fillers was increased from 360 to 1540 cm ^{2}/g.

It was determined, that 0,16 % the hydrophobic addition was optimum. It was showen, that after the GKG – 94 addition the moistureabsorbtion of the investigated fillers and the polymer compositions decreased in 2,2 – 2,6 times.

It was established, that an existence of the siliconorganic additions in compositions led to the bending strength rise with a modificator content increasing. A general increase of the filled compositions strength was equal 22 – 31 %.

Results of these investigations show, that fillers modification with the polyorganosiloxanes improve properties of composition materials because of their hydrophilic reduction.

ENDURANCE of ELECTROSPARK COVERAGES FROM a COMPOSITION Ag-CaF$_2$

Kryachko L.A., Zatovskiy V.G., Polotay V.V., Smirnov V.P., Polotay A.V.

I.N. Frantsevich Institute for Problems of Materials Science, NASU, Kiev, Ukraine

Fluoride of calcium (fluorite, CaF$_2$) is successful applied in hard-loading pair of abrasion, where the classical solid lubricants appear low-effective [1]. It is determined by its thermo-dynamic stability at heightened temperatures and appropriate physical-mechanical characteristics: high hardness in a combination to brittleness, that promotes simplification run-in of surfaces of abrasion, hardening of working layers and decreasing of their wear. The positive influence of the addition of fluorite on endurance of sliding electrical contacts on the basis of bronze in high-speed thermal-loaded current-collecting device [2] and silver - in current-collecting devices of a heightened resource [3] is also marked.

The aspiration to a miniaturization of products, and also economy of precious and scarce materials reduces in necessity of application of coatings instead of integral all-metal details. Thus in the field of an electrical engineering and the electronics engineering alongside with galvanic coatings a wide circulation have received electrospark, which plot on the details from copper or its alloys.

The purpose of the present work was a research tribotechnical and electric-contact properties of electrospark coatings from a composition Ag-CaF$_2$.

As fluorite is an insulator, and, besides, is badly witted with silver, the drawing of an electrospark layer from this composition on materials with a high thermal conductivity in usual conditions is connected to the large difficulties. At the same time it is revealed, that the lowering of a gradient of temperature on depth of a treated surface conducts to normalization of process of a deposition of a layer. Therefore we accepted additional measures, which have allowed to receive on details from copper, manufactured as rivets, electrospark working layer by thickness of 0.45 microns in the central part and up to 0,30 microns - on a rim, fig. 1.

The coatings plotted on second of operation conditions of installation "Elitron-22 A" during the 3rd min on each detail, then a surface layer flattened by a steel ball, which is fixed in the vibrator of the installation "M1-641".

Mass wear of the coating determined by weighing on analytical weight of the mark ВЛА-200-М.
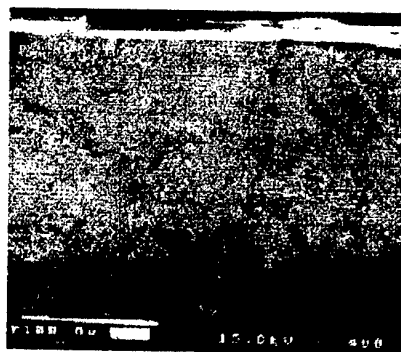
Fig. 1 - Microstructure of an electrospark coating from a composition Ag-CaF$_2$

The investigations carried out by the machine of friction on a technique stated in [4]. The rings from beryllium bronze served as contrary-body. Test specifications: speed of sliding of rings V = 0,5 m/s; contact pressing N$_K$= 1,0 N; a path of friction L = 10 km.

The results of investigations have shown, that the values of friction factor of the examined pairs are reduced during first 50-100 m of a path from 0,1 up to 0,06 and further remained rather stable (0,05 ... 0,07). As a result run-in on a working surface of a coverage the platform is shaped round which ambassador of 1 km of abrasion path has a diameter ~ of 0,5 mm.

The ambassador of 10 km of friction path the sizes of a working trace on a surface of a coverage increased up to 1,0 ... 1,2 mm, fig. 2. At the same time the common loss of a mass of a coverage defined by weighing, for all time of investigations has made 0,1 mg, that is in limits of an error of weight.

After long operation on a surface of a track there are fine scratches caused by hit of separate alternate corpuscle fluorite in a zone of friction. The decoding profilograph of the working trace which has been removed at driving indenter across a direction of friction, fig. 3, gives a value of maximum depth of the scratches at a level ~ 2 microns. As a whole, the condition of a trace

quite satisfactory, the presence of films on its surface visibly is not revealed.

Condition of a surface of a working trace in addition was evaluated by measurement of contact resistance on a specially developed technique [6].
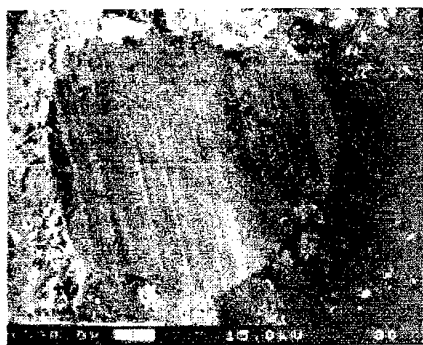
Fig. 2 - Working surface of a coverage after investigations (L = 10 km)
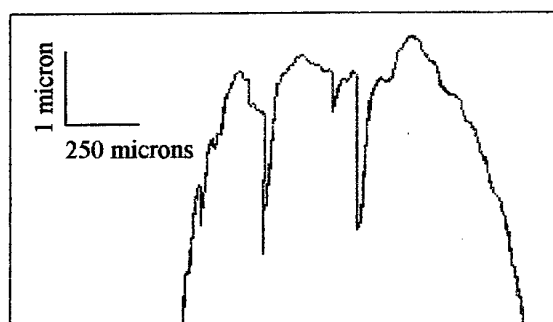
Fig. 3 – Profilograph of a surface of friction of a coverage from a composition Ag-caF2 after investigations

Fixing of values of a voltage drop U realized by a way traverse by a silver focusing prod of a working surface of a coverage with step 1 micron by contact pressing 0,5 sN. The voltage between a focusing prods and investigated surface in the broken condition made 100 mV.
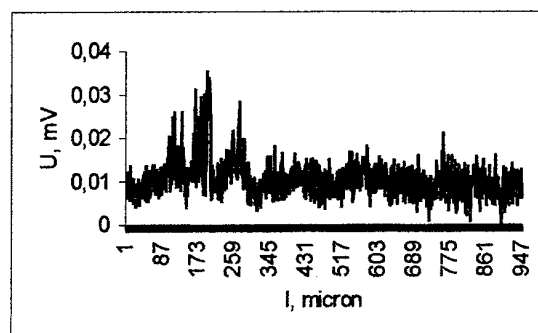
Fig. 4 – Change of a voltage drop across a path of friction

The results, which introduced in a fig. 4, testify to presence on a surface of a trace of areas with different conductance, which differ on an absolute value in 2-3 times. Apparently, it is a consequence frictional of interaction of contacting surfaces having a place at a trial on endurance, which has reduced to local film structures on them. It is necessary to assume that their nature and thickness do not call complete loss of conductance in the chosen test specifications.

Thus, the carried out researches confirm positive influence of fluorite inclusions on serviceability of contact details on the basis of silver.

REFERENCES

1. Шевчук М.Ф., Роик Т.А. Порошковые антифрикционные материалы для работы при повышенных температурах // Порошковая металлургия, 2001.- № 1 / 2. – С. 53-58.

2. Куранов В.Г., Иванов Г.В., Бобырев С.В. и др. Комбинированная контактная пара для прецизионных скользящих слаботочных контактов повышенного ресурса // Электрические контакты. Пути повышения качества и надежности / ИПМ АН УССР: Киев, 1981. – С. 95-100.

3. Затовский В.Г., Френкель А.Г. Структура и свойства материалов на основе оловянистой бронзы для высокоскоростных тяжелонагруженных токосъемников // Порошковая металлургия, 1995. - № 11/12. – С. 57-62.

4. Затовский В.Г. Особенности работы скользящих электрических контактов из композиционных самосмазывающихся материалов // Трение и износ, 1985. – № 1. – С. 107-113.

5. Крячко Л.А., Падерно В.Н., Коваленко О.И. Особенности структурообразования и поведения при эксплуатации слаботочных электроконтактных материалов, содержащих фторид кальция // Порошковая металлургия, 1992. - № 9. – С. 84-88.

6. Polotay V.V., Zatovskiy V.G., Polotay A. V. Microtribotest for studies of contact interaction of pair friction // Intern. Confer. "CERAM-2001". Abstracts. Kiev, IPMS. - 2001. – P. 231.

413

HEAT RADIATION OF LIQUID METALS AND ALLOYS

Panfilovitch K.B., **Sagadeev V.V.**, **Shmagina L.V.**, **Golubeva I.L.**
Kazan State Technological University, Kazan, Russia

The radiation heat exchange plays a determinative role in work of the high-temperature instruments and installations. Now there is no experimental base of data about the radiation of liquid metals and alloys. For determination their emissitivity factors it is offered to use the equations of the classical electromagnetic theory in some works.

There are no clear ideas of the nature of change of the spectral emissivity of metals at melting. Experimental monochromatic emissivity factors of a number of metals at $\lambda = 0,65$ microns do not change at melting. Authors [1] couldn't have a single meaning if the emissivity factor $\varepsilon_{0,65}$ change generally at melting of molybdenum, niobium, vanadium and titanium. The optical constants of iron and nickel don't change their meaning close to visible range of spectrum too [2,3]. In work [4] the increasing of emissivity factor was found at melting of copper $\varepsilon_{0,65}$ from 0,12 to 0,16. The spectral emissivity by the measurements of the authors rises for metals and decreases for semimetals. There is jump on 80 per cent for copper (fig.1).
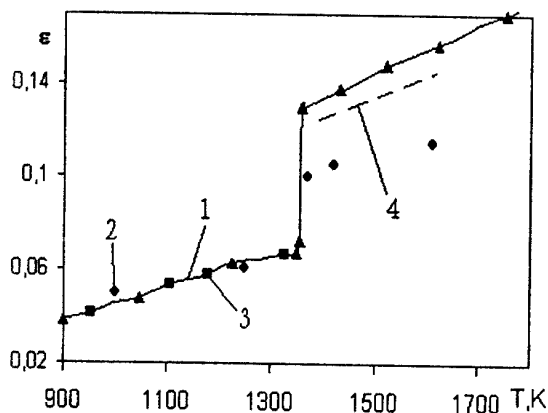
Fig.1 The amissivity factor of copper. 1 – our measurements, 2 - electromagnetic theory calculation. 3 – [7], 4 – [5].

The ratio of the emissitivity factor of liquid phase to the emissitivity factor of solid phase at melting temperature was measured by the authors in the range of wave distances from 1,69 to 10,6 microns on the retrofit, used earlier for research of the integral radiation of heat of liquid and solid metals [6]. Parts of spectrum were cut by a narrow-band filter. For Zn, Cd, Pb, Sn the change of the emis-

sitivity factor at melting in the nearest infra-red range (1,69 microns) isn't large but it rises sharply with the increasing of wave distance and reaches value $\varphi = 2,39$ at $\lambda = 10,6$ microns for Zn (fig.2).

In case of semimetals the value $\varphi < 1$ decreases with wave distance. The calculations of the emissitivity factor with the help of electromagnetic theory, considering possible to use it for liquid metals, don't guarantee adequate accuracy. There are results for copper in solid phase being in a good accordance with the experimental data (fig.1). But in liquid phase they are understated on 35 per cent.

The ratio of the spectral emissivities, calculated from the formula Hagen-Rubins, practically doesn't depend on wave distance and it is less than 1.
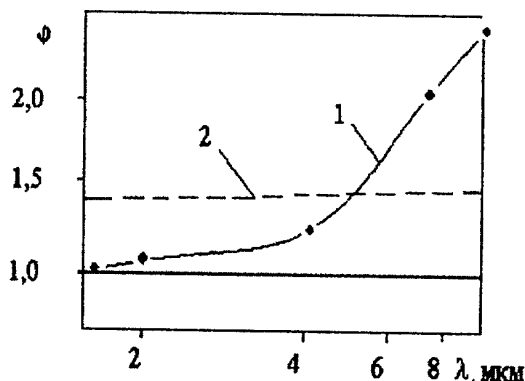
Fig.2 – The value φ for zinc. 1 – our measurements, 2 - electromagnetic theory calculation (formula of Hagin-Rubins).

The heat radiation was measured for alloys of metals. The spectral emissivities of Zn-Al alloy have the same values ε in the solid phase (fig.3). In liquid phase they considerably diverge due to sharp change of emissivity factor of zinc at melting point. The emissivity factor of Sn-Zn melt at low temperatures lightly depends on structure (fig.4) this dependence vanishes with the increasing of temperature. In experiments the metals were used in which the content of the main substance was 99,999% of a mass fraction.
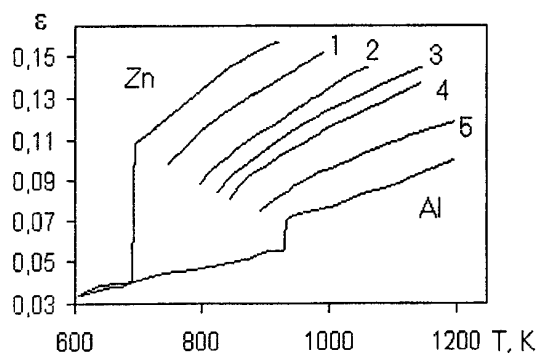
Fig.3 – The amissivity factor of alloys of zinc with aluminum (mass fraction): 1 – 0,8; 2 – 0,6; 3 – 0,5; 5 – 0,2.
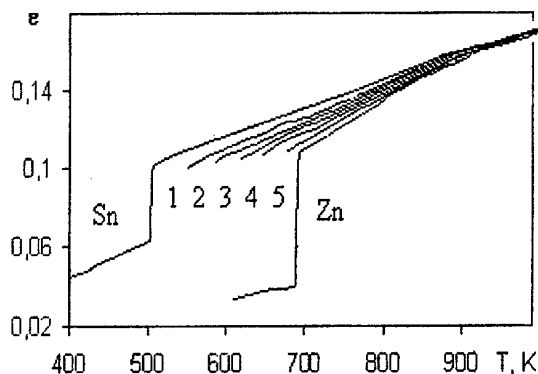
Fig.4 – The amissivity factor Sn-Zn alloy. Zinc content (mass fraction): 1 – 00,8; 2 0,0,6; 30,40,5; 4,8 0,4; 5,8 0,2 Zn
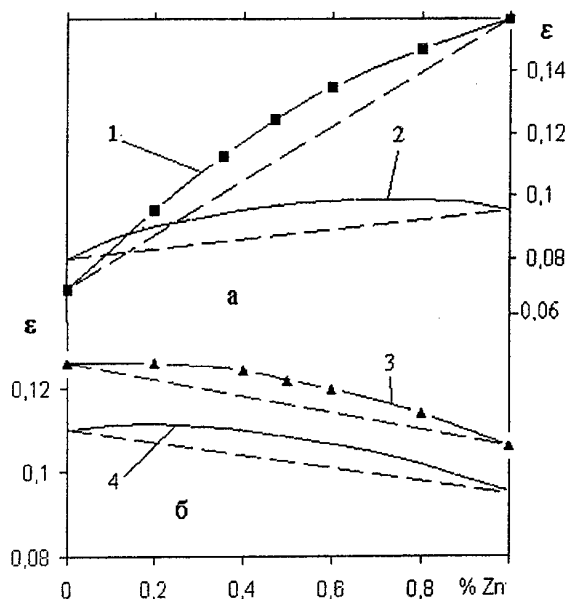
Fig.5 – Dependence of experimental data (1,3) and electromagnetic theory calculation (2,4) of amissivity factor of alloys Zn-Al (a) at T = 950 K and at T = 700 K on structure.

The amissivity factors Zn-Al and Zn-Sn melts depending on structure don't change additive (fig.5) The absolute values of the spectral emissivity of liquid alloys calculated with the electromagnetic theory only qualitatively come to an agreement about experiment. The amissivity factors of liquid alloys depending on structure repeat the nature of change of specific electrical resistance. It turned out that the deviations of the amissivity factor counted with the reproduce the deviations from additive dependence of experimental data of amissivity factors. Therefore it's possible to carry out approximate estimators ε of alloys with the help of ε of pure metals, calculating the deviations from additivity from the electromagnetic theory.

Literature.

1. Берзин Б.Я., Кац С.А., Чеховской В.Я. Спектральная излучательная способность жидких тугоплавких металлов //ТВТ. – 1976. – Т.14. - №3. – С.497 – 502.

2. Шварев К.М., Гущин В.С., Баум Б.А. Влияние температуры на оптические константы железа //ТВТ. – 1978. – Т.16. - №3. – С.520 – 526.

3. Гущин В.С., Шварев К.М., Баум Б.А., Гельд Л.В. Оптические свойства никеля при высоких температурах //Физика твердого тела. – 1978. – Т.20. – вып.6.С.1637 – 1642.

4. Пелецкий В.Э Исследование монохроматической излучательной способности жидкой меди //ТВТ. – 2000. – Т.38, №3, С.424 – 428.

5. Блох А.Г. Основы теплообмена излучением. /Под ред. А.М.Гурвича, -М.: Госэнергоиздат, 1962. – 351с.

6. Панфилович К.Б., Сагадеев В.В. Интегральная степень черноты твердых и жидких элементов //Промышленная теплотехника. 1990. Т.19, №5. С.66.

7.Латыев Л.Н. и др. Излучательные свойства твердых материалов: Справочник /Л.Н.Латыев, В.А.Петров, В.Я.Чеховской, Е.Н.Шестаков, Под ред. А.Е.Шейдлина. – М.: Энергия. 1974. – 471с.

STRUCTURAL PROPERTIES OF DETONATION-CREATED STEEL-ALUMINUM BIMETALLIC JOINTS

Litvishko T.N.
State Design Office Yuzhnoye, Dniepropetrovsk, Ukraine

The rocket-space industry uses bimetallic transfer elements for joining parts from different metals and alloys. So, for joining aluminum propellant tanks and titanium pressure vessels with ducts from a stainless steel the bimetallic elements steel-aluminum and steel-titanium are employed, for joining thruster's niobium combustion chamber with an injector - steel-niobium, and so on. At this the joint of bimetallic layers shall be strong and very often shall meet some specific requirements.

The Yuzhnoye SDO has elaborated and mastered technology of bimetallic joints production under use of explosion welding. The paper presents results of integrated investigations of bimetallic joints steel-aluminum 12X18H10T-A6-AMr6 and steel-copper-niobium 12X18H10T-M1-H65B2MЦ that were produced in order to determine criteria of layers joining's reliability and further optimization of technological parameters in the explosion welding. The investigation has been performed for layers of bimetallic joints produced under collision parameters close to optimal ones.

This investigation was performed under use of light microscopy, microhardness measurement, micro-roentgen-spectral analysis, raster electron microscopy and technological tests: resistance to layers separation, bending by an angle of up to 90^0, ultrasonic inspection and leak test with helium leak detector.

The quality, phase composition and structure characteristics of bimetallic joints are considerably influenced by technological parameters and chemical composition of metals to be welded.

The generalized analysis of metallographic examination's data has shown a presence of morphological inhomogeneity on borders between layers.

Bimetal 12X18H10T-A6-AMr6. The border between layers A6-12X18H10T is characterized by smooth waviness. In the contact zone some separate intermediate inclusions of 8-15 μm thickness are observed. The inclusions' microhardness is $H\mu = 2200...7200$ N/mm^2. The micro-roentgen-spectral analysis reveals that these inclusions have a chemical composition differing from initial one of materials to be joined. The inclusions have up to 88% Al, 12% Fe, 4% Cr and 3% Nb.

Apparently, the intermediate inclusions may be identified as a finely dispersed mixture of particles from A6 aluminum, 12X18H10T stainless steel and inclusions of intermetallic phase FeAl$_3$. The latter may dissolve up to 4% Cr and partly replaces iron by nickel.

The border between AMr6 and A6 has a regular waviness. In waves troughs and crests some intermediate inclusions are found with a microhardness $H_\mu = 330...660$ N/mm^2 of the following chemical composition: magnesium of 2,7...4,2%, manganese of 0,4...0,6% and aluminum as a rest.

At explosion welding the near-border layers are strengthened. The microhardness of layers is: 12X18H10T steel – $H_\mu=2900$ N/mm^2, A6 aluminum – $H_\mu=280...330$ N/mm^2 and AMr6 aluminum – $H_\mu=800...1200$ N/mm^2.

The separation strength is determined by properties of A6 aluminum and consists of 86...110 N/mm^2. The fractography analysis shows that fracture goes along the A6 layer and has a kind of viscous mechanism of serpentine spelling. The forced modes of explosion collision lead to a macro separation of samples observed during emergence of a crack on the border between 12X18H10T steel – intermediate inclusions – A6 aluminum and leap-type development of the crack in a direction of the deformation.

The fracture surface along the layers' separation AMr6-A6 is relatively uniform in its structure and has an appearance of small-cap-breaking. The dimension of indented facets is 10-20 μm and this

is a witness of metal deformative strengthening in the fracture zone.

Bimetal 12X18H10T-M1-H65B2MЦ. There are zones of various etching on borders between bimetallic layers: copper-niobium – 80...120 μm thickness, copper-steel – 40...60 μm. At this the microhardness of layers grows: up to $H_\mu=3500...4250$ N/mm^2 for niobium and up to $H_\mu=2400...3100$ N/mm^2 for steel; in the copper layer the microhardness grows only from the steel side and totals $H_\mu=1200...1400$ N/mm^2.

At the border with copper the niobium is more etchable and has a column-like structure of grains with variable dispersivity. The column-like crystals near copper has a thickness of less than 1 μm and at a distance of 10-12 μm they are considerably branched.

The copper on a border with niobium has no visible structure changes, and on a border with steel its grains are reduced, and a homophased structure is violated. In the copper a separation of excessive phases is observed, which phases are diminishing with a distance from the steel and often they decorate copper grains. However, through all the thickness the layer with changed structure differs from initial copper having pronounced deformative-bladed structure.

The examination of inter-phase distribution of elements has revealed a presence of diffusive zones on both borders of layers separation. The alloying elements of stainless steel penetrate into the copper to the depth of up to 50 μm. The copper's diffusion into niobium totals 10-15 μm.

The strength of layers breaking off is 200...270 N/mm^2. The failure goes through the copper layer at a distance of 0,01...0,05 μm from the border with steel. The failure surface is presented as facets of pit type with traces of serpentine sliding typical for the viscous type of breaking off. An emergence of combined brittle spelling is characterized by pronounced waviness and stream-like pattern that appear in materials subjected to a twinning during deformation.

So, the main criterium of bimetallic joints reliability may be adopted as a morphology of a surface between metal layers, which is formed during explosion action. These data may be determined on the basis of statistical processing of results obtained at metallography and fractography examinations and technological tests of samples. The phase and structure transformations during explosion welding have a considerable influence on a quality of layers integration. Their influence may be reduced or eliminated through correction of explosion load parameters, as well as through application of intermediate metal layers on the border of separation.

Evaporation of the refractory metals in ultrahigh vacuum.

Silantiev V.I.
Institute for magnetism, NAS of Ukraine, Kyiv, Ukraine

Evaporation of Mo, W and Re monocrystals has been studied.

Differential method of Lengmure (evaporation from open surface) permitting to anneal at temperatures up to 3300 K has been used for investigations. Evaporated substance was condensed through diaphragm onto changed Al substrates, which were cooled by liquid nitrogen. The condensate weight was determined by scales with accuracy of $4.4 \cdot 10^{-7}$ g. The temperature was changed by the optical micropyrometer ВИМП-15 with the error $\pm 0,5\%$. Experiments were carried out in ultrahigh vacuum setup with sorption pump, which works out vacuum of $\sim 1 \cdot 10^{-10}$ Pa. Mainly hydrogen, argon and a negligible amount of $N_2^+ + CO^+$ created the pressure in the chamber. At the maximum temperatures the pressure did not rise above 10^{-7} Pa.

The residual atmosphere composition at all stages of experiments was controlled by masspectometer.

Monocrystal samples with the deflection of crystallographic planes not more than 20-30' were investigated. The influence of the preliminary annealing and dissolved gases on the pressure has been studied. Thus, the reproducible data for the (110) plane of molybdenum were achieved only after stepped annealing with the exposure at the T=2700 K during 1 hour. The molybdenum vapour pressure in the temperature interval 2300-2700 K is lgP=9,41- (31900/T), and the sublimation energy is 146 kcal/mol. These values coincide properly with calculated ones and those, obtained by the other investigators.

After the measurements the samples aged at room temperature during 24 hours, then the measurements were carried out again. The vapour pressure was increased several times and described in terms lgP=10,84-(34200/T) and the sublimation energy – 156 kcal/mol. This points out the formation of compounds on the surface.

The preliminary annealing at the temperatures above the temperatures of measurements was carried out for another samples too and the volume and the surface were cleared out of the gas and. The more typical alloying admixture in metals is the carbon, which is not moved out by annealing. It possesses limited dissolution in the refractory metals and its concentration on the surface may reach considerable values up to monolayer. It results with the carbon on the surface acquires positive charge what leads to increase of the bond energy, in ones turn this must cause the blocking of the sublimation process.

On the other hand, increase of the carbon concentration more than the dissolution limit may lead to the formation of carbides and cause the increase of the sublimation velocities.

In detail the influence of carbon was studied in W monocrystals with the (100), (110) and (111) planes oriented parallel and perpendicular the growth axis with the carbon content of $5 \cdot 10^{-3}$, $3 \cdot 10^{-3}$ and $1 \cdot 10^{-3}$ weight % at the temperatures 2800-3350K. One observed the anisotropy of the sublimation properties either for the different planes or for the equivalent planes, but different oriented with the growth axis. Absolute values of the sublimation parameters and the anisotropy depended on the concentration of carbon. The less values of the vapour pressure ($\sim 40\%$) and the increase of the sublimation energy on 25 kcal/mol were observed for the small amounts of carbon.

After the decarburizing annealing of these samples during 20 hours at 2100 K and under the pressure of oxygen $\sim 1 \cdot 10^{-4}$ Pa the mentioned peculiarities disappeared and obtained data coincides perfectly with the calculated curve. The sublimation energy of pure W equaled 175 ± 1 kcal/mol.

We did not succeed in the perfect decarbonization of the plane (111) of tungsten; it obviously results from the peculiarity of its structure and the absorption ability. During evaporation of the decarbonized layer the noted peculiarities appeared again.

The rise in concentration of carbon (10^{-2} weight %) results in increasing the evaporation velocity up to 5 times and increasing of the sublimation energy, which is caused by the formation of carbides on the surface.

It is noteworthy, that the decarbonization is effective for the small amounts of carbon (10^{-3} weight %). The perfect decarbonization of the samples with the high concentration of carbon was not succeeded and their characteristics differ from those for pure tungsten.

Dissolution of carbon in the tungsten can be rise by doping with the small amounts of Re, at

that the evaporation velocity decreases almost by the order, i.e. to the values typical for tungsten with the small amount of C.

In the case of metals with hcp lattice in contrast to the metals with bcc lattice the influence of dopant on the anisotropic character of the properties must become more apparent. The aim is to investigate Re monocrystals with the relative residuary resistance equaled 600 and 8000 ($R_{res.}=R_{298K}/R_{4,2K}$) with carbon content·$10^{-2}$ weight % and ·10^{-3} weight % correspondingly. The planes (0001) and (10 $\overline{1}$0) were studied. For the different planes of Re with $R_{res.}$=600 small difference in sublimation parametres in the range of the high temperatures takes place, while for the more pure Re the value of anisotropy is rather high.

With the increasing of the purity of Re the sublimation energy for (0001) plane decreases and for (10 $\overline{1}$0) plane increases.

As in the case of W the blocking effect of carbon on the evaporation takes place in the case of Re. The more considerable anisotropy of the evaporation velocity for Re in comparison with W is typical, though the sublimation energy for different planes differs slightly.

It is noteworthy that the improvement of purity of Re results also in increasing anisotropy of the other properties of Re monocrystals.

ELECTROCHEMICAL STUDY OF THE PROTECTIVE PROPERTIES OF THE MONOLAYERS AND THIN FILMS ON ALUMINUM AND ON STAINLESS STEEL 316

Groysman A., Starosvetsky D.[1], Sukenic C.[2], Mandler D.[3], Meth S.[2], Shefer M.[3], Savchenko N.

Oil Refineries Ltd., Haifa, Israel
[1]Technion, Haifa, Israel
[2]Bar-Ilan University, Tel-Aviv, Israel
[3]Hebrew University, Jerusalem, Israel

In the present work we have studied the corrosion protection provided by monolayers and thin films. Plates made of stainless steel (SS 316) and aluminum (Al 1100) were used in our experiments as substrates. Stainless steel specimens were coated by organic monolayers of alkylthiols, alkylamines, alkylsilanes and combinations of alkylsilanes and TiO_2.

The monolayers for aluminum specimens were prepared with phenyltrimethoxysilane (PhTMOS) and methyltrimethoxysilane (MeTMOS), which were coated electrochemically, following a procedure that was recently developed.

Electrochemical measurements of the corrosion behavior of SS and aluminum specimens with and without monolayers and thin films were carried out using both conventional electrochemical techniques, such as potentiodynamic and potentiostatic polarization, and electrochemical noise measurements (ENM). The test media used for the stainless steel and for the aluminum specimens were 0.5 N and 100 ppm NaCl solutions, respectively. The temperature of the solutions was 25°C.

Protective characteristics of the films were estimated in accordance with the specimen resistance to pitting corrosion attack, in particular by comparing the characteristic potentials of pitting corrosion (pitting corrosion potential, E_{pit}, and repassivation potentials, E_{rp}) measured on specimens with and without the films.

The results measured by cyclic potentiodynamic polarization were compared with results obtained by using the ENM technique. Good correlation between these two different electrochemical methods was observed for the thin films on SS 316.

It was established that the protective properties of the films strongly depend on their type and method of preparation.

THE STRUCTURE AND THE PROPERTIES OF THE COATINGS FORMED BY PENTAGONAL CRYSTALLITES

Vikarchuk A.A., Volenko A.P., Krylov A.Yu., Yasnikov I.S.
Togliatti State University, Togliatti, Russia

An exotic pattern compounded of multi-fold and five-fold symmetry crystallites, forbidden by crystallography rules, can be obtained during electrodeposition of Ni and Cu. Such structures have been named pseudo-crystallites. The separate consideration of these structures is quite important, as in case of a considerable volumetric fraction in a deposit of such formations as five-fold or multi-fold symmetry crystallites, the coating's properties differs against the usual, for example, the completely different deformation mechanism are observed.

The purpose of our investigation was to determine the origin mechanism of the crystallites with the pentagonal symmetry and to study the structure and mechanical properties of the coatings formed by such crystallites. Here are the main experimental results that have been obtained in our laboratory:

1. The crystallites with the five-fold (pentagonal) symmetry are often encountered in Cu and Ni electrodeposits having <110> texture. In it's turn such texture can be obtained during the deposition with both high and low overvoltage value. In the case of low overvoltage values (for Cu about 10^{-3} V and 0.5 V for Ni) a lot of the five-fold symmetry crystallites are formed and in the case of high overvoltage (10^{-2} and 1 V accordingly) the coating contains twins of the growth origin (Fig.1).

2. At definite deposition conditions in a quite narrow field of current density variation it was possible to obtain coating completely consisting of five-fold symmetry crystallites (Fig.2). The crystallites had the {111} type planes at the solution-deposit boundary and reached the size of 50 µm while the coating thickness was about 80 µm.

3. The crystallites were compounded from a quite perfect five sectors, which were separated with sharp direct boundaries with one being different from the others by the contrast in electron microscope (Fig.1, 2, 4).

4. The etched samples and the cross-sections of the deposits shows that such crystallites, having the cone shape with <110> axis, are formed at later stages of crystal growth (3-4 µm from a

substrate) but not degenerate from initial clusters (Fig.3).

5. The careful electron microscope study revealed that the separating {111} type boundaries were the twin boundaries; four of them were perpendicular to {110} plane (<112>{111}) and the last one inclined (<110>{111}).

6. The diffraction from such crystallite had the five-fold symmetry; the discrepancy of 7,5° was distributed among 2 – 3 sectors' boundaries. The diffraction from a separate sector was as from f.c.c. lattice.

7. During the deposit growth the inner tension in coatings organized from pentagonal crystallites drops down at the thickness of 3-5 µm, acoustic emission intensity rises.

8. Twin lays parallel to sector boundaries and single dislocations have been observed some times in the large crystallites. In adjacent sectors the dislocations were with the same but the contrary Burger's vectors (Fig.1).

9. As the deposit thickness and accordingly the crystallite size grow up, the boundaries' crossing point splits in two, forming the non-twin boundary between them. The splitting are followed by dislocation emission along one of the boundaries (<110>{111}) (Fig.4).

These experimental results can't be explained by current theories and we put forward disclination model of pentagonal crystallites origin. In accordance to the model there is a partial disclination with module of Frank vector equal to 7° in the center of the crystallite and the five twin boundaries abrupt on the disclination axis. One of the boundaries being inclined to substrate plane {110} has a growth origin, and twinning dislocation movement has formed the others, which are perpendicular. This new model of the crystallite origin is capable to explain all available experimental results: cone shape of the five-fold crystallites, their quite big sizes and fast growth as compared to the other crystallites, their perfection at small sizes and defective structure at the big ones, texture and internal tension in the deposits, and at least the mechanism of twins origin in electrodeposited metals. It also explains the uniformity of all five sectors separated by twin

boundaries, which are crossed in the central point, and splitting of this point in two as crystallite grows up.

Figure 1

Figure 2

Figure 3

Figure 4

422

LIFE TIME MODELING OF MCrAlY COATINGS FOR INDUSTRIAL GAS TURBINE BLADES (experimental and calculation approach)

Krukovsky P., Tadlya K., Krukovsky S., Tadlya O., Rybnikov A.[1], Krukov I.[1], Mogaiskaya N.[1], Kolarik V.[2], Juez-Lorenzo M.[2]

Institute of EngeneeringThermophysics, Kiev, Ukraine
[1]Polsunov Central Boiler and Turbine Institute, St. Petersburg, Russia
[2]Fraunhofer-Institute fuer Chemische Technologie, Pfinztal, Germany

The life time of the blades in advanced stationary gas turbines for electric power generation is basicly controlled by the oxidation resistance of the coating and by interdiffusion processes at the coating / substrate interface. A typical transversal concentration profile of an oxide – forming element in the surface – near region of the alloy is shown schematically in Fig.1. (thickness of the coating is more then x_3
moving boundary)
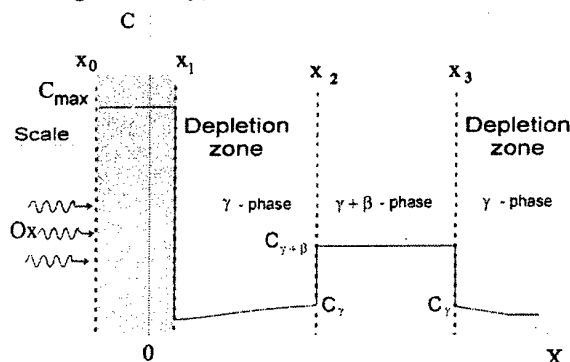
Fig. 1. Concentration profile of the alloying element Me (curve 1) and the oxidant Ox (curve 2)

In the case of the MCrAlY coatings the protection against oxidation is achieved by the formation of a thin Al_2O_3 layer on the coating surface (x_1-x_0). The Al, which generally is found as a β-NiAl phase in the coating, is consumed by both Al_2O_3 formation at the surface and by interdiffusion at the substrate – coating interface, producing aluminum depletion zones that increase with time and temperature.

A physical and mathematical model considering the Al concentration profile across the coating was applied according to [1]. In fig.1 $C_{\gamma+\beta}$ - average aluminum concentration in two-phase γ+β - region, C_γ - interfacial concentration of aluminum at the γ / γ+β interfaces. The physical model takes into account that during the oxidation the oxide surface x_0 moves outwards, while the boundaries x_1 move inwards the alloy, x_2 and x_3 move towards each other. Time, when the β-NiAl

phase is completely consumed (x_2 reaches x_3), may be assumed as a coating life time end.

The modern models for modeling the oxidation and diffusion processes in MCrAlY coatings (Fick's first and second law) like mentioned above usually can't use for lifetime prediction due to unknown models parameters for complicated MCrAlY coatings compositions. The physical and mathematical model under consideration comprises three key parameters, which must be estimated for the prediction of the oxidation and diffusion processes: the effective diffusion coefficient of aluminum D_{Al}, C_γ – interfacial concentration of aluminum at the γ / γ+β interfaces and k – oxidation rate constant.

The main innovative aspect of the approach described in the present work is the application of the Inverse Problem Solution technique (IPS) to determine the quantitative values of the model parameters [2]. This technique was considered in [3] for single-phase coating model.
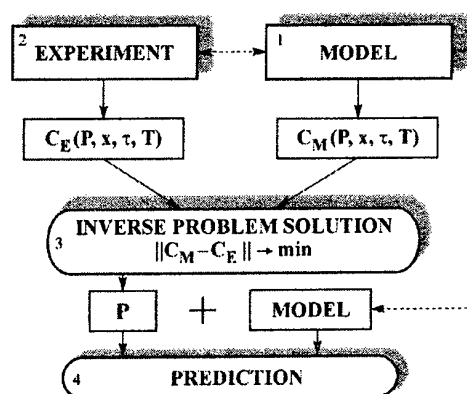
Fig. 2 Scheme of computational and experimental approach for oxidation and diffusion processes prediction using the IPS method

In the case of the lifetime modeling of MCrAlY coatings the concentration profile of Al across the coating thickness measured after a defined time τ_e of exposure to temperature is needed as input values only. All model parameters needed for the modeling like the D_{Al} coefficients are then

determined by the IPS technique and used for the forecast calculation. Thus the IPS technique allows an economic quantitative life time modeling, which is easily feasible in practice, and enables long term prediction using experimental data from some hundreds hours of exposure time, supposed that no change in the relevant mechanisms occurs.
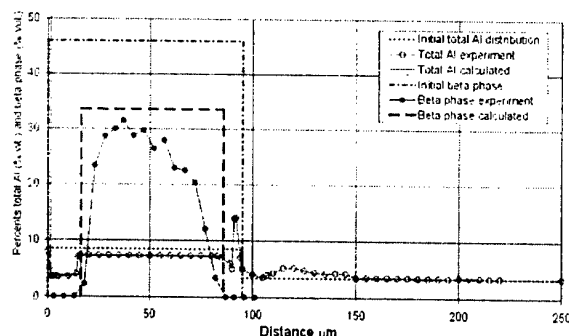
Fig. 3 Measured and calculated total Al concentration profile and beta phase across the coating and base metal after 1000 h at 950 C.

The approach (Fig.2) consists of four fundamental steps.
1. Design of a mathematical model or the use of an existing one.
2. Experiments with given experimentation time and temperature delivering input data for the model parameter estimation.
3. Estimation of the key parameters of the mathematical model for different temperatures (calibration of mathematical model).
4. Computational prediction of the alloying element distributions and coating life time end.
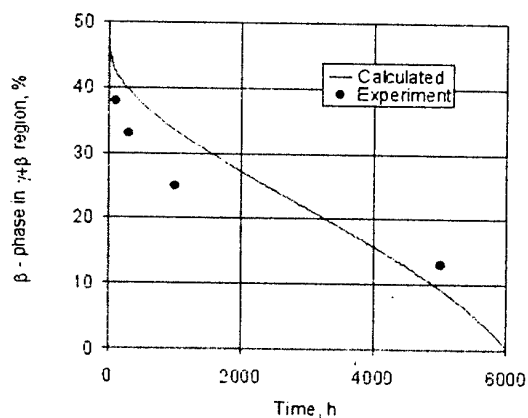
Fig. 4 The predicted and measured beta phase concentration during oxidation at 950 C and coating thickness 100 micron

Exposure experiments (Fig.3) were carried out in air at 900, 950 and 1000°C with an NiCoCrAlY coating with 8 % Al. The concentration profiles of

the elements Al across the coating thickness were determined by electron microprobe in the initial state and after 100, 300 and 1000 hours of oxidation. Fig.3 shows calculated concentration profiles after IPS technique implementation for coating thickness 95 micron.

Fig.4 gives predicted and measured beta phase concentration during oxidation. Time 6000 h means coating life time end. The model and ISP technique allow the beta phase life prediction for various coating thickness during oxidation (see Fig. 5).
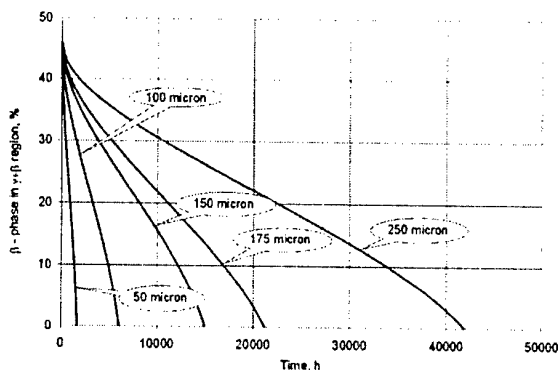
Fig. 5 The predicted beta phase life for various coating thicknesses during oxidation at 950 C

Conclusions:
1. The approach by Inverse Problem Solution showed to be a technically easily feasible way to obtain input values for the model parameter estimation.
2. The model calibrated by Inverse Problem Solution Technique and short time experiment data can be used for long time modeling and prediction of oxidation and diffusion processes in MCrAlY coatings.

References
1. E.Y.Lee, D. M. Chartier, R. R. Biederman and R. D. Sisson, Jr Modelling the microstructural evolution of M-Cr-Al-Y coatings during high temperature oxidation. Surface and coatings technology, 32 (1987) 19-39
2. P.G. Krukovsky, E.S. Kartavova, Inverse Problems in Engineering. Theory and Practice, ASME (1999) 403-408P.Krukovsky, V. Kolarik, K. Tadlya, A. Rybnikov, I. Kryukov, M. Juez-Lorenzo Lifetime Modelling of High Temperature Corrosion Processes. Proceedings of an EFC Workshop 2001 p 231-

STRUCTURE AND PROPERTIES OF POWDER COATINGS, SPRAYED BY HVOF GUNS OF NEW (TWO CHAMBERS) CONCEPT

Yevdokimenko Yu.I., **Kadyrov V.Kh., Kysil V.M., Korol' A.A., Podchernyaeva I.A.,**
Panasyuk A.D.
Institute for Problems of Materials Science of NAS of Ukraine, Kyiv, Ukraine

The technology of HVOF flame spraying is one of the main methods of the gas – thermal spraying, which combine high quality of produced coatings and high efficiency as well as simplicity of the used equipment. One of the drawbacks of this technology is complication, and in many cases impossibility of making refractory coatings from hard ceramic compounds. Thermodynamic analysis shows that the energy possibilities of HVOF allows to melt particles of refractory materials at the melting temperature up to 2500K (particularly – oxide powders) without increasing of the equipment's achieved heat rating. But known gas-dynamic layouts of burner devices for HVOF don't allow their full scale use.

In order to optimize of sprayed material particles heating and accelerating process in the HVOF burner channel on the base of maximum value of specific enthalpy criterion, the new conception of inner chamber process organization in the HVOF device burners was suggested [1,2].

This approach consists of functional division of the heating and accelerating sections of the particles for the expense of combination of consumptional and geometrical influence on the flow. New concept of gas dynamic burner channel with functional separation of dispersed powder heating and accelerating zones is aimed for:
- Disperse phase heating in transporting gas flow with high temperature and low velocity;
- Following accelerating of disperse phase in around sonic and supersonic flow;
- Accelerating of gas flow up to sonic velocity by means of consumption influence, which is reached by injection of certain portion of gas between heating and accelerating zones;
- Absence of convergent zones along the channel length.

On the basis of this concept the gas – dynamic channel, mathematical and software means of its calculation, construction of the burner based on the novel principles was worked out. The burner devices and installation for its testing were created. The maximum of particles enthalpy is achieved due to increasing of the time of their sojourn on the heating section in the base gas flow with high temperature and low speed. In the second section the accelerating of the heated particles is mainly carried out in near – and supersonic flow.

The discharging of the heating stage is made by serial introducing of the high temperature gas in the flow stream in two spaced on along the flow assemblies feed on the section of between which the optimal for heating particles by parameters of the flow. That is by variation of values of initial consumption coefficient it is possible to obtain optimal combination for the given geometry of the channel the temperatures and velocities of of two phase stream in the heating zone and to obtain maximal exit particles melt degree. Conditionally such burner can be called "two- chamber" one.

As a result of the experimental research of experimental burner installations the optimal technology spray parameters of different powder materials were developed. It was determined that the optimal, in terms of refractory materials coating quality, are the parameters with maximal possible for the given installation heat capacity. That can be reached at the parameters of maximal possible pressure in the combustion chamber for the stoihiometry ratio of fuel components.

The efficiency of use two – chamber burner was tested while overcoat by 4 types of coatings:
1. Al_2O_3 + 50% NiCr
2. (Al_2O_3 + SiC) + 50% NiCr
3. Al_2O_3 + 24% ZrO_2
4. stainless steel X18H9

The distinctions of their structure formation and capacities were studied.

For comparison, the coating from Al_2O_3 obtained by the HVOF method using traditional burner with supersonic distillating channel was studied.

In order to determine phase content, morphology of phase components, common porosity, shapes, and sizes of pores, the methods of microstructure analysis were used, the measurement of micro hardness as well as roentgen phase and micro X-ray analysis were carried out.

The quantitative and qualitative analyses of microstructure were carried out while using light microscope PMT – 3, special program of materials complex "SIAMS" which is equipped with computer device which allows to receive general enlargement more of 3000 (including optical till 1000).

The "SIAMS" system also allows to evolve each individual phase and make its quantitative analyses using computer graphics. The roentgen phase analysis on the diffractometer DRON – 3M, raster scan electronic Superprob GEOL 733 and micro X-ray analyzer were used for identification of the phase content.

Tribological parameters (friction coefficient f and wear rate I, mm/km) were studied by scheme shaft bush in the dry friction mode.

Data of metalography, durometery and phase analysis, and the results of tribological tests of studied coatings allow to make a conclusion that use of new construction of the burner for HVOF – coatings of the different grades has a prospect. The high-density coatings, which are adjoined to the surface of the undercoat, and, having fine structure, are produced from composite ceramic powders. Such coatings provides the high operation capacities.

Typical structure fragments of Al_2O_3-ZrO_2 coating are given on Fig.1

Thus, application of new burner design allows to obtain homogenous porousless coatings of perspective composite ceramic based on Al_2O_3-ZrO_2.

The comparable test of the Al_2O_3 coating which is received by HVOF – method with a help of the traditional burner, shows that it has big quantity of linear and cross-cut cracks, which significantly decrease durability and lead to the delamination of the material.
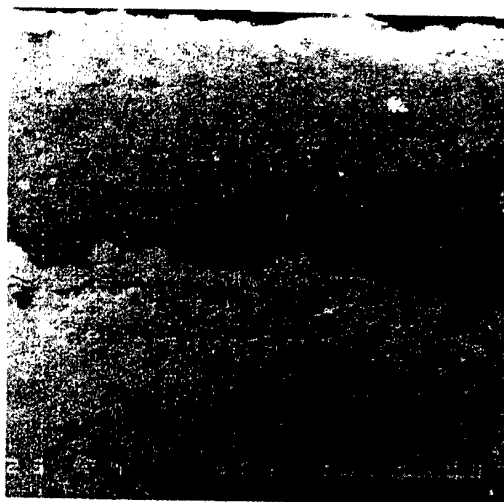
Fig.1. Al_2O_3-ZrO_2 coating cross section microstructure (electron microscopy), x230

1. Timoshenko V.I., Belotserkovets I.S., Galinsky V.P., Kisel V.M., Evdokimenko Yu.I., Kadyrov V.Kh. Investigation operations in burner devices for a high-speed gas-flame powder material spraying with using flow effect // Engineering physical journal. - 2001.- V.74, N 6.

2. Timoshenko V.I., Belotserkovets I.S., Galinsky V.P., Kisel V.M., Evdokimenko Yu.I., Kadyrov V.Kh. Investigation operations of acceleration, heating and melting the particles from refractory materials in burner devices for a gas-flame spraying // Engineering physical journal. - 2002. - V.75, N 2.

INVESTIGATION OF RADIATION DAMAGE IN IRON WITH BERYLLIUM COATINGS AFTER ALPHA-PARTICLES IMPLANTATION

Kadyrzhanov K.K., Kerimov E. A., Kislitsin S.B., Turkebaev T.E.
Institute of Nuclear Physics of National Nuclear Center, Almaty, Kazakhstan

The technique for creating of stable beryllium coatings on iron and research results of coatings stability under irradiation by alpha particles is presented.

Production of stable beryllium coatings on iron foils

According to thermodynamic approach, developed by authors of present publication [1,2] the stable at high temperatures layer enriched with beryllium on iron can be created when volume of the material will represent a saturated solid solution of beryllium in alpha iron. In this case diffusion penetration of deposited on the surface beryllium inside of material volume became negligible and stable structure with the high contents of beryllium, for example phase $FeBe_2$, in near to surface area is formed. As follow from equilibrium phase diagram iron – beryllium the concentration of beryllium in saturated solid solution in alpha iron at temperature 750^0 C makes 10 - 12%. One of possible way for creation of stable coating consist in deposition on thin alpha-iron film of beryllium layers with both sides of sample and annealing it at temperature 750^0C. Thickness of beryllium layers and duration of annealing period should be such, that during this period saturated solid solution beryllium – iron can generated in a matrix, and the excess of the beryllium on surface has generated the beryllium enriched $FeBe_2$ phase. The technique of stable beryllium coatings production was follow. The specimens have been made of the α-Fe foils (enriched by ^{57}Fe isotope up to 89 at. %), rolled to the thickness $\sim$ 10 μm and subject to homogenization annealing in vacuum at 800^0 C for 2 hours. The deposition of Be onto the iron foil have been carried out by magnetron sputtering. The thickness of deposited beryllium layer on the one side of specimen is 1.3 μm (side A). Thickness of beryllium layer on the another side of specimen is 0.9 μm (side B). Isothermal annealing series in vacuum has been carried out at temperature 720^0 C during 0.5, 1, 2, 5, 10, 15, 20, 50 and 100 hours. After each period of annealing the structure of specimen was determined by the technique of conversion electrons Mossbauer spectroscopy (CEMS) in back scattering

geometry, γ-ray technique in absorption geometry and X-ray difractometry. Control of deposited Be layer depth as well as determination of the iron concentration profile over the depth have been implemented by the Rutherford back scattering method (RBS) at the electrostatic accelerator UKP-2-1 (Kazakhstan Institute of Nuclear Physics). In result of set of annealing in described above system Be-Fe-Be stable phase distribution along the depth of specimen was formed. Phase $FeBe_2$ with beryllium concentration $\sim$ 66% is form near to both sides (A and B) of specimen. The $FeBe_2$ phase thickens along the depth of specimen is $\sim$ 0.7μm. Solid solution of beryllium in alpha iron with beryllium content $\sim$ 10% is form inside of specimen. The period for stable phase with different Be content formation is $\sim$ 10 hours. Further annealing up to 100 hours at temperature 720^0 C does not result in change of a structural - phase distribution in specimen.

Investigations of stability Be-Fe-Be system under alpha-particle irradiation

One side (side A) of sample with stable beryllium coating was subjected to irradiation by alpha particles on accelerator "Wezuvii" (Kazakhstan Institute of Nuclear Physics) for research of radiation resistance: stability of the phase structure, formation gas bubbles etc. Irradiation conditions were the following:

• Energy of irradiating particles - 330 keV,
• Total doze - $3·10^{16}$ particles /cm^2,
• Temperature of irradiation - 100^0 C.

Main purpose of the present researches was to determine the possible dissolution enriched with beryllium of $FeBe_2$ phase due to irradiation. Therefore energy an alpha of particles was selected so that longitudinal straggling of particles was 1.09 microns i.e. maximum of radiation damage was concentrated in near to surface region enriched by beryllium. Calculations of projected range of alpha particles with energy 330 keV in Fe(34%) + Be(64%) target by computer code "TRIM" give follow results: projected range = 1.09 um, longitudinal straggling = 1191 A [3]. So alpha particles with energy 330 keV satisfy to these requirements.

It is necessary to mark that the total doze of irradiation in circumscribed experiment is insufficient for formation of the gas porosity in the sample. This problem will be the subject of further researches. Now we concern only structure changes induced by alpha particle irradiation.
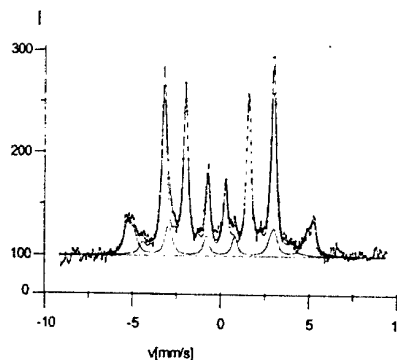
a) SEM spectra (side A) before irradiation
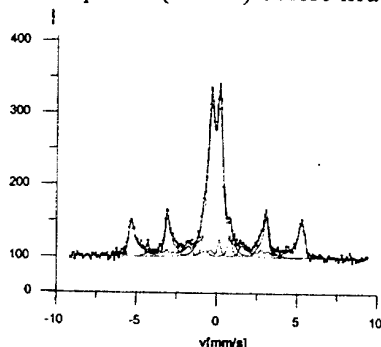
b) SEM spectra (side A) after irradiation
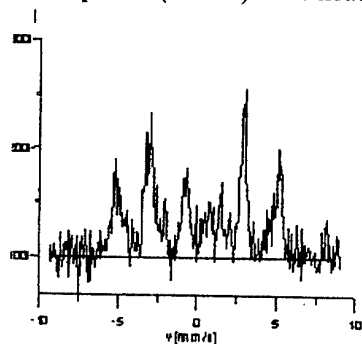
c) SEM spectra (side A) of irradiated sample after 5 hours annealing

Fig. 1. SEM spectra's of non irradiated (a), irradiated (b), irradiated - annealed specimen (c).

The structure of irradiated and after irradiated annealed specimen was studied by CEMS, X-ray, RBS, optical microscopy (OM) and scanning electron microscopy (SEM) technique.

OM and SEM investigations of the structure of irradiated surface shows that the irradiation up to such dozes does not call noticeable changes of surface texture. CEMS and X-ray investigation shows that takes place disturbance of the short-range order degree in the $FeBe_2$ phase, look, for example, fig. 1.

On fig. 6 SEM spectra's of non-irradiated (a), irradiated (b), irradiated and annealed specimen is presented. From comparison of spectra on fig 1a and 1b it is visible, that the disturbance of the short-range order degree or partial amorphization of $FeBe_2$ phase structure was observed. Consequent annealing at temperature 700^0 C (fig. 1c) results in recovery of phase structure. The X-ray diffractometry investigations confirm results of SEMS study. RBS measurements of depth distribution of Be and Fe near to irradiated surface shows: there are no visible changes of beryllium and iron content in that region. Therefore, it is possible to draw conclusion that the irradiation at small dozes does not result in essential disturbance of phase $FeBe_2$ structure and it is not observed induced by irradiation migration of beryllium into matrix of sample.

Conclusion

1. The beryllium coating on thin iron foil stable in temperature interval up to 750^0 C are obtained by means of magnetron sputtering method.

2. It is shown that the irradiation by alpha particles at room temperatures up to dozes $3\cdot10^{16}$ particles /cm^2 does not result in destruction of beryllium coating.

References

[1] Kadyrzhanov K.K., Turkebaev T.E., Udovsky A.L., NIM **B 103**, 38 (1995).

[2] Kadyrzhanov K.K., Kerimov E.A., Rusakov V.S., Turkebaev T.E., Udovsky A.L.. Proceeding of I. Eurasia Conference on Nuclear Science and its Application. 23-27 October 2000, Izmir, Turkey. Vol.2. p 760.

[3] Ziegler J.F., Biersack J.P., The stopping and range of ions in solids, Pergamon Press, New York, 1985.

FORMATION OF PROTECTIVE SELF-RECOVERING OXIDE LAYERS ON THE STAINLESS STEELS SURFACE DURING THE CONTACT TO HEAVY METALS COOLANTS

Yeliseyeva Olga, Fedirko Viktor, Tsisar Valentyn
Karpenko Physico-Mechanical Institute of NASU, Lviv, Ukraine

Accelerator Driven System (ADS) is the most prominent concept of hybrid reactors with respect to the transmutation potential and safety aspects. ADS consists of three main parts: an accelerator (for protons generating), target module (in which the protons produce free neutrons) and subcritical blanket (in which the fission reaction occurs).

Lead and lead-bismuth eutectic due to its excellent thermo-physical and nuclear properties are considered as candidates for target unit and coolant. Austenitic and 9-12 Cr martensitic steels are candidate structural materials for ADS design. The compatibility of heavy-liquid metals and structural materials is one of the key problems on the way of technological realization of the ADS concept.

The basis of protection of structural materials under the contact with aggressive heavy liquid metal mediums lays in the formation on the steel surface the protective oxide layers using the oxygen as a special admixture. Formation of oxide layer inhibits the dissolution of the steel components provided that the properties of the oxide layer are satisfactory. In general the oxide layer to be protective must possess by the optimal parameters (adherent, compact, coherent etc.) and ability to self-healing during long period of work. The quality of the coating depends on the level of oxygen activity in the heat medium, composition and structure of the solid material and character of the surface treatment.

At present time the transition oxygen concentration region from dissolution to oxidation is well known. In spite of the numerous experimental data the model representation of components interaction in such complex systems is not developed well.

In presented paper the results of investigations of interaction between ferritic-martensitic steels (EP823, T91 and Armco-iron-as a modeling material) and oxygen-contained liquid melts (Pb and PbBi) in the temperatures range 500-650°C. On the basis of obtained results the mechanisms of interactions as function of temperature and oxygen activity in the melts are determined. The special attention is emphasized on the process of protective oxide layer formation, which is able to self-recovering during long period of exploitation. The possible mechanism of transaction from passivation to intensive oxygen corrosion is presented.

FEATURES OF ACOUSTIC CONTROL OF STRUCTURE AND PHYSICAL AND MECHANICAL PROPERTIES OF HIGH-POROUS MATERIALS

Bezimyanniy Y.G.
Frantsevich Institute for Problems of Material Science of NAS of Ukraine, Kiev, Ukraine

Being designed for functional applications, high-porous (with porosity level to 95%) metal composites are promising materials to use in special equipment that works under extreme conditions. The composites are based on foam metals, knitted semifinished products, sintered discrete fibers and cellular structures and used as dempers, permeable materials, elements providing construction rigidity for heat-shielding systems etc. [1]. Operating properties of those materials are determined by their structures. Imperfection in technological operations does not provide the guarantee of high uniformity for material structural components, the absence of defects and, as a result, stable physical and mechanical characteristics. Therefore, controlling the structural state of the material and its physical and mechanical characteristics plays important role both in development of technology for material production and in the course of its production and operation. Nondestructive acoustic methods are traditionally applied for such control [2]. However, their application to high-porous materials shows substantial specific features that, first of all, related to the complex behavior of acoustic fields in such materials [3]. This problem is weakly reflected in the literature both in theoretical and practical aspects and therefore it is of great interest.

Fig.1. Specimen of foam nichrome having porosity of 95%.

Analysis of above high-porous materials structures has been performed. As an example, the structure of foam nichrome is given in Fig.1. On the base of the analysis performed mechanical models have been proposed. The models allow the determination of relation between elastic wave parameters, on the one hand, and the material physical and mechanical properties and structural parameters, on the other hand.
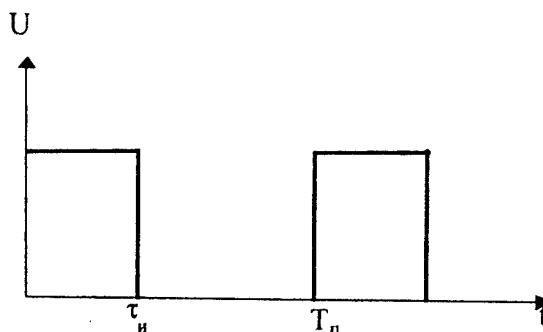
Fig.2. Oscillogram of the signal emitted into the specimen

Experimental research into mechanisms of acoustic fields formation for the running wave within those materials has been conducted. The mechanisms have been studied as a function of parameters of the signal emitted into the specimen (Fig.2 and 3) and degree of deformation in the material structural elements. The unique apparatus complex that measures acoustic characteristics of materials and original methods have been applied to provide experimental research. The elactic wave passed through the specimen of the material studied has been analyzed by time (Fig.4), energy and frequency (Fig.5) features. Elastic wave parameters proposed allow us to control the structural state and determine characteristics of elasticity and inelasticity of high-porous materials. Results of theoretical and experimental research have been compared.

The work done shows that behavior of acoustic fields in the high-porous materials is determined by wave sizes of the material structural components. For instance, when wave sizes of

mesostructural elements are small, the material behaves like uniform. In this case we can judge of material elasticity by the elastic wave velocity and of material inelasticity - by energy losses. Both of those characteristics are sensitive to the degree of material destruction. Changes of the front drop for the elastic wave impulse that occur during wave propagation within the material have been proposed to use as a measure for energy loss. Resonance effects of mesostructural elements are observed when wave sizes of the elements are close to 1. In this case resonance frequencies allow us to evaluate those elements sizes and control the degree of material destruction. Therefore, choosing parameters of the signal emitted into the specimen, we can control either effective macroscopic characteristics of the material or research the state of its structural elements at mesolevel.
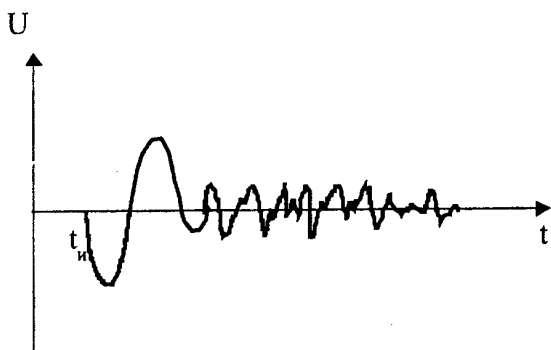
S

Fig.5. Spectrogram of the signal passed through the specimen of foam nichrome

References

[1] Современное материаловедение XXI век. Отв. Ред. И.К.Походня. Киев, Наук. думка, 1998.

[2] Й. Крауткремер, Г.Крауткремер: Ультразвуковой контроль материалов, Москва, Металлургия, 1991.

[3] Безымянняй Ю.Г.: Возможности акустических методов при контроле структуры и физико-механических свойств пористых материалов. Порошк. металлургия, 5-6, 2001, 23-33.

S

Fig.3. Spectrogram of the signal emitted into the specimen

U

Fig.4. Oscillogram of the signal passed through the specimen of foam nichrome

APPLICATION OF THE INVERSE PROBLEMS SOLUTION FOR RESEARCH OF MATERIALS THERMAL CONDUCTIVITY

Isayev K.B.
Frantsevich Institute for Problems of Materials Sciences of NASU, Kyiv, Ukraine

The thermal conductivity (TC) is the fundamental characteristic of substances and materials. Without its knowledge cannot be created new materials, to project various products, to simulate their thermal condition etc. Nowadays there are a great many methods for determination TC of materials, however, only some of them are realized in practice. There are, for example, stationary methods, method of monotone heating, methods of pulse heating and some other. There is a large quantity of the publications devoted these methods. For last some tens years they have allowed to determine thermal conductivity of a great many substances and materials. It is necessary to mark, that majority of these methods is labor-consuming, the equipment is made in single version, they have not a universality.

Any of traditional method does not allow to determine materials TC in wide ranges of heating rate and values of thermal conductivity, to spend researches materials TC, which at heating undergo to various physical-chemical transformations accompanying with allocation gas products (for example, metal hydrides, heat-shield materials with organic resins). The installations on the basis of stationary and pulse laser methods for determination of TC have the high price (especially laser method).

From all of these lacks the methods for determination of thermal physical properties based on solving of inverse problems of heat conduction (IPHC) are free. Plenty of these methods is developed now. However, only some of them were used for research of thermal physical properties of various materials. As a rule, authors of these methods are limited with demonstration of opportunities of the methods on model temperature fields.

In activity the research engineering of thermal conductivity (RETC) of different materials is offered. It consists of experimental determination of one-dimensional temperature fields in heat receiver (sample of researched material with thermal sensors) and use of these fields for the solution of inverse problems of heat conduction.

RETC consists of several stages. The first stage consists of heat receiver manufacturing out of researched material. Further, there is a stage of its test in conditions of one-sided heating. Outcome of these tests is the experimental temperature fields in samples of researched materials. This information is necessary for solving of inverse problem with using of additional information about a researched material and heat receiver. As a result of the solving IPHC is received thermal conductivity temperature dependence in frameworks of the originally chosen mathematical model of heat and mass transfer in the material.

The experimental information (temperature fields in samples of researched materials), additional information (data about specific heat and density of a material, distance of thermocouples from heating surface of heat receiver etc.) and also the results of the solving IPHC come in a database. All this information is used for the analysis of different factors influence on thermal physical properties of a material, and also for correction of mathematical model of heat and mass transfer in a researched material in case of need.

Investigation of materials with low (0.6 $Wm^{-1}K^{-1}$) and high (160 $Wm^{-1}K^{-1}$) thermal conductivity by the application of offered engineering for research an influence of different factors on temperature dependence of materials thermal conductivity is considered.

As a first asbestos cloth phenol composite (ACPC) was chosen. The material contains in the structure phenol-formaldehyde resin (48 %) and asbestos cloth. The analysis of influence both of kind and heating rate on effective thermal conductivity of this material was carried out. It was supposed, that specific volumetric heat (product of density on specific heat) of material is constant in all of investigated range of temperatures. In mathematical model of heat and mass transfer the presence of various physical-chemical processes (which take place at heating of ACPC) was not taken into account. The samples of this material were tested at convective and radiation one-sided heating. The temperature fields in samples ACPC are adduced.

As materials with high thermal conductivity the composites on a basis of aluminum-silicon alloy AL25 were investigated. The alloy AL25 consists

basically of aluminum and silicon (11-13%) and also small amount of the additives of metals (~4.5%), such as Cu, Mg and Ni. The research of influence of three powder additives: aluminum dioxide (22%), silicon carbide (18%) and mullite-silica (19%), on thermal physical properties of composites on the basis of alloy AL25 was carried out. The markings of compositions with these powders have the following kind: AL25+22, AL25+18, AL25+19. Samples of the composites were made by liquid punching with the further turning processing after crystallization and cooling. The temperature dependence of specific heat of these composites was taken into account on the solving of IPHC. This characteristic was determined on standard installation IT-c-400, in which the method of monotonous heating is realized.

The melt of lead (overheated up to temperature approximately 400°C) was used as a heat source for creating of temperature fields in samples of these composites. As an example the experimental temperature field in a sample of an alloy AL25 is adduced. This field is typical for all investigated composites on the basis of this alloy, which were tested in these conditions of one-sided heating.

For experimental determination of one-dimensional temperature fields in samples ACPC and composites of AL25 the designs of heat receivers developed in [1] were used. Two ways of thermocouples closing were tested on samples of the alloy AL25. The thermocouples were fixed in a cuts and apertures. For filling of cuts and apertures the copper powder was used. As a result of solving IPHC it is not influence of a way for thermocouples closing on thermal conductivity of this alloy.

The experimental temperature fields in samples of researched materials are the base information for determination TC of these materials by solving IPHC. For determination of temperature dependence of thermal conductivity of materials two methods for solving of inverse problems of heat conduction [2,3] were used.

Using the research engineering of thermal conductivity for investigation above presented materials allowed hold the next results.

Asbestos material. The thermal conductivity ACPC (it is a typical representative of heat-shielding materials with organic resin) in range of temperatures resin destruction has a minimum, which with increasing of heating rate displaces in area of high temperatures. The value of this

minimum is decreasing at the same time. Examination of the results of determination of temperature dependences TC of this material (they are obtained by results of experiments at different kinds of one-sided heating) has shown, that the minimum TC displaces in area of high temperatures approximately up to 100K/s.

It speaks that the thermal destruction displacement of phenol-formaldehyde resin in high temperature area takes place only up to this heating rate in the investigated range.

Composites on the basis of AL25. For this composites the injection in alloy AL25 the additives of silicon carbide, aluminum dioxide and mullitesilica is resulted to reduction of its thermal conductivity. This reduction becomes greater with increasing of temperature. It is generated first of all with that circumstance, that thermal conductivity of the additives in some times below this characteristic AL25 [4,5].

It is necessary also note, that for silicon carbide and aluminum dioxide sharp reduction of values of their thermal conductivity has a place with growth of temperature. So, according to data [4,5] temperature increase from 100°C up to 400°C leads to reduction of thermal conductivity values of these materials in 3-4 times. For a composite with mullitesilica such sharp reduction of thermal conductivity is absent.

References

1. Isayev K.B. Designs of heat receiver for determination of one-dimensional temperature fields in compact and powder materials. *IV Minsk Int. Forum: Heat/Masstransfer-2000*, **3**, 394 (2000) (in Russ.).
2. Isayev K.B. Heat-transfer in the destroying under one-sided heating composite materials. *Eng. Phys. J.*, **65**, No 6, 645 (1993) (in Russ.).
3. Krukovsky P.G. Universal approach to solution of inverse heat-transfer problems (method and software). *30th National Heat Transfer Conf., N. Y. (1995), ASME (UEC)*, **10**, 107 (1995).
4. Kingery W.D. Thermal conductivity: VI, Determination of conductivity of Al_2O_3 by spherical envelope and cylinder methods. *J. Amer. Ceram. Soc.*, **37**, No 2 (part II), 88 (1954).
5. Vasilos T. and Kingery W.D. Thermal conductivity: XI. Conductivity of some refractory carbides and nitrides. *J. Amer. Ceram. Soc.*, **37**, No 9, 409 (1954).

NOVEL PV MATERIAL BASED InN COATING: FABRICATION, STRUCTURAL AND OPTICAL PROPERTIES

Goryachev Yu. M., Malakhov V.Ya.

I. Frantsevich Institute for Problems of Materials Science, NAS, Kiev, Ukraine

The fabrication details, plus basic structural and optical properties of low temperature plasma enhanced reactionary sputtered (LTPERS) InN coatings are presented. RHEED and AFM studies of surface morphology of InN films were done. Optical absorption and reflectance spectra of InN textured films were taken to reproduce accurately dielectric function as well as to determine optical effective mass of electrons and the direct band gap energy (2.03 eV). Some TO (485 cm^{-1}) and LO (585 cm^{-1}) phonon features of indium nitride polycrystalline films in the NIR and Raman spectra are observed and discussed. The attractive possibilities of InN layers as top coatings of InN/Si tandem heterojunctions for potential application in PV devices including high efficiency space solar cells are discussed.

Over the last ten years, indium nitride has become the focus of growing interest as III-V semiconductor with direct band gap about 2.0 eV and therefore possessing of potential application in photonic devices such as LEDs, lasers, full color displays, especially high efficiency solar cells [1]. The physical properties of InN thin films obtained by different methods have been studied in numerous works [2-8] including ones of the author. However optical and electric parameters, such as dielectric and optical constants, energy gap, effective mass of carriers as well as phonon wavenumbers await for further more accurate definition. A lack of single crystal samples explains the situation regarding the above data. No structural or thermal properies of InN have been studied for epitaxial films on lattice-matched substrates. For this reason, this paper presents original structural and optical data for InN polycrystalline films synthesized previously and recently by LTPERS [6-8]. It also offers to use the potentional possibilities of InN/Si heterojunctions in PV devices, including high efficiency and radiation stable solar cell arrays for space destination.

Inasmuch as a dissociation temperature of InN films is about 650°C [2], therefore the low temperature growth technique is required. In our case, LTPERS equipment to synthesize InN thin films was used. Intensive Ti-wire evaporation, applied as getter, was carried out during all time of deposition process to reduce oxygen contamination inside of the reactor and in the growing films as well. High quality smooth surfaced Si, quartz, fluorite and compound ceramics were used as substrates. During film growth, the substrate temperature was about 350°C, due to intensive ion bombardment of the top electrode (anode) during sputtering process. Film thickness varied in the range 100-2000 nm. To determine the chemical composition of the sputtered InN films Auger spectrometer (JAMP-10) was used. The surface morphology and the microstructure of a cross-section of the films were investigated using Philips SEM5V scanning electron microscope plus standard atomic force microscope (AFM) equipment. The crystalline structure parameters of the sputtered films were determined using an X-ray diffractometer (DRON-3) employing Cu(kα) radiation, and also by means of the electronograph EG-100a. Reflectance and transmittance measurements in visible and NIR regions (25000-200 cm^{-1}) were carried out using a Bruker IFS-66 Fourier transform spectrometer (FTIR) and Carl Zeiss M40 grating spectrometer, respectively. A Raman spectrometer Dilor XY equipped with microscope, was used to study the phonon spectra of the nitride films.

X-ray diffraction patterns of α-InN (wurtzite) layers deposited on ceramic substrates demonstrate a very strong diffraction peak corresponding to the InN (002) plane. This suggests a textured crystalline structure of deposited layers, where the **c** axis is perpendicular to the plane of substrate. The same result was obtained from study of the RHEED pattern of InN film on ceramics (Fig. 1). These results plus an Auger-investigation, show that no outsider phases except InN one were presented in the films. Some off-stoichiometric In/N ratio, with an abundance of In inside nitride films was caused by nitrogen vacancies. A perceptible oxygen concentration was revealed in the films, probably leading to amorphous indium oxide partialy forming (bound oxygen). Moreover, other unactive oxygen molecules are incorporated in voids between the InN graines.
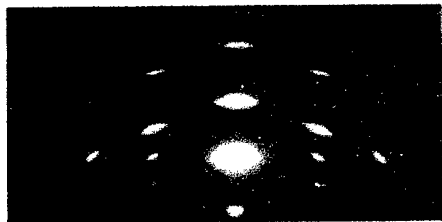
Figure 1. RHEED pattern of InN layer on SiO_2

Further transmittance and reflectance spectra in visible range were taken to determine the band gap energy of InN thin films on CaF_2 (fluorite) substrates. In this procedure the gap energy was derived from absorption coefficient spectrum of InN layer and yielded $E_g \cong 2.03$ eV which is very close to earlier value [6]. Moreover, the PDS method was used to explore some peculiarities in the free carriers absorption spectra for InN polycrystalline films deposited on different substrates. In order to obtain the necessary information about phonon features of InN films as well as to determine precisely some optical parameters the Drude-Lorentz formalism was used for dielectric function modeling procedure to reflectance spectra from both InN films surface and bare fluorite substrate. Final result shown a good agreement between experimental data and the calculated curve [7]. Also, in our opinion, reflectance peaks at 485 and 590 cm^{-1} respectively, are connected with TO and LO modes vibration of indium nitride [3-5]. An identical result was obtained from a study of Raman spectra for InN textured films (>1 μm thick) on ceramics. The broadening of the peak at 485 cm^{-1} in the Raman spectra of nitride layer (Fig. 2) is very close to that observed in the reflectance spectra. However, because of the imperfect crystalline structure of our samples, we can observe only two apparent optical phonon modes: $E_1(TO)$ at 485 cm^{-1} and $A_1(LO)$ at 585 cm^{-1}. For this reason, it was also difficult to find the main LO phonon mode at 694 cm^{-1}, as predicted by Osamura et al. [4].
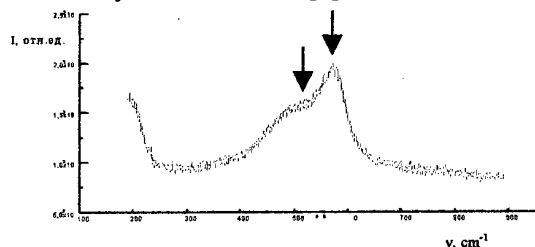
In order to estimate the potential possibilities of InN film material for solar cell fabrication, some theoretical and practical considerations were used. To achieve an optimum power conversion efficiency η for solar cells based on an InN n-layer (emitter) and p-Si (base), large α(E), minority carrier lifetime τ, diffusion length L (at least αL>3 for front side illumination) and surface recombination velosity S have to be combined. This can be achieved under compromise condition of optimum band gaps E_g (~1.0 and 2.0 eV) for an efficient tandem system consisting of several stacked single cells between a large I_{sc} or V_{oc} [1].

Summarizing, an appropriate solar cell base material should exhibit a proper energy gap and a strong absorbtion ($α_{InN} > 10^4$ cm^{-1}) adjusted to the solar spectrum, a dopability by carriers featuring high mobilities and long lifetimes. Another important advantage of an InN/Si heterojunction in future solar cells is a protective function including protection from radiation using the absorbtive InN layer as a top coating. The existing problem of heteroepitaxy of InN films on Si will be resolved by research into an appropriate buffer layer (e.g. AlN thin layer) on InN-Si interface, to match the lattice periods and improve of the heterojunction operating parameters. The fabrication of high quality heterojunctions with InN/Si and its further characterization are also of great importance for manufacturing of high efficiency solar cells for terrestrial and space applications.

References

1. Yamamoto A. et al., *Sol. Energy Mater. and Sol. Cells*, **35**, 53-60 (1994).
2. Ambacher O., *J. Phys. D: Appl. Phys.* **31**, 2653-2710 (1998).
3. Tansley T., Egan R. and Horrigan E., *Thin Solid Films*, **164**, 441-448 (1988).
4. Osamura K., Naka S. and Murakami Y., *J. Appl. Phys.*, **46**, 3432-3437 (1975).
5. Kwon H-J., Lee Y-H., *Appl. Phys. Lett.*, **69**, 937-940 (1996).
6. Tyagai V., Malakhov V. et al., *J. Sov. Phys. Semicond. (USA)*, **11**, 1257-1261 (1977).
7. Malakhov V., *Proc. of the Euromat'99*, **9**, 75-79 (1999).
8. Malakhov V., *Proc. of the TATF'2000*, Extended Abstract Booklet, 351-353 (2000).

Figure 4. Typical Raman spectra of InN layer deposited on ceramics.

THE INFLUENCE OF HEAT-RESISTANT COATINGS ON HIGH-TEMPERATURE STRENGTH OF NIOBIUM ALLOY OF THE SYSTEM Nb-W-Mo-Zr

Bukhanovsky V.V., **Borysenko V.A. and Kharchenko V.K.**

Institute for Problems of Strength National Academy of Sciences of Ukraine, Kyiv, Ukraine

A successful use of refractory metals and alloys in structures operating under conditions of high-temperature oxidizing and aggressive gaseous atmospheres depends, to a great extent, on the solution of problems associated with the development of reliable protective coatings.

This paper examines the strength, deformability, and load-carrying capacity of niobium alloy 5VMTs of the Nb-W-Mo-Zr system both in the initial state and with ceramic slip coatings based on molybdenum and hafnium silicides under conditions of short-term and long-term static tension in vacuum, inert medium, and in air in the temperature range from 290 to 2070 K. A procedure has been developed for assessing the damage accumulated in the niobium alloy/silicide-ceramic coating composite under high-temperature loading.

The investigation of the mechanical characteristics of the alloy and the composite was performed on plane and cylindrical five-fold proportional specimens using general-purpose high-temperature setups. The specimens were cut from a 2mm thick rolled plate and a rod 60 mm in diameter in the as-delivered condition (annealing for 2 hours at 1670 K).

On fabrication, the specimens were annealed for 1 hour at 1470 K to relieve internal stresses. A ceramic coating on the specimen working portion was formed by double dipping into a slip containing the silicides $MoSi_2 + Mo_5Si_2 + HfSi_2$ followed by a low- and high-temperature annealing and vacuum diffusive silicification for 8 hours at 1470 K with an activating agent. The specimens were annealed at 1670 K for 30 min on applying the first layer of the slip and at 2120 K for 30 min on re-applying the silicide-ceramic mixture of the same composition.

To investigate the effect of thermal treatment on the mechanical properties of niobium alloys, a part of the specimens was annealed according to the above stepwise temperature regime without applying a coating.

In the process of active tensioning of the specimens at the rate of 2 mm/min that corresponded to the relative strain rate $\sim 2.2 \cdot 10^{-3}$ s^{-1}, the stress-strain diagrams were recorded, from which we determined the proportionality limit σ_{pr}, offset yield stress $\sigma_{0.2}$, ultimate strength σ_r, relative elongation δ, and the relative uniform strain $\delta_{uniform}$ of the specimen.

Creep tests of alloy 5VMTs and the niobium alloy/silicide-ceramic coating composite were performed at temperatures of 1770, 1970, and 2020 K in vacuum, inert atmosphere, and in air. The values of the applied stresses were from 0.3 to 1.0 of the material offset yield stress at the corresponding temperature. The curves of high-temperature creep, long-term strength, and of 0.5% and 1.0% creep strengths were constructed from the test results. When processing the curves obtained, the creep strengths of the composite were determined, i.e., the stresses inducing strains of 0.5% and 1.0% within the test times of 0.1, 1.0, and 10 hours.

To study the ultimate states of the niobium alloy/heat-resistant coating composite in the course of high-temperature mechanical loading, a procedure has been developed, which is based on the metallographic investigation of the kinetics of initiation and growth of damages in the coating and in the matrix at different levels of plastic deformation of the specimen.

Both high-temperature thermal treatment according to the regime of applying the silicide-ceramic coating and the deposition of the coating itself were found to contribute to some decrease in the strength and, in particular, plastic characteristics of niobium alloys resulting, in a

number of cases, in the change in the mode of the material fracture from ductile intragranular to ductile intercrystalline one. Thus, both the ultimate strength and the offset yield stress for alloy 5VMTs decrease by 5 to 10% in the temperature range from 290 to 1770 K with the level of softening increasing with temperature. In this case, the relative elongation decreases from 7% to 27 % in the range between 290 and 1270 K and from 45% to 50% in the range between 1520 and 2070 K.

Deposition of a silicide-ceramic coating to alloy 5VMTS leads in the tests in vacuum to a decrease in its offset yield stress from 8% at 1270 K to 33% at 2020 K. In the tests in an inert atmosphere and in air, the extent of softening of the composite as compared to the parent material is much lower.

The relative elongation of the alloy 5VMTs/ceramic-coating composite in the temperature range from 1270 to 1970 K is 2 to 4 times lower as compared to the parent material with the maximum decrease in the plastic characteristics of the composite taking place in tests in air.

The investigation of the damage accumulated in the composite under conditions of high-temperature tension revealed that cracks in the ceramic coating initiate already at early stages of plastic deformation (up to 0.5%). When the tests were performed in air, we observed both the formation of new cracks and healing of the cracks that existed earlier. For strains in excess of 0.5 to 0.7%, the cracks initiated in the coating penetrate the matrix, and this is already impermissible from the standpoint of further safe operation of the structure.

As a result of the investigation of creep and long-term strength of the niobium alloy/silicide-ceramic coating composite, the values of the limits of 0.5% and 1.0% creep for the composites were obtained at temperatures of 1770 and 2020 K for the test times of 0.1, 1.0, and 10 hours. For instance, the creep strength of the composite inducing strains of 0.5% within the test time of 1 hour in argon is 25 MPa at 1770 K and 8 MPa at 2020 K. In air, the above values are higher accounting for 30 MPa at 1770 K and 10 MPa at 2020 K.

The results of the investigations were used in strength analysis for structural elements of the objects of rocket and space engineering operating under extreme conditions.

FEATURES OF MATERIAL RECRYSTALLIZATION DURING POWERFUL ELECTRIC PULSE TREATMENT

Barykin N.P., Valeev I.Sh, Kamalov Z.G., Trifonov V.G.

Institute for Metals Superplasticity Problems RAS, Ufa, RUSSIA

Conventional processes of strain-thermal treatment of materials for formation of fine-grained structure in them are rather high expensive and non-efficient. Treatment of materials by powerful current pulses, namely, powerful electric pulse treatment (PEIT), is an accelerated and efficient method for modifying structure and mechanical properties of metallic alloys.

The present paper considers structure change in materials during processing by powerful current pulses providing the rate of heating $\sim 10^6$-10^7 K/s. Flat samples of copper 99.9Cu and aluminum alloy Al6.0Mg0.6Mn at strain values from 0.3 to 1.6, produced by cold rolling were subjected to current pulses of various densities and duration $\sim 10^2$ µs, generated by a bank of capacitors. After that the samples were rapidly cooled to room temperature for about 1 µs. Reference samples were annealed in an electric resistance furnace.
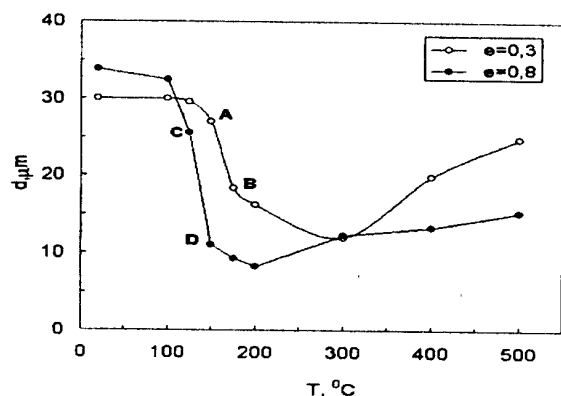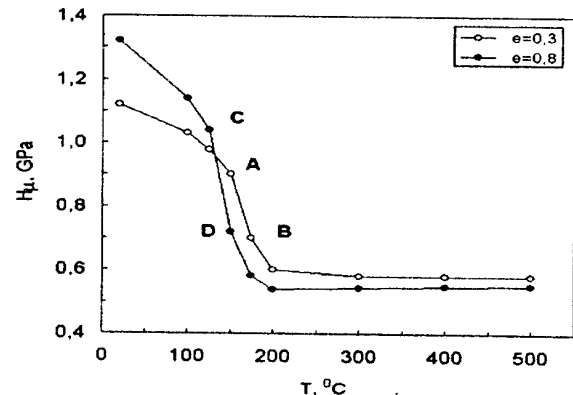
Fig.1. Dependence of microhardness (upper) and grain size (below) on temperature of annealing for copper 99.9Cu .

Figs. 1a, b show the dependence of changes in microstructure and grain size on temperature of annealing for copper 99.9Cu.

Changes in microhardness and mean grain size depending on conventional temperature of PEIT are shown in Fig.2.
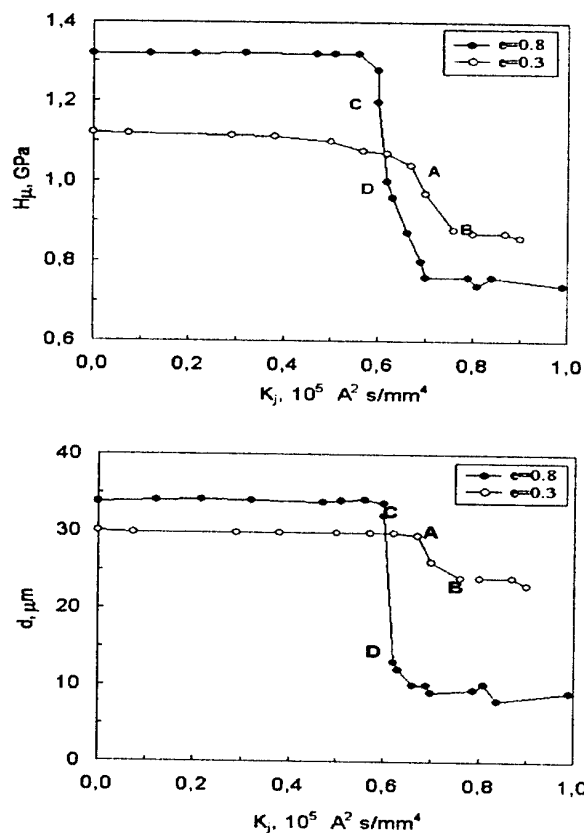
Fig.2. Dependence of microhardness (upper) and grain size (below) on power of PEIT for copper 99.9Cu.

Analyzing the obtained dependencies one can conclude that in spite of the qualitative similarity of static recrystallization and recrystallization during PEIT, there exist a number of significant differences between them. Firstly, thermal recrystallization occurs in the temperature range 100-200°C, while recrystallization during PEIT is realized at temperatures 500-600°C. Secondly, the decrease in microhardness during static annealing begins at temperatures significantly less than temperatures of recrystallization onset that, as known, is connected with redistribution of defects of a crystal

438

lattice whereas microhardness of samples during PEIT remains constant over a wide range of K_j (Fig.2a). Thirdly, during PEIT the significant decrease in grain size (portion AB for the strain e=0.3 and CD – for e=0.8) starts only after the significant decrease in microhardness as compared to the initial state. During static annealing the most significant decrease in grain size (areas AB and CD in Fig.1) occurs simultaneously with decreasing microhardness. During PEIT at e=0.8 the significant decrease in microhardness occurs already at once after grain refinement (below the point D).
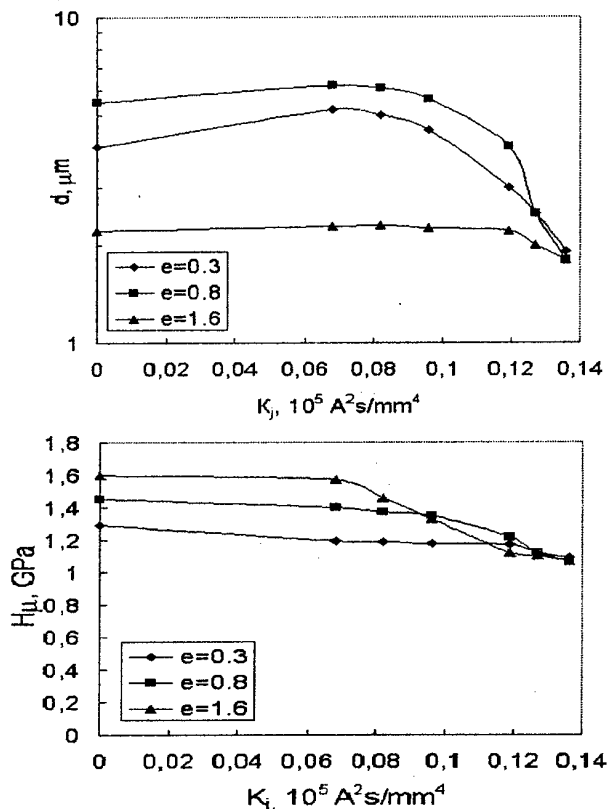
Fig.3. Dependence of microhardness (below) and grain size (upper) on temperature of annealing for the alloy Al6.0Mg0.6Mn.

Dependencies of microhardness and grain size on temperature of annealing for the alloy Al6.0Mg0.6Mn is shown in Fig.3.

As seen from the plot, the noticeable decrease in microhardness occurs over the temperature range 225-300°C at all strain values. The increase in the temperature of annealing up to 600°C does not leads to the noticeable change in microhardness being equal to 0.9 GPa. The refinement of granular structure occurs in all stress over the temperature range 300 – 400°C At annealing temperatures above 400°C grain coarsening starts in the samples and at the temperature 600°C the grain size in all three states achieves 80 μm and more.
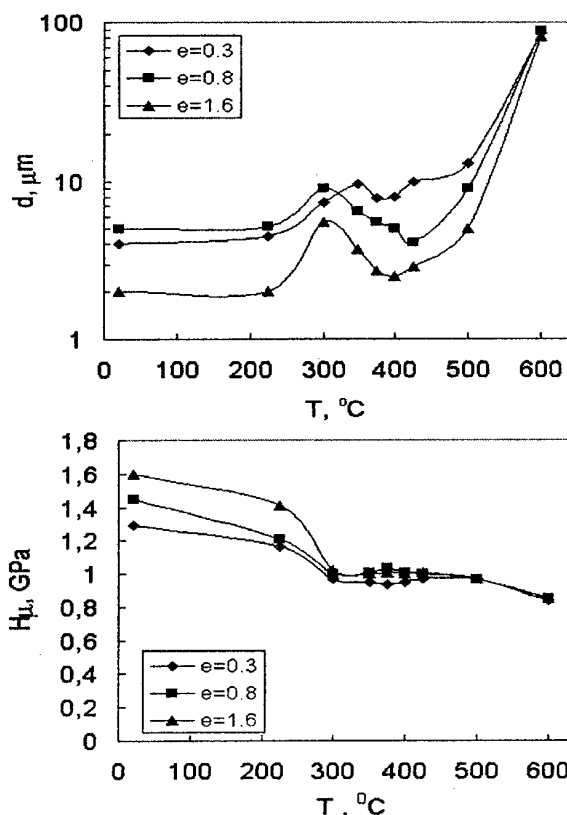
Fig.4. Dependence of microhardness (below) and grain size (upper) on power of PEIT for the alloy Al6.0Mg0.6Mn.

Changes in microhardness and grain size in samples out the alloy Al6.0Mg0.6Mn depending on conventional temperature of PEIT are shown in Fig. 4.

During PEIT the temperature range (150 500°C) over which microhardness decreases is wider as compared to static annealing. As the calculated temperature 500 – 600°C is reached the value of microhardness in all three states approaches one value and becomes equal to 1.1 GPa that is higher than at maximum temperatures of annealing. PEIT with the power $K_j>0,08 \cdot 10^5 A^2 sec/mm^4$ leads to refinement of granular structure and as the power achieves the value corresponding to the calculated temperature $\approx 600°C$ the minimal recrystallized grain size in all three states becomes 2 μm.

On the basis of the results of metallographic analysis and the measurement of microhardness one can conclude that powerful current pulses cause thermoactivated recrystallization of a material. Since processing is very short-term, coarsening cannot be realized fully though the samples heated to the premelting temperature. It has been established that PEIT provides formation of microstructure with grains finer than after annealing.

FORMATION OF METASTABLE STRUCTURES DURING ELECTRO-EROSION TREATMENT (EEO) OF STEELS[1]

Ploshkin V.V.
Moscow State Industrial University, Moscow, Russia

During EET of steel parts they undergo surface carburrizing (up to 6 %C wt.) with a further quenching from the liquid state of superficial layers with rates 10^3-10^6 K/s because of their superheating by the low-temperature plasma of electric discharges to temperature not higher than the boiling point of metal ($\approx$3000 °C). This leads to the formation of metastable phases and structural components of the so-called "white layer" (WL) and of the heat-affected zone (HAZ), drastically influencing their physico-chemical technological and exploitation properties.

During EET (in kerosene, with copper or carbo-graphitic electrodes as instrument, at medium currents 5 – 15A and length of pulses 10^{-3} c) of steels 20 and 45 (0,2 and 0,45 %C), the following peculiarities were observed.

1.   The graphite inclusions (nodules) in WL are non-spherical only from one side, facing the treated surface, and this is connected to the direction of heat flow, mainly on the stage of cooling. The analysis of the structure of such nodules (Fig. 1) has show /1/ that they are not "amorphous" carbon (soot), but a variety of spheroidal graphite, formed with the participation of fullerenes – fourth (after graphite, ddiamond and carbyn) allotropic form of crystalline carbon /2/.

2.   In Fig. 2 the microstructure consists of a *sequence* layers deposited one on other, including unetchable zones (4). The lower layer (1) in Fig/ 2 consists of a fine-grained white hypoentectic iron with disorderly arranged dendrites of austenite (products of its decomposition after cooling to room temperature) and of cementite as the result of a lower-speed of crystallization after repeated heating cycles.

In zone (2) a similar fine-grained structure contains additionally thin strata of secondary cementite. Layer (3) consists also of chemically inhomogeneous hypoentectic white iron, but with austenite dendrites, mainly oriented along the direction of heat flow. The size and orientation jf second order in the lower part of these dendrites witness somewhat lower rates of cooling in this zone.

Certain cementite crystals, including those arrayed along a crack, underwent etching (some of them not along all their lenght) and have acquired a distinct grayish hue. In our opinion this is the result of the transformation of *non-stoichiometric* cementite into *baikovite* /3, 4/. Taking into account the melting point of cementite (1257 °C) and the formation of a boundary between formation of baikovite was found to be 1200-1000°C and this correlates with published data.

During superfast cooling of higt-carbon melts (up to 5% wt.) /5/ a pseudoeutectic was obtained with distinct microvolumes consisting of a *homogeneous* solid solution of carbon in iron with 2,0 – 6,67 %C. They are not etched by nital and caustic sodium picrate. Taking into account that the unetchable part (4) of WL is formed at higher solidification rates than necessary for the obtaining of a superfine eutectic mixture of phases, and that upon heating it can be transformed into a heterogeneous mixture, it may be assumed that the formation of WL takes place without a diffusional redistribution of carbon concentration in the liquid solution. WL in zone (4) *is a strongly supersaturated solid solution of carbon in iron with the same carbon content as was in the liquid phase.*

3.   On the WL – HAZ boundary we have found a dark fringes along the oblong austenite grains or isolated of WL. This fringe is the result of a metastable contact-melting $\alpha Fe + Fe_3C \rightarrow$ *liquid*. It can be seen how the liquid phase penetrates from the WL into HAZ. This penetration is observed in places location where grains with molten boundaries are closely located to each other. In separate case we can even observe the fusion of different plots of the liquid phase into a common pool. The mechanism of the formation in separate microvolumes of a metastable liquid eutectic $\alpha Fe + Fe_3C$ can be explained with the use of phase diagrams of E. Schurmann and R. Schmied /6/, who determined

---

on the base of thermodynamic and thermochemical computations the separate eutectic points of equilibrium of either graphite or cementite with ferrite or austenite, namely *1102 and 1057 ^0C* correspondingly for the $^{\alpha}Fe + Fe_3C$ and $^{\alpha}Fe + grafite$ systems.

Most interesting is the metastable equilibrium, when the low-carbon phase in the interval *727-1525 ^0C* is not austenite, but a metastable ferrite. Yet in real conditions the crystallization of eutectics at high cooling rates and strong carburizing of the metal, with a big difference of solubilities of components, can be shifted to very low temperatures, even lower than *1000 ^0C*.

This is corroborates by the fact that such a contact melting and subsequent crystallization are accompanied at ≈ 1000 ^0C by austenitization of pearlite in this temperature range when lamellar pearlite is heated at rates 10^4-10^6 K/s. During cooling to low temperatures a martensite of low etching properties is formed, though in certain parts of the former pearlite grains the martensitie transformation was not total.

The existence of ferrite in contact with WL (see Fig. 3), that *is with a hypoeutectie white iron*, is also an evidence of thereality of the interaction of high-carbon phases (graphite and cementite) not only with $^{\gamma}Fe$, but with $^{\alpha}Fe$ too. The structure of WL is formed without intermixing of the metal, therefore we have a distinct boundary between the WL, the HAZ and the ferrite that remained untransformed as a separate phase (due to lack of time).

Conclusions

1. During EET of steels the formation of the microstructure of the surface layers takes place with a phisico-metallurgical paradox – *the temperatures of some of the phase transformations are being lowered with rising heating and cooling rates*. If the structure formation during EET occurred with speeds of heating lower than actual, ferrite would have had enough time to transform itself into $^{\gamma}Fe$ (only slightly later than pearlite) and the anomalous low-temperature contact melting could not occur.

2. In the WL of EET-treated steels we discovered *baikovite*, formerly identified in cast irons, treated with a laser beam.

3. The cheoretical previsions of E. Schurmann and Schmied were corroborated, according to them there exist metastable equilibrium *Fe – C* phase diagrams where the austenite phase is replaced by ferrite.

References

1. V.V. Ploshkin. Not fully spherical carbon nodules in the surface layers of steels after electro-erosion treatment. In the collection of scientific works of the Moscow State Industrial University. Vol. 1. Voscow. MSIU ed., 1999 (in Russian).

2. A.A. Zhukov. Fullerenes and the spheroidization of graphite in iron alloys. Metal Suience and Heat Treatment. 2000. No. 7. P. 3-6 (in Russian).

3. A.A. Zukov, M.A. Kristal, A.N. Kokora, Sneznoy R.L. La baikovite, une nouvelle structure dans les alliages fer-carbone. Memoires scientifiques de Revue de Metallurgie, 1972, № 3, p. 211 – 217

4. V.V. Ploshkin, A.A. Zhukov On the mechanism of transformation of decarburized cementite into baikovite. Physics and Chemistry of Materials Treatment.2001, No 6, p.169-172 (in Russian).

5. K.P. Bunin, G.I. Ivantsov, Ya.N. Malinotchka. Structure of Cast Iron. Moscow. Mashgiz. Ed. 1952, p. 163 (in Russian).

6. O. Kubashevsky. Handbook "Phase Diagrams of binary Sistems on the Iron Base". Moscow, Metallurgia ed. , 1985, p. 32-35 (in Russian).

Fig. 1. WL with graphite nodules (steel 20); x500; etched by nital
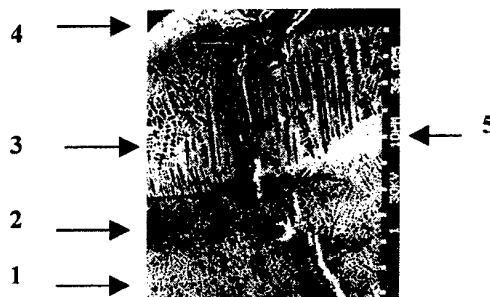
Fig. 2. Fragment of the microstructure of WL; etched by nital

Fig. 3. Structure of HAZ and of a thim layer of WL (steel 45); x500; etched by nital

441

THERMAL STABILITY AND MAGNETIC PROPERTIES OF Ni-P ELECTRODEPOSITED COATINGS

Babich M.G., Nakonechna O.I., Yeremenko G.V., Zakharenko M.I.
Department of Physics, National Taras Shevchenko university, Kyiv, Ukraine

The nature of the formation of localized magnetic moments in metal crystals is studied insufficiently. In particular, it is due to the role of peculiarities in exchange interaction of electrons to the character of the nearest atomic environment [1]. The Ni-based amorphous alloys take special place among the transition metal – metalloid (TM-M) – type amorphous alloys because we can consider such alloys as the model objects as they have one unpaired electron [2].

To better understand the magnetic nature of the Ni-based electrodeposited coatings we have been investigated the temperature dependencies of magnetic susceptibility $\chi(T)$ for $Ni_{18}P_{19}$ coatings of different thickness.

The $Ni_{81}P_{19}$ coatings with the thickness ranging from 12 to 43 μm have been electrodeposited onto electrotechnical ceramics (polycor) using the electrolyte given by Brenner et al. [3] at 74 °C with a constant current density of 200 mA/cm^2. The thickness of NiP layer could be controlled using different deposition times.

The temperature dependencies of magnetic susceptibility were obtained using the Faraday-type technique with automatic microbalance (the sensitivity was equal to 10^{-11} cm^3/g and accuracy was better than 1.5 5). An experimental temperature interval was T = 300 – 850 K. The heating rate not exceeded 8 K/min.

All the investigated coatings can be divided into two groups. The first group includes thin coatings (D ≤ 20 μm) and the second one includes the ribbons with D = 25 and 43 μm. To reveal the peculiarities of the coatings' structure we have carried out the X-ray diffraction studies, using FeK$_\alpha$ - radiation. For the ribbons of the first group the diffraction pattern is halo that evidences for their amorphous structure. For the rest coatings the diffraction pattern is the superposition of the above mentioned halo and weak Bragg peaks corresponding, to our mind, to the reflections from *f.c.c.* Ni(P)-type crystal inclusions. It is necessary to note that the intensity of the latter increases with the coating thickness. Consequently, the coating structure changes from

amorphous to amorphous-crystalline with D increase. Also, according to the X-ray diffraction analysis data the *f.c.c.* – phase has some greater value of the lattice period than that for pure nickel. That is related on our opinion to the Ni(P) solid solution formation.

The temperature dependencies of the magnetic susceptibility $\chi(T)$ for $Ni_{18}P_{19}$ coatings of different thickness D obtained by the Faraday method within the wide temperature range are shown at Figs. 1, 2. χ values for all coatings of the first group are smoothly decreased with temperature increasing. The $\chi(T)$ dependencies for the coatings of second group are rather significant, displaying a ferromagnetic-like shape. At the temperature range 530 –560 K a small increasing of χ is observed while heating due to crystallization of samples. The appropriate values of crystallization temperature T_x are listed in Table. This Table also contains the values of the Curie temperature of the samples in crystalline state.
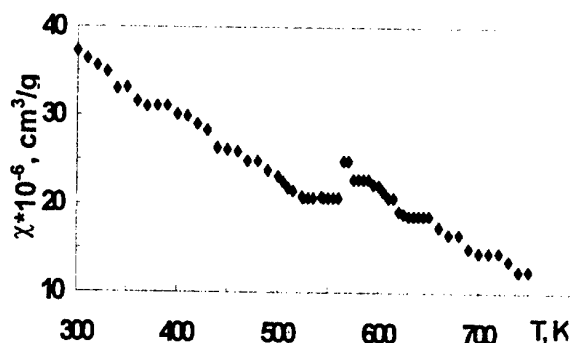
Fig.1. Temperature dependence of χ for as-deposited NiP coating of 12 μm thick.
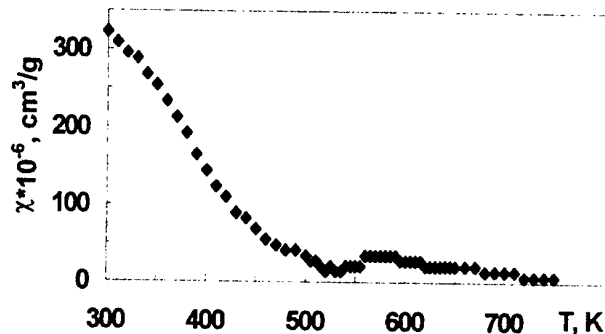
Fig.2. Temperature dependence of χ for as-deposited NiP coating of 43 μm thick.

Table.
The crystallization temperature T_x, the curie temperature T_C of $Ni_{81}P_{19}$ coatings with different thickness D

D, μm	T_x, K	T_C, K
12	565	585
16	540	592
18	530	590
25	565	570
43	560	565

The analysis of $\chi(T)$ shows that the experimental curves can be described by the superposition of three terms of susceptibility:

$$\chi = \chi_d + \chi_p + \chi_{cw},$$

where χ_{cw} is the Curie-Weiss paramagnetic term, χ_p is the Pauli paramagnetic and χ_d is the ion-core diamagnetic term. From the analysis of the χ_{cw} term we have obtained the values of mean localized magnetic moment μ and of localized magnetic moment per Ni atom μ_{Ni}. The latter one was found to be almost constant ($\leq 0.3\mu_B$) for the ribbons of the first group. Besides, it was found that χ values increase with D almost tenfold. So far, one can suppose that these experimental facts testify the presence of the ferromagnetic inclusions (or clusters) in such coatings. The contribution of clusters to magnetic properties of the coatings increases with their thickness.

Thus, for the investigated samples the coating thickness variations correspond to the cooling rate is changed almost tenfold. So, for thick layers the cooling rate is insufficient to form the absolute disordering state during quenching. Thus, the atomic crystal-like clusters could be saved in coating during electrodeposition.

These clusters essentially influence the magnetic properties of coatings. They cause the appearance of the ferromagnetic component of χ. So, we can consider that the presence of magnetic clusters in Ni-P amorphous alloys is not its characteristic feature but is determined, first of all, by the technological regimes of preparation.

Also, it was interesting to analyze the magnetic state of NI atoms in paramagnetic state. As it was mentioned above, the value of localized magnetic moment does not exceed $0.3\mu_B$. This value is significantly less that for pure paramagnetic Ni ($\mu_{Ni} = 1.66\mu_B$). To our mind, such difference in value associated with quenching of the spin

moment of atoms by an internal field. This phenomenon takes place due to d-electron transport peculiarities among components of the alloy and is known for crystalline alloys, too [4]. In the case of amorphous metallic alloys this phenomenon has to display more clearly due to the influence of two factors that lead to essential weakening of the interatomic exchange interaction. The first is the absence of the long-range order in amorphous alloys and, the second is the presence of P metalloid atoms for which d-states are empty. The above mentioned reasons evoke an essential decrease in the d-d bond formation probability between metallic atoms. Under these conditions the intratomic interaction becomes predominant. Therefore, when the orbital moment is quenched, the spin moment may be also quenched.

References

[1] F. Stein, G. Deitz, *J. Magn. Magn. Mater.*, 117 (1992) 45.

[2] R. Hasegawa, *J. Magn. Magn. Mater.*, 100 (1991) 1.

[3] A. Brenner, D.E. Couch, E.K. Williams, *J. Natl. Bur. Stand.*, 44 (1950) 109

[4] P.P. Kuz'menko, N.I. Zakharenko, *Dokl. AN UkrSSR (b)*, 8 (1975) 713 (in Russian).

443

STRUCTURE AND MAGNETIC PROPERTIES OF METAL COATED THERMOEXFOLIATED GRAPHITE

Babich M.G., Matzui L.Yu., Zakharenko M.I., Kapitanchuk L.M.[1], Brusilovets A.I.
National Taras Shevchenko university, Kyiv, Ukraine
[1]Paton Institute for Electric Welding NASU, Kyiv, Ukraine

Carbon-based materials find the increasingly wide industrial applications due to their unique combination of high corrosion resistance and thermal stability with low density. An active search for the novel materials that meet the modern requirements to be used in aircraft and automobile industry, space equipment, energetic has led to the creation of the carbon composite materials (CCM) [1]. However, the traditional technologies based on the usage of the carbon fibers or pyrolitic graphite are usually extremely power consuming. So the development of the new technologies of CCM production basing on the natural graphite is promising. The method of the chemical modifying of the thermoexfoliated graphite (TEG) surface to obtain the necessary complex of physical and chemical properties is the main method to create CCM [2]. The possibility of the uniform distribution of metal component through CCM volume, the possibility of the variation of phase composition of coating's content, the simplicity of fabrication determine the advantages of this method.

The investigated samples of TEG+Ni, Co, Fe were produced by the chemical modification method according to two alternative procedures. According to the first one graphite was preliminary thermoexfoliated and then the modifier was deposited on the surface of TEG particles through several successive chemical reactions: impregnation of TEG with metals acetate, drying and reduction of metals in the flow of hydrogen at the appropriate temperatures. The powders of modified TEG produced by this method had the density of (0.03 – 0.07)g/cm^3 which considerably exceeded the density of initial TEG. The second procedure consists in the impregnation of natural graphite, its heat treatment through thermal impact and subsequent reduction of metals.

The X-ray phase analysis (DRON-4 diffractometer, filtered CoK$_\alpha$-radiation) was used to study phase composition of the prepared composites. Scanning electron microscopy (JSM-840 microscope) was used to study morphology, shape and distribution of metal particles on the TEG surface. LAS-2000 system ("Riber", France) was used to determine the element composition of the obtained materials and the types of possible chemical compounds being formed at the sub-surface layers by SIMS and the Auger spectroscopy methods. It becomes possible to detect the change of the mentioned parameters in the depth of the samples through the ion etching of their surface (the etching rate was equal, as a rule, 0.3 nm/min).

Temperature dependencies of the magnetic susceptibility were obtained using the Faraday-type technique with automatic microbalance (the sensitivity was equal to 10^{-11} cm^3/g and accuracy was better than 1.5 %).

Detailed investigations of the samples prepared according to the first procedure have shown that modification of TEG yields homogeneous, uniformly distributed fine disperse impregnations of metal no more than 300 nm in size located both on the ends of TEG particles and on the surface of their layers moved apart by exfoliation. These impregnations consist of smaller crystallites about 10-50 nm in size. Therewith, the samples prepared by the second procedure contain essentially large-scaled metallic particles.

TEG+Ni. According to the data of the X-ray phase analysis the modification of TEG by Ni results in a formation of fine Ni particles on the surface of graphite that is confirmed by the sharp broadening of the appropriate diffraction peaks. The magnitude of magnetic susceptibility χ depends linearly on nickel content at T= 300K and its temperature dependence is typical for the ferromagnetics in general. It was found that the Curie temperature T_c depends noticeably on concentration of modifier in TEG and decreases with nickel content but still remains lower than for pure bulk nickel [3]. Taking into account the model proposed in [4], we could make a statement that the nature of such changes in T_c is directly related with the crystallite sizes L of modifier. The analysis of temperature dependencies of magnetic susceptibility revealed that calculated values of the paramagnetic Curie temperature θ

Table 1

Magnetic properties of TEG + Ni and sizes of Ni particles

Ni content, wt. %	T_c, K	μ_{Ni}, μ_B	θ, K	L, nm
10	589	1.48	596	5
30	611	1.64	599	11
50	612	1.72	600	12

practically do not depend on Ni content and localized moment per Ni atom μ_{Ni} increases with the increasing of c_{Ni}, finally approaching the value of $\sqrt{3}\mu_B$ which is characteristic to single unpaired d-electron. The mentioned parameters of the studied samples are listed in Table 1. Reasoning from the findings reported in Ref.[5] the described regularities of magnetic properties of TEG+Ni composites should be considered as an evidence of validity of the proposed mechanism of the Curie temperature decreasing in the nanoscaled Ni system.

TEG+Co. The specimens prepared according to the first procedure exhibit $\chi(T)$ behavior while heating that is typical for ferromagnetic amorphous metallic alloys [6] (as an example see Fig. 1). Starting from 530 K the susceptibility becomes to change non-monotonically. $\chi(T)$ is almost the same in the temperature range of 530 – 700 K and is increased with further heating for TEG +10% Co. The same but less pronounced peculiarities are observed for TEG = 30 % Co and TEG + 50% Co, therewith the temperature when the susceptibility becomes to rise is decreased (640 and 600 K, respectively). This circumstance permits to argue that the structure of the modifier-metal is almost amorphous at the initial stages of precipitation. At the latest stages the metal particles possess the crystalline structure that is typical for cobalt. This is confirmed by the X-rays diffraction data that proved the presence of both f.c.c. and amorphous cobalt in as-prepared materials. The investigation of element content of Co particles by Auger spectroscopy method has shown the presence of oxygen together with basic elements (Co, C). Oxygen is detected in surface layers of 15-30 nm thick. $\chi(T)$ curves for TEG+Co samples prepared by the second procedure is in general the similar to those described earlier. Meanwhile, the change of χ

after heating-cooling cycle is more pronounced that is the evidence of more non-equilibrium state of metallic particles. This fact dictates the improved resistance against oxidation just for these samples.
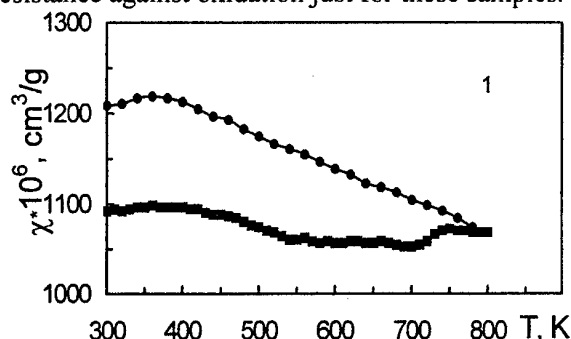
Fig. 1. $\chi(T)$ dependencies for TEG + 10 wt.% Co; ■ - heating, ● - cooling.

TEG+Fe. The shape of $\chi(T)$ curves for the samples prepared by the second procedure (maximum of χ at T~650-700 K and subsequent gradual decrease to almost zero values) displays the presence of ferromagnetic component and its partially amorphous structure The estimated value of T_c is equal to 802 K, that is in a good agreement with T_c value for Fe_3O_4.[3] The formation of this phase was also confirmed by the X-ray diffraction and SIMS. $\chi(T)$ curves for TEG+Fe samples prepared by the first procedure (Fe content 10, 30 and 50 wt.%) exhibit a considerable difference as compared to those described earlier: the absence of χ maximum at 650-700 K range and difference between susceptibility values measured while heating and cooling. Such behaviour evidences the formation of equilibrium crystalline phases at the stage of samples' preparation.

This work was supported in part by STCU through Grant #1618.

References

[1] H. Fucstner, F. Hoster et al., *J. Catalysis* 118 (1989) 502.

[2] F. Beguin, H. Messaoudi, *J. Mater. Chem.* 219 (1992) 957.

[3] S.V. Vonsovsky, *Magnetism,* Nauka, Moscow, 1971 (in Russian).

[4] V. Budarin, V. Diyuk, L. Matzui et al., IVMTC28 Abstr. (1999), p. 58.

[5] P.P. Kuz'menko, N.I. Zakharenko, *Metallofizika* 2 (1980) 44 (in Russian).

[6] R. Hasegawa, *Glassy metals: magnetic, chemical and structural properties,* CRC Press, Inc., Boca Raton, Florida, 1983.

STRUCTURE AND PROPERTIES OF DIFFUSION COATINGS ON WOLFRAMLESS FIRM ALLOYS

Hizhnjak V.G., **Dolgykh.**, **Karpets M.V.**[1]
National Technical University of Ukraine "KPI", Kiev, Ukraine
[1]Frantsevich Institute for Problems of Materials NAS of Ukraine, Kiev, Ukraine

Now the problem of decrease of the charge traditional hard alloys tool materials of marks BK, TK is solved wide application wolframless firm alloys of marks TH20, KHT16, KXH15

For increase stability of characteristics many-sided non sharpen back hard alloys plates with mechanical fastening frequently resort to drawing on working surfaces of coverings on a basis carbides transitive metals IV-V of groups of periodic system that allows to increase durability of tools in some times [1,2,3].

Among known coverings, witch coated on a surface of firm alloys, the greatest practical application have received single-layered coverings on a basis carbide the titan and multilayered coverings on a basis carbide titan TiC, nitrideTiN of titan and aluminium oxide Al_2O_3. Application of coverings on wolframless firm alloys is interfered by absence of technological receptions their drawing, and also incomplete character of the information on structure, structures and properties of coverings [4,5,6].

In the present work of a covering on the basis of the titan, vanadium and хрома on a surface of a firm alloy of mark TH20, rendered in an interval of temperatures $1223 - 1373^0C$ and time of endurance(quotation) 0,5 - 6 hours. Process of saturation by transitive metals carried out in the closed reactionary space at the lowered pressure with use as initial reagents of powders of the titan, vanadium, хрома, four-chloride carbon and the carbonaceous additive [3,4].

The samples received thus with coverings, and also initial alloys were investigated by X-ray diffraction, microstructural and durometerical methods analyses. It is established, that in some cases the phase structure of superficial and internal zones of initial alloys essentially differs. So for alloys TH20 the period of a crystal lattice of phase TiC in superficial zones thickness 10 – 15 micron appears lower, than cores. After cementation (temperature 1000^0C, time 2 hours) the maintenance of carbon in superficial zones is increased. It results in growth of parameter of a crystal lattice of phase TiC of alloy TH20 up to values of parameters of a lattice of the given phase of the central zone.

After diffusion metallizations of alloy TH20 by the titan, vanadium, lame the surface consists of zone carbides sating metal adjoining to the basic alloy and zones intermetallic on the basis of sating metal and никеля.

In alloys KXH15 after cementation phase Cr_7C_3 disappears. Besides at cementation of firm alloys saturation nickel - molybdenum of a sheaf carbon, which takes part at the subsequent chemical-thermal processing in formation carbides phases, takes place.

It is shown, that the phase structure of sheetings is determined by a kind of saturation and structure of an initial alloy. After diffusion metallizations of alloys TH20, KHT16 the titan, vanadium, lame the surface consists of a zone carbides sating metal adjoining to the basic alloy and zones intermetallic on the basis of sating metal and nickel. For coverings on basis KXH15 are characteristic presence directly at a basis of a zone of carbide Cr_7C_3.

It is necessary to note, that the sequence of formation and an arrangement carbides and intermetallics layers in a covering on the investigated alloys will well be coordinated to known representations about character of diffusion processes in a zone of saturation [7,8].

The analysis of a structure of alloys wich were subjected metallic diffusin by titanium and vanadium has shown, that is direct under a zone carbide accordingly TiC, VC the zone with the advanced porosity that gives to this zone a grayish shade is located. It is necessary to note, that microscopic metallography methods the zone with the advanced porosity comes to light in diffusion to a zone at thickness of a layer intermetallic metal 5,0 - 7,0 and has thickness a little bit big, than a layer intermetallic. At metallization of the

investigated alloys formation of a zone of intermetallic with participation accordingly the titan, vanadium, хрома is accompanied diffusion by removal of nickel bases in a covering. It results in development in the basic alloy of a zone of porosity. It is necessary to note, that preliminary cementation of firm alloys essentially reduces thickness of a zone of intermetallic and zones with the advanced porosity.

With the purpose of definition of features and laws with coverings researches of wear resistance were carried out at various modes of processing of steel.

Wear resistance determined in conditions of cutting and estimated on size of relative deterioration, which expected under the relation of the sizes of a facet of deterioration of a back surface to a way of cutting. Typical for the established dependences of relative deterioration on speed of cutting there is a displacement of speed of cutting at which the minimal relative deterioration is observed, aside the big speeds at decrease of relative deterioration with coverings in comparison with initial plates.

Serviceability of a covering sharply grows at speeds of cutting v > 150 m / minutes when it raises resistance hard alloys matrixes of diffusion to dissolution in a processable material [9,1].

Conclusions.

In work the opportunity of drawing on a surface wolframless firm alloys TH20, KHT16 and KXH15 coverings is shown on the basis of the titan, vanadium, хрома, a pine forest. The phase structures, microhardness of formed layers are determined kinetics of growth. It is established, that nickel of the basic alloy participates in formation of coverings.

It Is shown, that stability many-sided firm alloys plates with mechanical fastening with sheetings raises at processing steels in 2 - 5 times in comparison with initial. Coverings have shown peak efficiency on the basis of the titan.

The literature:

1. Верещака А.С. Третьяков И.П. Режущие инструменты с износостойкими покрытиями: М.: Машиностроение, 1986. – 192с.

2. Андриевский А.Р., Спивак И. И. Прочность тугоплавких соединений и материалов на их основе: Справочник. / Челябинск, Металлургия. Челябинское отделение. 1989 – 386с.

3. Лоскутов В.Ф., Хижняк В.Г., Куницкий Ю.А., Киндрачук М.В. Диффузионные карбидные покрытия. – К.: Технiка, 1991. – 168с.

4. Хижняк В.Г. Некоторые свойства и характеристики твердых сплавов ВК8 и Т15К6 с двухкомпонентными покрытиями // Вестник Национального Технического Университета Украины «КПИ». Машиностроение. – 1997. вып. 32. - 221 – 227с

5. Крючков В.Я. Исследование стойкости пластин из безвольфрамого твердого сплава ТН20. Станки и инструмент. 1987, №7, - 25 – 26с.

6. Коняшин И.Ю., Костяков В.И., Нарамовский И.В. Структура и свойства безвольфрамовых твердых сплавов после газового азотирования. Защитные покрытия на металлах. К., Наукова думка, 1988, вып.22., 69 – 73с.

7. Химико-термическая обработка металлов и сплавов./ Справочник. – М.: Металлургия, 1981. – 424с.

8. Третьяков В.И. Основы металловедения и технологии производства спеченных твердых сплавов. – М.: Металлургия, 1976. – 528с.

9. Методика испытаний металлорежущего инструмента. Общие машиностроительные нормативы режимов резания для технического нормирования работ на металлорежущих станках. Часть1. – М.: Машиностроение, 1974. – 406с.

INVESTIGATION OF TOTAL EMISSIVITIES OF THERMAL INSULATION MATERIALS AND COATINGS

Paderin L.
Central Aero-Hydrodynamic Institute (TSAGI), 140180, Zhukovsky, Moscow Region, Russia

The knowledge of total hemispherical emissivity of materials and coatings is of basic interest for the design and development of high temperature structures. Taking into account, that the radiant properties including total emissivity of materials and coatings are often most sensitive to the specific environments, first of all gaseous components, it is desirable to perform the investigations of above properties in simulated operating conditions. In many situations the directional emissivity is of practical interest also. By present time in the most degree base of data, provided the total emissivity temperature relations, have created for high conductive materials, first of all for metals. Investigation of thermal insulation materials and coatings on ones is more complicated problem. Therefore these materials have studied in significantly smaller degree. In the main, it is caused by the methodical difficulties, connected with heating and measuring temperature of test sample examined surface. Because of low heat conductivity the total emissivity measurements on these materials at high temperatures (T>1000K) require that the radiation heater and the radiation detector are to be located on the same side of the test sample. In this case, the measurement of the radiation flux emitted from the sample surface is complicated by the heater radiation, which is reflected from the sample simultaneously. Therefore, total hemispherical emissivity measurements are most complicated because the radiation detector is to be located at a relatively short distance from the test sample surface. This causes intensive radiant heat exchange between sample and radiation detector and, by it possible significant measurement errors in addition. The measurement of sample examined surface temperature create serious problem since the traditional contact and optical methods of temperature measurements are practically not applicable. Especially, it is related to hemispherical emissivity investigation of sample, which examined surfaces should be isothermal. Therefore, a new special method is to be created to measure sample surface temperatures taking into account the particularities of emissivity measurement method and facility. In literature, in particulary, [1, 2] the methods and facilities for normal emissivity measurements (total and spectral) of thermal insulation materials under vacuum conditions are presented above all. Information about measurements of the total hemispherical emissivity as well as directional emissivity of these materials at high temperature is not discussed.

In proposed paper some modifications of method and facility for measurements of total hemispherical and normal emissivities as well as directional emissivity are presented. Total emissivity is evaluated from the measurement of the heat flux radiated from the examined surface of a test sample, which rotates in an isothermal heating zone of controllable temperature, and comparing radiation fluxes from test samples and blackbody model at the same temperature. Each modification of facility comprises the following basic units: vacuum chamber, mechanism for rotating of a sample with adjustable speed, radiant heater, calorimeter type radiation detector, temperature sensors and thermal insulation outlined the heating zone. Unlike to known methods the radiation detector is placed inside of chamber immediately in heating zone, that permits to measure hemispherical radiant flux from a test sample. A test sample is either a disk of 120÷200 mm diameter or a square plate of 120 to 150 mm length. The sample thickness ranges from 0.1 to 50 mm. In particular, samples of up to some millimeters in thickness are to be manufactured of high conductive material. If the sample thickness is less than50 mm, an extra insulation corresponding differential thickness is arranged between the sample and its support. Concrete peculiarities and parameters of method and facility variants depend of emissivity type, operating conditions, temperature range of measurements and test sample parameters. The test facilities are optimized to get the sample surface as isothermal as possible, so that the potential systematic error caused by speed of rotating sample as well as by reflection of the heater radiation from the test sample surface are negligible. Prior to the measurements the radiation detector is calibrated under operating conditions in the setup by means a spherical model of a black

body under vacuum conditions (P<10 Pa). If the measurements are to be performed at gas pressure (P>10Pa), additional calibration of the detector is carried out for the prescribed pressure/temperature range using a reference sample of known and stable temperature dependent emissivity. At present time the existing methods and facilities enable the following measurements: 1) hemispherical and normal emissivities under vacuum conditions in temperature range $150K \geq T \leq 2000K$ and at adjustable air pressure, simulating operating conditions, in temperature range $500K \geq T \leq 1600K$, 2) directional emissivity in angle range $20° \geq \gamma \leq 85°$, where γ is the angle relatively normal to examined surface, under vacuum conditions in temperature range $600K \geq T \leq 1100K$. Absence of intermediate absorptive and reflective medium and elements between a test sample and radiation detector, contactless method for evaluating test sample temperature as well as calibration of radiation detector in operating conditions provide the high accuracy of measurement. The uncertainties assessed for measurements of hemispherical and normal emissivities to be lower than 5% and for measurements of directional emissivity to be lower than 8%. The developed methods and facilities in the following enable the investigations practically on any types materials, structure rigid and flexible components as tiles, honeycomb, blankets and other flat sample as well as of thermal control coating on ones. The test results of different materials and coatings are presented.

References

1.Izluchatelnie Svoistva Tverdih Materialov. Spravochnik pod red. A.E. Sheindlina, Izd. Energia, Moskva, 1974, 471 str.
2.Grial J. et al., Determination of high temperature Thermo-Radiative Properties of Composite Materials for Thermal Protection of Spacecraft, 3rd Europen Workshop on high temperature materials, Stuttgart, pp. 178-183

INVESTIGATION OF THE DIFFUSION-HARDENING ALLOYS STRUCTURE BASED ON Cu-Ga SYSTEM USING THE SYNCHROTRON RADIATION

Ancharov A.I., Grigoryeva T.F., Sharafutdinov M.R.
Institute of Solid State Chemistry and Mechanochemistry SB RAS, Novosibirsk, Russia

Diffusion-hardening alloys (DHA) or metallic glues is the name for compounds arising as a result of interaction of a solid metal powder and metal melt. Diffusion of the liquid component into a solid matrix results an appearance of the intermetallic compound with a melting point higher than that of the liquid component (by 150 to 400°K depending on the composition). Mixing the solid and liquid components, one can produce a paste that can solder different materials. Later on the soldered joint gets hard and provides mechanical, electrical and thermal connection. DHA have very broad application in different technologies. The main advantage of the DHA soldering as compared with the conventional one is the connection happens at ambient temperature or small heating. Therefore, there are no deformations due to inhomogeneous warming up when long (especially thin-walled) details are being connected. A simplest example of a DHA is the mixture of copper powder and melted gallium. Gallium melts at 30° C. Thus the soldering shall be done at small heating. One can see from the phase diagram of this system that interaction after preparation of the mixture of 66.6%(atom) of Ga with 33.3% of Cu will lead to appearance of the intermetallic compound $CuGa_2$. So, having carried out soldering at a temperature of 30°C, we obtain a compound which stays hard until 252°C. However, it is more convenient to use the Ga-Sn eutectic which have a melting point of 20.5°C. The role of powder was played by the metastable solution of Ga (20 at.%) in Cu, obtained by mechanochemical activation.

At first, it was planned to determine the rate of formation of the intermetallic compound and time of completion of the reaction by the data of X-ray structural analysis made with different time intervals. The work was carried out at the station of the 2nd channel of the VEPP-3 storage ring (BINP SB RAS). The investigations allowed us to reveal that 90% of the intermetallic compound forms during 7-8 hours from the beginning of the process. At the same time, it was found that 9

hours later there appears peaks corresponding to tin. Additional investigations carried out at the station of the 4th channel of VEPP-3 using the hard X-rays and two-coordinate detector based on Imaging Plate showed that the tin is strongly textured and can even be in the form of distorted single crystals. Shooting by the Laue method with the use of "white" SR confirmed this supposition.

Since the tin crystallization takes place after formation of the larger of part of the intermetallic compound, the tin can be located as streaks between the intermetallic grains. It is known, intermetallic compounds are fragile. A plastic tin streak should increase the strength of the soldered conjunction.

Application of the powder of metastable solid solution of tin in copper made it possible to increase the quantity of tin in a streak and to increase the strength of the soldered conjunction.

The described technology allowed us to realize soldering of four water-cooled copper ties to the vacuum chamber of the 4 meter long undulator at ambient temperature. This chamber has successfully sustained a 230°C warming-up.

ELECTROMAGNETIC STIMULATION OF CRACK HEALING IN TRANSPARENT DIELECTRICS

Feodorov V.A., Plushnikova T.N., Tjalin Yu.I., Chivanov A.V.
Derzhavin Tambov State University, Tambov, Russia

Strength characteristics of materials are determined by presence of defects: pores, microcracks and so on. However in practice not only detection of presence or absence of crack in material must be done. It is necessary to eliminate the defect, for example to prevent its development by healing.

The destruction of crystals is accompanied by plastic deformation, its intensity and degree of localization depends on a velocity of crack propagation. At stopping of a crack in alkali-halide crystals the plastic zones are formed, their structure is determined by a type of a destroying crack, geometry of a sample, properties of a material. It is known that in such crystals spontaneous and artificial healing of cracks possibly.

The purpose of this paper was to investigate experimentally the influence of electromagnetic radiation on processes of stress relaxation and healing of crack tip in alkali-halide.

The materials used in the present work were LiF, NaCl, KCl single crystals with impurity content 10^{-4} wt%, 10^{-3} wt% and 10^{-2} wt%. The size of the samples was 10x25x2 mm. The samples were cleft from big single crystals. The crack of asymmetrical cleavage was initiated on (100) plane by calibrated impact with energy $\approx$ 80 mJ. The point of crack initiation was situated at distance S_1 from axis of symmetry (fig. 1a). The degree of asymmetry was determined as $S_1/0.5S_2$, where S_2 is width of sample. The sample was cleft in two equal parts on (010) plane for preparation of "control" and "testing" crystals. Chemical etching revealed the dislocation structure.

At the first series of experiment crystals were heated in stove in the temperature range of 300 ÷ 773 K.

At the second series crystals were illuminated by tungsten lamps. The power of lamps was 20 and 100 W and the maximum energy in the spectrum was 1.06 and 1.24 eV correspondingly. The wavelengths were 350 ÷ 760 nm. The intensity of lighting was changed from 4 lx to 15 klx accordingly to power of lamp and lightfilter. The time of illumination was varied from 10 to 1500 hours.

In the third series the crystals subjected to action of ultraviolet and X-Ray radiation, with a wave length λ =250÷410 nm and λ =0,154 nm; λ =0,193 nm. An exposure of crystals by X-rays was made by X-ray diffractometer (DRON-2, DRON-0,5). The time of action varied from 3 minutes about 3 hours. Dose X-ray radiation 3R/min.
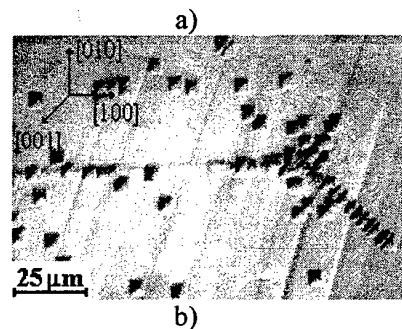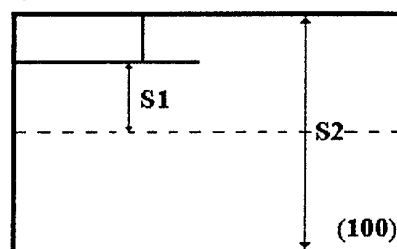
Fig. 1. a) Scheme of crack initiation. S_1 is distance between crack and axis of symmetry. S_2 is width of sample. b) The dislocation rosette of healing crack in LiF.

The behaviour of dislocations at tops of cracks is determined by the equation of equilibrium. At compiling of dislocations equilibrium (for dislocation emitted by a crack in a plane of a sliding) it is necessary to take into account stresses: operating on a dislocation from a leg of a crack $\tau^T(x_n)$, forces of an image τ_i, interaction of dislocations $\tau^D(x_n, x_j)$ and resistance of crystal to a shift τ_S. For the scheme of plastic current of a fig. 1b equations of equilibrium will look like the following:

$$\tau^T(x_n) + \sum \tau^D(x_n, x_j) - \tau_S - \tau_i = 0, \quad n = 1,2,...,m.$$

The behaviour of dislocations at tips of cracks will depend from a relation of stresses.

The plastic flow in the tip of a stopped crack in LiF single crystal was investigated by numerical modelling [1]. Two stages of dislocation structure formation in the tip of crack were discussed. The first stage is the formation of gliding lines in the moment of crack stop. The second is their evolution and partial crack healing. It was shown, that in condition of unloading a few dislocations moved out of crystal on the crack plane under affect of mutual repel and forces of reflection. As a result of the process the dislocation density is maximal at some distance from the crack tip. There is a dislocation free area nearly the crack tip.

It was experimentally found, that electromagnetic radiation changed dislocation structure at tip of the crack (fig. 2). The summary density of dislocations was lowered. The healing at the crack tip was observed [2].

a)

b)
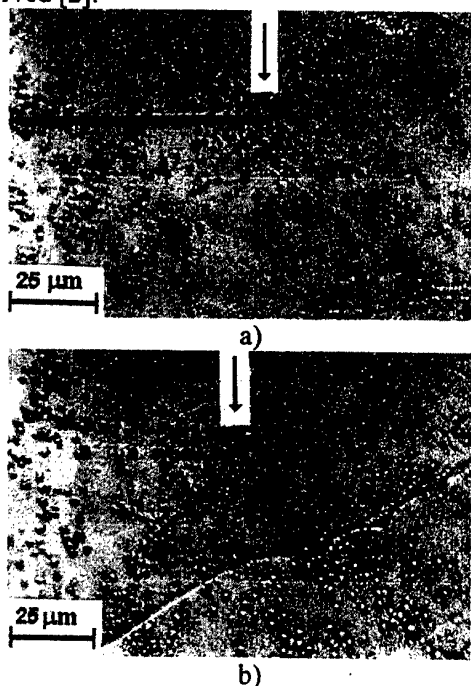
Fig. 2. Dislocation structure in neighbourhood of tip of cleavage crack in LiF single crystal to influence of X-Ray radiation E=6,25 keV: a) "Control" crystal, T=300 K. b) "Testing" crystal after t=5 min.

Electromagnetic radiation causes decreasing of mechanical stresses in tip of the crack of a reversible motion of dislocations and partial healing of the tip.

The exponential dependence of dislocation density both from temperature and from time of lighting was determined (fig. 3).

The intensity of healing and relaxation of stresses depends on material and spectrum of electromagnetic radiation. The processes of healing

and stress relaxation depend on intensity of electromagnetic radiation. The greatest effect is observed at action of a X-rays.

The influence of small doses X-ray radiation on processes of healing microcrack was investigated.

The action X-ray radiation results in stress relaxation in tip of cracks for account a reversible motion of dislocations was established. The intensity of healing and stress relaxation depends from a wave of length of a X-rays.
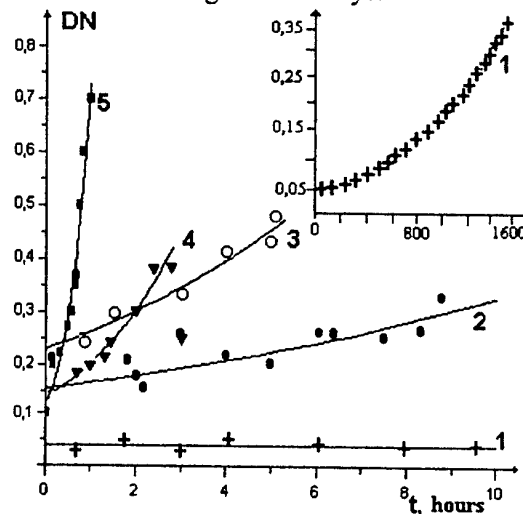
Fig. 3. The relationship between comparative changing of dislocations number at crack tip ($\Delta N/N$) and time (t) of treatment: 1. T=355 K, 2. λ=760 nm, 3. λ=350 nm, 4. λ=250÷410 nm, 5. λ=0,154 nm.

The effect of healing microcrack was incremented at diminution a wave of length. The mechanisms of stress relaxation and healing resulted from X-Ray radiation were discussed.

Conclusions

1. Electromagnetic radiation causes decreasing of mechanical stresses in tip of the crack and partial healing of the tip.

2. The intensity of healing and relaxation of stresses depends on material and spectrum of electromagnetic radiation.

3. The processes of healing and stress relaxation depend on intensity of electromagnetic radiation.

References

[1] G. Ortega and V. Reindbold. Iterative methods of a solution of systems of the non-linear equations with many unknown. Moscow, 1975, p.558.

[2] Feodorov V.A., Plushnikova T.N., Tjalin Yu.I. Healing of cracks, stopped in alkali-halide and calcite as a result of asymmetrical cleavage, Solid State Physics, 42, 4 (2000), 685-687.

452

RESEARCH OF MATERIAL'S CORROSIVE RESISTANCE OF COMPRESSOR BLADES WHICH ARE RETURNED TO SERVICE BY THE USE OF TITANIUM NITRIDE COATINGS

Tarasenko Yu.P., Tsariova I.N., Myshlyaev D.A.
Scientific and Production Company "Tribonika"

The surface protection of compressor blades in gas transfer equipment from atmospheric corrosion is one of the important problems.

At present time this task is salved, basically, at the cost of the use of anodic and cathodic protective coatings. However, in service conditions, because of medium's erosion action, the wear of protective coating occurs, and as a consequence of it, the intensification of corrosive processes is taking place. The task to increase the corrosive resistance of blades becomes the more vital in the development of repair and return to service techniques, which are intended to extend the service life of these critical parts.

The corrosion behavior of compressor blades' material – steel 12X13 – is studied in this work. The attacks of pearlite stainless steel under atmospheric corrosion are, basically, of pitting type. Under conditions of corrosive, industrial atmosphere and under humidity (especially in sea climate), when the action of active chlorine ions is enhanced, the nature of attacks is complicated up to pit and knife-line corrosion and to corrosion fatigue.

Owing to the physical simulation of different steps of pitting corrosion process are shown.

The pitting resistance of stainless steel 12X13 has been studied after the following technological operations such as machining, electropulse polishing, heat treatment (700°C, 2 hours) and after the applying of ion-plasma TiN coating. As a main method of study it was used the method of potential-dynamic, anodic, polarized curves in NaCl aqueous solution, which simulates the sea atmosphere. From the curves of forward and reverse direction there were determined parameters of pitting resistance (to GOST 9.912-89): potential of free corrosion E_{cor}, potential of pitting formation E_b, potential of repassivation E_{rp}, bases of pitting resistance:

The results of corrosion tests after different types of material's compressor blades treatment are given in the Table.

In initial condition the material had a negative value of potential of stable pitting formation. By electropulse polishing and owing to the surface microtexture's smoothing, the pitting resistance of stainless steel is increased. In this case, the parameter E_b displaces to the electropositive area, extending so the region of metal passive state. The heat treatment leads up to the further rise of all features. The increase of ΔE_{rp}. means that the repassivation, after pitting formation, is reached faster. The rise of anti-friction features is connected with the more uniform distribution of carbide phase and with the improvement of structure's homogeneity. The titanium nitride coating on steel favours the increase of E_b, ΔE_b, ΔE_{rp}. Here the presence of micro-porosity causes the local breakdown of the coating. Upon the whole, there is a positive effect of the cathodic coating owing to the electrochemical action of its portions on the anodic polarization of metal bared areas and to the maintenance of these portions in the passive state.

As result of technological operations, conducted on blades after service, the resistance to pitting corrosion is improved. The positive result of the use of titanium nitride coatings is confirmed by the results of climatic tests in salt-spray chamber (NaCl-46 g / l, t° = 35˚C), performed on compressor blades.

$$\Delta E_{rp} = E_{rp} - E_{cor}, \Delta E_b - E_{cor}$$

Type of treatment	Indexes of resistance, B				
	E_{cor}	E_b	E_{rp}	ΔE_b	ΔE_{rp}
1	-0,21	-0,09	-0,35	0,11	-0,14
2	-0,12	0,04	-0,31	0,16	-0,19
3	-0,16	0,003	-0,32	0,17	-0,16
4	-0,15	0,03	-0,14	0,18	0,004
5	-0,16	0,06	-0,15	0,23	0,02

1 - Initial condition (machining); 2 - Initial condition (machining + electropulse polishing); 3 - After use (machining + electropulse polishing); 4 - After use (machining + electropulse polishing + technical maintenance + electropulse polishing); 5 - After use (machining + electropulse polishing + technical maintenance + electropulse polishing + TiN coating).

PROPERTIES OF DIAMOND-LIKE FILM - POLYMER STRUCTURES USED FOR SOLAR MODULE ENCAPSULATION

Klyui N.I.[1], Korneta O.B.[2], Litovchenko V.G.[1], Makarov A.V.[1], Dykusha V.N.[1], Voronina O.O.[2]

[1]Institute of Semiconductor Physics, Kiev, Ukraine
[2]Kiev National University, Kiev, Ukraine

Introduction

In connection with gradually conventional energy sources exhaustion, at present the great attention is paid to alternative renewable energy source development. Among them the most prospective are solar and wind power station. A solar power station consists of solar batteries. The main part of the solar battery is a flat solar module (SM). For the module assembling mineral glass sheets are used as front and rear covers. Electrically connected and hermetically encapsulated solar cells (SC) are put between the covers. The covers are needed to protect the SCs against actions of degradation factors (rain, UV-radiation, dust, sand-storms etc.) and damage during transportation. Here special hardened glasses are used to increase endurance and strength of SM. Moreover, such glasses are needed to be of high transparency. The application of such materials provides long serviceability (10-25 years), but on the other hand, great financial expenditure is required.

The problem of cost decreasing for energy produced by SMs can be solved by means of component parts cost reducing. For this purpose, mineral glass cover can be replaced by a polymer one. At the same time, the SMs constructed with polymer application are of significantly less weight. However, modern polymer glasses has significant disadvantage, such as low hardness (SMs with polymer cover would be covered with small scratches during short time and lose the transparency), surface damage under the influence of ultraviolet radiation and atmospheric precipitation. (that also have influence on transparency). The mentioned disadvantages can be overcome applying special protective coverings on the polymer glass surface. Such covering must have good adhesion to the plastic, high hardness and transparency.

Present work is aimed to solving the mentioned problem by means of depositing DLC film on the surface of acrylic plastic.

Experimental

The DLC (a-C:H and a-C:H:N) films were deposited by RF glow discharge in a parallel plate reactor. The RF power (13.56 MHz) was applied to the lower electrode, the upper electrode was grounded. The gas mixture (CH_4, H_2 and N_2) was introduced through the upper electrsode in a showerhead flow configuration. The substrates for deposition were put directly on the lower electrode, which was cooled by water. The stainless steel chamber was evacuated to a base vacuum of about 10^{-4} Torr before each deposition run. The total pressure (P) of the reaction chamber was varied from 0.2 to 0.8 Torr. During a deposition process the RF-discharge power was fixed. The films obtained at different discharge power were deposited onto polymer substrate used for solar module production. The DLC films with different nitrogen contents were deposited from mixtures of methane, hydrogen and nitrogen by a gradual replacement of hydrogen by nitrogen. The nitrogen content in the gas mixture (P_{N2}) was changed from 0 to 30%. The film thickness was varied from 100 to 300 nm.

Optical constants of the films were measured by laser (λ=632.8 nm) and spectral ellipsometer. Transmittance spectra of the polymer+DLC film structures were also measured. The mechanical properties and wear resistance of the films were studied using a microhardness tester "Shimadzu HMV-2000, Japan) and 5130 Abraser device (USA), respectively. All measurements were carried out at room temperature.

Result and discussion

Tables 1 show results of light transmittance measurements obtained for a-C:H films deposited from CH_4:H_2 gas mixture at different RF-discharge power and total gas pressure in the reaction chamber. Integral transmission of the structures was measured using incandescent lamp.

Table 1. DLC-film thickness and DLC-film-polymer structure transparency in dependence on discharge power. (total pressure p=0.2Torr)

#	P_{rf}, W	T, %	d_{DLC}, nm
1	100	89	145
2	175	83.3	150
3	250	80	145

It is seen that increasing of RF-discharge power results in decreasing of DLC-film – polymer structure optical transparency. The transparency of the structure changes from 80% to 89%. The effect is connected with the light absorption in DLC film. Indeed, as was shown earlier [...], increasing of RF bias voltage of RF discharge power leads to formation of DLC-film with higher hardness, refractive index and extinction coefficient.

Obviously, increasing of k value is responsible for decreasing of the structure transparency. It should be pointed out that the transparency value is too high for effective use of the DLC-film – polymer structure for solar module encapsulation. Thus, it is evident that the DLC-film must meet requirements of high transparency, being at the same time rather hard, and, that is especially important, high wear resistance. For this aim, optimization of technological regimes at firm formation has to be carried out.

Table 2 DLC-film thickness and DLC-film-polymer structure transparency in dependence on total gas pressure. (RF-discharge power P_{rf}=175W)

#	p, Torr	T, %	d_{DLC}, nm
1	0.2	83.3	150
2	0.5	93	150
3	0.8	94	150

In the table 2 the results obtained for the DLC-film deposited at fixed RF-discharge power and various total gas pressure in reaction chamber are presented. One can see that significant increasing of the presented structure transparency is observed, when total gas pressure in the reaction chamber increases. The transparency may be increased up to 94%. Taking into account the transparency value for uncovered polymer (acrylic plastic) of 96.7%, the initial DLC-film transparency is close to 97.3%. Therefore, we can conclude that obtained transparency value is quite suitable for the DLC film application as a protective coating.

On the other hand the DLC-film – polymer structure demonstrates high wear resistance. It can be seen from abrasion test results, presented on fig.1. Indeed, there are many scratches on the uncoated polymer surface after abrasion test (fig.1b) while the polymer coated with DLC-film is almost undamaged.
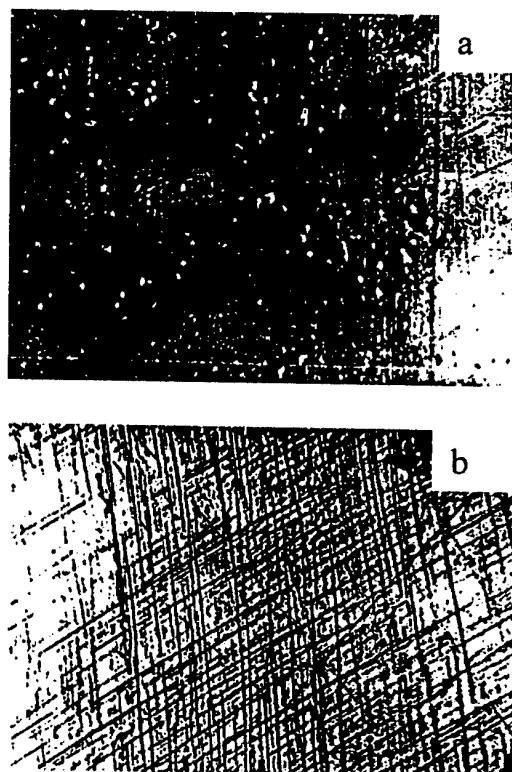
Fig. 1 Micrograph of DLC film –polymer structure (a) and uncoated polymer (b), after abrasion testing.

In conclusion, it has been shown that DLC-film can be successfully used as protective coating for solar module encapsulation.

References

1. A.Plessing, S.Degiampietro, P.Pertl Laminated film material for solar cell encapsulation and their influence on PV-module production and development // Proceeding of 2nd WCPSEC, pp.1915-1919

2. V.A.Semenovich, N.I.Klyui Diamond like carbon films: effect of deposition conditions on the optical properties // Journal of CVD.– 1995.- V.4, № 1.- P.29-37.

FORMATION OF COMPLICATED OXIDE COATINGS ON CARBON AND SILICON CARBIDE FIBERS BY THE SOL-GEL PROCESS

Zima T.M., Baklanova N.I., Karakchiev L.G., Lyakhov N.Z.
Institute of Solid State Chemistry and Mechanochemistry SB RAS, Novosibirsk, Russia*

Modern aerospace industry requires structural materials with low density, high strength and stability to oxidation at temperatures above 1000°C. The most promising materials are composites with ceramic matrix reinforced by ceramic and carbon fibers (CMC's). A thin barrier layer is deposited onto the fibers to increase the strength of the material. The major role of the barrier coating is to reflect microcracks that arise in the matrix. Besides, the coating provides connection between fibers and matrix, redistributes strain, acts as diffusion barrier and prevents fiber oxidation.

One of the methods to deposit the coatings onto fibers is sol-gel process. It allows obtaining multiple uniform coatings with controllable chemical composition, microstructure and density.

The goal of the present study is to study the thermal evolution and crystallization of sol-gel-derived coatings, composed of metal oxides and their mixtures, on carbon and SiC fibers.

Precursors for complicated oxide nanosized coatings were the sols of hydrated aluminium oxide (HAO), titanium dioxide (HTDO), zirconium dioxide (HZDO) and their binary mixtures. The sols were synthesized electrochemically from aqueous solutions of the corresponding metal chlorides. The concentration of disperse phase was varied within a broad range by diluting. The sols were deposited onto Nicalon cloth, TGN–2M cloth, carbon non-woven cloth by dipping, followed by treatment at 20-1000°C and 1350°C.

Sol properties were studied by means of Raman spectroscopy (RFS-100), auto-correlation spectroscopy of quasi-elastic light scattering, electron microscopy (H–600, Hitachi) using a cryofractographic BAF-400 Balzers device. Rheological properties of the systems were investigated with the help of a rotary viscosity meter "Rheostat–2.1". The phase composition of the samples during sol-gel-solid transition was

determined using X-ray diffraction (XRD) and thermal analysis. Crystallite size was estimated from the broadening of diffraction patterns. The coatings were studied by means of XRD and scanning electron microscopic (SEM) analysis.
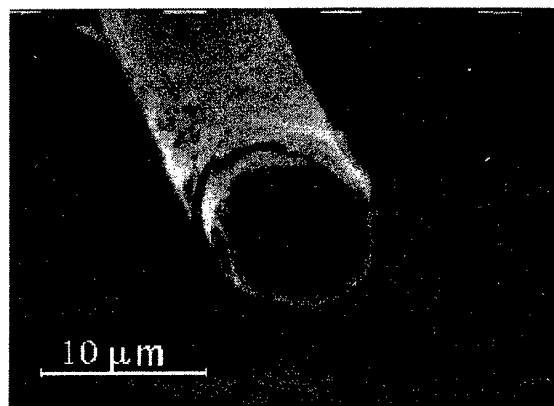
Figure 1. Sol-gel derived ZrO_2 coating on Nicalon fiber.
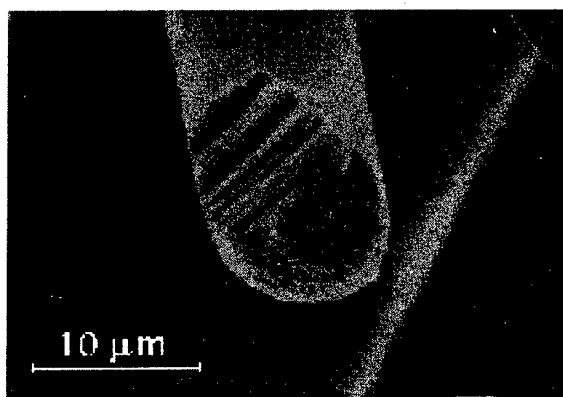
Figure 2. Sol-gel derived Al_2O_3-TiO_2 coating on Nicalon fiber.

The analysis of rheological curves suggests that HAO, HTDO, HZDO sols are stable, weakly structured systems. Concentrating them by evaporation causes the increase in pseudo-plasticity. During sol-gel transition, at the initial stage we observe a smooth increase of the system's density, then its sharp increase when 60–85 % of water is removed. Mixing sols we observe the

formation of gel. Gel formation rate, as well as the ability of sols to get homogenized and to get structured, depends on the nature of components and on their amounts. Immediately after mixing, the mixtures behave as Newton liquids. The character of structure formation changes with time. The particles of HZDO sol are spread uniformly; they are round with a mean diameter of about 5 nm. HTDO sol particles have a size of up to 10 nm; in zirconium-titanium sol, particle size is 11–15 nm. The particles have irregular disc-like shape and do not form any regular structure.

When treated at 25–900°C, the density of samples under investigation increases linearly. Specific surface and dispersity of the samples change in a more complicated manner. The size of alumina xerogel globules decreases with increasing temperature up to 450°C. Titanium dioxide conserved high dispersity till 450°C, anatase content being increased with temperature. A specific feature of the binary system Al_2O_3-TiO_2 is the stabilization of the amorphous state to 900°C and braking of the polymorphous transformation into TiO_2. Zirconium titanate is clearly observed in X-ray diffraction patterns of the ZrO_2-TiO_2 xerogel at temperatures above 600°C.

The microstructural observation of coatings deposited onto carbon and silicon carbide fibers show the dependence of the morphology of coatings on the properties of the sols of hydrated metal oxides. Fig. 1 shows a coating derived by dipping Nicalon twice into undiluted HZDO sol, followed by thermal treatment at 1000°C. One can see that undiluted sols and their mixtures form oxide layers that can be easily separated from the fiber and get cracked, depending on thermal treatment conditions. The use of diluted sols leads to the formation of thin layers composed of metal oxides or their mixtures on carbon and silicon carbide fibers. Fig. 2 shows an electron microscopic photograph of a coating formed after a single dipping of the Nicalon cloth into the binary mixture of the diluted aluminum oxide-titanium oxide sol with the component ratio 1:1, thermal treated at 1000°C. One can see that the coatings are dense, uniform in thickness, and they conserve topological features of the structure of monofilament surface. A distinguishing feature is the absence of monofilament binding to each other.

It is demonstrated that gel formation and drying are not accompanied by any noticeable growth of primary particles and aggregates. With increasing number of dippings, the uniformity of the thickness of coating is destroyed. The XRD data of multilayered coatings agree with the results obtained earlier for xerogels of the corresponding metal oxides and their mixtures.

Thus, it is demonstrated that the sol-gel procedure based on inorganic aqueous systems is a promising method to obtain complicated nanosized oxide coatings on carbon and silicon carbide fibers.

SPARK COATINGS FROM ALLOYS OF THE Ni–Cr–Al SYSTEM

Alfintseva R.A., Paustovskii A.V., Timofeeva I.I., Kurinnaya T.V., Kirilenko S.N., Pyatachuk S.G., and Kostenko A.D.

Institute for Problems of Materials Science, NAS of Ukraine, 3 Krzhizhanovsky Str., Kyiv, 03142, Ukraine

Investigations performed earlier [1, 2, 6] have shown that the conditions under which electrode materials form infinite solid solutions or intermetallic compounds with a low cold brittleness temperature should be considered most favorable. In this connection, spark coatings from alloys of the Ni–Cr–Al system on steel 45, which can combine high wear resistance and refractoriness were studied. As anodes for spark alloying (SA), the most characteristic alloys were chosen, namely, A1 which is a binary Ni–Cr alloy of eutectic composition according to the phase diagram presented in [3], A2 which is a ternary Ni–Cr–Al eutectic alloy according to data of work [4], A5 which is a ternary Ni–Cr–Al alloy located in the quasibinary Cr–Ni–A section according to data of work [5], and 6A which is a Ni–Cr–Al–Y alloy analogous to the second eutectic composition and is alloyed by 2 mass % of yttrium.

The influence of the phase composition of the anode on the following basic parameters of spark alloying of steel 45 were investigated:

- specific erosion of the anode Δa;
- gain in the cathode weight Δk measured for an area of 1 cm^2 at 1 s intervals;
- total erosion of the anode $\Sigma \Delta a$;
- total gain in the cathode weight $\Sigma \Delta k$ measured for the alloying time t = 10 min/cm^2;
-mean transfer coefficient of the material k$'$ = $\Sigma \Delta k / \Sigma \Delta a$ (at t = 10 min/cm^2).

SA was carried on an EFI-46A machine under the following conditions: a specific treatment time of 10 min/cm^2; an oscillation frequency of a vibrator of 100 Hz; a short circuit current of 1.5 A.

Electrodes for SA were made by two methods, namely, high-energy hot pressing in vacuum (HEHP) and melting in an arc furnace with a nonconsumable tungsten electrode in a protective atmosphere.

Cast and hot-pressed (HEHP) electrodes, as well as spark coatings from them were studied by microstructural X-ray analysis and X-ray phase microanalysis.

It has been shown that, in cast alloy 1A, a biphase eutectic structure, consisting of a Ni-based γ-solid solution and a Cr-based α-solid solution, is observed. An analogous phase composition is observed in hot-pressed alloy 1A.

In cast and hot-pressed alloys 4A and 6A, a triphase structure consisting of an α, γ, and β(Ni-Al) phase is observed.

In cast alloy 6A,the intermetallic phase Ni$_3$Y, located along boundaries of eutectic colonies, was detected. In hot-pressed alloy 6A, the oxide phase Y$_2$O$_3$ was identified.

Values of the parameters of SA of steel 45 with using anodes from aforementioned cast and hot-pressed alloys are presented in Table 1.

Table 1.

Chemical composition of the anode material, mass %	Initial state of anodes	Total weight gain $\Sigma \Delta k \cdot 10^{-3}$, g/cm^3	Total anode erosion $\Sigma \delta a \cdot 10^{-3}$, g/cm^3	Mean transfer coefficient k$'$=$\Sigma \Delta k$/ $\Sigma \Delta a$
1A Ni-50.5 Cr-49.5	Cast HEHP 900°C 1000°C	2.8 2.5 4.1	6.6 5.3 6.1	0.42 0.48 0.68
4A Ni-50.3 Cr-40.2 Al-9.5	Cast HEHP 900°C 1150°C	6.2 5.5 4.0	10.0 16.0 6.0	0.62 0.35 0.68
5A Ni-42.2 Cr-38.3 Al-19.5	Cast HEHP 900°C 1150°C	2.1 2.9 2.9	4.8 8.3 5.3	0.43 0.35 0.55
6A Ni-40.3 Cr-39.2 Al-19.5 Y -2.0	Cast HEHP 900°C 1100°C 1150°C	3.6 5.4 4.5 4.5	13.6 21.2 6.5 6.4	0.267 0.250 0.690 0.700

In the case of SA by cast alloys 1A, 4A, 5A alloys and by the same alloys obtained by the HEHP method at 1150°C, the mean transfer coefficients have almost the same values. In investigations of anodes pressed at 900°C, the values of the mean transfer coefficient are lower. This is connected with the smaller densities of anodes pressed at 900°C and differences in the phase composition as compared to anodes pressed at 1150°C. In SA by cast alloy 6A, the lowest transfer coefficient is observed. However, in SA

459

by hot-pressed alloy 6A, a 2.5-fold increase in the transfer coefficient is noted. It can be suggested that this is caused by the presence of the intermetallic compound Ni_3Y in cast alloy 6A, which results in its embrittlement and favors an increase in the fraction of the hard phase in erosion products of the cathode during SA.

The X-ray studies of spark coatings showed the presence of intermetallic phases containing iron and the metals of the anode. In the coating from alloy 1A (Ni-Cr), the intermetallic compounds NiAl, CrAl, and FeNi, as well as carbides FeC, and complex δ-NiOAl$_2$O$_3$ type oxides were detected. In the coatings from cast alloy 6A (Ni-Cr-Al-Y), a phase containing yttrium in the form of an oxide or an intermetallic component was not detected by radiographic analysis. In the case of SA by hot-pressed alloy 6A, the intermetallic phases NiAl, CrAl, FeNi, Al$_3$Y, and NiAlY were identified in the coating.

Wear resistance tests of the coatings were performed in a MT-68 test unit on 5x10.5x15 mm specimens in dry friction in air with a 65G steel counterbody.

In the tests, the friction coefficient f and the intensity of wear of a specimen I (mm/km) were determined.

The test conditions were as follows: a slip speed V = 10 m/s, a load of 5 kg. The test results are presented in Table 2.

Table 2.

Specimen No.	Initial state of the anode	Friction coefficient F	Wear I, μm/km
4A	Cast	0.27	175.5
	HEHP	0.27	50.5
6A	Cast	0.26	130.0
	HEHP	0.29	40.0
5A	HEHP	0.27	9.3
VK-3U*	sintered	0.30	10.0

* WC-Co-Cr

CONCLUSIONS

The investigations performed showed that, during SA of steel 45, intermetallic phases containing the metals of the anode and cathode formed. The wear resistance of the coatings obtained via SA by hot-pressed alloys is larger than that of the coatings obtained via SA by cast alloys. This is connected with the character of erosion of the cathode. The alloys of eutectic composition containing the intermetallic phase Ni-

Al and solid α-solution of chromium possess the largest wear resistance.

REFERENCES

1. Verkhoturov A.D., Podchernyaeva I.A., Pryadko L.F., and Egorov F.F., Electrode Materials for Spark Alloying. Moscow, Nauka, 1988.

2. Samsonov G.V., Verkhoturov A.D., Bovkun G.A., and Sychev V.S., Spark Alloying of Metallic Surfaces. Kiev, Naukova Dumka, 1985, 220 p.

3. Massalski B., Binary Alloy Phase Diagrams, ASTM. Metal Park, Ohio, 1 (1986), 842 p.

4. Kornilov I.I. and Mints R.S., Zhurn. Neorgan. Khim., No. 3, vol. III (1958) 699.

5. Kupchenko T.V., «Regularities of the substitution of aluminum in α+β eutectic alloys of the system», in: Phase Diagrams. Kiev, Naukova Dumka, 1984.

6. Verkhoturov A.D., Rogozinskaya A.A., and Timofeeva I.I., Formation of a Hardened Layer during Spark Alloying of Steels and Titanium Alloys. Moscow, Metallurgiya, 1989, 89 p.

THE RESISTANCE OF A CHROMIUM ALLOY AND YTTRIUM CHROMITE COATING IN THE CONDITIONS OF OXIDATION AND HIGH-TEMPERATURE SALT CORROSION

Oryshich I.V., Poryadchenko N.E., Zykova E.V.
Institute of problems of Materialscience NAS of Ukraine, Kiev, Ukraine

The traditional heat resisting alloys on a basis Ni, Co and Fe already have exhausted themselves: their working temperatures do not exceed 1100°C. Among metal materials the alloys on a basis chromium are represented as perspective one for gasturbine construction. Use as the additive to chromium of rare-earth metals (La, Y) in a combination with boron and elements (V, Ti, Ta) forming the carbides has allowed to receive a delute chromium alloy of system Cr-V-Ta-La [1], from which it is possible to produce rods, pipe, plates, sheet, foil and to use in little loading details working at above 1100° C. For protection against saturation of nitrogen during work in the conditions of high temperatures and agressive medium it was offered yttrium chromite coating [2].

In this work the heat resistance and resistance to high-temperature salt corrosion (HTSC) of a chromium alloy and the yttrium chromite coating put on him are investigated. The oxidation of an alloy was carried out on the samples by a diameter of 20mm and thickness of 5 mm in the muffle electric furnace at 900-1400° C for 1000 hours according to a technique [3], and HTSC - on cylindrical samples by a diameter of 10 mm and height 15 mm at 600-900° C for 20 hours according to a technique [4]. The tests of sulphate corrosion (SC) carried out both in pure sodium sulphate and in 90% Na_2SO_4+10% TE, where TE - threefold 48,7% $MgCl_2$, 38,2% KCl and 13,1% NaCl eutectic ($T_{m.p.}$=410°C), and of chlorite corrosion (CC) – in melted TE. The heat resistance of the materials was determined by the weight gain, the resistance to HTSC – by the weight losses. For the determination of the resistance of an alloy with the yttrium chromite coating the flat samples of a chromium alloy by the size 25x10x1 mm were used. The coating was formed by magnetron method. The thickness of he coatings in all cases was maintained at a level of 10 microns. In case of two-layer coating the thickness of a chromite layer was 7-8 microns and the thickness of a modified zirconium dioxide - 2-3microns.

As a result of the researches was established, that a kinetics of the oxidation of a chromium alloy submits practically to parabolic law, according to which the dependence of the weight gain (q) from time of exposure (t) is expressed by the formula q_p^2=k_pt. The determined quantities of a parabolic constant k_p for 900, 1000, 1100, 1200, 1300 and 1400° C is equal 0,002; 0,4; 0,7;4,4;64 and 324 $g^2m^{-4}h^{-1}$ accordingly. This will allow to determine q for any temperature and time of an exposure. The temperature dependence of heat resistance has an exponential dependence. The heat resistance of a chromium alloy many times over exceed those of the most heat resisting alloys on Ni, Co and Fe bases [3] and itself chromium [5]. It is connected with the positive influence of lanthanum, as lanthanum oxide form with chromium oxide a lanthanum chromite ($LaCrO_3$) at the bondary surface between the metal and the scale. The presence of lanthanum chromite in the scale strengthen her bond with the matrix of an alloy (coherence of the scale) and brake chromium diffusion in the scale and oxydgen diffusion into an alloy. It was revealed the chromium nitrites (Cr_2N) under the oxide layer by metallographic analysis as induvidul choins at 1200°C, then as rough segregation at 1300°C and the continuous layer at 1300°C. The constant k_p thus strongly grew, though the kinetic dependence remained approximately parabolic. Simultaneous nitrogenizattion and oxidation of an alloy caused appreciable deterioration of his heat resistance. So, the thickness of scale at the maximal exposure for 1000hr was increased from 15-20 microns at 1200°C up to 120-150 microns at 1300°C and 250-280 microns at 1400°C. In last two cases she was chopped off from a surface of samples, that testifies to low heat resistance of an alloy at this temperatures.

The resalts of researches of resistance of a chromium alloy to high-temperature sulphate and chlorite corrosion have shown (tab.1), that it is especially strongly shown in the melts of salts.

Table 1 - Dependence of the weigh losses (g/m^2) of an alloy from the temperature and composition of salts, t = 20 hr.

Composition of medium	Temperature, °C				
	600	700	800	900	1000
Na_2SO_4	0,1	0,15	0,28	10,0	122,0
90% Na_2SO_4 + 10 %TE	2,5	7,0	25,0	56,0	120,0
ТЭ	17,0	55,0	240,0	1200,0	4500,0

Table 2 - Dependence of the hot-corrosion resistance of an alloy (g/m^2) from the compostion of a coating

Composition of a coating	Oxidation, 1300°C, 100 hours.	90 % Na_2SO_4 +10 % TE, 20hours.	TE, 900°C, 20 hours.
Chromium alloy	21,0	56	1200
$YCrO_3$	1,2	2,5	22,0
$YCrO_3$ + ZrO_2 (Y_2O_3)	0,78	1,3	13,2

If the salt is in a firm condition, for example, $Na_2SO_4(T_{m.p.}$ =883°C), she (it) practically does not work on metal, and under a film of salt (salt) there is practically usual oxidation. Therefore pure (clean) salt Na_2SO_4 strongly influences metal, since 900° C, and its (her) mix with TE $(T_{m.p.}$ =550° C), as, however, and itself TE $(T_{m.p.}$=410°C), on all the investigated temperature interval. Let's note, that salt melts at rather low temperatures influence metal much stronger, than gas medium at much higher temperatures and exposure (1300° C, 100hr, tab. 2).

As a whole it is necessary to consider, that the resistance of an chromium alloy to SC is much higher, than known heat resisting and corrosion-proof alloys on Ni basis [6]. In chlorite melts he is exposed to corrosion rather strongly and his resistance much below, than above named. The kinetic dependence of sulpfate corrosion is between linear and parabolic (1<n<2), and chlorite submits to the approximately linear law (n~1,0). As against the heat resisting of Ni alloys given a chromium alloy is designed for work at temperatures of the order 1200°C.

The results of influence of protective coatings on the resistence of a chromium alloy to oxidation and HTSC are given in tab. 2.

It was established, that protective chromite and two-layer chromite- zirconium dioxide coating strongly raise resistance to oxidation and high-temperature sulphate and chlorite corrosion of a chromium alloy. In comparison with a metal matrix their resistance to oxidation grows in of ~25 times, resistance SC - in~40 times, and CC – in~90 times of a sample. Thus, a chromium alloy can be used up to 1200°C, and at higher - with application of the protective coating on base yttrium chromite and zirconium dioxide.

REFERENCES

1. Ракицкий А.Н., Трефилов В.И. //Порошковая металлургия.-1977, № 9.-С. 62-72. 2.Ракицкий А.Н., Зыкова Е.В., Порядченко Н.Е., Орышич И.В.//Сб. тр. Nowe Kerunki i badanie technologi Materialowych. redakcja naukova, J.Ranachowski, J.Raable, W.Petrovski. Warszawa: YPPT PAN. 1999. C. 329-332.

3. Никитин В.И. Расчет жаростойкости металлов. М.: Металлургия.- 1976.- 207 с.

4. Орышич И.В //Защита металлов.- 1981.- т. 17, № 1.- С. 74-79.

5. Салли А., Брэндз Э. Хром. М.: Металлургия.- 1971.- 360 с.

6. Никитин В.И // Изв. АН ССР. Металлы.-1985.- № 1.- С. 176-181

ESTIMATION OF THE PROTECTIVE PROPERTIES OF THE Y-Cr-O SYSTEM COATINGS BY ELECTROCHEMICAL METHODS

Scherbakova L.G., Zykova E.V., Poryadchenko N.E.
Institute of problems of Materialscience NAS of Ukraine, Kiev, Ukraine

For increase of heat resistance of the chromium-base alloys at the temperatures more than 1273 K in a nitrogen contaning medium it is used an yttrium chromite coating [1]. The protective properties of the coatings are substantially determined by their phase composition: the presence in a coating Y or Y-O phases worsens their heat resistance. Taking into account essential distinction in a chemical resistance and an electrochemical behaviour of chromium and yttrium and their oxides in acid electrolyte for an estimation of quality of coatings and presence in them of Y are offered to use electrochemical methods, in particular, anodic polarization of samples with coatings in various areas of potentials depending on the put tasks.

Technique of experiments

The Y-Cr coatings was deposited on the substrates of high chromium VKh-2K alloy by a ion-plasma method with the following annealings for the formation of necessary structure and composition. For realization of electrochemical researches a P-5848 potentiostat with KSP-4 self-recoder, standard 3-rd electrode cell with divided anodic and cathodic spaces, an chlorine-silver electrode of comparison and platinum auxiliary electrode were used. Polarization of the samples was carried out in 0,5 M H_2SO_4 solution at the room temperature in conditions of natural aeration.

The Y-Cr coating as against Cr and his basis alloys at anodic polarization does not passivate and in the field of steady passivation Cr is dissolved with speeds in 200-400 times above. Using these differences, the combined method of an estimation of thickness of the deposited coatings and distribution of Y deep into them was offered. It was carried out alternate galvanostatic laminoetching ($i=5mA/cm^2$) of coating with the following polarization in the field of steady Cr passivation. An operation was carried out before occurrence of ability for a surface to passivate anodically. From coulonometric measurements the thickness of a yttrium containing coating was counted.

For study of influence of phase composition, the regimes of forming annealing and the action of gaseous medium on the protective properties of coverings it was used the comparative analysis of the volt-ampere curves which have been taken off in area of Cr repassivation (E>1,15V). The anodic dissolution of chromium in this area of potentials is controlled by a stage of his oxidation up to Cr^{+6}. Moreover, the places of primary course of process are a various sort of the defects in a film of oxides, that allows to estimate their quality [2].

Results of experiments

Influence of composition of initial coverings. The Y-O coating does not passivate and in area of repassivation is dissolved with higher speeds, than VKh-2K substrate, owing to dissolution Y. The research of an anodic behaviour of the Y, Cr and O containing films in various ratio and sequence of deposition of layers has shown, that the currents of dissolution of coatings grow in a sequence YCr+YCrO+CrO<YCrO<YCr+YCrO< VKh-2K. The counted total defection of a coating (initial porosity and appearing one as result of dissolution Y) grows in this line with 1.4 up to 20.0%. The films formed on the surface of VKh-2K during oxidation in air (1473K, 5 hours) have the high protective characteristics. The process of anodic dissolution is realized only at the increase of the oxidizing potential of a system on 0,10-0,16V (E>1,3V) in comparison with the unprotected alloy. Hence, the increase of the chromium oxides contents especially as the top layer and the decrease of the yttrium contents in unannealing coatings it is resulted in improvement of their protective properties.

Properties of coatings after the annealing. A forming annealing (FA) in oxygen of Cr-Y containing coverings results to formation on all depth of stable $YCrO_3$ and Cr_2O_3 phases. The speed of anodic dissolution of such coatings sharply falls, the process of dissolution carries local character and is realized on the defective places and pores, share which does not exceed 0.3% of the area of a coating. The protective characteristics of monolayered YCrO and two-layered YCr+YCrO coatings after the forming

layered YCr+YCrO coatings after the forming annealing practically are the same. However, during the thermocycling (1473K, 200cycles) in a lesser degree, and at the tests in N_2(1473K, 5hours) in the greater degree it is occurred of the formation of defects in a YCrO coating, owing to what anodic overpotential decreases at simultaneous growth of currents of dissolution. The protective properties of a YCr+YCrO coating after the 5- hour exposure in N_2 at 1373K are kept, i.e. the temperature of nitrogenization essentially influences on the formation of defects in a coating. The inclination of a linear dependence lgi-E of the anodic curves received on the VKh-2K samples without and with the coatings without FA, after nitrogenization decreases, while on the samples with the coatings subjected FA, it remains constant. It is supposed, that the observable changes in the coatings without FA are connected with formation during

nitrogenization at T>1473K nitride Cr_2N, which is dissolved owing to the instability in acid medium. In the subjected FA coatings the formation of defects is connected, mainly, with the mechanical destructions of the coatings both at the thermocycling and at the nitrogenization.

Thus, use of an electrochemical methods allows to optimize composition of the initial coatings, the regimes of forming annealing and to supervise preservation of the protective properties of the coatings at the operation in nitrogen containing medium.

REFERENCES
1. Bega N, Jyabokritsky V., Kalashnikova L., Poryadchenko N. at al./Protective coatings at the metals. K.:Naukova dumka, 1991, v.26 p.61 (in Russian).
2. Jagupolskya L., Shcherbakova L., Gordonnya A.,Franzevitch I. DAN SSSR, 1984, v.287, p.938 (in Russian).

WORKING OUT OF LASER COVERAGES

FROM COMPOSITE MATERIALS

A.P. Shatrava

Physics-technological institute of metals and alloys, NAN of Ukraine, Kiev, Ukraine

One of actual tasks of contemporary machine-building is rise of resources of faultless engines work and mechanisms, going in conditions of high loading and intensive friction, limited lubricant. By Most effective decision of this task is use in pairs of friction of high technology antifriction materials.

By most perspective materials, answering to contemporary requirements on antifriction, wear resistance and to other properties, are composition materials. So, for example, for making of sliding bearings bushes start to widely to make use of composition: Bronze + reinforcing particles on iron base in global and lamella form.

In most cases such materials get by methods infiltration, baking, or by dint of dispersion standard materials on base Fe-Al; Fe-Cu and Cu-Al. However by most problem in given case is a size heterogeneity and irregularity of phase composition, low durability, and also efforts concentrators presence in structure, being generated during baking.

On other, the by volume production methods of composition materials are in row of cases ineffective and uneconomical. Above all things this related to that, that a most significance for detail work longevity have quality and official descriptions of her superficial working layer, and not detail in volume. For hardening and renewal of details surfaces all more frequent use the local influence methods with application of concentrated energy sources: laser and electronic ray, plasma arc, shock wave and oth., in that number and coverage's drawing methods by the medium of given energy sources.

For example, compatibility question of chafing materials attached to use of coverages. The questions, bearing upon forming processes of composition materials on details surfaces by the medium of laser hard facing, practically not studied.

Attached to selection of most meaningful criterions in given work basic attention spared to phase composition of coverage, as determinative, affecting physical and chemical properties of superficial layer, and to coverage quality with point of coupling durability viewing with surface of base and his operational properties. Originating from requirements to materials with point of viewing of optimum friction conditions and wear in researches object quality were select the compositions on base steel 9X18 and bronze OCS 3-8-6 with diverse by volume components maintenance in composition of cover material.

For laying of experimental process researches of laser hard facing of composition materials used an universal technological complex "Comet-2M" on the basis of CO_2-laser by nominal power 1 kW.

For process realization of laser hard facing were worked up and made proper adaptations, allowing to realize a serve of cover material in processing zone and to remove a purveyance in relation to laser radiation.

A given technological complex allows to realize a processing, as flat surfaces, so and rotation bodies surfaces on diverse set routines of heating (heating source shift speeds in relation to detail, serve reagent and inert gases, change of focusing spot diameter). A Laser powders hard facing from steel and bronze took in inert gas (Ar), which profited in quality of powder transporting (expense Gr = 20-30 l/h) attached to serve by dispersion 50-150 Mk.

As most effective coverage's drawing method used laser gas-powder hard facing with serve of cover material immediately in processing zone. Cover powder gave under corner 45(to axis of laser radiation after to moving of laser ray expense of which changed in limits (Gпm = 7-20 g/min).) (By power Closeness of thermal source put together Wp=1-4x108 W/м2.)

For lying of trials on wear of got coverages used installation of friction, on which the trials took around in conditions of dry friction.

For receipt technology optimization of composition coverage's were done experimental researches for three previously select factors: power of thermal source, speed of his shift and focusing diameter.

From findings visibly, that with power closeness growth the geometrical dimensions of

hard-faced layers increase. Increase they, also and with exposition time growth of thermal source.

For study of structurally phase composition of got coverage's and elements distribution morphology of composition structure were priced such parameters as: percent inclusions maintenance, middle inclusions dimension, middle inclusions area and oth.

The Most stable dimensions of steel and bronze inclusions and closeness of their packing typical for coverage's with 20% is by percent maintenance of one of constituents (Fig. 1).
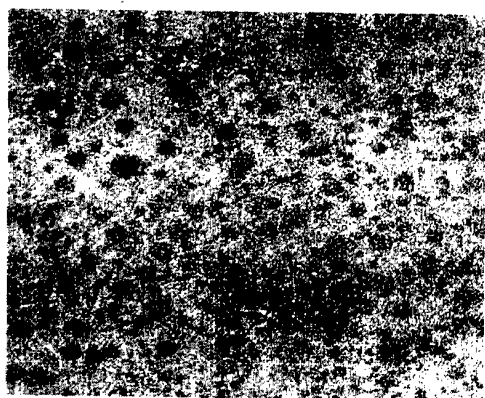
Fig. 1. Distribution in coverage of steel particles (20% Steel + 80% Bronze). Coverage height 1,95 mm. (Magnification. 300)

A structure-phase and h-rays analysis of single bronze inclusions and steel showed a presence in them, in first case of steel-containing phase, and in second bronze-containing phase. This explains, on visible that, that in process their coalition is able "put" some part of matrix.

With rise of amount of bronze in composition of material coverage's surface hardness smoothly rises for compositions to 40% maintenance of bronze, and after that severally falls, remaining, however above, than in initial steel. Rise of coverage hardness explains, presumably, by hardening of steel phase during heating and cooling (tempering from liquid fortune), which, not looking at augmentation of amount of bronze, raises general hardness. A tempering of steel phase with rise of amount of heat-conducting material is more effective. After that, beginning with composition with 40% bronze, a steel phase loses its integrity and gets across in inclusions in overhead part, and after that and on all coverage thickness.

For study of distribution of chemical elements in coverage's coverage to and after their trials on wear, took their h-rays analysis.

Results comparison of h-rays coverage's analysis to and after trials on wear shows considerable (on a par on 20 is 30%) copper maintenance augmentation on coverage surface after trials cycle. Given researches took on standards with pressure 15,3 MPa attached to trials on wear. This allows to draw a conclusion of bronze bearing-out on friction surface.

Balancing trials results on wear of composition coverage's attached to diverse loading one can be drawn a conclusion of that, that attached to small loading by best indexes describe coverage's with 20-30% bronze, and attached to more high coverage loading with 70-80% bronze (Fig. 2).
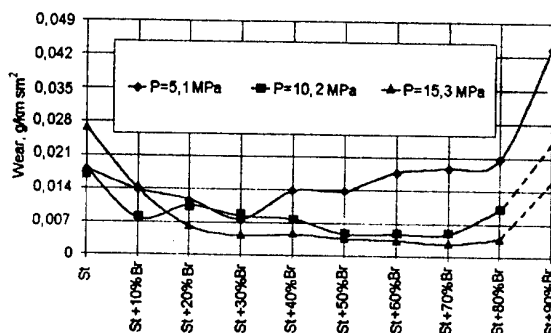
Fig. 2. Wear level of composite coverages of different stuff with different load.

Attached to rise of loading takes place intensive bearing-out of soft material on friction surface, (that is born out by data of h-rays analysis), and the evenly distributed steel (for compositions III of group) inclusions play a role "framework", which on one does not prevent to penetration of soft material on surface, and with other does not allow coverage to become deformed attached to high loading. Consequently, attached to raised loading a soft phase darts out on surface and is by hard smearing attached to friction, and hard carries on oneself basic loading.

Composition laser coverages were drifted on working surfaces of experienced details parties, which walked for trials in conditions of industrial exploitation. Comparative exploitation analysis of tooled details with initial, showed an essential (1,5 2,5 times) firmness rise first, that allowed to be accorded considerable economic effect.

466

TRIBOLOGICAL CHARACTERISTICS OF SPARK COATINGS OBTAINED FROM TiN AND TiB$_2$ BASED ELECTRODE MATERIALS WITH SUBSEQUENT LASER AND SOLAR RADIATION PROCESSING

Paustovsky.A.V., Frolov G.A., Tsyganenko V.S., Novikova V.I., Lityuga N.V., Kostenko A.D., Yegorov F.F.

Franthevich Institute for Problems of Materials Science of the Ukraine NAS, Kyiv, Ukraine

The refractory materials with plastic component addition are widely used for fabrication wear-resistance coatings in mechanical engineering [1]. To such materials concern TiN, TiB$_2$ with the additives Cr, Ni, Mo.

In the present work the combined coating methods are used: spark treatment (ST), spark treatment and laser processing (ST+LT), spark treatment and solar radiation (ST+SR).

As an electrode material the materials on base TiN+ (Cr, Ni), TiN+(Ni, Mo), TiB2+(Ni, Mo) are chosen. ST carried out in spark unit EFI-46A in a mode (I=1,5A, C=300 □F). Laser treatment is carried out in unit Quantum - 15 in a mode (E=2,5 J). A solar irradiation carried out in unit SGU-2 at a thermal flow of 11-12 MW/м^2.

Trybological investigations are carried out in unit MT-65 at sliding speed of V=10 м/sec at P=50 MPa under the circuit the stitch - in - shaft on air.

The characteristics of friction factor (f) and wear rate (I micron/km) are investigated.

It is established that friction factor (f) decreases by 40 % for all the materials in study after processing of steel ST+SR in comparison with a coating method ST+LT, and it is a little bit less, than for a coating from ST, excepting a TiB$_2$ based material, for which f is a little bit higher (Figure).

The wear rate is changed also ambiguously. So for TiB$_2$ - based material the values of wear rate are identical to all kinds of processing and have made 7,3. For TiN+(Cr,Ni) and TiN+(Ni,Mo) based materials the wear rate is less at ST+SR (3-7). The highest values of wear (12-17) are observed after ST+LT (Figure).

Thus, the comparative results for TiN and TiB$_2$ based materials at the combined coatings have shown that the friction factor after processing ST+SR for all specified materials is decreased by 40 % in comparison with coatings after ST+LT.

The wear rate values decrease by the factor of 3-5 for TiN-based coatings after ST+SR in comparison with such value after ST+LT.

The wear rate for all the kinds of processing is identical to TiB$_2$-based materials.
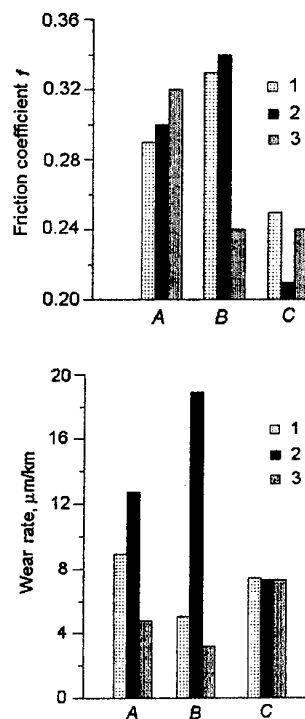
Figure. Friction coefficient f and wear intensity of the coatings from TiN-(Cr, Ni) (1), TiN-(Ni,Mo) (2), and TiB$_2$ - (Ni,Mo) (3). АST; ВST+LT; СST+SR

References

Verkhoturov A.D., Podchernyayeva I.A. Pryadko L.F., Yegorov F.F. Electrode materials for spark treatment. - Moscow: Science. 1988.

FEATURES OF GROWTH AND STRUCTURE OF IRON FILMS

O.K. Dvoynenko
Institute for Problems of Material Science of the National Academy of Sciences of Ukraine, Kyiv, Ukraine

Methods of thermal evaporation and constant current cathode sputtering are generally used for preparation of iron films.

The magnetron sputtering at constant current is the perspective method for a production of various material films.

The advantages of the films produced by the magnetron method are as follows: no porosity; high film adhesion to a substrate; a similarity of chemical compositions of the target and the film; the proximity of the film and bulk material properties at definite thicknesses.

The difficulty of magnetron preparation of iron films is connected with the shunting of the magnetic field by material of the target.

In the present work the shunting was diminished by means of the special target construction and its 10 - 15°C overheating as compared with Curie temperature. The target is shown on figure. It consisted of several rings. The surface of the working ring (1) was sputtered. Other rings (2,3) were served to cool the first one and to depress the shunting.
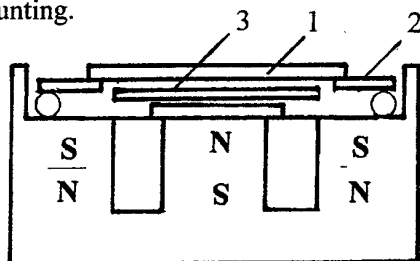
Figure. Scheme of magnetron target for sputtering.

The sputtering was made with the vacuum-pumping equipment with the built-in magnetron at the next parameters: the absolute pressure of Ar - 1.3 Pa; the voltage - 300-400 V; the cathode current - 2.2 A; the deposition rate ~1.5 nm/sec.

The structure of the films was analyzed by the electronograph EG type and X-ray diffractometer.

The influence of the film thickness on its structure was investigated for the films with thickness from 25 to 300 nm. The mixture of the body-centered (α) and face-centered (γ) phases of iron were found in the films of 25 -200 nm thickness.

The films with thickness more than 200 nm had the body-centered structure, like the structure of bulk iron specimen.

A nucleation of iron films don't depend from the substrate material and the deposition method [1-2]. The islands structure formation was observed at first growth stages. With the film thickness increasing the islands were merged and formed solid layers.

Super thin films were amorphous. With increasing of the film thickness the formation of the mixture of body-centered (α) and face-centered (γ) phases of iron was observed in case of epitaxial film growth [3-5].

In the present work the formation of two phases (α and γ) iron films was observed as in [3].

The formation of the unique α -structure was observed for the iron films with thickness over 200 nm.

Thin iron films evaporated on transparent substrates prepared by magnetron sputtering are perspective as matrixes for the biocorrosion study.

Using of these films allowed to measure and to compare the corrosion activity of different species of bacteria.

1. Takeshita H. et. all. Scanning tunneling microscopy study of ultrathin Fe films grown GaAs (001) surface// Jap. J. Appl. Phys. Pt 1. 1995. 34, N28. p. 1119-1122.
2. Fnidiki A.et all. Tb/Fe multilayered films studied by conversion electron Mossbauer spectrometry and Kerr effect//J. Phys. Sec. 4. 1992. 2, N3. p.251-255.
3. Detzel Th. Epitaxy and thermal behaviour of metastabile metal films// Progr. Surface Sci. 1995. 48, N1-4. p. 275-286.
4. Goigtlander B. et all. Epitaxial growth of Fe on Au(111): a scanning tunneling microscopy// Surface Sci. 1991. 225, N3. p. L529-L535.
5. Arnott M.et all. Growth and thermal properties of fcc iron films on Cu(100)// Surface Sci. 1992. 269-270. PtB. p.724-730.

Sc_2O_3 LASER MIRRORS

Andreeva A.F., Kasumov A.M.

Institute for Problems of Material Science of the National Academy of Sciences of Ukraine, Kyiv, Ukraine

The development of laser mirrors with strong beam stability and high working resource is urgent problem on nowadays. These mirrors are important under various applications such as the development of powerful eximer laser resonators, which are used in apparatus for metal cutting and quenching; printed - circuit cards production; automatic cutting of various materials and etc.

In this work the condensation conditions, optical and dielectric properties of the Sc_2O_3 thin films and $Sc_2O_3-SiO_2$ multilayer mirrors were investigated.

The SiO_2 films were evaporated in the vacuum $1 \cdot 3 \cdot 10^{-3} Pa$. The Sc_2O_3 films were obtained by using the metallic Sc reactive deposition method in O_2 atmosphere [1-3].

The Sc_2O_3 thin films had good dielectric and optical properties. Their specific electrical resistance constituted $\sim 10^{13} Ohm \cdot cm$ at 300K, dielectric loss $\sim 10^{-4}$, refractive index - 2.1. Films were highly transparent in the wide spectrum range and had small light dispersion loss.

The Sc_2O_3 films properties were practically independent on the O_2 pressure (P) and on the deposition rate (V) in the wide diapason of parameters at the evaporation.

In figure 1 the Sc_2O_3 thin films refraction index depending on P/V is shown. The value of the Sc_2O_3 thin films refraction index coincided with the data of the work [4].

The structure and properties of the Sc_2O_3 films were more dependent on the condensation temperature.

At T_c lower than 340^0C the quasiamorphous Sc_2O_3 films were formed. At $T_c \sim 340^0C$ their crystallization began and at $T_c \geq 350\ ^0C$ the cubic C-phase was stabilized, and the gradual increasing of the coherent dispersion blocks were observed. The refractive index, the absorption coefficient and the light dispersion loss were dependent on condensation temperature.

The photon energy dependence of the Sc_2O_3 films absorption index (α) is shown in figure 2 for the different condensation temperatures of films.
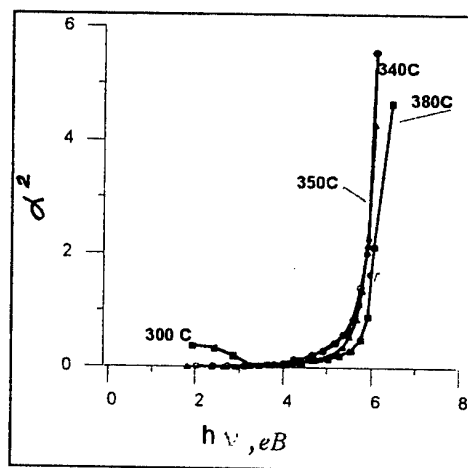
Figure 2. The square of absorption index (α^2) of Sc_2O_3 films as function of $h\nu$ for different condensation temperatures ($\bullet$ -330; $\bullet$ -340; $\bullet$ - 350; $\bullet$ -360; $\bullet$ -380^0C).

The edge of proper absorption range was about 5-6 eV. The Sc_2O_3 films were transparent in the spectral range 190 nm - 10 μm .

The absorption index was $\sim 10^4\ cm^{-1}$ in the transparency region. In the proper absorption region α was increased by the square law. The band gap of the Sc_2O_3 films was 6 eV. This value coincided with the published data [4].

The Sc_2O_3 films using is perspective as high refractive, protective and corrosion resistant layers,

Figure 1. Refractive index of the Sc_2O_3 thin films as function of P/V.

interference filters and laser mirrors for high energy optics [5-7].

The interference mirrors were obtained by the in-turn coating Sc_2O_3 and SiO_2 films with the formation of multilayer covering on optical SiO_2 substrate.

The laser mirrors based on Sc_2O_3-SiO_2 were obtained for using at the wavelengths $\lambda=0.193$-0.650 µm. The value of reflection coefficient maximum was determined by the number of Sc_2O_3-SiO_2 bilayers. Regarding the technical specifications its variability was from 50 to 99.7 %.

The interference mirrors of Sc_2O_3- SiO_2 had a very small light dispersion loss ($< 10^{-3}$ %) and a high resistance to powerful energy irradiation.

The light dispersion loss value depends on the condensation temperature (figure 3).

Figure 4. Spectral transmission of laser mirror before (a) and after (b) the permanent irradiation (2500 $W \cdot cm^{-2}$, 120 s).

The optical and dielectric parameters, the mechanical and wet-strength of Sc_2O_3-SiO_2 interference mirrors were compared to the parameters of the best mirrors according to published data [1, 2], as the result the irradiation strength of this mirrors was proved to be higher.

Figure 3. The light dispersion loss of SiO_2-Sc_2O_3 laser mirror σ as function of condensation temperatures T_c ($\lambda= 630$ nm).

The irradiation resistance was investigated by the constant and impulse signal operation.

At permanent irradiation the power of light stream applied was 20-2500 $W \cdot cm^{-2}$. At pulse irradiation was used the wave length 0.308 µm, the pulse duration - 70 ns, the beam diameter - 0.1-0.2 mm.

33 laser mirrors were investigated. The majority of mirrors (87%) did not change the parameters after permanent irradiation 2500 $W \cdot cm^2$ during 120 s.

In the figure 4 the spectral transmission of laser mirror before (a) and after (b) the permanent irradiation 2500 $W \cdot cm^{-2}$ during 120 s is shown. One can see, that the films mirrors did not change the optical characteristics. The threshold of mirrors destruction by pulse irradiation was higher than 3000 $W \cdot cm^{-2}$.

1. Андреева А.Ф. Получение и свойства пленок оксидов РЗМ // Порошковая металлургия. 1998. № 1–2 / 98. С.107 - 110.

2. Heitmann W. Reactively evaporated films of rare earth oxides // Vakuum-Technik. 1973. Band 22 № 2. P. 49 - 55.

3. Colen M., Bunshach R.F. Synthesis and characterization of Y_2O_3 deposits // J. Vac. Sci. and Technol. 1976. Vol.13. № 1. P.536-539

4. Абрамов В., Ермошкин А., Кузнецов А. Оптические свойства и электронная структура-Y_2O_3 и Sc_2O_3 // ФТТ. 1983. Т. 25. № 6. С. 1703 - 1711

5. Андреева А.Ф., Касумов А.М. Структура и оптические свойства пленок оксида скандия. Вопросы атомной науки и техники, вып 2(10), 1999, с.79-81.

6. Rainer F., Lowermilk W.H., Milan D. et al. Materials for optical coatings in the ultraviolet // Appl. Optics. 1985. Vol. 24 . № 4. P.496-500.

7. Andreeva A.F. et al. Growth conditions, optical and dielectric properties of Y_2O_3 films // Phys. stat. sol. (a). 1994. Vol. 145. P.441 - 446.

471

THE INFLUENCE OF THERMOCYCLING ON THE STABILITY OF THERMOELASTIC MARTESITE TRASFORMATION CHARACTERISTICS IN Fe-Ni-Co-Ti ALLOYS

Shevchenko O.M., Kozlova L.E.[1]
Institute of Materials Science Problems named by I.N.Frantsevich NAS of Ukraine, Kiev, Ukraine
[1] Institute of Magnetism NAS of Ukraine, Kiev, Ukraine

The aging Fe-Ni-Co-Ti alloys with thermoelastic martensite transformation are developed and investigated long enough [1-5]. Small temperature hysteresis and complete reverseability of $\gamma \leftrightarrow \alpha$ transformation in these alloys is reached by creating the micro-heterogeneous structure on austenite aging and using the magnetic ordering influence on the martensite transformation. Practical application of the above alloys with shape memory usually requires lengthy operation at the conditions of cyclic temperature variation. Thus, the influence of thermocycling over a temperature range of $\gamma \leftrightarrow \alpha$ transformation on features of the latter in Fe-Ni-Co-Ti alloys for a small number of thermocycles (30) was studied.

The alloys with different thermal hysteresis (H) of martensite transformation 1 – Fe-30.2%Co-18.0%Ni-7.8%Ti (H=40K), 2 – Fe-34.8%Co-19.3%Ni-7.2%Ti (H=95K), 3 - Fe-36.7%Co-17.9%Ni-8.1%Ti (H=125K), 4 – Fe-30.5%Ni-19.4%Co-5.6%Ti (H=25K), 5 – Fe-26.5%Ni-23.5%Co-6.6%Ti (H=270K) were melted in an induction furnace in argon atmosphere, hot rolled and homogenized at 1373K, then the specimens were water quenched from T=1423K and aged in a salt bath: alloys 1,2,3 at T=923K during 20, 10 и 2 min respectively, alloy 4 – at T=973K 30 min, and alloy 5 was investigated in the quenched state.

The characteristic temperatures of $\gamma \leftrightarrow \alpha$ transformation and the Curie point of austenite were found by examining the temperature dependencies of magnetic permeability and dilatometer changes on the thermocycling carried out in the required temperature interval in an apparatus measuring small-field magnetic permeability and dilatometer. Also shape memory effect was studied by the method of three points bending, metallographic and X-ray investigations were conducted at the room and low temperatures.

In alloys 1 and 4 the direct and reverse martensite transformations come about at subzero temperatures with narrow hysteresis (20 and 40K). On thermocycling in this temperature range a slight decrease of the austenite magnetic permeability (the less then 10% after 30 cycles) was observed, and also lowering the start temperature of direct martensite transition M_s (approximately to 5K) and raising the reverse transition temperature resulted in the hysteresis increase (~10K), figure 1a.

In the alloys with wide thermal hysteresis of $\gamma \leftrightarrow \alpha$ transformation (2, 3 and 5) the drop of magnetic permeability and dimension changes on cooling-heating reaches a significant value (up to 50%), figure 1b. And on each next cycle this drop decreases while exhibiting a tendency to reach a certain fixed value, which does not subsequently depend on the number of cooling-heating cycles. After the 20-th cycle the variations are practically unobservable. The M_s point does not substantially change. A shift of the reverse transformation start A_s to the lower temperatures and during the early 2-3 cycles an increase and then a decreasing of its finish temperature A_f is observed. Thus, at the outset of thermocycling some rise of the transformation hysteresis occurs, but as a result of that procedure the hysteresis of this type alloys reduces.

As it is known, the initial magnetic permeability of austenite is substantially higher than that of martensite. This is due to the magnetic-crystalline anisotropy of martensite crystals and high density of crystalline defects, because the martensite transformation is accompanied by the formation of dislocations and the appearance of various defects. With an increase in the number of $\gamma \leftrightarrow \alpha$ transformation cycles the number of defects in the structure increases (a multiplication and redistribution of dislocation occurs). It is most likely that in the process of a multitude of martensite $\leftrightarrow$ austenite transformations the change of the lattice leads to restructuring of the defect structure so that a stable reversibly inheritable distribution of crystal lattice defects is formed [6]. This improves the

472
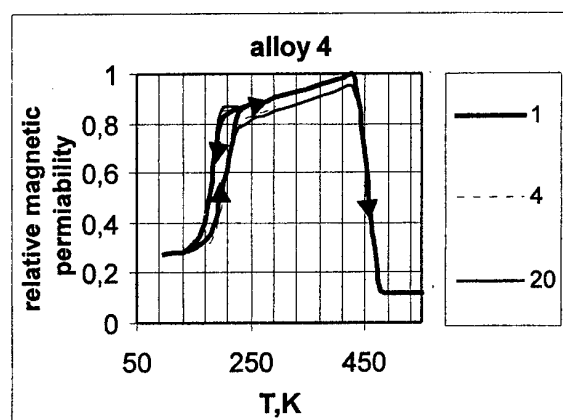
a
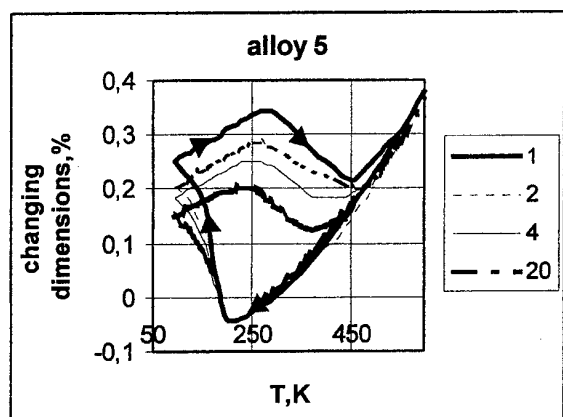
b

Figure 1. The changing of properties in Fe-Ni-Co-Ti alloys with different hysteresis of $\gamma \leftrightarrow \alpha$ transformation on thermocycling.

The martensite structure of Fe-Ni-Co-Ti alloys with narrow transformation hysteresis shows thinner plates and less height of its relief that evidences of smaller form deformation and, as a consequence, lower level of arising stresses. Owing to this the relaxation process does not occur and the coherency on the phase boundaries preserves.

Thus, thermocycling does not substantially influence the critical temperatures, hysteresis and degree of transformation in the alloys with narrow (up to 40K) hysteresis of $\gamma \leftrightarrow \alpha$ transition. In Fe-Ni-Co-Ti alloys with wide thermal hysteresis of martensite transformation the thermocycling in M_f-A_f range resulted in some decreasing of the hysteresis H, measured on the thermal curves at ½ change of the value, and also transformation degree (the quality of thermoelastic martensite). After ~20 cycles of cooling-heating the property stabilization is observed.

[1] Кокорин В.В., Гунько Л.П., Козлова Л.Е., ДАН СССР, 286, №4 (1986), 883-886.
[2] Kokorin V.V., Martensite Transformations in Inhomogeneous Solid Solutions, Kiev, Nauk. Dumka, 1987.
[3] Kokorin V.V., Shevchenko O.M., Materials Science Forum, 79-82 (1991), 545-550.
[4] Кокорин В.В., Гунько Л.П., Шевченко О.М., ФММ, №11 (1992), 119-123.
[5] Kokorin V.V., Gunko L.P., Shevchenko O.M., Scr. Metal., 28 (1993), 35-40.
[6] Brainin G.E., Driban V.A., Likhachev V.A., FMM, 47 (1979), 611.

the reverseability of martensite transformation and results in the decreasing of hysteresis on thermocycling the alloys with wide transformation hysteresis. However, because of the partial stress relaxation some quality of martensite loses thermoellastisity and is retained in the structure of the above alloys when overheating A_f. The X-rays investigations and incomplete disappearance of the martensite relief on the surface of polished metallographic specimens after thermocycling evidence of this fact. While heating the samples to higher temperatures, the effects due to multiple cycling disappear almost completely, as it leads to the destruction of the dislocation structure established in the process of multiple phase transitions and complete transformation of all martensite bulk to austenite.

473

STRONG PLASTIC DEFORMATION STRENGTH OF TECHNICAL PURE TITANIUM PRODUCED BY COLD HEARTH ELECTRON BEAM REMELTING

Minakov V.N., **Minakov N.V., Popchuk R.I., Puchkova V.U., Khomenko G.E., Schekin- Krotov V.A.**[1]

Institute for Problems of Materials Science by I.M.Frantsevich NAS of Ukraine, Kiev, Ukraine
[1]Joint Stock Company «FIKO», Kiev, Ukraine

Now a day leading titanium - manufacturers puts into operation cold hearts electron beam facilities with independent heat sources. Independent heat sources of Electron Beam and Plasma Melt processes allow to monitor and control the temperature of the molted metal zone and crystallization, to effect the structure and impurities distribution. The technology is based on cold hearth process with horizontal charge feed. Molten metal traverses continuously a horizontal water cooled heart from the feed stock melting region to mold where the ingot solidifies and at the bottom - withdrawn. Typically the four electron guns (EG) are used: two of them are for charge melting, the other two to maintain the controlled melt temperature. JSC "FIKO" has developed one fold electron-beam cold hearts process with cold cathode glow discharge electron guns. It can be used for manufacturing of ingots $\varnothing 630$mm, up to 5 tons by weight. The process of melting goes in electron-beam cold hearts furnace through intermediate poll, charge in the container (in large scale scraped condition) moves horizontally. This method allows to use up to 100 % scrap and wastes of titanium industry as raw material. Main advance of the JS FIKO technology is stable melting process. It is possible to provide the process of melting at 2,5 Pa. For comparison pressure less than $2,5 \times 10^{-2}$Pa is required to guarantee operation of the gun with the thermocathode.

JS FIKO electron beam process produces strong plastic deformation (SPD) ready commercially pure titanium.

Chemical composition of the technically pure titanium meets requirements of the ASTM B348 Grade 2 standard.
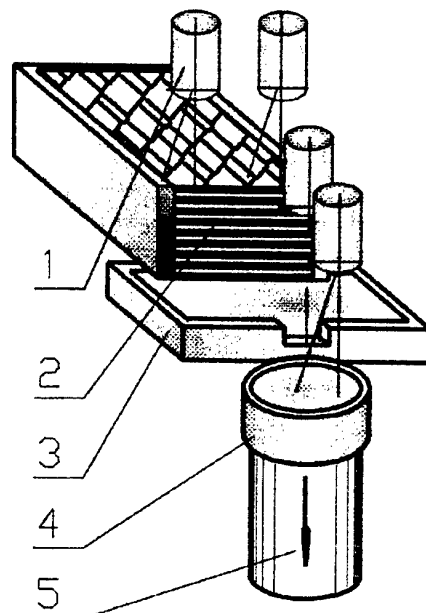
Fig,1 EBM unit at "FIKO" limited plant. 1 - Cold cathode glow discharge gun; 2 - feed stock; 3 - cold hearth; 4 - mould; 5 - ingot.

One of the main goal of the mill products manufacturing is to refine an legacy as cast state grain boundary structure. The ingot has been forged under the schema $\varnothing 630$mm $\rightarrow$ $\varnothing 250$mm $\rightarrow$ $\varnothing 120$mm. Commercially pure titanium structure and mechanical properties has been studded. Deformation parameters affects on the grain size. CP titanium with approximately ~ 1mm (fine grain) and 5mm (rough grain) has been produced. File grain produced in dynamic recrystallization process, whereas rough grain size corresponds to drawing out factor.

- Fine grain CP Titanium's (grain size 1-2 mm) mechanical properties are:
- yield stress σ_{02}=378,3 MPa,
- tensile strength - $\sigma = 467,7$ MPa,
- aspect ratio $\delta = 21,05\%$,
- reduction of area ψ =85,2%.

The mechanical properties of the magnetically controlled electro slag remelted (MEM)* titanium with a grain size 5 mm were used as an starting point .

JS FIKO CP titanium yield stress under the room and cryogenic temperature conditions exceeds MEM ones. Critical defects size decrease as a temperature reduction. Low temperature mechanical tests are useful to reveal CP titanium defects. JS FIKO CP titanium fracture could be characterized by high stress level. Grain boundaries, particles and other defects affected to the process of fracture.

As a temperature decrease from +20 to -196°C strong plastic deformation strength (modulus of plasticity) grows for all types of tested CP titanium.

T,°C	D, MPa	
	CP Titanium JS "FIKO"	CP Titanium "MEM"
20	900	650
-196	1050	1150

D - strength of the heavy plastic deformation or modulus of plasticity.

As a result of current study it should be mentioned that JS FIKO process could be used for grade 2 CP titanium production from scrap and low grade sponge.

* Special gratitude should be mentioned to prof. Kompan Ya.Yu for samples of MEM titanium, Paton Electric Welding Institute, Ukraine.
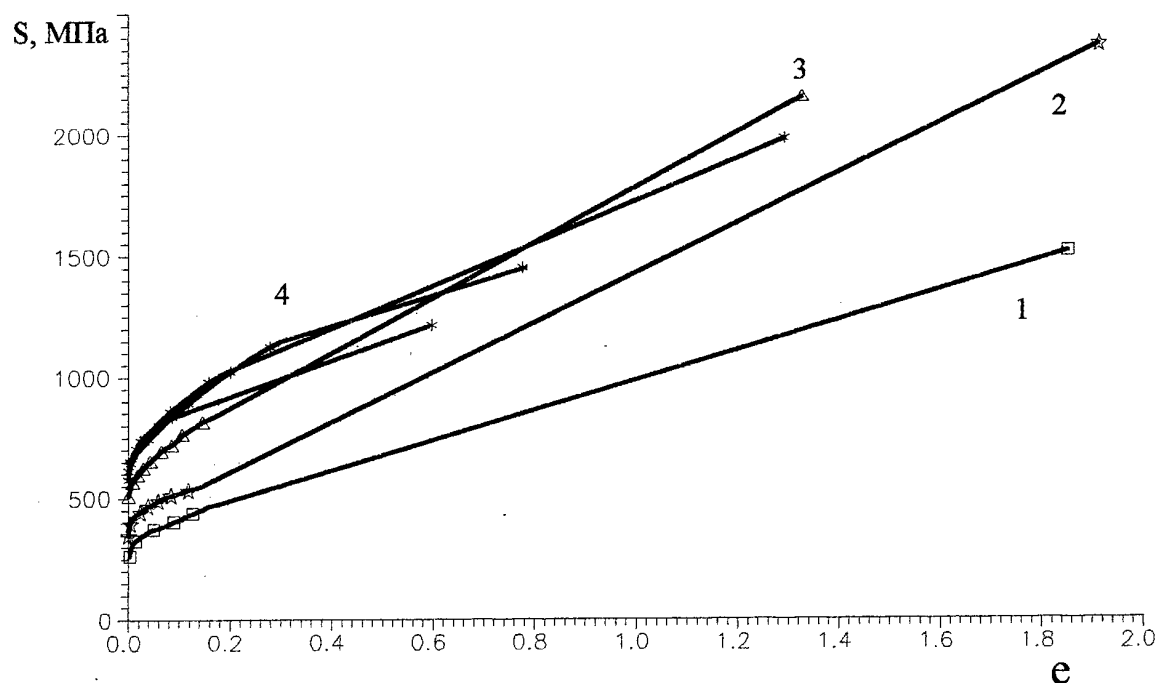
Fig. 2 True strength vs. True deformation for JS "FIKO" and MEM titanium: 1. MEM 20°C; 2. JS "FIKO" titanium 20°C; 3. MEM -196°C; 4. JS "FIKO" titanium -196°C.

475

THE RATING OF AN OPPORTUNITY OF USING TRIBOLOGICAL COATINGS OBTAINED FROM TiN, TiB$_2$ BASED MATERIALS AT THE RAISED TEMPERATURE IN CONDITIONS OF SOLAR ENERGY EFFECT

Frolov G.A., Paustovsky A.V., Tsyganenko V.S., Novikova V.I., Timofeeva I.I., Isayeva L.P., Lityuga N.V.

Frantsevich Institute for Problems of Materials Science, the Ukraine NAS, Kyiv, Ukraine

The prospective direction is use of a solar energy in technological processes of coating the wear resistant layers [1].

A coating on steel substrate is made by spark alloing (SA) with use of the electrode of materials on a basis TiN, TiB$_2$ based materials containing the additions of Cr, Ni, Mo. SA carried out in EFI-46A unit a mode of 1,5 A, C=300 ☐F. The processing of a surface by solar radiation was carried out in SGU-2 unit, involving mirror paraboloid concentrator for solar radiant energy, and supplied with Sun tracking system as well as with checkout set. The thermal flow is 11-12 MW/m^2.

The analysis of heating curves shows, that temperature on a steel substrate basically is determined by absorbent ability (the factor of blackness) of coating surface in study. Than above factor of blackness, the above temperature of a surface, the more intensively warming up on a substrate takes place. Temperature of a substrate of researched materials differed considerably from each other. It is explained to that the large share of heat is removed for the account of radiant cooling, i.e. by radiation with heated up surfaces.

At a choice of a coating it is necessary to prefer ones with greater absorbing ability, i.e. those samples, heating temperature of which was more. Just these coatings at heating will remove better heat at the expence of radiant of cooling.

The heat penetration curves for samples of three considered compositions show, that maximal absorbing ability (the most intensive warming up of a substrate) has a TiN- (Ni, Cr) material (Fig., curve4). For a material TiB$_2$- (Mo, Ni) the values of temperature for heating are a little bit lower (fig., curve 3). Lower absorbing ability has the material TiN- (Ni, Mo), however its values are higher, than for steel (Fig., curves 2, 1). Temperature steel substrate is minimal.

X-ray analysis of researched surfaces has established, that after SA initial coatings consist basically of intermetallides with small oxides content. After influence of a solar energy on spark coatings the amplification in intensity of reflections from an intermetallide phase is observed, that testifies to them annealing, and also occurrence complex oxide phases. It is revealed, that at a high temperature heat penetration in spark coatings the interaction of iron from a steel substrate with an electrode material occurs.

As it is revealed by metallograph analysis, a dense continuous film forms on a surface of a sample. This film heals cracks, roughness, and surface finish. Factor of friction of SA-coatings after processing by radiant energy decreases on 40 % in comparison with the raw coatings.

Thus, it is established, that the processing of spark coatings by radiant energy results not only in improvement of the materials tribological characteristics, but also raises absorbing ability of a material, that makes expedient their use in sites of friction, in which the significant share of heat is removed by radiation from a surface.
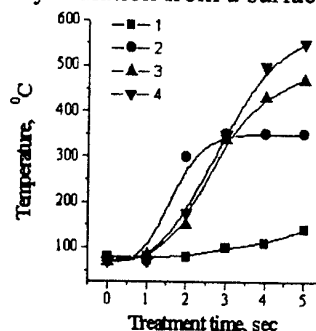
Figure. Warming temperature dependence (T, °C) of steel substrate on the time treatment for the materials: 1 – steel; 2 – TiN-(Ni, Mo); 3 – TiB$_2$-(Ni, Mo); 4 - TiN-(Cr, Ni).

Reference
[1] Podchernyayeva I.A., Lavrenko V.A., Frolov G.A., Dyuba A.D., Pasichny V.V. About laws of formation of a superficial layer in conditions of the

concentrated solar and laser hardening // Poroshkovaya Metallurgiya.-1994.- № 5/6.

PECULIARITIES OF STRUCTURE AND MORPHOLOGY OF CHROMOUM COATING MODIFIED BY SUPERHARD ALUMINIUM BORONCARBIDE $Al_3B_{48}C_2$ AND BORON SUBOXIDE $B_{13}O_2$

Kharlamov A.I., Khotynenko N.G., Kirillova N.V.[1]., Fomenko V.V.[2]., Sameluk A.V., Jacobi V.G.[3]., Trapalis Christos[4], Ushkalov L.N.

Institute for Problems of Materials Science NAS of Ukraine, Kiev, Ukraine
[1]National Taras Shevchenko University, Kiev, Ukraine
[2]National University of Food Technologies, Kiev, Ukraine
[3]Ashurst Technology Centre Inc., Toronto, Canada
[4]Institute of Materials Science, Athens, Greece

Superhard materials formed of light elements and, in particular, boron containing compounds are of important interest for creation of technology of wearproof chemically resistant tool materials with high mechanical strength and thermostability. Questions regarding the usage of superhard materials as a reinforcing addition to coatings deposited on working tools of a turning lathe, drill bitts are of especial significance. Their solutions aimed to increase their technological characteristics such as wear-resistance, thermostrength, hardness, long-life and etc.

In this work the results of researches of structure, of morphology and composition of modified chromium coating with aluminium boroncarbide $Al_3B_{48}C_2$ and boron suboxide $B_{13}O_2$ reinforcing additions deposed on drill bitts are presented. The coatings are obtained by electrochemical precipitation of chromium from electrolyte contained highly dispersed (< 1mkm) single crystal particles of aluminium boroncarbide and boron suboxide. The mode of the coating depositing was optimized by varying of technological parameters of chromium precipitation from electrolyte and of disperseveness of boron-containing compounds. To investigate structure, morphology and composition of coatings samples Scanning Electron Microscopy (SEM) equipped with Energy-Dispersive X-Ray Spectrometer (EDS), Scanning Auger Electron Spectroscopy and Microscopy and Secondary Ion Mass Spectrometry (SIMS) were employed. A portion of the research was carried out by Ashurst Technology Centre Inc. Toronto, Canada.

Microstructure and morphology of the coating surface are presented in fig.1 (a, b, c). Results of mass-spectroscopy measurements - in fig.2. The thickness of the coating is about 3 μm. The coatings consists mainly of chromium with a little concentration (about 1 %) of other elements or their compounds, which got into the coating during a process of the electrolysis. Elements such as B, O, $B_\delta O_y$, Ti,Cl, Al or their compounds are also detected in the composition of the coating. They were localized mainly on the interface between coating and a drill where their concentration is one order higher than in the chromium coating. Particles in shape of flakes (from 1 to 5 μm in size) are randomly distributed on the surface of the coating (fig.1,a.). Under the formation made of the flakes one can observe a layer which consists of more dispersed particles (fig.1,b.). A fragment of the chromium coating is displayed in fig.1 (c), on which a flaw led to cracking of the flakes but not to their exfoliating from the lower layer can be seen. Besides, flaws indicated exfoliating of the coating off iron base were not also observed. Consequently, adhesion of a modified coating to an iron base and efficient cohesion between the outer layer of flakes with an interjacent one consisting mainly of highly dispersed reinforcing additions is good enough. Probably, because of this feature, the drill bitts with such a coating exhibited at tests extremely high (more than 5 times with comparison of uncoated drills) performance.

478
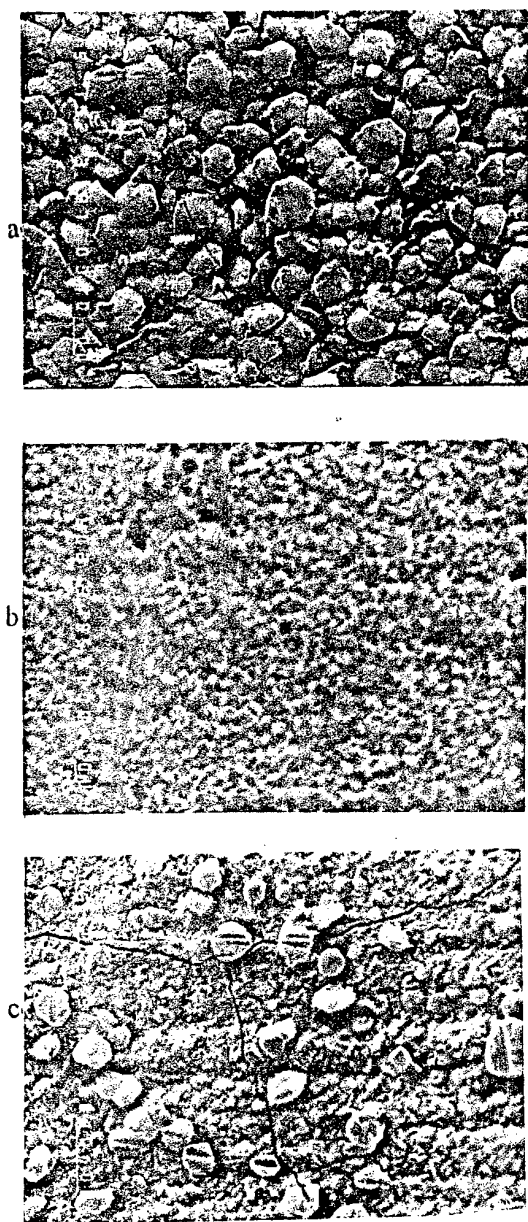
Fig. 1. Microstructure of outer (a) and inner (b) layers, and also a fracture (c) of chromium coating which characterizes high strength of cohesion between the layers.

Fig.2. By element composition of the chromium coating modified with high -hard aluminimum borocarbide $Al_3B_{48}C_2$ and boron suboxide $B_{13}O_2$ obtained through mass-spectroscopy measurements.

Thus, the presence of components of reinforcing additions ($Al_3B_{48}C_2$ and $B_{13}O_2$) on the interface iron / chromium facilitates to the growth of the coating adhesion and can at the same time be a remarking feature of this coating.

479

SOME STRUCTURAL-MICROMECHANICAL ADHESION CRITERIA OF MULTILAYER HEAT- PROTECTIVE COATINGS

Okatova G., Checan V., Markova L.V.
Powder Metallurgical Researche Institute, Minsk, Belarus

Introduction

A significant achievement in the field of creation of protective coatings on turbine blades is coatication of ceramic heat-shielding coatings (HSC) by the electron-beam spraying method [1,2].

A blade of the turbine with three-layer HSC is a complex interdependent system [3]. At the testing stages, there was flaking of a ceramics layer on some blades. Preliminary research determined that the flaking occured on the boundary of " a pore-free zone " (fig.1 on arrow 1) from the ceramics side.
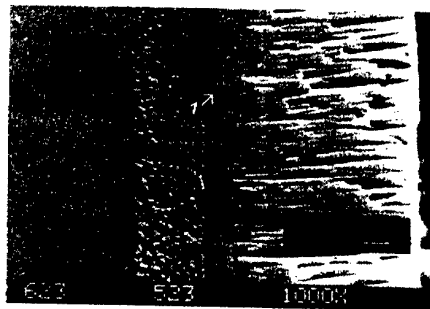
Fig.1. HSC microstructure on a cast rotor 1-st stage turbine blade

There was no definite answer to the questions of reason and conditions of formation of a pore-free zone and correlation of its size with conditions of ceramic layer formation.

The purpose of research was to establish structural - micromechanical criteria of good adhesion of multilayer HSC obtained by electron-beam spraying method.

Experiment

The research was carried out on 3 layer HSC: external ceramics $ZrO_2+Y_2O_3$, cermet Ni-Cr-Al-Y + ZrO_2-Y_2O_3 (up to 40 microlayers) and metal sublayer Ni-Cr-Al-Y. Coatings were put on cast rotor 1-st stage turbine bladings made from refractory alloy GS6F. The research blades had been selected for research according to its main structural attribute -the width of pore-free zone.

The research was carried out using the integrated method of coatings research designed in BRPA Powder Metallurgy [4]. As leading criterion for estimation of resistance to flaking, the method of micro-impressions, used for estimation of adhesive strength of coatings, was selected.

Results and discussion

The research of blades determined the types and measured the width of structural zones of ceramics. It turned out that on the lip, back and trough of feather of different blades the pore-free zone is either absent or has significantly varying width - from 2 up to 12 microns.

Results of microhardness measuring and estimation of resistance to the flaking of ceramics have shown, that

- microcracking in a pore-free zone on different blades is detected at loads from 0.25 up to 10 N and not always determined by the blade width;

- the poorest resistance had the blade with the pore-free zone zone width of 4-5 microns on the back and 6-10 microns on the trough - microcracking in the pore-free zone appeared already at micro impression with load of 0.25 N (fig.2);
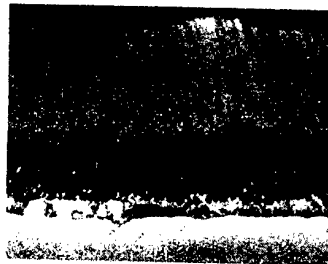
Fig.2. Microstructure of ceramics - cermet transition zone with a microhardness print at loads 0.1, 0.25 (on arrow. 1 with crack - separation on the boundary: pore-free zone - zone of columnar crystals) and 5 N, x400

- on blade PN before and after (the sample PNO) an annealing at absence of pore-free zone on the back and its presence on the trough (the size 6 and 8 microns), the best result is obtained: at micro-impression with all loads - from 0.1 up to 10 N microcracking is practically absent (only at load 10 N on blade PN a very small microcracking inside and on a print contour is found).

The microhardness in a pore-free zone of the blades inclined to cracking, is lower on ~1000 MPa, than in blades with higher resistance to development of cracks (PN, PNO).

In blade PN the microhardness of pore-free zone is 4750, in columnar zone it is lower - 3700 MPa; after annealing the microhardness in pore-

free zone has increased at 200 MPa, in columnar zone it increased at >1000 MPa.

Research in SEM after steep etching has shown that the pore-free zone has the same columnar structure as the main ceramics layer, but its crystals are very thin - 1 microns and fit closely to each other (fig.3.) The centers of microcrystals nucleation are microcrystals ZrO_2 in cermet microlayers. During directional growth, part of microcrystals suspends the growth of others - separate pores and lines of micropores begin to appear (fig.3, on arrows 2-4).
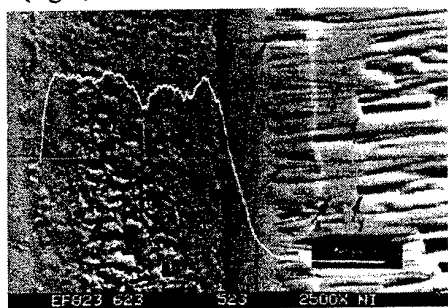
Fig.3. Microstructure of the ceramics - cermet transition zone with concentration distribution curve Ni

The microstructure in blade PN has essential difference from other blades: at a pore-free zone of grey colour there are the thin white interlayers (fig.4 on arrows 1, 2).
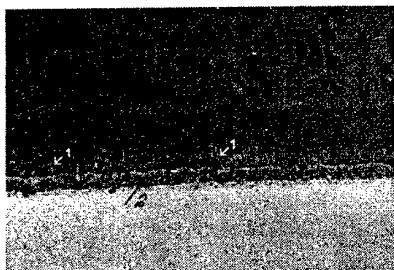
Fig.4. Microstructure of blade PN, x1000

After steep etching and research in SEM it was found that polyhedral microcrystals and "bridges" of connection of a cermet and ceramics serve as the basis of columnar microcrystals in pore-free ceramics zone of blade PN (fig.5).
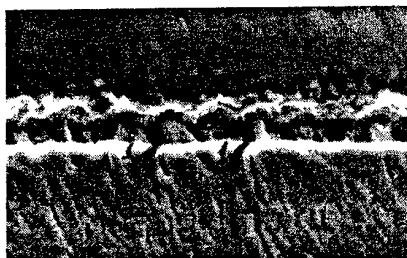
Fig.5. Microstructure of pore-free zone on the ceramics - cermet boundary, x2500

On a concentration curve it is visible that diffusive interaction in HSC goes on elements Ni, Cr Al, the zone of diffusion is placed in "pore-free" zone. The thinner is the zone, the higher is gradient of density on these elements.

On concentration curves in blade PN on particle lines - white "interlayers" horizontal areas are marked (fig.6).
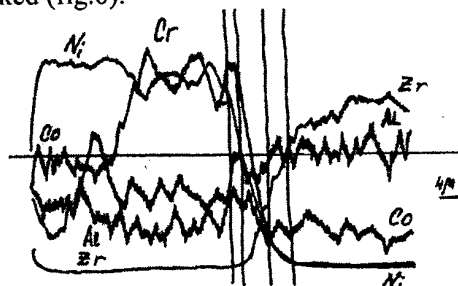
Fig.6. Concentration distribution curves Ni, Cr, Al, Co, Zr in a ceramics - cermet transition zone of blade PN

In a blade with strong cracking in ceramics the preferential phase is ZrO_2 with monoclinic lattice. In a blade without flaking the main phase is ZrO_2 - tetragonal.

Conclusion

From comparison of structure and Ni, Cr, Al distribution in "pore-free" zone it is obtained that in blade PN the pore-free ceramics zone has fine polyhedral structure, a metal framework of a special structure with higher strength which protects ceramic HSC layer obtained by electron-beam spraying method from flaking.

References

1. Movchan B.A., Malashenko I.S. The temperature-resistant coatings besieged in vacuo/under editing B.E.Paton. Kiev: Sciences. Dumka. 1983. 232 p.
2. N.I.Grechanjuk, V.A.Osokin etc. New materials and the coatings obtained with the electron-beam method. Theses of reports of the International conference. The materials and coatings in extreme conditions .... Kacively, Crimea, Ukraine. 2000, p.134.
3. Pimenova G.P. (Okatova G.P.), Markova L.V., Shavkunov A.V. The thin structure of the coatings obtained by an electron-beam method. In book: Electron-beam spraying and gas-thermal coatings.-Kiev, IEW of a name of E.A.Patona, 1988, p. 65-72
4. Roman O.V., Pimenova G.P. (Okatova G.P.), Markova L.V., Chekan V.A. A complex method electron probe analysis researches of coatings. Theses of reports of the International conference. Electronic microscopy. Czecho-slovakia, Nitra, 1983.

THE INFLUENCE OF ELECTROMAGNETIC MIXING ON THE STRUCTURAL CHARACTERISTICS OF ZIRCONIUM

Chernyavsky V.B., Verbylo M.A., Kreshchuk A.V., Zubenko A.I.
Physico-Technological Institute of Metals and Alloys of National Academy of Sciences of Ukraine (PTIMA NASU), Kiev, Ukraine

The metallurgy of zirconium has received intensive development after zirconium became the basic component of constructional alloys for atomic engineering.

Zirconium has several unique properties. Those are small section of capture of neutrons, high temperature melting and good corrosion properties. Therefore zirconium began to be used as a basis a constructional material of an active zone of nuclear reactors. It has required development of methods of reception zirconium "reactor cleanliness". I.e. in zirconium there should be a minimally necessary quantity of such impurity as H_2, O_2, Si, C, F, Hf etc.

Perspective method of zirconium refinement is electron-beam melting (EBM), allowing from initial metallurgical preparation of zirconium to receive an ingot of higher degree of cleanliness with regulated, lower contents of harmful impurity, which strongly influence mechanical and corrosion properties.

In PTIMA NAS of Ukraine calciumthermal zirconium of the mark CTZ-100, made on the Dneprodzherzhinsk State research-production enterprise "Zirconium", is remelt in ingots by a diameter of 270 mm, length 260 mm and weight 70 kg by a traditional method EBM and, using a method EBM with imposing of electromagnetic fields.

The basic purpose of the given work was realization of the comparative analysis of ingots zirconium received by various ways. For remelting of zirconium is used cold-bottom electron beam installation CEBI-1 supplied by system of electromagnetic stirring (EMS).

The average chemical compositions of the produced ingots agreed with technical requirements (TR). The special attention is given to the contents O_2 in metal. Since. O_2 being dissolved in Zr in plenties reduces plasticity, corrosion stability, changes crystal structure and orientation of allocation hydrides. Therefore TR the contents O_2 up to 0,1-0,12 % is limited. In our case the contents O_2 changes from 0,13 % at EBM up to 0,12 % at EBM with EMS.

The hardness of a matrix Zr on Brinell after various methods remelting was measured. Its level agreed TR, 170 kg / мм^2 applying EMS and are little bit higher, 176 kg / мм^2 without EMS. That is explained, on all probability raised contents O_2 in Zr, remelted by a traditional method EBM. With the purpose of revealing local volumetric liquation the microhardness from periphery to the center of a sample was measured at loading 20. At remelt of an alloy both with EMS and without EMS the level of hardness has made 184,8 kg / mm^2, that indirectly testifies to uniformity of structures.

Researches macrostructure along an ingot has shown the tendency to crushing a grain in Zr remelted with EMS, large degree of a regularity in an arrangement of acicular dendrites on all extent of an ingot.

According to the literary data, Zr undergoes during cooling from melt phase transformation at temperature 862^{0}C: the high-temperature β-phase with body-centered by a lattice passes in low-temperature an α-phase with hexagonal close-packed by a lattice. This transition has the extremely large meaning in technology of processing Zr and its alloys, since as a result of this transition there is a structure determining all properties of a material in all ranges of working temperatures (300-380^{0}C and up to 1000-1200^{0}C).

Really, at research of microstructure Zr CTZ-100, after etching, the presence of packages and plates making these packages, low-temperature of an a-phase allocated on borders of grains of a former β-phase is found out.

Researches of microstructure Zr, after electron beam remelting, we carried out on samples cut out from the top, central and bottom parts on height of an ingot. The microstructure of an alloy without electromagnetic hashing is characterized homogeneous enough under the geometrical

characteristics by packages of an a-phase. Width of packages of top, center and bottom of an ingot have practically identical meanings 0.33 - 0.36 mm; width of plates makes 0.007 - 0.01mm; distance between plates makes on the average 0.001 mm.

Investigating microstructure Zr with EMS, the significant crushing of structural components is observed structural orderliness: width of packages has decreased up to 0.15-0.22 mm, plates making packages, are characterized by two standard sizes. The plates by the sizes of 0.02-0.04 mm make 70% of the areas microsection, and 30 % of the areas microsection borrow plates of width 0.005-0.006 mm. Distance between plates makes on the average 0.0005 mm.

The observable structural changes testify, on all probability, to aspiration of an alloy with EBM to more equilibrium condition, about reduction of a degree liquation, about the greater degree of homogenization melt.

In the top part of an ingot both without EMS, and with EMS are observed shell-like porousness, that,

probably, testifies about raised gas-full in the top part of an ingot, owing to reference in this area of harmful impurity and gases, that is characteristic for zoned melting. And it on all probability explains faltering growth of plates in the top part of an ingot and less ordered orientation of packages.

The preliminary conclusions, which can be made of work, testify to positive influence EMS on feature of the structural characteristics. But for more complete picture of influence EMS it is necessary to carry out additional researches with precise differentiation of parameters melting and speed of crystallization. Namely, control of temperature overheating volumetric and in a zone focal of a stain, multiplicity of processing at different powers, speed of cooling of an ingot in process crystallization. To carry out metallographic the control of a parity of residual quantity high-temperature and lowtemperature of phases and influence of their volumetric quantity on a level of the physics-mechanical characteristics of an alloy. I.e. to connect technological parameters of process of melt and having filled with the functional characteristics of the received material.

INVESTIGATIONS FOR INFLUENCE OF COMBINED ACCELERATED IMPACT OF OUTER SPACE FACTORS ON PHYSICAL PROPERTIES OF FUNCTIONAL SPACE-APPLICATION COATINGS

Gavrylov R.V., Pokhyl Yu.O., Agashkova N.N., Pristiuk M.M., Triolo J. J.[2], Pedolsky H.[3]
Special Research and Development Bureau for Cryogenic Technologies B.Verkin Institute for Low Temperature Physics and Engineering, NASU, Kharkov, Ukraine
[2] NASA, Washigton, DC, USA
[3] «Orbita» Ltd, Kensington, MD, USA

In this report, represented are results of investigations for influence of simultaneous accelerated impact of laboratory- simulated outer-Space environment factors (SEF), such as: - flux of protons (p$^+$) and electrons (e$^-$), electromagnetic radiation of artificial Sun, vacuum ultra- violet (VUV) radiation and vacuum, on properties of functional material, being a thin composite coating layer, produced by vacuum evaporation method.

In the course of studies, there were made investigations and measurements (prior to, and after impact by SEF) of the following parameters:
- surface morphology;
- integral coefficient of irradiation, ($\square$);
- coefficient of reflection [R($\square$)] within 200...1800 nm wavelength range;
- coating masses losses, at accuracy to 10^{-4} g.

Totally, two experimental series have been carried out.

In first experimental series, test- samples of coatings were irradiated by integral (p+)- and (e-)- flux by dosage D = $6*10^{15}$ cm^{-2}, which corresponded to five years of materials' stay on geostationary orbit/ As a source of artificial Sun radiation within 200...2500 nm wavelength range, there was employed "IS- 160" type Xenon lamp-based Sun- simulator. The artificial Sun radiation intensity made up I=$1,4*10^3$W/m^2, which corresponded to a unitary dose of para-atmospheric Sun. Total irradiation time was 100 hours. With purpose to simulate VUV- radiation of Sun within (5...200nm) wavelength band, there was employed gas- jet source of light, the GJS. Maximum flux of VUV - radiation made up 0.125 W/m^2, which ensured an irradiation- dosage in equivalent to 1 year of outer Space environment.

After exposure to the simultaneous accelerated impact by all the above- listed SEF the integral coefficient of irradiation, ($\square$, has increased from 56% up to 67%.

Figure 1 represents a characteristic diagram of change in reflection- ability of a coating, before (curve I) and after (curve II) impact by SEF.
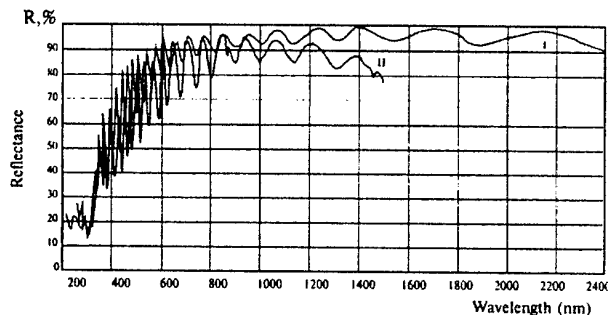
Figure 1: #1 Series of Experiments. Characteristic curves for reflection- coefficient of a test- sample investigated

It is obvious from Figure 1 that character of spectral dependency R($\square$) after irradiation is similar to that of initial test- sample (i.e., curves (II) and (I), correspondingly); however, the curve (II) is situated notably lower than curve (I), at almost twice as increased oscillations amplitude. Decrease of reflection- coefficient does not exceed ~ 15 % in entire range. Decrease of visible- band reflected- light intensity (350 < $\square$ < 800 nm) can be assumed for by occurrence of surface- roughness, whose value is commensurable or even in exceed of incidental light wavelength.

Analysis of data gained at investigation of surface morphology has shown that coating surface structure has undergone dramatic changes. An irradiated coating surface possesses a lot of different non- homogeneities, like: cracks, pores,

roughness, lamination of coating layer out of substrate.

In second experimental series, coating- surfaces were irradiated by integral (p^+)- and (e^-)- flux with energy E= 150 keV, after 72 irradiation hours which corresponded to 720 hours of materials' stay on geostationary orbit. Dosage D = $5*10^{12}$cm^{-2} made up Maximum VUV- radiation flux made up 0,125 W/m^2, which has enabled authors to expose materials to test- dosage in equivalent of 720 hours of materials' radiation in outer Space on geostationary orbit.

Integral coefficient irradiation ($\square$ of coatings has not changed after impact by SEF.
Figure 2 represents a characteristic diagram of change in reflection- ability of a coating, before curve (I), and after curve (II), impact by SEF, in #2 series of experiments.
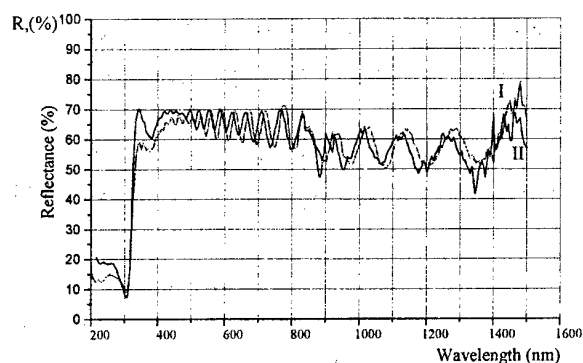
Figure 2: #2 Series of Experiments. Characteristic curves for reflection- coefficient of a test- sample investigated:

After irradiation, character of spectral dependency R($\square$) is similar to that of initial test- sample; however, the reflection- coefficient has reduced by about 10%, whereby oscillations amplitude has increased by 3...5%. Major changes of test- sample reflection- coefficient occurred within 350...800 nm wavelength range.

Investigations for surface- morphology have shown that coating- surface structure has undergone some changes. An irradiated coating surface includes different sorts of non- homogeneities, like: cracks, pores, roughness etc.

Analysis of data thus obtained, enables one to pronounce the following findings:

1. Decrease of reflected- light intensity in visible range, as well as increase of oscillations- amplitude at reflection- characteristics diagram after SEF- impact, can be explained by change of surface- structure under impact of SEF.

2. Test - samples investigated in #1 series of experiments, have undergone greater changes than those in #2 series. For example, coating- surface has eroded to comparably greater extent, and with greater amount of cracks. These features are related, presumably, to facts that in #2 session, irradiation dosage was less by 1000 times.

3. Coating- surface structural changes, delineated by this present paper, can be assumed for by either of three potentially possible physical mechanisms.

First, irradiation material's by charge particles brings to accumulation of charges in para- surfacial layer, strong Coulomb interactivity among charges, and hence, to origination of cracks within coating structure.

Secondly, combined impact on material by (p+)- and (e-)- flux results in impregnation of para- surfacial layer with hydrogen (due to effect of re- combination), bringing to embrittlement of coating and to decreasing of composite- material adhesion- strength.

Thirdly, occurrence of surface roughness, commensurable with incidental- light wavelength, is a bright evidence that under attack of vacuum ultraviolet radiation, the coating- surface must have undergone some etching erosion.

NOTE: this work has been accomplished in the scope of #9 Contract among SR&DB- ILTPh&E- NASU and NASA, USA (2000).

CHANGING OF MECHANICAL PROPERTIES OF STRUCTURAL MATERIALS UNDER THERMAL- AND FORCE- CYCLING REGIME

Pokhyl Yu.O. ,Lototskaya V.A.

Special Research & Development Bureau for Cryogenic Technologies of Institute for Low Temperature Physics & Engineering, NAS of Ukraine (SR&DB ILTPE NASU), Kharkov, Ukraine

Elements of constructions and devices intended to be employed at low- temperature thermocycling (LTTC), are subjected to thermocyclic mechanical stresses of 1st and 2nd type. These stresses can result in change of material's structural state and hence, in alternation of compound structural - sensitive physical & mechanical properties thereof. It is, therefore, actually important: to study the effect of LTTC on mechanical properties of cryogenic- application materials, as well as to look for the ways for maintaining these characteristics in stability.

The present report provides a brief review of results gained originally at studies implemented at SR&DB ILTPE NASU and dedicated to study of the influence of LTTC effect on mechanical properties of a series of commercial cryogenic materials, such as stainless steels, titanium- and aluminium-based alloys.

The studies have been carried out on experimental set-up (engineered by experts of SR&DB specifically for variable temperature thermo- cycling of materials), in a wide 423 to 4.2K temperature- range, and in combination with tensile- loading stresses [1]. Choice of LTTC- regimes and loading magnitudes were determined with regard to the would be application field of materials.

Parameters of LTTC- regimes relate to the external factors which are acting on material's structural- state. The internal factors, which controle the mechanical behavior of materials, are: type of material' s crystal- lattice, initial structural state, thermal-physical properties, material' s susceptibility to phase - transformations, stacking fault energy, anisotropic characteristics of materials' physical & mechanical properties, as well as actual modes of plastic deformation: slipping or twinning.

It has been found [2] that with steels, the degree of metal- phase stability is a definite factor that can essentially vary the character of mechanical characteristic dependencies ($\sigma_{0,2}$, σ_u, δ) on quantity of thermal cycles. It is known that in dependence on: (i) material' s stability (such as presence of cooling-induced martensite and/ or deformation-induced martensite) and (ii) subsequent test- temperature, either hardening, or softening of materials can occur.

Structural investigations have shown [3], that the increasing of steels yield stress $\sigma_{0,2}$ after LTTC is connected with crushing of initial size of grain $\overline{d}$. Increasing of martensite phases density during LTTC (cooling a-martensite in steel 03Cr18Ni8 and deformed e-martensite in steel Cr18Ni10Òi) is the cause of the crushing. The Hardening in this case is described by the equation of a Hall – Petch: $\sigma = \sigma_j + K \cdot \sqrt{\overline{d}}$. The parameters ($\sigma_j$, K) of the Hall - Petch equation are determined by power of boundaries between initial FCC γ- austenite and formed BCC α-martensite, or HCP ε-phase.

Softening of Cr18Ni10Ti steel that occurs under low temperature deformation at 77K, is related to the fact that beginning of plastic flow is specified not by deformation of initial austenite, but by supplementary deformation caused (by shear way) by nucleation of α-and ε-martensites, under stresses below value of yeild- stress for the initial austenite [4]. Under influence of LTTC and external stresses, a large quantity of stacking faults are originated within initial austenite. Then under low temperature deformation they start to act as multiple sources of intensive $\gamma \Rightarrow \varepsilon$ transformation. Simultaneously with it, the $\varepsilon \Rightarrow \alpha$ transformation occurs in the sheets of ε- phase which is originated during thermocycling. It should be noted that $\varepsilon \Rightarrow \alpha$ transformation also giving contribution (although to somewhat lesser) to make the exterior stress lowering. The increase of transformation- intensity after definite amount of thermal cycles (being pre- computed for a given sort of steel of a given stability- degree) can explain the fact of ultimate strength decrease for thermocyclic samples. The more is the quantity of thermal cycles, -the greater is amount of ε-and α-

martensites born in the process of thermocycling, the less is intensity of transformation at subsequent deformation, the more inner stresses are accumulated in residual austenite and the less intensive plastic deformation is developed in newly- born and comparatively strongest BCC α - martensite . All these processes add together to hardening the thermo- cycled material.

Thus, by regulating the intensity of either heardening α-, or plasticizing ε- martensites nucleation, one can obtain a pre- determined effect of hardening and / or plastification for structurally- unstable steels. This effect is the basis for method of cryogenic thermocyclic treatment of materials (CTCT). As a result of CTCT- technologies, steel with simultaneously enhanced strength- and plasticity- parameters can be obtained.

Influence of LTTC on mechanical properties of materials can be essentially liberated by stabilization of metastable materials (with FCC or HCP lattice): either through change of chemical composition (for example, of 03Cr18Ni10 steel with 0,14% nitrogen, and/ or Cr-Ni-Mn steel), or due to thermo-mechanical treatment (of pseudo-α alloy 19 (Ti- Al- Nb- Zr) .

At the same time however, qualitative and quantitative evolution of structural state was found within structural stable materials with HCP lattice (alloy Ti-(3,5-5%) Al) being subjected to LTTC regime: 300$\Leftrightarrow$77K under stress $\sigma_{n} = 0,9\sigma_{0,2}^{300K}$. Such the evolution proves to ensure both hardening and plasticating effects at 4,2K operational temperature simultaneously, after N=300 cycles [5].

With HCP α-alloy PK-20 (system Ti-Zr-Al), increase of macroscopic mechanical properties was found at 293K -after thermocycling within total N=200 cycles under $\sigma = 0,7\sigma_{0,2}^{293K}$ in the temperature interval 310-77K, whereby maximum increase was registered after 100 cycles. It should be noted that such a behavior is not yet clear to explorers and thus requires further structural investigations.

The LTTC tests done for thermally non-hardened pseudo-α-alloy Ti- (3,5-5) Al- (0,8-2) Mn system, fabricated by means of powder- metallurgy , with pressing force of 400 and 800 MPa, [6]), have shown that in regard to alloy produced at

400MPa, the LTTC effect results in somewhat decreased strength at 293K. The failure is of brittle character. However, with regard to alloy produced at 800 MPa, the LTTC process has caused practically no effect on material' s mechanical properties.

In this case the presence, size, quantity and unhomogenious distribution pores, to be determined relative density of a material, area of contact between particles are structural factors to be responded to mechanical properties of alloy.

The LTTC in the temperature interval 77K- 423K under loading $\sigma = 0,2\sigma_{U}^{423K}$ does not practically influence the strength- and plasticity- properties of FCC aluminium alloy AMg6, while the aluminium alloy 01983T3 has become notably decreasing at its mechanical properties after 100 thermocycles. This latter example is assumed as a fact that at heating alloy to the ultimate limit of a thermocycle (423K), an effect of collective recrystalization takes place within the alloy, which is followed by coagulation of second-phase precipitation along grain- boundaries. These processes result in decreased energy of microcracks- nucleation along the grain-boundaries , and are manifested macroscopically as a brittle intergranular alloy- failure at 77K.

Thus we resume, that versatile purposeful variation of the structural - phase states in combination with LTTC modes, can result in obtaining a novel material with pre- planned complex of optimal mechanical properties.

References
1. V.K. Chernetsky, N.I. Mokry, L. M. Volikova// Soviet Patent #1711035, Int. Class. G 01, # N 3/ 60, published Feb 07, 1992 Moscow, Bulletin #5
2. E.M.Medvedev, V.Ya. Illichev, A.I. Zaharchenko, E.S. Kirilov Pre- Printed Paper, ILTPh&E- NASU, 1975
3. E.M.Medvedev, F.F.Lavrentev, T.M.Kurmanova, Pre- Printed Paper, ILTPh&E- NASU, 1976
4. L.V.Skibina, V.Ya. Illichev, V.A.Lototskaya, "Problemy Prochnosti " #2, 1976, p. 71
5. F.F.Lavrentev, Yu.A.Pokhil, P.P.Dudko, Cryogenics, March, 1983, p. 170.
6. A.I.Telegon, G.I.Masliy, E.L.Fertman et al "Applied Cryogenic & Vacuum Materials Science" "Naukova Dumka", Kiev, 1991, p. 35.

487

NUMERICAL ANALYSIS OF THE X-RAY DIFFRACTION AND INVESTIGATION OF THE ALUMINIUM SINGLE CRYSTALS SUBSTRUCTURE, WHICH WAS FORMED UNDER THE INFLUENCE OF INTENSE ULTRASONIC VIBRATIONS

Bazelyuk G.Ya., **Ryaboshapka K.P.**, **Skrypnyk Yu.V.**
Kurdyumov Institute for Metal Physics, National Academy of Sciences of Ukraine, Kyiv, Ukraine

A dislocation structure formed in aluminium single crystals under the influence of intense ultrasonic vibrations (the amplitude of the relative deformation amounted to $\sim 5 \cdot 10^{-4}$) was investigated by the method of the double mass spectrometry. With the help of the personal computer and developed mathematical procedure, the analysis of the azimuth distribution in the intensity of scattered X-rays was performed. As a result, it appeared possible to represent a complex shape of separate maxima in experimental single- or multiple-peak double reflection curves by a series of peaks that are described by simple Gauss or Lorentz distribution laws. It was estimated that the complexity of the one-peak double reflection curves of aluminium single crystals at the initial state (just after the growth) is the outcome of the superposition of simple intensity distributions (of Gauss or Lorentz type) of X-rays scattered by several independently reflecting and slightly misaligned crystal blocks, contained in the diffracting volume of the metal (see Fig.1).
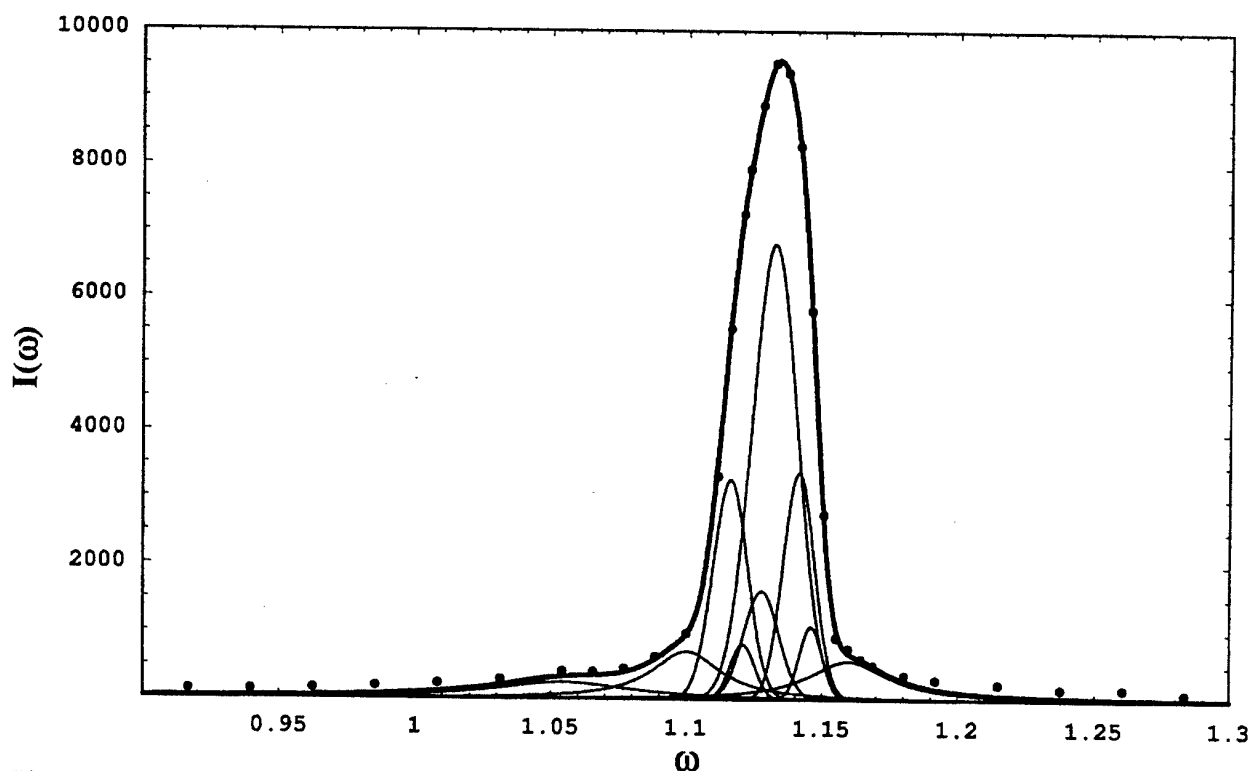
Fig. 1   The double reflection curve of the aluminium single crystal at the initial state (after the growth).

It was shown that ultrasonic irradiation leads to an increase in the misalignment of the neighbouring crystal blocks. It is manifested in an increase of the integral width and in the developing of the multiple-peak structure in the double reflection curves (see Fig. 2).
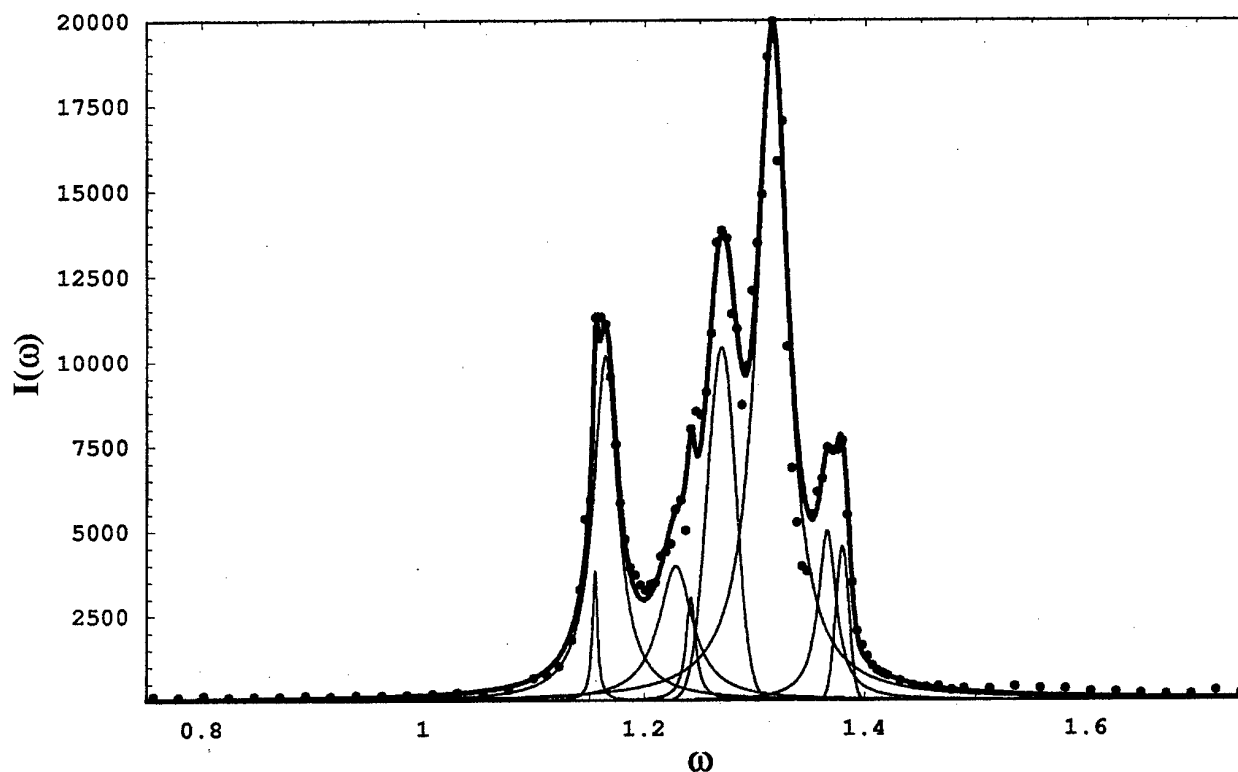
Fig. 2   *The double reflection curve of the ultrasonically irradiated aluminium single crystal with the amplitude of the relative deformation of $5 \cdot 10^{-4}$ at 773 K*

These effects can be connected with an increase in the dislocation density at the block boundaries, where the scattering of the acoustic energy is the most intense. The adopted mathematical procedure for the double reflection curves analysis provides an opportunity to determine the number of blocks participating in the diffraction of the X-rays along with the distribution laws for their misalignments.

THE EFFECT OF PULSE LASER RADIATION ON THE THICK FILM RESISTORS BASED ON Ni_3B

Paustovsky A.V., Rud' B.M., Shelud'ko V.E., Tel'nikov E.Ya., Rogozinskaya A.A.
Frantsevich Institute for Problems of Materials Science NAS of Ukraine, Kiev, Ukraine

Of the new compounds which have found the use as the functional phase for fabrication of the thick film resistors (TFR) used in microelectronics, metal borides hold an important place. It's due to their high refractoriness, chemical stability and possibility of producing the resistors over a wide range of nominal value with low magnitude of temperature coefficient of electrical resistance (TCR) on their base.

Presented here are the results of research of the phase constitution, electrical resistance and the structure of Ni_3B–based TFR surface under the influence of the laser radiation (LR).

The composition on the base of Ni_3B powder and glass-binder was adopted as the object for investigation. The dispersivity was 5 μm. The making of TFR was realized with the method of paste mask printing on the dielectrical 22XC or BK94 substrate followed by the heat treatment in the travelling ПЭК–8 oven. The thickness of the resistor film made up δ=35 μm. The samples were processed with "Квант-15" laser in "severe" (λ=1.06μm, τ=4 ms, E= 0.5–1.5 J, $\varnothing_S$= 1 mm) and "soft" (with the application of attenuator filter and defocusing to 1.5 mm) regimes. The X-ray phase analysis was carried out with X-ray diffractometer ДРОН-3М in $CuK\alpha$ – filtrated radiation. Digital Instruments Nanoscope D3000 Atomic Force Microscope was used to characterize in tapping mode the TFR morphology. The electrical resistance was defined by means of Щ–302 combined digital instrument. In order to estimate the temperature value in the laser focus we utilized well–known analytical expressions [1]. Inasmuch the radius of Gaussian beam is more than the film thickness the temperature may be approximately calculate on the assumption that layer of limited thickness may be substituted by half–space:

$$T(0,t) = \frac{2\varepsilon * W_P}{\lambda} \times \left(\frac{at}{\pi}\right)^{0.5}, \qquad (1)$$

and when employing exact solution for Gaussian source under the assumption of half–space:

$$T(0,0,t) = \frac{\varepsilon * W_P r}{\lambda * \pi^{0.5}} arctg\left[\left(\frac{4at}{r^2}\right)^{0.5}\right], \qquad (2)$$

where $\varepsilon = 1- R$ – absorbent ability; R – reflection factor; W_P – density of radiation power; λ and a – thermal conductivity and thermal diffusivity respectively; r – radius of laser spot; t – pulse duration.

Fig.1 depicts the optical image of original TFR film. As it is heat–treated, the burn-out of organic binder, the melting-down of glass–binder and formation of the globules from 2-5 to 25 μm in size occur.
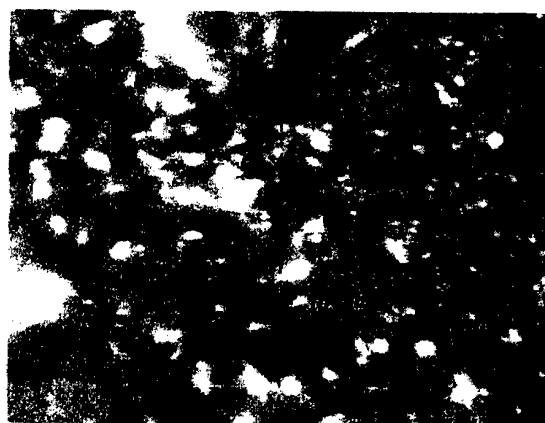
10$^{\mu}$m

Fig. 1. The optical image of original TFR film

Shown in Fig.2 is the 3D – image of surface section (1×1 μm). One can see rather–ordered globular structure with the degree of roughness R_Z = 2.97 nm. The outcomes of the cross–section analysis of this surface demonstrate that the value of RMS (root means square) is 0.992 nm. Between the globules one can see the hollows from 0.05 to 5.96 nm in depth.

After irradiating with the energy E = 0.5 J the burning-off of the globules takes place. In this case the conglomerates of larger size form (from 200 to 350 μm). The surface roughness increases to R_Z = 68.84 nm. After irradiating with the energy E = 1-1.5 J the further burning-off of TFR surface is observed. The degree of roughness is different (R_Z = 46.95 – 70.25 nm). On some surface section the "scaled" structure is formed (Fig. 3 ,4).

490
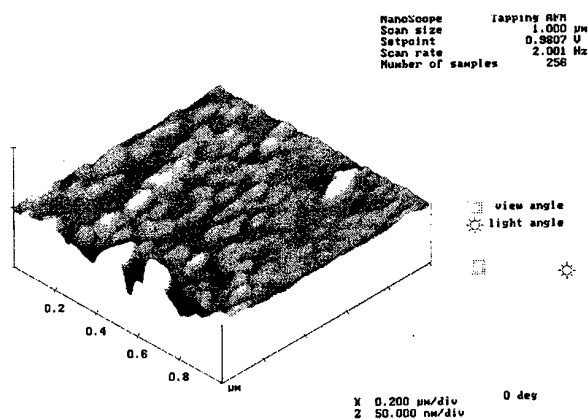
Fig. 2. 3D – image of TFR surface (1×1 µm) before irradiating

electrical resistance changes in the range from 1.4 –2.5 Ohm to 120 MOhm (initial value — 0.14-0.16 Ohm). In the "soft" regime ($\varnothing_S$ = 1 mm) the electrical resistance changes from 0.18 to 0.34 Ohm (initial value — 0.12-0.21 Ohm). When defocusing to $\varnothing$=1.5 mm the electrical resistance changes: from 0.5 –1.8 Ohm to 120 MOhm (R_{INI} = 0.14 – 0.2 Ohm) in "severe" regime and in "soft" one — 0.19 – 0.25 Ohm (R_{INI} = 0.14 – 0.18 Ohm).
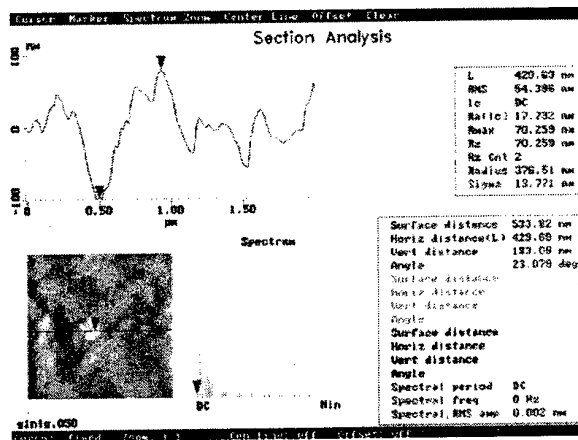
Fig.4 The cross–section analysis of the TFR surface after radiating with E = 1 J

REFERENCES

1. Duley W.W., Laser Processing and Analysis of Materials, Plenum Press, N.Y. and L., 1983

Fig. 3. The optical image of the TFR surface after radiating with E = 1 J

The data on X–ray phase analysis show that in TFR the following change of the phase constitution occurs under the action of LR. In the initial film the appearance of metallic nickel that combines at the stage of heat treatment is noted. After radiating (E = 0.5 J) the intensity of metallic nickel spectral line decreases. The spectral lines of the solid solution $NiAl_2O_4$, silicide nickel – Ni_3Si appear in addition to intensive lines of α–Al_2O_3. When increasing the energy to 1–1.5 J the phase of $NiAl_2O_4$ vanishes and nickel, α–Al_2O_3, Ni_3Si phases remain.

The magnitude of the electrical resistance are determined by the change of the surface topology and the phase constitution of the film. In the regime of "severe" radiation (for $\varnothing_S$ = 1 mm) the

491

STRUCTURE AND PHASE STATE OF SPARK COATINGS

Bondar V.I., Gubin Yu.V.[1], Danil'chenko V.E., Paustovsky A.V.[1], Semirga A.M.
Kurdyumov Institute of Metal Physics of NAS of Ukraine, Kiev, Ukraine
[1]Franthevich Institute for Problems of Materials Science of NAS of Ukraine, Kiev, Ukraine

The choice of alloyed electrodes composition and optimal regimes of spark treatment (ST) can be realized on base of utilization of fundamental regularities of phase-structural and stress state formation in electrode and surface materials. In this investigation a phase content and residual stress distribution are determined in hard-alloy spark coatings on steel surface.

Spark treatment carry out on "Elitron" equipment in air medium with regimes: current 0,5-2,8 A, treatment time 1-5 min. The base surface is carbon steel У8. The alloyed electrode is hard alloy T15K6 on tungsten carbide base. Phase analysis and determination of residual stresses (RS) carried out by X-ray method on the same specimens. X-ray investigations were carried out on "DRON-3" X-ray unit with utilization of cobalt or molibdenum anode radiation. RS were determined by non-destruction $\sin^2\psi$ X-ray method. Laser treatment was carried out on "QUANT-18M" equipment in air atmosphere with 8 ms pulse duration. The laser radiation energy was increased consecutive on 2 to 20 J to avoid melting regime. The surface of specimen was treated by reciprocal overlapping of laser spots (20-25%).

X-ray investigations of surface after spark treatment of У8 steel showed that the exist sufficient difference between the phase content of T15K6 electrode and coating material. In coating structure not discovered diffraction reflexes of base structure component-tungsten carbide WC. Also not discovered diffraction reflexes of Co plastic addition. It is observed reflexes of TiC carbide, W_2C carbide hexagonal lattice and clean tungsten volume-central cube lattice. This phases are products of initial WC carbide dissociation. Parameter of TiC carbide lattice is decreased in the coating. This connected with TiC partial dissociation, carbon loss and nitrogen substitution of carbon in near-electrode space. This connected with small TiN formation energy in contrast with TiC. The austenite thin layer was formed in surface layer of У8 steel on all treatment regimes. The carbon concentration in austenite is equal

(1,2-2) weight % by determination of lattice parameter magnitude.

For heterophase coatings it is advisable to determine RS in each phase component. It is connected with significant difference in thermal properties, elastic modulus, thermal broadening coefficients and structural transformation volume effects. Such selective measurements in different phases can be made X-ray method only. The Davidenkov method made middle RS values in all the volume of coating. This method is not correct to investigation of separate heterophase components. Coating material have complicate structure-stress state. In TiC carbide were formed tension stresses up to 150 MPa. However, in phases W and W_2C were determined pressure residual stresses with 110 and 200 MPa magnitude accordingly. Both tensile and pressure residual stresses have maximum magnitude on surface of coating. Magnitude of residual stresses decrease sufficiently on 5-8 μm depth.

Austenite streak do not have RS independently with its thickness and carbon content. Stress relaxation in austenite phase it is connected with decreasing of specific volume by α-γ transformation. This discovered phenomenon can be useful because such thin layer leads to decreasing of residual stresses on coating-base boundary. This residual stresses leads to decreasing coating material adhesion and limitation of deposited material thickness. Residual stresses with more magnitude are formed in boundary with base on intensive spark treatment. However, austenite layer relaxation ability were increased simultaneously with RS growth. This phenomenon is connected with austenite layer depth growth and increasing of α-γ transformation volume effect under increasing of carbon content. Dependence of γ-α carbon steel transformation volume effect can be explained by such expression: $(\Delta V/V)_{\gamma-\alpha} = 2,5+1,08p$. Where p is carbon content in weight per cents. This expression can be characterize also stress relaxation degree by austenite streak on increasing of carbon content in this streak. Besides that plastic austenite streak can be play buffer role

between the base and fragile coating components in conditions of micro-stroke mechanical loading in wear-resistance coating details exploitation process.

Sufficient stress relaxation in all phase contents begin by laser pulse treatment with $0,3 J/mm^2$ energy density. RS were practical completely relaxed on near-melting area. Spark coating phase content was maintained completely. Austenite streak was relaxed on process of laser treatment.

More intensive heating brings to melting of spark coating and surface alloyed layer with convective mixing of components and practically new alloyed layer formation.

The coating phase components dislocation density was calculated on data of X-ray reflexes half-width. Dislocation density is equal $(1,7-3)10^{-10}$ cm^{-2}. Laser melting increase dislocation density up to $6 \cdot 10^{10}$ sm^{-2}.

HYDROABRASIVE WEAR-RESISTANCE OF CONCENTRATORS FOR ULTRASOUND TREATMENT

Paustovsky A.V., Perevyazko V.A., Gubin Yu.V.
Franthevitch Institute for Problems of Materials Science of NAS of Ukraine, Kiev, Ukraine

Ultrasound dimensional treatment is perspective method for production of prototypes and small specimen series of glass, graphite, ferrite, ceramics, poly- and single crystal diamonds, high strength and construction ceramics. High-precision details of this materials find wide sphere of application: rigging elements, punches, draw plates, instrument, plungers, fuel equipment, bearings and other motor details; details of optical systems, pumps and high-pressure equipment; details for watch, electronic and microfabrication industries; details and groups which operate on high temperature, corrosive surrounding, high loading and abrasive.

Efficiency of ultrasound treatment depends on concentrators work part wear-resistance. These concentrators are operatete on hydro-abrasive conditions.

This type of destruction correlates in complex form with physic-mechanical and strength characteristics of concentrators alloys.

Wear-resistance of steel, hard-alloy and concentrators of other materials do not allow to determine the mechanical characteristics, which correlate with destruction magnitude.

The theory of fragile destruction mechanics, which proposed by Kolesnicov and Cherepanov allow to tie together influence of some structure parameters on wear-resistance; nano-dimension of matrix phase grain, presence and dispersion of strengthen hard phase.

Wear-resistance of materials under the conditions of hydro-abrasive medium increases:

a) with decreasing of matrix phase grain dimension;

b) with decreasing of non-deformation phase content in structure;

c) with decreasing of elastic module;

In order to have full picture of destruction mechanism we have studied the regularities and features of different materials concentrators destruction. This allowed to study the structure and properties of alloys for operation in hydro-abrasive wear conditions.

As a result of the investigation the new materials on nickel base for ultrasound treatment concentrators with high operation characteristics are worked out.

Structure and properties of composite coatings from the nitride CrN and TiN

V. Gorban

Institute for Problems of Material Science, National Academy of Sciences of Ukraine, Kiev, Ukraine.

The existing dependence of the characteristics of friction on a crystal lattice gives the basis to assume, that nitrides with HCP lattice have more wear resistance, than metals with FCC- and BCC-latttce. The adhesion activity of nitrides, makes contribution to wear resistances level its minimum is of characteristic Cr nitrides. This explains a minimum level of coupling of Cr nitrides with steel and other metals in comparison with others nitrides.

The work purpose is research of the structure, phase composition, properties and serviceability of composite coatings on the basis of nitrides CrN and TiN in conditions of high temperatures and contact loadings.

The coating was obtained by the ion-plasma sprayinig of Cr and Ti in nitrogen environment. The ratio of thickness of multiple coatings was chosen as 4:1 at thickness of a layer of nitride CrN 0.4 microns.

Serviceability of the given coatings was compared with that of gas-thermal and galvanic coatings from the chromium-based alloys.

The research of structure of multiple coatings of nitrides CrN + TiN has shown, that the technology allows to ensure the chosen ratio of thicknesses. X-ray structure analysis of the given coatings has revealed a phase of nitrides CrN and firm solution (TiCr) N. Chromium is distributed rather uniformly on layers, and titanium has the precisely expressed concentration dependence. The peak minimum of titanium is on a layer of nitride CrN, and maximum - on nitride TiN.

It is known, that the increase of quantity of phase boundaries results in the increase of hardness in layered composite coatings, that is confirmed by research of the characteristics the of microhardness of multiple coatings in nitrides CrN + TiN. For a two-layer coating the hardness is at the level of 16-19 GPa, for four-layer coating - 18-21 GPa, and for twenty-four-layer one it reaches the level of 26-29 GPa.

Multiple coatings of nitrides CrN + TiN are characterized by high stability of structure and, as a consequence, of operational properties in the temperatures range up to 1300 K (Tables 1).

Tables 1. Researches of influence of annealing temperature on microhardness of coatings from the nitride CrN and nitride TiN.

Material	Nit. comp comp.	Annealing temperature, K			
		1000	1100	1200	1300
CrN	15,0	15,0	13,0	12,0	11,0
CrN+TiN	21,0	20,0	20,0	18,0	16,0

The hardness of coverings is reduced from 21 up to 16 ГПа after 1 hour annealing at temperature 1300 K. Similar dependence is characteristic and for coatings from the chromium-base alloys. The stability of the characteristics composition coatings of nitrides CrN + TiN is confirmed with the given dependences of changes of force of friction on temperature of tests of coatings from the chromium-base alloys (Fig. 1).
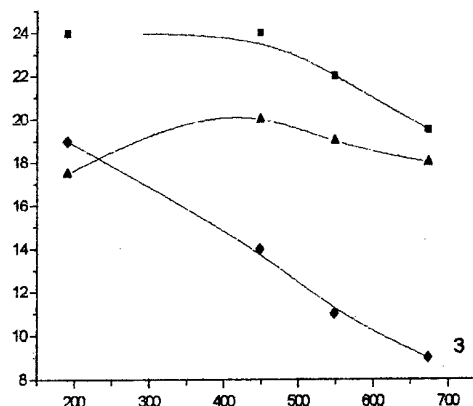
Fig. 1 Dependence of force of friction on temperature of tests and method of production of coatings. 1. - coatings from the chromium-based alloys; 2 - ion-plasma coatings of nitrides CrN; 3 - multiple coatings of nitrides CrN + TiN

The obtained data show, that alloys the insignificant decrease of frictional forces with temperature is characteristic of coatings from the chromium-based, and the considerable decrease of frictional forces (more than twice) is marked for multiple coatings of nitrides CrN + TiN.

The research of coatings after friction has revealed, that the absence of appreciable superficial hardening and saturation by oxygen concerns to features composition coatings of nitrides CrN. The sharp increase of the contents of oxygen in a superficial layer of friction with 6-8 till 20-24 of % on weight and of hardness with 4-5 till 8-10 GPa is characteristic for a coatings from the chromium-base alloys. Composition coatings of nitrides CrN + TiN the stability both contents of oxygen, and level of microhardness is characteristic. It is in most cases marked insignificant (with 17 up to 14 GPa) decrease of hardness at the expense of formation of a thin superficial film of a material rider (iron) on a surface coatings of nitride CrN.

The conclusion is made, that for composition coatings of nitride CrN mechanisms of structural changes, mass transfer and the oxidations of superficial layers bring in the insignificant contribution in wear resistance of a material.

The research of influence of temperature and technology of drawing on time of stabilization of force of friction of coatings from the chromium-base alloys coincides in due course formations of secondary structures on a surface of friction.

In work the research of hardness composition coatings of nitrides CrN + TiN with the help of automatic record of the diagram of depth of cave-in diamond indenters is carried out at small loadings. It has allowed to receive the additional data. Except for importance of common hardness, the application of small loadings enables to estimate hardness of separate layers composition coatings. The estimation of the elastic and plastic characteristics of a material by a method of account of the cave-in, given common depth, and depth of introduction indentors after removal of loading is carried simultaneously spent.

The estimation of influence of various modes of friction and temperature on the service characteristics of various coatings from the chromium-base alloys is carried spent. Is shown, that irrespective of conditions of friction for composition coatings of nitrides CrN + TiN higher parameters wear resistence and corrosion stability are characteristic. So, in conditions of boundary friction at loading 10 MPa, speeds of sliding 14 м/s, temperature of tests 473 K and way of 500 kms friction of deterioration composition coatings of nitrides CrN + TiN has made 1 micron and rider (pig-iron) - 4 microns. For chromium galvanic coatings in similar conditions of deterioration has made 8 and 9 microns accordingly.

The conclusions about the contribution of an elastic and plastic component on wear resistance of coatings from the chromium-base alloys are made.

Literatura.

1. Andrievski P.A., Anisimov I.A., Anisimov V.A. Formirovanie struktyry i tverdosti mnogosloynux kondensatov na osnove nitridov Ti, V, Cr // Fisika i ximij organicheskix materialov. - 1992.- N2.- C. 99-102.

Cajxametov P.X., Karpman M.G., Fetisov G.P. Mnogokomponentnue nitridnue ion-plasma pokrytij na jsnove Ti, V, Cr // Vetallovedenie i termicheskaj obrabotca metallov.- 1993.- N9.- C. 8-11.

496

SECTION E. EXPERIMENTAL DATA OBTAINED FROM PERFORMANCE OF MATERIALS AND COATINGS IN ON LOCATION HAZARD CONDITIONS

STUDY OF THERMAL REGIMES OF RE-ENTRY SPACE VEHICLES USING CRYSTAL INDICATORS OF MAXIMAL TEMPERATURE

Timoshenko V.P.
NPO Molniya, Moscow, Russia, e-mail: moltim@dol.ru

The problems of thermal regimes measurement for re-entry space vehicles are related to most complicated due to necessity of large number temperature sensors installation, weight and layout limitations on cable lines and telemetry equipment. As a rule even at stages of experimental development of new space vehicles it is necessary to limit installation of temperature measurement means by the rather small amount due to mentioned technical difficulties.

One of the way to increase information volume about a thermal condition of hot structures and thermal protection of re-entry vehicles is applying indicators of maximum temperatures. Each indicator of such type allows estimate only one value of maximal temperature reached for all flight time. But it is not require any cables and measurement electronic equipment onboard a descent vehicle.

Most widely used indicators of maximum temperatures are thermal paints. However they are not resistive to mechanical loads as well as to moisture action especially at landing of vehicle on water surface. For estimation of maximum temperature in a given point of a surface it is necessary to apply several types of thermal paints. And the accuracy of measurements essentially depends on number of used paints and size of labels that can be plotted in an investigated zone in view of real temperature gradients influence. Similar lacks have melting plugs from special alloys sometimes also used as indicators of maximal temperatures.

One of rather new means for temperature levels registration are the crystal indicators of maximal temperatures (CIMT). They have good accuracy, small dimensions, high resistance to environment actions and provide a capability of maximum temperature evaluation in rather wide range by only one sensor.

The method of maximum temperature evaluation is based on X-ray analysis of atomic crystal lattice parameters for indicating material which vary depending on a level of temperature and time of heating.

As such indicating material the crystals of silicon carbide or technical diamond are usually used which were undergo previously to irradiation by neutrons. Under the action of irradiation some defects of crystal lattice are formed as a result of atoms displacement concerning their starting positions. Thus there is some extension (on 3-4 %) of crystal lattice which can be measured with accuracy by methods of the X-ray analysis.

After neutron irradiation the crystals of silicon carbide have no residual radioactivity therefore it is not required applying or any measures of a radiation safety.

During measurement process under the action of high temperatures (more 100°C) in crystals occurs so-called annealing of defects - atoms step-by-step return to places of their steady positions in nodes of crystal lattice. This process occurs the faster than temperature is higher and than longer time of heating. As a result there is a gradual recovery of crystal lattice that is removal of the extension induced by irradiation.

The quantitative analysis of a degree of recovery of crystal lattice of the indicator is carried out using X-ray diffraction methods by comparison diffraction angles of X-radiation on atoms of indicating material before and after heating.

For evaluation of maximum temperature values it is necessary to know a history of heating. In particular if the heating takes place at constant temperature it is necessary to know only time of heating. If temperature in measuring point varies during experiment for definition of maximum temperature value it is necessary to know at least in a dimensionless form dependence of a

499

temperature variation with real time of experiment. On the one hand it is definite limitation of a method however in many cases dependence of temperature variation with time is known or can be more or less precisely obtained by a computational way.

The design arrangement of CIMT depends on area of their applying. Crystal element by itself has relatively small size (about 0.3 mm) and can be easily lost. Therefore for convenience of handling it is often installed in metallic or ceramic container.

The technical parameters of CIMT on the basis of SiC are characterized by the following data:
- measured temperature range is from 150°C to 1450°C,
- time interval of the measured temperatures action is from 30 seconds to about 10 days,
- measurement error in all temperature range is 5-20°C, (less for constant temperature levels and more for complex non-steady thermal modes).

The applying CIMT is specially justified for such objects where the usual thermocouples or can not be applied in general or can be installed only in rather restricted number.

In aerospace engineering CIMT for the first time were widely used for estimation of external heat loads on heat protection at flight tests of experimental space vehicles BOR-4 and BOR-5. Later obtained experimental information successfully was used at designing and flight tests of the orbital spacecraft BURAN.

Now CIMT are successfully applied both at bench and at flight tests of materials and structural elements of various space vehicles.

On the Fig.1 the exterior CIMT sensitive element is presented and also shown a fragment of Carbon-Carbon sample with three CIMT, glued on its external surface. This sample was used for research of catalycity in conditions of a high frequency plasmatron.

On the Fig.2 is shown general view of a descent vehicle FREGAT and Carbon-Carbon panel of the FOTON capsule at which CIMT were used for measurement of thermal regimes during re-entry flight in the Earth atmosphere.
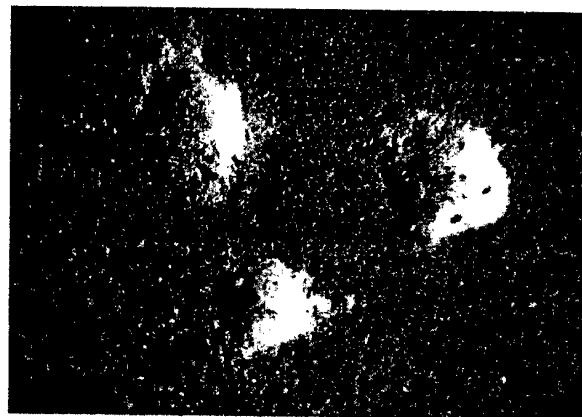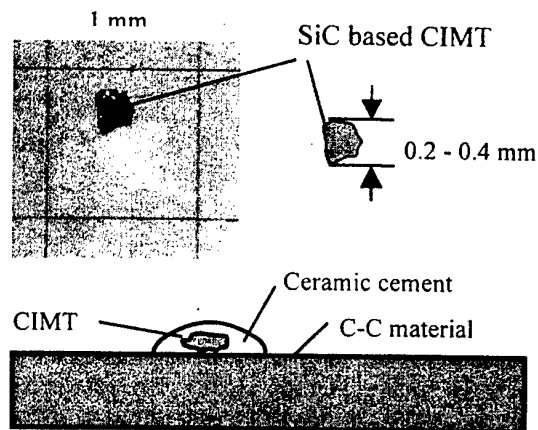
Fig.1 CIMT and its installation on C-C structure
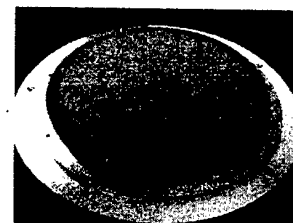
Fregat   Foton

Fig.2 Application of CIMT for temperature measurements in TPS of re-entry capsules

500

WETTING OF TiC BY NON-REACTIVE LIQUID METALS

Frage N., Froumin N., Dariel M.P.

Department of Materials Engineering, Ben-Gurion University of the Negev, P.O.Box 653, Beer-Sheva, Israel

Over the past years, the wetting behaviour of TiC by non-reactive metals has been the subject of several investigations. The purpose of the present study was to relate the wetting of titanium carbide by non-reactive metals (Ag, Au, Cu, Sn) to the thermodynamic properties of these metal-ceramic systems.

The interaction on the metal-ceramic interface depends on the thermodynamic stability of the ceramic phase and on the thermodynamic properties of the liquid metallic solutions. The non-reactive metals, investigated in the present study, do not form a carbide phase and the solubility limits of carbon are very low. Thus, if some titanium carbide dissolves in a liquid metal, it leads to titanium transfer to the melt and graphite precipitation at the interface, according to reaction TiC = [Ti] + C (gr). The amount of precipitated graphite depends on the amount of titanium that is transferred into the melt and is related to the equilibrium titanium concentration in the molten solutions in contact with the carbide phase. The equilibrium titanium concentration depends on the thermodynamic properties of the liquid metallic solutions and, in particular, on the activity of titanium.

The Au-Ti, Sn-Ti and Cu-Ti solutions exhibit a negative departure from ideal behaviour, while the Ag-Ti solution displays a strong positive departure. Thus, the driving force for TiC dissolution in the liquid metals increases from the Ag-Ti to the Au-Ti system. The TiC/Ag system may be considered as being completely non-reactive. The large negative departure of the Au-Ti system from ideal behaviour should lead to enhanced titanium transfer from the carbide phase to liquid Au. The contact angle is a measure of the chemical interaction that takes place between the liquid and the substrate and therefore, a relatively low contact angle was expected for Au(Ti) alloys.

The effect of the carbon content of the carbide phase on the wetting behavior may also be related to titanium transfer through the metal-ceramic interface. The decreasing carbon content in the carbide phase leads to increased titanium activity and to enhanced titanium transfer into the metallic (liquid) phase. The equilibrium titanium content in the metal solution, which is in a contact with sub-stoichiometric titanium carbide, was estimated. The decrease of the carbon content in the carbide phase leads to a remarkable increase of the titanium content in the liquid metals.

Wetting experiments were performed using the sessile drop technique in a vacuum furnace (10^{-3} Pa) at 1150°C for all alloys.

The initial contact angle for all the Ib metals was of the order of 120°-to-130° and 105° for Sn. The initial contact angle did not change in the TiC/Ag and TiC/Au systems that exhibit a strong non-wetting behavior. The contact angle in the TiC/Cu and TiC/Sn systems decreased to slightly below 90°. The non-wetting to wetting transition that occurs in the TiC/Sn and TiC/Cu systems may be attributed to the partial dissolution of titanium carbide in the molten metals.

The actual contact angle in TiC/Au system is surprisingly high and is accounted for by the transformation of carbidic carbon on the TiC surface into graphite. This result was confirmed by investigation of two Au-Ni alloys (3.7 at% and 7.5 at% Ni) and two Au-Fe alloys (7.1 and 15.8 at%Fe) on a TiC substrate.

The direct addition of titanium to the liquid metals as well as decreasing of the carbon content in the ceramic phase improves significantly the wetting of the TiC substrate by the non-reactive metals. However, the actual contact angles in TiC/Au system were surprisingly high. This inconsistency with the thermodynamic predictions can be accounted for by the analysis of the isothermal sections of the ternary phase diagrams. Two schematic isothermal sections are shown in Fig.1. One section (thin lines) corresponds to a system, in which the metallic liquid solution is characterized by a moderate departure from ideal behavior, e.g., the Cu-Ti system.
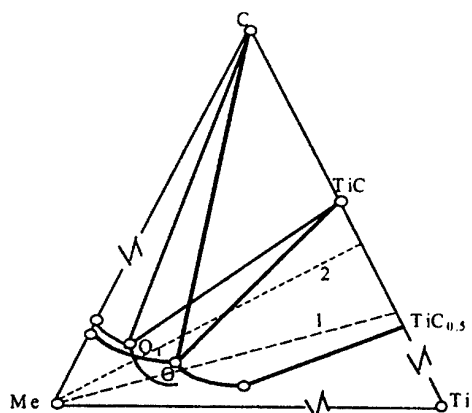
Fig.1. The schematic view of the 1400K isothermal section of the ternary phase diagram.

Point O_1 corresponds to three-phase equilibrium and is located at relatively low titanium content in the metallic melt. The second isothermal section (thick curves) describes a system in which a very strong departure in the liquid metal

It is apparent from Fig.1 that line (2) that links the Me corner with the point corresponding the titanium carbide that has a moderate departure from stoichiometry does not cross the graphite containing regions in TiC/Cu-like systems. This line, however, does cross the graphite-containing region for systems in which the titanium activity in the metallic solution is low. In that case, the interaction between the ceramic and the metal phases leads to graphite formation at the interface. If the departure from carbide stoichiometry is strong enough, line (1) crosses only the two-phase region (liquid metal and TiC_x) and no graphite formation is expected. Thus, the relatively high contact angle in the TiC/Au system may be attributed to the formation of a graphite interlayer at the metal-ceramic interface. Hence, if the C/Ti ratio is low enough ($x<0.6$), all non-reactive metals wet the carbide substrate.

Even though this study proves the preponderant role played by the presence of Ti in the molten metal in determining of wetting behaviour, the exact mechanism by which Ti affects wetting is not yet resolved. In particular, it has not yet been settled whether it is the formation of a sub-stoichiometric, near-surface TiC_x layer with a marked metal-like electronic structure or an enhanced chemical interaction at the substrate-molten metal interface that determines the wetting behaviour.

The results of the wetting experiments were confirmed by joining of TiC plate with plain carbon steel 1080. Altering of near-surface layer of a stoichiometric titanium carbide by a heat treating under hydrogen atmosphere at 850K was sufficient to allow joining the ceramic to the steel by Ag-Cu alloy at 780°C.
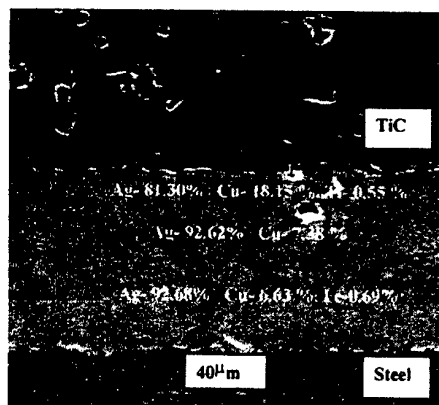
Fig.2. The microstructure of the joint between TiC and 1080 steel.

Transfer of Ti from a thin layer of sub-stoichiometric carbide and of Fe from the steel to the braze take place in the course of the joining process. Adequate bonding of TiC to steel with a filler layer thickness of about 50μm was observed (Fig.2).

502

ENHANCED MASS-TRANSPORT AT LARGE DEPARTURES FROM STOICHIOMETRY IN TiC$_x$

Dariel M.P., Klein O., Frage N.
Department of Materials Engineering, Ben-Gurion University of the Negev, Beer-Sheva, Israel

Titanium monocarbide has a NaCl structure that consists of two interpenetrating, Ti and C, fcc sublattices. At equiatomic composition, each Ti atom is surrounded by six carbon nearest neighbors, located at 0.216 nm, and twelve Ti nearest neighbors distanced at 0.306 nm. Titanium carbide is stable over a range of x = C/Ti ratios, that extends from 0.5 to close to 1. At sub-stoichiometric compositions in TiC$_x$ (x < 1), some of the carbon sites are unoccupied and at the lowest x ratio, 50% of the carbon sites are empty. The structure and properties of non-stoichiometric monocarbides have been the subject of numerous studies [1].

As far as the early seventies, unusual large rates of mass transport were observed in TiC$_x$ at large departures from stoichiometry [2]. Enhanced sintering was reported by Ordinyan [3] at low 0.5<x <0.7 values and excessive grain growth was observed at the range of carbon content. Mass transport processes take place essentially by diffusion in the solid state. The self-diffusion coefficients of Ti and of C have been determined by Sarian [4]. The diffusion of each species takes place on its own sublattice. That of carbon is greatly facilitated by the large concentration of structural empty carbon sites, the diffusion of titanium proceeds also by a vacancy mechanism but only by thermal vacancies generated on the Ti sublattice. The diffusivities of carbon, not surprisingly, are higher by several orders of magnitude than those of Ti, the latter were reported to be independent of the carbon content in TiC$_x$. All diffusion processes involved in sintering or in grain growth, in the two component system, TiC$_x$, occur via an ambipolar diffusion mechanism. The effective ambipolar diffusion coefficient, $\tilde{D}$, can be expressed as

$$\tilde{D} = D_{Ti}D_C / (D_{Ti} + D_C)$$ where

D_{Ti} and D_C are the intrinsic diffusivities of Ti and C, respectively in TiC$_x$. Since $D_C \gg D_{Ti}$, essentially $\tilde{D} \cong D_{Ti}$, we expect that mass transport in TiC$_x$ be dominated by the diffusion of the slowest species, namely Ti, along its fastest path. The substantial dependence of mass transport, both in sintering and, as observed, in grain growth, stands in apparent conteradiction with the reported lack of dependence of the self diffusion coefficients of Ti on the carbon content in TiC$_x$.

In view of this inconsistency, we decided to reexamine the experimental evidence upon which the commonly accepted conclusion regarding the carbon concentration dependence of D_{Ti} was based.

Sarian examined four TiC$_x$ samples, one of which only, TiC$_{0.67}$, had a carbon content x < 0.8. Contrary to the other samples, the TiC$_{0.67}$ could not have been grown from the melt because at this composition it does not melt congruently. Sarian reported only one single data point for this sample, the results regarding a diffusion annneal carried out at 2150°C. We conclude that Sarian's conclusion, regarding the lack of dependence of the Ti self-diffusion coefficients in TiC$_x$ and which seems to have gained common acceptance, is at best well established only for the upper carbon content range, x > 0.8.

Sintering, along its different stages, involves usually several different diffusion mechanisms. In contrast, grain growth involves usually one single diffusion mechanism possibly based on grain-boundary diffusion. The mean grain size, $\overline{D}$, after a grain-growth treatment of t duration, relates to the operating diffusion coefficient through a simple expression of form:

$$\overline{D} \propto C(D_{Ti}t)^{1/n}, \text{ with usually } n \approx 2 .$$

Within a systematic study of the grain growth, various TiC$_x$ samples with 0.5 < x <0.8, were synthesized by reacting stochiometric TiC with appropriate amounts of TiH$_2$ at 1150°C for three hours. In the course of this treatment single phase TiC$_x$ was produced and the carbon content was ascertained by lattice constant measurements and using the previously published data. Grain growth treatments were performed at different temperatures. The grain size of the polished and etched samples was determined using an image analysis software. The grain size after a standard treatment at 1300°C for one hour carried out on

three TiC_x samples with different x values is shown in Fig.1. In some instances the time dependence of the grain growth was examined and the results showed a nearly perfect $\overline{D} \propto t^{1/2}$ behavior.

The results corroborated the previously reported enhanced mass transport effects at large departures from stoichiometric composition. These results, as mentioned, are in gross contradiction with the assumption that the diffusion of Ti is independent on the carbon content in TiC_x. In order to provide an explanation to these observations, we put forward the a model which focuses on the immediate environment of the Ti atoms within a lattice containing a high concentration of carbon vacancies.

The carbon vacancies at the the sintering and grain growth treatment temperatures are distributed randomly on their sublattice, since the order-disorder temperatures are below 1000K. In such a lattice, each Ti atom will have in its immediate neighborhood a statistical distribution of vacant carbon sites. Since Ti, on its own sublattice, diffuses by a vacancy mechanism, its diffusion coefficient can be expressed by the well known relation $D_{Ti} = Do \exp(-Q/RT)$ where

$$Q = \Delta H_{Ti}^f + \Delta H_{Ti}^m$$ and the enthalpy terms are associated with the formation of a Ti vacancy and its migration. The generation of a Ti vacancy is associated with the breaking up of the bonds
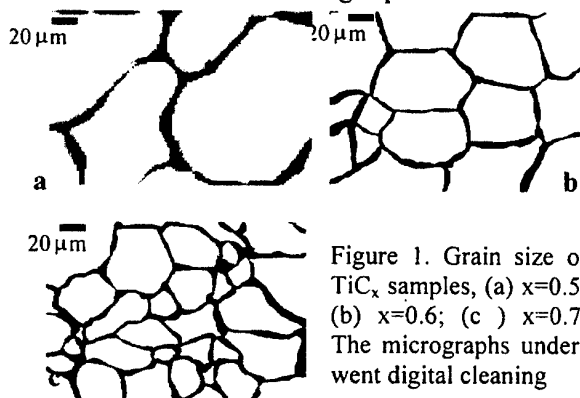
Figure 1. Grain size of TiC_x samples, (a) x=0.5; (b) x=0.6; (c) x=0.7. The micrographs underwent digital cleaning

linking that atom to its immediate neighbors, namely the C atoms. We assume as a first approximation that $\Delta H_{Ti}^f = m\Delta H_{Ti-C} + \Delta H_{Ti}^0$, where m stands for the number of neighboring C atoms (at most 6), H_{Ti-C} represents the enthalpy associated with one Ti-C bond and ΔH_{Ti}^0, the total enthalpy associated with second nearest neighbors, i.e. Ti atoms. Obviously the larger the

number of C vacancies around a given Ti atom, the lower the enthalpy needed to form that vacancy. For reasons of brevity, we neglect at this stage any discussion regarding the effect of the local vacancy concentration on ΔH_{Ti}^m and on ΔH_{Ti}^0. Since the enthalpy term appears in the exponential, we also neglect all local situations in which a Ti atoms is surrounded by less than all six vacant carbon sites. The diffusion coefficient, taking into account the dependence of the statistical probability of six surounding vacant carbon sites, on the carbon-to metal ratio, x, can be written as: $D_{Ti} = D_0'(1-x)^6 \exp\left(-Q'/RT\right)$

(eq.1) where $Q' = \Delta H_{Ti}^0 + \Delta H_{Ti}^m{}'$. Clearly $Q' \ll Q$, and, therefore, this particular local configuration determines the actual diffusivity of the Ti atoms. In order to check the validity of this model, we plotted in Fig.2, the normalized values of $\overline{D}$, the grain-size, along with the normalized $\sqrt{D_{Ti}}$ values fom eq.1, as a function of x. Both the grain size and the $\sqrt{D_{Ti}}$ values were normalized with respect to their value at x = 0.5. The good agreement supports the validity of the model that has been put forward.
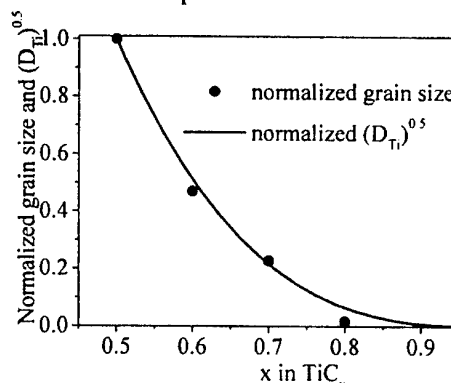
Figure 2. Normalized grains-size and $(D_{Ti})^{1/2}$ as a function of x.

References

1. A.I.Gusev, A.A.Rempel, A.J.Magerl, "Disorder and Order in Strongly Non-Stoichiometric Compounds", Springer, (2001).
2. R.A.Andriyevskii et.al., Powder Metallurgy 6 (174), 22 (1977).
3. S.S.Ordanyan et al., Powder Metallurgy 8 (68), 26 (1968); ibid, 7 (199), 43 (1979).
4. S.Sarian, J.Appl.Phys. 39, 3305 (1968); ibid, 40, 3515 (1960)

504

ANTIOXIDIZING PROTECTIVE COATINGS ON CARBON MATERIALS FOR EXPLOITATION UNDER EXPERIMENTAL CONDITIONS

Kostikov V.I., Kravetskiy G.A., Rodionova V.V.
FSUE «NIIGrafit», Moscow, Russia

Carbon materials cannot be used for a long time in gaseous oxidizing atmospheres at temperatures over 500°C in view of intensive oxidation of carbon. To protect parts made of carbon materials, NIIGrafit Institute has developed a number of formulations and techniques for applying coatings, which ensure serviceability of carbon parts in oxidizing atmospheres in a wide temperature range.

Given hereinbelow are some data on structure and properties of the coatings developed.

Plasma spraying is a technique for applying coatings onto local portions of parts, as well as for protecting large-size parts. A technology has been developed for plasma application of high-melting metal oxides (ZrO_2, TiO_2, Al_2O_3, Cr_2O_3, etc) onto carbon materials. Ways are shown for increasing the oxidation resistance of plasma coatings via creating multicomponent coatings, such as Al_2O_3 – Al useful for protection of arc furnaces electrodes. The investigation of interaction between the oxides and carbon has made it possible to recommend the following temperature ranges for the coatings usage: ZnO_2:1800 to 2000°C, Al_2O_3:1200 to 1300°C.

Slip-baking coatings are characterized by a high technological effectiveness, possibility of applying onto large-size parts of complex configuration, simplicity of the equipment required.

NIIGrafit has developed a member of formulations ensuring the exploitation of carbon parts up to 1500°C. Of great interest is a coating based on molybdenum disilicide and high-melting borosilicate glass which possesses a healing ability for defects and relaxation of stresses arising in the coating from the difference in coefficients of thermal expansion of the substrate and the coating. The coating has been successfully used for protection of wing edges of the spacecraft «Buran», as well as for creation of an experimental short-life gas-turbine engine with employment of carbon-carbon materials (thermally stressed sections of a combusion chamber and a nozzle box). The slip-baking multicomponent coatings based on Ti, Zn, Hf borides ensure the serviceability of carbon parts in a wide temperature range: from 600 to 1800°C.

Coatings based on silicon carbide and applied by the method of chemical reaction from a vapor phase (CVR-process) or chemical deposition from a vapor phase (CVD-process) are used jointly with the slip-baking coatings in view of a high brittleness of the silicon carbide coating leading to its cracking. The slip-baking coating is capable of healing cracks in the carbide layer. In its turn, silicon carbide has good «barrier» properties diffusion of carbon into the oxide surface coatings.

Structural particularities of the coatings and their physic mechanical properties are given.

505

INVESTIGATION OF CONSTRUCTION HEAT-SHILDING DURING THE INFLUENCE OF INCREASED RADIANT HEAT FLOWS

Gotovtsev G.D., Klishin A.F.
Lavochkin Association, Himky, Russian Federation

Under conditions of a single action of increased radiant heat flows structural (including building) materials with lowered thermostability are heated up to self-ignition point. Facility, permitting to conduct accelerated tests of materials, was developed for investigation of thermostability parameters of materials during radiant heating. The facility allows to create radiant heat flow that can be controlled both in magnitude and duration. Initial directed heat flow from the source of radiant heating passes through the diaphragm that shapes the diameter of the beam, and then the radiation power passes through the densitometer and falls on the target made of investigated material. In order to define the temperature of self-ignition point and target heating rate, the temperature variations are measured in time in the area of the radiant flow influence on the working and back side of the target. The beginning and the end of tests are set by the time of operation of controlled shutter installed between the diaphragm and the target. The tests of heat protection of different construction materials have been carried out using the same procedure. The efficiency of application for some thin-layer coating materials which makes a boiling stratum during heating, thus protecting investigated material from ignition, has been defined.

PECULARITIES OF GRINGING THE CERAMIC POWDERS FOR COVERING THE CAST IRON MOLDS

Baranova T.F.
Federal State Unitary Enterprise "Obninsk Research and Production Enterprise "TECHNOLOGIYA", Obninsk, Russia

The ceramic filler consisting of the mullite-corrunduim/chamot/zircon/clay/electrocorundum mixture is used to manufacture the antiburning paint for the cast iron molds in molding the cast iron and aluminium alloys.

The quality of the coating applied depends directly on the ceramic powder dispersiveness which must be optimal and correspond with the specific surface of 5500-6000 cm^2/g. In case of less dispersiveness the smooth state and thickness of the coating are not ensured. In case of higher extent of dispersiveness the stable hiding power of the paint cannot be attained (the paint does not wet the surface of the mold). The paint can also stick to the mold surface.

The process of producing the fine-dipersed powders (specific surface of 5500-6000 cm^2/g) from the staring raw materials with grains 3-0,1 mm in size using new surfactants based on polysiloxane polymers of various structures has been developed. The time of griding in the ball mills 200 litres in valume at 47-55 rpm is reduced one half (from 80-100 to 40-60 hours) depending on the hardness and starting size of powders grains, on the quality of the surfactants being injected. The dependencies of the powders dispersiveness and the coating quality on the surfactant type (hydrophilic and hydrophobic) are determined.

HIGH-TEMPERATURE OXIDATION RESISTANCE OF CERAMIC MATRIX COMPOSITES Si_3N_4/C_f

Kelina I.Yu., Plyasunkova L.A., Chevykalova L.A., Dotsina E.S.
Federal State Unitary Enterprise "Obninsk Research and Production Enterprise "TECHNOLOGIYA", Obninsk, Russia

In the last few years the composite ceramics has received much recognition as a new class of advanced materials having high physical/mechanical characteristics and unique combination of these properties. With respect to these characteristics the ceramics compares favourably (in spite of its brittleness) with metals and alloys. The main field of application of ceramic matrix composites (CMC) is engine manufacturing. Taking into account that the engine components are exposed in real working conditions to heated air and fuel combustion products, it becomes obvious that CMCs being used must be resistant to high temperature oxidation.

The composites with C_f fiber reinforced silicon nitride matrix are of interest among CMCs being developed actively now. Si_3N_4/C_f system is promising for high-temperature applications due to high oxidation resistance of Si_3N_4 matrix at the temperatures up to 1500°C, due to the application for reinforcing the discrete and continuous carbon fibers and due to the attainment of actually theoretical composite material density thanks to the use of hot pressing technology.

The aim of this work is to study the high-temperature oxidation resistance of Si_3N_4/C_f CMCs reinforced with carbon fibers of various brands of home and foreign manufacture which have varying content of fiber. The studies were carried out in the air at moderate (1100°C) and ultimate (1500°C) temperatures.

The process of oxidation of CMCs Si_3N_4/C_f proceeds in two directions. On the one hand the oxidation of Si_3N_4 at the temperatures being considered occurs with mass increment due to the forming of the silicon dioxide film (passive oxidation mode). On the other hand the carbon fiber oxidation with a mass loss begins because the resulting carbon oxides CO_2 and CO being formed are gaseous products.

The process of high temperature oxidation of Si_3N_4/C_f CMCs reinforced with the discrete carbon fibers in a wide range of temperatures (1100-1500°C) has been studied. The studies were carried out based on a series of specimens the content of which varied depending on the type of sintering activator (MgO, Y_2O_3), type of carbon fiber of home (UNKP-5000) and foreign (T300, M60J Torayca, Japan) manufacture and depending on its content from 5 to 40 volume %.

The specimens for the study were manufactured by hot pressing at 1750 – 1850°C in nitrogen atmosphere in graphite molds. This ensured the protection of carbon fibers against oxidation in the course of high-temperature sintering.

The process of high-temperature oxidation of CMC has been studied by the methods of scanning electron microscopy and optical microscopy, X-ray-phase and spectral analyses with respect to the formation nature and composition of oxide film, state of matrix and fibers. The physical/mechanical properties of specimens before and after high-temperature oxidation were evaluated. The dependence of mass on time, fiber type and its volume content are presented.

The essential differences in the mode of composites in the course of oxidation have been detected. Interconnection between the speed of oxide film formation (and its composition) and sintering activator quantity and quality in the Si_3N_4/C_f system have been found. The advantages of MgO sintering activator over Y_2O_3 activator during the use of CMC at temperatures above 1100°C are shown.

The analysis of surface layer microstructure have demonstrated that the oxidation process was running irregularly on mutually perpendicular edges. It proceeds more actively in the plane perpendicular to crystallographic axis "C" of the fiber.

The essential differences in the mode of composites in the course of oxidation at 1100°C and 1500°C have been detected. The changes in morphology of oxidized layer were observed in

the process of temperature increase: from amorphous state to various content of crystalline phases SiO_2.

The structure and integrity of the imported fibers T-300 and M60J remain at 1100°C. These fibers manifested themselves more resistant to oxidation than fibers of home manufacture. The UKN (УКН) fibers change their structure in the course of oxidation and represent thin filaments consisting of spherical-shape particles 0.1-0.2 µm in size (figure 1).

It is shown that the high speed formation of oxide film takes place during a short-time oxidation at 1500°C. Dense film with high content of crystalline phases and 40-200 µm in thickness is formed. Thereby the sealing of pores, self-healing of microcracks and termination of mass losing take place. In so doing the carbon fibers retain their integrity in all CMCs.

The studies of specimens with interlayers made from continuous fibers have shown that in the whole temperature range 1100 – 1500°C the fibers burned up completely with various extent of structure degradation (figure 2).

The fibers in Si_3N_4-MgO matrix retain their integrity in all instances (figure 3, 4) which is due to less quantity of sintering activator and consequently to less quantity of glass-forming components in the ceramics and also due to the peculiarities of the oxidation of matrix itself in this temperature range.

The studies carried out have demonstrated the necessity for increasing the CMC resistance to high-temperature oxidation by creating the protective coatings for fibers and the comprehensive protection of the whole article.

Fig. 1

Fig. 2

Fig. 3

Fig. 4

ANALYSIS OF MECHANISM OF OXIDATION OF MATERIALS ON THE BASIS CARBON BY OF THE INFLUENCE OF STREAM COMBUSTION PRODUCTS WITH TEMPERATURE UNDER 4500 K

Osipov V.P., Panin S.D.
Moscow Bauman State Technical University, 2nd Baumanskaja Str., 107005, Moscow, Russia

In present time there accumulated a considerable experience of calculations of value ablation of carbon-carbon materials nozzles SPRM. The model [1] which takes into account kinetic, transitional and diffusive oxidation regimes by active components (H_2O, CO_2, O_2, OH) stream combustion products is proved data of full-scale test engines.

The mass speed of ablation in kinetic mode is representing by equation

$$m_i = K_{0i} \frac{p}{RT_w} \exp\left(-\frac{E}{RT_w}\right) C_{ie}, \quad C_{ie} -$$ concentration of active components of stream.

The values of coefficient K_0 for common reaction of oxidation are determined experimentally. For carbon-carbon material there provided tests on liquid-propellant rocket engine (kerosene + nitric acid, $T_0 = 3350$ K). The test value ablation and calculated value, when $K_0 = 3000$ m/c are present on fig.1.
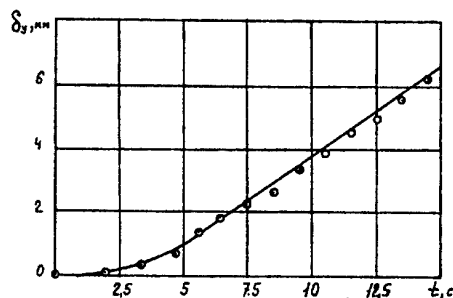
Fig.1 Calculated and test thickness of ablation of throat nozzle LPRE

This value of K_0 was used in calculations of thickness of ablation carbon-carbon materials of throat nozzles SPRM and coincidence with data of test was observed.

The classic test for determining of constants of kinetic oxidation is carried by temperature of wall $T_w = $const., but in conditions of nozzle of SPRM

the temperature of wall is considerably changing in time. Speed of mass ablation goes with finite rate of mass transfer $m = m + t_p \dfrac{dm}{dt}, t_p$ - time of relaxation.

The influence of finite rate of mass transfer is determined by

$$\left(1 - t_p \frac{1}{T_w} \frac{dT_w}{dt}\left(1 + \frac{E}{RT_w}\right)\right).$$

In initial times ($T_w \sim 1000$ K, $\dfrac{dT_w}{dt} = 3 \cdot 10^4$ K, E = $1,7 \cdot 10^5 \dfrac{kJ}{mol}$,) the influence of finite rate has degree (1-50t_p). In work [2] they say, that t_p of mass transferring more t_p of conductivity for 5-6 degree. Then in processes of mass transfer $t_p \sim 10^{-4}$ sec and influence of finite rate don't exceed 5%.

The transition to propellant with temperature of combustion products under 4500 K may require considerable correction of existing approbating models – for $T_w > 4000$ K be able reactions C+H, C+NO and other. The calculations of thickness ablation and temperature fields carbon-carbon throat of nozzle hypothetical SPRM ($p_0 = 14$MPa, stagnation temperature $T_0 = 4500$ K) had by method [3] shows, that temperature of wall $T_w = 3900$ K to 50 sec in throat. When entering the nozzle $T_w > 4000$ K. The pressure is not less than 9 MPa and sublimation mode is hardly to be expected.

The diffusion regime of oxidation is realized and mass rate of ablation $m = \dfrac{\alpha}{c_p} B_m$, where $\dfrac{\alpha}{c_p}$ is parameter of transfer (coefficient of mass trans-

fer), B_m is generalized force (potential function of condition) or oxidizing potential

$$B_m = M_c \sum \frac{C_i}{M_i}, \text{ where}$$

M_c - molar mass of carbon.

According to methodology [1] estimations of maximum value of oxidizing potential was done in terms of thermodynamic equilibrium [4]. The calculations were executed by conventional formula of propellant with redundancy of carbon in condensed phase. Maximum value of oxidizing potential and thermal effect of ablation are shown on fig.2,3.
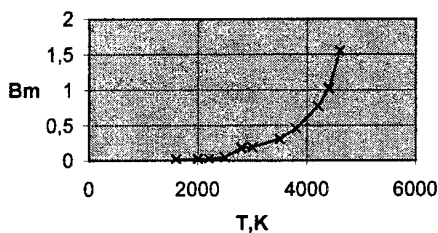
Fig.2 Change of oxidizing potential

These data confirm existence of the temperature range with invariable value of oxidizing potential. The intensity growth oxidizing potential B_m for reason of atomic hydrogen is observing at $T_w >$ 3000 K, but contribution of nitrogen is unimportant.
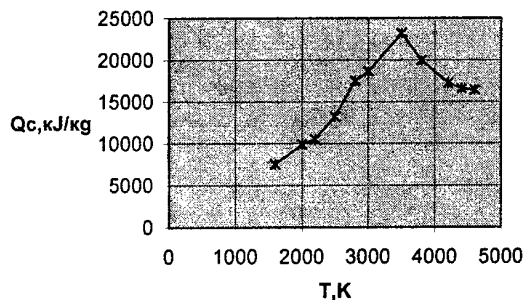
Fig.3 Change of thermal effect

Data are received maximum value. The growth of ablation rate because of increase of oxidizing potential brings to the growth thermal effect of abla-

tion mQ_c in boundary condition of equation for conductivity.
It begins to reduce the temperature of wall and returns process in limits of usual models.

References

1. V.I.Boyarintsev, U.V.Zvyagin. Investigation of destruction graphitic materials at high temperature // Thermophysics of high temperature, 1975, V.13 -№5, pp.1045-1051.
2. A.V.Luicov. Heat and Mass transfer: Reference book. M.: Energy, 1978. – p.480.
3. A.A.Shishkov, S.D.Panin, B.V.Rumyantsev. Working processes in solid propellant rocket motors. M.: Mashinostroenie, 1988. – p.240.
4. G.B.Sinyarev, N.A.Vatolin, B.G.Trusov, G.K.Moiseev. Application ECM for thermodynamic calculations metallurgical processes. M.: Science, 1982. – p.261

CAPACITY TO EXPLOSION-PROOF PROTECTION FOR METALS AND METALLIC COATINGS

Author: Senior Scientific Researcher I, ROMAN EREMIEA Ph.D.Eng, General Director
National Institute for Mine Safety and Explosion-Proof Protection - INSEMEX Petroşani, Romania

The metallic materials and coatings of housings for equipments or for their parts in industrial installations may become sources of ignition for flammable gaseous mixtures through mechanical sparks and/or over-heated surfaces.

The author identified the tendency to ignition by mechanical sparks and/or over-heated surface for the main metallic materials and identified original solutions for an explosion-proof protection.

The paper presents in detail the tendency to ignition by mechanical sparks of metals, through analytical determination, as well the results of the laboratory tests carried out on different industrial metals and protective coatings in explosive atmosphere with combustible gases.

The annex presents, in Xerox-copied format, the diagram for the ignition tendency by mechanical sparks of the main metals for general industrial use. The explosion-proof protective solutions that result after research studies shall classify into:
• Protective solutions that result after an optimum design and choice of the metal nature;
• Protective coatings with spark-proof, static-proof and corrosion-proof properties.

INVESTIGATION OF FAILURE OF FIBERGLASS PLASTIC AND CARBON-CARBON COMPOSITION MATERIALS UNDER CONDITIONS OF FLIGHT IN DUSTY ATMOSPHERE

Mikhatulin D.S., Polezhaev Yu.V., Reviznikov D.L.[1]

IVTAN (Institute of High Temperatures) Scientific Association, Russian Academy of Sciences, Moscow, 127412 Russia

[1]Moscow State Aviation Institute (Technical University), Moscow, 125080 Russia

The flight of a hypersonic flying vehicle (HV) in an atmosphere containing rain (snow, dust, etc.) formations is accompanied by both thermochemical and thermal-erosion failure of external thermal shielding. The highest degree of such effect is observed at the leading edges of wings and at the stagnation points of frontal surfaces. In view of this, it is of interest to perform an integrated study of heat transfer and erosion failure of heat-shielding materials under conditions of horizontal flight of an HV at different parameters of flight, espeially, at the beginning of motion when entering a cloud of formations identified above.

In this study, we simulate the horizontal flight of an HV first in a clean atmosphere and then in a dusty cloud. Taken to be the initial moment of time was the moment when the HV in the state corresponding to that of flight in a clean atmosphere enters a dusty cloud. The transition period starts from quasistationary thermochemical failure of fiberglass plastic in the nondusty flux to thermal-erosion failure in the dusty cloud; it is this latter cloud that is studied by us up to relaxation to the quasistationary rate of thermal-erosion failure. Meant by this is a constant rate of failure that may be such only under conditions of a constant thermal state of the surface layer, i.e., when, at the moment of particle impact, the temperature profile in the surface layer is one and the same. The period being studied is the period of variation of the temperature profile from the initial period, which corresponds to the quasistationary profile under the thermochemical effect of the clean gas flow before the HV entry into the cloud, to the final period, which corresponds to the quasistationary profile under the thermal-erosion effect of the dusty gas flow under conditions of flight inside the cloud. In so doing, the results of experimental investigations involving ground studies into the fiberglass resistance to the supersonic effect of heterogeneous flows are extended to the flight conditions.

A characteristic feature of the material being investigated (fiberglass plastic) is the marked dependence effective enthalpy of erosion failure of H_{er} on the integral mean temperature T_s (a drop with increasing temperature of heating of the surface layer). This effect must be included in the prediction of the behavior of materials of fiberglass plastic under fight conditions.

In order to calculate heat fluxes under conditions of supersonic heterogeneous flow past a blunt body, use is made of a semiempirical model [1] that defines the coefficient of enhancement of convective heat transfer relative to its value of α_0 in a dust-free flow.

Various procedures may be employed to calculate the convective heat transfer in the neighborhood of the forward critical point under conditions of dust-free flow past a spherical blunting. We used the Fay-Riddell formula.

Therefore, the process of simulation of thermal-erosion failure under flight conditions includes the following steps, the determination of the gasdynamic parameters of incident flow by the reassigned trajectory data, the calculation of the parameters of gas in the shock layer between the shock wave and the body subjected to flow, the calculation of motion and heat transfer of particles in the shock layer and the determination of the parameters of collision between particles and obstacle, the calculation of the parameters of heat transfer of the structure subjected to dust-free flow, and the simultaneous solution of equations of pulsed failure and heat transfer in the material subjected to failure.

We treat the neighborhood of the forward stagnation point of a spherical blunting with an infinite extent of the cloud and constant parameters of incident flow, determined using the standard atmosphere model. The equation of motion for a solitary particle in compressed gas

behind the shock wave is used to determine the rate of collisions between particles and object. The drag coefficient of particles is calculated by Henderson's formula.

On analyzing the variation of the surface temperature T_w in the initial stage of the process, one can conclude that, for large particles, the variation of the temperature profile in the surface layer first proceeds by way of "cutting off" its high-temperature part to a depth equal to the crater depth. This is followed by the heating to the temperature T_m and the recovery of thermochemical failure with considerable values of time from the beginning of the process. It is only at a high altitude H and at a low concentration of particles, when the convective heat transfer α is relatively low, that the temperature of thermochemical failure does not recover even after the first particle impact.

The effect of the temperature dependence of the effective enthalpy of erosion failure on the thickness $\overline{\Delta}_T$ of material carried away may be judged by the difference of the curves corresponding to this quantity for different parameters from the straight line Δ_0. For this factor, the effect of the nonstationary stage is significant. This shows up most clearly in the case of a small particle diameter (d_p=5 μm), when the average temperature of the heated layer remains rather high during the extensive initial stage. In so doing, the time dependence of the thickness $\overline{\Delta}_0$ - of material carried away in the nonstationary stage is substantially nonlinear, this leading to a considerable excess of $\overline{\Delta}_T$ over $\overline{\Delta}_T$, the thickness of the layer carried away at a constant enthalpy H_{er}=const (in the latter case, the rate of carryover is constant and the dependence is linear). In view of the foregoing, the temperature dependence of the effective enthalpy of erosion failure H_{er} must be included in such estimates.

An increase in the flight altitude leads to a variation of the affecting parameters. An analysis of this venation reveals the existence of two contradictory factors which define the effect of the flight altitude on the intensity of failure of heat shielding. On the one hand, the increase in the rate of collision of particles with the surface predetermines the intensification of failure, and, on the other hand, the increase in the effective enthalpy H_{er} is indicative of the increasing resistance of the material to failure. For all

particle sizes, an increase m altitude leads to a drop of T_s as a result of the decrease in the total coefficient of heat transfer and of the increase in the crater depth with increasing velocity of particle impact. This leads to a decrease in the rate of erosion failure $\overline{U}_{er}$, which is most pronounced in the case of particles of small diameters and in the case of low altitudes, when the weakening of the decelerating effect of the shock layer on particles is of considerable importance.

The effect of the radius of hemisherical blunting of the frontal sirface R_N on the rate of erosion failure is analyzed. An increase in R_N is accompanied, on the one hand, by a decrease in the rate of collision of particles with the obstacles, which promotes the heating of the surface layer, and, on the other hand, by a decrease in the heat-transfer coefficient. As a result of the effect of these contradictory factors, the temperature of the surface layer and the effective enthalpy of erosion failure prove to be rather conservative to the venation of the blunting radius for the treated panicle sizes, and the venation of the intensity of failure is largely defined by the decrease in the rate of collision.

A more significant effect is made by the concentration of panicles in the flow. An increase in the concentration G_p leads to an increase in the heat flux and promotes a rise of the temperature of the heated layer. However, this tendency is suppressed by the reduction of the time between collisions. As a result, for all treated particle diameters, T_s drops with increasing G_p, this leading to a decrease in $\overline{U}_{er}$. In this case, this correlation is less conspicuous with increasing particle diameter.

INTERACTION OF RAREFIED SUPERSONIC GAS FLOWS AND RADIATION FLUX WITH STRUCTURAL MATERIALS OF SPACECRAFT OUTER COATINGS

Abramovskaya M., Aksyutenko A., Bass V., Percheritsa L., Smelaya T.
Institute of Technical Mechanics of National Academy of Science (NAS) and
National Space Agency (NSA), Dniepropetrovsk, Ukraine

The brief review of basic results of fundamental and applied research performed by the research staff of employees of the Department of Rarefied Gas Dynamics of the Institute of Technical Mechanics of NAS and NSA is submitted.

The investigations into the features of interaction of rarefied gas supersonic flows with the materials of space vehicle (SV) other coatings was necessitated by consideration of a wide scope of scientific and applied problems in the fields of rarefied gas dynamics, molecular gas dynamics and satellite photometry.

In this report attention was focused on the experimental investigations carried out with the aid of the vacuum aerodynamic facility (VAU-2M) ITM NAS and NSA [1]. The installation was put into operation in 1988 with direct financial support of RSC "Energia" and State design office "Yuzhnoye".

Measurement results of impulse exchange coefficients and scattering indicatrixes of neutral rarefied supersonic flows (velocity $4 \div 8$ km/s) interaction with main structural materials of SV outer coatings (screen-vacuum thermal insulation, aluminium-and-magnesium alloys, solar batteries fragments, ceramic coatings, etc.) are presented. The force measuring results are generalized in the framework of a hypersonic approcsimation of a diffuse model with variable accommodation coefficients of normal P_n and tangential P_τ component of impulse. A root-mean-square error of the measuring did not exceed 6 %. The obtained results are in agreement with the results of scattering indicatrixes measurements on the same surfaces.

The results of data processing on aerodynamic drag of six passives spherical Simulated Earth Satellites (SES) made of different structural materials launched in the framework of space program "Variation" are discussed. The experiment was carried out on the basis of a joint decision of several organizations: ITM (Ukraine), "Nauka" and "Cosmos" (Russian federation). The satellites were put in the orbit in pairs and separated from SV "Resurs-F" 25.05,89, 18.07,89 and 01.08,92. Other coatings materials for these satellites were chosen on the basis of the analysis of experimental results obtained on VAU-2M installation. During the whole period of SES existence they were regularly observed with the aid of space checkout facilities. In so doing, orbits element and ballistic coefficients of coordination between real satellite deceleration and one value measured under laboratory conditions were correlated. Qualitative and quantitative coincidence of full-scale and laboratory experiments allows to develop an adequate enough model of the basic physical features of interaction of high-speed rarefied gas flows with streamlined surfaces on the VAU-2M installation and their recalculation to full-scale conditions of flight.

At present problems of reliable aerodynamic support of space projects and programs are often arise. The realization of the "Venus – Galley" international project may serve as an example. At SV flight in gas-and-dust comet atmosphere (relative velocity ~ 80 km/s) the energy of interaction of dust particles of a mass up to 1 gm with outer coatings materials is commensurable with the energy of a micronuclear explosion. Methodical aspects of investigations of a hypersonic flow about "Vega" spacecraft and simultaneous action of solar radiation are discussed [4].

The results of systematic research of aerodynamic characteristics of the orbital SV and the implanted research probe (penetrator) also at various modes of their motion in a Mars atmosphere (design "Mars – 96") are given.

New physical and mathematical models have been considered to describe mass transfer processes and

the glow characteristics in the SV locality, including the calculation three-dimensional free-molecular flows taking into account the interaction of propulsion systems jets with the structure elements [2]. Attention is fixed on the role of physical and numerical experiments in the investigations of the luminous radiation level and induced pollution of onboard devices and equipment owing to the collisions of structural materials mass loss products among themselves and with free stream particles.

Priority attention has been paid to the development of efficient numerical algorithms allows to take into account of interference effects, structure elements cross shading and program realization of such algorithms.

The existing physical analogy between the processes of molecular and radiation flux has allowed the developed software to be adopted with reference to the solution of modern problems of geodynamics of a satellite photometry and radiative heat exchange. The results of complex numerical studies of disturbances acting on the part of forces of a nongravitational origin on geodynamic satellites and satellites of global navigational systems ("Etalon", "Glonass", GPS) are presented. The analysis of the obtained results has shown that in the calculation of forces of solar pressure acting on these satellites the influence of structure elements mutual shading effects becomes determining.

A priori numerical analysis of nongravitational disturbances acting on Etalon SES with regard to the structure elements reflective power has shown the good agreement with laser long-range measurement results processed subsequently.

The examples of application of computational aerodynamics methods for the solution of various satellite photometry problems are demonstrated.

A special attention is given to the discussion of the results obtained in the field of SV outer molecular and radiation heat exchange. The mathematical methods developed to calculate aerogasdynamic characteristics were modified conformably to problems of SV outer molecular and radiation heat exchange. The main sources of SV elements outer heating include: direct solar radiant energy fluxes, molecular thermal radiation fluxes ("kinetic" heating and heating as a result of a recombination

of the upper atmosphere atomic oxygen on streamlined surfaces), and also of Earth's infrared radiant energy fluxes and solar radiant energy fluxes reflected by its surface. It is shown that at small altitudes (~200–300 km) molecular fluxes essentially contribute to total heat fluxes on the SV structure elements of large sizes (orbital complexes, reusable apparatus, etc.). The magnitude of these fluxes substantially depends on a molecular composition of the Earth's upper atmosphere and its variations caused by solar and geomagnetic activity. It is underlined that in the development of SV thermal control systems it is necessary to take into account all kinds of outer radiant energy fluxes since at small altitudes the radiant energy fluxes going from the Earth can reach value ~40 % as compared to direct solar radiant energy fluxes [1].

The scientific program of individual aerophysical experiments on studying the kinetics interphase and intermolecular interaction planed to be fulfilled and realized onboard an International Space Station [4] is presented.

References

1. Bass V.P. A technical mechanics. –2001. – № 1. –P. 52–63. (in Russian)
2. Bass V.P. A technical mechanics. –2001. – № 1. –P. 63–85 (in Russian)
3. Bass V.P. A space science and technology. – 2000. –Vol.6. –№ 4. –P. 57–60. (in Russian)
4. Rijov Yu. A., Bass V.P., Kovtunenko V.M. u. a. Rarefied Gas Dynamic. New York and London Plenum Press. –1982. –Vol.1. –P. 503–511.

TRIBOLOGICAL INVESTIGATION IN OPEN SPACE AROUND THE MOON

Yarosh V.M., Moisheev A.A., Bronovets M.A.[1]

Lavochkin Scientific and Production Association, Khimki, Russia

[1]Interdisciplinary Scientific Tribology Council, Moscow, Russia

INTRODUCTION

Further development of cosmonautics is connected with creation of satellites, space stations and space vehicles with long life times. While this, significant interest gives work of friction units in open space, because according to working environment a complete row of mechanisms and assemblies work out of pressurized compartments and could be influenced by open space factors. And besides, for us very important to know correctness the overhead testing of the antifriction materials and friction units in vacuum equipments.

FRICTION SIMULATOR (FS)*
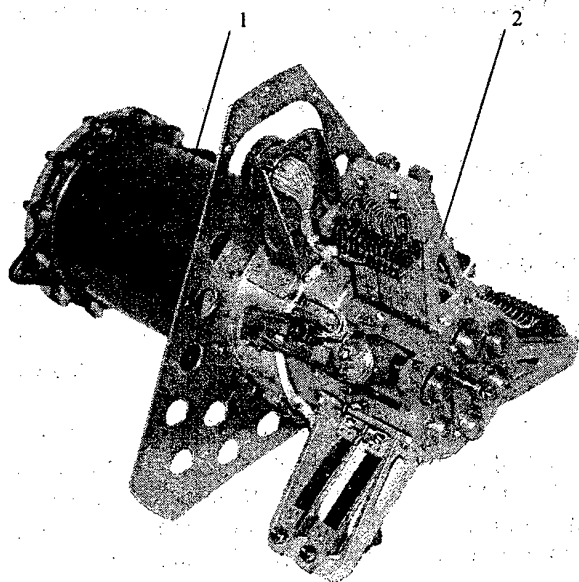
Figure 1 Friction simulator
1) Electromechanical hermetic driver
2) Test friction units block

FS was built for investigation of tribological parameters of antifriction materials and coatings in laboratory facilities and in vacuum or gas environments as well, and also on-board of any S/C in the open space environment.

*The Institute of Optical-Physical Measurements under the leadership of prof. A.A.Silin designs FS device; it's laboratory tests were executed in the same Institute under the leadership of prof. E.A.Dykhovskoi

FS -device set includes:
- Autonomous FS unit (dimensions: 315 x 230 x 180 mm, mass is 4,0 kg);
- Two five-channels strain meter converters (dimensions: 225 x 170 x 120 mm, mass is 1,5 kg);
- Control unit of the tested assemblies (dimensions: 240 x 180 x 60 mm, mass is 1,5 kg).

In device are using two schemes of the friction testing: "shaft-bush" (1) (back-to-back overlap coefficient of the friction surface approximates to 1) and "disc-indenter" (2) (back-to-back overlap coefficient of the friction surface approximates to 0). Simultaneously nine friction assemblies could be tested: three assemblies "shaft-bush" and six assemblies "disc-indenter"**.

Taking into account, that FS device should work in high vacuum environment, decision to investigate tribological parameters of widely using VNII NP-212 hard lubrication coating (HLC) in S/C friction assemblies was taken; lubricate component of it is MoS_2.

Choosing of loading-speed test regimes of the samples testing was done by samples model tests from the same materials in specially manufactured unified module UMT- scheme "shaft-bush" on vacuum facility VK-1.

FS -device working on board the spacecraft

Special control unit (SCU) for the friction assemblies control was designed in order to execute experiment in space; radio commands were transmitted to BUT from the Earth, and FS device and two strain meter converters via SCU were connected to S/C. Flying FS device, two strain meter converters and SCU by the special frame were installed at the external surface of the S/C structure; S/C was designed to the moon mission. In order to provide referenced temperature mode FS device with the equipment set was covered by MLI. In order to increase degree of vacuum in the testing samples zone, a hole of 70 mm in diameter was cut in MLI.

**Choice of the specimen materials and load-velocity regimes provides under leadership of prof. Yu.N.Drozdov and dr.S.L. Gafner (A.A.Blagonravov Research Machinery Institute RAS)

During the 15-month active work of the space station around Moon the testing friction units with hard lubricant expose to influence the space environment. 18 communication contacts were performed with FS device. During mentioned period, sum device working time was 128 hours.

Results of tests in far space

It is well known that in the course of flight the S/C itself changes properties of ambient environment, by creating its proper atmosphere around it, which forms due to desorption, sublimation and erosion of materials from the exterior surface of vehicle, imminent losses of gas and its condensate from the pressurized compartments.

The FS instrument was installed on the "LUNA-22" S/C under thermal protection, in which a through-hole was cut in order to increase the value of vacuum in the area of testing units. Basing on available experience of development and operation of different S/C mechanisms in the conditions of outer space, it is possible to suppose that a pressure around the testing units of friction was about 10^{-4} - 10^{-5} Pa.

First FS device switch-on was executed in 32 days after the launch of the S/C. FS -device staying in duty mode during long period of time was planned in order to determine action of the space environment onto the structure and measurement systems of FS -device, onto evaporating process of adsorbed gases, water vapors and cleaning of the antifriction coating surface.

Friction coefficients at the Moon orbit

First seconds of testing friction assembly's work showed practically the same friction torque that had been received at the launch site. This could be explained by the fact that "input" surface layer of the lubricant coating didn't change during 32 days under the open space factors action.

Throw 1,5 – 2,0 min test friction coefficient have value for scheme "shaft-bush" 0,24-0,22 and for scheme "disc-indenter" 0,16-0,15. Friction coefficient to the end of the first communication contact decrease for "shaft-bush" to 0,14-0,10 and for "disc-indenter" to 0,10-0,09.

Beginning high value of the friction coefficient of installed friction, and, further stabilized at the value of 0,06-0,04.

It is interesting to note influence of FS device presence time in not working mode onto start friction coefficient during tests according to scheme "shaft-bush". If time of not working device mode was from 20 to 76 days, then start friction coefficient increased up to the value of 0,21, and while 1 day - from 0,1 up to 0,15. These results show, that MoS_2 in the coating has so called "stop-effect", - increases friction torque while start, depending on time interval of friction assembly staying in not working mode. The same result we were showing on the scheme "disk-indenter".

During all exploitation period in the space, temperature inside FS body and temperature of two strain meter converters, staying in not working position, had average values of 10 - 12 °C. During FS work temperature of its body was increased up to 28 - 35°C and its value depended on duration of FS functioning.

CONCLUSION

1. The autonomous instrument FS, intended for the tribological tests according to kinematics configurations: "shaft-bush" and "disc-indenter" was developed and manufactured. It was installed on the exterior surface of the "LUNA-22" S/C and during 15 months it was subjected to the series of successful measurements of tribological characteristics on the Moon orbit.

2. The tests on the Moon orbit established a tendency of reducing of the friction coefficient to some limit value after the beginning of work of the joints, which keeps independently on the number of activation's of the instrument and duration of non-movable contact. The starting friction factor increased depending on the duration of the FS instrument being in the switched off state. This argues that MoS_2 has the so-called "stop-effect".

3. On the basis of acquired results of ground and flight tests of samples of pairs of friction it is implied to develop the guideline/technical documentation (GTD) necessary for provision of tests and certification of antifriction materials on the endurance under affect of factors of the outer space and the bringing of GTD in accordance with the international requirements.

APPLICATION OF COMPOSITE MATERIAL "IPM-301" AT TRIBO-JUNCTIONS OF SPACE RADIOMETRIC SYSTEM "R-400"

Kostornov A., Yuga A., Chevichelova T., Simeonova Yu.[1], Nazarsky T.[1]

Frantsevitch Institute for Problems of Material Science NUAS, Kiev, Ukraine

[1]Space Research Institute of the Bulgarian Academy of Sciences, Sofia, Bulgaria

The complex of research equipment onboard the MIR Space Station used to study the Earth from space under the Priroda International Program comprised, among others, the Bulgarian Scanning Radiometric System R-400 [1]. It measured the own radiothermal emission of the Earth's surface in the microwave range of the electromagnetic spectrum. For the purpose, a twopolarization scanning antenna was used, operating in space vacuum.

The requirements for reliable operation in space posed a specific tribological problem to be solved in the process of designing the tribojunctions of the antenna mechanism. A unique self-lubricating composite dry-friction material was used, operating within the temperature range from +50°C to -30°C.

Space conquer revealed the complex nature of the tribological processes taking place in vacuum, in the absence of oxygen and moisture in a highly diluted medium, without convection cooling and traditional lubrication [2]. Under these conditions, contact interaction takes place at higher temperature and plastic deformation, with increasing adhesion causing intensive wear, scuffing, and seizure at the contact place [3]. This is the reason why failures in space are sometimes of tribological nature.

Accounting for these peculiarities, in constructing the tribojunctions of the system R-400, a new copper-based composite material was used, alloyed with Mn and P, and containing Pb in the form of globular formations. The material was developed at the Institute for Problems of Material Science of the National Academy of Sciences of Ukraine. At the Space research Institute of the Bulgarian Academy of Sciences it was studied and put to a complex test, after which it was used at the tribojunctions of the system R-400 [4].

The studies revealed that the material represents a heterogeneous, relatively plastic compound containing solid phases. Its structure is shown in Fig.1. The study of the structure performed by the quick electron defraction method (80 kev) revealed that it represents a superposition of the three cubic lattices of Cu, Mn, and P. The basic lattice is the copper one, and the biggest lattice is the lead one. Lead is present in the form of an oxide that does not impair the constant of the Cu lattice.

Phosphorus forms a solid phase (Cu_3P) located along the grains boundary. It restricts plastic deformation and obstructs the formation of scuffing centers at the contact place under dry friction in vacuum.

Manganese also forms a solid phase that improves the material's strength, not impairing its plasticity.
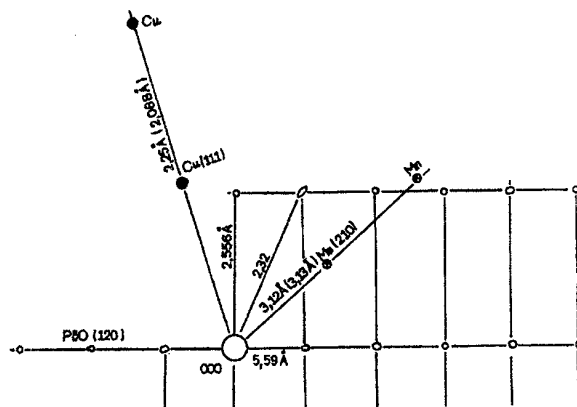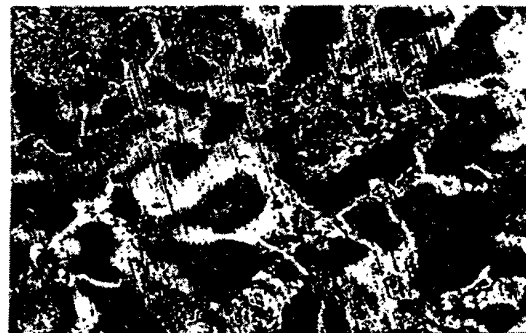
Fig.1 - Structure of the material: microstructure and defractogram

Under dry friction, as a result of increased temperature and plastic deformation as well as the difference in diffusion coefficients and linear expansion of Cu and Pb, a stimulated diffusion of lead towards the surface is observed. The analysis of the friction surface, performed by the method of the Auger-electron spectroscopy proves this. On the spectrogram of the surface under dry friction in vacuum, a manifested peak of Pb at 96 ev is observed. Its intensity increases depending on the friction regime.

The X-ray microanalysis reveals that, under dry friction in air, a layer of oxidized lead is formed on the surface while under friction in vacuum a layer of reduced metal lead is formed. The quantity and surface distribution of the latter depend on its distribution within the material's structure and the friction regime. These two factors determine to a great extent the antifriction parameters of the surface and its adaptability in operation. The change of the friction coefficient points to the same fact. Under friction in air it drops from 0.34 to 0.18-0.20; under friction in vacuum (3.10^{-4} Pa) it drops down until it reaches the stable value of 0.16 which is due to the formation of a surface lead layer acting as a solid lubricant.

Experience shows that reduced metal lead as a lubricating material features more stable triboparameters in the process of operation which

confirms the trouble-free operation of the tribocouples of the antenna mechanism of R-400 in space conditions in the course of 5 years [5].

REFERENCE

1. Nazarsky T., Dimitrov G., Levchev Ch. The PRIRODA Project for remote sensing of geophysical parameters from board of the MIR Orbital Station, Bulgarian Geophysical Journal, Bulg.Acad.Sci., vol.XIX, Nr.3, Sofia, 1993 (in Bulgarian).
2. Silin, A.A.. Friction in space vacuum, Friction and Wear, issue Nr.1, 1989, 1 (in Russian).
3. Drozdov Yu.N., Pavlov V.G., Pouchkov V.P. Friction and wear under extreme conditions, M., Machine Construction, 1986, p.51-61 (in Russian).
4. Simeonova Yu., Nazarsky T. Application of Composite Materials in the design of space apparata. Intern.Congress "Mechanical Engineering Technologies'97", Sofia, Sept.1997, Proceedings, vol.4, p.104.
5. Nazarsky T., Dimitrov G. et al. Studies with the microwave scanning radiometric system R-400 under the PRIRODA International Research Project for Remote Sensing of the Earth from space, 10 Years Since the SHIPKA Space Project, Jubilee Research Session, June 1998, Sofia, Proceedings, 1998 (in Bulgarian).

PROBLEM OF MATERIALS AT ECONOMIC HIGH-SPEED START OF THE SATELLITE IN SPACE

Nerus M.
Institute for problems of materials NAS of Ukraine, Kiev, Ukraine

Necessity to delivering in space of a plenty of technological cargoes demands search of new less expensive ways of their delivery in circumterraneous space that would provide economy of means up to 50 %.

Search conducts both on a way of creation of electrodynamic accelerators, and on a way of creation of artillery systems capable to deliver a cargo in space [1, 2, 3].

It represent the most perspective a way of the dispersal of a shell mixed in many stages in the vacuum accelerator (a vacuum gun). At the first stage the shell is dispersed as in the usual instrument by influence of pressure upon a bottom of a shell on technology MIAIBN. At the second stage there is a mixed active - jet dispersal of a shell. At the third stage - active dispersal due to adiabatic expansion of the saved up gases.

Additional dispersal of a shell on a final site of a trunk is made on the electrodynamic accelerator. After the second stage there is a burning in a trunk of elements of a design of jet engines that results in increase of energy of a working body in out-of-shell space. Components of a working body are selected such that they could provide necessary speed of dispersal of a shell in a trunk.

The range of speeds of dispersing can be within the limits of 3000 ... 11200 m/sec. The circuit with additional dispersal of a shell on a trajectory after its output from a trunk of the dispersed device is on occassion possible.

For simplification of the circuit of work of dispersing device the stage of electrodynamic dispersal can be excluded.

Calculation of movement of a shell is made on the equations:

$$M\frac{dV}{dt} = P_K S, \quad (1)$$

$$P = m\omega_u + F_c P_c - F_c P_h, \quad (2)$$

$$A = E = \frac{P_1 V_1}{\gamma - 1}\left[1 - \left(\frac{V_2}{V_1}\right)^{1-\gamma}\right] = \frac{mV^2}{2}, \quad (3)$$

$$V = \sqrt{\frac{2A}{m}}. \quad (4)$$

For decrease of expenses for overcoming of forces of resistance of environment to movement of a shell in a trunk the vacuum before a shell is created.

The vacuum artillery system "Apogee-N" for economic high-speed deducing cargoes in space is shown on fig. 1.
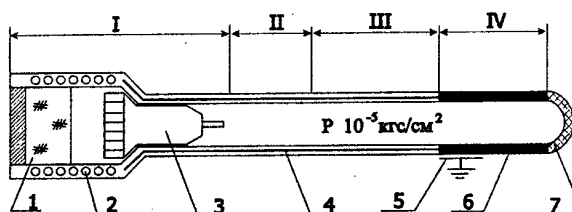
Figure 1. The vacuum artillery system "Apogee-N"

I - an active site of dispersal, II - an active-jet site of dispersal, III - active (an adiabatic site of dispersal), IV - an electrodynamic site of dispersal.
1 - a powder charge, 2 - the plasmagenerator, 3 - a shell, 4 - a trunk, 5,6 - electrodes, 7 - the vacuum hatch.

The problem of materials at high-speed dispersal of the device is solved by application new high-energy fuels for the charges of dispersal burnt during work, high-strength materials for units of rocket engines, low - frictional materials for pair friction the "trunk - shell", new high-strength and wearproof materials for units and details of the vacuum dispersing device. In a design of installation are used new composit materials "Trainer", "Luner" and "Shield".

The problem of decrease of expenses for overcoming of forces of friction at movement of a shell on directing is solved by application of new technology of its moving. At dispersal the shell goes in a trunk in a gas pillow. Kinetic friction of pair friction "shell - trunk" passes in internal friction between layers of the gas environment.

$$F_{END} \geq 10^3...10^5 F_{BG}. \qquad (5)$$

The Problem of decrease of initial weight of the device removed in space is solved by application in the discrete rocket engine high-energy fuels with the big share of low-molecular components. Capacity of the rocket engine and weight of the device removed in space expect under the formula:

$$M_0 = M_K e^{\frac{U_R}{W_H}}, \qquad (6)$$

где

M_0 — Initial weight of the device;
M_K — Final weight of the device;
U_R — Speed of the device after burning out of fuel;
W_H — Speed of the expiration of a working body.

Speed of the device on an output from the vacuum dispersing device will consist of the sum of speeds at each stage

$$V_d = V_1 + V_2 + V_3 + V_{ed}, \qquad (7)$$

where

V_1 — Speed of the device after active dispersal at the first stage, the formula (1);
V_2 — Speed of the device after active-jet dispersal at the second stage, the formula (2);
V_3 — Speed of the device after an adiabatic site of dispersal, the formula (3), (4);
V_{ed} — Speed of electrodynamic dispersal.

The examined way of dispersal of a shell allows to provide necessary speeds removing of a shell in space at speeds of a throwing 8...11,2 km/sec with or to create high enough starting speeds (3...7 km/sec) with the further additional dispersal of the device on a trajectory.

Calculations show, that at application of vacuum artillery system for removing cargoes in space, decrease of expenses on 30...50 % is provided.

List of the Literature

1. Urukov B.A. About some problems of development of electrodynamic accelerators. – Col. J.V.Kondratjuka's (O.G.Shargeja) space and terrestrial orbits. - Dnepropetrovsk, Sich, 1996.
2. Nerus M.A. Anti-asteroid hyperhigh-speed thermochemical gun big barrel energy. –"Arsenal of XXI century ", №1, 1999. - p. 54-55
3. Nerus M. A. From a gun - to the Moon, or a hyperhigh-speed throwing of a shell. –"Arsenal of XXI century", №2, 1999. - p. 44-45.

DEVELOPMENT OF THERMAL RESISTANT AND INSULATING STRUCTURES OF ADVANCED REUSABLE AEROSPACE SYSTEMS

Gofin M.Y.

NPO Molniya, Moscow, Russia, e-mail: molgof@dol.ru

The design problems and peculiarities of regular, nonregular and specific zones of thermal protection and hot structures are analyzed for reusable space vehicles BURAN, SPACE-SHUTTLE, HERMES as well as for experimental space vehicles BOR-4 and BOR-5.

Special attention is concentrated on thermal protection design in areas of fuselage connection with wing, fin and carbon-carbon hot structure elements. Also are considered joints of movable and unmovable aggregates and also removable hatches and panels. Advantages and disadvantages of various thermal protection types are discussed. Special requirements to their exploitation, service and repair are described.

Scheme of the HERMES wing leading edge hot structure element installation

Schemes of seals for hatch of BURAN forward landing gear

HEAVY WEAR, HIGH TEMPERATURE AND HIGH STRESSES APPLICATION OF DETONATION POWDER SPRAYED COATINGS.

Kadyrov V.
Institute for Problems of Materials Science of NAS of Ukraine, Kyiv, Ukraine

Nowadays modern metal and nonmetal coatings do really penetrate many areas of manufacture and research. Such areas are: aircraft industry, nuclear, metalworking, textile, petrochemical and polymer production, metallurgy and steel industry [1,2,3].

Creating various purposes coatings on a base substrate is an essential part of modern manufacturing process and is an important direction in designing advanced materials with unique properties in future. There are several different technologies to apply coatings to substrates including conventional plasma, vacuum plasma, wire arc metallizing, high velocity oxy-fuel (HVOF), gas detonation processes. Among these processes HVOF and gas detonation technologies are capable of creating premium quality coatings with low porosity and high adhesion to substrate, suitable for applications in extreme wear, heat and corrosion aggressive surroundings. There are several limitations of high velocity oxygen fuel process, including large volumes of the combusted gases, high thermal flux to the substrate to be sprayed on and short lifetime of supersonic nozzle. These disadvantages are related to the fundamental nature of this technology and are not present in gas detonation coating process, which has physically different mechanisms of particle heating and acceleration. This report discusses considerations, which affected the design decisions in the creation of the advanced gas detonation coating processes and equipment [4].

With simple and cheap operation and excellent coating quality this promising process represents important direction in coating technology and is used in various branches of industry.

Gas detonation equipment was originally developed and patented in USA by Union Carbide Corp. In 1955 [1] and independently in 1969 at the IPM NAS of Ukraine (Kyiv). A typical gas detonation coating process consist of the following stages. A portion of fuel gas mixture (oxygen and acetylene, for example) is fed through a mixer into a tubular barrel closed at one end. Simultaneously, a powder of the sprayed material is injected through a powder feeder before the explosion is triggered by a spark plug. Combustion of the gas mixture leads to a detonation effect and formation of a high-pressure ultrasonic wave, which propagates the hot gas stream and heats and accelerates the powder particles. The resulting powder particle velocity can be as high as 1200 m/s. Collision of the powder with the substrate forms a high density coating with strong adhesion. After the one spraying cycle is finished, the powder and the fuel mixture are injected again, and the process repeats at rates of up to 15 shorts/sec.

Technical parameters of different detonation guns developed by different research and commercial groups in Ukraine, Russia and western countries are described.

The main advantages of ADM-2D (IPM of NASU and NIC "ADM") detonation process and the gun are as follows:
- Safe and efficient
- Improved design of gas distribution system
- Use less combustible natural fuel
- Eliminates the use of nitrogen
- Continuous supply of the combustion gas mixture
- No mechanically moving parts (valves, gas distributors)
- Higher firing frequency (frequency of 55Hz was demonstrated)
- Efficient use of powder
- Low (150 °C- can be further reduced by air or CO_2 flow) temperature of substrate sprayed on
- Operates over a broad range of gas flow rates and gas mixture proportions
- Ability to coat thin foils, plastics and composite materials
- Minimal power supply requirements (220V, 50/60 Hz , 200watts
- High reliability, longer life time of chamber and barrel, cheap maintenance

Properties of detonation are described.

Coating properties can be tailored by processing parameters:

- Spray protocol (stand off distance, powder flow, number of passes, etc.)
- Substrate condition (composition, temperature, preheating
- Controlling the microstructure (particle size effects, porosity/density effects
- Phase structure

Detonation coatings are the best for many applications in aircraft, metallurgy, metal working and other industries with severe working part stresses and environment. It is caused by the following coating properties:

- Good mechanical properties over a wide temperature range
- High resistance to thermal and mechanical cycling
- Good dense layers
- High hardness and resistance to wear
- Resistance to corrosion and high temperature oxidation
- Resistance to erosion and cavitation

By detonation process can be sprayed broad range of materials, including metals, ceramics, alloys and composites. The ideal coating material does not exist, and it is often necessary to find a suitable coating such that the combined coating/substrate system can satisfy the operating conditions. The choice of any coating for a given application depends on operating environment, the substrate material, the coating availability and economics.

Detonation gun coatings of ceramic and cermet materials have achieved widespread application on gas turbine engines (new coatings and repair) and their use continues to grow. The coatings are used in increasingly demanding environments, thus successful utilization requires a thorough understanding of their structure. Areas of application within the engine can be roughly separated into low and high temperature regimes (below and above 650 °C) At low temperature, impact/fretting wear (e.g. midspans on compressor blades) erosion resistance (e.g. knife edge seals) and various seals and bearings (e.g. bearing journals and bevel gears) are of concern. At high temperature, impact/fretting wear (e.g. turbine blade Z-notches), gas path seals (e.g. outer air seals) and thermal barriers (e.g. combustors and aerofoils) are of interest. Each area requires

one or more coating type to satisfy the specific requirements to a given engine. The most common coating types include tungsten carbide-cobalt, alumina, chromium carbide-nickel chromium, a new family of cobalt based alloys with alumina or chromia dispersions. Even with the introduction of more advanced engines, the tungsten carbide-cobalt and chromium carbide-nickel chromium families of materials continue their dominance in the low temperature regime. The low temperature application of detonation coating include protection against impact and fretting (fan and compressor blades), fretting (variable vane synchronising rings and bearings, compressor rotor tube), sliding adhesive and fretting (bleed manifold expansion joint liner and sleeves, bearing seal housing), adhesive (oil pump gears).

High temperature applications are include not only ceramic and cermet materials but chromium carbide-nickel chromium materials, which have been used for many years and are frequently still the best choice. The high temperature applications of detonation coatings include protection against fretting wear (stator shroudes-vanes), impact-fretting wear (blades), rubbing wear (blades).

References.
1. Poorman R.M., Sargent H.B., Lamprey R., Method and Apparatus Utilizing Detonation waves for Spraying and Other Purposes. U.S. Patent 2,714,563, 1955.
2. Кадыров В.Х., Щепетов В.В. Войтов В.А., Износостойкость детонационных покрытий из порошков Ni-Al-Si, Ni-Al-B в условиях граничной смазки., Порошковая металлургия, 1989, №11, стр. 74-76.
3. Kadyrov V., Detonation Coating Technology, Journal of Japan Thermal Spray Society, vol.29#4, Dec.1992, pp48-61
4. Kadyrov V., Advanced Gas Detonation Coating Process DEMETON, Proceedings of the 14th Inter. Thermal Spray Conf. May, 1995, Kobe, Japan, pp. 417-425

GAS - ANALYTIC MEASUREMENTS OF BURNING PROCESSES

Vladislav F. Primiskii
J-S. Society "Ukranalit", Kyiv, Ukraine

Utilization of solid man-made wastes is one of the actual problems of large mega-polices. In Kiev a waste-burning plant "Energia" operates more than 20 years; annually it burns about 50% products of the city vital activity.

In 1998-2000 the specialists of "Ukranalit" developed and included in the technological process a multi-level system of ecology monitoring and control of burning process in accordance with the results of gas analysis.

The lower system level consists of four sets of gas-analytic technological complexes TK-1. Each complex consists of high-temperature gas analyzer O_2 -151EchO1(0-20%), which measures oxygen concentration directly in the burning zone, and multi-channel gas analyzer 325 FA01 (CO=0-10%,CH=0-5000ppm,CO_2 =0-20%).

High-temperature probe of the gas analyzer for O_2 measurement is introduced directly into flame zone via a flange in its wall. The length of the probe made of stainless steel can be various. On the probe end a special high-temperature (600-1200 ^{0}C) sensor (ZiO_2) is located which measures O_2 concentration in the burning zone. The necessity of oxygen control in power plants, burning various kinds of fuel, is determined by the necessity to provide optimal proportion fuel/air in the process of burning. Considering that usually plants operate by the air excess factor more than 1, the decrease of the oxygen concentration in released gases by 1% allows to decrease fuel loss by 2%. The information signal from the sensor is transmitted via a special cable inside the probe onto the electronic block with digital indicator board located inside the box TK-1.

In the gas analyzer, using the method of infra-red spectroscopy, concentrations of CO, CH and CO_2 are automatically measured in the gas output of each kettle. Gas analyzers 151EchO1- electronic block and 325 FA01 -are mounted in a thermostatic box.

The box is mounted on the outer wall of the kettle. Measured information from each of gas analyzers is transmitted by control on a computer in the controller's office by a special cable 1000m by length.

Gas-analyzing system TK-1 allows to effect real-time measurements of the composition of gas mixture in the burning zone and to correct the proportion fuel/air. The TK-1 set provided the optimization of burning processes and allowed to save 5-6% of fuel.

The system higher level is an ecology complex EK-1, which is mounted on gas outputs behind dust electric filters. EK-1 is based on gas analyzer "Spectr 4", in which multi-input optic cuvette was used for the first time. This allows to measure concentrations of CO, SO_2 and NO in wide range: CO (0-4.0g/m^3), NO(0-5.0g/m^3), NO_2(0-6.0g/m^3) and SO_2(0-0.5 g/m^3).

Measured information is also transmitted from EK-1 via a cable in the controller's office on the monitor.

Thus, for the first time we implemented day-long persistent control of gas medium in technological processes of wastes combustion. The system use allowed to optimize burning process, to decrease fuel consumption and toxic gases release into atmosphere and to increase the quantity of burned wastes per a specific fuel unit. Computer processing of measured information allowed to archive the measurement results thus enabling to trace deviations from normal technological process by the results of gas-analytical measurements.

At minor finishing, the system consisting of the sets TK-1 and EK-1 may be recommended for introduction on power plants- heat-electrical plants and boiler-rooms, and in technological processes, connected with the processes of burning natural gas and mazut.

POLYURETHAN ENAMEL

Kuksenko V.S., Vettegren V.I., Nikiforov V.V.[1]
A.F. Ioffe Physico-Technical Institute Russian Academy of Science, Saint-Petersburg, Russia
[1]State Unitary Enterprise "Central Institute of Materials", Saint-Petersburg, Russia

For protection corrosion of metals in hard working condition (at very wide temperature range including working in tropics) during a very long time (20 years and more) new generation of paint and varnish materials on base of polyurethan binder are developed.

Such materials are not produced in Russia. For protection of metal corrosion are used the film-forming paint and varnish materials on base of epoxy and polyvinyl chloride. They have low values of stability in very hard working conditions at ultra violet light.

We developed new paint and varnish materials They are enamels on base of production in Russia

hydroxyl containing polyesters strengthened by polyisocyanates.

New enamels have a very stability in influence of ultra violet light, moisture, and corrosion active gases and salts.

They have very high adhesion on metals, strength, and elasticity.

New enamels are abrasive stable.

They spread well. Shagreen is absent.

The enamels can format the good covers at low temperatures.

THE EFFECT OF Γ-IRRADIATION ON MAGNETIC PROPERTIES OF AMORPHOUS ALLOYS Fe-Si-B

Maslov V., Nosenko V., Taranenko L., Neimash V.[1], Povarchuk V.[1]
Institute of Metallo-Physics, National Academy of Sciences of Ukraine, Kiev, Ukraine
[1]Institute of Physics, National Academy of Science of Ukraine, Kiev, Ukraine

The effectiveness and reliability of the inductiv elements of electric circuits (different transformers, choke coils, etc.) depends from the properties of magnetic cores that are the parts of inductive elements. Magnetic cores are usually made of transformer steel, permalloy, ferrite. Recently, above-mentioned traditional materials are being successfully replaced with the amorphous alloys produced by rapid quenching from the melt since their properties exceed the properties of conventional crystalline soft-magnetic materials. Iron based amorphous alloys (base system Fe-Si-B) posses high value of the saturation induction Bs= 1.4 – 1.6 T, the Curie temperature Tc (380-450C), specific electric resistance; they have low loss in the core (130-160Wt/kg under B=0.2T and 100khz), and can be produced easily and effectively. The range of amorphous alloys applications available currently may be extended into new areas. Namely, they could be used for the manufacturing of inductive elements of electronic and electro-technical devices for space apparatus, control and safety systems for nuclear power plants (devices for secure turn-off, sensitive elements of sensors measuring pressure, moving, or vibration), deflection systems for charge particles accelerators. These applications require information about the changes of magnetic characteristics under irradiation regarding the magnitude of changes and also their tendency. The data on the influence of different radiation conditions on the atomic structure, thermal stability, and crystallization of amorphous alloys have been already known from different publications. However, there is not data concerning the influence of γ-irradiation on the magnetic properties of the thermo-treated magnetic cores made of amorphous ribbons, which can be used in such devices. It created the reason for present investigation. This research is also to investigate the stability of irradiated and non-irradiated magnetic cores in dependence from time.

The influence of hard γ-irradiation (Co^{60} with the energy of γ-quanta of 1.2 Mev, exposing dose

~$2*10^9$ R) on the dynamic (1kHz) magnetic properties of the thermo-treated toroidal magnetic guide made of $Fe_{78.5}Si_6B_{14}Ni_1Mo_{0.5}$ (marked as MG-3) and $Fe_{75.5}Si_2Ni_{3.5}Mo_3$ (MG-8) alloys of Metglas 2826MB type produced by rapid quenching has been investigated. A standard induction-non-interrupted method was used for measuring magnetic properties of cores (frequency 1kHz). The saturation induction (B_s), half-width of dynamic hysteresis loop H_c at B=0.2T, magnetic permeability (both initial μ_i in the field of 0.1A/m and maximal μ_{max}), and also the field achieved at μ_{max} ($H\mu_{max}$), which characterizes the slope of $\mu(H)$ curve were determined. As-quenched ribbons from MG-3 and MG-8 alloys were tested as for the presence of diffusion hallo on the X-Ray diffraction curve in the range of the first peak. This testing demonstrated that they were similar as for "X-Ray amorphousness". The temperature of the beginning of crystallization and the formation of primary crystals α-Fe(Si) were determined of 480C and 520C correspondingly for these two alloys at the heating rate 20K/min that indicated their rather high thermal stability. The Curie temperature Tc was determined of 363C for MG-3 (due to higher Mo content) and 276C for MG-8 alloy. The initial magnetic permeability of both alloys in the as-quenched state was not high (≈350) because of the great concentration of different structural defects. These defects and the quenching conditions stipulate significant quenching stresses in such material as well as the differences in local chemical and topological atomic structure. In its part it may result in the occurrence of magnetic anisotropy and conditions for fixing magnetic domains. The negative impact of the factors mentioned is usually eliminated by thermo-treating leading to structural relaxation and, consequently, to the improved properties up to the level inherent in the unique amorphous state of metal alloys.

Due to the relaxation completed the amount of H_c and μ_i achieves the minimal and maximal values correspondingly at the annealing temperature of T_a ~420°C, which is the optimal temperature for

528

the alloys investigated. It is seen from the dependencies of μ_1 and coercive force H_c presented for the MG-3 alloy on the Fig.1.
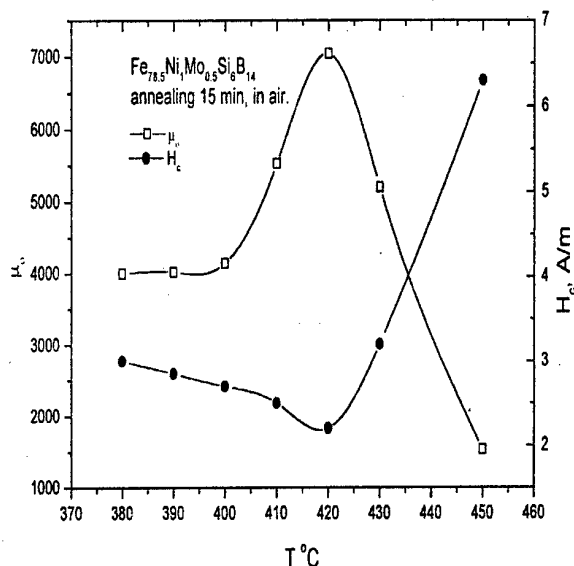
Fig.1 μ_0 and H_c behavior at heat treatment MG-3

Fig.2 The influence of gamma-irradiation and long exposure (to 25 month) at the room temperature on the magnetic permeability of MG-3 and MG-5 alloys. 1 – nonirradiated; 2 – irradiated after thermo-treating; 3 - irradiated before thermo-treating.

The magnitude of B_s is revealed to be the same before and after irradiation. However, the main properties of magnetic soft materials, such as coercive force and magnetic permeability have decreased as a result of irradiation. There are definite peculiarities in the influence of irradiation on ribbon in dependence from if the ribbon was irradiated in just as-quenched state ("γ+TO") or if it was irradiated after thermo-treating ("TO+γ"). The values of μ_1 and H_c have decreased by 28-58% in the both alloys investigated. At that, μ_{max} intends to increase.

The properties of MG-8 are changing under irradiation more significantly than the properties of MG-3. The irradiation influence more essentially the properties of magnetic cores made of as-quenched ribbons than of the ribbons thermo-treated before the irradiation. It was revealed that the changes of magnetic properties of magnetic cores caused by irradiation are capable of relaxing during long exposures at the room temperature. The relaxing of coercive force is less detectable then the changes of magnetic permeability μ_1. The changes are different in dependence from alloy content and the mode of irradiation, as it shown by Fig.2.

The deterioration of the magnetic properties of previously thermo-treated alloys under irradiation could be explained by the formation of the short-range-order structure defects.

These defects are capable of changing the conditions of atomic exchange interaction and, consequently, influencing the formation of magnetic domains and the mobility of their boundaries. Slow annealing of defects at the room temperature is probably the cause of the gradual relaxation of magnetic properties. In the case of irradiation before thermo-treating the radiation defects and radiation-induced diffusion may influence the annealing of quenching stresses in the material.

BEHAVIOR OF n-Si ELECTRICAL PARAMETERS AFTER A HIGH-TEMPERATURE 1 MeV ELECTRON IRRADIATION

Neimash V., Kras'ko N., Kraitchinskii A., Tischenko V., Voitovych V., Simoen E.[1], Claeys C.[2]
Institute of Physics, National Academy of Science of Ukraine, Kiev, Ukraine
[1]IMEC, Leuven, Belgium
[2]E.E. Dept, KU Leuven, Belgium

The lattice defects induced by a "low" temperature irradiation of silicon are not stable at room temperature. It is well known that the A-centres, that are traditionally key recombination levels in lifetime engineering by particle irradiation, are completely annealed after some minutes at 350°C and after 2-3 years at room temperature. This annealing behaviour can be an important problem for the practical application of radiation-based defect engineering of silicon materials and components. One possible path for solving this problem is performing the irradiation at high temperatures. In this case the parameters of the irradiated devices are stable at room temperature during almost unlimited time. Therefore the study of the nature and properties of radiation defects (RDs), induced in silicon during a high-temperature irradiation, has strong technological potential. One side-aspect to be concerned with in Czochralski (CZ) silicon is the formation of oxygen containing thermal donors (TDs) that are generated at temperatures in the range 350-500 °C. The influence of "hot" nuclear radiation on TD generation is very poorly investigated.

The purpose of our work was to obtain information about the nature and rate of RDs and TDs generation under a 1 MeV electron irradiation at 450°C of n-type CZ Si. We investigated the influence of that "hot irradiation" on the conductivity at 20°C by the 4-probe method, while the RDs were studied by the Deep Level Transient Spectroscopy (DLTS) method. The concentration of free electrons at room temperature was calculated from the conductivity, assuming that the mobility is constant. The investigated samples were parallelepipeds with sizes of 10x5x3 mm. They were heated up to 450°C by the absorption of power from the electron radiation (a current density $I = 8$ $\mu A/cm^{-2}$ has been employed). The scheme of the "hot" irradiation experiment is shown in fig. 1. The 1 MeV electron beam (3) illuminates perpendicular one of the major sides of the sample. A hole (4) with a diameter 1,2 and a depth of 5 mm was drilled in one of small sides to house a platinum thermocouple, which was used for temperature control and as support for the sample. Full absorption of 1 MeV electrons happens in silicon at a depth of 2 mm. The temperature difference between the irradiated and dark side of the sample did not exceed 0.5°C due to thermal conduction. Therefore, TDs were generated during irradiation in the region close to face 2 in fig. 1, while the dark side (1 in a fig. 1) was heated to 450°C without direct exposure to electron damage.
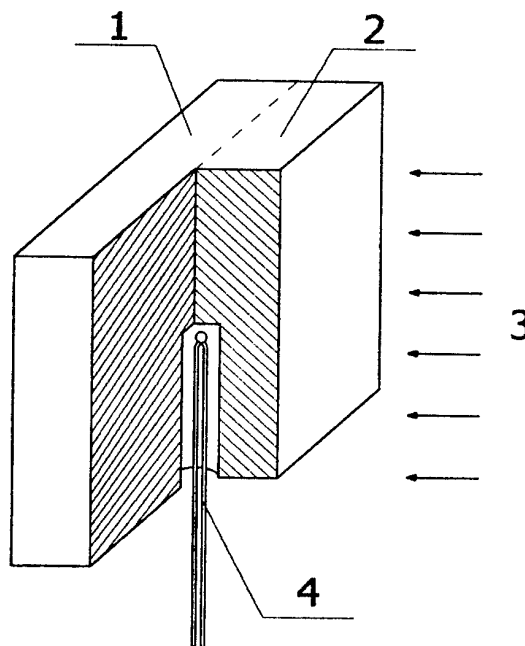
Fig. 1. Schematic sample configuration for the "hot" electron irradiation.

The initial parameters of the investigated samples are shown in Table. 1, namely, the carrier concentration (n_0), the interstitial oxygen concentration (N_O) and the substitutional carbon concentration N_C.

Table 1

№ sample	n_0 10^{13} cm^{-3}	N_O 10^{17} cm^{-3}	N_C 10^{16} cm^{-3}
1	9,1	<5	<5
2	10,5	9	<5

The study of the sample with the small oxygen concentration (№1) should provide information on the generation of RDs at 450°C. TD generation in such crystals is very small. The sample with the high oxygen concentration is expected to be affected by simultaneous RD and TD generation during the 450°C electron irradiation.

DLTS on Au Schottky barriers revealed clearly the generation of an acceptor type of radiation defect (activation energy - E_C – 0.3 eV) in n-Si after "hot" electron irradiation. The DLTS-spectra for both sides of sample № 2 after the thermal-radiation treatment are illustrated in fig. 2. The absolute trap concentration cannot be accurately determined because of the large relative density, but is estimated to be of the same order of the background donor concentration.

THERMOPHYSICAL PROPERTY DATABASE OF MATERIALS

Vinogradov Yu.K., Lopatin V.I.[1], Vanitcheva N.A.
Moscow State Aviation Institute (Technical University) MAI
[1]International Engineering University

The application of materials in hazard conditions depend on their thermophysical properties and properties of media, in which these materials are used. Thermophysical property database developed by the authors includes more than 2000 tables of physical characteristics of different gases and liquids. The tables have been drawn up by means of analysis and generalization of more than 470 original literature sources. The experimentally studied regions of the reference parameters have been expanded to cover and very low temperatures, including the extreme states.

The improved system of data presentation allowed us to include the following new features:
* the thermodynamic data for ionized states of a number of substances;
* the thermodynamic and transport property data for the critical region of a large number of substances;
* new experimental thermodynamic tables for alkali metals and mercury;
* the database covers a number of new substances such as deuterium and other isocompounds of hydrogen.

Thermophysical property database developed by the authors is based on "Handbook of Physical Properties of Liquids and Gases", by N. B. Vargaftik, Yu. K. Vinogradov and V. S. Yargin which was published by Begell House Inc., USA, 1996. Collected in this book is a large and comparatively new experimental material on thermophysical properties of liquids and gases. HPLG (Handbook of Physical Properties of Liquids and Gases) relational database uses Visual FoxPro 5.0 for Windows 98 providing full integration into the family of applied Microsoft and the quick search of the information of the user's concern. The service programs of operational search as well as those of sampling selection organization by a single or several criteria from table data are performed by Visual FoxPro5.0 for Windows 98 and SQL language.

HPLG database enables:
* to make the search of thermophysical properties of different substances both by the groups of substances and by separate properties,
* to look up the whole table or to move smoothly in the table represented on to the monitor screen, as well as to show on the screen the reference to the sources used while constructing the data table,
* to make the data selection from the tables by a single or several criteria and to give the results as separate tables or graphs,
* to represent the table data in different system units,
* to perform the interpolation on table values, to replace and to modify the source tables.

A service of thermophysical property table value interpolation has been developed, since the tables are usually given by the authors for round temperature and pressure values, which is not always good for the users. The service allows to calculate an interpolation error by a residual term value, which is especially important, as the values obtained by interpolation in the field of dramatic thermophysical properties change (e.g., in the field of the phase transfer or critical area) may prove to be unreliable. Two-argument interpolation ability is provided for.

The database also uses a service of representing the table data by thermophysical properties in different system units. The user, after opening the Units menu, can choose the measurement units of this or that thermophysical property of the substance.

The database service can comprise that of working with references. This is an effective search and output of references applied for particular table construction on to the computer's display. Sampling selection organization from a full or a particular list of references by a single or a few parameters is provided for.

The description service gives brief description of substances used in each particular group, table comments, approximation and other equations and coefficient values of these equations, as well as the most typical graphs of thermophysical properties and their errors.

This database is demonstrated to day at this conference. We should be very glad to discuss is disadvantages and advantages with the colleagues.

EXPERIMENTAL INVESTIGATION OF HIGH-TEMPERATURE MATERIAL HEAT-SHILDING PROPERTIES

Zelenov I.A., <u>Klishin A.F.</u>
Lavochkin Association, Himky, Russian Federation

The hyperthermal heat-shielding materials widely applied in engineering are intended to provide in conditions of operational thermal actions given level of permissible temperatures of structural items these materials are put on. Contrary to hyperthermal heat insulation the series of such heat-shielding materials at a particular level of thermal actions is partly blown (destroyed), thus taking a part of applied heat flow.

With the help of gas-dynamic plasmotrone facility with two-dimensional nozzle the tests of the samples with thin-layer hyperthermal covering (TLHC), intended for short-lived protection of a metal construction from the influence of a heat flow, were carried out. Tests of the rectangular type samples (with dimensions in plane near 200 x 350 mm) were conducted at lowered environmental pressure near 16,5 mbar and heat flow from 15 kW/m^2 up to 40 kW/m^2. Experimentally, using temperature variations of substratum and working surface of the sample, the parameters of heat-shielding coating material's destruction are determined: temperature of destruction and the heat-shielding effect of inflation of destruction products' vapor in near-wall stratum. It was shown, that these parameters directly depends on the level of applied heat flow, and temperatures of destruction for the investigated material were from 550°K up to 700°K.

The results of the tests have been used for improving of heat-shielding coating of TLHC thickness procedure of calculation for metal structural items with different permissible temperature of operation.

ENDURANCE CARBIDES AND BORIDES OF COVERAGES ON У8A STEEL

Higniak V.G., Korol V.I., Kostenko A.D. [1], Loskutova T.V.
National Technical University of Ukraine "KPI", Kiev, Ukraine
[1]Frantsevich Institute for Problems of Materials NAS of Ukraine, Kiev, Ukraine

Work capacity of articles, which one are in contact interplay, in many cases is instituted by their wear [1]. Common means of strife with it is the lubricant, which one safeguards interacting parts from forward contact. However at heightened temperatures, in conditions of high off loading the lubricant can not be utilized. In many cases for the applicable operation of dodges on interacting surfaces put wear-resistant coatings. The in-service experience of parts of ambulances, instruments and technological casing hardware with protective coating has shown, that on aspects of deterioration of composition a coating - ground the phenomena cracking at early stages of operation are proper [1,2,3].

Carbides coating on a surface of steel У8A 4 hours in a self-contained reaction space plotted at the temperature of 1323 K and soak period at underpressure. As starting reagents have utilized dusts of transitional metals (titanium, vanadium, chrome), perchloromethane, carbon containing of the component [3]. Bodies coating realized in carbide of boron at the temperature of 1198 K and soak period 4 hours [2]. Phase composition of coatings instituted on a X-ray diffractometer ДРОН 2.0 in copper radiating. The metallurgical surveys realized on an optical microscope « Neophot 21 ». A microhardness metered on a gear ПМТ - 3, furnished system permitting to record the curve of a loading in coordinates an offloading on indentor - depth of an intrusion of a pyramid.

Microhardness, index of microfragility carbides and borides of coatings, adhesion of a coatings and fundamentals instituted under the method of application [4] at analysis of the curve of impression indentor of a gear ПМТ - 3. At formation of radial fracture of length With on the curve an off loading - the strain will be deviated a site at an off loading Pт, that allows to define microhardness on a following proportion

$$\sigma_{M\Pi} = P_\tau / C^2 .$$

The fracture, is disposed on boundary coverage - steel, mirrors a level of an adhesion a coverage -

ground, and the magnitude Pт $/C^2$ institutes a stress of a bond liftoff of a coating $\sigma_{B\Pi}$.

As an index of microfragility it is offered to utillize a dimensionless index g, reflective an off loading of crack initiation Pт, size of radial fracture with, gross capacity on indentor the launcher and sizes of a friable impression at an off loading of the launcher - dн

$$\gamma = C^2 P_p / d_H^2 P_{mp}$$

Thus the index of microfragility mirrors correlation between a microhardness and microhardness for particular structural and tension of diffusive bed.

The tribotechnical trials conducted on the ambulance of abrasion of a MT - 68 under the circuit a barrel - rod [5]. As a material opposite skew field have utilized 65Г steel, well-tried and tempered on hardness HRC 51. The trials conducted at off loading 5-10 MPa and slip velocities of 5-15 m/s. A wear evaluated on variation of linear dimensions of a sample of abrasion, referred to a path. A flat surface not adjusted is model allows to supervise during abrasion of a feature of deterioration of composition coating - steel and to place the moment of a beginning of breaking down of a coating and kinetics of shaping of a hitch of a wear. A wear evaluated on resizing a hitch in time.

Besides the trials test on abrasive and erosive stability were held.

The analysis of received datas has shown, that a maximum level of adhesive interplay with steel У8A have carbides of a coating including chromes and borides of a coating.

In operation is established, that the off loading of crack initiation Pт, echoing property of a coating material to an elasto-plastic strain in a zone of contact with indentor to the moment of a beginning of driving of fracture, depends on many

factors. The ambiguous dependence Pт from a microhardness is confirmed by that factor, that the lowest values Pт were fixed for carbides coating VC, and highest for boride FeB. Thus value of a microhardness of datas of coating differ unsignificantly.

The least sizes of fracture were established for coatings such as VC and FeB. The coatings with a maximal microhardness, such as TiC, (Ti, V) C, differ by maximum ratings of an index of microfragility and low-level values of microhardness. The coatings $Cr_{23}C_6$, Cr_7C_3 are characterized by high microhardness and low index of microfragility, yielding however by magnitude of an index of microfragility to boride FeB.

As is indicated in operation in conditions of a sliding friction without lubricant the lowest values of a friction coefficient for slip velocities, accepted in operation, (5-15 m/s) and load range (5-10 MPa) were established for coatings TiC, (Ti, V) C - 0,23. In ascending order of friction coefficient of a coating it is possible to arrange in a following series: carbides of chrome - 0,25, carbides of a vanadium - 0,27, borides ferri lactas - 0,28.

The experimental outcomes, received in operation, have shown, that carbides and borides of a coating 30 times effectively increase endurance of steel У8A in 2,5 - depending on a method of trials.

Thus the highest outcomes have shown:
- At abrasion slip without lubricant without preliminary reseat of conjugated surfaces - coverage such as VC, V_2C;
- At a sliding friction without lubricant with preliminary reseat of surfaces - coverage such as (Ti,V)C, TiC;
- At abrasive deterioration - coating such as Cr_7C_3, $Cr_{23}C_6$;
- At erosive deterioration - coating such as TiC, (Ti,V) C.

In operation the necessity of usage for an adequate estimation of different aspects of deterioration of protective coating of such performances of a material is rotund: microhardness, index of microfragility, adhesive interplay in composition steel - coating.

It is possible to consider, that microhardness, index of microfragility are in effective performances complementary a microhardnesses and reflective influencing of a tension, the patterns, presence of defects of a coating material on his stability to deterioration at different test specifications.

1. Костецкий Б.И. Сопротивление изнашиванию деталей машин. – М. – К.:Машгиз, 1959. – 478 с.
2. Химикотермическая обработка металлов и сплавов: Справ. – М.: Металлургия, 1981. 424 с.
3. Лоскутов В.Ф., Хижняк В.Г., Куницкий Ю.А., Киндрачук М.В. Диффузионные карбидные покрытия. К.: Техніка, 1991. – 168 с.
4. Хижняк В.Г., Дудка А.И., Хижняк О.В. Определение микрохрупкости карбидных покрытий с использованием метода кинетической микротвердости. //Изв. Вузов. Черная металлургия .- 1996. -№9. –83 с.
5. Мамыкин Э.Т., Ковпак М.К., Юга А.И. и др. Комплекс машин и методика определения антифрикционных свойств материалов при трении скольжения // Порошковая металлургия. – 1973. №1 – с. 67-72

ON ULTRASONIC ELECTRIC ARC METAL SPRAYING ONTO THE CRANK-UP PINS OF DIESEL ENGINES BY FLUX-CORED WIRES

Sergeyev V.V., **Spiridonov Yu.L.**, **Tret'yak M.S.**[1], **Chuprasov V.V.**[1], **Lunyov A.N.**[2], **Zharkov L.K.**, **Sergeyev M.V.**[2]

Scientific-Industrial Complex "Yuna", Kazan, Russia
[1] National Academy of Sciences, Minsk, Belourus'
[2] Kazan State Technical University, Kazan, Russia

Rebuilding of worn-out machine parts and recovery of their high service characteristics gradually lost due to wear is one of the most important problems of repairing technology. A method for rebuilding of worn-out machine parts is the method of electric arc metal spraying rapidly introducing now into everyday practice. The method is very effective and is distinguished by low expenses and manufacturing cost. At our enterprise, this method is successfully used for more than ten years to recover the worn-out pins of crankshafts used in the carburettor internal combustion engines of light cars (of up to 80 h.p. in power). At the same time, the rebuilding of worn-out crank-ups of high power diesel engines didn't give any positive results. In the process of spraying, the coatings were applied by spraying the wires of grade 65 G.

Studying the characteristics of coatings, we established the fact that it is necessary to provide high adhesion, hardness and low porosity of coatings with proper regard for heavy-duty operational conditions of crank-up pins in diesel engines where the specific loads exceed more than 60 MPa. In the now-existing metal-spraying pistols, spraying of compressed air through the cylindrical nozzle with inlet pressure of 5-6 MPa uses the large-drop mechanism of wire melting. As a result, there forms a coating that possesses large porosity, low bonding strength, and hardness due to small velocity of particles flight, insufficient dispersion of parts in metal melt, intensive burn-out of alloy components, especially carbon, from wire; there burns out of up to 60 % of carbon and 15 % manganese and silicon. As a consequence, the porous and soft coating in operation of diesel engine was densified due to high specific loads and the engine began to "knock". The velocity of particles flight at a distance of 150 mm is no more than 160 m/s. A smaller distance is not used habitually due to some peculiarities of crankshafts design.

In order to eliminate the above-mentioned drawbacks, we developed the metal-spraying pistol with ultrasonic outflow of air. We carried out the calculations of the pistol gasodynamic characteristics to obtain the optimal ultrasonic outflow of air, and also the calculations of the nozzle exit section parameters at which the additional reduction of metallized jet takes place. The metal-spraying pistol makes it possible to adjust the rate of air outflow; the calculated rate of outflow varies from 340 m/s to 430 m/s. In doing it, the air-metallization jet with the spray-cone angle of no more than 9^0 is being formed. In the present-day pistols, it is impossible to obtain the spray-cone angle of no less than 40^0. As the spraying metal, use is made of the flux-cored wire PP-TP-1. Use of such wires makes it possible to regulate the chemical and phase composition of the coating in wide limits, and ensure thereby the desired service characteristics such as wear-resistance, corrosion resistance, hardness, and density; it offers new possibilities for increasing the service life of parts reclaimed. So, the flux-cored wires which are based on iron and which have aluminium, manganese, and chromium in their blends are meant for creation of wear-resistant coating that run under conditions of sliding friction (frequently with limited or poor lubrication) or during short periods of time at dry friction conditions.

Sizes of the sprayed particles and their granulometric composition influence significantly on the service characteristics of coatings. They do not only specify the particles velocity and temperature but also the chemical composition of a coating influencing upon the completeness of chemical reactions run in two-phase jet and on surface. We managed to obtain particles of 150 μm in dia (90 %); the maximum of their distribution is in the range of 50-100 μm, which is significantly smaller as compared with the subsonic outflow of air where the overwhelming majority of particles has the diameter of more than

100 μm. We can thus confirm the fact that influence of gasodynamic forces of ultrasonic air jet on formation of particles of 100 μm in dia is dominating.

In the course of studies of coating microstructure we established that all coating have a peculiar laminar structure, insignificant porosity, and small quantity of unmelted particles. The oxide layers are thin ; at X1000 magnification, there observed, in some separate particles, martensite, pearlite, troostite, and also oxides along the boundary surfaces. Thickness of the deformed particles in a coating is approximately 10 μm. Distribution of phases in a coating is highly uniform , without any aggregations. We observed some separate local aggregations of porosity which may probably caused by metal-spraying pistol operation. Coating porosity is on the average 4,5%; we must note that porosity near the boundary surface "coating-base" is higher which is connected with operation of synthetic corundum at sandblasting.

Measurements of coating hardness showed that it varies from section to section. The measurements of coating hardness prior to grinding gave the value of 51-56 HRC. After grinding and removal of layer of 1,0 mm thick hardness decreased and was only of 42-47 HRC. Hardness of a similar coating at its application with subsonic metal-spraying pistol was no more than 37 HRC and mounted to 28-36 HRC.

Adhesion is one of most important characteristics that determines the operational capabilities and service life of the part repaired and it must obviously be sufficiently high, at least, not smaller than the value of pressure applied by the connecting rod upon the crank-up pin via the insertion piece.

At the same time, in the course of studies on influence of detonation coatings on the substrate's strength characteristics we established the fact that all characteristics of strength deteriorate as adhesion increases and it results in premature rupture of parts. The bonding strength of electric arc coatings PP-TP-1 applied by using the ultrasonic air jet was more than 52 MPa; the force of current has not exerted any significant influence on adhesion, but increase in velocity of air jet outflow (or increase of air flowrate) results in increase of adhesion from 29 MPa to 52 MPa.

Owing to these studies, the technological process of rebuilding the worn-out crank-up pins of diesel engines has been successfully introduced into the practice of maintenance shops. At present, we have succeeded in rebuilding of more than 2000 crankshafts of buses "IKARUS". The maximal run between repairs is more than 150000 km. Also rebuilt is more than 120 crankshafts of trucks "KAMAZ"; here, the run with no any traces of wear is 60000 km. We have rebuilt also three crankshafts of the bus "Mercedes" with failure-free run from 72000 to 81000km.In all these cases, service of crankshafts is continued.

In the scientific-industrial complex "Yuna" there was built the shop for repairing the crankshafts, camshafts, and other parts of automobiles and agricultural motor-vehicles by gas thermal spraying.

In this shop there are three stadions for rebuilding of parts by ultrasonic electric arc metal– spraying, plasma installation UPU–8, gas-flame installation, two machines for crankshafts grinding, automated sandblasting chamber, and other equipment.

DETONATION SPRAYING AS THE EFFECTIVE TECHNOLOGY FOR INCREASING LIFE-TIME OF HEAVY-DUTY GTE COMPRESSOR BLADES

Sergeyev V.V, Spiridonov Yu.L., Lunyov A.N.[1]
Scientific-Industrial Complex ZAO "Yuna", Kazan, Russia
[1]Kazan State Technical University, Kazan, Russia

To eliminate the self-excited vibration, a number of various blade designs of high-, medium-, and low-pressure compressors is equipped with the antivibration flanges which form, when touching in -between along their corresponding contact surfaces, the strengthening ring. When acted upon by the natural airstream and inevitable vibrations, the contact surfaces of flanges have to run at rigid, extremal conditions: if, for example, the blade temperatures vary from 230K to 730K, the contact surfaces suffer from high specific pressures accompanied by severe vibration. As a result, there occurs very rapid wear of blades and their further deterioration of operation may result in blade breakdown and creation of emergency situations. The analysis of different methods for increasing wear-resistance of the flange contact surpaces showed that the most promising method is the method of coatings application by detonation spraying. This method makes it possible to ensure the wear-resistant coatings of different composition on the contact surfaces of antivibration flanges of GTE compressor blades. The coating compositions used possess high physico-mechanical properties such as adhesion, cohesion, hardness, wear resistance, porosity, and the like.

With detonation spraying, coatings are sprayed due to the action of detonation products (oxygen and gaseous fuel mixtures) on particles (granules) of powder. At detonation explosion of fuel mixture in the set-up tube, the particles are heated-up, accelerated, and sprayed on a part. The speed at which the powder particles reach a part is equal to 700 m/s.

To ensure high quality of coatings, we have developed the "compact" powder VK-15 in which the features of detonation spraying are taken into account; in composition, it consists of tungsten carbide (WC) and cobalt. To these features can be related such ones as the oxidizing medium, action of shock waves and high-speed flows, products of detonation, disintegration of powder particles with different masses, and high temperature.

One of most efficient techniques for elimination of harmful action on the powder sprayed is the creation of special composite powders; unlike the mechanical mixture VK-15, such special powder is distinguished by compact structure of every granule where the disperse hardening WC particles are distributed uniformly in the cobalt matrix. This matrix reliably protects WC particles from harmful action of oxidizing medium of detonation products. All the powder granules each are constructed with due regard for the basic requirements imposed on baked hard alloys: optimal combination of solid hardening phase of WC and plastic matrix made from cobalt; absence or minimal interaction between them in powder production process. WC phase size is $3...5$ μm and the distance between them is $0,4...1\mu m$. The size of a granule itself is $20...40\mu m$; it is sufficiently hard and cannot be disintegrated under the action of shock waves and high pressures of detonation products. This specially developed powder took the name "compact" powder VK-15V.

For purposes of detonation spraying, we have developed the detonation set-up (DS) which makes it possible to adjust the temperature and kinetic parameters of detonation products within wide range of values. The rate of the set-up fire is $6,6$ cycles per second; it makes it possible to reduce time of powder granules stay in detonation products without any deterioration of coating characteristics. Also provided is the pulse delivery of powder into the set-up tube; this feature ensures strictly preset position of compact powder cloud in the set-up tube; alongside a significant economy of materials, it makes it possible to impart equal speed to powder particles. The set-up design makes it possible to adjust the powder cloud position in its tube (time of delay). Also provided is a possibility to adjust temperature and rate of detonation products using propane as gaseous fuel instead of acetylene, and adding inert gas in gas mixture composition.

After evaluation of technological DGS regimes by a degree of their action, we divided, on conditional basis, the coating spraying regimes into "soft", "moderate", and "rigid" regimes. In "soft" regime, the temperature and kinetic parameters of detonating mixture are minimal,

whereas in "rigid" regime they are maximal. In the course of our studies, we have examined a number of coating characteristics and established the fact that in studying the wear-resistance of coatings in the presence of fretting corrosion, an increase of temperature and kinetic parameters of detonation products results in changes of coatings wear type. If, for example, the average linear wear for the coatings VK-15V and VK-15 sprayed in "soft" regimes was correspondingly 0,8 and 3 µm, the wear observed in "rigid" regimes was 2,8 and 5,1 µm, respectively (Fig.1). After testing, the friction path, the coatings VK-15 appear as the smooth polished lustrous surfaces without any signs of destruction. At the same time, in " rigid" regimes we can observe cracks and the process of spalling on the friction path. The phenomenon is caused by the fact that WC particles of compact powder are reliably protected from the action of decarbonization and that there are more plastic cobalt bonds in a coating and considerably smaller quantity of intermetallides and fragile double carbides. In connection with the fact that the blades of high–and medium-pressure compressors suffer from high temperatures. We studied wear-resistance of coatings at temperatures of up to 873 K and revealed that wear nature remains unchangeable until the temperature 773 K is reached and that the wear is minimal.

At higher temperatures (more than 773 K) the wear nature dramatically changes and we observe significant local damages whose depth increases with increase of temperature.
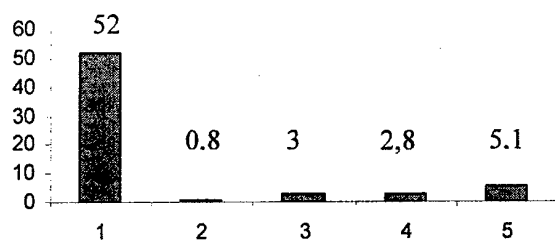
Fig.1. Comparison of wear-resistance of detonation coatings from titanium alloy in the presence of fretting corrosion: T=293 K, 1.VT-8; 2.VK-15V,"soft" regime; 3.VK-15, "soft' regime; 4. VK-15V, "rigid" regime; 5. VK-15, "rigid" regime.

The herein-presented studies made it possible to reveal a significant influence of detonation spraying, i.e., thermodynamic parameters, upon the structural phase of coatings and adhesion. Up to 59% of WC content in coatings VK-15V

sprayed in "soft" regimes is retained (from the initial composition of 85 %).

When spraying in the "rigid" regimes, we managed to retain no more than 20 % of WC. Microhardness increases here from 9,2 GPa to 18 GPa, whereas the content of free cobalt decreases from 12% to 1%.

When spraying in "rigid" regimes, content of fragile phases – intermetallides and double carbides – drastically increases in the coatings VK-15V.Adhesion of coatings increases from 68 MPa to 150 MPa and the structure of coating VK-15V sprayed in "soft" regimes is improved; the number of pores , broken surfaces, and oxide inclusions is significantly reduced.

The phases are distributed uniformly which is confirmed by studies of coatings in the characteristic rays.

In the course of our studies, we have established a significant influence of temperature and kinetic parameters of detonation products on the fatigue strength in the specimens made from titanium alloys; such influence is exerted to the largest degree by the detonating mixture composition. The rate of the negative reaction of WC reduction, changes of structural inhomogeneity of coatings and their adhesion were varied most effectively due to the action of temperature and the rate of detonation products efflux. Both parameters were varied at increase or decrease of oxygen content in the detonating mixture, dilution of mixture by inert gas, and use of less heat–generating fuel gas; in other words, the regimes were changed from "rigid" to "soft" regimes. In the "rigid" regime, we observe a decrease in the fatigue limit of titanium alloy from 480 MPa (without coating) to 100 MPa. Adhesion, structural inhomogeneity, phase variations, microhardness are in this case maximal. In "soft" regimes, the fatigue limit increases up to 300 MPa. At the same time, a slight increase of temperature and rate of detonation products ("moderate" regime) increases the fatigue limit up to 380 MPa.

Making use of the special "compact" powder VK–15 and adjusting the temperature and kinetic parameters within wide range, we can thus create wear-resistive coatings as applied to the specific conditions of GTE compressor blade service.

Based on the results of the herein-presented studies of coatings, we established the fact that the coatings suffering from fretting corrosion and cyclic loads inherent for GTE compressor blades in operation must be sufficiently plastic and capable to relax stresses caused by external loads (even at the expense of adhesion).

EROSION RESISTANCE OF "SiC SKELETON CEMENTED DIAMOND" MATERIALS

Gordeev S.K., Guglin D.N, Danchyukova L.V., Zhukov S.G.

Central Research Institute for Materials, Saint Petersburg, Russia

Carbide materials are known to have good mechanical properties, even at high temperatures. As a special group silicon carbide ceramics is formed both as sintered (SiC) or reaction-bonded (Si/SiC). High hardness and wear-resistance, low coefficient of thermal expansion (CTE) and excellent stability at high temperatures in air characterize the group. The combination of properties of silicon carbide ceramics provides significant advantages by their specific parameters and mostly by specific elastic modulus. Properties of SiC-ceramics are further improved via reinforcement, for instance, by whiskers and fibers.

Analyzing the combination of properties of SiC-ceramics and other materials shows that one of the best reinforcement materials for them is diamond. It has excellent mechanical and thermal properties, comparing very favorably with silicon carbide. This is the reason why we consider reinforcement of SiC-ceramics by diamond particles to result in production of composites with unique combination of elasticity, thermal conductivity, hardness and wear resistance.

We have developed novel superhard materials and named them SiC-skeleton cemented diamond (ScD). ScD represents a group of superhard materials, in which diamond particles are cemented by a silicon carbide matrix (or skeleton) [1]. It may be supposed that a combination of two phases with high hardness (diamond and silicon carbide) in one material makes it extremely high wear-resistant. The main feature of ScD distinguishing it from the known superhard materials (diamond, cBN), is a possibility to produce ScD in the form of articles of complex shapes and large sizes, thus using the net-shape technology. This feature allows to consider ScD as a special type of engineering ceramics with unique properties by wear resistance, rigidity, thermal conductivity, CTE. By controlled varying composition and properties of materials, as well as production of gradient materials with non-uniform distribution of diamond particles throughout the material volume it is possible to easily adapt ScD for different fields of application. High hardness

and wear resistance of ScD allow us to expect its stability in extreme conditions such as in conditions of abrasive particles stream.

The studies were aimed to determine erosion resistance of ScD materials and to compare them with other wear resistant materials.
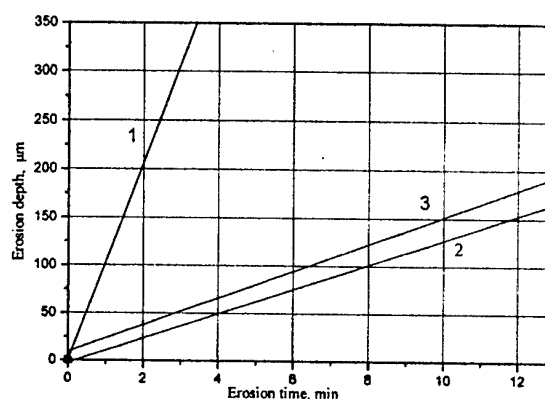
Fig.1. Dynamics of erosion of cemented carbide BK-6 (1) and of ScD materials based on diamond powders 10-14 μm (2) and a mixture of grains 50-63 μm (60%) and 10-14 μm (40%) (3)

Wear resistance was determined by a method analogous to ASTM G76 [2]. The gas blast erosion used a stream of high-pressure gas to accelerate a stream of particles through a nozzle towards to test sample. The sample was held at the distance and angle of the nozzle for the test system. Working distance in our experiments was 40 mm. Angles of impact were 45° and 90°. Nozzle size was 7.6 mm diameter and 80 mm long. Aluminium oxide with particle size 250-500μm was used as erodent material. For the studies we used samples 20 mm diameter, which were placed in a stream of abrasive particles so that one of the surfaces was totally covered by the stream. Wear was determined by gravimetric measurement and then calculated as volume wear and erosion depth.

The studies have shown that wear resistance of both ScD materials and cemented carbide linearly

increases with time of tests (Fig.1). It is seen that erosion resistance of ScD materials compares much favorably with wear resistance of cemented carbide.

The obtained results of wear resistance of ScD prepared from diamond micropowders have shown that ScD materials have high wear resistance (Table 1). Wear resistance of ScD is 10 times greater compared with cemented carbide (BK-6). The greatest resistance was obtained on materials prepared of the mixture of diamond micropowders. One of the reasons maybe attributed to an increased volume concentration of diamonds in such materials. However, the dependence on concentration is not linear: relative diamond consumption of the "mixture" materials turns out to be significantly less in comparison with materials prepared from narrow diamond grain range micropowders.

Table 1. Erosion resistance of ScD and cemented carbide

Diamond particle size (μm) in composition of ScD	Wear rate, μm/min (at angle of impact)	
	90°	45°
10-14	10.2	9.9
20-28	26.7	-
(20-28)+(2-3)	2.3	2.1
(50-63)+(10-14)	13.0	13.2
Cemented carbide BK-6	105	102

Thus, during the studies it was determined that ScD materials have high erosion resistance. Wear resistance of ScD materials significantly depends on the material structure, whereas methods for optimization of the material structure and achievement of extremely high wear resistance are known.

References

1. Sergey Gordeev, Thommy Ekström Novel Diamond Applications: Diamond Engineering Materials//Superhard Tool Materials on the Turn of the Centuries: Production, Properties, Applications. Inter. Conf., 4-6.07.2001, Kiev, 2001
2. M.J. Neale and M.Gee Guide to Wear Problems and Testing for Industry//William Andrew publ., New York, USA, 2001, 150 p.

ANTIBURNING PAINT FOR COATING THE CAST IRON EQUIPMENT USED IN CASTING ALUMINIUM AND CAST IRON ALLOYS

Baranova T.F., Kelina I.Ju., Savanina N.N.
Federal State Unitary Enterprise "Obninsk Research and Production Enterprise "TECHNOLOGIYA", Obninsk, Russia

Antiburnig paint (ABP) is intended for coating cast iron molds, in particular grinding bodies (balls) and cast iron lingots for aluminium alloy casting. The main parts of ABP: a filler with aluminosilicate composition (for instance, mullite-corundum chamot, mortar, etc.) and a binder (liquid glass, aluminoboronphospate concentrate).

The filler ensures high thermal resistance and refractoriness of the coating. High dispersity of the filler powders is responsible for the technological stability of the ABP suspension.

The hiding power and a smooth coating surface of ABP depend on the ratio of the suspension components. They are optimum at $\gamma = 1.12 - 1.16$ g/cm^3.

Factory tests were carried out at Close Stock Company "KUUSKOSKI" (Vyborg, Leningrad region) in the process of aluminium casting: 200 lingots were filled 10 – 12 times during one cycle of filling (a total of three cycles with the duration of 4 hours each were carried out). It was found that the quality of the paint is suited to the requirements placed upon it. The paint compares well with home made analogs in its characteristics and it is superior to home made analogs in labour consumption for stripping the spent coating and in the consumption of the paint per one ton of products.

The service life of the molds in case of casting the cast iron balls 25 – 120 nm in diameter is 500 – 1000 fillings.

STUDY OF MATERIAL'S CONDITION OF TURBINE BLADES IN GAS TRANSFER EQUIPMENT AFTER USE

Tsariova I.N., Tarasenko Yu.P., Myshlaev D.A., Sorokin V.A.
Scientific and Production Company "Tribonika"

The working blades are the most critical components in gas transfer equipment. They operate in severe conditions being simultaneously attacked by high temperature and stresses. In the case of long-duration use and in the consequence of fatigue processes, of corrosive and erosive medium attacks, the physicochemical and structural changes take place, which have an effect on the serviceability of blades.

In order to determine the remaining service time and the possibility to recondition (return to service) the material serviceability, we have studied the state of blades in nickel heat-resistant alloy of low-pressure turbine (LPT) with running time of ≈ 21000 hours.

The alloy's phase composition after use is established by X-ray analysis and by metallography: γ-solid solution of alloying elements (Cr, Co, W, Mo, Ti, Al, Fe, C, B) in nickel, intermetallide strengthening γ-phase $Ni_3(TiAl)$ and carbonitrides of complex composition.

As a result of heat action the surface of blade's edge was exposed to a high-temperature oxidation with $NiCr_2O_4$ formation and it was depleted by alloying elements. The thickness of defective layer is 15-40 μm. The studies of sub-structure of γ-phase in the depth up to 10 μm have revealed the presence of the dispersion in the structure of the grain with blocks' size from 120 to 350 nm. The commination of sub-grains is a consequence of dislocations' collective motion and of sub-grains' formation at plastic deformation processes. The micro-deformations in FFC-Ni grains on the surface layer of blades exceed by one order the micro-deformations in the core of blades.

By the method of X-rays "sliding" beam it was received the density distribution of chaotic and boundary dislocations along the depth of surface layer. The maximum density of defects takes place on the depth of 2-3 μm. In the core of blade's edge and blade's lock the dislocation's structure has changed slightly.

The structural studies are confirmed be the results of mechanical tests. According to the micro-hardness measurements along the indentation's depth it was determined the strong strengthening in the layer of 1,5 μm. The surface micro-hardness exceeds by $\sim$ 2 times the hardness of the base and is equal to 800 kg/mm^2. The thickness of modified zone is equal to 100 μm. The strength of edge's metal after use is higher than in blade's tail. It was noted the decrease of impact toughness.

The shown modifications of the structure and of physical - mechanical features are typical for the established stage of the fatigue – strain hardening. As per micro-hardness and modulus of elasticity the index of material ductility was determined. It was revealed the significant degradation of ductile features after use.

To estimate the remaining service time it was applied the method, which is based on the correlation of ductility coefficient and long-term strength. The conclusion was done about a high degree of the brittle failure's probability in the case of further blades' use and also about the expediency of repair in due time.

On the basis of performed studies it was developed the technology to recondition the serviceability (i.e. return to service) of blades in low-pressure turbine. The technological cycle includes: the operations of surface's machining and electro-pulse treatment, the reconditioning heat treatment, the applying of ion-plasma heat resistant coating.

The proposed repair-reconditioning technology allows to extend the service life of turbine blades.

COVERS FOR THE INVESTIGATION OF STRESSED – STRAINED STATE FOR THE CERAMIC CONSTRUCTIONS

Railyan V.S., Rusin M.Yu., Pestov A.V., Gratsiansky Yu. A., Irkov V.I.
Federal State Unitary Enterprise "Obninsk Research and Production Enterprise
"TECHNOLOGIYA", Obninsk, Russia

Wide applications of new materials, especially ceramics, in engineering leads to the need for improvement of conventional methods of research and development, in particular the methods estimation of stressed – strained state of the constructions. The mostly often used approach to stressed – strained state of the constructions is tensimetry. At comparatively low temperature $T < 373K$ the wire tensoresistors are used successfully. At higher temperatures this method gives large errors cuused by the difference of thermophysic characteristics of ceramics, tensoresistors material and the adgesive used. The compensating methods, used in studies of metallic constructions are not very effective for ceramics. To widen the range of investigation one should use the peculiar features of ceramics, i.e. dielectric properties and porosity. These features make it possible to apply directly to the ceramic surface the sensitive element of the sensor, produced powderlike electricity conducing materials.

At creation of the conducting of the layer at the expense of filling with electricity conducting fine disperse powder, its resistance when heated will depend mainly on the thermal expansion of the ceramics.

The results are presented for the research of deformation of the surface of ceramics samples at thermal loading up to 400^0C. The powder on the base of tin oxide as used as a high temperature cover. The alloy of silver, applied directly to their sample under investigation was used for electric contacts. Also the results are presented of research in estimation of the surface deformation at room temperature using the high- resistance graphite covers.

Theoretically and experimentally are grounded the methods for sensitivity increase in estimation of deformations in ceramic constructions of technical ceramics in comparison to conventional tensimetry using wire sensors. The relations of cover electrophysical properties and surface temperature are shown. The results of the investigation prove that the current conducting covers on the base of tin oxide are able to work for estimation of mechanical deformation as a result of thermal impact at temperatures up to 400^0C.

PERFLUOROPOLYMER-CONTAINING HYDROPHOBIC HETEROGENEOUS CATALYST

Muidinov M.R.

Institute of Problems of Chemical Physics of RAS, Chernogolovka, 142432 Moscow region, Russia

Removal of trace amounts of hydrogen in atomic power stations, electrochemical and radiochemical plants, in closed systems (such as space systems or the underwater fleet), all with high requirements to safety, is an especially actual problem. For its solution, the catalysts, which stably burn down trace amounts of hydrogen at room temperature and often in wet conditions, are required.

In the literature, the way of stability improvement of palladic catalysts, which permits to retain high catalytic activity during hydrogen oxydation at a relative humidity of reaction medium higher than 70 %, is not discovered.

Best present-day industrial hydrophobic catalyst is obtained with the use of Teflon F-4DW suspension as hydrofobizator. The particle sizes for the dust of this suspension make parts of a micrometer. They significantly (approximately on the order of magnitude) exceed pore sizes of the support, so the particles do not penetrate into its bulk and do not protect its surface entirely during impregnation [1]. In the course of hydrogen oxydation up to the water, the hydrated layer is promptly formed on unprotected surface of the hydrophilic support of the industrial catalyst. On such support, the surface of catalytic agent proper is also coated with water, and, as a result, its activity is sharply reduced. Therefore, known catalytic systems for burning down the hydrogen can effectively oxidize molecular hydrogen up to the water only at high enough temperature (60-100 °C) and considerable gas phase hydrogen content (> 3 % vol.).

The method of updating the catalysts for hydrogen burning down offered by us consists in forming thin (2-5 nm) polymeric coverage by graft polymerization of fluoromonomer adsorbed on the support surface. Such method, while rising hydrophobicity, longevity, endurance and stability of a catalyst support, allows retaining of:
♦ high specific rate of catalytic process of hydrogen burning down at a relative humidity of reaction medium higher than 70 %;

♦ high specific surface area of the catalyst.

Besides, the modified catalyst acquires stability to inhibitors of process of catalytic oxydation of hydrogen and does not lose high catalytic activity in the course of time.

The catalysts have passed approbation in model life-support systems of the closed objects [2, 3].

Chemically bound with catalyst carrier surface and evenly distributed, fluoropolymer coating is thinner than suspension coverage in some thousand times. Thus, practically entire surface of the catalytic agent proper becomes accessible for participation in catalytic process. During oxidation the products of catalytic reactions (water) easily leave from surface of the hydrophobic catalyst, and consequently the developed porous structure of catalyst support is retained, and the surface of the catalytic agent proper is not blocked.

After modifying the heterogeneous catalyst by perfluoropolymers, the process of hydrogen oxydation on its surface becomes possible at the temperature of 20-25 °C and for hydrogen contents of 0.05 % vol., i.e. the reburning of hydrogen can be carried out at a room temperature and, as against known catalysts, at contents two order of magnitude smaller than its dangerous concentration in the environment. The results of the trials of the hydrophobic heterogeneous catalyst are presented in Tables 1 and 2.

Thus, the advantages of hydrophobized catalyst are:
♦ invariance of specific surface area of the heterogeneous catalyst;
♦ absence of necessity in frequently technically complex process of preheating the catalyst (ensuring the absence of the opened hot surfaces, the protection from sparking and so on);
♦ catalyst stability to different blocking catalytic poisons and inhibitors;
♦ heightened operation durability;

- support surface hydrophobicity;
- opportunity of hydrogen oxydation on catalyst surface at the temperature of 20-25 °C and hydrogen contents of 0.05-0.5 % vol.;
- heightened conversion of hydrogen - up to 97 %;
- heightened supply of hydrogen-containing air - up to 50-80 l/h;
- small breakthrough of hydrogen - 0.002 % vol. at the hydrogen content of 0.09 % vol. and its conversion of 97 %.

The developed technique of hydrophobization of the support surface of heterogeneous catalyst is useful for catalysts of different processes, not only of molecular hydrogen burning down, i.e. has universal character.

References

1. Scherbakova M.V., Shepelin V.A., Dzisyak A.P., Alfimov V.I. Khimicheskaya promyshlennost, 1986, № 3, 167-170 (in Russian).

2. Muidinov M.R. Stable perfluoropolymer-containing hydrophobic heterogeneous catalyst for burning down fire-dump. Tekhnika mashinostroeniya, 2001, № 1, 76-88 (in Russian).

3. Muidinov M.R. Surface-modified, stabilized, hydrophobic heterogeneous catalyst containing perfluoropolymer for burning down fire-dump. Abstracts of the reports of 3-rd International Conference "Chemistry of highly organized substances and scientific foundations of nanotechnology" (June 2001, St.-Petersburg). St.-Petersburg, 2001, p. 369.

Table 1
Catalytic oxydation of hydrogen in flowing conditions with the use of hydrophobized catalyst [1]

Test number	Air supply, l/h	Hydrogen content, % vol.	Relative humidity, %	T_{input}, °C	T_{exit}, °C	Hydrogen conversion, %
1	78	0.047	84	23	23	68.1
2	55	0.066	86	25	25	89.4
3	84	0.200	67	20	20	90.0
4	63	0.470	81	25	25	90.0
5	42	0.090	80	23	23	97.8
6	55	0.440	84	23	23	97.0
7	60	0.300	75	20	20	93.0

Table 2
Comparative performances of industrial and modified catalysts

Catalyst	Gas mixture supply, l/h	Hydrogen content, % vol.	T, °C	Relative humidity, %	Hydrogen conversion, %
Industrial	3	3	80	≥70	≤95
Modified	50-80	0.05-0.5	25	≥70	≤97

---

[1] The unmodified catalyst at these values of humidity and temperature does not work.

MEASURING RATE OF CORROSION IN STRUCTURES MADE OF LOW-CARBON STEEL USING THE ELECTRIC RESISTANCE METHOD

Ivanenko K.O., Kopan Yu.V.[1], Revo S.L., Hutoryanska N.V., Sementsov Yu.I.[2]
National Taras Shevchenko University, Kyiv, Ukraine
[1]Ukraine Center for Standardization and Metrology, Kyiv, Ukraine
[2]"TMSpecmash" Ltd., Kyiv, Ukraine

Low-carbon steel is widely used in water and gas pipe-lines, in construction of bridges and other structures owing to its inexpensive and hi-tech features. Over the years of a long life of various metallic structures, composition of surface metal layers is changed, microcracks are formed and partially closed in it (for instance, due to oxides formation). As a result, service life of such structures is decreased. Development of a forecasting method for operation of such structures is an important economic task.

With this purpose, we use a method for measuring electric resistance of a corrosion gauge. This gauge (Fig. 1) comprises a closed loop of four identical wire parts of the same composition as structure 5 whose corrosion is being monitored. Part 1 is fixed on electric insulators 6-7 made of epoxy resin and is dyed with the same paint as the structure. Parts 2-4 are insulated from corrosion with epoxy resin. Loop 1-4 is a Wheatstone bridge and is coupled to the measuring instrument through electric contacts 8-11. The instrument supplies constant current to diagonal 10-11 of the bridge and measures
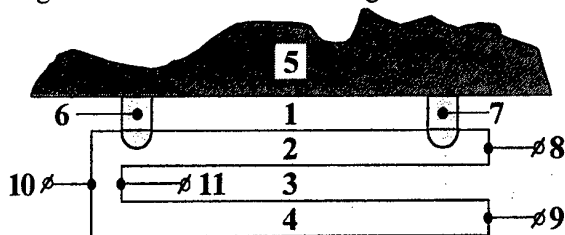
Figure 1. Diagram of the corrosion gauge

difference of potentials on diagonal 8-9. An error in measuring electric resistance caused by temperature variations is reduced in this way. The difference between the corrosion gauge and strain gauge is that electric resistance of corrosion gauge is changed due to corrosion while electric resistance of the strain gauge – due to mechanical strain. Moreover, composition of the corrosion gauge is the same as the structure's being monitored while the composition of the strain gauge wire is special and standard. Bridge circuit coupling of the corrosion gauge (Fig.1) is

reasonable to measure, for instance, atmospheric corrosion during a short term (up to 6 months). For constant corrosion monitoring when electric resistance of the gauge if greatly increased, part 1 of the wire is sufficient to be used as gauge, and it should be coupled to a standard tensiostation. Standardization of corrosion gauges is needed. For structures of low-carbon steel (steel 3), we tested the wire of 0.5 in diameter, the length of the part 1 being 0.5 m. Penetration of corrosion h (mm) was calculated by formula (1)

$$h = \frac{r}{2R}(R - R_t),\qquad(1)$$

where r – radius of the wire (mm), R – initial electric resistance of the wire part being corroded (Ω), R_t – current value of the electric resistance. For convenience, the scale of the device was division graduated h by formula (1).

Atmospheric corrosion of one of the bridges over Dnipro river in Kiev was studied in June-August, 2001. Fig.2 shows the results of the study. Measuring was done in the hours of the day when
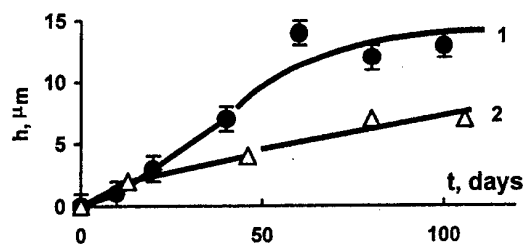
Figure 2. Corrosion penetration h to low-carbon steel (steel 3) in Dnipro's damp atmosphere in summertime (1) and wintertime (2) t

the gauge was dry. Following Fig. 2, the corrosion rate is 20 μm/year in winter and 40 μm/year in summer, and the annual average is 30 μm/year. Protective anti-corrosion coating is based on nitrocellulose enamel. Without a protective coating the corrosion rate is 100-150 μm/year. Thus, the corrosion gauge can be also used to define efficiency of protective coatings.

EXPERIENCE OF USE OF NEW CERMET USING THE PLASMA SPRAYING METHOD TO COAT THE FRICTION COUPLES

Tkachenko S.G., Kudenko G.E.[1], Nikitin A.E., Tukov V.G.
PKP Delta, Donetsk, Ukraine
[1]GP PPES P/O Donetskugol, Donetsk, Ukraine

In this paper are given the results of development of a new two-component gas and thermal coating designed to restore the geometrical sizes of worn surfaces of landing places and friction bearings of a heavily charged shafts of metal rolling equipment.

The service behaviour of coatings must meet the requirements of hardness, wearing capacity [1], corrosion resistance.

In spite of the fact that the plasma spraying of coatings is known for a while [2], the manufacturing of those in real conditions is complicated by the high cost of special materials and the complexity of technological processes which have to ensure the stable service behaviour of the coatings [3, 4, 5].

That's why the authors stated the problem of choice of the coating composition and the development of the technological process of spraying in specific industrial setting. As a result of experiments the authors have developed the technological process of application of two-component coating formed from Cr and Cr oxide with volumetric hardness 60 – 65 units HRC and the layer thickness up to 1.5 mm using the plasma spraying equipment Kiev-7.

The given metallograph experiments and field tests certify that the obtained coating meet all the established requirements. The study of the microstructure showed the following:
1) the coating has a good adherence with the base (Fig. 1)
2) the coating has a low porosity (Fig. 2,3) and is uniformly distributed on the surface of the article (Fig. 2)
3) the coating has a high micro- (Fig. 3,4 5) and macro hardness

Currently this coating is used to restore the geometrical sizes of face .bearing seals and landing places of metal rolling equipment shafts, as well as some studies are done to amplify the field of application of the coating, some experiments are conducted to study the possibility of the coatings use to increase the life cycle of face sealing, shafts and protective bushings of pump axes and the working surface of stop valves.

Fig. 1 – Microstructure of the coating x 250

Fig. 2 – Microstructure of the coating x 100

548
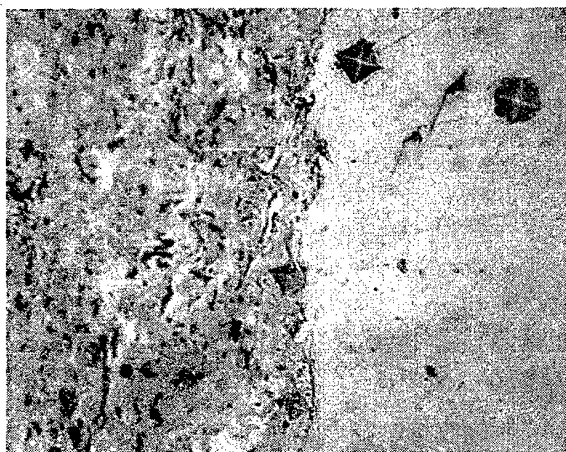
Fig. 3 – Microstructure of the coating x 500
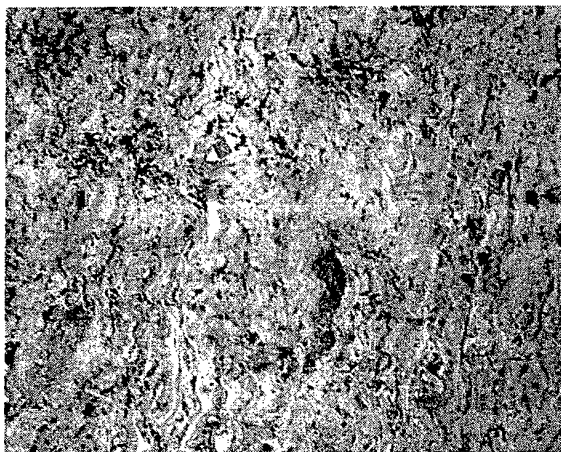
Fig. 4 – Microstructure of the coating x 500
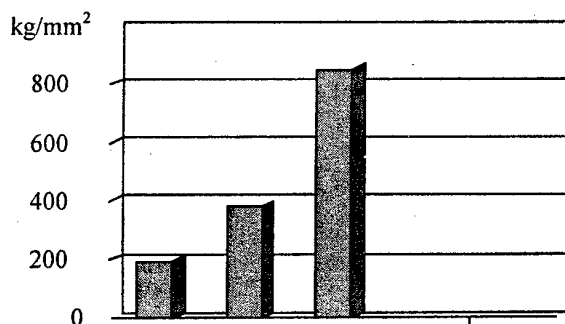
1 – base material,
2 – transition layer
3 – studied coating.

Fig. 5 – Histogram of microhardnes distribution in the volume of the sample

At present stage the metallographic and phase structural analysis of the coating material is conducted.

The technology of the coating application is on the stage of patenting.

List of references:

1. Крагельский И.В., Добычин М.Н., Комбалов В.С. Основы расчетов на трение и износ. - .:"Машиностроение". 1977. – 526с.
2. Кречмар Э. Напыление металлов, керамики и пластмасс. Инж. Э.Кречмар с участием инж. Г. Шварца. Пер. с нем. инж. Е.М. Стрельцовой и Д.Н. Маневич. Под ред. конд. тех. наук М.Е.Морозова и инж. И.А.Немковского.   – М.:   " Машиностроение ". 1966. – 432 с.
3. Сидоров А.И. Восстановление деталей машин напылением и наплавкой. – М.: "Машиностроение". 1987. – 189 с.
4.Хасуй Ацуси. Техника напыления. Перевод с японского С.Л.Масленникова. - М.: "Машиностроение".1975. – 288 с.
5.Борисов   Ю.С.,   Борисова   А.Л. Плазменные порошковые покрытия. - К.:"Техника".1986. – 223 с.

FOAM CERAMIC FILTERS FOR METAL MELTS: REALITY AND PROSPECTS

Antsiferov V.N., Porozova S.E.
Scientific Centre of Powder Material Study, Perm, Russia

The popular nowadays in metallurgy and machinery the item production of secondary alloys needs additional methods for metal cleaning. Rather cheap and available method for metal quality improvement is the filtration through volume filters - they are (together with filling of refractory pieces) foam ceramic filters (FCF) [1,2]. They are sufficiently much used in the West, but are of little use in Russia. FCF manufactured by doubling of polymeric matrix (fig.1) allows to improve moulding quality concurrent with the decrease of incurred charges [2,3].
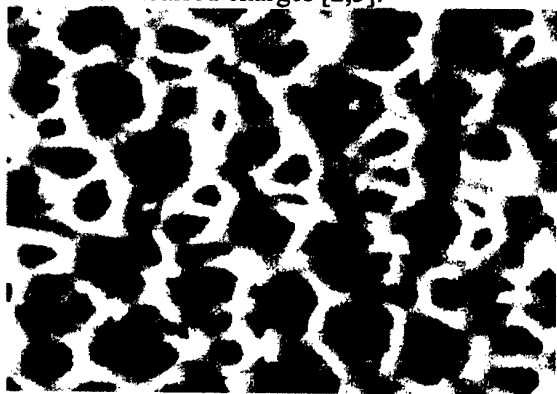
Fig.1. FCF structure. ×10

It seems that FCF apparent advantages must actively promote them in foundry. Meanwhile, the works can get only filters manufactured by Corning Inc., Foseco Inc., Hi-Tech Ceramics and some others. Russian and Byelorussia developments are not in the market of mass quantity because there is no stable demand caused by homeland industry crisis rather than the lack of information and clear instructions on implementation. Trying to use FCF the enterprises face such problems as filter placing in gating system or pouring basin; metal "solidification" followed by full clogging of filter; filter failure by metal jet.

If the problem of placing can be settles more or less successfully, metal "solidification" is difficult to overcome. It is caused by cooling effect of the filter due to, the first, by temperature difference of metal and alloy, and the second, by parting of metal jet and increasing of specific surface. The

less is the filter cell, the more is the contribution of the second element. The metal "solidification" reveals especially strong during filtration of high temperature alloys. In the cases the metal goes through the filter, the overcooling structures occur (e.g. interdendritic graphite in iron).

In domestic literature the similar problem is discussed concerning fillings – the most widespread variant of volume filters [4]. The lines of problem settlement: either filter heating, or metal overheating. The first variant is difficult to accomplish technologically for FCF. The second variant can not be realized at the works without filling temperature control (the latter is typical to many Russian enterprises).

The foundries interested in metal quality use some types of filters already and are not glad to change it. Necessary to demonstrate FCF distinct advantages. Only filling parameters optimization helps to prove it because laboratory tests on aluminium alloys showed that it is possible not only to improve the alloy, but to worse it as well [5]. Many authors note the governing role of adhesive effect during metal cleaning through volume filters [3,6]. In this case the dependence of filtration quality from alloy composition and filter material is apparent. The choice of optimum material for various alloys needs a large number of experiments and data analyses. For example, the experience gained in Scientific Centre of Powder Material Study [7] lets to manufacture filters by doubling of polymeric matrix (with minimum finishing) on the basis of any ceramic matrix.

Filtration through volume filters is, in essence, the strong and practically not used at present instrument for influence on alloys microstructure and properties. So, when studying FCF influence on microstructure and properties of duralumins and silumins [7-8] it was shown that filtration allows to decrease the volume part and dimension of intermetallic inclusions and to increase the content of alloy elements in aluminium hard solution, to increase the casting alloy strength. The quantitative characteristics of alloy microstructure and strength

changes can be considered as specific filter influence.

During the experiments carried on together with Piston Engine Design Bureau specialists on the foundry bay of JSC "AvtoVAZ" there was made the comparative characteristics of two filter types (FCF and silica grid TУ 6-11-318-78) when casting B124 complex alloy. It is noted that filters (even grid) change phase crystallization conditions and results in phase alloy change recorded even after heat treatment. When standard heat treating they observed the absence of the hardening phase in dispersion-hardened alloy.

FCF influences greatly the alloy, therefore, its joint use with modifiers require corresponding researches. Rather successful use of FCF based on chemically bound silicon carbide on filling unmodified grey iron in loam moulds (SPETSLIT, Ltd., Perm) permits to change the sizes and distribution type of graphite inclusion and to decrease the ferrite content in ferrite-pearlitic base. Therewith, the strength increased by 25 % with simultaneous increase of plasticity. The use of the similar filter for grey iron Gh190 (Table 52205 Standard VAZ-FIAT), modified ФC65 and CK resulted in washed-out filter material in the process of filtration.

In some cases incorrect task set by the researches can result in negative conclusions. So comparing the results of steel filtration through sintered corundum and FCF chemically bound at 1600 ^{0}C, the authors [9] arrive at conclusion about FCF inapplicability, though it is clear that it is a matter of limits applied to chemically bound materials only.

FCF are filtering materials with huge potential. Using them we can produce both more clear and homogeneous alloys and alloys with different and controlled composition. And finally, if to use the idea expressed in L.M. Akselrod's and others' paper [10], under definite filling conditions the filter surface can be self-cleaning. Important to understand that various types of filtering materials

most likely are not competitors because depending on real production requirements it is necessary to choose the optimal variant. The problem of FCF implementation possesses large intellectual capacity and requires serious research and experimental work.

References:
1. Stepanova V.D., Kim S.P. Straight-line Flow Systems for Refining of Aluminium and its Alloys Abroad // Non-ferrous Metals, 1990, № 9, p.90-93.
2. Staroverov Yu. S., Chernov Yu.A. Foam Ceramic Filters in Foundry and Steelmaking Abroad // Refractories. 1992, № 1, p.38-40.
3. Brockmeyer J.W., Aubrey L.S. Application of Ceramic Foam Filters in Molten Metal Filtration // Ceramic Engineering and Science Proceedings. 1987, 8 (1-2), p.63-74.
4. Ten E.B. Definition of Allowable Optimal Initial Temperature for Filter // High School Proceedings. Ferrous Metallurgy. 1994, № 3, p.59-62.
5. Silumin Structure and Properties Change when Filtering through Ceramic Foam Filter / S.E. Porozova, A.M. Makarov, V.B. Kulmetyeva. // High School Proceedings. Non-ferrous Metallurgy. 2000, № 1, p.20-22.
6. Ten E.B. Mechanism for Molten Metal Filtering Refining // Foundry, 1990, № 9, p.5-6.
7. Antsiferov V.N., Porosova S.E. High-porous Permeable Materials Based on Alumosilicates. Perm: PSTU, 1996, 207 p.
8. Porosova S.E. Ceramic Foam Filter as the Factor Influencing on Silumin Structure and Properties // MiTOM. 2001, № 8. P.35-37.
9. Svyazhin A.G., Romanovich D.A. Filtration of Non-ferrous Inclusions // High School Proceedings. Ferrous Metallurgy. 1997, № 3, P.16-19.
10. .Technology Development for Manufacturing Refractory Delaying the Metal Channel Closing / L.M. Akselrod, G.G. Melnikova, G.O. Bodina // Refractory and Techn. Ceramics. 2001, № 2, p.22-26.

LAYERED ANTISHOCK COMPOSITIONS BASED ON Al-Si$_3$N$_4$ COMPOSITE MATERIAL

Gilyov V.G.
Centre of Powder Material Sciences, Perm, Russia

It known that different materials are used as armour: steel, light alloys, ceramics. And contradictory demands are placed on armour materials: high hardness and fracture toughness, therefore, the tendency to develop heterogeneous materials is seen, to these can be related structural heterogeneous tripsteels and layered compositions materials (CM). One way to settle the problem is the layered structures made of hard ceramic layers and tough interlayers of metal alloys.

We tried to produce the layered items with hard layers of composite (Al—Si$_3$N$_4$ type), where Al – the alloy based on aluminium, Si$_3$N$_4$ - reinforcing component of porous ceramics of elements [1]. The paper [1] describes in details the production of ceramics, Me-Si$_3$N$_4$ composites were obtained by impregnation of porous Si$_3$N$_4$-ceramics with melt under pressure.

Ceramics of elements is interesting as the filler for CM, because it features high porosity adjustable within large limits, thin porous structure of elements, the presence of fibre-like crystals of silicon nitride and large inter-element pores which make easier quick impregnation under pressure moulding [2].

There are examined the anti-bullet barriers structures with armour layer of Al-Si$_3$N$_4$ type composite based on 2 aluminium alloys: AK4M2 and AЛ-23-1 reinforced by porous Si$_3$N$_4$ ceramics of elements. These barriers were produced by hot metal stamping. For this purpose they filled the mould with the melt, then put heated ceramic plates and carried on the moulding cycle. For creation of barrier structural elements in ceramics such as grids in tough interlayers and perforation, the preliminary holes or slots were made.

And as the result the following compositions were produced:

1. Fibered – F. For its production they use the fibered ceramics consisting of pore fibers of reactively sintered silicon nitride (thickness of 0.5-2.0 mm) forming the frame. After impregnation with aluminium alloy the composite parts reinforced by ceramic fibers have the hardness of 50-60 HRC. Interfiber binding interlayers made of aluminium alloy serve as the tough component in this structure.

All other barrier types possess disperse CM structure formed by impregnation of ceramic of elements of 0.01-0.03 mm thickness [1], hardness of 20-45 HRC as a function of Si$_3$N$_4$ volume fraction.

2. Layered – L (fig. a). The structure consists of composite layer and matrix alloy layer.

3. Grid – G. In this one-layer structure the composite layer is divided into cells by interlayers of matrix alloy, they form the grid and divide all armour (its thickness).

4. Layered-grid – LG (fig. b). Consists of composite layer divided by grid inter- layers of aluminium alloy (G type structure) and a base of matrix alloy.

5. Layered-perforated - LP (fig. c). Differs from the layered structure by the presence (in composite) of bars, diameter 1.5 – 2.3 mm, of matrix alloy made together with the base and hardening the layers connection (rivetted joint effect).

Anti-bullet resisting tests were as follows: firing with TT gun (V$_0$=440 m/s, d = 9 mm) or AKM submachine-gun (V$_0$=715 m/s, d=7.62 mm), distance – 3 and 5 m. The samples – discs of 60 mm during tests were fastened on periphery in hard steel holder. Test numerical index: bullet flying speed after interaction with the barrier tested. The bullet speed was measured according to the methods

based on the principle of contact interlocking of route basic sections.

Due to the variety of geometric parameters of sample structures and different test condition it is advantageous to introduce the convenient and universal value for comparative estimation of anti-bullet resistance. For this characteristic it is worthwhile to accept the change value of bullet kinetic energy during interaction with barrier relative to its thickness and bullet section area:

$$\overline{\sigma_{eff}} = \frac{m(V_o^2 - V_\kappa^2)}{hS}, \qquad (1)$$

a   b
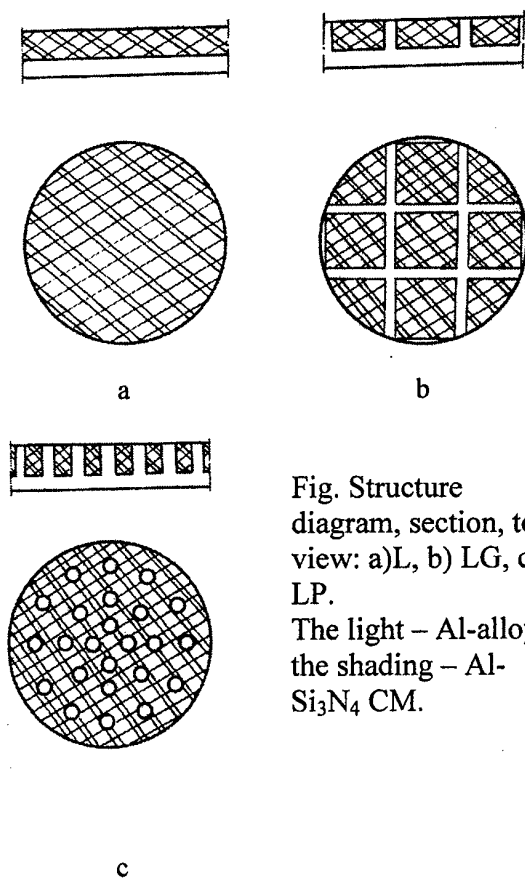
Fig. Structure diagram, section, top view: a)L, b) LG, c) LP.
The light – Al-alloy, the shading – Al-Si₃N₄ CM.

c

It characterises the effective dynamic resistance to bullet penetration through the barrier and the strength dimensions. This value possesses the general nature because it depends both on armour component properties and on their dimension relation, mutual position and interaction; characterises the structure as a whole and can serve as the

optimising parameter for the composition, micro- and microstructure and technological factors.

There are studied: the influence of Si_3N_4 in composite, element thickness in ceramics, dimension relation in structure.

Shown high anti-bullet strength of layered and layered-grid barriers, data concerning the parameters influence of ceramics composition and structures. Ceramics elements (0.03 mm thickness) used for reinforcing at incomplete nitriding of silicon blanks and large phase of α-Si_3N_4 provide the best quality of impregnation, composite hardness, anti-bullet strength and long life of barriers.

No punching of layered barriers based on AЛ23-1 alloy with composite layer of 45 vol. % Si_3N_4 and hardness of 35 HRC by AKM gun bullet of 5.45 mm, V_0=750 m/s at surface density of 390 g/dm².

References:
1. V.G. Gilyov, V.N. Antsiferov. High-Porous Materials Based on Reactive-Sintered Silicon Nitride. // Perm State Tech. University. Perm, 1998, p.199.
2. V.N. Antsiferov, V.G. Gilyov, V.P. Grigoryev et al. Wear Resistance of the Composite Materials based on Aluminium Alloys with Nitride Silicon as Reinforcing Phase. // Metal Study and Metal Heat Treatment.1993.# 1, p.16-18.

553

WELDING WASTE GAS CLEANING ON HONEYCOMB CATALYST CARRIERS

Antsiferov V.N.[1], Khanov A.M., Sirotenko L.D., Matygullina E.V.
Perm State Technical University, Perm, Russia
[1] Scientific Centre of Powder Material Study, Perm, Russia

At present welding fabrication ranks the third on the vocational diseases level. The most urgent are the works connected with the search for welding waste gas cleaning in closed volumes and in the places beyond the reach of stationary ventilation. Current cleaning systems – portable small filter-ventilation units - do not provide harmful agents elimination from welding sites up to the limiting concentration. For the most part it is caused by the fact that neutralization set of these units consists of container with activated carbon of short service life, rather high pressure loss of filling layer and does not eliminate carbon monoxide.

For welding waste gas cleaning the most promising is the implementation of block carriers of honeycomb structure allowing to perform effective catalytic transformation of toxic nitrogen oxides and carbon into biologically inert compounds. It is known honeycomb structures have some advantages. They are: small and permanent hydrodynamic resistance to gas flow during operation, high allowable flow speed, absence of local overheating peculiar to filled catalysts which result in catalyst deactivation. Straight-channel structure helps to work with dusted gas flows without filtration.

The most popular technology for honeycomb structure manufacturing is the extrusion, honeycomb block erection of ceramic relief plates or metal corrugated bands. The authors have developed the technology for honeycomb structure manufacturing by extrusion moulding of ceramic masses [1]. Extrusion moulding of plasticized ceramics permitting to mould the items of complex spatial structure is developed and studied rather well. Extrusion moulding is based on definite structural and mechanical properties of systems moulded, their ability to decrease plastic strength under mechanical influences, and to restore it again after stress relief. Thanks to this, under the mechanic forces of moulding machine (screw, blades, means for wear into holes) the mass becomes less tough, acquire plasticity and can be pressed through the die. After the die and stress relief there occurs the toxicotropic restoration of

plastic strength, the mould items becomes fit for future transportation and finishing.

We have developed the laboratory and pilot-industrial equipment, as well as the auxiliaries for production of honeycomb structure materials based on plasticized ceramics [2]. The frame creating equipment helps to produce rectangular, hexagonal round structures. Previously the authors used in their studies silica porcelain with sintering temperature about 1200 ^{0}C. There were carried on special rheologic investigations, received the theoretic relations for calculation of perforated matrix thickness ensuring its operation without failure. Aiming to cheapen the honeycomb structure technology and, consequently, the equipment for welding waste gases cleaning we fulfilled the researches connected with the choice of more accessible but technological raw material. Raw materials of local deposits for production of building materials were chosen as the research objects. In Perm Region red-burn clays are widely spread. They possess more low sintering temperature (900-950 °C) in comparison with silica porcelain, easy to mould. Their main defect – high shrinkage if sintered. So as to lower the shrinkage, special filling agents were introduced into the mass. Rheologic researches of various raw materials made possible to choose the deposit with the most technological material. In the samples they defined structural and physical-and-mechanical properties. Essentially the samples of red-burn clay are highly competitive with silica porcelain on mechanical characteristics.

In design of filter-absorption plant they use the honeycomb blocks with cells 3x3mm.

The copper-chromium spinel catalyst was chosen as the cheap and effective one. Known that the present catalyst possesses good activity and thermal stability, low temperature, operates in excess of oxygen. The content of active component in catalyst – 10 mass % . The prototype of filter-absorption plant for welding was made [3]. The neutralization set consists of metal casing with heat insulation coating; heating block made as ceramic

honeycomb block in the cells of which Ni-Cr alloy spiral is installed; block catalysts of honeycomb structure positioned in succession. The pneumatic machine serves as the draft initiator providing the required gas flow speed. The researches were carried on under conditions of natural process of welding waste gas neutralizing. They used electrodes of the most popular УОНИ-13/45 grade issuing the largest volume of harmful agents. In the process of work the reactor length, flow rate of gas mixture passed and temperature in reactor were varied. It is found when the reactor length increases and the flow rate of gas mixture decreases there occurs the growth of nitrogen oxides transformation, temperature dependence is of extreme character because at $<300\ ^0C$ the reducer (CO) oxidises actively. Maximum degree of nitrogen oxides transformation at the catalysts tested equals to 60%. Activation energy for reducing reaction Nox amounts to 36.5 Kj/mol Nox. The process takes place in kinetic area and is limited by the stage of chemical interaction of reagents.

In addition to gas catalyst neutralization unit the filter-absorption plant has the air intake, the filter-absorber of hard particles, the draft initiator. The plant operates as follows. The draft initiator produces vacuum in the plant. Polluted air comes in mechanical filter for mechanical dust cleaning of welding aerosol. Then the air passed through the heating block is heated up to required temperature of $300\ ^0$ C. Further, the heated air comes on block catalysts of honeycomb structure for nitrogen oxides reducing and carbon monoxide oxidation. The purified air goes out the back wall of gas neutralization unit. The plant was tested with satisfactory results – with electrodes issuing harmful gases at relation of NOx:CO equal or less than 3:4. In case of the plant implementation for welding with other electrodes we recommend to supply gas-reducer (e.g. CH4) in catalyst block.

References:
1. V.N. Antsiferov, L.D. Sirotenko, Yu.S.Klyachkin, A.M. Khanov. Composition Oxide Materials and Honeycomb Structures. Perm State Techn. University, Perm, 1999, 92 p.
2. A.M. Khanov, L.D. Sirotenko, E.V. Matygullina. Matrix Strength at Honeycomb Material Extruding. Machinery Bulletin. #4, 1995, p.3-6.
3. O.A. Onorin, E.V. Matygullina, A.M. Khanov, M.N. Ignatov. Filter-Absorption Unit for Welding Waste Gas Cleaning// Welding. 1998. # 10. P. 37-39.

ALLOYS OF ALUMINIUM FOR THIN-FILM METALLIZATION OF GREAT INTEGRATED CIRCUIT

Novosjadlui S.P., Melnyk P.I.
Stephanyk Precarpathian university

Thin a film of aluminium, which are widely used for formation of thin-film metallization of integrated circuits (IC) of small and an average level of metallization, became unsuitable for the big integrated circuits (BIC). It is caused by such factors:

- intensive interaction Al and Si at heat treatments which resulted in short circuits p-n transitions;
- low stability for the refusals, caused by mass tranfer due to electrodiffusion and corrosion;
- the low temperature of began recrystallisation results to that at heat treatment there is a significant growth of granularity of films;
- high tensions it is compressed of compression result in growth hillocks which become the centres of electrocorrosion destruction.

For elimination of these lacks by us the following technologies are developed:

- manufacturing alloys of aluminium alloyed by rare metals and on their basis of targets for magnetronic formations of metallized films of AlHo-1, AlSiHo-1;
- modifying a film surface of aluminium by ionic alloy of Al +, B+, B4, Sb+, which provides their high corrosion and electromigratory stability;
- formation of an alloyed aluminium film by magnetronic dispersion of the combined target of alloy AK-1, into which working zone probes from an alloy refractory (Ti, Zr, Hl, V, Nb, Ta, Cr, Mo, W) and rare metals (Sc, Y, La, Ho) are entered.

Such technology simply allows to change the following physical and chemical properties of films:

- the factor of passivation is increased;
- decrease thermal intensity in folms and hillocks;
- adhesion films to functional layers is increased;
- time of corrosion destruction decreases on the order and more;
- film granularity and and roughness of edges decreases at a photo-lithographic process;
- alloy aluminium impurity with cations and anions becomes effective means of translation of stationary electrode aluminium films in area of positive values;

The specified technology of metallization is used at formation of structures of the big integrated circuits which work in extreme modes of operation on temperature, humidity and capacity of dispersion.

CONTROL SYSTEM FOR FAST THERMAL PROCESSES

Reznik S.V.[(1)], Anuchin S.A.[(2)], Rusin M.Ju.[(2)], Trofimov A.I.[(3)]

[(1)]Bauman Moscow State Technical Universiry, Moscow, Russia

[(2)]Obninsk Research and Production Enterprise "Technologiya", Obninsk, Russia

[(3)]Obninsk Institute of Nuclear Power Engineering, Obninsk, Russia

Ceramic materials are widely used in thermostressed structures owing to their high thermal, chemical, electrical resistance, high strength and radiotransparency. The upper limit of the operating temperature range depending on the product type is 1300 – 2200°C. Conventional procedures and devices for measuring thermophysical and optical characteristics are used at much lower temperatures.

To solve this problem, a setup for measuring thermophysical and optical properties of the structural ceramic materials under one-sided radiation heating in a wide temperature range has been developed.

This method and the algorithm of solving the inverse problem of heat exchange make possible a comprehensive determination of thermophysical and optical properties under dynamic conditions.

A high rate of ceramic specimen heating causes rigid requirements imposed upon the control system (CS): high speed of response and accurate temperature measurements. A great number of measurements and the following processing of measurements are impossible without the use of the computers.

A control system with the use of a personal computer (PC) and advanced technical approachers has been developed. A block-diagram of the control system is shown in Fig.1. The program of the setup control incorporates a mathematical model of the object to be controlled. It selects its parameters in accordance with the variation of the thermophysical · characteristics with the temperature. The dynamic programming method offers maximum control accuracy and minimum time of the object response to the control action.

The metering system (MS) possesses a low-pass digital filter which filters off high-frequency interference. Since the temperature in different points of the specimen varies depending on the thermocouple position relative to the frontal
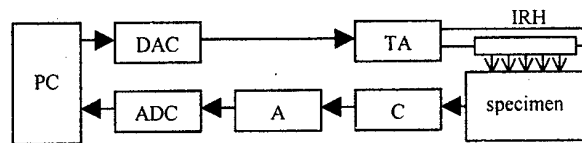
Fig. 1 PC – personal computer
DAC – digital-to-analog converter
ADC – analog-to-digital converter
TA – thyristor amplifier
IRH – infrared heaters
C – commutator
A – amplifier

surface (Fig.2), the time of the channel inquiry in MS varies with the rate of the temperature variation in this point. It allows the metering system to inquire more often the channels with a higher rate of the temperature variation without the increase of speed of response of the whole system but with the increase of the temperature control accuracy.
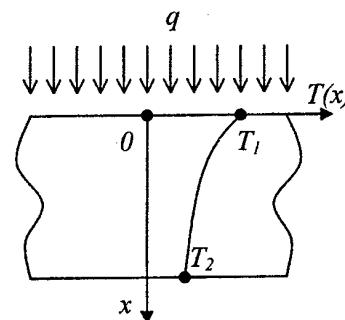
Fig. 2 Distribution of temperature in the specimen depending on the distance from the frontal surface

The experimental data obtained are further processed with the help of the programme for solving the inverse problem of heat exchange.

The control system is then connected to the computer printer port but the connection to a bus with a higher speed is planned later on.

In summary it should be noted that the setup in question has made it possible to reduce the duration of the experiment at the expense of the unsteady-state stage of heat exchange and automation of the whole process of measurements, to extend the temperature range of the experimental data. The thermal tests of the specimens from structural ceramics NIASIT 8PP in the temperature range from 50 to 800°C have been carried out. The data obtained are in good agreement with the material ratings. The error of the temperature dependence of the thermal conductivity is within ±10%.

Thus the modification of the setup and the control system will extend the capabilities and improve the efficiency of the investigations on heat exchange in materials and coatings.

FOAM METALS - PERSPECTIVE DAMPERS OF SHOCK WAVES

Danchenko Y.V., Kulakov S.V.

Research Center of Powder Material Science, Perm, Russia

Barriers of porous and foam materials are used for damping of shock waves (SW), arising in an environment at explosion of explosive charge. The foam metals or so-called high-porosity permeable cellular metals (HPCM), having a structure in the form of polygon cells bound into spatial skeleton, in the best way combine the properties of the above mentioned dampers. This is favoured by maximum pore volume (85-97 %) and minimum quantity in them of rigid component (15-3 %) distributed as a three-dimensional lattice (Figure 1).
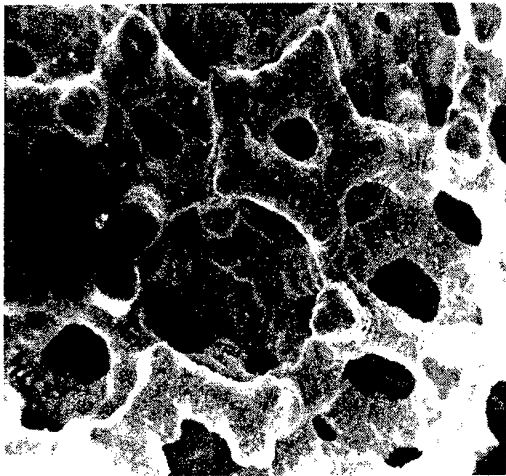
Fig. 1. Structure of HPCM. x10

To check experimentally the above mentioned statement it was investigated the propagation of shock waves through barriers of foam metals in near and far zones of explosion. The damping processes were studied using HPCM of copper-nickel alloy and "sandwiches" made of a foam metal plate with outside sheets of stainless steel, and the structural and geometrical characteristics of a foam metal - porosity, cell diameter and thickness - were varied.

The sequence of SW propagation through foam metal was recorded by ionization contact sensors and frequency meter via synchronizer.

It has been determined that in a near zone of explosion the SW speed is reduced 2-4 times when increasing the layer thickness of a foam metal from

5 to 35 mm and reducing its cell diameter and density (fig. 2a). When using a combined barrier consisting of HPCM and metal sheets with considerably different dynamic compressibility, the effect of SW attenuation is indicated more considerably (fig. 2b).
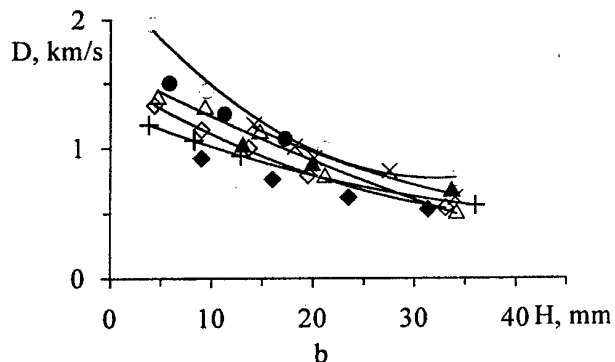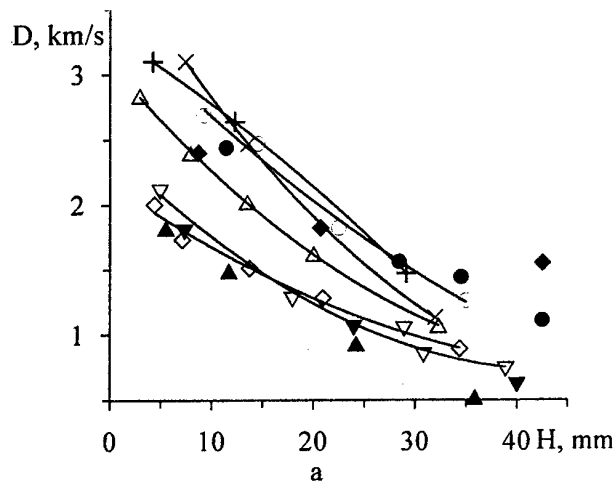
a: d_c, mm/ρ, g/sm^3: ○ - 4,08/0,59; ● - 3,5/0,6; ◇ - 0,8/0,9; ◆ - 0,8/0,47; △ - 2,0/0,94; ▽ - 0,8/1,24; ▼ - 2,0/1,14; ▲ - 0,8/1,28; + - 4,08/1,22; ✕ - 2,0/0,31. 6: d_c, mm/ρ, g/sm^3: ○ - 4,08/0,3; ● - 3,5/0,6; ◇ - 0,8/0,9; ◆ - 0,8/1,28; △ - 2,0/1,23; ▲ - 3,5/0,4; + - 2,0/0,61; ✕ - 2,0/0,61.

Fig. 2. Speed shock waves damping in HPCM (a) and sandwich barriers based on HPCM (b)

The foam metals have advantage on reduction of SW speed and pressure compared to the most efficient dampers made of lead and foam materials with a polymeric matrix. After HPCM barriers the slow increase of SW pressure front is also observed (fig. 3a), and at small thickness the combined barriers have the advantage, and with

increasing the HPCM thickness the effect of a metal plate weakens (fig. 3b).

established and role of high porosity element and metal plate has been determined.
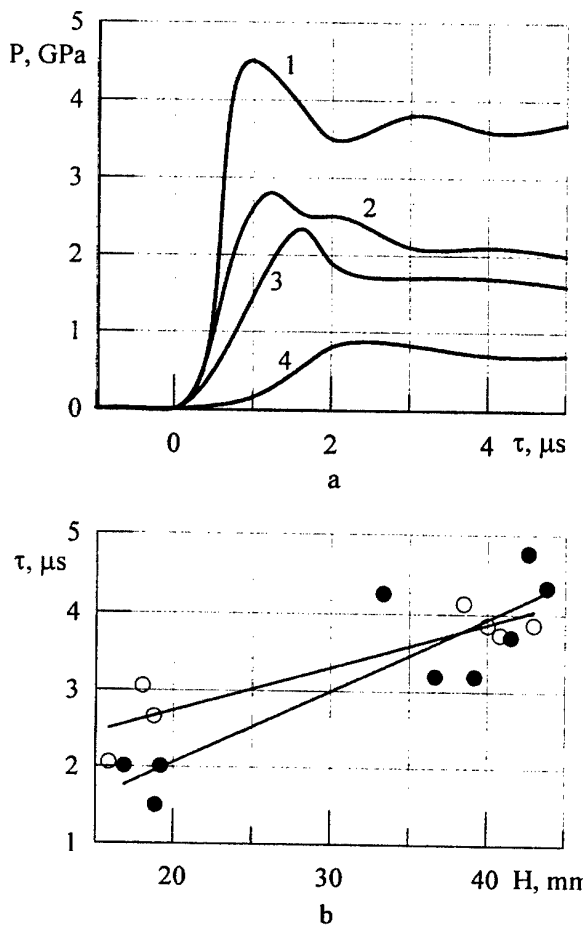
Barrier thickness, mm: 1 – 11; 2 – 18; 3 – 28; 4 – 39.
P_{max}, GPa: 1 – 4,5; 2 – 3,2; 3 – 2,5; 4 – 0,9.
◯ - combined damper; ● - HPCM damper.

Fig. 3. Pressure increase (a) and rate of pressure increase (b) in HPCM damper in near explosion zone

d_c, mm: 1 – 3,5; 2 – 2,2; 3, 4 – 0,8.
ρ, g/sm³: 1 – 0,6; 2 – 0,14; 3 – 0,4, 4 – 1,27.
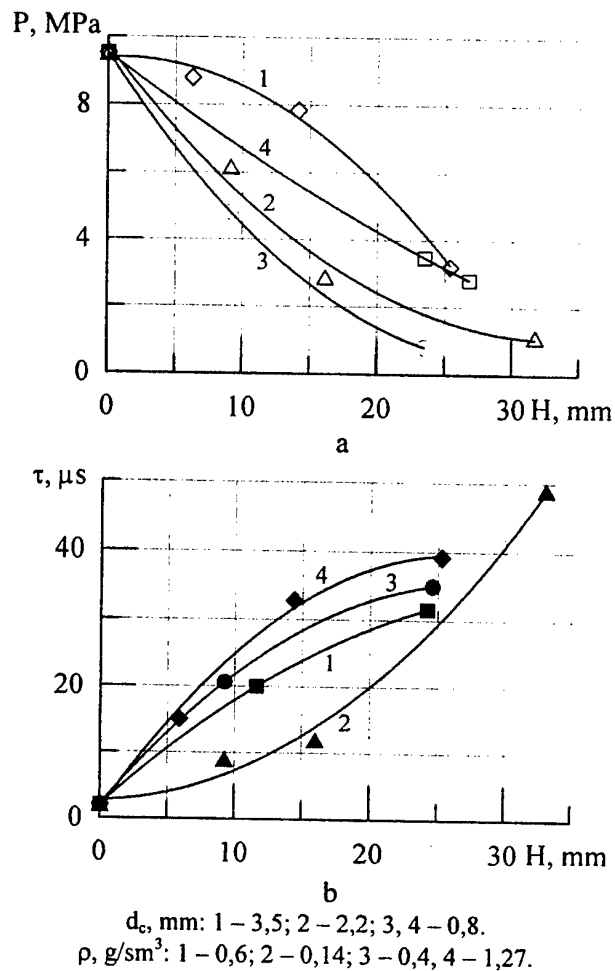
Fig. 4. Structural and geometrical characteristics of HPCM dampers versus short wave parameters

Mitigation of SW maximum pressure 5-9 times and increase of its growth time 3-6 times take place when HPCM dampers are arranged outside of detonation product direct influence, and the damping is indicated in a greater degree for close-meshed low density structures (fig. 4).

It has been revealed, that the foam metals have good protective properties resisting to a detonation transfer. It is provided by reduction of pressure transmitted to an initiated charge, and diffusion of SW front, that transforms SW into isoentropic compression wave and reduces heating of the centers stimulating a detonation. Distinctive features of combined damper operation have been

DEVELOPMENT AND INVESTIGATION OF FRICTION CARBON MATERIALS TERMAR

Kostikov V.I., Demin A.V., Kulakov V.V., Kenigfest A.M.
FSUE "NIIGrafit", Moscow, Russia

Brakes for modern aircraft are employed in rather complex and stressed conditions. In this connection a complex of quite different requirements is imposed upon materials of the most important constituents of the brakes, friction elements.

First and foremost, these materials must have for efficient braking a sufficient value of friction coefficient, which is to be ultimately stable in quite different conditions of exploitation (taxing, rejected take-off, emergency landing) and independent of natural conditions (humidity, contamination, etc.)

The main necessary features of the friction materials also involve their ability to rapidly and efficiently absorb kinetic energy of an aircraft released under braking conditions, which ensures protection against overheating of the remaining parts of the landing gear.

Carbon-carbon composites to the utmost extent meet the present-day requirements. Due to their high mechanical strength under static and dynamic loads, high heat capacity and thermal conductivity, temperature stability of the above characteristics, good frictional properties, they have no competitors in the described field of application.

The friction carbon materials for the recent decades have found a wide spread in brake devices of aircrafts, racing cars and high-speed rail-way transport due to a number of advantages over the previously used prototype, friction cermet, the main of them being:
- stable high frictional characteristics under various exploitation conditions;
- high wear resistance ensuring a considerable service life to braces: exploitation up to 2000 and over of take-offs and landings (the frictional cermet ensures 500 take-offs and landings at most);
- high static and dynamic strength at elevated temperatures, a sufficiently high ability to absorb energy, thereby ensuring an efficient braking under extreme conditions and opportunity

of further exploitation of brakes (impracticable in case of frictional cermet);
- low weight making it possible to substantially save the flying mass at the appropriate increase of a lode-carrying capacity.

Among over than 16000 aircraft wheels annually produced in the world, in 60 % of cases use is made of friction carbon disks. The word-wide annual output of such discs exceeds 500000 pieces.

The developer of all the friction carbon materials produced on industrial scale in Russia (and USSA), combined by the general title Termar, was FSUE "NIIGrafit". The materials Termar-TD, Termar-DF, Termar-CTD, and Termar-ADF were employed or are being employed up to now in aircrafts Tu-154M, Tu-160, AN-124 («Ruslan»), An-225 («Mriya»), Tu-204, the space shuttle «Buran».

Friction carbon materials, fully called as friction carbon-carbon composites, comprise a skeleton consisting of carbon fibers bound by a carbon matrix.

According to foreign production technology for friction carbon materials, a porous skeleton made of carbon felt is infiltrated with a carbon matrix mainly via a high-temperature pyrolysis of hydrocarbon gases (natural gas).

The principal particularity of the production technology for the Termar materials is the use, as a source for obtaining the matrix, of a liquid organic binder, cal-tar pitch. The multistage technology involves mixing the material components, molding performs, their heat treatment in order to convert the organic binder into a carbon matrix, several cycles of additional pitch densification of the performs and heat treatment to form an optimal structure ensuring the required frictional properties, machining to obtain discs, applying a protective coating.

The technology developed makes it possible to properly control frictional characteristics of the

material so as to obtain a material of high density, thereby increasing its ability to absorb energy released under braking and minimizing the possibility of the effect of environment and exploitation conditions on its properties, which is highly dangerous for the materials of foreign production.

The optimization of materials and their production technology was based on results of investigation of influence of structure and characteristics of the material and its components, as well as the exploitation conditions on performance characteristics, study of the material structural changes in the course of exploitation.

Using methods of optical, scanning, and transmission electron microscopy, Raman spectroscopy, there have been revealed profound changes in the structure and morphology of surface layers conditioned by thermal and force actions of friction. A mechanism of phenomena occurring on friction surfaces of the carbon materials is suggested.

CARBON-ARC EVAPORATION OF IMPURITIES FROM REFRACTORY COMPOUNDS OF ZIRCONIUM AND SILICIUM

Kravchenko L.P., Kurochkin V.D., Tsurpal L.A.

Institute for Problems of Material Science, NAS of Ukraine, Kyiv, Ukraine

Refractory compounds of zirconium and silicium are widely used as materials working at extreme conditions. Some of them are used for resistant coatings protecting constructions against high temperatures. Experimental study of materials at temperatures above 2500 K is rather difficult task. This article presents investigations high temperature reactions employing emission spectrometry of carbon-arc in atmosphere of argon and air. Temperature of materials to be studied may be easily varied by changing arc current and depth of electrodes. Process of evaporation was registered by intensities of spectral lines of elements studied. This method allows to study reactions at temperature up to 4000 K.

Temperature of the bottom of electrode was measured by means of several methods. First of them is specially designed facility for comparison of radiation with standard tungsten lamp and high resolution spectrometer, used as monochromator. For not too high temperatures results of measurements were validated by ordinary used method employing calibration by melting points of well known materials.

To study the low of evaporation from materials inserted into electrode crate we used kinetic equation of the form:

$$dC/dt = k\,(C_0 - C)^n, \qquad (1)$$

where C_0 and C are initial and current concentrations, k - rate constant, n - reaction order.

Reaction order were determined from evaporation curves by half-value period ($T_{1/2}$) of C_0 on standards, prepared from above mentioned compounds. Typical curves represent dependence of intensity of spectral line of element studied on time (fig.1). Reaction order were found from slope of the straight line in coordinates ($lgT_{1/2}$, lgC). Values measured appears to be in the range 1.1 - 1.2 that are very close to 1.0. Therefore evaporation rate of an element may be written by kinetic equation of the first order. Solution of equation results in:

$$\ln(C_0/C) = k\,t \qquad (2)$$

Values C_0/C were measured from relations of areas under evaporation curves for the given time:
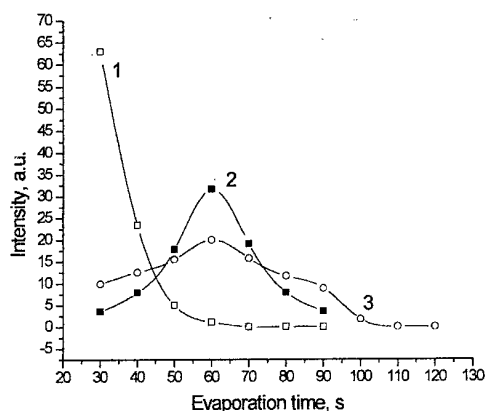
Fig.1 Kinetic of intake of Al_2O_3 from ZrB_2 in graphite anode of air arc at current 20 A.
1 - T = 2400 K, 2 - T= 2300 K, 3 - T = 2200 K.

$$C = C_0(1 - \int_0^t Idt / \int_0^T Idt) \qquad (3)$$

where t - current time, T - the time of total evaporation of an element.

Experiments show that curves in coordinates ($\ln(C_0/C)$ - t) are indeed straight lines and rate constants k were determined from the slope of the lines (Fig.2).
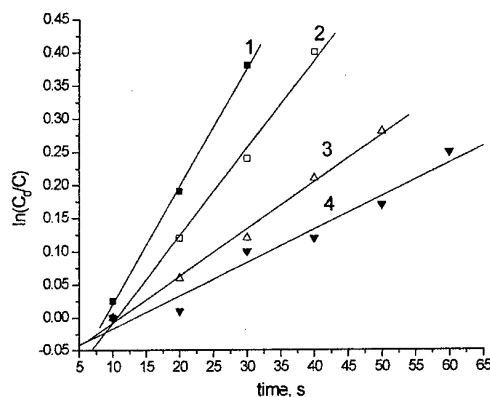
Fig.2 Determination of rate constants of thermal dissociation of Al_2O_3 from ZrC in air arc at current 20 A. 1 - T = 2350 K; 2 - T= 2200 K; 3 - 1940 K; 4 - T= 1800 K (depth of electrodes are 3, 4.2, 6, 7 mm respectively)

From known rate constants at the given temperatures activation energies of process thermal dissociation have been calculated. Chemical reactions of reduction by carbon have been studied preliminary in argon arc on some oxides, chlorides and fluorides with well known thermal constants. Results are presented in the table 1.

Table 1. Measured activation energies of carbon-arc dissociation in argon.

Matrix	Activation energy, kJ/mol
BaO	142
MgO	293
NaF	100
CaO	92
AgCl	84
NaCl	84

Evaporation of Al_2O_3 from carbon or TiC matrix in air arc indicates that reaction probably proceeds through the stage of formation of unstable compounds. Reductions of aluminum oxide may proceed by to ways:

$$Al_2O_3 + 3C = 2Al + 3CO \qquad (4)$$
$$2\,Al_2O_3 + 6C = Al_4C_3 + 6CO \qquad (5)$$
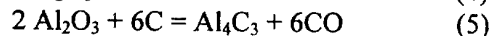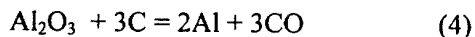
Free enthalpy of reaction (4) at temperature of a sample of about 2000 K is positive (ΔG = 62.8 kJ/mol) so this reaction is impossible. According to [2, 3] reaction (5) is possible and results in formation of unstable aluminum carbide having enthalpy of vaporization 353.7 kJ/mol. Measured activation energy E_a for Al_2O_3 is 175.8 kJ/mol. Comparison of activation energies with enthalpies of sublimation indicates that there is correlation between them. Measured E_a lies in the range 0.4 - 0.6 of ΔH_s^0. These results indicate that intake of vapors into discharge plasma is not simple evaporation but accompanied by chemical heterophase reactions of powders studied with carbon. Proposed method allows to study processes in electrodes at high temperatures in direct current arc.

By this method were investigated kinetic of thermal dissociation such refractory additions as MgO, Fe_2O_3, TiO_2 in zirconium silicides Zr_2Si, $ZrSi_2$, Zr_5Si_3 and also ZrO_2, Si_3N_4.

REFERENCES

1. Kurochkin V., Kravchenko L. Interaction of a Spark Discharge with W-Cu electrodes Alloyed by REE // High Temperature Materials and Processes. - 2000.- v.19. - No 6.- P. 427 - 433.

2. Термодинамические свойства неорганических веществю Справ.под ред. Зефирова А.П.- М.: - Атомиздат, 1965, С.460.

3. Куликов И.С. Термическая диссоциация соединений. - М.: Металлургия, 1969.

INVESTIGATION OF BIOMATERIALS BASED ON BIOLOGICAL HYDROXYAPATITE FOR EXTREME ENVIRONMENTS OF ALIVE ORGANISMS

Brusko A.T.[1], **Sulyma V.S.**[1], **Ivanchenko L.A.**[2], **Podruchniak E.P.**[3], **Pinchuk N.D.**[2]

[1] Institute of traumatology and orthopedic of MSA of Ukraine, Kyiv, Ukraine

[2] Institute for Problems of Materials Science of NAS, Kyiv, Ukraine

[3] Institute of gerontology of MSA of Ukraine, Kyiv, Ukraine

Present-day medicine uses more actively biological materials for replacement of bone defects, which arise owing to traumas or diseases of an osteal tissue. The introduction of an implant in an osteal tissue of an alive organism results in building extreme conditions in a local field new created of a bone, and, probably, and all organism. Study of a response of an organism on introduction in it of simulated substitutes of fields of a bone represent a serious problem. The successful solution of this problem is important for a choice of biomaterials with given properties from a wide spectrum of materials developed in the given time.

The character of modifications in a field of an implantation can be investigated by X-ray method per day of operation and at different stages of an adhesion or gystomorphological by examinations of fields new created of a bone after deduction animal of experiment.

We have proposed [1,2] to use a composite material in surgery that is based on bioactive biological hydroxyapatite, which is the mineral in bone tissue obtained by heat treatment of bones. Such biomaterials are more economical than analogous ones that contain synthetic hydroxyapatite and they represent the use of cheap natural raw material in technological processes involving appreciably lower energy consumption.

In the present work are submitted results of X-ray and gystomorphological examinations of new created osteal tissue fields of adult dogs which were implanted biomaterials on the basis of biological hydroxyapatite after synthetically built apimetaphyseal and diaphyseal defects tibiae of a bone. The implants by the way of granules of different dimension and with the various contents hydroxyapatite were made by a method of a low-temperature sintering.

The postoperative term experimental animal transited without complications, the adhesion of wounds descended by a first intention, support of pelvic extremities was saved.

It is by X-ray method fixed, that in 3 weeks after an implantation of all kinds granules around of an implant the nonuniform density of an osteal tissue with indistinct contours are observed. Through 13 and 15 weeks the sharpness of contours was even more lost. In 26-30 weeks a rather small part of an implant was saved invariable on X-ray density.

It is fixed in gystomorphological examinations rezults, that in 3 weeks of stay of an implant in an osteal tissue around of its granules the heavy-bodied web new creates osteal beams is founded. From the party intratrabecular of hollows osteal beds grew in a biomaterial the veins and osteogen with shaping of islands of an osteal tissue. The depth of a germination of an osteal tissue compounded 1,5-2 mm. It is observed directly opposition of an osteal tissue on granules of a biomaterials. In 13-15 weeks after an implantation are formed web osteal beams permeated volume of a implant.

The majority of implants granules gave in to a degradation, fragmentation and sequential replacement by an osteal tissue. In a fig. are submitted comparative dynamics of shaping of an osteal tissue around of biogranules of two types (with glass phase and without it) on different terms of observation. At an implantation of biomaterials contained glass phase, the rate of an osteogenesis was a little bit higher, than at an implantation of biomaterials which are not contained glass phase. It is necessary to note, that the maximum rate of creating of a new osteal tissue is observed in more later terms of implant stay in alive organisms.
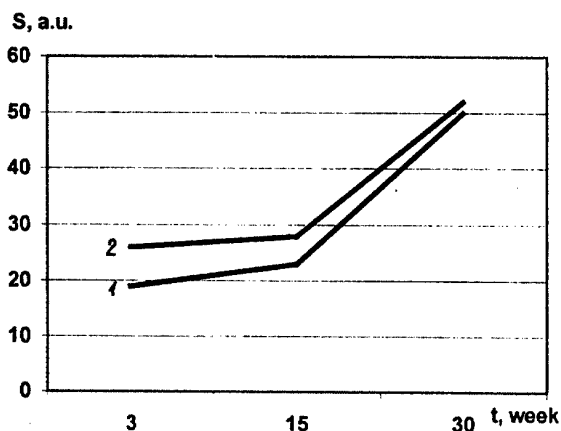
Figure. Relative area of new created osteotissue around of biomaterial a granules (160-500) micron in different terms after its implantation (1 - with glass phase; 2 - without glass phase).

The dynamic overseeing by shaping of an osteal tissue around of granules of different dimension has not revealed sharp differences. It is observed nevertheless at use of larger implant granules (it is more 500 micron) the major rate of shaping of an osteal tissue in the term between 3-15 weeks after implantation.

The results of X-ray and gystomorphological of examinations of implants on the basis of biological hydroxyapatite have found absence of inflammatory process of separate fields and all organism as a whole at all stages of observations. The high adhesion new created of an osteal tissue with a surface of biogranules of a biomaterial without development fibrous of a sheath is revealed, that testifies to adequate interaction of a stuff with adjacent tissues. The positive property of utilized biomaterials is availability of a porosity of beads, that promotes shaping of a heavy-bodied web osteal beams and permeation of an osteogen in pores of granules and space between granules.

The glass-reinforced granules of biomaterials based on biological hydroxyapatite seem to have suffered some surface dissolution since their tips appear rounded off after implantation and major relative area of new created osteotissue around particles is possibly due to some greater resorption.

These results indicate that silicate ion dissolved from bioactive glass-ceramic synthesed by us also plays the essential role in forming the osteoapatite in the living bone of mammals.

References

1. L.A.Ivanchenko, E.P.Podrushnyak, T.I.Fal`kovs`ka, et al. New biocomposites based on bone hydroxyapatite and the scope for using them in biology and medicine // Probl. Osteologii. - Vol. 1, - Nos.2/3. - 1998 - P. 102-104.
2. L.A.Ivanchenko, T.I.Fal`kovs`ka, N.D. Danilenko e.a. Structure and properties of a high-porosity glass ceramic containing biological hydroxyapatite // J. Powder Metalurgy and Metal Ceramics. - Vol.38. - Nos.9-10. - 1999. - P. 448-453.

COMPOSITE METAL-POLYMER POROUS MATERIALS FOR GASES DEHUMIDIFICATION AND FUEL DEWATERING

Ilyuschenko A.Ph., Pilinevich L.P., Tumilovich M.V., Savich V.V., Kravtsov A.G.[(1)], Ryabchenko I.A.[(1)]

Powder Metallurgy Research Institute of the NAS of Belarus, Minsk, Belarus

[(1)]Mechanics of Metal-Polymer Systems Research Institute of the NAS of Belarus, Gomel, Belarus

Complex cleaning and dewatering of gases, fuel and lubricants from mechanical impurities is a promising application for porous permeable materials (PPM) which are determined by their structural and capillary properties [1].

Effectiveness of removing mechanical impurities by porous materials is determined by shape and sizes of pores and material thickness. Moisture separation depends, first of all, on capillary properties of pores surface. Adhesion interaction takes place during the contact between water and hard surface, which influences effectiveness of moisture separation.

Characteristics of adhesion between a compact hard body and a liquid are not the same as compared to adhesion between a porous body and a liquid. On porous surface edge angle θ is not true, but is a seeming edge angle. Porosity if a hard surface increases a seeming edge angle, if the true one is less than 90°. Higher porosity of a hard surface may lead to significant reduction of wetting even in a case of hydrophilic surfaces. That's why water-repellency is not a function only of a wetting angle and for its estimation we need to use parameters of porous structures correlating to water-repellency.

A porous material is usually considered as a system of open cylinder capillaries with an average diameter of d. Capillary pressure $P=4\sigma \cos\theta/d$ (σ - surface tension) causes suction of liquid into a capillary. In conditions of complete wetting $\theta = 0$, $\cos \theta = 1$, and P is maximal. At non-complete wetting, when $\theta > 0°$, $\cos \theta < 1$, value of P reduces. At $\theta > 90°$, $\cos \theta$ changes its sign and, correspondingly, capillary pressure changes its direction as well preventing ingress of moisture into pores (anti-capillary pressure). Cosine of edge wetting angle for porous and polymer materials, determined according to method [2] is presented in Figure 1.

In Fig.1 you can see that bronze has the least value of cos θ from all metals, and PTFE - from polymers. The following investigations [3] showed that the least moisture-absorption capacity was determined for PPM from bronze and PTFE

powders, and the highest - for PPM from titanium and copper powders. At the same time porous titanium holds moisture at the highest temperature comparing to other materials. Investigations of water yielding capacity of different PPM during their drying at 100 °C showed that PPM from titanium powder have high moisture capacity and high ability to hold it [3].
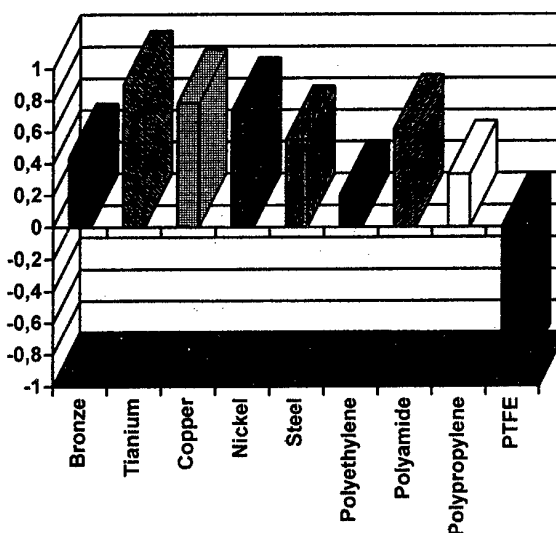
Figure 1. Cosine of edge water wetting angle for different materials.

Taking all the mentioned above into consideration at least two PPM with different parameters of porous structure and physical and physical-chemical properties are necessary for effective separation of water vapor and droplets from fuel, lubricants and compressed gases.

Thus, for cleaning and dewatering fuel a composite metal-polymer PPM (MPPM) was developed consisting of two layers. Substrate was made of sintered bronze powder (thickness 3-4 mm) which provides mechanical strength, necessary cleaning fineness and permeability, and a thin selective hydrophobic layer is precipitated in vacuum when a PTFE block is exposed to focused

CO_2-laser radiation and generation at certain modes of ultra-fine fibre [4]. Porosity of a fibre PTFE layer can reach 80-90%, it can be formed on quite complex-shaped parts. Technology enables to control porosity according to thickness. A MPPM like that enables to separate water from fuel and liquid oil. At the same time PTFE serves as a water-repellent, which is practically not permeable for water and other polar liquids. General look and structure of a filter element are presented in Fig. 2.
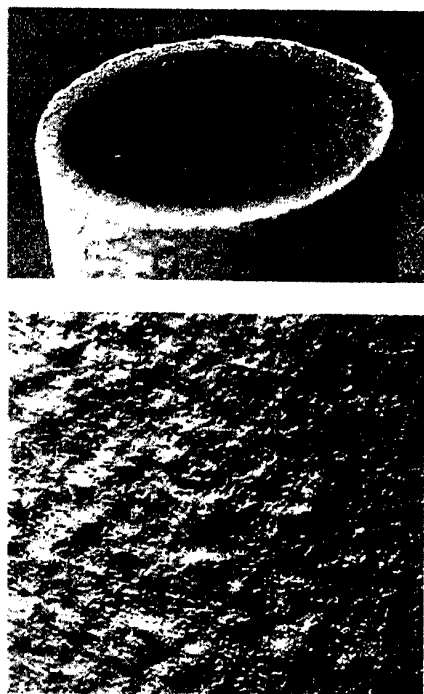
Figure 2. Structure of porous material «PTFE - bronze» for fuel dewatering.

A test sample of filter element from this MPPM was tested at Minsk Motor Works on summer diesel fuel with density of 0.84 g/cm3 and viscosity of 3.6 cSt for its corresponding to standard requirements for filters of rough and fine cleaning. Test results have showed that cleaning completeness for mechanical impurities was 95-98 % and can be increased by optimization of porous structure of metal porous layer, and completeness of moisture separation from diesel fuel was 100 % at any test mode.

To dry compressed air and other gases we have developed two types of double-layer MPPM based on porous titanium - with a selective PTFE layer produced according to the technology mentioned before, and a selective layer from HPPE fibre deposited according to «Melt-blowing» method [5]. A selective layer provides cleaning from mechanical impurities and moisture droplets. A layer from porous titanium with big pores has high moisture absorption and moisture capacity to pro-

vide vapour condensation and holding of formed droplets in pores. Tests have showed close character of both types of MPPM, and lower cost of MPPM with a selective layer from HPPE. In Figure 3 you can see general look and structure of a filter from the last material.
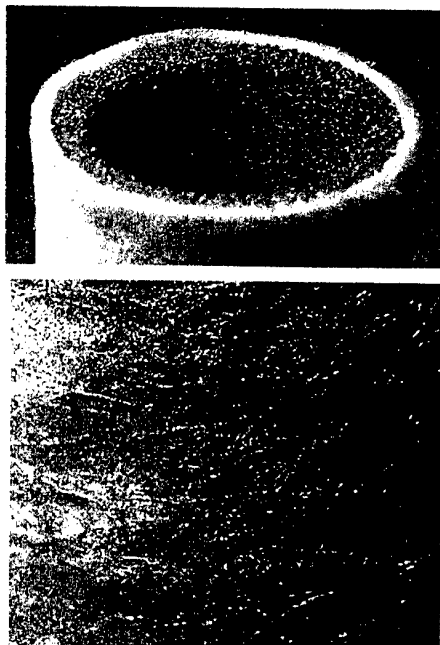
Figure 3. Structure of porous «HPPE - titanium» material for drying compressed air.

Dew point when drying air with MPPM with a selective layer form HPPE fibre reduces to -5 °C, completeness of cleaning from droplets and vapors reaches 99.99 %.

The investigations carried out have showed that MPPM «PTFE - bronze» is the most effective for water separation from fuel and lubricants; «PTFE - titanium» or «HPPE - titanium» - for drying compressed gases.

1. P.A. Vityaz, V.M. Kaptsevich, V.K. Sheleg. Porous Powder Materials and Parts Made from Them // Minsk, «Vysheishaya Shkola», 1987, 164 p. (in Russian).
2. A.Ph. Ilyuschenko, L.P. Pilinevich, M.V. Tumilovich Porous Powder Materials for Effective Cleaning Gases and Liquids // Proceedings of PM2001 Congress & Exhibition, Nice, France, 22-24 October, 2001, vol.1, p. 369-374.
3. P.A. Vityaz, V.K. Sheleg, V.V. Savich and others. Definition of Edge Angle for Capillary-Porous Materials // «Zavodskaya Laboratoriya».- vol.51, 1985, #4, p. 53-55 (in Russian).
4. L.F. Ivanov Physics and Technology of Laser Processing PTFE into Fibre-Porous Materials // Theses for Ph.D. degree, Gomel, IMMS, 1998 (in Russian).
5. V.A. Goldade, A.V. Makarevich, L.I. Pinchuk and others Polymer Fibre «Melt-Blowing» Materials // Gomel, IMMS, 2000, p.254 (in Russian).

ROLE OF MICRO-PLASMA-CHEMICAL TREATMENT IN CONDITIONS OF CONTROLLED ELECTRIC DISCHARGE TO INCREASE HEAT-RESISTANCE OF HEAT-RESISTANT BLADES OF <u>TURBO-FORCE ENGINE</u> (TFE)

Chigrinova N.M., Chigrinov V.Y., Tsareva I.N.[1], Alfintseva R.A.[2]

Powder Metallurgy Research Institute of NAS of Belarus, Minsk, Belarus

[1]«Tribonika» Technical-Scientific Company, N. Novgorod, Russia

[2]Frantsevich Problems of Material Science Research Institute of NAS of Ukraine, Kiev, Ukraine

Investigations of structure-formation peculiarities and basic properties of gas-pumping devices of gas TFE turbines produced from ЦНК-7 alloy under affecting energy of charged flow of particles during impulse discharges were carried out after their micro-plasma-chemical treatment in low-voltage controlled discharge by modifying transformed structure with an acoustic impulse.

At the same time functional composite coatings based on nickel with introducing alloying elements (Cr, Al, Y) promoting increase of heat-resistance were formed on surfaces under investigation. Thickness of coatings on samples was 30-60 mkm.

Phase composition, morphology, microhardness, roughness and heat-resistance of two coatings formed in changing micro-plasma-chemical treatment conditions were studied.

Phase compositions of formed coatings were determined with the help of «Дрон-3М» and «Дрон-4» diffractometers in symmetric shooting according to Bragg-Brentano using Cu-K$_\alpha$-radiation. Coating microhardness was determined according to Knupp's method, roughness was controlled according to R$_a$ parameter on roughness-indicator 296, heat-resistance - according to the standard method.

It is know that different phases may form - hard solution of alloying elements in ГЦК-Ni (γ-phase) and intermetallide phases: NiAl (β-phase), Ni$_3$Al (γ-phase), Ni$_2$Al$_3$ (δ-phase) - depending on element composition of coatings and temperature of interaction according to the diagram of the «Ni-Al-Cr» system phase conditions.

It was determined that a coating based on Ni-Cr-Al, despite its formation mode, is a Ni-hard solution of alloying elements with lattice period of a ≈3.59-3.60 A°. Presence of texture was determined in the direction (002). On the sample, where yttrium was introduced into its coating, we have produced a coating close in its phase composition to the conditional diagram, but there were some differences: first, increase of ГЦК-Ni lines intensity (111), second, reflexes of β-phase at the background level. Nevertheless, quantity of this intermetallide phase is small (about 5%).

Besides, broadening, asymmetry and increase of lines intensity (111)-Ni is observed. At high reflection angles reflexes are observed. Intermetallide NiAl (β-phase) phase is identified. Asymmetry of the peak (111) can be stipulated by coherency of crystal lattices γ- and β-phases.

In difractograms of Ni-Al-Cr coatings, produced according to combined scheme of micro-plasma-chemical treatment including ultrasound effect having higher plasticity, we have determined formation of significant ДУПЛЕТ at 2θ=42°÷45° angles and additional β-phase. In the result of pointing out the line (110) of β-phase intensity of the ГЦК-Ni peak reduces. Increase of intermetallide phase leads to increase of microhardness for these coatings.

Introduction of Yttrium into coating composition leads to significant changes in phase composition: formation of Ni$_3$Al reflexes (γ-phase) and chromium carbides Cr$_{23}$C$_6$ (or Cr$_3$C$_2$). High intensity of intermetallide phase lines proves of its high concentration in the coating.

It is known that NiAl intermetallide phase is more preferable for protection of turbine blade working surface from high-temperature oxidation, which forms in the coating of the mentioned composition produced according to combined treatment scheme with ultrasound effect. Mechanism of β-NiAl -phase is similar to

exhaustion of protective properties of heat-resistant coatings at high operational temperatures (~ 1000 °C), and in the result of that Ni_3Al + hard Ni solution form with the following oxidation (to NiO, $NiAl_2O_4$).

Coating based on Ni-Cr-Al with optimal concentration of $\gamma+\beta$ - phase, formed according to the combined scheme with ultrasound effect, has the highest heat-resistance.

STUDY OF INFLUENCE OF BORON STATE AS INITIAL REAGENT ON MODE OF BORON SUBOXIDE SYNTHESIS AND ITS PROPERTIES

Kharlamov A.I., Khotynenko N.G., Kirillova N.V.[1], Trapalis Ch.[2], Fomenko V.V.[3], Goydina S.V., Shatscikh C.K., Gubareni N.I.

Institute for Problems of Materials Science NAS of Ukraine, Kiev, Ukraine
[1]National Taras Shevchenco University, Kiev, Ukraine
[2]Institute of Materials Science, Athens, Greece
[3]National University of Food Technologies, Kiev, Ukraine

In the last year, growing interest to suboxide phases of boron could be explained regarding, first of all, their high hardness (diamandand CBN are better of some phases only) and lightness. In the present paper results of study of boron anhydride interaction with powderous boron of two different modifications are reported. The aim of the investigation is to study the nucleation and growth mechanisms in heterogeneous system of suboxide boron phase and find out nature of inheriting by the yield of properties of one of precursors, in particular, boron. In the investigation the most spread commercial powders of two modification of boron, black amorphous (B_{am}) and rhombohedrical (Br) were used. It is common practice to suppose that their difference in reaction capabilities is great. But the most important is that this two powderous borons were chosen because of their significant difference of their particles morphology. Characterisation of as initial boron powders as products of their synthesis was carried out by means of crystal-optical, X-Ray, chemical, electron microscopy and IR-spectroscopy methods.

It was found out that B_{am} obtained through crecking of borines and B_r obtained through magnium thermal reduction of B_2O_3 differs not only by the order of crystallity. Boron powders TEM images (fig.1,a) show B_{am} consist of homogenous in shape (like balls) particles but significantly various in size, diameter of which is from 30 to 150 nm. Specific surface (S_s) of B_{am} measured by means of the BET method employing an ASAP-2000M device is 9,3 m^2/g. In IR transmission spectra of B_{am} the characteristic lines of the lattice absorption are absent. Powder of B_{cr} consist of homogenous enough particles in shape of splinters (fig.1,b) with the size of which is 0,5-1 mkm. In the yield there are also individual bigger particles in shape of rods and 3-5 mkm in length and particles in shape of right rectangles with size less than 0,5mkm. Specific surface of B_{cr} powder is 3,4 m^2/g. Thus, initial boron reagents significantly differ not only in its inner structure (X-Ray, IR-spectra) but also apparently (dispersity and morphology of particles) that obviously has to affect on properties of products synthesized. Temperature and kinetic functions of B_2O_3 interactions with as B_{am} as B_{cr} boron were investigated at 1000-1500°C using a vacuum furnace with the tungsten heaters and carbon free crucibles. Reaction capabilities of boron modifications under investigation with B_2O_3 were compared and studied as in vacuum as in the medium of inert gas by means of high-temperature derivatogroph. In conditions comparable temperature at which reactions with B_{am} starts is approximately 160 °C lower within all heating rates than that when B_{cr} was used and at 20 degree/min rate of heating is 1260 and 1420°C, respectively. Temperature of the reaction start practically does not depend on nature of reaction medium but its decreasing is observed when rate of heating was lowered. Derivatograms of boron interaction with $B_2O_{\#}$ contain two (endo- and exothermal) peaks which characterize B_2O_3 melting (T=340°C) and boron suboxid phase formation, respectively. Influence of initial boron state is performed not only on temperature-time parameters of B_2O_3 reduction process but also on chemical composition of powderous suboxide boron, its dispersity and what is the most important, morphology of its particles (fig.1,c,d). According to results of chemical analysis, the phase with composition $B_{6,3}O$ is formed from B_{am} whereas when Bcr is used the phase of $B_{6,5}O$ composition is obtained. X-ray spectra of products obtained of B_{am} and B_{cr}. are similar and correspond B_6O phase. However, respect of relative intensities of main peaks in X-ray patterns of both products is remarkably different. IR transmission spectra of $B_{6,3}O$ and $B_{6,5}O$ powders also differ when the absorption lines are considered (fig.2). But the most interesting fact is

that varying in dispersity, powder-like $B_{6,3}O$ and $B_{6,5}O$ are remarkably different when their particles surface morphology observed. Moreover, morphology of both products particles clearly enough resembles morphology of appropriate initial boron reagents. For example, $B_{6,3}O$ particles are a bit circular in shape. It is worth noticing that some of $B_{6,3}O$ particles have passing through hollows which are of right shape.

Thermostability in air of B_{am}, B_{cr}, $B_{6,3}O$ and $B_{6,5}O$ investigated in non isothermal mode testifies on considerably higher temperatures of boron suboxide oxidation. It is that $B_{6,5}O$ oxidation occurs at temperature as low as 535°C, whereas $B_{6,3}O$ is already oxidized at T=445°C.

Therefore, obtained results undoubtedly proves that boron suboxide also gets in some extent the reaction capability of initial boron, when inheriting the morphology of initial boron during process of its synthesis.

PARABOLOIDAL ANTENNAE AS A BASE FOR CREATING SOLAR HIGH-TEMPERATURE POWER INSTALLATIONS

Pasichny V., Tsyganenko V., Lykhodid S.
Institute for Problems of Materials Science named after Frantsevitch National Academy of Sciences of Ukraine, Kyiv, Ukraine

Using the concentrators of solar radiation for solar furnaces is one of the ways for mastering renewable ecologically pure solar energy. This process is restrained to a considerable extent by the absence of the serial production of optical concentrating systems which are expensive enough. The two concentrators of 2,8 and 5,0 m diameter were created in the IPMS NASU of Ukraine (IPMS) in 1973 by gluing small plane mirrors (facets) onto the surface of metal antennae of parabolic profile. Their almost 30 years operation has shown the possibilities to realize the wide range of high-temperature processes [1] with their help and has confirmed the expediency and perspective of using obsolete antennae as a basis of solar furnaces. This method makes it possible to reduce considerably their cost and time of manufacturing. The multiple-stage technology for applying the reflecting layer and the analytical method for determination of the facets optimum dimensions [2] are developed in the IPMS. The purpose of the given work is to analyze available constructions of paraboloidal antennae as a potential base of solar furnaces (SF) after the operating service life of these expensive modern mechanical articles is over. Reflector-type antennae of radio-technical systems for the super-high frequency (SHF) convert the radiation of point source into the system of parallel beams. But they also can be used with the opposite purpose as concentrators of solar radiation which bring the parallel solar beams in focus. For this purpose orate antennae can be used. Reflector-type antennae for the microwave range are of their kind. They differ by their construction because the range of the problems being solved with their help is very wide. Focusing reflectors (mirrors) of the antennae can be of various profiles such as paraboloid, truncated paraboloid, paraboloidal cylinder, cone, sphere etc. They can be all metal, cribrate, reticular for reducing their weight. Almost half a century orate antennae of various profiles are used in the following systems: wireless distance and superdistance communication [3], control of artificial earth satellites [4], radiolocation [5], radioastronomy.

All these systems differ by the high degree of the concentration of microwave antennae equipment because the linearity of SHF waves propagation requires using retransmitting (radio relay) stations equipped by the systems of the following two types:
- the systems using direct wave radiated by a transmitter;
- the systems using the waves reflected by the troposphere or ionosphere heterogeneities. They are radio relay, troposphere and satellite communication lines.

Great reflector-type aerials (GRTA) used on the whole in space satellite communication and radio-astronomy represent the special class. The concept GRTA is used both for accentuating great linear dimensions (tens meters and more) and great electric dimensions which are assumed conditionally to be above 500-1000λ. Such classification which is carried out relatively the spheres of application of antenna system equipped by reflectors makes it possible to determine potential heat power of each system when they are used as solar furnaces. The systems of radio relay communication are equipped by paraboloidal, spherical and elliptic reflector measuring from 1 up to 9 meters.

The system of troposphere and ionosphere communication are equipped paraboloidal reflectors (round and square) measuring from 9 up to 20 meters.

The systems of satellite communication (ground) are equipped by paraboloidal and horn-paraboloidal reflectors measuring from 5 up to 25 meters. The GRTA are manufactured on the whole in the form of paraboloid measuring from 20 up to 300 meters. The systems of radar detection are equipped by paraboloidal, spherical and other reflectors (the on-board reflectors measuring from o,6 up to 2 meters and ground ones – from 2 up to 12 meters. All the enumerated systems include the reflectors of the diameter being equal from 0,2 up to 300 m. The expected heat power of these antennae overlap the range

573

from 0,2 up to 30000 kW when they are used as solar furnaces.

The adduced data are evidence of the great nomenclature of available antennae and the wide range of the power of the concentrators being manufactured on their basis. The experience and calculations show that the temperature - 1700-2000 K of the objects in such solar furnaces can be obtained easily enough with their help. It makes it possible to use these solar furnaces not only in materials science as it has been noted above but in power engineering also. In particular, the processes of solar energy thermo-chemical conversion and its accumulation in hydrogen converted gas being obtained or are under thorough investigation in some countries. Usually the temperature of these processes is not above 1300 K. The temperatures in the Stirling engine are even lower. The combination of the last with the concentrators of solar radiation is considered to be one of the three the most prospective solar power systems in the plans of the US Department of Energy (DOE) which are made for the period till 2020 year [7].

The power of such concentrators of solar radiation can be calculated approximately by the following formula:

$$N_t = AS_mR_n, \qquad (1)$$

where R_n –normal solar radiation, KWt/m^2; S_m – useful power of concentrator maximum cross-section, m^2; A – efficiency of the optical system being equal to the relation of the energy obtained in the concentrator focal area to the incident energy.

In the case of the concentrator direct orientation at the Sun the coefficient A can be assumed to be equal to 0,6 –0,7, but many factors influence upon its value and the concise analysis of them is given in the address.

It would be noted that movable paraboloidal antennae covering the greatest possible trajectory of the Sun movement along the sky are the most prepared for being used. All the immovable or partly movable systems the profile of which differs from the paraboloidal one need the supplementary analysis concerning their use as SF. Movable enough antennae do not exceed usually 60-70 m by the diameter. Immovable

antennae can have the limited using during the time of light day under the condition of their fixed guidance on the optimum point of the Sun trajectory. As an example the radiotele- scope of ∅30 m can be mentioned which belongs to the branch of Physical Institute of the RAS (Katsively, Crimea, Ukraine). It is made of concrete and guided by the summer Sun at noon. During 2-3 hours it can produce about 350 kW of heat power with its gradual decrease.

For example, it is enough for supplying a great sanatorium with hot water.

So, "a store" of radio-antennae accumulated all over the world is a considerable basis for the creation of solar power installation of various purposes ensuring the prolongation of the operation service life of very expensive articles by 30 – 40 and more years.

Literature:
1. Pasichny V. Some aspects of concentrated solar energy technological using// RENEWABLE ENERGY. Energy Efficiency, Policy and the Environment : World Renewable Energy Congress V (September 1998, Florence, Italy).- Pergamon, 1998, part IV.- P. 2114-2117.
2. Pasichny V., Uryukov B. Solar Energy Concentrators with Optimal Plane Mirror Facets// Proceedings of the World Renewable Energy Congress VI, 1-7 July 2000, Brighton, UK.- Part 2, p.p. 1100-1113.
3. Куликов В.В. Современные системы беспроводной дальней связи// Москва: изд. «Наука».- 1968.- 230 c.
4. Корсунский Л.Н. Распространение радиоволн при связи с искусственными спутниками Земли// Москва: изд. «Сов. радио».- 1971.- 207 c.
5. Драбкин А.Л., Е.Б. Коренберг, С.Е. Меркулов. Антенны// Москва: изд. "Радио и связь".- 1995.- 152 c.
6. Цейтлин Н.М. Антенная техника и радиоастрономия// Москва: изд. «Сов. радио».- 1976.- 350 c.
7. Rannels James. The DOE office of solar energy technologies' vision for advancing solar technologies in the new millennium // Solar Energy.- 2000, Vol. 69, N 5, p.p. 363-368.

ELECTRONIC PROPERTIES OF $YBa_2Cu_3O_{7-\delta}$ OBTAINED UNDER HIGH PRESSURE

Nemoshkalenko V.V., Shevchenko A.D.
Kurdyumov Institute for Metal Physics, N.A.S. of the Ukraine, Kyiv, Ukraine

Introduction

Studying an effect of external actions on peculiarities of electronic properties of high-temperature superconductors (HTSC) in a normal state is one of the actual problems for HTSC physics. These characteristics as is known, determine peculiarities of superconductivity. Interest for studying the electronic properties of $YBa_2Cu_3O_{7-\delta}$ is due to the fact, that in $YBa_2Cu_3O_{7-\delta}$ as well as in classical superconductors of A15, C15 structures, etc.[1] in a normal state the crystalline lattice instability being a sign of superconductivity takes place. For example, in $YBa_2Cu_3O_{7-\delta}$ (the compound of orthorhombic 1-2-3 structure) obtained by a standard technology of solid-phase synthesis the crystalline lattice instability connected with oxygen vacancy ordering by their shifting along the axis 0 was observed radiographically at about 17 OK[2]. In this case a symmetry of 1-2-3 compound was not changed. It should be noted, that in the home and foreign literatures the publications dealing with experimental studying the physical properties of usual "porous" HTSC obtained by the standard solid-phase synthesis technology are consistently increased. As is known, critical parameters of porous HTSC are very sensitive to external actions and they degrade to attack by moisture, corrosive atmosphere, thermal cycling or ageing in the course of time, ets. [3]. These factors inhibit to use the porous HTSC widely in practice. As was mentioned above [4] an agregate state of 0 atoms in pores of the porous HTSC is varied, at liquid-netrogen temperature. This fact effects also negatively on superconducting characteristics of the porous $HTSC_S$ and on their operating stability. Therefore the investigations of physical properties and, in particular, of electronic ones in porouless HTSC, to be obtained under high pressure are clean. There are no, however, the works dealing with studying the physical properties of HTSO ceramics obtained under high pressure up to the present* This work deals with the investigation of physical properties and, in particular, at 78 and 300K of the X-ray emission fluorescent $CuL\alpha_{1,2}$ and $OK\alpha_{1,2}$ spectra in HTSC ceramics $Yba_2Cu_3O_{7-\delta}$ (δ=0,06 and 1,00), obtained under high pressure in order to study the peculiarities of the electronic structure of these compounds.

Experimental Results and Discuss

The technology for obtaining HTSO under high-pressure is developed by Shevchenko, and behaviour peculiarities of the temperature coefficient of thermal expansion (α) in $YBa_2Cu_3O_{7-\delta}$ are also developed by him[5]. It was found, that the relation $\alpha(T)$ at about 17OK has that peculiarities which can be connected with appeared polar effect. Theoretical calculations of the relation OC(T) given in the framework of the polaron model[5] showed that these is a good agreement between both the calculated and experimental curves $\alpha(T)$. In this work the spectra $CuL\alpha_{1,2}$ and $OK\alpha_{1,2}$ were investigated by using the samples $YBa_2Cu_3O_{7-\delta}$ (δ= =0,06 and 1,00) prepared by powder sintering of 1-2-3 compound under high-pressure (20 Kbar) in the high-pressure solid-phase chambers ("the Ghechevitsa"-type) and under a hydraulic press with 20001 force. Under thermobarometric treatment of 1-2-3 compound powders the oxygen loss was removed by special technological methods providing for leek-pro of ness of the high-pressure chamber where 1-2-3 compound powder surrounded by special shielding medium was placed! A temperature of super-conducting transition T_c was controlled by a magnetic measuring method of the temperature magnetization relations. T_c was 92K but below T_C with appearing Maisner effect a diamagnetic response was observed. The samples $YBa_2Cu_3O_{7-\delta}$ were investigated by structural X-rays under high-pressure by using a diffractometer (DRON-2-type) with filtered copper radiation. As showed the structural X-ray analysis of the samples (7-δ= 6,94) they have the distinct orthorhombic structure 1-2-3 with the following parameters of a crystalline lattice: a = 3.833 Å, b = 3.896 Å, c = 11,693 Å. A content of oxygen (7-δ) in these samples was determined by the known structural criteria setting before in the literature for HTSC ceramics of $YBa_2Cu_3O_{7-\delta}$ obtained by a standard synthesis technology. As is known, as a result of the multiple X-ray investigations of $YBa_2Cu_3O_{7-\delta}$ the oxygen loss in $YBa_2Cu_3O_{7-\delta}$ was found to be accompanied by an orthorhombic-tetragonal transition of 1-2-3 compound. This transition is accompanied by varying parameters of the crystalline lattice in an orthorhombic phase. With decreasing oxygen coefficient (7-δ) from 7,0 to 6,0 both the parameter of the crystalline lattice, c, and the difference (c/3-b) are

found to increase, The criterium (b-a) being characteristic of a degree of orders of the 0 atoms and vacancies has a maximal value for the orthophase and equals zero for a tetragonal modification of 1-2-3 compound. An interaction between 0 content and crystal-lographic parameters of 1-2-3 compound is found in a literature. One is described by the following equation r=65(n − 1) − 0.5, where n = $c/3\sqrt{ab}$-1. An index of oxygen is determined as (7-δ). For 1-2-3 compounds with (7-δ) = 6,0 in the tetragonal phase there were the following parameters of o o the crystalline lattice: a = 3.86 Å, c= 11.83 Å. The electronic structure of metal oxydes $YBa_2Cu_3O_{7-\delta}$ (δ = 0,06; 1,00) obtained under high pressure has been studied by the X-ray fluorescence $CuL\alpha_{1,2}$ − and $OK\alpha_{1,2}$ − bands. The first ones of them represent the valence (d − symmetry) electrons of Cu atoms while the seconds do the valence (p − symmetry) electrons of 0 atoms. The spectra have been obtained by using a device (GARF-1-type) having a crystal-mono-chromator RbAP at 78K and 300K. In the first case the samples were liquid-nitrogen cooled but in the second one they were water-cooled. The transition δ=0,06–δ=1,0 is accompanied by a notable broadening of their widths. Usually such an increase of spectral line width is connected with growing uncoupled spin density or with changing local symmetry of 3-d metal atom surroundings. The last fact seems to play a determining part in the broadening of the bands $CuL\alpha_{1,2}$ owing to changing structure of a compound while with toiown increasing of, $Cu\pm state$ balances in the compounds being close to δ=1,0 a mean spin density on Cu atoms is not promoted for increasing. The comparison of the $OK\alpha_{1,2}$-bands of metallooxide ceramics shows their essential chonging intensities in the area of lower values of phonon energies that is due to chan-ging δ − interactions as in the case of metalloceramics obtained by usual technology[6], providing for chemical bonds between 0 atoms and surroundings. In its turn, with increasing energy of centre of gravity in the $OK\alpha_{1,2}$-bands from 525,1 eV for $YBa_2Cu_3O_6$ to 525,4 eV for $YBa_2Cu_3O_{6.94}$ the fact is showed, that delocalized valence p-electrons of 0 atoms in HTSC increases as well. A change in the $CuL\alpha_{1,2}$-band structure vs the temperature of the sample $YBa_2Cu_3O_{6.94}$ is also setted by the authors. As shows Fig.1
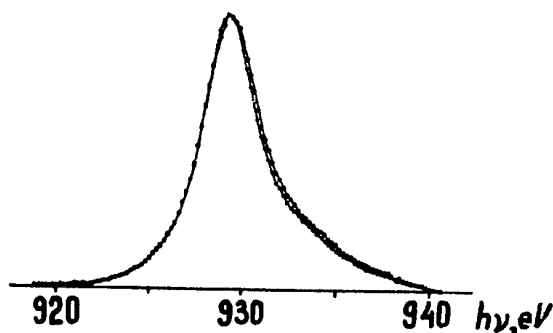
Fig. 1. The X-ray $CuL\alpha_{1,2}$-bands of the compounds $YBa_2Cu_3O_{6.94}$ at 78K(∘−∘−∘−∘), at 300K (•−•−•−•).

a superconducting state transition of the compound $YBa_2Cu_3O_{6.94}$ is accompanied by increasing intensity of the $CuL\alpha_{1,2}$-band in its short-wave region including the Fermi one. Besides this, the transition mentioned results in short-wave shift (by 0,15 eV) of the centre of gravity of the band. Both the facts show an increasing density of the valence d-electrons on Cu atoms and increasing contributions of the d-electrons near the Permi level into density of the electron states.

References

1. Shevchenko A.D., Ustable lattice superconduc-tivity, "Metallurgiya", Moscow, 1985. −105 P.
2. Alexandrov O.V., Ivanenko O.M., Karasik V.R., Kiselyeva K.V. Structure ustable high temperature superconductor $YBa_2Cu_3O_7$ in the field low temperature// Sol. St. Phys. − 1988.− 30, N7.– P.2052-2057.
3. High temperature superconductors, bd. by D.Nelson, M. Wittinkhem, T.Johrge, Mir. − 1988. − 400 P.
4. Broslavets Yu.Yu., Zeientsov V.V., Fesenko T.N. et al., Levitatsiya Keramiki $YBa_2Cu_3O_7$ and nonsuperconducting materials in nonuniform magnetic field.//Pulse lazers and their applications. − 1988. − P.104-107.
5. Alexandrov A.S., Kornilovich P.E., Shevchen-ko A.D., Shulzhenko A.A., Thermal expansion of $YBa_2Cu_3O_7$// Sol. St. Phys. − 1990– 32, N1. − P.303-305.
6. Nemoshkalenko V.V., Kornyushin Yu.V., Ereshchenko A.A. et al., Influence of thermal adieus on properties of ittrievoi ceramics// Metallofizika. − 1988 − 10, N6.– P.6-10.

DANTURES MANUFACTURE EMPLOYING PLASMA TECHNOLOGIES

Besov A.V.
National Technical University "KPI", Kiev, Ukraine

In orthopedic stomatology an important problem, when a fixed denture manufactured, is to provide tight cohesion of a facing cover with a metallic body of a denture. Strength of cohesion of metal with polymer and ceramics approached due to the use of traditional dental-technical technologies often does not meet requirements put before it [1].

To increase strength of cohesion and improve esthetic of denture's appearance a new technology was developed. The main feature of which is to depose by means of plasma spraying devices a retentive porous metallic layer (micropearl) on the surface of a denture's body. The layer can vary within wide range from 50 to 300 mkm in width [2].

In terms of chemical composition a sprayed layer of micropearls is identical or close to that of the bridge-like denture's body material (stainless steel, nickel-chromium alloys, cobalt-chromium alloys (CCA), titanium). In order to depose a cover on a small-sized dental-technical items under conditions of stomatological institutions a plasma device of small dimensions and low power (0.5...2.0 kW) which is electrically supplied on usual mains was designed.

Suitable modes of intermediate cover layers spraying on materials used for a metallic base of dentures were worked out through investigation of the influence of plasmatron current, kind of plasma forming gases and its consumption, range of spraying and size of sprayed particles on strength of the cover cohesion with a substrate. Metallic alloys used in stomatology along with titanium, cuprum, gypsum were taken to form a substrate.

Optimal spraying modes permit to obtain covers with required thickness in dependence upon duration of the spraying process (30...120 sec.).
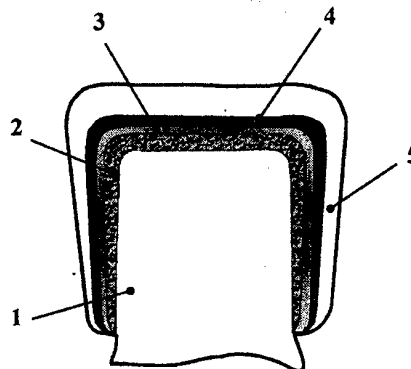
Fig. 1. Scratch of a metal-ceramic denture with retentive layers sprayed.
1. Teeth protethed.
2. Metallic crown.
3. Plasma retentive cover of CCA powder.
4. Plasma retentive cover of aluminum oxide.
5. Porcelain.

Stomatologic covers have to meet certain requirements on density and strength. Therefore, investigations of their physical-mechanical properties were carried out following standard methods.

Investigations of plasma sprayed cover microstructures showed that covers have a porous sandwich-like structure. When retentive layers sprayed on a monolithic metal denture, there is a smooth transition from the base material to the porous metal of the retentive layer to which, in its turn, elements of a facing cover fit. Thus, considerable growth of the surface area that occurs during the plasma spraying favors to better mechanical cohesion of the facing cover with the retentive layer of micropearls. Strength of cohesion of samples was measured by the normal detachment method.

Results of tests revealed that the use of plasma sprayed retentive layers of micropearls increases strength of cohesion 3...5 times in comparence with traditional methods [3,4].

Employing of the plasma spraying in orthopedic stomatology permits:
- reduce time and labor force consuming, when dentures manufactured;
- decrease net costs and improve esthetic qualities of dentures.

References:

1. Копейкин В. Н. Ошибки в ортопедической стоматологии// М.: Медицина, 1986-174с.
2. Бесов А. В. Способ изготовления порошковых материалов для плазменного напыления ретенционных покрытий //Патент РФ №2151668 от 27.06.2000г.
3. Бесов А. В. Исследование прочности сцепления плазмонапыленных композиций с облицовочным покрытием// Вестник национального технического университета Украины «Киевский политехнический институт». Машиностроение.-вып.41-2001.-с.246-250.
4. Гальченко В. В., Бесов А. В., Павленко А. В. и др. Улучшение качества эстетических покрытий несъемных зубных протезов//Український стоматологічний альманах.2002.-№1-с.41-43.

EXPERIMENTAL RESULTS OF A CAST COMPOSIT MATERIAL INDUSTRIAL USE AT EXTREMAL EXPLOITATION CONDITIONS

Zatulovsky A.S., Zatulovsky S.S.., Nguen Van Tan [1], Vu Van Mieng[1]
Physico-technological institute of metals and alloys NAN of Ukraine, Kiev, Ukraine
[1]Institute of machine building technologies of ministry of industry of Vietnam, Hanoi, Vietnam

The object of this experimental study is heterogeneous cast composite material (CCM), consisting of plastic matrixes (bronze, brass), reinforced by the high modulus steel granules (the cast shot from a carbon steel) (Ill. 1). CCM may be referred to irregular isotropic matrix systems in which geometric parameters, in determined degree, are random quantities, which, however, depend on a some manyfactoral law. Characteristics of such sort of materials most rationally to find experimentally for concrete CCM with provision of particularities of structure, which considerably affect on a level of working performance data of the material.
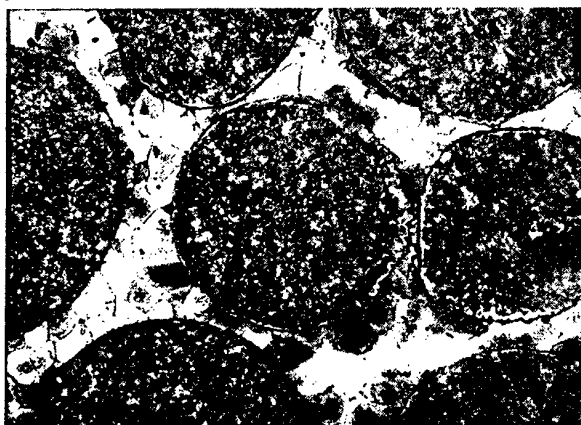
Ill.1.

Experimental tribotechnical tests of CCM and production usage an triboparts carry out at a number of plants of Ukraine, uniquely have proved the advantages of new material in comparison with traditional ones. The results have interest for Vietnam industry with standpoint of increasing of firmness and reliability of functioning of machines and equipment, reductions of volumes of use of expensive ferro-alloy and ligatures, which at present time are imported in this country. The study of CCM adaptation in production is executed within the framework of International research program of development and use of new constructional and functional materials with increased working performance.

At first stage the perspective applications of CCM are determined, interested enterprises and the concrete details, fabrication of which from the composite actually for production and will give the maximum technical-economic effect. Taking into account for dimensions of chosen troboparts, conditions of their usage the CCM compositions and optimum technological parameters of making of half-finished products with use the method of fluid-hard consolidation were selected. The technology is adapted to conditions of pilot production of Institute of technology of machine building (IMBT, c. Hanoi). The most acceptable decisions are found experimentally to the following technological operations: 1) preparation reinforcing elements and matrix alloys; 2) CCM half-finished products consolidation ; 3) finish processing of products from CCM.

Tribotechnical test of the CCM samples, which make in IMBT, practised in Frantsevich Institute of Problems of Materials science of the NAN of Ukraine by the machine of friction MT-68, on air, without lubricant in pair with 65Г steel under constant load 5 kg and velocities of friction 5, 10, 15 m/c. The results have shown that CCM wear-resistance vastly exceed this property of traditional material – wear-resistant bronze БрО5Ц5С5, for which in these conditions is fixed the disastrous wear-out and intensive carrying the material from sample to counter-body are recorded. Significant increase to wear-resistance of CCM in 4-10 once observe after termal processing the CCM samples (hardening in water with 840 ^{0}C + high tempering under 600 ^{0}C). It is installed that optimum CCM structure: reinforcing granules – high dispersed sorbit of tempering furlough, $H\mu$ - 240 kg/mm^2; the matrix - grain of α - solution, $H\mu$ - 140 kg/mm^2; the clear border of contact of phases, without intermetallides forming.

As a result of trobotechnical test is stated that CCM has the essential advantages on wear capability, carrying abilities, stability under increased temperature and loads in contrast with mono-materials that is connected with presence in structure of contact layer high modulus reinforcing

elements (the steel granules), which 1) prevent the development of plastic deformation (creep); 2) hold up formation and development of rifts in wear process. Besides, in the extreme conditions of dry friction on the contact surface of bushing from CCM - steel shaft (more than 45 HRC) are formed strong and plastic separating films, reducing factor of friction. The studies have shown that separating films have the complex construction and consist of the copper and iron oxidises and dispersed products of wear-out of granules.

On developed technologies the tribodetails are made from CCM (the sliding bearings) of different equipment and machines (the ill. 2). Information about production CCM usage in conditions of friction during 0,5 - 1 yeas is presented in table.
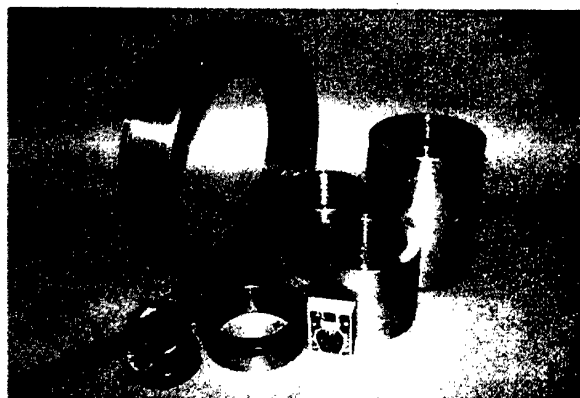
Ill. 2

The results of experimental study and earlier data are indicate that CCM safely works in the high loaded elements of friction at extreme conditions of lubricant absence absence or its limited presenting at loads before 15 MPa, velocities of friction before 20 m/c, temperature before 850 ^{0}C.

CCM ability to work is confirmed by earlier 3-6 years of operation on series of major concerns of Ukraine and others countries. Firmness of details from CCM in 2-5 once above, than it of bronze, brasses, powdered composites as iron - graphite, bronze - graphite, wear-resistant cast iron that provides increase to reliability and firmness of the working elements of friction, reduction of idle times because of repair of equipment, economy of energy and material expenses, including deficit and expensive colour alloys, ligatures and modifiers. Secondary non-ferrous metals, scrap of copper alloys using for production of CCM products reduces the cost and technical-economic advantage at high wear-resistant CCM using, including in mass branches of machine building: in energy, metallurgy, car, agricultural and others areas of machine building.

№	Name of product from	Plant, on which test is organised	Instead of what material CCM is used	Increase of the usage period
1.	Bearing of sought-after part of tractor (bulldozer)	Repair plant	Bronze	in 4,0 times
2.	Bearing supporting element of transporter of coal dust (TH467)	Heat power station Ninh Binh	Bronze, wearresistant cast iron	in 3,0 times
3.	Slide bearing (KH0309) of molding machines	Sweet factory	Bronze	in 5,0 times
4.	Slide bearing of coffee dryer	State farm Ltichav	Wearresistant cast iron	in 5,0 times

580

OPTICAL FURNACE FOR BOTH INVESTIGATION OF MATERIALS THERMAL PROPERTIES AND PROTECTIVE COATINGS OBTAINED

Frolov Alexander A., Frolov Gennady A., Podchernjaeva Irina A.
Frantsevich Institute for Problems of Materials Science, NAS of Ukraine, Kiev, Ukraine

The elevated power optical furnace "Crystal-M" with xenon radiation sources was developed in the IPMS of NAS of Ukraine on the basis of the equipment described in [1], for study of the high temperatures physicochemical processes. It is possible to develop various methods high-temperature treatment of materials and obtaining protective coatings on metals and ceramic materials.

The optical furnace consists of three ellipsoidal reflectors. The ДКСШРБ-10000 lamps are disposed in one focus of every ellipsoidal reflector. Three mirror reflectors were placed symmetrically respectively of the equipment axis. Here by on the installation axis was a region out off light fluxes, which was higher more then 20 sm. over the focal zone. The sensing units and devices for experimental processes registration were in this region. The second focuses of mirrors are combined in to one focal zone in which a treated material was been.

Over 2 kW of the concentrated light energy flux (CLEF) was concentrated in the general focal spot of 10 mm in diameter. Maximal magnitude of the average light energy flux density, E, in the focal spot was $E=1,4 \cdot 10^4$ kW/m^2 for the lamp current, I = 300A. This corresponded of equilibrium radiation of absolute black body at the temperature $T_{a.b.b.} = 4000$ K. The maximal magnitude of the average light energy flux density in a focal spot of a diameter of 6 mm at I=300A is $E=1,6 \cdot 10^4$ kW/m^2, $T_{a.b.b.} = 4100$ K.

The fusion experiments for high-melting oxide-coated compounds, such as HfO$_2$ ($T_{melt} = 3103$ K) and ZrO$_2$ ($T_{melt} = 2973$ K) were carried out. It was shown that the majority of high-melting oxides could be melted in this optical furnace, under condition of the sufficiently level of a heat insulation of melt zone.

The optical furnace "Crystal-M" was used for model action of the working conditions of the materials, which were used in the extreme high temperature conditions as well.

Isotropic compact-grained graphite, so-called "graphinol" was investigated in the article [2]. This material was developed expressly for needs of the space and nuclear industry and it had high resistance to thermal shock at the entry of space-ship into planets atmosphere. On opinion of authors "graphinol" is an ideal object for study of an ablation of graphite materials at the peak thermal loads conditions.

The energy light flux density for the "Crystal-M" installation had high sufficiently magnitude. Therefore this installation could be used for the simulation model of a thermal shock procedure. The definition method of an efficient thermal conductivity was developed for the lamellar graphite contained materials.
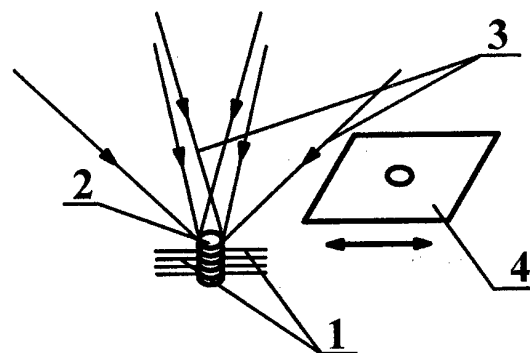
Fig.1. The scheme of measuring of a thermal conduction for lamellar heat-insulating materials in the optical furnace: 1-sample; 2-thermocouples; 3-stream of light radiation; 4- shutter blind.

The thermocouples, 1, were placed in a cylindrical sample, 2, on the different distance from the sample surface irradiated by the CLEF. It was necessary to obtain maximal homogeneity of the light flux falling down on a sample surface to carry out the study of thermal properties. For this purpose three light emitters were installed so that the general focal zone was disposed by 20 mm higher respectively of the optical focus of each emitter. For the lamp current I = 300A, the energy light flux density was $E = 1 \cdot 10^4$ kW/m^2. The impulses of CLEF, 3, moved to a sample. These impulses form was rectangular. The shutter blind, 4, regulated the impulse length.

The dynamics of thermal field's change was defined in experiments. For this purpose the time change thermocouples indications were recorded.

The thermocouples coordinates were defined on X-ray image. The coefficient of efficient thermal conductivity $\lambda(T)$ was defined by the picking out method of its values in the equation (1).

$$\rho c \frac{\partial T}{\partial \tau} = \frac{\partial}{\partial y}\left[\lambda(T)\frac{\partial T}{\partial y} \right] \quad (1)$$

Here ρ, c- density and a heat capacity of a material; τ- time; y - coordinate.

The numerical calculations results using two independent programs were compared with the change temperature dynamic measured by the thermocouples. The time dependencies of both surface temperature and sample backside temperature were used as the boundary conditions. The sample surface temperature was measured by a photoelectric pyrometer or by the thermocouple. The latter "instantaneously" given to a surface after light flux was shut with the shutter blind. The sample backside temperature was measured during the experimental time by thermocouple. The values of efficient thermal conductivity coefficient were obtained on the installation "Crystal-M" for the graphite containing materials. These values were coordinated with the literary data.

The high-energy light flux density in the focal area of the optical furnace "Crystal-M" allowed us to carried out experiments for obtain of high-temperature coatings using the CLEF method.

It was shown [3,4], the surface treatment of high-performance steels by CLEF using xenon lamps radiation one can consider as a method of obtaining of functional gradient materials having a higher level of the physical-chemical properties. Under conditions of CLEF a heterogeneous gradient system formed on a surface resulting from the processes of high temperature oxidation, phase formation and convective mass transfer of alloying elements. The properties of layers obtained are predicted by both the choice of the alloying composite components and of the treatment regimes. For example, the shliker coating using the composition powder based on LaB_6 with Ni-Cr bunch was deposited on the steel 3 surface under the action of CLEF. The velocity of anodic dissolution of such coated samples in 3 % solution NaCl in on active area was decreases a almost by four orders in comparison with an initial surface of steel due to formation of the before treatment. It was possible as a result to formation of the $LaCrO_3$ lanthanum chromite in a scale. The same effect took place for the material based on Al_2O_3 - SiC/Si_3N_4 system due to the formation of mullites of the Al_2O_3 - SiO_2 in a scale.

The high cleanliness of the optical heat processes allowed us to use the developed optical furnace for development of protective ceramic coatings technology for special applications. For obtaining of such coatings the materials of substrate and coatings should have particular properties:

1 - the physicochemical properties of a substrate ceramics should be corresponded with the coat material properties;

2 – the materials of substrate and coats should have the high heat resistance in order to keep the processing conditions in a local focal zone with heavy gradients of temperature and high speeds of heating.

This problem was successfully solved for Nb_2O_5 and $LiNbO_3$ protective coatings obtain. Here by large size products were obtained using such materials by scanning a processing surface in a focal zone. Thus, the Nb_2O_5 coating dishes of the volume up to 5 litres and some other products were obtained. These products have been tested in industry conditions during thermochemical treatment of high purity niobium compounds, [5].

REFERENCES

1. Балбашов А.М. Коротун М.М. Условия выращивания монокристаллов тугоплавких веществ методом Чохральского с радиационным нагревом // Изв. АН СССР. Сер. Физическая - 1975. – Т. 39. - №1.-С. 222-224.

2. Клейн К.А.,Джентилмен Р.Л. Использование интегрального метода теплового баланса для определения формы кратеров, возникающих в графите под действием излучения лазера // Аэро - космическая техника.- 1987, №-11.- С.76-85.

3. Подчерняева И.А., Лавренко В.А., Швец В.А., Фролов А.А. Формирование коррозионно-стойких слоёв на низколегированной стали с использованием концентрированного солнечного излучения // Порошковая металлургия. – 2000.-№ 11/12 .-С. 119-124.

4. Подчерняева И.А., Лавренко В.А., Швец В.А., Фролов А.А. Тепленко М.А Формирование коррозионно-стойкого слоя на стали при её взаимодействии с композитом на основе Si_3N_4 - Al_2O_3 в условиях светотермической обработки // Порошковая металлургия. – 2001.-№ 1/2 .-С 58-60.

5. Фролов А.А. Керамические материалы для получения высокочистых соединений ниобия и тантала // Стекло и керамика. - 1992.-№7.- С. 14-15.

SPECTRAL (λ = 0,65 mkm) AND INTEGRAL EMISSIVITY OF LaB_6–MeB_2 BASED CATHODE MATERIALS

Taran A.A., Ostrovski E.K., Komozynski P.A., Paderno Yu.B.[1], Filippov V.B.[1]
Zhukovsky National Aerospace University "Kharkov Avia Institute", Kharkov, Ukraine
[1]Frantsevich Institute for Problems of Material Scienses of NASU of Ukraine, Kiev, Ukraine

The knowledge of real (thermodynamic) temperature of cathode elements is necessary both for determination of work function of thermionic materials and for evaluation of power, which is needed for heating of a cathode assemble up to working temperatures. It is impossible without determination of spectral ε_λ and integral ε_T emissivities of a cathode material.

Spectral emissivities of only several rare-earth borides in powder form and their temperature dependence [1] are known up to date. There is also some data available for the hot-pressed composites in LaB_6 - ZrB_2 system [2]. However, the creation of a data base on thermal physical properties for all materials used in emission electronics is necessary.

The results of ε_λ and ε_T measurements of zone-melting cathode materials in LaB_6 – MeB_2 systems (Me = Zr, Hf, V) are presented in this work.

The ε_λ and ε_T as a function of temperature, annealing time at different temperatures, and diboride phase content have been studied.

For LaB_6– ZrB_2 it has been shown that ε_λ decreases from 0,85 to 0,68 with the increase of temperature and of ZrB_2 content. However, for systems with HfB_2 and VB_2 ε_λ is practically not temperature dependent. Time dependencies for LaB_6– ZrB_2 show that ε_λ decreases with the increase of annealing time, which may indicate the occurrence of surface structure rearrangement.

The ε_T behavior for different cathode materials as a function of above mentioned parameters is also discussed in the present report.

Literature:

1. Serebrjakova T.I., Paderno Yu.B., Samsonov G.V. Emission coefficients of powders of some refractory compounds /Optics and spectroscopy. – 1960. – V.8, № 2. – P. 410-412 (in Russian).
2. Zapadaeva T.E., Nikolaeva E.E., Ordan'jan S.S.., Petrov V.A. Emissivity and resistivity of composites in LaB_6– ZrB_2 system /Powder metallurgy. – 1987. – № 7. – P. 75-78.

INVESTIGATION OF TRIBOLOGY CHARACTERISTICS OF MODELLING COMPOSITIONS ON THE BASE OF DUCTILE METALS WITH INORGANIC COMPOUNDS IN VACUUM

Solntsev V.P., Skorokhod V.V., Frolov G.A., Kostornov A.G., Kostenko A.D.
Institute for Problems of Materials Science of National Academy of Science of Ukraine

For new engineering, capable long to operate long in a near-earth orbit, and also in conditions of Mars and Venus planets it is necessary to develop new generation of the wear-resistant materials intended for friction junctions of space vehicles and planet research vehicles. Besides these materials may be of interest for friction junctions of vacuum settings. Since the space vacuum, the ambients at Mars and Venus present extreme conditions and, as a rule, do not suppose application of liquid lubricants searching of materials which may show a maximum level of the functional properties in these conditions, is an actual problem.

At creation of the wear-resistant materials intended for operation in conditions of a drying friction and vacuum, first of all it is necessary to consider the factor of the composition which determines dissipative properties of a material and its ability to self-realization of nonlinear mechanisms of the adaptation, resulting in curing structural defects. Accumulated experience on creation of powder wear-resistant materials displays, that such materials are obtained at heterogenization their structures by introduction of ingredients, having high characteristics of hardness and elasticity. In conditions of friction such materials have localization of a plastic deformation owing to what it is not observed avalanche setting as a result of accumulation of a free energy of lattice imperfections. At friction of heterogeneous compositions the stream of a mechanical energy is in part transformed owing to elastic interaction in thermal, thus augmenting kinetic parameters of system. There is a strain-relief crystallization, recovery, recrystallization and diffusive processes of mass transfer are accelerated. In essence in such materials there are processes of the nonlinear interaction, resulting in to selfrecovery or self-curing of system. Para of friction is open dynamic system which stability is determined by set of the processes initiated in a material by an external stream of energy.

Kinetic characteristics of this material are determined by a crystalline structure of the matrix, the phases present in it and character of their interaction with a matrix.

At study of link between setting during friction and a crystalline structure of metal in [1, 2] it was shown, that rubbing pairs of the metals having Body-Centred Cubic Lattices (BCCL) or Face-Ceentred Cubic Lattices (FCCL), intensively wear out at setting. The intensity of a wear of these metals grows at increase of sliding speed. At the same time rubbing pairs from the metals having a hexagonal lattice wear out at setting to a less degree and have lower friction coefficient, than FCCL and BCCL metals. Their intensity of a wear is diminished with increase of sliding speed. This circumstance speaks distinction of opportunities of origin of dot imperfections in cubic and hexagonal crystals [3].

In heterogeneous systems the role of the factor of a crystalline structure matrix of a material uniquely is not defined. Therefore vanadium and titanium were selected as a matrix of compositions metals with a lattice BCCL and Hexagonal Close Packing (HCP). These metals owing to the specific physical-mechanical and functional properties are of interest for creation of new generation of functional materials. As heterogenizated phases the wide spectrum of different physico-chemical nature compounds (carbides, borides, silicides, oxides, chalcogenides, transition metals, covalent compounds B_4C, SiC, AlN, Si_3N_4, intermetallides of titanium and a vanadium) was applied. The vanadium and titanium are rather active metals. Therefore the factor of physico-chemical interaction of a proeutectoid constituent with a matrix, observed at sintering compositions, also was taken into account at the analysis of tribological properties. Thus comparison of tribological properties of compositions was carried out also in view of isomorphism of proeutectoid constituents in each of matrix.

In the table tribological characteristics of compositions on a base of vanadium and titanium, obtained in vacuum at sliding speed 1 m/s and

loading 2 MPa are shown. As rider the steel 45 (HRC 50÷52) was applied. The contents of heterogenizated phase (φ) was 15÷ 18 vol. %. Thus for a clear vanadium the friction coefficient (f) was equal 0,8, a wear (i) - 0,1 g/km, and for titanium - $f = 0,32$ and $i = 0,05$ g/km.

The analysis of experimental results allows to conclude, that at heterogenization structures with hard compound intensity of a wear as vanadium - the representative of metals with BCCL lattice, and titanium - with HCP lattice efficiently decrease. Compositions on a base of titanium have a smaller friction coefficient, than on a base of vanadium. It allows to conclude, that antifriction, connected with crystalline structure of a matrix, also is saved. Hard compounds with a high coefficient of elasticity essentially reduce rate of a wear. At the same time solid lubricants in the greater degree reduce only a friction coefficient. In cases when in a composition there is no hardening phase, their influence on intensity of a wear is developed only at small sliding speeds and loadings. Character of friction and a wear sharply varies, if in compositions there are both solid

phases-reinforcers, and solid lubricants. Their share influence is most expressed, if during friction the chemical processes, resulting in formation of secondary structures with dynamic character of stability, are excited. It is peculiar to the systems containing chalcogenide components. The intensity of a wear is diminished in 5 - 10 times at rather small densities of chalcogenide component (up to ~1,5 %). Such compositions have all necessary elements of processes of self-organizing and undoubtedly become defining for new generation of materials of space assignment.

References

1. Носовский И.Г., Исаев Э.В., Костецкий Б.И. О роли кристаллического строения при трении и схватывании металлов // Докл. АН СССР. – 1971. – Т.198, №1. – С.78-82.
2. Костецкий Б.И. Трение, смазка и износ в машинах. – Киев: Техника, 1970. – 396с.
3. Любарский И.М., Пелетник Л.С., Металлофизика трения. – М.: Металлургия, 1976. – 176с.

Table

Tribilogical characteristics of compositions on a base of vanadium and titanium

φ	TiB_2	SiC	B_4C	TiC	MoS_2	ZrO_2	VC	MoSe
Compositions on a base of vanadium								
f	0,55	0,57	0,56	0,54	0,25	0,54	0,55	0,22
i, г/км	0,0078	0,0021	0,0057	0,0092	0,0126	0,0093	0,0107	0,0163
Compositions on a base of titanium								
f	0,32	0,44	0,31	0,32	0,34	0,33	0,30	0,20
i, г/км	0,0003	0,00027	0,00015	0,0008	0,0014	0,0001	0,0004	0,0011

SECTION F. POTENTIAL AND CONTEMPORARY TECHNOLOGIES FOR RECYCLING INDUSTRIAL WASTE AIMED TO PRODUCTION STRUCTURAL, HEAT-INSULATIVE, FACING AND OTHER MATERIALS

COAL GASIFICATION AND WASTES UTILIZATION IN BLAST FURNACES

Tovarovskiy Iosif Grigor'evich
Iron and Steel Institute NAS of Ukraine by name of Z.I. Nekrasov, Dnepropetrovsk, Ukraine

The traditional structure of fuel balance of the metallurgical works with use of natural gas as a substitute of coke in the usual conditions of Ukraine is inefficient because of high cost of natural gas, which has come nearer, and in a number of cases has exceeded cost of quantity, replaced with it of coke. The task of rationalization of structure of fuel balance by shrinking the consumption of natural gas can be decided by replacement it by coke gas on the technology, earlier developed by Iron and Steel Institute [1,2].

The energy requirements of other metallurgycal manufactures, first of all coke ovens, instead of used in Blast Furnaces coke gas, the products of not coking coals gasification are offered. As units for coal gasification Blast Furnaces removed from operation on balance of metal can be used [3-5].

The known gas producers with the compact lay working in a mode of a slag drip at raised pressure, structurally come nearer to the Blast Furnace, but it is less on volume [6]. In usual on balance of metal conditions are liberated Blast Furnaces, suitable for performance of function of coal gasification. The received reducing gas can be used as for injecting in others Blast Furnaces for replacement of natural gas and coke [5,7], and for use in other technological and power units as a high-heating fuel.

The main feature of use of the Blast Furnace as a gas producer is that temperature of gases, departing from a stock column, should exceed a level, at which there is an intensive stressing of pitches adversely influencing a condition of gas pipelines and complicating technology. Most intensively pitches are allocated in an interval 300 – 500 °C, and at temperatures is higher 840°C there is their breaking-up. As the maintenance of temperature of a top gas at a level, demanded on the specified conditions, (> 500°C) is inadmissible on conditions of a service of the equipment of charging, it is necessary to apply untraditional reception - sharp refrigeration of gas at a run-out from a melting stock column.

Essence of reception that above a stock level of materials, which have at the bottom edge of a shaft top, on a circle establish tuyeres for injecting cooled top gas (50-80°C), that allows after melting it with mine gas to receive temperature of a 300-500°C top gas, departing from the furnace. The heat-eliminating gas recirculate in the system. Off-site gas can be added to it. The quantity of recirculating gas can be determined from simple balance ratio of gas components. At a choice coals it is necessary to prefer hard (non-bitumnious) coals, which allocate at heating insignificant quantity of pitches and are accessible enough.

The scheme of technology includes (Fig.1):
- Charging with coal in the Blast Furnace of "coolants", which quantity and calorific capacity provide a decrease of temperature of gases, departing from stack, up to 840-1000°C, and the makeup does not include easy reducible oxides, forming in stack CO_2 and H_2O;
- Injecting above the charge surface, which have at the bottom edge of the furnace throat, cooled gases ensuring after mixing with mine gas the preset value of top gas temperature, allowed on service condition of the equipment;
- Refrigeration of a part of a top gas up to minimal - possible temperature, it compression and injection through tuyeres, located above the charge surface of materials (recycling);
- Selection of "coolants" with the maximum - possible contents of useful components (iron, manganese etc.), that raises the energy-economic efficiency of technology and makes it multi-purpose.

At use the Blast Furnace as a producer furnace there is an opportunity of use in quality of "coolants" of gas not only moisture and gases, but also solid lump materials charged with coal. These materials contain fluxing additives and other useful components extracted in melts (pig-iron and slag) as passing products of a coal gasification.

Expediently for these purposes to use metallurgical slags - vessel, welding, ferromanganese, silicomanganese with extraction of useful components in a melt. In such a way, alongside with power, the economic and ecological problems of the operation and branch

are solved. Use of metallurgical slag in quality of "coolants" of gas solved the important technological task: As they do not contain easy reducible oxides, giving back oxygen in stack by a "indirect" way, the waste gas does not replenish gaseous with products of reduction (CO_2 and H_2O), which decrease its caloricity, and the heat pickup at direct reduction of oxides increases the "coolant" properties of the slag additives.
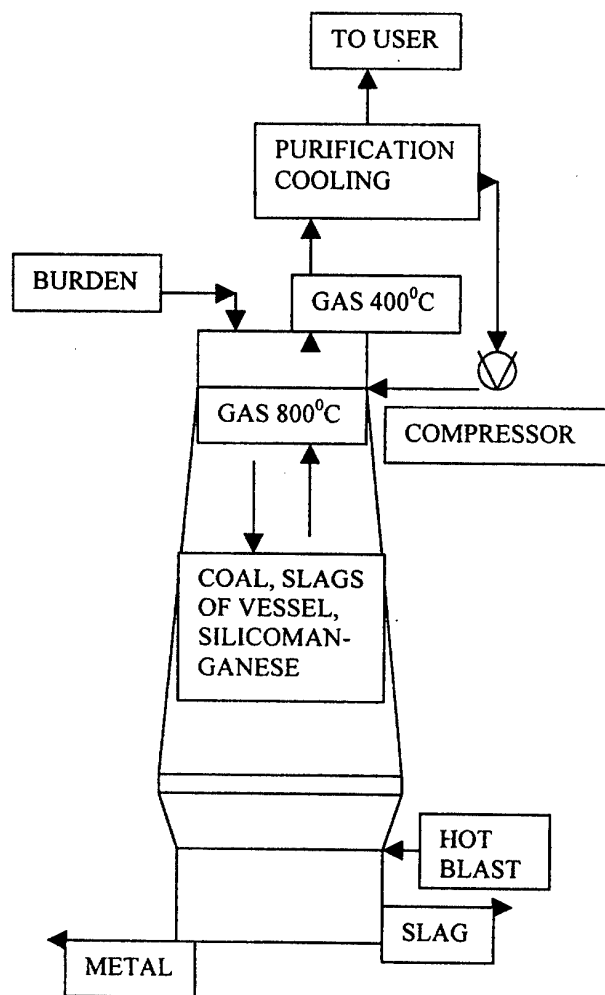
FIG.1. SCHEME OF COAL GASIFICATION
AND WASTES UTILIZATION IN THE
BLAST FURNACE

For an estimation of opportunities of offered technology have executed account of expected smelting characteristics. As fuel have accepted a hard (non-bitomnious) coal, that give minimum pitches in the Blast Furnace and complications, connected to it of technology, and as "coolants" - a self-fluxing mix of a silicon-manganese slag (SMS) and vessel slag (VS). In account for 1 kg of coal is spent: 0,1 kgs SMS and 1,34 kgs VS; is

generated 3,33 $м^3$ of gas (5680 kj/$м^3$); 0,38 kgs of metal with the contents of manganese 15,7 %; 1,25 kgs of slag. At existing in Ukraine and Europe the prices of an expense for ingoing materials there is less cost of the made metal, therefore cost of gas is close to zero, and the fabricated metal with the contents 15,7 % of manganese can mix to non-manganese metal others Blast Furnaces for a conclusion from their burden the manganese additives, that will raise efficiency of the blast-furnace smelting.

While run on the specified technology a Blast Furnace of volume 2000 $м^3$ the quantity of gasification coal will make at least 1500 t/day, manufacture of gas 3,33×1000×1500/24 = 208000 $м^3$/h, and metal 0,38×1500 = 570 t /day. At the expense of the made gas can be released 33000 $м^3$/h of natural gas, that will match to annual economic benefit 23 million Dollars USA at capital expenses, commensurable with expenses on dismantling of the Blast Furnace.

BIBLIOGRAPHY
1.   'Blast furnace smelting with blowing of coke gas' V.F.Pashinskiy, I.G. Tovarovskiy, P.E. Kovalenko, N.G. Boykov. Kiev: "Technika", 1991, 104 p.
2.   Tovarovskiy I.G., Severnyuk V.V., Lyalyuk V.P, 'The analysis of parameters and processes of the blast-furnace smelting'. Dnepropetrovsk: "Porogi", 2000, 420 p. (Ru).
3.   'Exploration of high-temperature properties of non coking coal in conditions of blast-furnace smelting'. I.G. Tovarovskiy, N.A. Gladkov, A.S.Nesterov etc. Stal. Moskow, 1996, # 11, p.14-16 (Ru).
4.   Patent of Russian Federation # 1770362. C 21 B. 7 / 00. Shaft Furnace . I.G. Tovarovskiy, S/I/ Suchkov, V.I. Babiy etc. Bulletin of inventtions.1992. # 39, p.78.
5.   'Production and application of coal gasification products in blast-furnace smelting'. I.G. Tovarovskiy, I.I. Solodkiy, I.Ya. Tolmachev etc. Moskov: Chermetinformatsiya.1992, 101 p.(Ru).
6.   Shilling G-D., Bonn B., Kraus U. 'Coal Gasification'. Translation from German. Moskov."Nedra", 1986, 175 p. (Ru).
7.   Tovarovskiy I.G., Homich V.N., Boyarovskaya G.P. 'Efficiency of use of coal gasification products in quality of blast additives in blast-furnace smelting'.Moskov: Stal, 1982. # 6, p. 5 - 11

RECYCLING OF THE BIOLOGICAL – INERT MULTICOMPONENT ALLOYS

Maksyuta I.I., Anikin Y.P.
Physico-Technological Institute of Metals and Alloys of National Academy of Sciences of Ukraine (PTIMA NASU), Kiev, Ukraine

Composition and technology of a new generation of bio-inert and highly refined alloys on a Co - Cr- Mo- Ni basis with an enhanced corrosion ressistance and exploitation characteristics, which are complied with the ISO-standards for the medicine- aimed alloys were developed in the Physico-Technological Institute of Metals and Alloys, NASU. These alloys are used for a generally applied medical products manufacturing, i.e. artificial limbs, jaw- face surgery and orthopedics materials, surgery string, etc.

However, during cast items manufacturing from alloys, there are more than 50 % scrap from full item weight and its reuse are not desirable because of increased content of gases and presence of unmetal inclusions.

The experiment was aimed at the development of a new technologycal processes of the medical alloys Co - Cr- Mo и Ni - Cr- Mo based wastes extra refining with the consequent obtaining of the complete cycle of medical wastes recovery and getting the billets, that are complied with the ISO-standards for the medicine- aimed alloys.

Solution of the aforesaid problem is described in the paper. It includes implementation of the ecological friendly technological scheme with a double- stage vacuum-induction (VIM) and electron-beam skull melting with electromagnetic stirring of melt (EBM) during the alloys waste melting. Due to this highly refined from the detrimental impurities (S, Zn, Pb, As, Bi etc.), unmetallic inclusions and gases (O_2, H_2, N_2), alloy can be obtained. Thus it will have an advanced corrosion resistance inside biological body i.e. their bio compatibility, and as a consequence - assurance in a reduced negative organism's response for the implantation.

Technical process and methodology:

DOUBLE-STAGE melting process:
1. Double Vacuum-induction melting- VIM+ VIM;

2. Vacuum-induction melting + Electronic-beam melting VIM+ EBM

Development of the medical wastes technologycal process forsaw an investigation of the influence of the technological parameters, e.g. the charge introduction, its mass and content, the pressure of residual gases, the regimes of the EB heating power regulation, the time and direction of the electro-magnetic stirring, the consumption and temperature of the cooling water, etc., on the alloys properties, as well as on the duration of the melting, electric energy consumption, and metal losses due to evaporation. With the use of expendable thermocouples the integral temperature of melts in crucibles and its distribution within the depth of the bath was measured.

The following research techniques is used in the paper:
- theoretical analysis of the local melt heating with the scanning electron beam and its refining from admixtures, non-metal inclusions (oxides, nitrides, carbides)and gases (O_2, N_2 ,H_2)
- modeling of heating processes and melt stirring in the crucible, melt refining, ingots olidifying;
- full-scale experiments.

The investigation of properties of casting materials was conducted by methods of optical and electron-microscope metallography, chemical, phase, roentgenographic and microroentgenospectral metallographic analyses, as well as high temperature differential thermal analysis. Physical and mechanical properties were studied by standard techniques in compliance with the standards adopted in Ukraine. Casting properties of the alloys were also studied by method developed in the same institute with the use of a special sampler that takes.

CONCLUSION

1. Optymal technological schemes and routines of complete recovery cycle for multycomponent biologically inert alloys Co - Cr & Ni - Cr based are established:

591

-double-stage melting **VIM+ VIM** at a mass ratio of 1:1 of clean charge materials and casting wastes.
-double-stage melting **VIM+ EBM** at a ratio of 100 % of nonconditioned casting wastes;
both cycles require first refining stage i.e. VIM to be conducted at a high temperature of melt overheating, chamber pressure decrease from 6. 7 $*10^{-1}$ Pa to 6, 7 $* 10^{-3}$ Pa and minimal time of melt exposure to the ceramic crucible. Overheating at 323-373 K above the liquid's temperature is sufficient for decontamination.
- Pouring of metal in steel or chill mould, crystallization on air.

2. After the complete recycling cycle on the recommended routines, utilizing 50...100 % by weight of casting wastes, certified billet for all alloys types gains the following features :
- minimum melting loss, alloys chemical composition is preserved within the standards for each metal quality;
-essential alloys refining: amount of gases is 5-7 times lower, maintenance of oxygen, hydrogen and nitrogen in sum does not exceed 10-15 ppm;
-non-metallic inclusions (nitride, oxides, oxynitride) are dispersing (grind down), amount of coarse-grained globular oxides and oxynitride is 2-4 times lower;
-dense cast billet macrostructure with minimal pipe and least quantity of casting pores, high castability that enables casting of thin walls wares;
-homogeneous microstructure with grinded grain and lowered amount of massive carbide emissions and eutectics.

-decreasing of segregation coefficient of alloys elements due to intensive melt stirring during **VIM** (calculated on results of researches on MRSA " COMECA MS 46");
-complex of physics-mechanical characteristics, required by standard ISO 5832 (hardness, HB, yield point **(YP)**, ultimate tensile strength (UTS), δ,%,, φ,%)
– within the certificates for each metal quality);
-corrosion resistance in 10% solution of NaCl at T = 50 ^{0}C, for 100 a hours exceeds analogues.
-a toxicological alloys analysis after complete recycling cycle has not revealed any harmful admixtures.

3. As a refining degree criterion R = (Rgas+ R inclusion), % conditionally choosen complex index, which depends on lowering level of contamination by gases and non-metallic inclusions after each consequent melting stage. Calculations revealed, that each VIM melting stage diminishes R value by 15...20 % on everage, and by 25... 30 % after EBM stage.

4. It's necessary to note that increase of temperature and melt overheating period duration with the purpose of admixtures evaporation and dissociation processes intensification, lead to the destruction of ceramic crucible fettling on **VIM** stage and multiplies losses of doping materials on both stages.

THE BEHAVIOR OF HIGHPOROUS HETEROGENEOUS MATERIAL IN ENVIRONMENTS OF POWERFUL ENERGY FLUXES ACTION

Efremov V.P., Fortov V.E., Ostrik A.V.[1], Potapenko A.I.[1]

Hight Energy Density Research Center Russian Academy of Science, Moscow, Russia
[1]Central Institute of Physics and Technology MoD RF, Sergiev Posad, Russia

The action of powerful energy flux upon condensed matter is a suitable method for the study of thermal characteristics in the broad area of phase diagram. The interest in porous matter is stimulated by their use as protection material for bodies, irradiated by different energy fluxes. At present one of the most perspective mean of protection is using on surface of irradiated body a bumper shields of heterogeneous material with tungsten covered hollow glass microballoons (GMB) as a filler and rubber as a binder (fig.1).
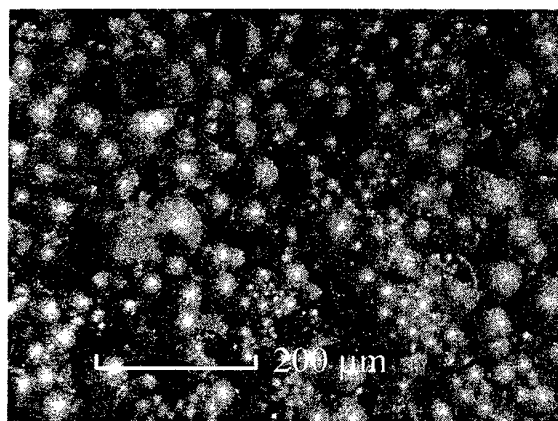
Fig.1. tungsten covered hollow GMB.

The aim of the paper is the investigation of pulse electron and X-ray beam action upon the perspective design materials. For the task solution it is necessary to build on the base of experimental data the mathematical model of high porous insulator material, irradiated by powerful energy flux, as well as numerous and experimental determination of thermal properties of this material.

The behavior of investigated GMB-rubber material in shock waves generated by powerful pulse is assumed to be complex [1]. Effects that need to be considered include energy deposition, heat transfer, porosity influence, features of fabrication, GMB crushing and size distribution [2]. There are the following phenomena, which are of primary interest:

- initial pressure generation in the GMB filled material;

- pressure evolution and shock wave motion in the material.

The pulse action of powerful electron beam or X-ray beam on sandwich structure with bumper shield is considered. Initial pressure generation is defined by Gruneisen's factor of material, which depends on material structure. It is presumed that all microballoons has uniform density. The glass and the tungsten are considered as porous matter [3].

Crushed microballoons (see fig.1) may appear at material fabrication. Effective characteristics (the density, bulk modulus and Gruneisen's factor) for the microballoon's crack, as well as for the crack-rubber mix, are calculated using mass part and volume part of tungsten and glass in the filling and the part of crushed GMB.

The metal covered GMB was considered as two-layer sphere. The effective Gruneisen's factor for metal covered GMB was determined by using of percolation model [4]
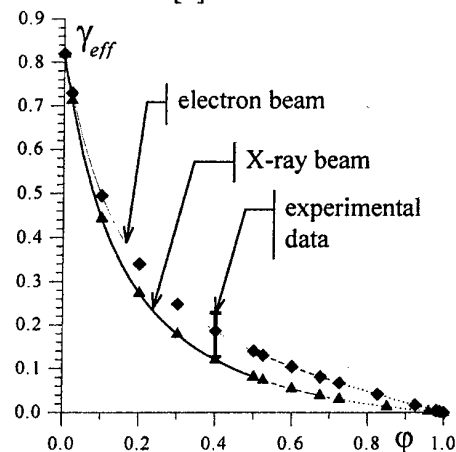
Fig.2. The comparison with experimental data.

Calculated dependences of the effective Gruneisen's factor as function of filling volume part for electron and X-ray pulse action are shown on fig.2 and compared with experimental data, obtained by measuring the particle velocity in the material with laser interferometer system. Investigated samples in these experiments are loaded by electron beam of 290 keV with pulse duration 100 μs. Calculated values are in good agreement with experimental one.

It was interest to exam the influence of GMB characteristics on effective Gruneisen's factor of

the material. The GMB diameter, one's wall thickness, tungsten mass part and GMB crushed percent are varied. In all cases Gruneisen's factor decrease with filling volume part increasing. Also Gruneisen's factor decrease with GMB diameter increasing, as well as wall thickness, covering mass part and crack percent decreasing (fig. 3). The differences in the GMB characteristics lead to differences in initial pressure generation in the GMB filled material (fig. 4) [2].
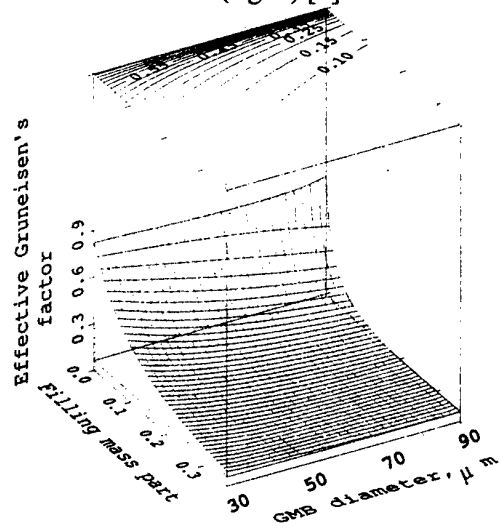
Fig.3. The Grunaisen's factor vs structure of material.
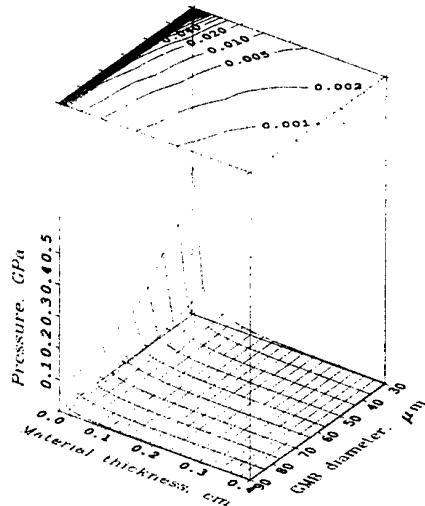
Fig.4. The initial pressure field vs structure of material.

The area of initial pressure is a reason of shock wave. For the simulation of wave propagation the one-dementional Lagrangian code was used. GMB-rubber heterogeneous material was treated as homogeneous porous elastic-plastic solid. The differential equation of state is used [4].

Two-layer sandwich structure (GMB-rubber bumper shield with organoplastik) was examined.

Shock wave forming and moving are numerically studied. Tungsten mass part was varied. Microstructural analysis of the composite material after the pulse action was made. Areas of filler spall and the flux energy density leading to the GMB-rubber material spall was determined. Results of numerically study for various types of protection materials are shown in figure 5 (solid lines corresponds to 3.3 µs after irradiation, dashed – 5.3 µs; rhombus – 21.5% of tungsten, circles – 8.8% of tungsten). After passing the shock wave through the contact border of materials amplitudes of its positive and negative parts are increased.
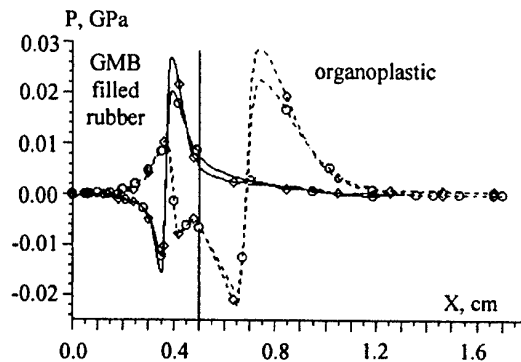
Fig.5. Shock waves transition.

In conclusion, presented model allows to describe interaction of powerful pulse beams with heterogeneous insulator material and can be use for optimisation of protection properties of composite material.

This work has been done due to support of Russian Base Scientific Foundation.

1. *Ostrik A., Potapenko A.* Numerical investigation of the beam mechanical action on heterogeneous materials. // Proc. of Int. Conf. "SWCM-98", S.-Petersburg. 1998. P. 156-158.
2. *Efremov V., Ostrik A., Potapenko A., Fortov V..* Pressure generation by pulse volume energy deposition in heterogeneous material with hollow microballoons. // Chemical Ph. Report. 2000. V.19. №2. pp.32-43.
3. *Kanitkin N.N., Kuzmina L.V.* Quantum-statistical hugoniots of porous substances. // Proc. of Int. Conf. "SWCM-98", S.-Petersburg. 1998. P. 174.
4. *B. Demidov, V. Efremov, V. Fortov et. al.* // J. of Technical Ph. 1998, V.68, №10. P.117.

HEAT INSULATING AND ADSORBING MATERIALS BASED ON PRODUCTS OF WASTES VAPOR THERMOLYSIS

Aristarkhov D.V., Zhuravsky G.I.[(1)], Polessky E.P.[(1)]

Scientific and production company "Ecology Energy", Moscow, Russia

[(1)]Luikov Heat and Mass Transfer Institute, National Academy of Belarus, Minsk, Belarus

Traditional thermal technologies of processing industrial wastes (pyrolysis, gasification burning) have reached at present a high level of development. Efficient technological schemes have been developed, modern equipment is manufactured and used.

At the same time harsher requirements to technologies of wastes recycling requires the need for creating basically new methods and equipment.

One of promising trends of creating ecologically and energetically efficient technologies is steam thermolysis, i.e. thermal destruction of organic wastes in a media of overheated water steam.

The studies conducted in this work show that qualitative materials for heat insulation, adsorbents for purifying gaseous and liquid emissions can be obtained by steam treatment of plant biomass wastes (wood, lignin).

Materials for filler structures produced from wood wastes according to this technology meet all quality criteria. (positive decision on invention application N20013765/12 June 5, 2001, the Russian Federation).

Following are average indexes of such materials: density 630 –1190 kg/cu.m, thermal conductivity in dry condition at 25+1°C and density of 830 kg/cu.m is 0.12 -.0.18 Wt/mK, compressive stress limit equals 233 kg/cu.cm, sorptive humidification for 72 hours at relative humidity of 98% is within 0.5 – 4.0%.

Experimental studies showed that up to 0.3 kg of activated carbon can be obtained from 1 kg of absolutely dry wood wastes by steam thermolysis with a considerable reduction (compared with a traditional technology) of environmental pollution.

One stage of obtaining active carbon (one technological processes includes stages of carbonization and activation) results not only in

reduction of waste releases but in saving energy resources.

The present work puts forward a new scheme of obtaining active carbon from rubber wastes (positive decision on invention application N 200127875/12 of Nov. 9. 2000 and N 2000127874/06/06 of 09. 2000, Russian Federation).

By this scheme the process of rubber wastes recycling results in an ecological effect due to wastes processing, in an economical effect due to obtaining valuable technical materials.

Experimental works on obtaining adsorbents from rubber wastes by the above mentioned scheme proved that recycling 1 ton of wastes can result in obtaining 400 kg of liquid fuel (mazut 40), 450 kg of activated carbon and up to 1.4 Gigo-calorie of thermal energy. The process is completely self-sufficient.

Analysis of the activated carbon samples obtained from worn out tires showed that a specific adsorptive surface is at least 120 sq.m/g, Iodine number is128 g/kg, dibutylphtalate is at least 100 cu.cm/g, ash content is up to12%, mass Sulfur content is about 1.2%, Carbon content is 87-90%.

Direct wastes burning results in release to the atmosphere of considerable quantity of toxic compounds: flu ash, heavy metals compounds, oxides of Sulfur and Nitrogen, Chlorine compounds as well as super-toxic substances (dioxines, poli-aromatic Carbons)

Typical for the technology of burning, gasification and pirolysis is osmophoric pollution of the atmosphere. These technologies produce odorants – odorifrous substances which might not have resorptive influence on a human being but cause reflective reaction of the organism. The organism reacts to osmophoric pollution by feeling smell, changing the brain bio-electric activity, light sensitivity etc.

In order to prevent odorants exhaust, their concentration should be reduced considerably lower than maximum permissible concentration, which is quite a complicated problem.

During steam thermolysis of organic wastes, formation of odorants and high-toxic compounds is suppressed or stops completely.

This is explained by the following factors:
- thermolysis of chlorine-organic compounds in steam medium with no oxygen and with reducing atmosphere leads to dehydrochlorination with formation of CHl i.e. formation of molecular chlorine required for production of dioxines is excluded;
- water vapor in a gas-vapor mixture reduces partial pressure of gaseous decomposition products which hampers secondary reactions and formation of high-toxic compounds;
- condensation of water vapor results in concentration of thermolysis products and their purification from soot particles.

Concentration of thermolysis products leads to higher specific combustion heat, creates conditions for direct (without additional fuel) combustion of theses products with a considerably lower environmental pollution compared with direct wastes burning.

Vapor thermolysis of plant biomass results in formation of gaseous, liquid, and solid products. Gaseous products include organic acids (formic, acetic, propionic), furfurol, carbon oxide and dioxide as well as water vapor.

Liquid products of biomass vapor thermolysis contain mainly water and organic acids solved in it, as well as tars. Solid products composition of biomass thermolysis at 200°C slightly differs from initial composition of wood biomass, and at higher temperatures solid products are oxygen-enriched. According to known hygienic quality criteria, solid products of wood biomass low-temperature thermolysis meet the requirement for construction materials, and products of high-temperature thermolysis can be used as adsorbents to purify liquid and gaseous wastes.

During vapor-thermal impact on rubber wastes, organic compounds are destroyed and solid, liquid, gaseous products are formed. Their quantitative yield and qualitative composition are determined by composition of the products and operating conditions of vapor treatment (temperature, heating speed, means of heat application, speed of decomposition products evacuation from thermolysis zone). Analysis of rubber wastes thermolysis of gaseous products showed that they don't contain high-toxic compounds (dioxines, benzopyrens, plolychlorided biphenyls etc).

INVESTIGATION FOR REMAKING OF PRIMARY SOLID ALLOY AND TUNGSTEN WIRE WASTES IN SOLAR FURNACE

Pasichny V.V., Uvarova I.V., Babutina T.E.
Institute for Problems of Materials Science NAS of Ukraine, Kyiv, Ukraine

Tungsten is one of the most precious materials for modern technique. It is known as a main component of heat-resistant and refractory alloys. There are no tungsten sources of raw materials in Ukraine. That is why the conservation and repeated use of tungsten holding industrial wastes are very signify. The oxidation and following reduction and carbidization are the well-known process for tungsten solid alloy wastes remaking. This process is carried out in common electric furnaces. After primary oxidation the wastes are converted often by chemical methods. All of these methods demand considerable energy expenditure. One of the ways for energy economy is the using of renewable energy sources in particular solar energy. As it is evidence of wide experience of material investigations in IPM NAS of Ukraine the using of solar furnaces is more convenient for oxidation of metals since in this case it can be possible to achieve the temperature near 3500 in air medium directly. Some limitations for solar furnaces using are the one-sided heat supply, irregular distribution of energy density, dependence on season, daily time and weather.

The aim of this work was to carry out the investigation of mechanism and kinetic for oxidation of tungsten hard alloys and tungsten wire wastes and establish the optimal heat treatment regimes at radiation heating, which imitates concentrated solar radiation.

Taking into consideration the specific character of solar furnaces and necessary to work off the research principles the experiments were carried out at heat treatment in optical furnace with a xenon lamp in 3 kW [1]. This equipment permits to carry out dosated heating of individual small samples on fixed horizontal surface and determines the weight and structural phase transformation in materials. Moreover it is a possibility for complete transformation from compact sample to oxide powder or powder mixture of different oxides by hand manipulation. Defocussing of samples fulfilled regulation of heat parameters. Temperature was measured by thermocouple.

The researches were carried out on the tungsten fiber samples, pressed to definite porosity. The influence of sample porosity weight and temperature on the oxidation kinetics was studied. The dependences of oxidation degree against time are shown in Figure.
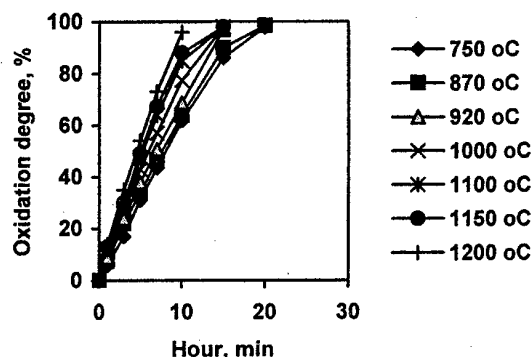
Figure Dependences of oxidation degree against time at different temperatures and the same porosity at ≈ 70 %.

As can be seen from this data the tungsten oxidation passes on linear low from the beginning. The process is described by following kinetic linear equation

$$W = kc$$

k- coefficient of reaction rate of simple equation:

$$k = (1/t)\ln(c^o/c)$$

c^o and c — the initial and current concentration, correspondingly.

All of the samples were heated on the stainless steel backing of 2-mm. thicknesses. At energy density of 12 KW/cm^2 on the backing level and 18-20 KW/cm^2 on the sample surface the noticeable process of wire oxidation started. Weak gassing due to oxide sublimation, quick oxidation of separate fibers, which was situate nearer to focus, the appearance of separate micromelting places in hottest zones, change of the sample color into light-yellow one in zones, closing to hottest one were observed. Immovable position of oxidizing samples resulted in gradual delay of oxidation for

lower layers due to screening by the upper oxide layers forming on the surface.

As a result approximately one quarter of sample volume became non-oxidized after 25-30 min. of being heated. Taking into account inefficiency of such immovable position of oxidizing samples the following experiments were accompanied by mechanical turning over of oxidizing sample promoting its destruction to parts, drusen and at least the oxide powders. The powder obtained in such a way was the uniform light yellow color being peculiar to WO_3. Since completeness of such conversion was established by sight the duration of the oxidation was rather subjective kind. But the obtained experimental dependence of heating duration against sample weight was straight line.

The dependence of the weight increase against heating duration at oxidation of tungsten wire deviated slightly from a straight line owing to increase of quantity of flying sublimate. Gassing was observed during the whole heating time for all the samples at chosen conditions. Since the oxide looses was desired the method for the determination of their amount was developed: they were equal to 3,0±0,4 % under chosen condition.

The samples of the hard alloys (WC-6Co, WC-8Co, WC-15Co, WC-20 Co) were chosen for the investigation of the oxidation. The samples of necessary length (about 10 mm) were made of cutting prism of the sectional view 5x5. Thermal cutting on the laser module KTM-1 created in the IPMS on the bases of installation KVANT-12 was performed. The optimal conditions of heating for equal oxidation of all the sample sides without burn-off were found. Such heating level was obtained by the irradiancy of 18 W/cm^2 on the sample surface.

The linear low of tungsten hard alloys oxidation was characterized by parallel growth of all the sample sides in the directions of its axis of symmetry. As a result the total sample volume became in two-three times larger than the initial one. It cased the approach of this sample surface to the focal plane and corresponding increase of the irradiancy. The compensation for the increase of the sample thickness was realized by periodic moving its surface off the focal plane.

The first visual signs of the oxide layer growth were shown between 3-6-th minutes. Later the growth and the deformation of the oxides began.

After 30-35 the noticeable delay of oxidation due to screening of the radiant flux by oxide layer. As a result of the experiments increase of the sample weight and their thickness depending on heating duration has been obtained. The weight and the thickness of oxidized hard alloy parts after being separated from sample were determined too.

The obtained experimental data have permitted to determine general tendencies of oxidation for different materials containing tungsten and can characterize the process of waste remaking as a whole.

Thus, the principle possibility for tungsten containing waste remaking by use of concentrated solar radiation was established. At the next stage of investigation it is necessary to carry out the experiments in solar furnaces directly taking into account the scale factor of treating object, the working up of the special technical devices for permanent separating of oxidized parts.

1. Pasichny V.V., Powder metallurgy and metal ceramics, 1995, 7/8, pp. 475-483.

APPLICATION OF ELECTROPLATING WASTE FOR PRODUCTION OF ENAMEL COATINGS

Kochetov G.M., Emelianov B.M.
National University of Construction and Architecture, Kiev, Ukraine

Wastewater and the sludge of industrial plants contain significant amount of toxic components polluting the environment. Considerable dissonance between volume of the waste accumulation and their utilization now is dominating fact in Ukraine. The utilization of heavy metals from those waste, on the one hand, allows to save valuable natural raw materials and power resources, and, on the other, to solve the important ecological problem.

There are some technologies, allowing to apply electroplating sludge as a component of different construction materials: brick, tile, concrete, etc. However, sanitary assessments of these materials, have revealed, that notwithstanding positive technological results, environmental parameters of them are far from being appropriate for application, due to permanent leaching and migration of heavy metal ions into the environment. Therefore, for the time being the above sludge-treatment technologies do not allow to conserve valuable resources and prevent environmental pollution.

We have developed technology for utilization of nickel-containing sludge as materials for an enamel industry. It is moreover important since until now only pure nickel and cobalt oxides have been used as a coupling in ground enamel coatings. According to the known data the problem for replacement of pure oxides by nickel-containing waste of industrial plants is not positively solved. Selection of galvanic sludge for the goal of replacement is explained by the presence in sludge of some component besides nickel, in particular, copper and zinc, which are favorable for the characteristics of an enamel coating. However, the galvanic sludge commonly contains chromium and this metal is known as such that decrease of ground enamels quality. The chromium problem is also solved in this research.

were studied by using of standard techniques and compared with standard enamels obtained in similar conditions.

In this research as a raw material for replacement of nickel and cobalt oxides in the ground enamel we propose to use enriched galvanic sludge from one Ukrainian plant. The sludge contains substantional amount of moisture (up to 80%). Therefore, for more convenient storage and transportation the first stage of the sludge treatment includes it contraction, dewatering. Obtained materials were abbreviated as Nickelit. Next two methods of Nickelit processing were developed: 1) chemical and 2) thermal.

Chemical enrichment

For removal of undesirable contamination of Nichelit with Cr(III) compounds chemical method based on amphoteric properties of chromium hydroxide was used. Chemically enriched Nickelit can be used for replacement of coupling oxides in the ground enamels. Chemical analysis shown that chromium content in processed Nickelit is not exceeds 3,0 % (in recalculated to oxide).

Additional thermal enrichment

The method of thermal enrichment of chemically processed Nickelit is based on a fact that Nickelit contains also significant amount of chemically bonded water, which is not possible to remove by preliminary dewatering. The product of high-temperature processing (further Nickelit-T) was crushed till powder in vibrating mill and carefully mixed up before using.

Chemically and thermally enriched Nickelit has up to 70 of % of Nickel (III) oxide. This material was used in laboratory conditions for replacement of the individual nickel oxide in ground enamels. Mixture for ground enamel was prepared in standard conditions taking to account nickel contents in Nickelit-T.

Preparation of initial mixture for enamel, it processing was performed in standard conditions. Basic physical-chemical and mechanical properties of the obtained ground enamels,

Results of the experiment showed that the main working characteristics and physical-chemical

properties of ground enamels obtained from Nickelit-T meet standard requirements. Moreover mechanical stability (stress) and heat resistance are higher for the materials proposed.

We suggest mathematical model for simulation of properties of Nickelit-T-containing enamel depending on its chemical composition. This model was tested for calculation of thermal expansion coefficient. Coefficients obtained from the model are in good agreement with those obtained from experiment.

The proposed mathematical model can be used for theoretical prediction of ground enamel's properties.

The technology has been tested at the industrial sites and we recommend it for large-scale implementation. Our technology ensures waste-minimization and replacement of expensive production inputs.

SAFETY OF METAL AND CONCRETE CONTAINERS IN THE CONDITIONS OF INTENSIVE THERMAL, RADIATION AND IMPACT EFFECTS

Guskov V.D., Korotkov G.V., Rutman Yu.L.
KBSM (Special Mechanical Engineering Design Office), S.-Petersburg, Russian Federation

Overloading of the Spent Nuclear Fuel (SNF) storage facilities of nuclear reactors and necessity to transport the SNF is a complicated ecological problem requiring an immediate solution. An effective and cost-effective way of its solution is to use special metal and concrete containers (MBK) for storage and transportation of the SNF. The MBKs have been developed by the KBSM (Special Mechanical Engineering Design Office), S.-Petersburg. Concrete in such constructions has been used for the first time and that required for complicated science-consuming researches. In the base of such researches were results received during development of special facilities of high strength. In present time a cycle of research and development and experimental works has been performed having shown safety of the MBK with the SNF in diverse extreme conditions provided in the RF regulations and the IAEA recommendations.

Special super heavy concrete of highly strength (V 110) and highly strength plastic steels have been applied in the MBK. The concrete and steel of the MBK are working in the extreme conditions, stipulated by radiation processes, intensive thermal emissions of the SNF, a safety requirement in emergency conditions (an impact on a hard foundation with a velocity of V = 13,3 m/s, fire etc.). The extreme thermal load on the MBK is 30-80 kWt/m^2 during half an hour. Plastic deformations of the metallic protective elements under an impact are characterized by Odquist parameter $e_0 \approx 0,95 ... 1$. An influence of the factors mentioned on the MBK has been studied on the base of systems approach; both on the basis of special mathematical models and on the basis of unique stand equipment experimentally. One of the most important properties is provided by application of special protective elements (PE), which absorb impact energy through their plastic deformation in the MBK construction. The difficulty of calculation and design of such elements was in necessity of simultaneous account of as geometrical, so physical non-linearities of their deformation process (change of the contact area and the PE configurations, operation in the deep plastic deformation zone). The difficulties mentioned have been overcome through a calculation methodology specially developed, which was based on a principally new method of task solutions of limit equilibrium. Special mathematical models have been used too for thermal and mass exchange process analysis.

Special attention has been given to radiation and chemical processes in the conditions of elevated temperature influence and to longevity issues.

A cycle of calculation and experiments has been completed by tests of large-scale and full-scale MBK models. Systemic behavior studies of diverse materials (concrete, metal, sealing elements) in the extreme conditions of the MBKs operation have allowed to give the MBKs safety warranties and recommend them for serial production.

POLYMER-WOOD MATERIALS BASED ON POLYMER WASTES

Mamunya Ye.P., Myshak V.D., Lebedev E.V.
Institute of Macromolecular Chemistry, National Academy of Sciences of Ukraine, Kyiv, Ukraine

The new composite polymer wood materials (PWM) are thermoplastic polymer matrix filled with up to 70 % of woodcutting. The attractive properties of PWM are good mechanical characteristics, possibility of the processing by traditional methods of plastics processing and low price of PWM. Using the thermoplastic polymer waste for PWM production solves two problem at once: 1) preventing environment pollution by means of polymer waste recycling, 2) obtaining new materials suitable for goods production.

Extrusion, pressing and die-casting are the methods for PWM processing into the goods. The extrusion expects of high polymer melt homogeneity and appointed wood fractional composition. Therefore this method has not enough perspective for mixed polymer waste and poor quality woodcutting recycling.

If the wood flour (woodcutting with small particle size) with relatively low concentration (up to 20%) is used to provide the necessary melt flow then the injection molding could be used for PWM production.

More suitable for PWM production is pressing method. This method allows using different mixed polymer waste, different type of woodcutting (sawdust and chip with particle size from 0.1 to 10 or more mm) and also plants waste. At the same time the acceptable quality level PWM is obtained due to the reinforcing and compactibilising behavior of wood phase.

The following variants of pressing methods may be marked out:
A) Direct pressing of the mixture of milled polymer and wood chips;
B) Pressing of the polymer-wood mixture previously homogenized in the melt.

Furthermore the B method may be divided on the following variants:
B1) After homogenization polymer-wood paste is cooled and serves as semi-finished product (sfp) for further pressing. Before pressing a carpet is formed from the sfp. After that the carpet is heated and pressed.
B2) After homogenization polymer-wood paste is formed as continuos wide strip. The strip is cooled and cut to obtain semi-finished product

as plates for further pressing. The plate is heated before pressing.
B3) The portion of hot homogenized polymer-wood paste is injected into the die mold and formed.

All above-mentioned variants have merits and demerits. Variant A is most favorable for processing of wood chips with particle size more than 10 mm. This wood chips make the external appearance of goods similar to the natural wood. At the same time the product strength is the same as strength of material obtained by means of another variants, but the product water resistance is essentially lower.

Variant B1 allows to segregate the stages of PWM obtaining and product formation. The product pressing technology is similar to the well-known technology of resin-bonded chipboard. The main problem of this technology is the carpet heating stage. This is due to the low thermal conductivity of the granulated polymer-wood sfp. The HF (high frequency) heating are most favorable for initial carpet heating whilst the IR (infrared) emission heating is the least efficient.

Variant B2 is the same as the B1 excluding the carpet formation stage from sfp.

Variant B3 is most efficient since it exclude the semi-finished product (carpet or plate) heating stage. However this technology expects the high spread rate of the hot melt within the die mold because of the high cooling rate of the melt. In this case the melt is not able to fill up the die mold regions remote from the melt injection. Therefore obtaining large area thin-walled product by means of the B3 method is difficult.

Properties of PWM depend on many factors such as composition of the polymer matrix, content of the wood phase, size of wood particles, interaction on the polymer-wood boundary, etc.

The distinctive feature of the wood chip filler is the presence of reactive groups that can come into chemical and intermolecular interaction with polymer matrix. One more feature is the filler porous structure providing a good coupling with polymer. The possibility to rise both chemical interaction and hydrogen bond

formation between secondary PE and cellulose functional groups was earlier shown by IR study of the secondary PE filled with wood.

The different level of wood component influence on the composite strength and structure formation within the polymer matrix for primary and secondary PE was shown by the DSC comparative study of PWM (see Table).

Polymers and composites	Tensile strength σ, MPa	Melting heat ΔH, kJ/kg	Relative melting heat decrease, $\delta(\Delta H)$, %
Primary PE	12.6	108.9	-
Secondary PE (SPE)	11.5	108.1	-
70 PE + + 30 Wood	10.9	97.6	10.4
70 SPE + + 30 Wood	13.8	93.3	14.0

It can be seen from the Table that the melting heat decrease occurs for both secondary and primary PE filled with wood, but for secondary PE the value of $\delta(\Delta H)$ is bigger. Therefore, the rise of chemical interaction between secondary PE and wood results in crystallization suppression within the polymer matrix and increases the composite strength σ.

The pressing technology of obtaining PWM looks mainly like the technology of obtaining chipboard and wood-fiber board. The process includes steps of wood drying, cold mixing with polymer, hot and cold pressing (method A). However, in this case, the high waterproofness can not be achieved because of the partial wood wetting with the polymer as a result of the both non-homogeneity of the mixture and high polymer melt viscosity, although, the strength of material is high enough. The hot blending step insertion into the technological process (i.e. blending of the polymer in the melt state with ground wood (method B)) results in the drastic improvement of PWM characteristics. The impact of large shear deformations in the course of the composite blending in the mixer ensures the uniform spreading of polymer melt on wood particle surface. Homogeneous mass comes into the grinder and after that it can be kept as granulated semi-fabricate, which comes then into the forming equipment (method B1).

When the polymer blend is used for PWM production hot blending gives especially good effect. When PWM is obtained by method B1 the

composite waterproofness improves greatly (water absorption ΔW and swelling ΔS are decreased considerable), tensile strength σ_t increases and bending strength σ_b remains almost unchanged. Polymer-wood mass homogenization at the temperature higher than polymer melting point results in semi-fabricate formation, which has wood particles covered completely with the polymer layer. The following pressing leads to the filling of the capillary-porous wood structure with the polymer present on the wood particle surface and therefore, improves PWM waterproofness. The strength increases due to the removal of defects, such as wood particle parts non-wetted with the polymer.

These regularities occur also for PWM on base of blends PS-PVC and PE-PVC. Extreme effects of rise and reduction PWM parameters appear when contents of one polymer component is small (5-10 %). These effects can explain by change of the polymer matrix structure with adding second polymer.

Dependencies of strength (σ_t and σ_b) and water resistance (ΔW and ΔS) have the contrary character. Increase of strength and decrease of ΔW, ΔS occurs for the same compositions. It allows us to conclude that main factor defining parameters of PWM are interaction polymer matrix – wood. Interaction polymer - polymer have less meaning. Really, maximal ΔW value of poor blend PE-PS achieves 1 %, whilst PWM on base of this blend increase up to 22 %. Consequence, additions improving interaction polymer – wood can considerable rise properties of PWM.

Consequently, when secondary polymers are used for obtaining the polymer-wood materials it is possible to improve the composite characteristics due to formation of both chemical and hydrogen bonds between functional groups of the polymer and wood. The insertion of the step of hot polymer-wood blending into the technological process of PWM production makes it possible to improve drastically the waterproofness and strength of the resulting material.

PARAMAGNETIC FEATURES OF SOME ADSORBENTS OBTAINED FROM VARIOUS PRODUCTION WASTE

Ryabikin Yu.A., Zashkvara O.V, Mansurova R.M.[(1)], Mansurov Z.A.[(1)]
Institute of Physical and Technology ME&S RK, Almaty, Kazakhstan
[(1)]Combustion Problem Institute, Almaty, Kazakhstan

Decision of ecological problems of different nature, including radiation ecology, brings up sharply a question of getting high effective and inexpensive adsorbents. Last time the adsorbents on carbonaceous materials basis have more and more distribution. Important advantage of such adsorbents is that they can be obtained from industry and agriculture waste. Costs for such adsorbents getting is small, therefore their production is advantageous. At that two problems are essentially decided: waste utilisation takes place that improves ecological situation in itself and effective and economically advantageous adsorbents are obtained. The such spent adsorbents substitution by new ones is often more advantageous than their regeneration.

Various sledges obtained as waste of some metallurgy productions, thermoelectric power station employment, woodworking industry and agricultural productions, (stones of fruits and berries, various nut shells and so on) as different clays can be used as materials for getting of substances.

In this report some results concerning overcarbonization process study by electron paramagnetic resonance (ESR) method of as Turgai sludge and Chilic clay (TSCC) mixture with the ratio 1:1 and some different objects as results on overcarbonization of walnut shell (WS), grape stones (GS) and birchen sawdust (BS) are presented.

Turgai sludge constitutes the aluminum industry waste. The mixture composition TSCC 1:1 contains Fe_3O_4 (32,6%), CuO (4,1%), MnO (8,2%), PbO (5,5%), CdO (4,3%) and 3% of other oxides. Material overcarbonization process was executed in quartz reactor with use of propane-butane gas mixture. The overcarbonization of TSCC 1:1 during 30 min was carried out at temperatures 450^0C, 550^0C, 650^0C, 750^0C and 900^0C. The organic materials overcarbonization was carried out in argon atmosphere at various temperatures.

In ESR spectrum of initial sample TSCC a line, due to Fe^{+3} ions, with wide $\Delta H=84 Oe$ and $g=2,11$ dominates. Besides this line there is one more ESR line due also Fe^{+3} ions but with wide $\Delta H=7 Oe$ and $g=4,3$. On ESR spectrum from Fe^{+3} ions with $g=2,11$ a weak six-component spectrum of bivalent manganese ions was laid which parameters approach to ones of Mn^{+2}- spectrum in MnO lattice. But already at first overcarbonization temperature 450^0C this spectrum is not recorded. It fails too observe at more high overcarbonization temperatures the spectrum of Fe^{+3} ions with $g=4,3$. This, to a great extent, is connected with the fact that line intensity with $g=2$ grows sharply at first overcarbonization temperatures, and at 550^0C it achieves a maximum, and its excess over initial sample is 300-fold. When overcarbonization temperature being further increase, not less violent decrease of resonance signal intensity occurs. Unfortunately, intensive signal from Fe^{+3} ion cluster denuded the possibility to record ESR signal of carbonaceous sediment formed under overcarbonization of these materials. Nevertheless, it has been discovered a correlation between obtained dependence of magnetic resonance signal intensity on ovecarbonization temperature with carbide mechanism of materials overcarbonization. It has been shown that in this system the basic overcarbonization process begins higher 550^0C, when iron clusters with significantly large dimensions forming. This leads to generation of large quantities of carbon Fe_2C, which decomposition products free carbon isolation.

Carbonized organic materials are rather widely used as adsorbents. ESR method has been applied for study of carbonized materials, nevertheless their paramagnetic features strike up to now by their variety. According to known literature data the unpaired electrons concentration dependence on carbonization temperature of organic materials passed through a maximum in temperature diapason from 400^0C to 600^0C. Such dependencies obtained by as for walnut shell (WS) and grape stones (GS) show an availability of two maxima. The first is in 160^0C-200^0C range, and the second (basic) - in 350^0C - 400^0C range. The rations of these maxima

intensities for both these samples is approximately equal to 3,9.

When carbonization process of classical sample (birchen sawdust) being study, we also found out two maxima on dependence curve of ESR signal intensity on carbonization temperature. But in this case the ration of basic maximum to low-temperature one was about 150-fold, and, probably in early investigation the first maximum was simply neglected. We connect the presence of intensive first maximum in the samples of WS and GS with isolation of large quantity of tarry substances during carbonization process For investigation of paramagnetic features change after metal salt adsorption WS, carbonized in atmosphere of air and argon at temperature 800^0C, was selected. ESR spectrum of initial WS samples, carbonized in air at $T=800^0C$ consists of two lines: narrow line free radical, with concentration of unpaired electrons $N=7 \cdot 10^{16}$sp/g and line width $\Delta H=6,2$Oe, and broad one from Fe^{+3} ions with $\Delta H=100$Oe and $N=8 \cdot 10^{18}$sp/g. In these samples after salts sorption of followed metals row – Cd, Mo, Fe, Co, Mn, they were generated paramagnetic complexes – metal-carbon-unpaired electrons (Me-C-unp.el.), which had different ESR line widths (47Oe, 46Oe, 15Oe, 12Oe and 29Oe) and different concentration of unpaired electrons ($8 \cdot 10^{20}$, $1,3 \cdot 10^{20}$, $0,2 \cdot 10^{20}$, $0,1 \cdot 10^{20}$, $0,6 \cdot 10^{20}$sp/g), correspondingly. Free radical states concentration

after adsorption in dependence on metal kind changed only by 1,5-2-fold. And the concentration of Co-C-unp.el. and Cd-C-unp.el. complexes exceeds Fe^{+3} ion concentration in initial sample by 1,3-fold and by 100-fold, correspondingly.

Carbonized at 800^0C in argon atmosphere WS was activated by 0,1N solution HCl. After that in WS ESR spectrum the line of Fe^{+3} ions disappear, and free radical states concentration became $N=1,4 \cdot 10^{19}$sp/g. After adsorption of Cd and Cu salts by these samples the ESR spectrum of these samples consists of two lines The broad line is due to paramagnetic complexes Me-C-unp.el, and narrow one – to free radical states with $N=4,6 \cdot 10^{16}$sp/g for both metal complexes. For the complex Cd-C-unp.el. – $N=1,6 \cdot 10^{19}$sp/g, $\Delta H=280$Oe; and for the complex Cu-C-unp.el. - $N=1,1 \cdot 10^{19}$sp/g, $\Delta H=14$Oe.

Thus, paramagnetic complexes of Me-C-unp.el. kind are generated as a results of metal adsorption. Summary concentration of unpaired electrons in the samples after adsorption is always higher than in initial samples. It requires supplementary explanation, but it is evident that paramagnetic features of these substances plays important role in adsorption metal processes.

PROPERTIES OF AlB POWDER OBTAINED BY CRUSHING Al - B COMPOSITE PRESENTING INDUSTRIAL WASTE

Mironovs V., Muktepavela F.[(1)]

Technical University, Riga, Latvia
Institute of Solid State Physics, University of Latvia, Riga, Latvia

1.Introduction

Mechanical disintegration of materials is widely used in various powder technologies. Powder production at crushing is accompanied by numerous acts of fracturing. High density of dislocations and network of microcracks has been obtained in this case. When the process of milling takes place in the active medium, like, in the air, oxides and other chemical compounds may be formed both on external and internal interfaces. As a result, powders obtained through crushing may serve as a way of producing a new heterogeneous material [1,2].

The aim of this paper is to show the possibility of utilization of waste of commercially produced Al-B fiber composites by crushing in the air. The structure and mechanical properties of obtained AlB powders and sintered compacts were investigated. Adhesion on Al/Al and Al/B interfaces at various temperatures and cleanliness of surfaces have been studied on bimetallic joints as model objects.

2.Experimental procedure

Estonian DSL type and Fritch's disintegrators were used for crushing. The samples, showing lack of bonding between fibers and matrix, were specially chosen. During crushing of such material, the free boron fibers served as additional deforming rigid elements.

The microhardness method was used for estimation mechanical properties of powder particles. The depth dependence of microhardness characterizes the mechanical properties of particles both in near-surface layers and in the bulk. The Vickers microhardness tests were performed by the original device described in [3], which is insensitive to vibration and is suitable for accurate hardness measurements over a load range from 3 mN to 2 N. Under the load range from 2 to 10 N measurements were made by the microhardness tester PMT-3. Structure investigations were carried out using Neophot-30 microscope, SEM and X-ray diffractometer. Sintering of powders was carried out after their cold pressing. The temperature of sintering varied from 393K up to 910K. Tests of mechanical strength of sintered samples were carried out on compression by machine WPM-500.

3. Results and discussion

After disintegration powder particles had diameter from 0.5 to 1.0 mm. The length of boron fibers was 2 mm . X-ray analysis of the powders showed that no new phases such as AlB_2 and AlB_{12} appear after disintegration. Boron and aluminum lines were broadened. For boron it is connected with its fine dispersed quasi amorphous state which is caused by fibers production method. Elastic stresses of deformation nature caused the broadening of the aluminium lines. Influence of oxide complexes, mixed with metal during disintegration is also possible.

Structural observations have shown that aluminium powders are strongly deformed by crushing. In the overstressed regions the large cracks could be seen. Each of Al powder particle is structurally inhomogeneous. Boron fibers were frequently broken but showed no evidence of interaction with aluminium.

The results of Al powder particle microhardness measurements are presented in Fig.1. For comparison, in the same figure values of microhardness for aluminium matrix in composite (curve 3) is shown. As it is seen the powder particles after disintegration have much higher microhardness than aluminium matrix in the composite. In the near -surface layer microhardness is even higher. It can be assumed that we deal with strongly deformed state of aluminium. However, the results of microhardness measurements for powder annealed did not confirm this conclusion. Annealing at 800 K caused the reduction of strengthening only in the

surface layer, while microhardness in the bulk did not change, being 2-3 times higher than that of aluminium in the composite matrix before disintegration.
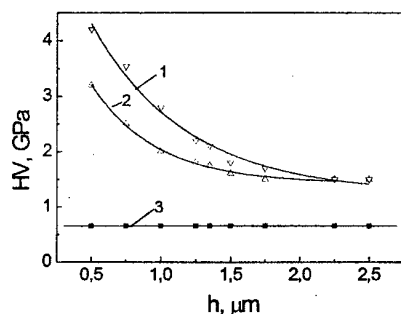
Fig.1 The dependence of microhardness on the indentation depth for aluminium powder after disintegration (1), after annealing at 800K (2) and Al matrix of the as-prepared Al-B fiber composite (3).

From these data it could be inferred that oxide compounds occur in the Al powder particles hardening them simultaneously. It is in agreement with the results of X-ray analysis and structural observations. Deep oxidation of aluminium is possible due to oxygen penetration through developed network of dislocations, grain boundaries and microcracks, which appear in the regions of stress concentrating during material disintegration. Every Al powder particle presents itself as a "composite". As it concerns boron fibers, their microhardness after disintegration corresponded to the initial value and was about 70 GPa.

Powder compacts were obtained. Received after cold pressing powders samples were monolithic and kept together, however, easily brittle failured at small loading. Sintering of such samples at 393K has resulted in some increase of their srength on compression which value did not exceed 10 MПa. Sintering at higher temperatures resulted in gradual increase of strength which at 910K has made already 90 MПa. It is interesting, that character of failure could be treated as q quasi brittle with some share of plasticity. Sintered samples had small density (2.2 g/cm^3) and represented dielectric. Stable oxides determine also the strength and adhesion on the Al/B and Al/Al interfaces. Investigations of the adhesion show that the adhesion strength of the Al/Al joints increases under annealing at 400 K while their softening after annealing at 800 K was observed.

The strength of Al/B joints increased only under annealing at 800 K. The effect of annealing on the deformation behaviour of atomically-clean and oxidized interfaces is quite different. These data together with the results of our fractographic investigations allow to conclude that annealing leads to ..., increase of the adhesion and plasticity of the oxidized interface layer.

In summary we shall notice, that, Al-B powder possessing high hardness properties can be successfully applied as an abrasive material for doping grinding pastes. Another example of applying the Al-B powder is fabricating the powder based grinding tools. For that purpose Al-B powder was mixed with polymer filler and then pressed and polymerized. The obtained samples containing 30-60% Al-B were used for fabricating the abrasive wheel which could be applied to the treatment of glass, metals and ceramics.

The received data about mechanical and physical properties of sintered AlB ceramic have preliminary character and demand the further researches. However, it is possible to notice, that new AlB ceramics consequently its small density and also sufficient strength at small brittleness is perspective for use as isolators and other designs, it is especial in transport mechanical engineering.

References

1.A.Benghalem and D.G.Morris, Acta Met. et Mat., 1994 ,42, 4071.
2. M.Oehring, Z.H.Yan, T.Klassen and R.Borman,Phys.Stat.Sol.A,1992, 131, 671.
3.G.P.Upit and S.Varchenya, In Sci. Instruments, Zinatne, Riga, 1986, p.12.

REFINEMENT OF SUPERALLOYS SCRAP BY METHODS OF VACUUM REMELTING

Dobkyna Yuliya[1], **Dr. Myalnitsa H.F.**[2]
[1]Physico-Technological Institute of Metals and Alloys (PTIMA) NAS of Ukraine, Kiev, Ukraine
[2]SPE "Mashproekt", Nikolaev, Ukraine

A complex of research activities for establishing the thermal stability of the cast alloys structure CHS88UVI and CHS104VI type (like IN738, Rene41) has been conducted. These alloys were recovered from non – return wastes, which had been generated during the casting of blades on gas turbine engine (GTE).

Two stages process, that included vacuum thermal melting with directional crystallization (VTMDC) and subsequent vacuum induction melting was employed. VTMDC process was carried out in the PMP-4M unit that had been usually used for cast blades production. Regeneration of components of the solid solution of alloy from high temperature compounds was realized in the second stage. In addition there was conducted the refinement of the superalloys scrap from metallic admixture and non-metallic inclusions.

The recycling high temperature alloys for gas turbine engines is of great concern to Ukrainian specialty metallurgy. It is a basic problem since there are a lot of companies, which produce these engines for aviation, ship building and energetic.

The vacuum induction melting is a common method for recycling vacuum grade superalloy scrap. However this method is insufficient while applied for refining scrap contaminated by non-metallic inclusions. The problem is one of the "hottest" for recycling of used or rejected blades of gas turbine engines. The blades were coated by non-metallic phases that were difficult to separate by means of ordinary mechanical and chemical operations. Moreover a part of the phases located on internal surfaces of a refrigerated blade. Since these scraps cannot be classified as pedigree ones they should be used at the charges of lower grades alloys. This option doesn't seem to be sound enough from economic considerations. Another unacceptable option is recycling the scraps abroad on toll bases. Therefore a development of the newest approaches based on combination of different recycling methods is an urgent point.

We would like to present a new two- stage refining technology in vacuum. It consists of filtration process followed by deep refining of a melt under specific conditions. So superalloy scraps are remelted in vacuum- thermal furnace designed for unidirectional solidification of a melt at the first stage. This process was mentioned already in the report about the results of our researches, which confederate during the Canada conference. After That a semi-finished product is remelted in vacuum-induction furnace with a peculiar temperature condition. The first stage recycling is characterized by alloy refining from exogenous non-metallic inclusions and dissolved gases. This process runs during scraps remelting under vacuum in the melting device PMP-4M, where solidification by zones of an alloy takes place after complete melting of metal. It causes a complete removal from the alloy of non-metallic phases and detrimental elements. The special ceramic mold was designed for providing deep filtration process. This effect can be reached due to the application of a unique multilevel construction of the mold and a common filter. The mold is set into a graphite box and covered with graphite shots. The reluctant ambient of a mold is reached by carbon presence in the melting device. The possibility of another oxidation of a melt is prevented in such a way.

The scraps set into upper part of a mold are melted by induction heating over a wide range of superalloy's solidus-liquidus temperatures (1270 – 1335 °C). Then a melt is heated up to melting point of nickel (1450 °C). So a nickel partition, which prevents a charge getting a mold bottom, is melted. The molten alloy soaks throw a filter under gravity power and gets released from exogenous inclusions. The additional refinement is reached through unidirectional solidification of alloy, which starts from bottom of a mold on three inoculating crystals. These superalloy monocrystals initiate solidification with orientation. The exogenous inclusions, which still remain in a melt, are pushed aside by crystallization front and located at tops of three forming ingots. The parts of the alloy admixed by the inclusions are separated by shearing.

In the same cases such complex refining procedure is insufficient for usage of produced alloy for casting the high performance blades. The additional specific vacuum induction melting is applied. The process runs under 0,133 Pa pressure. The rigid temperature control and vigorous induction mixing provide the conditions favorable for additional melt refinement. Our specific vacuum induction melting slightly differs by electric power consumption and termination from the traditional one. The experimental melts were carried out in 8-kg capacity UPPF-2 furnace. The traditional scraps from Cr-bearing Ni-based high temperature alloys ChS88U and ChS104 were used. These grades are applied for production of blades of power gas turbine engines and gas pumping devices. The scraps were sheared and processed by the first stage of refining. The semi-finished products were subjected to the second stage of refining. The alloy was cast into ceramic molds, which had been heated up to 1000° C. The molds were manufactured by lost wax process.

The average chemical compositions of the produced ingots agreed with technical requirements. Particularly the content of detrimental admixtures and gases are in specification due to the second stage of the recycling ($Mg \approx 0.01$, $Sn < 0.0005$; $Sb < 0.001$; $Bi < 0.005$; $In < 0.001$; $Cb < 0.00005$; $O_2 < 0.0035$; $H_2 < 0.0003$). Therefore it is obvious that the produced ingots should be applied in high performance castings production.

Macrostructure of the produced ingots was characterized by the dense and homogenous structure, the absence of zonal segregation and insufficient shrinkage porosity. These facts evidence chemical homogenization of the ingots through there longitude. Spectrochemical analyses, which had been carried out showed the same effects.

Microstructure of the polished specimens cut out from upper, middle and bottom ingot's zones and in longitudinal and cross sections was examined. Its characteristic features are spheroidization of shapes of the carbides, low content of nitride and carbo-nitride non-metallic inclusions and virtually complete absence of $M_{23}C_6$ and MC phases.

The mechanical properties of ChS88U and ChS104 were measured on the cast coupons, which had been produced under vacuum along with the castings for blades. They are the technical requirement as well.

APPLICATION OF THERMALLY EXPANDED GRAPHITE FOR WATER SURFACE SPILLAGE COLLECTING

Vishnyakov L.R., Moroz V.P., Kossiguin E.P., Kovalchuk N.M., Sinaiskiy B.M.
Frantsevich Institute for Problems of Materials Science, National Academy of Sciences, Kyiv, Ukraine

The problem of minimization of ecological disasters which are accompanied by oil spillage is associated with difficulties of its collection from the water surface.

The oil spillage as a result of tanker damages is typically localized by booms, then mechanically collected using special means. However this method has the following disadvantages: the collected product may contain water, thus excluding its further usage; and, besides, the water surface has remainder oil spots due to a non-sufficient cleaning thus creating additional ecological problems, time consuming and high cost.

The most efficient removal of the oil from the water surface is achievable through the sorbent use [1-2]. It is known that thermally expanded graphite (TEG) has a greater potential as sorbent for various oil products being a high modification of the natural graphite, having a developed surface and good adhesion to the most organic compounds [3]. The sorptive capacitance of TEG can reach 60 g/g, it is fully hydrophobic.

However, a number of problems remains not overcome: selection of a proper grade of TEG powder, need of a certain procedure of powder preparation for its transportation to the spilled areas.

There are considerable resources of natural graphite available in Ukraine thus allowing to become a producer and exporter of new potential sorbent for Ukraine. So, the Institute for Problems of Materials Science, NAS of Ukraine, is now involved in the search of an efficient use of TEG for oil spillage cleaning application.

This paper describes a comparative study of TEG powder properties of ГАК-2, ГСМ-1 grades and pyrolitic graphite. To prepare the TEG powder, a technology was used which included the chemical treatment of natural graphite powder by solutions of concentrated sulfuric acid added with potassium bichromate (4 wt.%) and thermal treatment of resultant oxidized graphite to up to 1000 ^{0}C in a continuous furnace [4].

The thermal treatment yielded 200-300 times expanded graphite particles along the C-axis, which had a worm-like structure.

The sorbent surface and chemical compositions were examined using scanning microprobe analysis on the COMEBAX SX-50 instrument. It was found that the TEG particles had a worm-like form. Bulk density is an important feature of TEG as sorbent, which correlates with its specific area. The properties of the TEG grades studied are shown in Table

Properties of studied TEG grades

Characteristic	Grade		
	ГАК-2	ГСМ-1	Pyrog-raphite
Particle size along, microns transverse, microns	1041.0 291.0	1064.0 331.2	708.0 220.0
Bulk density, g/dm^3	6.32	2.88	17.5
Ash, % maximum	0.6	0.55	1.2
Chemical composition, % Sulfur Carbon	0.22 99.6	0.2 9.,8	0.4 99.2

As experiments have shown, all the TEG powders increase their bulk densities with sulfur and ash contents. On the other hand, a reverse relationship is observed of powder bulk density of worm-like powder size and carbon amount.

It was found through the chemical composition analysis, the bulk density of more «pure» powders was lower. Thus, for instance, such elements as iron, silicon, aluminum, etc. in the ГСМ-1 are in significantly smaller quantities as in the ГАК-2 powder and pyrolitic graphite.

The sorbents were evaluated for potential under laboratory conditions. To determine the sorptive capacity of TEG powders, a broad cylindrical reservoir was filled with water and added with oil. The TEG powder was uniformly distributed all over the surface of reservoir and mixed. The powder containing absorbed oil was then collected using a metallic screen. The collected matter was weighed. The sorptive capacity is defined as $(m-m_g)/m_g$, where m is the weight of powder with absorbed oil and m_g is the weight of TEG powder in grams.

As experiments have shown, all the used TEG powders had high hydrophoby degree and were easy collected from the water surface after the oil absorption.

The studies concluded the sorptive capacity of TEG powders of 47 g/g, 41 g/g, 36 g/g, respectively for ГСМ-1, ГАК-2 powders and pyrolitic carbon, the values are better than for known sorbents, which not exceeding 10 g/g. This agent only absorbs the organic liquid, which can be 70-80% recycled during subsequent processing, thus notifying another important feature.

The sorptive capacity study of compacted TEG powders showed their efficiency for use in the oil cleaning. Moreover, the powder does not drown and can be removed from the surface without leaving traces.

To resolve the problem of TEG transportation emerged from its low bulk density, we are in stage of developing a technology of powder compacting and encapsulating using porous materials.

The study confirmed the potential of thermally expanded graphite for collecting the oil products from the water surface.

REFERENCES

1. V.Arens, and O.Griden. Efficient sorbents for oil spillage collecting// ЭкиП, 1997, No.2, P. 32-37.
2. M.Perederiy. Sorptive materials made of coal// XTT, 2000, No. 1, P.35-44.
3. I.Chernish, I.Karpov, and G.Prikhodko. Physical and chemical properties of graphite and compounds . Kiev: Naukova Dumka, 1990, 200 p (In Russian).
4. L.Vishnyakov, T.Chizhankov, V.Moroz et al. Designing of new sealing composite materials made of reinforced thermally expanded graphite. In Proceed. of reports «Researches in composite material area», Institute for Problems of Materials Science, NAS of Ukraine. 1995. P.128-139 (In Russian).

PREPARATION OF WC AND WC-Co HARD ALLOY MIXTURE BY REDUCTION-CARBIDIZATION OF OXIDEZED TUNGSTEN WASTES

Babutina T.E., Uvarova I.V.
Institute for Problems of Materials Science NAS of Ukraine, Kyiv, Ukraine

The problem of remaking of tungsten containing wastes is very important for Ukraine not having own reserves of tungsten mineral.

Using the thermochemical method for regeneration tungsten wastes supposes two main operations: oxidation of wastes with the subsequent reduction – carbidization. There are some methods for realization operations of reduction – carbidization, which can be conditionally divided to two groups: traditional technologies with carbon using [1] and without carbon technologies with methane/hydrogen atmosphere using [1, 2].

In [3] the method of simultaneous reduction – carbidization of oxidized tungsten wastes in the methane/hydrogen atmosphere of a precision controlled composition is offered. But creation the methane/hydrogen atmosphere of a precision controlled composition demands application of the special equipment for the control of gas mixture.

In this work the products of thermodestruction of high hydrocarbons is offered to use as gas atmosphere. This process is remarkable for a maximum simplicity and does not demand using of the gas communications or balloon.

The data obtained into the half-industrial muffle and laboratory furnaces were compared. The previously oxidized WC-Co hard alloy industrial wastes and tungsten wire wastes were used. In the case of reduction – carbidization of hard alloys oxidized wastes the carbon was added into the mixture. Requisite quantity of carbon was added in accordance with stoichiometry WC. The reduction – carbidization of tungsten wire was carried out without using of carbon.

The high hydrocarbon destructs at temperatures 450 – 750 °C. At first there is a hydrogen appearance. Then C-C connection breakage is observed. Thus in a hot zone of furnace high hydrocarbon instantly decompose gassing hydrogen, which creates a reducing atmosphere. At a further destruction the lowest hydrocarbon forms

and reduction – carbidization atmosphere is created. The atmosphere composition is determined by following reactions:

$$MeO+H_2=Me+H_2O \qquad (1)$$
$$CH_4+ H_2O=CO+ 3H_2 \qquad (2)$$
$$CO+ H_2O=CO_2+H_2 \qquad (3)$$
$$CH_4+CO_2=2C+2H_2O \qquad (4)$$
$$C+CO_2=2CO \qquad (5)$$
$$C+H_2O=CO+H_2 \qquad (6)$$
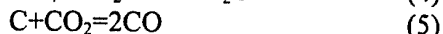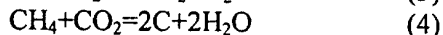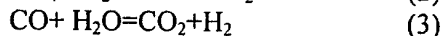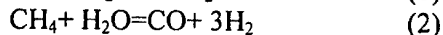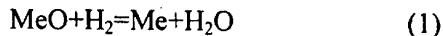
The manufacture of tunggsten carbide depends on the thermodynamics of systems containing its constituent elements.

The detailed analyze of thermodynamics of the hydrogen-carbon-oxygen-tungsten (cobalt-tungsten) system equilibrium being reviewed in [4, 5] were made. Reduction – carbidization was carried out according to the thermodynamic data. Thus, it was possible to avoid carbon losses, which is characteristic for process spending into hydrogen medium. Also upsetting of redundant carbon taking places during reduction – carbidization into methane/hydrogen atmosphere at deviation the composition from equilibrium was not observed.

The different temperature-time dependence for processing reduction – carbidization was studied. Phase composition and quantity of oxygen, bound and free carbons in the final products of reactions were determined by X-ray and chemical analysis. Specific surface areas were determined by the thermal nitrogen desorption.

It was shown that in all cases specific surface areas were decreased at increasing of process time.

As can be resulted the kinetic data for tungsten oxide reduction – carbidization stepwise transformation WO_3 in W though a phase of dioxide WO_2 and then the transformation into WC though a phase W_2C was found. In this case the process is controlled by diffusion and depends on temperature and process time. Reduction WO_3 was finished at 900 °C. Carbidization was began at 1000 °C and finished at 1100 – 1150 °C into laboratory and half-industrial muffle furnace

accordingly. Specific surface area was 2,4 – 2,7 m²/g for WC received into laboratory furnace and 2,3 m²/g for WC received into half-industrial muffle furnace. The contents of oxygen were 0,6 – 0,8 % at all cases and maximum quantity of free carbon were 0.5 %.

The reduction – carbidization of mixture $CoWO4+WO_3$ was studied in presence and absence of carbon differently. Stoichiometric WC composition could be obtained only at the presence of carbon. At using of carbon from a gas phase received by decomposing of high hydrocarbon process occurred slowly and phases of Co_3W_3C+ free carbon were obtained under the same conditions.

The difference in passing of reduction – carbidization for $CoWO_4+WO_3$ as against WO_3 connected with the presence of cobalt in mixture. Cobalt is known as the activator [6,7] influencing on carbidization of a chemical mixture $CoWO4+WO_3$, when it does not combine in intermetallic. In this case it accelerate the reaction of methane decomposition and increase the coefficient of carbon diffusion, as it is in four degree higher in cobalt against one in WC. The appearance of Co_7W_6 and Co_3W intermetallic phases decreases the carbidization degree strongly [8]. Carbidization of Co_7W_6 intermetallic includes the stage of Co_3W_3C formation with following production of WC+Co mixture.

$$Co_7W_6+2C\rightarrow2Co_3W_3C+Co \qquad (7)$$
$$\underline{Co_3W_3C+4C\rightarrow6WC+6Co} \qquad (8)$$
$$Co_7W_6+6C\rightarrow6WC+Co \qquad (9)$$
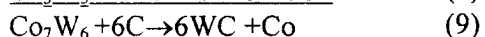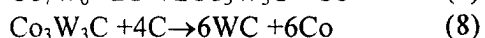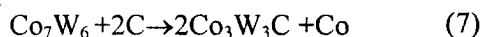
As can be seen in [8] the carbidization rate increase in the presence of cobalt 7% and decrease at the cobalt content of higher 7%. Investigated wastes relate to type of hard alloys containing cobalt higher liminal 7%. Thus, the fact of whole carbidization in mixture $CoWO_4 + WO_3$ was observed only in the presence of carbon. Reduction-carbidization of such mixture at the analogical temperature-time condition has taken place with the Co_3W_3C intermetallic formation without carbon.

In the case of WO_3 reduction-carbidization stochiometric WC was produced without hard carbon. According to thermodynamic data and the component concentration [8] the carbon activity in the mixture of CH_4/H_2 and CO/CO_2 increase in the row:

$$CO<C_{hard}<CH_4$$

Thus, carbidization of tungsten by mixture CH_4/H_2 is the most convenient in comparison of hard carbon. At high hydrocarbon thermodestruction had also obtained the mixture of methane and higher hydrocarbons with hydrogen.

Produced powders with high specific surface area had been used in galvanophoretic coatings and shown the increasing of corrosion and abrasive resistance in 3-5 times.

References

1. Пат. 3953194 США. Способ регенерации цементированных карбидов, 1976. Опубл. 20.06.75.

2. Васкевич Н.К., Сенчихин В.К., Третьяков В.И. К вопросу получения смесей WC –Co // Цвет. Металлургия. –1984. - № 2. –С. 34 – 37.

3. Термохимический способ регенерации отходов твердых сплавов с применением метановодородной газовой среды прецизионного состава / Бондаренко В.П., Павлоцкая Э.Г., Мартынова Л.М., Мошкун В.Ф.// Прогрессивные методы и средства обеспечения качества изготовления деталей машин. – Н.Новгород, 1992. – С.108 – 109.

4. G. Kris Schwenke, Thermodynamics of the hydrogen – carbon – oxygen – tungsten system, as applied to the manufacture of tungsten and tungsten carbide//15th International Plansee Seminar, Eds.G. Kneringer, P. Rodhammer and H. Wildner, Plansee Holding AG, Reutte, 2001, Vol.2, p.647 - 661

5. Петухов А.С. Химические и фазовые превращения при восстановлении и карбидизации сложных вольфрам кобальтовых соединений. 1.Термодинамическая оценка вероятности реакций восстановления и карбидизации сложных вольфрам кобальтовых оксидных систем // Порошковая металлургия. – 1990.- №4. – С.35-39.

6. Третьяков В.И., Сенчихин В.К., Васкевич Н.К. и др. // Влияние кобальта на процесс карбидизации вольфрама метаном // Порошковая металлургия. – 1990. - №11. – с.32-36

7. Ushiima K., Fuqii K., Mechanism of WC formation from WO₃ added Co₃O₄ and Co//G.Gap. Int. Met. – 1978. – №9.- p.876 – 881

8. Васкевич Н.К., Сенчихин В.К., Третьяков В.И. Некоторые вопросы термодинамики карбидизации вольфрама// Порошковая металлургия. – 1985. – №6. – с.69-73

UTILIZATION OF FERROALLOYS WASTES UNDER CAST IRON MODIFICATORS PRODUCTION

V.Masliuk, O. Shinsky[1], V. Kurovsky,V.Litovka[1]
Institute for Problems of Materials Science of NASU, Kyiv, Ukraine
Physico-Technological Institute of Metals and Alloys Science of NASU, Kyiv, Ukraine

Preparation of smelted ferroalloys (on the base of ferrosilicon, silicomanganese, silicocalcium and others) is obliged to produce wastes in the powder kind.

Last investigations in Ukraine and abroad have shown perspectives to utilize these wastes by pressing with addition of metallic powders for modifying briquettes production.

Some comparative figures about economical efficiency of master alloys/briquettes are shown :
energy consumption - kWh/hour/MT - 1500+-200/140+-20
magnesium solution, % 70+-10/100
comparative consumption,%,100/75+-5

Analysis of well-known briquettes are shown, that they have some binder elements, which will introduce in melt in kind of slag.

Proposed briquettes do not have binder elements and do not impurity liquid metal.

In some explorations we have clarified precise conditions of mechanical pressurizing, magnesium content, some alloying elements.

Briquettes density is dependent from their dimensional characteristics. Mechanical strength is dependent from porosity, that's why one of the most important under briquettes technology production are : pressure effort, weight, dimension and briquettes content.

As a result of investigation is shown, that under porosity rising is positive attendance on raised temperature. As a reverse, content of graphite spheroidization is lowering under weight growing of each briquette..

In comparison with alloying elements of analogic content briquettes have ensured production of graphite portions with larger dimension and more bigger content of ferrite in cast iron, that we can explain by presence of dispersed components in briquettes (Ferro, ferrosilicon), which has a crystallization centers during graphitization.

Regimes of briquettes-modifocators also influence on durability of their solubility in cat iron. And dependent from pressurizing has an external characteristics.

Briquettes-modificators of optimal developed contents and regimes of production have been tested in production conditions with positive effect under casting of high-stressed castings (crankshafts, transmission case, etc.) by ductile and vernacular graphite cast irons, and relied their competitiveness with others more expensive modificators in kind of alloyed modificators.

LIST OF PARTICIPANTS

A

AKSENOV V.B.
Siberian Physic -Technical Institute, Tomsk, Russia
Tel.: (3822) 53-3209
Fax: (3822) 53-3034
E-mail: chum@phys.tsu.ru

ABELL S.
University of Birmingham, Birmingham, United Kingdom
Tel.: (44 121) 414-5232
Fax: (44 121) 414-5232
E-mail: j.s.abell@bham.ac.uk

ABENOJAR J.
Universidad Carlos III de Madrid, Spain
Tel.: (3491) 624-9914, 624-9485, 624-9401
Fax: (3491) 624-9430
E-mail: abenojar@ing.uc3m.es

ABRAMOV YE.V.
State Firm «Central Design Office «Arsenal», Kyiv, Ukraine
Тел: (044) 483-36-11
Fax: (044) 444-3611

ABRAMOVSKAYA M.
Institute of Technical Mechanics of NASU and NASUU, Dniepropetrovsk, Ukraine
Tel.: (0562) 47-2588
Fax: (0562) 47-3413
E-mail: bass@pvv.dp.ua

ADEEV V.M.
Frantsevich Institute for Problems of Materials Science, NASU, Kyiv, Ukraine
Tel.: (044) 444-0294, 444-1573
Fax: (044) 444-2131
E-mail: vadima2001@mail.ru

AGASHKOVA N.N.
Verkin Technologies Institute for Low Temperature Physics and Engineering, NAS of Ukraine, Kharkov, Ukraine
Tel.: 322-293,322-019, 300-364, 300-355
Fax: 322-293, 321-292
E-mail: gavrylov@cryocosmos.com, moril@cryocosmos.com

AKSYUTENKO A.
Institute of Technical Mechanics of NASU and NASUU, Dniepropetrovsk, Ukraine
Tel.: (0562) 47-2588
Fax: (0562) 47-3413
E-mail: bass@pvv.dp.ua

ALEXANDROVA L.I.
Bakul Institute for Superhard Materials Science, NASU, Kyiv, Ukraine
Tel.: (044) 430-1126
Fax: (044) 468-8625
E-mail: prikhna@iptelecom.net.ua, frd@ism.kiev.ua

ALEXEEV M.K.
Federal State Unitary Enterprise «Obninsk Research and Production Enterprise «TECHNOLOGIYA», Obninsk, Russia
Tel.: (08439) 96-887
Fax: (08439) 64-575
E-mail: info@technologiya.ru, onpptechn@kaluga.ru

ALFINTSEVA R.A.
Frantsevich Institute for Problems of Materials Science, NASU, Kyiv, Ukraine
Tel.: (044) 444-0256

ANCHAROV A.I.
Institute of Solid State Chemistry and Mechanochemistry SB RAS, Novosibirsk, Russia
Tel.: (3832) 39-4145
E-mail: ancharov@mail.ru

ANDREEVA A.F.
Frantsevich Institute for Problems of Materials Science, NASU, Kyiv, Ukraine
Tel.: (044) 444-8218
E-mail: andreeva@ipms.kiev.ua

ANDRIEVSKI R.A.
Institute of Problems of Chemical Physics RAS, Chernogolovka, Russia
Tel.: (096) 522-3577
Fax: (096) 522-3577
E-mail: ara@icp.ac.ru

ANIKIN Y.P.
Physics and Technology Institute for Metals and Alloys, NAS of Ukraine, Kyiv, Ukraine
Tel.: (044) 444-3550, 444-1210
Fax: (044) 444-3550, 444-1210
E-mail: maksyuta@ptima.kiev.ua, anikin@ptima.kiev.ua

ANTONOVICH YA.V.
Institute of Machine Reliability National Academy of Sciences of Belarus, Minsk, Belarus
Tel.: (017) 284-2401
Fax: (017) 284-24-01
E-mail: nanotech@inmash.bas-net.by

ANTSIFEROV V.N.
Research Center of Powder Material Science, Perm, Russia
Tel.: (3422) 39-1119, 39-1127
Fax: (3422) 39-1122
E-mail: director@pm.pstu.ac.ru, kpmc@pm.pstu.ac.ru

ANUCHIN S.A.
Bauman Moscow State Technical University, Moscow, Russia
Tel.: (095) 263-6705
Fax: (095) 261-0107

ARINKIN S.M.
Lykov Heat and Mass Transfer Institute, National Academy of Belarus, Minsk, Belarus
Tel.: 284-1351, 284-13-19
Fax: 284-1515
E-mail: sergey_demidkov@tut.by

ARISTARKHOV D.V.
Scientific and production company «Ecology Energy»,
Moscow, Russia
Tel.: (095) 482-4345
Fax: (095) 482-4345
E-mail: WW@esc.ru, ee@esc.ru, vas@hmti.ac.by

ASHIKHMIN V.P.
Institute for Solid-State Physics, Materials Science and
Technology at National Science Center «Kharkov
Institute of Physics and Technology» (ISSPMST NSC
KIPT), Kharkov, Ukraine
Tel.: (0572) 3503530
Fax: (0572) 35-1688
E-mail: sayenko@kipt.kharkov.ua

AZHAZHA ZH.S.
Institute for Solid-State Physics, Materials Science and
Technology at National Science Center «Kharkov
Institute of Physics and Technology» (ISSPMST NSC
KIPT), Kharkov, Ukraine
Tel.: (0572) 3503530
Fax: (0572) 35-1688
E-mail: sayenko@kipt.kharkov.ua

B

BABICH M.G.
Shevchenko Kyiv National University, Kyiv, Ukraine
Tel.: (38044) 266-2335
E-mail: babich@mail.univ.kiev.ua

BABUTINA T.E.
Frantsevich Institute for Problems of Materials Science,
NASU, Kyiv, Ukraine
E-mail: uvarova@materials.kiev.ua

BAGLYUK G.A.
Frantsevich Institute for Problems of Materials Science,
NASU, Kyiv, Ukraine
Tel.: (044) 444-3364
E-mail: dep.40@materials.kiev.ua

BAKLANOVA N.I.
Institute of Solid State Chemistry and
Mechanochemistry SB RAS, Novosibirsk, Russia
Tel.: (3832) 32-9600
Fax: (3832) 322847
E-mail: servis_ins@online.sinor.ru,
lena@mill.solid.nsc.ru

BAKULIN V.N.
Institute of Applied Mechanics RAS, Moscow, Russia
Tel.: (095) 192-4615
Fax: (095) 192-4615
E-mail: rvv@page.net.ru

BARABASH M.YU.
Frantsevich Institute for Problems of Materials Science,
NASU, Kyiv, Ukraine
Tel.: (044) 570-7823, 444-1090
Fax: (044) 444-1090
E-mail: ybar@mail.valtek.kiev.ua,
olik@materials.kiev.ua

BARABASH O.M.
Kurdyumov Institute for Metal Physics, NASU, Kyiv,
Ukraine
Tel.: (044) 444-3061
Fax: (044) 444-3061
E-mail: korzhova@materials.kiev.ua

BARANOV V.L.
Puhov Institute of Power Engineering Simulation
Problems NASU of Ukraine, Kyiv, Ukraine
Tel.: (08439) 96-659, 99-041,96-875
Fax: (08439) 64-575
E-mail: info@technologiya.ru, onpptechn@kaluga.ru

BARANOVA T.F.
Federal State Unitary Enterprise «Obninsk Research
and Production Enterprise «TECHNOLOGIYA»,
Obninsk, Russia
Tel.: (08439) 96-659, 99-041,96-875
Fax: (08439) 64-575
E-mail: info@technologiya.ru, onpptechn@kaluga.ru

BARSCHEVSKA A.K..
Frantsevich Institute for Problems of Materials Science,
NASU, Kyiv, Ukraine
Tel.: (044) 444-2401
Fax: (044) 444-2401
E-mail: vish@i.com.ua

BARYKIN N.P.
Institute for Metals Superplasticity Problems, RAS, Ufa,
Russia
Tel.: (3472) 25-3750, 25-3815
Fax: (3472) 25-3759
E-mail: imsp11@anrb.ru, aigirsh@rambler.ru

BASS V.
Institute of Technical Mechanics of NASU and NASUU,
Dniepropetrovsk, Ukraine
Tel.: (0562) 47-2588
Fax: (0562) 47-3413
E-mail: bass@pvv.dp.ua

BAZELYUK G.YA.
Kurdyumov Institute for Metal Physics, NASU, Kyiv,
Ukraine
Tel.: (044) 444-9590, 444-1548
E-mail: rkp@imp.kiev.ua, skrypnyk@i.com.ua

BEDNAYA K.L.
Research-and-Production Corporation «Technology-
2000» Ltd, Kharkov, Ukraine
Tel.: (0572) 92-2167
Fax: (0572) 16-2180
E-mail: kt_2000@ukr.net, kgv_2000@mail.ru

BELOTSERKOVETS I.S.
Institute of Technical Mechanics of NASU and NASUU,
Dniepropetrovsk, Ukraine
Tel.: (0562) 46-1051, 47-2465
Fax: (0562) 47-3413
E-mail: itm@tim3.dp.ua, galinskyv@mail.ru

BELOUSOVA V.I.
Urals State Technical University (USTU- UPI),
Ekaterinburg, Russia
Tel.: (3432) 5-2361, (3432) 75-9420, (08439) 6-6317
Fax: (34392) 5-2361, (08439) 6-6317
E-mail: polytech@mtf.ustu.ru, frantish@freemail.ru,
kerambet@ok.ru

BELYAEVA E.I.
Institute of Solid State Chemistry and
Mechanochemistry SB RAS, Novosibirsk, Russia
Tel.: (3832) 32-9600
Fax: (3832) 322847
E-mail: lena@mill.solid.nsc.ru

BEREZANSKAYA V.
Frantsevich Institute for Problems of Materials Science,
NASU, Kyiv, Ukraine
Tel.: (044) 444-1124
E-mail: SLYS@materials.kiev.ua

BESOV A.V.
NTUU «Kyiv Polytechnic Institute», Kyiv, Ukraine
Tel.: (044) 441-1546
E-mail: oksana@materials.kiev.ua

BEZIMYANNIY Y.G.
Frantsevich Institute for Problems of Materials Science,
NASU, Kyiv, Ukraine
Tel.: (044) 444-2055
Fax: (044) 444-2131

BLOSCHANEVICH A.M.
Frantsevich Institute for Problems of Materials Science,
NASU, Kyiv, Ukraine
Tel.: (044) 444-1191
E-mail: lavrenko@svitonline.kiev.ua

BOBONAZAROV KH.
Khujand Scientific Center of Tajik Academy of
Sciences, Khujand, Tajikistan
Tel.: 5-1774
E-mail: khush@khj.tajik.net

BOEHMERT J.
Forschungszentrum Rossendorf e.V., Institut für
Sicherheitsforschung, Dresden, Germany
E-mail: brit@eurocom.od.ua

BOGATCHEV E.A.
Open Joint-Stock Company «KOMPOZIT», Institute of
Metals, Korolev, Russia
Tel.: (095) 513-2306, 513-2180
Fax: (095) 516-0628, 516-0617
E-mail: eug-bogatchev@mail.ru,
kompozit.mat@g23.relcom.ru

BOGATIRIOVA J.D.
Physics and Technology Institute for Metals and Alloys,
NAS of Ukraine, Kyiv, Ukraine
Tel.: (044) 444-1424
Fax: (044) 444-3542
E-mail: kompozit@inec.Kyiv.ua

BOGOMOLOVA O.A.
Institute of the Theoretical and Applied Mechanics SB
RAS, Novosibirsk, Russia
Tel.: (3832) 30-4273
Fax: (3832) 34-2268
E-mail: shulgin@itam.nsc.ru, vetal@sibnet.ru

BOLGAR A.S.
Frantsevich Institute for Problems of Materials Science,
NASU, Kyiv, Ukraine
Tel.: (044) 444-1290
Fax: (044) 444-2131
E-mail: bas@materials.Kyiv.ua, kopa@alex-ua.com

BOLOTOVA L.
Baikov Institute of Metallurgy and Material Science,
RAS, Moscow, Russia
Tel.: (095) 135-9652
Fax: (095) 135-4455
E-mail: chern@ultra.imet.ac.ru

BONDAR V.I.
Kurdyumov Institute for Metal Physics, NASU, Kyiv,
Ukraine
Tel.: (044) 444-9588, 444-3577
E-mail: danila@imp.Kyiv.ua

BONDARENKO M.E.
Frantsevich Institute for Problems of Materials Science,
NASU, Kyiv, Ukraine
Tel.: (044) 444-0256
Fax: (044) 444-2131
E-mail: leonid@materials.Kyiv.ua

BONDARENKO T.
Frantsevich Institute for Problems of Materials Science,
NASU, Kyiv, Ukraine
Tel.: (044) 444-3573
E-mail: zyrin@ipms.Kyiv.ua rs@ipms.Kyiv.ua

BORISENKO V.A.
Institute for Problems of Strength, NASU, Kyiv, Ukraine
Tel.: (044) 295-6030
Fax: (044) 296-1684
E-mail: v.krivenyuk@ipp.adam.Kyiv.ua,
nick@ipp.adam.Kyiv.ua

BOROVINSKAYA I.P.
Institute of Structural Macrokinetics and Materials
Science
RAS, Chernogolovka, Moscow region, Russia
Tel.: (09652) 46-244, 962-8007
Fax: (09652) 962-8025
E-mail: inna@ism.ac.ru

BORTS B.
Institute for Solid-State Physics, Materials Science and
Technology at National Science Center «Kharkov
Institute of Physics and Technology» (ISSPMST NSC
KIPT), Kharkov, Ukraine
E-mail: borts@kipt.kharkov.ua

BORYSENKO V.A.
Institute for Problems of Strength, NASU, Kyiv, Ukraine
Tel.: (044) 295-6030, 296-5657
Fax: (044) 296-1684
E-mail: nick@ipp.adam.Kyiv.ua

BRAKHNOV N.
Frantsevich Institute for Problems of Materials Science,
NASU, Kyiv, Ukraine
Tel.: (044) 444-1124
E-mail: SLYS@materials.Kyiv.ua

BRATANICH T.I.
Frantsevich Institute for Problems of Materials Science,
NASU, Kyiv, Ukraine
Tel.: (044) 444-1533
Fax: (044) 444-2131
E-mail: tibrat@ipms.Kyiv.ua

BRITAVSKAYA E.
South Ukrainian State Pedagogical University, Odessa,
Ukraine
E-mail: brit@eurocom.od.ua

BRONOVETS M.A.
Interdisciplinary Scientific Tribology Council, Moscow,
Russia
E-mail: brnovets@ipmnet.ru

BRUSILOVETS A.I.
Shevchenko Kyiv National University, Kyiv, Ukraine
Tel.: (044) 266-2335, 266-2384
E-mail: babich@mail.univ.Kyiv.ua,
matzui@mail.univ.Kyiv.ua

BRUSKO A.T.
Institute of Traumatology and Ortopedic of MSA of
Ukraine, Kyiv, Ukraine
Tel.: (044) 216-1633, 216-6983

BUKHANOVSKY V.V.
Institute for Problems of Strength, NASU, Kyiv, Ukraine
Tel.: (044) 295-6030, 296-5657
Fax: (044) 296-1684
E-mail: nick@ipp.adam.Kyiv.ua

BUNCHUK J.P.
State Design Office Yuzhnoye, Dniepropetrovsk,
Ukraine
Tel.: (0562) 92-5113, 92-0866
Fax: (0562) 92-5113
E-mail: kbu@public.ua.net, bunchuc@a-teleport.com

BUNIN V.A.
Institute of Structural Macrokinetics and Materials
Science
RAS, Chernogolovka, Moscow region, Russia
Tel.: (09652) 4-6240, 4-6357, (095) 962-8007
Fax: (095) 962-8040
E-mail: bunin@ism.ac.ru, Inna@ism.ac.ru

BURKAT G.K.
Special Design Bureau «Tekhnolog» at the Saint-
Petersburg State Technological Institute
(Technical University), Saint-Petersburg, Russia
Tel.: (812)100-3898
Fax: (812) 100-3898
E-mail: alcen@comset.net

BURLACHENKO Y.V.
Frantsevich Institute for Problems of Materials Science,
NASU, Kyiv, Ukraine
Tel.: (044) 456-9263, 533-2632

BUTENKO T.I.
Cherkassy State Technological University, Cherkassy,
Ukraine
Tel.: +38 (0472) 43-3680, 42-2148, 43-01-10
Fax:+38 (0472) 43-23-54, 42-2165
E-mail: bosh@gate.chiti.uch.net

BYAKOVA A.V.
NTUU «Kyiv Polytechnic Institute», Kyiv, Ukraine
Tel.: (044) 213-3569, 559-3443
Fax: (044) 213-3569
E-mail: byakova@vic.com.ua

BYCHKOV T.A.
JSC «ELKAM-Neftemash», Perm, Russia
Tel.: (3422) 45-3288
E-mail: nasos@pisem.net, KuraevaEN@mh.ru

C

CHECAN V.
Powder Metallurgy Research Institute of NAS of
Belarus, Minsk, Belarus
Tel.: (0375) 239-9883, 232-8581
Fax: (0375) 210-0574
E-mail: chekan@srpmi.minsk.by

CHEPEL S.N.
Physics and Technology Institute for Metals and Alloys,
NAS of Ukraine, Kyiv, Ukraine
Tel.: (044) 444-3515, 444-1155
Fax: (044) 444-1210
E-mail: metal@ptima.Kyiv.ua, root@u_cast.Kyiv.ua

CHEPELEVICH V.G.
Mozyr State Pedagogical Institute, Mozyr, Belarus
Tel.: 3750215125438
E-mail: mozvuz@mail.gomel.by

CHERNEGA S.M.
NTUU «Kyiv Polytechnic Institute», Kyiv, Ukraine
Tel.: (044) 441-1423, 241-7606
E-mail: carolin@ukrpost.net

CHERNENKO N.
Federal State Unitary Enterprise «NIIGrafit», Moscow,
Russia
E-mail: grafit@aha.ru

CHERNYAVSKY V.B.
Physics and Technology Institute for Metals and Alloys,
NAS of Ukraine, Kyiv, Ukraine
Tel.: (044) 444-2350
Fax: (044) 444-1210
E-mail: verbylo@ptima.Kyiv.ua

CHERNYSHOV G.
Bauman Moscow State Technical University, Moscow,
Russia
Tel.: (095) 263-6277, 267-1729
Fax: (095) 261-4257, 267-7130
E-mail: aleshin@bmstu.ru, Niikmtp@mx.bmstu.ru

CHERNYSHOV L.I.
Frantsevich Institute for Problems of Materials Science,
NASU, Kyiv, Ukraine
Tel.: (044) 444-2073
Fax: (044) 444-2131
E-mail: chern@materials.Kyiv.ua

CHERNYSHOVA T.
Baikov Institute of Metallurgy and Material Science
RAS, Moscow, Russia
Tel.: (095) 135-9652
Fax: (095) 135-4455
E-mail: chern@ultra.imet.ac.ru

CHEVTCHENKO S.
Institute for Solid-State Physics, Materials Science and
Technology at National Science Center «Kharkov
Institute of Physics and Technology» (ISSPMST NSC
KIPT), Kharkov, Ukraine
E-mail: borts@kipt.kharkov.ua

CHEVYCHELOVA T.M.
Frantsevich Institute for Problems of Materials Science,
NASU, Kyiv, Ukraine
Tel.: (044) 444-0256, 444-2524
E-mail: brodnikov@alfacom.net

CHEVYKALOVA L.A.
Federal State Unitary Enterprise «Obninsk Research
and Production Enterprise «TECHNOLOGIYA»,
Obninsk, Russia
E-mail: info@technologiya.ru

CHIGRINOV V.Y.
Powder Metallurgy Research Institute of NAS of
Belarus, Minsk, Belarus
E-mail: chigrin@mail.bn.by

CHIGRINOVA N.M.
Powder Metallurgy Research Institute of NAS of
Belarus, Minsk, Belarus
E-mail: chigrin@mail.bn.by

CHIVANOV A.V.
Derzhavin Tambov State University, Tambov, Russia
Tel.: (0752) 35-2614
Fax: (0752) 71-0307
E-mail: feodorov@tsu.tmb.ru, plushnik@mail.ru

CHUJKO A.A.
Institute for Surface Chemistry, NAS of Ukraine, Kyiv,
Ukraine
Tel.: (044) 444-1135
Fax: (044) 444-3567
E-mail: user@surfchem.freenet.Kyiv.ua

CHUMLYAKOV YU.I.
Siberian Physic-Technical Institute, Tomsk, Russia
Tel.: (3822) 53-3209
Fax: (3822) 53-3034
E-mail: chum@phys.tsu.ru

CHUPRASOV V.
Lykov Heat and Mass Transfer Institute, National
Academy of Belarus, Minsk, Belarus
Tel.: (103-75-172) 84-1521
Fax: (103-75-172) 28-42212
E-mail: kls@hmti.ac.by, office@hmti.oc.by

CLAEYS C.
IMEC, Leuven, Belgium
E-mail: claeys@imec.be, simoen@imec.be

D

DAN'KO S.V.
Frantsevich Institute for Problems of Materials Science,
NASU, Kyiv, Ukraine
Tel.: (044) 444-1573
Fax: (044) 444-2131
E-mail: altifer@ipms.Kyiv.ua, sftm@nas.gov.ua

DANCHENKO Y.V.
Research Center of Powder Material Science, Perm,
Russia
Tel.: (3422) 39-1110
Fax: (3422) 39-1122
E-mail: dan@pm.pstu.ac.ru

DANCHYUKOVA L.V.
Central Research Institute for Materials, Saint
Petersburg, Russia
Tel.: (812) 278-9341, 278-9178, 271-4469
Fax: (812) 274-4639
E-mail: carbid@pop3.rcom.ru

DANILCHENKO V.E.
Kurdyumov Institute for Metal Physics, NASU, Kyiv,
Ukraine
Tel.: (044) 444-3577
E-mail: danila@imp.Kyiv.ua

DANILOV P.A.
Institute for Solid-State Physics, Materials Science and
Technology at National Science Center «Kharkov
Institute of Physics and Technology» (ISSPMST NSC
KIPT), Kharkov, Ukraine
E-mail: gabelkov@kipt.kharkov.ua

DANYLENKO V.M.
Frantsevich Institute for Problems of Materials Science,
NASU, Kyiv, Ukraine
Tel.: (044) 444-3364
E-mail: dep.40@materials.Kyiv.ua

DARIEL M.P.
Ben-Gurion University of the Negev, Beer-Sheva, Israel
E-mail: nfrage@bgumail.bgu.ac.il

DEKHTERUK V.
Frantsevich Institute for Problems of Materials Science,
NASU, Kyiv, Ukraine
Tel.: (044) 444-2371

DEKHTYAR O.I.
Kurdyumov Institute for Metal Physics, NASU, Kyiv, Ukraine
Tel.: 444-9560 (сл.), 248-4195 (д.)
Fax: 444-0120
E-mail: dekhtyar@imp.Kyiv.ua

DELLITH J.
Institut fur Physikalische Hochtechnologie, Jena, Germany
Tel.: (49 36 41) 20-6103, 20-6107, 20-6106
Fax: (49 36 41) 20-6199
E-mail: Jan.Dellith@ipht-jena.de

DEMICHEV V.I.
Open Joint-Stock Company «KOMPOZIT», Institute of Metals, Korolev, Russia
Tel.: (095) 513-2091, 513-2326
Fax: (095) 516-0617
E-mail: kompozit.mat@g23.relcom.ru

DEMIN A.V.
Federal State Unitary Enterprise «NIIGrafit», Moscow, Russia
E-mail: grafit@aha.ru

DEREV'YANKO O.V.
Frantsevich Institute for Problems of Materials Science, NASU, Kyiv, Ukraine
Tel.: (044) 444-2255
Fax: (044) 444-2131
E-mail: raitch@ipms.Kyiv.ua

DLUGUNOVICH V.A.
Institute of Physics, National Academy of Sciences, Minsk, Belarus
E-mail: tsaruk@dragon.bas-net.by

DMITRUK N.L.
Institute for Physics of Semiconductors, NAS of Ukraine, Kyiv, Ukraine
E-mail: romanyuk@isp.Kyiv.ua

DOBKYNA Y.
Physics and Technology Institute for Metals and Alloys, NAS of Ukraine, Kyiv, Ukraine
Tel.: (044) 444-3550
Fax: (044) 444-1210
E-mail: dobkyna@ptima.Kyiv.ua

DOBROVOLSKY V.D.
Frantsevich Institute for Problems of Materials Science, NASU, Kyiv, Ukraine
Tel.: (044) 444-3364

DOLGYKH
NTUU «Kyiv Polytechnic Institute», Kyiv, Ukraine
Tel.: (044) 441-1423
E-mail: vdolgih@ukr.net

DOLMATOV V.YU.
Special Design Bureau «Tekhnolog» at the Saint-Petersburg State Technological Institute (Technical University), Saint-Petersburg, Russia
Tel.: (812)100-3898
Fax: (812) 100-3898
E-mail: alcen@comset.net

DONCHENKO M.I.
NTUU «Kyiv Polytechnic Institute», Kyiv, Ukraine
Tel.: (044) 216-8337

DOTSINA E.S.
Federal State Unitary Enterprise «Obninsk Research and Production Enterprise «TECHNOLOGIYA», Obninsk, Russia
E-mail: info@technologiya.ru

DRANENKO A.S.
Frantsevich Institute for Problems of Materials Science, NASU, Kyiv, Ukraine
Tel.: (044) 444-2531
Fax: (044) 444-2131
E-mail: dvor@ipms.Kyiv.ua

DUB S.N.
Bakul Institute for Superhard Materials Science, NASU, Kyiv, Ukraine
Tel.: (044) 430-1126
Fax: (044) 468-8625
E-mail: prikhna@iptelecom.net.ua, frd@ism.Kyiv.ua

DUBIKOWSKY L.
Frantsevich Institute for Problems of Materials Science, NASU, Kyiv, Ukraine
Tel.: (044) 444-2425
Fax: (044) 488-3821

DUBININ N.E.
Institute of Metallurgy Ural's Division of RAS, Ekaterinburg, Russia
Tel.: +7 3432 67-8924, 28-5312
Fax: +7 3432 67-8918
E-mail: faza@imet.mplik.ru, faza@imet.sco.ru, m_o_l_a@mail.ru

DUBOK V.
Frantsevich Institute for Problems of Materials Science, NASU, Kyiv, Ukraine
Tel.: (044) 444-7256
Fax: (044) 444-2131
E-mail: dubok@ipms.Kyiv.ua

DUBOVIK T.V.
Frantsevich Institute for Problems of Materials Science, NASU, Kyiv, Ukraine
Tel.: (044) 444-0002, 444-0101
Fax: (044) 444-2131
E-mail: imorozov@materials.Kyiv.ua, panavic@materials.Kyiv.ua

DUBROVSKAYA G.N.
Cherkassy State Technological University, Cherkassy, Ukraine
Tel.: +38 (0472) 43-3680, 42-2148, 43-01-10
Fax:+38 (0472) 43-23-54, 42-2165
E-mail: bosh@gate.chiti.uch.net

DUROV O.V.
Frantsevich Institute for Problems of Materials Science, NASU, Kyiv, Ukraine
Tel.: (044) 444-6201
Fax: (044) 444-3017
E-mail: naidich@ipms.Kyiv.ua

622

DVORINA L.A.
Frantsevich Institute for Problems of Materials Science,
NASU, Kyiv, Ukraine
Tel.: (044) 444-2531
Fax: (044) 444-2131
E-mail: dvor@ipms.Kyiv.ua

DVOYNENKO O.K.
Frantsevich Institute for Problems of Materials Science,
NASU, Kyiv, Ukraine
Tel.: (044) 444-8218
E-mail: andreeva@ipms.Kyiv.ua

DYACHENKO O.P.
Federal State Unitary Enterprise «Obninsk Research
and Production Enterprise «TECHNOLOGIYA»,
Obninsk, Russia
Tel.: (08439) 96-875, 62-687
Fax: (08439) 64-575
E-mail: info@technologiya.ru, onpptechn@kaluga.ru

DYADECHKO O.G.
Frantsevich Institute for Problems of Materials Science,
NASU, Kyiv, Ukraine
Tel.: (044) 444-2401
Fax: (044) 444-2401
E-mail: vish@i.com.ua

DYKUSHA V.N.
Institute for Physics of Semiconductors, NAS of
Ukraine, Kyiv, Ukraine
Tel.: (044) 265-6202, 265-6290, 265-1866
Fax: (044) 265-8342
E-mail: klyui@isp.Kyiv.ua

DYMENKO V.V.
Paton Electric Welding Institute, NAS of Ukraine, Kyiv,
Ukraine
Tel.: (044) 261-5966
Fax: (044) 286-0486

E

EEREMIEAROMAN
National Institute for Mine Safety and Explosion-Proof
Protection – INSEMEX Petroşani, Romania
Tel.: +40 (054) 54-6277
Fax: +40 (054) 54-6277
E-mail: insemex@comtrust.ro

EFREMOV V.P.
Hight Energy Density Research Center, Russian
Academy of Science, Moscow, Russia
Tel.: (095) 485-09-63
E-mail: efremov@ihed.ras.ru

EGAMOV M.CH.
Khujand Scientific Center of Tajik Academy of
Sciences, Khujand, Tajikistan
Tel.: 51-232
E-mail: muchtor@khj.tajik.net

ELANSKY G.N.
Moscow Evening Metallurgical Institute, Moscow,
Russia
Tel.: (095) 361-1480
Fax: (095) 361-1443
E-mail: protasov_ds@zsmk.ru

EMELIANOV B.M.
National University of Construction and Architecture,
Kyiv, Ukraine
Tel.: (044) 241-55-38, 241-55-87
Fax: (044) 248-11-30
E-mail: gena_kochetov@hotmail.com,
pohorila@ukma.Kyiv.ua

EREMENKO V.V.
Verkin Technologies Institute for Low Temperature
Physics and Engineering, NAS of Ukraine, Kharkov,
Ukraine
Tel.: 322-293, 321-223, 322-019
Fax: 322-293, 335-593, 321-292
E-mail: eremenko@ilt.kharkov.ua

ERMISHKIN V.A.
Baikov Baikov Institute of Metallurgy and Materials
Science, RAS, Moscow, Russia
E-mail: powder@imet.mplik.ru

ERSHOVA N.I.
Federal State Unitary Enterprise «Obninsk Research
and Production Enterprise «TECHNOLOGIYA»,
Obninsk, Russia
Tel.: (08439) 96-640, 96-819
Факс(08439) 64-575
E-mail: onpptech@kaluga.ru, onpptechn@kaluga.ru

EVTUSHOK T.M.
Frantsevich Institute for Problems of Materials Science,
NASU, Kyiv, Ukraine
Tel.: (044) 444-1481

F

FEDIRKO V.
Karpenko Physico-Mechanical Institute, NASU, Lviv,
Ukraine
Tel.: (0322) 65-4343
Fax: (0322) 64-9427
E-mail: olga.yeliseyeva@brasimone.enea.it,
fedirco@ipm.lviv.ua

FEDOROV V.
Shevchenko Kyiv National University, Kyiv, Ukraine
Tel.: (044) 266-2384
E-mail: vovch@mail.univ.Kyiv.ua,
matzui@mail.univ.Kyiv.ua

FEDOROV V.A.
Derzhavin Tambov State University, Tambov, Russia
Tel.: (0752) 35-2614
Fax: (0752) 71-0307
E-mail: feodorov@tsu.tmb.ru, plushnik@mail.ru

FILIPPOV V.B.
Frantsevich Institute for Problems of Materials Science,
NASU, Kyiv, Ukraine
E-mail: dep60@ipms.Kyiv.ua

FILONOV A.
Join-Stock Company «Revda Non Ferrous Metals
Processing Works», Revda, Sverdlovsk reg., Russia
E-mail: KuraevaEN@mh.ru

FIRSTOV S.A.
Frantsevich Institute for Problems of Materials Science,
NASU, Kyiv, Ukraine
Tel.: (044) 444-0294, 444-1124, 444-0051
Fax: (044) 452-5523
E-mail: fsa@materials.Kyiv.ua

FISCHER W.
Space Infrastructure Division of ASTRIUM GmbH,
Bremen, Germany
E-mail: sreznik@bmstu.ru

FIYALKA L.
Frantsevich Institute for Problems of Materials Science,
NASU, Kyiv, Ukraine
Tel.: (044) 444-2371

FLIS A.A.
Frantsevich Institute for Problems of Materials Science,
NASU, Kyiv, Ukraine
Tel.: (044) 444-2471
E-mail: flis@imp.Kyiv.ua

FOMENKO V.V.
National University of Food Technologies, Kyiv, Ukraine
Tel.: (044) 221-7833

FOMICHEV A.S.
Frantsevich Institute for Problems of Materials Science,
NASU, Kyiv, Ukraine
Tel.: (044) 444-3090
Fax: (044) 444-2131
E-mail: dep6@materials.Kyiv.ua

FORTOV V.E.
Hight Energy Density Research Center, Russian
Academy of Science, Moscow, Russia
Tel.: (095) 485-09-63
E-mail: efremov@ihed.ras.ru, potapenko@ihed.ras.ru

FRAGE N.
Ben-Gurion University of the Negev, Beer-Sheva, Israel
E-mail: nfrage@bgumail.bgu.ac.il

FREIK D.
Stefanyk Physics-Chemical Institute at Precarpathian
University, Ivano-Frankivsk, Ukraine
Tel.: (0342) 59-6082
E-mail: freik@pu.if.ua

FROLOV A.A.
Frantsevich Institute for Problems of Materials Science,
NASU, Kyiv, Ukraine
E-mail: frolov@edu-ua.net

FROLOV G.A.
Frantsevich Institute for Problems of Materials Science,
NASU, Kyiv, Ukraine
Tel.: (044) 444-0492, 459-5944
E-mail: frolov@alfacom.net

FROLOVA E.G.
Puhov Institute of Power Engineering Simulation
Problems, NASU of Ukraine, Kyiv, Ukraine
Tel.: (044) 459-5944
E-mail: frolov@alfacom.net

FROUMIN N.
Ben-Gurion University of the Negev, Beer-Sheva, Israel
E-mail: nfrage@bgumail.bgu.ac.il

FUJIMURA T.
"VISION DEVELOPMENT CO., LTD", Tokyo, Japan
Tel.: 03(3561) 3480
Fax: 03(3561) 3490
E-mail: vision@luvenet.com

FURSOV S.G.
Institute for Solid-State Physics, Materials Science and
Technology at National Science Center «Kharkov
Institute of Physics and Technology» (ISSPMST NSC
KIPT), Kharkov, Ukraine
Tel.: (0572) 35-6612, 35-6355
Fax: (0572) 35-3983
E-mail: admin@kipt.kharkov.ua, igor@kipt.kharkov.ua

FUSCHICH O.I.
Frantsevich Institute for Problems of Materials Science,
NASU, Kyiv, Ukraine
Tel.: (044) 444-1571
Fax: (044) 444-2131
E-mail: dir@ipms.Kyiv.ua

G

GAB A.I.
Vernadskii Institute of General and Inorganic Chemistry,
NAS of Ukraine, Kyiv, Ukraine
Tel.: (044) 444-0111
Fax: (044) 444-3070
E-mail: GAB@ionc.kar.net, iness@ionc.kar.net

GAB I.I.
Frantsevich Institute for Problems of Materials Science,
NASU, Kyiv, Ukraine
Tel.: (044) 444-3017
Fax: (044) 444-3017
E-mail: naidich@ipms.Kyiv.ua

GABELKOV S.V.
Institute for Solid-State Physics, Materials Science and
Technology at National Science Center «Kharkov
Institute of Physics and Technology» (ISSPMST NSC
KIPT), Kharkov, Ukraine
E-mail: gabelkov@kipt.kharkov.ua

GALINSKY V.P.
Institute of Technical Mechanics of NASU and NASUU,
Dniepropetrovsk, Ukraine
Tel.: (0562) 46-1051, 47-2465
Fax: (0562) 47-3413
E-mail: galinskyv@mail.ru

GAMEZA L.M.
Institute of Machine Reliability, National Academy of
Sciences of Belarus, Minsk, Belarus
Tel.: (017) 284-2401
Fax: (017) 284-24-01
E-mail: nanotech@inmash.bas-net.by

GAVRYLOV R.V.
Verkin Technologies Institute for Low Temperature
Physics and Engineering, NAS of Ukraine, Kharkov,
Ukraine
Tel.: 322-293,322-019, 300-364, 300-355
Fax: 322-293, 321-292
E-mail: gavrylov@cryocosmos.com

GAVRYLYUK V.P.
Physics and Technology Institute for Metals and Alloys,
NAS of Ukraine, Kyiv, Ukraine
Tel.: (044) 444-1322, 444-0280
E-mail: vladIlch@hotmail.com

GAWALEK W.
Institut fur Physikalische Hochtechnologie, Jena,
Germany
Tel.: (49 36 41) 206103
Fax: (49 36 41) 206199
E-mail: Wolfgang.Gawalek@ipht-jena.de

GERASIMJUK G.I.
Frantsevich Institute for Problems of Materials Science,
NASU, Kyiv, Ukraine
Tel.: (044) 444-3573
Fax: (044) 444-2131
E-mail: dep25@materials.Kyiv.ua

GETMAN O.I.
Frantsevich Institute for Problems of Materials Science,
NASU, Kyiv, Ukraine
Tel.: (044) 444-3415
Fax: (044) 444-2131
E-mail: vv@pani.Kyiv.ua

GILYOV V.G.
Research Center of Powder Material Science, Perm,
Russia
Tel.: (3422) 39-1110
Fax: (3422) 39-1122
E-mail: mak@pm.pstu.ac.ru

GOFIN M.Y.
NPO «Molniya», Moscow, Russia
E-mail: molgof@dol.ru

GOKHMAN A.
South Ukrainian State Pedagogical University, Odessa,
Ukraine
E-mail: brit@eurocom.od.ua

GOLOVKOVA M.E.
Frantsevich Institute for Problems of Materials Science,
NASU, Kyiv, Ukraine
Tel.: (044) 444-3364, 444-0294

GOLUBEVA I.L.
Kazan State Technological University, Kazan, Russia
Tel.: (8432) 194-374, 750-682
Fax: (8432) 369-942
E-mail: roustam@dionis.kstu.ru, panfilovitch@kstu.ru

GORBACHUK N.P.
Frantsevich Institute for Problems of Materials Science,
NASU, Kyiv, Ukraine
Tel.: (044) 444-1290
Fax: (044) 444-2131
E-mail: bas@materials.Kyiv.ua

GORBAN V.
Frantsevich Institute for Problems of Materials Science,
NASU, Kyiv, Ukraine
Tel.: (044) 444-2524

GORCHAKOVA L.I.
Federal State Unitary Enterprise «Obninsk Research
and Production Enterprise «TECHNOLOGIYA»,
Obninsk, Russia
Tel.: (08439) 96-887
Fax: (08439) 64-575
E-mail: info@technologiya.ru, onpptechn@kaluga.ru

GORDEEV S.K.
Central Research Institute for Materials, Saint
Petersburg, Russia
Tel.: (812) 278-9341, 278-9178, 271-4469
Fax: (812) 274-4639
E-mail: carbid@pop3.rcom.ru

GORDIYENKO S.P.
Frantsevich Institute for Problems of Materials Science,
NASU, Kyiv, Ukraine
Tel.: (044) 444-01-01
Fax: (044) 444-2131
E-mail: panavic@materials.Kyiv.ua,
imorozov@materials.Kyiv.ua, bas@materials.Kyiv.ua

GORYACHEV YU.M.
Frantsevich Institute for Problems of Materials Science,
NASU, Kyiv, Ukraine
Tel.: (044) 444-2371
E-mail: malakhov@ipms.Kyiv.ua

GOTOVTSEV G.D.
Lavochkin Scientific and Production Association, Himky,
Russia
Tel.: (095) 575-5916, 575-5516
Fax: (095) 573-3595
E-mail: gotovtsev@hotmail.com

GOYDINA S.V.
Frantsevich Institute for Problems of Materials Science,
NASU, Kyiv, Ukraine
Tel.: (044) 444-0256

GRACHEV V.V.
Institute of Structural Macrokinetics and Materials
Science RAS, Chernogolovka, Moscow region, Russia
Tel.: +7 (09652) 46-381
Fax: +7 (095) 962-8025
E-mail: vlad@ism.ac.ru, inna@ism.ac.ru

GRACHEVA L.I.
Institute for Problems of Strength, NASU, Kyiv, Ukraine
Tel.: (044) 295-6030
Fax: (044) 296-1684
E-mail: v.krivenyuk@ipp.adam.Kyiv.ua,
nick@ipp.adam.Kyiv.ua

GRATSIANSKY YU.A.
Federal State Unitary Enterprise «Obninsk Research
and Production Enterprise «TECHNOLOGIYA»,
Obninsk, Russia
Tel.: (08439) 96-797
Fax: (08439) 64-575
E-mail: onpptech@kaluga.ru, onpptechn@kaluga.ru

GRECHANYUK N.I.
Scientific Production Enterprise «Gecont», Vinnitsa,
Ukraine
Tel.: (0432) 555-5751
Fax: (0432) 26-1941
E-mail: Gecont@ukr.net

GRETCHANNIKOV E.E.
Mozyr State Pedagogical Institute, Mozyr, Belarus
Tel.: 3750215125438
E-mail: mozvuz@mail.gomel.by

GREVNOV L.M.
Research Center of Powder Material Science, Perm,
Russia
Tel.: (3422) 39-1119, 39-1127
Fax: (3422) 39-1122
E-mail: director@pm.pstu.ac.ru, kpmc@pm.pstu.ac.ru

GRICEL P.V.
Molodechno Powder Metallurgy Plant, Molodechno,
Belarus
Tel.: (1773) 32-498, 32-345
E-mail: zpm@molodecno.by, molzpm@mail.ru

GRIGOREV O.N.
Frantsevich Institute for Problems of Materials Science,
NASU, Kyiv, Ukraine
Tel.: (044) 444-1481

GRIGORYEVA T.F.
Institute of Solid State Chemistry and
Mechanochemistry SB RAS, Novosibirsk, Russia
Tel.: (3832) 39-4145
E-mail: ancharov@mail.ru

GRINCHUK P.S.
Lykov Heat and Mass Transfer Institute, National
Academy of Belarus, Minsk, Belarus
Tel.: (0172) 84-2250, 84-2775, 84-2205
E-mail: gps@hmti.ac.by, orabi@hmti.ac.by,
pnv@hmti.ac.by

GRISHCHISHYN D.A.
Frantsevich Institute for Problems of Materials Science,
NASU, Kyiv, Ukraine
Tel.: (044) 444-3364
E-mail: dep.40@materials.Kyiv.ua

GRISHCHISHYNA L.N.
Frantsevich Institute for Problems of Materials Science,
NASU, Kyiv, Ukraine
Tel.: (044) 444-3364
E-mail: dep.40@materials.Kyiv.ua

GROYSMAN A.
Oil Refineries Ltd., Haifa, Israel
Tel.: 972-4-8788623
Fax: 972-4-8788371
E-mail: GALEC@orl.co.il

GRUSHENKO A.
Zhukovsky National Aerospace University «Kharkov
Aviation Institute», Kharkov, Ukraine

GRUSHENKO O.
Zhukovsky National Aerospace University «Kharkov
Aviation Institute», Kharkov, Ukraine

GUBAR E.Y.
Cherkassy State Technological University, Cherkassy,
Ukraine
Tel.: +38 (0472) 43-3680, 42-2148, 43-01-10
Fax:+38 (0472) 43-23-54, 42-2165
E-mail: bosh@gate.chiti.uch.net

GUBARENI N.I.
Frantsevich Institute for Problems of Materials Science,
NASU, Kyiv, Ukraine
Tel.: (044) 444-0256
Fax: (044) 444-2131
E-mail: leonid@materials.Kyiv.ua

GUBENKO S.I.
National Metallurgical Academy of Ukraine,
Dnepropetrovsk, Ukraine
Tel.: (0562) 41-0357
Fax: (0562) 41-0357
E-mail: sgubenko@email.dp.ua

GUBIN YU.V.
Frantsevich Institute for Problems of Materials Science,
NASU, Kyiv, Ukraine
Tel.: (044) 444-0256, 444-4961

GUGLIN D.N.
Central Research Institute for Materials, Saint
Petersburg, Russia
Tel.: (812) 278-9341, 278-9178, 271-4469
Fax: (812) 274-4639
E-mail: carbid@pop3.rcom.ru

GUJDA V.V.
Institute for Solid-State Physics, Materials Science and
Technology at National Science Center «Kharkov
Institute of Physics and Technology» (ISSPMST NSC
KIPT), Kharkov, Ukraine
Tel.: (0572) 35-6612, 35-6355
Fax: (0572) 35-3983
E-mail: gujda@kipt.kharkov.ua

GUMENIUK S.V.
Frantsevich Institute for Problems of Materials Science,
NASU, Kyiv, Ukraine
Tel.: (044) 444-1534, 294-5645
Fax: (044) 444-2034
E-mail: gbag@rambler.ru, celt@materials.Kyiv.ua

GURIN I.
Institute for Solid-State Physics, Materials Science and
Technology at National Science Center «Kharkov
Institute of Physics and Technology» (ISSPMST NSC
KIPT), Kharkov, Ukraine
Tel.: (0572) 356-612, 356-484
Fax: (0572) 353-983
E-mail: igor@kipt.kharkov.ua

GURIN V.
Institute for Solid-State Physics, Materials Science and
Technology at National Science Center «Kharkov
Institute of Physics and Technology» (ISSPMST NSC
KIPT), Kharkov, Ukraine
Tel.: (0572) 356-612, 356-484
Fax: (0572) 353-983
E-mail: gurin@kipt.kharkov.ua

GUSAKOV A.G.
Belarussian State University, Minsk, Belarus
Tel.: (017) 209-5462
E-mail: MichaelZheludkevich@scnsoft.com

GUSEV E.L.
Unified Institute for Physical Technical Problems of the
North Siberian Division, RAS, Yakutsk, Russia
Tel.: (411) 244-67-80
E-mail: e.l.gusev@ipng.ysn.ru

GUSKOV V.D.
KBSM (Special Mechanical Engineering Design Office),
Saint-Petersburg, Russia
Tel.: (812) 542-8894
Fax: (812) 542-8894
E-mail: conby@infopro.spb.su

H

HABISREUTHER T.
Institut fur Physikalische Hochtechnologie, Jena,
Germany
Tel.: (49 36 41) 206103
Fax: (49 36 41) 206199
E-mail: Tobias.Habisreuther@ipht-jena.de

HAMITSAEV A.S.
Federal State Unitary Enterprise «Obninsk Research
and Production Enterprise «TECHNOLOGIYA»,
Obninsk, Russia
Tel.: (08439) 96-797
Fax: (08439) 64-575
E-mail: info@technologiya.ru, onpptech@kaluga.ru

HERDT R.
Institut fur Physikalische Hochtechnologie, Jena,
Germany
Tel.: (49 36 41) 20-6103, 20-6107, 20-6106
Fax: (49 36 41) 20-6199
E-mail: Robert.Herdt@ipht-jena.de

HIZHNJAK V.G.
NTUU «Kyiv Polytechnic Institute», Kyiv, Ukraine
Tel.: (044) 441-1423
E-mail: carolin@ukrpost.net, vdolgih@ukr.net

HOLENEVICH V.A.
Frantsevich Institute for Problems of Materials Science,
NASU, Kyiv, Ukraine
Tel.: (044) 444-2401
Fax: (044) 444-2401
E-mail: vish@i.com.ua

HOLOPTSEV V.V.
Institute of Applied Physics, Nizny Novgorod, Russia
E-mail: holo@appl.sci-nnov.ru

HOMENKO E.V.
Frantsevich Institute for Problems of Materials Science,
NASU, Kyiv, Ukraine
Tel.: (044) 444-1181
Fax: (044) 444-2131
E-mail: 29min@ipms.Kyiv.ua

HUTORYANSKA N.V.
Shevchenko Kyiv National University, Kyiv, Ukraine
Tel.: (044) 266-2367
Fax: (044) 266-2367
E-mail: ivanenko@phys.Kyiv.ua,
revo@phys.univ.Kyiv.ua

I

ILCHENKO V.D.
Physics and Technology Institute for Metals and Alloys,
NAS of Ukraine, Kyiv, Ukraine
Tel.: (044) 444-1322, 444-0280
E-mail: vladllch@hotmail.com

ILYUSCHENKO A.PH.
Powder Metallurgy Research Institute, NAS of Belarus,
Minsk, Belarus
E-mail: alexil@srpmi.belpak.minsk.by

IRKOV V.I.
Federal State Unitary Enterprise «Obninsk Research
and Production Enterprise «TECHNOLOGIYA»,
Obninsk, Russia
Tel.: (08439) 96-797
Fax: (08439) 64-575
E-mail: info@technologiya.ru, onpptech@kaluga.ru

ISAYEV K.B.
Frantsevich Institute for Problems of Materials Science,
NASU, Kyiv, Ukraine
Tel.: (044) 444-0081
Fax: (044) 444-2131
E-mail: isayev_k@gala.net

ISAYEVA L.P.
Frantsevich Institute for Problems of Materials Science,
NASU, Kyiv, Ukraine
Tel.: (044) 444-0256, 444-0492
E-mail: frolov@alfacom.net

ITSENKO A.I.
Frantsevich Institute for Problems of Materials Science,
NASU, Kyiv, Ukraine
Tel.: (044) 444-0002, 444-0101
Fax: (044) 444-2131
E-mail: imorozov@materials.Kyiv.ua,
panavic@materials.Kyiv.ua

IVAKIN E.
Institute of Physics, National Academy of Sciences,
Minsk, Belarus
Tel.: (095) 132-8229
Fax: (095) 135-7672
E-mail: ralchenko@nsc.gpi.ru

IVANCHENKO L.A.
Frantsevich Institute for Problems of Materials Science,
NASU, Kyiv, Ukraine
Tel.: (044) 444-3364
Fax: (044) 450-4487
E-mail: pinchuk_natalie@mail.ru

IVANCHEV S.S.
Saint-Petersburg Department of the Boreskov Institute
of Catalysis, SB RAS, Saint-Petersburg, Russia
E-mail: ivanchev@SM2270.spd.edu

IVANCHUK A.
Frantsevich Institute for Problems of Materials Science,
NASU, Kyiv, Ukraine
Tel.: (044) 444-1486
Fax: (044) 444-2131
E-mail: dir@ipms.Kyiv.ua

IVANENKO E.A.
Shevchenko Kyiv National University, Kyiv, Ukraine
Tel.: (044) 444-3364, 444-0294

IVANENKO K.O.
Shevchenko Kyiv National University, Kyiv, Ukraine
Tel.: (044) 266-2367
Fax: (044) 266-2367
E-mail: ivanenko@phys.Kyiv.ua,
revo@phys.univ.Kyiv.ua

IVANOVA I.I.
Frantsevich Institute for Problems of Materials Science,
NASU, Kyiv, Ukraine
Tel.: (044) 444-0294, 444-1124, 444-0051
Fax: (044) 452-5523
E-mail: fsa@materials.Kyiv.ua, epp@materials.Kyiv.ua

IVLEVA T.P.
Institute of Structural Macrokinetics and Materials
Science, RAS, Chernogolovka, Moscow region, Russia
E-mail: sepl@ism.ac.ru, tanja@ism.ac.ru

J

JACOBI V.G.
Ashurst Technology Centre Inc., Toronto, Canada
Tel.: (416) 820-3030

JUEZ-LORENZO M.
Fraunhofer-Institute fuer Chemische Technologie,
Pfinztal, Germany
Tel.: +49 (721) 464-0147
Fax: +49 (721) 464-0111
E-mail: vk@ict.fhg.de

K

KADYROV V.
Frantsevich Institute for Problems of Materials Science,
NASU, Kyiv, Ukraine
Tel.: (044) 444-0590
Fax: (044) 450-4080
E-mail: valkad@alfacom.net

KADYRZHANOV K.K.
Institute of Nuclear Physics of National Nuclear Center,
Almaty, Kazakhstan
Tel.: (3272) 54-5143, 54-6467
Fax: (3272) 54-6517
E-mail: kadyrzhanov@inp.kz

KALININ D.YU.
Bauman Moscow State Technical University, Moscow,
Russia
Tel.: (095) 263-6705
Fax: (095) 261-3614
E-mail: dmitry_kalinin@mail.ru

KAMALOV M.M.
Institute of Solid State Physics RAS, Chernogolovka,
Russia
Tel.: (096) 522-2066
E-mail: myshlyae@issp.ac.ru

KAMALOV Z.G.
Institute for Metals Superplasticity Problems, RAS, Ufa,
Russia
Tel.: (3472) 25-3750, 25-3815
Fax: (3472) 25-3759
E-mail: imsp11@anrb.ru, aigirsh@rambler.ru

KANTSEDAL V.P.
Institute for Solid-State Physics, Materials Science and
Technology at National Science Center «Kharkov
Institute of Physics and Technology» (ISSPMST NSC
KIPT), Kharkov, Ukraine
Tel.: (0572) 3503530
Fax: (0572) 35-1688
E-mail: sayenko@kipt.kharkov.ua

KAPITANCHUK L.M.
Paton Electric Welding Institute, NAS of Ukraine, Kyiv,
Ukraine
Tel.: (38044) 266-2335, 266-2384
E-mail: matzui@mail.univ.Kyiv.ua,
zakharenko@mail.univ.Kyiv.ua

KAPLENKO O.G.
Institute for Solid-State Physics, Materials Science and Technology at National Science Center «Kharkov Institute of Physics and Technology» (ISSPMST NSC KIPT), Kharkov, Ukraine
Tel.: (0572) 35-6612, 35-6355
Fax: (0572) 35-3983
E-mail: gurin@kipt.kharkov.ua, admin@kipt.kharkov.ua

KARACHENTSEV N.V.
Novokuznetsk Department of KemSU, Novokuznetsk, Russia
E-mail: protasov_ds@zsmk.ru

KARAKCHIEV L.G.
Institute of Solid State Chemistry and Mechanochemistry, SB RAS, Novosibirsk, Russia
Tel.: (3832) 32-9600
Fax: (3832) 322847
E-mail: lena@mill.solid.nsc.ru

KARIMOV S.N.
Khujand Scientific Center of Tajik Academy of Sciences, Khujand, Tajikistan
Tel.: 51-232
E-mail: muchtor@khj.tajik.net

KARPENKO V.D.
State Works of Carbon Carbon Composite Materials «Uglecompozit», Zaporozhye, Ukraine
Tel.: (0612) 35-3171
Fax: (0612) 35-5273
E-mail: kvd@vuglecomp.zp.ua

KARPETS M.V.
Frantsevich Institute for Problems of Materials Science, NASU, Kyiv, Ukraine
Tel.: (044) 444-1290
Fax: (044) 444-2131
E-mail: bas@materials.Kyiv.ua

KARVATSKIY A.YA.
NTUU «Kyiv Polytechnic Institute», Kyiv, Ukraine
Tel.: (044) 274-4052, 241-6870, 241-8609
Fax: (38 044) 274-4052, 241-6870
E-mail: anton@fizmat.Kyiv.ua

KASHCHEYEV I.D.
"NVF Ognjeuporniye Materyaly & Teploviye Agregaty" Ltd, Pervouralsk, Russia
Tel.: (3432) 5-2361, (3432) 75-9420, (08439) 6-6317
Fax: (34392) 5-2361, (08439) 6-6317
E-mail: polytech@mtf.ustu.ru, frantish@freemail.ru, kerambet@ok.ru, buran@obninsk.com

KASUMOV A.M.
Frantsevich Institute for Problems of Materials Science, NASU, Kyiv, Ukraine
Tel.: (044) 444-8218
E-mail: andreeva@ipms.Kyiv.ua

KASUMOV M.M.
Institute for Surface Chemistry, NAS of Ukraine, Kyiv, Ukraine
Tel.: (044) 444-1135
Fax: (044) 444-3567
E-mail: user@surfchem.freenet.Kyiv.ua

KATSUHIKO KISHITAKE
Kyushu Institute of Technology, Kitakyushu, Japan
Tel.: (81-22) 217-5214
Fax: (81-22) 217-5178
E-mail: slava@iamp.tohoku.ac.jp

KAYUK V.G.
Frantsevich Institute for Problems of Materials Science, NASU, Kyiv, Ukraine
Fax: (044) 444-2131

KAZO J.
Shevchenko Kyiv National University, Kyiv, Ukraine
Tel.: (044) 510-7837, 227-1027, 266-2326
Fax: (044) 510-7837, 266-2326
E-mail: HVitaly@mail.ru

KELINA I.YU.
Federal State Unitary Enterprise «Obninsk Research and Production Enterprise «TECHNOLOGIYA», Obninsk, Russia
Tel.: (08439) 96-640, 96-819
Факс(08439) 64-575
E-mail: onpptech@kaluga.ru

KENIGFEST A.M.
Federal State Unitary Enterprise «NIIGrafit», Moscow, Russia
E-mail: grafit@aha.ru

KEPICH T.
Shevchenko Kyiv National University, Kyiv, Ukraine
Tel.: (044) 510-7837, 227-1027, 266-2326
Fax: (044) 510-7837, 266-2326
E-mail: HVitaly@mail.ru

KERIMOV E. A.
Institute of Nuclear Physics of National Nuclear Center, Almaty, Kazakhstan
Tel.: (3272) 54-5143, 54-6467
Fax: (3272) 54-6517
E-mail: kadyrzhanov@inp.kz, skislitsin@inp.kz, turkebaev@inp.kz

KHANOV A.M.
Perm State Technical University, Perm, Russia
Tel.: (3422) 39-1119
Fax: (3422) 39-1122
E-mail: patent@pm.pstu.ac.ru, director@pm.pstu.ac.ru

KHARCHENKO V.K.
Institute for Problems of Strength, NASU, Kyiv, Ukraine
Tel.: (044) 295-6030, 296-5657
Fax: (044) 296-1684
E-mail: nick@ipp.adam.Kyiv.ua

KHARLAMOV A.I.
Frantsevich Institute for Problems of Materials Science, NASU, Kyiv, Ukraine
Tel.: (044) 444-0256
E-mail: dep73@ipms.Kyiv.ua

KHOLOMEEV G.A.
Institute for Solid-State Physics, Materials Science and Technology at National Science Center «Kharkov Institute of Physics and Technology» (ISSPMST NSC KIPT), Kharkov, Ukraine
E-mail: gabelkov@kipt.kharkov.ua, sayenko@kipt.kharkov.ua

KHOMENKO G.E.
Frantsevich Institute for Problems of Materials Science, NASU, Kyiv, Ukraine
Tel.: (044) 444-1573
Fax: (044) 444-2131
E-mail: minakov@ipms.Kyiv.ua, altifer@ipms.Kyiv.ua

KHOMICH A.
Institute of RadioEng. & Electronics, Fryazino, Russia
Tel.: (095) 132-8229
Fax: (095) 135-7672
E-mail: ralchenko@nsc.gpi.ru

KHOMKO T.V.
Frantsevich Institute for Problems of Materials Science, NASU, Kyiv, Ukraine
Tel.: (044) 444-0256
Fax: (044) 444-2131
E-mail: leonid@materials.Kyiv.ua

KHORUJAYA V.G.
Frantsevich Institute for Problems of Materials Science, NASU, Kyiv, Ukraine
Tel.: (044) 444-3090
Fax: (044) 444-2131
E-mail: dep6@materials.Kyiv.ua

KHORUNOV V.F.
Paton Electric Welding Institute, NAS of Ukraine, Kyiv, Ukraine
Tel.: (044) 227-2677, 227-1434
Fax: (044) 227-2677
E-mail: khorunov@ukrpack.net

KHOTYNENKO N.G.
Frantsevich Institute for Problems of Materials Science, NASU, Kyiv, Ukraine
Tel.: (044) 444-0256

KHRAMTSOV V.D.
Research Center of Powder Material Science, Perm, Russia
Tel.: (3422) 39-1160, 39-1119 .
Fax: (3422) 39-1122
E-mail: director@pm.pstu.ac.ru, patent@pm.pstu.ac.ru

KHYZHUN O.YU.
Frantsevich Institute for Problems of Materials Science, NASU, Kyiv, Ukraine
Fax: (044) 444-2131

KIKUCHI R.
Materials Science and Mineral Engineering, University of California, Berkeley, USA
Fax: 81-424-75-0650
E-mail: wmfjindo@din.or.jp, kmjindo@issp.u-tokyo.ac.jp

KIREEVA I.V.
Siberian Physica -Technical Institute, Tomsk, Russia
Tel.: (3822) 53-3209
Fax: (3822) 53-3034
E-mail: chum@phys.tsu.ru

KIRILENKO S.N.
Frantsevich Institute for Problems of Materials Science, NASU, Kyiv, Ukraine
Tel.: (044) 444-0256

KIRILLOVA N.V.
Shevchenko Kyiv National University, Kyiv, Ukraine
Tel.: (044) 221-0216

KISLITSIN S.B.
Institute of Nuclear Physics of National Nuclear Center, Almaty, Kazakhstan
Tel.: (3272) 54-5143, 54-6467
Fax: (3272) 54-6517
E-mail: kadyrzhanov@inp.kz, skislitsin@inp.kz, turkebaev@inp.kz

KLEIN O.
Ben-Gurion University of the Negev, Beer-Sheva, Israel
E-mail: nfrage@bgumail.bgu.ac.il

KLISHIN A.F.
Lavochkin Scientific and Production Association, Himky, Russia
Tel.: (095) 575-5916, 575-5516
Fax: (095) 573-3595
E-mail: gotovtsev@hotmail.com

KLOCHKOV L.A.
Frantsevich Institute for Problems of Materials Science, NASU, Kyiv, Ukraine
Tel.: (044) 444-1501

KLYUI N.I.
Institute for Physics of Semiconductors, NAS of Ukraine, Kyiv, Ukraine
Tel.: (044) 265-6202, 265-6290, 265-1866
Fax: (044) 265-8342
E-mail: mak@gelio.isp.Kyiv.ua klyui@isp.Kyiv.ua, lvg@isp.Kyiv.ua

KOBELEVA L.
Baikov Institute of Metallurgy and Material Science RAS, Moscow, Russia
Tel.: (095) 135-9652
Fax: (095) 135-4455
E-mail: chern@ultra.imet.ac.ru

KOBYAKOV V.P.
Institute of Structural Macrokinetics and Materials Science RAS, Chernogolovka, Moscow region, Russia
Tel.: 444-9560
Fax: 444-0120
E-mail: dekhtyar@imp.Kyiv.ua

KOCHETOV G.M.
National University of Construction and Architecture, Kyiv, Ukraine
Tel.: (044) 241-55-38, 241-55-87
Fax: (044) 248-11-30
E-mail: gena_kochetov@hotmail.com

KOKHANA I.M.
Frantsevich Institute for Problems of Materials Science,
NASU, Kyiv, Ukraine
Tel.: (044) 444-2401
Fax: (044) 444-2401
E-mail: vish@i.com.ua

KOKHANIY V.O.
Frantsevich Institute for Problems of Materials Science,
NASU, Kyiv, Ukraine
Tel.: (044) 444-2401
Fax: (044) 444-2401
E-mail: vish@i.com.ua

KOLARIK V.
Fraunhofer-Institute fuer Chemische Technologie,
Pfinztal, Germany
Tel.: +49 (721) 464-0147
Fax: +49 (721) 464-0111
E-mail: vk@ict.fhg.de

KOLISNICHENKO O.V.
Paton Electric Welding Institute, NAS of Ukraine, Kyiv,
Ukraine
Tel.: 220-0914, 261-5034
E-mail: ytyurin@i.com.ua, ytyurin@paton.Kyiv.ua

KOLOKOLOV L.I.
Federal State Unitary Enterprise «Obninsk Research
and Production Enterprise «TECHNOLOGIYA»,
Obninsk, Russia
Tel.: (08439) 96-797
Fax: (08439) 64-575
E-mail: info@technologiya.ru, onpptech@kaluga.ru

KOLOMIETS L.L.
Frantsevich Institute for Problems of Materials Science,
NASU, Kyiv, Ukraine
Tel.: (044) 444-3415
Fax: (044) 220-4094
E-mail: kolom@ukrnet.net

KOLOTYLO D.M.
Kyiv National University of Economic, Kyiv, Ukraine
Tel.: (044) 459-6180
E-mail: danielkolotilo@mail.ru

KOLOTYLO O.D.
Frantsevich Institute for Problems of Materials Science,
NASU, Kyiv, Ukraine
Tel.: (044) 444-1191
E-mail: kolotyloAM@gala.net

KOLYANDA S.I.
Institute for Solid-State Physics, Materials Science and
Technology at National Science Center «Kharkov
Institute of Physics and Technology» (ISSPMST NSC
KIPT), Kharkov, Ukraine
Tel.: (0572) 35-6612, 35-6355
Fax: (0572) 35-3983
E-mail: admin@kipt.kharkov.ua

KOMOZYNSKI P.A.
Zhukovsky National Aerospace University «Kharkov
Aviation Institute», Kharkov, Ukraine
E-mail: dep60@ipms.Kyiv.ua

KONCHA A.A.
South Ukrainian State Pedagogical University, Odessa,
Ukraine
Tel.: (0482) 64-7753, 61-0823, 20-8181
E-mail: storm_x@aport.ru

KONDRATENKO O.S.
Institute for Physics of Semiconductors, NAS of
Ukraine, Kyiv, Ukraine
E-mail: romanyuk@isp.Kyiv.ua

KONYASHIN I.YU.
Boart Longyear GmbH & Co. KG, Technical
Development Centre, Burghaun, Germany
Tel.: +49-6652-82412
Fax: +49-6652-82490
E-mail: IKonyashin@boartlongyear-eu.com

KOPAN A.R.
Frantsevich Institute for Problems of Materials Science,
NASU, Kyiv, Ukraine
Tel.: (044) 444-1290
Fax: (044) 444-2131
E-mail: kopa@alex-ua.com

KOPAN YU.V.
Ukraine Center for Standardization and Metrology, Kyiv,
Ukraine
E-mail: kopa@alex-ua.com

KORABLYOVA E.A.
Federal State Unitary Enterprise «Obninsk Research
and Production Enterprise «TECHNOLOGIYA»,
Obninsk, Russia
Tel.: (08439) 96-875, 62-687
Fax: (08439) 64-575
E-mail: info@technologiya.ru, onpptechn@kaluga.ru

KORDYUK A.A.
Kurdyumov Institute for Metal Physics, NASU, Kyiv,
Ukraine
Tel.: (044) 444-9538
E-mail: kord@imp.Kyiv.ua

KORNETA O.B.
Shevchenko Kyiv National University, Kyiv, Ukraine
Tel.: (044) 265-6202, 268-3578
Fax: (044) 265-8342
E-mail: kornet@mail.univ.Kyiv.ua,
voronina@mail.univ.Kyiv.ua

KOROL V.I.
NTUU «Kyiv Polytechnic Institute», Kyiv, Ukraine
Tel.: (044) 441-1423
E-mail: carolin@ukrpost.net

KOROL' A.A.
Frantsevich Institute for Problems of Materials Science,
NASU, Kyiv, Ukraine
Tel.: (044) 444-1191, 444-0590, 444-2201, 444-1321
Fax: (044) 444-2131
E-mail: valkad@alfacom.net

KOROTKOV G.V.
KBSM (Special Mechanical Engineering Design Office),
Saint-Petersburg, Russia
Tel.: (812) 542-8894
Fax: (812) 542-8894
E-mail: conby@infopro.spb.su

KORZHOVA N.P.
Frantsevich Institute for Problems of Materials Science,
NASU, Kyiv, Ukraine
Tel.: (044) 444-3061
Fax: (044) 444-3061
E-mail: korzhova@materials.Kyiv.ua

KOSINSCAIA A.V.
Physics and Technology Institute for Metals and Alloys,
NAS of Ukraine, Kyiv, Ukraine
Tel.: (044) 444-1424
Fax: (044) 444-3542
E-mail: kompozit@inec.Kyiv.ua

KOSTENKO A.D.
Frantsevich Institute for Problems of Materials Science,
NASU, Kyiv, Ukraine
Tel.: (044) 441-1423
E-mail: carolin@ukrpost.net

KOSTIKOV V.I.
Federal State Unitary Enterprise «NIIGrafit», Moscow,
Russia
E-mail: grafit@aha.ru

KOSTORNOV A.G.
Frantsevich Institute for Problems of Materials Science,
NASU, Kyiv, Ukraine
Tel.: (044) 444-1571
Fax: (044) 444-2131
E-mail: dir@ipms.Kyiv.ua

KOSTYAKOV V.N.
Physics and Technology Institute for Metals and Alloys,
NAS of Ukraine, Kyiv, Ukraine
Tel.: (044) 444-3515, 444-1155
Fax: (044) 444-1210
E-mail: metal@ptima.Kyiv.ua, root@u_cast.Kyiv.ua

KOSTYUK B.D.
Frantsevich Institute for Problems of Materials Science,
NASU, Kyiv, Ukraine
Tel.: (044) 444-6201
Fax: (044) 444-3017
E-mail: naidich@ipms.Kyiv.ua

KOSYGIN E.P.
Frantsevich Institute for Problems of Materials Science,
NASU, Kyiv, Ukraine
Tel.: (044) 444-2401
Fax: (044) 444-2401
E-mail: vish@i.com.ua

KOTENKO V.A.
Frantsevich Institute for Problems of Materials Science,
NASU, Kyiv, Ukraine
Tel.: (044) 444-1481

KOVAL A.
Frantsevich Institute for Problems of Materials Science,
NASU, Kyiv, Ukraine
Tel.: (044) 444-22-64, 444-1201
E-mail: maslyuk@materials.Kyiv.ua

KOVALCHUK N.M.
Frantsevich Institute for Problems of Materials Science,
NASU, Kyiv, Ukraine
Tel.: (044) 444-2401
Fax: (044) 444-2401
E-mail: vish@i.com.ua

KOVALEV L.K.
Moscow State Aviation Institute, Moscow, Russia
E-mail: prikhna@iptelecom.net.ua

KOZINA G.K.
Bakul Institute for Superhard Materials Science, NASU,
Kyiv, Ukraine
Tel.: (044) 430-3441
E-mail: ngolovko@radgeo.freenet.Kyiv.ua

KOZLOVA L.E.
Institute for Magnetism, NASU, Kyiv, Ukraine
Eeл: (044) 444-9591
E-mail: kozlova@imag.Kyiv.ua

KOZYRSKI E.N.
Belarussian State University, Minsk, Belarus
Tel.: (017) 209-5462
E-mail: MichaelZheludkevich@scnsoft.com,
mmmmm@tut.by

KRACUNOVSKA S.
Institut fur Physikalische Hochtechnologie, Jena,
Germany
E-mail: prikhna@iptelecom.net.ua

KRAITCHINSKII A.
Institute of Physics, NAS of Ukraine, Kyiv, Ukraine
Tel.: (044) 265-3973, 265-0825, 265-9958
Fax: (044) 265-1589
E-mail: kraitch@iop.Kyiv.ua

KRAS'KO N.
Institute of Physics, NAS of Ukraine, Kyiv, Ukraine
Tel.: (044) 265-3973, 265-0825, 265-9958
Fax: (044) 265-1589
E-mail: krasko@iop.Kyiv.ua

KRAVCHENKO L.P.
Frantsevich Institute for Problems of Materials Science,
NASU, Kyiv, Ukraine
Tel.: (044) 444-2024
Fax: (044) 444-2131
E-mail: vkur@ipms.Kyiv.ua

KRAVCHENKO V.S.
Frantsevich Institute for Problems of Materials Science,
NASU, Kyiv, Ukraine
Tel.: (044) 4441191
E-mail: lavrenko@svitonline.Kyiv.ua

KRAVETSKIY G.A.
Federal State Unitary Enterprise «NIIGrafit», Moscow, Russia
E-mail: grafit@aha.ru

KRAVTSOV A.G.
Mechanics of Metal-Polymer Systems Research Institute of NAS of Belarus, Gomel, Belarus
E-mail: alexil@srpmi.belpak.minsk.by

KRESHCHUK A.V.
Physics and Technology Institute for Metals and Alloys, NAS of Ukraine, Kyiv, Ukraine
Tel.: (044) 444-2350
Fax: (044) 444-1210
E-mail: verbylo@ptima.Kyiv.ua

KRIUSHIN V.
Frantsevich Institute for Problems of Materials Science, NASU, Kyiv, Ukraine
Tel.: (044) 444-1486
Fax: (044) 444-2131
E-mail: dir@ipms.Kyiv.ua

KRIVORUCHKO E.M.
Lebedev Rubber Research Institute, Saint-Petersburg, Russia
Tel.: +7 (812) 251-4028, 251-5227
Fax: +7 (812) 251-4813
E-mail: vniisk@mail.rcom.ru, ypsokol@mail.rcom.ru

KRUKOV I.
Polsunov Central Boiler and Turbine Institute, Saint-Petersburg, Russia
Tel.: (812) 550-8227
Fax: (812) 550-8227
E-mail: rybnicov@online.ru

KRUKOVSKY P.
Institute of Engeneering hermophysics, Kyiv, Ukraine
Tel.: (044) 446-9281, 441-7304
Fax: (044) 446-6091
E-mail: kruk@i.Kyiv.ua

KRUKOVSKY S.
Institute of Engeneering hermophysics, Kyiv, Ukraine
Tel.: (044) 446-9281, 441-7304
Fax: (044) 446-6091
E-mail: kruk@i.Kyiv.ua

KRYACHKO L.A.
Institute for Problems of Materials Science, NASU, Kyiv, Ukraine
Teл.: (044) 444-2474
E-mail: 29min@ipms.ua

KRYLOV A.YU.
Togliatti State University, Togliatti, Russia
E-mail: A.Krylov@vaz.ru

KSHNJAKIN V.S.
Sumy Institute for Surface Modification, Sumy, Ukraine
Tel.: 220-0914, 261-5034
E-mail: ytyurin@i.com.ua

KUDENKO G.E.
GP PPES P/O Donetskugol, Donetsk, Ukraine
E-mail: olesya@eradig.donetsk.ua,
delta2@gppes.donetsk.ua

KUDIN V.G.
Shevchenko Kyiv National University, Kyiv, Ukraine
E-mail: nodid@mail.univ.Kyiv.ua

KUIMOV S. D.
Join-Stock Company «Revda Non Ferrous Metals Processing Works», Revda, Russia
Tel.: (3422) 45-3288
E-mail: KuraevaEN@mh.ru

KUKSENKO V.S.
Ioffe Physico-Technical Institute, RAS Saint-Petersburg, Russia
Tel.: (812) 247-1445, 247-9139
Fax: (812) 247-1017
E-mail: Victor.Kuksenko@pop.ioffe.rssi.ru

KULAKOV S.V.
Research Center of Powder Material Science, Perm, Russia
Tel.: (3422) 39-1110
Fax: (3422) 39-1122
E-mail: dan@pm.pstu.ac.ru

KULAKOV V.V.
Federal State Unitary Enterprise «NIIGrafit», Moscow, Russia
E-mail: grafit@aha.ru

KULIKOVA G.I.
Federal State Unitary Enterprise «Obninsk Research and Production Enterprise «TECHNOLOGIYA», Obninsk, Russia
Tel.: (08439) 96-887
Fax: (08439) 64-575
E-mail: info@technologiya.ru, onpptechn@kaluga.ru

KURAKIN V.I.
Federal State Unitary Enterprise «Obninsk Research and Production Enterprise «TECHNOLOGIYA», Obninsk, Russia
Tel.: (08439) 96-797
Fax: (08439) 64-575
E-mail: info@technologiya.ru, onpptech@kaluga.ru

KURILOV A.G.
Research-and-Production Corporation «Technology-2000» Ltd, Kharkov, Ukraine
Tel.: (0572) 92-2167
Fax: (0572) 16-2180
E-mail: kt_2000@ukr.net, kgv_2000@mail.ru

KURILOV G.V.
Research-and-Production Corporation «Technology-2000» Ltd, Kharkov, Ukraine
Tel.: (0572) 92-2167
Fax: (0572) 16-2180
E-mail: kt_2000@ukr.net, kgv_2000@mail.ru

KURINNAYA T.V.
Frantsevich Institute for Problems of Materials Science,
NASU, Kyiv, Ukraine
Tel.: (044) 444-0256

KURKOVA D.I.
Frantsevich Institute for Problems of Materials Science,
NASU, Kyiv, Ukraine
Tel.: (044) 444-3017
Fax: (044) 444-3017
E-mail: naidich@ipms.Kyiv.ua

KUROCHKIN V.D.
Frantsevich Institute for Problems of Materials Science,
NASU, Kyiv, Ukraine
Tel.: (044) 444-2024
Fax: (044) 444-2131
E-mail: vkur@ipms.Kyiv.ua

KURYACHII A.P.
Central Aero-Hydrodynamic Institute, Zhukovsky,
Moscow Region, Russia
Tel.: (095) 556-4172
Fax: (095) 556-4337, 911-0019
E-mail: sasha@kura.aerocentr.msk.su

KUSNETSOVA T.
Frantsevich Institute for Problems of Materials Science,
NASU, Kyiv, Ukraine
Tel.: (044) 444-2524, 444-8286
E-mail: dep53@ipms.Kyiv.ua

KYSIL V.
Frantsevich Institute for Problems of Materials Science,
NASU, Kyiv, Ukraine
Tel.: (044) 450-4963, 444-1191
Fax: (044) 444-2131
E-mail: vyakysil@i.com.ua

L

LAKIZA S.M.
Frantsevich Institute for Problems of Materials Science,
NASU, Kyiv, Ukraine
Tel.: (044) 444-3573
E-mail: dep25@ipms.Kyiv.ua

LAPTEV A.V.
Frantsevich Institute for Problems of Materials Science,
NASU, Kyiv, Ukraine
Tel.: (044) 444-2101
Fax: (044) 444-2131
E-mail: shat@ipms.Kyiv.ua

LASHNEVA V.
Frantsevich Institute for Problems of Materials Science,
NASU, Kyiv, Ukraine
Tel.: (044) 444-7256
Fax: (044) 444-2131
E-mail: dubok@ipms.Kyiv.ua

LAVRIV L.V.
Frantsevich Institute for Problems of Materials Science,
NASU, Kyiv, Ukraine
Fax: (044) 444-2131

LEBEDEV E.V.
Institute of Macromolecular Chemistry, NAS of Ukraine,
Kyiv, Ukraine
Tel.: (044) 559-3722, 559-4695
Fax: (044) 552-4064
E-mail: ihvs@ukrpack.net

LEDOVSKAYA L.N.
Institute for Solid-State Physics, Materials Science and
Technology at National Science Center «Kharkov
Institute of Physics and Technology» (ISSPMST NSC
KIPT), Kharkov, Ukraine
Tel.: (0572) 3503530
Fax: (0572) 35-1688
E-mail: sayenko@kipt.kharkov.ua

LEGKAYA T.N.
Kurdyumov Institute for Metal Physics, NASU, Kyiv,
Ukraine
Tel.: (044) 444-3061
Fax: (044) 444-3061
E-mail: korzhova@materials.Kyiv.ua

LELEKA S.V.
NTUU «Kyiv Polytechnic Institute», Kyiv, Ukraine
Tel.: (044) 274-4052, 241-6870, 241-8609
Fax: (044) 274-4052, 241-6870
E-mail: sleleka@fizmat.Kyiv.ua

LEPESHKIN Y.D.
Baikov Baikov Institute of Metallurgy and Materials
Science, RAS, Moscow, Russia
E-mail: powder@imet.mplik.ru

LESHOK A.V.
Molodechno Powder Metallurgy Plant, Molodechno,
Belarus
Tel.: (1773) 32-498, 32-345
E-mail: zpm@molodecno.by, molzpm@mail.ru

LEVASHOV E.A.
Research Center of SHS at the Institute of Steel and
Alloys, Moscow, Russia
Tel.: (095) 236-5298
E-mail: levashov@shs.misis.ru

LINNIK YU.A.
Institute for Solid-State Physics, Materials Science and
Technology at National Science Center «Kharkov
Institute of Physics and Technology» (ISSPMST NSC
KIPT), Kharkov, Ukraine
Tel.: (0572) 3503530
Fax: (0572) 35-1688
E-mail: sayenko@kipt.kharkov.ua

LISENKO A.A.
Frantsevich Institute for Problems of Materials Science,
NASU, Kyiv, Ukraine
Tel.: (044) 444-3364
E-mail: dep.40@materials.Kyiv.ua

LISNYAK V.V.
Shevchenko Kyiv National University, Kyiv, Ukraine
E-mail: nodid@mail.univ.Kyiv.ua

634

LISOVSKY A.F.
Bakul Institute for Superhard Materials, NASU, Kyiv,
Ukraine
Tel.: (044) 430-3505
Fax: (044) 468-8632
E-mail: frd@ism.Kyiv.ua

LITOVCHENKO V.G.
Institute for Physics of Semiconductors, NAS of
Ukraine, Kyiv, Ukraine
Tel.: (044) 265-6202, 265-6290, 265-1866
Fax: (044) 265-8342
E-mail: mak@gelio.isp.Kyiv.ua klyui@isp.Kyiv.ua

LITVISHKO T.N.
State Design Office Yuzhnoye, Dniepropetrovsk,
Ukraine
Tel.: (0562) 92-0866
Fax: (0562) 92-5113
E-mail: kbu@public.ua.net

LITYUGA N.V.
Frantsevich Institute for Problems of Materials Science,
NASU, Kyiv, Ukraine
Tel.: (044) 444-0256, 444-0492
E-mail: frolov@alfacom.net

LITZKENDORF D.
Institut fur Physikalische Hochtechnologie, Jena,
Germany
Tel.: (49 36 41) 206103
Fax: (49 36 41) 206199
E-mail: Doris.Litzkendorf@ipht-jena.de

LJASHENKO V.I.
Frantsevich Institute for Problems of Materials Science,
NASU, Kyiv, Ukraine
Tel.: (044) 444-1501

LLJASHENKO M.I.
Sumy Institute for Surface Modification, Sumy, Ukraine
Tel.: 220-0914, 261-5034
E-mail: ytyurin@i.com.ua

LOGINOV JU.V.
JSC «Perm Research Technological Institute» (JSC
«PNITP'), Perm, Russia
Tel.: (3422) 45-3288
E-mail: nasos@pisem.net, KuraevaEN@mh.ru,
nasos@perm.raid.ru

LOGUNOV A.V.
Open Joint-Stock Company «KOMPOZIT», Institute of
Metals, Korolev, Russia
Tel.: (095) 513-2211, 513-2124, 513-2180
Fax: (095) 516-0617
E-mail: razumov@aif.ru, kompozit.mat@g23.relcom.ru

LOPATA A.T.
Institute for Solid-State Physics, Materials Science and
Technology at National Science Center «Kharkov
Institute of Physics and Technology» (ISSPMST NSC
KIPT), Kharkov, Ukraine
E-mail: borts@kipt.kharkov.ua

LOPATIN V.I.
International Engineering University
Tel.: (095) 785-0770
Fax: (095) 158-4029
E-mail: v.lopatin@race.ru

LOPATO L.M.
Frantsevich Institute for Problems of Materials Science,
NASU, Kyiv, Ukraine
Tel.: (044) 444-3573
Fax: (044) 444-2131
E-mail: dep25@materials.Kyiv.ua

LOSKUTOV V.F.
NTUU «Kyiv Polytechnic Institute», Kyiv, Ukraine
Tel.: (044) 441-1423, 241-7606
E-mail: carolin@ukrpost.net

LOSKUTOVA T.V.
NTUU «Kyiv Polytechnic Institute», Kyiv, Ukraine
Tel.: (044) 441-1423
E-mail: carolin@ukrpost.net

LOTOTSKAYA V.A.
Verkin Technologies Institute for Low Temperature
Physics and Engineering, NAS of Ukraine, Kharkov,
Ukraine
Tel.: 322-019, 300-349
Fax: 321-292
E-mail: mail@cryocosmos.com

LOUTFY R.L.
Materials and Electrochemical Research Corporation,
Tucson, USA
Tel.: 1-520-574-1980
Fax: 1-520-574-1983
E-mail: Shapovalov@mercorp.com

LOVCHIKOV K.V.
Lebedev Rubber Research Institute, Saint-Petersburg,
Russia
Tel.: +7 (812) 251-4028, 251-5227
Fax: +7 (812) 251-4813
E-mail: vniisk@mail.rcom.ru, ypsokol@mail.rcom.ru

LUBYANOI D.A.
West Siberian Steel Corporation, Novokuznetsk, Russia
Tel.: (3843) 59-2879
E-mail: protasov_ds@zsmk.ru

LUCHKA M.V.
Frantsevich Institute for Problems of Materials Science,
NASU, Kyiv, Ukraine
Tel.: (044) 444-2055
Fax: (044) 444-2131
E-mail: tat_zest@yahoo.com, miron@ipms.Kyiv.ua

LUDVINSKAYA T.A.
Frantsevich Institute for Problems of Materials Science,
NASU, Kyiv, Ukraine
Tel.: (044) 444-1501, 444-3522
E-mail: dep15@ipms.Kyiv.ua

LUNIN A.I.
Moscow Technical University, Moscow, Russia
E-mail: nikonov@vniiht.ru

LUNYOV A.N.
Kazan State Technical University, Kazan, Russia
Tel.: (8432) 384-623
Fax: (8432) 435-935
E-mail: root@una.kazan.ru

LUZGINOVA N.V.
Siberian Physic-Technical Institute, Tomsk, Russia
Tel.: (3822) 53-3209
Fax: (3822) 53-3034
E-mail: chum@phys.tsu.ru

LYAKHOV N.Z.
Institute of Solid State Chemistry and
Mechanochemistry, SB RAS, Novosibirsk, Russia
Tel.: (3832) 32-9600
Fax: (3832) 322847
E-mail: servis_ins@online.sinor.ru,
lena@mill.solid.nsc.ru

LYKHODID S.
Frantsevich Institute for Problems of Materials Science,
NASU, Kyiv, Ukraine
Fax: (044) 444-2131

LYSENKO S.I.
Frantsevich Institute for Problems of Materials Science,
NASU, Kyiv, Ukraine
Tel.: (044) 444-3090
Fax: (044) 444-2131
E-mail: dep6@materials.Kyiv.ua

M

MAIBORODA V.P.
Frantsevich Institute for Problems of Materials Science,
NASU, Kyiv, Ukraine
Tel.: (044) 444-3364, 444-0294

MAKARA V.A.
Shevchenko Kyiv National University, Kyiv, Ukraine
Tel.: (044) 510-7837, 227-1027, 266-2326
Fax: (044) 510-7837, 266-2326
E-mail: nodid@mail.univ.Kyiv.ua

MAKARENKO G.N.
Frantsevich Institute for Problems of Materials Science,
NASU, Kyiv, Ukraine
Tel.: (044) 444-1501

MAKAROV A.V.
Institute for Physics of Semiconductors, NAS of
Ukraine, Kyiv, Ukraine
Tel.: (044) 265-6202, 265-6290, 265-1866
Fax: (044) 265-8342
E-mail: mak@gelio.isp.Kyiv.ua

MAKSIMOVA G.M.
Frantsevich Institute for Problems of Materials Science,
NASU, Kyiv, Ukraine
Tel.: (044) 444-3364, 444-0294

MAKSYMOVA S.V.
Paton Electric Welding Institute, NAS of Ukraine, Kyiv,
Ukraine
Tel.: (044) 227-2677, 227-1434
Fax: (044) 227-2677
E-mail: khorunov@ukrpack.net

MAKSYUTA I.I.
Physics and Technology Institute for Metals and Alloys,
NAS of Ukraine, Kyiv, Ukraine
Tel.: (044) 444-3550, 444-1210
Fax: (044) 444-3550, 444-1210
E-mail: maksyuta@ptima.Kyiv.ua

MALAKHOV V.YA.
Frantsevich Institute for Problems of Materials Science,
NASU, Kyiv, Ukraine
Tel.: (044) 444-2371
E-mail: malakhov@ipms.Kyiv.ua

MALASHENKOV S.P.
Institute for Surface Chemistry, NAS of Ukraine, Kyiv,
Ukraine
Tel.: (044) 444-1135
Fax: (044) 444-3567
E-mail: user@surfchem.freenet.Kyiv.ua

MALKHANOVA O.G.
Institute of Metallurgy, Ural's Division of RAS,
Ekaterinburg, Russia
Tel.: +7 3432 67-8924, 28-5312
Fax: +7 3432 67-8918
E-mail: faza@imet.mplik.ru, faza@imet.sco.ru,
m_o_l_a@mail.ru

MAMUNYA YE.P.
Institute of Macromolecular Chemistry, NAS of Ukraine,
Kyiv, Ukraine
Tel.: (044) 559-3722, 559-4695
Fax: (044) 552-4064
E-mail: yemamun@i.Kyiv.ua

MANDICH N.V.
HBM Electrochemical and Engineering Co., Lansing,
Illinois, USA
E-mail: drnenad@ix.netcom.com

MANDLER D.
Hebrew University, Jerusalem, Israel
E-mail: MANDLER@vms.huji.ac.il

MANSUROV Z.A.
Combustion Problem Institute, Almaty, Kazakhstan
Tel.: (3272) 62-7279
Fax: (3272) 92-5811
E-mail: icp@nursut.kz

MANSUROVA R.M.
Combustion Problem Institute, Almaty, Kazakhstan
Tel.: (3272) 62-7279
Fax: (3272) 92-5811
E-mail: icp@nursut.kz

MAREK E.V.
Frantsevich Institute for Problems of Materials Science,
NASU, Kyiv, Ukraine
Tel.: (044) 444-1501

MARKOV V.G.
Central Aero-Hydrodynamic Institute, Zhukovsky,
Russia
Tel.: (095) 192-4615, (411) 244-67-80
Fax: (095) 192-4615
E-mail: rvv@page.net.ru; e.l.gusev@ipng.ysn.ru

MARKOVA L.V.
Powder Metallurgy Research Institute, NAS, Belarus,
Minsk, Belarus
Tel.: (0375) 239-9883, 232-8581
Fax: (0375) 210-0574
E-mail: gppo@mail.ru, chekan@srpmi.minsk.by

MARKOVSKY E.A.
Physics and Technology Institute for Metals and Alloys,
NAS of Ukraine, Kyiv, Ukraine
Tel.: (044) 444-1322, 444-0280
E-mail: vladllch@hotmail.com

MARTINEZ D.
Platforma Solar de Almeria, Tabernas, Spain
E-mail: sreznik@bmstu.ru

MARTÍNEZ M.A.
Universidad Carlos III de Madrid, Spain
Tel.: (3491) 624-9914, 624-9485, 624-9401
Fax: (3491) 624-9430
E-mail: abenojar@ing.uc3m.es, fvelasco@ing.uc3m.es,
jmota@ing.uc3m.es, mamc@ing.uc3m.es

MARTSENYK P.S.
Frantsevich Institute for Problems of Materials Science,
NASU, Kyiv, Ukraine
Tel.: (044) 444-3090
Fax: (044) 444-2131
E-mail: dep6@materials.Kyiv.ua

MARTYUKHIN I.
Frantsevich Institute for Problems of Materials Science,
NASU, Kyiv, Ukraine
Tel.: (044) 444-3255, 444-3039
E-mail: olmi@alfacom.net

MASLOV V.
Kurdyumov Institute for Metal Physics, NASU, Kyiv,
Ukraine
Tel.: (044) 444-3241, 444-3505
Fax: (044) 444-3505
E-mail: maslov@imp.Kyiv.ua

MASLYUK V.
Frantsevich Institute for Problems of Materials Science,
NASU, Kyiv, Ukraine
Tel.: (044) 444-22-64, 444-1201
E-mail: dir@materials.Kyiv.ua,
tkach@materials.Kyiv.ua, maslyuk@materials.Kyiv.ua,

MASUDA-JINDO K.
Tokyo Institute of Technology, Tokyo, Japan
Fax: 81-424-75-0650
E-mail: wmfjindo@din.or.jp, kmjindo@issp.u-tokyo.ac.jp

MATROSOV A.L.
Scientific and Technological Company TECHMA Ltd,
Cheboksary, Russia
Tel.: (8352) 45-3948
Fax: (8352) 45-0901
E-mail: techma@chuvashia.ru

MATSEVITY YU.M.
Podgorny Institute for Mechanical Engineering
Problems, NAS of Ukraine, Kharkov, Ukraine
Tel.: (0572) 94-5514
Fax: (0572) 94-4635
E-mail: matsevit@ipmach.kharkov.ua

MATYGULLINA E.V.
Perm State Technical University, Perm, Russia
Tel.: (3422) 39-1119
Fax: (3422) 39-1122
E-mail: patent@pm.pstu.ac.ru, director@pm.pstu.ac.ru

MATZUI L.
Shevchenko Kyiv National University, Kyiv, Ukraine
Tel.: (044) 266-2384
E-mail: matzui@mail.univ.Kyiv.ua

MEDVEDEV A.S.
Institute of Solid State Physics RAS, Chernogolovka,
Russia
Tel.: (096) 522-2066
E-mail: myshlyae@issp.ac.ru

MELESHEVICH K.A.
Frantsevich Institute for Problems of Materials Science,
NASU, Kyiv, Ukraine
Tel.: (044) 444-3090
Fax: (044) 444-2131
E-mail: dep6@materials.Kyiv.ua

MELESHKO A.I.
Open Joint-Stock Company «KOMPOZIT», Institute of
Metals, Korolev, Russia
Tel.: (095) 513-2091, 513-2326
Fax: (095) 516-0617
E-mail: kompozit.mat@g23.relcom.ru

MELNIKOV V.S.
Institute of Geochemistry, Mineralogy and Ore-
Formation, NASU, Kyiv, Ukraine
Tel.: (044) 444-0570

MELNYK P.I.
Stephanyk Precarpathian University, Ivano-Frankivsk,
Ukraine
E-mail: nsp@pu.if.ua

METH S.
Bar-Ilan University, Tel-Aviv, Israel
E-mail: Sukenc@mail.biu.ac.il

MEZHYLOVSKA L.
Stefanyk Physic-Chemical Institute at Precarpathian
University, Ivano-Frankivsk, Ukraine
Tel.: (0342) 59-6082
E-mail: freik@pu.if.ua

MIKHAILOV O.
Frantsevich Institute for Problems of Materials Science,
NASU, Kyiv, Ukraine
Tel.: (044) 444-3255, 444-3039
E-mail: olmi@alfacom.net

MIKHATULIN D.S.
United Institute for High Temperature, RAS, Moscow,
Russia
Tel.: (095) 484-2888, 485-8255
Fax: (095) 450-7755, 485-8366
E-mail: mikhatulin@ihed.ras.ru

MILMAN Y.V.
Frantsevich Institute for Problems of Materials Science,
NASU, Kyiv, Ukraine
Tel.: (044) 444-3061
Fax: (044) 444-3061
E-mail: korzhova@materials.Kyiv.ua

MINAKOV N.V.
Frantsevich Institute for Problems of Materials Science,
NASU, Kyiv, Ukraine
Tel.: (044) 444-0294, 444-1573
Fax: (044) 444-2131
E-mail: altifer@ipms.Kyiv.ua, vadima2001@mail.ru,
minakov@ipms.Kyiv.ua

MINAKOVA A.V.
Frantsevich Institute for Problems of Materials Science,
NASU, Kyiv, Ukraine
Tel.: (044) 444-0294, 444-1573
Fax: (044) 444-2131
E-mail: altifer@ipms.Kyiv.ua, vadima2001@mail.ru,
minakov@ipms.Kyiv.ua

MINAKOVA R.V.
Frantsevich Institute for Problems of Materials Science,
NASU, Kyiv, Ukraine
Tel.: (044) 444-1181
Fax: (044) 444-2131
E-mail: 29min@ipms.Kyiv.ua

MIRONOVA A.G.
Institute for Solid-State Physics, Materials Science and
Technology at National Science Center «Kharkov
Institute of Physics and Technology» (ISSPMST NSC
KIPT), Kharkov, Ukraine
E-mail: gabelkov@kipt.kharkov.ua

MIRONOVS V.
Technical University, Riga, Latvia
Tel.: (371) 708-9270
Fax: (371) 741-9153
E-mail: mironovs@bf.rtu.lv

MOGAISKAYA N.
Polsunov Central Boiler and Turbine Institute, Saint-
Petersburg, Russia
Tel.: (812) 550-8227
Fax: (812) 550-8227
E-mail: rybnicov@online.ru

MOISHEEV A.A.
Lavochkin Scientific and Production Association, Himky,
Russia
E-mail: brnovets@ipmnet.ru

MOLCHANOVSKAYA G.M.
Frantsevich Institute for Problems of Materials Science,
NASU, Kyiv, Ukraine
Tel.: (044) 444-3364, 444-0294

MOLYAR A.G.
Frantsevich Institute for Problems of Materials Science,
NASU, Kyiv, Ukraine
Tel.: (044) 444-1534, 444-3053, 444-3364

MORDOVETS N.M.
Frantsevich Institute for Problems of Materials Science,
NASU, Kyiv, Ukraine
Tel.: (044) 444-3061
Fax: (044) 444-3061
E-mail: korzhova@materials.Kyiv.ua

MORDYUK B.N.
Kurdyumov Institute for Metal Physics, NASU, Kyiv,
Ukraine
Tel.: (044) 444-9572, 444-0521
E-mail: prokop@imp.Kyiv.ua, galina@imp.Kyiv.ua

MOROZ A.L.
Frantsevich Institute for Problems of Materials Science,
NASU, Kyiv, Ukraine
Tel.: (044) 444-1538
Fax: (044) 444-2131
E-mail: agkost@ipms.Kyiv.ua

MOROZOV I.A.
Frantsevich Institute for Problems of Materials Science,
NASU, Kyiv, Ukraine
Tel.: (044) 444-0002, 444-0101
Fax: (044) 444-2131
E-mail: imorozov@materials.Kyiv.ua

MOROZOVA R.A.
Frantsevich Institute for Problems of Materials Science,
NASU, Kyiv, Ukraine
Tel.: (044) 444-0002, 444-0101
Fax: (044) 444-2131
E-mail: imorozov@materials.Kyiv.ua

MOSHCHIL V.E.
Bakul Institute for Superhard Materials Science, NASU,
Kyiv, Ukraine
Tel.: (044) 430-1126
Fax: (044) 468-8625
E-mail: prikhna@iptelecom.net.ua, frd@ism.Kyiv.ua

MOSKALENKO S.A.
Frantsevich Institute for Problems of Materials Science,
NASU, Kyiv, Ukraine
Tel.: (044) 444-6201
Fax: (044) 444-3017
E-mail: naidich@ipms.Kyiv.ua

MOTA J.M.
Universidad Carlos III de Madrid, Spain
Tel.: (3491) 624-9914, 624-9485, 624-9401
Fax: (3491) 624-9430
E-mail: jmota@ing.uc3m.es,

MOULTANOVSKY A.
Bergstrom Climate Systems, Inc., Rockford, Illinois,
USA
Tel.: 1-815-873-4440
Fax: 1-815-873-4688
E-mail: amoult98@aol.com, AMoult@bergstrominc.com

MUIDINOV M.R.
Institute of Problems of Chemical Physics, RAS,
Chernogolovka, Russia
E-mail: makarov@icp.ac.ru

MUKTEPAVELA F.
Institute of Solid State Physics, University of Latvia,
Riga, Latvia
Tel.: (371) 726-1132
Fax: (371) 711-2583
E-mail: famuk@latnet.lv

MURATOV V.B.
Frantsevich Institute for Problems of Materials Science,
NASU, Kyiv, Ukraine
Tel.: (044) 444-1290
Fax: (044) 444-2131
E-mail: bas@materials.Kyiv.ua

MURZIN A.
Sevastopol National Technical University, Sevastopol,
Ukraine .

MURZIN L.
Sevastopol National Technical University, Sevastopol,
Ukraine

MYALNITSA H.F.
SPE «Mashproekt», Nikolaev, Ukraine
Tel.: (0512) 29-7122
Fax: (0512) 22-0379
E-mail: dobkyna@ptima.Kyiv.ua

MYKHAJLYONKA R.
Stefanyk Physics-Chemical Institute at Precarpathian
University, Ivano-Frankivsk, Ukraine
Tel.: (0342) 59-6082
E-mail: freik@pu.if.ua

MYSHAK V.D.
Institute of Macromolecular Chemistry, NAS of Ukraine,
Kyiv, Ukraine
Tel.: (044) 559-3722, 559-4695
Fax: (044) 552-4064
E-mail: vdmyshak@i.com.ua

MYSHLYAEV D.A.
Scientific and Production Company «Tribonika», Nizny
Novgorod, Russia
Tel.: (8312) 32-0301
Fax: (8312) 32-0301
E-mail: apotapov@sandy.ru

MYSHLYAEV M.M.
Baikov Baikov Baikov Institute of Metallurgy and
Materials Science, RAS, Moscow, Russia
Tel.: (096) 522-2066, (2522) 2066
Fax: (096) 524-9701, (252) 49701
E-mail: myshlyae@issp.ac.ru

N

NAGORNY P.A.
Bakul Institute for Superhard Materials Science, NASU,
Kyiv, Ukraine
Tel.: (044) 430-1126, 468-8625, 468-8987
Fax: (044) 468-8625, 468-8987
E-mail: prikhna@iptelecom.net.ua, frd@ism.Kyiv.ua

NAIDICH YU.V.
Frantsevich Institute for Problems of Materials Science,
NASU, Kyiv, Ukraine
Tel.: (044) 444-6201
Fax: (044) 444-3017
E-mail: naidich@ipms.Kyiv.ua

NAKONECHNA O.I.
Shevchenko Kyiv National University, Kyiv, Ukraine
Tel.: (38044) 266-2335
E-mail: babich@mail.univ.Kyiv.ua,
les@mail.univ.Kyiv.ua

NAYDEK V.L.
Physics and Technology Institute for Metals and Alloys,
NAS of Ukraine, Kyiv, Ukraine
Tel.: (044) 444-3515, 444-1155
Fax: (044) 444-1210
E-mail: metal@ptima.Kyiv.ua, root@u_cast.Kyiv.ua

NAZARSKY T.
Space Research Institute of the Bulgarian Academy of
Sciences, Sofia, Bulgaria
E-mail: dandolov@space.bas.bg

NEIMASH V.
Institute of Physics, NAS of Ukraine, Kyiv, Ukraine ·
Tel.: (044) 265-3973, 265-0825, 265-9958
Fax: (044) 265-1589
E-mail: vova@neimash.Kyiv.ua

NEKLYUDOV I.M.
Institute for Solid-State Physics, Materials Science and
Technology at National Science Center «Kharkov
Institute of Physics and Technology» (ISSPMST NSC
KIPT), Kharkov, Ukraine
Tel.: (0572) 3503530
Fax: (0572) 35-1688
E-mail: sayenko@kipt.kharkov.ua

NEMIROVSKY JU.V.
Institute of the Theoretical and Applied Mechanics, SB
RAS, Novosibirsk, Russia
Tel.: (3832) 30-4273
Fax: (3832) 34-2268
E-mail: shulgin@itam.nsc.ru, vetal@sibnet.ru

NEMOSHKALENKO V.V.
Kurdyumov Institute for Metal Physics, NASU, Kyiv,
Ukraine

NERUS M.
Frantsevich Institute for Problems of Materials Science,
NASU, Kyiv, Ukraine
E-mail: nerus@ukrpost.net

NESHPOR I.P.
Frantsevich Institute for Problems of Materials Science,
NASU, Kyiv, Ukraine
Tel.: (044) 444-1501, 444-3522
E-mail: dep15@ipms.Kyiv.ua

NEVEROVSKAYA A.YU.
Lebedev Rubber Research Institute, Saint-Petersburg,
Russia
Tel.: (812) 100-3898
Fax: (812) 251-4813
E-mail: alcen@comset.net

NGUEN VAN TAN
Institute of Machine Building Technologies of Ministry of
Industry of Vietnam, Hanoi, Vietnam
Tel.: 04 8353113
Fax: 04 8359235

NIKIFOROV V.V.
State Unitary Enterprise «Central Institute of Materials»,
Saint-Petersburg, Russia
Tel.: (812) 278-9114
Fax: (812) 110-7660

NIKITIN A.E.
PKP Delta, Donetsk, Ukraine
E-mail: olesya@eradig.donetsk.ua,
delta2@gppes.donetsk.ua, o_vaall@mail.ru

NOSENKO V.
Kurdyumov Institute for Metal Physics, NASU, Kyiv,
Ukraine
Tel.: (044) 444-3241, 444-3505
Fax: (044) 444-3505
E-mail: nosenko@imp.Kyiv.ua

NOVIKOVA V.I.
Frantsevich Institute for Problems of Materials Science,
NASU, Kyiv, Ukraine
Tel.: (044) 444-0256
E-mail:frolov@alfacom.net

NOVOSELOVA I.A.
Vernadskii Institute of General and Inorganic Chemistry,
NAS of Ukraine, Kyiv, Ukraine
Tel.: (044) 444-0111
Fax: (044) 444-3070
E-mail: GAB@ionc.kar.net, iness@ionc.kar.net

NOVOSJADLUI S.P.
Stephanyk Precarpathian University, Ivano-Frankivsk,
Ukraine
E-mail: nsp@pu.if.ua

O

OGENKO V.M.
Institute for Surface Chemistry, NAS of Ukraine, Kyiv,
Ukraine
Tel.: (044) 444-1135
Fax: (044) 444-3567
E-mail: user@surfchem.freenet.Kyiv.ua

OKATOVA G.
Powder Metallurgy Research Institute, NASB, Minsk,
Belarus
Tel.: (0375) 239-9883, 232-8581
Fax: (0375) 210-0574
E-mail: gppo@mail.ru, chekan@srpmi.minsk.by

OKATOVA T.P.
Powder Metallurgy Research Institute, NASB, Minsk,
Belarus
Tel.: +38 (0472) 47-6536

OKHRIMENKO G.
Institute for Problems of Strength, NASU, Kyiv, Ukraine
Tel.: (044) 295-9613
Fax: (044) 296-1684
E-mail: rum@ipp.adam.Kyiv.ua

OKHRIMENKO V.V.
Frantsevich Institute for Problems of Materials Science,
NASU, Kyiv, Ukraine
Tel.: (044) 444-2401
Fax: (044) 444-2401
E-mail: vish@i.com.ua

OLIKER V.E.
Frantsevich Institute for Problems of Materials Science,
NASU, Kyiv, Ukraine
Tel.: (044) 444-1090
Fax: (044) 444-1090
E-mail: olik@materials.Kyiv.ua

OREKHOV V.T.
State Unitary Enterprise All-Russian Research Institute
of Chemical Technology, Moscow, Russia
E-mail: nikonov@vniiht.ru

ORLOVA E.A.
Special Design Bureau «Tekhnolog» at the Saint-
Petersburg State Technological Institute
(Technical University), Saint-Petersburg, Russia
Tel.: (812)100-3898
Fax: (812) 100-3898
E-mail: alcen@comset.net

ORLOVSKY V.Y.
Paton Electric Welding Institute, NAS of Ukraine, Kyiv,
Ukraine
Tel.: (044) 444-261-5244
Fax: (044) 227-2366
E-mail: Leco@carrier.Kyiv.ua

ORYSHICH I.V.
Frantsevich Institute for Problems of Materials Science,
NASU, Kyiv, Ukraine
Tel.: 044 (444-8286)

OSIPOV V.P.
Bauman Moscow State Technical University, Moscow,
Russia
Tel.: (095) 263-7568, 263-6793
Fax: (095) 261-0107
E-mail: sdpanin@sm.bmstu.ru

OSTRIK A.V.
Institute of Problems of Chemical Physics RAS,
Chernogolovka, Russia
Tel.: (254) 506-65
E-mail: ostrik@pool-7.ru

OSTROVSKI E.K.
Zhukovsky National Aerospace University «Kharkov
Aviation Institute», Kharkov, Ukraine
E-mail: dep60@ipms.Kyiv.ua

OSWALD B.
OSWALD Elektromotoren GmbH, Miltenberg, Germany
E-mail: prikhna@iptelecom.net.ua

OVCHINNIKOV I.N.
Bauman Moscow State Technical University, Moscow,
Russia
E-mail: powder@imet.mplik.ru

P

PADERIN L.YA.
Central Aero-Hydrodynamic Institute, Zhukovsky,
Russia
Tel.: (095) 556-4172
Fax: (095) 556-4337, 911-0019
E-mail: sasha@kura.aerocentr.msk.su

PADERNO YU.B.
Frantsevich Institute for Problems of Materials Science,
NASU, Kyiv, Ukraine
E-mail: dep60@ipms.Kyiv.ua

PANASHENKO V.M.
Frantsevich Institute for Problems of Materials Science,
NASU, Kyiv, Ukraine
Tel.: (044) 444-0101
Fax: (044) 444-2131
E-mail: panavic@materials.Kyiv.ua

PANASYUK A.D.
Frantsevich Institute for Problems of Materials Science,
NASU, Kyiv, Ukraine
Tel.: (044) 444-1191, 444-0590, 444-2201, 444-1321
Fax: (044) 444-2131
E-mail: lavrenko@svitonline.Kyiv.ua

PANCHENKO E.YU.
Siberian Physic-Technical Institute, Tomsk, Russia
Tel.: (3822) 53-3209
Fax: (3822) 53-3034
E-mail: chum@phys.tsu.ru

PANFILOVITCH K.B.
Kazan State Technological University, Kazan, Russia
Tel.: (8432) 194-374, 750-682
Fax: (8432) 369-942
E-mail: panfilovitch@kstu.ru

PANICHENKO S.
Bauman Moscow State Technical University, Moscow,
Russia
Tel.: (095) 263-6277, 267-1729
Fax: (095) 261-4257, 267-7130
E-mail: aleshin@bmstu.ru, Niikmtp@mx.bmstu.ru

PANICHKINA V.V.
Frantsevich Institute for Problems of Materials Science,
NASU, Kyiv, Ukraine
Tel.: (044) 444-3415
Fax: (044) 444-2131
E-mail: vv@pani.Kyiv.ua

PANIN S.D.
Bauman Moscow State Technical University, Moscow,
Russia
Tel.: (095) 263-7568, 263-6793
Fax: (095) 261-0107
E-mail: sdpanin@sm.bmstu.ru

PANOV E.N.
NTUU «Kyiv Polytechnic Institute», Kyiv, Ukraine
Tel.: (044) 274-4052, 241-6870, 241-8609
Fax: (044) 274-4052, 241-6870
E-mail: admin@fizmat.Kyiv.ua

PARTCH R.
Clarkson University CAMP, Potrdam NY, USA
Tel.: (263) 36-401-
Fax: (044) 444-2131
E-mail: poke@ipms.Kyiv.ua

PASCUK S.E.
Molodechno Powder Metallurgy Plant, Molodechno,
Belarus
Tel.: (1773) 32-498, 32-345
E-mail: zpm@molodecno.by, molzpm@mail.ru

PASICHNY V.
Frantsevich Institute for Problems of Materials Science,
NASU, Kyiv, Ukraine
Fax: (044) 444-2131

PATON B.E.
Paton Electric Welding Institute, NAS of Ukraine, Kyiv,
Ukraine
Tel.: (044) 261-5966
Fax: (044) 286-0486

PAUSTOVSKII A.V.
Frantsevich Institute for Problems of Materials Science,
NASU, Kyiv, Ukraine
Tel.: (044) 444-0256

PAVLYUCHENKO V.N.
Saint-Petersburg Department of the Boreskov Institute
of Catalysis, SB RAS, Saint-Petersburg, Russia
E-mail: pavlyuch@SM2270.spd.edu

PAVLYUKEVICH N.V.
Lykov Heat and Mass Transfer Institute, NASB, Minsk,
Belarus
Tel.: (0172) 84-2250, 84-2775, 84-2205
E-mail: pnv@hmti.ac.by

PECHKOVSKY E.P.
Frantsevich Institute for Problems of Materials Science,
NASU, Kyiv, Ukraine
Tel.: (044) 444-0294, 444-1124, 444-0051
Fax: (044) 452-5523
E-mail: fsa@materials.Kyiv.ua, epp@materials.Kyiv.ua

PEDOLSKY H.
"Orbita" Ltd, Kensington, MD, USA
Tel.: 322-293,322-019, 300-364, 300-355
Fax: 322-293, 321-292
E-mail: gavrylov@cryocosmos.com,
moril@cryocosmos.com

PELEVIN F.V.
Bauman Moscow State Technical University, Moscow,
Russia
Tel.: 263-6917, 263-6040
E-mail: pelevin.f.v@mtu-net.ru

PERCHERITSA L.
Institute of Technical Mechanics of NASU and NASUU,
Dniepropetrovsk, Ukraine
Tel.: (0562) 47-2588
Fax: (0562) 47-3413
E-mail: bass@pvv.dp.ua

PERELMAN V.
Lomonosov Moscow Institute of Fine Chemical
Technology, Moscow, Russia
Tel.: 447-6283
Fax: 434-7111
E-mail: perelman@mtu-net.ru

PERESELENTSEVA L.N.
Frantsevich Institute for Problems of Materials Science,
NASU, Kyiv, Ukraine
Tel.: (044) 444-2401
Fax: (044) 444-2401
E-mail: vish@i.com.ua

PEREVYAZKO V.A.
Frantsevich Institute for Problems of Materials Science,
NASU, Kyiv, Ukraine
Tel.: (044) 444-0256, 444-4961

PERMYAKOVA I.J.
Derzhavin Tambov State University, Tambov, Russia
Tel.: (0752) 35-2614
Fax: (0752) 71-0307
E-mail: ushakov@tsu.tmb.ru, feodorov@tsu.tmb.ru

PERMYAKOVA T.V.
Frantsevich Institute for Problems of Materials Science,
NASU, Kyiv, Ukraine
Tel.: (044) 444-1533
Fax: (044) 444-2131
E-mail: tibrat@ipms.Kyiv.ua

PESTOV A.V.
Federal State Unitary Enterprise «Obninsk Research
and Production Enterprise «TECHNOLOGIYA»,
Obninsk, Russia
Tel.: (08439) 96-797
Fax: (08439) 64-575
E-mail: info@technologiya.ru, onpptech@kaluga.ru

PETIT D.
Laboratoire d'Etudes Thermiques, Ecole Nationale
Superieure de Mecanique et d'Aerotechnique,
Futuroscope, France
E-mail: sreznik@bmstu.ru

PETROVA A.M.
Frantsevich Institute for Problems of Materials Science,
NASU, Kyiv, Ukraine
Tel.: (044) 444-3255
Fax: (044) 444-2131
E-mail: dir@ipms.Kyiv.ua

PETUKHOV A.
Minsk Motor Factory, Minsk, Belarus
E-mail: kls@hmti.ac.by

PETUKHOV A.
Frantsevich Institute for Problems of Materials Science,
NASU, Kyiv, Ukraine
Tel.: (044) 444-1533
E-mail: olgak@materials.Kyiv.ua

PILINEVICH L.P.
Powder Metallurgy Research Institute, NASB, Minsk,
Belarus
E-mail: alexil@srpmi.belpak.minsk.by

PILIPENKO A.V.
Institute for Solid-State Physics, Materials Science and
Technology at National Science Center «Kharkov
Institute of Physics and Technology» (ISSPMST NSC
KIPT), Kharkov, Ukraine
E-mail: gabelkov@kipt.kharkov.ua

PINCHUK N.D.
Frantsevich Institute for Problems of Materials Science,
NASU, Kyiv, Ukraine
Tel.: (044) 444-3364
Fax: (044) 450-4487
E-mail: pinchuk_natalie@mail.ru,
pinchuk_natalie@ukrpost.net

PIRYATINSKII YU.P.
Institute of Physics, NAS of Ukraine, Kyiv, Ukraine
E-mail: romanyuk@isp.Kyiv.ua

PISARENKO V.
Frantsevich Institute for Problems of Materials Science,
NASU, Kyiv, Ukraine
Tel.: (044) 444-2524, 444-8286
E-mail: dep53@ipms.Kyiv.ua

PIVINSKY I.Y.
«NVF Kerambet» Ltd, Obninsk, Russia
Tel.: (3432) 5-2361, (3432) 75-9420, (08439) 6-6317
Fax: (34392) 5-2361, (08439) 6-6317
E-mail: kerambet@ok.ru, buran@obninsk.com

PLOSHKIN V.V.
Moscow State Industrial University, Moscow, Russia
E-mail: mgni-info@mtu-net.ru

PLOTNIKOV I.V.
Institute of Applied Physics, Nizny Novgorod, Russia
E-mail: holo@appl.sci-nnov.ru

PLUSHNIKOVA T.N.
Derzhavin Tambov State University, Tambov, Russia
Tel.: (0752) 35-2614
Fax: (0752) 71-0307
E-mail: feodorov@tsu.tmb.ru, plushnik@mail.ru

PLYASUNKOVA L.A.
Federal State Unitary Enterprise «Obninsk Research
and Production Enterprise «TECHNOLOGIYA»,
Obninsk, Russia
E-mail: info@technologiya.ru

PODCHERNYAEVA I.A.
Frantsevich Institute for Problems of Materials Science,
NASU, Kyiv, Ukraine
Tel.: (044) 444-1191, 444-0590, 444-2201, 444-1321
Fax: (044) 444-2131
E-mail: lavrenko@svitonline.Kyiv.ua

PODREZOV YU.N.
Frantsevich Institute for Problems of Materials Science,
NASU, Kyiv, Ukraine
Tel.: (044) 444-1538
Fax: (044) 444-2131
E-mail: agkost@.materials.Kyiv.ua

PODRUCHNIAK E.P.
Institute of Gerontology of MSA of Ukraine, Kyiv,
Ukraine
Tel.: (044) 295-5484

POGREBNJAK A.D.
Sumy Institute for Surface Modification, Sumy, Ukraine
Tel.: 220-0914, 261-5034
E-mail: ytyurin@i.com.ua

POKHYL YU.O.
Verkin Technologies Institute for Low Temperature
Physics and Engineering, NAS of Ukraine, Kharkov,
Ukraine
Tel.: 322-293,322-019, 300-364, 300-355
Fax: 322-293, 321-292
E-mail: gavrylov@cryocosmos.com,
moril@cryocosmos.com

POKROPIVNY A.V.
Frantsevich Institute for Problems of Materials Science,
NASU, Kyiv, Ukraine
Tel.: (263) 36-401-
Fax: (044) 444-2131
E-mail: poke@ipms.Kyiv.ua

POKROPIVNY V.V.
Frantsevich Institute for Problems of Materials Science,
NASU, Kyiv, Ukraine
Tel.: (263) 36-401-
Fax: (044) 444-2131
E-mail: poke@ipms.Kyiv.ua

POLESSKY E.P.
Lykov Heat and Mass Transfer Institute, National
Academy of Belarus, Minsk, Belarus
Tel.: (017) 284-2241, 284-2478
Fax: (017) 232-1325
E-mail: vas@hmti.ac.by, vvl@hmti.ac.by

POLETAEV E.B.
Physics and Technology Institute for Metals and Alloys,
NAS of Ukraine, Kyiv, Ukraine
Tel.: (044) 444-3515, 444-1155
Fax: (044) 444-1210
E-mail: metal@ptima.Kyiv.ua, root@u_cast.Kyiv.ua

POLEZHAEV YU.V.
Institute of High Temperatures Scientific Association,
RAS, Moscow, Russia
Tel.: (095) 484-2888, 485-8255
Fax: (095) 450-7755, 485-8366
E-mail: mikhatulin@ihed.ras.ru

POLOTAY A.V.
Institute for Problems of Materials Science, NASU, Kyiv,
Ukraine
Тел.: (044) 444-2474, 444-1571, 444-3401, 444-3315
E-mail: 29min@ipms.ua, polotay@materials.Kyiv.ua,
dep20@ipms.Kyiv.ua

POLOTAY V.V.
Institute for Problems of Materials Science, NASU, Kyiv,
Ukraine
Тел.: (044) 444-2474, 444-1571, 444-3401, 444-3315
E-mail: 29min@ipms.ua, polotay@materials.Kyiv.ua,
dep20@ipms.Kyiv.ua

POLTAVTSEV N.I.
Institute for Solid-State Physics, Materials Science and
Technology at National Science Center «Kharkov
Institute of Physics and Technology» (ISSPMST NSC
KIPT), Kharkov, Ukraine
E-mail: gabelkov@kipt.kharkov.ua

POMARIN Y.M.
Paton Electric Welding Institute, NAS of Ukraine, Kyiv,
Ukraine
Tel.: (044) 444-261-5244
Fax: (044) 227-2366
E-mail: Leco@carrier.Kyiv.ua

PONOMAREV S.S.
Frantsevich Institute for Problems of Materials Science,
NASU, Kyiv, Ukraine
Tel.: (044) 444-0294
Fax: (044) 444-2131

POPCHUK R.I.
Frantsevich Institute for Problems of Materials Science,
NASU, Kyiv, Ukraine
Tel.: (044) 444-1573
Fax: (044) 444-2131
E-mail: minakov@ipms.Kyiv.ua, altifer@ipms.Kyiv.ua

POPOV A.
Shevchenko Kyiv National University, Kyiv, Ukraine
Tel.: (044) 510-7837, 227-1027, 266-2326
Fax: (044) 510-7837, 266-2326
E-mail: HVitaly@mail.ru

POPOV V.P.
Frantsevich Institute for Problems of Materials Science,
NASU, Kyiv, Ukraine
Tel.: (044) 444-2255
Fax: (044) 444-2131
E-mail: raitch@ipms.Kyiv.ua

POPOVITCH P.
Facultät für Physik, Tubingen universität, Tubingen,
Deutschland
E-mail: nodid@mail.univ.Kyiv.ua

POROZOVA S.E.
Research Center of Powder Material Science, Perm,
Russia
Tel.: (3422) 39-1110
Fax: (3422) 39-1122
E-mail: director@pm.pstu.ac.ru, patent@pm.pstu.ac.ru

PORYADCHENKO N.E.
Frantsevich Institute for Problems of Materials Science,
NASU, Kyiv, Ukraine
Tel.: 044 (444-8286)

POTAPENKO A.I.
Central Institute of Physics and Technology MoD RF,
Sergiev Posad, Russia
Tel.: (095) 485-09-63
E-mail: a.potapenko@mail.ru, potapenko@ihed.ras.ru

POVARCHUK V.
Institute of Physics, NAS of Ukraine, Kyiv, Ukraine
Tel.: (044) 265-3973
Fax: (044) 265-1589
E-mail: vova@neimash.Kyiv.ua,
povarchuk@iop.Kyiv.ua

POZNIAK L.A.
Frantsevich Institute for Problems of Materials Science,
NASU, Kyiv, Ukraine
Tel.: (044) 444-1534, 294-5645
Fax: (044) 444-2034
E-mail: gbag@rambler.ru, celt@materials.Kyiv.ua

PRIKHNA T.A.
Bakul Institute for Superhard Materials Science, NASU,
Kyiv, Ukraine
Tel.: (044) 430-1126
Fax: (044) 468-8625
E-mail: prikhna@iptelecom.net.ua

PRILUTSKII E.V.
Frantsevich Institute for Problems of Materials Science,
NASU, Kyiv, Ukraine
Tel.: (263) 36-401-
Fax: (044) 444-2131
E-mail: poke@ipms.Kyiv.ua

PRIMISKII V.F.
J-S. Society «Ukranalit», Kyiv, Ukraine
Tel.: 269-9913
Fax: 269-9912, 269-9913
E-mail: ukr@analit.relc.com

PRISTIUK M.M.
Verkin Technologies Institute for Low Temperature
Physics and Engineering, NAS of Ukraine, Kharkov,
Ukraine
Tel.: 322-293,322-019, 300-364, 300-355
Fax: 322-293, 321-292
E-mail: gavrylov@cryocosmos.com,
moril@cryocosmos.com

PROKOPENKO G.I.
Kurdyumov Institute for Metal Physics, NASU, Kyiv,
Ukraine
Tel.: (044) 444-9572, 444-0521
E-mail: prokop@imp.Kyiv.ua

PROSUNTSOV P.V.
All-Russian Institute on Aviation Materials, Moscow,
Russia
Tel.: (095) 263-8623
E-mail: copyserv@mtu-net.ru

PRYKHOD'KO I.
Nekrasov Iron and Steel Institute NAS of Ukraine,
Dnepropetrovsk, Ukraine
Tel.: (0562) 46-1051
E-mail: pryhodko@fregat.dp.ua

PSHENICHNA O.V.
Frantsevich Institute for Problems of Materials Science,
NASU, Kyiv, Ukraine
Tel.: (044) 444-1321
E-mail: ngolovko@radgeo.freenet.Kyiv.ua

PUCHKOVA V.U.
Frantsevich Institute for Problems of Materials Science,
NASU, Kyiv, Ukraine
Tel.: (044) 444-0294, 444-1573
Fax: (044) 444-2131
E-mail: altifer@ipms.Kyiv.ua, vadima2001@mail.ru

PYATACHUK S.G.
Frantsevich Institute for Problems of Materials Science,
NASU, Kyiv, Ukraine
Tel.: (044) 444-0256

PYLYPENKO N.P.
Physic-Technical Institute, NAS of Ukraine, Donetsk,
Ukraine
Tel.: (0622) 55-5121
E-mail: tatjana@konstant.fti.ac.donetsk.ua

R

RABINOVICH O.S.
Lykov Heat and Mass Transfer Institute, National
Academy of Belarus, Minsk, Belarus
Tel.: (0172) 84-2250, 84-2775, 84-2205
E-mail: gps@hmti.ac.by, orabi@hmti.ac.by,
pnv@hmti.ac.by

RAGULYA A.
Frantsevich Institute for Problems of Materials Science,
NASU, Kyiv, Ukraine
Tel.: (044) 444-1533
E-mail: olgak@materials.Kyiv.ua

RAILYAN V.S.
Federal State Unitary Enterprise «Obninsk Research
and Production Enterprise «TECHNOLOGIYA»,
Obninsk, Russia
Tel.: (08439) 96-797
Fax: (08439) 64-575
E-mail: onpptech@kaluga.ru, onpptechn@kaluga.ru

RALCHENKO V.
General Physics Institute, RAS, Moscow, Russia
Tel.: (095) 132-8229
Fax: (095) 135-7672
E-mail: ralchenko@nsc.gpi.ru

RAYCHENKO O.I.
Frantsevich Institute for Problems of Materials Science,
NASU, Kyiv, Ukraine
Tel.: (044) 444-2255
Fax: (044) 444-2131
E-mail: raitch@ipms.Kyiv.ua

RAZUMOVSKII I.M.
Open Joint-Stock Company «KOMPOZIT», Institute of
Metals, Korolev, Russia
Tel.: (095) 513-2211, 513-2124, 513-2180
Fax: (095) 516-0617
E-mail: razumov@aif.ru

RED'KO V.P.
Frantsevich Institute for Problems of Materials Science,
NASU, Kyiv, Ukraine
Tel.: (044) 444-3573
Fax: (044) 444-2131
E-mail: dep25@materials.Kyiv.ua

REKADA M.
Quebec University of Montreal, Montréal, Québec,
Canada
Tel.: 1-514-735-7117
E-mail: mdrekada@sympatico.ca

REVIZNIKOV D.L.
Moscow State Aviation Institute, Moscow, Russia
Tel.: (095) 158-4894
E-mail: reviz@k806.mainet.msk.su

REVO S.L.
Shevchenko Kyiv National University, Kyiv, Ukraine
Tel.: (044) 444-3364, 444-0294
Fax: (044) 266-2367
E-mail: revo@phys.univ.Kyiv.ua

REZNIK S.V.
Bauman Moscow State Technical University, Moscow,
Russia
Tel.: (095) 263-6705
Fax: (095) 261-0107
E-mail: sreznik@serv.bmstu.ru

RIZHGOV V.P.
Institute for Solid-State Physics, Materials Science and
Technology at National Science Center «Kharkov
Institute of Physics and Technology» (ISSPMST NSC
KIPT), Kharkov, Ukraine
Tel.: (0572) 35-6612, 35-6355
Fax: (0572) 35-3983
E-mail: igor@kipt.kharkov.ua, gujda@kipt.kharkov.ua

RODIONOVA V.V.
Federal State Unitary Enterprise «NIIGrafit», Moscow,
Russia
E-mail: grafit@aha.ru

ROGOZINSKAYA A.A.
Frantsevich Institute for Problems of Materials Science,
NASU, Kyiv, Ukraine
Tel.: (044) 444-0256, 444-2524
Fax: (044) 444-2131
E-mail: brodnikov@alfacom.net

ROGUL T.
Frantsevich Institute for Problems of Materials Science,
NASU, Kyiv, Ukraine
Tel.: (044) 444-2524, 444-8286
E-mail: dep53@ipms.Kyiv.ua

ROMASHIN A.G.
Federal State Unitary Enterprise «Obninsk Research
and Production Enterprise «TECHNOLOGIYA»,
Obninsk, Russia
Tel.: (095) 255-2394, 546-3592, (08439) 96-763
Fax: (08439) 64-575
E-mail: onpptechn@kaluga.ru

ROSTOVCHIKOV V.A.
JSC «Perm Research Technological Institute» (JSC
«PNITP"), Perm, Russia
Tel.: (3422) 45-3288
E-mail: nasos@pisem.net, KuraevaEN@mh.ru,
nasos@perm.raid.ru

ROZHKOV Y.V.
"NVF Ognjeuporniye Materyaly & Teploviye Agregaty"
Ltd, Pervouralsk, Russia
Tel.: (3432) 5-2361, (3432) 75-9420, (08439) 6-6317
Fax: (34392) 5-2361, (08439) 6-6317
E-mail: polytech@mtf.ustu.ru, buran@obninsk.com

RUD` B.M.
Frantsevich Institute for Problems of Materials Science,
NASU, Kyiv, Ukraine
Tel.: (044) 444-0256, 274-2975, 444-2371
Fax: (044) 444-2131
E-mail: post@ipms.Kyiv.ua, dir@ipms.Kyiv.ua

RUDENSKAYA N.A.
Institute of Solid State Chemistry, Ural Branch of RAS,
Ekaterinburg, Russia
Tel.: (3432) 49-3524, 74-5370
Fax: (3432) 74-4495
E-mail: shveikin@ihim.uran.ru

RUDYK N.D.
Frantsevich Institute for Problems of Materials Science,
NASU, Kyiv, Ukraine
Tel.: (044) 444-0294, 444-1573
Fax: (044) 444-2131
E-mail: altifer@ipms.Kyiv.ua, minakov@ipms.Kyiv.ua

RUSANOVA L.N.
Federal State Unitary Enterprise «Obninsk Research
and Production Enterprise «TECHNOLOGIYA»,
Obninsk, Russia
Tel.: (08439) 96-887
Fax: (08439) 64-575
E-mail: info@technologiya.ru, onpptechn@kaluga.ru

RUSIN M.YU.
Federal State Unitary Enterprise «Obninsk Research
and Production Enterprise «TECHNOLOGIYA»,
Obninsk, Russia
Tel.: (08439) 96-797
Fax: (08439) 64-575
E-mail: info@technologiya.ru

RUTKOVSKIY A.
Frantsevich Institute for Problems of Materials Science,
NASU, Kyiv, Ukraine
Tel.: (044) 444-1486
Fax: (044) 444-2131
E-mail: dir@ipms.Kyiv.ua

RUTMAN YU.L.
KBSM (Special Mechanical Engineering Design Office),
Saint-Petersburg, Russia
Tel.: (812) 542-8894
Fax: (812) 542-8894
E-mail: conby@infopro.spb.su

RYABAKOV A.G.
State Unitary Enterprise All-Russian Research Institute
of Fine Chemical Technology, Moscow, Russia
E-mail: nikonov@vniiht.ru

RYABCHENKO I.A.
Mechanics of Metal-Polymer Systems Research
Institute, NASB, Gomel, Belarus
E-mail: alexil@srpmi.belpak.minsk.by

RYABIKIN YU.A.
Institute of Physical and Technology ME&S RK, Almaty,
Kazakhstan
Tel.: (3272) 54-6413, 54-5281
Fax: (3272) 54-6224
E-mail: gaitinov@satsun.sci.kz, bolotov@satsun.sci.kz

RYABOSHAPKA K.P.
Kurdyumov Institute for Metal Physics, NASU, Kyiv,
Ukraine
Tel.: (044) 444-9590, 444-1548
E-mail: rkp@imp.Kyiv.ua, skrypnyk@i.com.ua

RYBNIKOV A.
Polsunov Central Boiler and Turbine Institute, Saint-
Petersburg, Russia
Tel.: (812) 550-8227
Fax: (812) 550-8227
E-mail: rybnicov@online.ru

RYUMSNYNA T.A.
Donetsk National Technical University, Donetsk,
Ukraine
Tel.: (0622) 55-9515
E-mail: ryumshina@donapex.net

S

SADYKOV F.A.
Institute for Metals Superplasticity Problems, RAS, Ufa,
Russia
Tel.: (3472) 25-3750, 25-3815
Fax: (3472) 25-3759
E-mail: imsp11@anrb.ru, aigirsh@rambler.ru

SAGADEEV V.V.
Kazan State Technological University, Kazan, Russia
Tel.: (8432) 194-374, 750-682
Fax: (8432) 369-942
E-mail: roustam@dionis.kstu.ru, panfilovitch@kstu.ru

SALVATORI S.
Third University of Rome, Department of Electronics,
Rome, Italy
Tel.: (095) 132-8229
Fax: (095) 135-7672
E-mail: ralchenko@nsc.gpi.ru

SAMELUK A.
Frantsevich Institute for Problems of Materials Science,
NASU, Kyiv, Ukraine
Tel.: (044) 444-2524, 444-8286
E-mail: dep53@ipms.Kyiv.ua

SAMSONOV V.I.
Federal State Unitary Enterprise «Obninsk Research
and Production Enterprise «TECHNOLOGIYA»,
Obninsk, Russia
Tel.: (08439) 96-763
Fax: (08439) 64-575
E-mail: info@technologiya.ru

SARTINSKA L.L.
Frantsevich Institute for Problems of Materials Science,
NASU, Kyiv, Ukraine
Tel.: (044) 444-2371
Fax: (044) 444-2131
E-mail: sart@ipms.Kyiv.ua

SAVANINA N.N.
Federal State Unitary Enterprise «Obninsk Research
and Production Enterprise «TECHNOLOGIYA»,
Obninsk, Russia
Tel.: (08439) 96-659, 99-041,96-875
Fax: (08439) 64-575
E-mail: info@technologiya.ru, onpptechn@kaluga.ru

SAVCHENKO N.
Oil Refineries Ltd., Haifa, Israel
Tel.: 972-4-8788623
Fax: 972-4-8788371
E-mail: GALEC@orl.co.il

SAVCHUK YA.M.
Bakul Institute for Superhard Materials Science, NASU,
Kyiv, Ukraine
Tel.: (044) 430-1126, 468-8625, 468-8987
Fax: (044) 468-8625, 468-8987
E-mail: prikhna@iptelecom.net.ua, frd@ism.Kyiv.ua

SAVENKO V.S.
Mozyr State Pedagogical Institute, Mozyr, Belarus
Tel.: 3750215125438
E-mail: mozvuz@mail.gomel.by

SAVICH V.V.
Powder Metallurgy Research Institute, NASB, Minsk,
Belarus
E-mail: alexil@srpmi.belpak.minsk.by

SAYENKO S.YU.
Institute for Solid-State Physics, Materials Science and
Technology at National Science Center «Kharkov
Institute of Physics and Technology» (ISSPMST NSC
KIPT), Kharkov, Ukraine
E-mail: gabelkov@kipt.kharkov.ua

SCHEKIN-KROTOV V.A.
Joint Stock Company «FIKO», Kyiv, Ukraine
Tel.: (044) 201-6136
Fax: (044) 264-0546

SCHERBAKOVA L.G.
Frantsevich Institute for Problems of Materials Science,
NASU, Kyiv, Ukraine
Tel.: 044 (444-8286)

SCHERBAKOVA L.N.
Frantsevich Institute for Problems of Materials Science,
NASU, Kyiv, Ukraine
Fax:: (044) 444-2131

SCHMIDT CH.
Institut fur Physikalische Hochtechnologie, Jena,
Germany
Tel.: (49 36 41) 20-6103, 20-6107, 20-6106
Fax: (49 36 41) 20-6199
E-mail: Christa.Schmitd@ipht-jena.de

SEMENOVA E.L.
Frantsevich Institute for Problems of Materials Science,
NASU, Kyiv, Ukraine
Tel.: (044) 444-30-90
E-mail: selena@materials.Kyiv.ua

SEMENTSOV YU.I.
"TMSpecmash" Ltd., Kyiv, Ukraine
Tel.: (044) 461-9937
Fax: (044) 461-9942
E-mail: tmlab@i.com.ua

SEMIRGA A.M.
Kurdyumov Institute for Metal Physics, NASU, Kyiv,
Ukraine
Tel.: (044) 444-9588, 444-3577
E-mail: danila@imp.Kyiv.ua

SENKOVENKO M.YU.
Institute of the Theoretical and Applied Mechanics, SB
RAS, Novosibirsk, Russia
Tel.: (3832) 30-4273
Fax: (3832) 34-2268
E-mail: shulgin@itam.nsc.ru, vetal@sibnet.ru

SENYUT V.
Institute of Machine Reliability, NASB, Minsk, Belarus
Tel.: (017) 284-2401
Fax: (017) 284-2401
E-mail: nanotech@inmash.bas-net.by

SEPLYARSKII B.S.
Institute of Structural Macrokinetics and Materials
Science, RAS, Chernogolovka, Russia
E-mail: sepl@ism.ac.ru, tanja@ism.ac.ru

SEREDA G.N.
Federal State Unitary Enterprise «Obninsk Research
and Production Enterprise «TECHNOLOGIYA»,
Obninsk, Russia
Tel.: (08439) 96-802, 98-484
Fax: (08439) 64-575
E-mail: info@technologiya.ru, onpptechn@kaluga.ru

SERGEYEV M.V.
Kazan State Technical University, Kazan, Russia
Tel.: (8432) 384-623
Fax: (8432) 435-935
E-mail: root@una.kazan.ru

SERGEYEV V.V.
Scientific-Industrial Complex «Yuna», Kazan, Russia
Tel.: (8432) 435-935
Fax: (8432) 435-935
E-mail: root@una.kazan.ru

SERGIENKO N.V.
Bakul Institute for Superhard Materials Science, NASU,
Kyiv, Ukraine
Tel.: (044) 430-1126
Fax: (044) 468-8625
E-mail: prikhna@iptelecom.net.ua, frd@ism.Kyiv.ua

SHALUNOV E.P.
Scientific and Technological Company TECHMA Ltd,
Cheboksary, Russia
Tel.: (8352) 45-3948
Fax: (8352) 45-0901
E-mail: techma@chuvashia.ru

SHAPOVAL A.A.
NTUU «Kyiv Polytechnic Institute», Kyiv, Ukraine
Tel.: (044) 252-3643
Fax: (044) 444-2131
E-mail: admin@fizmat.Kyiv.ua

SHAPOVALOV V.I.
Materials and Electrochemical Research Corporation,
Tucson, USA
Tel.: 1-520-574-1980
Fax: 1-520-574-1983
E-mail: Shapovalov@mercorp.com

SHARAFUTDINOV A.R.
Bauman Moscow State Technical University, Moscow,
Russia
Tel.: (095) 263-6705
Fax: (095) 261-3614
E-mail: ml_shaman@mail.ru

SHARAFUTDINOV M.R.
Institute of Solid State Chemistry and
Mechanochemistry, SB RAS, Novosibirsk, Russia
Tel.: (3832) 39-4145
E-mail: ancharov@mail.ru

SHARAPOV V.M.
Cherkassy State Technological University, Cherkassy,
Ukraine
Tel.: +38 (0472) 43-3680, 42-2148, 43-01-10
Fax:+38 (0472) 43-23-54, 42-2165
E-mail: bosh@gate.chiti.uch.net

SHATALOV V.V.
State Unitary Enterprise All-Russian Research Institute
of Chemical Technology, Moscow, Russia
E-mail: nikonov@vniiht.ru

SHATRAVA A.P.
Frantsevich Institute for Problems of Materials Science,
NASU, Kyiv, Ukraine
Tel.: (044) 444-1310
Fax: (044) 444-0250
E-mail: vladIIch@hotmail.com

SHATSCIKH C.K.
Frantsevich Institute for Problems of Materials Science,
NASU, Kyiv, Ukraine
Fax:: (044) 444-2131

SHCHERBAK I.A.
Frantsevich Institute for Problems of Materials Science,
NASU, Kyiv, Ukraine
Tel.: (044) 444-1290
E-mail: bas@materials.Kyiv.ua

SHEFER M.
Hebrew University, Jerusalem, Israel
E-mail: MANDLER@vms.huji.ac.il

SHELUD`KO V.E.
Frantsevich Institute for Problems of Materials Science,
NASU, Kyiv, Ukraine
Tel.: (044) 444-0256, 274-2975, 444-2371
Fax: (044) 444-2131
E-mail: post@ipms.Kyiv.ua, dir@ipms.Kyiv.ua

SHESTAKOV S.I.
Bakul Institute for Superhard Materials Science, NASU,
Kyiv, Ukraine
Tel.: (044) 443-9544
Fax: (044) 467-5625
E-mail: ism1@kibor.Kyiv.ua

SHEVCHENKO A.D.
Kurdyumov Institute for Metal Physics, NASU, Kyiv,
Ukraine
Tel.: (044) 444-10-05
Fax: (044) 444-2561

SHEVCHENKO O.M.
Frantsevich Institute for Problems of Materials Science,
NASU, Kyiv, Ukraine
Tel.: (044) 444-3364

SHEVCHUK N.V.
Frantsevich Institute for Problems of Materials Science,
NASU, Kyiv, Ukraine
Tel.: (044) 444-1290
E-mail: bas@materials.Kyiv.ua

SHEVYAKOVA EH.P.
Institute for Solid-State Physics, Materials Science and
Technology at National Science Center «Kharkov
Institute of Physics and Technology» (ISSPMST NSC
KIPT), Kharkov, Ukraine
E-mail: gabelkov@kipt.kharkov.ua

SHIGANOV I.
Bauman Moscow State Technical University, Moscow,
Russia
Tel.: (095) 263-6277, 267-1729
Fax: (095) 261-4257, 267-7130
E-mail: aleshin@bmstu.ru, Niikmtp@mx.bmstu.ru

SHILOVITCH T.
NTUU «Kyiv Polytechnic Institute», Resources-
Economy Technique Research Center, Kyiv, Ukraine
Tel.: (044) 241-6870
Fax: (044) 241-8609
E-mail: admin@fizmat.Kyiv.ua

SHKATULAK N.M.
South Ukrainian State Pedagogical University, Odessa,
Ukraine
Tel.: (0482) 23-4098
Fax: (0482) 732-5103
E-mail: usov@balkan.farlep.net

SHLAPAK A.M.
Frantsevich Institute for Problems of Materials Science,
NASU, Kyiv, Ukraine
Tel.: (044) 444-1431
E-mail: dep69@ipms.Kyiv.ua

SHMAGINA L.V.
Kazan State Technological University, Kazan, Russia
Tel.: (8432) 194-374, 750-682
Fax: (8432) 369-942
E-mail: roustam@dionis.kstu.ru, panfilovitch@kstu.ru

SHTERN M.
Frantsevich Institute for Problems of Materials Science,
NASU, Kyiv, Ukraine
Tel.: (044) 444-3039
E-mail: olmi@alfacom.net

SHULGIN YU.F.
Kuzmashzavod, Novokuznetsk, Russia
Tel.: (3843) 42-8781
E-mail: protasov_ds@zsmk.ru

SHULISHOVA O.I.
Frantsevich Institute for Problems of Materials Science,
NASU, Kyiv, Ukraine
Tel.: (044) 444-1290
E-mail: bas@materials.Kyiv.ua

SHULYAKOVSKY A.V.
Bauman Moscow State Technical University, Moscow,
Russia
Tel.: (095) 263-6705
Fax: (095) 261-3614
E-mail: a_shulyakovskyk@mail.ru

SHVEIKIN G.P.
Institute of Solid State Chemistry, Ural Branch of RAS,
Ekaterinburg, Russia
Tel.: (3432) 49-3524, 74-5370
Fax: (3432) 74-4495
E-mail: shveikin@ihim.uran.ru

SIDORKO V.R.
Frantsevich Institute for Problems of Materials Science,
NASU, Kyiv, Ukraine
Tel.: (044) 444-30-90
E-mail: selena@materials.Kyiv.ua

SILANTIEV V.I.
Institute for Magnetism, NASU, Kyiv, Ukraine
Tel.: (044) 444-9568
Fax: (044) 444-1020
E-mail: vbar@imag.Kyiv.ua

SILENKO P.M.
Frantsevich Institute for Problems of Materials Science,
NASU, Kyiv, Ukraine
Tel.: (044) 444-1431
E-mail: dep69@ipms.Kyiv.ua

SIMAN N.
Frantsevich Institute for Problems of Materials Science,
NASU, Kyiv, Ukraine
Tel.: (044) 444-2371

SIMEONOVA YU.
Space Research Institute of the Bulgarian Academy of
Sciences, Sofia, Bulgaria
E-mail: dandolov@space.bas.bg

SIMOEN E.
IMEC, Leuven, Belgium
E-mail: claeys@imec.be, simoen@imec.be

SINAISKIY B.M.
Frantsevich Institute for Problems of Materials Science,
NASU, Kyiv, Ukraine
Tel.: (044) 444-2401
Fax: (044) 444-2401
E-mail: vish@i.com.ua

SIROESHCO G.S.
Molodechno Powder Metallurgy Plant, Molodechno,
Belarus
Tel.: (1773) 32-498, 32-345
E-mail: zpm@molodecno.by, molzpm@mail.ru

SIROTENKO L.D.
Perm State Technical University, Perm, Russia
Tel.: (3422) 39-1119
Fax: (3422) 39-1122
E-mail: patent@pm.pstu.ac.ru, director@pm.pstu.ac.ru

SIROVATKA V.L.
Frantsevich Institute for Problems of Materials Science,
NASU, Kyiv, Ukraine
Tel.: (044) 444-1090
Fax: (044) 444-1090
E-mail: olik@materials.Kyiv.ua

SITALO V.G.
State Design Office Yuzhnoye, Dniepropetrovsk,
Ukraine
Tel.: (0562) 92-5113, 92-0866
Fax: (0562) 92-5113
E-mail: kbu@public.ua.net, bunchuc@a-teleport.com

SKACHEDUB A.A.
State Unitary Enterprise All-Russian Research Institute
of Chemical Technology, Moscow, Russia
E-mail: nikonov@vniiht.ru

SKACHKOV V.
Zaporozhye State Engineering Academy, Zaporozhye,
Ukraine
Tel.: (0612) 60-1517
Fax: (0612) 35-5273
E-mail: kvd@vuglecomp.zp.ua

SKOROKHOD V.V.
Frantsevich Institute for Problems of Materials Science,
NASU, Kyiv, Ukraine
Tel.: (044) 444-2264
Fax: (044) 444-2131
E-mail: dir@materials.Kyiv.ua

SKRIFVARS M.
SICOMP AB, Pitea, Sweden
E-mail: mikael.skrifvars@sicomp.se

SKRYPAI A.A.
Frantsevich Institute for Problems of Materials Science,
NASU, Kyiv, Ukraine
Tel.: (044) 444-1290
Fax: (044) 444-2131
E-mail: bas@materials.Kyiv.ua

SKRYPKA N.N.
Physics and Technology Institute for Metals and Alloys,
NAS of Ukraine, Kyiv, Ukraine
E-mail: ver@materials.Kyiv.ua

SKRYPNYK YU.V.
Kurdyumov Institute for Metal Physics, NASU, Kyiv,
Ukraine
Tel.: (044) 444-9590, 444-1548
E-mail: rkp@imp.Kyiv.ua, skrypnyk@i.com.ua

SLOBODYANIK N.S.
Shevchenko Kyiv National University, Kyiv, Ukraine
E-mail: nodid@mail.univ.Kyiv.ua

SLYS I.
Frantsevich Institute for Problems of Materials Science,
NASU, Kyiv, Ukraine
Tel.: (044) 444-1124
E-mail: SLYS@materials.Kyiv.ua

SLYUNYAEV V.N.
Frantsevich Institute for Problems of Materials Science,
NASU, Kyiv, Ukraine
Fax: (044) 444-2131

SMELAYA T.
Institute of Technical Mechanics of NASU and NASUU,
Dniepropetrovsk, Ukraine
Tel.: (0562) 47-2588
Fax: (0562) 47-3413
E-mail: bass@pvv.dp.ua

SMIRNOV K.L.
Institute of Structural Macrokinetics and Materials
Science, RAS, Chernogolovka, Russia
Tel.: (252) 46-267
Fax: (095) 962-8025
E-mail: kosm@ism.ac.ru

SMIRNOV V.P.
Institute for Problems of Materials Science, NASU, Kyiv, Ukraine
Тел.: (044) 444-2474, 444-1571, 444-3401, 444-3315
E-mail: 29min@ipms.ua, polotay@materials.Kyiv.ua, dep20@ipms.Kyiv.ua

SNOPKO V.N.
Institute of Physics, National Academy of Sciences, Minsk, Belarus
E-mail: tsaruk@dragon.bas-net.by

SOBESKI A.S.
Belarussian State University, Minsk, Belarus
Tel.: (017) 209-5462
E-mail: MichaelZheludkevich@scnsoft.com, mmmmm@tut.by

SOKOLOV YU.P.
Lebedev Rubber Research Institute, Saint-Petersburg, Russia
Tel.: +7 (812) 251-4028, 251-5227
Fax: +7 (812) 251-4813
E-mail: vniisk@mail.rcom.ru, ypsokol@mail.rcom.ru

SOLNTSEV V.P.
Frantsevich Institute for Problems of Materials Science, NASU, Kyiv, Ukraine
Tel.: (044) 444-1201
E-mail: solntsev_kutuz@mail.ru

SOLNTSEVA T.
Frantsevich Institute for Problems of Materials Science, NASU, Kyiv, Ukraine
Tel.: (044) 444-22-64, 444-1201
E-mail: solntsev_kutuz@mail.ru

SOLONIN S.M.
Frantsevich Institute for Problems of Materials Science, NASU, Kyiv, Ukraine
Tel.: (044) 444-3415
Fax: (044) 220-4094
E-mail: kolom@ukrnet.net

SOLONIN YU.M.
Frantsevich Institute for Problems of Materials Science, NASU, Kyiv, Ukraine
Fax: (044) 444-2131

SOLOZHENKO V.L.
Bakul Institute for Superhard Materials Science, NASU, Kyiv, Ukraine
E-mail: romanyuk@isp.Kyiv.ua

SOROCHINSKAYA O.V.
Saint-Petersburg Department of the Boreskov Institute of Catalysis, SB RAS, Saint-Petersburg, Russia
E-mail: pavlyuch@SM2270.spd.edu, mikael.skrifvars@sicomp.se

SOROKIN V.A.
Scientific and Production Company «Tribonika», Nizny Novgorod, Russia
Tel.: (8312) 32-0301
Fax: (8312) 32-0301
E-mail: apotapov@sandy.ru

SPIRIDONOV YU.L.
Scientific-Industrial Complex «Yuna», Kazan, Russia
Tel.: (8432) 435-935
Fax: (8432) 435-935
E-mail: root@una.kazan.ru

STARCHENKO I.M.
Institute of Solid State and Semiconductors Physics, NASB, Belarus, Minsk
Tel.: (0172) 284-12-78
Fax: (0172) 284-08-88
E-mail: star@ifttp.bas-net.by

STAROSVETSKY D.
Technion, Haifa, Israel
Tel.: 972-4-8788623
Fax: 972-4-8788371
E-mail: GALEC@orl.co.il, Sukenc@mail.biu.ac.il, MANDLER@vms.huji.ac.il

STELMAKH L.S.
Institute of Problems of Chemical Physics, RAS, Chernogolovka, Russia
Tel.: (09652) 46-395
E-mail: stelm@ism.ac.ru

STELMAKH O.
Shevchenko Kyiv National University, Kyiv, Ukraine
Tel.: (044) 266-2384
E-mail: vovch@mail.univ.Kyiv.ua, matzui@mail.univ.Kyiv.ua

STETSYUK T.V.
Frantsevich Institute for Problems of Materials Science, NASU, Kyiv, Ukraine
Tel.: (044) 444-3017
Fax: (044) 444-3017
E-mail: naidich@ipms.Kyiv.ua

STOLIN A.M.
Institute of Structural Macrokinetics and Materials Science, RAS, Chernogolovka, Russia
Tel.: (09652) 46-395
E-mail: amstolin@ism.ac.ru

STUS N.V.
Shevchenko Kyiv National University, Kyiv, Ukraine
E-mail: nodid@mail.univ.Kyiv.ua

SUBBOTIN V.I.
Frantsevich Institute for Problems of Materials Science, NASU, Kyiv, Ukraine
Tel.: (044) 444-1501, 444-3522
E-mail: dep15@ipms.Kyiv.ua

SUCHKOVA G.A.
Institute of Solid State Chemistry and Mechanochemistry, SB RAS, Novosibirsk, Russia
Tel.: (3832) 32-9600
Fax: (3832) 322847
E-mail: lena@mill.solid.nsc.ru

SUDAVTSOVA V.S.
Shevchenko Kyiv National University, Kyiv, Ukraine
E-mail: vsudavtsova@univ.Kyiv.ua

SUKENIC C.
Bar-Ilan University, Tel-Aviv, Israel
E-mail: Sukenc@mail.biu.ac.il

SUKHAREVA T.
Institute for Solid-State Physics, Materials Science and
Technology at National Science Center «Kharkov
Institute of Physics and Technology» (ISSPMST NSC
KIPT), Kharkov, Ukraine
Tel.: (0572) 356-612, 356-484
Fax: (0572) 353-983
E-mail: admin@kipt.kharkov.ua, igor@kipt.kharkov.ua

SUKHODOLOV A.
Institute of Physics, NASB, Minsk, Belarus
Tel.: (095) 132-8229
Fax: (095) 135-7672
E-mail: ralchenko@nsc.gpi.ru

SULYMA V.S.
Institute of Traumatology and Ortopedic of MSA of
Ukraine, Kyiv, Ukraine
Tel.: (044) 216-1633, 216-6983

SURKOV A.E.
Institute for Solid-State Physics, Materials Science and
Technology at National Science Center «Kharkov
Institute of Physics and Technology» (ISSPMST NSC
KIPT), Kharkov, Ukraine
E-mail: gabelkov@kipt.kharkov.ua

SURZHENKO A.B.
Institut fur Physikalische Hochtechnologie, Jena,
Germany
Tel.: (49 36 41) 206103
Fax: (49 36 41) 206199
E-mail: Oleksiy.Surzhenko@ipht-jena.de

SURZHENKO O.
Institut fur Physikalische Hochtechnologie, Jena,
Germany
E-mail: prikhna@iptelecom.net.ua

SUZDAL'TSEV E.I.
Federal State Unitary Enterprise «Obninsk Research
and Production Enterprise «TECHNOLOGIYA»,
Obninsk, Russia
Tel.: (08439) 96-797
Fax: (08439) 64-575
E-mail: info@technologiya.ru, onpptech@kaluga.ru

SVERDUN V.B.
Bakul Institute for Superhard Materials Science, NASU,
Kyiv, Ukraine
Tel.: (044) 430-1126
Fax: (044) 468-8625
E-mail: prikhna@iptelecom.net.ua, frd@ism.Kyiv.ua

T

TADLYA K.
Institute of Engeneering Thermophysics, Kyiv, Ukraine
Tel.: (044) 446-9281, 441-7304
Fax: (044) 446-6091
E-mail: konst@ittf.Kyiv.ua, temerline@yahoo.com,
sudak@ittf.Kyiv.ua

TADLYA O.
Institute of Engeneering Thermophysics, Kyiv, Ukraine
Tel.: (044) 446-9281, 441-7304
Fax: (044) 446-6091
E-mail: konst@ittf.Kyiv.ua, temerline@yahoo.com,
sudak@ittf.Kyiv.ua

TAKASHI NAKAMURA
Tohoku University, Sendai, Japan
Tel.: (81-22) 217-5214
Fax: (81-22) 217-5178
E-mail: slava@iamp.tohoku.ac.jp

TARAN A.A.
Zhukovsky National Aerospace University «Kharkov
Aviation Institute», Kharkov, Ukraine
E-mail: dep60@ipms.Kyiv.ua

TARANENKO L.
Kurdyumov Institute for Metal Physics, NASU, Kyiv,
Ukraine
Tel.: (044) 444-3241, 444-3505
Fax: (044) 444-3505
E-mail: nosenko@imp.Kyiv.ua, lyubov@istu.Kyiv.ua

TARASENKO YU.P.
Scientific and Production Company «Tribonika», Nizny
Novgorod, Russia
Tel.: (8312) 32-0301
Fax: (8312) 32-0301
E-mail: apotapov@sandy.ru

TARASOV A.F.
South Ukrainian State Pedagogical University, Odessa,
Ukraine
Tel.: (0482) 64-7753, 61-0823, 20-8181
E-mail: storm_x@aport.ru

TARASOV P.V.
Institute for Solid-State Physics, Materials Science and
Technology at National Science Center «Kharkov
Institute of Physics and Technology» (ISSPMST NSC
KIPT), Kharkov, Ukraine
E-mail: gabelkov@kipt.kharkov.ua

TCHETANOV B.V.
State Enterprise «VIAM», Moscow, Russia
Tel.: (095) 263-8911
Fax: (095) 267-6177
E-mail: admin@viam.ru

TEL`NIKOV E.YA.
Frantsevich Institute for Problems of Materials Science,
NASU, Kyiv, Ukraine
Tel.: (044) 444-0256, 274-2975, 444-2371
Fax: (044) 444-2131
E-mail: post@ipms.Kyiv.ua, dir@ipms.Kyiv.ua

TEPLENKO M.A.
Frantsevich Institute for Problems of Materials Science, NASU, Kyiv, Ukraine
Fax: (044) 444-2131

TIMOFEEV A.N.
Open Joint-Stock Company «KOMPOZIT», Institute of Metals, Korolev, Russia
Tel.: (095) 513-2211, 513-2124, 513-2180
Fax: (095) 516-0617
E-mail: kompozit.mat@g23.relcom.ru

TIMOFEEVA I.I.
Frantsevich Institute for Problems of Materials Science, NASU, Kyiv, Ukraine
Tel.: (044) 444-0256, 444-0492
E-mail: frolov@alfacom.net

TIMOSHENKO E.S.
South Ukrainian State Pedagogical University, Odessa, Ukraine
Tel.: (0482) 64-7753, 61-0823, 20-8181
E-mail: storm_x@aport.ru

TIMOSHENKO M.
Commercial Bank "Premierbank"
Tel.: (0562) 45-1053
E-mail: mtimoshenko@premierbank.dp.ua

TIMOSHENKO V.
Institute of Technical Mechanics of NASU and NASUU, Dniepropetrovsk, Ukraine
Tel.: (0562) 46-1051
Fax: (0562) 47-3413
E-mail: timoshenko@itm3.dp.ua

TIMOSHENKO V.P.
NPO «Molniya», Moscow, Russia
E-mail: moltim@dol.ru

TISCHENKO V.
Institute of Physics, NAS of Ukraine, Kyiv, Ukraine
Tel.: (044) 265-3973, 265-0825, 265-9958
Fax: (044) 265-1589
E-mail: tischenko@iop.Kyiv.ua

TJALIN YU.I.
Derzhavin Tambov State University, Tambov, Russia
Tel.: (0752) 35-2614
Fax: (0752) 71-0307
E-mail: feodorov@tsu.tmb.ru, plushnik@mail.ru

TKACHENKO G.
Frantsevich Institute for Problems of Materials Science, NASU, Kyiv, Ukraine
Tel.: (044) 450-4963, 444-1191
Fax: (044) 444-2131
E-mail: cosmos@ipms.Kyiv.ua, vyakysil@i.com.ua

TKACHENKO L.
Frantsevich Institute for Problems of Materials Science, NASU, Kyiv, Ukraine
Tel.: (044) 444-22-64, 444-1201
E-mail: tkach@materials.Kyiv.ua

TKACHENKO S.G.
PKP Delta, Donetsk, Ukraine
E-mail: delta2@gppes.donetsk.ua

TOLKACHEV A.N.
Institute of Solid State and Semiconductors Physics, NASB, Belarus, Minsk
Tel.: (0172) 284-12-78
Fax: (0172) 284-08-88
E-mail: star@ifttp.bas-net.by

TOLOCHKO N.K.
Technical Acoustics Research Institute, NASB, Vitebsk, Belarus
E-mail: alexil@srpmi.belpak.minsk.by

TONKOVID A.N.
Government Plant of Powder Metallurgy, Brovary, Ukraine
Tel.: (294) 50-182, 52-265
Fax: (294) 50-585, 62-924
E-mail: pmplant@realtel.net.ua

TOVAROVSKIY I.G.
Nekrasov Iron and Steel Institute, NASU, Dnepropetrovsk, Ukraine
Tel.: (0562) 47-4548 (сл.), 46-6955 (дом.)
Fax: (056) 776-5324
E-mail: iosif@tig.dp.ua

TRAPALIS CHRISTOS
Institute of Materials Science, Athens, Greece
Tel.: 3-01-65-03-336

TRET'YAK M.S.
NASB, Minsk, Belarus
Tel.: (103-75-172) 84-1521
Fax: (103-75-172) 28-42212
E-mail: office@hmti.oc.by

TRIFONOV V.G.
Institute for Metals Superplasticity Problems, RAS, Ufa, Russia
Tel.: (3472) 25-3750, 25-3815
Fax: (3472) 25-3759
E-mail: imsp11@anrb.ru, aigirsh@rambler.ru

TRIOLO J.J.
NASA, Washington, DC, USA
Tel.: 322-293,322-019, 300-364, 300-355
Fax: 322-293, 321-292
E-mail: gavrylov@cryocosmos.com, moril@cryocosmos.com

TROFIMOV A.I.
Federal State Unitary Enterprise «Obninsk Research and Production Enterprise «TECHNOLOGIYA», Obninsk, Russia
Tel.: (08439) 96-802
Fax: (08439) 64-575
E-mail: info@technologiya.ru

TROPINOV A.
Scientific Private Company «ALINEKA», Kyiv, Ukraine
Tel.: (044) 248-6187
Fax: (044) 248-6187
E-mail: alineka@Kyiv-page.com.ua

TROPINOVA I.
Scientific Private Company «ALINEKA», Kyiv, Ukraine
Tel.: (044) 248-6187
Fax: (044) 248-6187
E-mail: alineka@Kyiv-page.com.ua

TSARIOVA I.N.
Scientific and Production Company «Tribonika», Nizny
Novgorod, Russia
Tel.: (8312) 32-0301
Fax: (8312) 32-0301
E-mail: apotapov@sandy.ru

TSISAR V.
Karpenko Physico-Mechanical Institute, NASU, Lviv,
Ukraine
Tel.: (0322) 65-4343
Fax: (0322) 64-9427
E-mail: olga.yeliseyeva@brasimone.enea.it,
fedirco@ipm.lviv.ua

TSURPAL L.A.
Frantsevich Institute for Problems of Materials Science,
NASU, Kyiv, Ukraine
Tel.: (044) 444-2024
Fax: (044) 444-2131
E-mail: vkur@ipms.Kyiv.ua

TSYGANENKO V.S.
Frantsevich Institute for Problems of Materials Science,
NASU, Kyiv, Ukraine
Tel.: (044) 444-0256, 444-0492
E-mail: frolov@alfacom.net

TUKOV V.G.
PKP Delta, Donetsk, Ukraine
E-mail: delta2@gppes.donetsk.ua

TUMILOVICH M.V.
Powder Metallurgy Research Institute, NASB, Minsk,
Belarus
E-mail: alexil@srpmi.belpak.minsk.by

TURKEBAEV T.E.
Institute of Nuclear Physics of National Nuclear Center,
Almaty, Kazakhstan
Tel.: (3272) 54-5143, 54-6467
Fax: (3272) 54-6517
E-mail: turkebaev@inp.kz

TYURIN YU.N.
Paton Electric Welding Institute, NAS of Ukraine, Kyiv,
Ukraine
Tel.: 220-0914, 261-5034
E-mail: ytyurin@i.com.ua, ytyurin@paton.Kyiv.ua

U

UMANSKY A.P.
Frantsevich Institute for Problems of Materials Science,
NASU, Kyiv, Ukraine
Tel.: (044) 444-1321
Fax: (297) 92-273

URYUKOV B.
Frantsevich Institute for Problems of Materials Science,
NASU, Kyiv, Ukraine
Tel.: (044) 450-4963, 444-1191
Fax: (044) 444-2131
E-mail: cosmos@ipms.Kyiv.ua, vyakysil@i.com.ua

USHAKOV I.V.
Derzhavin Tambov State University, Tambov, Russia
Tel.: (0752) 35-2614
Fax: (0752) 71-0307
E-mail: ushakov@tsu.tmb.ru, feodorov@tsu.tmb.ru

USHERENKO S.M.
Institute of Pulse Processes, Minks, Belarus
Tel.: (375) 172 32-5196
Fax: (375) 172 32-8411
E-mail: impuls@BN.BY

USHKALOV L.N.
Frantsevich Institute for Problems of Materials Science,
NASU, Kyiv, Ukraine
Tel.: (044) 444-0256
E-mail: leonid@materials.Kyiv.ua

USKOVA N.A.
Frantsevich Institute for Problems of Materials Science,
NASU, Kyiv, Ukraine
Tel.: (044) 444-1534, 444-3053, 444-3364

USOV V.V.
South Ukrainian State Pedagogical University, Odessa,
Ukraine
Tel.: (0482) 23-4098
Fax: (0482) 732-5103
E-mail: usov@balkan.farlep.net

UVAROV V.
Kurdyumov Institute for Metal Physics, NASU, Kyiv,
Ukraine
E-mail: uvarov@imp.Kyiv.ua

UVAROVA I.V.
Frantsevich Institute for Problems of Materials Science,
NASU, Kyiv, Ukraine
E-mail: uvarova@materials.Kyiv.ua

V

VALEEV I.SH.
Institute for Metals Superplasticity Problems, RAS, Ufa,
Russia
Tel.: (3472) 25-3750, 25-3815
Fax: (3472) 25-3759
E-mail: imsp11@anrb.ru, aigirsh@rambler.ru

VALEEVA A.KH.
Institute for Metals Superplasticity Problems, RAS, Ufa,
Russia
Tel.: (3472) 25-3750, 25-3815
Fax: (3472) 25-3759
E-mail: imsp11@anrb.ru, aigirsh@rambler.ru

VANITCHEVA N.A.
Moscow State Aviation Institute, Moscow, Russia
Tel.: (095) 556-6655, 556-9011, 158-4118
E-mail: vinograd@pt.comcor.ru

VATOLIN N.A.
Institute of Metallurgy Ural's Division of RAS,
Ekaterinburg, Russia
Tel.: +7 3432 67-8924, 28-5312
Fax: +7 3432 67-8918
E-mail: faza@imet.sco.ru, m_o_l_a@mail.ru

VDOVENKO V.A.
Government Plant of Powder Metallurgy, Brovary,
Ukraine
Tel.: (294) 50-182, 52-265
Fax: (294) 50-585, 62-924
E-mail: pmplant@realtel.net.ua

VECHER A.A.
Belarussian State University, Minsk, Belarus
Tel.: (017) 209-5462
E-mail: MichaelZheludkevich@scnsoft.com

VELASCO F.
Universidad Carlos III de Madrid, Spain
Tel.: (3491) 624-9914, 624-9485, 624-9401
Fax: (3491) 624-9430
E-mail: fvelasco@ing.uc3m.es

VELIKANOVA T.YA.
Frantsevich Institute for Problems of Materials Science,
NASU, Kyiv, Ukraine
Tel.: (044) 444-3090
Fax: (044) 444-2131
E-mail: dep6@materials.Kyiv.ua

VERBYLO D.G.
Frantsevich Institute for Problems of Materials Science,
NASU, Kyiv, Ukraine
Tel.: (044) 444-1538
Fax: (044) 444-2131
E-mail: agkost@ipms.Kyiv.ua

VERBYLO M.A.
Physics and Technology Institute for Metals and Alloys,
NAS of Ukraine, Kyiv, Ukraine
Tel.: (044) 444-2350
Fax: (044) 444-1210
E-mail: verbylo@ptima.Kyiv.ua

VERESCHAKA V.M.
Frantsevich Institute for Problems of Materials Science,
NASU, Kyiv, Ukraine
Tel.: (044) 444-2401
Fax: (044) 444-2401
E-mail: vish@i.com.ua

VERETENNIKOVA M.V.
Special Design Bureau «Tekhnolog» at the Saint-
Petersburg State Technological Institute
(Technical University), Saint-Petersburg, Russia
Tel.: (812)100-3898
Fax: (812) 100-3898
E-mail: alcen@comset.net

VETTEGREN V.I.
Ioffe Physico-Technical Institute, RAS, Saint-
Petersburg, Russia
Tel.: (812) 247-1445, 247-9139
Fax: (812) 247-1017
E-mail: victor.vettegren@pop.ioffe.rssi.ru

VIKARCHUK A.A.
Togliatti State University, Togliatti, Russia
E-mail: A.Krylov@vaz.ru, yasn@infopac.ru

VIKULIN V.V.
Federal State Unitary Enterprise «Obninsk Research
and Production Enterprise «TECHNOLOGIYA»,
Obninsk, Russia
Tel.: (08439) 96-875, 62-687
Fax: (08439) 64-575
E-mail: info@technologiya.ru, onpptechn@kaluga.ru

VINOGRADOV YU.K.
Moscow State Aviation Institute, Moscow, Russia
Tel.: (095) 556-6655, 556-9011, 158-4118
E-mail: vinograd@pt.comcor.ru

VISHNYAKOV L.R.
Frantsevich Institute for Problems of Materials Science,
NASU, Kyiv, Ukraine
Tel.: (044) 444-2401
Fax: (044) 444-2401
E-mail: vish@i.com.ua

VISHNYAKOVA E.L.
Frantsevich Institute for Problems of Materials Science,
NASU, Kyiv, Ukraine
Tel.: (044) 444-2401
Fax: (044) 444-2401
E-mail: vish@i.com.ua

VITYAZ P.A.
Institute of Machine Reliability, NASB, Minsk, Belarus
Tel.: (017) 284-2401
Fax: (017) 284-24-01
E-mail: nanotech@inmash.bas-net.by

VLASOV A.
General Physics Institute, RAS, Moscow, Russia
Tel.: (095) 132-8229
Fax: (095) 135-7672
E-mail: ralchenko@nsc.gpi.ru

VLASOV A.A.
NTUU «Kyiv Polytechnic Institute», Kyiv, Ukraine
Tel.: (044) 213-3569, 559-3443
Fax: (044) 213-3569
E-mail: byakova@vic.com.ua

VOITOVYCH V.
Institute of Physics, NAS of Ukraine, Kyiv, Ukraine
Tel.: (044) 265-3973, 265-0825, 265-9958
Fax: (044) 265-1589
E-mail: vova@neimash.Kyiv.ua, krasko@iop.Kyiv.ua,
kraitch@iop.Kyiv.ua, tischenko@iop.Kyiv.ua

VOLENKO A.P.
Togliatti State University, Togliatti, Russia
E-mail: A.Krylov@vaz.ru, yasn@infopac.ru

VORONINA O.O.
Shevchenko Kyiv National University, Kyiv, Ukraine
Tel.: (044) 265-6202, 268-3578
Fax: (044) 265-8342
E-mail: voronina@mail.univ.Kyiv.ua

VOROPAEV A.G.
Belarussian State University, Minsk, Belarus
Tel.: (017) 209-5462
E-mail: MichaelZheludkevich@scnsoft.com

VOSKOBOINIK I.V.
Frantsevich Institute for Problems of Materials Science,
NASU, Kyiv, Ukraine
Tel.: (044) 444-3061
Fax: (044) 444-3061
E-mail: korzhova@materials.Kyiv.ua

VOVCHENKO L.
Shevchenko Kyiv National University, Kyiv, Ukraine
Tel.: (044) 266-2384
E-mail: vovch@mail.univ.Kyiv.ua,
matzui@mail.univ.Kyiv.ua

VOVKOTRUB N.E.
Shevchenko Kyiv National University, Kyiv, Ukraine
E-mail: vsudavtsova@univ.Kyiv.ua

VOZNYAKOVSKIJ A.P.
Special Design Bureau «Tekhnolog» at the Saint-
Petersburg State Technological Institute
(Technical University), Saint-Petersburg, Russia
Tel.: (812)100-3898
Fax: (812) 100-3898
E-mail: alcen@comset.net

VOZNYAKOVSKY A.P.
Lebedev Rubber Research Institute, Saint-Petersburg,
Russia
Tel.: +7 (812) 251-4028, 251-5227
Fax: +7 (812) 251-4813
E-mail: vniisk@mail.rcom.ru, ypsokol@mail.rcom.ru

VU VAN MIENG
Institute of Machine Building Technologies of Ministry of
Industry of Vietnam, Hanoi, Vietnam
Tel.: 04 8353113
Fax: 04 8359235

VYAZOVIKIN I.V.
Voronezh Technological Institute, Voronezh, Russia
Tel.: (044) 444-8286
Fax: (044) 444-2131
E-mail: vyaz@ipms.Kyiv.ua

VYAZOVIKINA N.V.
Frantsevich Institute for Problems of Materials Science,
NASU, Kyiv, Ukraine
Tel.: (044) 444-8286
Fax: (044) 444-2131
E-mail: vyaz@ipms.Kyiv.ua

W

WENDLAND ST.
RÖTECH G.m.b.H., Mühlheim –an-der-Ruhr, Germany
Tel.: +49 (208) 444-2167
Fax: +49 (208) 47-8117
E-mail: Wendland@t-online.de

WENDT M.
Institut fur Physikalische Hochtechnologie, Jena,
Germany
Tel.: (49 36 41) 20-6103, 20-6107, 20-6106
Fax: (49 36 41) 20-6199
E-mail: Michael.Wendt@ipht-jena.de

Y

YAGODKIN V.V.
Frantsevich Institute for Problems of Materials Science,
NASU, Kyiv, Ukraine
Tel.: (044) 444-3364
E-mail: dep.40@materials.Kyiv.ua

YAKUSHKINA V.S.
Federal State Unitary Enterprise «Obninsk Research
and Production Enterprise «TECHNOLOGIYA»,
Obninsk, Russia
Tel.: (08439) 96-875, 62-687
Fax: (08439) 64-575
E-mail: info@technologiya.ru, onpptechn@kaluga.ru

YANTSEVITCH C.V.
NTUU «Kyiv Polytechnic Institute», Kyiv, Ukraine
Tel.: (044) 441-1423, 241-7606
E-mail: carolin@ukrpost.net

YAROSH V.M.
Lavochkin Scientific and Production Association, Himky,
Russia
E-mail: brnovets@ipmnet.ru

YASNIKOV I.S.
Togliatti State University, Togliatti, Russia
E-mail: A.Krylov@vaz.ru, yasn@infopac.ru

YAZYKOV A.V.
Novokuznetsk Department of KemSU, Novokuznetsk,
Russia
E-mail: protasov_ds@zsmk.ru

YEGOROV F.F.
Frantsevich Institute for Problems of Materials Science,
NASU, Kyiv, Ukraine
Tel.: (044) 444-0256

YELISEYEVA O.
Karpenko Physico-Mechanical Institute, NASU, Lviv,
Ukraine
Tel.: (0322) 65-4343
Fax: (0322) 64-9427
E-mail: olga.yeliseyeva@brasimone.enea.it

YENEVICH V.G.
Frantsevich Institute for Problems of Materials Science,
NASU, Kyiv, Ukraine
Tel.: (044) 444-1181
Fax: (044) 444-2131
E-mail: 29min@ipms.Kyiv.ua

YEPIFANTSEVA T.
Frantsevich Institute for Problems of Materials Science,
NASU, Kyiv, Ukraine
Tel.: (044) 444-3255, 444-3039
E-mail: olmi@alfacom.net

YEREMENKO G.V.
Shevchenko Kyiv National University, Kyiv, Ukraine
Tel.: (38044) 266-2335
E-mail: babich@mail.univ.Kyiv.ua,
les@mail.univ.Kyiv.ua, zakharenko@mail.univ.Kyiv.ua

YEVDOKIMENKO YU.
Frantsevich Institute for Problems of Materials Science,
NASU, Kyiv, Ukraine
Tel.: (044) 450-4963, 444-1191
Fax: (044) 444-2131
E-mail: cosmos@ipms.Kyiv.ua, vyakysil@i.com.ua

YUKIO IDE
Yamaguchi Prefectural Industrial Technology Institute,
Ube, Japan
Tel.: (81-22) 217-5214
Fax: (81-22) 217-5178
E-mail: slava@iamp.tohoku.ac.jp

YURCHUCK V.L.
Frantsevich Institute for Problems of Materials Science,
NASU, Kyiv, Ukraine
Tel.: (044) 444-1534, 294-5645
Fax: (044) 444-2034
E-mail:gbag@rambler.ru, vyur@rql.net.ua

YURYEVA E.I.
Institute of Solid State Chemistry, Ural Branch of RAS,
Ekaterinburg, Russia
Tel.: (3432) 74-5331
Fax: (3432) 74-4495
E-mail: Yuryeva@ihim.uran.ru

Z

ZADVORNY A.
Institute for Solid-State Physics, Materials Science and
Technology at National Science Center «Kharkov
Institute of Physics and Technology» (ISSPMST NSC
KIPT), Kharkov, Ukraine
Tel.: (0572) 356-612, 356-484
Fax: (0572) 353-983
E-mail: admin@kipt.kharkov.ua, igor@kipt.kharkov.ua

ZAGNY V.V.
Institute of Technical Mechanics of NASU and NASUU,
Dniepropetrovsk, Ukraine
Tel.: (0562) 46-1051, 47-2465
Fax: (0562) 47-3413
E-mail: itm@tim3.dp.ua, galinskyv@mail.ru

ZAKHARENKO M.I.
Shevchenko Kyiv National University, Kyiv, Ukraine
Tel.: (38044) 266-2335
E-mail: zakharenko@mail.univ.Kyiv.ua

ZAKHAROVA E.G.
Siberian Physic-Technical Institute, Tomsk, Russia
Tel.: (3822) 53-3209
Fax: (3822) 53-3034
E-mail: chum@phys.tsu.ru

ZAKORZHEVSKY V.V.
Institute of Structural Macrokinetics and Materials
Science, RAS, Chernogolovka, Russia
Tel.: (09652) 46-244, 962-8007
Fax: (09652) 962-8025
E-mail: zakvl@ism.ac.ru

ZASHKVARA O.V.
Institute of Physical and Technology ME&S RK, Almaty,
Kazakhstan
Tel.: (3272) 54-6413, 54-5281
Fax: (3272) 54-6224
E-mail: gaitinov@satsun.sci.kz, bolotov@satsun.sci.kz

ZATOVSKIY V.G.
Institute for Problems of Materials Science, NASU, Kyiv,
Ukraine
Тел.: (044) 444-2474, 444-1571, 444-3401, 444-3315
E-mail: 29min@ipms.ua, polotay@materials.Kyiv.ua

ZATULOVSKY A.S.
Physics and Technology Institute for Metals and Alloys,
NAS of Ukraine, Kyiv, Ukraine
Tel.: (044) 444-3542
Fax: (044) 444-3542
E-mail: kompozit@inec.Kyiv.ua

ZATULOVSKY S.S.
Physics and Technology Institute for Metals and Alloys,
NAS of Ukraine, Kyiv, Ukraine
Tel.: (044) 444-3542
Fax: (044) 444-3542
E-mail: kompozit@inec.Kyiv.ua

ZEISBERGER M.
Institut fur Physikalische Hochtechnologie, Jena,
Germany
E-mail: prikhna@iptelecom.net.ua

ZELENOV I.A.
Lavochkin Scientific and Production Association, Himky,
Russia
Tel.: (095) 575-5916, 575-5516
Fax: (095) 573-3595
E-mail: gotovtsev@hotmail.com

ZGADKEIVICH M.L.
Paton Electric Welding Institute, NAS of Ukraine, Kyiv,
Ukraine
Tel.: 220-0914, 261-5034
E-mail: ytyurin@i.com.ua, ytyurin@paton.Kyiv.ua

ZHARKOV L.K.
Scientific-Industrial Complex «Yuna», Kazan, Russia
Tel.: (8432) 435-935
Fax: (8432) 435-935
E-mail: root@una.kazan.ru

ZHDANOVSKII V.A.
Institute of Physics, NASB, Minsk, Belarus
E-mail: tsaruk@dragon.bas-net.by

ZHELUDKEVICH M.L.
Belarussian State University, Minsk, Belarus
Tel.: (017) 209-5462
E-mail: MichaelZheludkevich@scnsoft.com

ZHUKOV S.G.
Central Research Institute for Materials, Saint
Petersburg, Russia
Tel.: (812) 278-9341, 278-9178, 271-4469
Fax: (812) 274-4639
E-mail: carbid@pop3.rcom.ru

ZHUNKOVSKII G.L.
Frantsevich Institute for Problems of Materials Science,
NASU, Kyiv, Ukraine
Tel.: (044) 444-1481

ZHURAVKOV A.
Shevchenko Kyiv National University, Kyiv, Ukraine
Tel.: (044) 266-2384
E-mail: vovch@mail.univ.Kyiv.ua,
matzui@mail.univ.Kyiv.ua

ZHURAVSKY G.I.
Lykov Heat and Mass Transfer Institute, National
Academy of Belarus, Minsk, Belarus
Tel.: (017) 284-2241, 284-2478
Fax: (017) 232-1325
E-mail: vas@hmti.ac.by, vvl@hmti.ac.by

ZIMA T.M.
Institute of Solid State Chemistry and
Mechanochemistry, SB RAS, Novosibirsk, Russia
Tel.: (3832) 32-9600
Fax: (3832) 322847
E-mail: servis_ins@online.sinor.ru,
lena@mill.solid.nsc.ru

ZORIN V.
Frantsevich Institute for Problems of Materials Science,
NASU, Kyiv, Ukraine
Tel.: (044) 444-1486
Fax: (044) 444-2131
E-mail: dir@ipms.Kyiv.ua

ZUBENKO A.I.
Physics and Technology Institute for Metals and Alloys,
NAS of Ukraine, Kyiv, Ukraine
Tel.: (044) 444-2350
Fax: (044) 444-1210
E-mail: verbylo@ptima.Kyiv.ua

ZUBRO S.
Lomonosov Moscow Institute of Fine Chemical
Technology, Moscow, Russia
Tel.: 447-6283
Fax: 434-7111
E-mail: perelman@mtu-net.ru

ZVONARIOV E.V.
Powder Metallurgy Research Institute, NASB, Minsk,
Belarus
Tel.: (7522) 31-2246

ZYKOVA E.V.
Frantsevich Institute for Problems of Materials Science,
NASU, Kyiv, Ukraine
Tel.: 044 (444-8286)

ZYRIN A.
Frantsevich Institute for Problems of Materials Science,
NASU, Kyiv, Ukraine
Tel.: (044) 444-3573
E-mail: zyrin@ipms.Kyiv.ua

For publishing materials are prepared by:

L. Chernyshev
D. Levina
O. Onoprienko
O. Koryak
T. Pirnach

Web master

N. Minakov